

Second Edition

GAS **Chromatography**



Edited by **Colin F. Poole**

GAS CHROMATOGRAPHY

SECOND EDITION

This page intentionally left blank

GAS CHROMATOGRAPHY

SECOND EDITION

Edited by

COLIN F. POOLE

Department of Chemistry, Wayne State University, Detroit, MI, United States



ELSEVIER

Elsevier

Radarweg 29, PO Box 211, 1000 AE Amsterdam, Netherlands

The Boulevard, Langford Lane, Kidlington, Oxford OX5 1GB, United Kingdom

50 Hampshire Street, 5th Floor, Cambridge, MA 02139, United States

Copyright © 2021 Elsevier Inc. All rights reserved.

No part of this publication may be reproduced or transmitted in any form or by any means, electronic or mechanical, including photocopying, recording, or any information storage and retrieval system, without permission in writing from the publisher. Details on how to seek permission, further information about the Publisher's permissions policies and our arrangements with organizations such as the Copyright Clearance Center and the Copyright Licensing Agency, can be found at our website: www.elsevier.com/permissions.

This book and the individual contributions contained in it are protected under copyright by the Publisher (other than as may be noted herein).

Notices

Knowledge and best practice in this field are constantly changing. As new research and experience broaden our understanding, changes in research methods, professional practices, or medical treatment may become necessary.

Practitioners and researchers must always rely on their own experience and knowledge in evaluating and using any information, methods, compounds, or experiments described herein. In using such information or methods they should be mindful of their own safety and the safety of others, including parties for whom they have a professional responsibility.

To the fullest extent of the law, neither the Publisher nor the authors, contributors, or editors, assume any liability for any injury and/or damage to persons or property as a matter of products liability, negligence or otherwise, or from any use or operation of any methods, products, instructions, or ideas contained in the material herein.

Library of Congress Cataloging-in-Publication Data

A catalog record for this book is available from the Library of Congress

British Library Cataloguing-in-Publication Data

A catalogue record for this book is available from the British Library

ISBN: 978-0-12-820675-1

For information on all Elsevier publications visit our website
at <https://www.elsevier.com/books-and-journals>

Publisher: Susan Dennis

Acquisitions Editor: Kathryn Eryilmaz

Editorial Project Manager: Liz Heijkoop

Production Project Manager: Kumar Anbazhagan

Cover Designer: Greg Harris

Typeset by TNQ Technologies



Contents

Contributors xi

1. Milestones in the development of gas chromatography

WALTER G. JENNINGS AND COLIN F. POOLE

- 1.1 Introduction 1
- 1.2 The invention of gas chromatography 1
- 1.3 Early instrumentation 2
- 1.4 Early column developments 3
- 1.5 Interfacing glass capillary columns to injectors and detectors 6
- 1.6 The Hindelang conferences and the fused-silica column 7
- 1.7 Increasing sophistication of instrumentation 9
- 1.8 Decline in the expertise of the average gas chromatographer 15
- References 16
- Further reading 17

2. Theory of gas chromatography

LEONID M. BLUMBERG

- 2.1 Introduction 19
- 2.2 Nomenclature and other conventions 20
- 2.3 General definitions and conventions 23
- 2.4 Solute-column interaction 23
- 2.5 Properties of ideal gas 29
- 2.6 Flow of ideal gas in open tubes 33
- 2.7 Solute migration and elution 37
- 2.8 Peak spacing and reversal of elution order 45
- 2.9 Peak width 48
- 2.10 Performance metrics 67
- 2.11 Optimization 73
- References 92

3. Column technology: open-tubular columns

FRANK L. DORMAN AND PETER DAWES

- 3.1 Introduction 99
- 3.2 Overview of the fused-silica drawing process 100

- 3.3 The preform—raw material 100
- 3.4 Surface chemistry 101
- 3.5 Drawing of the capillary from the preform 101
- 3.6 Protective coating 103
- 3.7 Alternative protective coatings 104
- 3.8 Cleanroom environment 105
- 3.9 Quality monitoring 105
- 3.10 Observations on handling of fused-silica capillary tubing 107
- 3.11 Column technology—coating the stationary phase 108
- 3.12 Stationary phases 111
- 3.13 Coating techniques 112
- 3.14 Column technology—quality evaluation 114
- 3.15 Column technology—summary 116
- References 116

4. Column technology: porous layer open-tubular columns

JAAP DE ZEEUW

- 4.1 Introduction 117
- 4.2 Challenges in porous layer open-tubular (PLOT) column chemistry 117
- 4.3 Measurement of restriction of PLOT columns 119
- 4.4 Manufacture of PLOT columns 119
- 4.5 Stabilization of adsorption layers 121
- 4.6 Behavior of adsorbents 122
- 4.7 PLOT columns in gas chromatography—mass spectrometry 123
- 4.8 Types of capillary tubing 123
- 4.9 Most commonly used adsorbents 124
- 4.10 Summary 138
- References 140

5. Column technology: packed columns

COLIN F. POOLE

- 5.1 Introduction 141
- 5.2 Gas-liquid chromatography 142
- 5.3 Gas-solid chromatography 158
- References 161

6. Column classification and structure-retention relationships

COLIN F. POOLE

- 6.1 Introduction 165
- 6.2 Stationary-phase classification 167
- 6.3 Structure—retention relationships 181
- References 186

7. Multidimensional and comprehensive gas chromatography

JOHN V. SEELEY

- 7.1 Introduction 191
- 7.2 A graphical representation of 2D GC separations 193
- 7.3 Backflushing 2D GC 195
- 7.4 Heartcutting 2D GC 200
- 7.5 Comprehensive 2D GC 203
- 7.6 Conclusions 211
- References 213

8. Sample introduction methods

ANDREW TIPLER

- 8.1 Introduction 217
- 8.2 Choosing a sample introduction system 218
- 8.3 Supporting devices 218
- 8.4 The cold on-column injector 223
- 8.5 The flash vaporization injector 229
- 8.6 The split/splitless injector 231
- 8.7 The programmable-temperature vaporizing (PTV) injector 240
- 8.8 The gas sampling valve 246
- 8.9 The liquid sampling valve 247
- Acknowledgments 247
- References 249

9. Headspace gas chromatography

MICHAEL J. SITHERSINGH AND NICHOLAS H. SNOW

- 9.1 Introduction 251
- 9.2 Fundamentals of headspace extraction 253
- 9.3 Instrumentation and practice 257
- 9.4 Method development considerations 262
- Acknowledgments 264
- References 264

10. Thermal desorption gas chromatography

ELIZABETH WOOLFENDEN

- 10.1 General introduction to thermal desorption 267
- 10.2 Brief history of thermal desorption—essential functions and performance characteristics 270
- 10.3 The evolution of TD technology—important milestones 276
- 10.4 Using thermal desorption to enhance analysis of complex liquid and solid samples 285
- 10.5 Sampling options for thermal desorption 288
- 10.6 An introduction to thermal desorption applications 288
- 10.7 Breath monitoring 290
- 10.8 Air monitoring 291
- 10.9 Chemical emissions from everyday products to indoor and in-vehicle air 295
- 10.10 Toxic chemical agents and civil defense 299
- 10.11 Direct thermal desorption of residual volatiles 299
- 10.12 Odor/fragrance profiling and VOC “fingerprinting” 301
- 10.13 Forensic applications 306
- 10.14 Monitoring manufacturing and other industrial chemical processes 309
- Appendix A 309
- Appendix B 314
- References 316

11. Pyrolysis-gas chromatography

KAREN D. SAM

- 11.1 Introduction 325
- 11.2 Molecular theory 326
- 11.3 Instrumentation 329
- 11.4 Applications 330
- References 342

12. Conventional detectors for gas chromatography

COLIN F. POOLE

- 12.1 Introduction 343
- 12.2 Ionization-based detectors 345
- 12.3 Bulk physical property detectors 358
- 12.4 Optical detectors 360
- 12.5 Electrochemical detectors 366
- References 367

13. Molecular spectroscopic detectors for gas chromatography

ARIEL M. O'BRIEN AND KEVIN A. SCHUG

- 13.1 Introduction 371
- 13.2 Milestones 372
- 13.3 Gas chromatography Fourier transform infrared spectroscopy 373
- 13.4 Gas chromatography vacuum ultraviolet spectroscopy 382
- 13.5 Comparison of techniques 390
- 13.6 Conclusions and future outlook 394
- References 394

14. Mass spectrometric detectors for gas chromatography

DAVID J. HARVEY

- 14.1 Introduction 399
- 14.2 Gas chromatography—mass spectrometry interfaces 399
- 14.3 Ionization techniques 402
- 14.4 Methods of mass separation 409
- 14.5 Modes of operation 414
- 14.6 Data analysis 417
- 14.7 Sample preparation 420
- 14.8 Conclusions 420
- References 423

15. Ion mobility detectors for gas chromatography

MARIA JOSE CARDADOR, NATIVIDAD JURADO-CAMPOS AND
LOURDES ARCE

- 15.1 Introduction 425
- 15.2 IMS operation 426
- 15.3 IMS device components 427
- 15.4 Types of IMS instruments 430
- 15.5 Limitations of IMS 432
- 15.6 Fundamentals of GC-IMS 432
- 15.7 Types of IMS coupled to GC 433
- 15.8 Data obtained from GC-IMS instruments 434
- 15.9 Treatment of IMS data 435
- 15.10 Advantages and disadvantages of GC-IMS analysis 438
- 15.11 Applications 439
- References 442

16. Speciation and element-selective detection by gas chromatography

QILIN CHAN AND JOSEPH A. CARUSO

- 16.1 Introduction to plasma-based detectors 449
- 16.2 GC-ICPMS 451
- 16.3 GC-MIP and GC-GD 454
- 16.4 Sample preparation for GC—plasma spectroscopy 457
- 16.5 Advances in applications of GC—plasma spectroscopy 457
- 16.6 Conclusions and perspectives 462
- References 462

17. Field and portable instruments for gas chromatography

STANLEY D. STEARNS

- 17.1 History 469
- 17.2 Design challenges 472
- 17.3 Sample introduction 472
- 17.4 Column configurations 474
- 17.5 Detectors 476
- 17.6 Gas supply 477
- 17.7 Power management 478
- 17.8 Prototyping 481
- 17.9 Commercial portable GCs currently available 482
- 17.10 Future trends 482
- Acknowledgments 485
- References 485

18. Preparative gas chromatography

LEESUN KIM AND PHILIP J. MARRIOTT

- 18.1 Introduction 487
- 18.2 Application scale of preparative gas chromatography 488
- 18.3 Experimental techniques for analytical-scale prep-GC 489
- 18.4 Case studies: applications 494
- 18.5 Conclusions 502
- Acknowledgments 502
- References 502

19. Data acquisition and integration

YURI KALAMBET

- 19.1 Introduction 505
- 19.2 Equipment control and signal measurement 506

- 19.3 Peak search 508
19.4 Errors caused by discretization (data rate) and conversion (bit price value) 512
19.5 Smoothing 514
19.6 Peak identification 517
19.7 Quantification 518
References 521

20. Data analysis methods for gas chromatography

KARISA M. PIERCE, TIMOTHY J. TRINKLEIN, JEREMY S. NADEAU
AND ROBERT E. SYNOVEC

- 20.1 Introduction 525
20.2 Preprocessing 527
20.3 Pattern recognition 533
20.4 Calibration 540
20.5 Experimental method optimization 541
20.6 Conclusion 542
References 542

21. Validation of gas chromatographic methods

BIEKE DEJAEGER, JOHANNA SMEYERS-VERBEKE AND
YVAN VANDER HEYDEN

- 21.1 Introduction 547
21.2 Regulatory aspects 548
21.3 Method validation items 548
21.4 Accuracy profiles 559
References 559

22. Physicochemical measurements (inverse gas chromatography)

ADAM VOELKEL

- 22.1 Introduction 561
22.2 Gas–solid inverse gas chromatography 562
22.3 Bulk properties of polymers and polymers blends 569
References 573

23. Separation of stereoisomers by gas chromatography

CECILIA CAGLIERO, BARBARA SGORBINI, CHIARA CORDERO,
ERICA LIBERTO, PATRIZIA RUBIOLO AND CARLO BICCHI

- 23.1 Introduction 581
23.2 Chiral stationary phases for enantioselective gas chromatography 583

- 23.3 Determination of the enantiomeric distribution 595
23.4 Strategy for achieving chiral recognition 596
23.5 Total analysis systems and chiral recognition of complex samples 604
23.6 Micropreparative enantioselective gas chromatography 604
23.7 Conclusions 606
References 606

24. Sample preparation for gas chromatography

COLIN F. POOLE

- 24.1 Introduction 615
24.2 Isolation and concentration techniques using physical methods 616
24.3 Sample cleanup by column chromatography 635
24.4 Microchemical reactions for modification of target compound 638
References 648

25. Petrochemical applications of gas chromatography

JULIANA CRUCELLO, NATHÁLIA DE AGUIAR PORTO,
ROGÉRIO MESQUITA CARVALHO,
ALEXANDRE DE ANDRADE FERREIRA,
CARLOS ALBERTO CARBONEZI AND
LEANDRO WANG HANTAO

- 25.1 Introduction 655
25.2 Column selection according to sample volatility 659
25.3 Introduction to organic geochemical analyses 660
25.4 Refinery oil assays 663
References 669

26. Gas chromatographic analysis of essential oils

K. HÜSNÜ CAN BAŞER AND TEMEL ÖZEK

- 26.1 Definitions: what is essential oil? What are fragrances? 675
26.2 GC phases used in the analysis of essential oils and aroma chemicals 676
26.3 Separation criteria and techniques 676
26.4 Retention index 679
26.5 Qualitative and quantitative aspects 679
26.6 GC-MS libraries 679
26.7 Conclusions 680
References 681

27. Gas chromatographic analysis of lipids

CRISTINA CRUZ-HERNANDEZ AND FRÉDÉRIC DESTAILLATS

- 27.1 Introduction 683
- 27.2 Fatty acid analysis by GC as methyl ester derivatives 684
- 27.3 Analysis of free fatty acids and acylglycerols 690
- 27.4 Analysis of sterols, sterol esters, stanyl esters, and steryl glycosides 691
- 27.5 Analysis of waxes 693
- References 693

28. Gas chromatographic analysis of carbohydrates

A.C. SORIA, A. MENA, A.I. RUIZ-MATUTE AND M.L. SANZ

- 28.1 Introduction 703
- 28.2 Sample preparation 704
- 28.3 Derivatization 708
- 28.4 Chromatographic conditions for the analysis of carbohydrates 713
- 28.5 Structural elucidation of low-molecular-weight carbohydrates 716
- 28.6 GC-MS analysis of oligo- and polysaccharides 719
- 28.7 Comprehensive two-dimensional gas chromatography 720
- References 721

29. Gas chromatographic applications in metabolomics

SZE HAN LEE, MAINAK MAL, KISHORE KUMAR PASIKANTI AND ERIC CHUN YONG CHAN

- 29.1 Overview of metabolomics 727
- 29.2 Analytical tools in metabolomic research 728
- 29.3 GC-MS-based metabolomics 728
- 29.4 Metabolomics of solid samples 733
- 29.5 Metabolomics of liquid samples 735
- 29.6 Future directions 737
- References 737

30. Applications of gas chromatography in forensic science

ABUZAR KABIR AND KENNETH G. FURTON

- 30.1 Introduction and scope 745
- 30.2 Analysis of bulk drug for identification, impurity profiling, and drug intelligence purpose 747
- 30.3 Gas chromatography in forensic toxicology 753
- 30.4 Analysis of ignitable liquid residues from fire debris 760
- 30.5 Analysis of explosives 761

- 30.6 Gas chromatographic analysis of organic gunshot residues (OGSRs) 764

- 30.7 Analysis of forensic trace evidence 767
- 30.8 Forensic environmental analysis 768
- 30.9 Analysis of human odor profile 772
- 30.10 Analysis of human decomposition products 774
- 30.11 Field-portable gas chromatograph for onsite sample analysis 776
- 30.12 Gas chromatography in food forensics 777
- 30.13 Analysis of chemical warfare agents (CWAs) 778
- 30.14 New developments in gas chromatography with forensic implications 779
- References 780

31. Applications of gas chromatography to multiresidue methods for pesticides and related compounds in food

MILAGROS MEZCUA, M. ANGELES MARTINEZ-UROZ AND AMADEO R. FERNANDEZ-ALBA

- 31.1 Introduction 793
- 31.2 Multiresidue methods for pesticides in crops 794
- 31.3 Multiresidue methods for pesticides in animal origin products 798
- 31.4 Multiresidue methods for pesticides in processed food 799
- 31.5 Multiresidue methods for pesticides in baby food 802
- 31.6 Conclusions 804
- Acknowledgments 804
- References 804

32. Gas chromatographic analysis of wine

SUSAN E. EBELER

- 32.1 Introduction 807
- 32.2 Stationary phases 808
- 32.3 Multidimensional separations 810
- 32.4 Detectors and hyphenated techniques 812
- 32.5 Sample preparation 815
- Summary 821
- References 822

33. Gas chromatographic analysis of emerging and persistent environmental contaminants

FRANK L. DORMAN AND ERIC J. REINER

- 33.1 Introduction 836
- 33.2 Polychlorinated biphenyls 838
- 33.3 Dioxins 843

- 33.4 Organochlorine pesticides 848
- 33.5 Halogenated flame retardants 851
- 33.6 Polybrominated diphenyl ethers 853
- 33.7 Other halogenated flame retardants 853
- 33.8 Perfluorinated compounds 859
- 33.9 Polycyclic aromatic hydrocarbons 859
- 33.10 Other compounds not specifically discussed 861
- 33.11 Summary 861
- References 862

- 34. Gas chromatography in space exploration
MARIA CHIARA PIETROGRANDE
 - 34.1 Introduction 865
 - 34.2 Technological and operating constraints in space GC 866
 - 34.3 Prebiotic chemistry in Titan's atmosphere: the Cassini–Huygens mission 867
 - 34.4 Prebiotic chemistry in comet environments: Rosetta mission 867

- 34.5 Search for key chemical biomarkers: Mars exploration 869
- 34.6 Search for chirality in space 871
- 34.7 Conclusions and perspectives 872
- References 872

- 35. Gas chromatographic analysis of chemical warfare agents
PHILIP A. SMITH
 - 35.1 Introduction and background 875
 - 35.2 Analytical considerations for sampling and gas chromatographic analysis of CWA-related compounds 887
 - 35.3 GC applications for biomedical CWA analyses 895
 - 35.4 Conclusion 896
 - References 896

- Index 901

Contributors

- Lourdes Arce** Department of Analytical Chemistry, University of Córdoba, Institute of Fine Chemistry and Nanochemistry, Córdoba, Spain
- Carlo Bicchi** Dipartimento di Scienza e Tecnologia del Farmaco, University of Torino, Torino, Italy
- Leonid M. Blumberg** Advachrom, Wilmington, DE, United States
- Cecilia Cagliero** Dipartimento di Scienza e Tecnologia del Farmaco, University of Torino, Torino, Italy
- K. Hüsnü Can Başer** Anadolu University, Eskisehir, TR, Turkey
- Carlos Alberto Carbonezi** Division of Geochemistry, PETROBRAS Research and Development Center (CENPES), PETROBRAS, Rio de Janeiro, RJ, Brazil
- Maria Jose Cardador** Department of Analytical Chemistry, University of Córdoba, Institute of Fine Chemistry and Nanochemistry, Córdoba, Spain
- Joseph A. Caruso** University of Cincinnati, Cincinnati, OH, United States
- Rogério Mesquita Carvalho** Division of Chemistry, PETROBRAS Research and Development Center (CENPES), PETROBRAS, Rio de Janeiro, RJ, Brazil
- Qilin Chan** University of Cincinnati, Cincinnati, OH, United States
- Eric Chun Yong Chan** Department of Pharmacy, National University of Singapore, Singapore
- Chiara Cordero** Dipartimento di Scienza e Tecnologia del Farmaco, University of Torino, Torino, Italy
- Juliana Crucello** Institute of Chemistry, University of Campinas (UNICAMP), Campinas, SP, Brazil
- Cristina Cruz-Hernandez** Nestlé Research, Vers-chez-Les-Blanc, Lausanne, Switzerland
- Peter Dawes** Analytical Science, SGE, Ringwood, VIC, Australia
- Nathália de Aguiar Porto** Institute of Chemistry, University of Campinas (UNICAMP), Campinas, SP, Brazil
- Alexandre de Andrade Ferreira** Division of Geochemistry, PETROBRAS Research and Development Center (CENPES), PETROBRAS, Rio de Janeiro, RJ, Brazil
- Bieke Dejaegher** Department of Analytical Chemistry, Applied Chemometrics and Molecular Modeling, Vrije Universiteit Brussel (VUB), Brussels, Belgium
- Frédéric Destailats** Nestlé Nutrition Research, Vevey, Switzerland
- Jaap de Zeeuw** Restek Corporation, Middelburg, The Netherlands
- Frank L. Dorman** Biochemistry and Molecular Biology, The Pennsylvania State University, University Park, PA, United States
- Susan E. Ebeler** Department of Viticulture and Enology, One Shields Avenue, University of California, Davis, CA, United States
- Amadeo R. Fernandez-Alba** Pesticide Residue Reseach Group, University of Almeria, La Canada de San Urbano, Almeria, Spain
- Kenneth G. Furton** Department of Chemistry and Biochemistry, Florida International University, Miami, FL, United States
- Leandro Wang Hantao** Institute of Chemistry, University of Campinas (UNICAMP), Campinas, SP, Brazil
- David J. Harvey** Target Discovery Institute, Nuffield Department of Medicine, University of Oxford, Oxford, United Kingdom

- Walter G. Jennings** Food Science, University of California, Davis, CA, United States
- Natividad Jurado-Campos** Department of Analytical Chemistry, University of Córdoba, Institute of Fine Chemistry and Nanochemistry, Córdoba, Spain
- Abuzar Kabir** Department of Chemistry and Biochemistry, Florida International University, Miami, FL, United States
- Yuri Kalambet** Ampersand Ltd., Moscow, Russian Federation
- Leesun Kim** Ulsan National Institute of Science and Technology, Ulsan, South Korea
- Sze Han Lee** Department of Pharmacy, National University of Singapore, Singapore
- Erica Liberto** Dipartimento di Scienza e Tecnologia del Farmaco, University of Torino, Torino, Italy
- Mainak Mal** Department of Pharmaceutical Technology, Brainware University, Kolkata, India
- Philip J. Marriott** School of Chemistry Monash University, Clayton, VIC, Australia
- M. Angeles Martinez-Uroz** Pesticide Residue Research Group, University of Almería, La Canada de San Urbano, Almería, Spain
- A. Mena** Instituto de Química Orgánica General (CSIC), Madrid, Spain
- Milagros Mezcua** Pesticide Residue Research Group, University of Almería, La Canada de San Urbano, Almería, Spain
- Jeremy S. Nadeau** Department of Chemistry, University of Washington, Seattle, WA, United States
- Ariel M. O'Brien** Department of Chemistry & Biochemistry, The University of Texas, Arlington, TX, United States
- Temel Özek** Anadolu University, Eskisehir, TR, Turkey
- Kishore Kumar Pasikanti** Accelerating Therapeutics for Opportunities in Medicine (ATOM) Consortium, San Francisco, CA, United States
- Karisa M. Pierce** Department of Chemistry and Biochemistry, Seattle Pacific University, Seattle, WA, United States
- Maria Chiara Pietrogrande** Department of Chemistry, University of Ferrara, Ferrara, Italy
- Colin F. Poole** Department of Chemistry, Wayne State University, Detroit, MI, United States
- Eric J. Reiner** Biochemistry and Molecular Biology, The Pennsylvania State University, University Park, PA, United States
- Patrizia Rubiolo** Dipartimento di Scienza e Tecnologia del Farmaco, University of Torino, Torino, Italy
- A.I. Ruiz-Matute** Instituto de Química Orgánica General (CSIC), Madrid, Spain
- Karen D. Sam** Applications Lab, CDS Analytical, Oxford, PA, United States
- M.L. Sanz** Instituto de Química Orgánica General (CSIC), Madrid, Spain
- Kevin A. Schug** Department of Chemistry & Biochemistry, The University of Texas, Arlington, TX, United States
- John V. Seeley** Oakland University, Department of Chemistry, Rochester, MI, United States
- Barbara Sgorbini** Dipartimento di Scienza e Tecnologia del Farmaco, University of Torino, Torino, Italy
- Michael J. Sithersingh** KR Consultants, Parsippany, NJ, United States
- Johanna Smeyers-Verbeke** Department of Analytical Chemistry, Applied Chemometrics and Molecular Modelling, Vrije Universiteit Brussel (VUB), Brussels, Belgium
- Philip A. Smith** US Department of Labor, Salt Lake Technical Center, Sandy, UT, United States
- Nicholas H. Snow** Chemistry and Biochemistry, Seton Hall University, South Orange, NJ, United States
- A.C. Soria** Instituto de Química Orgánica General (CSIC), Madrid, Spain
- Stanley D. Stearns** Valco Instruments Co. Inc., Houston, TX, United States
- Robert E. Synovec** Department of Chemistry, University of Washington, Seattle, WA, United States
- Andrew Tipler** PerkinElmer Inc., Shelton, CT, United States

Timothy J. Trinklein Department of Chemistry,
University of Washington, Seattle, WA, United
States

Yvan Vander Heyden Department of Analytical
Chemistry, Applied Chemometrics and Molecular
Modelling, Vrije Universiteit Brussel (VUB), Brus-
sels, Belgium

Adam Voelkel Institute of Chemical Technology
and Engineering, Poznan University of Technology,
Poznań, Poland

Elizabeth Woolfenden Markes International
Limited, 1000 Central Park, Western Avenue,
Bridgend, United Kingdom

Milestones in the development of gas chromatography

Walter G. Jennings^{1,†}, Colin F. Poole²

¹Food Science, University of California, Davis, CA, United States; ²Department of Chemistry, Wayne State University, Detroit, MI, United States

1.1 Introduction

This article was started by the senior author Walter Jennings, who was unable to complete it due to poor health. Walter passed away in the summer of 2012. Sections 1.2–1.6 are a personal account of the early days of gas chromatography seen through the eyes of one of the major pioneers and innovators in this field. With only minor editorial changes made by the junior author, these are presented as Walter intended. As the junior author, I am responsible for Sections 1.7 and 1.8. These sections extend Walter's comments on the early days of gas chromatography to the present day and benefited from the detailed notes he provided me with.

1.2 The invention of gas chromatography

In 1952, A.J.P. Martin and R.L.M. Synge were both awarded Nobel Prizes for their work in the field of liquid/solid chromatography. Martin, in

his award address, suggested it might be possible to use a vapor as the mobile phase. Some years later, James and Martin used ethyl acetate vapor to desorb a mixture of fatty acids that had been affixed to an adsorbent and placed in a tube. The vapor stream eluting from that tube was directed to an automated titration apparatus, resulting in a graph showing a series of “steps” that reflected the sequential additions of base as each eluted acid was neutralized by automated titration [1]. Many practitioners have for far too long considered this as the starting point of gas chromatography.

In 2008, Leslie Ettre published an article in which he stated, “... the activities of Professor Erika Cremer and her students at the University of Innsbruck, Austria, in the years following the Second World War, represented the true start of their continuous involvement in gas chromatography” [2]. After exploring Ettre's arguments and conducting some research myself, I fully agree with his conclusions. I now believe that the

[†] Author W.G. Jennings is deceased.

theoretical basis for gas chromatography was first conceived by Erika Cremer, an Austrian scientist at the University of Innsbruck, Austria, in the late 1940s during the period of the Second World War. As Ettre points out, this was a period when women, especially in Germanic countries, were expected to confine their activities to “children, church, and kitchen”. In spite of her “superb Ph.D. thesis work,” she had great difficulty in finding a position. Her opportunity came in 1940 when the war started, and university teachers were drafted. She obtained an academic position at the University of Innsbruck, Austria (then a part of Germany), in the Institute of Physical Chemistry. It was here that she and her students (with major credit to Fritz Prior) constructed the first prototype of a gas chromatograph (GC) (Fig. 1.1) and, after a long delay that was probably attributable to the war, published the results of their research in 1951 [3,4]. At this time she was promoted to professor and, some 20 years later, to director of the

University's Institute of Physical Chemistry. Professor Dr. Cremer, by all accounts a brilliant woman scientist, died in 1996.

1.3 Early instrumentation

By 1953, several petroleum companies, primarily in Great Britain and the Netherlands, were exploring this new analytical technique, and in 1954, a few flavor chemists (including this author) were building crude chromatographs, many of them based on an article by N. H. Ray [5]. Ray inserted thermal conductivity cells into a Wheatstone bridge, whose outlet connected to a strip chart recorder, thus generating a Gaussian peak for each eluting solute; this was (to my knowledge) the first gas chromatogram as we know it today. The schematics and chromatograms published by Ray encouraged a number of readers (including the author) to build similar chromatographs. Almost every part of these crude instruments had to be

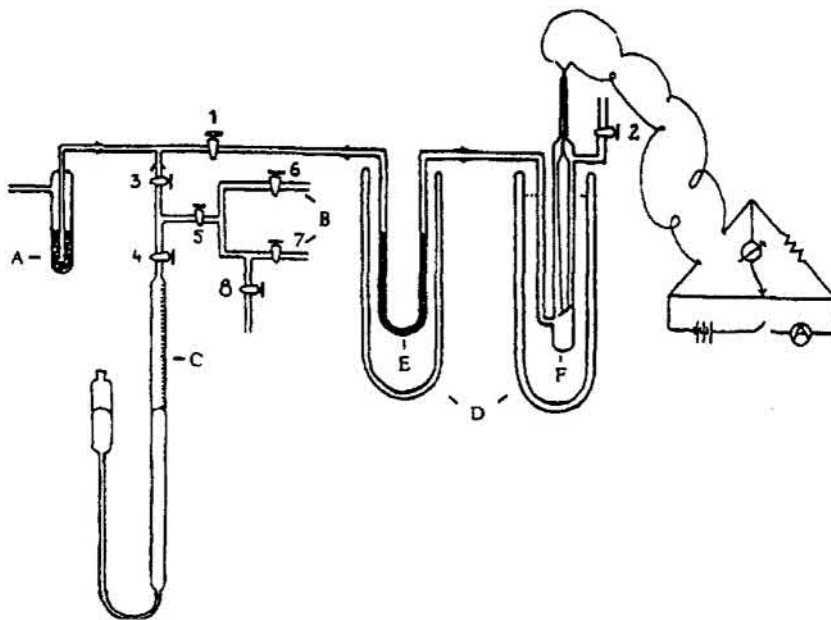


FIGURE 1.1 The gas chromatographic system used in Prior's work, in 1945–1947. (A) adsorbent for purification of the carrier gas (hydrogen); (B) sample inlet system; (C) buret containing mercury with niveau glass for sample introduction; (D) Dewar flask; (E) separation column (containing silica gel on activated carbon); and (F) thermal conductivity detector. From Ref. O. Bobleter, *Exhibition of the first gas chromatographic work of Erika Cremer and Fritz Prior*, *Chromatographia* 43 (1996) 444–446; Copyright Friedr. Vieweg and Sohn.

self-designed and self-made, but this introduced the days of the packed column; supports, such as granules of diatomaceous earth, were coated with a variety of high-boiling fluids (e.g., diethylene glycol succinate, DEGS) and, in our earliest efforts, packed into copper columns, typically 3–6 m long with internal diameters of about 6 mm, and (usually) coiled. It was soon recognized that copper columns were quite active, and most workers switched, first to stainless steel and then to coiled glass tubing of similar dimensions. The reminiscences of many of the early pioneers in gas chromatographic instrumentation are summarized in Ref. [6].

1.3.1 Early commercial instruments

The first companies to manufacture GCs in Europe were Griffin and George (London) and Metropolitan Vickers Electric (Manchester), but the US instrument companies had a greater impact on the development of this new area [7]. PerkinElmer was one of the first companies to market a GC; in May of 1954, they introduced their Model 154 Vapor Fractometer. The temperature of the column oven was adjustable from room temperature to 150°C, and it offered a “flash vaporizer” with a rubber septum permitting syringe injection into the carrier gas stream. The detector was a thermal conductivity cell. The instrument was a great success and sold widely [8]. In early 1956, PerkinElmer followed up with their Model 154-B, with a temperature range from room temperature to 225°C and could be fitted with an optional rotary valve offering a variety of sample loops for the injection of gas samples.

1.4 Early column developments

All of the early instruments utilized packed columns, some coiled, some U-shaped. Packed columns all have one thing in common: they possess a high resistance to gas flow, and this

limits the practical length of the column, usually to a few meters. In much later days, some packed columns approached an efficiency equivalent to our current 0.32 mm internal diameter capillary columns (ca. 3000 plates per meter), but because of their length limitations, they could achieve perhaps 35,000 theoretical plates while a 30 m open-tubular 0.25 mm internal diameter column should be capable of three times that efficiency, merely because it is three times longer.

It was at the 1958 Second International Symposium on Gas Chromatography in Amsterdam that Marcel Golay, who was then a consultant to PerkinElmer, introduced the theory of open-tubular capillary columns and demonstrated their superiority to packed columns [9]. (*There is no connection between the old PerkinElmer referred to here and the PerkinElmer of today, they are entirely different companies.*) These columns demanded much smaller sample injections, necessitating more sensitive detectors than the thermal conductivity detectors that were in common use at the time. Fortunately, James E. Lovelock had invented an electron-capture detector in 1957 [10], and in 1958 the flame ionization detector appeared; some credit this to Harley, Nel, and Pretorius [11], and others to McWilliams and Dewar [12,13]; these increased detector sensitivities by ca. 10^3 – 10^6 . The invention and development of the flame ionization detector are discussed in more detail in Ref. [14]. Early capillary columns were of plastic and copper tubing; the former had serious temperature limitations and the latter was active; this led to stainless steel tubing. PerkinElmer had filed for and been granted patents on the open-tubular concept, essentially worldwide. I purchased two PerkinElmer wall-coated open-tubular (WCOT) columns at different times, only to find that the columns available from them produced abominable results. PerkinElmer apparently recognized this fact, because they essentially abandoned their research efforts on WCOT columns, outsourced their production, and redirected their efforts to columns whose interiors

were first coated with a support material (e.g., diatomaceous earth) and then with the stationary phase. These were dubbed “support coated open-tubular (SCOT) columns.” PerkinElmer continued to rigorously enforce the patent on WCOT (and SCOT) columns, but under considerable pressure (especially from the applicant) they were forced to issue one license, to Hansjurg Jaeggi, a former assistant of Kurt Grob in Switzerland. Under Swiss law, if a patent bars a Swiss from conducting his or her business, a license must be issued. Jaeggi had been and still was making excellent glass WCOT columns. The high quality of his columns led PerkinElmer to later propose that they collaborate, but, probably because of the acrimonious battle he had gone through to obtain his license, he wanted nothing more to do with PerkinElmer and refused their offer. His obituary, written by Konrad Grob, makes interesting reading [15].

1.4.1 Do-it-yourself glass capillary columns

In 1965, Desty et al. invented an elegantly simple machine for drawing long lengths of coiled glass capillaries [16]. Besides the fact that this was much less expensive tubing, it also had a smoother interior *and it was transparent*. For the first time, it was possible to scrutinize the layer of stationary phase as it existed on the column wall; soon it was obvious that when a new unused column exhibiting a thin uniform film of stationary phase was exposed to higher temperatures, the stationary phase collected into beads that were randomly scattered over the inner surface. Almost immediately scores of scientists realized that many of the low-viscosity fluids that worked well in packed columns were unsatisfactory for WCOT columns and should be replaced with high-viscosity materials that would retain their high viscosity even at higher temperatures. Low-viscosity silicone fluids (e.g., OV 101) were replaced with high-viscosity silicones (e.g., OV 30, a viscous paste-like silicone), and experimenters soon began producing much more stable columns.

1.4.2 The positive results of patent enforcement

The low quality of the PerkinElmer WCOT columns and enforcement of their patent led many scientists to begin making their own columns for their own use. This caused investigators in many other fields, who would have preferred to purchase useable columns from an outside source and confine their research to some other field, to now have to make columns; scores of scientists were now studying and publishing on methods of pretreating, deactivating, and coating columns. Their combined results were responsible for many of the advances in column improvements, and they soon surpassed the results that had been generated by Perkin Elmer [17].

1.4.3 Mileposts in coating WCOT capillary columns

Golay had coated his original glass open-tubular columns by completely filling them with a dilute solution of stationary phase in a low-boiling solvent, sealing one end, and then drawing the column, open end first, through an oven [18]. As used by Golay, the column could be coiled only after coating, a distinct drawback. The method was improved by Ilkova and Mistrykov [19], who coiled and then filled the column and sealed one end. The open end of the filled column was fed into a heated oven by supporting the column on a rotating rod fitted with a drive roller at the entrance to the column oven, thus literally screwing the rest of the column into the oven.

Up until just a few years ago, all chemistry departments at the multicampus Universities of California system frowned on applied research, and chemistry department faculties drifting away from pure organic chemistry or pure physical chemistry rarely survived to tenure. Analytical chemistry was essentially forbidden. There were many faculty members scattered through various other departments who were analytical

chemists, and eventually they formed a “Group in Analytical and Environmental Chemistry,” open to anyone in any department who had interests in the analytical side. At one time I chaired that group for several years and it still exists. At this time, my title was “Professor of Food Science and Technology and Chemist in the Experiment Station.” This had several advantages: for one thing, those with just the academic title worked 9 months per year, while the Experiment Station operated 11 months a year. My department chairman tolerated what he called my “dabbling” in gas chromatography, but insisted that I should also be working on subjects “more aligned with the food industries”; he suggested “circulation cleaning,” which was just emerging. Swallowing what I wanted to say, I assigned a new Ph.D. student (Malcolm Bourne) to the project, built a miniature circulation pipeline, and helped him bake radiolabeled tristearin onto glass microscope slides and strips of stainless steel of similar width and length. These were inserted into the rapid circulating system, and the levels of radioactivity measured every 2 minutes. Inevitably, semilog plots of our cleaning curves showed a rapidly dropping curve that terminated in a straight line with a slight downward slope. All at once Bourne realized that he was looking at two first-order reactions that were occurring simultaneously. The baked film of tristearin existed only at one of two energy levels, a loosely bound system, and a much more tightly bound system—nothing in between. Spatial estimates indicated that the tightly bound form was not a monolayer, but could be up to at least 20 molecular thicknesses [20–22]. He also discovered that by manipulating time and temperature, he could change the ratio of the two species. Bourne went on to study the kinetics of cleaning in much greater depth and made quite a name for himself. I went back to my “dabbling,” then slowly realized that my newly gained knowledge on removal of thin films was just the reverse of achieving more stable coatings of stationary phases to the column surface.

This may have guided me as I attempted to modify our column coating apparatus. After replacing the opaque lid of the oven with a glass lid, it was obvious that the solution was superheated and evaporated in a series of minor explosions, leaving blotches of stationary phase randomly scattered over the surface of the column. I decided to introduce the column into the oven through a preheater made from a short curved length of 1/8 inch stainless steel tubing lagged with an electrically heated wire and heated to 150°C: the column's passage through the curved preheater was not smooth; indeed, it scraped the walls and vibrated. To avoid breakage, I introduced graphite powder into the loop. The column continued to vibrate, but more gently. In retrospect, that vibration at this point on its passage into the oven would also discourage superheating. It may have been dumb luck, but from then on, the evaporation of the solvent occurred smoothly. We were routinely producing very stable columns with uniformly thin coatings.

1.4.4 Commercial column manufacturers

At this point, one of my Ph.D. students, Robert Wohleb, suggested that we had a marketable product and should establish a column production company. When I broached this suggestion with my department chairman, he called in the dean. After much discussion, they agreed that I could engage in this activity only if I agreed to several restrictions: (1) as long as I was a full-time professor, I could receive no remuneration from this venture; (2) there could be no connection between my university research and activities of the company; (3) I could not get involved in the day-to-day activities of the company. I could, *on my own time*, answer trouble-shooting questions and engage in educational activities. J&W Scientific was founded in 1974; I constructed two drawing machines in my machine shop at home and left them with

Wohleb as I departed on my second sabbatical leave, this time in Karlsruhe, Germany. Sandy Lipsky had launched his company, Quadrex, slightly ahead of J&W.

1.4.5 Bonded, cross-linked, and/or immobilized stationary phases

In 1975, J&W noticed a sudden drop in column sales from several regular customers; fortunately, we had been using (and saving) bar codes to trace every step each column went through. The bar codes on all of the columns those customers had been buying showed they had all gone through the same coating machine in the same general time period. I called several of the buyers and asked if they were having problems with our columns and was shocked when they replied, “no, the columns are great—they never wear out.” This was serious, we were putting ourselves out of business. In checking that coating machine, it was discovered that the thermocouple on the preheater through which the column entered the oven had failed some time ago and was giving much lower readings. Over the past few weeks, the technician on the machine had simply compensated for the low reading by boosting the voltage. Instead of 150°C, that preheater was close to 300°C. The stationary phase we were using (SE-54) contained 1% vinyl. Our R&D head, Rand Jenkins, realized that serendipity had smiled on us! He immediately ordered materials and began adding vinyl-containing compounds, to our coating solutions, hoping that the phase would not only cross-link but also connect with some surface hydroxyls. With some pretty harsh testing, we found that the columns exposed to these higher preheater temperatures were much more rugged, and the deposited phase could not be removed with solvent rinsing. At the next “Advances in Chromatography” meeting in Houston, we announced the “Bonded Phase Column.” If the technician on that machine had reported the failing thermocouple, we would simply have replaced it and none of this would

have happened. It turned out that Kurt Grob in Switzerland had (independently) been working along these same lines. Checking on the dates that both parties had ordered vinyl chemicals, Rand was just about 5 days ahead.

1.4.6 Further improvements in stationary phases

In the late 1950s and extending into the 1960s, gas chromatographers dealt with a plethora of stationary phases. Petroleum chemists, dealing with nonpolar products, favored phases such as squalane, a fully saturated hydrocarbon (C₃₀H₆₂) on the basis of like-attracts-like. The upper temperature limit for Squalane is 125 degrees, and a higher temperature paraffin, Apolane 87 (C₈₇H₁₇₆), was sometimes used instead. Chemists dealing with more polar products needed more polar stationary phases, and they turned to high-boiling esters such as diethylene glycol succinate (DEGS). As more and more scientists entered the field, the range of stationary phases exploded to over 200 different phases, most of which were gradually discarded. The polysiloxane stationary phases are now widely used and have been reviewed by Blomberg [23] and Haken [24].

1.5 Interfacing glass capillary columns to injectors and detectors

Attaching these relatively fragile glass capillaries to injectors and detectors via leak-proof connections soon became a problem; some workers punched holes in small disks of silicone rubber, which were then substituted for the ferrules supplied with 1/16 inch Swagelok fittings, but all too frequently, as the nut on the Swagelok fitting was tightened to the point that there were no leaks, the compressive strain on the glass caused breakage at that point. Others tried lead disks, with similar effects. I was on sabbatical leave at the nuclear research

institute in Karlsruhe, Germany, when a clerk in the supply room called my attention to a sheet of plastic heavily infused with graphite. After sliding Swagelok caps onto both column ends, I wound small strips of this around both ends of a glass capillary, removed the stock ferules from the Swagelok connectors to the inlet and detector, and connected the column. As I tightened the connections to a point where there was no leakage and found that the column was still intact, I was delighted. The company that made these graphitized sheets was just a few miles outside of Karlsruhe, and I paid them a visit. They were very cordial and gave me a number of samples. On my return to the United States, J&W ordered several steel dies dimensioned on the inner measurements of a 1/16 inch Swagelok fitting and began pressing ferules. These went on the market in 1975; they were a great success, and I have always regretted my failure to patent that product.

1.6 The Hindelang conferences and the fused-silica column

The first symposium restricted to open-tubular (capillary) columns was organized by Rudolf Kaiser and chaired by Dennis Desty in 1975; this was the first of the four Hindelang conferences and was held in an isolated village in the Bavarian Alps. Ettre visited Kaiser, first to voice his opposition to holding the meeting, and then proposed a delay, arguing that it was being held "far too early," but many other workers in the field were enthused by the idea. I still regard the first Hindelang conference as the most exciting meeting I have ever attended. It attracted nearly everybody that was working with glass capillary columns. We listened to presentations from our associates in the morning and spent afternoons and evenings gathered around tables seating perhaps eight participants, drinking strong German brews and exchanging views on chromatography, with the emphasis

on WCOT columns. It was then that Golay approached me; he was feeble at the time and steadied by Ettre. He wanted to talk about J&W's method of coating columns. I explained that the first step was his idea of feeding a filled column, open end first, into a heated oven. Ilkova and Mistrykov's idea of screwing the coiled column into the oven showed real ingenuity: my pre-heater contribution would have been proposed by anyone that could actually see the operation taking place. Now that I have reached (and probably surpassed) Golay's age at the time, I believe I can now understand his curiosity, and I hope he realized that another of his brilliant ideas had borne fruit. He departed courteously, and I was left to continue my attempts to visit every table and meet every participant. I did meet virtually all the experts, absorbed a great deal of knowledge, and left filled with new ideas and a desire to get home quickly where I could get back to work in my own lab.

There are many types of glass, but we will restrict our interests to those studied for their chromatographic interest by Dandeneau and Zerenner: soda lime, borosilicate, uranium, potash soda lead, and fused silica (Table 1.1) [25]. At the third Hindelang conference, I presented a paper on multiple short-pass capillary chromatography, in which one of my Ph.D. students (James A. Settlage) had recycled a butane injection 16 times through two 7.5 m columns to achieve 1170 theoretical plates per second and generated 850,000 theoretical plates in those 16 passes in less than 12 min [26]; as I finished, several members of the audience rushed to the podium with congratulations; at a final synopsis of the meeting, Desty cited also this paper, but I knew they were all wrong. The most significant paper was that of Dandeneau and Zerenner [25], releasing the fused-silica column. When Dandeneau presented his paper, very few people realized its importance. Sandy Lipsky, who had started Quadrex about the same time that J&W was founded, was one, and I was another. Both Lipsky and I had been trying to convert

TABLE 1.1 Approximate compositions for glass materials used for capillary column fabrication.

Glass type	Metal oxide percent composition (w/w)									
	SiO ₂	Al ₂ O ₃	Na ₂ O	K ₂ O	CaO	MgO	B ₂ O ₃	PbO	U ₂ O ₃	BaO
Soda lime	68	3	15		6	4	2			2
Borosilicate	81	2	4				13			
Uranium glass	76	3	4	2			14		1	
Potash soda lead	56	2	4	9				29		
Fused silica ^a	100									

^a Typically contains less than 1 ppm total metals.

industrial analysts to WCOT glass capillaries, with but scant success. Industrial analysts realized the superiority of results generated by these columns, but they also recognized their fragility. Downtime is rarely critical in academia, but in industry it can be very serious; glass capillaries break easily, packed columns lasted longer. However, this fused-silica column changed everything! Here was a capillary column that was both strong and flexible, but because it was both labor-intensive and materials-intensive, it was much more expensive.

Fused-silica columns have immense tensile strength, permitting an extremely thin column wall, which in turn makes a flexible column. This permitted drawing long lengths of straight tubing, which can then be coiled. Interfacing these to detectors and injectors was now a simple task; no longer must we flame straighten the ends of the column, it was already inherently straight! But the outer surface of drawn silica requires protection. Like all silica-based glasses, fused silica is subject to flaws at its surface, and flaws grow at a rate determined by stress—and coiling this long straight piece of fused silica places it under stress—as the flaw grows larger, the column snaps at that point. To protect the outer surface, Hewlett Packard first coated the columns with a coating of polysiloxane, but this ended up as a very sticky column. DuPont then came forward with a polyamide coating that was applied during the drawing process. Later

they changed to a polyimide; this seals surface flaws in the tubing. It is usually applied in several thin coats during the drawing process.

Not everyone recognized the advantages of the fused-silica column; indeed, in spite of my vigorous protests, my partners at J&W dismissed it as “a gimmick.” 2 weeks later, it was impossible to give, let alone sell, a glass capillary column, and J&W made the conversion to fused silica. At this point, things became very “touchy.” The vast majority of scientists working in gas chromatography had careers based on glass capillary columns—drawing, deactivation, coating, etc.—now those careers were passé. I had a seminar scheduled for Milan, Italy, where I was warmly received—until my first slide was shown. It was a fused-silica column. Several attendees left the room, and the atmosphere took on a chill. Very few in this audience wanted to hear how their futures might be affected. Shortly thereafter, Georges Guiochon organized a chromatography symposium in Cannes, France. The GC column portion of the meeting was chaired by Gerhardt Schomburg. As he called the meeting to order, he announced that there would be “no discussion of fused-silica columns.” As the meeting proceeded, several attendees expressed their objections to the opening restriction and announced that they had come to the meeting just to learn more about the fused-silica column. With obvious distaste, Schomburg turned to me and said, “tell them

something about fused silica." At this time, I had been exploring on-column injections with fused silica, sometimes trapping samples within the fused-silica tubing by folding the flexible tube into a "U" shape in a Dewar flask filled with liquid nitrogen, then withdrawing the "U" and reinserting it into a flask of heated oil for injection. This approach demanded a flexible tube and would have been impossible with glass capillary tubing. An obviously uncomfortable Schomburg interrupted me with the observation that "flexibility appeals only to Americans, and only because they are too clumsy to handle glass." A few months later, J&W was selling Schomburg fused-silica columns.

1.7 Increasing sophistication of instrumentation

Table 1.2 provides a timeline for important developments in instrumentation [8,26,27]. The essential elements of instruments were developed by the early 1960s, with further developments occurring in short bursts of innovation and advances in technology followed by longer periods of evolutionary changes and consolidation. Many advances were catalyzed by advances in column technology or electronics. For example, the advent of the microprocessor brought about a radical change in instrument design and use. From this point onward, instrument functions were monitored and controlled by networks of circuits communicating with each other and with a central controller. This paved the way for the emergence of the keyboard instrument controlled by software running on a personal computer, which dominated instruments for laboratory use by the early 1990s. A significant milestone in achieving full automation of instrument operation was the introduction of electronic pressure control in the early 1980s. This allowed carrier gas and support gas pressure and flow rates to be set and monitored by electromechanical devices

communicating with a central processor. With the introduction of robotic autosamplers at about the same time, the GC could now operate without human intervention, 24 h operation became standard practice for routine analysis in high sample throughput environments, and GCs were deployed to remote locations and monitored electronically with only occasional visits for service and routine maintenance. Electronic pressure control was central to a series of advances in programmed and large-volume injection techniques, multidimensional-column chromatography, and retention-time locked methods. The complex functions of gas chromatography had been reduced to those of a black box analyzer 50 years after its invention, but still evolutionary changes continue in technology with the view of minimizing the importance of the skill and knowledge of the operator in the production of data [27].

1.7.1 Column heating

Apart from the use of liquid thermostats in the early days of gas chromatography, the column heater in a GC is typically a forced-circulation air oven, the temperature of which can be changed in a controlled manner with time for temperature-programmed separations. Good temperature control is essential to obtain reproducible retention times and to avoid peak distortions associated with temporal and spatial oven temperature gradients. A low thermal mass for the oven is also important since it allows rapid cooling after temperature programming. Typically, forced air-circulation ovens can maintain a higher rate of heating at lower temperatures than higher temperatures due to the greater amount of heat lost to the surrounding environment as the temperature ramp progresses. For fast gas chromatography, some manufacturers have addressed this problem with the oven inside an oven concept or more directly using resistive heating achieved through

TABLE 1.2 Important advances in technology that impacted gas chromatography.

1955	First commercial instrument (thermal conductivity detection)
1955–60	Rapid growth in technology Invention of ionization detectors Interfaces for coupling to mass spectrometry Microsyringes produced commercially Temperature programming introduced
1960–70	Period of technical advances First open-tubular columns introduced Transistors replace vacuum tubes Improvements in detector technology Stable rubidium sources introduced for TID Improved FPD (several designs) Pulsed ECD introduced
1970–80	Period of consolidation and refinement Microprocessor-based instruments introduced Self-made glass open-tubular columns increasingly used Computing integrators introduced for data handling Fused-silica open-tubular columns introduced in 1979 and catalyzes further changes in column and instrument technology
1980–90	Period of technical advances Gum and immobilized phases developed Columns with thick-film stationary phases developed Wide-bore open-tubular columns developed Fundamental basis for injection mechanisms developed On-column and PTV injection developed Large-volume injection described Autosamplers for unattended injection developed
1990–2000	Period of consolidation and refinement Keyboard instrumentation (PC control of operation and data handling) Electronic pneumatic control Selectable elemental detection (SED) Pulsed flame photometric detector developed (FPD)

TABLE 1.2 Important advances in technology that impacted gas chromatography.—cont'd

1955	First commercial instrument (thermal conductivity detection)
	Electron-capture detector with pulsed discharge source developed (ECD)
	More versatile and affordable spectroscopic detectors (MS, FTIR)
	Solid-phase microextraction affords a new approach to sampling and sample introduction
	First microfabricated gas chromatograph on a chip introduced but fails commercially
	Field portable instruments move gas chromatography out of the laboratory
	Introduction of comprehensive two-dimensional gas chromatography
2000–Present	Slowing down in the growth of technology
	Micro-GC instruments for fast gas chromatography developed
	Capillary columns with ionic liquid stationary phases introduced
	Gas generators start to replace pressurized gas cylinders
	Programmable robotic systems used to automate sample preparation
	Resistive heating of columns introduced as an alternative means of temperature control to convection ovens

the use of a metallic heating element to transfer heat to the column by conduction [28]. Fast gas chromatography makes use of short columns of small internal diameter, thin film columns, higher carrier gas flow rates, and fast temperature program rates (Table 1.3) [29]. For the fastest separations, the limiting instrument conditions become the available column inlet pressure, maximum oven temperature program rate,

maximum detector sampling rate, detector sensitivity and noise level, and sample introduction (initial bandwidth). Contemporary laboratory instruments can usually meet the requirements for fast gas chromatography (first entry in Table 1.3), but special-purpose instruments are required for very fast gas chromatography (second entry in Table 1.3). The entries in Table 1.3 reflect what is within the capability of commercial instruments with little modification (first entry) and the limits of current technology requiring special purposing of instruments (second entry). From the perspective of separation speed, the capability of gas chromatographic instruments limits performance more so than column technology in contemporary practice.

TABLE 1.3 Instrumental parameters for fast gas chromatography.

(i) Fast gas chromatography (separation times <10 min)
Peak widths 0.5–2 s
Columns 5–15 m with I.D. 0.25–0.1 mm
Temperature program rates 20–60°C min ⁻¹
Column inlet pressure <15 bar Data acquisition rate 50 Hz
Mobile phase velocity 1.4 × u _{opt}
(ii) Very fast gas chromatography (separation time in seconds)
Peak widths 50–200 ms
Columns 2–10 m and I.D. 0.1–0.05 mm
Temperature program rates >60°C min ⁻¹
Data acquisition rates 50–200 Hz

1.7.2 Sample introduction

The limited sample capacity and low carrier gas flow rates associated with open-tubular columns make sample introduction more difficult than for packed columns. A thermostated flash

vaporization chamber in which the evaporated sample is mixed with carrier gas and divided between a stream entering the column (carrier gas flow) and a stream vented to waste (split flow) was the first practical solution to this problem. Split injection can be used to generate extremely small bandwidths for high peak capacity separations but discriminates against less volatile compounds and the quantitative analysis of wide boiling-point mixtures is difficult, and for samples present in dilute solution, detectability is limited by the small amount of sample transferred to the column. The splitless injection technique was devised (actually discovered accidentally [30]) to overcome some of the deficiencies of split injection for the analysis of mixtures in dilute solution through the transfer of relatively large sample volumes to the column. The gas flow through a splitless injector is relatively low, and the sample is introduced into the column over a comparatively long time (30–60 s), relying on cold trapping and/or solvent effects to refocus the compounds at the head of the column. The importance of these refocusing mechanisms was not fully understood at first and much of our current knowledge of the injection mechanism owes a great deal to the exemplary studies of Konrad Grob and the publication in 1986 of his classic book on split and splitless injection [30].

The programmed-temperature vaporizer (PTV) injector is perhaps the most versatile injector developed for gas chromatography. It facilitates split and splitless injection as well as new approaches for large-volume injection with solvent elimination [31]. The PTV injector has a low thermal mass to allow rapid heating and cooling. The sample is introduced at a relatively low temperature and then raised ballistically to a temperature sufficient for rapid volatilization of the highest-boiling sample components. Slow sample introduction at a low temperature with solvent elimination facilitates the injection of

large sample volumes (usually <1 mL) for trace analysis. The PTV injector was originally introduced in Europe in the 1980s, but it was over a decade later before it gained traction in the United States. For much of this time it was an option but not heavily promoted or supported by instrument companies based in the United States. This was probably due to a combination of commercial preferences and the not-invented-here syndrome.

The production of wide-bore fused-silica capillary columns coated with immobilized stationary phases in the early 1980s allowed the syringe needle to be introduced directly into the column and eliminated the problem of removal of the stationary phase by the relatively large volume of solvent released inside the column by the syringe [32]. These advances in column technology facilitated the development of cold on-column injection where the sample is introduced as a liquid into the column inlet and subsequently vaporized. Discrimination because of volatility differences was virtually eliminated and the risk of sample decomposition minimized. With secondary cooling of the injector, the oven temperature could be kept well above the boiling point of the solvent while maintaining the column inlet at a much lower temperature. This is important for using on-column injection in high-temperature gas chromatography. Dirty samples present a problem owing to contamination of the sample introduction zone, which leads to poor chromatography and unreliable quantification. Both on-column and PTV injection afford high accuracy and precision. These injectors also facilitated the direct coupling of other chromatographic systems to gas chromatography, such as liquid chromatography and supercritical fluid chromatography [33]. In the 1980s, Carlo Erba manufactured an instrument for on-line liquid chromatography–gas chromatography, but the uptake was poor and the system was discontinued.

The array of sample introduction methods for gas chromatography and an understanding of the mechanistic details on which they rely were complete by the end of the 1980s and modifications since then have been evolutionary. The most visible change is the shift from manual to automated sample introduction systems that accept samples in vials and can be programmed for sequential analysis of each or selected vials in a batch. The introduction of solid-phase microextraction in the early 1990s simplified sample preparation and handling steps using a syringe containing a retractable sorbent fiber compatible with solvent-free sample introduction [34]. By the turn of the century, this had become one of the most popular sampling/sample introduction techniques in gas chromatography. It can be seen as the forerunner of the liquid-phase microextraction techniques developed over the last decade or so [35]. Together these microextraction formats are responsible for achieving a better scaling of sample size requirements to sample utilization capabilities of capillary columns and are having a considerable impact on laboratory working practices.

1.7.3 Detectors

Gas chromatography is blessed by a number of robust and sensitive detectors based on gas-phase ionization processes (e.g., flame ionization, thermionic ionization, electron capture, and photoionization), bulk property (thermal conductivity), optical (flame photometric, chemiluminescence, and atomic emission), electrochemical (electrolytic conductivity), and advanced spectroscopic (mass spectrometry and infrared and far-UV spectroscopy) detection principles. Many of these detectors were introduced during the initial phase of the development of gas chromatography and are still used today in a modified form reflecting changes in enabling technology. The exception is the (Hall) electrolytic conductivity detector, which, because of its large detector volume and basis

in wet chemical processes, is less used today. Interfacing of modern detectors to capillary columns is not normally difficult except for fast gas chromatography where the detector volume and data acquisition rates limit the use of some detectors. The flame ionization detector facilitated many of the early developments in capillary columns (Section 1.4). This detector has a low dead volume, a high sensitivity for nearly all carbon-containing compounds, and an extremely wide linear response range. Other detectors were developed in response to the need for element-selective or structure-selective detection. These detectors allowed the analysis of target compounds at low concentrations in complex samples and made an important contribution to the rapid acceptance of gas chromatography in laboratories performing routine analysis as well as research laboratories.

A special mention should be made of the coupling of gas chromatography with mass spectrometry (GC-MS). This coupling dates almost from the beginning of gas chromatography, but in the early days the practical problems and high cost meant that the combination was confined to a few research laboratories. When packed columns dominated the practice of gas chromatography, separators were required to reduce typical column flow rates to the vacuum-handling capacity of the ion source of the mass spectrometer. Separators based on a jet, glass fritted tube, or diffusion membrane design allowed sample enrichment while simultaneously reducing the gas flow to the ion source. Separators disappeared nearly completely with the introduction of fused-silica open-tubular columns, which could be routed from the column oven through a heated transfer line directly into the ion source of the mass spectrometer. During the time that instrumentation for gas chromatography was advancing, so were all aspects of mass spectrometry, which became more powerful, affordable, reliable, and available to laboratories with low-skilled personnel. The great advantage of the mass

spectrometer as a detector is its ability to provide structural information for identification using different ionization approaches and through techniques such as tandem mass spectrometry. Another advantage is its high sensitivity and selectivity as a detector in the selected ion or high-resolution mode.

1.7.4 Data handling

In the early days of gas chromatography, peak quantification was done by purely manual measurements of peak heights, although it was recognized that peak area measurement was fundamentally better but more difficult. The product of the peak height and the peak width at half height could be used as an approximate area measurement, but this was neither fast nor (usually) accurate, especially for narrow peaks. Approaches based on planimetry and cut-and-weigh procedures could afford reasonable accuracy but demanded considerable skill to achieve acceptable results and were slow and tedious. Electromechanical devices such as the ball-and-disk integrators and integrating amplifiers were early attempts at automating this time-consuming process. These devices were rather limited in range and speed of response. The advent of microprocessors in the early 1970s ushered in the computing integrator, which took over the labor-intensive process of data management, eventually resulting in devices that could record a chromatogram simultaneously with data acquisition and, when the separation was complete, instantly generate reports in tabular form of all sorts of descriptive information from the chromatogram, including the calculation of peak areas. It was not long before mainframe computers were in use to handle data produced from a number of instruments simultaneously. The development of the personal computer and the rapid growth in processor speed and memory, however, had a greater impact and resulted in data management being handled by software running on a dedicated

personal computer with information being archived locally and/or centrally on a laboratory information network server. Today, the large amount of data produced by capillary columns (especially when coupled to a mass spectrometer) can be handled by a personal computer, which simultaneously functions as the system manager controlling and monitoring all aspects of the chromatograph. What has not changed is that the methods used to manipulate the chromatographic data for display and calculation are considered proprietary information, requiring an act of faith that what is provided as a printout or on screen is exactly what happened in the column [36]. What is clear, however, is that it would be nearly impossible to persuade scientists to return to the status quo before the electronic age of data handling as laboratory productivity would be severely limited.

1.7.5 Comprehensive gas chromatography

Sometimes the separating power of gas chromatography, even when augmented by the identification power of spectroscopic detectors such as mass spectrometry, is still insufficient to accurately determine the composition of a sample. This problem is tackled in contemporary studies using comprehensive gas chromatography. Comprehensive separations have their origins in multidimensional gas chromatography developed in the early 1960s after the introduction of the Dean's switch for controlling the flow direction of a gas stream at a T-piece using pressure changes [37]. Modern microfabricated versions of this device remain at the heart of many developments in multicolumn separation systems. Multidimensional (typically two-dimensional) gas chromatography employs two independent columns connected to each other by an interface [38]. In early versions a fraction of the chromatogram, a heartcut, from the first column was isolated by cold trapping and then released by thermal desorption for separation on the second

column. The disadvantage of this approach is that the fraction collected at the interface contains no information about the separation on the first column. In the 1980s, Siemens marketed a remarkable instrument for its time, the SiChromat-2, which had two independently controlled air-circulation ovens, housing the two columns, connected by a T-piece to isolate, focus, and reinject fractions from the first column to the second by live switching based on the Deans' switching mechanism. This instrument likely contained the most complex pneumatic system of any instrument of its generation and required considerable skill in its operation. It had to compete for preference with a new generation of affordable and easy-to-use gas chromatography–mass spectrometry systems, however, and was not a commercial success. In the early 1990s, Phillips introduced comprehensive gas chromatography in which the whole separation on the first column was transferred to a second column of different selectivity, the two columns being connected through a modulation interface [39]. In this case, the chromatogram is recorded as a two-dimensional contour plot with the planar axes consisting of the independent retention times for each compound on the two columns and the vertical axis is related to the amount of each compound. This technique was not an instant success, but after further refinements in modulator design, a decade later it had entered the main stream of commerce. These instruments are at the cutting edge of instrument development where capabilities are pushed to match column performance. The function of the modulator is to arrest, concentrate, and launch a fraction of the material contained within each peak of the chromatogram from the first column and transfer them as a series of pulses of constant frequency to the second column [40]. To avoid overlap of individual separations on the second column, each chromatogram must be complete in less time than the cycle time of the modulator. Thus, the second-column separations must be very fast with a total separation

time measured in seconds. This requires incredibly small injection bandwidths, short second columns of small internal diameter, fast detector response times, and repetitious and fast changes in instrument operating conditions. Comprehensive gas chromatography generates a large amount of data, especially when mass spectrometry is used as a detector, and challenges remain in how best to make these data available to the user in a form convenient for analysis. In these instruments, one can perhaps see a vision of the future of single-column gas chromatography (based on technology developed for the second-dimension separation) while at the same time highlighting the limitations of current technology for gas chromatography.

1.8 Decline in the expertise of the average gas chromatographer

At present, the success in the commercial sector in gas chromatography has resulted in a situation not all that different from a narcotic dependency. To be classed as an expert in gas chromatography, all that seems to be necessary is the wherewithal to purchase a GC and a column. Today, those tasked to operate a GC do not need to even make an injection, columns have become classified as laboratory supply items, and data as something that appears on a printout at the end of an experiment. When I was first introduced to gas chromatography in the 1970s, it was necessary to make, modify, and continuously improve columns and instruments to meet the needs of each application. Expert chromatographers of this time were of necessity well versed in troubleshooting and thoroughly knowledgeable of the principles and practice at what often appeared to outsiders as the dark arts of separations. On account of the immense powers of separations, virtually any unskilled individual can produce data today; even the village idiot can inject a sample and obtain peaks that are interpreted as “usable data.” This has

led to a continuing decline in the expertise of the average practicing chromatographer from the mid-1980s to the present time. This can be perilous, because everything from column selection to troubleshooting skills is based on a fundamental knowledge of chromatographic principles, the absence of which degrades the quality and usefulness of the information acquired by these instruments. To address these problems requires a massive educational effort before the knowledge is lost and the usefulness of gas chromatography to decision-makers is called into question. When I first started to make my way in gas chromatography, I never thought that such a reversion would occur so quickly, and as retirement approaches, that intellectually I might leave the field in a poorer state than when I entered it. There is no doubt that advances in technology have delivered better instruments and columns but now in the hands of less qualified operators; this does not always lead to better-quality data.

References

- [1] A.T. James, A.J.P. Martin, Gas-liquid partition chromatography: the separation and microestimation of volatile fatty acids from formic to dodecanoic acid, *Biochem. J.* 50 (1952) 679–690.
- [2] L.S. Ettre, The beginnings of gas adsorption chromatography 60 years ago, *LC-GC N. Am.* 26 (2008) 48–51.
- [3] F. Prior, Determination of Adsorption Heats of Gases and Vapors by Application of the Chromatographic Method in the Gas Phase, Doctoral theses, University of Innsbruck, Innsbruck, Austria, 1947 (in German).
- [4] O. Bobleter, Exhibition of the first gas chromatographic work of Erika Cremer and Fritz prior, *Chromatographia* 43 (1996) 444–446.
- [5] A.N.H. Ray, Gas chromatography, I–II, *J. Appl. Chem.* 4 (1954) 21–25, 82–85.
- [6] L.S. Ettre, A. Zlatkis (Eds.), 75 Years of Chromatography – a Historical Dialogue, Elsevier, Amsterdam, 1979.
- [7] H.A. Laitinen, G.W. Ewing, A History of Analytical Chemistry, Division of Analytical Chemistry, American Chemical Society, Washington, 1977, pp. 303–304.
- [8] L.S. Ettre, The early development and rapid growth of gas chromatographic instrumentation in the United States, *J. Chromatogr. Sci.* 40 (2002) 458–472.
- [9] M.J.E. Golay, in: D.H. Desty (Ed.), *Gas Chromatography 1958 (Amsterdam Symposium)*, Butterworths, London, 1958, pp. 139–143.
- [10] J.E. Lovelock, S.R. Lipsky, Electron affinity spectroscopy – a new method for the identification of functional groups in chemical compounds separated by gas chromatography, *J. Am. Chem. Soc.* 82 (1960) 431–433.
- [11] J. Harley, W. Nel, V. Pretorius, Flame ionization detector for gas chromatography, *Nature* 181 (1958) 177–178.
- [12] I.G. McWilliam, R.A. Dewar, in: D.H., Desty (Eds.), *Gas Chromatography 1958 (Amsterdam Symposium)*, Butterworths, London, 1958, p. 142.
- [13] I.G. McWilliam, The origin of the flame ionization detector, *Chromatographia* 17 (1983) 241–243.
- [14] L.S. Ettre, The invention, development and triumph of the flame ionization detector, *LC GC* 15 (2002) 364–373.
- [15] K. Grob, Hansjurg Jaeggi – obituary, *J. High Resolut. Chromatogr.* 12 (1989) 459.
- [16] D.H. Desty, J.N. Haresnape, B.H.F. Whyman, Construction of long lengths of coiled glass capillary, *Anal. Chem.* 32 (1960) 302–304.
- [17] K. Grob, The role of column technology in capillary gas chromatography, *J. High Resolut. Chromatogr.* 7 (1984) 252–257.
- [18] M.J.E. Golay, in: D.H. Desty (Ed.), *Gas Chromatography 1958 (Amsterdam Symposium)*, Butterworths, London, 1958, pp. 36–55.
- [19] E.L. Ilkova, E.A. Mistrukov, A simple versatile method for coating glass capillary columns, *J. Chromatogr. Sci.* 9 (1971) 569–570.
- [20] M.C. Bourne, W.G. Jennings, Existence of two soil species in detergency investigations, *Nature* 197 (1963) 1003.
- [21] M.C. Bourne, W.G. Jennings, Kinetic studies of detergency. I Analysis of cleaning curves, *J. Am. Oil Chem. Soc.* 40 (1963) 517–523.
- [22] M.C. Bourne, W.G. Jennings, Kinetic studies of detergency. II Effect of age, temperature, and cleaning time on rates of soil removal, *J. Am. Oil Chem. Soc.* 40 (1963) 523–530.
- [23] L. Blomberg, Current aspects of the stationary phase in gas chromatography, *J. High Resolut. Chromatogr.* 5 (1982) 520–533.
- [24] J.K. Haken, Developments in polysiloxane stationary phases in gas chromatography, *J. Chromatogr.* 300 (1983) 1–77.

- [25] R.D. Dandeneau, E.H. Zerenger, An investigation of glasses for capillary chromatography, *J. High Resolut. Chromatogr.* 2 (1979) 351–356.
- [26] W. Jennings, J.A. Settlege, R.J. Miller, Multiple short pass glass capillary gas chromatography, *J. High Resolut. Chromatogr.* 2 (1979) 441–443.
- [27] K.D. Bartle, P. Myers, History of gas chromatography, *Trends Anal. Chem.* 21 (2002) 547–557.
- [28] A.Z. Wnag, H.D. Tolley, M.L. Lee, Gas chromatography using resistive heating technology, *J. Chromatogr. A* 1261 (2012) 46–57.
- [29] C. Cruz-Hernandez, F. Destailates, Recent advances in fast gas chromatography: application to the separation of fatty acid methyl esters, *J. Liq. Chromatogr. Relat. Technol.* 82 (2009) 1672–1688.
- [30] K. Grob, *Classical Split and Splitless Injection in Capillary Gas Chromatography*, second ed., Huethig, Heidelberg, 1986, 1992.
- [31] W. Engewald, J. Teske, J. Efer, Programmed temperature vaporizer-based injection techniques for injection in capillary gas chromatography, *J. Chromatogr. A* 856 (1999) 259–278.
- [32] K. Grob, *On-column Injection in Capillary Gas Chromatography*, second ed., Huethig, Heidelberg, 1991.
- [33] K. Grob, *On-line Coupled LC–GC*, Huethig, Heidelberg, 1991.
- [34] J. Pawliszyn, *Solid-phase Microextraction: Theory and Practice*, Wiley-VCH, New York, 1997.
- [35] C.F. Poole (Ed.), *Liquid-phase Extraction*, Elsevier, Amsterdam, 2020.
- [36] N. Dyson, *Chromatographic Integration Methods*, The Royal Society of Chemistry, Cambridge, UK, 1998.
- [37] K.M. Sharif, C.T. Chin, C. Kulsing, P.J. Marriott, The microfluidic Deans switch: 50 years of progress, innovation and application, *Trends Anal. Chem.* 82 (2016) 35–54.
- [38] P.Q. Tranchida, D. Sciarrone, P. Dugo, L. Mondello, Heart-cutting multidimensional gas chromatography: a review of recent evolution, applications, and future prospects, *Anal. Chim. Acta* 716 (2012) 66–75.
- [39] C. Meinert, U.J. Meierhenrich, A new dimension in separation science: comprehensive two-dimensional gas chromatography, *Angew. Chem. Int. Ed.* 51 (2012) 10460–10470.
- [40] H.D. Bahaghighat, C.E. Freye, R.E. Synovec, Recent advances in modulator technology for capillary two dimensional gas chromatography, *Trends Anal. Chem.* 113 (2019) 379–391.

Further reading

- [1] A. Gerontas, New technologists of Research in the 1960s: the case of the reproduction of automated chromatography specialists and practioners, *Sci. Educ.* 23 (2014) 1681–1700.
- [2] G.M. Gross, V.R. Reid, R.E. Synovec, Recent advances in instrumentation for gas chromatography, *Curr. Anal. Chem.* 1 (2005) 135–147.

Theory of gas chromatography

Leonid M. Blumberg

Advachrom, Wilmington, DE, United States

2.1 Introduction

Analytical gas chromatography (GC), Fig. 2.1, is a technique of separation of components of mixtures (*samples*) with the purpose of obtaining information about their molecular composition. The information obtained from a chromatographic analysis can include a chromatogram (a graphical image of a detector output), information regarding the heights and the areas of *resolved* (adequately separated) peaks in a chromatogram, their molecular identity, etc.

This chapter is mostly based on its previous edition [1]. As before, it is assumed here that the reader is familiar with the basic GC concepts and structures such as the *capillary*, i.e., *open-tubular* column (OTC), *carrier gas* as the *mobile phase* in GC, liquid and solid *stationary phases*, the key mechanisms of the interaction of the solutes *migrating* (being carried by the carrier gas) through a column with the stationary phase, temperature and/or pressure programming, etc. Several chapters of this volume and other sources [2–12] could help to refresh this information.

A theory of GC can be tailored to emphasize different aspects of GC operations. It might be focused, for example, on accurate prediction of retention times and degree of separation of all

or some predetermined components of the sample. As the computerized calculations are usually acceptable for such predictions, complexity of the models becomes a relatively minor issue compared to their accuracy. It might become necessary for the accurate predictions to account for such generally minor factors as nonideal carrier gas, effects of the liquid stationary phase surface, nonuniform column stationary-phase thickness, etc. These factors, however, are outside of the main concern of this chapter. Its main focus is on the effect of the operational parameters of GC analysis on its *general performance*. The theory presented here is designed to address such issues as the effect of column dimensions, carrier gas type and flow rate, temperature programming, and other factors on duration of analysis, the number of peaks that can be resolved, detection limits (DLs), and the trade-offs between these performance factors. To get simple and insightful mathematical descriptions of these relations, simplicity of the basic models becomes more important than their accuracy. As a general trend, this chapter favors simplicity over unnecessary accuracy. The aforementioned and other similar minor secondary factors complicating the models are typically ignored.

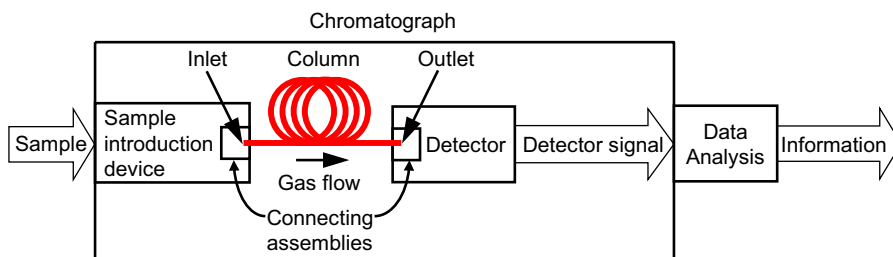


FIGURE 2.1 Block diagram of a chromatographic system.

Temperature programming known from Griffiths, James, and Phillips since 1952 [13] is an indispensable technique used in the analyses of complex mixtures. It can reduce the time of analysis of a complex sample by an order of magnitude compared to isothermal analysis and, by reducing the peak widths, can substantially improve their detectability. The first theoretical study of general performance of temperature-programmed GC is known from Giddings, who outlined the theory and came close to finding optimal heating rate [14]. Although Giddings did not explicitly express this point of view, he essentially treated the void time as the basic clock in chromatography and found that the optimal heating rate should be inversely proportional to the void time. The view of the void time as the basic clock in chromatography is the basis for more recently developed techniques of method translation and retention locking in chromatography [15], as well as for expressing optimal heating rate in terms of temperature per void time [16]. An important contribution to the theory of temperature-programmed GC came from Habgood and Harris, who [17–19] extended the concepts of plate number and plate height previously known only for isothermal GC, to temperature-programmed GC.

This chapter is an overview of the current state of GC theory with the emphasis on temperature-programmed GC. The isothermal GC is viewed as a temperature-programmed GC with zero heating rate. The chapter starts with the review of relevant theoretical

information regarding interaction of organic compounds with liquid polymers, properties of ideal gases, and flow of ideal gases. This information is then used as a basis for addressing such core issues of GC theory as formation of retention times and other parameters of eluting solutes; formation of peak spacing and factors affecting reversal of peak order; and formation of peak widths. This material is used then as the basis for the study of the column optimization—the optimal flow rate, optimal heating rate, and optimal trade-off between a column separation performance, analysis time, and DL.

Only the **analytical** GC is considered in this chapter. The scope of the chapter is primarily limited to the most widely used **capillary** (open-tubular) columns. Other constraints introduced in the chapter are highlighted by the **bold-face** type in the text.

2.2 Nomenclature and other conventions

2.2.1 Abbreviations

DL	detection limit
EOF	efficiency-optimized flow rate
FID	flame-ionization detector
GLC	gas–liquid chromatography
MDA	minimal detectable amount
MDC	minimal detectable concentration
MS	mass spectrometer
OTC	open-tubular column
PLOT	porous layer open tubular (column)
RTL	retention time locking

SOF speed-optimized flow rate
WCOT wall-coated open-tubular column

2.2.2 Subscripts

a asymptotic parameter (parameter of a solute that was highly retained at the beginning of a heating ramp)
Def recommended default parameter
i parameter at a column inlet
init initial parameter at the beginning of a heating ramp
max maximum, except for speed-optimized conditions
middle parameter in the middle of the heating ramp
min minimum, except for speed-optimized conditions
o parameter at a column outlet
Opt speed-optimized parameter
opt optimal parameter, except for speed-optimized conditions
R parameter at retention time
ref reference parameter
st parameter at standard temperature and pressure

2.2.3 Symbols (local symbols used only shortly before or after their introduction are not listed)

Symbol	Description
D	Solute diffusivity in gas
d	Column internal diameter
d_c	Internal diameter of column tubing
d_f	Stationary-phase film thickness
D_g	Gas self-diffusivity
D_{pst}	Solute diffusivity in gas at standard pressure and arbitrary temperature
D_S	Solute diffusivity in stationary phase
F	Gas flow rate, Eq. (2.43)
f	Gas specific flow rate, Eq. (2.45)
f_{crit}	Critical specific flow rate, Eq. (2.54)
G	Gibbs free energy, Eq. (2.7)

g	Dimensionless Gibbs free energy, Eq. (2.7)
G_H	Enthalpy, Eq. (2.7)
G_p	Peak formation factor, Eq. (2.154)
G_S	Entropy, Eq. (2.7)
H	Plate height (apparent), Eqs. (2.122), (2.123)
\mathcal{H}	Local and/or instant plate height (solute spatial dispersion rate), Eq. (2.107)
h	Dimensionless plate height, Eq. (2.148)
j	James–Martin compressibility factor, Eq. (2.39)
j_G	Giddings compressibility factor, Eq. (2.130)
j_H	Halász–Hartmann–Heine compressibility factor, Eq. (2.51)
k	Retention factor, Eq. (2.3)
K_c	Distribution constant, Eq. (2.6)
L	Column length
ℓ	Dimensionless column length, Eq. (2.50)
M	Molar mass
N	Plate number (apparent), Eq. (2.121)
\mathcal{N}	Intuitive plate number, Eqs. (2.117) and (2.125)
n	Running peak capacity, Eq. (2.180)
Δn	Incremental peak capacity, Eq. (2.180)
n_c	Peak capacity of chromatographic analysis, Eq. (2.180)
P	Relative pressure, Eq. (2.26)
ΔP	Relative pressure drop, Eq. (2.26)
p	Pressure
Δp	Pressure drop, Eq. (2.26)
\mathcal{P}_0	Throughput, Eq. (2.241)
p_a	Ambient pressure
p_g	Gauge pressure, Eq. (2.26)
\mathcal{P}_i	Performance parameter, Eq. (2.240)
p_{st}	Standard pressure, 1 atm
Q	Transport efficiency, Eqs. (2.126) and (2.153)
\mathcal{R}	Molar gas constant, 8.31447 J/(K mol)
R_s	Resolution of two consecutive peak, Eq. (2.172)

R_T	Heating rate, Eq. (2.63)	X_r	Sensitivity of ΔT_R to relative change in r_T , Eq. (2.90)
r_T	Dimensionless heating rate, Eq. (2.69)	X_T	Parameter in Eqs. (2.167) and (2.220)
s	Running separation capacity, Eq. (2.176)	X_θ	Sensitivity of ΔT_R to $\Delta\theta_{\text{char}}$, Eq. (2.89)
Δs	Separation of two peaks, incremental separation capacity, Eqs. (2.175) and (2.178)	X_σ	Gas parameter, Table 2.6
s_c	Separation capacity of chromatographic analysis, Eq. (2.177)	z	Distance from column inlet
Δs_{char}	Characteristic separation capacity, Eq. (2.197)	β	Phase ratio, Eq. (2.8)
T	Temperature	ζ	Dimensionless distance from column inlet, Eq. (2.31)
T_{char}	Characteristic temperature, Eq. (2.13)	η	Gas viscosity
ΔT_{char}	Difference in characteristic temperatures of two solutes	η_{st}	Gas viscosity at standard temperature
ΔT_M	Void temperature increment, Eq. (2.73)	θ_{char}	Characteristic thermal constant, Eq. (2.13)
T_{norm}	Normal temperature, 298.15K (25°C)	$\Delta\theta_{\text{char}}$	Difference in characteristic thermal constants of two solutes
T_R	Solute elution temperature	θ_{charG}	Generic characteristic thermal constant Eq. (2.18)
ΔT_R	Difference in elution temperatures of two solutes	A	Linear dynamic range, Eq. (2.256)
T_{st}	Standard temperature, 273.15K (0°C)	λ	Mean free path
t	Time	μ	Solute mobility, Eq. (2.3)
t_{anal}	Analysis time	μ_{eff}	Solute effective mobility, Eq. (2.60)
t_M	Void time, Eq. (2.48)	μ_R	Mobility of eluting solute
t_m	Gas propagation time, Eq. (2.47)	ξ	Gas empirical parameter, Table 2.2
$t_{M,\text{char}}$	Void time at characteristic temperature	ρ_n	Noise spectral density
$t_{M,R}$	t_M in static analysis under conditions existed at time t_R in dynamic analysis	σ	Peak width (standard deviation) in time domain
$t_{M,\text{ref}}$	Void time at reference temperature	$\tilde{\sigma}$	Width (standard deviation) of a solute zone
$t_{m,\text{sol}}$	Solute mobile time, Eq. (2.58)	σ_T	Peak width (standard deviation) in temperature domain
t_{mol}	Mean time between molecular collisions	σ_z	Temporal width of migrating solute zone
t_R	Retention time	v	Average molecular speed
Δt_R	Retention time difference of two solutes	Φ	Function defined in Eq. (2.42)
$t_{R,\text{stat}}$	Retention time in static analysis	φ	Dimensionless film thickness, Eq. (2.9)
u	Gas velocity, Eq. (2.28)	Ω	Gas pneumatic resistance, Eq. (2.30)
\bar{u}	Gas average velocity, Eq. (2.38)	ω	Solute immobility, Eq. (2.3)
v	Solute velocity	$\bar{\omega}$	Distance-averaged immobility, Eq. (2.87)
X_{all}	Parameter in Eq. (2.255)	ϑ	Parameter defined in Eq. (2.101)
X_D	Gas parameter, Table 2.2	ϑ_S	Parameter defined in Eq. (2.102)
X_i	Parameter in Eq. (2.238)		

2.3 General definitions and conventions

Conditions of GC analysis are *static* (as in *isothermal isobaric* GC) if they do not change with time. Otherwise, the conditions are *dynamic* (as in temperature- and/or pressure-programmed GC). The conditions could be *uniform* (the same at any place along the column length) or *nonuniform*. Gas decompression along the column is a typical cause of nonuniform conditions [2] causing gas velocity to increase in the direction from the inlet to the outlet.

Throughout this chapter, temperature (T) can be expressed in degrees Celsius ($^{\circ}\text{C}$) or in units of *absolute temperature* (in kelvin, K). However, T in all equations is assumed to be the **absolute temperature** unless the contrary is explicitly stated. On the other hand, temperature intervals and the differences between two absolute temperatures can be expressed in $^{\circ}\text{C}$ units.

Two types of *open-tubular columns* (OTC) also known as the *capillary columns* are used in GC. The internal walls of the *wall-coated* open-tubular (WCOT) column are coated with absorbing liquid polymer film. The internal walls of the *porous-layer* open-tubular (PLOT) column are covered with a solid porous layer having large adsorbing surface. The WCOT columns play the dominant role in GC, and only they are considered in this chapter. In this context, the terms **OTC**, **WCOT column**, **capillary column**, and **column** are synonyms. Typically, the thickness of a stationary liquid film in OTC is much smaller than the *column tubing internal diameter* (d_c). In these cases, the difference between d_c and the diameter (d) of the internal open space can be ignored.

2.4 Solute–column interaction

2.4.1 Solute distribution between mobile and stationary phases

Let z and t be, respectively, the distance traveled by a solute *zone* (a packet of solute molecules) from the inlet and the time of that travel

(*migration*). A solute migrating through a column might interact with the column stationary phase (might be partially absorbed by liquid stationary phase or adsorbed on solid stationary phase). As a result, the net *velocity*,

$$v = \frac{dz}{dt} \quad (2.1)$$

of migration of the zone at some location (z) along the column can be smaller than the carrier gas local *velocity* (u) at the same location. The relationship between v and u can be expressed as

$$v = \mu u \quad (2.2)$$

where μ is the mobile phase fraction of the solute (defined below).

Different *solutes*—components of a sample—might be differently distributed between the stationary phase and the inert carrier gas in a column. As a result, different solutes might migrate through the column with different velocities (v) and elute from the outlet at different *retention times*—thus being *separated* from each other. This means that.

Different distribution of different solutes between the stationary phase and the carrier gas resulting from the different interaction of the solutes with the stationary phase in a column is the root cause of the solute separation.

The distribution of a solute between the column phases can be expressed in several equivalent ways [2]:

$$k = \frac{a_{\text{stat}}}{a_{\text{mob}}}, \quad \mu = \frac{a_{\text{mob}}}{a}, \quad \omega = \frac{a_{\text{stat}}}{a} \quad (2.3)$$

where $a = a_{\text{mob}} + a_{\text{stat}}$, a_{mob} and a_{stat} are, respectively, the total amount of the solute and its amounts in the mobile and the stationary phases. Parameters k , μ , and ω are, respectively, the solute *retention factor* [2,20] (*capacity factor* [4,5], *capacity ratio* [20], *partition ratio* [3,7,17]), *mobility* [2] (originally introduced by Consden et al. [21], it is also known as the *retardation factor* [6,20], the *retention ratio* [5], and the *frontal ratio* [4]), and *immobility* [2] (*interaction level* [2]).

It follows directly from their definitions in Eq. (2.3) that parameters k , μ , and ω relate to each other as

$$\begin{aligned} k &= \frac{1-\mu}{\mu} = \frac{\omega}{1-\omega}, & \mu &= 1-\omega = \frac{1}{1+k}, \\ \omega &= 1-\mu = \frac{k}{1+k} \end{aligned} \quad (2.4)$$

and are bound by conditions:

$$0 \leq k \leq \infty, \quad 0 \leq \mu \leq 1, \quad 0 \leq \omega \leq 1 \quad (2.5)$$

Parameters μ and ω are complementary to each other. If $\mu = 0$, then $\omega = 1$. Conversely, if $\omega = 0$, then $\mu = 1$. This justifies the complementary terms for these parameters such as the mobility (μ) and the immobility (ω). The latter represents a measure of a solute interaction with a column stationary phase (its affinity to the phase). As such measure, the solute immobility (ω) is similar to the retention factor (k). However, ω is a normalized measure (changing from 0 to 1) while k is not.

As parameters k , μ , and ω are interdependent with each other, either one is sufficient for all evaluations that depend on a solute distribution between the phases. However, a need for the simplicity and transparency of interpretation of theoretical results justifies preferential choice of one parameter over the others depending on the type of evaluations. Thus, the mobility (μ) most directly affects, Eq. (2.2), the solute velocity (v); the immobility (ω) most directly affects their separation [22,23]; and the retention factor most directly relates to thermodynamics of a solute–column interaction—the next topic.

2.4.2 Characteristic parameters of a solute–column interaction

GC utilizing columns with liquid stationary phase is known as *gas–liquid chromatography*

(GLC) and as *partition GC* [24]. This is the most frequently used type of GC by far and the subject of primary attention in this chapter.

The equilibrium of a solute distribution between two phases (stationary liquid polymer phase and mobile gas phase in partition GC) can be described by the *distribution constant* [2,20] (*partition constant* [3–5,7,8,24,25]):

$$K_C = \frac{C_{\text{stat}}}{C_{\text{mob}}} \quad (2.6)$$

where C_{mob} and C_{stat} are the concentrations of the solute in the mobile and the stationary phase, respectively. The dependence of K_C on temperature (T) can be described by the integrated *van't Hoff equation* representing an *ideal thermodynamic equilibrium model* [5,26] (Fig. 2.2A):

$$K_C = e^g, \quad g = \frac{G}{T} = -\frac{G_S}{\mathcal{R}} + \frac{G_H}{\mathcal{R}T} \quad (2.7)$$

(ideal thermodynamic model)

where G , G_S , G_H , and g are the *Gibbs free energy*, *entropy*, *enthalpy*, and *dimensionless Gibbs free energy* [2,23], respectively, of a solute transfer from stationary to mobile phase, and $\mathcal{R} = 8.31,447 \text{ J}/(\text{K mol})$ is the *molar gas constant*. As an example, parameters G_S and G_H of several solutes are listed in Table 2.1. Generally, T can be nonuniform, i.e., it can be different at different locations (z) along the column. In this case, K_C is also nonuniform, i.e., it is a function $K_C(z)$ of z . This condition exists in, e.g., *thermal gradient GC* (discussed later). It is assumed throughout this chapter that, unless the contrary is explicitly stated, T and K_C are **uniform**.

It follows from Eqs. (2.3), (2.6), and (2.7) that

$$k = \frac{K_C}{\beta} = \frac{e^g}{\beta}, \quad \beta = \frac{\text{stationary phase volume}}{\text{gas volume}} \quad (2.8)$$

where β is the *phase ratio*. Generally, the stationary-phase film thickness and/or

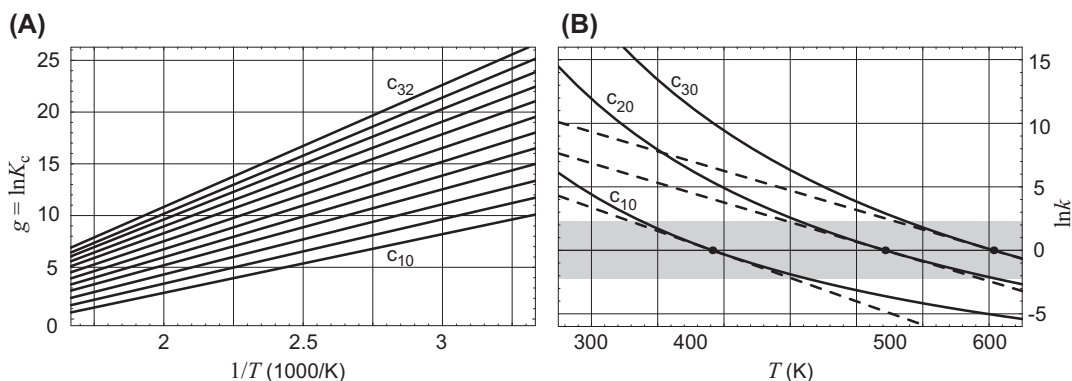


FIGURE 2.2 Thermodynamic properties of n-alkanes in 5% diphenyl-dimethyl polysiloxane polymer: (A) dimensionless Gibbs free energies (g , Eq. 2.7) of a solute transfer from stationary to mobile phase versus inverse temperature ($1/T$), (B) $\ln k$ versus T (Eq. 2.10 at $\varphi = 0.001$). Within shaded area in (B) where $0.1 \leq k \leq 10$, a tangent line to $\ln k(T)$ -curve at $k = 1$ closely approximates the curve itself. From L.M. Blumberg, *Temperature-Programmed Gas Chromatography*, Wiley-VCH, Weinheim, 2010. Adapted with permission.

thermodynamic properties can be nonuniform [28]. In this case, the numerator and the denominator of Eq. (2.8) represent local volumes in narrow vicinity of each coordinate z , and β can be nonuniform. However, it is assumed throughout this chapter that β is **uniform**.

For capillary column having its internal walls coated with thin liquid stationary-phase *film*, β can be expressed as

$$\beta \approx \frac{1}{4\varphi}, \quad \varphi = \frac{d_f}{d} \quad (2.9)$$

where d_f and φ are, respectively, the stationary-phase film *thickness* and *dimensionless thickness* [2]. Eq. (2.8) becomes (Fig. 2.2B):

$$k = 4\varphi e^g \quad (2.10)$$

which, in the case of ideal thermodynamic model, Eq. (2.7), becomes

$$\ln k = \frac{G_H}{RT} - \frac{G_S}{R} + \ln(4\varphi) \quad (2.11)$$

(ideal thermodynamic retention model)

The ideal thermodynamic model of Eq. (2.7) (two-parameter model based on parameters G_S

and G_H) is not the only known thermodynamic model in GC [2,5,29–34]. More complex three-parameter models [31–34] can provide more accurate retention time prediction. However, as stated in the Introduction, accurate retention time prediction is out of scope of this chapter. Simpler models are sufficient for theoretical study of performance of GC analyses—the main focus of this chapter.

The model in Eq. (2.7), although relatively simple, has its own shortcomings. Its two parameters, G_H and G_S , change with temperature and solute concentration. The dependence of G_H and G_S on a solute concentration can be negligible if stationary-phase *overloading* is avoided when relatively small sample amounts are analyzed. It is assumed throughout this chapter that, unless otherwise explicitly stated, a column is **not overloaded** and the solute concentration does not affect parameters G_H and G_S . As for the dependence of these parameters on temperature, it is negligible if the solute migration is evaluated within a relatively narrow temperature range (less than $\pm 50^\circ\text{C}$ [2]) around the temperature at which the parameters were found (measured, calculated, etc.).

TABLE 2.1 Thermodynamic parameters of several solutes in 5% phenyl-dimethyl polysiloxane polymer [34]. Also included are the solute molecular weights (M) and boiling points (T_b).

#	Name	M [27] g/mol	G_H kJ/mol	G_S J/mol/K	T_b [27] °C	T_{char} °C	θ_{char} °C
1	Heptane	100.2	30.2	49.3	98.4	43.7	27.7
2	Octane	114.2	34.5	55.2	125.7	67.8	28.
3	Nonane	128.3	38.8	61.5	150.8	88.4	28.
4	2-Octanone	128.2	40.2	60.3	173.6	105.7	29.7
5	Decane	142.3	43.1	67.5	174.1	107.3	27.9
6	2-Octanol	130.2	41.	61.9	180.	107.5	29.4
7	1-Octanol	130.2	43.9	65.7	194.4	120.1	29.3
8	Undecane	156.3	40.	55.1	196.8	122.5	32.6
9	5-Nonanol	144.3	44.6	66.5	193.	123.5	29.3
10	2-Nonanol	144.3	45.2	67.6	193	125.4	29.2
11	1-Nonanol		48.1	71.3		136.9	29.1
12	5-Decanol		48.8	72.2		139.7	29.1
13	2-Decanone	156.3	48.5	71.4	210.1	140.3	29.3
14	Dodecane	170.3	43.7	59.8	216.3	140.4	32.5
15	Tridecane	184.4	47.5	64.6	235.4	156.8	32.3
16	Tetradecane	198.4	51.3	69.4	253.7	171.7	32.1
17	Pentadecane	212.4	55.	74.1	270.6	185.3	31.8

Sorted by ascending T_{char} . T_{char} and θ_{char} are at $\varphi = 0.001$.

Even when its parameters (G_H and G_S) are fixed quantities, the use of the ideal thermodynamic model in theoretical studies of temperature-programmed GC is highly problematic because it, in Giddings' words [35], "always leads to rather formidable integrals whose solutions are not easily obtained" [14,17]. Fortunately, within a moderately wide range, $0.1k_0 \leq k \leq 10k_0$, of retention factors (k) around some predetermined retention factor k_0 , the difference between actual $\ln k(T)$ -curve for a

solute and the tangent line to that curve at $k = k_0$ is small (Fig. 2.2B) so that, in column performance evaluations, the tangent line can be used as a *linear retention model* [2] described below.

The linear model has chromatographic justification. During the heating ramp covering a wide temperature range, all solutes elute with approximately equal retention factors (k_R) [2,14] (see also Section 2.7.6). The solutes also migrate through the major portion of a column length with retention factors that are not much larger than $10k_R$ [2]. This suggests that a linear retention model can be used for evaluation of the key elution parameters of the solutes in temperature-programmed GC analyses. A choice of $k_0 = 1$ leads to the simplest transformation (see further) of parameter G_S and G_H into parameters of a linear retention model, and vice versa [2]. It also helps that, at optimal or near-optimal heating rate, retention factors of eluting solutes are not far from unity [2].

Let $\ln k(T)$ be some (not necessarily ideal) model of a solute-column interaction where functions $\ln k(T)$ for all solutes are roughly similar to the ones in (Fig. 2.2B). The tangent line at $k = 1$ for each solute can be treated as the solute linear retention model [2]:

$$\ln k = -\frac{T - T_{char}}{\theta_{char}} \quad (\text{linear retention model}) \quad (2.12)$$

where

$$T_{char} = T|_{k=1}, \quad \theta_{char} = -\left(\frac{d(\ln k(T))}{dT}\right)\Big|_{k=1}^{-1} \quad (2.13)$$

Both parameters (T_{char} and θ_{char}) of the straight line in Eq. (2.12) are measured in units of temperature. Their examples for several solutes are listed in Table 2.1.

Quantity T_{char} —the *intercept* of the line in Eq. (2.12)—is the *characteristic temperature* of the

solute–column interaction—the temperature at which $\ln k = 0$. In a typical isothermal and temperature-programmed analysis, the solutes generally elute in the order of increasing their T_{char} .

Parameter θ_{char} is the *characteristic thermal constant* of the interaction. The *slope* of the line in Eq. (2.12) is equal to $-1/\theta_{\text{char}}$. Following are the reasons for describing the solute–column interaction via parameter θ_{char} rather than via the slope.

- Quantity θ_{char} is measured in temperature units, while the slope is measured in less intuitive inverse temperature units.
- Temperature (T) increase reduces k . As a result, $\ln k(T)$ has a *negative slope*, while parameter θ_{char} is conveniently a positive quantity equal to the temperature increase that reduces k in Eq. (2.12) by a factor $e \approx 2.72$.
- From a more general perspective, k is an almost exponentially declining function of T . In some disciplines (physics, medicine, etc.) the exponentially (or almost exponentially) declining quantities (mass, concentration, strength, etc.) are characterized by the *half-life time*—the time during which the quantity declines by a factor of 2. (It is easier to comprehend that the half-life strength of some medicine, e.g., is 12 h rather than that the slope of reduction of natural logarithm of the strength of the medicine is 0.06 h^{-1} .) In other disciplines (electronics, mechanics, etc.), quantities exponentially declining with time are characterized by the *time constant*—the time during which the quantity declines by a factor of $e \approx 2.72$. As a concept, the time constant is less intuitive than the half-life time. On the other hand, the time constant is more convenient to handle mathematically. They relate to each other as (half-life time) $\approx 0.7(\text{time constant})$. The characteristic thermal constant (θ_{char}) is analogous to the time constant.

- Functions $K_c(T) = \text{Exp}(G/T)$, $\ln K_c(T) = G/T$, and $k(T) = \text{Exp}(G/T)/\beta$, Eqs. (2.7) and (2.8), represent interdependent quantities (K_c and k), but all have different slopes. Thus, the slope of $K_c(T)$ is different from those of $\ln K_c(T)$ and $k(T)$. Not only that, but the slope of the same parameter depends on the way it is described. Thus, the slope of $K_c(T)$ is different from that of $\ln K_c(T)$. On the other hand, the characteristic thermal constant (θ_{char}) of all these quantities is the same. When T changing from T_{char} to $T_{\text{char}} + \theta_{\text{char}}$, both K_c and k become e -times smaller regardless of equations describing these parameters as functions of T .

Example 2.1. Quantity θ_{char} typically ranges between 25 and 40°C [2] (see also examples in Table 2.1). If $\theta_{\text{char}} = 30^\circ\text{C}$, then raising T from T_{char} to $T_{\text{char}} + 30^\circ\text{C}$ reduces both K_c and k by a factor of 2.72, raising T by 1°C , from T_{char} to $T_{\text{char}} + 1^\circ\text{C}$, reduces both K_c and k by $(1^\circ\text{C})/(30^\circ\text{C}) \approx 3.3\%$, in order to reduce k or K_c by a factor of 2, T should be raised from T_{char} by $30^\circ\text{C} \times \ln 2 \approx 21^\circ\text{C}$. The latter is close to published experimental results [35–37].

The topic of this chapter is theoretical evaluation of the factors affecting performance of GC analyses and their optimization. Among these factors are the effects of a column temperature and heating rate not on each particular solute, but general trends in such effects on all solutes. The linear retention model is sufficiently accurate for such evaluations and is the only known model that leads to broad theoretical solutions [2]. The theory reviewed in this chapter is based on that **linear retention model**.

The significance of T_{char} and θ_{char} goes beyond their role of parameters in linear retention model of Eq. (2.12). Their definitions in Eq. (2.13) are not related to any particular model and are valid for any model. Quantities T_{char} and θ_{char} can serve as parameters in an ideal two-parameter thermodynamic model, as well as parameters of a three-parameter thermodynamic model [34].

If parameters, G_H and G_S , of the ideal two-parameter model in Eq. (2.7) are known, then parameters T_{char} and θ_{char} could be found from Eqs. (2.11) and (2.13) as [2]:

$$\begin{aligned} T_{\text{char}} &= \frac{G_H}{G_S - \mathcal{R} \ln(4\phi)}, \\ \theta_{\text{char}} &= \frac{\mathcal{R} G_H}{(G_S - \mathcal{R} \ln(4\phi))^2} \end{aligned} \quad (2.14)$$

These transformations were used for calculation of T_{char} and θ_{char} in Table 2.1. If necessary, T_{char} and θ_{char} could be transformed back to G_H and G_S [2]:

$$G_H = \frac{\mathcal{R} T_{\text{char}}^2}{\theta_{\text{char}}}, \quad G_S = \mathcal{R} \left(\frac{T_{\text{char}}}{\theta_{\text{char}}} + \ln(4\phi) \right) \quad (2.15)$$

Substitution of Eq. (2.15) in Eq. (2.11) yields [2]:

$$\ln k = \frac{T_{\text{char}}}{\theta_{\text{char}}} \left(\frac{T_{\text{char}}}{T} - 1 \right) \quad (2.16)$$

(ideal thermodynamic model)

which is the same ideal thermodynamic model as the one in Eq. (2.11) only differently expressed. Eq. (2.16) makes it obvious that, as mentioned earlier, $k = 1$ at $T = T_{\text{char}}$ and that $(-1/\theta_{\text{char}})$ is the slope of $\ln k$ at $T = T_{\text{char}}$.

Having clear chromatographic interpretation, characteristic parameters T_{char} and θ_{char} provide insight into chromatographic properties of the solutes (their expected elution temperatures in temperature-programmed analyses, dependence of the temperatures on the heating rate, etc.). This cannot be said about thermodynamic parameters G_H and G_S in Eq. (2.11). While having clear thermodynamic interpretation, they tell little about chromatographic properties of the solute. Thus, the fact that decane in Table 2.1 has $G_H \approx 43.15$ kJ/mol and $G_S \approx 67.5$ J/mol/K tells little about, say, its elution temperature in a typical temperature-programmed analysis, while $T_{\text{char}} = 107.3^\circ\text{C}$ indicates that decane will elute in such analysis at about 107.3°C .

Several applications of parameters T_{char} and θ_{char} are demonstrated in this chapter. Among them are evaluations of optimal heating rate, prediction of reversal of a solute elution order as a function of the heating rate, evaluation of diffusivity of an arbitrary solute with a known T_{char} . Outside this chapter, the characteristic parameters were also used for prediction of the peak distribution maps in GC \times GC [38]. The concept of characteristic parameters extended to LC (liquid chromatography) was used for evaluation of optimal mixing rate (the rate of programmable change in solvent composition) in gradient LC. This suggests that characteristic parameters of a solute-column interaction can serve as a common ground for representation of different retention mechanisms. There are other applications for these parameters. One of them could be quantitative evaluation of the effects of column aging. In a recent publication [39], the effect of a column heating to high temperature on parameters G_H and G_S of several solutes was measured and tabulated. Transformation of these parameters into T_{char} and θ_{char} using Eq. (2.14) led to a chromatographically meaningful conclusion that the heating reduced T_{char} by 3–4°C and reduced θ_{char} by 4%–6%. For a solute eluting during a typical heating ramp, reduction of T_{char} by some ΔT_{char} results in about the same reduction in elution temperature [2], reduction in θ_{char} is an indication of proportionally higher sensitivity of k to the change in column temperature, Eq. (2.13).

As follows from Eq. (2.14), characteristic parameters depend on film thickness. If two columns have the same stationary-phase type of different film thicknesses, then Eqs. (2.14) and (2.15) can be used for transforming T_{char} and θ_{char} of each solute in one column into these parameters in another column. However, such transformations are somewhat cumbersome [2]. A simple approximate transformation for T_{char} can be obtained from the approximation [2]:

$$\frac{T_{\text{char}2}}{T_{\text{char}1}} = \left(\frac{\varphi_2}{\varphi_1} \right)^{0.07} \quad (2.17)$$

It shows that T_{char} is a weak function of the film thickness. Thus, doubling the film thickness, i.e., doubling φ , causes about 5% increase in T_{char} of each solute. Similar transformation for θ_{char} is described later.

2.4.3 Relations between characteristic parameters

The characteristic temperature (T_{char}) of a solute can be any temperature within the range of GC analyses and beyond. As a general trend, the solutes with larger boiling points have larger T_{char} . The values of characteristic thermal constant (θ_{char}) are typically confined within 25–40°C range [2] (see also examples in Table 2.1). For a given solute, parameters T_{char} and θ_{char} are independent of each other and essentially are the parameters of the solute chromatographic identity in relation to a give column. However, there is a general trend, Fig. 2.3. The solutes having larger T_{char} (and eluting at higher temperatures) have generally larger θ_{char} . In addition to that, film thickness slightly affects θ_{char} . The trends in Fig. 2.3 can be described as [2]:

$$\begin{aligned} \theta_{\text{charG}} &= \theta_{\text{char,st}} \left(\frac{T_{\text{char}}}{T_{\text{st}}} \right)^{0.7}, \\ \theta_{\text{char,st}} &= 22^\circ\text{C} \cdot (10^3 \varphi)^{0.09} \end{aligned} \quad (2.18)$$

where θ_{charG} is the expected value of θ_{char} for the solute with a given T_{char} . A solute for which $\theta_{\text{char}} = \theta_{\text{charG}}$ (i.e., its actual θ_{char} is equal to the expected θ_{char} for the solute's T_{char}) is called herein as the *generic* one [2]. In view of that, θ_{charG} can be interpreted as the characteristic thermal constant of a *generic solute* and can be called as the *generic characteristic thermal constant*.

Example 2.2. In a column with $\varphi = 0.001$, a generic solute having $T_{\text{char}} = 423.15\text{K}$ (150 °C) has $\theta_{\text{charG}} \approx 30^\circ\text{C}$. A (possibly different) generic solute that has the same T_{char} in a column of

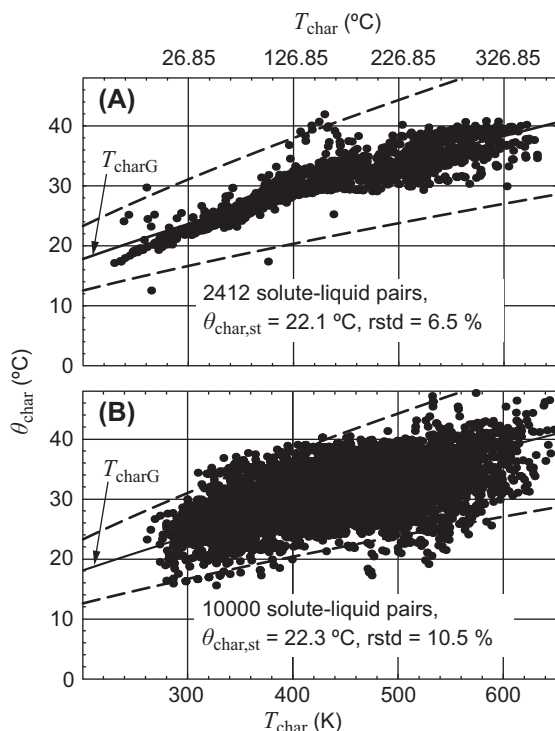


FIGURE 2.3 Maps of ($T_{\text{char}}, \theta_{\text{char}}$) pairs (the dots) for (A) 2412 combinations of more than 1000 solutes in eight liquid polymers [2] and (B) about 10,000 combinations generated from the data in Refs. [30,40]. In all cases, $\varphi = 0.001$. Each dot in (B) represents one of 212 solutes in one of 50 stationary phases characterized in Ref. [40]. (Some 20 or so solutes represented in (B) appear in both sources [30,40].) Quantity $\theta_{\text{char,st}}$ listed in each graph corresponds to respective least square fits, solid lines, of Eq. (2.18). The dashed lines mark $\pm 30\%$ distances from the solid lines, rstd is relative standard deviation of vertical departures of the dots from the solid line. Panel A from L.M. Blumberg, *Temperature-Programmed Gas Chromatography*, Wiley-VCH, Weinheim, 2010. Adapted with permission.

equal diameter, but twice as thick stationary phase of the same type has $\theta_{\text{charG}} \approx 32^\circ\text{C}$.

2.5 Properties of ideal gas

2.5.1 Theoretical relations

It is assumed throughout this chapter that the carrier gas is an **ideal gas** [2,26,41]. This means

that relationship between its mass (m_g), pressure (p), temperature (T), and volume (V) is governed by the *ideal gas law*:

$$pV = \frac{\mathcal{R} m_g T}{M} \quad (2.19)$$

where M is the gas *molar mass*. Several molecular properties of ideal gas are important for GC. Among them are *average molecular speed* (v), *mean free path* (λ), *mean time between collisions* (t_{mol}), *self-diffusivity* (D_g), and *viscosity* (η). They relate to each other and to other gas properties as [2,26,41,42]:

$$v = \sqrt{\frac{8\mathcal{R}T}{\pi M}}, \quad \lambda = \frac{4v\eta}{5p}, \quad t_{\text{mol}} = \frac{\pi\eta}{4p},$$

$$D_g = \frac{3\pi}{20} \cdot \frac{\eta v^2}{p} \quad (2.20)$$

The values of some of these parameters and others, introduced later in this section, are listed in Table 2.2.

2.5.2 Viscosity

Among gas parameters in Eq. (2.20), only the average molecular speed (v) can be calculated from *a priori* known molar mass (M) of the gas. Other parameters are expressed via the gas viscosity (η) — a measure of its resistance to flow. Ideally, as is assumed throughout this chapter, η is **independent of pressure**. Although theoretical expressions for η are known, they are either complex or not sufficiently accurate for practical applications [26,41,43]. Instead, empirical expressions are used in GC [2,43–45].

TABLE 2.2 Molecular and other properties of several gases.

Gas	He	H ₂	N ₂	Ar
<i>Molecular properties:</i>				
M (molar mass), g/mol	4.003	2.016	28.01	39.95
λ_{st} (mean free path at $p = p_{\text{st}}$, $T = T_{\text{st}}$), μm	0.177	0.112	0.0604	0.0641
v_{st} (average molecular speed at $T = T_{\text{st}}$), km/s	1.20	1.69	0.454	0.38
η_{st} (viscosity at $T = T_{\text{st}}$), $\mu\text{Pa}\cdot\text{s}$	18.69	8.362	16.84	21.35
$D_{g,\text{st}}$ (self-diffusivity at $p = p_{\text{st}}$, $T = T_{\text{st}}$), cm^2/s	1.26	1.12	0.162	0.144
<i>Empirical parameters:</i>				
ξ (parameter in Eq. 2.21)	0.685	0.698	0.710	0.750
X_D (parameter in Eqs. 2.24 and 2.25)	0.456	0.544	0.693	0.686
<i>Combinations:</i>				
$X_D \lambda_{\text{st}}$, μm	0.081	0.061	0.042	0.044
$(X_D \lambda_{\text{st}})/(X_D \lambda_{\text{st}})_{\text{hydrogen}}$	1.33	1	0.689	0.721
$X_D v_{\text{st}}$, km/s	0.548	0.92	0.315	0.261
$(X_D v_{\text{st}})/(X_D v_{\text{st}})_{\text{hydrogen}}$	0.596	1	0.342	0.284
$X_D^2 D_{g,\text{st}}$, cm^2/s	0.262	0.331	0.078	0.068
$D/D_{\text{hydrogen}} = X_D^2 D_{g,\text{st}} / (X_D^2 D_{g,\text{st}})_{\text{hydrogen}}$ (Eqs. 2.24 and 2.25)	0.79	1	0.24	0.21

$p_{\text{st}} = 1 \text{ atm}$, $T_{\text{st}} = 0^\circ\text{C}$. Quantities D_{hydrogen} and D are the diffusivities of the same solute in hydrogen and in another gas, respectively. In the source [2], quantity X_D was denoted as γ_D .

From L.M. Blumberg, *Temperature-Programmed Gas Chromatography*, Wiley-VCH, Weinheim, 2010. Adapted with permission.

The following two are the simplest at their accuracies [2,45]:

$$\eta = \left(\frac{T}{T_{st}}\right)^{\xi} \eta_{st} \quad (2.21)$$

$$\eta = \eta_{st0} \left(\frac{T}{T_{st}}\right)^{\xi(T)}, \quad \xi(T) = \xi_0 + \xi_1 \frac{T - T_{st}}{T_{st}} \quad (2.22)$$

Parameters η_{st} (the gas viscosity at 0°C) and ξ in Eq. (2.21) are listed for several carrier gases in Table 2.2. Parameters in Eq. (2.22) are listed in Table 2.3. All parameters were obtained by the least square fittings of Eqs. (2.21) and (2.22) to numerical data [43] within $300\text{K} \leq T \leq 600\text{K}$ and $250\text{K} \leq T \leq 750\text{K}$, respectively [2]. Eq. (2.21) is simpler than Eq. (2.22), but Eq. (2.22) is more accurate (Table 2.4). The data in Table 2.4 show that, only when Eq. (2.21) is used within the *extended temperature range* ($250\text{K} \leq T \leq 750\text{K}$), its errors for viscosity of nitrogen and argon can be larger than the errors in the source of numerical viscosity data [43]. In all other cases compiled in Table 2.4, the errors added by Eqs. (2.21) and (2.22) can be ignored because they are smaller [2] than the errors specified in the source [43] for its numerical data.

In the rest of this chapter, **only** Eq. (2.21) is used for evaluation of gas viscosities. Eq. (2.22) might be useful in designing pneumatic control systems in GC instruments where higher accuracy of viscosity calculation might be necessary.

The numerical values of parameters η_{st} and ξ in Table 2.2 for helium, hydrogen, and nitrogen

TABLE 2.3 Gas viscosity parameters in Eq. (2.22).

Gas	He	H ₂	N ₂	Ar
η_{st0} ($\mu\text{Pa}\cdot\text{s}$)	18.63	8.382	16.62	21.04
ξ_0	0.6958	0.6892	0.7665	0.8131
ξ_1	-0.0071	0.005	-0.0378	-0.0426

From L.M. Blumberg, *Temperature-Programmed Gas Chromatography*, Wiley-VCH, Weinheim, 2010. Adapted with permission.

TABLE 2.4 The largest % errors in numerical viscosity data in the source [43] (Primary errors), and additional errors due to Eqs. (2.21) and (2.22).

Gas	He	H ₂	N ₂	Ar
Primary errors	1	2	2	no data
Additional errors from Eq. (2.21), $300\text{K} \leq T \leq 600\text{K}$	0.2	0.2	0.8	0.8
Additional errors from Eq. (2.21), $250\text{K} \leq T \leq 750\text{K}$	0.5	0.5	2	2.5
Additional errors from Eq. (2.22), $250\text{K} \leq T \leq 750\text{K}$	0.1	0.2	0.4	0.4

The additional errors are the largest % difference between the numerical data in the source [43] and the data obtained from Eqs. (2.21) and (2.22).

From L.M. Blumberg, *Temperature-Programmed Gas Chromatography*, Wiley-VCH, Weinheim, 2010. Adapted with permission.

are different from those reported in other sources [45,46]. As shown elsewhere [2], the viscosity based on the data in Table 2.2 is expected to be more accurate than viscosity based on the previously reported data [45].

2.5.3 Solute diffusivity in gas

Solute *diffusion* in gas plays dual—positive and negative—role in GC separation process. On the one hand, the diffusion is the mechanism that transports the solutes from the gas to the stationary phase and back. In that regard, the diffusion is essential for the separation process in GC. On the other hand, the diffusion broadens the peaks, thus reducing their separation. It is important that only the existence of the diffusion broadens the peaks. However, as shown later, because it reduces the time of transporting the solutes to and from the column walls,

Larger solute diffusivity in the gas proportionally reduces the analysis time under optimal conditions without reducing the number of peaks that a column can resolve.

Diffusivity (D) [2,41] (*diffusion coefficient* [5,26,41,47–49]) of a solute is a measure of the rate of its diffusion in the gas. For some solutes, D can be found from *Fuller–Giddings empirical expression* [48]:

$$D = \frac{10^{-3} \sqrt{1/M_g + 1/M_{\text{sol}}}}{\left(V_g^{1/3} + (\Sigma V_{\text{sol}})^{1/3}\right)^2} \cdot \frac{\text{atm}}{p} \cdot \left(\frac{T}{\text{K}}\right)^{1.75} \cdot \text{cm}^2/\text{s} \quad (2.23)$$

where M_g and M_{sol} are molecular weights of the gas and the solute, respectively, while V_g and V_{sol} are dimensionless empirical quantities known as the *molecular diffusion volume* of the gas and the *atomic diffusion volume increments* of a solute, respectively. The values of these quantities for some gases and solutes can be found in several sources [48,49].

While Eq. (2.23) is suitable for evaluation of diffusivity of some solutes (those few with known parameters V_g and V_{sol}), it is structurally too complex and not suitable for broad theoretical evaluations. One of the difficulties with using Eq. (2.23) is that it does not provide a simple way of accounting for the fact that the solutes generally tend to elute in the order of increase in the size of their molecules. The following two equations more directly account for this effect [2]:

$$D = X_D^2 D_{g,\text{st}} \cdot (10^3 \varphi)^{0.09} \cdot \frac{p_{\text{st}}}{p} \cdot \left(\frac{T_{\text{char}}}{T_{\text{st}}}\right)^{-1.25} \left(\frac{T}{T_{\text{st}}}\right)^{1+\xi} \quad (2.24)$$

$$D = \frac{X_D^2 D_{g,\text{st}} \cdot (10^3 \varphi)^{0.09}}{k^{0.1}} \cdot \frac{p_{\text{st}}}{p} \cdot \left(\frac{T}{T_{\text{st}}}\right)^{\xi-0.25}, \quad (0.1 \leq k \leq 30) \quad (2.25)$$

where gas parameters $D_{g,\text{st}}$ and X_D as well as their products $X_D^2 D_{g,\text{st}}$ for several gases are listed in Table 2.2.

Several observations can be made regarding expected accuracy of Eqs. (2.23), (2.24), and (2.25).

1. An error (ΔD) in evaluation of a solute diffusivity (D) eventually leads to the errors in theoretical prediction of peak widths [2], which, in the worst case, can be proportional to $\sqrt{\Delta D/D}$. As long as $\Delta D/D < 1$, the relative peak width error is smaller (maybe much smaller) than half of the relative error ($\Delta D/D$) in D .
2. When the effects of operational parameters (column dimensions, carrier gas type, column temperature, heating rate, etc.) on a column performance are considered, the diffusivity errors are typically canceled out and can be ignored.
3. Eqs. (2.24) and (2.25) are the approximations of Eq. (2.23). Therefore, the errors in Eq. (2.23), reported [48] to have 6.7% standard deviation and actually reaching 40% and beyond in some cases, should be the benchmark for judging the significance of the errors in Eqs. (2.24) and (2.25).
4. The additional errors in Eqs. (2.24) and (2.25) are expected to be within $\pm 8\%$ at the edges of 25–325°C temperature range [2]. This means that the contribution of the additional errors is not dominant.
5. Eq. (2.24) describes D as a function of a solute characteristic temperature (T_{char}) and a column temperature (T). In this equation, D is proportional to $T^{1+\xi}$ where, according to Table 2.2, quantity $(1 + \xi)$ ranges between 1.685 and 1.75, i.e., for all gases, it is close to 1.75th power of T in Eq. (2.23).
6. In the studies of a column performance, it is desirable [2] to express D as a function of measurable parameters such as column temperature and solute retention factor (k). Eq. (2.25) does that. All solutes that were highly retained at the beginning of a heating ramp elute with roughly the same theoretically predictable elution retention factor [2]. In this case, k in Eq. (2.25) is a fixed quantity and D is proportional to $T^{\xi-0.25}$ where quantity $(\xi - 0.25)$ is about 0.5 for argon and about 0.45 for other gases in

Table 2.2 [50]. This might appear as contradicting with Eq. (2.23) where D is proportional to $T^{1.75}$. However, there is no contradiction. According to Eq. (2.23), the diffusivity of a particular solute is proportional to about $T^{1.75}$. However, also according to Eq. (2.23), the diffusivity of a solute having larger molecule is generally lower than the diffusivity of the one having smaller molecules. During a heating ramp, the solutes having larger molecules generally elute at higher temperatures. Eq. (2.25) reflects the combined effect of these two phenomena. Their net quantitative effect of $D \sim T^{0.4}$ for helium and hydrogen has been experimentally confirmed elsewhere [50].

7. Transition from Eqs. (2.24) to (2.25) is based on approximation $T_{\text{char}}/T \approx k^{0.08}$ verified for $0.1 \leq k \leq 30$ and probably valid for retention factors larger than 30 [2].
8. Strictly speaking, Eqs. (2.24) and (2.25) are valid only for n-alkanes [2]. However, observation of a large number of GC chromatograms suggests that, whenever there is an n-alkane peak in a chromatogram, its width is not noticeably different from the widths of its neighbors, whatever they are. As a result, it is reasonable to use Eqs. (2.24) and (2.25) for evaluation of diffusivities of all solutes.

2.6 Flow of ideal gas in open tubes

From the point of view of the gas flow, a column is a *tube*. It is assumed throughout this chapter that a column (and, therefore, a tube) is **uniform**, **long** ($L \gg d$), has **circular cross-section**, and the flow in it is **laminar** [2] and **mass conserving**¹ (no material flows through the tube walls).

Several pressure parameters are known in chromatography: the *inlet pressure* (p_i), the *outlet pressure* (p_o), the *ambient pressure* (p_a), the *gauge pressure* (p_g), the *pressure drop* (Δp), the *relative pressure* (P), and the *relative pressure drop* (ΔP). Some of these parameters relate to others as:

$$\Delta p = p_i - p_o, \quad p_g = p_i - p_a, \quad P = \frac{p_i}{p_o},$$

$$\Delta P = \frac{\Delta p}{p_o} \quad (2.26)$$

Due to gas viscosity, the *longitudinal velocity* (u_r) of the gas flow in a tube has the *parabolic profile* (Fig. 2.4) [2,5]:

$$u_r = \left(1 - \left(\frac{2r}{d}\right)^2\right) u_{r,\text{max}} \quad (2.27)$$

Let A_{gas} be the total cross-sectional area open for the gas flow, and dA be an area of a small element in that cross section. A *cross-sectional average*,

$$u = u(z) = \frac{1}{A_{\text{gas}}} \int u_r dA, \quad A_{\text{gas}} = \frac{\pi d^2}{4} \quad (2.28)$$

of all longitudinal velocities (u_r) in a cross section located at *longitudinal coordinate* z (the distance from the inlet) of the tube is the gas *linear velocity* (briefly, *velocity*) at z . According to *Darcy's law*,

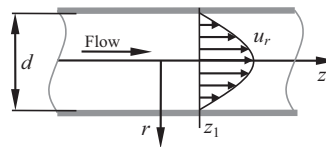


FIGURE 2.4 Parabolic profile, Eq. (2.27), of longitudinal velocities (u_r) in an open tube.

¹ There is evidence [154] that this assumption might be incorrect for helium at 200°C or higher temperature.

gas velocity (u) at location z along a tube can be found as [2,4,5,51,52]:

$$u = -\frac{1}{\Omega} \cdot \frac{\partial p}{\partial \zeta} \quad (2.29)$$

where Ω and ζ are, respectively, the tube *pneumatic resistance* and *dimensionless distance* from the inlet defined as:

$$\Omega = \frac{32L\eta}{d^2} \quad (2.30)$$

$$\zeta = \frac{z}{L} \quad (2.31)$$

The gas is a *compressible* fluid. The volume of its fixed mass is proportional to its temperature (T) and inversely proportional to pressure, Eq. (2.19). This implies [2]:

$$pu = (\text{fixed quantity}) \quad (2.32)$$

In mass-conserving flow of gas, the product pu is uniform (the same at any location along the tube).

Solving the system in Eqs. (2.29) and (2.32), one can express the gas velocity (u) at any location along the tube as a function of pressure (p) at that location as [2] (Fig. 2.5):

$$u = \frac{p_i^2 - p_o^2}{2\Omega p} \quad (2.33)$$

$$p = p_i \sqrt{1 - j_2 \zeta}, \quad u = \frac{u_i}{\sqrt{1 - j_2 \zeta}}, \quad j_2 = \frac{p_i^2 - p_o^2}{p_i^2} \quad (2.34)$$

These equations further yield for u as a function of p_i , p_o , and z :

$$u = \frac{d^2 p_i j_2}{64L\eta \sqrt{1 - j_2 \zeta}} \quad (2.35)$$

At $\zeta = 1$, u becomes the *outlet velocity* (u_o):

$$u_o = \frac{d^2 (p_i^2 - p_o^2)}{64L\eta p_o} \quad (2.36)$$

Gas compressibility complicates relations between pneumatic parameters. They are substantially simpler at the following two decompression extremes:

$$\text{decompression is } \begin{cases} \text{weak,} & \text{when } |\Delta p| \ll p_o \\ \text{strong,} & \text{when } \Delta p \gg p_o \end{cases} \quad (2.37)$$

When the decompression is *weak* (Fig. 2.5A), the gas pressure (p) and velocity (u) are almost uniform. On the other hand, when the decompression is *strong* (Fig. 2.5C), p and u are substantially nonuniform—the difference in their values at the inlet and the outlet is large. Under typical GC conditions, gas decompression is weak and

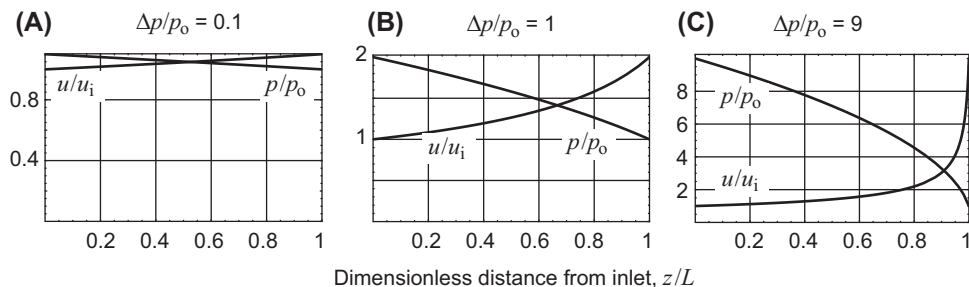


FIGURE 2.5 Pressure (p) and velocity (u) as functions, Eq. (2.34), of a distance (z) from a tube inlet and relative pressure drop ($\Delta p/p_o$). The change of quantities p and u along the tube is small when $\Delta p/p_o = 0.1$, gets larger when $\Delta p/p_o = 1$, and is very large when $\Delta p/p_o = 9$. From L.M. Blumberg, *Temperature-Programmed Gas Chromatography*, Wiley-VCH, Weinheim, 2010. Adapted with permission.

can be ignored when relatively short wide-bore columns ($d \geq 0.32$ mm) operate with detectors working at atmospheric pressure. Conversely, the decomposition is strong in all cases of GC-MS ($p_o = 0$) and in the analyses of complex mixture utilizing relatively long narrow-bore columns.

Because the gas velocity (u) can change with the distance from the inlet, the *time-averaged velocity* (briefly, *average velocity*),

$$\bar{u} = \frac{L}{t_M} \quad (2.38)$$

of the gas is frequently used in GC as a single gas velocity measure. It relates to the gas outlet velocity (u_o) as [2,4,6,24]:

$$\bar{u} = ju_o, \quad j = \frac{3(p_i + p_o)p_o}{2(p_i^2 + p_i p_o + p_o^2)} \approx \begin{cases} 1, & |\Delta p| \ll p_o \\ \frac{3}{2\Delta P}, & \Delta p \gg p_o \end{cases} \quad (2.39)$$

where j is the *James–Martin compressibility factor*. While presenting a well-known and conceptually simple relation of parameters \bar{u} and u_o , the last expression is incomplete. It describes \bar{u} as a function of three pneumatic parameters, p_i , p_o , and u_o of which only two can be mutually independent [2] while the third is a function of the other two. For example, if quantities p_o and u_o in a given tube are known, then p_i is predetermined by the tube dimensions. This means that Eq. (2.39) is insufficient for finding \bar{u} for a given u_o without additional information about the relationship between p_i , p_o , and u_o . That relationship is described in Eq. (2.33). Solving together Eqs. (2.33) and (2.39), one can find that \bar{u} is a function of p_o and u_o [2]:

$$\bar{u} = \frac{3u_o}{2} \cdot \frac{A}{(1+A)^{3/2} - 1}, \quad A = \frac{2\Omega u_o}{p_o} \quad (2.40)$$

The physics of several important relations in GC (flow rate, plate height, etc.) are more directly expressed as functions of u_o rather than as functions of \bar{u} . On the other hand, it is easy to measure \bar{u} using Eq. (2.38), while it is more difficult to measure u_o . In view of that, it is useful to be able to compute u_o from \bar{u} . A solution of Eq. (2.40) for u_o can be expressed as [2,53]:

$$u_o = \frac{p_o}{2\Omega} \cdot \left(\Phi^2 \left(\frac{\Omega \bar{u}}{p_o} \right) - 1 \right) \quad (2.41)$$

For an arbitrary variable x , function $\Phi(x)$ is defined as

$$\Phi(x) = \frac{1}{9} \left(-3 + 4x + X_+^{1/3} + X_-^{1/3} \right) \quad (2.42)$$

where

$$X_+ = 2(X_1 + 27\sqrt{X_2}), \quad X_- = 2(X_1 - 27\sqrt{X_2}),$$

$$X_1 = (3 + 8x)(36 + 3x + 4x^2),$$

$$X_2 = x(3 + 4x)(24 + 3x + 4x^2)$$

These cumbersome expressions describe a monotonic slightly convex function $\Phi(\cdot)$ (Fig. 2.6).

Another measurable parameter of the gas flow is the *flow rate*. The *volumetric flow rate* (briefly, *flow rate*, F) is the volume of gas that flows through any cross section of the tube—the volume measured at standard pressure (p_{st}) and at some predetermined temperature regardless of actual pressure (p) and temperature (T) at that cross section. Quantity F can be found as [2]:

$$F = \frac{\pi d^2 p u T_{\text{norm}}}{4 p_{st} T} = X_{FA} p u, \quad X_{FA} = \frac{\pi d^2 T_{\text{norm}}}{4 p_{st} T} \quad (2.43)$$

It is assumed in Eq. (2.43) and throughout this chapter that F is always measured at *normal temperature*, $T_{\text{norm}} = 298.15\text{K}$ (25°C). As the flow is mass conserving, F is the same at any cross section of the tube. Thus, F at the inlet is the same as it is at the outlet and through any

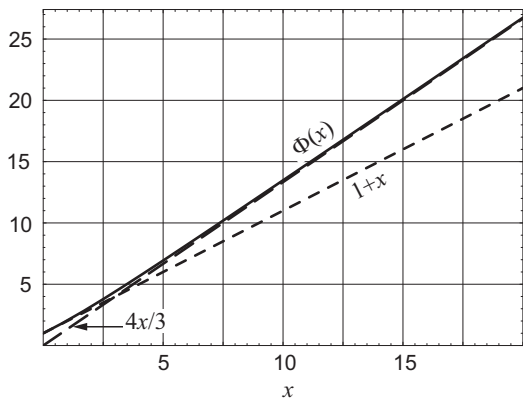


FIGURE 2.6 Function $\Phi(x)$ (solid line —) and its tangent lines: $1 + x$ at $x = 0$ (short dashes - - -), and $4x/3$ at $x = \infty$ (long dashes - - -).

cross section along the way. Substitution of Eqs. (2.33) and (2.30) in Eq. (2.43) yields:

$$F = \frac{\pi d^4 (p_i^2 - p_o^2) T_{\text{norm}}}{256 L \eta p_{\text{st}} T} \quad (2.44)$$

The factors affecting performance of GC column are easier to identify and evaluate if they are expressed not as functions of F , but as functions of *specific flow rate* (f) [2,11]:

$$f = \frac{T}{T_{\text{norm}}} \cdot \frac{F}{d} \quad (2.45)$$

– the flow rate per unit of a tube diameter (d). Factor (T/T_{norm}) included in the definition of f removes the dependence of f on the specifics of the flow rate measurement in GC. Due to Eqs. (2.43) and (2.33), Eq. (2.45) can be rearranged as [2]:

$$f = \frac{\pi d p u}{4 p_{\text{st}}} = \frac{\pi d \cdot (p_i^2 - p_o^2)}{8 p_{\text{st}} \Omega} = \frac{\pi d^3 (p_i^2 - p_o^2)}{256 L p_{\text{st}} \eta} \quad (2.46)$$

The absence of parameter T_{norm} in Eq. (2.46) is an indication of the independence of quantity f of the temperature conventions in the measurement of F .

Another important parameter of the mobile-phase flow is the *void time* (t_M), which plays the role of a basic time clock in chromatography [2,15] and, from that perspective, is not only a pneumatic parameter, but also a chromatographic parameter. Let $t_m = t_m(z)$ be the mobile phase (carrier gas in GC) *propagation time*—the time:

$$t_m = t_m(z) = \int_0^z \frac{dz}{u(z)} \quad (2.47)$$

– the average time of migration of the gas molecules from inlet to arbitrary location z along the column. The *void time* (t_M) is the average time of migration of the gas molecules from the inlet to the outlet. If L is the column length, then:

$$t_M = t_m(L) = \int_0^L \frac{dz}{u(z)} \quad (2.48)$$

For known operational conditions, t_M can be found as [2]:

$$t_M = \frac{32 \ell^2 \eta}{j_H \Delta p} \quad (2.49)$$

where

$$\ell = \frac{L}{d} \quad (2.50)$$

$$j_H = \frac{3(p_i + p_o)^2}{4(p_i^2 + p_i p_o + p_o^2)} \approx \begin{cases} 1, & |\Delta p| \ll p_o \\ \frac{3}{4}, & \Delta p \gg p_o \end{cases} \quad (2.51)$$

Parameters ℓ and j_H are the tube *dimensionless length* and the *Halász–Hartmann–Heine compressibility factor* [54]. Eq. (2.49) shows that t_M is proportional to quantity $(L/d)^2$. It should be noticed, however, that this is true for the cases where Δp is the same for all column dimensions.

This is not how the columns operate in GC. Lower pressure is typically required for shorter and wider-bore columns, while higher pressure is required for longer and narrower-bore ones. What typically is more or less the same for all columns is the gas specific flow rate (f) [2]. On the other hand, pressure is a strong function of a column dimension. As a result, t_M in a realistic GC is not proportional to $(L/d)^2$ as it appears from Eq. (2.49). Expressing t_M as a function [2],

$$t_M = t_M(d, L, f) = \frac{\pi^2 d^4 p_o^3}{1536 p_{st}^2 \eta f^2} \left(\left(1 + \frac{256 L p_{st} \eta f}{\pi d^3 p_o^2} \right)^{3/2} - 1 \right)$$

$$= \begin{cases} \frac{\pi d L p_o}{4 p_{st} f}, & |\Delta p| \ll p_o \\ \sqrt{\frac{64 \pi L^3 \eta}{9 d p_{st} f}}, & \Delta p \gg p_o \end{cases} \quad (2.52)$$

of column parameters and f exposes a more complex but also more realistic dependence of t_M on column dimensions. It shows that, at the same f for all column dimensions, t_M is not proportional to the factor $(L/d)^2 \eta$ as it appears from Eq. (2.49). Rather, t_M at fixed f is complex function of tube dimensions (d and L) and gas viscosity (η). The function becomes simpler at the extremes of the gas decompression. When the decompression is weak, t_M is proportional to the product dL and is independent of η . When the decompression is strong, t_M is proportional to $\sqrt{\eta L^3/d}$.

Eq. (2.52) plays a key role in a column optimization [11] discussed in Section 2.11 of this chapter. To make sense of the middle (general) term of Eq. (2.52), let's introduce the *borderline inlet*

pressure ($p_{i,B}$) and the *critical specific flow rate* (f_{crit}) as²:

$$p_{i,B} = \sqrt{2} p_o, \quad f_{crit} = f \text{ at } p_i = p_{i,B} \quad (2.53)$$

Under these conditions, Eq. (2.46) yields:

$$f_{crit} = \frac{\pi d^3 p_o^2}{256 L p_{st} \eta} \quad (2.54)$$

allowing one to more compactly express the general form of Eq. (2.52):

$$t_M(d, f, f_{crit}) = \frac{\pi^2 d^4 p_o^3}{1536 f^2 p_{st}^2 \eta} \left(\left(1 + \frac{f}{f_{crit}} \right)^{3/2} - 1 \right) \quad (2.55)$$

suggesting that conditions of the weak ($|\Delta p| \ll p_o$) and the strong ($\Delta p \gg p_o$) gas decompression can be also expressed as $f \ll f_{crit}$ and $f \gg f_{crit}$, respectively. Eqs. (2.38) and (2.55) yield for \bar{u} as a function of f :

$$\bar{u} = \frac{1536 L p_{st}^2 \eta f^2}{\pi^2 d^4 p_o^3} \left(\left(1 + \frac{f}{f_{crit}} \right)^{3/2} - 1 \right)^{-1} \quad (2.56)$$

A large collection of mathematical expressions describing relations between various pneumatic parameters of a tube can be found elsewhere [2,53].

2.7 Solute migration and elution

A solute *zone* is a packet of solute material in a column. Its width is measured in units of *distance* along the column. Elution of a solute zone out of a column outlet results in a chromatographic *peak* representing the rate of flow of the solute material from the outlet as function of time (t) [2,55]. The widths of the peaks are measured in

² The definition of $p_{i,B}$ here is different from that in Ref. [2] where $p_{i,B} = 2p_o$.

units of *time*. Typically, the peaks are observed as components of a chromatogram—a visual representation of a detector output. It is important to recognize that the solute zones within a column and the peaks in a chromatogram are different things. The first mathematical moment of a solute zone (its *center of mass*) is the longitudinal distance (z) of the zone from the column inlet [2]. The first mathematical moment of a peak is its *retention time* (t_R). First moments of symmetrical peaks and zones coincide with their apexes.

The time (t_e) when the center of mass of the zone is at the outlet, i.e., when $z = L$, is the zone *elution time*. Strictly speaking, t_R and t_e could be slightly different from each other [2,55]. Here is why. Suppose that during its migration within a column, the zone was perfectly symmetric. During its elution, the solute material still remaining in the column continues to diffuse and its zone continues to broaden. As a result, the second half of the solute material elutes slightly longer than its first half. This makes the peak slightly tailing and t_R slightly delayed compared to t_e . The difference between t_R and t_e is practically insignificant [2] and can be ignored. Frequently, the difference is not even recognized. Although it is ignored in the rest of this chapter, it is important to recognize the existence of the difference between t_R and t_e for better understanding the elution process. (See also the footnote to Eq. (2.110)).

In a study of temperature-programmed analyses, it might be more convenient to deal with the solute elution temperatures than with the peak retention times. A solute *elution temperature* (T_R) is a column temperature at the peak retention time. The latter depends on such secondary factors of temperature programming as the column dimensions, carrier gas type, flow rate, etc., that, in equally scaled temperature programs (see further) do not affect T_R . As a result, considering T_R rather than t_R makes it possible to bypass the effects of the secondary factors, to simplify the study, and to come up with more general results.

2.7.1 General equations of a solute migration and elution

Due to its decompression along a column, the gas velocity (u) can be a function, Eq. (2.34), of z (be nonuniform). Due to the temperature-dependent gas viscosity, u in a temperature-programmed analysis can also change with t (be dynamic). Pressure programming in isothermal GC analysis also causes dependence of u on t . Another parameter in Eq. (2.2), the solute mobility (μ) can also be a time-dependent quantity. In fact, the change in μ with t is the whole purpose of the temperature programming in GC. In addition to being a dynamic quantity, μ can be nonuniform. A nonuniform μ in GC can result from nonuniform temperature in *thermal gradient* GC [56–63] and/or from nonuniform film thickness in otherwise uniform column [28].

In a general case of nonuniform dynamic conditions, a solute retention time (t_R) can be found from integration of Eq. (2.1) with solute velocity (v) described in Eq. (2.2) where parameters u and μ and, therefore, parameter v can be functions, $u = u(z, t)$, $\mu = \mu(z, t)$, and $v = v(z, t)$, of time (t) and distance (z) traveled by the solute since its injection. Eqs. (2.1) and (2.2) can be integrated as [2,64]:

$$\int_0^{t(z)} \mu(z(t), t) dt = t_{m, \text{sol}}(z) \quad (2.57)$$

$$t_{m, \text{sol}}(z) = \int_0^z \frac{dz}{u(z, t(z))} \quad (2.58)$$

where $t_{m, \text{sol}}(z)$ is the *solute mobile time*—the time that, on its way from the inlet to distance z , the solute spent in the gas [64]. Different solutes can have different $t_{m, \text{sol}}(z)$ at the same z . Quantity $t_{m, \text{sol}}(z)$ can also be different from the mobile phase (carrier gas in GC) propagation time, $t_m(z)$, Eq. (2.47). Quantity $t_m(z)$ is the time of migration of a single gas packet from inlet to z —the sum of

the small time intervals $dt_m(z)$ of migration of the packet over all small distances (dz) comprising z . On the other hand, $t_{m,\text{sol}}(z)$ is the sum of the small time intervals $dt_m(z)$ of migration of different gas packets over distances dz —each gas packet overlapping with a given solute when the solute is at z .

Generally, the system of Eqs. (2.57) and (2.58) can only be solved numerically. However, analytical solutions can be found for some typical GC analyses [2]. One of such typical analyses is the uniform heating of a uniform column. Non-uniform thermodynamic conditions and their effect on the *peak focusing* are considered later. For now, it is assumed that, in addition to previous assumption that a column is uniform, it is also **heated uniformly**, unless otherwise stated explicitly. Therefore, thermodynamic parameters (k , μ , and ω) of the solutes, as well as the gas viscosity (η) are uniform.

2.7.2 Isobaric analysis

When the column and its heating are uniform, quantities η and μ , being functions of temperature (T), become functions $\eta = \eta(T(t)) = \eta(t)$ and $\mu = \mu(T(t)) = \mu(t)$, of only the time (t) (but not of the distance, z). If, in addition to that, the analysis is *isobaric* (inlet and outlet pressures, p_i and p_o , are fixed during the analysis), then the column pressure (p) at any z is function $p(z)$ of only z (but not of t) and then system of Eqs. (2.57) and (2.58) can be reduced to a single equation [2]:

$$\int_0^{t_R} \mu_{\text{eff}}(T(t)) dt = t_{M,\text{ref}} \quad (\text{isobaric}) \quad (2.59)$$

where $t_{M,\text{ref}}$ is the *reference void time*—the void time at some arbitrarily chosen predetermined *reference temperature* (T_{ref}), and

$$\mu_{\text{eff}}(T(t)) = \frac{\eta(T(t))}{\eta(T_{\text{ref}})} \mu(T(t)) \quad (2.60)$$

is the solute *effective mobility* [2] (*effective propagation factor* [15]).

Eq. (2.59) has interesting implications. It implies that, in an *isobaric analysis* with any temperature program, $T(t)$,

The net effect of a temperature-depended solute mobility (μ) and gas viscosity (η) on a solute retention time (t_R) and on its elution temperature (T_R) can be lumped in a single quantity—the effective solute mobility (μ_{eff}).

The net effect of the column dimensions, carrier gas type, and the gas initial conditions on a solute retention time (t_R) can be expressed via a single parameter—the static void time ($t_{M,\text{ref}}$) measured at some predetermined fixed reference temperature (T_{ref}).

Other than through its effect on the void time ($t_{M,\text{ref}}$) at some predetermined fixed temperature (T_{ref}), gas decompression along a column has no effect on a solute retention time (t_R) and on its elution temperature (T_R).

Eq. (2.59) can be also expressed as [2]:

$$\int_0^{t_R/t_{M,\text{ref}}} \mu_{\text{eff}} \left(T \left(\frac{t}{t_{M,\text{ref}}} \right) \right) d \frac{t}{t_{M,\text{ref}}} = 1 \quad (\text{isobaric}) \quad (2.61)$$

implying that the void time (t_M) plays a special role in the formation of retention times. It acts as a basic *time clock* of chromatography and a fundamental *scaling factor* of a chromatogram. It follows from Eq. (2.61) that the effect of a temperature program, $T(t)$, on peak retention times comes not from T as function of the clock time (t), but from T as a function of t in relation to t_M . This is why reporting only the temperature program without reporting the void time or providing sufficient information for its calculation (column dimensions, temperature, flow rate, etc.) in the same analysis is not informative. The same heating rate, say, $10^\circ\text{C}/\text{min}$, can be too fast for some columns and conditions and too slow for others. On the other hand, $10^\circ\text{C}/t_M$ is close to optimum for all columns and conditions [16] (see optimal heating rate, further).

When the medium is static (isobaric and isothermal), Eq. (2.59) yields:

$$t_R = \frac{t_M}{\mu} = (1+k)t_M \quad (\text{static analyses}) \quad (2.62)$$

2.7.3 Method translation and retention time locking

The proportionality of the peak retention times in isobaric temperature-programmed analyses to the void time measured at one set of static conditions indicates the scalability of the peak retention times and is the basis for *method translation* and *retention time locking* (RTL) concepts [2,15,65] and techniques [66–71].

The facts underlying the GC method translation can be summarized as follows [15]. Let $t_{M,A}$ and $t_{M,B}$ be the void times in isobaric temperature-programmed analyses A and B, possibly utilizing columns of different diameters and lengths as well as different carrier gases. Let also $t_{R,A}$ and $t_{R,B}$ be the retention times of peaks representing the same solute in A and B, respectively. Then $t_{R,A}$ and $t_{R,B}$ are proportional to $t_{M,A}$ and $t_{M,B}$, respectively, i.e., $t_{R,B}/t_{M,B} = t_{R,A}/t_{M,A}$ as long as:

- both columns have the same stationary phase type and relative film thickness (φ)
- the time domains of the temperature programs in A and B, possibly consisting of several temperature ramps and holds, are scaled in proportion to their void times, i.e., [2]:
 - both temperature programs have equal number of temperature ramps and holds
 - the corresponding hold temperatures are the same in temperature programs of both analyses while their hold times, $t_{\text{hold},A}$ and $t_{\text{hold},B}$, are proportional to respective void times: $t_{\text{hold},B}/t_{M,B} = t_{\text{hold},A}/t_{M,A}$

- the heating rates, $R_{T,A}$ and $R_{T,B}$, of the corresponding temperature ramps are inversely proportional to the respective void times: $R_{T,B} t_{M,B} = R_{T,A} t_{M,A}$

The RTL can be viewed as the method translation in reverse. While the latter is based on the timescaling of the temperature program in proportion to the void time, the former is based on adjusting the void time (t_M) to a given temperature program [15]. A typical application of the RTL can be to restore a required t_M changed due to changing a column from one to another of the same type (but possibly different dimensions) or due to trimming a column when it becomes necessary [67,71]. A typical way of restoring t_M is by adjusting pressure.

The theory of GC method translated and RTL is proven to *isobaric* temperature-programmed analyses [15] satisfying the earlier listed requirements. The theory also applies to nonisobaric analyses—combinations of arbitrary temperature and pressure programming, but only under extreme conditions of gas decompression—the decompression is either weak or strong [2]. The latter includes all GC-MS applications. The most practically important cases of simultaneous temperature and pressure programming are the *isorheic* [72] (*constant flow*) temperature-programmed analyses. A rigorous proof of the theory for isorheic analysis with intermediate gas decompression is unknown. On the other hand, it is not proven that the method translation and RTL *do not work* for isorheic analyses with moderate decompression. Both GC method development and RTL are widely used in the practice of development and maintenance of the methods for isobaric and isorheic analyses.

More complex method translation and RTL techniques applicable to combinations of arbitrary temperature and pressure programming are also known [70].

2.7.4 Linear heating ramp and linear retention model

Eq. (2.59) is valid for any retention model (μ could be any function of T) and for any temperature program, $T(t)$. However, under these broad conditions, Eq. (2.59) can be solved only numerically. Narrowing the scope to the *linear heating ramp* and linear retention model brings evaluation of Eq. (2.59) one step closer to the closed-form (analytical) solutions.

The linear heating ramp, $T(t)$, can be described as:

$$T = T(t) = T_{\text{init}} + R_T t \quad (2.63)$$

where T_{init} is the *initial temperature* of the ramp, and R_T is a fixed *heating rate* (in *isothermal analysis*, $R_T = 0$). The scope is further limited to linear and to ideal thermodynamic models of a solute retention. Due to Eqs. (2.4), (2.12), and (2.16), the solute mobility (μ) of the linear and ideal thermodynamic retention models can be expressed as:

$$\mu = \left(1 + \exp \frac{T_{\text{char}} - T}{\theta_{\text{char}}}\right)^{-1} \quad (2.64)$$

(linear retention model)

$$\mu = \left(1 + \exp \left(\frac{T_{\text{char}}}{\theta_{\text{char}}} \cdot \left(\frac{T_{\text{char}}}{T} - 1 \right) \right)\right)^{-1} \quad (2.65)$$

(ideal thermodynamic model)

The former is the basis for the closed-form solutions obtained further while the latter can be used for numerical verification of those solutions.

From Eqs. (2.64) and (2.21), the integrand (μ_{eff}) in Eq. (2.60) for the linear retention model can be expressed as

$$\mu_{\text{eff}}(T(t)) = \left(\frac{T_{\text{ref}}}{T(t)} \right)^{\xi} \left(1 + \exp \frac{T_{\text{char}} - T(t)}{\theta_{\text{char}}} \right)^{-1} \quad (2.66)$$

(isobaric analysis, linear retention model)

Eq. (2.59) becomes:

$$\int_0^{t_R} \left(\frac{T_{\text{ref}}}{T(t)} \right)^{\xi} \left(1 + \exp \frac{T_{\text{char}} - T(t)}{\theta_{\text{char}}} \right)^{-1} dt = t_{M,\text{ref}} \quad (2.67)$$

Unfortunately, a closed-form solution of this integral even with linear $T(t)$ is unknown. A suitable approximation of its integrand can be adopted due to the following considerations. A solute that is not significantly retained at the beginning of a heating ramp (its T_{char} is not significantly different from T_{init}) does not stay in a column for a long time so that the change in T during the solute migration is relatively small. On the other hand, if a solute is significantly retained at the beginning of the ramp, then it continues to stay near the column inlet until T gets closer to the solute characteristic temperature (T_{char}). Again, during the solute migration through the major portion of the column length, the change in T is relatively small. In both cases, a meaningful migration of a solute takes place when T is reasonably close to T_{char} [2]. On top of that, the factor $(T_{\text{ref}}/T)^{\xi}$ in Eq. (2.67) is a relatively weak function of T so that, during all or major portion of the solute migration, $(T_{\text{ref}}/T)^{\xi}$ remains close to $(T_{\text{ref}}/T_{\text{char}})^{\xi}$. After replacing in it $(T_{\text{ref}}/T)^{\xi}$ with $(T_{\text{ref}}/T_{\text{char}})^{\xi}$, Eq. (2.67) becomes:

$$\left(\frac{T_{\text{ref}}}{T_{\text{char}}} \right)^{\xi} \int_0^{t_R} \left(1 + \exp \frac{T_{\text{char}} - T(t)}{\theta_{\text{char}}} \right)^{-1} dt = t_{M,\text{ref}} \quad (2.68)$$

The integral in this expression has a closed-form solutions described shortly.

2.7.5 Dimensionless heating rate and void temperature increment

Expressing its heating rate (R_T) in dimensionless form simplifies and broadens the solutions of Eq. (2.68) for the linear heating ramp described in (2.63).

It follows from Eq. (2.68) that the significance of a change in a column temperature (T) depends on the relation of that change to the solute characteristic thermal constant (θ_{char}). This is true for linear, ideal, and more complex three-parameter thermodynamic models [31–34] of solute–column interaction of which the linear retention model is an approximation in vicinity of $T = T_{\text{char}}$. Additionally, as follows from Eq. (2.61), the rate (R_T) of the temperature change is meaningful only in relation to the void time rather than to the absolute time scale. These observations suggest that *dimensionless heating rate* (r_T) can be defined as [2]:

$$r_T = \frac{R_T t_{M,\text{char}}}{\theta_{\text{char}}} \quad (2.69)$$

where $t_{M,\text{char}}$ is void time statically measured at a solute characteristic temperature (T_{char}). To distinguish it from the dimensionless heating rate (r_T), quantity R_T can be called as the *absolute heating rate*.

Generally, r_T can be different for different solutes and, therefore, can be function of T . However, in isobaric analysis with linear heating ramp, this is essentially not the case. Indeed, during the isobaric linear heating ramp, both components of the ratio $t_{M,\text{char}}/\theta_{\text{char}}$ in Eq. (2.69) change in approximate proportion with $T^{0.7}$. For θ_{char} , this follows from the facts that $\theta_{\text{char}} \approx \theta_{\text{charG}}$ (Fig. 2.3) where, according to Eq. (2.18), $\theta_{\text{charG}} \sim T^{0.7}$. The proportionality $t_{M,\text{char}} \sim T^{0.7}$ follows from Eq. (2.49) where t_M at constant pressure is proportional to gas viscosity (η), which, according to Eq. (2.21), is proportional to T^ξ where $\xi \approx 0.7$ (Table 2.2). As a result, $t_{M,\text{char}}/\theta_{\text{char}}$ at a constant pressure is essentially independent of T , and, therefore, r_T at a fixed R_T is essentially independent of T . One can conclude that

In isobaric analyses with linear heating ramp, the dimensionless heating rate (r_T) is approximately the same for all solutes.

From Eqs. (2.49), (2.21), and (2.18), r_T for all solutes can be estimated as [2]:

$$r_T \approx \frac{R_T t_{M,\text{ref}}}{\theta_{\text{charG,ref}}} \quad (2.70)$$

where $\theta_{\text{charG,ref}}$ is θ_{char} of generic solute having $T_{\text{char}} = T_{\text{ref}}$, i.e., according to Eq. (2.18),

$$\theta_{\text{charG,ref}} = \theta_{\text{char,st}} \left(\frac{T_{\text{ref}}}{T_{\text{st}}} \right)^{0.7} \quad (2.71)$$

Example 2.3. If $\theta_{\text{char,st}} = 22^\circ\text{C}$, $R_T = 10^\circ\text{C}/\text{min}$, $T_{\text{ref}} = 423.15\text{K}$ (150°C), and $t_{M,\text{ref}} = 1\text{ min}$, then, $\theta_{\text{charG,ref}} \approx 22^\circ\text{C} \times (273.15/423.15)^{0.7} \approx 30^\circ\text{C}$, and $r_T \approx 0.33$ for any generic solute.

Any temperature can be chosen as T_{ref} . However, for consistency of all forthcoming numerical examples and recommendations, it is desirable to base them on the same T_{ref} . In this chapter, $T_{\text{ref}} = 423.15\text{K}$ (150°C)—a round number approximately in the middle of GC temperature range—is used in all numerical evaluations.

Combining Eqs. (2.63) and (2.70), one can express retention time of a peak eluting at temperature T_R as:

$$t_R = \frac{\Delta T_R t_{M,\text{ref}}}{\theta_{\text{charG,ref}} r_T}, \quad \Delta T_R = T_R - T_{\text{init}} \quad (2.72)$$

In addition to the dimensionless heating rate, also useful is the *void temperature increment* (*dead temperature* [14], *void temperature* [15], *hold-up temperature* [2]), ΔT_M —the temperature change during the time interval equal to the void time (t_M):

$$\Delta T_M = R_T t_M \quad (2.73)$$

As shown later, the optimal ΔT_M is close to 10°C for all GC analyses [16,73].

To emphasize the fact that ΔT_M and t_M in Eq. (2.73) are measured at the same reference temperature (T_{ref}), the former can be expressed as:

$$\Delta T_{M,\text{ref}} = R_T t_{M,\text{ref}} \quad (2.74)$$

If $\Delta T_{M,\text{ref}}$ for some $t_{M,\text{ref}}$ is known, then R_T and r_T could be found from Eqs. (2.74) and (2.69) as:

$$R_T = \frac{\Delta T_{M,\text{ref}}}{t_{M,\text{ref}}} \quad (2.75)$$

$$r_T = \frac{t_{M,\text{char}}}{\theta_{\text{char}}} \cdot \frac{\Delta T_{M,\text{ref}}}{t_{M,\text{ref}}} \quad (2.76)$$

Eq. (2.75) suggests that the same heating rate can be expressed in the absolute form of the temperature change per time unit and in the *normalized* form as $\Delta T_M/t_M$.

Example 2.4. If $t_M = 0.5$ min and $R_T = 15^\circ\text{C}/\text{min}$, then $\Delta T_M = 15^\circ\text{C}/\text{min} \times 0.5$ min = 7.5°C , and R_T can be also expressed in the normalized form as $R_T = 7.5^\circ\text{C}/t_M$.

Eqs. (2.70) and (2.74) yield:

$$r_T \approx \frac{\Delta T_{M,\text{ref}}}{\theta_{\text{charG,ref}}} \quad (2.77)$$

which, together with Eq. (2.18), allows one to find ΔT_M as:

$$\Delta T_{M,\text{ref}} = r_T \theta_{\text{char,st}} \left(\frac{T_{\text{ref}}}{T_{\text{st}}} \right)^{0.7} \quad (2.78)$$

2.7.6 Migration and elution parameters

Eq. (2.68) can be used for finding retention times (t_R) of a particular solute under particular operational conditions in a column with particular stationary phase and its relative thickness. To find t_R , one needs to know column dimensions, carrier gas type, flow rate, etc. This might be unnecessary if, for the solutes eluting during a linear heating ramp, their *elution temperatures* (T_R) rather than retention times (t_R) are considered, i.e., if the *time domain* (t -domain)

representation of peaks is replaced with their *temperature domain* (T -domain) representation. This representation can be used only for the peaks eluting during the heating ramps. The T -domain representation typically yields simpler, more general, and more insightful solutions [2], and is the dominant representation in this chapter.

Let k_{init} , μ_{init} , and ω_{init} be *initial retention factor*, *initial mobility*, and *initial immobility* of a solute, i.e., the solute parameters in Eq. (2.3) at the beginning of a heating ramp. A solute is *highly interactive* (with the column) if $k_{\text{init}} \gg 1$, or equivalently, $\mu_{\text{init}} \ll 1$, or $\omega_{\text{init}} \approx 1$. Following are some solutions of Eq. (2.68) [2]. They are the simplest when expressed via the solute immobility (ω):

$$\omega = \omega(\zeta) = \omega_{\text{init}} \omega_a(\zeta) \quad (2.79)$$

where $\zeta = z/L$ is the solute dimensionless distance, Eq. (2.31), from the column inlet, and

$$\omega_a = \omega_a(\zeta) = e^{-r_T \zeta} \quad (2.80)$$

is the solute *asymptotic migration immobility*—the immobility that the solute would have if it was highly interactive ($\omega_{\text{init}} \approx 1$). At $\zeta = 1$, a solute migration immobility becomes its *elution immobility* (ω_R). Eqs. (2.79) and (2.80) become:

$$\omega_R = \omega_{\text{init}} \omega_{R,a}, \quad \omega_{R,a} = \omega_a(1) = e^{-r_T} \quad (2.81)$$

where $\omega_{R,a}$ (Fig. 2.7) is the solute *asymptotic elution immobility*—the elution immobility it would have if it was highly interactive.

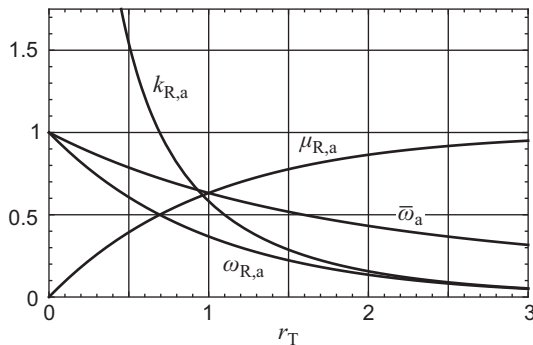


FIGURE 2.7 Asymptotic elution parameters in Eqs. (2.81)–(2.83) and (2.87).

Combining Eq. (2.79) with Eqs. (2.4) and (2.12), one can find other migration parameters of the solute, such as $k(\zeta)$, $\mu(\zeta)$, and $T(\zeta)$ corresponding to the time when the solute is located at $z = \zeta L$ [2]. At $\zeta = 1$, the solute migration parameters become its elution parameters. The asymptotic elution immobility ($\omega_{R,a}$) of a highly interactive solute is described in Eq. (2.81). Other asymptotic elution parameters of this solute can be found from Eqs. (2.4), (2.12), and (2.81) as [2] (Figs. 2.7 and 2.8):

$$\mu_{R,a} = 1 - e^{-r_T} \quad (2.82)$$

$$k_{R,a} = 1/(e^{r_T} - 1) \quad (2.83)$$

$$T_{R,a} = T_{\text{char}} + \theta_{\text{char}} \ln(e^{r_T} - 1) \quad (2.84)$$

For small and large r_T values, these parameters can be approximated as:

$$\mu_{R,a} \approx \begin{cases} r_T, & r_T < 0.3 \\ 1, & r_T > 3 \end{cases}, \quad (2.85)$$

$$k_{R,a} \approx \begin{cases} 1/r_T, & r_T < 0.3 \\ 0, & r_T > 3 \end{cases}, \quad (2.85)$$

$$T_{R,a} \approx T_{\text{char}} + \theta_{\text{char}} \cdot \begin{cases} \ln r_T, & r_T < 0.3 \\ r_T, & r_T > 3 \end{cases}$$

At $r_T = \ln 2 \approx 0.7$, Eqs. (2.83) and (2.84) yield $k_{R,a} = 1$ and $T_{R,a} = T_{\text{char}}$ indicating that each

highly interactive generic solute elutes at the column temperature equal to the solute characteristic temperature, and it elutes with retention factor of 1. The optimal r_T ($r_{T,\text{Opt}}$), close to 0.4 (see further), is lower than 0.7 indicating that, at $r_T = r_{T,\text{Opt}}$, the solute elution temperatures are lower than their T_{char} by about $0.7\theta_{\text{char}}$, which for the reference generic solutes ($T_{\text{char}} = 150^\circ\text{C}$, $\theta_{\text{charG,ref}} = 30^\circ\text{C}$) means $T_{R,a} \approx T_{\text{char}} - 21^\circ\text{C}$.

Also important for column performance evaluations is the distance-averaged immobility of a solute:

$$\bar{\omega} = \int_0^1 \omega(\zeta) d\zeta \quad (2.86)$$

which, from Eqs. (2.79), (2.80), and (2.82), can be found as [2] (Fig. 2.7):

$$\bar{\omega} = \omega_{\text{init}} \int_0^1 e^{-r_T \zeta} d\zeta = \omega_{\text{init}} \bar{\omega}_a,$$

$$\bar{\omega}_a = \frac{1 - e^{-r_T}}{r_T} = \frac{\mu_{R,a}}{r_T} \quad (2.87)$$

The errors in theoretical values of $T_{R,a}$ and $\mu_{R,a}$ relative to their counterparts found from computer simulations based on ideal thermodynamic model are shown in Fig. 2.9. When

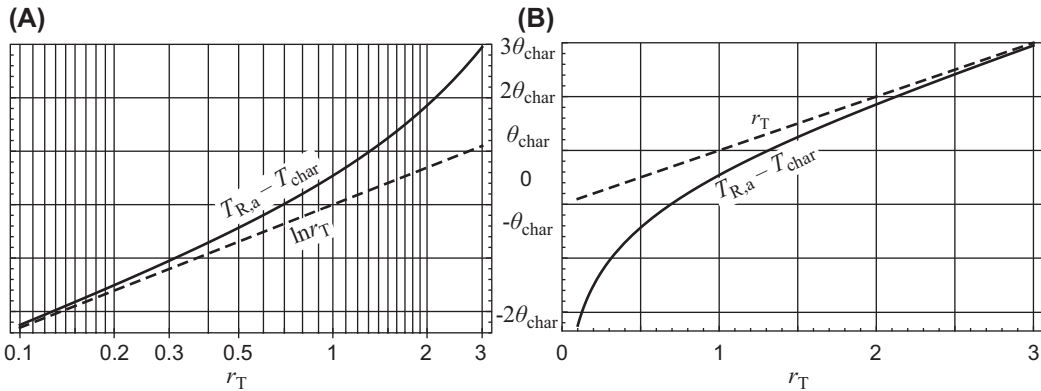


FIGURE 2.8 Departure ($T_{R,a} - T_{\text{char}}$, solid lines) of a solute elution temperature ($T_{R,a}$) from its characteristic temperature (T_{char}) versus dimensionless heating rate (r_T) in logarithmic (A) and linear (B) scale. The dashed lines are the tangents to the solid lines at $r_T \rightarrow 0$ in the logarithmic, and at $r_T \rightarrow \infty$ in the linear scales for r_T .

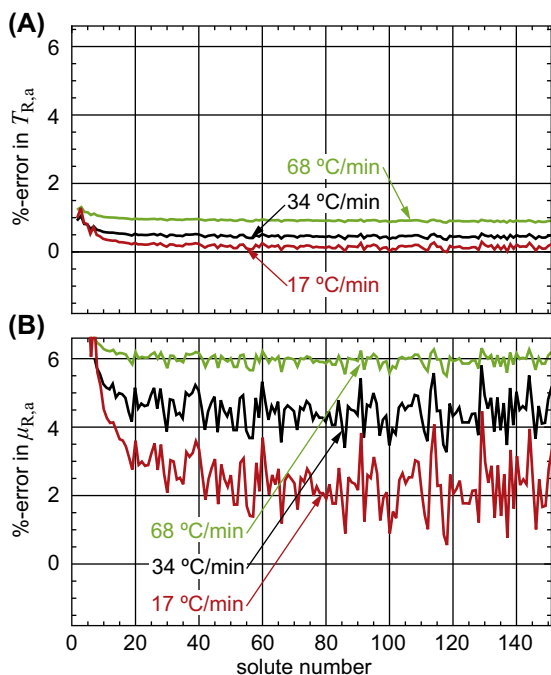


FIGURE 2.9 Relative errors in theoretical values of (A) $T_{R,a}$ and (B) $\mu_{R,a}$, Eqs. (2.84) and (2.82), compared to their counterparts T_R and μ_R found from computer simulations base on ideal thermodynamic model in Eqs. (2.11) and (2.16). Solutes and stationary phase: 147 pesticides in a column with 1701-type (14% cyanopropylphenyl-methyl polysiloxane) stationary-phase polymer. Column: 10 m \times 0.1 mm \times 0.1 μ m. Initial and reference temperatures: $T_{init} = 25^\circ\text{C}$, $T_{ref} = 150^\circ\text{C}$. Gas: helium isobaric at $p_o = 1$ atm and the flow of 0.8 mL/min at T_{ref} ($t_{M,init} = 0.279$ min, $t_{M,ref} = 0.354$ min). Temperature program: $T = T_{init} + R_T t$ with R_T shown in the graphs. The normalized equivalent of heating rate $R_T = 34^\circ\text{C}/\text{min}$ is $12^\circ\text{C}/t_{M,ref}$. Characteristic parameters of the pesticides were obtained as described elsewhere [2].

evaluating the significance of the errors in theoretical retention parameters in this chapter, it should be recognized that the parameters are not intended for prediction of chromatograms, but for evaluations of column performance and its optimizations. Thus, if solute elution temperatures ($T_{R,a}$) transformed into retention times were treated as theoretically predicted retention times in a chromatogram, then, say, 1%

inaccuracy in Fig. 2.9A might be unacceptable. In this chapter, however, it is only important that the analysis time is proportional to $T_{R,a}$. In that case, larger than 1% inaccuracy is acceptable. Similarly, $\mu_{R,a}$ is used further for theoretical predictions of peak widths, which, in practical evaluations, are typically measured with larger than 10% inaccuracy.

2.8 Peak spacing and reversal of elution order

Peak *spacing* is the distance between two peaks [74,75]. It can be expressed as the *temporal spacing*, i.e., the difference (Δt_R) in the peak retention times (t_R), or as the *thermal spacing*, i.e., the difference (ΔT_R) in the peak elution temperatures (T_R).

As follows from Eq. (2.84), ΔT_R of highly interactive solutes depends on the differences (ΔT_{char} and $\Delta \theta_{char}$) in their characteristic temperatures and characteristic thermal constants, respectively. The former can be as large as hundreds of $^\circ\text{C}$ while the latter seldom exceeds 10°C . As a result, ΔT_{char} dominates the peak spacing so that the solutes generally elute in the order of increased T_{char} —solute with larger T_{char} generally elute later than those with lower T_{char} . This might not be the case for closely spaced solutes for which ΔT_{char} is comparable with $\Delta \theta_{char}$. The elution order of such solutes depends on ΔT_{char} and $\Delta \theta_{char}$, and it also depends, Eq. (2.84), on dimensionless heating rate (rT). As a result, a change in the heating rate might reverse the elution order of two solutes and the time order of the corresponding peaks.

The thermal spacing, $\Delta T_R = T_{R,B} - T_{R,A}$, of solutes A and B can be estimated as [2]:

$$\begin{aligned}\Delta T_R &\approx \Delta T_{char} + X_\theta \Delta \theta_{char}, \\ \Delta T_{char} &= T_{char,B} - T_{char,A}, \\ \Delta \theta_{char} &= \theta_{char,B} - \theta_{char,A}\end{aligned}\quad (2.88)$$

where quantity

$$X_\theta = \frac{r_T}{1 - e^{-r_T}} + \ln(1 - e^{-r_T}) \quad (2.89)$$

is the *sensitivity* of the thermal spacing of two solutes to the difference ($\Delta\theta_{\text{char}}$) in their characteristic thermal constants. The sensitivity is a function of r_T . It has negative value and the magnitude getting monotonically smaller with increasing r_T , Fig. 2.10. As a result, X_θ has the following properties.

1. The slower is the heating, the larger is the effect of the difference $\Delta\theta_{\text{char}}$ on the peak thermal spacing (ΔT_R). Conversely, the faster is the heating, the less sensitive is the ΔT_R to $\Delta\theta_{\text{char}}$.
2. When quantities ΔT_{char} and $\Delta\theta_{\text{char}}$ for a given solute pair have different signs, the heating rate does not affect the sign of their thermal spacing (ΔT_R), and therefore, the heating rate does not affect the solute elution order.
3. Conversely, when quantities ΔT_{char} and $\Delta\theta_{\text{char}}$ for a given solute pair have (a) the same signs and (b) comparable magnitudes, a change in a heating rate can change the sign of ΔT_R and, therefore, *reverse* the solute elution order.

Example 2.5. Typically, the largest value of the difference $\Delta\theta_{\text{char}}$ for two solutes having close

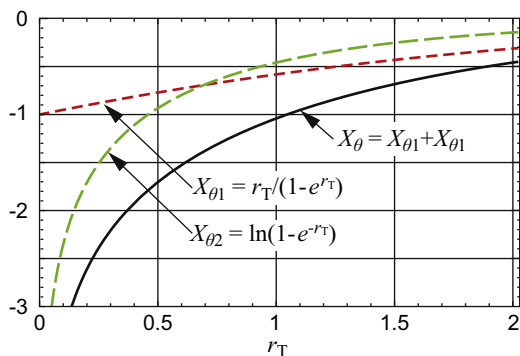


FIGURE 2.10 Sensitivity (X_θ), Eq. (2.89), of thermal spacing of two peaks to the difference ($\Delta\theta_{\text{char}}$) in characteristic thermal constants of corresponding solutes.

T_{char} values does not exceed 30% of generic θ_{char} (θ_{charG}) for that T_{char} (Fig. 2.3). For $T_{\text{char}} = 423.15\text{K}$ (150°C), $\theta_{\text{charG}} \approx 30^\circ\text{C}$ and $|\Delta\theta_{\text{char}}| < 9^\circ\text{C}$. For $r_T = 0.35$ (near optimal heating rate, see further), Eq. (2.89) yields: $X_\theta = -2.1$. Therefore, $|X_\theta \Delta\theta_{\text{char}}| < 20^\circ\text{C}$. If ΔT_{char} and $\Delta\theta_{\text{char}}$ for two solutes have the same sign, then changing the heating rate can change the solute elution order. The elution order change is unlikely if $|\Delta T_{\text{char}}| > 20^\circ\text{C}$.

Since changing the heating rate can change the order of two closely spaced peaks, it might be also useful to know the *sensitivity* of the peak spacing to the change in the heating rate. That sensitivity (X_r) can be defined as the change in ΔT_R per unit of relative change (dr_T/r_T) in r_T , i.e., [2]:

$$X_r = \frac{d(\Delta T_R)}{dr_T/r_T} \quad (2.90)$$

Eqs. (2.88) and (2.89) yield (Fig. 2.11) [2]:

$$X_r = \frac{d(\Delta T_R)}{dr_T/r_T} = \frac{r_T^2 e^{r_T}}{(e^{r_T} - 1)^2} \Delta\theta_{\text{char}} \quad (2.91)$$

Eq. (2.91) can be also expressed as

$$d(\Delta T_R) = X_r \frac{dr_T}{r_T} = \frac{r_T^2 e^{r_T} \Delta\theta_{\text{char}}}{(e^{r_T} - 1)^2} \frac{dr_T}{r_T} \quad (2.92)$$

Fig. 2.11 shows that, in the most practically important region of moderate heating rates, $X_r \approx \Delta\theta_{\text{char}}$. As a result,

$$d(\Delta T_R) \approx \Delta\theta_{\text{char}} \frac{dr_T}{r_T}, \quad r_T \leq 0.75 \quad (2.93)$$

Example 2.6. Let $\Delta\theta_{\text{char}} = 10^\circ\text{C}$, $r_T = 0.35$, $dr_T/r_T = 0.1 = 10\%$. The former represents more or less worst-case scenario of nearly the largest possible value of $\Delta\theta_{\text{char}}$ (Example 2.5). Eq. (2.93) yields: $d(\Delta T_R) = 1^\circ\text{C}$. This means that a 10% change in dimensionless heating rate can change thermal spacing of two peaks by up to 1°C . How significant is this change? Let σ and σ_T be the standard deviations of a peak in time and

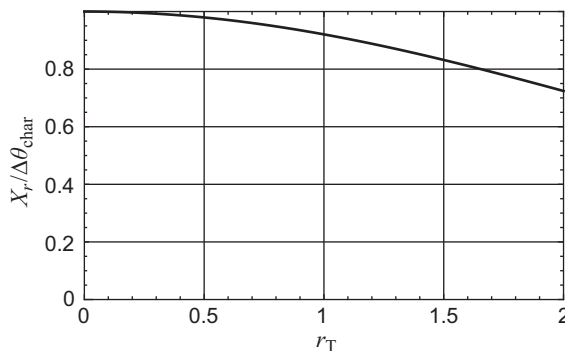


FIGURE 2.11 Normalized sensitivity ($X_r/\Delta\theta_{\text{char}}$, Eq. (2.91), of thermal spacing (ΔT_R) of two solutes to relative change (dr_T/r_T) in dimensionless heating rate.

temperature domain, respectively. They relate as $\sigma_T = R_T\sigma$. Under optimal conditions in a column with plate number N , σ_T can be estimated as [2] $\sigma_T = 40^\circ\text{C}/Q$ where $Q = \sqrt{N}$, which can be estimated as $Q = \sqrt{L/d}$. For a conventional $25\text{ m} \times 0.25\text{ mm}$ column, $Q \approx 320$ and $\sigma_T \approx 0.125^\circ\text{C}$. The latter indicates that the magnitude (1°C) of the change in the peak spacing is eight times larger than σ_T , i.e., an identifiable reversal of the peak order. Thus, the order of two peaks separated by $4\sigma_T$ could change without changing the magnitude of their spacing.

Eq. (2.93) can be used not only for the evaluation of a possibility of reversal of the peak order, but also for evaluation of requirements for the accuracy of method parameters of a GC analysis. According to Eq. (2.69), r_T in a given column is proportional to R_T . Therefore, a relative change (dr_T/r_T) in r_T in a given column with a given gas flow is equal to relative change (dR_T/R_T) in R_T . However, a change in R_T is not the only cause of a change in r_T . Eq. (2.69) also shows that r_T is proportional to the void time (t_M), which, due to Eq. (2.50), is inversely proportional to pressure drop along a column and, when column pressure and temperature are fixed, t_M is proportional to $(L/d)^2$. This implies that a column replacement, trimming the column end, etc., can also change r_T . The relative change in r_T due to changing L/d is two times larger than relative change in L/d . This suggests that, to

reduce the possibility of the reversal of the peak order, a combined effect of the relative error in the heating rate, the relative error in pressure drop, and twice the relative error in the ratio L/d should be tightly controlled.

Example 2.7. Suppose that, to prevent a measurable reversal of a peak order, a possible change in ΔT_R should not exceed σ_T . According to Example 2.6, this can be achieved when

$$\frac{dr_T}{r_T} < \frac{40^\circ\text{C}}{\Delta\theta_{\text{char}}\sqrt{N}} \approx \frac{4}{\sqrt{N}} \quad (\text{for } d(\Delta T_R) < \sigma_T) \quad (2.94)$$

For a conventional $25\text{ m} \times 0.25\text{ mm}$ column, $\sqrt{N} \approx 320$. Therefore, the change in r_T should not exceed 1.25%. For more efficient columns, the acceptable change in r_T should be even smaller in inverse proportion to \sqrt{N} .

The last example suggests that the combined effect of the relative errors in all factors affecting r_T should not exceed 1% or be even smaller especially in the analyses using high-efficiency columns. The errors in the column dimensions including the ones caused by a column trimming can be much larger than that [76]. Fortunately, the problem has a simple solution. What's important in the final count is not each error, but their combined effect on r_T , i.e., according to Eq. (2.69), on the product $R_T t_M$. This indicates that adjusting t_M by adjusting the column pressure, i.e., the earlier described RTL [15] can compensate

for the effect of the changes in column dimensions and operational conditions on r_T .

This discussion can also serve as an illustration of advantages of evaluating the properties of temperature-programmed analysis in the T -domain. The definitive results were obtained without specifying column dimensions, carrier gas type, its flow rate, etc., that might be necessary if retention times rather than elution temperatures were considered.

2.9 Peak width

There are many *peak width* metrics in chromatography. *Standard deviation* (σ) of a peak [2–7,10,17,20], *half-height width* (w_h), *base width* (w_b) [3,6,20], *area-over-height width* (w_A) [2,77], 2σ -width [6], 4σ -width [5], 6σ -width [78], and 8σ -width [79] are some of them. Quantity w_h is typically easy to measure by “a ruler and a pencil.” Metric $w_A = (\text{peak area})/(\text{peak height})$ is typically reported by commercial data analysis devices (integrators). If a peak shape is not *a priori* known, then only σ can be theoretically predicted from parameters of a chromatographic analysis. As a result, the choice for this study was between the metric of σ and its multiples. Each multiple has its own justification. Typical justifications are based on the assumption of *Gaussian peaks* [2,5,6]. Thus, starting from van Deemter et al. [80], the choice of the 4σ -width metric is typically justified by the fact that, for Gaussian peaks, $w_b = 4\sigma$. However, for non-Gaussian peaks, the relationship between w_b and σ might be different [2]. For *exponential peaks*, e.g., $w_b = \sigma$ [2]. In this chapter, **σ is the only peak width metric**, unless otherwise is explicitly

stated, and the terms *peak width* and *peak standard deviation* are treated as synonyms.

A way to theoretically predict the peak widths in chromatograms is through the study of evolution of the widths of the *solute zones* during their migration in the column. These widths (the standard deviations, $\tilde{\sigma}$, of the zones) are measured in units of distance along a column.

2.9.1 Plate height in uniform static chromatography

For the most part, the material of this section is suitable not only for GC but also for other separation techniques operating under uniform static conditions.

The width (σ) of a peak produced by elution of a solute zone can be found as³:

$$\sigma = \frac{\tilde{\sigma}_0}{v_0} \quad (2.95)$$

where v_0 and $\tilde{\sigma}_0$ are, respectively, the solute zone velocity and width (standard deviation) at the column outlet. In a column operating under uniform static conditions and *ideal* or nearly ideal (sharp) sample introduction, the *variance* ($\tilde{\sigma}^2$) of a solute zone can be found from one of the following two expressions known from Golay [81]:

$$\tilde{\sigma}^2 = \mathcal{H}z, \quad \tilde{\sigma}^2 = \mathcal{D}t \quad (\text{uniform static conditions}) \quad (2.96)$$

where z is the distance from the inlet and t is the solute migration time to z . At the column outlet, these equations become:

$$\tilde{\sigma}_0^2 = \mathcal{H}L \quad (\text{uniform static conditions}) \quad (2.97)$$

$$\tilde{\sigma}_0^2 = \mathcal{D}t_R \quad (\text{uniform static conditions}) \quad (2.98)$$

³ Subject to clarification in the footnote to Eq. (2.110).

where [81,82]:

$$\mathcal{H} = \frac{2(D + kD_S)}{u} + \frac{\vartheta^2 d^2 u}{96D} + \frac{2\vartheta_S^2 d^2 \varphi^2 (1 + \varphi)^2 u}{3D_S} \quad (2.99)$$

$$\mathcal{D} = \mathcal{H}v = \mathcal{H}\mu u \quad (2.100)$$

$$\begin{aligned} \vartheta &= \frac{\sqrt{1 + 6k + 11k^2}}{1 + k} = \sqrt{11 - 16\mu + 6\mu^2} \\ &= \sqrt{1 + 4\omega + 6\omega^2} \end{aligned} \quad (2.101)$$

$$\begin{aligned} \vartheta_S &= \frac{\sqrt{k}}{1 + k} = \sqrt{(1 - \mu)\mu} = \sqrt{(1 - \omega)\omega} \\ &= \sqrt{\mu\omega} \end{aligned} \quad (2.102)$$

and D_S is a solute diffusivity in stationary phase. In overwhelming majority of GC analyses, WCOT columns are used. In these columns, $\varphi \ll 1$ and D_S is typically so small compared to D [83] that for all practically significant retention factors $kD_S \ll D$. Eq. (2.99) can be simplified as:

$$\mathcal{H} = \frac{2D}{u} + \frac{\vartheta^2 d^2 u}{96D} + \frac{2\vartheta_S^2 d^2 u}{3D_S} \quad (\text{WCOT columns}) \quad (2.103)$$

Quantities \mathcal{H} and \mathcal{D} are the solute *spatial* and *temporal dispersion rates*. The former is the rate of increasing $\tilde{\sigma}^2$ per unit of distance traveled by the solute along the column, while latter is the rate of increasing $\tilde{\sigma}^2$ per unit of the solute migration time. The half-value ($D_{\text{eff}} = \mathcal{D}/2$) of \mathcal{D} is known in chromatography as *effective diffusion coefficient* [5], *dynamic diffusion constant* [84], *dispersion coefficient* [85], *effective diffusivity* [86,87], and under other names. Both D_{eff} and \mathcal{D} are measured in units of $\text{length}^2/\text{time}$ (e.g., cm^2/s). While D_{eff} is better known in chromatography than \mathcal{D} is, the analogy of the latter with \mathcal{H} is more transparent. Quantity \mathcal{D} is also in line with treatment of dispersion in general math [88].

The rate (\mathcal{H}) of increase in $\tilde{\sigma}^2$ per unit of a solute displacement along a column is known

as a column *plate height* that can be measured in units of $\text{length}^2/\text{length}$ [2] (such as mm^2/m —an increase in $\tilde{\sigma}^2$ in millimeters-squared per 1 m of a solute migration along the column). However, as a matter of practical convenience, the units of $\text{length}^2/\text{length}$ are typically reduced to the units of length, and \mathcal{H} is typically expressed in units of length (e.g., mm). This, however, does not change the fact that \mathcal{H} is the rate of the dispersive increase in the spatial variance ($\tilde{\sigma}^2$) of a solute zone per distance unit of its migration. Golay was notorious in equal parallel theoretical treatment of parameters \mathcal{H} and \mathcal{D} . The goal seems to stress the conceptual similarity of a mysterious (in his time and even now) parameter \mathcal{H} with more familiar concept of diffusion coefficient as the rate of broadening of a solute zone. Additional discussion of this topic can be found elsewhere [2].

Although Eqs. (2.97) and (2.98) have similar structure, and parameters \mathcal{H} and \mathcal{D} represent similar concepts, some difference in components of Eqs. (2.97) and (2.98) as well as in parameters \mathcal{H} and \mathcal{D} speaks decisively in favor of greater utility in chromatography of parameter \mathcal{H} over parameter \mathcal{D} .

First, the column length (L) is typically a *priori* known parameter. Therefore, in order to find $\tilde{\sigma}_0$ from Eq. (2.97), one needs to find only one unknown solute-dependent parameter (\mathcal{H}), while, in order to find the same $\tilde{\sigma}_0$ from Eq. (2.98), one needs to find two unknown solute-dependent parameters (\mathcal{D} and t_R).

Furthermore, \mathcal{H} as a function, Eqs. (2.99) and (2.103), of gas velocity (u) has chromatographically important minimum:

$$\mathcal{H}_{\min} = \sqrt{\frac{(1 + 6k + 11k^2)d^2}{12(1 + k)^2} + \frac{16Dd_f^2 k}{3(1 + k)^2 D_S}} \quad (2.104)$$

that is typically affected only by one solute parameter—its retention factor (k). The values of \mathcal{H}_{\min} are confined within relatively narrow

range for all values of k . As a result, \mathcal{H}_{\min} can be (and typically is) treated as a *column parameter* (a *column plate height*) rather than a solute parameter. This is not the case for \mathcal{S} , which, according to Eq. (2.100), can be zero when $\mu \rightarrow 0$ so that the relative range of its variation has no limit. These are the main reasons why the plate height is known as one of the key parameters of a column performance, while \mathcal{S} (or D_{eff}) is seldom considered in chromatography.

The name *plate height* for the spatial dispersion rate (\mathcal{H}) came from the earlier known concept of H.E.T.P. (“height of equivalent theoretical plate”) introduced by Peters in 1922 [89] as a way of comparing packed distillation towers (columns) with the ones assembled from discrete plates (trays). In 1941, Martin and Singe adopted the concept of H.E.T.P. (“height equivalent to one theoretical plate”) for chromatographic columns [25]. It was initially thought that H.E.T.P. represented a *separation stage* and that the stage-to-stage transition was the sole reason for the broadening of the solute zones. Inconsistency of this perception became obvious when van Deemter et al. published their celebrated 1956 paper [80] where it was found that H.E.T.P. in a packed column was rooted in the solute diffusivity. In 1957, a scientific committee of 10 leading experts in the field including Martin and Golay agreed that “a theoretical plate is an abstract term with no physical significance other than as a measure of the relative variance of a peak” [90]. A few years later, Giddings suggested that the “current trend is to abandon the postulates that gave birth to the concept of HETP and speak of it as a general parameter for the measuring zone spreading” (Giddings and Kelly [91], page 96). “Despite the absence of the theoretical plate model ..., [parameter \mathcal{H}] retains the name *plate height* for historical continuity” (Giddings [5], page 97). Additional details regarding the history of the *plate height* concept can be found elsewhere [2].

2.9.2 Peak width in nonuniform dynamic chromatography

As a result of the carrier gas decompression along the column, the gas velocity increases in the direction from the column inlet to the outlet. The conditions of solute migration become coordinate dependent, i.e., nonuniform. Temperature and/or pressure programming adds to that the dynamic conditions of time-dependent change in the solute velocity. As a result, Eq. (2.97) can no longer be used for finding the variances ($\tilde{\sigma}_0^2$) of the eluting solute zones, which are necessary for finding the widths (σ) of the peaks in chromatograms. A more general approach taking into account nonuniform dynamic conditions becomes necessary.

If a medium of a solute migration is uniform and static, the plate height (\mathcal{H}) for a given solute migrating in the medium is uniform and static—it does not change with distance along the column or with time. Eq. (2.97) can be viewed as the definition of \mathcal{H} , i.e., \mathcal{H} can be defined as:

$$\mathcal{H} = \tilde{\sigma}_0^2/L \quad (\text{uniform static conditions}) \quad (2.105)$$

Otherwise, \mathcal{H} can be a *local* quantity changing with distance and/or time and Eq. (2.97) cannot be used for finding $\tilde{\sigma}_0$. The distance-dependent changes in nonuniform medium could be *abrupt* (as in a narrow region around connection of two columns having different diameters, different stationary phases, etc.) or *gradual* (as in the case of a solute velocity change due to the gas decompression). A medium of a solute migration is *smooth* if the local plate height (\mathcal{H}) and velocity gradient ($\partial v/\partial z$) do not significantly change within the solute zone. For example, nonuniformity caused by the gas decompression along a GC column is smooth [2]. The variances ($\tilde{\sigma}^2$) of a solute zone migrating in smooth medium

can be found from the following ordinary differential equation [2,86,87]:

$$\frac{d\tilde{\sigma}^2}{dz} = \mathcal{H} + \frac{2\tilde{\sigma}^2}{v} \cdot \left. \frac{\partial v(z,t)}{\partial z} \right|_{t=t(z)}, \quad (2.106)$$

(smooth medium)

where $\tilde{\sigma}^2 = \tilde{\sigma}^2(z)$, $\mathcal{H} = \mathcal{H}(z, t(z))$, $v = v(z, t(z))$, and $t(z)$ is the time required for the center of mass (z) of the zone to arrive to location z . The gradient, $\partial v / \partial z$, of the solute velocity is considered to be a known function of independent variables z and t . For example, if nonuniformity is caused only by the gas decompression along the column and the column pressure is fixed, then $\partial v / \partial z = (du/dz)\mu$ where du/dz can be found from differentiation of u in Eq. (2.35) with ζ defined in Eq. (2.31). The local plate height in Eq. (2.106) is defined as [2,86,87]:

$$\mathcal{H} = \lim_{\tilde{\sigma} \rightarrow 0} \frac{d\tilde{\sigma}^2}{dz} \quad (2.107)$$

The definition is based on the following considerations. Due to its decompression, the gas velocity increases in the direction from inlet to outlet. As a result, the front of a solute zone in the column travels faster than its tail causing the zone expansion in addition to its dispersive expansion. As the decompression-related zone expansion is accompanied by the zone acceleration, the net outcome is that a broader zone elutes faster and does not cause broadening of the peak in chromatogram. This suggests that, from the point of view of the broadening of peaks in chromatograms and their resolution, the decompression-related zone expansion is almost nonconsequential [2,86,87]. Therefore, it is necessary to identify only the dispersive component of the zone broadening—the one that causes the peak broadening in chromatograms. The derivative $(d\tilde{\sigma}^2/dz)$ in Eq. (2.107) is the dispersion rate, which, in uniform

medium, is the same as the plate height (\mathcal{H}) in Eq. (2.96). As the decompression cannot expand a zero-wide zone, the limit in Eq. (2.107) excludes the decompression-related zone expansion from affecting the local plate height (\mathcal{H}) in Eq. (2.107). So defined \mathcal{H} can be found from Eqs. (2.99) or (2.103) where some or all parameters can be local quantities that can depend on distance and/or on time.

Eq. (2.107) excludes the effects of all nondispersive factors of the zone broadening. It has been developed for chromatography in general [86,87] and is valid beyond GC [92].

More general alternatives of Eq. (2.106) are known [2,87,93–95]. However, only the **smooth medium** is considered in this chapter and only Eq. (2.106) and its transformations are considered further. It is more general than all previously considered models on the zone broadening in a nonuniform dynamic medium [85,96]. Thus, as shown further, the well-known *Giddings compressibility factor* [96] follows [86] from Eq. (2.106).

Only the **uniform heating** of the columns is considered in this chapter from now on, unless contrary is explicitly stated. As a result, the solute mobility (μ) is uniform. Eq. (2.2) yields $\partial v / \partial z = (\partial u / \partial z)\mu$ simplifying Eq. (2.106) as:

$$\frac{d\tilde{\sigma}^2}{dz} = \mathcal{H} + \frac{2\tilde{\sigma}^2}{u} \cdot \left. \frac{\partial u(z,t)}{\partial z} \right|_{t=t(z)} \quad (\text{uniform } \mu) \quad (2.108)$$

When gas decompression along a column is weak and can be ignored (relatively short and wide columns operating at atmospheric outlet), Eq. (2.108) converges to the form used by Golay [81]:

$$\frac{d\tilde{\sigma}^2}{dz} = \mathcal{H} \quad (\text{uniform medium}) \quad (2.109)$$

Finally, when conditions are also static (no temperature and pressure programming), and the sample introduction is ideal ($\tilde{\sigma}^2(0) = 0$),

Eq. (2.109) can be expressed in the form of Eq. (2.105).

In addition to spatial standard deviation ($\tilde{\sigma}$), the solute zone can be described by its *temporal width* (σ_z)—a temporal equivalent of $\tilde{\sigma}$. Extending Eq. (2.95) for the peak width (σ) in a chromatogram to the column interior, σ_z can be defined [2,86,95] as the time⁴:

$$\sigma_z = \sigma_z(z) = \frac{\tilde{\sigma}(z)}{v(z, t(z))} \quad (2.110)$$

required for $\tilde{\sigma}$ -wide zone located at z and migrating with velocity v to travel the distance $\tilde{\sigma}$. Comparing Eqs. (2.95) and (2.110), one can conclude that:

$$\sigma = \sigma_z(L) \quad (2.111)$$

the width (σ) of a peak in a chromatogram is the temporal width (σ_z) of the eluting solute zone (the zone at the column outlet). Substitution of $\tilde{\sigma}(z)$ from Eq. (2.110) in Eq. (2.106) transforms the latter into equivalent ordinary linear differential equation for $\sigma_z^2 = \sigma_z^2(z)$ as a function of z [2,95]:

$$\frac{d\sigma_z^2}{dz} = \frac{\mathcal{H}}{v^2} - \frac{2\sigma_z^2}{v^2} \frac{\partial v(z, t)}{\partial t} \Big|_{t=t(z)} \quad (2.112)$$

In static medium (like isothermal isobaric GC), $\partial v(z, t)/\partial t = 0$. Eq. (2.112) becomes [86]:

$$\frac{d\sigma_z^2}{dz} = \frac{\mathcal{H}}{v^2}, \quad (\text{static medium}) \quad (2.113)$$

One can view the ratio \mathcal{H}/v^2 on the right-hand side of this equation as a single parameter.

In that case, there is certain symmetry between Eqs. (2.109) and (2.113). The former describes the uniform, but possibly dynamic medium, while the latter—the static, but possibly nonuniform one. In both cases, the right-hand side is represented by a single *a priori* known parameter of a column and its operation. On the other hand, Eqs. (2.108) and (2.112) can be viewed as extensions of Eqs. (2.109) and (2.113), respectively, to nonuniform dynamic medium.

It is assumed in this chapter that the gas decompression along a column is **the only source** of nonuniform conditions in GC. This incorporates the assumption of the uniform μ . Accounting for Eqs. (2.2), (2.33), and (2.34), Eq. (2.113) can be expressed as:

$$\frac{d\sigma_z^2}{dz} = \frac{4096\mathcal{H}L^2\eta^2}{d^4j_2^2p_1^2\mu^2} \left(1 - j_2\frac{z}{L}\right), \quad (\text{static GC}) \quad (2.114)$$

Its integration, assuming that all parameters are uniform (independent of z) and recognizing that $\sigma = \sigma_z(L)$, yields:

$$\sigma^2 = \frac{2048\mathcal{H}L^3\eta^2(p_1^2 + p_0^2)}{d^4\mu^2(p_1^2 - p_0^2)^2}, \quad (\text{static GC}) \quad (2.115)$$

2.9.2.1 Plate height and plate number in nonuniform static chromatography

In uniform static medium, solute velocity (v_o) at the column outlet is the same as its velocity (v) at any location along the column and at any time. As a result, the void time (t_M) can be found

⁴ Its notation might suggest that the temporal width (σ_z) of the zone having its center of mass at z is the zone temporal standard deviation, i.e., σ_z^2 is the variance, $\text{var}[t(z)]$, of the time, $t(z)$, required for the solute zone to migrate through coordinate z [55]. Actually, σ_z^2 is slightly different from $\text{var}[t(z)]$ [2]. During the short time of the zone migration through coordinate z , the zone expands. This fact affects $\text{var}[t(z)]$, but it does not affect σ_z^2 causing the difference between the two. However, the difference (in the order of d/L [2]) is practically insignificant and is typically ignored [96] as it is done here by equating σ (the peak standard deviation) and $\sigma_z(L)$ (the temporal width of the zone at the outlet).

as $t_M = L/u_0$. Eqs. (2.2), (2.62), and (2.97) allow one to express Eq. (2.95) as:

$$\sigma = \frac{t_R}{\sqrt{\mathcal{N}}} \quad (\text{uniform static medium}) \quad (2.116)$$

where t_R is the peak retention time, and

$$\mathcal{N} = \frac{L}{\mathcal{H}}, \quad (\text{uniform static medium}) \quad (2.117)$$

is a column *plate number* in uniform static medium [2,5,97,98].

The definition, Eq. (2.117), of the “number of theoretical plates” (\mathcal{N}) was introduced by Glueckauf [98] in 1955, who also demonstrated that \mathcal{N} defined in Eq. (2.117) can be found as:

$$\mathcal{N} = \frac{t_R^2}{\sigma^2}, \quad (\text{uniform static medium}) \quad (2.118)$$

(in the source [98], quantities t_R and σ were expressed in terms of their volumetric equivalents). The key advantage of Eq. (2.118) over Eq. (2.117) is that Eq. (2.118) allows one to find \mathcal{N} from externally measurable parameters t_R and σ , without the need to know a column internal parameter \mathcal{H} . With \mathcal{N} known from measurements, \mathcal{H} can be found from Eqs. (2.117) and (2.118) as:

$$\mathcal{H} = \frac{L}{\mathcal{N}}, \quad (\text{uniform static medium}) \quad (2.119)$$

$$\mathcal{H} = \frac{L \sigma^2}{t_R^2}, \quad (\text{uniform static medium}) \quad (2.120)$$

In 1957 and 1958, Eq. (2.118) was recommended [90,99] as the definition of the *plate number* (N) in static medium (uniform and nonuniform):

$$N = \left(\frac{t_R}{\sigma} \right)^2, \quad (\text{static medium}) \quad (2.121)$$

In 1959, Giddings and coworkers demonstrated that, in *nonuniform* static medium in general and in GC with its compressible carrier gas in particular, \mathcal{N} in Eq. (2.117) and N in Eq. (2.121) can be different from each other

[96,100]. Consequently, the plate height (H) found from expression:

$$H = \frac{L}{N}, \quad (\text{static medium}) \quad (2.122)$$

extending Eq. (2.119) to nonuniform static medium, can be different from the local plate height (\mathcal{H}) even if \mathcal{H} itself is uniform. Quantity H was called the *apparent (measured, observed) plate height* [96,100]. From Eq. (2.121), H can be also expressed as [96,100]:

$$H = \frac{\sigma^2 L}{t_R^2}, \quad (\text{static medium}) \quad (2.123)$$

In another development, Purnell demonstrated in 1960 [101] that it is N in Eq. (2.121) rather than \mathcal{N} in Eq. (2.117) that defines the column “separation power.” This solidified, from perspective of a column performance, the primacy of N in Eq. (2.121) over \mathcal{N} in Eq. (2.117) with \mathcal{H} defined in Eq. (2.107).

Currently, Eqs. (2.121) and (2.122) are officially recommended [20] and widely recognized [3,4,6–10,17,102–104] as the definitions of, respectively, the *plate number* (N) and the *plate height* (H) in chromatography. The same terminology and notations are adopted in this chapter. To maintain the distinction between H and N , Eqs. (2.121) and (2.122), on the one hand, and \mathcal{H} and \mathcal{N} , Eqs. (2.107) and (2.117), on the other, the latter two are called here as the *local plate height* and the *intuitive plate number* (previously called as the *directly counted plate number* [2]), respectively. The distinctions go beyond the terminology. They reflect different concepts.

According to Eq. (2.107), \mathcal{H} is the rate of dispersive increase of the variance of the solute zone during its migration along the column. This rate is associated in chromatography with the concept of the *plate height* [90,91]. According to Eq. (2.117), if \mathcal{H} is uniform, then \mathcal{N} is the number of \mathcal{H} -long segments—the plates—in the column length. As H in Eq. (2.122) can be different from \mathcal{H} , it does not represent the rate

of dispersive increase of the variance of the solute zone during its migration along the column and, therefore, H is different from the true concept of the plate height in chromatography. Similarly, N in Eq. (2.121) can be different from the number, \mathcal{N} , Eq. (2.117), of the \mathcal{H} -long segments—the plates—in the column length. Therefore, N does not represent what its name suggests it does. In other words, while \mathcal{H} and \mathcal{N} are the metrics of the true physical processes of the zone migration and dispersion within a column, quantities H and N are their apparent (fictitious) counterparts that are not true to their historically adopted names. On the other hand, while \mathcal{H} and \mathcal{N} describe the physics of the zone dispersion processes, H and N describe their effects on the column performance.

Eq. (2.117) defines the intuitive plate number (\mathcal{N}) in uniform static medium. Actually, Eq. (2.117) stands even if the medium is nonuniform (e.g., nonuniform solute velocity), as long as \mathcal{H} is uniform, i.e.,

$$\mathcal{N} = \frac{L}{\mathcal{H}}, \quad (\text{uniform } \mathcal{H}) \quad (2.124)$$

Generally, however, when \mathcal{H} is nonuniform, the intuitive planet number can be found as the sum [2]:

$$\mathcal{N} = \int_0^L d\mathcal{N} = \int_0^L \frac{dz}{\mathcal{H}}, \quad (\text{static medium}) \quad (2.125)$$

of the intuitive plate numbers, $d\mathcal{N} = dz/\mathcal{H}$, in all short segments of length dz in the column length (L).

Giddings demonstrated [105] that, in static medium with nonuniform mobile-phase velocity (u) and uniform \mathcal{H} , $H \geq \mathcal{H}$ so that $H = \mathcal{H}$ only when u is uniform. This also implies that $N \leq \mathcal{N}$ so that $N = \mathcal{N}$ only when u is uniform. In other words, H can never be lower (better) than \mathcal{H} and N can never be higher (better) than \mathcal{N} . The

equalities, $H = \mathcal{H}$ and $N = \mathcal{N}$, can be achieved only when u is uniform.

More generally, in static medium where both u and \mathcal{H} can be nonuniform, $H \geq \mathcal{H}$ so that $H = \mathcal{H}$ only when the ratio \mathcal{H}/u is uniform [106]. In other words.

In nonuniform medium, H can never be lower (better) than \mathcal{H} and, therefore, N can never be higher (better) than \mathcal{N} in Eq. (2.125). The equalities, $\mathcal{H} = H$ and $\mathcal{N} = N$ are achieved only when u and \mathcal{H} change along the column in proportion to each other.

As mentioned earlier, quantity N defined in Eq. (2.121) is called as the “plate number” [20] for historic reasons. Actually, however, it is a practically convenient theoretical fiction that might be different from the actual numbers (\mathcal{N}), Eqs. (2.124) and (2.125), of plates in the column. This might be the case even if \mathcal{H} is uniform [96] (if u is not). As quantity $N = (t_R/\sigma)^2$ does not represent what its name says it does, its use in theory and practice of chromatography can be justified only if its utility justifies that, regardless of its physical meaning. One can notice in that regard that N is calculated as the *square* of the ratio t_R/σ just to be followed by taking the *square root* of N in calculations of such key parameters of column performance as peak capacity, resolution, and others [107]. This suggests that, while the ratio t_R/σ is an important parameter, squaring it to be followed by taking the square root of the square is an unnecessary complicating redundancy. It is more straightforward to deal, instead of N , with quantity:

$$Q = \frac{t_R}{\sigma}, \quad (\text{static medium}) \quad (2.126)$$

relating to N as $Q = \sqrt{N}$. As shown further, not only the use of Q instead of N eliminates the complicating redundancy of calculating the square of $(t_R/\sigma)^2$ to be followed by calculating the square root of that square, but, unlike N , quantity Q (previously denoted as \mathcal{P} , E , and E_c) has its own transparent meanings [22,23,108–112].

Quantity N is typically associated with various concepts of column efficiency. This goes back to the origins of theory of *column chromatography* [25]. In some sources (including earlier publications of this author), N was associated with a column *separation efficiency*. From that perspective, parameter Q in Eq. (2.126), relating to N as $Q = \sqrt{N}$, might be interpreted as an alternative measure of the *separation efficiency*. However, this interpretation could be misleading. Indeed, the plate number concept is valid not only for chromatographic columns, but also for inert tubes ($k = 0$) incapable of any separation. Furthermore, according to Eq. (2.104), the plate height of an inert tube is lower than that of a column ($k > 0$) with the same internal diameter. Consequently, the N and Q of inert tube are larger than their counterparts in a column of the same internal diameter and length. However, because it can make no separation, it would be misleading to say that the tube has higher *separation efficiency*. The efficiency that parameters N and Q represent is the *efficiency of transporting* a sharp single peak to the outlet of a column or a tube. The larger are the parameter N and Q , the narrower are the peaks in relation to their retention times, Eqs. (2.121) and (2.126). It has been suggested to call Q the column *transport efficiency* [111,112]. In this chapter, the short term, *efficiency*, is also used for Q , recognizing that Q is not interpreted as the separation efficiency. The advantages of parameter Q over N were discussed in several publications [22,23,108–112]. Eq. (2.122) for the plate height can be expressed as:

$$H = \frac{L}{Q^2}, \quad (\text{static medium}) \quad (2.127)$$

2.9.2.2 Plate height in nonuniform static GC

If column parameters and operational conditions are known, its local plate height (\mathcal{H}) defined in Eq. (2.107) can be found from Eq. (2.103). However, it is not \mathcal{H} , but the (apparent)

plate height (H) defined in Eq. (2.122) that affects the performance of a column operating under nonuniform conditions caused in GC by the gas compressibility [96,100,101].

The peak width (σ) can be found as $\sigma = \sigma_z(L)$, Eq. (2.111), where $\sigma_z^2(z)$ is solution of Eq. (2.113), or as $\sigma = \tilde{\sigma}_o/v_o$, Eq. (2.95), where $\tilde{\sigma}_o^2 = \tilde{\sigma}^2(L)$ and where $\tilde{\sigma}^2(z)$ is a solution of Eq. (2.108). Assuming that the sample introduction is ideal ($\sigma_z(0) = 0$, $\tilde{\sigma}^2(0) = 0$), both approaches yield:

$$\sigma^2 = \frac{L}{\mu^2} \left(\frac{2048\eta^2 L^2 (p_1^2 + p_o^2)}{d^4 (p_1^2 - p_o^2)^2} \left(\frac{2D}{u} + \frac{\vartheta^2 d^2 u}{96D} \right) + \frac{2\vartheta_S^2 d_f^2}{3D_S \bar{u}} \right) \quad (2.128)$$

This, together with Eqs. (2.36), (2.38), (2.39), (2.62), and (2.123), yields the known *Giddings equation* [2,96,100]:

$$H = \frac{L\sigma^2}{t_R^2} = j_G \cdot \left(\frac{2D}{u} + \frac{\vartheta^2 d^2 u}{96D} \right) + \frac{2\vartheta_S^2 d_f^2 \bar{u}}{3D_S} \quad (2.129)$$

where j_G is the *Giddings compressibility factor*, which, accounting for Eq. (2.39), can be expressed as [2,96,100]:

$$j_G = \frac{j^2 (p_1^2 + p_o^2)}{2p_o^2} = \frac{9(p_1^2 + p_o^2)(p_1 + p_o)^2}{8(p_1^2 + p_1 p_o + p_o^2)^2} \quad (2.130)$$

Quantity j_G changes between 1 for weak gas decompression (relatively wide and short columns with atmospheric outlet pressure) and 1.125 for strong decompression (GC-MS and relatively narrow and long columns). In many cases, the variation of j_G is practically insignificant and can be ignored.

A *thin-film column* is a one where the last (the d_f -dependent) term in Eq. (2.129) is significantly smaller than the other terms and can be ignored. A column has an *intermediate film thickness* or is a

thick film if the last term in Eq. (2.129) is comparable or larger than the other terms, respectively. If the film thickness effect on H is not negligible, then accounting for it is complex [113]. The tendency toward increasing the film thickness usually comes from the need for increasing the column *loadability*. This makes it possible to inject larger sample amount and to lower (improve) the DL for low-concentration components without overloading the column by large-concentration components present in the same sample. However, increasing the film thickness beyond the level where its effect on H can be ignored substantially reduces the column separation performance. Another way of increasing the loadability is not only to increase the film thickness but also to proportionally increase column length, diameter, and film thickness. This also increases H . A comparative analysis of the two approaches shows that an increase in the film thickness alone is only beneficial when the effect of the film thickness on H is small. Beyond that, the proportional increase in the column dimensions and film thickness offers better trade-off between the column separation performance, analysis time, and DL . From now on, **only the thin-film columns** are considered. Eq. (2.129) becomes:

$$H = j_G \cdot \left(\frac{2D}{u} + \frac{\vartheta^2 d^2 u}{96D} \right) \quad (2.131)$$

This expression is simpler than Eq. (2.129). However, it is still unsuitable for practical use and practice-oriented theoretical studies. Due to carrier gas decompression, quantities u and D change along the column. They can be measured at an arbitrary location as long as it is the same for both parameters. This implies that both u and D are always measured at the pressure that is the same for both of them. It can be the inlet pressure (p_i), the outlet pressure (p_o), or pressure (p) at any location along the column. If there is significant difference between p_o and p_i , then (due to strong gas decompression) outlet (u_o) and inlet (u_i) gas velocities are different from each other and their measurement becomes impractical. This is especially true for GC-MS where u_o approaches infinity. To adopt Eq. (2.131) to practical needs, it should be expressed via parameters that are practically easy to measure and to set up. Such parameters could be the inlet pressure (p_i), the average gas velocity (\bar{u}), the flow rate (F), or specific flow rate (f), Eq. (2.45), and others. When expressed via parameters f , F , and \bar{u} , Eq. (2.131) becomes [2,114,115] (Figs. 2.12, 2.13⁵):

$$H = H(f) = \left(\frac{B_f}{f} + C_{ff} \right) j_G, \quad (2.132)$$

$$B_f = \frac{\pi d D_{\text{pst}}}{2}, \quad C_{ff} = \frac{d \vartheta^2}{24 \pi D_{\text{pst}}}$$

⁵ There are widely published experimental $H(\bar{u})$ plots for the same column [6,9,10,155] that are reproduced from single 1979 source [155] and that contradict to the theoretical $H(F)$ plots in Fig. 2.13. According to theory, Eq. (2.143) and Fig. 2.13, H_{\min} is the same for nitrogen, hydrogen, and helium. On the other hand, it was experimentally found that H_{\min} for the three gases is 0.22, 0.26, and 0.28 mm, respectively [155]. This serves as the basis for widely accepted claim that nitrogen and helium are, respectively, the most and the least efficient carrier gases. The difference, however, can be attributed to experimental errors. One of them could be the known insufficiently fast detector electronics [156] for newly invented fast capillary column [157] used in the experiments [155]. As the dependence of H_{\min} on the carrier gas contradicts to theory and, as it is based on a single experiment with obvious potential error, it cannot be treated as the established fact without targeted detailed experimental verification. The gas dependence of H_{\min} is not considered in this chapter.

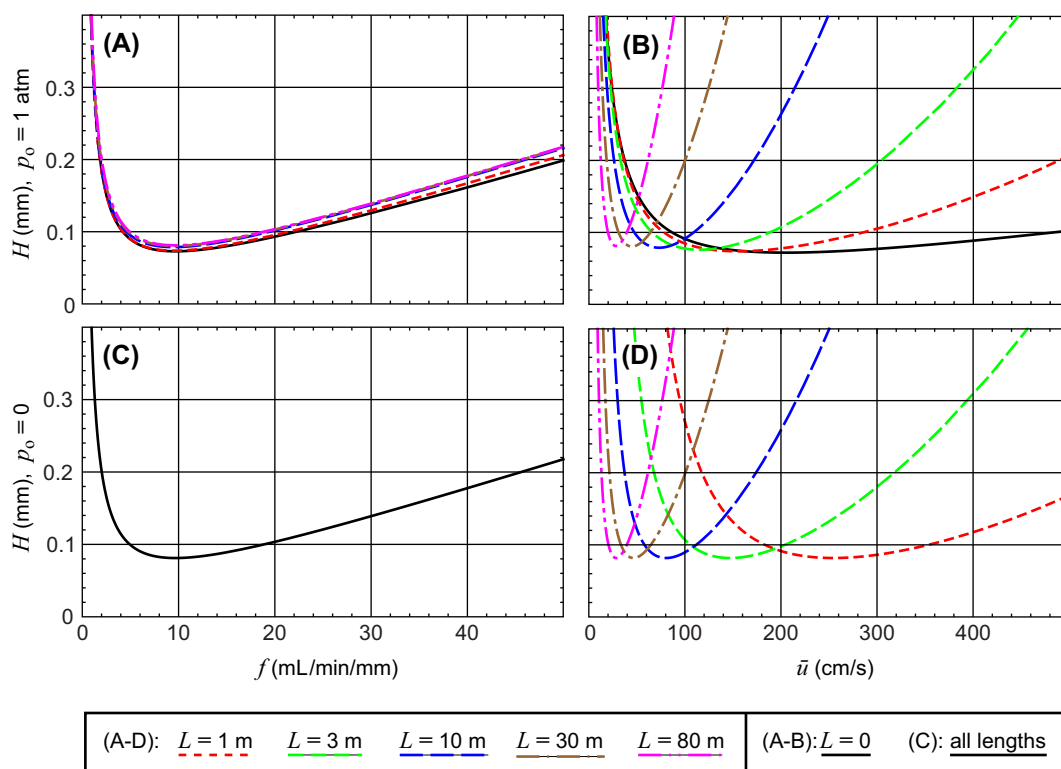


FIGURE 2.12 Plate height (H) versus hydrogen-specific flow rate (f), average velocity (\bar{u}), column lengths (L), and outlet pressure (p_o). Conditions: $d = 0.1$ mm, $T = 150^\circ\text{C}$, $\phi = 0.001$, $k = 2$. The choice of $k = 2$ is explained in Example 2.10.

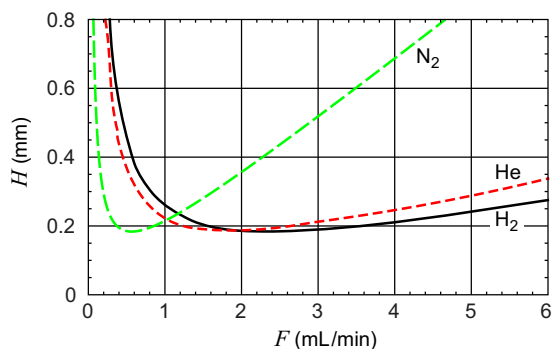


FIGURE 2.13 Plate height (H) versus flow rate (F) for three carrier gases. Conditions: $d = 0.25$ mm, $L = 25$ m, $p_o = 1$ atm, $T = 150^\circ\text{C}$, $k = 2$, $\phi = 0.001$.

$$H = H(F) = \left(\frac{B_F}{F} + C_F F \right) j_G, \quad (2.133)$$

$$B_F = \frac{\pi d^2 D_{\text{pst}} T_{\text{norm}}}{2T},$$

$$C_F = \frac{T \vartheta^2}{24\pi D_{\text{pst}} T_{\text{norm}}}$$

$$H = H(\bar{u}) = \left(\frac{A_1 A_2}{\Phi(A_1 \bar{u})^2 - 1} + \frac{d^2 \vartheta_{G1}^2 (\Phi(A_1 \bar{u})^2 - 1)}{48 A_1 A_2} \right) j_G, \quad (2.134)$$

$$A_1 = \frac{32\eta L}{d^2 p_o}, \quad A_2 = \frac{4D_{\text{pst}} p_{\text{st}}}{p_o}$$

where D_{pst} is the solute diffusivity in the gas at standard pressure ($p_{\text{st}} = 1$ atm). Due to Eq. (2.25), quantity D_{pst} can be found as:

$$D_{\text{pst}} = \frac{X_D^2 D_{\text{g,st}} \cdot (10^3 \phi)^{0.09}}{k^{0.1}} \cdot \left(\frac{T}{T_{\text{st}}} \right)^{\xi - 0.25}, \quad (0.1 \leq k \leq 30) \quad (2.135)$$

The gas-specific parameters $D_{\text{g,st}}$, X_D , and ξ in this equation are listed for several gases in Table 2.2. Unlike equations for $H(f)$ and $H(F)$, equation for $H(\bar{u})$ cannot be generally expressed in the form $(B/\bar{u} + C\bar{u})$, but only in relatively rare cases when the gas decompression is negligibly weak:

$$H = \frac{B_{\text{weak}}}{\bar{u}} + C_{\text{weak}} \bar{u}, \quad B_{\text{weak}} = \frac{2D_{\text{pst}} p_{\text{st}}}{p_o}, \quad C_{\text{weak}} = \frac{d^2 \vartheta_{\text{G1}}^2 p_o}{96D_{\text{pst}} p_{\text{st}}}, \quad (\Delta p < < p_o) \quad (2.136)$$

When the decompression is strong, H can be expressed as [2,116]:

$$H = \frac{B_{\text{GCMS}}}{\bar{u}^2} + C_{\text{GCMS}} \bar{u}^2, \quad B_{\text{GCMS}} = \frac{81d^2 D_{\text{pst}} p_{\text{st}}}{1024L\eta}, \quad C_{\text{GCMS}} = \frac{L\eta \vartheta_{\text{G1}}^2}{3D_{\text{pst}} p_{\text{st}}}, \quad (\Delta p > > p_o) \quad (2.137)$$

The optimal values (f_{opt} , F_{opt} and \bar{u}_{opt}) of variables (f , F and \bar{u}) corresponding to the minimum (H_{min}) in H can be found as [2]:

$$f_{\text{opt}} = \sqrt{\frac{B_f}{C_f}} = \frac{2\sqrt{3}\pi D_{\text{pst}}}{\vartheta} \quad (2.138)$$

$$F_{\text{opt}} = \sqrt{\frac{B_F}{C_F}} = \frac{2\sqrt{3}\pi D_{\text{pst}} d}{\vartheta} \cdot \frac{T_{\text{norm}}}{T} \quad (2.139)$$

$$\bar{u}_{\text{opt}} = \frac{18432Lp_{\text{st}}^2 D_{\text{pst}}^2 \eta}{d^4 p_o^3 \vartheta^2} \cdot \left(\left(\frac{512\sqrt{3}Lp_{\text{st}} D_{\text{pst}} \eta}{d^3 p_o^3 \vartheta} + 1 \right)^{3/2} - 1 \right)^{-1} \quad (2.140)$$

$$= \begin{cases} \frac{8\sqrt{3}D_{\text{pst}} p_{\text{st}}}{dp_o \vartheta}, & \Delta p \ll p_o \\ \frac{3}{4} \sqrt{\frac{\sqrt{3}dD_{\text{pst}} p_{\text{st}}}{2L\eta \vartheta}}, & \Delta p \gg p_o \end{cases}$$

The latter follows from f_{opt} due to Eq. (2.56). Expressions for $H(p_i)$ and $p_{i,\text{opt}}$ could be found elsewhere [2].

Which expression for H is more suitable for studies of a column performance and for guiding practical method development for GC analyses? To answer this question, several factors should be considered. Among them are the simplicity of expression for H , simplicity of expressions for optimal values of its parameters, and simplicity of controlling these parameters in practical applications.

Comparing Eqs. (2.132)–(2.134) for $H(f)$, $H(F)$, and $H(\bar{u})$ as well as Eqs. (2.138)–(2.140) for f_{opt} , F_{opt} and \bar{u}_{opt} one finds that the structure of function $H(\bar{u})$ is substantially more complex than that of the other two. Similarly the structure of expression for \bar{u}_{opt} is substantially more complex than that of expressions for f_{opt} and F_{opt} . Moreover, the difference is not only in the structure of equations, but also in the number of variables affecting optimal parameters.

Eqs. (2.138)–(2.140) show that all optimal parameters depend on the solute diffusivity (D_{pst}) in the carrier gas and on the solute retention factor (through parameter ϑ , Eq. 2.101). The former depends, Eq. (2.25), on the carrier gas type, temperature (T), and k , which, in turn, also depends on T . Overall, all optimal parameters depend on the carrier gas type, column temperature, and solute retention.

Eq. (2.138) shows that no other parameters affect f_{opt} . It follows from Eqs. (2.135) and (2.138) with data in Table 2.2 that, for columns and conditions in Fig. 2.12, $f_{\text{opt}} = 9.72$ mL/min/mm, Table 2.5, not only for all column lengths and outlet pressures in Fig. 2.12, but also for all column diameters.

In addition to parameters affecting f_{opt} , quantity F_{opt} is proportional to column diameter (d), depends on the choice of the flow measurement temperature (T_{norm} in this chapter), and differently depends on T than f_{opt} does.

On the other hand, in addition to its dependence on the factors affecting f_{opt} (carrier gas type, T , and k), quantity \bar{u}_{opt} also substantially depends on gas viscosity (η), column internal diameter (d), length (L), and outlet pressure (p_o). What's more, the additional dependencies (on η , d , L and p_o) in \bar{u}_{opt} are not proportional and not even linear, but more complex. The effects of L and p_o on $H(\bar{u})$ and on \bar{u}_{opt} are illustrated in Fig. 2.12B and Fig. 2.12D and in Table 2.5 showing that \bar{u}_{opt} is different for different column lengths (L) and that the dependence of \bar{u}_{opt} on L at $p_o = 1$ atm (like in GC-FID) is different from that at $p_o = 0$ (GC-MS). Add to that the dependence, Eq. (2.140), of \bar{u}_{opt} on d (not shown in Fig. 2.12 and Table 2.5), and it becomes obvious that choosing \bar{u}_{opt} in practical method development is not a simple task

Example 2.8. For columns and conditions in Fig. 2.12, \bar{u}_{opt} in GC-MS ($p_o = 0$) changes from 28.5 cm/s for $L = 80$ m (the longest column that can be used in fast single-column analyses of complex mixtures [117]) to 255 cm/s for $L = 1$ m

TABLE 2.5 Quantities \bar{u}_{opt} and f_{opt} for the columns and conditions in Fig. 2.12.

L (m)	0	1	3	10	30	80
\bar{u}_{opt} (cm/s), $p_o = 1$ atm	206	158	118	74.1	45.1	28.1
\bar{u}_{opt} (cm/s), $p_o = 0$	∞	255	147	80.5	46.5	28.5
f_{opt} (mL/min/mm), any p_o	9.72					

(a popular choice for the secondary column in GC \times GC [118]).

Expressions for $p_{i,\text{opt}}$ are almost as complex as they are for \bar{u}_{opt} [2].

Eqs. (2.132) and (2.133) can be expressed in the following symmetric forms including parameters f_{opt} and F_{opt} , Eqs. (2.138) and (2.139), and directly exposing the effects of departure of f and F from their optima [2]:

$$H(f) = \frac{H_{\text{min}}}{2} \cdot \left(\frac{f_{\text{opt}}}{f} + \frac{f}{f_{\text{opt}}} \right) \quad (2.141)$$

$$H(F) = \frac{H_{\text{min}}}{2} \cdot \left(\frac{F_{\text{opt}}}{F} + \frac{F}{F_{\text{opt}}} \right) \quad (2.142)$$

where the lowest plate height (H_{min}) can be found from Eq. (2.132) as:

$$H_{\text{min}} = \frac{j_G d \vartheta_{G1}}{2\sqrt{3}} \quad (2.143)$$

The Giddings compressibility factor (j_G), Eq. (2.130), in this equation represents the dependence of H_{min} on the gas decompression. It changes from the weak to the strong gas decompression within the range $1 \leq j_G \leq 1.125$, Eq. (2.130). Eq. (2.143) becomes:

$$H_{\text{min,weak}} = \frac{d\vartheta_{G1}}{2\sqrt{3}}, \quad H_{\text{min,strong}} = \frac{\sqrt{27}d\vartheta_{G1}}{16} \quad (2.144)$$

When the length (L) of a column operated at atmospheric p_o increases, H_{min} also increases due to the increase in j_G , Fig. 2.12A and B. On the other hand, in GC-MS ($p_o = 0$), the decompression is strong regardless of L . As a result, L no longer affects j_G and H_{min} .

A symmetric form, similar to Eqs. (2.142) and (2.141), does not generally exist for $H(\bar{u})$ —another disadvantage of expressing H as a function of \bar{u} . However, in the extreme cases of the

weak and the strong gas decompression, $H(\bar{u})$ can be expressed as [2]:

$$H(\bar{u}) = \frac{H_{\min, \text{weak}}}{2} \cdot \left(\frac{\bar{u}_{\text{opt, weak}}}{\bar{u}} + \frac{\bar{u}}{\bar{u}_{\text{opt, weak}}} \right), \quad (\Delta p << p_o) \quad (2.145)$$

$$H(\bar{u}) = \frac{H_{\min, \text{strong}}}{2} \cdot \left(\left(\frac{\bar{u}_{\text{opt, strong}}}{\bar{u}} \right)^2 + \left(\frac{\bar{u}}{\bar{u}_{\text{opt, strong}}} \right)^2 \right), \quad (\Delta p >> p_o) \quad (2.146)$$

where, according to Eq. (2.140):

$$\begin{aligned} \bar{u}_{\text{opt, weak}} &= \frac{8\sqrt{3}D_{\text{pst}}p_{\text{st}}}{dp_o\vartheta}, \quad \bar{u}_{\text{opt, strong}} \\ &= \frac{3}{4} \sqrt{\frac{\sqrt{3}dD_{\text{pst}}p_{\text{st}}}{2L\eta\vartheta}} \end{aligned} \quad (2.147)$$

Unlike the structure of symmetric functions $H(f)$ and $H(F)$, Eqs. (2.141) and (2.142), that do not depend on the degree of gas decompression, the structure of symmetric functions $H(\bar{u})$ strongly depends on the decompression. When the decompression is weak ($\Delta p \ll p_o$), the structure of $H(\bar{u})$, Eq. (2.145), is similar to that of $H(F)$ and $H(f)$. However, when the decompression is strong, the structure of $H(\bar{u})$, Eq. (2.146), is different reflecting much stronger sensitivity of $H(\bar{u})$ to departure of \bar{u} from \bar{u}_{opt} . For comparison, it follows from Eqs. (2.141) and (2.142) that, regardless of the degree of the gas decompression, a factor-of-two departure of f and F from their optima raises H above H_{\min} by 25% ($H = 1.25H_{\min}$). The same is true for $H(\bar{u})$, but

only at the weak gas decompression, Eq. (2.145). The picture is different for $H(\bar{u})$ at strong gas decompression, Eq. (2.146), where the same factor-of-two departure of parameter \bar{u} from \bar{u}_{opt} more than doubles H ($H = 2.125H_{\min}$). The curves in Fig. 2.12B illustrate the transition of $H(\bar{u})$ from weak decompression for short columns to strong decompression for the long ones. The curve for $L = 0$ illustrates Eq. (2.145) and the curve for the longest 80 m column approximately illustrates Eq. (2.146). All curves in Fig. 2.12D illustrate Eq. (2.146).

All in all, the facts that

- \bar{u}_{opt} can change within a wide range, Fig. 2.12B and D and Table 2.5, when column diameter is fixed
- the range of variation of \bar{u}_{opt} becomes even wider when different column diameters are considered
- $H(\bar{u})$ is substantially more sensitive to variations of $\bar{u}/\bar{u}_{\text{opt}}$ than to variations of f/f_{opt} or F/F_{opt}

substantially complicate theoretical prediction and practical optimization of \bar{u} . These factors are the likely reasons why the values of \bar{u}_{opt} for many useful applications are not known from the literature.⁶ On the other hand, f_{opt} is independent of column dimensions and of operational parameters η and p_o . Simple recommendations for optimal flow rate proportional to $d \times f_{\text{opt}}$ published in 1999 [115] and reproduced further in this chapter for several gases are consistently recommended for several generations of commercial GC instruments manufactured by Hewlett–Packard Co (Palo Alto, CA) and then by Agilent Technologies (Santa

⁶ Frequently recommended values of \bar{u}_{opt} (35 cm/s for helium and 50 cm/s for hydrogen) are approximately suitable only for typical (25 m × 0.25 mm) columns and only for some unknown combination of outlet pressure, column temperature, and solute retention. For a 1 m × 0.1 mm column in GC-MS (a frequent choice of the secondary column in GC×GC [118]) under conditions in Fig. 2.12, $\bar{u}_{\text{opt}} \approx 250$ cm/s, Fig. 2.12D ($\bar{u}_{\text{opt}} \approx 200$ cm/s for helium). This is some five times larger than the typically recommended value. It follows from Eq. (2.146) that lowering \bar{u} compared to \bar{u}_{opt} by a factor of 5 would increase H compared to H_{\min} by more than 12.5 times.

Clara, CA) since 1994. Recently, Restek Corporation (Bellefonte, PA) included the same recommendations in its column catalogs. Similar recommendations are now extended to GC \times GC [119].

Several decades ago, specifying \bar{u} was the most typical way of describing the gas flow conditions in GC analyses. The very purpose of considering $H(\bar{u})$ and \bar{u}_{opt} here was to demonstrate their complexity and to discourage their use. From now on, the dependence $H(\bar{u})$ and expressions for \bar{u}_{opt} are no longer considered in this chapter.

The independence of f_{opt} from column dimensions makes it possible to isolate (as was done elsewhere [2,119] and later in this chapter) a study of the effects of the column dimensions on the column performance from the effects of the flow rate on that performance. However, for practical purposes, it is eventually necessary to know the optimal flow rate (F_{opt}) for a particular column under particular operational conditions rather than f_{opt} for a class of columns and operational conditions. The explicit recommendations for choosing optimal f and F are provided further after discussion of suitable choices for the reference temperature and retention factors in determining these optima. The final recommendations also account for the fact that the optimal temperature-programmed f_{opt} and F_{opt} are different from their isothermal counterparts. On top of that, the importance of minimizing H in a given time rather than minimizing it in a given column is also considered. Some of these considerations are based on evaluation of the *dimensionless plate height* [2,5,120]:

$$h = \frac{H}{d} \quad (2.148)$$

allowing one to express Eqs. (2.142) and (2.141) as:

$$h = \frac{h_{\text{min}}}{2} \cdot \left(\frac{F_{\text{opt}}}{F} + \frac{F}{F_{\text{opt}}} \right) \quad (2.149)$$

$$h = \frac{h_{\text{min}}}{2} \cdot \left(\frac{f_{\text{opt}}}{f} + \frac{f}{f_{\text{opt}}} \right) \quad (2.150)$$

where

$$h_{\text{min}} = \frac{H_{\text{min}}}{d} = \frac{j_G \vartheta}{2\sqrt{3}} \approx 1 \quad (2.151)$$

Eqs. (2.127) and (2.148) yield:

$$Q = \sqrt{\frac{L}{dh}} \quad (2.152)$$

2.9.2.3 Plate height, efficiency, and optimal flow in temperature-programmed GC

The definition in Eq. (2.126) of the transport efficiency (Q) (as well as the definition in Eq. 2.121 of the plate number) in static analysis is not suitable for temperature-programmed GC analyses and for dynamic chromatography in general. Indeed, as shown further, all highly interactive solutes (highly retained at the beginning of a heating ramp) elute during the linear heating ramp with roughly the same peak widths [2] while their retention times (t_R) gradually increase. As a result, quantity Q in Eq. (2.126) might increase with time by an order of magnitude or more making Q a time-dependent quantity rather than a column parameter and a key metric in evaluation of a column performance. However, based on the approach proposed by Habgood and Harris in 1960 [17–19,121], the definition in Eq. (2.126) can be generalized to include static and dynamic analyses in general and isothermal and temperature-programmed GC analyses in particular.

The retention time (t_R) in static analysis can be expressed as, Eq. (2.62), $t_R = t_M/\mu$ where $\mu = 1/(1+k)$ is the solute mobility—the solute fraction in mobile phase. As a result, Eq. (2.126) can be expressed as $Q = t_M/(\mu\sigma)$. In the case of dynamic conditions, quantities t_M and μ can

be interpreted as the void time ($t_{M,R}$) at the solute retention time and the mobility of the eluting solute (μ_R)—its mobile phase fraction at the time of the solute elution. In other words, $t_{M,R}$ and μ_R are the parameters measured at static conditions that are the same as the conditions in dynamic analysis existing at the peak retention time. The definition of the column efficiency (Q) in static and dynamic analyses can be generalized as $Q = t_{M,R}/(\mu_R\sigma)$. This is essentially the original *Habgood–Harris definition* of N in temperature-programmed GC [17,18] transformed into definition of Q as $Q = \sqrt{N}$. The definition has a problem. While $t_{M,R}$ and μ_R in it are *statically* measured parameters, quantity σ is the peak width in actual *dynamic* analysis. The mixture of the measurement conditions complicates the concept of the dynamic Q and its theoretical prediction based on the column and its operational parameters. The choice of dynamic conditions and their combinations is unpredictably large (multislope temperature programming combined with multislope pressure programming in GC, similar combinations in gradient LC, etc.). As a result, the very meaning of the concept of column efficiency (Q) in dynamic analysis becomes uncertain. The following definition [1] does not have this problem.

The efficiency (Q) for a solute in dynamic analysis is the efficiency for that solute in static analysis under conditions existing in the dynamic analysis at the solute elution time (t_R)

In other words:

$$Q = \frac{t_{M,R}}{\mu_R\sigma_{\text{statR}}} \quad (2.153)$$

where σ_{statR} is the width of the peak corresponding to the solute in static analysis under conditions existing in dynamic analysis at time t_R . This definition is equally valid for static and dynamic analyses.

A purpose of knowing Q is to predict the peak width (σ) in a chromatogram. Thus, in static

analysis, if Q is known, then σ can be found from Eq. (2.126) as $\sigma = t_R/Q$. However, σ_{statR} found from Eq. (2.153) can be different from the actual peak width (σ) in dynamic analysis. In temperature-programmed GC, e.g., the difference can result from the change in the local plate height during the analysis due to the change in the column temperature. To reduce the difference between σ_{statR} in Eq. (2.153) and the actual σ in dynamic analysis, Giddings introduced [14] a concept of the *significant temperature*, $T_s = 0.9T_R$ (in kelvins), to use T_s in Eq. (2.153) instead of T_R . Unfortunately, this approach has limited utility. It probably helps in cases of isobaric single-ramp temperature programming at typical rates. However, its extension to pressure programming in GC or to gradient LC is questionable. On the other hand, a definition of the efficiency should be suitable for a wide range of dynamic techniques.

The definition of Q in Eq. (2.153) allows one to resolve the aforementioned controversies. First, the definition itself (unlike its prototype [17,19]) provides a better certainty to the concept—the parameters in it are as certain as they are in any static analysis. Second, a separate parameter—the *peak formation factor* (G_p)—can be introduced to relate the actual peak width (σ) in dynamic analysis to its static counterpart (σ_{statR}) in Eq. (2.153) so that:

$$\sigma = G_p\sigma_{\text{statR}} \quad (2.154)$$

This together with Eq. (2.153) allows one to find σ as:

$$\sigma = \frac{G_p t_{M,R}}{Q\mu_R} \quad (2.155)$$

Quantity G_p has its own merit. It quantifies the relative difference between the actual peak width (σ) in dynamic analysis and the peak width (σ_{statR}) in static analysis under conditions existing in dynamic analysis at the solute elution time. If G_p is known, then, from Eq. (2.62), (2.127), and (2.154), Q and H in Eq. (2.153) can

be found from parameters of dynamic analysis as:

$$Q = \frac{G_p t_{M,R}}{\mu_R \sigma} \quad (2.156)$$

$$H = \left(\frac{\mu_R \sigma}{G_p t_{M,R}} \right)^2 L \quad (2.157)$$

In GC with uniform heating, $G_p \approx 1$. Assuming that $G_p = 1$ reduces Eq. (2.156) to its original Habgood–Harris form [17,19]:

$$Q = \frac{t_{M,R}}{\mu_R \sigma} \quad (2.158)$$

Eqs. (2.155) and (2.157) become:

$$\sigma = \frac{t_{M,R}}{Q \mu_R} \quad (2.159)$$

and $H = (\mu_R \sigma / t_{M,R})^2 L$.

Typically, Q in a given analysis is roughly the same for all solutes and can be treated as a fixed quantity. In addition to that, it follows from Eq. (2.82) that μ_R is approximately the same for all highly interactive solutes in isobaric analysis. Furthermore, according to Eqs. (2.159), (2.49), and (2.21) together with the data in Table 2.2:

$$\sigma = \sigma(\Delta p, Q) = \frac{32 \eta_{st}^2}{j_H Q \Delta p \mu_R} \left(\frac{T_R}{T_{st}} \right)^\xi \sim T_R^{0.7} \quad (2.160)$$

In other words,

the width (σ) of a peak corresponding to a highly interactive solute (highly retained at the beginning of the heating ramp) eluting at temperature T_R during isobaric linear heating ramp is proportional to $T_R^{0.7}$.

Example 2.9. A peak eluting at 250°C (523.15K) is about 16% wider than the peak eluting at 150°C (423.15K).

Compared to isothermal analyses where the peak widths can increase during the analysis by more than an order of magnitude, it is reasonable to suggest that,

all peaks generated during a heating ramp have roughly the same width.

Eq. (2.160) expresses σ as function of pressure drop (Δp). What is typically known is the flow rate (F) or specific flow rate (f). Substitution of Eq. (2.52) in Eq. (2.159) yields:

$$\begin{aligned} \sigma = \sigma(f, Q) &= \frac{\pi^2 d^4 p_o^3}{1536 p_{st}^2 \eta Q \mu_R f^2} \\ &\left(\left(1 + \frac{256 L p_{st} \eta f}{\pi d^3 p_o^2} \right)^{3/2} - 1 \right) \\ &= \frac{1}{Q \mu_R} \begin{cases} \frac{\pi d L p_o}{4 p_{st} f}, & |\Delta p| \ll p_o \\ \sqrt{\frac{64 \pi L^3 \eta}{9 d p_{st} f}}, & \Delta p \gg p_o \end{cases} \end{aligned} \quad (2.161)$$

Due to proportionality of F to f , Eq. (2.45), this equation can be transformed into dependence of σ on F .

The peak width (σ) is measured in units of time. For the peaks eluting during the heating ramp, one can also consider the T -domain equivalent (σ_T) of the $time$ -domain (t -domain) σ , defined as:

$$\sigma_T = R_T \sigma \quad (2.162)$$

and measured in units of temperature. From Eqs. (2.69) and (2.159), σ_T can be expressed as:

$$\sigma_T = \frac{\theta_{char} r_T}{Q \mu_R} \frac{t_{M,R}}{t_{M,char}} \quad (2.163)$$

For highly interactive solutes, $\mu_R = \mu_{R,a}$. From Eqs. (2.82) and (2.87), one has:

$$\sigma_{T,a} = \frac{r_T t_{M,R} \theta_{char}}{(1 - e^{-r_T}) t_{M,char} Q} = \frac{t_{M,R} \theta_{char}}{t_{M,char} Q \bar{\omega}_a} \quad (2.164)$$

Ignoring typically small relative difference between $t_{M,R}$ and $t_{M,char}$, one can approximate $\sigma_{T,a}$ as:

$$\sigma_{T,a} \approx \frac{\theta_{char}}{Q \bar{\omega}_a} \quad (2.165)$$

To use this equation, one needs to know Q , which, in turn, requires knowing H . A general exact theoretical expression for H in a temperature-programmed analysis is unknown. Approximate integration of Eq. (2.106) for isobaric single-ramp temperature-programmed analysis shows that typical temperature programming causes minor increase in minimal plate height and, therefore, minor reduction in maximal Q [2]. This is in agreement with known experimental data [17,19]. More significant is the difference in expression for f_{opt} . The latter can be expressed as [2]:

$$f_{\text{opt}} = X_T f_{\text{opt,iso}} = \frac{2\sqrt{3}\pi D_{\text{pst}} X_T}{\vartheta} \quad (2.166)$$

where $f_{\text{opt,iso}}$ (Eq. 2.138) is f_{opt} in isothermal analysis and

$$X_T = \begin{cases} 1, & \text{isothermal conditions} \\ 0.82 \sqrt{\frac{1 + 4\omega_R + 6\omega_R^2}{1 + 4\bar{\omega} + 6\bar{\omega}^2}}, & \text{isobaric heating ramp} \end{cases} \quad (2.167)$$

where ω_R and $\bar{\omega}$ are the elution ω and the distance-averaged ω , Eqs. (2.81) and (2.87), respectively.

Example 2.10. As shown further, the optimal r_T in temperature-programmed analysis with linear heating ramp is close to 0.4. At $r_T = 0.4$, Eqs. (2.81), (2.4) and (2.87), and then Eq. (2.167) yield: $\omega_R = 0.67$, $k_R = 2.03$, $\bar{\omega} = 0.824$, and $X_T = 0.716$. Therefore, f_{opt} for a solute eluting with $k = 2$ in temperature-programmed analysis is about 72% of f_{opt} for the solute migrating with $k = 2$ in isothermal analysis. These numerical results serve as a basis for other numerical values in this chapter.

The difference in f_{opt} in isothermal and temperature-programmed analyses was taken into account in a study of column optimization in GC \times GC [119] where the primary column operates under temperature-programmed conditions while each secondary column runs under essentially isothermal conditions.

2.9.2.4 Thermal gradients and peak focusing

It has been assumed so far that the column temperature (T) is uniform, i.e., the *thermal gradients* (T -gradients) do not exist ($\partial T/\partial z = 0$). This constraint is removed in this and only this section. It is assumed here that the T -gradients can exist ($\partial T/\partial z \neq 0$) and that they can move along a column, i.e., a coordinate (z) where the T -gradient has a fixed value g_T ($\partial T/\partial z = g_T$) can move along the column. It is generally assumed (mistakenly in most cases) that the negative T -gradients ($\partial T/\partial z < 0$) can substantially *focus* (*sharpen*) the peaks and, by that, substantially improve their separation and/or speed of analysis [57,58,61].

The earliest known description of the moving negative T -gradients in gas-phase separations was published by Zhukhovitskii et al. in 1951 [56]—a year earlier than Griffiths et al. described [13] the technique with “varying the temperature” (the temperature programming, as it is known today). Soon after, the conventional (uniform) temperature programming became a dominant technique in GC [122]. However, the interest in the negative moving T -gradients in GC never abated [57–63].

The negative T -gradients in GC cause negative gradients ($\partial\mu/\partial z < 0$) in the solute mobility (μ -gradients), which, as follows from Eq. (2.2), can cause negative gradients ($\partial v/\partial z < 0$) in the solute velocities (v -gradients). The negative v -gradients cause the front of a solute zone within a column to migrate slower than its tail causing, in turn, the zone compression (sharpening). It was generally expected that the zone compression within a column should inevitably result in *focusing* (sharpening) the peaks in chromatograms. Moreover, typically, no distinction is made between the solute zones within a column and the chromatographic peaks. As a result, the zone compression is typically equated with the peak focusing. This probably was (and is) the single most significant factor in sustaining the interest in negative T -gradients.

Following side effects of the negative v -gradients are frequently overlooked:

- The same negative v -gradient that compresses a solute zone (by causing the front of the zone to travel slower than its tail) also reduces the distance between two neighboring zones (by causing the leading zone to travel slower than the trailing one). This phenomenon is especially significant for the most critical closely spaced zones. As a result, the net effect of the v -gradients on the zone (and the peak) separation can be questioned.
- For the T -gradients to cause significant v -gradients, the solutes should be sufficiently retained, i.e., their retention factors (k) should be sufficiently high or, equivalently, their mobility (μ) should be sufficiently low. This tends to slow down the zone migration and elution, which, in turn, broadens the chromatographic peaks and reduces the speed of analysis.

The existence of these conflicting effects questions the ability of the v -gradients to improve the separation performance and speed of analysis. Moreover, it even questions the significance of the gradient. Gas decompression in GC provides an exemplary illustration of the outcome of these observations. Suppose that the column and its heating are uniform, and the only source of non-uniform solute velocities is the gas decompression causing the gas and the solute velocity acceleration in direction from the inlet to the outlet. This phenomenon is opposite to the focusing and might be expected in a significant peak defocusing (broadening). Indeed, due to the velocity acceleration in direction from inlet to outlet, the front of a solute zone migrates faster than its tail causing the zones broadening. In the worst case scenario of GC-MS, the widths of the eluting zones approach infinity. According to conventional logic of peak focusing, this case of the peak defocusing should result in infinitely wide peaks. However, nothing close to that happens. The very zone acceleration that broadens them up to infinity also accelerates their migration so that, while the widths of the eluting zones

approach infinity, their elution velocities also approach infinity. The net result of almost infinitely wide zones eluting with almost infinite velocity is the peak broadening by up to ... 6.1% (square root of j_G , Eq. 2.130). In other words, an enormous (up to infinity) zone broadening within GC column, has barely noticeable (6% in the worst case) defocusing of peak in chromatograms. In addition to theoretical predictions [59,60], this example should moderate the expectations for the peak focusing due to negative v -gradients.

The results of theoretical studies of the effects of v -gradients in chromatography (not only GC) can be summarized as follows [59,60]. There is a *performance baseline* for chromatographic analyses—the *ideal basic separation* (infinitely sharp sample introduction, uniform column, and uniform conditions of a solute migration, no gas decompression in GC, constant plate height, etc.). The theory [59,60] shows that

- Adding v -gradients to an ideal basic separation cannot enhance its potential separation performance and/or speed of analysis.
- Adding v -gradients to nonideal separation can reduce the harmful effects of nonideal conditions and, by that, improve the separation performance and/or speed of analysis, but not beyond that available from ideal basic separation.

The examples where the negative v -gradients improve the separation by compensating nonideal adverse conditions are known [59,123]. A reader interested in additional details regarding the v -gradients can find them elsewhere [59,60].

2.9.2.5 Incorrect plate height equation

The equation:

$$H = \frac{B}{\bar{u}} + C\bar{u} \quad (2.168)$$

typically attributed to Golay or to van Deemter, dominates the literature and the university courses on GC theory [6,7,9,10,12,124,125]. Its coefficients (B and C) are frequently not specified at all [124,125] or defined as [6,7,9,10,12]:

$$B = 2D, \quad C = \frac{(1 + 6k + 11k^2)d^2}{96(1 + k)^2D} + \frac{2kd_f^2}{3(1 + k)^2D_S} \quad (2.169)$$

where all parameters are the same as those in Eq. (2.103) except for the diffusivity (D) (see further). Eqs. (2.168) and (2.170) imply that, in a simple case of a thin-film column ($d_f = 0$), the optimal \bar{u} (\bar{u}_{opt}) minimizing H can be found as [6,7,9,10,12]:

$$\bar{u}_{\text{opt}} = \sqrt{\frac{B}{C}} = \frac{D}{d} \sqrt{\frac{48(1 + k)^2}{1 + 6k + 11k^2}}, \quad (d_f = 0) \quad (2.170)$$

It might appear at the first glance that Eq. (2.168) is identical to Eq. (2.103). However, this appearance is deceptive. Eq. (2.103) is correct, while Eq. (2.168) is not. There are several substantial differences between Eq. (2.168), *incorrectly attributed to Golay*, and the time-tested correct Eq. (2.103) that directly follows from the equation rigorously proven by Golay [81]:

- average gas velocity (\bar{u}) in Eq. (2.168) replaces local gas velocity (u) in Eq. (2.103)
- in Eq. (2.169), the solute diffusivity (D) in the gas is assumed to be measured at the standard pressure (1 atm), while, in Eq. (2.103), it is a local property measured at local pressure and temperature
- the form of Eq. (2.168) implies that its coefficients (B and C) are independent of \bar{u} , which, according to Eq. (2.134), is not correct.

A theoretical proof or experimental verification of Eq. (2.168) is unknown.

The history of adoption of Eq. (2.168a) and its harm to GC theory and practice are briefly described further. Additional details can be found elsewhere [2,126].

Several workers contributed to the introduction of Eq. (2.168) at the early stages of the development of the plate height theory when GC-MS with its strong gas decompression along the column was unknown and when the use of the high column pressure causing significant gas decompression was a rare exception [127].

In 1956, Keulemans and Kwantes [128] suggested [128] that the van Deemter equation [80] can be expressed in a simple form of a *mathematical hyperbola* $H = A + B/u + Cu$ where A , B , and C were independent of u . This was the first step toward Eq. (2.168). The hyperbola version of Eq. (2.103) is:

$$H = B/u + Cu \quad (2.171)$$

The assumption that B and C in it are independent of u is generally *incorrect*. It can be approximately correct only when the gas decompression along the column is weak, i.e., when the column pressure drop, $\Delta p = p_i - p_o$, is negligible compared to outlet pressure p_o ($\Delta p \ll p_o$). In contemporary GC, this requirement might be satisfied in short wide-bore columns operating at $p_o = 1$ atm. In most cases, however, in order to change u , a substantial change in p_i might be required. This, in turn, causes substantial change in the local pressure (p) within a column, which, in turn, substantially changes the local diffusivity (D) of the solute in the gas, which, in turn, changes parameters B and C in Eq. (2.169) when u changes. The net result is that changing u also changes B and C in Eq. (2.171). With its parameters, B and C , changing together with the changes in u , Eq. (2.171) is not a mathematical hyperbola [80], and its structure, implying that B and C are constants, is incorrect.

The next and the final step was made by Purnell and Quinn in 1960 [129], who expressed Eq. (2.171) in the form of Eq. (2.168), i.e., replaced the local gas velocity (u) in Eq. (2.171) with variable \bar{u} in Eq. (2.168). The latter was defined as "the compressibility-averaged carrier gas velocity."

No proof or even explanation of validity of the replacement was given.

Several workers immediately adopted Eq. (2.168) in their studies in the early 1960s. Soon, however, the error was recognized [130] and retractions followed [127,131]. Nevertheless, Eq. (2.168) survived, and with rare exceptions [96,116], it is generally treated as a settled issue. There are several possible explanations for it. Eq. (2.168) has a simple structure, and in the case of substantial gas decompression, the average gas velocity (\bar{u}) in incorrect Eq. (2.168) is easier to measure than the gas local velocities (u) in correct Eq. (2.103) where u can be different at different locations along the column. The problem is, however, that Eq. (2.168) substantially distorts the reality. Another possible explanation of persistence of incorrect Eq. (2.168) is that, while being widely recommended, it is not taken seriously. Eq. (2.168) is not used for solving real theoretical or practical problems in GC (e.g., theoretical prediction of \bar{u}_{opt}). Rather, Eq. (2.168) is used as a simple mental picture (a picture—not a mathematical equation) of dependence, $H(\bar{u})$, of H on \bar{u} that has a minimum at some optimal \bar{u} . No one, even the workers advocating Eq. (2.168), proposed specific recommendations for \bar{u}_{opt} found from Eq. (2.168) and suitable for all practical columns in practical GC analyses (including GC-MS).

The correct $H(\bar{u})$, Eq. (2.134), is substantially more complex than incorrect Eq. (2.168), and the correct equation for \bar{u}_{opt} , Eq. (2.140), is substantially more complex than incorrect one in Eq. (2.170). For one thing, the correct \bar{u}_{opt} substantially depends on the column length (L) and outlet pressure (p_o), Fig. 2.12, Table 2.5. These dependencies are not represented in incorrect Eq. (2.170) for \bar{u}_{opt} . The numerical values of \bar{u}_{opt} obtained from Eq. (2.170) are incorrect for majority of practical applications, especially for GC-MS.

Not only Eq. (2.168) is the source of incorrect \bar{u}_{opt} values, but its very structure is misleading.

It distorts, e.g., the importance of optimization of \bar{u} . According to Eq. (2.168), a twofold departure of \bar{u} from \bar{u}_{opt} in any direction ($\bar{u} = 0.5\bar{u}_{\text{opt}}$ or $\bar{u} = 2\bar{u}_{\text{opt}}$) makes H larger (worse) than H_{min} by 25% ($H = 1.25H_{\text{min}}$). This is incorrect for many practical applications and especially for GC-MS. According to correct Eq. (2.146) for $H(\bar{u})$ in GC-MS, the twofold departure of \bar{u} from \bar{u}_{opt} more than doubles H compared to H_{min} ($H = 2.125H_{\text{min}}$), indicating that the column operation in GC-MS is substantially more sensitive to departures of \bar{u} from \bar{u}_{opt} than the incorrect Eq. (2.168) suggests. This causes the following “double-jeopardy” outcome. The error of incorrect theoretical prediction of \bar{u}_{opt} from Eq. (2.168) is the largest in GC-MS—exactly where an incorrect setting of \bar{u}_{opt} is the most harmful.

The dominant proliferation of incorrect Eq. (2.168) in the literature and in university courses is a substantial reason for confusions and mistrust in theory among practicing GC method developers.

2.10 Performance metrics

2.10.1 Metrics

An improvement in the separation performance can be considered as the primary goal of a column optimization. However, the separation performance is not the only performance factor in chromatography. Other factors are the *analysis time* and the *DL*. With no upper limit to the analysis time and no requirement for detection of low-concentration components, any separation performance could be possible. Therefore, a column optimization is a matter of obtaining the best trade-off between the separation, the time, and the DL where the focal point of optimization is the separation.

The metrics of separation performance in static and dynamic GC analyses were discussed

elsewhere [22,80,101,107,109,132–134]. Following is a brief review.

The most widely known metrics of separation performance of a chromatographic analysis are the resolution and the peak capacity. The *resolution* (R_s) of peaks A and B is defined as [20]:

$$R_s = \frac{\Delta t_R}{\bar{w}_b}, \quad \Delta t_R = t_{R,B} - t_{R,A}, \quad (2.172)$$

$$\bar{w}_b = \frac{w_{b,A} + w_{b,B}}{2}$$

where $t_{R,A}$ and $t_{R,B}$ are the retention times of peaks A and B, and $w_{b,A}$ and $w_{b,B}$ are their *base widths* defined as “the segment of the peak base intercepted by the tangents drawn to the inflection points on either side of the peak” [20]. For *Gaussian peaks*, $w_b = 4\sigma$. R_s becomes [5,107,122]:

$$R_s = \frac{\Delta t_R}{4\bar{\sigma}}, \quad \Delta t_R = t_{R,B} - t_{R,A}, \quad (2.173)$$

$$\bar{\sigma} = \frac{\sigma_A + \sigma_B}{2}, \quad (\text{Gaussian peaks})$$

The roots of the definition in Eq. (2.172) go back to the celebrated van Deemter et al. [80] 1956 paper stating that “a simple case [of peak separation] is obtained when the tangents of the elution curves of the subsequent solutes just touch at the base of the chromatogram.” The actual definition in Eq. (2.172) was proposed by Phillips in 1958 [135] and formally recommended by the leading authorities in chromatography [136] “as one which might be useful for the time being”. The “time being” still continues now—more than 60 years after its posting—as the resolution, R_s , remains the dominant metric of separation of peak pairs in chromatography [20].

Right from its introduction, R_s was met with skepticism as being “unnecessarily cumbersome” [135] and “difficult to use in most cases” [137]. Following are some shortcomings of R_s [22,134].

- If the peak shape is not known a priori, then w_b cannot be theoretically predicted from

known operational conditions of a GC analysis.

- If peaks are not Gaussian, then quotient 4 in Eq. (2.173) has no justification. For *exponential peaks*, e.g., $w_b = \sigma$ [2] (not $w_b = 4\sigma$ as for Gaussian peaks).
- R_s is not an *additive* metric: for consecutive peaks A, B, and C having different widths, $R_{s,AB} + R_{s,BC} \neq R_{s,AC}$.

These and other shortcomings of R_s [22,134] make it unsuitable for theoretical studies. But this is not all. Another, maybe the most significant, shortcoming is discussed further after introduction of peak capacity.

There are several different definitions of peak capacity in chromatography [134]. The one adopted in this chapter is slightly different from the original Giddings' definition [133], but identical to the definition that Giddings and Davis used in their studies of peak overlap statistics [5,138]. Following are several preliminary definitions [11,22] leading to the *Giddings–Davis* definition of the peak capacity of a chromatographic analysis [5,138].

Let t_A and t_B be the retention times of two peaks. The *separation* (Δs) of two peaks is the number of σ -slots (σ -long intervals) between their retention times [11,22]. If σ is the same for both peaks, then:

$$\Delta s = \frac{\Delta t}{\sigma}, \quad \Delta t = t_B - t_A, \quad (\sigma_B = \sigma_A = \sigma) \quad (2.174)$$

Otherwise:

$$\Delta s = \Delta s_{AB} = \int_{t_A}^{t_B} \frac{dt}{\sigma} \quad (2.175)$$

Generally, t_A and t_B do not have to be the peak retention times, but any time markers in the separation space of a chromatogram. In that case, Δs in Eq. (2.175) is the *separation capacity* of the time interval (t_A, t_B). One can also define the *running*

separation capacity (s)—the separation capacity of the interval from the void time (t_M) to an arbitrary time t within the separation space—and the separation capacity of the analysis (s_c) [11,22]:

$$s(t) = \int_{t_M}^t \frac{dt}{\sigma} \quad (2.176)$$

$$s_c = \int_{t_M}^{t_{\text{anal}}} \frac{dt}{\sigma} \quad (2.177)$$

It follows from Eqs. (2.175) and (2.176) that:

$$\Delta s = \Delta s_{AB} = s(t_B) - s(t_A) \quad (2.178)$$

and that, unlike R_s , metric Δs is an additive one, i.e., $\Delta s_{AC} = \Delta s_{AB} + \Delta s_{BC}$. This allows one to view the separation capacity (Δs) of any subspace of the separation space of a chromatogram as the incremental separation capacity. It can be approximated as:

$$\Delta s \approx \frac{\Delta t}{\bar{\sigma}}, \quad \Delta t = t_B - t_A, \quad \bar{\sigma} = \frac{\sigma_A + \sigma_B}{2} \quad (2.179)$$

For Gaussian peaks, the approximation error does not exceed 5% as long $\sigma_A \leq \sigma_B \leq 2\sigma_A$ [134].

The separation capacities (Δs , s , s_c) represent the numbers of σ -slots in respective separation spaces. Let Δs_{min} be the smallest number of σ -slots sufficient for resolving (identifiably and quantifiably separating) two consecutive peaks. Assuming that Δs_{min} is the same for all consecutive peaks (regardless of their height and widths), the incremental peak capacity (Δn) of an arbitrary interval, the running peak capacity (n), and the peak capacity of the analysis (n_c) can be defined as [11,22]:

$$\Delta n = \frac{\Delta s}{\Delta s_{\text{min}}}, \quad n = \frac{s}{\Delta s_{\text{min}}}, \quad n_c = \frac{s_c}{\Delta s_{\text{min}}} \quad (2.180)$$

The last equation is the Giddings–Davis definition of the peak capacity [5,138]. Since all

definitions of the separation capacity and the peak capacity are based on the peak standard deviation, both concepts are suitable for any peak shape.

It is frequently assumed that 6σ separation ($\Delta s_{\text{min}} = 6$, $R_s = 1.5$) is necessary for resolving two peaks by a simple data-analysis system [124,137]. Sometimes, $\Delta s_{\text{min}} = 8$ is considered [79]. For more powerful data analyses based on peak deconvolution, $\Delta s_{\text{min}} \leq 1$ might be sufficient for resolving two peaks [139–141]. Most frequently, however, n_c based on $\Delta s_{\text{min}} = 4$ ($R_s = 1$) is assumed.

Comparing with each other the metrics of the peak separation, the separation capacities, and the peak capacities of different intervals, one can notice that all of them represent a system of mutually compatible metrics. Thus, the separation (Δs) of two peaks is the number of σ -slots between the peaks while the incremental separation capacity (Δs) is the number of σ -slots between arbitrary time markers in a chromatogram. Furthermore, s is Δs when $t_A = t_M$, and s_c is s when $t = t_{\text{anal}}$. Similar relations exist between the peak capacities, which relate to the respective separation capacities by simple relations of proportionality.

There is an inevitable question. Why was it necessary for Giddings to introduce [133] the new concept of the peak capacity (n_c) of chromatographic analysis at the time (1967) when the concept of resolution was already well established? Why was it necessary to introduce the new concept of n_c rather than to simply extend the concept of the resolution (R_s) of two arbitrary peaks to the resolution (R_{sc}) of the peaks at t_M and at t_{anal} and treat it as the peak capacity? The first answer is that Eq. (2.173) for the resolution (R_s) makes sense only for Gaussian peaks, while the separation capacity and the peak capacity are defined for any peak shape. Suppose that this problem does not exist, i.e., all peaks are Gaussian. Was it necessary in this narrower case to introduce n_c rather than extending R_{sc} ?

Let's compare R_{sc} for Gaussian peaks with n_c at $\Delta s_{\min} = 4$ —both in static analyses with the same fixed Q . Eqs. (2.62), (2.126), (2.177), and (2.180) yield:

$$s = Q \ln(t/t_M) = Q \ln(1+k), \quad (\text{static}) \quad (2.181)$$

$$n_c = \frac{Q}{4} \ln \frac{t_{\text{anal}}}{t_M}, \quad (\text{static}, \Delta s_{\min} = 4) \quad (2.182)$$

On the other hand, Eqs. (2.126) and (2.173) yield for $t_{R,A} = t_M$ and $t_{R,B} = t_{\text{anal}}$:

$$R_{sc} = \left(\frac{1 - t_{\text{anal}}/t_M}{1 + t_{\text{anal}}/t_M} \right) \frac{Q}{2} < \frac{Q}{2} \quad (\text{Gaussian peaks}) \quad (2.183)$$

As expected, n_c increases when t_{anal} increases. However, this is not the case with R_{sc} . As it has been established earlier [22], the last equation shows that, no matter how long a static analysis lasts and how many resolvable peaks it generates, the resolution of the last and the first peak does not exceed the fixed number $Q/2$. In short, at some t_{anal} , the R_{sc} simply stops working as the peak separation metric. This might be the most significant shortcoming of R_s explaining why it was necessary to introduce the concept and the metric of the peak capacity in addition to the already well-established metric of R_s . The key reason for that goes back to the basics. While the separation (Δs) of two peaks represents a certain concept (the number of σ -slots between the peak retention times) expressed in Eq. (2.175), the resolution (R_s) is a mathematical expression, Eq. (2.172) or (2.173), without a clear underlying concept. It has been earlier suggested in this text that R_s is unsuitable for theoretical studies. The last observations reinforce this suggestion.

The introduction of the transparent metric Δs , Eq. (2.175), of the separation of two peaks makes R_s —the metric that is “unnecessarily cumbersome” [135] and “difficult to use in most cases” [137]—a redundant metric that can be

abandoned in favor Δs —a member of mutually compatible transparent metrics. In practical evaluations, an approximation $\Delta s \approx \Delta t/\bar{\sigma}$, Eq. (2.178), can be used. Comparing this approximation with the definition, Eq. (2.173), of R_s suggests that, first, the approximation $\Delta s \approx \Delta t/\bar{\sigma}$ is suitable for any peak shape while R_s in Eq. (2.173) is only suitable for Gaussian ones, and second, $\Delta s \approx \Delta t/\bar{\sigma}$ is an approximation that can be reverted to an exact definition, Eq. (2.175), of Δs as soon as the approximation error becomes unacceptable, while R_s in Eq. (2.173) is the definition that does not work in many theoretically and practically important cases.

On the other hand, although it is certainly desirable to use one metric, Δs , in theoretical and practical applications instead of two— R_s in practical applications and Δs in theoretical studies— R_s will probably continue to dominate the practice. For two closely spaced Gaussian peaks, R_s can be approximated as [107,132]:

$$R_s \approx \frac{\sqrt{N}}{4} \frac{k_A}{1+k_A} (\alpha - 1), \quad (\text{Gaussian}, \quad |\alpha - 1| \ll 1) \quad (2.184)$$

The separation (Δs) of two closely spaced peaks of any shape can be approximated as [22,23]:

$$\Delta s = Q\omega_A \Delta g, \quad (|\Delta g| \ll 1) \quad (2.185)$$

where $\omega = k/(1+k)$ is a solute *immobility* (its fraction in the stationary phase), Eqs. (2.3) and (2.4), while [22,23].

$$\Delta g = g_B - g_A = \ln \frac{k_B}{k_A} = \ln \alpha \quad (2.186)$$

is the *separability* of solutes A and B—the difference in their dimensionless Gibbs free energies (g_A and g_B), Eqs. (2.7) and (2.10). One can conclude that, for closely spaced Gaussian peaks, Δs and R_s relate to each other as [22,23]:

$$R_s \approx \Delta s/4 \quad (\text{closely - spaced Gaussian peaks}) \quad (2.187)$$

On the other hand, while (as demonstrated earlier) R_s might not even make sense if the peaks are not closely spaced or are substantially non-Gaussian, Δs is meaningful for any spacing of peaks of any shape. If Q is the same for all solutes, then Δs for peaks A and B of any spacing and any shape in *static* analysis can be expressed as [22,23]:

$$\Delta s = Q\bar{\omega}_g\Delta g \quad (2.188)$$

where

$$\bar{\omega}_g = \frac{1}{\Delta g} \int_{g_A}^{g_A+\Delta g} \omega dg = \frac{\ln(1 + (e^{\Delta g} - 1)\omega_A)}{\Delta g}, \quad (2.189)$$

(static media)

is the *separability-averaged immobility* of all solutes that could elute between solutes A and B. In the essence, the separation (Δs) of peaks A and B is the sum of the separations of consecutive pairs of peaks that exist (or could exist) between peaks A and B. The last two expressions together with Eqs. (2.4) and (2.10) yield:

$$\Delta s = Q \ln \frac{1 + k_B}{1 + k_A}, \quad (\text{static media}) \quad (2.190)$$

The same result follows from Eqs. (2.178) and (2.181).

For peaks A and B appearing during heating ramp in temperature-programmed analysis, Eq. (2.175) can be expressed in temperature domain as:

$$\Delta s = \Delta s_{AB} = \int_{T_A}^{T_B} \frac{dT}{\sigma_T} \quad (2.191)$$

As all highly interactive solutes elute during a linear heating ramp with approximately equal widths, their separation (Δs_a) can be expressed as:

$$\Delta s_a = \frac{\Delta T}{\sigma_{T,a}}, \quad \Delta T = T_B - T_A \quad (2.192)$$

where $\sigma_{T,a}$ is the width of a highly retained peak within (T_A, T_B) ranges. For better accuracy, $\sigma_{T,a}$ can be the width of a peak in the middle of (T_A, T_B) ranges. From Eqs. (2.84) and (2.165), the last equation can be expressed for generic solutes in isobaric analysis as:

$$\Delta s_a \approx Q\bar{\omega}_a \frac{\Delta T_{\text{char}}}{\theta_{\text{char}G}}, \quad \Delta T_{\text{char}} = T_{\text{char}, B} - T_{\text{char}, A} \quad (2.193)$$

The temperature change during its migration causes the change in the solute immobility (ω)—its fraction in the stationary phase, Eq. (2.3). Quantity $\bar{\omega}_a$ in the last equation for Δs_a is the column-length-averaged ω , Eq. (2.87), of a highly interactive solute. For nongeneric solutes (having different θ_{char}), the last expression becomes, from Eq. (2.88):

$$\Delta s_a \approx \frac{Q\bar{\omega}_a}{\theta_{\text{char}}} (\Delta T_{\text{char}} + X_\theta \Delta \theta_{\text{char}}),$$

$$\Delta \theta_{\text{char}} = \theta_{\text{char}, B} - \theta_{\text{char}, A} \quad (2.194)$$

where function X_θ of r_T is defined in Eq. (2.89).

2.10.2 Benchmarks

As will be seen shortly, the separation capacity (s_c) of chromatographic analysis plays a key role in optimization of heating rate in temperature-programmed analysis. However, both s_c and the peak capacity (n_c) of chromatographic analysis are less suitable for *column comparison*. Indeed, s_c substantially depends on analysis time (t_{anal}) or on temperature range (ΔT) of a heating ramp that can be different for *different samples* analyzed in *the same column* under *the same operational conditions*. Compare, e.g., analyses of two different samples using the same column, under the same operational conditions. Suppose that the last component of one sample elutes at, say, 200°C while a different last component of a different sample elutes at 300°C. If s_c is the separation capacity of the analysis lasting till the last peak, then s_c of the first

analysis would be substantially smaller than that of the second analysis. This, however, depends not on the column or its operational conditions, but solely on the difference between the samples, indicating that s_c is not suitable for comparison of the columns. The same is true for n_c . The separation capacity (Δs) of a specific predetermined interval in the separation space of a chromatogram can be more suitable for column comparison.

Let's define the *exponential interval* (t_A , t_B) in static analysis and its separation capacity (Δs_{exp}) as, respectively, a one where $t_B/t_A = e$ ($e \approx 2.72$) and

$$\Delta s_{\text{exp}} = \Delta s_{AB} \Big|_{t_B=et_A} \quad (2.195)$$

Quantity Δs_{exp} does not depend on the sample, but only on a column and its operational conditions, and, therefore, is suitable for column comparison. The same is true for the peak capacity, $\Delta n_{\text{exp}} = \Delta s_{\text{exp}}/\Delta s_{\text{min}}$, where Δs_{min} is a fixed quantity. It follows from Eqs. (2.178) and (2.181) that:

$$\Delta s_{\text{exp}} = Q, \quad (\text{static analysis, fixed } Q) \quad (2.196)$$

leading to a transparent interpretation of parameter Q (in addition to its definition as $Q = t_R/\sigma$, Eq. 2.126):

If the transport efficiency (Q) of a column in static analysis is the same for all peaks, then Q is the separation capacity of an exponential interval in that analysis.

This observation suggests that Q can be used as a *benchmark* of the separation capacity of static (isothermal isobaric) GC analysis.

Example 2.11. According to Eq. (2.181), static analysis occupying three consecutive exponential intervals (i.e., lasting till $1 + k = e^3 \approx 20$) has $s_c = Q \ln 20 \approx 3Q$. Its 4σ peak capacity is $n_c = s_c/4 \approx 0.75Q$. In other words, Q is close to potential peak capacity of a typical isothermal GC analysis.

Consider now a θ_{charG} -wide temperature interval within heating ramp, where θ_{charG} is the characteristic thermal constant of generic solute

having characteristic temperature T_{char} , Eq. (2.18). The separation capacity for highly retained solutes eluting during θ_{charG} -wide temperature interval is the *characteristic separation capacity* (Δs_{char}). Substitution of $\Delta T_{\text{char}} = \theta_{\text{charG}}$ in Eq. (2.193) and accounting for Eq. (2.87) yields for isobaric analysis (Fig. 2.14):

$$\Delta s_{\text{char}} = Q \bar{w}_a = \frac{(1 - e^{-r_T})Q}{r_T} \quad (2.197)$$

As $\bar{w}_a < 1$ (Fig. 2.14), $\Delta s_{\text{char}} < Q$. In a slow heating ramp, i.e., when $r_T \ll 1$, \bar{w}_a is close to unity and

$$\Delta s_{\text{char}} = Q, \quad (r_T \ll 1) \quad (2.198)$$

A column transport efficiency (Q) is the characteristic separation capacity (Δs_{char}) of a slow ($r_T \ll 1$) isobaric temperature-programmed analysis.

Similarly to Δs_{exp} in static analysis, Δs_{char} does not depend on the sample, but only on a column and its operational conditions, and, therefore, is suitable for column comparison. The same is true for *characteristic peak capacity*, $\Delta n_{\text{char}} = \Delta s_{\text{char}}/\Delta s_{\text{min}}$, where Δs_{min} is a fixed quantity.

Eq. (2.198) indicates that Q can serve as a *benchmark* for separation capacity of a linear heating ramp. Expressed in terms of temperature range, the equations for characteristic separation capacity (Δs_{char}) are equally valid for all columns

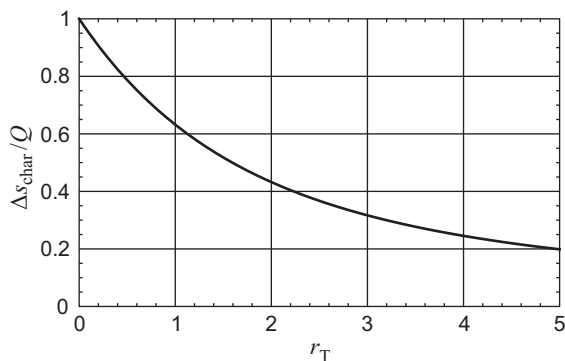


FIGURE 2.14 Characteristic separation capacity (Δs_{char}), Eq. (2.199), of isobaric temperature-programmed analysis with dimensionless heating rate r_T , Eq. (2.69).

and samples, carrier gas types and flow rates, heating rates, etc. The solutes with larger T_{char} have larger θ_{charG} and generally elute at higher temperatures. For the ones with $T_{\text{char}} \approx 150^\circ\text{C}$ (approximately a middle of GC temperature range) $\theta_{\text{charG}} \approx 30^\circ\text{C}$, Eq. (2.18), for all known pairs of stationary phases and solutes.

Example 2.12. The estimate $\theta_{\text{charG}} \approx 30^\circ\text{C}$ indicates that Δs_{char} is the separation capacity (Δs_{a}) of approximately 30°C -wide temperature range of a linear heating ramp.

It is shown below that, at optimal heating rate, $r_{\text{T,Opt}} = 0.4$. Eq. (2.197) yields:

$$\Delta s_{\text{char,Opt}} \approx 0.8Q \quad (2.199)$$

Example 2.13. Eq. (2.199) and the estimate that Δs_{char} is the separation capacity (Δs_{a}) of approximately 30°C -wide temperature range (Example 2.12) imply that Q is the optimal separation capacity ($\Delta s_{\text{a,Opt}}$) of approximately 37.5°C -wide temperature range. This further implies that the optimal separation capacity of 150°C -wide temperature range (say, from 75 to 225°C) is $4Q$, and that of 225°C -wide temperature range (say, from 35 to 260°C) is $6Q$. Accordingly, the 4σ peak capacities of 150 and 225°C wide temperature intervals are, respectively, Q and $1.5Q$.

One way or another,

A column transport efficiency (Q) can serve as a benchmark for the separation capacity and the peak capacity of isothermal and temperature-programmed analyses.

It can be added in closing that the concepts of Δs_{exp} and Δn_{exp} are suitable for static LC. Furthermore, the characteristic parameters can also be defined in LC [110,142] extending metrics Δs_{char} and Δn_{char} to LC. This makes it possible not only to compare performance of GC or LC columns among themselves, but also to compare the column performance in different separation techniques. Moreover, relationships $\Delta s_{\text{exp}} = \Delta s_{\text{char}} = Q$, Eqs. (2.196) and (2.198), as

well as $\Delta s_{\text{char,Opt}} \approx 0.8Q$, Eq. (2.199), are valid in LC [110,143] indicating that Q can serve as the separation capacity benchmark in both techniques.

2.11 Optimization

2.11.1 Targets of column optimization

Two types of separation performance can be considered—the *specific* and the *general* separation performance [22]. The former is concerned with separation of closely spaced peaks representing specific solutes. It depends on the column kinetics and selectivity thermodynamics and can be measured by metrics such as peak resolution, separation, etc. Changing column temperature in static analysis or heating rate in dynamic analysis can substantially change the separation of two solutes, or nullify it, or even reverse their elution order. These outcomes (like the total absence of separation of two specific solutes) might happen not because this temperature or that heating rate is generally unsuitable, but only because they are unsuitable for a specific solute pair. On the other hand, the *general separation performance* is concerned with issues such as the number of peaks that a given separation technique or a given analysis can resolve (identifiably and quantifiably separate) or the number of resolved peaks that can be packed in a certain subspace of the separation space of a given analysis, etc. These properties can be represented by respective peak capacities. The peak capacity depends, Eq. (2.180), on the column separation performance and on the ability of the data analysis system to identify and quantify poorly separated peaks. This chapter is concerned only with the optimization of the trade-off between a column general separation performance and time where there is no need to bring in the picture the properties of data analysis systems. The key metric of a column separation performance characterization and optimization is the separation capacity.

A column optimization considered here can be called as the *speed optimization*, which is obtaining the shortest analysis time at a *required separation capacity* (s_c) of the column (at a given number of σ -slots in a chromatogram). As shown further, this optimization is different from, say, obtaining the highest s_c in a given column. Eq. (2.197) for the characteristic separation capacity of highly interactive solutes (Δs_{char})—a benchmark of a column performance in temperature-programmed analysis—shows that the performance depends on two factors—the column transport efficiency (Q) and the dimensionless heating rate (r_T). Therefore, the goal of a column optimization can be split into two goals—optimization of Q and optimization of r_T . The latter is the heating rate (R_T) expressed in relation to the solute characteristic thermal constants and the void time (t_M), Eq. (2.69). Therefore, the speed optimization of Q can be formulated as obtaining a required Q at the shortest t_M . From Eqs. (2.52) and (2.152), the latter can be expressed as a function of Q [11]:

$$t_M = t_M(d, Q, f) = \frac{\pi^2 d^4 p_0^3}{1536 p_{\text{st}}^2 \eta f^2} \left(\left(1 + \frac{256 Q^2 p_{\text{st}} \eta}{\pi d^2 p_0^2} h f \right)^{3/2} - 1 \right) = \begin{cases} \frac{\pi d^2 Q^2 p_0}{4 p_{\text{st}}} \frac{h}{f}, & |\Delta p| \ll p_0 \\ \frac{8 d Q^3}{3} \sqrt{\frac{\pi \eta}{p_{\text{st}}}} \frac{h^3}{f}, & \Delta p \gg p_0 \end{cases} \quad (2.200)$$

2.11.2 Optimal flow rate

A column transport efficiency (Q) in dynamic analysis is defined, Eq. (2.153), as Q in static (isothermal isobaric) analysis under conditions existing in dynamic (temperature- and/or pressure-programmed) analysis at a solute elution time. Therefore, optimization of Q in dynamic analysis can be reformulated as optimization of Q in static analysis.

The earliest study of speed optimization of Q is known from Scott and Hazeldean (1960) [144]. Ignoring gas compressibility, they described the following optimization procedure. A column operating at optimal flow rate (F_{opt}) has minimal plate height (H_{min}) and maximal $Q(Q_{\text{max}})$. Let $t_{M,\text{opt}}$ be the optimal void time under these conditions. If F is doubled to $F = 2F_{\text{opt}}$, then H will increase by 25%, Eq. (2.142). By using 25% longer column with otherwise the same parameters, the Q_{max} will be restored. However, the new t_M , equal to $0.5 \times 1.25 t_{M,\text{opt}} = 0.625 t_{M,\text{opt}}$, will be 37.5% shorter than $t_{M,\text{opt}}$, demonstrating that, by simultaneous variation of F and the column length (L), t_M can be reduced without reducing Q . These ideas were the basis for further developments of speed optimization of Q accounting for the gas decompression [1,145] as described further.⁷

The speed optimization of the flow rate (F) is formulated as finding its optimum (F_{opt}) that leads to the shortest t_M at a required Q .

The optimal F minimizing t_M at a *required* Q might be different from the optimal F (F_{opt}) minimizing H and, therefore, maximizing Q in a *given* column. To distinguish these flow rates, F_{opt} is called as the *efficiency-optimized flow rate* (EOF)

⁷ In the original Scott–Hazeldean analysis [144], simultaneous variation of average gas velocity (\bar{u}) and column length (L) was considered and the concept of optimum practical gas velocity ($\text{OPGV} = 2\bar{u}_{\text{opt}}$) was introduced. Unfortunately, the original study was based on incorrect plate height expression $H = B/\bar{u} + C\bar{u}$ (see Section 2.9.3 Incorrect plate height equation). As a result, although the OPGV was recommended without reservations and is frequently assumed to be suitable for all GC applications, the concept is meaningful only in a narrow case of the weak gas decompression and cannot be utilized in practically important applications with strong decompression such as GC-MS and others [2].

[115], while F minimizing t_M at a required Q is called as the *speed-optimized flow rate* (SOF) [115] and denoted as F_{Opt} (Capital “O” in subscript “Opt”). Accordingly, the specific flow rate minimizing t_M at a required Q is called as the *specific speed-optimized flow rate* (SSOF) and denoted as f_{Opt} . From Eq. (2.45), the SOF (F_{Opt}) can be found from f_{Opt} as:

$$F_{\text{Opt}} = df_{\text{Opt}} \frac{T_{\text{norm}}}{T} \quad (2.201)$$

suggesting that optimization of the flow rate (F) can be reduced to optimization of the specific flow rate (f). As shown below, both (F_{Opt} and f_{Opt}) directly relate to their efficiency-optimized counterparts (F_{opt} and f_{opt}). Eqs. (2.138) and (2.139) show that F_{Opt} depends on column diameter (d), while f_{opt} does not and, therefore, is suitable for the columns of all diameters. Additionally, f_{opt} does not depend on the choice of the flow measurement temperature ($T_{\text{norm}} = 25^\circ\text{C}$, in this chapter), while F_{Opt} does.

2.11.2.1 Strong gas decomposition

It is convenient to start the analysis of a gas flow optimization from the case of a *strong gas decomposition* along the column, i.e., when $\Delta p \gg p_o$. These are the most demanding and most typical applications because the decomposition is strong in all GC-MS analyses and in analyses of complex mixtures requiring relatively long, relatively narrow columns. It follows from Eq. (2.200) that, at any fixed f (optimal or not):

$$t_M \sim Q^3 \quad (\text{strong decomposition, fixed } d \text{ and } f) \quad (2.202)$$

It also follows from Eq. (2.200) at strong decomposition that t_M has a minimum ($t_{M,\text{Min}}$) at a given Q and d when quantity h^3/f has a minimum. To find this minimum, let's express Eq. (2.150) as (Fig. 2.15A):

$$\frac{h^3 f_{\text{opt}}}{f} = \frac{h_{\text{min}}^3 \cdot f_{\text{opt}}}{8 \cdot f} \left(\frac{f_{\text{opt}}}{f} + \frac{f}{f_{\text{opt}}} \right)^3 \quad (2.203)$$

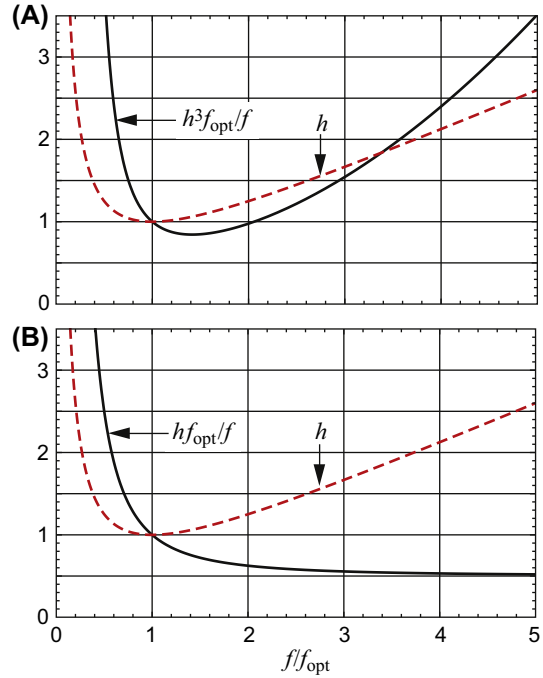


FIGURE 2.15 Quantities $h^3 f_{\text{opt}}/f$ and $h f_{\text{opt}}/f$ as functions of f , Eqs. (2.203) and (2.222), solid lines. Functions h of f , Eq. (2.150) are included for the references. Quantity $h^3 f_{\text{opt}}/f$ in (A) has a minimum at $f = f_{\text{opt}} = \sqrt{2} f_{\text{opt}}$. Quantity $h f_{\text{opt}}/f$ in (B) approaches its lowest level at infinitely large f .

This expression and, therefore, t_M have a minimum at:

$$f_{\text{Opt}} = \sqrt{2} f_{\text{opt}} \quad (\text{strong decomposition}) \quad (2.204)$$

As $f = f_{\text{Opt}}$ yields the lowest h^3/f at a fixed Q , it also yields, according to Eq. (2.200), the lowest t_M ($t_{M,\text{Min}}$) at fixed Q and the largest Q at a fixed t_M . In other words,

At $f = f_{\text{Opt}}$, the void time (t_M) is the shortest for a given efficiency (Q), or, conversely, Q is the largest for a given t_M

For practical applications, one needs to transform f_{Opt} into F_{Opt} , which, from Eqs. (2.201) and (2.204), can be expressed as:

$$F_{\text{Opt}} = \sqrt{2} F_{\text{opt}} \quad (\Delta p \gg p_o) \quad (2.205)$$

At $f = f_{\text{Opt}}$ Eq. (2.150) yields for the *optimal dimensionless plate height* (h_{Opt}) in a speed-optimized column:

$$\begin{aligned} h_{\text{Opt}} &= \frac{h_{\text{min}}}{2} \left(\frac{1}{\sqrt{2}} + \sqrt{2} \right) \\ &= \frac{3h_{\text{min}}}{2\sqrt{2}} \approx 1.061h_{\text{min}} \quad (\Delta p \gg p_o) \end{aligned} \quad (2.206)$$

This means that the speed optimization increases the plate height (h_{Opt}) by about 6% compared to its efficiency-optimized value (h_{min}). This, according to Eq. (2.152), reduces the column efficiency by practically negligible 3% compared to its original maximum ($Q_{\text{max,col}}$) for the same column at $f = f_{\text{opt}}$. However, to sustain the theoretical assumption of a fixed efficiency in Eq. (2.200), the lost efficiency can be regained by using a longer column, i.e., replacing the original L_{orig} -long column with the one having the *optimal length* (L_{Opt}):

$$L_{\text{Opt}} = \frac{3L_{\text{orig}}}{2\sqrt{2}} \approx 1.061L_{\text{orig}} \quad (\Delta p \gg p_o) \quad (2.207)$$

Let $t_{M,\text{opt}}$ and $t_{M,\text{Opt}}$ be t_M at f_{opt} and f_{Opt} respectively. Two versions ($t_{M,\text{Opt},L}$ and $t_{M,\text{Opt},Q}$) of $t_{M,\text{Opt}}$ can be considered. The former is $t_{M,\text{Opt}}$ in a column of a fixed length while the latter is in the column of a fixed efficiency. When quantities $t_{M,\text{Opt},L}$ and $t_{M,\text{Opt},Q}$ are compared with each other, it is assumed that all parameters (column diameters, carrier gas types, etc.) other than the column length and efficiency are the same in both cases. It can be noticed that $t_{M,\text{Opt},Q}$ is also the shortest t_M ($t_{M,\text{Min}}$) that can be obtained at a given Q (in a column of a given diameter, with a given carrier gas, etc.). However, for the symmetry of notations, it is more convenient to keep the notation $t_{M,\text{Opt},Q}$ rather than $t_{M,\text{Min}}$ when comparing the quantity represented by these notations with $t_{M,\text{Opt},L}$.

It follows from Eq. (2.52) at $\Delta p \gg p_o$ that the relative reduction in t_M at a fixed L is proportional to the relative increase in \sqrt{f} . As a result,

$$\begin{aligned} \frac{t_{M,\text{Opt},L}}{t_{M,\text{opt}}} - 1 &= \sqrt{\frac{1}{\sqrt{2}}} - 1 \approx -0.16 \\ &\text{(strong decompression)} \end{aligned} \quad (2.208)$$

On the other hand, it follows from Eq. (2.200) at $\Delta p \gg p_o$ that the relative reduction in t_M at a fixed Q is proportional to the relative reduction in $\sqrt{h^3/f}$. As a result (Fig. 2.15A),

$$\begin{aligned} \frac{t_{M,\text{Opt},E}}{t_{M,\text{opt}}} - 1 &= \sqrt{\frac{1}{8} \cdot \frac{1}{\sqrt{2}} \left(\frac{1}{\sqrt{2}} + \sqrt{2} \right)^3} - 1 \\ &= \sqrt{\frac{27}{32}} - 1 \\ &= -0.0814 \quad (\Delta p \gg p_o) \end{aligned} \quad (2.209)$$

The 16% smaller $t_{M,\text{Opt},L}$ compared to $t_{M,\text{opt}}$ comes at a cost of the earlier shown 3% smaller column efficiency (Q), while the 8% smaller $t_{M,\text{Opt},Q}$ compared to $t_{M,\text{opt}}$ comes at no reduction in Q . In other words, using SOF in a *given column* reduces the time and the efficiency by 16% and 3%, respectively, compared to those at EOF in the same column. On the other hand, using SOF in 6% longer column reduces the time by 8% with no loss in efficiency compared to their counterparts in the original column at EOF. Practically, probably no method developer would consider changing the column when considering the choice between EOF and SOF. This suggests that

The practical outcome of choosing SOF instead of EOF is 16% shorter time and 3% lower Q .

This also suggests that

SOF is practically always preferable to EOF, and there is no practical reason for using EOF instead.

All forthcoming recommendations are based only on SOF, while EOF is only used as an intermediate step in calculations of SOF. If necessary, however, one can find EOF (F_{opt}) from SOF as $F_{\text{opt}} = F_{\text{Opt}}/\sqrt{2}$, Eq. (2.205).

How does $t_{\text{M,Opt}}$ depend on the carrier gas type? Eqs. (2.52) and (2.200) describe the dependence of t_{M} on gas viscosity (η). Substitution of $f = f_{\text{Opt}}$ in Eq. (2.52) or in Eq. (2.200) and accounting for Eqs. (2.204) and (2.138) shows how $t_{\text{M,Opt}}$ also depends on a solute diffusivity (D_{pst}) at standard pressure. For a given gas, parameters η and D_{pst} are mutually dependent quantities. As a result, dependence of $t_{\text{M,Opt}}$ on η and D_{pst} does not provide a complete picture of dependence of $t_{\text{M,Opt}}$ on the gas type. Accounting for Eqs. (2.135), (2.21), and (2.20) yields:

$$t_{\text{M,Opt}} = \frac{8\sqrt{5\sqrt{2}L^3\vartheta_{\text{G1}}}}{3\sqrt{3\pi\sqrt{3}d}} \frac{k^{0.05}}{(10^3\phi)^{0.045}} \left(\frac{T}{T_{\text{st}}}\right)^{0.125} \frac{1}{X_{\text{D}v_{\text{st}}}},$$

($\Delta p > > p_o$)

(2.210)

This shows that $t_{\text{M,Opt}}$ is inversely proportional to the product $X_{\text{D}v_{\text{st}}}$ listed for several gases in Table 2.2. The key component in this product is the average molecular speed (v_{st}) of a gas at standard pressure and temperature. Relative values of $t_{\text{M,Opt}}$ of hydrogen in relation to $t_{\text{M,Opt}}$ of other gases are listed in Table 2.6.

At strong gas decomposition, a column with hydrogen at SOF has 40% shorter void time (and analysis time) than the same column with helium at SOF.

The peak width at strong gas decomposition can be expressed as [11][158]:

$$\sigma = \frac{8L}{3\mu_{\text{R}}} \sqrt{\frac{\pi\eta h}{p_{\text{st}} f}} \quad (\text{strong decomposition})$$

(2.211)

which, from Eqs. (2.150), (2.204), (2.166), yields at $f = f_{\text{Opt}}$:

$$\sigma_{\text{Opt}} = \frac{2L}{\mu_{\text{R}}} \sqrt{\frac{2\pi h_{\text{min}}\vartheta_{\text{G1}}\eta}{3\sqrt{3}\pi D_{\text{pst}}p_{\text{st}}X_{\text{T}}}} \quad (f = f_{\text{Opt}})$$

(2.212)

Remarkably [2,11,117,158],

At strong gas decomposition at SOF, the column diameter has no effect on the peak width (the latter is proportional to the column length).

From Eq. (2.211), one can also find σ at $f \rightarrow \infty$. This would be the narrowest peak width (σ_{min}) that can be obtained in a column of a given length in isothermal analysis at a given temperature or in temperature-programmed analysis with a given dimensionless heating rate. It is interesting that

$$\frac{\sigma_{\text{min}}}{\sigma_{\text{Opt}}} = \sqrt{\frac{2}{3}} \approx 0.82$$

(2.213)

In a column with strong gas decomposition at SOF, further flow rate increase up to infinity can only reduce the peak width by less than 20%.

TABLE 2.6 Flow-related parameters of several gases.

Gas	Units	Conditions	Equation	H ₂	He	N ₂	Ar
$f_{\text{iso},150}$	mL/min/mm	Isothermal	Eq. (2.217)	10	8	2.4	2.1
X_{σ}	ms/m	150°C	Eq. (2.215)	4.4	7.3	12.4	15.0
$t_{\text{M,Opt,hydrogen}}/t_{\text{M,Opt}}$	1	Weak decomposition	Eq. (2.223)	1	0.8	0.24	0.21
$t_{\text{M,Opt,hydrogen}}/t_{\text{M,Opt}}$	1	Strong decomposition	Eq. (2.210)	1	0.6	0.34	0.28
$t_{\text{M,Opt,hydrogen}}/t_{\text{M,Opt}}$	1	Same p_o , p_i and Q	Eq. (2.224)	1	0.45	0.5	0.4

Substitution of Eqs. (2.135), (2.21) and (2.20) in Eq. (2.212) expresses σ_{Opt} via a gas-dependent product $X_{D^{\text{vst}}}$ (Table 2.2) as:

$$\sigma_{\text{Opt}} = \frac{4}{3} \sqrt{\frac{10}{\sqrt{3}\pi}} \sqrt{\frac{h_{\text{min}} \vartheta_{\text{G1}}}{X_T}} \left(\frac{T}{T_{\text{st}}}\right)^{0.125} \frac{Lk^{0.05}}{\mu_{\text{R}}(10^3\varphi)^{0.045}} \frac{1}{X_{D^{\text{vst}}}} \quad (2.214)$$

The essence of this relationship can be expressed as

$$\sigma = \frac{X_{\sigma} L}{\mu_{\text{R}}} \quad (2.215)$$

where the values of X_{σ} for several gases at predetermined reference conditions are listed in Table 2.6 [11]. This is the simplest way of predicting σ in isothermal and temperature-programmed analyses at strong gas decompression in general and in GC-MS in particular [11,108,117,159].

2.11.2.2 Practical recommendations

As follows from Eq. (2.45), F is proportional to the column internal diameter (d) and to specific flow rate (f) independent of d . It is convenient, therefore, to recommend f_{Opt} leaving the method developer to find F_{Opt} from known f_{Opt} as described further.

Quantity f_{Opt} can be found from f_{opt} using Eq. (2.204). According to Eqs. (2.166) and (2.167), f_{opt} depends on the carrier gas type and its temperature (through solute diffusivity, D_{pst} in the gas), on a solute retention factor and diffusivity in the gas (through parameter ϑ and D_{pst}). On top of that, f_{opt} values in isothermal and temperature-programmed analyses are different from each other. The specific value of f_{opt} for several gases can be found from following considerations. The ratios of D_{pst} for the same solute in different gases are listed in Table 2.2. Therefore, if f_{opt} is known for one gas, its values for other gases can be found accordingly. Furthermore, it is convenient to recommend f_{Opt} for one temperature, to find F_{Opt} at that temperature, and to consider the need for the temperature adjustment of F_{Opt} after that. With

these considerations, the solute retention factor (k) remains the only unknown parameter in calculation of f_{opt} . A reasonable choice is $k = 2$, Example 2.10.

Parameter F_{Opt} at reference temperature, $T_{\text{ref}} = 150^{\circ}\text{C}$ (approximate middle of GC temperature range) can be found from Eqs. (2.45) and (2.204) as:

$$F_{\text{Opt,ref}} = \frac{T_{\text{norm}}}{T_{\text{ref}}} f_{\text{Opt,ref}} d = \sqrt{2} \frac{T_{\text{norm}}}{T_{\text{ref}}} f_{\text{opt,ref}} d \quad (2.216)$$

If $f_{\text{opt,ref}}$ corresponds to specific conditions, then the corresponding F_{Opt} is optimal only for those conditions. It is convenient to view F_{Opt} as the *default* value [119] (F_{Def}) for the respective optimum and consider the evaluation of its closeness to the actual optima for other conditions as a separate issue. Eq. (2.216) can be expressed as:

$$F_{\text{Def,ref}} = f_{\text{Ref}} d \quad (2.217)$$

where

$$f_{\text{Ref}} = \sqrt{2} \frac{T_{\text{norm}}}{T_{\text{ref}}} f_{\text{opt,ref}} \quad (2.218)$$

For isothermal analysis with hydrogen at 150°C in a column with $\varphi = 0.001$ and solute with $k = 2$, $f_{\text{opt,ref}} = 9.72 \text{ mL/min/mm}$ (Table 2.5). One has:

$$f_{\text{Ref}} = f_{\text{iso,150,H2}} = \sqrt{2} \frac{298.15\text{K}}{423.15\text{K}} \frac{9.72 \text{ mL}}{\text{min mm}} \approx \frac{10 \text{ mL}}{\text{min mm}} \quad (2.219)$$

Similar parameters for other gases can be found from $f_{\text{iso,150,H2}}$ using the diffusivity ratios in Table 2.2. Accounting for Eq. (2.166) and assuming that, in temperature-programmed analyses, $X_T = 0.7$ (Example 2.10), Eq. (2.217) can be expressed as:

$$F_{\text{Def,150}} = f_{\text{iso,150}} X_T = f_{\text{iso,150}} \begin{cases} 1, & \text{isothermal conditions} \\ 0.7, & \text{temperature program} \end{cases} \quad (2.220)$$

with $f_{\text{iso},150}$ values compiled for several gases in Table 2.6 [11,115,119]. In isobaric temperature-programmed GC, the flow rate changes during the analysis.

The recommended default can be implemented in isobaric analysis by choosing the column pressure so that, at 150°C, the flow rate is equal to $F_{\text{Def},150}$ calculated as $F_{\text{Def},150} = f_{\text{Def},150}d$ with $f_{\text{Def},150}$ selected according to Eq. (2.220).

2.11.2.3 Weak gas decompression

It follows from Eq. (2.200) that at weak gas decompression, i.e., when $|\Delta p| \ll p_o$,

$$t_M \sim Q^2 \quad (\text{weak decompression, fixed } d \text{ and } f) \quad (2.221)$$

It also follows from Eq. (2.200) that, at weak decompression, the void time (t_M) is the shortest at a given Q and d when quantity hf_{opt}/f is the lowest. To find the lowest hf_{opt}/f , Eq. (2.150) can be expressed as (Fig. 2.15B):

$$\begin{aligned} \frac{hf_{\text{opt}}}{f} &= \frac{h_{\text{min}}}{2} \cdot \frac{f_{\text{opt}}}{f} \left(\frac{f_{\text{opt}}}{f} + \frac{f}{f_{\text{opt}}} \right) \\ &= \frac{h_{\text{min}}}{2} \cdot \left(1 + \frac{f_{\text{opt}}^2}{f^2} \right) \end{aligned} \quad (2.222)$$

This quantity and, therefore, t_M do not have a minimum, but approach their lowest levels when f approaches infinity. It means that increasing the flow rate and the column length so that the column efficiency remains fixed always reduces t_M (and the analysis time). This is a more formal expression of the original 1960 Scott–Hazeldean model of a column speed optimization [144]. It does not tell the whole story, however.

Under realistic conditions, an unlimited increase in the flow rate (F) and in the column length (L) in order to reduce t_M without reducing efficiency (Q) inevitably leads to high pressure drop and strong gas decompression. This means that the weak gas decompression does not have

a property of *closure*—the speed optimization at weak decompression inevitably transitions to conditions that are outside of the weak decompression.

Equations describing the speed optimization accounting for transitioning from weak to strong gas decompression along the column are complex. The essential results are illustrated in Figs. 2.16 and 2.17. The minor effect of the Giddings compressibility factor (j_G), Eq. (2.130), on column performance at weak gas decompression was ignored in Figs. 2.16 and 2.17 and in their discussion.

Fig. 2.16 illustrates the transitional parameters F_{Opt}^* and L_{Opt}^* —the SOF and the optimal column length, respectively, corresponding to the shortest t_M at a fixed Q in the region of transitioning from the weak to the strong gas decompression. These parameters can be different from their respective counterparts, F_{Opt} and L_{Opt} , Eqs. (2.205) and (2.207), at strong decompression.

Example 2.14. Consider a $5 \text{ m} \times 0.53 \text{ mm}$ column with hydrogen at 150°C and at $p_o = 1 \text{ atm}$. For this column, $F_{\text{Opt}} = 5.3 \text{ mL/min}$ (Eq. (2.220), Table 2.6) and, from Eq. (2.205),

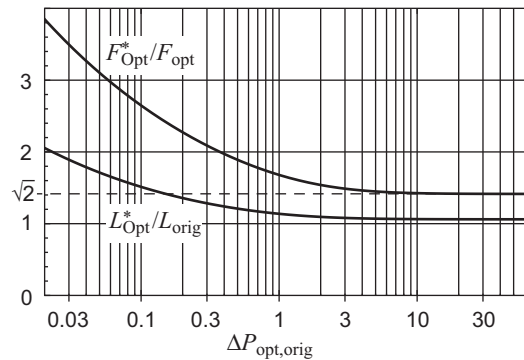


FIGURE 2.16 Dependence of F_{Opt}^* and L_{Opt}^* minimizing t_M at fixed Q on relative pressure drop ($\Delta P_{\text{opt,orig}} = \Delta p_{\text{opt,orig}}/p_{o,\text{opt,orig}}$) at $F = F_{\text{Opt}}$ in original L_{orig} -long column. At strong gas decompression (large $\Delta P_{\text{opt,orig}}$), F_{Opt}^* and L_{Opt}^* approach their strong decompression counterparts (F_{Opt} and L_{Opt}) described in Eqs. (2.204) and (2.207).

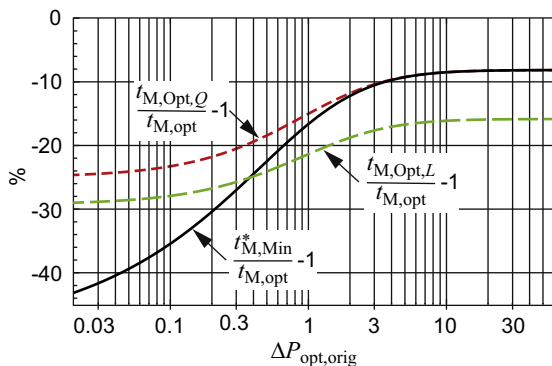


FIGURE 2.17 Relative reductions in void times compared to the void time ($t_{M,opt}$) at $F = F_{opt}$ in original L_{orig} -long column having efficiency $Q_{max, orig}$ and relative pressure drop $\Delta P_{opt,orig}$. Quantity $t_{M,Min}^*$ is t_M in completely optimized column, i.e., at $F = F_{opt}^*$ in a L_{opt}^* -long column (Fig. 2.16). Quantity $t_{M,opt,Q}$ is t_M at $F = F_{opt} = \sqrt{2}F_{opt}$ in L_{opt} -long column where $L_{opt} = 1.061L_{orig}$, Eq. (2.207). Using $L = 1.061L_{orig}$ keeps the column efficiency at the level of $Q_{max, orig}$ when F is increased from F_{opt} to $\sqrt{2}F_{opt}$. Quantity $t_{M,opt,L}$ is the void time at $F = \sqrt{2}F_{opt}$ in original (L_{orig} -long) column. Not increasing the column length when F is raised from F_{opt} to $\sqrt{2}F_{opt}$ reduces the column efficiency by practically negligible 3% compared to its original maximum $Q_{max, orig}$.

$F_{opt} = 3.75$ mL/min. At this flow, $\Delta P_{opt,orig} \approx 0.025$ (one of the lowest practical pressure drops). One can find from Fig. 2.16 that, at $\Delta P_{opt,orig} = 0.025$, $F_{opt}^* \approx 3.6 F_{opt} \approx 13.5$ mL/min. According to Eq. (2.141), this flow rate causes about 1.94-fold increase in a column plate height compared to its minimum (H_{min}) at $F = F_{opt}$. To preserve the column efficiency, the column should be made 1.94 times longer, i.e., $L_{opt}^* \approx 9.7$ m. Fig. 2.16 confirms that. The net reduction in t_M compared to the one in the original 5 m-long column at $F_{opt} = 3.75$ mL/min can be found from Fig. 2.17.

Choosing $F = F_{opt}^*$ and $L = L_{opt}^*$ according to Fig. 2.16 results in the shortest possible $t_M(t_{M,Min}^*)$ for a required Q . What if, ignoring

the fact that the gas decompression might not be strong, the column is optimized for the strong decompression, i.e., if F and L are chosen as $F = F_{opt}$ and $L = L_{opt}$ where F_{opt} and L_{opt} are the speed optimization parameters, Eqs. (2.204) and (2.207), at strong gas decompression? This can be viewed as a partial speed optimization in comparison with the complete speed optimization where $F = F_{opt}^*$ and $L = L_{opt}^*$. How large is the difference between $t_{M,Min}^*$ in the complete optimization on the one hand, and $t_{M,opt,Q}$ or $t_{M,opt,L}$ on the other ($t_{M,opt,Q}$ is t_M at $F = F_{opt}$ and $L = L_{opt}$ while $t_{M,opt,L}$ is t_M at $F = F_{opt}$ at a fixed L)? Is it worth it to go “extra mile” with all accompanying complications to achieve $t_{M,Min}^*$ instead of $t_{M,opt,Q}$ or $t_{M,opt,L}$ obtainable at known conditions? The answers to these questions can be found in Fig. 2.17 where all three parameters are normalized to the same $t_{M,opt}$ —the void time in a given column at EOF.

Example 2.15. $\Delta P_{opt,orig} = 0.025$ (5 m \times 0.53 mm column with hydrogen at $F = F_{opt}$). Fig. 2.17 shows that, at $\Delta P_{opt,orig} = 0.025$ (practically the lowest $\Delta P_{opt,orig}$), $t_{M,Min}^*$ at complete speed optimization is 42% lower than $t_{M,opt}$ in efficiency-optimized column ($F = F_{opt}$) yielding $Q_{max,orig}$. In comparison, at a simpler partial speed optimization without changing the column length, $t_{M,opt,L}$ is 29% lower than $t_{M,opt}$ while yielding $Q = 0.97Q_{max, orig}$, Eq. (2.151) at $F = \sqrt{2}F_{opt}$.

In practically the weakest gas decompression ($\Delta P_{opt,orig} = 0.025$), the partial speed optimization at $F = \sqrt{2}F_{opt}$ without changing the column length yields 13% lower time saving and 3% lower Q compared to the complete speed optimization. Nevertheless, being the simplest one, the partial optimization can be recommended as the best practical choice at the weak and the strong decompression. Alternatively, Figs. 2.16 and 2.17 can be used for the complete speed optimization.

Only the partial speed optimization with $F = \sqrt{2}F_{\text{opt}}$ without changing the column length is considered further. It is assumed from now on that the SSOF $f_{\text{opt}} = \sqrt{2}f_{\text{opt}}$, Eq. (2.204), is optimal for **any decompression**.

Using the transformations similar to those that led to Eq. (2.210), one can find that $t_{\text{M,Opt}}$ corresponding to $f = f_{\text{opt}}$ at weak gas decompression can be expressed as:

$$t_{\text{M,Opt}} = \frac{dLk^{0.1}\vartheta_{\text{G1}}}{8\sqrt{6}(10^3\phi)^{0.09}} \frac{p_o}{p_{\text{st}}} \left(\frac{T}{T_{\text{st}}}\right)^{0.25-\xi} \frac{1}{X_{\text{D}}^2 D_{\text{g,st}}}, \quad (|\Delta p| \ll p_o) \quad (2.223)$$

This shows that $t_{\text{M,Opt}}$ is inversely proportional to the product $X_{\text{D}}^2 D_{\text{g,st}}$. The data in Table 2.6 suggest that

At weak gas decompression, a column with hydrogen at SOF has 20% shorter void time (and analysis time) than the same column with helium at SOF.

2.11.2.4 Fixed pressure

It has been assumed so far that a GC instrument can provide any pressure necessary for a column optimization. This reflects overwhelming majority of practical applications. It can be also added that, although commercial GC instruments cannot provide unlimited pressure, the practically available pressure is not a fundamental limiting factor in GC instrumentation [11] and the pressure that a GC instrument can provide can be increased if higher pressure becomes practically necessary. Nevertheless, for completeness of the study, the speed optimization under a limited pressure deserves consideration. The problem can be formulated as that of the speed optimization under a *fixed pressure*. Conversely, the previously considered conditions when pressure required for a column optimization was available can be called as the case of *adjustable pressure*.

From Eqs. (2.50), (2.152), t_{M} in Eq. (2.49) for fixed pressure can be expressed as:

$$t_{\text{M}} = \frac{32Q^4 h^2 \eta}{j_{\text{H}} \Delta p} \quad (2.224)$$

In order to maintain constant h in this equation, the specific flow rate (f) should be fixed. Eq. (2.226) implies:

$$t_{\text{M}} \sim Q^4 \quad (\text{fixed } \Delta p \text{ and } f) \quad (2.225)$$

$$t_{\text{M}} \sim 1 / \Delta p \quad (\text{fixed } Q \text{ and } f) \quad (2.226)$$

Eq. (2.224) also implies that if a column pressure is fixed, then t_{M} is the shortest for a required Q when h is the smallest i.e., according to Eq. (2.150), at $f = f_{\text{opt}}$. In other words,

$$f_{\text{Opt}} = f_{\text{opt}} \quad (\text{fixed } \Delta p) \quad (2.227)$$

Eq. (2.224) does not directly contain column dimensions L and d reflecting the fact that, at fixed Δp , the variation of L and d effects t_{M} only through their effect on parameters (Q and h). It follows from Eq. (2.46) that, in order to maintain fixed f (to maintain fixed h) when p_o and p_i are fixed, the ratio d^3/L should be fixed. This, in turn, implies that, in order for two columns (A and B) to have efficiencies Q_{A} and Q_{B} at the same pressure and the same h , the column diameters (d_{A} and d_{B}) and lengths (L_{A} and L_{B}) should relate to their efficiencies as:

$$\frac{d_{\text{B}}}{d_{\text{A}}} = \frac{Q_{\text{B}}}{Q_{\text{A}}}, \quad \frac{L_{\text{B}}}{L_{\text{A}}} = \left(\frac{Q_{\text{B}}}{Q_{\text{A}}}\right)^3 \quad (2.228)$$

This together with Eq. (2.225) implies that

$$Q \sim d, \quad t_{\text{M}} \sim d^4 \quad (\text{fixed } \Delta p \text{ and } f) \quad (2.229)$$

One can also consider changing the carrier gas while keeping pressure and column efficiency fixed and using optimal flow in both cases. Eq. (2.222) shows that, under these conditions, t_{M} is proportional to the gas viscosity, η (Table 2.2). The values of $t_{\text{M,Opt}}$ of hydrogen in relation to $t_{\text{M,Opt}}$ of other gases are listed in Table 2.6.

At the same Δp and Q , a column with hydrogen at SOF has 55% shorter void time (and analysis time) than the same column with helium at SOF.

It is interesting that, because η of nitrogen is about 10% lower than η of helium,

The analysis with nitrogen is about 10% faster than the analysis with helium when both yield the Q at same Δp .

Example 2.16. Pressure required for operation of a 100 m \times 0.1 mm column with nitrogen at $f = f_{\text{opt}}$ is about 600 kPa—close to the pressure limit in some GC instruments. The same 100 m \times 0.1 mm column with helium at $f = f_{\text{opt}}$ requires more than twice as high pressure. Instead, one can choose a column with different dimensions that require 600 kPa pressure at $f = f_{\text{opt}}$ of helium. It follows from Eqs. (2.20), (2.46), (2.138) and (2.152) that the diameters (d_A and d_B) and the lengths (L_A and L_B) of columns A and B yielding the same efficiency (Q) at the same pressure and optimal conditions for each carrier gas relate as:

$$\frac{d_B}{d_A} = \frac{L_B}{L_A} = \frac{X_{D,B}\lambda_{\text{st},B}}{X_{D,A}\lambda_{\text{st},A}}$$

where X_D and λ_{st} are gas parameters in Table 2.2. Accordingly, the helium counterpart of 100 m \times 0.1 mm column with nitrogen is a 193 m \times 0.193 mm column (a 180 m \times 0.18 mm column that can be assembled from commercially available shorter 0.18 mm columns can be used for experimental verification of this example). The void time in this column with helium at $f = f_{\text{opt}}$ is about 10% larger than the void time in 100 m \times 0.1 mm column with nitrogen at $f = f_{\text{opt}}$. This is in contrast with the adjustable pressure while using the same column where, as follows from Table 2.6, optimal analysis with helium at weak and strong gas decompression is, respectively, almost twice and more than three times as fast as optimal analysis with nitrogen.

Comparing performance at predetermined operational conditions (like at a predetermined Δp) is more fundamental than comparing it in columns of predetermined dimensions [111,146]. After all, a method developer can change the column if necessary, but not the maximum Δp available from the GC instrument. This suggests that comparing Q and t_M at the same Δp in (possibly different) columns with helium and nitrogen is more revealing than comparing these parameters (Q and t_M) in the same column with helium and nitrogen. Therefore, the fact that nitrogen is 10% faster than helium at the same Δp and Q (Example 2.16) can be viewed as the ultimate result. The price for the time saving should also be compared on operational or performance level (not on the level of column dimensions), which, in this case, is the column loadability and MDC (minimum detectable concentration) [1,11,108]. For columns of the same optimal efficiency (Q_{Opt}), the loadability is proportion to d^3 [108] (also see further). To produce the same optimal Q_{Opt} at the same Δp , a column with nitrogen should be 1.93 times narrower compared to the one with helium (Example 2.16). As $1.93^3 \approx 7.2$, one can conclude, ignoring a relatively minor 10% time saving with nitrogen, that [1,11,108],

The price for using nitrogen instead of helium for obtaining the same efficiency in the same time at the same pressure is sevenfold lower column loadability and, therefore, sevenfold higher (worse) MDC.

2.11.2.5 Column diameter and pressure

Optimizing specific flow rate (f) is not the only way of reducing the void time (t_M) at a required column efficiency (Q). According to Eq. (2.200), t_M at a fixed Q and f strongly depends on the column internal diameter (d):

$$t_M \sim d^2 \quad (\text{weak decompression, fixed } f \text{ and } Q) \quad (2.230)$$

$$t_M \sim d \quad (\text{strong decompression, fixed } f \text{ and } Q) \quad (2.231)$$

In both cases, reducing d reduces t_M at the same Q . Therefore, it is desirable to always use the smallest possible d , taking into account that reducing d can increase the strains on the system components. Smaller d requires faster detectors, sharper sample introduction capable of smaller injection amounts. It also can increase (worsen) the MDC, etc.

Reducing d at a fixed f and Q inevitably increases the inlet pressure (p_i) according to relationship:

$$p_i = \sqrt{p_o^2 + \frac{256hQ^2p_{st}nf}{\pi d^2}} \quad (2.232)$$

that follows from Eqs. (2.46) and (2.152). Accordingly, it follows from Eq. (2.226) that increasing pressure reduces t_M at a fixed Q and f , i.e., operating a column at the highest possible pressure yields the shortest possible t_M at a required Q . If Δp and f are fixed, then $Q \sim d$, $t_M \sim d^4$, Eq. (2.229). It is impossible in this case to change d without changing Q . However, reducing d reduces t_M more significantly than it does Q , and the choice of d can be considered as a way of obtaining a required Q at the highest available pressure. Eq. (2.224) guarantees that Q will be obtained at the shortest t_M possible for a column of a given type in a given instrument.

Giddings [147] was the first to recognize that operating a column at maximum available pressure results in its best separation–time trade-offs. The same was later confirmed by Knox and Saleem [131]. However, the maximum instrumental pressure does, indeed, typically limit the column performance in LC, but it is not a dominant performance limiter in GC. To operate at the largest practically available instrumental pressure (10 bar), a GC column should have so small d (0.05 mm and lower) that its loadability and, therefore, the DL for low concentration solutes can get far above (worse) the typically acceptable levels. As a result, the lowest acceptable d (close to 0.1 mm), but not the largest

available pressure is typically the dominant factor limiting the separation–time trade-off in GC.

2.11.2.6 Closing remarks

Specific flow rates optimizing speed of analysis at several pressure conditions can be summarized in a single expression:

$$f_{\text{Opt}} = f_{\text{opt}} \cdot \begin{cases} \sqrt{2}, & \text{adjustable pressure} \\ 1, & \text{fixed pressure} \end{cases} \quad (2.233)$$

In a column with a given diameter and a given carrier gas,

Speed optimization of a column flow leads to the shortest analysis times at a predetermined column efficiency and to the largest efficiency at a predetermined analysis time.

When column pressure is fixed, optimal flow for maximal efficiency is the same as that for minimal void time at a given efficiency. Only when a GC instrument can supply pressure required for speed optimization, the latter can reduce the analysis time compared to that at maximal efficiency of a given column. The time savings (16%–29% at least) are practically useful, but not dramatic. From theoretical perspective, it is not the amount of the time saving that counts the most, but the very fact that the questions of the flow optimization for the best separation–time trade-off are answered. Even more important is the fact that the approach to the speed optimization of the flow rate can be extended to optimization of other parameters such as a column heating rate.

Finally, as mentioned earlier, practical cases when pressure available in a GC instrument is insufficient for the flow optimization are relatively rare. It is assumed from now on that, unless otherwise is explicitly stated, **optimal pressure is always available**.

Optimal flow rate depends on temperature. Assuming that parameter ξ (Table 2.2) can be approximated as $\xi = 0.7$, it follows from Eqs. (2.201), (2.204), (2.166), and (2.134) that (Fig. 2.18A)

$$F_{\text{Opt}} \sim T^{-0.55} \quad (2.234)$$

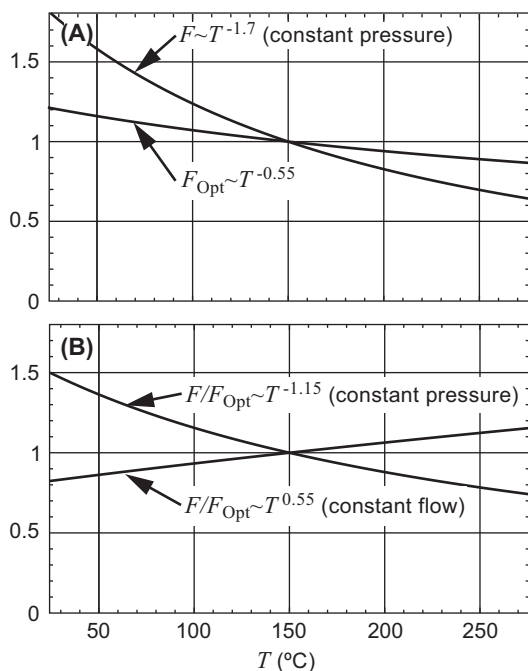


FIGURE 2.18 Normalized (to unity at 150°C) flow rates in temperature-programmed analyses versus column temperature (T). (A) Actual flow rate (F , Eq. (2.235), at constant pressure, and optimal flow rate (F_{Opt} , Eq. (2.234). (B) Relative values of F/F_{Opt} at constant pressure and constant flow.

Experimental verification and additional discussion of this relation can be found elsewhere [2,50]. It is interesting to compare F_{Opt} with actual flow (F) in a column during a heating ramp. It follows from Eqs. (2.46) and (2.21) that actual flow rate in isobaric analysis is (Fig. 2.18A):

$$F \sim T^{-1.7} \quad (2.235)$$

The last two expressions show that the ratio F/F_{Opt} changes during a temperature-programmed analysis in both constant pressure and constant flow modes (Fig. 2.18B). In other words, there is a mismatch of actual and optimal flow in both operational modes. At constant flow, the mismatch is significantly smaller than it is at constant pressure. This is not the only

and probably not the most important advantage of the constant flow mode. It is practically important that constant gas flow leads to more consistent detector operations [160].

2.11.3 Optimal heating rate

Among the factors affecting separation capacity (s_c) of GC analysis is the heating rate (R_T). The dependence of characteristic separation capacity (Δs_{char}) of a linear heating ramp—a benchmark of the separation capacity for highly interactive (strongly retained at the beginning of the heating ramp) solutes—on dimensionless heating rate (r_T) is described in Eq. (2.197) and illustrated in Fig. 2.14. The slower is the heating rate, the larger is Δs_{char} and s_c . At $r_T = 0$ and, therefore, at $R_T = 0$ (isothermal analysis), Δs_{char} and s_c are the highest. Unfortunately, highest s_c comes at the expense of substantially longer analysis time (t_{anal}), which, in the case of analysis of a complex mixture, can become prohibitively long. Using temperature programming can substantially reduce t_{anal} . However, it also reduces Δs_{char} and s_c . These considerations suggest that there can be a point of the best trade-off between s_c and t_{anal} .

The optimal heating rate ($R_{T,Opt}$) is the one that leads to the shortest analysis time (t_{anal}) at required separation capacity (s_c) and to the largest s_c at a given t_{anal} .

As does its benchmark (Δs_{char} , Eq. (2.197), the separation capacity (s_c) of the entire GC analysis depends on the column efficiency (Q) and on the dimensionless heating rate (r_T). In addition to that, s_c also depends on the temperature range (ΔT) that can be different for different samples. The analysis time (t_{anal}) also depends on r_T and ΔT .

Suppose that, at some operational conditions, s_c is larger than necessary and it is desirable to reduce it in order to reduce t_{anal} . Two ways of doing so can be considered. One can increase r_T and by that lower s_c and t_{anal} . One can also

keep r_T constant, but reduce Q together with reducing t_M . The implementation of the latter approach requires additional explanation. If the heating rate (R_T) did not change, then making t_M shorter would reduce r_T , Eq. (2.70), violating the requirement of constant r_T . To compensate for shorter t_M , R_T can be made proportionally larger so that reducing t_M would not reduce r_T . When r_T is fixed, the ratio t_{anal}/t_M is fixed and reducing t_M proportionally reduces t_{anal} . Comparing the two approaches of reducing s_c in order to reduce t_{anal} , one can choose the more *effective* one in which the same reduction in s_c causes larger reduction in t_{anal} or the same reduction in t_{anal} requires smaller reduction in s_c .

Consider now a very slow heating ramp with r_T close to zero. Suppose that r_T is doubled. As $2r_T$ is still close to zero, this might have barely noticeable effect on s_c while significantly reducing t_{anal} . On the other hand, the alternative approach of reducing Q together with reducing t_M reduces both s_c and t_{anal} and, therefore, is less effective than increasing r_T alone. However, at some point of further increasing r_T , it can become significant so that its further increase will not only reduce t_{anal} , but also reduce s_c , Eq. (2.197) and Fig. 2.14. At some point, this approach can become less effective than its alternative—reducing Q without changing r_T . The optimal r_T ($r_{T,\text{Opt}}$) is the one with the following properties:

- At $r_T < r_{T,\text{Opt}}$, increasing r_T is *more effective* for trading smaller s_c for smaller t_{anal} than reducing Q while keeping r_T fixed
- At $r_T = r_{T,\text{Opt}}$, both alternatives are *equally effective*
- At $r_T > r_{T,\text{Opt}}$, increasing r_T is *less effective* for trading smaller s_c for smaller t_{anal} than reducing Q while keeping r_T fixed

The relationship between Q and t_M depends on the column pressure conditions, which,

from Eqs. (2.200) and (2.224), can be summarized as:

$$t_M = X_i Q^i \quad (2.236)$$

where

$$i = \begin{cases} 2, & \text{weak decompression, any } p_o \text{ and } \Delta p \\ 3, & \text{strong decompression, any } p_o \text{ and } \Delta p \\ 4, & \text{any decompression, fixed } p_o \text{ and } \Delta p \end{cases} \quad (2.237)$$

$$X_i = \begin{cases} \frac{\pi d^2 p_o h}{4 p_{\text{st}} f}, & i = 2 \\ \frac{8d}{3} \sqrt{\frac{\pi \eta h^3}{p_{\text{st}} f}}, & i = 3 \\ \frac{32 h^2 \eta}{j_H \Delta p}, & i = 4 \end{cases} \quad (2.238)$$

Consider, e.g., strong decompression when $t_M \sim Q^3$. In this case, at $r_T = r_{T,\text{Opt}}$, i.e., when equal change in s_c results in equal change in t_{anal} for both alternatives, the ratio s_c^3/t_{anal} is flat, i.e., $d(s_c^3/t_{\text{anal}})/dr_T = 0$. The same is true for other pressure conditions, i.e.,:

$$\frac{d\mathcal{P}_i}{dr_T} = 0, \quad i = (2, 3, 4), r_T = r_{T,\text{Opt}} \quad (2.239)$$

where

$$\mathcal{P}_i = \frac{s_c^i}{t_{\text{anal}}} \quad (2.240)$$

can be viewed as a column *performance parameter*—the larger is the \mathcal{P}_i , the better is the performance.

It is interesting to notice that quantity \mathcal{P}_i is meaningful with the indexes (i) other than (2, 3, 4) in Eq. (2.239) for $r_{T,\text{Opt}}$ [16]. Specifically, quantities:

$$\mathcal{P}_0 = 1/t_{\text{anal}}, \quad \mathcal{P}_1 = s_c/t_{\text{anal}} \quad (2.241)$$

are, respectively, the analysis *throughput* (the number of analyses per time unit) [1] and the *average speed of analysis* (the average number s -slots per time unit) [16,22].

Theoretical evaluation of quantity s_c and, therefore, \mathcal{P}_i is complex [1]. Their experimentally found maxima together with the corresponding $R_{T,Opt}$ are shown in Fig. 2.19. Representing the following experimental conditions. Column (HP-5): 30 m \times 0.32 mm, gauge pressure: 11.75 psi, initial temperature: 50 °C, final temperature: 320 °C. Other conditions are listed in Table 2.7.

Fig. 2.19 shows that $R_{T,Opt}$ depends on pressure conditions represented by index i in \mathcal{P}_i ,

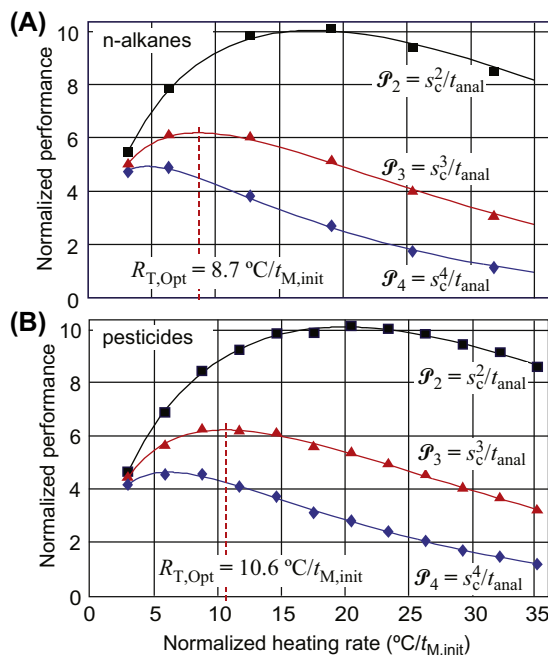


FIGURE 2.19 Experimental performance parameters (\mathcal{P}_i), Eq. (2.240), for (A) even-numbered n-alkanes $\text{C}_{10}\text{--}\text{C}_{36}$, and (B) 10 pesticides (unknown, aniline, unknown, dichlorvos, vernolate, lindane, chlorpyrifos-methyl, malathion, dieldrin, mirex). From L.M. Blumberg, M.S. Klee, *Optimal heating rate in gas chromatography*, J. Microcolumn Sep. 12 (2000) 508–514. Adapted with permission.

TABLE 2.7 Experimental conditions for Fig. 2.19.

	n-alkanes	Pesticides
Film thickness (μm)	0.25	0.32
Carrier gas	Helium	Hydrogen
Void time (min)	1.272	0.596
Lowest heating rate ($^{\circ}\text{C}/\text{min}$)	2.5	5
Highest heating rate ^a ($^{\circ}\text{C}/\text{min}$)	40	65

^a Other heating rates: from $5^{\circ}\text{C}/\text{min}$ to the highest in $5^{\circ}\text{C}/\text{min}$ increments.

and for the same pressure conditions, it is different to some degree for the two samples. A general recommendation for choosing a default heating rate in temperature-programmed analyses can be based on the following considerations.

A column operation at maximum pressure available from GC instruments (\mathcal{P}_4) is relatively rare and can be ignored in choosing general recommendation for the *default heating rate* ($R_{T,Def}$) in temperature-programmed GC. Of the other two pressure conditions—strong (\mathcal{P}_3) and weak (\mathcal{P}_2) gas decompression—the former is not only the most typical (it includes all GC-MS applications), but it is also the most demanding as the strong decompression typically exists in analyses of complex samples requiring relatively long and narrow columns and temperature programming. On the other hand, the weak decompression typically exists in analyses of relatively simple samples using relatively short and wide columns. On top of that, relatively simple samples are typical candidates for isothermal analyses. It is reasonable, therefore, to choose $R_{T,Def}$ that is optimal for strong gas decompression. The optimal rates ($R_{T,Opt}$) for n-alkanes and pesticides at strong decompression are (Fig. 2.19 for \mathcal{P}_3) 8.7 and $10.6^{\circ}\text{C}/t_M$, respectively justifying $R_{T,Opt} = 10^{\circ}\text{C}/t_M$ as a reasonable common outcome [15,16,148].

Several additional details should be considered in choosing $R_{T,Def}$.

In vicinity of their maxima, the \mathcal{P}_i -curves are rather flat. As a result, choosing $R_{T,Def} = 10^\circ\text{C}/t_M$ instead of optimal $8.7^\circ\text{C}/t_M$ for n-alkanes or $10.6^\circ\text{C}/t_M$ for pesticides leads to unnoticeable reduction in the column performance.

Is it reasonable to recommend a certain $R_{T,Def}$ based only on two types of sample in a single column type? To answer this question, one can recall that the elution temperature (T_R) of any solute in any column in temperature-programmed analysis mostly depends on its characteristic parameters (T_{char} and θ_{char}) and dimensionless heating rate (r_T) [2]. The dependence of the elution temperatures ($T_{R,a}$) of highly interactive solutes (highly retained at initial temperature of the heating ramp) on T_{char} , θ_{char} , and r_T is described in Eq. (2.84). Under typical (optimal or near-optimal) conditions, $T_{R,a}$ of a given solute is close to its T_{char} so that all solutes generally elute in the order of increase in their T_{char} . A particular solute can have substantially different T_{char} in two different columns. Thus, T_{char} of a polar solute in a polar column can be substantially larger than its T_{char} in an apolar column. Similarly, T_{char} of an apolar solute in an apolar column can be substantially larger than its T_{char} in a polar column [34]. What's important, however, is that two possibly different solutes that have the same T_{char} in possibly different columns will elute at almost equal T_R as long as r_T is the same in both cases. Moreover, all solutes having the same T_{char} in different columns have approximately the same θ_{char} (Fig. 2.3). As a result, equal r_T in analyses of different samples in different columns correspond to equal normalized heating rates ($^\circ\text{C}/t_M$). This explains why the normalized optimal heating rate is expected to be approximately the same in all analyses. The experimental difference between $R_{T,Opt}$ in Fig. 2.19 can be attributed to several secondary factors. One of them is caused by relatively

thinner stationary-phase film in n-alkane experiments ($\varphi = 0.00,078$) compared to that in pesticide experiments ($\varphi = 0.001$) (Table 2.7). Increasing the former to $\varphi = 0.001$ would increase $R_{T,Opt}$ for n-alkanes at strong gas decompression from 8.7 to $8.9^\circ\text{C}/t_M$. There were other possible reasons for the difference. The results of Fig. 2.19, but based on a different column and sample with hydrogen and helium as carrier gas, was confirmed by another group of workers [149].

The normalized value of the heating rate depends on t_M . The latter, in isobaric temperature-programmed analysis, is proportional to temperature-dependent gas viscosity (η), Eq. (2.49). The normalized heating rates in Fig. 2.19 were found from isobaric analyses with initial temperature (T_{init}) of 50°C . In other words, the recommended default ($R_{T,Def}$) can be specified as:

$$R_{T,init,Def} = 10^\circ\text{C}/t_{M,init}, \quad (\text{isobaric}, T_{init} = 50^\circ\text{C}) \quad (2.242)$$

Although recommending ($R_{T,Def}$) (in $^\circ\text{C}/t_M$) is practically convenient, what actually affects the column performance is the dimensionless heating rate (r_T). Moreover, as shown earlier, r_T in isobaric temperature-programmed analysis with linear heating ramp is essentially the same for all solutes. Quantity r_T is a theoretically important parameter affecting solute migration and elution, Eqs. (2.80)–(2.85), (2.88)–(2.93), as well as the column performance overall. From Eqs. (2.18), (2.69), and (2.242), one has for the default r_T ($r_{T,Def}$) corresponding to $R_{T,Def}$ at 50°C :

$$r_{T,Def} = 0.4 \quad (2.243)$$

Simply recommending $R_{T,Def} = 10^\circ\text{C}/t_M$ can be confusing. It was found for initial temperature of 50°C , Eq. (2.242). What if, in isobaric temperature-programmed analysis, the initial temperature (T_{init}) of a heating ramp is not 50°C as it was in the experiments for Fig. 2.19? And should the default R_T in constant flow

mode be the same as it is in constant pressure mode? It is desirable to come up with the default value at the same temperature in all cases. In this chapter, that reference temperature (T_{ref}) is 150°C. From Eqs. (2.18), (2.78), and (2.139), the default void temperature increment ($\Delta T_{M,\text{ref,Def}}$) at $T_{\text{ref}} = 150^\circ\text{C}$ can be estimated as $\Delta T_{M,\text{ref,Def}} = 12^\circ\text{C}$. From Eq. (2.75), the recommended *reference default heating rate* ($R_{T,\text{ref,Def}}$) becomes:

$$R_{T,\text{ref,Def}} = 12^\circ\text{C}/t_{M,\text{ref}} \quad (2.244)$$

One can still use the $10^\circ\text{C}/t_M$, Eq. (2.242), as the isobaric default if T_{init} is close to 50°C (say, $35^\circ\text{C} \leq T_{\text{init}} \leq 60^\circ\text{C}$). However, the $12^\circ\text{C}/t_{M,\text{ref}}$ leads to a more consistent setting regardless of T_{init} in constant pressure and constant flow mode. This means that, whatever is the actual programming mode and its actual T_{init} , the absolute default heating rate $R_{T,\text{Def}}$ (in $^\circ\text{C}/\text{min}$) should be calculated from Eq. (2.244) with $t_{M,\text{ref}}$ measured at $T = T_{\text{ref}}$. If, however, the analysis is isobaric with $T_{\text{init}} = 50^\circ\text{C}$, then either default will result in the same absolute $R_{T,\text{Def}}$ (in $^\circ\text{C}/\text{min}$).

Example 2.17. Suppose that, in isobaric analysis with $T_{\text{init}} = 50^\circ\text{C}$, $t_{M,\text{ref}} = 0.5$ min. According to Eqs. (2.21) and (2.49), t_M at any other temperature including T_{init} can be found from $t_{M,\text{ref}}$ as $t_{M,\text{init}} = (T_{\text{init}}/T_{\text{ref}})^\xi t_{M,\text{ref}}$, which, at $\xi \approx 0.7$ (Table 2.2), yields $t_{M,\text{init}} \approx 0.415$ min. One can verify that both recommendations, Eqs. (2.242) and (2.244), yield the same absolute default heating rate setting, $R_{T,\text{Def}} = 24^\circ\text{C}/\text{min}$.

Although the default heating rates in Eqs. (2.242) and (2.244) are recommended for all pressure conditions, they were actually based on the optimal rates at strong gas decompression, as explained earlier. Of course, one can also choose, if necessary, the R_T that is best for operations at maximum instrumental pressure or at weak decompression. The rates are, respectively, about $5^\circ\text{C}/t_{M,\text{init}}$ and $20^\circ\text{C}/t_{M,\text{init}}$ (Fig. 2.19 for

\mathcal{P}_4 and \mathcal{P}_2) at $T_{\text{init}} = 50^\circ\text{C}$ or about 6 and $24^\circ\text{C}/t_{M,\text{ref}}$.

The recommended default heating rates are summarized in Table 2.8. The elution parameters of highly interactive solutes at these defaults are compiled in Table 2.9.

2.11.3.1 Generic temperature program

It was assumed so far that the heating ramp starts simultaneously with the sample introduction. This approach has a shortcoming. The solutes that are insufficiently retained at initial temperature (T_{init}) of the ramp would be poorly retained if the analysis was isothermal at T_{init} . Raising the temperature during migration of these solutes further reduces their retention and separation. This can be avoided by preceding the ramp with holding the initial temperature fixed for some *hold time* (t_h) prior to the ramp. The hold time can be chosen on the following basis. The retention factors of highly interactive solutes eluting during isobaric heating ramp approach their asymptotic level $k_{R,a} = 1/(e^{r_T} - 1)$, Eq. (2.83).

A *balanced* single-ramp temperature program [23] starts with the initial hold of duration:

$$t_{\text{hb}} = (1 + k_{R,a})t_{M,\text{init}} = \frac{t_{M,\text{init}}}{1 - e^{-r_T}} \quad (2.245)$$

The solute eluting at the end of this hold has retention factor $k_{R,a}$ —the same as the asymptotic retention factor for the solutes eluting during the ramp. Switching from the hold to the ramp at this time results in a small departure of k from

TABLE 2.8 Equivalent alternative recommendations for default heating rate.

Default parameter	r_T	$R_{T,\text{init}}$	$R_{T,\text{ref}}$
Units ^a	1	$^\circ\text{C}/t_{M,\text{init}}$	$^\circ\text{C}/t_{M,\text{ref}}$
Parameter value	0.4	10	12

^a $t_{M,\text{init}}$ and $t_{M,\text{ref}}$ are t_M at, respectively, $T_{\text{init}} = 50^\circ\text{C}$ in isobaric analysis and $T_{\text{ref}} = 150^\circ\text{C}$ in any analysis.

TABLE 2.9 Asymptotic elution parameters, Eqs. (2.81)–(2.83), (2.87), and (2.167), of the solutes eluting during the heating ramp at $r_T = 0.4$.

Parameter	$k_{R,a}$	$\mu_{R,a}$	$\omega_{R,a}$	$\bar{\omega}$	X_T
Value	2	0.33	0.67	0.82	0.71

Asymptotic elution parameters are the ones of the highly interactive solutes (the ones that are highly retained at the beginning of a heating ramp).

$k_{R,a}$ for the solutes eluting shortly after the switching followed by the rapid approach of k to $k_{R,a}$ for majority of solutes eluting during the ramp [23].

A balanced single-ramp temperature program at the recommended default heating rate, Table 2.8, can be considered as the *generic* temperature program. It can be used as the starting point at the beginning of method development if nothing is known about the best (possibly, multiramp) temperature program for the analysis being developed. According to Table 2.9, $k_{R,a}$ in generic analysis is 2. Eq. (2.245) yields for the *default initial hold time* ($t_{h,Def}$) in generic analysis:

$$t_{h,Def} = 3t_{M,init} \quad (2.246)$$

In other words, the *generic temperature program*, $T_{gen}(t)$, is:

$$T_{gen}(t) = \begin{cases} T_{init}, & t \leq 3t_{M,init} \\ T_{init} + R_{T,Def}(t - 3t_{M,init}), & t > 3t_{M,init} \end{cases} \quad (2.247)$$

Example 2.18. For conditions $T_{init} = 50^\circ\text{C}$, $t_{M,ref} = 0.5$ min, Example 2.17 yields: $t_{M,init} \approx 0.415$ min, $R_{T,Def} = 24^\circ\text{C}/\text{min}$. Therefore, $t_{h,Def} = 1.245$ min. These are the parameters of generic temperature program for analysis with $T_{init} = 50^\circ\text{C}$, $t_{M,ref} = 0.5$ min.

2.11.4 Detection limit and trade-off triangle

The DL is another factor of a column performance trade-off (in addition to the separation capacity, s_c , and analysis time, t_{anal}). Following is a brief review of the issues related to DL. Additional information can be found elsewhere [11].

The DL is a metric of ability of a chromatographic system to detect and quantify small amounts of solutes in a sample. The DL is typically limited by the *baseline noise* in a chromatogram. The larger is the noise, the larger (the worse) is the DL. The noise can come from carrier gas impurities, column bleeding typically increasing with temperatures, detector electronics, etc. All noise sources except for the detector noise can be viewed as the external ones. If necessary, the noise coming from these sources can be reduced. Thus the noise due to the gas impurities can be reduced by using purer carrier gas, the column bleeding can be reduced by using *low-bleed columns* and lower temperatures. On the other hand, some factors affecting a detector noise are part of a GC instrument design and cannot be change by a system operator. In that regard, the detector noise ultimately controls the detection limit of a GC instrument.

Each GC system has a (digital or analog) *noise filter*. The baseline noise level depends on the width (σ_{filt}) of the filter *impulse response* [150]—the width of the filter's output resulted from extremely narrow input pulse. Typically, a method developer can control σ_{filt} (by choosing a number of data points per peak or by other means available in GC system). However, there are limits to the utility of that control. Increasing σ_{filt} reduces the noise. On the other hand, too wide σ_{filt} can broaden the peaks and make some of them unresolvable. Therefore, it is necessary to maintain a certain balance between σ_{filt} and the widths (σ) of the peaks in a

chromatogram. Quantitative characteristics of that balance depend on the structure of the baseline noise. For example, the level of the *white noise* [150]—a typical type of detector noise—is inversely proportional to $\sqrt{\sigma_{\text{filt}}}$. Only the **white noise** is considered further. It is also assumed from now on that, by varying the data rate during the analysis if necessary [151,152], σ_{filt} is always chosen so that the ratio $\sigma/\sigma_{\text{filt}}$ is **the same in all analyses**. As a result, the noise level is inversely proportional to $\sqrt{\sigma}$, i.e., [11].

$$(\text{noise level}) \sim \sqrt{\frac{\rho_n}{\sigma}} \quad (2.248)$$

where ρ_n is the noise *spectral density* [150]. It is assumed further that the **carrier gas type and flow rate do not affect ρ_n and a detector response**.

Two metrics of DL can be considered: the *minimum detectable amount* (MDA) and the MDC [11,153]. Both metrics are solute-specific. The MDA of a given solute is its *amount* at a predetermined *signal-to-noise ratio*. The MDC of a given solute is its *concentration* at a predetermined *signal-to-noise ratio*.

The MDA is suitable for the situation where the *same amount of sample* can be injected in a column of any dimensions without overloading the column. This might happen where only a small amount of sample is available. In this case, *there is no conflict between the MDA, the separation capacity, and the analysis time* [11]. Thus, when column diameter and length get smaller in proportion with each other, the column maximum efficiency remains unchanged while the analysis time gets shorter. Along with that, the peaks become sharper so that the *signal-to-noise ratio* for the same sample amount increases (improves). This means that MDA gets lower (better) while the analysis time gets shorter without changing the column separation capacity. If necessary, shorter analysis time can be traded for larger separation capacity. The relationships of MDA and column

dimensions can be quantified by the following relations of proportionality [11]:

$$\text{MDA} \sim \sqrt{\frac{\rho_n}{f\mu_R}} \begin{cases} d\sqrt{Qhp_o}, & \text{weak decompression} \\ Q\sqrt{dh^3\eta}, & \text{strong decompression} \end{cases} \quad (2.249)$$

Different situation might exist in analyses of complex samples where, in order to prevent column overloading and substantial broadening of larger peaks, a reduction in column dimensions must be accompanied by the reduction in the amount of injected sample. To maintain the same margin of a column overloading for all column dimensions, a sample injected in any column should have the *same concentration* (rather than the same amount). MDC becomes a suitable metric of detection limit. The conflict between the need to prevent a column overloading by the high concentration components and to detect low concentration components creates a conflict between separation capacity, analysis time, and MDC. From now on, **only the MDC** is considered as a metric of DL.

The *largest sample amount* (A_{max}) that does not overload a column (or causes the same relative level of overloading) is proportional to the product $\varphi d_c^{5/2} \sqrt{L}$ [11], i.e.,

$$A_{\text{max}} \sim \varphi d_c^{5/2} \sqrt{L} \quad (2.250)$$

Dependence of MDC on method parameters and properties of a chromatographic system can be described by the following relations of proportionality [11]:

$$\text{MDC} \sim \frac{1}{d^2 \varphi} \sqrt{\frac{p_o \rho_n}{Q \mu_R f h}}, \quad (\text{weak decompression}) \quad (2.251)$$

$$\text{MDC} \sim \frac{1}{\varphi} \sqrt{\frac{\rho_n \sqrt{\eta}}{d^5 \mu_R \sqrt{f h}}}, \quad (\text{strong decompression}) \quad (2.252)$$

These expressions describe, among other things, the dependence of MDC on column diameter and efficiency (Q). It is interesting that, at strong gas decompression, MDC does not depend on Q at a given d (and, therefore, on column length). This means that

The variations of a column length in order to obtain the shortest analysis time at a predetermined separation performance or to obtain the best separation performance at a predetermined analysis time do not affect MDC.

Eventually, one needs to know the trade-offs between s_c , t_{anal} and MDC, i.e., how these components of a column performance relate to each other. Only the **optimal** conditions ($f = f_{\text{Opt}}$, $r_T = r_{T,\text{Opt}}$) for the most demanding operations with the **strong gas decompression** are considered further. One has [11]:

$$\text{MDC} \sim X_{\text{all}} \sqrt{s_c^{15}/t_{\text{anal}}^5} \quad (2.253)$$

where

$$X_{\text{all}} = X_\sigma^3 \sqrt{\rho_n}/\varphi \quad (2.254)$$

and X_σ is the gas-related parameter defined in Eq. (2.215) and listed for several carrier gases in Table 2.6. These equations not only highlight the relationship between the column performance parameters s_c , t_{anal} , and MDC, but they also identify the key factors (φ , ρ_n , and X_σ) affecting the column performance. The latter (X_σ) represents the effect of the carrier gas on the trade-off between s_c , t_{anal} , and MDC.

Example 2.19. According to Table 2.6, X_σ for helium is about 60% of that for hydrogen. Due to the factor X_σ^3 in Eq. (2.254), MDC in a system with hydrogen as a carrier gas is about five times lower (better) than MDC in a system with helium with possibly different columns chosen to produce the same separation capacity in the same time. To be more specific, consider two GC-MS analyses: one is based on a 10 m \times 0.1 mm column with helium and another on a 17 m \times 0.17 mm column with hydrogen. Under

optimal conditions, both analyses have the same efficiency and the same void time. As a result, the width of a peak corresponding to the same solute and the noise spectral density (ρ_n) are the same in both cases. However, according to Eq. (2.250), the sample amount that can be injected in a column with hydrogen is about five times larger ($1.7^3 \approx 4.9$) than that amount for a column with helium. This means that, to yield the same signal-to-noise ratio in both cases, the analysis with hydrogen could have five times lower concentration of the trace-level components than the analysis with helium. In other words, the analysis with hydrogen has five times lower (better) MDC than the analysis with helium.

The trade-off between a column separation power, analysis time, and DL is sometimes illustrated by a *trade-off triangle* (*triangle of compromise* [11,73]). Eq. (2.253) is a quantitative description of that triangle under different operational conditions (at strong gas decompression). However, to construct the triangles at several conditions, some metrics of a column performance should be modified.

Quantity s_c can be viewed as a *direct metric* of a separation performance in the sense that larger value of the metric corresponds to better separation performance. On the other hand, MDC and t_{anal} can be viewed as *inverse metrics* in the sense that larger values of the metrics correspond to poorer performance. For better visualization of Eq. (2.253), it is desirable that all performance metrics in the expression were direct. Such direct counterparts of MDC and t_{anal} are the *linear dynamic range* (Λ) of a chromatogram (the ratio of the largest undistorted *peak height* to the noise):

$$\Lambda \sim \frac{1}{\text{MDC}} \quad (2.255)$$

and the *throughput*, $\mathcal{P}_0 = 1/t_{\text{anal}}$, Eq. (2.241), (the number of analyses per time unit). Eq. (2.253) becomes (Fig. 2.20):

$$X_{\text{all}}^2 s_c^{15} \mathcal{P}_0^5 \Lambda^2 = \text{constant} \quad (2.256)$$

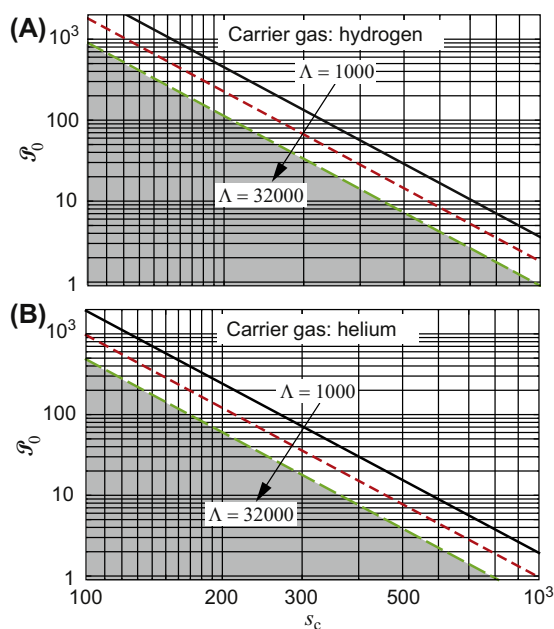


FIGURE 2.20 Trade-offs, Eq. (2.256), between separation capacity (s_c), throughput (\mathcal{P}_0), and dynamic range (Λ). Three levels of Λ are shown for each carrier gas. Each next level is $4\sqrt{2}$ times larger than the previous one and, as follows from Eq. (2.252), corresponds to twice as large column diameter. Each line in the graphs can be viewed as a side of a triangle of separation–time–MDC trade-off. A triangle corresponding to the same Λ for hydrogen is larger (better) than that for helium.

Expression similar to Eq. (2.256) can be also constructed for the weak gas decompression. However, the most demanding trade-offs between s_c , \mathcal{P}_0 , and Λ exist in analyses of complex mixtures typically requiring strong gas decompression. From that perspective, Eq. (2.256) can be viewed as description of the *ultimate trade-off triangle*.

References

- [1] L.M. Blumberg, Theory of gas chromatography, in: C.F. Poole (Ed.), *Gas Chromatography*, Elsevier, Amsterdam, 2012, pp. 19–78.
- [2] L.M. Blumberg, *Temperature-Programmed Gas Chromatography*, Wiley-VCH, Weinheim, 2010.

- [3] M.L. Lee, F.J. Yang, K.D. Bartle, *Open Tubular Gas Chromatography*, John Wiley & Sons, New York, 1984.
- [4] G. Guiochon, C.L. Guillemin, *Quantitative Gas Chromatography for Laboratory Analysis and On-Line Control*, Elsevier, Amsterdam, 1988.
- [5] J.C. Giddings, *Unified Separation Science*, Wiley, New York, 1991.
- [6] L.S. Ettre, J.V. Hinshaw, *Basic Relations of Gas Chromatography*, Advanstar, Cleveland, Ohio, 1993.
- [7] W. Jennings, E. Mittlefehldt, P. Stremple, *Analytical Gas Chromatography*, second ed., Academic Press, San Diego, 1997.
- [8] C.F. Poole, *The Essence of Chromatography*, Elsevier, Amsterdam, 2003.
- [9] R.L. Grob, E.F. Barry (Eds.), *Modern Practice of Gas Chromatography*, fourth ed., John Wiley & Sons, Hoboken, New Jersey, 2004.
- [10] H.M. McNair, J.M. Miller, *Basic Gas Chromatography*, second ed., John Wiley & Sons, Inc, Hoboken, New Jersey, 2009.
- [11] L.M. Blumberg, Multidimensional gas chromatography: theoretical considerations, in: L. Mondello (Ed.), *Comprehensive Chromatography in Combination with Mass Spectrometry*, Wiley, Hoboken, NJ, 2011, pp. 13–63.
- [12] K. Dettmer-Wilde, W. Engewald, *Practical Gas Chromatography: A Comprehensive Reference*, Springer-Verlag, Berlin, 2014.
- [13] J. Griffiths, D. James, C.S.G. Phillips, *Gas chromatography*, *Analyst* 77 (1952) 897–904.
- [14] J.C. Giddings, Theory of programmed temperature gas chromatography: the prediction of optimum parameters, in: N. Brenner, J.E. Callen, M.D. Weiss (Eds.), *Gas Chromatography*, Academic Press, New York, 1962, pp. 57–77.
- [15] L.M. Blumberg, M.S. Klee, Method translation and retention time locking in partition GC, *Anal. Chem.* 70 (1998) 3828–3839.
- [16] L.M. Blumberg, M.S. Klee, Optimal heating rate in gas chromatography, *J. Microcolumn Sep.* 12 (2000) 508–514.
- [17] W.E. Harris, H.W. Habgood, *Programmed Temperature Gas Chromatography*, John Wiley & Sons, Inc., New York, 1966.
- [18] H.W. Habgood, W.E. Harris, Retention temperature and column efficiency in programmed temperature gas chromatography, *Anal. Chem.* 32 (1960) 450–453.
- [19] H.W. Habgood, W.E. Harris, Plate height in programmed temperature gas chromatography, *Anal. Chem.* 32 (1960) 1206.
- [20] IUPAC, Nomenclature for chromatography, *Pure Appl. Chem.* 65 (1993) 819–872.

- [21] R. Conden, A.H. Gordon, A.J.P. Martin, Qualitative analysis of proteins: a partition chromatographic method using paper, *Biochem. J.* 38 (1944) 224–232.
- [22] L.M. Blumberg, Metrics of separation performance in chromatography. Part 1. Definitions & application to static analyses, *J. Chromatogr. A* 1218 (2011) 5375–5385.
- [23] L.M. Blumberg, M.S. Klee, Quantitative comparison of performance of isothermal and temperature-programmed gas chromatography, *J. Chromatogr. A* 933 (2001) 13–26.
- [24] A.T. James, A.J.P. Martin, Gas-liquid partition chromatography: the separation and micro-estimation of volatile fatty acids from formic acid to dodecanoic acid, *Biochem. J.* 50 (1952) 679–690.
- [25] A.J.P. Martin, R.L.M. Synge, A new form of chromatogram employing two liquid phases. 1. A theory of chromatography. 2. Application to the micro-determination of the higher monoamino-acids in proteins, *Biochem. J.* 35 (1941) 1358–1368.
- [26] W.J. Moore, *Physical Chemistry*, fourth ed., Prentice-Hall, Inc., Englewood Cliffs, 1972.
- [27] R.C. Weast, M.J. Astle, W.H. Beyer, *CRC Handbook of Chemistry and Physics*, 69th ed., CRC Press, Inc., Boca Raton, Florida, 1988.
- [28] M.W.-H. Li, H. Zhu, M. Zhou, J. She, Z. Li, K. Kurabayashi, X. Fan, Peak focusing based on stationary phase thickness gradient, *J. Chromatogr. A* 1614 (2020).
- [29] D.E. Bautz, J.W. Dolan, L.R. Raddatz, L.R. Snyder, Computer simulation (based on a linear-elution-strength approximation) as an aid for optimizing separation by programmed-temperature gas chromatography, *Anal. Chem.* 62 (1990) 1560–1567.
- [30] S.N. Atapattu, K. Eggers, C.F. Poole, W. Kiridena, W. Koziol, Extension of the system constants database for open-tubular columns: system maps at low and intermediate temperatures for four new columns, *J. Chromatogr. A* 1216 (2009) 1640–1649.
- [31] E.C.W. Clarke, D.N. Glew, Evaluation of thermodynamic functions from equilibrium constants, *Trans. Faraday Soc.* 62 (1966) 539–547.
- [32] F. Aldaeus, Y. Thewalim, A. Colmsjö, Prediction of retention times of polycyclic aromatic hydrocarbons and *n*-alkanes in temperature-programmed gas chromatography, *Anal. Bioanal. Chem.* 389 (2007) 941–950.
- [33] B. Karolat, J. Harynuk, Prediction of gas chromatographic retention time via an additive thermodynamic model, *J. Chromatogr. A* 1217 (2010) 4862–4867.
- [34] L.M. Blumberg, Distribution-centric 3-parameter thermodynamic models of partition gas chromatography, *J. Chromatogr. A* 1491 (2017) 159–170.
- [35] J.C. Giddings, Elementary theory of programmed temperature gas chromatography, *J. Chem. Educ.* 39 (1962) 569–573.
- [36] A.B. Fialkov, A. Gordin, A. Amirav, Extending the range of compounds amenable for gas chromatography – mass spectrometric analysis, *J. Chromatogr. A* 991 (2003) 217–240.
- [37] E. Grushka, Chromatographic peak capacity and factors influencing it, *Anal. Chem.* 42 (1970) 1142–1147.
- [38] K.A. Stevenson, L.M. Blumberg, J.J. Harynuk, Thermodynamics-based retention maps to guide column choices for comprehensive multi-dimensional gas chromatography, *Anal. Chim. Acta* 1086 (2019) 133–141.
- [39] V.E. Shiryaeva, A.A. Korolev, T.P. Popova, A.Y. Kanateva, A.A. Kurganov, The stability study of thermodynamic parameters of sorption of light hydrocarbons on poly [Trimethylsilyl (Propyn-1)] at different temperatures, *J. Chromatogr. Sci.* 57 (2019) 778–783.
- [40] C.F. Poole, S.K. Poole, Separation characteristics of wall-coated open-tubular columns for gas chromatography, *J. Chromatogr. A* 1184 (2008) 254–280.
- [41] W. Kauzmann, *Kinetic Theory of Gases*, W. A. Benjamin, Inc., New York, 1966.
- [42] Y.S. Touloukian, S.C. Saxena, P. Hestermans, *Thermal Conductivity, Nonmetallic Liquids and Gases*, IFI/Plenum, New York, 1970.
- [43] Y.S. Touloukian, S.C. Saxena, P. Hestermans, *Viscosity*, IFI/Plenum, New York, 1975.
- [44] J.T.R. Watson, *Viscosity of Gases in Metric Units*, Her Majesty's Stationery Office, Edinburgh, 1972.
- [45] J.V. Hinshaw, L.S. Ettre, The variation of carrier gas viscosities with temperature, *J. High Resolut. Chromatogr.* 20 (1997) 471–481.
- [46] L.S. Ettre, Viscosity of gases used as the mobile phase in gas chromatography, *Chromatographia* 18 (1984) 243–248.
- [47] J. Crank, *The Mathematics of Diffusion*, second ed., Clarendon Press, Oxford, 1989.
- [48] E.N. Fuller, P.D. Schettler, J.C. Giddings, A new method for prediction of binary gas-phase diffusion coefficients, *Ind. Eng. Chem.* 58 (1966) 19–27.
- [49] V.R. Maynard, E. Grushka, Measurement of diffusion coefficients by gas-chromatography broadening techniques: review, in: J.C. Giddings, E. Grushka, R.A. Keller, J. Cazes (Eds.), *Advances in Gas Chromatography*, vol. 12, Marcel Dekker, Inc., New York, 1975, pp. 99–140.
- [50] L.M. Blumberg, W.H. Wilson, M.S. Klee, Evaluation of column performance in constant pressure and constant flow capillary gas chromatography, *J. Chromatogr. A* 842 (1–2) (1999) 15–28.
- [51] H. Darcy, *Les Fontaines Publiques de la ville de Dijon*, Dalmont, Paris, 1856.
- [52] H. Darcy, *The Public Fountains of the City of Dijon*, Kendall Hunt Publishing Co., Dubuque, IA, 2004.

- [53] L.M. Blumberg, Relations between pneumatic parameters of ideal gas in a column with uniform permeability, *Chromatographia* 41 (1995) 15–22.
- [54] I. Halász, K. Hartmann, E. Heine, Column types in gas chromatography, in: A. Goldup (Ed.), *Gas Chromatography 1964*, The Institute of Petroleum, London, 1965, pp. 38–61.
- [55] J.Å. Jönsson, Dispersion and peak shapes in chromatography, in: J.Å. Jönsson (Ed.), *Chromatographic Theory and Basic Principles*, Marcel Dekker, New York, 1987, pp. 27–102.
- [56] A.A. Zhukhovitskii, O.V. Zolotareva, V.A. Sokolov, N.M. Turkel'taub, A new method of chromatographic analysis, *Dokl. Akad. Nauk SSSR* 77 (1951) 435–438.
- [57] R.W. Ohline, D.D. DeFord, Chromatography, the application of moving thermal gradient to gas liquid partition chromatography, *Anal. Chem.* 35 (1963) 227–234.
- [58] W.A. Rubey, Operational theory and instrumental implementation of the thermal gradient programmed gas chromatography (TGPGC) mode of analysis, *J. High Resolut. Chromatogr.* 15 (1992) 795–799.
- [59] L.M. Blumberg, Outline of a theory of focusing in linear chromatography, *Anal. Chem.* 64 (1992) 2459–2460.
- [60] L.M. Blumberg, Limits of resolution and speed of analysis in linear chromatography with and without focusing, *Chromatographia* 39 (1994) 719–728.
- [61] J.B. Phillips, V. Jain, On-column temperature programming in gas chromatography using temperature gradients along the capillary column, *J. Chromatogr. Sci.* 33 (1995) 541–550.
- [62] H.D. Tolley, S.E. Tolley, A. Wang, M.L. Lee, Moving thermal gradients in gas chromatography, *J. Chromatogr. A* 1374 (2014) 189–198.
- [63] P. Boeker, J. Leppert, Flow field thermal gradient gas chromatography, *Anal. Chem.* 87 (2015) 9033–9041.
- [64] L.M. Blumberg, Migration and elution equations in gradient liquid chromatography, *J. Chromatogr. A* 1599 (2019) 35–45.
- [65] W.D. Snyder, L.M. Blumberg, Constant peak elution temperature with GC columns of different diameter. How to increase analysis speed with little or no loss in resolution, in: P. Sandra, M.L. Lee (Eds.), *Proceedings of the Fourteenth International Symposium on Capillary Chromatography*, Baltimore, USA, May 25–29, 1992, ISCC92, Baltimore, USA, 1992, pp. 28–38.
- [66] B.D. Quimby, V. Giarrocco, M.S. Klee, Speed Improvement in Detailed Hydrocarbon Analysis of Gasoline Using 100 μm Capillary Column, Application Note 228-294, Hewlett-Packard Co, vol. 43, Wilmington, DE, 1995, 5963-5190E.
- [67] V. Giarrocco, B.D. Quimby, M.S. Klee, Retention Time Locking: Concepts and Applications, Application Note 228-392, Hewlett-Packard Co, vol. 23, Wilmington, DE, 1997, pp. 5966–5962469E.
- [68] F. David, D.R. Gere, F. Scanlan, P. Sandra, Instrumentation and applications of fast high-resolution capillary gas chromatography, *J. Chromatogr. A* 842 (1999) 309–319.
- [69] P. Sandra, F. David, High-throughput capillary gas chromatography for the determination of polychlorinated biphenyls and fatty acid methyl esters in food samples, *J. Chromatogr. Sci.* 40 (2002) 248–253.
- [70] L.M. Blumberg, Method Translation in Gas Chromatography, 2003. USA patent 6634211.
- [71] N. Etxebarria, O. Zuloaga, M. Olivares, L.J. Bartolomé, P. Navarro, Retention-time locked methods in gas chromatography, *J. Chromatogr. A* 1216 (2009) 1624–1629.
- [72] C. Costa Neto, J.T. Köffer, J.W. De Alencar, Programmed flow gas chromatography. Part I, *J. Chromatogr.* 15 (1964) 301–313.
- [73] M.S. Klee, L.M. Blumberg, Theoretical and practical aspects of fast gas chromatography and method translation, *J. Chromatogr. Sci.* 40 (2002) 234–247.
- [74] J.C. Giddings, Use of multiple dimensions in analytical separations, in: H.J. Cortes (Ed.), *Multidimensional Chromatography Techniques and Applications*, Marcel Dekker, Inc., New York and Basel, 1990, pp. 1–27.
- [75] D.E. Bautz, J.W. Dolan, L.R. Snyder, Computer simulation as an aid in method development for gas chromatography. I. The accurate prediction of separation as a function of experimental conditions, *J. Chromatogr.* 541 (1991) 1–19.
- [76] W. Jennings, The “replacement” column, a recurring problem in gas chromatography, *Restek Adv.* 1 (2006) 2.
- [77] B. Yan, J. Zhao, J.S. Brown, J. Blackwell, P.W. Carr, High-temperature ultrafast liquid chromatography, *Anal. Chem.* 72 (2000) 1253–1262.
- [78] J.M. Davis, Statistical theory of spot overlap in two-dimensional separations, *Anal. Chem.* 63 (1991) 2141–2152.
- [79] R.E. Murphy, M.R. Schure, J.P. Foley, Effect of sampling rate on resolution in comprehensive two-dimensional liquid chromatography, *Anal. Chem.* 70 (1998) 1585–1594.
- [80] J.J.J. van Deemter, F.J. Zuiderweg, A. Klinkenberg, Longitudinal diffusion and resistance to mass transfer as causes of nonideality in chromatography, *Chem. Eng. Sci.* 5 (1956) 271–289.

- [81] M.J.E. Golay, Theory of chromatography in open and coated tubular columns with round and rectangular cross-sections, in: D.H. Desty (Ed.), *Gas Chromatography 1958*, Academic Press, New York, 1958, pp. 36–55.
- [82] L.M. Blumberg, Extension of Golay plate height equation for open-tubular columns, *J. Chromatogr. A* 1524 (2017) 303–306.
- [83] J.M. Kong, S.J. Hawkes, Diffusion in silicone stationary phases, *J. Chromatogr. Sci.* 14 (1976) 279–287.
- [84] M.J.E. Golay, The dynamic diffusion constant within fluid flow in an open straight tube with an elliptical cross-section, *J. Chromatogr.* 196 (1980) 349–354.
- [85] H. Poppe, J. Paanakker, M. Bronckhorst, Peak width in solvent-programmed chromatography. I. General description of peak broadening in solvent-programmed elution, *J. Chromatogr.* 204 (1981) 77–84.
- [86] L.M. Blumberg, T.A. Berger, Variance of a zone migrating in a non-uniform time invariant linear medium, *J. Chromatogr.* 596 (1992) 1–13.
- [87] L.M. Blumberg, Variance of a zone migrating in a linear medium. II. Time-varying non-uniform medium, *J. Chromatogr.* 637 (1993) 119–128.
- [88] E. Zauderer, *Partial Differential Equations of Applied Mathematics*, second ed., John Wiley & Sons, New York, 1989.
- [89] W.A. Peters, The efficiency and capacity of fractionating columns, *J. Ind. Eng. Chem.* 14 (1922) 476–479.
- [90] W.L. Jones, S. Dal Nogare, D.H. Desty, M.J.E. Golay, A.I.M. Keulemans, A.J.P. Martin, S.S. Ober, C.S.G. Phillips, J. Thoburn, E. Williams, Standard nomenclature considerations and recommendations, in: V.J. Coates, H.J. Noebels, I.S. Fagerson (Eds.), *Gas Chromatography*, Academic Press, New York, 1958, pp. 315–317.
- [91] J.C. Giddings, R.A. Keller, in: E. Heftmann (Ed.), *Theoretical Basis of Partition Chromatography, Chromatography*, Reinhold Publishing Corp., New York, 1961, pp. 92–111.
- [92] L.M. Blumberg, Theory of gradient elution liquid chromatography with linear solvent strength: Part 2. Peak width formation, *Chromatographia* 77 (2014) 189–197.
- [93] K. Lan, J.W. Jorgenson, Theoretical investigation of the spatial progression of temporal statistical moments in linear chromatography, *Anal. Chem.* 72 (2000) 1555–1563.
- [94] K. Lan, J.W. Jorgenson, Spatial and temporal progressions of spatial statistical moments in linear chromatography, *J. Chromatogr. A* 905 (2001) 47–57.
- [95] J. Leppert, L.M. Blumberg, P. Boeker, Equation for evolution of temporal width of a solute band migrating in chromatographic column, *J. Chromatogr. A* 1612 (2020) 460645.
- [96] J.C. Giddings, S.L. Seager, L.R. Stucki, G.H. Stewart, Plate height in gas chromatography, *Anal. Chem.* 32 (1960) 867–870.
- [97] A.B. Littlewood, *Gas Chromatography: Principles, Techniques, and Applications*, second ed., Academic Press, New York, 1970.
- [98] E. Glueckauf, Theory of chromatography. The “theoretical plate” concept in column separations, *Trans. Faraday Soc.* 51 (1955) 34–44.
- [99] D.H. Desty, E. Glueckauf, A.T. James, A.I.M. Keulemans, A.J.P. Martin, C.S.G. Phillips, Nomenclature recommendations, in: D.H. Desty, C.L.A. Harbourn (Eds.), *Vapor Phase Chromatography*, Academic Press, London, 1957, pp. xi–xiii.
- [100] G.H. Stewart, S.L. Seager, J.C. Giddings, Influence of pressure gradients on resolution in gas chromatography, *Anal. Chem.* 31 (1959) 1738.
- [101] J.H. Purnell, The correlation of separating power and efficiency of gas-chromatographic columns, *J. Chem. Soc.* (1960) 1268–1274.
- [102] E.F. Barry, R.L. Grob, *Columns for Gas Chromatography*, John Wiley & Sons, Hoboken, New Jersey, 2007.
- [103] J.H. Purnell, *Gas Chromatography*, John Wiley & Sons, Inc., New York, 1962.
- [104] A.I.M. Keulemans, *Gas Chromatography*, second ed., Reinhold Publishing Corp., New York, 1959.
- [105] J.C. Giddings, Plate height of nonuniform chromatographic columns. Gas compression effects, coupled columns, and analogous systems, *Anal. Chem.* 35 (1963) 353–356.
- [106] L.M. Blumberg, Erosion of efficiency in non-uniform linear chromatography, *J. High Resolut. Chromatogr.* 16 (1993) 31–38.
- [107] J.P. Foley, Resolution equations for column chromatography, *Analyst* 116 (1991) 1275–1279.
- [108] L.M. Blumberg, *Comprehensive two-dimensional gas chromatography: metrics, potentials, limits*, *J. Chromatogr. A* 985 (2003) 29–38.

- [109] L.M. Blumberg, Metrics of separation performance in chromatography. Part 2. Separation performance of a heating ramp in temperature-programmed gas chromatography, *J. Chromatogr. A* 1244 (2012) 148–160.
- [110] L.M. Blumberg, G. Desmet, Metrics of separation performance in chromatography: Part 3. General separation performance of linear solvent strength gradient liquid chromatography, *J. Chromatogr. A* 1413 (2015) 9–21.
- [111] L.M. Blumberg, G. Desmet, Kinetic performance factor – a measurable metric of separation-time-pressure tradeoff in liquid and gas chromatography, *J. Chromatogr. A* 1567 (2018) 26–36.
- [112] L.M. Blumberg, Kinetic performance factor – a proportional metric for comparing performance of differently structured liquid chromatography columns, *J. Chromatogr. A* 163 (2020) 461101.
- [113] L.M. Blumberg, Theory of fast capillary gas chromatography. Part 4: column performance vs. Liquid film thickness, *J. High Resolut. Chromatogr.* 22 (1999) 501–508.
- [114] L.M. Blumberg, Theory of fast capillary gas chromatography. Part 1: column efficiency, *J. High Resolut. Chromatogr.* 20 (1997) 597–604.
- [115] L.M. Blumberg, Theory of fast capillary gas chromatography. Part 3: column performance vs. Gas flow rate, *J. High Resolut. Chromatogr.* 22 (1999) 403–413.
- [116] P.A. Leclercq, C.A. Cramers, Optimum performance of capillary GC columns as a function of tube diameter and film thickness under various operation conditions, *J. High Resolut. Chromatogr.* 8 (1985) 764–771.
- [117] L.M. Blumberg, F. David, M.S. Klee, P. Sandra, Comparison of one-dimensional and comprehensive two-dimensional separations by gas chromatography, *J. Chromatogr. A* 1188 (2008) 2–16.
- [118] M.S.S. Amaral, Y. Nolvachai, P.J. Marriott, Comprehensive two-dimensional gas chromatography advances in technology and applications: biennial update, *Anal. Chem.* 92 (2020) 85–104.
- [119] L.M. Blumberg, Flow optimization in one-dimensional and comprehensive two-dimensional gas chromatography (GC × GC), *J. Chromatogr. A* 1536 (2018) 27–38.
- [120] J.C. Giddings, Evidence on the nature of eddy diffusion in gas chromatography from inert (nonsorbing) column data, *Anal. Chem.* 35 (1963) 1338–1341.
- [121] J.C. Giddings, Plate height theory of programmed temperature gas chromatography, *Anal. Chem.* 34 (1962) 722–725.
- [122] C.A. Cramers, P.A. Leclercq, Strategies for speed optimization in gas chromatography: an overview, *J. Chromatogr. A* 842 (1999) 3–13.
- [123] A. Wang, S. Hynynen, A.R. Hawkins, S.E. Tolley, H.D. Tolley, M.L. Lee, Axial thermal gradients in microchip gas chromatography, *J. Chromatogr. A* 1374 (2014) 216–223.
- [124] J.V. Hinshaw, Practical gas chromatography, *LCGC North Am* 31 (2013) 932–937.
- [125] N.H. Snow, Temperature programmed GC: why are all those peaks so sharp? *LCGC North Am* 37 (2019) 450–456.
- [126] L.M. Blumberg, Plate height formula widely accepted in GC is not correct, *J. Chromatogr. A* 1218 (2011) 8722–8723.
- [127] D.H. Desty, A. Goldup, W.T. Swanton, Performance of coated capillary columns, in: N. Brenner, J.E. Callen, M.D. Weiss (Eds.), *Gas Chromatography*, Academic Press, New York, 1962, pp. 105–135.
- [128] A.I.M. Keulemans, A. Kwantes, Factors determining column efficiency in gas-liquid partition chromatography, in: D.H. Desty (Ed.), *Vapor Phase Chromatography*, Academic Press, London, 1957, pp. 15–29.
- [129] J.H. Purnell, C.P. Quinn, An approach to higher speed in gas-liquid chromatography, in: R.P.W. Scott (Ed.), *Gas Chromatography 1960*, Butterworth, Washington, 1960, pp. 184–198.
- [130] B.O. Ayers, R.J. Loyd, D.D. DeFord, Principles of high-speed gas chromatography with packed columns, *Anal. Chem.* 33 (1961) 986–991.
- [131] J.H. Knox, M. Saleem, Kinetic conditions for optimum speed and resolution in column chromatography, *J. Chromatogr. Sci.* 7 (1969) 614–622.
- [132] H.A.C. Thijssen, Gas-liquid chromatography a contribution to the theory of separation in open hole tubes, *J. Chromatogr.* 11 (1963) 141–150.
- [133] J.C. Giddings, Maximum number of components resolved by gel filtration and other elution chromatography methods, *Anal. Chem.* 39 (1967) 1027–1028.
- [134] L.M. Blumberg, M.S. Klee, Metrics of separation in chromatography, *J. Chromatogr. A* 933 (2001) 1–11.
- [135] W.L. Jones, R. Kieselbach, Units of measure in gas chromatography, *Anal. Chem.* 30 (1958) 1590–1592.
- [136] A.J.P. Martin, D. Ambrose, W.W. Brandt, A.I.M. Keulemans, R. Kieselbach, C.S.G. Phillips, F.H. Stross, Nomenclature recommendations, in: D.H. Desty (Ed.), *Gas Chromatography 1958*, Academic Press, New York, 1958, p. xi.

- [137] G. Guiochon, Comparison of the performances of the various column types used in gas chromatography, in: J.C. Giddings, R.A. Keller (Eds.), *Adv. Chromatogr.*, vol. 8, Marcel Dekker, New York, 1969, pp. 179–270.
- [138] J.M. Davis, J.C. Giddings, Statistical theory of component overlap in multicomponent chromatograms, *Anal. Chem.* 55 (1983) 418–424.
- [139] B.J. Prazen, C.A. Bruckner, R.E. Synovec, B.R. Kowalski, Second-order chemometric standardization for high-speed hyphenated gas chromatography: analysis of GC/MS and comprehensive GC×GC data, *J. Microcolumn Sep.* 11 (1999) 97–107.
- [140] F. Gong, Y.-Z. Liang, F.-T. Chau, Combination of GC-MS with local resolution for determining volatile components in si-Wu decoction, *J. Sep. Sci.* 26 (2003) 112–122.
- [141] X. Shao, G. Wang, S. Wang, Q. Su, Extraction of mass spectra and chromatographic profiles from overlapping GC/MS signal with background, *Anal. Chem.* 76 (2004) 5143–5148.
- [142] L.M. Blumberg, Theory of gradient elution liquid chromatography with linear solvent strength: Part 1. Elution and retention parameters of a solute band, *Chromatographia* 77 (2014) 179–188.
- [143] L.M. Blumberg, G. Desmet, Optimal mixing rate in linear solvent strength gradient liquid chromatography. Balanced mixing program, *J. Chromatogr. A* 1476 (2016) 35–45.
- [144] R.P.W. Scott, G.S.F. Hazeldean, Some factors affecting column efficiency and resolution of nylon capillary columns, in: R.P.W. Scott (Ed.), *Gas Chromatography 1960*, Butterworth, Washington, 1960, pp. 144–161.
- [145] L.M. Blumberg, Theory of fast capillary gas chromatography. Part 2: speed of analysis, *J. High Resolut. Chromatogr.* 20 (1997) 679–687.
- [146] P.A. Bristow, J.H. Knox, Standardization of test conditions for high performance liquid chromatography columns, *Chromatographia* 10 (1977) 279–289.
- [147] J.C. Giddings, Comparison of the theoretical limit of separating ability in gas and liquid chromatography, *Anal. Chem.* 36 (10) (September 1964) 1890–1892.
- [148] T.A. Berger, Separation of a gasoline on an open tubular column with 1.3 million effective plates, *Chromatographia* 42 (1996) 63–71.
- [149] M. van Deursen, H.-G. Janssen, J. Beens, G. Rutten, C.A. Cramers, Design consideration for rapid-heating columns applied in fast capillary gas chromatography, *J. Microcolumn Sep.* 13 (2001) 337–345.
- [150] A. Papoulis, *Probability, Random Variables, and Stochastic Processes*, McGraw-Hill Book Co., New York, 1965.
- [151] L.M. Blumberg, D. Smith, A Continuous Sampling Rate Adjustment Algorithm for Digital Chromatographic Signals, Abstracts of 1985 Pittsburgh Conference & Exposition on Analytical Chemistry and Applied Spectroscopy, New Orleans Convention Center, LA, USA, 1985, p. 436. February 25 - March 1, 1985, Pittcon.
- [152] L.M. Blumberg, Antialiasing Filters for Continuously Varying Sampling Rate Conversion, Proceedings of ICASSP 86 IEEE-IECEJ-ASJ International Conference on Acoustics, Speech, and Signal Processing, Keio-Plaza Inner Continental Hotel, Tokyo, Japan, April 7–11, 1986, IEEE, New York, 1986, pp. 2595–2598.
- [153] T.H.M. Noij, *Trace Analysis by Capillary Gas Chromatography. Theory and Methods*, Ph. D. Thesis, Technical University of Eindhoven, Netherlands, 1988.
- [154] J.E. Cahill, D.H. Tracy, Effects of permeation of helium through the walls of fused silica capillary GC columns, *J. High Resolut. Chromatogr.* 21 (1998) 531–539.
- [155] T.A. Rooney, Theory of chromatography, in: R.R. Freeman (Ed.), *High Resolution Gas Chromatography*, Hewlett-Packard Co., 1979, pp. 7–21.
- [156] J.C. Sternberg, Extracolumn contributions to chromatographic band broadening, in: J.C. Giddings, R.A. Keller (Eds.), *Adv. Chromatogr.*, vol. 2, Marcel Dekker, Inc., New York, 1966, pp. 205–270.
- [157] R.D. Dandeneau, E.H. Zerenner, An investigation of glasses for capillary chromatography, *J. High Resolut. Chromatogr.* 2 (1979) 351–356.
- [158] L.M. Blumberg, T.A. Berger, Molecular basis of peak width in capillary gas chromatography under high pressure drop, *Anal. Chem.* 65 (1993) 2686–2689. In this issue.
- [159] M.S. Klee, J. Cochran, M. Merrick, L.M. Blumberg, Evaluation of conditions of comprehensive two-dimensional gas chromatography that yield a near-theoretical maximum in peak capacity gain, *J. Chromatogr. A* 1383 (2015) 151–159. In this issue.
- [160] L.M. Blumberg, T.A. Berger, M.S. Klee, Constant flow versus constant pressure in a temperature-programmed gas chromatography, *J. High Resolut. Chromatogr.* 18 (1995) 378–380.

Column technology: open-tubular columns

*Frank L. Dorman*¹, *Peter Dawes*²

¹Biochemistry and Molecular Biology, The Pennsylvania State University, University Park, PA, United States; ²Analytical Science, SGE, Ringwood, VIC, Australia

3.1 Introduction

In the early days of gas chromatography (GC), practitioners commonly used packed columns that were self-manufactured in their respective laboratories. Early users of the technique had to be capable of not only the instrumental aspects but also the column manufacturing. Commercial manufacturing of GC columns is a relative newcomer to the field, having been in existence for about the last 50 years. When commercial manufacturing first began, packed columns were the only columns used in the practice of GC. This may seem surprising to more recent users of the technique, and packed column GC has almost completely been replaced by wall-coated open-tubular (WCOT) capillary columns made from flexible fused-silica tubing. While there have been numerous advances made to the science of GC as a result of the use of these materials, Marcel Golay [1] is largely credited with first considering the benefits of the open-tubular column format. In the 1960 and 1970s, these columns were carefully manufactured using glass capillaries, based on the work of Desty [2].

Due to the inflexibility and fragility of these columns, however, they remained beyond the ability of many chromatographers. It was the innovation of drawn fused-silica capillary tubing that really moved the WCOT glass capillary format to commercial success. The work of Dandeneau and Zerenner [3] of Hewlett Packard Corporation as well as of Lipsky [4] made the WCOT capillary format available to all practitioners, and its importance cannot be overlooked. Due to the advantages of the WCOT capillary format, and the ease of use, capillary GC is possibly the most powerful common separation technique readily available to the analytical community. While only a subset of organic and organometallic compounds are amenable to a GC analysis (estimates are generally between 10% and 20%), it is generally the technique of choice due to its high efficiency and resolving power.

The introduction of thin-wall flexible fused-silica capillary tubing to GC by Dandeneau and Zerenner in 1979 was the important step that was needed to make capillary GC the widely utilized analytical technique that it is today.

Conventional glasses that were used up to that point are generally thought of as being inert and unlikely to react with the compounds, but in reality they are highly reactive when passing nanogram or smaller quantities of analytes down a long narrow capillary tube with high residence time at elevated temperatures. In conventional glasses such as soda glass and borosilicate glass, there is a very large percentage of metal oxides and other materials that may interact with the analyte molecules. These metal oxides may also cause catalytic breakdown of the polymer stationary phase at elevated temperatures.

Synthetic fused-silica material is very pure silicon dioxide, but it still has to be treated correctly to achieve the levels of inertness required in modern capillary GC columns. Correctly drawn and treated fused-silica tubing is the first essential ingredient of a high-quality fused-silica capillary column.

The inertness that can be achieved with fused-silica capillary columns was the driving force for their introduction, but there are other reasons for its successful adoption. Previously, the glass capillary columns that had an inside diameter of 0.25 mm had an outside diameter of around 1.0 mm. This meant that the tubing was not flexible, was fragile, and the curvature meant that it could not be inserted for any distance into a fitting. In addition, the large annular area at the end of the column added a significant dead volume, and so real skill was required to be able to make connections without getting some degree of peak tailing and loss of resolving power. Fused-silica capillary material has a thin wall and is flexible, making it very easy to work with compared to the earlier glass columns, and being thin walled it became very easy to make low or even zero dead volume connections.

An additional advantage of fused silica that the manufacturers understand well was that the glass coils that were previously used for GC columns were extremely slow to draw down to size and then bend it into a coil. The

speed of the process was in the order of 1 m min^{-1} , and it was normal in capillary column production to have banks of glass-drawing machines making the coils very slowly. With thin-wall fused-silica capillary tubing and the techniques used to draw flexible fiber optic material, the draw speed of the tubing can be in the order of hundreds of meters per minute but more usually is at a rate of around 20 m min^{-1} . So instead of producing a long 60-m column in over an hour, enough fused-silica tubing is commonly produced in a few minutes. With the old glass technology, capillary columns would be far more expensive than what analysts are accustomed to with modern fused-silica columns, and it is unimaginable how the worldwide demand would have been met (at a reasonable price).

3.2 Overview of the fused-silica drawing process

Companies producing fused-silica capillary tubing consider the techniques as proprietary, and so there is very little disclosure of ideas and technology between manufacturers of the tubing. The information given here is somewhat a general overview from the lessons of drawing fused-silica tubing for over 30 years. There will be different views on the appropriate procedures for producing fused-silica tubing.

3.3 The preform—raw material

The starting material for the fused-silica capillary tubing is known as a preform. The preform is a large high-purity synthetically produced fused-silica tube. There are three common ways of producing the preform material, but the most usual is continuous flame hydrolysis. Silane is oxidized to form silicon dioxide, and the resulting silicon dioxide dust is fused thermally onto a boule, which is like a big lump of pure fused silica. The boule can then be melted

and formed into the dimensionally very precise preform tube that is required.

In the past, fused silica was formed by feeding silicon tetrachloride into a hydrogen/oxygen flame in an additive process, forming a boule. The SiCl_4 process has fallen out of favor not only because of the large amounts of chlorine and hydrochloric acid that were formed in the process but also because GC columns formed in this manner always tended to have an excessively acidic character.

The hydroxyl concentration in the preform from the preferred hydrolysis process is very low, at below the 1-ppm level, and the metal impurities (metal oxides) are also less than 1 ppm. This is fortuitous because this is exactly what is needed for the production of capillary GC columns; however, it only happens because this is the property required for the much larger fiber optic manufacturing industry where this level of purity is required to achieve the stringent optical properties.

The dimensions of the preforms are typically in the range of 20-mm outside diameter with an inside diameter of around 14 mm, depending on the size required for the finished tubing. The dimension of the preform needs to relate to the ratio of the outside diameter to inside diameter of the drawn capillary tube. Under ideal drawing conditions, the ratio of outside diameter to inside diameter will be similar to the same ratio in the preform.

To achieve the required dimensional tolerances of the finished capillary, the preforms require quite remarkable tolerances, for example, often better than a 10- μm variation on the 20-mm outside diameter.

3.4 Surface chemistry

One of the long-term issues regarding fused-silica capillary tubing is the surface chemistry. There have been many different ways proposed on how to treat the capillary tubing to obtain the

ideal surface characteristics for inertness of the finished column, "coatability" of the surface with the stationary phase, and the forming of the covalent bonds between the stationary phase and the glass surface. What is often not discussed is what can be done as part of the drawing process that can have a dramatic impact on the surface chemistry and the quality of the capillary column that is ultimately produced. Without this control and knowledge, it is very difficult to reliably produce many batches of capillary columns even with surface chemistry normalization treatments. A common problem for many capillary column manufacturers is that a column type can be made consistently for a long period of time and then batches of the column fail to coat correctly and meet specifications. Producing capillary columns for many years was perceived as a black art until factors in the drawing process became better understood through careful experimentation with capillary drawing conditions and measurement of parameters such as the wettability of the fused-silica inner wall through contact angle measurements to determine silanol concentrations on the inner surface. In this way, it was eventually possible to understand the seemingly insignificant changes in the drawing process that had such a great impact on the GC capillary column manufacturing process.

3.5 Drawing of the capillary from the preform

The process of pulling a capillary tube from a large preform tube has been likened to "pulling toffee;" there are no dies to form the fiber. The end of the fused silica is brought to a very precisely controlled temperature and a molten thread is pulled from the preform. The dimensions of the capillary thread are managed by accurate pulling speed of the capillary combined with precise feed speed of the preform.

The ratio of draw speed to feed speed (draw ratio) predominantly determines the dimension of the capillary tube derived from the larger preform. For typical dimensions of capillary GC columns, a very high draw ratio is used where, from every meter of preform, over 4000 m of capillary is produced. As in fiber optic production, it is possible to draw tubing for capillary GC at enormous speeds of hundreds of meters per minute, but there are other considerations in chromatography tubing, which will be touched upon later. Typically, draw speeds are in the range of 10–40 m min⁻¹.

Because very fine molten glass tubing is being pulled in a steady state, it is easy to imagine that vibrations will be transmitted to the capillary causing imperfections and stress points in the finished tubing. For this reason, it is critical that no vibrations are transmitted into the draw system and so shock-absorbing mounts are used throughout the machine. In addition, motors, gearboxes, and anything that moves on the tower must not introduce a vibration or any unevenness in the force that is applied to the capillary as it is pulled. Long hours have been spent when designing and building the towers to find the source of the most imperceptible unevenness of movement or force.

For conventional glasses such as soda glass or borosilicate glass, the melt temperature is in the range of 600–800°C. The high-purity fused silica has a melt temperature in the order of 2000°C, which must be very precisely controlled within the range of a few degrees.

Many years ago, a gas/oxygen flame was used for heating or even a hydrogen/oxygen flame. Precise control of the gas flows while monitoring the temperature of the neck down point of the preform enabled a surprisingly accurate temperature control but the fuel/oxygen ratios also had an impact on inner surface chemistry of the capillary tubing (Fig. 3.1).

The standard furnace heating system for fused-silica drawing is now an inductively



FIGURE 3.1 Neck down area on a fused-silica preform.

heated graphite furnace. A graphite core in the furnace (termed a susceptor) is heated inductively, which in turn radiates heat to the fused-silica preform. Of course, the heated graphite would ignite in the presence of air and to prevent this as well as to protect the capillary from contamination, the furnace is purged with argon.

To control the level of acid and moisture content inside the preform during the draw process, it is also usual to purge the preform with inert gas. Some also use the purge gas pressure to finely control the dimensions of the resulting capillary.

The dimensional control of fused-silica capillary columns has steadily improved, making it possible to establish more stringent dimensional specifications on the finished capillary. These tight dimensions are maintained through automated feedback loops on the drawing tower. Positioned just below the furnace is a two-axis laser micrometer, which is used to measure the dimensions of the drawn fiber. It is not possible to measure the inside diameter of the tubing, but this can be inferred from the outside diameter measurement, provided a narrow range of drawing conditions have been used and the ratio of outside diameter to inside diameter is maintained the same as the preform. The laser micrometer measurement of the outside diameter of the capillary is then used in a feedback loop to

control the feed and draw speeds to maintain the required outside diameter. This permits an extremely tight control of the diameter of the capillary tube and consequently the inside diameter.

In GC, reproducible analyte retention from column to column is required, which begins with the fused-silica capillary tubing. The inside diameter is critical for consistent gas flow characteristics of the column, and the smallest difference in the inside diameter of a capillary will have a substantial impact on gas flow or more correctly gas velocity through the column and therefore retention times. The gas flow through the column for a given pressure is proportional to the inside diameter to the power of 4 (flow $\approx ID^4$), so on a 0.25-mm ID fused-silica column a 10- μm difference in diameter will give a 17% increase in gas velocity, which is very significant.

Despite statements to the contrary, the inside diameter does not have a significant impact on the phase ratio of the column, which is an important parameter in determining retention characteristics. Because most WCOT GC columns are coated statically (described later), the phase ratio is directly related to the concentration of the coating solution. For a given coating solution, the phase ratio will stay the same for successfully coated columns irrespective of the inside diameter of the column. The phase thickness may be slightly different if the tubing ID changes but the retention characteristics remain the same.

The two-axis laser micrometer on the tower also measures the ovality of the tubing as it is drawn and a further feedback loop on the preform feed system precisely adjusts the positioning of the preform in the furnace to correct misalignment and ovality that develop during the draw. Ovality must be controlled for the same reasons that consistent inside diameter of the capillary tubing is required. Ovality of the tubing creates additional problems in making connections in analytical chemistry applications, particularly with Press-Fit connectors and metal ferrules, which are being used more frequently with fused-silica material.

3.6 Protective coating

It is well known that glass fractures easily and yet fine fused-silica tubing is extremely flexible and can even be tied in knots. Glass is inherently strong and flexible provided the surface does not have surface defects. Cracks will nucleate and grow from very small defects on the glass surface. Moisture and even dust particles in the air settling on the unprotected fused silica are enough to damage the surface and make the tubing extremely fragile. As soon as the drawn capillary exits the furnace and has cooled sufficiently, a protective layer must be applied.

The first fused-silica capillary GC columns had a protective silicone coating, which worked until a higher-temperature capability was required. Polydimethylsiloxane, when used as the stationary phase inside the column where oxygen is excluded, can easily be operated in excess of 300°C, but the same material on the outside of the column in air fails catastrophically at as low as 220°C. If the exterior cladding was not thermally stable at the temperatures used in GC separations, it would severely restrict the applicability of GC. Polyimide was quickly settled on as an appropriate material. Polyimide is widely used in the electronics industry and forms a strong coating that hermetically seals and protects the fused silica. The problem with polyimide is that it can be extremely difficult to work with.

The polyimide resin is applied to the fused silica through a pressurized die through which the capillary tubing is pulled soon after it exits the furnace. A very uniform and well-controlled coating can be applied, but the polyimide must be cured quickly by passing it through a thermal curing system. The manufacturer's material on the polyimide resins suggests curing the material by heating over very long periods of time, for optimum performance. Curing the material too fast at too high temperature will cause bubbles in the polyimide coating, which of course leads to a weak very-poor-quality fused-silica capillary. In the continuous capillary drawing

process, minimal time is available to cure the polyimide before it comes in contact with the take-off wheel pulling the fused-silica capillary. If a tower needs to be run at 20 m min^{-1} and it is a 9-m-high tower, for example, there is less than half a minute to get the polyimide cured hard enough before it must pass over the take-off roller.

With the pressurized coating tips that are now used, thinner better-controlled coatings can be applied, which can be more rapidly cured. Multiple coatings can be applied as the capillary is taken through a series of rollers, coating applicators, and curing ovens.

Ultimately, the thickness of the cured polyimide coating needs to be around $15 \mu\text{m}$ to ensure good protection of the fused silica. In the SGE process, two coatings are applied as shown in

the schematic diagram (see Fig. 3.2), but some manufacturers apply more than this.

The final online check in the drawing process is a second two-axis laser micrometer monitoring the capillary tube before it is wound onto the spool. This checks the thickness and consistency of the polyimide coating. Again, the inline measurement allows feedback into the coating systems during the run (Table 3.1).

3.7 Alternative protective coatings

One of the limitations in GC is imposed by the polyimide coating. Polyimide is one of the best polymer materials in terms of its upper temperature limit, but conventional polyimide-clad fused silica will become weak with any

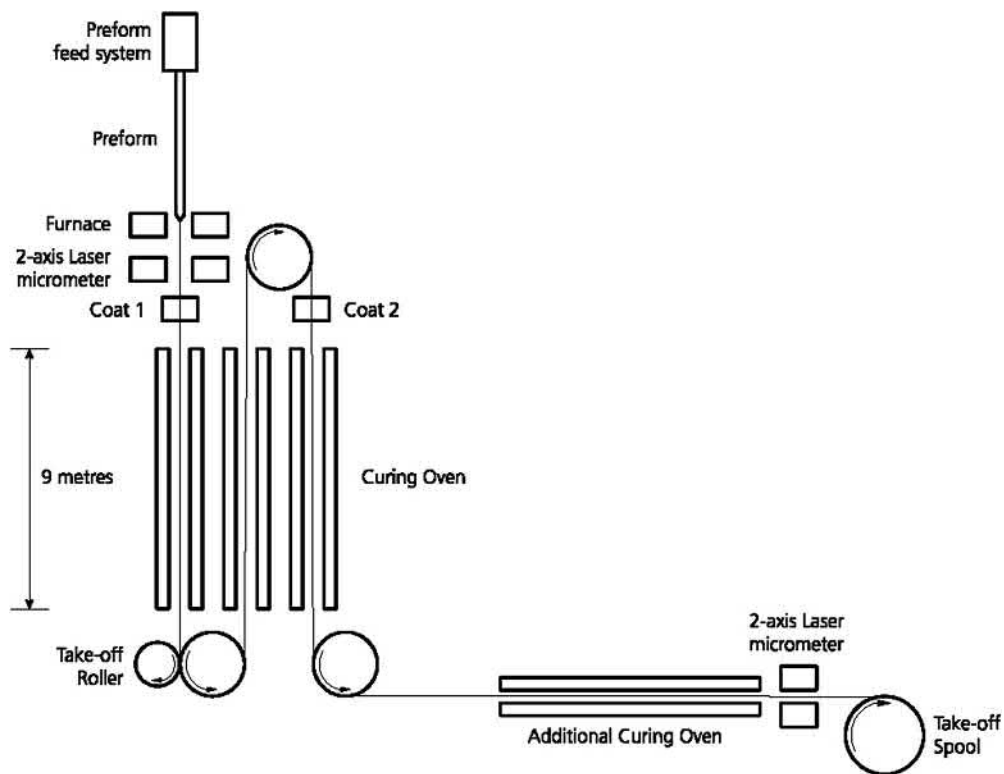


FIGURE 3.2 Fused-silica draw tower configuration.

TABLE 3.1 Standard SGE dimensional specifications for some of the different sizes of fused silica.

Nominal inside diameter (mm)	ID tolerance (μm)	Outside diameter (μm)	OD tolerance (μm)	Ovality (μm)	Polyimide coating (μm)
0.100	± 3	363	± 12	≤ 5	≥ 15
0.150	± 5	363	± 15	≤ 5	≥ 15
0.250	± 5	363	± 15	≤ 5	≥ 15
0.320	± 5	430	± 20	≥ 5	≥ 15
0.530	± 10	680	± 25	≤ 10	≥ 15

prolonged use above 370°C. Stationary phases for GC have long been available that will operate at much higher temperatures than this, such as the carborane–siloxane phases that can be operated to 480°C and silphenylene phases to 400°C. Several alternatives to deal with these higher required temperatures have been developed.

Aluminum-clad fused silica will operate to 500°C for very long periods of time and is produced by quenching molten aluminum onto the fused-silica capillary as it emerges from the furnace. The limitation of this material is that when the capillary is thermally cycled (as happens in GC), cracks in the aluminum coating develop. The problem comes about because of the mismatch in coefficients of thermal expansion between the fused silica and the thin aluminum coating. If an aluminum-clad fused-silica column is cooled slowly from the end of a temperature program run ($<10^\circ\text{C min}^{-1}$), it remains strong, but with rapid cooling, as used in capillary GC, the thin layer of aluminum cracks causing immediate weakening to the point that it becomes fragile; consequently, the aluminum-clad fused silica is of limited use in capillary GC.

The most successful solution for extending the temperature limit of fused-silica tubing is a high-temperature polyimide material. It is not disclosed why this material can achieve higher temperatures, but it is now used as standard by some manufacturers and does not deteriorate even at temperatures up to 420°C. The material

is 10 times more expensive than traditionally used polyimide resins, but the benefits outweigh the costs even for low-temperature applications.

3.8 Cleanroom environment

As has already been discussed, the unprotected capillary tube is extremely susceptible to damage from particles and moisture. Some drawing towers are incased in a controlled environment directly around the tower and others are operated in a cleanroom environment (Fig. 3.3).

Special attention is given to maintaining low humidity, as moisture, when the capillary is stressed by bending, will cause stress corrosion of the fused silica and weakening of the tubing. In addition, the conditioned air in the room is filtered to reduce particles that lead to point defects in the material and ultimately unexpected breaks in material that otherwise appears strong (Fig. 3.4).

3.9 Quality monitoring

Following the drawing process with the tubing on large spools, it must be checked for what are described as “point defects” and general strength. All material is run through a proof tester, which loads the material as it is wound over its entire length. The load should be below



FIGURE 3.3 Upper level of drawing towers in a controlled environment room.



FIGURE 3.4 Lower level of SGEs three drawing tower facility.

the expected failure point. Breakages from this test will lead to the entire batch being rejected. A useful tool to quantitatively monitor the quality of the material being produced is a tensile testing system, which loads samples of the tubing under stress to failure. Again, standards

for required failure stress are maintained (Figs. 3.5 and 3.6).

Following proof testing, and confirmation of dimensional tolerances from the several-kilometer-long continuous length of fused silica, the material needs to be wound off into the



FIGURE 3.5 Continuous proof testing machine.

lengths required for subsequent processing coating, whether it is for producing GC capillary columns, deactivated tubing, or producing into PEEK jacketed material (PEEKsil) for liquid chromatography transfer lines or columns.

It is also normal at this point to verify that the internal surface chemistry of the fused silica is as specified for the application the material is intended.

3.10 Observations on handling of fused-silica capillary tubing

Naturally people are conscious of not damaging the 15- μm -thick polyimide protective coating, but consideration must also be given to the inner bore of the tubing. The tubing is inherently straight, but if it is bent, stress is induced in fused silica, which then leads to crack propagation and failure. The greatest point of stress in the tubing is on the outer radius of tubing, but there is also stress induced in the bore of the tube, and damage to this inner wall will cause the tubing to be just as weak.

The types of things that will damage the fused silica from the bore are as follows:

- Chemically leaching of the bore of fused silica, which should not be necessary if the tubing has been drawn correctly.
- Packing fused silica with particles will scratch the bore of the material, making the tubing extremely brittle. In LC applications, this is sometimes done, but it is essential that the fused silica is reinforced and cannot be bent. By doing this, it can be possible to work with such columns, but the ultimate pressure before the tubing fails is reduced enormously.
- An observation that we do not have an adequate explanation for is when moisture-containing gas is pushed through a fused-silica capillary at a high velocity, even for a few seconds, the material becomes instantly extremely fragile. If gas must be pushed through fused-silica capillary tubing that has not had its inner surface modified in any way, the gas must be moisture-free.
- The smaller the radius that fused silica is coiled, the greater the stress on the material, which is not hard to imagine, but this stress is



FIGURE 3.6 Tensile testing of capillaries.

also highly dependent on the outside diameter of the tubing. For a given radius bend in the tubing, the stress at the surface goes up proportionally to the diameter.

Finally, when it is necessary to cut the fused silica, never snap it. The stress induced with such a violent action may be transmitted some distance into the tubing and can cause the material to be very weak for up to a meter from the break. In addition, particles of polyimide and

glass will contaminate the bore of the capillary, leading to activity and poor peak-shape issues. The fused silica should only be cut with a light scratch through the polyimide to the fused-silica surface underneath and gently pulled apart to give a square nonjagged break.

3.11 Column technology—coating the stationary phase

3.11.1 Surface preparations

As discussed in the previous section, surface pretreatment may not always be necessary if control of the chemistry in the bore of the tubing is possible during tubing manufacturing. In general, however, tubing pretreatment is done for several reasons: preparation of the surface for application of the stationary phase, increasing the column surface inertness, dehydration, changing the surface silanol content, or etching to increase roughness or surface area for some specific applications. Depending on what steps are to follow, the fused-silica surface may benefit from further processing or modification.

The only step to make a WCOT GC column that is truly required is the actual coating of the stationary phase. All of the other possible steps are optional, but they can severely impact the overall quality of the column that is produced. It is possible to coat many stationary-phase polymers directly onto untreated fused-silica columns, even if they have a variable surface chemistry. In order to make a high-efficiency, low-bleed column with excellent inertness, it is usually necessary to employ a number of additional steps prior to the actual coating of the stationary phase.

3.11.2 Leaching

Leaching is used to deionize the tubing surface through rinsing with acid solutions. Specifically, leaching solubilizes metal ions and

allows them to be removed from the surface of the column bore. Secondary to this removal of ions, leaching also increases the surface silanol concentration, which may be beneficial under certain circumstances as it allows for additional sites, which may serve as connection points for deactivation and/or stationary-phase molecules. While leaching could be carried out with caustic solutions, these materials are considerably more aggressive to the glass structure; therefore, leaching is usually carried out using acid solutions and most commonly hydrochloric acid. The concentration of this solution is also variable, but typically 1%–5% HCl solutions are used.

Contact time also plays a critical role in the leaching process, and leaching can be done using either static or dynamic techniques, but static is usually preferred. In this process, a plug of the leaching solution is moved through the column using an inert gas. This solution then “wets” the column surface. Once the plug of solution exits the other end of the column, both ends are sealed. Flame sealing is generally considered to provide the highest inertness, but other sealing devices can be used. The column is then heated (typically 200–250°C) and held at a final temperature for a period of time (typically 1–10 h). It is important to maintain constant temperature over the entire column.

Following leaching, the column will have high water content on the surface, in addition to the HCl. This must be removed prior to deactivation.

3.11.3 Rinsing and dehydration

Rinsing is necessary to remove the acid solution used in the leaching process. Deionized water may seem an obvious candidate for this procedure, but prolonged exposure to deionized water can cause a column to become very active. For this reason, rinsing should occur with the minimum amount of time and solution necessary to achieve removal of the leached material.

Additionally, the same solution used for leaching is typically used due to the activity that arises with the use of deionized water alone. Procedurally, the column ends are reopened, and the column is rinsed with the leaching solution. The rate of rinsing plays an important role, and slower rates often produce a better chromatographic surface. Typically, rinsing rates of 1 cm s^{-1} are reported [5]. Once a plug has been rinsed through the column (typically the plug should be about 25% of the total column volume), the column must then be dehydrated immediately. Dehydration occurs by following the plug with an inert gas and then heating the column to between 200 and 250°C and allowing the gas to continue to purge the column bore for approximately 1 h.

3.11.4 Surface deactivations

The deactivation of the column surface primarily serves two main purposes: First, the surface energy can be more closely matched to the stationary-phase molecules that will ultimately be coated. Second, the inertness of the column surface is increased by chemical modification of the acidic silanol sites that are present on either the untreated or acid-leached surface of the tubing. While the stationary phase can be directly coated onto the column surface in many cases, it is generally assumed that in order to produce a column of high inertness and durability, the column surface must be deactivated. This is true even for stationary phases that would normally wet the untreated or undeactivated tubing surface. As discussed in the first part of this chapter, it may be possible to minimize many of these column handling steps if direct control of the tubing chemistry is available. Since most users of GC do not have their own source of tubing, these steps are likely necessary. Additionally, only a few commercial column manufacturers (most notably SGE and Chrompack) actually manufacture their own tubing; so these steps are almost universal.

Deactivation can generally be divided into two classes: pinpoint and polymeric. While the end goal of each of these is the same, the method of reaching that goal is different. The idea behind a pinpoint deactivation is to react each silanol group with a chemical functionality, which derivatizes the acid moiety to something more neutral. In order to accomplish this, relatively small reactant molecules should be used to minimize steric hindrance of nearby silanols once a specific point has been reacted. Depending on the surface concentration and position of the silanols, this may be particularly difficult, especially if using highly functionalized reactants that contain larger moieties (e.g., triphenylchlorosilane). In a polymeric deactivation, much larger reactant molecules are used. These molecules are generally designed to react with one silanol and then cover, or mask, adjacent silanols. Mostly based on the research of Lee [6,7] and utilizing hydrosilane monomers or oligomers, polymeric deactivations can basically be described as a very thin layer of stationary-phase-like material that can be linked to the column surface through reaction with a surface silanol. Both techniques have benefits, but the end result can be the same if the chemistry is performed properly.

Pinpoint deactivation is typically carried out using either chlorosilanes or disilazanes. Each reacts with surface silanols, producing either HCl or NH₃ as the leaving group following bonding with the surface. This produces a silyl-ether connection from the surface of the tubing to the silicon of the deactivation reagent. Numerous reagents are commercially available from several sources at purities that typically do not require further processing. In some cases, these materials may be directly synthesized, but due to the wide variety available (Gelest, Silar, etc.), this is rarely necessary. The functionalities used are "tuned" to match the chemistry of the stationary phase that will ultimately be coated. For some manufacturers, a separate deactivation is used for every stationary phase offered, while for others very few different deactivations are

employed. It is arguable if a different deactivation is truly necessary for each possible stationary phase, given that most commercially available GC columns are of acceptable quality for most separations. For the most demanding applications, however, there may be an advantage in terms of inertness, bleed level, and lifetime. Finally, the deactivation reagent may also include functionalities that allow for direct chemical bond to the stationary phase. Most commonly this is done using vinyl groups in the deactivation layer and in the stationary phase to allow for bonding following application of the stationary phase.

Pinpoint deactivation is performed by treating the dehydrated tubing with a solution of the deactivation reagent. Since the possible reagents are too numerous to mention here, we will consider the use of a mixture of trimethylchlorosilane and dimethylvinylchlorosilane as a reasonable material. The ratios of these reagents will be adjusted to yield an overall vinyl percentage of typically 1%–10%. The vinyl groups are then available for bonding to the stationary-phase polymer, which also likely uses vinyl functionalities for this same purpose. The deactivation solution is made at a concentration ranging typically from 1% to 10% in a suitable solvent (dichloromethane). A plug of this material is then pushed through the column using an inert gas, much like the leaching process described earlier. When the plug exits the other end of the column, both ends are sealed again, and the column is heated to the temperature necessary to catalyze the reaction with the surface silanols. This temperature is usually in the range from 200°C to as high as 400°C, depending on the chemistry of the specific materials. Once the deactivation has occurred (time of heating varies between 2 and 10 h), the column is solvent-rinsed and then is ready for application of the stationary phase. If the column is to be used as a deactivated guard tubing, or for a retention gap, it is now ready for use, following a thermal cycle that runs to maximum operating temperature in an inert gas inner atmosphere.

3.12 Stationary phases

The coating of the stationary phase is again a similar procedure, regardless of the stationary phase being coated in most cases. In general, a stationary-phase polymer is either purchased from a supplier (Ohio Valley, GE, etc.) or directly synthesized as is typically done by most commercial suppliers of GC columns. A specified amount of the polymer, based on the desired stationary-phase film thickness, is dissolved in a suitable low-boiling solvent (e.g., pentane), forming a “coating solution.” The coating solution also likely contains other reagents used for cross-linking catalysis, further column deactivation, and immobilization. The types of compounds used for this are both widely varied and proprietary, but several have been discussed in the open literature such as peroxides and azo compounds [8].

Selection of the best stationary phase is likely the most important parameter in developing a GC separation. The selectivity of the analytes of interest and the stationary phase has a larger impact on the resulting compound resolution than any other parameter. For this reason, many stationary phases are commercially available, yet practitioners usually restrict themselves to very few actual materials. Most separations are performed using either a polydimethylsiloxane (PDMS, or a “-1” column) or a 5%polydiphenyl/95%polydimethylsiloxane (a “-5” column). In terms of selectivity, these stationary-phase moieties are very similar; so it can be concluded that most GC separations are run on essentially the same stationary-phase chemistry—an unfortunate situation. Users of GC often rely on the separation efficiency, or theoretical plates, to obtain resolution of their intended analytes. While this technique does have a very high efficiency, stationary-phase selectivity should still be considered first when choosing a capillary GC column. Modern WCOT GC stationary phases generally fall into

one of four categories: nonpolar polysiloxanes, functionalized polysiloxanes, polar nonsiloxanes, and other hybrid materials.

Nonpolar polysiloxanes comprise the largest group of materials, including the 1- and 5-type materials already mentioned. Additional phases employing arylene (or silphenylene) functionalities in the siloxane backbone have also received considerable attention due to their decreased levels of bleed and increased resistance to damage from oxygen. While substitution of arylene functionalities in place of the oxygen in the polymer backbone does change the stationary-phase selectivity relative to the pendant-substituted materials, the overall polarity is often indistinguishable. Most manufacturers offer both chemistries and often denote the arylene polymers as “MS” columns to indicate that they are preferred with mass spectrometric detectors, which may benefit from reduced bleed levels. Many of these columns use a poly(tetramethyl-1,4-silphenylenepolysiloxane), but many other moieties have been investigated, and many are commercially available under a variety of names [9]. The use of these materials generally improves the performance of the GC column, and, as a result, most new stationary phases that have been commercialized employ this type of chemistry, often in addition to the more typical pendant substitution of the silicon in the polysiloxanes.

Functionalized polysiloxanes, employing both arylene functionalities in the polymer backbone and pendant moieties, account for the greatest number of commercially available stationary phases, even if they are not the most used. Substitution of the dimethyl groups in PDMS with high concentrations of diphenyls (20%–65%), trifluoropropylmethyl, cyanopropylphenyl, bis-cyanopropyl, and many other moieties makes up a large range of possibilities for the analytical chemist to choose from. These materials allow for additional modes of interaction of the stationary phase with the analytes of

interest, other than what is offered by PDMS or five phases alone. For functionalized analytes, these materials generally offer improved selectivity, but do so sometimes at the cost of efficiency. Specifically, columns using high cyanopropylphenyl, or bis-cyanopropyl functionalities, often have about 2/3 of the efficiency of a PDMS column with similar dimensions. This is likely due to the polymer structure and a corresponding reduction in diffusivity as compared to PDMS polymers. Even with this decrease in efficiency, the increase in selectivity makes this a more than beneficial tradeoff, especially in the case of demanding separations such as FAME isomers, dioxins, or PCB congeners.

Polar, nonsiloxanes are a category that includes the waxes. Based on polyethylene glycol (PEG), and similar materials, these materials offer the highest polarity of the common stationary phases. For analytes that can hydrogen-bond to the stationary phase, these materials offer the highest selectivity. The difficulty with the materials in this category is their thermal limitations. In general, temperatures between 250 and 280°C represent the maximum isothermal temperatures for these materials. Additionally, these polymers often have increased levels of bleed and decreased efficiency as compared to the siloxanes and are usually not bonded. As a result, they are now viewed as more specialty-purpose materials, whereas a decade or two ago, they were considered general-purpose phases. Often, unless the PEG materials are absolutely necessary, polar-substituted siloxanes may allow for adequate selectivity without the drawbacks of these materials. For example, polytrifluoropropylsiloxanes (DB-210, Rtx-200, etc.) are very good choices for the separation of phenolics, and their increased thermal properties and improved efficiency make them a rather good choice as compared to the PEG materials for many applications.

There are also a number of materials that do not easily fit into any of the aforementioned categories. These hybrid materials are as diverse as

wax/polysiloxanes blends, ionic liquids, liquid crystals, and nonhydrocarbon arylene materials, most notably the polycarboranes. Each of these materials has value to the field of WCOT GC as they allow for selectivity not achieved with the PDMS-like materials. For example, the ionic liquids have received considerable interest for polar compound separations and as second-dimension GC \times GC materials. To date, they have not achieved the efficiency or the thermal stability of many of the polysiloxanes, but they do have very different solubility properties. The polycarboranes have seen application for many high-temperature separations such as high-temperature simulated distillation. These materials can be operated well in excess of 400°C, but they may exhibit a Lewis acid–base reaction with compounds such as carboxylic acids, so they remain a specialty material. Polycarboranes have also seen use for PCB congener analysis where they exhibit a very different elution order compared to many of the functionalized polysiloxanes and thus, are excellent as primary or confirmatory analysis columns for these separations.

3.13 Coating techniques

Modern commercial columns are generally coated using static coating techniques. Static coating implies that the column will be fully filled with a coating solution, and then the solvent will be slowly removed using evacuation under controlled temperature leaving the stationary-phase polymer behind as a thin layer. The benefit of static coating is that it produces the most uniform stationary phase, but the stationary phase must wet the deactivated surface and stay intact until the solvent has been removed and the column is thermally processed. If this becomes too difficult of a challenge, then the older technique of dynamic coating can be employed.

Dynamic coating requires less time than static coating and is often useful for scouting new column chemistries and the coating process may only take a few minutes. In dynamic coating, a viscous coating solution (5%–25% wt/vol) of the stationary phase is dissolved into a suitable solvent (pentane, dichloromethane, etc.) and an immobilization or a cross-linking reagent is added to this solution. The immobilization reagent, as previously mentioned, is generally in the 1%–5% wt/vol concentration range and is used to initiate cross-linking of the polymer molecules and also bonding of the stationary phase to the deactivation layer. The coating solution is then pushed through the tubing using relatively high pressure (due to the viscosity) at a controlled rate. As the plug nears the other end of the tubing, care must be taken to keep the same flow rate of the coating solution, so buffer columns or other devices are used to be able to control this rate. As the concentrated plug moves through the column, a layer of the stationary phase is deposited on the tubing wall. One of the limitations of dynamic coating is that the concentration of the stationary phase in the plug decreases as the plug moves through the column. This has the net effect of producing a gradient of stationary-phase thickness in the column. The stationary phase will be thicker at the end of the column where the plug was introduced and the exit end of the column will have a thinner stationary phase. Ultimately this produces a column that will exhibit different capacity factors for the analytes, depending on the direction of the installation into the GC. Also, if only portions of the column are used, as in GC \times GC, each portion will have slightly different capacity factors as well. Finally intended film thickness is not usually determinable without empirical knowledge of the process. While there are formulas for estimation of the stationary-phase thickness that would be produced given the flow rate of the plug and the viscosity of the solution, they are only approximations. If a column is to be coated using

dynamic techniques, then the film thickness may only be determined through actual isothermal testing of the final product. Following the coating, the stationary phase is bonded and cross-linked in a similar manner to a column coated by static techniques.

In static coating, a dilute coating solution (ca. 0.1%–1.0% wt/vol) is made using a suitable solvent, and immobilization reagent is added. The column is then completely filled with this solution. The concentration of the coating solution is determined by the intended film thickness as based on the following equation [5]:

$$\text{film thickness } (\mu\text{m}) = 2.5 \times \text{Column i.d. (mm)} \\ \times \% \text{concentration coating solution}$$

As previously mentioned, this coating solution will produce stationary-phase films on dissimilar i.d. columns so that the phase ratio is constant.

Once the coating solution has filled the entire column, one end of the column is sealed and vacuum is applied to the other end following immersion into a constant temperature environment. While the temperature is not necessarily high, it is usually a few degrees above ambient so that an even evaporation rate is maintained as the solvent vaporizes and is pulled away from the bore of the tubing. This process can be quite slow and represents the major drawback of static coating. Some longer columns with narrow i.d. (ca. 105 m \times 0.25 mm i.d.) may take a week or more to be properly evacuated.

There is a real art in sealing the one end of the column before applying the vacuum. It is important to not have a void at this location prior to sealing. Since the solvents used are flammable, flame sealing is not possible; so manufacturers use a variety of materials to make this seal. This is also considered proprietary and is often the cause for coating failures if the seal is improperly made.

Once the solvent has been completely removed, there will be a thin layer of stationary

phase left of the inside surface of the column. The column can now be thermally processed to initiate the cross-linking and bonding.

Depending on the immobilization reagents used, the thermal curing of the column may be done at a variety of temperatures. In general, peroxide catalysts require 250°C to initiate the cross-linking and bonding reaction, though many different materials are used. The coated column is connected to an inert gas stream and then heated to this initiation temperature where it is then held for a period of time (1–2 h) to allow the reaction to occur. Depending on the product, the column may be solvent-rinsed a final time to remove unbonded stationary phase. The “rinse-out” during this step should be small (less than 10%) or the column will likely be of questionable quality. Columns with high rinse-out are usually short-lived in the analytical laboratory, and repeated thermal cycling will cause the stationary phase to migrate toward the column exit slowly over time. This causes a continual change in capacity factor, and possibly selectivity, depending on the analytes. Rinse-out is often a quality measurement that commercial

manufacturers will determine prior to final commercialization of a stationary phase.

3.14 Column technology—quality evaluation

The final step in the manufacturing of capillary GC columns is to ensure the quality of the completed device. These same tests can also be used in the analytical laboratory that ultimately uses the columns to verify initial performance and as continuing verification of column performance as the column ages in normal use. For many years, the most common column performance test mixture was referred to as the “Grob mix” [10]. As developed in 1978, the Grob mix uses the target compounds listed in [Table 3.2](#).

These compounds are typically injected at higher concentration in split mode, so that injection port inertness is not as critical. For many years, the analysis of this mixture was considered to give a thorough evaluation of column reactivity, probing both acid- and base-reactive

TABLE 3.2 The Grob test mixture compounds.

<i>n</i> C10-FAME
<i>n</i> C11-FAME
<i>n</i> C12-FAME
2,3-Butanediol
Dicyclohexylamine
2,6-Dimethylaniline
2,6-Dimethylphenol
2-Ethylhexanoic acid
Nonanal
1-Octanol
Undecane (C11)
Decane (C10)

sites, as well as allowing for characterization of retention behavior. Due to the range of volatility, temperature-programmed analysis is necessary with this test mixture. When using temperature programming, the solute–stationary phase and solute–column surface interactions are reduced, relative to a lower-temperature isothermal analysis. This also serves to reduce the ability of this test to rigorously test the column inertness beyond a certain point. When it was first developed, column inertness was not nearly as high as it is today, and it was a more appropriate probe, even though it was a temperature-programmed analysis. Despite its limitations, the Grob test is still a viable way to determine column degradation in an analytical laboratory.

More recently, as column technology has continued to advance, a test mixture proposed by Luong, Graz, and Jennings [11] has received attention. Utilizing more reactive probes and lower on-column concentrations, this approach also uses either a late-eluting solvent or no solvent at all. The theory is that the solvent causes a “masking” of reactive sites, and that by having no solvent in front of the analytes as they move

through the column it is possible to get a more accurate test of a column's reactivity. Table 3.3 lists the compounds proposed in this work, but several column-manufacturing companies have adopted variations on this mixture, and the industry seems to be switching to a more rigorous test of column reactivity.

This test mixture has the added advantage of also being able to be analyzed under isothermal conditions due to the more limited range of volatility. This allows, as previously stated, a better interaction of the solute with both the stationary phase and the column surface. It is the combination of late-eluting (or no) solvent, analyte reactivity, and isothermal analysis that allows this mixture, or similar mixtures, to be better probes of today's higher-inertness columns. These mixtures could also be easily adapted into working analytical laboratories as continuing system control standards so that column degradation through routine use can be measured. This would allow for determination of when system maintenance was necessary or when the column had to be replaced.

TABLE 3.3 Test mix proposed by Luong, Graz, and Jennings.

Propionic acid
Octane
Nitrobutane
4-Picoline
Trimethyl phosphate
1,2-Pentanediol
Propylbenzene
1-Heptanol
3-Octanone
Decane

3.15 Column technology—summary

Modern WCOT GC columns are highly efficient, robust, and have generally high inertness. Advances in tubing manufacturing, column preparation, deactivation, and stationary-phase chemistry have all led to continued improvements since these formats were first considered. These columns represent what is generally the best separation technique for the compounds that are amenable to this technique, although there are still opportunities for further advancement. Stationary-phase chemistries still need to be developed to allow for increased resolution of many compounds, as efficiency does not solve all of the analytical challenges faced by chromatographers. Even though it is possible to obtain a column with several hundred thousand theoretical plates, selectivity is still the main tool when separating compounds of similar functionality and vapor pressure. Additionally, though not specifically discussed in this chapter, low thermal mass columns and new column formats are being explored, which promise to extend the range of analyses that capillary GC is capable of being used for and increase the ease of use for the practitioner.

References

- [1] M.J.E. Golay, in: V.J. Coates, H.J. Noebels, I.S. Fagerson (Eds.), *Gas Chromatography*, Academic Press, New York, NY, 1958.
- [2] D.H. Desty, J.N. Haresnape, B.H.F. Whyman, *Anal. Chem.* 32 (1960) 302.
- [3] R. Dandeneau, E.H. Zerenner, *J. High Resolut. Chromatogr.* 2 (1979) 2.
- [4] S.R. Lipsky, W.J. McMurray, M. Hernandez, J.E. Purcell, K.A. Billeb, *J. Chromatogr. Sci.* 18 (1980) 1.
- [5] K. Grob, *Making and Manipulating Capillary Columns for Gas Chromatography*, Huethig, Basel, Heidelberg, New York, 1986.
- [6] K.E. Markides, B.J. Tarbet, C.M. Schregenberger, J.S. Bradshaw, M.L. Lee, *J. High Resolut. Chromatogr.* 8 (1985) 741.
- [7] C.L. Woolley, R.C. Kong, B.E. Richter, M.L. Lee, *J. High Resolut. Chromatogr.* 7 (1984) 329.
- [8] B.E. Richter, J.C. Kuei, N.J. Park, S.J. Crowley, J.S. Bradshaw, M.L. Lee, *J. High Resolut. Chromatogr.* 6 (1983) 371.
- [9] P.R. Dvornic, R.W. Lenz, *High Temperature Siloxane Elastomers*, Huethig & Wepf, Basel, Heidelberg, New York, 1990.
- [10] K. Grob Jr., G. Grob, K. Grob, *J. Chromatogr.* 156 (1978) 1–20.
- [11] J. Luong, R. Graz, W. Jennings, *J. Sep. Sci.* 30 (2007) 2480–2492.

Column technology: porous layer open-tubular columns

Jaap de Zeeuw

Restek Corporation, Middelburg, The Netherlands

4.1 Introduction

Solid adsorbents have unique selectivity and characteristics that result in separations that are not possible using liquid stationary phases. The adsorption process allows the retention of very volatile components at higher temperatures, which creates conditions that make it easier to quantify them. Several types of adsorbents have found wide application in industry: molecular sieves are used for the separation of inert gases, and porous polymers (based on styrene divinylbenzene) are used for the separation of more polar compounds.

Adsorption materials are available in capillary columns, where retention is generated by a layer of adsorbent particles deposited on the inside wall of capillary tubing. Such capillaries are called PLOT (porous layer open tubular) columns, and they have several beneficial characteristics: they are highly efficient with high theoretical plate numbers, and they can be used at high operating temperatures.

However, PLOT columns can be challenging to make. Particles can be dislodged from the adsorbent layer and form restrictions within

the PLOT column, so manufacturing controls must be put in place to prevent this. Effective control procedures measure restrictions and use these values to control PLOT column quality. With good manufacturing controls, it has also been possible to apply PLOT technology to metal columns (MXT), allowing process-type applications to take full advantage of these developments [1].

4.2 Challenges in porous layer open-tubular (PLOT) column chemistry

PLOT columns allow separations combining adsorption chromatography with high-resolution capillary columns. The adsorbent is usually coated as a layer of particles on the inside wall of the capillary. The challenge is to make that layer stable. The layer usually consists of particles that are 0.1–2 microns in diameter. The stability of such a layer depends on the particle size, its physical characteristics, and the way the layer is built. If the layer is not stable, particles can leave their position and can “elute” from a PLOT column.

Fig. 4.1 shows an example of a PLOT column with unstable coating. When installed, sections of the layer can elute causing spikes on the baseline. Sudden changes in flow/pressure, or even shipping of the column, can initiate this process.

Fig. 4.2 shows a schematic of a layer where pockets are present. The moment the carrier gas pressure above the layer decreases (for instance, when a backflush is initiated), these pockets can blow up, releasing particles into the flow stream where they can create blockages and cause the following challenges:

- Retention times can change as restrictions build up.
- Higher pressures are required for the same flow setting.
- Columns need different pressures to operate optimally, depending on the restriction.
- Particles hit the detector, causing contamination.

Therefore, stabilization of the adsorption layers is important. Even if a top-quality PLOT column is being used, it is always best practice to have a mechanism in place to catch any



FIGURE 4.1 Example of solid particles eluting from an unstable PLOT column.



FIGURE 4.2 Schematics of a PLOT column particle-based layer where “pockets” are present.

eluting particles. Fortunately, there are several ways to ensure protection.

First, it is possible to catch loose particles by connecting a section of liquid-phase coated column at the end of the PLOT column. If a siloxane-coated section is used, the siloxane will act as a “glue,” trapping particles or segments that are released. Such a section is referred to as a “particle-trap.” The downside of this arrangement is that it requires a connector. Restrictions can also build up inside the connector (Fig. 4.3), resulting in higher inlet pressures that change as the restriction changes due to continued buildup during use.

A second method is to use a PLOT column that contains an integrated particle trap. Integrated particle trap PLOT columns contain a deposit of siloxane in both end sections of the PLOT column. This way, no connections are required. Still, there is some risk that particles will accumulate inside an integrated particle trap, forming restrictions, or that particles eventually will get through the column.

Because there is always some risk of particle release during transportation, the most practical recommendation is to always first flush the PLOT column if it is to be connected with valve- or flow-switching systems. To flush PLOT columns, use a 30%–50% higher flow and ramp it up to its maximum allowable temperature. During this flush, any dislodged particles will elute,

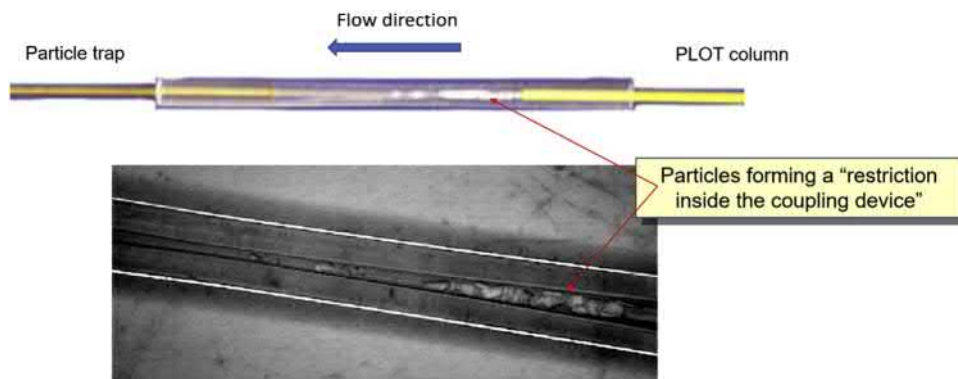


FIGURE 4.3 Restriction plug formed in the connection device used for coupling a particle trap to a PLOT column.

allowing you to use the column with more confidence.

4.3 Measurement of restriction of PLOT columns

PLOT columns will always have a higher restriction simply because the column has lower permeability due to the adsorption layer. Fig. 4.4 shows a way to measure the restriction

$$F = \frac{\text{tr}_1 \text{ of unretained component} \text{ [on uncoated tubing]}}{\text{tr}_2 \text{ of unretained component} \text{ [on column to test]}}$$

Ideal "open path": Flow-restriction factor "F" = 1.00

PLOT column with Flow-Restrictions: Flow restriction factor "F" = 0.2-0.8

FIGURE 4.4 Measuring the flow restriction factor is an effective way to measure the degree of restriction (resistance) in a PLOT column.

of PLOT columns, resulting in a flow restriction factor. This factor is defined using fixed capillary dimensions and measuring the impact on the retention time of an unretained component. Ideally, in an open tube, this factor is 1.00. If a layer is present, the ID of the PLOT column will change and any irregularity in the layer will also contribute to the restriction. This factor can be used during product quality testing to increase PLOT column reliability [2].

The flow restriction factor also makes it possible to measure reproducibility among different columns. Fig. 4.5 shows data obtained from commercial columns coated with porous polymers. There are large deviations in the flow restriction factor, but that can be controlled during manufacturing by using optimized coating and stabilization techniques.

4.4 Manufacture of PLOT columns

The manufacture of PLOT columns is quite different from liquid-phase coated columns. It requires specialized technology, and very few manufacturers can produce these columns. While liquid-phase columns mainly involve dissolving a polymer in a suitable solvent and depositing it on the capillary wall, adsorbents need a stable suspension and require different

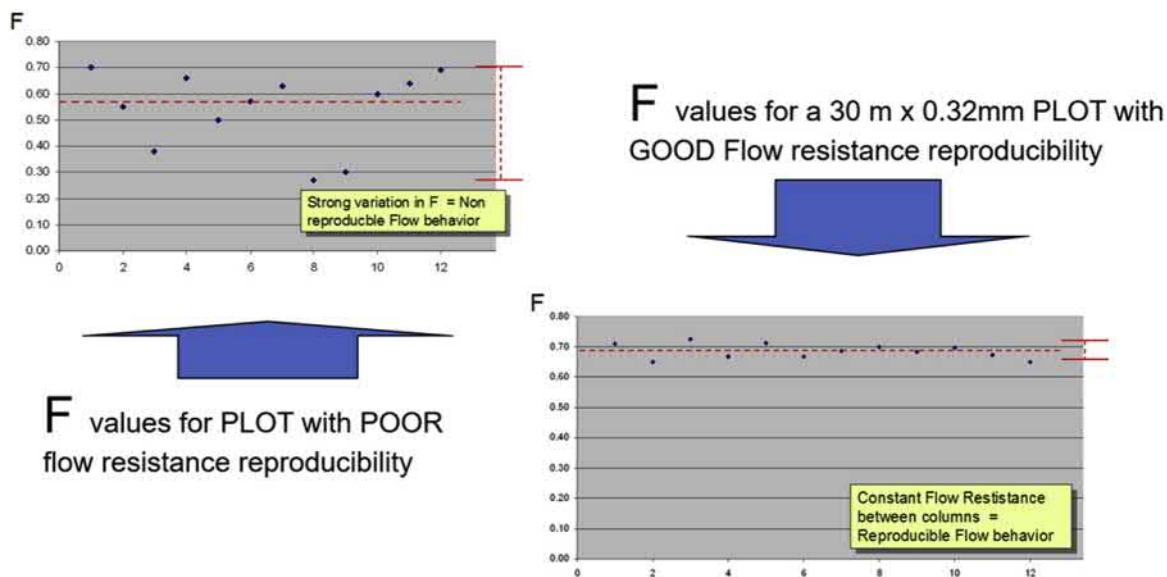


FIGURE 4.5 Example of a PLOT column series with good and bad particle stability: the difference is clearly shown by variation in the flow restriction factor.

coating techniques to build the thick layers that are necessary for good performance.

Dynamic coating has been used successfully for coating alumina adsorbent [3,4]. The trick here is to create a thixotropic suspension; the moment the alumina layer is deposited, it solidifies. Static coating is also possible, but it requires extremely stable suspensions because coating takes several days. One can speed up the coating process by using high-pressure static coating. In situ polymerization was described by Hollis in 1973 [5]. This technique is utilized for the preparation of PLOT columns with molecular sieves, zeolite, porous polymer, and silica. For the preparation of the column, a solution of monomer and catalyst is inserted into a column. Next, the column is heated for polymerization, producing a porous layer inside the column. After the reaction, the residue solvents, monomer, and catalyst are removed from the column by gas purging. This process removes solvent residues and activates the porous layer by freeing up the active

sites. More details are given by Mohnke and Heybey [6].

A new method for PLOT column coating was presented at ISCC-40, Riva del Garda, 2016. Here the column is filled with a suspension and is positioned in a centrifuge [7]. By spinning for 30–60 min at 3500 rpm, the particles are deposited on one side creating a crescent layer (Fig. 4.6). Because the deposition process uses gravitation force, the layer is built by the size of the particles, which adds stability. Initially, one expects such crescent layers not to be efficient, but in adsorption chromatography the particles do not have to be deposited as a homogeneous layer. We observe high efficiencies on several types of PLOT columns that have a clotty appearance, indicating irregular deposition of the solid phase. Because retention is caused by a surface process (adsorption), the coating does not need to be as homogeneous as we prefer for liquid phases. Fig. 4.7 shows a separation of solvents on a 30 m × 0.53 mm crescent



FIGURE 4.6 Cross view of a crescent PLOT column after spin coating for 60 min at 3500 rpm.

PLOT column that has about 1200 plates per meter. This technique makes it possible to prepare PLOT columns quickly in any diameter and length, and it does not require very stable suspensions.

4.5 Stabilization of adsorption layers

The stability of PLOT columns depends on the type of adsorbent material used. Alumina particles adhere together strongly, while porous polymers (such as the divinylbenzene types) develop a static electric load that makes formation of stable layers quite challenging.

Stability improves by using submicron or nanoparticles. Often, binders are added to improve stability. Binders are materials, such as salts or polymers, that will not negatively affect the retention and selectivity of the porous layer.

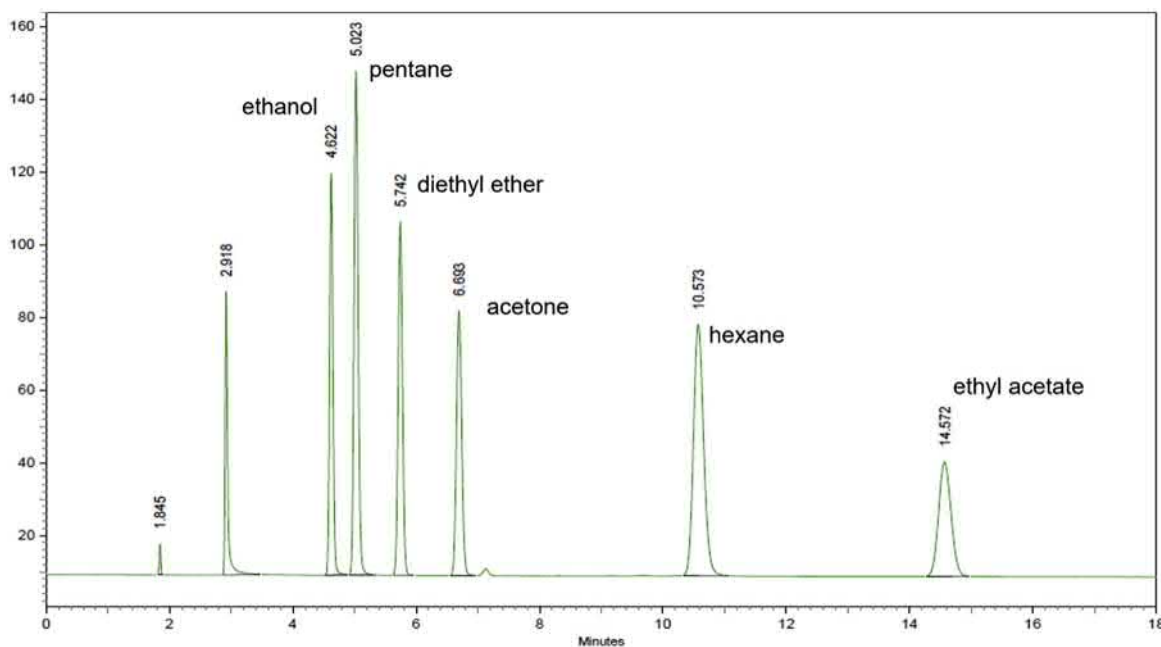


FIGURE 4.7 Separation of solvents on crescent styrene divinyl benzene/dimethyl acrylate PLOT column. After 60 min at 3500 rpm, 30 m \times 0.53 mm, Oven at 150°C.

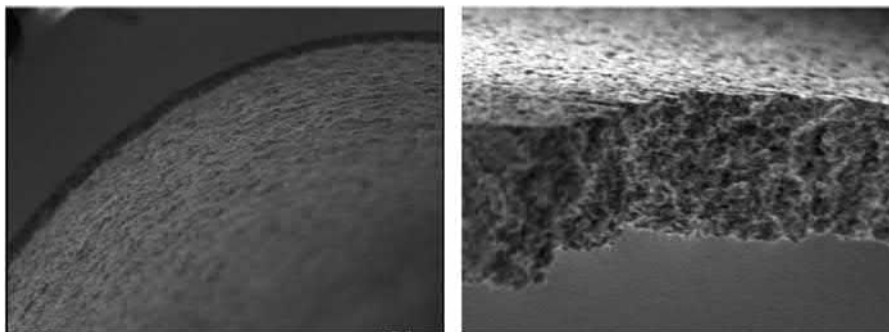


FIGURE 4.8 Example of a PLOT column with an integrated porous layer. Particles are not present, which will reduce any particle issues. Segments still can be ripped off due to large pressure variations.

However, the best way to enhance stability is to create a totally porous layer and eliminate the particles altogether. Fig. 4.8 shows an example of such an integrated porous structure: a porous layer of a styrene divinylbenzene derivative where the layer is not formed by particles. Such structures are strong, but even here, under extreme conditions, segments of the porous layer can release and can cause a restriction.

4.6 Behavior of adsorbents

Liquid stationary phases are commonly used in GC and their characteristics are well known.

That makes the use of solid adsorbents quite challenging because they behave very differently. For example, Fig. 4.9 shows the difference in impact on peak shape for liquid and solid phases. Overload of a liquid phase (polydimethylsiloxane or polyethylene glycol) will result in a leading peak. Higher amounts will push the peak backward and retention times will increase.

In contrast, when adsorbents are overloaded, the behavior is opposite that of liquid phases. Instead of a “leading” peak, we observe a “tailing” peak. The more we inject, the bigger the tail becomes and the peak will elute at a shorter retention time. Note that the tail due to

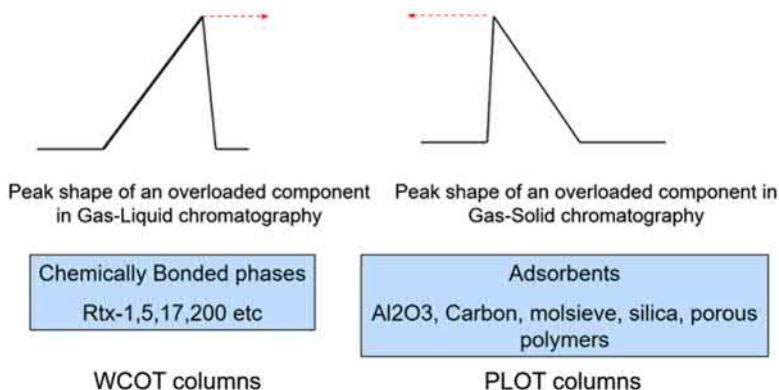


FIGURE 4.9 Impact of component concentration on peak elution profile using PLOT and WCOT column. Using PLOT the overloaded peak starts to tail and move forward, and with liquid phases the peak starts to lead and move backward.

overload always ends at the same position (Fig. 4.10).

This means that any components that elute in front of this peak may start to coelute. For several PLOT column types, different selectivities are available, which provides options for maximizing resolution of a highly overloaded peak. An example is shown in Section 4.9.1 discussing alumina.

4.7 PLOT columns in gas chromatography—mass spectrometry

Very often analysts ask if PLOT columns can be used with a mass spectrometer (MS). The challenge here is twofold: the high vacuum present in the MS and the relative low flows used with mass spectrometry. In general, the mostly commonly used PLOT columns are 0.53 mm ID because they have thick layers that provide maximum capacity (loadability) and retention. But to limit the flow for MS applications, 0.25 mm or 0.32 mm ID PLOT columns may be considered. The biggest challenge is that the vacuum in the ion source of the MS will make the linear velocity at the exit end of the column extremely high, increasing the risk of particle release, which could cause contamination of the ion source.

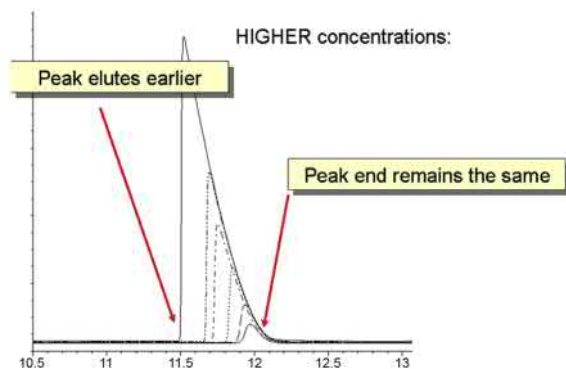


FIGURE 4.10 Impact of injected amount on peak shape and retention for adsorbents.

Fortunately, this scenario can easily be prevented by coupling the PLOT column with restriction tubing. Using a 5 m x 0.15–0.25 mm fused-silica capillary coated with 0.2–0.5 μm polysiloxane will help in two ways: (1) it will mitigate the pressure drop caused by the vacuum, and (2) if a particle is released, the siloxane coating will trap it. This setup can be used for 0.53 and 0.32 mm ID PLOT columns housed in either fused silica or metal tubing.

Although we may not be working under optimal flow conditions, we can still benefit from the high selectivity, loadability, and retention that PLOT columns offer. The only remaining challenge is to make a leak-free coupling when connecting columns in mass spectrometry. In our lab we have the best results with the Sil-Tite μ -Unions (Restek, USA), [8].

4.8 Types of capillary tubing

PLOT columns are primarily available in fused-silica capillary tubing. Most often, 0.53 mm ID tubing is used and is coated with 10–50 μm layers of adsorbent because thick layers are preferred for higher loading capacity. Adsorption is a surface process, and therefore, loadability is inherently limited. The 0.53 mm ID also operates at higher column flow, which reduces band broadening and helps to maximize sensitivity, especially when using a thermal conductivity detector. Most adsorbents are also available in smaller inner diameters, such as 0.32 and 0.25 mm ID. The 0.25 mm fused-silica columns are routinely used in portable GC platforms, where chip (MEMS) injection and detection techniques are used. Around 1990, such portable analyzers were introduced by Microsensor Technologies (MTI). Later other companies (Agilent, Q-Micro, Inficon) started using this technology, offering very fast, accurate, and sensitive portable gas analyzers [9].

In addition to fused-silica tubing, PLOT columns are also available in metal tubing. Restek

Corporation offers Molsieve 5A and 13X, Alumina BOND, and Q-type porous polymer phases in their metal (MXT) capillary tubing. Such columns are virtually unbreakable and are especially preferred for use in multicolumn analyzer systems. They also can be coiled in very tight diameters, allowing small ovens to be used. The chromatographic performance of the metal columns is comparable with the results obtained using fused-silica columns.

In practice, the biggest challenge with metal tubing is cutting the columns and even this is not difficult. A simple way to accomplish this is to use the same ceramic blades that are used for fused silica. Most of these ceramic blades have two different sides: a rough and a sharp side. Use the sharp side of the wafer to make a score. Ref. [10] provides a YouTube video showing how it is best done.

4.9 Most commonly used adsorbents

After the release of alumina as the first adsorbent, molecular sieves, carbon, silica, salt-coated, and porous polymer PLOT columns were introduced. Many of these are available in most common dimensions (0.25–0.53 mm ID) and in fused silica as well as metal. The most frequently used are the 0.53 mm ID columns in 25–30 m lengths because they provide the highest sample capacity. Table 4.1 provides an overview of most PLOT column adsorbents and their key application fields.

4.9.1 Alumina

Alumina has a unique selectivity for light hydrocarbons. This allows C1–C5 hydrocarbons, including all unsaturated isomers, to be separated with the highest possible resolution. Fig. 4.11 shows an analysis of impurities in crude 1,3 butadiene (peak 11) on an Rt-Alumina BOND/MAPD column. Methyl acetylene (peak 12) is an important component in this matrix.

On potassium chloride–deactivated alumina, methyl acetylene, 1,2-butadiene, and pentane will elute just before the 1,3-butadiene peak, so if the 1,3-butadiene sample is overloaded, it will elute earlier and overlap the target analytes. Sodium sulfate or MAPD deactivation solves this problem; it results in a higher polarity alumina surface, which makes methyl acetylene elute after the 1,3-butadiene peak.

The selectivity of alumina can be tuned using organic salts, such as potassium chloride, sodium sulfate, or sodium molybdate. Such columns are already in use, but they have limitations including temperature stability and low response factors for propadiene and acetylene. New-generation alumina columns provide significantly higher response factors, especially for propadiene (Fig. 4.12) and can be used up to 250°C. These columns usually have the acronym MAPD in the name, referring to methyl acetylene and propadiene.

Because of their selectivity, these new alumina columns can also be used for very fast analyses. Such columns not only allow accurate trace analysis of hydrocarbon impurities, but also can elute higher hydrocarbons faster and with good peak shape. By using specific types of alumina and an intensive deactivation ($\text{Al}_2\text{O}_3/\text{CFC}$), it also became possible to use alumina columns for refrigerant analysis [11]. Despite improved deactivation, some halogenated hydrocarbons will still decompose due to the catalytic activity of alumina. Recently it was also shown that hydrogen isomers and isotopes can be separated under subambient conditions using alumina columns treated with sodium sulfate and manganese sulfate salt deactivation [12].

4.9.1.1 Behavior of alumina: selectivity

Alumina surfaces behave with more polar characteristics if the column is used at lower temperatures. That means, if one wants more retention for polar analytes, the alumina columns must be operated at lower temperature. This can be done by decreasing the starting

TABLE 4.1 Applications for PLOT column adsorbents.

Adsorbent	Applications
Al ₂ O ₃ with deactivation salts	C1–C10 hydrocarbons, hydrogen isomers
KCl, Na ₂ SO ₄ , Na ₂ MoO ₄	C1–C5 isomers of unsaturated hydrocarbons
Al ₂ O ₃ /MAPD	C1–C10 and traces methyl acetylene and propadiene
Al ₂ O ₃ /CFC	Chlorofluorocarbons (CFCs)
Molecular sieve 5A	Noble gases, oxygen, nitrogen, C1–C3, carbon monoxide, nitrous oxide (N ₂ O), hydrogen spin isomers, H ₂ , D ₂ , T ₂ , HD, HT, DT
Molecular sieve 13X	Oxygen, nitrogen, C1–C3, carbon monoxide, naphthenes–paraffins C4–C12
Molecular sieve for argon/oxygen	Traces Ar in O ₂ and O ₂ in Ar, H ₂ , N ₂ , O ₂ , CO, C1–C3
Porous polymer, styrene divinylbenzene, Q-type	Hydrocarbons C1–C3, natural gas, refinery gas, CO ₂ , N ₂ O, NF ₃ , SF ₆ , solvents, sulfur gases, Freons, and water-containing samples
Porous polymer, ethylene glycol	Hydrocarbons C1–C3, polar solvents, trace H ₂ S,
dimethylacrylate polymer, U-type	COS in ethylene/propylene, SO ₂ , Freons
Carbon	Light hydrocarbons C1–C5, CO, CO ₂ , H ₂ , SO ₂ , CFCs
Silica	Light hydrocarbons C1–C10, C1–C4 isomers, sulfur gases, CFC, semipolar compounds, samples containing moisture
Inorganic salts, Lowox	Oxygenated hydrocarbons, range C1–C7, trace oxygenates in C1–C12 streams

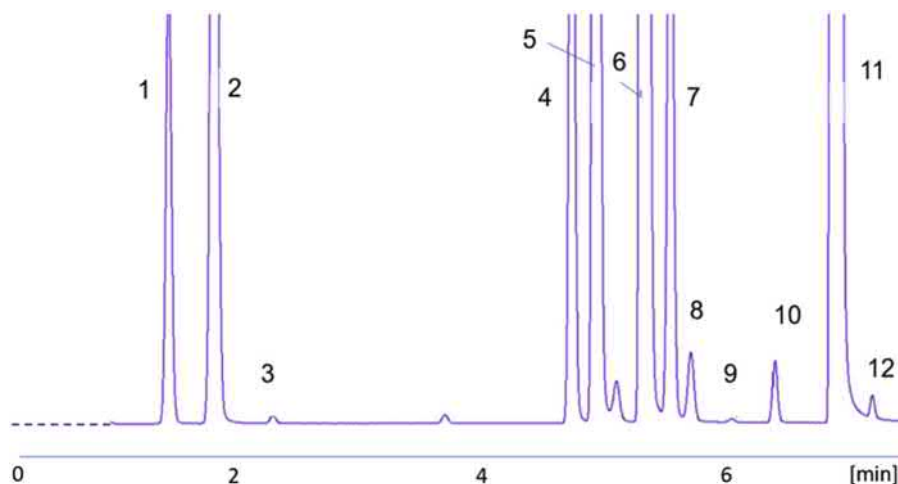


FIGURE 4.11 Impurities in crude 1,3 butadiene. Column: Rt-Alumina BOND/MAPD (50 m × 0.53 mm); oven: 70°C, 3 min → 200°C, 16.6°C min⁻¹; carrier gas: He, 11.5 psi; injection split: 1:5; peaks identification: 1. isobutane, 2. *n*-butane, 3. propadiene, 4. *trans*-2 butene, 5. 1-butene, 6. isobutene, 7. *cis*-2-butene, 8. isopentane, 9. *n*-pentane, 10. 1,2-butadiene, 11. 1,3-butadiene, 12. methyl acetylene.

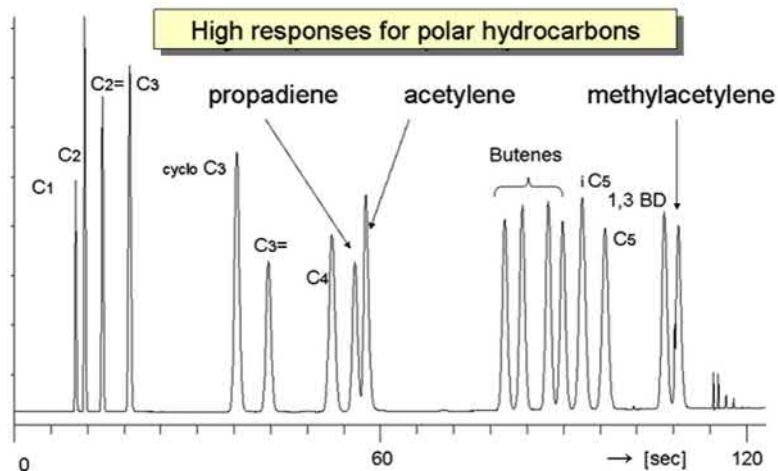


FIGURE 4.12 Fast analysis of C1–C5 using Al_2O_3 with special MAPD deactivation. Note the high responses of methyl acetylene, acetylene, and propadiene. Column: Rt-Alumina BOND/MAPD (15 m \times 0.53 mm); carrier He, 100 kPa; oven: 60°C, 0.5 min \rightarrow 150°C, 60°C min^{-1} ; injection split.

temperature, using a longer isothermal time at the starting temperature, using a higher gas flow, or using a slower temperature program. All these actions will reduce the elution temperature, which makes the alumina behave more polar as a result, the separations will change.

For example, at lower temperatures, polar hydrocarbons will move to the back of the chromatogram relative to *n*-alkanes. The biggest impact is observed with acetylene and propadiene, which can be positioned anywhere before or after the butane peak. Fig. 4.13 shows the position when changing the initial time at 60°C. Flow also has a big impact as shown in Fig. 4.14 where higher flow results in lower elution temperatures moving the polar hydrocarbons back. For further explanation of this impact, see Ref. [4,13].

4.9.1.2 Behavior of alumina: impact of water and other impurities

If water enters the alumina column, it will act as a deactivating agent and retention and selectivity will change. Water can be present in the sample, the carrier gas, or be introduced via a

leak. The impact of water depends on the amount as well as the column operating temperature.

Fig. 4.15 shows the impact of an injection of 4.5 μL of water into an alumina column. The result is about 15% shorter retention times and the relative position of propyne and 1,3-butadiene has changed. The water impact is reversible, as by heating the column for 3 h at 200°C the original retention is restored. The Rt-Alumina BOND/MAPD column can be used up to 250°C, which will shorten regeneration time significantly as water will elute faster. In practice, there are several actions one can take if water is suspected to be present:

- If water is present in the carrier gas, use moisture filters (traps) and check for leaks.
- If water is in the sample:
 - Selectively remove water from the sample. Note that this may also cause analyte loss.
 - Use a temperature program up to the maximum allowable operating temperature of the alumina column and remove the water after every analysis. This will take about 7–10 min.

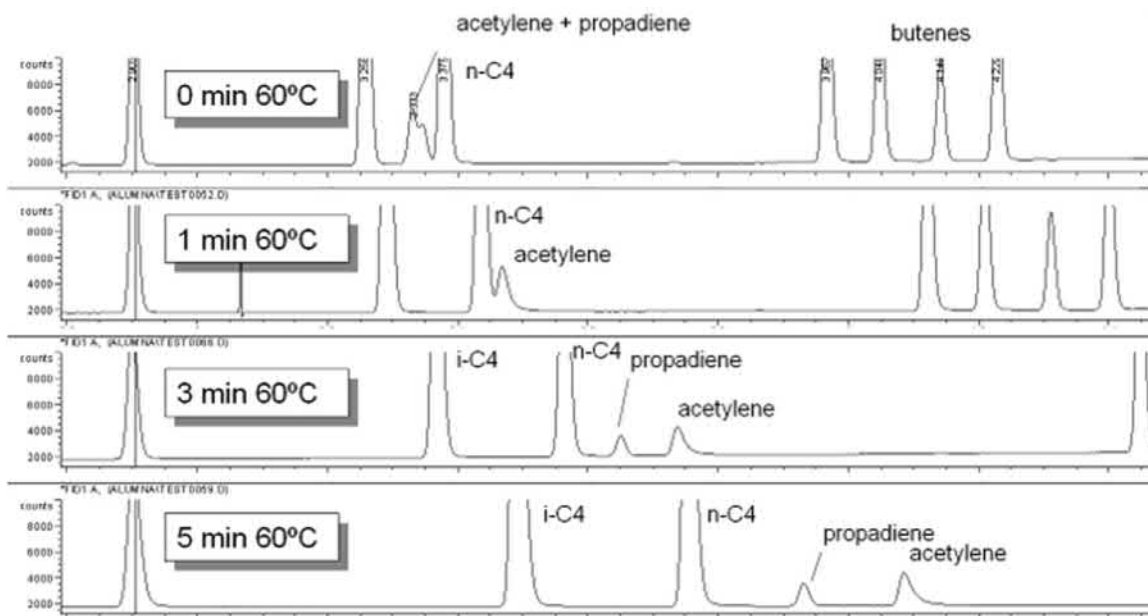


FIGURE 4.13 Impact of initial oven temperature and time on the relative position of acetylene and propadiene on an alumina PLOT column. Lower initial temperature and longer initial times will position acetylene and propadiene back in the chromatogram.

- If water levels are low, around 1–3 ppm, one can do 10–20 analysis and when a targeted peak elutes outside of its integration window, condition the column at the maximum allowable operating temperature for 30 min to remove the accumulated water.
- Use a thick-film PEG precolumn to retain the water. Water will elute after octane on most PEG phases. The first eluting peaks are injected onto an alumina column, then the water is backflushed or switched to a second detector if it has to be quantified. In this case we need a valve or Deans' switching setup.

Besides water, other polar molecules in the sample matrix can also affect retention, but water has by far the biggest impact. In order of decreasing impact: acids, alcohols, aldehydes, ketones, ethers, carbon dioxide, and sulfur compounds.

4.9.2 Molecular sieves

To get separation of even more volatile compounds, one needs a higher surface area. Molecular sieves (zeolites) have very high surface areas because of their structures. Type 5A consists of calcium aluminosilicate with an effective pore diameter of 5 Å, whereas type 13X is comprised of sodium aluminosilicate with an effective pore diameter of 10 Å.

The first molecular sieve glass capillary columns were introduced by Mohnke [14]. Later fused-silica columns became available for all common dimensions. To obtain a separation at temperatures above ambient, a thick layer is required (Fig. 4.16). Typical molecular sieve PLOT columns have up to 50 μm layers in 0.53 mm ID tubing.

4.9.2.1 Permanent gases/carbon monoxide

The zeolite consists of a well-defined porous structure, which generates retention even for

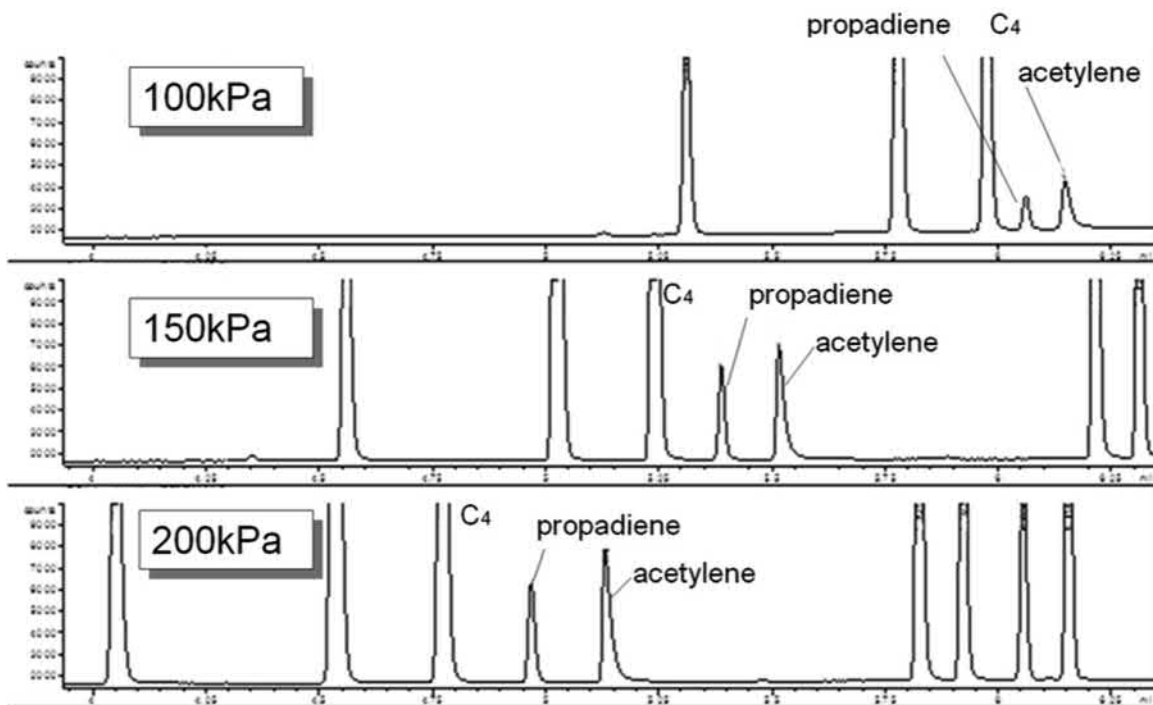


FIGURE 4.14 Impact of flow on the relative position of acetylene and propadiene on an alumina PLOT column. Higher flow will result in lower elution temperature, which will push these peaks back in the chromatogram.

the most volatile gas at moderate temperatures. It will separate all the noble gases including carbon monoxide at temperatures above 25°C (Fig. 4.17).

Here a pulsed-discharge ionization detector was used allowing low levels of permanent gases to be detected. When reducing the oven temperature to -148°C , one can even separate hydrogen isotopes including their spin isomers [15].

Adsorbents behave in a more polar fashion when operated at lower temperatures. As was true for alumina, the selectivity of zeolite molecular sieves is temperature-dependent. As a result, the relative position of carbon monoxide (being a polar compound) changes drastically when analysis is done at 40, 80, or 120°C (Fig. 4.18).

Molecular sieves will strongly adsorb water, resulting in a decrease of retention times. They are routinely used in GC filtration devices as drying agents. If water remains on the molecular sieve, the position of the carbon monoxide peak will change and this peak will move closer to methane. Conditioning for a few hours at 200°C or for 20 min at 300°C will totally regenerate the column. Sometimes oxygen and carbon monoxide show some activity, resulting in a tailing, low-response peak. Usually conditioning a molecular sieve column at high temperature in air will help to improve the peak shape.

4.9.2.2 Naphthenes and paraffins

Molecular sieve 13X is often used to separate naphthenes (cycloalkanes) from paraffins. Its larger pore diameter generates an interesting

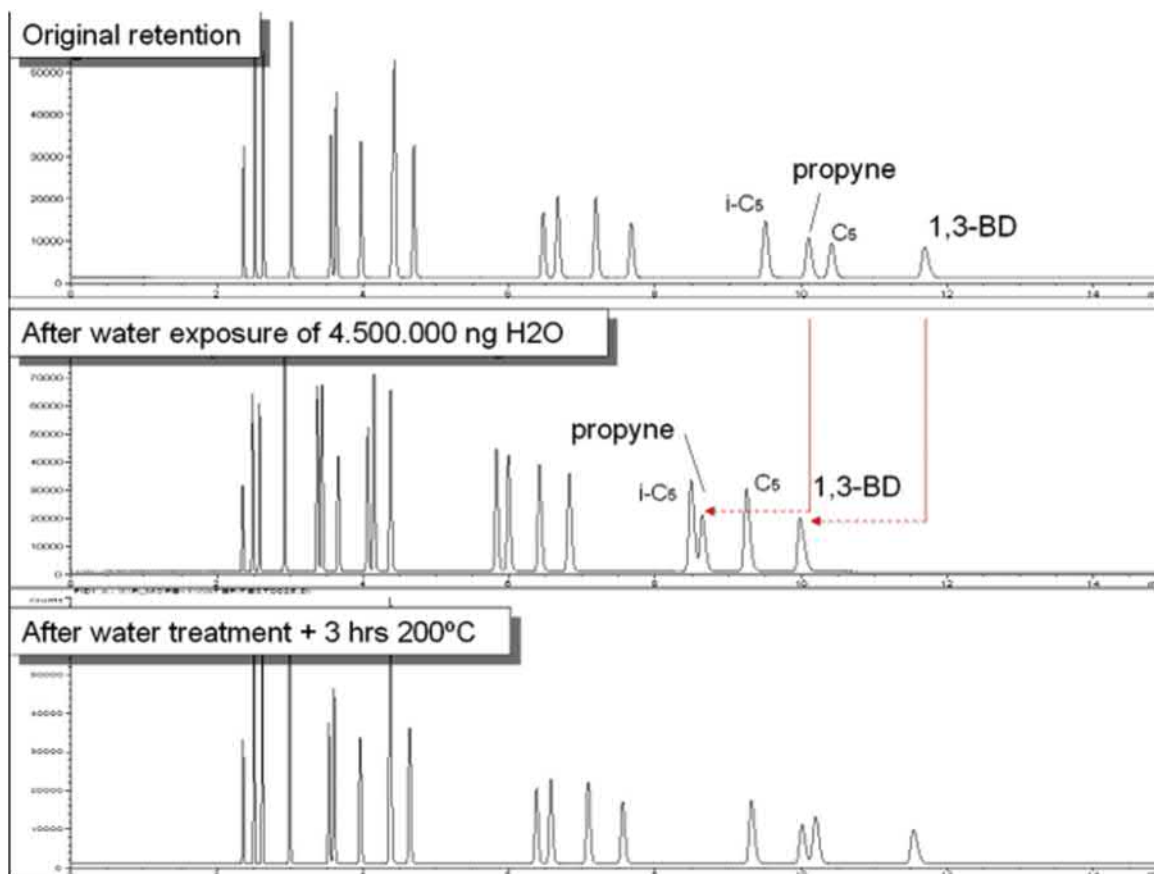


FIGURE 4.15 Impact of water on the retention and selectivity of alumina.

sieving effect. Retention of 13X molecular sieve columns is very high because of its high surface area. Once coated as a PLOT using submicron particles, temperatures of 500°C are required just to elute C10–C12 naphthenes/paraffins. Fig. 4.19 shows an example of this separation using a metal (MXT) capillary column. Metal is required as fused silica cannot be used here because the polyimide coating will pyrolyze very quickly above 400°C.

4.9.2.3 Nitrous oxide/stack injection

Nitrous oxide can be analyzed using porous polymer PLOT columns, but retention is very low and it elutes close to carbon dioxide. As

carbon dioxide is usually present in relatively high amounts, it will impact quantification. Nitrous oxide has a high affinity for the 5A molecular sieve resulting in very high retention. Its molecular diameter is small enough to enter the pores and be retained. At 250°C, nitrous oxide still has a capacity factor of about 2. Because of the high retention, it is possible to inject large volumes or perform multiple injections (stack injection) before starting the oven program. Fig. 4.20 shows a chromatogram for a 250 ppm gas standard on a Molsieve 5A PLOT column where $10 \times 100 \mu\text{L}$ injections were performed. Because of the high retention, nitrous oxide will be focused and elutes as a single, sharp

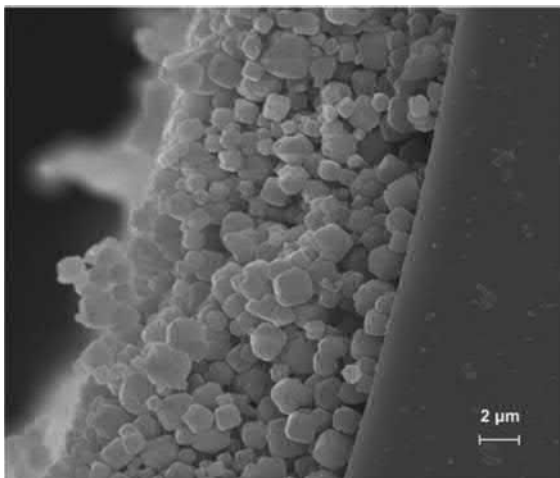


FIGURE 4.16 SEM picture of a molecular sieve-coated PLOT column.

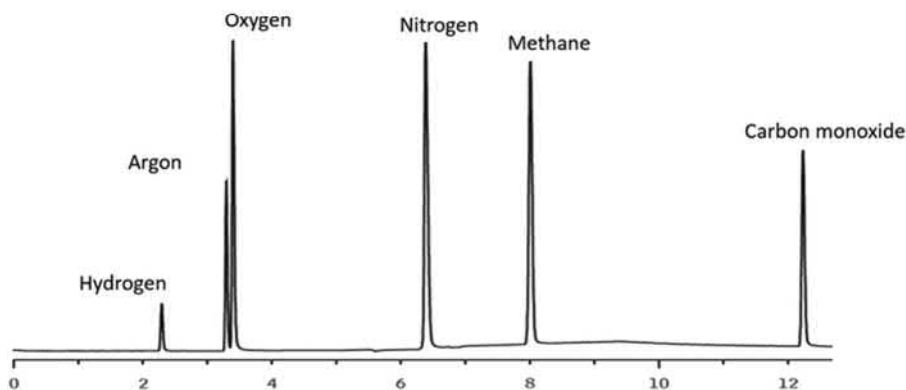


FIGURE 4.17 Permanent gases and CO at 50 ppm on a Molsieve 5A PLOT column. Column: Rt-Msieve 5A PLOT (30 m \times 0.53 mm ID, 50 μ m); injection: 5 μ L sample loop, 6-port Valco valve; carrier gas: He, 5 mL min⁻¹; oven temp.: 27°C, 5 min \rightarrow 100°C, 10°C min⁻¹, 5 min; detector: Valco PDD, 150°C.

peak. At 40°C, carbon monoxide is poorly retained and will always move through the molecular sieve column, which explains the 10 separate peaks for carbon monoxide. Using a Molsieve 5A column and larger volume injections, it is possible to determine sub-ppm levels of nitrous oxide with a thermal conductivity detector. Electron-capture detection is often used if low ppb levels of nitrous oxide need to be measured.

4.9.2.4 Special zeolites for argon and oxygen

The separation of argon from oxygen is challenging as shown in Fig. 4.17. At 30°C, both peaks are just baseline resolved using a 30 m capillary column. Because they elute very quickly, the initial injection bandwidth has a significant impact on the separation. The injection volumes must be very small to maintain the separation, but this reduces sensitivity. One can improve sensitivity by using subambient column temperatures.

Another challenge is that the separation rapidly becomes compromised if one of the two gases is present at a relatively high concentration. Special zeolite-based molecular sieves that significantly improved the separation of argon and oxygen were proposed in 2015 [16].

Fig. 4.21 shows the difference in selectivity of the specific zeolite compared to a Molsieve 5A column.

Resolution is almost four times higher, which makes this material interesting for the trace analysis of argon in oxygen or trace oxygen in argon. Injection volumes can be larger as a higher injection error can be tolerated while still obtaining baseline separation. Lastly, significantly higher temperatures can be used for this application.

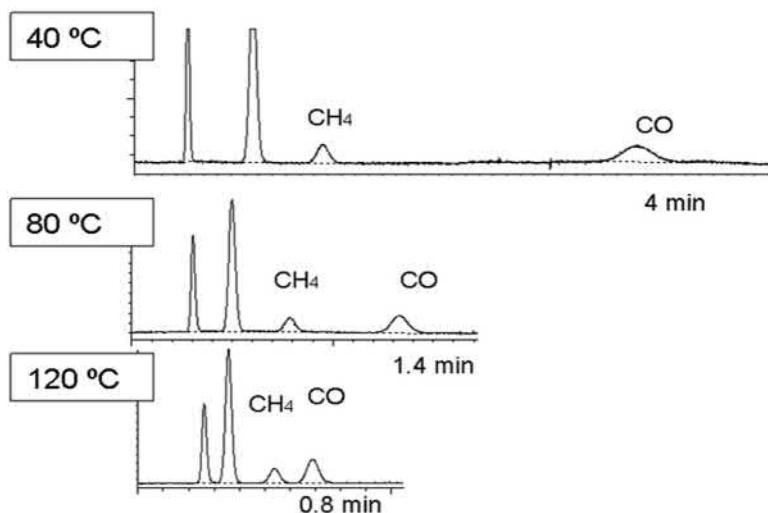


FIGURE 4.18 Impact of temperature on Molsieve 5A separation: Molsieve PLOT columns behave in a less polar fashion at higher temperatures, resulting in a relatively fast elution of carbon monoxide.

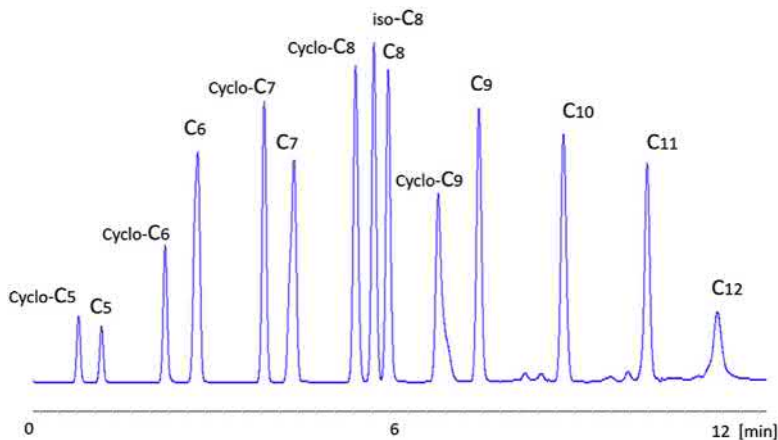


FIGURE 4.19 Naphthenes and paraffins separated on an MXT-Sieve 13X column (2.6 m \times 0.53 mm). Oven: 90°C \rightarrow 450°C, 30°C min⁻¹; carrier gas: H₂, 15 mL min⁻¹.

4.9.3 Carbon

Several types of carbon adsorbent are commonly used in chromatography; most are based on a highly porous carbon structure often referred to as a carbon molecular sieve. Commercial names used as packing material are ShinCarbon and Carboxen. Deposited in a capillary

column, there are CarboPLOT, CarbonPLOT, CarboBOND, and Carboxen-type PLOT columns.

Activated carbon surfaces are of interest because of their low polarity and large surface area. Carbon adsorbents have significantly lower retention compared to zeolite molecular sieves and are mostly used for analyzing gases such

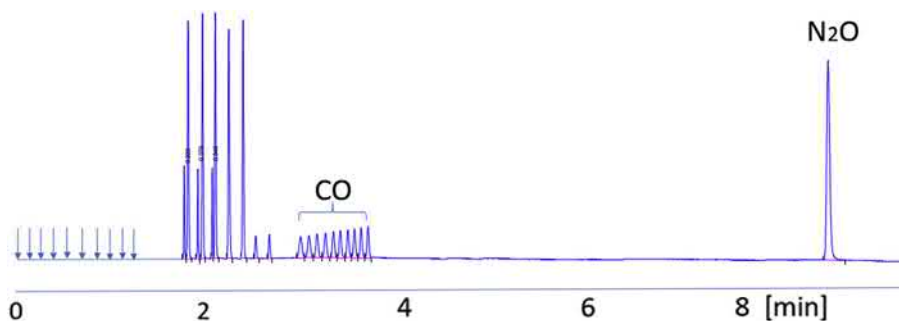


FIGURE 4.20 Nitrous oxide on Molsieve 5A using stack of 10 injections. Column: Rt-Msieve 5A (15 m \times 0.53 mm); oven: 40°C, 1 min \rightarrow 200°C, 20°C min⁻¹; carrier gas: He, 7 mL min⁻¹; injection: 10 \times 100 μ L stacked; time between injections: 10 s; Detector: TCD.

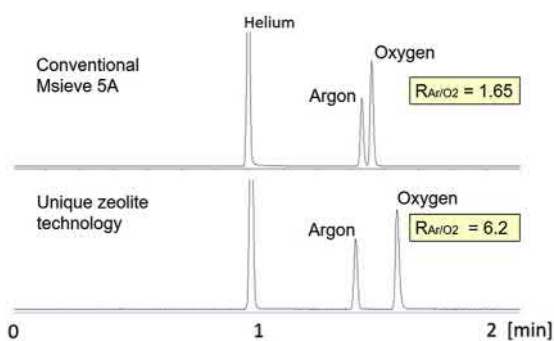


FIGURE 4.21 Separation of argon and oxygen using an optimized zeolite molecular sieve. Column: 30 m \times 0.53 mm; Oven: 30°C; Carrier gas: H₂; injection: split; Detection μ -TCD.

as hydrogen, nitrogen, oxygen, carbon monoxide, methane, and carbon dioxide. Carbon is the only adsorbent that separates and elutes carbon monoxide and carbon dioxide as sharp peaks. Even a 2 m packed column already shows good separations (Fig. 4.22). Here the 0.53 mm metal column was packed with ShinCarbon material. The 0.53 mm ID micropacked capillary can be installed in standard capillary injectors and operated with split, direct, or valve injection. Carbon adsorbents are not sensitive to water. Water elutes as a “hump” within a few minutes at 150°C.

When carbon adsorbents are used in PLOT columns, the challenge is to build stable layers

of 10 μ m or more to separate carbon monoxide from air. This can be difficult because thick layers of carbon are not easy to make. Also, in practice one has to be careful with flow/pressure changes because particles may elute. Particle traps are often required (see Section 4.2).

There are different ways to make carbon-type PLOT columns including dynamic or static coating with suspensions and in situ pyrolysis or formation of carbon nanotubes. Regardless of the technique, the key is to create enough surface area.

Because of the retention requirements for carbon monoxide separation from air, most carbon-type stationary phases are used in a packed column format. However, the separation of acetylene from the main ethylene matrix shown in Fig. 4.23 is a unique application for a capillary PLOT carbon column. If impurity analysis is the goal, it is usually preferred to have the impurity elute before the main component. The carbon column shows ideal selectivity as carbon materials are nonpolar, making acetylene (peak 2) elute before ethylene. Note that the ethylene peak is tailing due to overload, see Section 4.6.

The application of porous carbon for unsaturated hydrocarbons needs special attention. Higher temperatures are required to elute C₂ and C₃, which may cause a loss of response for unsaturated hydrocarbons. Fig. 4.24 shows the

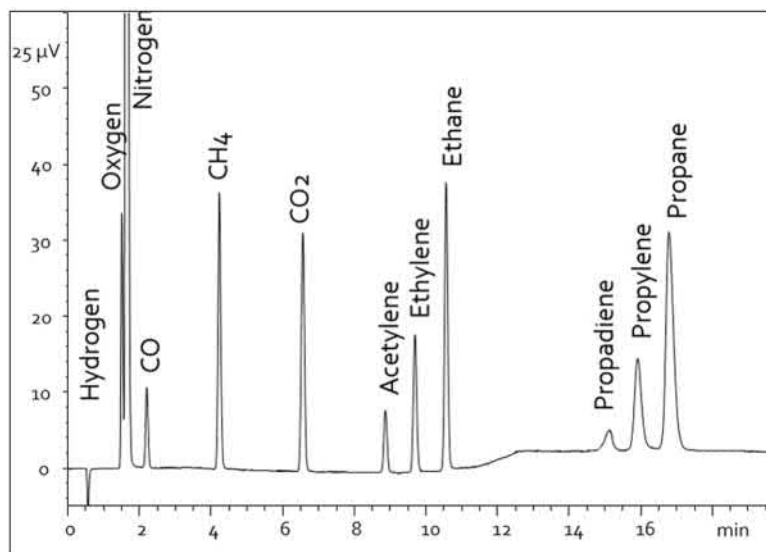


FIGURE 4.22 Gases on a micropacked ShinCarbon column (100/120 mesh, 2 m × 0.53 mm); oven: 40°C; carrier gas: He, 3.7 mL min⁻¹; injection: split, 1:10; detection: μ-TCD.

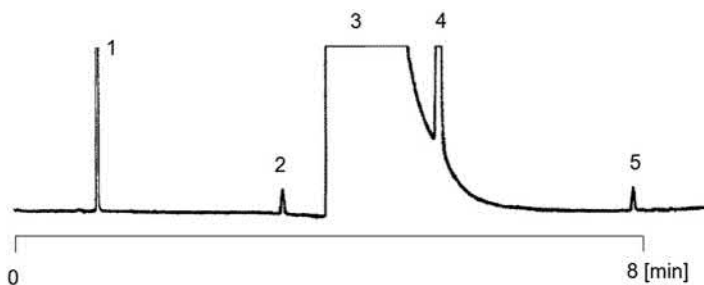


FIGURE 4.23 Acetylene (3 ppm) in ethylene. Column: Agilent J&W CarboBOND (25 m × 0.53 mm); oven: 35°C, 4 min → 180°C, 30°C min⁻¹; carrier: He, 40 kPa; Courtesy: Agilent Technologies, application note 1433.

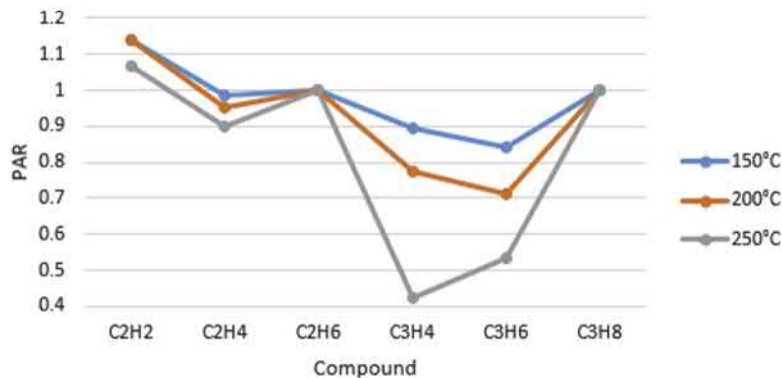


FIGURE 4.24 Reactivity of carbon adsorbents. Higher temperatures will have an immediate impact on the response signal of unsaturated hydrocarbons. A similar stationary phase was used as in Fig. 4.22.

response for C2 and C3 hydrocarbons when the analysis is done at 150, 200, and 250°C, respectively. The unsaturated hydrocarbons ethylene, propylene, and propadiene especially show a significantly lower response. For optimal results, the elution temperature for C2–C3 unsaturated hydrocarbons should be kept as low as possible. This can be realized by using high flows or flow programming. Because of their high retention, carbon PLOT columns can also be useful to analyze high-volatility halogenated and fluorinated compounds.

4.9.4 Silica gel

Silica gel is not widely used as a stationary phase for GC, with only a few specific applications developed for this material. It remains interesting though because it shows high retention for hydrocarbons, and it also elutes a range of semipolar compounds.

Commercialization of silica-coated columns (e.g., Agilent J&W Gaspro and Agilent J&W CP-Silica PLOT columns) showed that, in terms of selectivity, it does very well in the C1–C3 range, but C4 isomers tend to elute closer together as is the case with porous polymer

columns. Silica PLOT columns can be used up to about 250°C, which allows elution of up to C10 hydrocarbons. Armstrong et al. present a good comparison between silica and alumina adsorbents [17].

A useful characteristic of silica is that it elutes sulfur compounds at ppb levels. The sulfur compounds are well resolved from hydrocarbons, which make the ppb analysis of hydrogen sulfide and carbonyl sulfide in propylene/propane possible using a selective sulfur detector. One of the big challenges using silica is, similar to that in high-performance liquid chromatography, that the manufacture of reproducible silica surfaces is very difficult. One of the issues is that the variation of trace sulfur response is difficult to control between columns as well as between suppliers. This specific application can also be performed using a polar porous polymer U-type column (Figs. 4.31 and 4.32). Silica-coated columns also are much less sensitive to moisture, which is a big advantage over alumina; however, the poor selectivity for C4–C5 hydrocarbon isomers limits their use for light hydrocarbons. Besides sulfur compounds, highly volatile chlorofluorocarbon compounds and ethers can be separated with good peak shapes (Fig. 4.25).

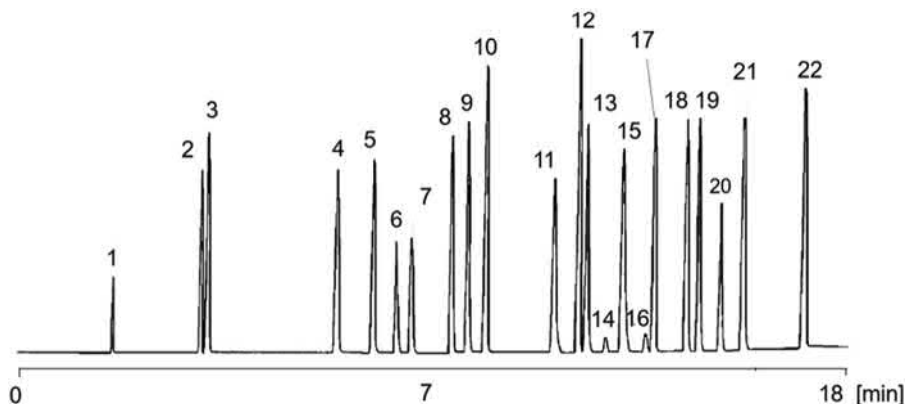


FIGURE 4.25 Halogenated hydrocarbons on silica-type PLOT column. Column: Agilent J&W GS-GasPro (30 m × 0.32 mm); carrier: He, 30 cm s⁻¹; Oven: 130°C, 4 min → 225°C at 10°C min⁻¹; injector: split injection. Detector: FID. Peak identification: 1. CH₄, 2. CHClF₂, 3. CCl₂F₂, 4. ClCF₂CF₂Cl, 5. CHCl₂F, 6. CCl₃F, 7. CF₂Br₂, 8. CH₃I, 9. CH₂Cl₂, 10. *trans*-ClCH=CHCl, 11. CF₃CCl₃, 12. *cis*-ClCH=CHCl, 13. CHCl₃, 14. ?, 15. CCl₄, 16. ?, 17. CH₃CH₂I, 18. CH₂Br₂, 19. CHCl₂Br, 20. C₄F₉I, 21. CHClBr₂, 22. CH₃CH₂CH₂I. Courtesy: Agilent Technologies, application note C532.

4.9.4.1 Silica as packed precolumn

Silica gel can also be used in packed precolumns, in particular for the determination of low levels (sub-ppm) of oxygen in hydrocarbon streams. Normally this application is done using a porous polymer primary column connected to a Molsieve 5A column using a valve, but often the porous polymer will irreversibly adsorb small amounts of oxygen. Silica gel has proven to be quite good for trace oxygen, and it will also retain C_{2+} hydrocarbons, so it can be used efficiently as a precolumn, where the first eluting composite peak is transferred into a molecular sieve column. This way it is possible to measure permanent gases and carbon monoxide at desired trace levels using a pulsed-discharge ionization detector.

4.9.5 Inorganic salts

Several unique PLOT columns have been developed (Agilent J&W Lowox, Agilent J&W GS-OxyPLOT) that are highly selective for oxygenated compounds [18]. Through proprietary technology, these columns have very high polarity. Methanol elutes after C14, allowing oxygenated compounds to be separated from a paraffin matrix (Fig. 4.26).

Because of the high retention and selectivity for oxygenated compounds, it is possible to inject relatively large sample volumes at low temperatures and still obtain a focused injection band. Selectivity for oxygenated compounds is so high that good separations for a large range of oxygenated components can be obtained even on a short $10\text{ m} \times 0.53\text{ mm}$ column (Fig. 4.27).

The determination of oxygenates at trace levels is important in hydrocarbon processing because traces of these compounds are known as “catalyst-killers.” Using oxygen-selective columns allows the accurate analysis of ppb levels of oxygenates. Often such oxygen-specific PLOT columns are used in conjunction with a

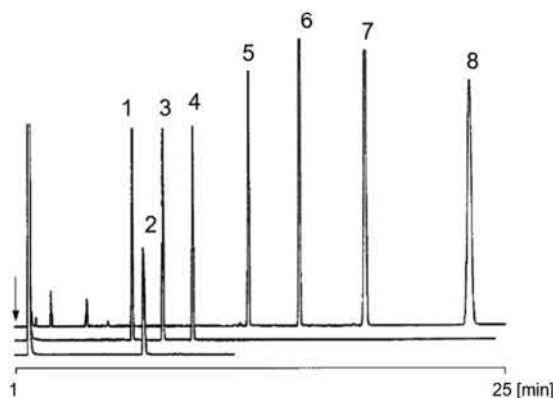


FIGURE 4.26 Methanol and hydrocarbons on Agilent J&W Lowox showing high polarity. Column: J&W Lowox ($10\text{ m} \times 0.53\text{ mm}$); temperature: 175°C , 2 min $\rightarrow 290^\circ\text{C}$, $10^\circ\text{C min}^{-1}$; carrier: He, 70 kPa; injector: valve into split, $T = 250^\circ\text{C}$; detector: FID, $T = 250^\circ\text{C}$. Peak identification: 1. C14, 2. methanol, 3. C15, 4. C16, 5. C18, 6. C20, 7. C20, 8. C22, 9. C24. Courtesy: Agilent Technologies, application note A1363.

nonpolar polydimethylsiloxane precolumn. The majority of oxygenated compounds elute in the C1–C7 range from the nonpolar precolumn. Injecting this fraction onto the polar PLOT column completely separates all oxygenates from hydrocarbons, allowing trace oxygenates to be measured in all types of hydrocarbon matrices, including naphthas. The stack injection technique, which is discussed in Section 4.9.2.3, is also applicable for oxygenates using oxygen-specific PLOT columns [19]. Because the stationary phase is based on a salt, such columns can be used up to very high temperatures with only minor bleed, allowing high sensitivity settings. Typical applications go as high as 300°C .

4.9.6 Porous polymers

Both molecular sieves and alumina-type materials have a strong physical interaction with polar analytes, such as alcohols, aldehydes, ethers, and water. Porous polymers, consisting of a skeleton of divinylbenzene, characteristically will elute all types of compounds, both

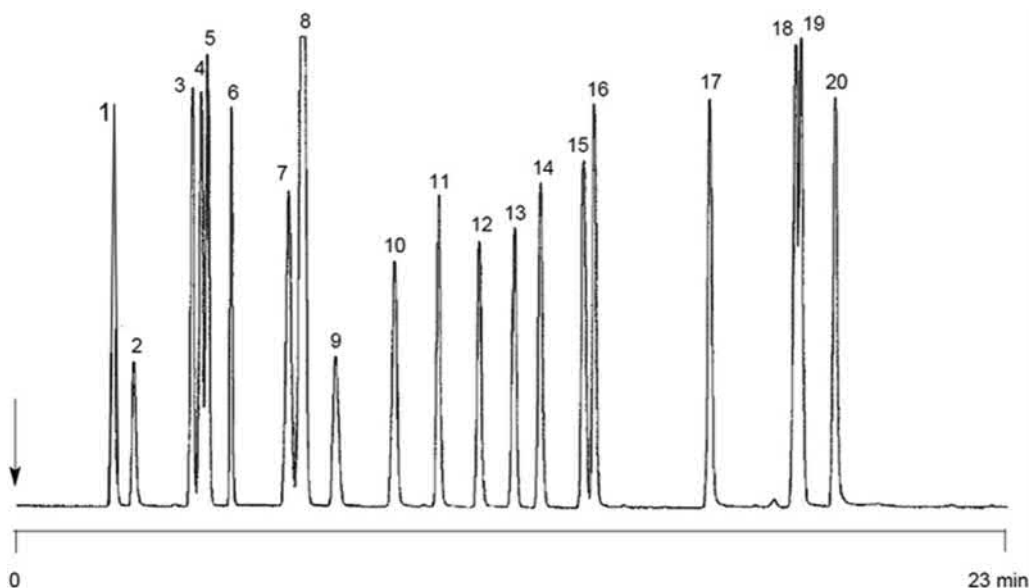


FIGURE 4.27 Selectivity of oxygenate-specific, salt-coated PLOT column. Column: Agilent J&W Lowox (10 m \times 0.53 mm); temperature: 50°C, 5 min \rightarrow 270°C, 30°C min⁻¹; carrier: He, 41 cm s⁻¹; injector: valve, 50 μ L, T = 150°C; detector: FID, T = 300°C; concentration range: 10–50 ppm. Peak identification: 1. diethylether, 2. acetaldehyde, 3. ethyl-*t*-butyl ether, 4. methyl-*t*-butyl ether, 5. diisopropyl ether, 6. propanal, 7. *t*-amylmethyl ether, 8. propyl ether, 9. isobutanal, 10. butanal, 11. methanol; 12. acetone; 13. isovaleraldehyde, 14. valeraldehyde, 15. 2-butanone, 16. ethanol, 17. 1-propanol, 18. *t*-butanol, 19. Iso butanol, 20. 1-butanol. Courtesy: Agilent Technologies, application note A1613.

polar and nonpolar. It is also insensitive to water and elutes it as a normal peak. This means that water-containing samples can be analyzed because the water will not have any effect on the retention of a porous polymer PLOT column. With porous polymers, the development of isothermal methods at lower temperatures, without using regeneration programs to remove water, is possible. The absolute retention is quite high, at about ten times that of liquid phases. Despite the relatively thick layers (10–20 μ m), porous polymer columns are highly efficient. This is in sharp contrast to liquid phases, where a 10 μ m polydimethylsiloxane column will lose 70%–80% of its efficiency due to resistance to mass transfer in the liquid phase. For these reasons, porous polymer PLOT columns are a useful addition to adsorption column technology

since they first became commercially available in 1988 [20]. However, selectivity for hydrocarbons on these columns is not as good as for alumina. The retention is not high enough to separate the inert gases. Most applications dealing with gases use a combination of a porous polymer and a Molsieve or alumina columns.

4.9.6.1 Types of porous polymers

Porous polymers are generally copolymers of styrene-divinylbenzene. Their polarity can be changed by incorporating polar groups such as vinylpyridine or ethylene glycol-dimethylacrylate groups. Typical trade names for porous polymer packing materials for packed columns used today are Porapak and HayeSep. As capillary columns, four types are available: Q, QS, S, and U. Table 4.2 summarizes their

TABLE 4.2 Porous polymer PLOT columns in order of increasing polarity (DVB = divinylbenzene).

Type	Composition	Temperature stability
Q	DVB–styrene	250–300°C
QS	DVB–low vinyl pyridine	250°C
S	DVB–high vinyl pyridine	250°C
U	DVB–ethylene glycol–dimethyl acrylate	190°C

characteristic properties. Differences in their selectivity are illustrated in Fig. 4.28. Note that with increasing polarity, the polar hydrocarbon acetylene (peak 4) will move back in the chromatogram relative to ethane (peak 2) and ethylene (peak 3).

The “Q” is the most popular type and also the most nonpolar, usable up to 300°C. As with liquid phases, temperature stability decreases with increased polarity. Temperature stability also depends on manufacturer specifications. As porous polymer PLOT columns have adsorbent layers of 10–20 μm , one can expect quite a high background when used at maximum operating temperatures. Though the phase will survive, a high background is not beneficial for sensitivity. The Q-type column is

very hydrophobic, meaning there is little interaction with polar compounds. For instance, water elutes from a Q-type PLOT column before many solvents with much lower boiling points. This is illustrated in Fig. 4.29, where despite a much lower boiling point (56°C), acetone elutes much later than water.

Porous polymers can be modified to perform specific applications. For instance, there is a Por-aPLOT amines-type adsorbent where a basic modification is applied, allowing a reasonable peak shape for ammonia and elution of low levels of volatile amines. The challenge is that the basic modification has a negative impact on the elution of other polar compounds, such as alcohols [21]. However, the peak shape of polar volatiles as well as sulfur gases on a U-BOND porous polymer column is very good (Figs. 4.30–4.32). Even highly polar compounds, such as methanol, formaldehyde, and water show good peak shapes.

Sulfur gases elute with good peak symmetry on Rt-U-BOND porous polymer columns. Fig. 4.31 shows the separation of 1 ppm of carbonyl sulfide and hydrogen sulfide in a natural gas matrix. Peaks are nearly Gaussian, making this adsorbent suitable for trace sulfur gas analysis. Another characteristic property of Rt-U-BOND porous polymer columns is that both sulfur gases are well resolved from ethane/

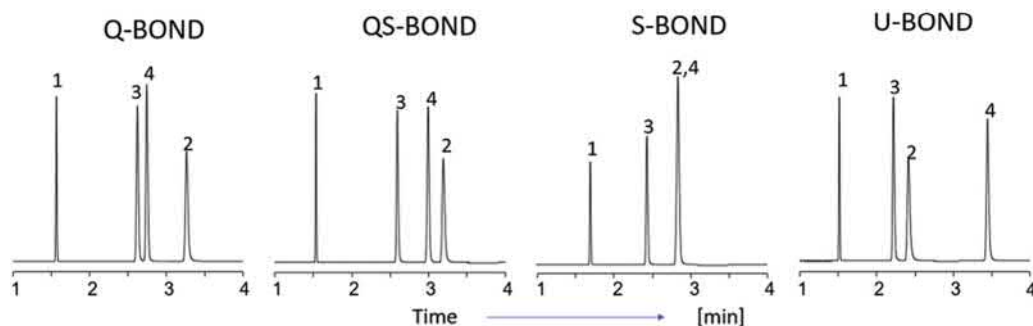


FIGURE 4.28 Separation of C2 isomers on different porous polymer PLOT columns. Column: Rt-BOND (Q, QS, S, and U) (30 m \times 0.53 mm, 20 μm); flow: He, 4.5 mL min^{-1} ; oven: 40°C, 3 min, \rightarrow 100°C, 20°C min^{-1} ; injection: split; detection: FID; peak identification: 1. methane, 2. ethane, 3. ethylene, 4. acetylene.

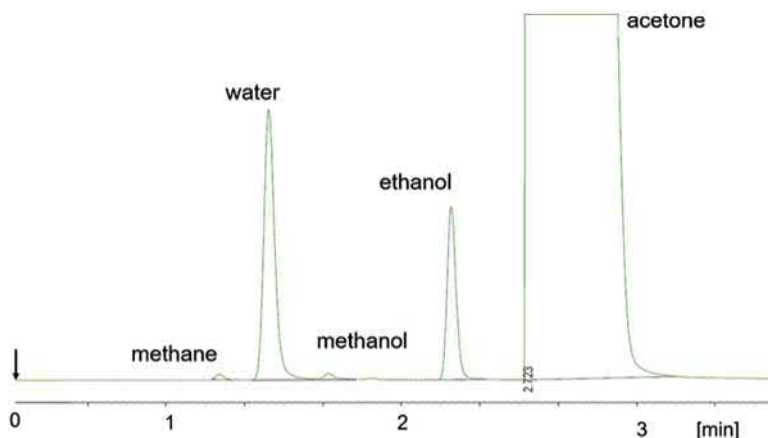


FIGURE 4.29 Water in acetone. Column: Rt-Q-BOND (30 m \times 0.53 mm, 20 μ m); oven: 200°C; carrier: He, 20 kPa; detector: μ -TCD; injection: split.

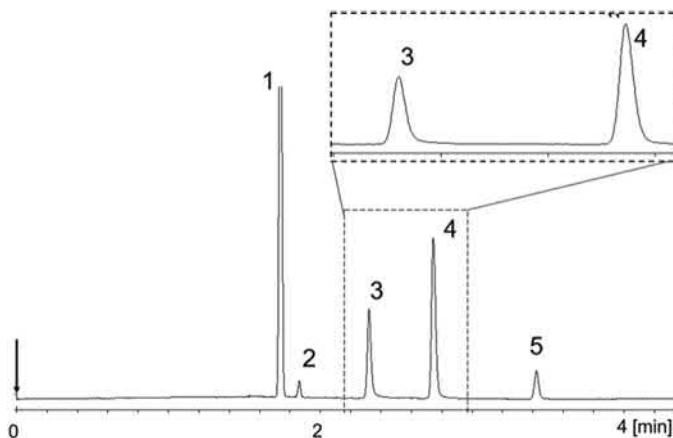


FIGURE 4.30 Polar volatiles on polar porous polymer PLOT column. Column: Rt-U-BOND (30 m \times 0.53 mm, 20 μ m); oven: 100°C; detection: μ -TCD; peak identification: 1. $N_2 + O_2 + CO$, 2. CO_2 , 3. formaldehyde, 4. water, 5. methanol.

ethylene as well as propane/propylene, facilitating the trace analysis of low levels of sulfur compounds in C2/C3 streams (Fig. 4.32). This application cannot be done on thick-film, nonpolar liquid phases because the carbonyl sulfide peak coelutes with propane, causing quenching of the detector response with sulfur-selective detectors.

4.10 Summary

Using adsorption materials as stationary phase in GC remains fascinating as selective separations can be realized for highly volatile compounds. Today there are a wide range of adsorption materials available as PLOT or packed columns, but one needs to realize the

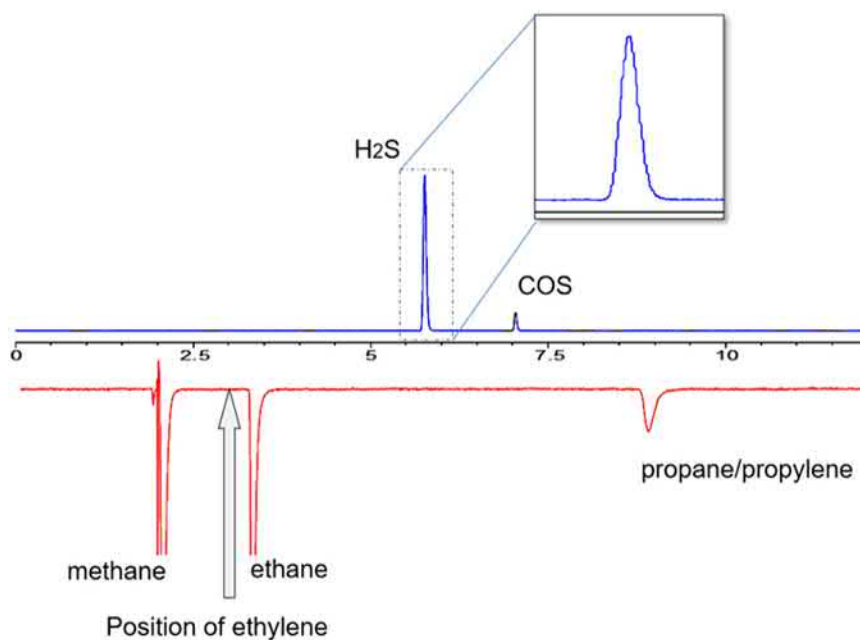


FIGURE 4.31 Sulfur gases in natural gas. Column: Rt-U-BOND (30 m \times 0.32 mm, 10 μ m); oven: 40°C, 5.0 min, 10°C min⁻¹ to 220°C, 2.0 min; detection: PFPD; carrier gas: He, 10 psi; Sample: 1 ppm in natural gas.

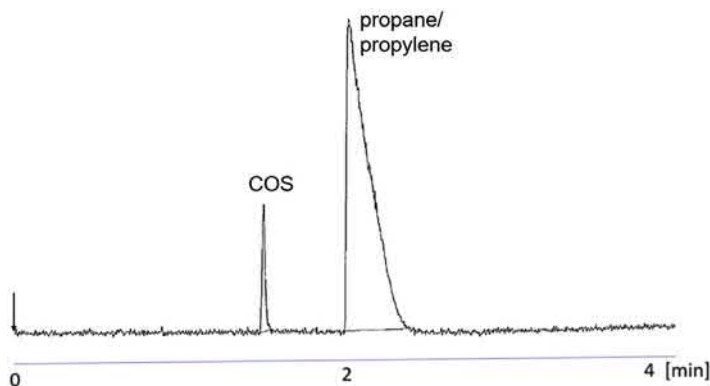


FIGURE 4.32 COS in propane/propylene. Column: Rt-U-BOND (30 m \times 0.53 mm, 20 μ m); oven: 50°C; carrier: He, 3.9 psi; detection: SCLD; injection: 0.5 μ L, split 1:10; sample: 700 ppb COS in propane/propylene, ratio 30:70.

limitations of such materials. They will generate retention for volatile compounds, but there is always some catalytic activity to consider. This also means the use of hydrogen as a carrier gas may impact recovery.

Practically PLOT columns are more vulnerable than WCOT columns, and one has to be more careful with carrier gas pressure changes, flows, and valve switching applications.

Despite this, the adsorbents open unique opportunities to realize fast separations of volatile compounds. Also, injection bandwidth is a key parameter to consider. The injection of volatile compounds and gases is challenging as the size of sample volumes will impact injection bandwidth and may compromise early eluting components. Choosing column dimensions and sample size entering the column remains essential for the best results.

References

- [1] R. Majors, J. de Zeeuw, LC-GC N. Am. Vol. 28 (10) (Oct. 2010).
- [2] J. De Zeeuw, B. Bromps, T. Vezza, R. Morehead, G. Stidsen, Am. Lab. 42 (5) (2010) 38.
- [3] R.C. M de Nijs, J. de Zeeuw, J. Chromatogr. 279 (1983) 41–48.
- [4] W. Schneider, J. Frohne, H. Brudereck, J. Chromatogr. 155 (1978) 311–327.
- [5] O.L. Hollis, J. Chromatogr. Sci. 11 (1973) 335e342.
- [6] M. Mohnke, J. Heybey, J. Chromatogr. 471 (1989) 37e53, [https://doi.org/10.1016/S0021-9673\(00\)94153-0](https://doi.org/10.1016/S0021-9673(00)94153-0).
- [7] US patent 20180340920; <https://patents.google.com/patent/US20180340920A1/en>.
- [8] <https://www.restek.com/catalog/view/47081/23882>.
- [9] J. de Zeeuw, R. van Hove, J. Curvers, L. Verhoeve, Am. Lab. (Dec. 2002) 25–27.
- [10] <https://www.restek.com/Technical-Resources/Technical-Library/Video-Library/How-to-Cut-a-Metal-Capillary-GC-Column>.
- [11] T. Vezza, J. de Zeeuw, PIN, April-May, 2011.
- [12] W. Wang, et al., Fusion Eng. Des. 137 (December 2018) 56–60.
- [13] J. de Zeeuw, R. Morehead, T. Vezza, B. Bromps, American Lab., October 2011.
- [14] M. Mohnke, W. Saffert, Preprints of the 4th International Symposium on Gas Chromatography, Hamburg, Germany, 1962, p. 214e219. June 13e16.
- [15] https://inis.iaea.org/collection/NCLCollectionStore/_Public/32/004/32004817.pdf?r=1&r=1.
- [16] Proceedings 39th International Symposium on Capillary Chromatography, ISCC, Dallas, Texas, USA, 2015.
- [17] D.A. Armstrong, G.L. Reid, J. Luong, Curr. Sep. 15 (1996) 1.
- [18] J. de Zeeuw, N. Vonk, M. Mohnke, D. Estel, C. Duvekot, Int. lab. (1999) 18–22, april.
- [19] J. Luong, R. Gras, H. Cortes and R. Mustacich, J. Chromatogr. Sci. 44 (2006) 219–226.
- [20] J. de Zeeuw, R.C.M. De Nijs, J.C. Buijten, J.A. Peene, M. Mohnke, J. High Resolut. Chromatogr. 11 (1988) 162–167.
- [21] M. Mohnke, R. Schmidt, B. Schmidt, J.C. Buijten, P. Mussche, J. Chromatogr., A 667 (1–2) (April 29, 1994) 334–339, [https://doi.org/10.1016/0021-9673\(94\)89085-4](https://doi.org/10.1016/0021-9673(94)89085-4).

Column technology: packed columns

Colin F. Poole

Department of Chemistry, Wayne State University, Detroit, MI, United States

Frequently used stationary phases [hydrocarbon, highly fluorinated, poly(siloxane), ethers and esters, and poly(ethylene glycol)] and supports [diatomaceous earths, fluorocarbon powders, and glass beads] for the preparation of packed columns for gas chromatography are described. Classification methods are discussed for stationary-phase selection with an emphasis on the solvation parameter model. The basic theory of band broadening and its effect on column design and the contribution of interfacial adsorption to the general retention mechanism are outlined. Common adsorbents for gas–solid chromatography [inorganic oxides, carbon, molecular sieves, and porous organic polymers] and their typical applications are discussed. The chapter contains all the material required to select, prepare, and characterize packed columns for gas chromatography together with the theory required to understand band broadening and retention.

5.1 Introduction

Since the early 1980s wall-coated, open-tubular (WCOT) columns and porous-layer

open-tubular (PLOT) columns have dominated the practice of analytical gas chromatography. This was a rather abrupt change in general practice since packed columns were used almost universally up until that time. Open-tubular columns of capillary dimensions provide significant improvements in peak capacity due to their higher permeability and WCOT columns are more inert than packed columns. On the other hand, only a limited number of liquids form stable films on the smooth walls of open-tubular columns, while virtually any liquid of low volatility can be handled using packed columns. Consequently, when the purpose is to determine specific physicochemical properties of a liquid employed as a stationary phase, for example, by inverse gas chromatography, packed columns are generally the only realistic choice. Packed columns can hold a significantly larger volume of stationary phase and are better suited to the needs of process gas chromatography at the pilot plant scale and laboratory preparative gas chromatography when isolation of all but a few milligrams of product is desired. Packed columns are also better suited to handling samples containing a significant amount of involatile or thermally unstable matrix components.

TABLE 5.1 Representative properties of different column types for gas chromatography.

Column type	Phase ratio	H_{\min} (mm)	u_{opt} (cm s ⁻¹)	Permeability (10 ⁷ .cm ²)
Classical packed	4–200	0.5–2	5–15	1–50
Micropacked	50–200	0.02–1	5–10	1–100
Packed capillary	10–300	0.05–2	5–25	5–50
SCOT	20–300	0.5–1	10–100	200–1,000
WCOT	15–500	0.03–0.8	10–100	300–20,000

These materials and their breakdown products usually accumulate on the packing at the head of the column, which is easily exchanged periodically for fresh packing material.

Some characteristic properties of the various types of packed columns are summarized in Table 5.1 [1,2]. Classical packed columns with an internal diameter >2 mm and packed with particles in the 100–250- μm range are the most widely used and are easily prepared in the laboratory. Micropacked columns have diameters <1 mm and are packed with particles of a similar size to classical packed columns [3,4]. These should be distinguished from packed capillary columns, which typically have an internal diameter <0.6 mm and are packed with particles in the 5–20- μm range [5,6]. Columns with narrow internal diameters facilitate fast temperature programming and particles of small diameters enhance performance. On the other hand, the low permeability of packed capillary columns limits column length and requires instruments modified for high-pressure operation. Support-coated open-tubular (SCOT) columns are capillary columns containing a liquid phase coated on a surface covered with a layer of porous solid material (support) leaving an open passageway at the center of the column. They are a hybrid of packed and open-tubular columns with properties that are a compromise between those of the two column types. As open-tubular column technology evolved,

SCOT columns were left with few real advantages and are no longer in general use.

5.2 Gas–liquid chromatography

Classical packed columns for gas–liquid chromatography are prepared by coating a support with the desired liquid phase and transferring the coated support (packing material) to an empty column of appropriate dimensions for the separation. Columns are generally made of glass, stainless steel or passivated nickel tubing [7], glass-lined or silicon-coated stainless steel [8], or Teflon and coiled to fit the column oven and connect with the injector and detector inlets. Metal columns are preferred for applications where mechanical stability and high temperatures are important, but, unless internally coated with a film of glass or silicon, are unsuitable for thermally labile compounds. Hot metal surfaces tend to be catalytically active and degrade labile compounds. Glass columns, with silanized surfaces, are the most inert but are more fragile than metal columns. Teflon columns are limited to low temperatures and are used for the separation of highly reactive chemicals degraded by glass and metal surfaces.

5.2.1 Frequently used stationary phases

Since the beginning of gas chromatography, thousands of substances have been used as

stationary phases [9–15]. Many of these were technical products with a variable or undefined composition, or had similar separation properties to other stationary phases but an inferior temperature operating range, and have long since been abandoned. The development of stationary-phase classification schemes, such as the Rohrschneider–McReynolds' system of phase constants, played an important role in rationalizing stationary-phase selection during the early development of gas chromatography by identifying redundant stationary phases with (near) identical separation properties. As a result, the number of stationary phases actively used has declined considerably and these can be grouped under a few general headings, namely: (1) hydrocarbons and perfluorocarbons; (2) poly(siloxanes); (3) ethers and poly(esters); (4) ionic liquids; (5) liquid crystals; and (6) chiral stationary phases.

It is desirable that the stationary phase has a wide liquid temperature operating range. The lower operating temperature is usually close to the melting point of the stationary phase or glass transition temperature for a polymer. The maximum allowable operating temperature is usually determined by the thermal stability of the stationary phase or its vapor pressure. Practical considerations dictate that the stationary phase should be uncreative, adequately wet common supports, and have reasonably solubility in a volatile organic solvent.

High-molecular-weight hydrocarbons such as hexadecane, squalane, Apolane-87, and Apiezon greases have long been used as low-selectivity stationary phases (Table 5.2). All hydrocarbon phases are susceptible to oxidation and should be used with carrier gases having a low oxygen content. Apolane-87 is the most resistant to oxidation of the common hydrocarbon phases

TABLE 5.2 Structure and properties of some frequently used stationary phases for packed-column gas chromatography.

Trade name	Structure and properties
Squalane	2,6,10,15,19,23-Hexamethyltetracosane. Obtained by the complete hydrogenation of squalene isolated from shark liver oil. Common impurities squalene and batyl alcohol.
Apiezon	A series of hydrocarbon greases prepared by the high-temperature treatment and molecular distillation of lubricating oils. Ill-defined composition containing unsaturated hydrocarbons and carbonyl and carboxylic acid-containing impurities. Colored samples should be purified by chromatography over charcoal and alumina before use. Apiezon MH prepared by hydrogenation of purified apiezon greases.
Apolane-87	24,24-Diethyl-19,29-dioctadecylheptatetracontane (C ₁₈ H ₃₇) ₂ CH(CH ₂) ₄ C(C ₂ H ₅) ₂ (CH ₂) ₄ CH(C ₁₈ H ₃₇) ₂ , molecular weight 1222, melting point ≈ 28–34°C
Fomblin YR	Poly(perfluoroalkyl ether) –[(OCFCF ₃ CF ₂) _n (OCF ₂) _m] _n –, average molecular weight 6–7 × 10 ³
OV-1	Poly(dimethylsiloxane), average molecular weight >10 ⁶ , melting point ≈ 100°C
OV-101	Poly(dimethylsiloxane), average molecular weight ≈ 3 × 10 ⁴ , viscosity 1500 cP
OV-3	Poly(dimethylmethylphenylsiloxane) containing 10 mol % methylphenylsiloxane
OV-7	Poly(dimethylmethylphenylsiloxane) containing nominally 20 mol % methylphenylsiloxane, average molecular weight ≈ 1 × 10 ⁴ , viscosity 500 cP
OV-11	Poly(dimethylmethylphenylsiloxane) containing nominally 35% methylphenylsiloxane monomer

(Continued)

TABLE 5.2 Structure and properties of some frequently used stationary phases for packed-column gas chromatography.—cont'd

Trade name	Structure and properties
OV-17	Poly(methylphenylsiloxane), average molecular weight $\approx 4 \times 10^4$, viscosity 1300 cP
OV-22	Poly(methylphenyldiphenylsiloxane) containing 65 mol % phenyl
OV-25	Poly(methylphenyldiphenylsiloxane) containing 75 mol % phenyl, average molecular weight 1×10^4 , viscosity $< 1 \times 10^5$
OV-105	Poly(cyanopropylmethyltrimethylsiloxane) containing 10 mol % cyanopropylmethylsiloxane
OV-225	Poly(cyanopropylmethylphenylmethylsiloxane) containing 50 mol % cyanopropylmethylsiloxane, average molecular weight 8×10^3 , viscosity 9×10^3 cP
OV-275	Poly(dicyanoalkylsiloxane) containing 70 mol % dicyanopropylsiloxane and 30 mol % dicyanoalkylsiloxane, average molecular weight 5×10^3 , viscosity 2×10^4 cP
QF-1	Poly(trifluoropropylmethylsiloxane), average molecular weight $\approx 2 \times 10^5$, viscosity $\approx 1 \times 10^4$
PPE-5	Poly(phenyl ether) $C_6H_5O(C_6H_5O)_3C_6H_5$, meta linked,
DOP	Diocetyl phthalate $C_6H_4(COOC_8H_{17})_2$, ortho substitution
EGS	Poly(ethylene glycol succinate) $HO(CH_2)_2[OOC(CH_2)_2COO(CH_2)_2]_nOH$
EGAD	Poly(ethylene glycol adipate)
DEGS	Poly(diethylene glycol succinate) $HO(CH_2)_2O(CH_2)_2[OOC(CH_2)_2COO(CH_2)_2O(CH_2)_2]_nOH$
CW20M	Carbowax 20 M, a poly(ethylene glycol) with an average molecular weight 14,000, $HO(CH_2CH_2O)_nCH_2CH_2OH$, melting point about $60^\circ C$
FFAP	The product obtained by condensing Carbowax 20 M with 2-nitroterephthalic acid
TCEP	1,2,3-Tris(2-cyanoethoxy)propane $(CH_2OCH_2CH_2CN)_3$
QBA FOS	Tetra-n-butylammonium perfluorooctanesulfonate
QBA MPS	Tetra-n-butylammonium 4-morpholinepropanesulfonate
QBA OS	Tetra-n-butylammonium octanesulfonate
QBA BES	Tetra-n-butylammonium 2-[bis(2-hydroxyethyl)amino]ethanesulfonate
QBA TS	Tetra-n-butylammonium 4-toluenesulfonate
QBA FMS	Tetra-n-butylammonium trifluoromethanesulfonate
QBA PIC	Tetra-n-butylammonium picrate
QBP TS	Tetra-n-butylphosphonium 4-toluenesulfonate
QBP Cl	Tetra-n-butylphosphonium chloride
QEA TS	Tetra-n-ethylammonium 4-toluenesulfonate
DEA TS	Di-n-ethylammonium 4-toluenesulfonate

because of its low concentration of tertiary hydrogen atoms. Both squalane and Apiezon may contain polar impurities that can be removed by column chromatography prior to use. The hydrocarbon stationary phases are primarily used for the separation of hydrocarbons and as low-selectivity reference phases in column classification schemes [9,11,16]. They have poor support deactivating properties and are poor solvents for polar compounds.

Highly fluorinated liquids are used for the separation of reactive compounds and for the separation of other highly fluorinated compounds, such as Freons [9,17]. Volatile metal halides, interhalogen compounds, and the hydrogen compounds of halides, sulfur, and phosphorus tend to destroy conventional phases. The low cohesive energy of highly fluorinated stationary phases results in lower retention compared with the analogous hydrocarbon phases facilitating the separation of thermally

labile compounds at lower temperatures. Most highly fluorinated liquids have poor support wetting characteristics leading to low column efficiency and incomplete support coverage at low phase loadings. The most useful stationary phases contain either ether or ester “anchor” functional groups, such as the poly(perfluoroalkyl ether) oil Fomblin YR, to assist in film formation and stabilization. They are generally considered special-purpose stationary phases and little used for general applications.

The poly(siloxanes) used in packed-column gas chromatography are generally linear polymers synthesized from monomers containing methyl, vinyl, phenyl, 3,3,3-trifluoropropyl, or 3-cyanoalkyl groups. By varying the monomer composition, polymers with a range of solvent properties can be prepared (Table 5.3) [9–15,18]. The poly(dimethylsiloxanes) are low-selectivity stationary phases, similar to the hydrocarbon phases but with wider liquid temperature ranges.

TABLE 5.3 Characteristic properties of packed-column stationary phases.

Stationary phase	Temperature range		System constants (121°C)				
	Minimum	Maximum	<i>e</i>	<i>s</i>	<i>a</i>	<i>b</i>	<i>l</i>
Squalane	20	120	0.13	0.01	0	0	0.58
Apolane-87	35	260	0.17	0	0	0	0.55
Fomblin YR	30	250					
OV-1	100	350					
OV-101	<20	350	0.02	0.19	0.13	0	0.50
OV-3	<20	350	0.03	0.33	0.15	0	0.50
OV-7	<20	350	0.06	0.43	0.17	0	0.51
OV-11	<20	350	0.10	0.54	0.17	0	0.52
OV-17	<20	350	0.07	0.65	0.26	0	0.52
OV-22	<20	300	0.20	0.66	0.19	0	0.48
OV-25	<20	300	0.28	0.64	0.18	0	0.47
OV-105	<20	275	0	0.36	0.41	0	0.50
OV-225	<20	250	0	1.23	1.07	0	0.47

(Continued)

TABLE 5.3 Characteristic properties of packed-column stationary phases.—cont'd

Stationary phase	Temperature range		System constants (121°C)				
	Minimum	Maximum	<i>e</i>	<i>s</i>	<i>a</i>	<i>b</i>	<i>l</i>
OV-275	25	250	0.21	2.08	1.99	0	0.29
QF-1	<20	250	-0.45	1.16	0.19	0	0.42
PPE-5	0	200	0.23	0.83	0.34	0	0.53
DOP	20	130	0	0.80	1.00	0	0.57
EGS	90	220					
EGAD	100	225	0.13	1.39	1.82	0.21	0.43
DEGS	20	200	0.34	1.53	1.75	0.17	0.37
CW20M	60	225	0.32	1.26	1.88	0	0.45
FFAP	50	250					
TCEP	20	170	0.20	1.82	1.79	0.24	0.33
QBA FOS	<20	220	0	1.09	1.62	0	0.40
QBA MPS	<20	180	0	1.75	3.54	0	0.55
QBA OS	<20	180	0.27	1.14	3.53	0	0.50
QBA BES	<20	170	0.25	1.76	3.67	0	0.38
QBA TS	55	200	0.16	1.58	3.30	0	0.46
QBA FMS	112	240	0	1.58	2.14	0	0.42
QBA PIC	90	200	0.10	1.56	1.42	0	0.45
QBP TS	44	230					
QBP CI	83	230	0.24	1.85	5.42	0	0.47
QEA TS	85	190	0.33	2.05	3.43	0	0.30
DEA TS	105	210					

Replacing methyl with phenyl groups increases the dipolarity/polarizability and hydrogen-bond basicity of the poly(siloxanes) with little change in the liquid temperature range (Table 5.3). Poly(siloxanes) with cyano groups on α -carbon atoms and fluorine atoms on α - and β -carbon atoms have low thermal stability and are not used for gas chromatography. Poly(siloxanes) with 2-cyanoethyl, 3-cyanopropyl, and 3,3,3-trifluoropropyl groups have suitable thermal stability and facilitate the synthesis of

poly(siloxane) stationary phases with high dipolarity/polarizability and hydrogen-bond basicity. The cyanoalkyl- and 3,3,3-trifluoropropyl-containing poly(siloxanes) have complementary selectivity. The poly(cyanoalkylsiloxane) phases with a high incorporation of cyanoalkyl groups are some of the most cohesive and polar stationary phases in common use. They are also susceptible to oxidation and hydrolysis requiring the use of high-purity carrier gases.

The dialkyl phthalates, poly(ethers), poly(esters), and poly(ethylene glycols) are a further group of stationary phases that cover a wide polarity range, with the poly(ethylene glycols) being the most important because of their complementary properties to the poly(siloxane) stationary phases (Table 5.3). The dialkyl phthalates are moderately polar and weak hydrogen-bond basic stationary phases [19]. The meta-linked poly(phenyl ethers) with five- or six-rings are moderately polar liquids with exceptionally low vapor pressure for their low molecular weight. The poly(ester) stationary phases are represented by a wide range of resinous composite materials derived from the reaction of a polybasic acid with a polyhydric alcohol [9,11,13,20]. The most widely used are the succinate and adipate esters of ethylene glycol, diethylene glycol, and butanediol. The stability of these materials at high temperatures is questionable and they are also slowly degraded by oxygen and water that might be present in the carrier gas or samples. Exchange reactions with samples containing alcohols, acids, amines, and esters are also possible. They have been replaced in many of their applications by the more stable poly(cyanoalkylsiloxanes).

Poly(ethylene glycols) are widely used for the separation of volatile polar compounds and have good support deactivating properties [9–15]. Carbowax 20 M is one of the most popular phases for packed-column gas chromatography. Condensing Carbowax 20 M with 2-nitroterephthalic acid produces a new phase, FFAP, recommended for the separation of organic acids. The poly(ethylene glycols) are degraded by oxygen, moisture, strong acids, and Lewis acids at high temperatures.

The ionic liquid stationary phases are organic salts of low melting point with a wide liquid temperature range (Table 5.3) [21,22]. Those used in gas chromatography are mainly alkylammonium, alkylphosphonium, and 1,3-dialkylimidazolium salts with weak nucleophilic anions, such as sulfonate and tetrafluoroborate.

The long-range Coulombic forces present in ionic liquids resist the escape of ions into the gas phase resulting in the virtual absence of significant vapor pressure over a wide temperature range. In many cases, the upper temperature limit is established by the thermal stability of the ionic liquid rather than its vapor pressure. Ionic liquids with weak nucleophilic anions possess low chemical reactivity and transformation reactions are relatively rare. Nucleophilic displacement reactions with alkyl halides and proton transfer and other acid/base reactions with amines have been observed in a few cases. The unique selectivity of the ionic liquids is a result of their strong hydrogen-bond basicity and significant capacity for dipole-type interactions (Table 5.3). The hydrogen-bond basicity of the ionic liquids is primarily a property of the anion and is influenced by the size and charge localization on the anion. Ions that can delocalize charge (e.g., picrate and perfluoroalkanesulfonate) are weaker hydrogen-bond bases and less dipolar than other ionic liquids. The halide anions have relatively small atomic radii and no mechanism for charge delocalization. They are the most basic of the ionic liquid stationary phases.

Liquid-crystal stationary phases are used for the separation of positional or geometrical isomers of rigid molecules [23]. Well over 200 liquid-crystal phases have been used in gas chromatography. They are of a variety of chemical types but all have a markedly elongated, rigid, rod-like structure in common. The most common types are Schiff bases, esters, and azo and azoxy compounds. In most cases, the order of elution is in accord with the solute length-to-breadth ratios with differences in vapor pressure and solute polarity also being important. Long and planar molecules fit better into the ordered structure of the liquid-crystal phase, whereas nonlinear and nonplanar molecules do not permeate so easily between the liquid-crystal molecules of the stationary phase and elute faster from the column.

When single stationary phases fail to provide an adequate separation but the poorly resolved components are different on the individual phases, then the use of a mixture of stationary phases (mixed solvent) or column packings (mixed bed) is a viable approach for the separation. The mixed-bed approach is the most versatile and economical one and, in the absence of specific interactions between stationary phases, results in similar separations to the mixed-solvent approach [1,12,24]. The window diagram method affords a convenient approach for identification of the optimum separation conditions [25]. In addition to the optimal binary stationary-phase composition and elution order, the window diagram method can also provide the required column length and the total separation time.

5.2.2 Supports

An ideal support would have sufficient surface energy to cause the stationary phase to wet the surface as a thin, stable film while sufficiently inert to eliminate solute interactions with the surface. It should have a large surface area to weight ratio (facilitates the preparation of columns with a high phase loading), a regular shape with a narrow range of cross-sectional

diameters (facilitates the preparation of columns of high efficiency), be mechanically stable (facilitates general handling), and be a good conductor of heat (facilitates rapid thermal equilibrium). No such ideal support exists but the diatomaceous earths represent a reasonable compromise and are the most widely used supports [26,27].

Diatomite (diatomaceous earth) is a natural product composed of the skeletons of single-celled alga found in large beds in various parts of the world. The skeletal material is essentially amorphous silica with small amounts of alumina and metallic oxide impurities. High-temperature processing ($>900^{\circ}\text{C}$) is used to agglomerate and strengthen the natural material. The presence of complex iron oxides gives this material its characteristic pink color. Thermal processing of the diatomite in the presence of a small amount of sodium carbonate results in the formation of a white material in which metal impurities are converted to colorless sodium silicate. Typical physical properties are summarized in Table 5.4. The pink supports are relatively hard and have a high packing density, a relatively large surface area, and a high loading capacity. They are used in both analytical and preparative gas chromatography. The white supports are more

TABLE 5.4 Characteristic properties of chromosorb supports.

Property	P	W	G ^a	A ^b	750 ^c
Color	Pink	White	Oyster	Pink	White
Apparent pH	6.5	8.5	8.5	7.1	8.0
Free fall density (g mL ⁻¹)	0.38	0.18	0.47	0.40	0.37
Packed density (g mL ⁻¹)	0.47	0.24	0.58	0.48	0.36
Surface area (m ² g ⁻¹)	4.0	1.0	0.5	2.7	0.5–1.0
Maximum liquid loading (%)	30	15	5	25	12

^a A specially prepared white support that is harder, more robust, inert, and has a higher density than typical white supports (a given column volume contains approximately 2.5 times the amount of Chromosorb G, and therefore liquid phase, as Chromosorb W of the same nominal phase loading).

^b Possesses the mechanical strength and high loading capacity of pink supports with a reduced surface activity approaching that of the white supports (used for preparative chromatography).

^c Most inert of the white supports.

friable, less dense, and have a lower surface area and loading capacity. They are used primarily for analytical separations. Supports with a mesh range of 80–100 (177–149 μm) or 100–120 (149–125 μm) are a reasonable compromise between column efficiency (proportional to d_p , the average particle diameter) and column pressure drop (proportional to $(1/d_p^2)$ for analytical separations). For polar compounds, severe tailing, decomposition, and loss of injected mass by adsorption are observed for some compounds and are associated with the presence of metallic impurities, principally iron, and silanol groups on the support surface. Acid and/or base washing to remove metal impurities and silanization of silanol groups are the most widely used methods for support deactivation [12]. Silanol groups are converted to silyl ethers by reaction with dimethyldichlorosilane (DMCS), hexamethyldisilazane (HMDS), trimethylchlorosilane (TMCS), or by a combination of these reagents. Highly silanized supports are not wet by polar liquids and are unsuitable for preparing packings with polar stationary phases. For strongly acidic or basic compounds, tailing reducers may be required to improve chromatographic properties. To be effective, the tailing reducer should be a stronger acid or base than the compounds to be separated. For amines, the tailing reducer could be a few percent (w/w) potassium hydroxide or poly(ethyleneimine). For acidic compounds, phosphoric acid or trimer acid is suitable. These active substances also act as subtractive agents (acidic tailing reducers absorb bases, etc.) and must be compatible with the stationary phase. Potassium hydroxide and phosphoric acid, for example, catalyze the depolymerization of poly(ester) and poly(siloxane) stationary phases.

Less commonly used supports include fluorocarbon powders, glass beads, and dendritic salt. The fluorocarbon powders, for example, Kel-F (a hard chlorofluorocarbon powder) and Teflon-6 (an agglomerated poly(tetrafluoroethylene) porous polymer), are used primarily as supports for the separation of corrosive compounds. They

have low surface energy and can be difficult to coat, often requiring special techniques [12]. Column efficiencies are often low compared with diatomaceous earth supports and the maximum operating temperature depends on the softening point of the support material, typically $<250^\circ\text{C}$. Glass beads with a narrow size distribution can be used to prepare efficient columns but have a low loading capacity ($<0.5\%$ w/w). Because of their controlled shape and size, they were used primarily in theoretical studies of band broadening.

5.2.3 Coating and packing techniques

The preparation of a packed column is a multistep process in which the liquid phase in a suitable volatile solvent is mixed with the support, the solvent removed by evaporation, and the dry packing added to the empty column. No special apparatus, not usually found in chemical laboratories, is required for this process. Column packings are prepared on a weight-for-weight basis and quoted as percent liquid phase (% w/w). The required weight of solid support is added to the required amount of stationary phase dissolved in sufficient solvent to completely cover the support. The solvent should be a good solvent for the stationary phase, free of stabilizers and involatile contaminants, and sufficiently volatile for easy evaporation. The most common coating/evaporation procedures are the rotary evaporator technique, pan-dry method, slurry filtration method, and column adsorption method [12]. Since diatomaceous supports are fragile, they should be handled gently during the coating procedure. After coating the damp packing is air-dried, oven-dried, or dried in a fluidized bed dryer. The latter is faster and usually gives packings of higher efficiency and permeability, probably due to removal of fine particles by the gas passing through the packing. Mechanical sieving prior to coating and fluidized bed drying after coating are the preferred methods of minimizing the deleterious effects of fines on column

performance. If an accurate value for the phase loading is required, it can be determined by either Soxhlet extraction or combustion on a sample of the dried and conditioned packing [12].

Columns of 0.5–3.0-m length and 2–4-mm internal diameter can be packed by the tap-and-fill method, aided by suction. Longer columns are more difficult to pack and require a combination of suction at the free end and pressure applied to the packing reservoir attached to the other end. One end of the column is terminated with a glass wool plug, attached to a water aspirator, and small aliquots of packing added via a filter funnel attached to the opposite end. The column bed is consolidated as it forms by gentle tapping of the column sides with a rod or with the aid of an electric vibrator. When the column has been packed to the required length, the funnel is removed and the empty segment of the column (the length of this segment is determined by the design of the column injector) is filled with a glass wool plug. Column preparation is completed by placing the column in the oven of the gas chromatograph and connecting it to the carrier gas flow from the injector end only. The temperature of the oven is then increased to about 20°C above the highest temperature to be used at for the planned separations (but never above the maximum allowed operating temperature for the stationary phase) and held there for several hours (usually overnight). This conditioning step removes volatile impurities and contaminants from the column packing and ensures that when the column is placed into service, a stable detector baseline is obtained.

After column conditioning, a few preliminary tests are performed to ensure that the performance of the column meets expectations. Column efficiency is determined with a simple test mixture containing compounds with weak specific interactions (e.g., *n*-alkanes and aliphatic ketones), an activity test with a polar test mixture reflecting the functional groups

expected to be present in the samples, and a resolution test using a mixture that reflects the intended column use. These tests provide information on column efficiency, absolute retention, peak tailing, separation factors, and resolution of target compounds suitable for demonstrating both column quality and that the column is fit for purpose. Columns with a plate number between 1500 and 2500 per meter are suitable for analytical applications (plate number varies with the phase loading and support type). An unusually high column inlet pressure indicates support attrition, possibly as a result of mechanical breakdown during the coating and packing procedure. Excessive tailing or adsorption of polar test compounds indicates residual column activity. Column performance might be restored by on-column silanization of support silanol groups using one of the many available column-conditioning reagents.

5.2.4 Packed columns for preparative-scale gas chromatography

Preparative-scale gas chromatography requires the use of larger amounts of stationary phase than analytical separations to achieve high sample throughput [12,28]. For simple separations, short, wide columns are generally used (e.g., 1–3 m × 6–10 cm I.D.) For difficult separations, long, narrow columns (e.g., 10–30 m × 0.5–1.5 cm I.D.) are preferred. Wide-bore columns cannot be coiled and purpose-designed instruments to accommodate long columns are required for their use. A coarser support material with a narrow particle-size distribution, for example, 35–80 mesh (500–177 μm), is used to facilitate operation at a reasonable inlet pressure. Reproducibly packing wide-bore columns with reasonable efficiency is more difficult due to the uneven radial packing density resulting from particle-size segregation (the larger particles accumulate closer to the wall). To minimize radial heterogeneity, the

shake, turn, and pressure packing method is recommended. The column is shaken in the radial direction and is rotated along its long axis while being packed and periodically pressurized. Packing with suction and vertical tamping affords a faster approach.

5.2.5 Classification of stationary phases

Many methods of classifying stationary phases to facilitate column selection for method development have been proposed and abandoned over the long history of gas chromatography [12,29]. Most early classification scales attempted to rank stationary phases according to their solvent strength (or polarity) and solvent selectivity. Single-value scales of solvent strength are unable to provide information that is useful for column selection, since multiple and independent interactions are involved in solute–solvent interactions. Scales of free energy or retention index differences for prototypical compounds were in use for many years but were shown to be unreliable [30]. The system of phase constants introduced by Rohrschneider and further developed by McReynolds are the best known of this type and can be found in some stationary-phase catalogs [11]. The modern approach to stationary-phase classification is based on Abraham’s solvation parameter model [1,22,31,32]. This model assumes that the transfer of a solute from the gas phase to the stationary phase occurs in three steps: the formation of a cavity in the stationary phase of the same size as the solute, transfer of the solute to the cavity with reorganization of the solvent molecules around the cavity, and the setting up of solute–solvent interactions recognized as dispersion, of a dipole type (orientation and induction), and hydrogen bonding. The master equation for gas chromatography is given as

$$\log SP = c + eE + sS + aA + bB + lL \quad (5.1)$$

where SP is some free energy–related retention property, such as a partition constant or

retention factor. The uppercase letters are solute descriptors, which define the capability of the solute to participate in the defined intermolecular interactions, but are not important for the present discussion. The capability of the stationary phase to enter into complementary interactions with those of the solute is indicated by the lowercase letters known as system constants. The *e* system constants are determined by electron lone-pair interactions, the *s* system constants by interactions of a dipole type, the *a* system constant by the hydrogen-bond basicity of the stationary phase, the *b* system constant by the hydrogen-bond acidity of the stationary phase, and the *l* system constant by the opposing contributions from cavity formation and dispersion interactions. The equation constant, *c* term, is not a fundamental property of the stationary phase and is determined by a number of factors related to the physical characteristics of the column and statistical contributions from fitting the model to the experimental data.

The system constants for some common stationary phases are summarized in Table 5.3 [1,22,31]. The system constants are only loosely scaled to each other so that differences in any column can be read directly but small differences along rows must be interpreted cautiously. Two features in this table stand out. None of the common stationary phases are significant hydrogen-bond acids (*b* system constant) and this interaction is unimportant for selectivity optimization. In the case of EGAD, DEGS, and TCEP, the small *b* system constant is more likely a reflection of impurities in the stationary phase produced during synthesis or while in use. The second feature of note is that electron lone-pair interactions (*e* system constant) are generally weak and of limited variation. They afford few opportunities to optimize selectivity. Fluorine-containing stationary phases have negative *e* system constants representing the tighter binding of electron pairs compared with hydrocarbons. The remaining three system constants account for most of the selectivity differences among the

TABLE 5.5 Typical ranges for the system constants at 121°C for alkylammonium and alkylphosphonium ionic liquids and nonionic stationary phases.

System constant	Range	
	Ionic liquids	Non-ionic liquids
<i>e</i> (electron lone-pair interactions)	0.07–0.50	0–0.037
<i>s</i> (dipole-type interactions)	1.4–2.1	0–2.1
<i>a</i> (solvent hydrogen-bond basicity)	1.4–5.4	0–2.1
<i>b</i> (solvent hydrogen-bond acidity)	0	0
<i>l</i> (cohesion and dispersion interactions)	0.44–0.55	0.37–0.58
(Associated anions)	0.26–0.37	

stationary phases in Table 5.3. The *l* system constant is always an important contributing factor to retention and mainly reflects changes in the cohesion of the stationary phases. It has small values for polar stationary phases, which retain compounds of low polarity weakly, and large values for low-polarity stationary phases, which retain compounds of low polarity more strongly. The *l* system constant is also strongly correlated to the partial molar Gibbs free energy of solution for a methylene group and is an indication of the spacing between alternate compounds in a homologous series. The ionic liquids with weakly associating ions have remarkably low cohesion for polar stationary phases due to the effect of the Coulombic fields on interionic distances. Ionic liquids with associating ions have similar cohesion to polar nonionic stationary phases. The stationary phases in Table 5.3 differ significantly in their capacity for dipole-type interactions (*s* system constant). For the poly(siloxane) stationary phases, the *s* system constant changes predictably with the type of substituent (methyl < phenyl < trifluoropropyl < cyanopropyl) attached to the polymer backbone. Poly(siloxane) stationary phases with a high incorporation of cyanoalkyl groups are among the most dipolar stationary phases used in gas chromatography. The poly(ethylene glycol) stationary phases are slightly less dipolar than the poly(ester) stationary

phases, and both are intermediate with respect to the dipolarity range for the poly(siloxanes) containing cyanoalkyl substituents. The ionic liquid stationary phases are all dipolar with some examples being the most dipolar of all stationary phases. All of the dipolar stationary phases are also hydrogen-bond bases (*a* system constant). The ionic liquids possess the widest range of hydrogen-bond basicity and include the highest ranked stationary phases for this interaction (Table 5.5). A notable feature of the polar stationary phases is the characteristic family difference for the *s/a* system constants ratio. This is the principal reason for retention of the different types of polar stationary phases for selectivity optimization.

A smaller number of stationary phases can be identified from those in Table 5.3 as a starting point for method development (Table 5.6). The system constants (and the intermolecular interactions they represent) are temperature-dependent and not highly correlated [33]. Thus, the system constants in Table 5.3 should be considered reliable for selectivity optimization at temperatures in the region of 120°C but less so at significantly different temperatures. System constants also depend on the phase loading for mixed retention mechanisms, which affects selectivity [34]. The general strategy for selectivity optimization is to choose a single

TABLE 5.6 Classification of common stationary phases into selectivity groups for method development.

Group	Type of stationary phase	Examples of group membership	Basis of selectivity
I	Hydrocarbons and poly(dimethylsiloxanes)	Squalane Apolane-87, OV-1	Low cohesion and very weak polar interactions.
II	Poly(methylphenylsiloxanes) < 50% methylphenylsiloxane monomer	OV-3, OV-11, OV-105, PPE-5	Low cohesion and moderate polar interactions ($s/a > 2$)
III	Poly(trifluoropropylmethyl-siloxanes)	QF-1	Moderate cohesion, intermediate dipolarity, low hydrogen-bond basicity, electron lone-pair interactions reduce retention ($s/a > 5$)
IV	Poly(cyanoalkylphenyl-siloxanes)	OV-225, OV-275, TCEP	High cohesion and strong dipolarity and hydrogen-bond basicity ($s/a \approx 1$)
V	Poly(ethylene glycols)poly(esters)	CW20M, DEGS	Intermediate cohesion, dipolarity, and hydrogen-bond basicity ($s/a < 1$)
VI	Ionic liquids	QBA TS, QBP Cl	See Table 4.5

stationary phase from each group in Table 5.6 for screening of the selectivity groups and, once a suitable group is identified for the separation, to fine-tune the selection by exploring other phases within the same group. Stationary-phase selection has to take into account the temperature operating range for the stationary phases as well as their selectivity.

5.2.6 Retention models

Any model devised to explain retention in packed-column gas chromatography has to take into account the distribution of the stationary phase on the porous support surface. For liquids that wet the support, the stationary phase is first adsorbed as a monomolecular and multimolecular layer over the entire support surface. As the phase loading is increased, it collects in the fine pores initially and then progressively appears in the large cavities at the same time as the adsorbed layer thickens up. The structured layer formed close to the support surface has more order than in the bulk liquid and different retention properties. Although surface forces are short range, their effect can be transmitted by the

successive polarization of adjacent molecules to a considerable depth in the liquid. This structured layer, then, may be of considerable thickness and will dominate the retention mechanism at low phase loadings. At high phase loadings, the presence of bulk liquid will come to dominate the retention mechanism. In addition, variation of the phase loading will result in nonlinear changes in the surface area of the gas–liquid interface as pores of different sizes fill with liquid at different rates. At high phase loadings, it is assumed that the gas–liquid interfacial area approaches a limiting value, approximately equal to the support surface area less than the area of its narrow pores and channels. For liquids that do not wet the support surface readily, the stationary phase will be present as droplets primarily at the outer grain surface allowing exposure of the sample to adsorption sites directly on the support surface at low phase loadings. At higher phase loadings, coalescence to a continuous film will occur and interactions with the support surface then depend primarily on the competition between the bulk (or structured) liquid phase and the sample for surface active sites on the support. Support deactivation

is then important to minimize these interactions but also to facilitate wetting of the support surface by liquids with poor support wetting characteristics.

Taking the aforementioned considerations into account, a general model for retention in gas–liquid chromatography has to consider contributions from interfacial adsorption at the support and/or liquid interfaces, as well as partition at the gas–liquid and bulk liquid–structured liquid interfaces. This results in the general model [35–37]

$$V_N^* = V_L K_L + \delta V_L + (K_S - K_L) + (1 - \delta) A_{LS} K_{DSL} + A_{GL} K_{GL} + A_{LS} K_{GLS} \quad (5.2)$$

where V_N^* is the net retention volume per gram of packing, V_L the volume of liquid phase per gram of packing, K_L the gas–liquid partition constant, δ_a constant constrained to have values of 1 when the film thickness is less than or equal to the thickness of the structured layer (d_s) and 0 when the film thickness exceeds the thickness of the structured layer, K_S the gas–liquid partition constant for the structured liquid layer, A_{LS} the liquid–solid interfacial area per gram of packing, $K_{DSL} = d_s(K_S - K_L)$, A_{GL} the gas–liquid interfacial area per gram of packing, K_{GL} the adsorption coefficient at the gas–liquid interface, and K_{GLS} the coefficient for adsorption at the liquid–solid interface. Although Eq. (5.2) provides a general description of the retention process, it is rather awkward to use. The equation contains five unknowns (K_L , K_S , K_{DSL} , K_{GL} , and K_{GLS}) requiring data for the packing characteristics (V_L , A_{GL} , and A_{LS}) for at least five columns prepared from the same support at different phase loadings to obtain a numerical solution. In addition, there is no exact method of defining the thickness of the structured layer, which must be established by a trial and error procedure. The general assumption in deriving Eq. (5.2) is that the individual retention mechanisms are independent and additive. This will

be true for conditions where the infinite dilution and zero surface coverage approximations apply (i.e., small sample sizes where the linearity of the various adsorption and partition isotherms are unperturbed and solute–solute interactions are negligible).

At intermediate to high phase loadings, the contributions of the structured liquid phase to retention are expected to be small, allowing Eq. (5.2) to be simplified [37–39]

$$V_N^*/V_L = K_L + (A_{GL}K_{GL} + A_{LS}K_{GLS})(1/V_L) \quad (5.3)$$

from which the gas–liquid partition constant can be determined by (usually) a linear extrapolation from a plot of V_N^*/V_L against $1/V_L$. This observation is consistent with the view that adsorption at the support–liquid interface is dominant for phases of low polarity and at the gas–liquid interface for polar phases. Some representative examples are shown in Fig. 5.1 for several compounds on the polar stationary phases Carbowax 20 M and poly(dicyanoalkylsiloxane) OV-275. For solutes retained solely by gas–liquid partition (e.g., nitromethane, dioxane, and ethanol) on Carbowax 20 M, the plots have a zero slope. The n-alkanes are retained by a mixed retention mechanism indicated by the positive slope and a significant intercept at $1/V_L = 0$. Interfacial adsorption is important for all compounds on OV-275 and is the dominant retention mechanism for the n-alkanes, which have a near-zero intercept, indicating that gas–liquid partitioning is of minor importance to their retention.

Since there is no good method for measuring A_{GL} , Eq. (5.3) is rarely used to determine K_{GL} but a qualitative assessment of the general contribution of interfacial adsorption to the retention mechanism can be obtained by comparison of the true gas–liquid partition constant obtained from Eq. (5.3) by extrapolation and the value measured with the assumption that retention occurs only by gas–liquid partition. These calculations indicate that interfacial

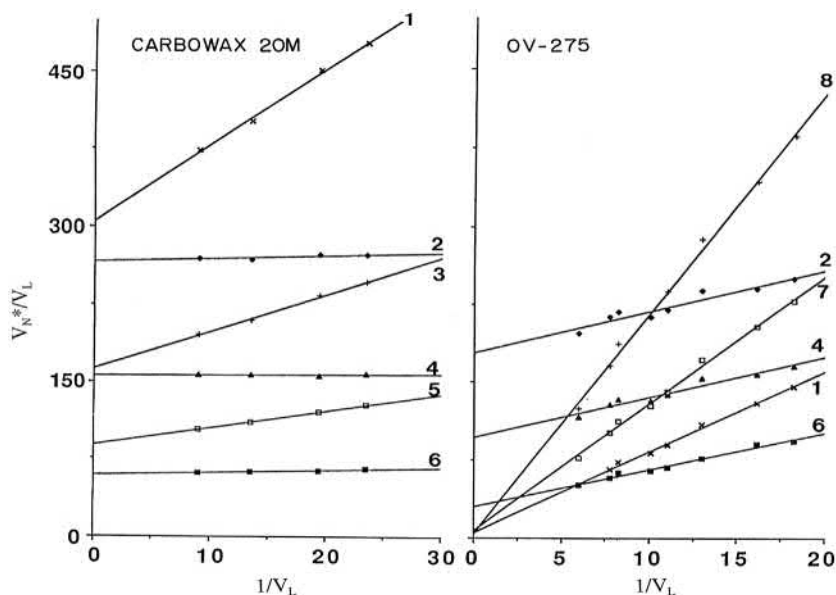


FIGURE 5.1 Plot of V_N^*/V_L against $1/V_L$ for different compounds on poly(ethylene glycol), Carbowax 20 M, and poly(cyanoalkylsiloxane), OV-275, stationary phases at 80.8°C. Identification: 1 = dodecane; 2 = nitromethane; 3 = undecane; 4 = dioxane; 5 = decane; 6 = ethanol; 7 = tridecane; and 8 = tetradecane. From Ref. C.F. Poole, S.K. Poole, *Foundations of retention in partition chromatography*, *J. Chromatogr. A* 1216 (2009) 1530–1550; copyright Elsevier.

adsorption is not a rare retention mechanism, and although gas–liquid partition tends to dominate in most cases, interfacial adsorption should not be ignored. Since the contribution from interfacial adsorption depends on the phase loading, temperature, type of stationary phase and support, and properties of the sample, it is impossible to prescribe exact circumstances when it is important; however, the following general comments serve to indicate when it is a likely contributor to retention. Interfacial adsorption tends to be more important at lower temperatures and for a mixed retention mechanism it may fall to zero at a sufficiently high temperature. Interfacial adsorption makes a larger relative contribution to the retention mechanism at lower phase loadings due to a combination of a larger accessible liquid surface area and a smaller bulk liquid volume. For nonpolar phases, interfacial adsorption can generally be related to support properties and,

at intermediate temperatures, possibly eliminated by adequate support deactivation. Interfacial adsorption is usually significant for most compounds on cohesive stationary phases and is commonly observed for solutes of low polarity on polar stationary phases.

5.2.7 Band-broadening mechanisms

As a sample migrates along the column, its distribution about the zone center increases in proportion to its residence time in the column. The extent of band broadening determines the column efficiency, which is expressed by convention as either the plate number (N) or plate height (H) for the column, and is controlled by a set of kinetic factors affected by column design. The plate number and plate height are calculated from the peak profile as indicated in Table 5.7. These terms have their origin in the

TABLE 5.7 Calculation of the plate number (N) and plate height (H) for a packed column assuming that peaks can be approximated by a Gaussian model.

$N = (t_R/\sigma_t)^2 = a(t_R/w)^2$	t_R = solute retention time
	σ_t = peak standard deviation
	a = constant that depends on the peak width
	w = a measure of the peak width
	w_h = peak width at half height and $a = 5.54$
	w_b = peak width at base and $a = 16$
$H = L/N$	L = column length

plate theory of chromatography, long since abandoned. Modern models of band broadening are based on rate theories that are better able to account for experimental observations as well as facilitating column design [1,40–44]. Rate theory considers three general contributions to band broadening, which can be identified as flow anisotropy (eddy diffusion), axial diffusion, and resistance to mass transfer. These terms, except where noted, are considered independent and additive. In general, rate models are able to account for the main features of band broadening but are not exact for packed columns.

The space between particles in a packed bed is made up of a network of interconnected channels of varied dimensions that depend on the size and shape of the particles and their packing density. For any channel, the mobile-phase velocity falls close to zero near the particle surface and increases rapidly toward the channel center. In addition, individual streamlines are not straight since molecules are forced to continually change direction by the obstacles (packing material) in their way. The heterogeneity of the mobile-phase velocity and path lengths for different streamlines results in band broadening compared with passage through an open tube. Band broadening resulting from these conditions is relaxed to some extent by radial diffusion, which allows solute molecules to sample multiple streamlines as they migrate along the

column. The contribution of flow anisotropy (eddy diffusion) to the plate height, H_E , can be estimated from $H_E = 2\lambda d_p$, where λ is the column packing factor (a dimensionless parameter with typical values between 0.5 and 1.5) and d_p is the average particle size. Band broadening by flow anisotropy can be minimized using a homogeneous bed packed with small particles of a narrow size range at a high packing density. The column pressure drop will ultimately determine the most practical particle size and column length. For typical operating pressures (<10 bar), this corresponds to an average particle size of about 100 μm and columns <5 m long.

The contribution to the plate height from molecular diffusion in the mobile phase arises from the tendency of the solute band to diffuse away from regions of high to lower concentration. Its contribution to the plate height, H_L , is proportional to the diffusion coefficient in the mobile phase, D_M , the tortuosity (obstruction) factor of the column, γ , and the time the solute spends in the mobile phase (inversely proportional to the mobile phase velocity u), $H_L = 2\gamma D_M/u$. The tortuosity factor typically has values of 0.6–0.8 that depend on the packing density over the length of the column [45]. Diffusion coefficients in the stationary phase are about 10^4 times smaller than in gases and the contribution to band broadening from axial diffusion in the stationary phase can generally be neglected.

During migration along the column, solute molecules are continually and reversibly transferring to and from the stationary phase. This process is not instantaneous because a finite time is required for the molecules to transfer to the interface between phases and enter the stationary phase by diffusion. Those solutes close to the interface enter the stationary phase almost immediately, whereas those some distance away enter sometime later. However, since the mobile phase is moving during this time interval, those molecules that remain in the mobile phase will be swept along the column and dispersed away from those molecules that entered the stationary phase almost immediately. Dispersion occurring in the stationary phase is exactly analogous to that in the mobile phase. Thus, those molecules that were close to the surface will be swept along in the mobile phase and dispersed from those molecules still diffusing to the interface. The combined peak observed at the column outlet is broadened about its band center, which is where it would have been if equilibrium was instantaneous, provided the degree of nonequilibrium is small. The process described earlier is called resistance to mass transfer, and the mobile-phase contribution, H_M , is given by $wudp^2/D_M$ where w is an empirical packing factor with values typically between 0.02 and 5. The stationary-phase contribution to resistance to mass transfer, H_S , is given by $2kd_f^2u/3D_s(1+k)^2$ where k is the retention factor, d_f the film thickness, and D_s the solute diffusion coefficient in the stationary phase. In practice, to account for the influence of convection (band broadening resulting from exchange of solute between streams moving at different velocities), the flow anisotropy term must be coupled with the mobile-phase resistance to mass transfer term, as indicated further [40]:

$$H_{MC} = 1/(1/H_E + 1/H_M) \quad (5.4)$$

where H_{MC} is the contribution to the plate height resulting from the coupling of flow anisotropy and resistance to mass transfer in the mobile phase. At typical mobile-phase velocities for packed columns, the coupling concept is of minor importance but, at high mobile-phase velocities, it is better able to explain experimental observation of the change in the total plate height. In particular, it accounts for the flattening out of the ascending portion of the van Deemter curve observed at high mobile-phase velocities compared with the uncoupled approach.

In gas chromatography, the mobile phase is incompressible and results in a pressure gradient along the column. As a consequence, diffusion constants in the mobile phase and the mobile-phase velocity vary in a nonlinear manner with the fraction of the column length explored. For columns operated at an average mobile-phase velocity in the region of the optimum value, a reasonable approximation for the total plate height (obtained by summing the individual contributions discussed earlier) is given by

$$\begin{aligned} H &= 2\lambda d_p + 2\gamma D_{M,0}/u_0 + [f_g(k)] \left(d_p^2/D_{M,0} \right) u_0 \\ &\quad + [f_s(k) d_f^2/D_s u_{AV}] \\ f_g(k) &= (1 + 6k + 11k)/96(1+k)^2 \\ f_s(k) &= 2k/3(1+k)^2 \end{aligned} \quad (5.5)$$

where the subscript zero is added to indicate that the parameter is specified as the value at the column outlet and the empirical constant w has been replaced by a functional dependence on the retention factor derived exactly for an open-tubular column and used as an approximation for a packed column. All terms containing u_0 should be multiplied by a function dependent on

the column inlet/outlet pressure ratio, P , but since for the usual range of conditions in gas chromatography it has values between 1 and 1.1, it is often omitted for simplicity [43]. For gas–solid chromatography the stationary-phase mass transfer term is replaced by a function describing the kinetics of adsorption and desorption from a solid surface, which is often the dominant term in the plate height equation for inorganic oxides and chemically bonded adsorbents [5,6,43].

Variation of the column plate height against the mobile-phase velocity is a hyperbolic function commonly described by the van Deemter equation [40–42,44]

$$H = A + B/u + (C_S + C_M)u \quad (5.6)$$

The equation coefficients can be superficially assigned to A = flow anisotropy, B = axial diffusion, and the C terms the contributions from resistance to mass transfer in the stationary and mobile phases to the column plate height. The coefficients of the van Deemter equation are empirical, however, and are not simply related to the various terms in Eq. (5.5). An important general contribution of the van Deemter equation was the illustration that an optimum mobile-phase velocity existed for a column at which its highest efficiency is realized, H_{\min} . Some typical values are summarized in Table 5.1. Since the region around u_{opt} is usually shallow with a fairly flat ascending portion at $u > u_{\text{opt}}$, for less demanding separations columns are often operated at $u > u_{\text{opt}}$ to reduce the separation time with a modest reduction in column performance.

5.3 Gas–solid chromatography

Gas–solid chromatography is used for applications that can broadly be characterized as those difficult to achieve by gas–liquid chromatography at normal operating temperatures [9,10,12,42,46]. These include the separation of

gases, solvents, and volatile hydrocarbons and halocarbons (typically compounds containing <12 carbon atoms and with a boiling point <200°C) [47]. Retention results from adsorption on surfaces with different types and number of active sites providing for complementary selectivity to liquids and an enhanced capability for the separation of isomers and isotopomers [48]. The distribution of energetic sites is usually determined by fitting retention data to various isotherm models to facilitate an understanding of retention mechanisms [49]. Reversed-flow gas chromatography provides an alternative approach to inverse gas chromatography for isotherm measurements [50]. The carrier gas can play a significant role in the separation process by competing with analyte molecules for adsorption at active sites on the stationary phase [51]. Selectivity, therefore, can be modified by the selection of the carrier gas and by the use of gas mixtures. One or more of the following features may be detrimental to applications in gas–solid chromatography: (i) sample size–dependent retention and asymmetric peak shapes resulting from nonlinear adsorption isotherms; (ii) the presence of chemically active adsorption sites resulting in irreversible binding of some analytes; (iii) the high surface areas and adsorption energies of adsorbents can result in excessive retention for compounds of low volatility and for polar compounds; (iv) column efficiency is often less favorable for adsorbents compared to liquids; (v) some adsorbents are catalytically active; and (vi) the reproducible preparation of adsorbents is generally more difficult than the synthesis of liquid stationary phases. Most adsorbents are sufficiently robust to allow dry packing of columns.

5.3.1 Inorganic oxides

The most important inorganic oxide adsorbents are silica gel and alumina. These are

available as spherical porous beads in a wide range of particle sizes with surface areas of 5–500 m² g⁻¹ and pore diameters of 8–150 nm. Retention is controlled by the specific surface area, surface deactivation method, the thermal history of the adsorbent, and the capability of analytes to participate in specific interactions, such as hydrogen bonding, with surface functional groups. The different surface functional groups (silanol groups in the case of silica and aluminum ions in the case of alumina) result in different selectivity for these adsorbents. Since both adsorbents tenaciously adsorb moisture, reproducible retention requires the rigorous exclusion of moisture from the carrier gas and samples. Mixing these adsorbents with a diatomaceous support or coating a diatomaceous support with a layer of fine-particle adsorbent (dusted columns) reduces retention and simultaneously improves efficiency [52]. A more general approach to control retention and selectivity is to coat the adsorbent with a small amount of liquid stationary phase or an inorganic salt [48,53]. Alkali metal salts (potassium chloride and carbonate, sodium sulfate, etc.) at loadings of 0.5%–30% (w/w) are common salt modifiers. At low loadings of salt or liquid phase, retention is reduced with less effect on selectivity, while at higher loadings, a mixed retention mechanism dominates and selectivity may be changed significantly from that of the bare adsorbent. Inorganic salts have their own adsorption characteristics that are different from silica and alumina, and in the case of liquid phases, adsorption at the liquid interface and gas–liquid partition are possible contributors to the retention mechanism.

5.3.2 Carbon adsorbents

Graphitized carbon blacks and carbon molecular sieves are the main types of carbon

adsorbents used in gas–solid chromatography [54]. Graphitized carbon blacks have low porosity with surface areas from about 5 to 100 m² g⁻¹. Ideally, they behave as nonspecific adsorbents with retention dominated by dispersion interactions. In reality, the presence of a small number of polar sites associated with surface oxygen complexes introduces strong specific interactions with polar compounds. Low loadings of liquid phase (0.2%–5% w/w) are frequently used to mask high-energy adsorption sites and to modify selectivity. Coating graphitized carbon blacks with phosphoric acid or potassium hydroxide facilitates the separation of organic acids and amines. The flat surfaces of graphitized carbon blacks are particularly well suited to the separation of structural and geometrical isomers.

Carbon molecular sieves consist of small graphite crystallites cross-linked to yield a disordered cavity-aperture structure. They are microporous with a large surface area, 200–1200 m² g⁻¹, and a pronounced retention of organic compounds. Primary applications include the separation of inorganic gases, hydrocarbons containing less than four carbon atoms, and the separation of small polar molecules such as water and formaldehyde. Higher-molecular-weight compounds may be irreversibly bound at typical operating temperatures.

5.3.3 Molecular sieves

Molecular sieves (zeolites) are artificially prepared alkali metal aluminosilicates. For gas–solid chromatography, the most common types are calcium aluminosilicate (type 5A) with an effective pore diameter of 0.5 nm and sodium aluminosilicate (type 13X) with an effective pore diameter of 1 nm. The molecular sieves are microporous with a tunnel-like pore

structure of similar dimensions to small molecules. Retention is primarily controlled by molecular size, whether the analyte can enter the pore structure of the molecular sieve, and by the strength of adsorption interactions with the internal pore surface. They are used primarily for the separation of gases and low-molecular-weight hydrocarbons [55].

5.3.4 Porous organic polymers

A number of porous organic polymer beads prepared from different monomers and cross-linking reagents with a range of surface areas and pore sizes are used in gas–solid

chromatography (Table 5.8) [12,46,56,57]. Beads with pore diameters <10 nm are used primarily for the separation of gases and those with larger pore diameters for volatile organic compounds (Table 5.9). Compared with other adsorbents their surfaces are relatively inert, facilitating the separation of polar compounds with little difficulty. The natural microporosity of polymer beads results in modest column efficiency. The retention mechanism is not well understood. At low temperatures, adsorption is expected to be the dominant mechanism, while at higher temperatures, it is possible that the porous polymers behave as highly extended liquids with solvation properties.

TABLE 5.8 Physical properties of porous polymer beads for packed-column gas chromatography.

Porous polymer	Monomers	Surface area (m ² g ⁻¹)	Average pore diameter (nm)	Temperature limit (°C)
Chromosorb 101	STY-DVB	30–40	300–400	275
Chromosorb 102	STY-DVB	300–400	8.5–9.5	250
Chromosorb 103	STY	15–25	300–400	275
Chromosorb 104	ACN-DVB	100–200	60–80	250
Chromosorb 105	Polyaromatic	600–700	40–60	250
Chromosorb 106	STY	700–800	5	225
Chromosorb 107	Acrylic ester	400–500	8–9	225
Chromosorb 108	Acrylic ester	100–200	25	225
Porapak N	STY-DVB-VPO	225–500	9	200
Porapak P	STY-DVB-EVB	100–200	7.5–10	250
Porapak Q	EVB-DVB	500–850	7.5–10	250
Porapak R	STY-DVB-VPO	450–600	7.5–10	250
Porapak S	STY-DVB-VP	300–550	7–9	250
Porapak T	EGDMA	250–450	9	200
Porapak PS	Silanized P			
Porapak QS	Silanized Q			250
Tenax-GC	DPO	19–30	25–7500	375

TABLE 5.9 Common packed-column applications of porous polymers.

Polymer	Application
Chromosorb 101 Porapak P and PS	Esters, ethers, ketones, alcohols, hydrocarbons, fatty acids, aldehydes, and glycols. Not recommended for amines and anilines.
Chromosorb 102 Porapak Q	Light and permanent gases, volatile carboxylic acids, alcohols, glycols, ketones, hydrocarbons, esters, nitriles, and nitroalkanes. Not recommended for amines, anilines. Nitrated by nitrogen oxide gases.
Chromosorb 103 Porapak S	Amines, amides, alcohols, aldehydes, hydrazines, and ketones. Not recommended for acids, amines, glycols, and nitriles. Reacts with nitroalkanes.
Chromosorb 104	Nitriles, nitro compounds, sulfur gases, ammonia, carbon dioxide, vinyl chloride, moisture in solvents, and xylenols. Not recommended for amines and glycols.
Chromosorb 105 Porapak N	Aqueous mixtures of formaldehyde, acetylene from lower hydrocarbons, and most gases. Not recommended for glycols, acids, and amines.
Chromosorb 106 Porapak QS	Alcohols, C ₂ –C ₅ carboxylic acids, alcohols, and sulfur gases. Not recommended for glycols and amines.
Chromosorb 107 Porapak T	Formaldehyde from water and acetylene from lower hydrocarbons. Sulfur compounds. Not recommended for glycols and amines.
Chromosorb 108	Gases, water, alcohols, aldehydes, and glycols.
Porapak R	Esters, ethers, nitriles, and nitro compounds. Not recommended for glycols and amines.
Tenax-GC	High-boiling polar compounds, diols, phenols, methyl esters of dicarboxylic acids, amines, diamines, ethanalamines, amides, aldehydes, and ketones.

References

- [1] C.F. Poole, *The essence of chromatography*, Elsevier, Amsterdam, 2003.
- [2] T.J. Bruno, A review of capillary and packed column gas chromatography, *Separ. Purif. Methods* 29 (2000) 27–61.
- [3] T. Herraiz, G. Reglero, M. Herraix, R. Alonso, M.D. Cabuzundo, Micropacked capillary columns: suitable alternative to very thick capillary columns, *J. Chromatogr.* 388 (1987) 325–333.
- [4] M. Inoue, Y. Saito, I. Ueta, T. Miura, H. Ohkita, K. Fujimura, et al., Rapid temperature-programmed separation and retention prediction on a novel packed-capillary column in gas chromatography, *Anal. Sci.* 26 (2010) 687–691.
- [5] R.J. Jonker, H. Poppe, J.F.K. Huber, Improvements of speed of separation in packed column gas chromatography, *Anal. Chem.* 54 (1982) 2447–2456.
- [6] M.M. Robinson, K.D. Bartle, P. Myers, High-pressure microcolumn gas chromatography, *J. Microcol.* (September, 10 1998) 115–123.
- [7] D.C. Fenimore, J.H. Whitford, C.M. Davis, A. Zlatkis, Nickel gas chromatographic columns: an alternative to glass for biological samples, *J. Chromatogr.* 140 (1977) 9–15.
- [8] Y. Takayama, T. Takeichit, Preparation of deactivated metal capillary for gas chromatography, *J. Chromatogr.* 685 (1994) 61–78.
- [9] G.E. Baiulescu, V.A. Ilie, *Stationary Phases in Gas Chromatography*, Pergamon Press, Oxford, 1975.
- [10] K.K. Unger (Ed.), *Packings and Stationary Phases in Chromatographic Techniques*, Dekker, New York, 1990.
- [11] H. Rotzsche, *Stationary Phases in Gas Chromatography*, Elsevier, Amsterdam, 1991.
- [12] C.F. Poole, S.K. Poole, *Chromatography Today*, Elsevier, Amsterdam, 1991.
- [13] J.A. Yancey, Liquid phases used in packed columns. Part I: polysiloxane liquid phases, *J. Chromatogr. Sci.* 23 (1985) 161–167.
- [14] J.A. Yancey, Liquid phases used in packed columns. Part II: use of liquid phases which are not polysiloxanes, *J. Chromatogr. Sci.* 23 (1985) 370–377.

- [15] E.F. Barry, R.L. Grob, *Columns for Gas Chromatography: Performance and Selection*, Wiley, New York, 2007.
- [16] C.F. Poole, R.M. Pomaville, T.A. Dean, Proposed substitution of Apolane-87 for squalane as a nonpolar reference phase in gas chromatography, *Anal. Chim. Acta* 225 (1989) 193–203.
- [17] R.M. Pomaville, C.F. Poole, Thermally stable highly-fluorinated stationary phases for gas chromatography, *Anal. Chim. Acta* 200 (1987) 151–169.
- [18] J.K. Haken, Development in polysiloxane stationary phases in gas chromatography, *J. Chromatogr.* 300 (1984) 1–77.
- [19] G. Park, C.F. Poole, Solvation in weak complexing n-octyl phthalate and n-octyl tetrachlorophthalate solvents by gas chromatography, *J. Chromatogr. A* 726 (1966) 141–151.
- [20] R.F. Koupps, R.S. Henly, Characteristics of EGS and DEGS polyesters in packed GC columns, *J. Chromatogr. Sci.* 12 (1974) 127–130.
- [21] C.F. Poole, K.G. Furton, B.R. Kersten, Liquid organic salt phases for gas chromatography, *J. Chromatogr. Sci.* 24 (1986) 400–409.
- [22] C.F. Poole, S.K. Poole, Ionic liquids as stationary phases for gas chromatography, *J. Sep. Sci.* 34 (2011) 888–900.
- [23] Z. Witkiewicz, J. Oszezudowski, M. Repelewicz, Liquid-crystalline stationary phases for gas chromatography, *J. Chromatogr. A* 1062 (2005) 155–174.
- [24] G.J. Price, The use and properties of mixed stationary phases in gas chromatography, *Adv. Chromatogr.* 28 (1989) 113–163.
- [25] J.H. Purnell, Window analysis: an approach to total optimization in chromatography, in: F. Bruner (Ed.), *The Science of Chromatography*, Elsevier, Amsterdam, 1985, pp. 363–379.
- [26] D.M. Ottenstein, Column support material for use in gas chromatography, *J. Chromatogr. Sci.* 25 (1987) 536–546.
- [27] J.F. Paltraman, E.A. Walker, Techniques in gas chromatography part 1. Choice of solid supports, *Analyst* 92 (1967) 71–82.
- [28] A. Zlatkis, V. Pretorius (Eds.), *Preparative Gas Chromatography*, Marcel Dekker, New York, 1971.
- [29] C.F. Poole, S.K. Poole, Characterization of the solvent properties of gas chromatographic liquid phases, *Chem. Rev.* 89 (1989) 377–395.
- [30] B.R. Kersten, C.F. Poole, K.G. Furton, Ambiguities in the determination of McReynolds stationary phase constants, *J. Chromatogr.* 411 (1987) 43–59.
- [31] C.F. Poole, T.O. Kollie, S.K. Poole, Recent advances in solvation models for stationary phase characterization and the prediction of retention in gas chromatography, *Chromatographia* 34 (1992) 281–302.
- [32] M.H. Abraham, C.F. Poole, S.K. Poole, Classification of stationary phases and other materials by gas chromatography, *J. Chromatogr. A* 842 (1999) 79–114.
- [33] S.K. Poole, T.O. Kollie, C.F. Poole, The influence of temperature on the mechanism by which compounds are retained in gas-liquid chromatography, *J. Chromatogr. A* 664 (1994) 229–251.
- [34] Q. Li, C.F. Poole, Influence of interfacial adsorption on the system constants of the solvation parameter model in gas-liquid chromatography, *Chromatographia* 52 (2000) 639–647.
- [35] J.R. Condon, C.L. Young, *Physicochemical Measurements by Gas Chromatography*, Wiley, Chichester, 1979.
- [36] R.N. Nikolov, Identification and evaluation of retention mechanisms in gas-liquid chromatographic systems, *J. Chromatogr.* 241 (1982) 237–256.
- [37] C.F. Poole, S.K. Poole, Foundations of retention in partition chromatography, *J. Chromatogr. A* 1216 (2009) 1530–1550.
- [38] B.R. Kersten, C.F. Poole, The influence of concurrent retention mechanisms on the determination of stationary phase selectivity in gas chromatography, *J. Chromatogr.* 399 (1987) 1–31.
- [39] R.C. Castells, Determination of gas-liquid partition coefficients by gas chromatography, *J. Chromatogr.* 1037 (2004) 223–231.
- [40] J.C. Giddings, *Dynamics of Chromatography – Part 1*, Marcel Dekker, New York, 1965.
- [41] E. Grushka, L.R. Snyder, J.H. Knox, Advances in band spreading theories, *J. Chromatogr. Sci.* 13 (1975) 25–37.
- [42] J.H. Knox, Band spreading in chromatography: a personal view, *Adv. Chromatogr.* 38 (1998) 1–49.
- [43] G. Guiochon, C.L. Guillemin, *Quantitative Gas Chromatography for Laboratory Analyses and On-Line Process Control*, Elsevier, Amsterdam, 1988.
- [44] S.J. Hawkes, Modernization of the van Deemter equation for chromatographic zone dispersion, *J. Chem. Educ.* 60 (1983) 393–398.
- [45] P. Thumneum, S. Hawkes, The obstruction factor γ in gas chromatography, *J. Chromatogr. Sci.* 14 (1981) 576–578.
- [46] C.J. Cowper, A.J. DeRose, *The Analysis of Gases by Chromatography*, Pergamon Press, Oxford, 1983.
- [47] L. Henrich, Recent advances in adsorption chromatography for analysis of light hydrocarbons in petrochemical-related materials, *J. Chromatogr. Sci.* 26 (1988) 198–203.

- [48] J.J. Cai, Y.L. Xing, M.L. Yang, X.B. Zhao, Preparation of modified gamma-alumina as stationary phase in gas-solid chromatography and its separation performance for hydrogen isotopes, *Adsorption* 19 (2013) 919–927.
- [49] J. Roles, G. Guiochon, Determination of the surface energy distribution using adsorption-isotherm data obtained by gas-solid chromatography, *J. Phys. Chem.* 95 (1991) 4098–4109.
- [50] F. Roubani-Kalantzopoulou, Determination of isotherms by gas-solid chromatography applications, *J. Chromatogr. A* 1037 (2004) 191–221.
- [51] V.G. Berezkin, I.V. Malyukova, The influence of the carrier gas on the retention parameters and height equivalent to the theoretical plate in gas–solid chromatography, *Russ. Chem. Rev.* 67 (1998) 761–781.
- [52] W.K. Al-Thamir, J.H. Purnell, R.J. Laub, Enhancement of gas–solid chromatographic column performance by inert solid dilution, *J. Chromatogr.* 188 (1980) 79–88.
- [53] K. Naito, M. Endo, S. Moriguchi, S. Takei, Characterization of modified alumina as an adsorbent for gas–solid chromatography, *J. Chromatogr.* 253 (1982) 205–215.
- [54] H. Grajek, Rediscovering the problem of interpretation of chromatographically determined enthalpy and entropy of adsorption of different adsorbates on carbon materials. Critical appraisal of literature data, *J. Chromatogr. A* 1145 (2007) 1–50.
- [55] T.G. Andronikashvili, V.G. Berezkin, N.A. Nadiradze, L.Y. Laperashvili, Increased effectiveness of chromatographic columns packed with zeolites in the separation of mixtures of some organic compounds, *J. Chromatogr.* 365 (1986) 269–277.
- [56] R. Arshady, Beaded polymer supports and gels. 1 manufacturing techniques, *J. Chromatogr.* 586 (1991) 181–197.
- [57] G. Castello, G. D’Amato, Effect of solute polarity on the performance of Porapak type porous polymers, *Chromatographia* 23 (1987) 839–843.

Column classification and structure-retention relationships

Colin F. Poole

Department of Chemistry, Wayne State University, Detroit, MI, United States

6.1 Introduction

A simplified blueprint for developing a separation method starts with the principle that the minimum resolution required for the most difficult to separate peak pair in a mixture establishes the difficulty of obtaining a separation and the time required to elute the last peak in the sample under the conditions established by the first criteria fixes the separation time. Peak widths and separation speed are mainly controlled by kinetic parameters while the capability of the stationary phase to differentiate between two compounds (selectivity) is a thermodynamic function. To a large degree, the two contributions to the separation can be treated independently and optimized separately, facilitating different approaches to a partial or complete optimization of a separation. The gas phase is close to ideal for typical separation conditions and selectivity can be considered a property of the stationary phase and column temperature alone.

For any column, resolution is impossible without selectivity or retention. Thus, all separations require a separation factor $\alpha > 1$ and a retention factor $k > 0$. Small changes in the separation factor and retention factor from their minimum values have a significant impact on resolution and the ease of obtaining a useful separation (required plate number, N_{req}) (Table 6.1) [1]. In choosing a separation system, the system with the highest separation factor will facilitate faster separations. The effect of the plate number on a separation is the most predictable separation parameter and can assume a wide range of values in gas chromatography. Its variation by changing the characteristic column dimensions allows many separations to be achieved for moderately complex mixtures under conditions where the separation factor and retention factor are far from optimum. Increasing the column length increases resolution only by the square root of the column length, while the increase in the separation time is proportional to the column

TABLE 6.1 Plate count required for a peak resolution of 1 for different separation conditions.

Retention factor	Separation factor	N_{req}	Retention factor	Separation factor	N_{req}
3	1.005	1,150,000	0.1	1.05	853,780
3	1.01	290,000	0.2	1.05	254,020
3	1.02	74,000	0.5	1.05	63,500
3	1.05	12,500	1.0	1.05	28,200
3	1.10	3,400	2.0	1.05	15,800
3	1.20	1,020	5.0	1.05	10,160
3	1.50	260	10	1.05	8,540
3	2.00	110	20	1.05	7,780

length. The maximum column length is ultimately determined by the available column inlet pressure, which increases with the column length. A better strategy to increase the plate number is to reduce the column radius at a fixed column length (Table 6.2) [2]. For the same stationary phase and temperature, observed retention factors are dependent on the column phase ratio (for a partition system the ratio of the volume of gas phase to stationary phase in the column). Thick-film columns, which have a low phase ratio, have a lower intrinsic efficiency (a result of additional band broadening resulting from slow mass transfer in the stationary phase), but thick-film columns then provide greater

resolution of volatile compounds through optimization of the retention factor range. Thick-film columns also facilitate the separation of volatile compounds at more convenient temperatures. The opposite argument applies to compounds of low volatility and provides the rationale for the manufacture of columns containing the same stationary phase with different phase ratios.

Nearly all separations in gas–liquid chromatography are achieved with hydrogen, helium, or nitrogen as the carrier gas. Although the choice of carrier gas does not significantly affect the separation factor for typical isothermal separation conditions, it can still affect resolution

TABLE 6.2 Characteristic properties of some representative open-tubular columns.

Length (m)	Internal diameter (mm)	Film thickness (μm)	Phase ratio	H_{min} (mm)	Column plates number	Plate per meter
30	0.10	0.10	249	0.06	480,000	16,000
30	0.10	0.25	99	0.08	368,550	12,285
30	0.25	0.25	249	0.16	192,000	6,400
30	0.32	0.32	249	0.20	150,000	5,000
30	0.32	0.50	159	0.23	131,330	4,380
30	0.32	1.00	79	0.29	102,080	3,400
30	0.32	5.00	15	0.44	68,970	2,300
30	0.53	1.00	132	0.43	70,420	2,340
30	0.53	5.00	26	0.68	43,940	1,470

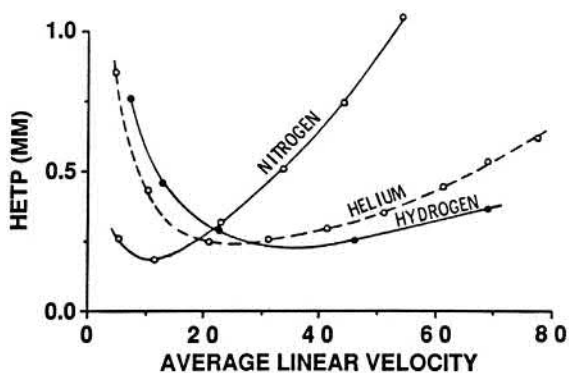


FIGURE 6.1 Plot of the column plate height against the mobile phase velocity (van Deemter plot) for a thin-film column with different carrier gases. From Ref. C.F. Poole, *The essence of chromatography*, Elsevier, Amsterdam, 2003; copyright Elsevier.

through its effect on efficiency and the optimum mobile-phase velocity for the separation. Differences in gas-phase diffusion coefficients favor the choice of hydrogen and helium for separations on thin-film columns at mobile-phase velocities at or above the optimum value for the column (Fig. 6.1). In addition, the value for the optimum mobile-phase velocity moves to higher values for gases of higher diffusivity favoring faster separations without loss of resolution. For thick-film columns ($>0.5 \mu\text{m}$), slow diffusion in the stationary phase makes a significant contribution to band broadening compared with mass transfer in the mobile phase. Thick-film columns should be operated close to the optimum velocity, with the choice of carrier gas being less significant and nitrogen often selected because of cost and/or safety considerations.

6.2 Stationary-phase classification

Numerous methods have been described to rank columns in terms of a single-value scale based on polarity (solvent strength) or multiple-value scales based on selectivity [3–7]. Qualitatively polarity is well understood, but since no

compound is uniquely polar and might be used to probe the polarity of other substances, it lacks a suitable operational scale. Indirect measurements of polarity such as those scales related one way or another to the reluctance of a polar stationary phase to dissolve a methylene group can only determine the cohesion of the stationary phase and its capability for dispersion interactions. In addition, column rankings based on polarity are less informative for column selection than multiple parameter selectivity scales [4,5,8]. The selectivity of a stationary phase is defined as its relative capability to participate in individual intermolecular interactions, such as dispersion, orientation, induction, and hydrogen bonding. Early attempts to define multiparameter selectivity scales were based on the system of phase constants introduced by Rohrschneider and subsequently modified and applied to a large number of stationary phases by McReynolds [9–11], solvent selectivity triangles [12], Hawke's polarity indices [13], solubility parameters [14], free energy or entropy scales for the solvation of prototypical compounds [15–17], and Abraham's solvation parameter model [4,18,19]. These approaches are compared elsewhere [4,5,8,9,17]. Only the system of Rohrschneider/McReynolds phase constants and the system constants derived from the solvation parameter model are important today.

The Rohrschneider/McReynolds system of phase constants is founded on the assumption that intermolecular interactions are additive, and their individual contribution to retention can be evaluated from the difference in isothermal retention index values for a series of prototypical compounds on the stationary phase to be classified and on squalane, adopted as a nonpolar reference phase, with all measurements at a standard temperature of 120°C . The phase constants (retention index differences) for five prototypical compounds (Rohrschneider) or 10 compounds (McReynolds) were used to compare the contribution of different solute interactions for each stationary phase.

This approach was abandoned after many years of use because of a number of practical and fundamental problems [20]. Two issues of particular note are the difficulty of identifying prototypical compounds to represent singular interactions and the demonstration that the retention index differences are composite terms that depend mainly on the choice of standard substances used to determine the retention index values rather than the capability of the prototypical compounds to interact with the stationary phase.

6.2.1 Solvation parameter model

The solvation parameter model is a fundamental model based on the parameterization of the cavity model of solvation for the transfer of neutral compounds from a gas phase, in which intermolecular interactions are absent (ideal gas assumption), to a condensed phase requiring formation of a solute-sized cavity (disruption of solvent–solvent interactions) accompanied by the formation of solute–solvent (stationary phase) interactions that depend on the complementary properties of the solute and the stationary phase [1,4,18,19,21]. Cavity formation is an endoergic process that opposes transfer from the gas phase and is expected to be less favorable for polar stationary phases due to stronger solvent–solvent interactions. The strength of solute–solvent interactions favors transfer of the solute from the gas phase and must exceed the free energy required for cavity formation. Retention in gas–liquid chromatography, therefore, will depend on the cohesive energy of the stationary phase, represented by the free energy required for cavity formation, the formation of additional dispersion interactions of a solute–solvent type, and on solute–solvent interactions that depend on the complementary character of the polar properties of the solute and the stationary phase. The appropriate form of the solvation

parameter model for retention in gas–liquid chromatography is set out as follows: Eq. (6.1)

$$\log K = c + eE + sS + aA + bB + lL \quad (6.1)$$

The gas–liquid partition coefficient, K , is the relevant free energy parameter for modeling retention but is not as easily determined as the retention factor, k . The two terms are connected through the phase ratio, β , by the relationship $K = k\beta$. When the retention factor is used in Eq. (6.1), the phase ratio is subsumed by the model intercept term, c , which is a system and statistical property with no other physical meaning. The upper case letters in Eq. (6.1) are the descriptors that encode solute properties, and the lower case letters in italics are system constants that encode the complementary properties of the stationary phase. The specific interactions are identified as follows: eE is the contribution from electron lone-pair interactions that occur between polarizable molecules; sS is the contribution from interactions of a dipole type that occur between molecules with a permanent dipole moment and/or with polarizable molecules due to interactions between a permanent dipole and an induced dipole; and the aA and bB terms represent the contributions of hydrogen bonding with the solute behaving as either a hydrogen-bond acid, A descriptor, or a hydrogen-bond base, B descriptor. Since a solute hydrogen-bond acid will interact with a solvent hydrogen-bond base, the a system constant is a measure of the hydrogen-bond basicity of the stationary phase, and in the same way, the b system constant is a measure of the hydrogen-bond acidity of the stationary phase. The lL term is a measure of the opposing contributions of cavity formation and dispersion interactions to the retention process. The sign of the lL term (positive or negative) provides an indication of the relative importance of cavity formation (breaking solvent–solvent interactions) and dispersion interactions (formation of solute–solvent dispersion interactions).

To characterize the selectivity of a stationary phase, that is to calculate the values of the system constants in Eq. (6.1), requires the experimental determination of the retention factors at a constant temperature for a varied group of compounds with known descriptor values. Several descriptor databases for a large number of compounds are available [22–25] as well as commercial [26] and free-to-access internet resources [27]. The descriptors used in this chapter are from the WSU experimental descriptor database [25]. For each column and temperature, a sufficient number of solutes are required to provide statistically meaningful values for the system constants and to explore a wide-enough descriptor space for the models to have useful predictive properties. The descriptor values for a collection of compounds with acceptable retention properties for convenient measurement must also have low cross-correlation to facilitate extraction of the true system constants by multiple linear regression analysis. The aforementioned criteria are met by using different compounds to characterize columns of different selectivity and/or evaluated at different temperatures. This allows all column types to be

classified at any temperature and is more flexible than methods that employ a group of prototypical compounds to define each interaction. A brief description of the methods used to determine descriptors is given in Table 6.3.

6.2.2 System constants database for open-tubular columns

The system constants fully describe all stationary-phase interactions and provide a logical basis for stationary-phase classification. System constants databases at 20°C intervals over the temperature range 60–140°C for 52 open-tubular columns [28], from 160 to 240°C for 14 open-tubular columns [29–31], to higher temperatures for nine open-tubular columns [32], and for the full temperature operating range for four ionic liquid stationary phases [33–36] are available. These databases facilitate the comparison of the separation properties of different stationary phases, afford a link between chromatographic selectivity and monomer composition for polymeric stationary phases, and enable the identification of selectivity-

TABLE 6.3 Solute descriptors used in the solvation parameter model and methods for their determination [22–25].

Descriptor	Method of determination
E	Excess molar refraction ($\text{cm}^3\text{mol}^{-1}/10$). For liquids, it can be calculated from the refractive index and characteristic volume. For solids, computer-estimated values for the refractive index can be used. For solids may be determined together with the other descriptors using chromatographic methods.
S	Dipolarity/polarizability descriptor usually determined by experiment. Initially estimated by gas chromatography on polar stationary phases but more commonly by liquid–liquid partition together with chromatographic methods today.
A	The effective or summation hydrogen-bond acidity descriptor. Originally determined from complexation constants in inert solvents for monofunctional hydrogen-bond acids and bases. The effective values broadened to allow for multiple solute–solvent interactions. They are commonly determined by liquid–liquid partition and chromatographic measurements today.
B	The effective or hydrogen-bond basicity descriptor. Determined as described for the A descriptor.
L	The gas–liquid partition coefficient for the solute on n-hexadecane at 298 K. For volatile compounds, it can be determined directly. For compounds of low volatility, it is determined by back calculation from gas chromatographic retention measurements on nonpolar stationary phases.

equivalent stationary phases with different or unknown stationary phase compositions. In addition, the databases can be used to assist in column selection and identification of initial separation conditions for method development. The columns included in the system constants database and their declared stationary phase compositions are summarized in Table 6.4.

Most stationary phases possess some capacity for electron lone-pair interactions (*e* system constant), but selectivity for these interactions is

rather limited except for fluorine-containing (PMTS) and poly(ethylene glycols) (PEG) stationary phases. None of the poly(siloxane) and poly(ethylene glycol) stationary phases are hydrogen-bond acids (*b* system constant is zero) [37]. Only the ionic liquid stationary phases in the database have significant hydrogen-bond acidity [38,39]. In practice, the important considerations for selectivity optimization for poly(siloxane) and poly(ethylene glycol) stationary phases are differences in cohesion/dispersion

TABLE 6.4 Stationary-phase chemistries and column identities for the system constants database.

Column	Type	Identity
PDMSO	Poly(dimethylsiloxane)	DB-1, SolGel-1
PMOSO	Poly(methyloctylsiloxane)	SPB-Octyl
PMPS-5	Poly(dimethyldiphenylsiloxane) 5% diphenylsiloxane monomer	HP-5, DB-5, OV-5, SPB-5, PTE-5
PMPS-20	20% diphenylsiloxane monomer	Rtx-20
PMPS-35	35% diphenylsiloxane monomer	DB-35
PMPS-50	50% diphenylsiloxane monomer	Rxi-17
PMPS-65	65% diphenylsiloxane monomer	Rtx-65
PMPS	Poly(methylphenylsiloxane)	Rtx-50, Rxi-50, HP-50 ⁺
SASO-5	Silarylene–siloxane and similar copolymers 5% 1,4-bis(dimethylsiloxane)phenylene	DB-5ms, ZB-5ms, Rxi-5Sil MS, HP-5TA
SASO-35	35% 1,4-bis(dimethylsiloxane)phenylene	DB-35ms
SASO-50	50% 1,4-bis(dimethylsiloxane)phenylene	DB-17ms
CBSO-5	Carborane–siloxane copolymer 5% phenyl	Stx-500
PMTS-35	Poly(dimethylmethyltrifluoropropylsiloxane) 35% methyltrifluoropropylsiloxane	DB-200
PMTS-50	Poly(methyltrifluoropropylsiloxane)	DB-210
PCPM-06	Poly(cyanopropylphenyldimethylsiloxane) 6% cyanopropylphenylsiloxane monomer	DB-1301, DB-624
PCPM-14	14% cyanopropylphenylsiloxane monomer	DB-1701

TABLE 6.4 Stationary-phase chemistries and column identities for the system constants database.—cont'd

Column	Type	Identity
PCPM-50	50% cyanopropylphenylsiloxane monomer	DB-225
PCM-50	Poly(cyanopropylmethylsiloxane)	DB-23
PCPS	Poly(biscyanopropylsiloxane)	SP-2340
SACPS-88	Bis(cyanopropylsiloxane)- <i>co</i> -methylsilylene 88% bis(cyanopropylsiloxane) monomer	HP-88
SACPS-90	90% bis(cyanopropylsiloxane) monomer	BPX90
PEG	Poly(ethylene glycol) Modified with nitroterephthalic acid	HP-20M, HP-INNOWax, EC-Wax, AT-Wax, DB-WAXetr, SolGel-Wax DB-FFAP
PAG	Poly(ethylene glycol)- <i>co</i> -propylene oxide	PAG
Rtx-Volatiles	Application specific/proprietary structure	Rtx-Volatiles
Rtx-VGC		Rtx-VGC
DB-608		DB-608
Rtx-440		Rtx-440
Rtx-Dioxin		Rtx-Dioxin
Rtx-Dioxin2		Rtx-Dioxin2
Rtx-OPPesticide		Rtx-OPPesticides
Rtx-CLPesticides		Rtx-CLPesticides
Rtx-TNT		Rtx-TNT
Rtx-TNT2		Rtx-TNT2
DB-XLB		DB-XLB
DB-VRX		DB-VRX
SLB-IL100	1,9-Di(3-vinylimidazolium)nonane bis(trifluoromethylsulfonyl)imide	SLB-IL100
SLB-IL60	1,12-Di(tripropylphosphonium)dodecane bi(trifluoromethylsulfonyl)imide	SLB-IL60
SLB-IL61	1,12-Di(tripropylphosphonium)dodecane bis(trifluoromethylsulfonyl)imide trifluoromethanesulfonate	SLB-IL61
SLB-IL76	Tri(tripropylphosphoniumhexanamido)triethylamine bis(trifluoromethylsulfonyl)imide	SLB-IL76

properties, dipole-type interactions, and stationary-phase hydrogen-bond basicity. These intermolecular interactions are temperature dependent and differences in selectivity at one temperature are not necessarily the same as those at a different temperature. Plots of the system constants as a continuous function of temperature are called system maps and allow a straightforward evaluation of the effect of temperature on selectivity. An example of a system map is shown in Fig. 6.2 for the poly(cyanopropylphenyldimethylsiloxane) stationary phase DB-1701 [29]. The shape of the plots is an indication that polar interactions persist to quite high temperatures and also that changes in selectivity due to polar interactions are larger at lower temperatures. The additional dispersion interaction that polarizable molecules experience on account of their loosely held lone-pair electrons represented by the e system constant is the only interaction that increases retention at higher temperatures. In several cases, the sign of the e system constant is negative at low temperatures and positive at higher temperatures. Although electron lone-pair interactions are relatively more important at higher temperatures, they remain comparatively weak interactions in

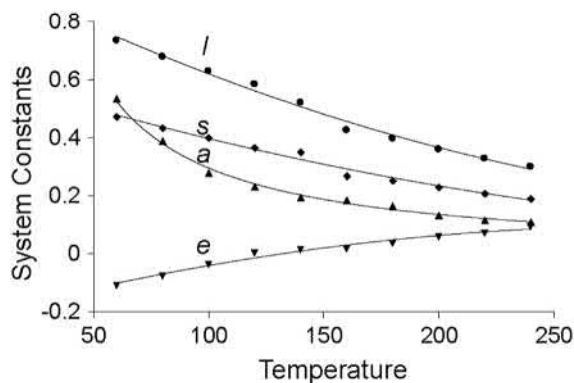


FIGURE 6.2 System map for the poly(cyanopropylphenyldimethylsiloxane) stationary phase PCPM-14. From Ref. S.N. Atapattu, C.F. Poole, *Solute descriptors for characterizing retention properties of open-tubular columns of different selectivity in gas chromatography at intermediate temperatures*, *J. Chromatogr. A* 1195 (2008) 136–145; copyright Elsevier.

most cases, only important for the separation of low polarity and polarizable molecules, such as polycyclic aromatic hydrocarbons.

The poly(dialkylsiloxane) stationary phases (PDMSO and PMOSO) are low-selectivity stationary phases characterized by low cohesion and weak polar interactions. Separations are governed mainly by dispersion interactions with good selectivity for the separation of nonpolar compounds. The PMOSO stationary phase is less dipolar and hydrogen-bond basic than the PDMSO stationary phases and as a reference point is the least selective of the stationary phases in Table 6.4. Replacing dimethylsiloxane monomers by diphenylsiloxane monomers for poly(dimethyldiphenylsiloxane) stationary phases (PMPS) results in an orderly change in the capability of the stationary phase for dipole-type interactions and in their hydrogen-bond basicity (Fig. 6.3). The changes in the system constants are approximately linear up to about 50% diphenylsiloxane monomer. Given that the cavity/dispersion term, l system constant, changes only slightly with diphenylsiloxane monomer composition, the principal

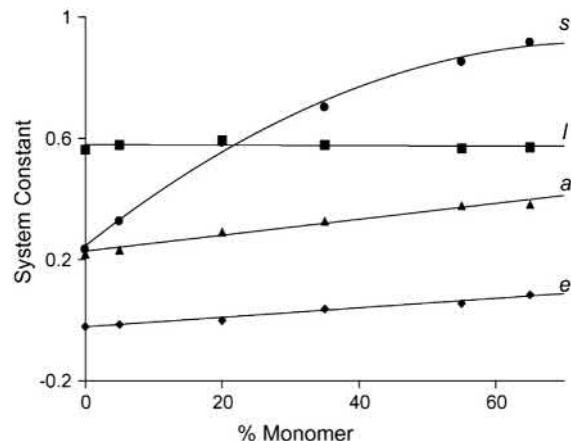


FIGURE 6.3 Plot of the system constants for the poly(dimethyldiphenylsiloxane) stationary phases as a function of the diphenylsiloxane monomer composition at 100 °C. From Ref. C.F. Poole, S.K. Poole, *Separation characteristics of wall-coated open-tubular columns for gas chromatography*, *J. Chromatogr. A* 1184 (2008) 254–280; copyright Elsevier.

selectivity difference among these phases is due to the variation in the ratio of dipole-type to hydrogen-bond base interactions [40]. There are small selectivity differences for stationary phases prepared from methylphenylsiloxane monomers compared with those prepared from dimethylsiloxane and diphenylsiloxane monomers with the same nominal composition of functional groups [31]. Stationary phases prepared from diphenylsiloxane monomers are more thermally stable and are generally preferred for most applications. The poly(dimethyldiphenylsiloxane)

stationary phases containing 5% diphenylsiloxane are the most widely used general-purpose stationary phases for gas chromatography. There are five examples of this type of stationary phase in Table 6.4. For these columns, which vary in film thickness from 0.10 to 1.50 μm , there is no selectivity dependence on film thickness. A mean value of the system constants for these columns provides a typical value for the system constants and the standard deviation an indication of their dispersion for similar columns obtained from different sources, Table 6.5 [28].

TABLE 6.5 Mean and standard deviation (SD) of the system constants for poly(dimethyldiphenylsiloxane) and silarylene–siloxane copolymers with nominal separation properties equivalent to 5% diphenylsiloxane monomer and poly(ethylene glycol) stationary phases.

Temperature ($^{\circ}\text{C}$)	<i>e</i>		<i>s</i>		<i>A</i>		<i>l</i>	
	Mean	SD	Mean	SD	Mean	SD	Mean	SD
<i>Poly(dimethyldiphenylsiloxane) PMPS-5</i>								
60	-0.100	0.009	0.421	0.014	0.393	0.010	0.702	0.005
80	-0.060	0.005	0.384	0.013	0.317	0.011	0.631	0.006
100	-0.029	0.001	0.338	0.009	0.257	0.003	0.569	0.008
120	0		0.311	0.013	0.214	0.008	0.516	0.005
140	0.019	0.004	0.288	0.010	0.187	0.001	0.471	0.001
<i>Silarylene–siloxane copolymer SASO-5</i>								
60	-0.105	0.007	0.453	0.022	0.440	0.080	0.724	0.012
80	-0.063	0.009	0.413	0.030	0.347	0.034	0.662	0.015
100	-0.024	0.007	0.370	0.025	0.284	0.024	0.608	0.023
120	0		0.345	0.021	0.236	0.020	0.556	0.024
140	0.029	0.006	0.318	0.032	0.189	0.013	0.507	0.022
140	0.241	0.014	1.218	0.043	1.727	0.057	0.426	0.021
<i>Poly(ethylene glycol) PEG</i>								
60	0.215	0.027	1.696	0.042	2.753	0.084	0.619	0.013
80	0.222	0.018	1.571	0.009	2.461	0.049	0.567	0.011
100	0.228	0.013	1.442	0.022	2.182	0.049	0.514	0.015
120	0.237	0.012	1.323	0.028	1.943	0.051	0.468	0.018
140	0.241	0.014	1.218	0.043	1.727	0.057	0.426	0.021

The indication is that slight selectivity differences exist for the columns evaluated. Inserting monomers containing stiffening groups (e.g., phenylene, carborane, diphenyl ether, etc.) into the backbone of poly(siloxane) stationary phases enhances their thermal stability by inhibiting the formation of cyclic siloxanes. These phases, designated SASO and CBSO in Table 6.4, generally have the extension ms added to the name of the nominally equivalent poly(dimethyldiphenylsiloxane) stationary phase and are designed for demanding applications where low column bleed is important. The silarylene-siloxane copolymers containing 5% 1,4-bis(dimethylsiloxane)phenylene with nominally similar separation properties to PMPS-5 columns are not selectivity equivalent, Table 6.5, and show greater variation by source. The DB-XLB stationary phase has an undisclosed composition but is said to have similar separation properties to PMPS-5 stationary phases. Selectivity equivalence can be evaluated by a correlation plot of the system constants for the two column types as a function of temperature. For two columns to be selectivity equivalent, the system constants will be aligned on the diagonal line with a slope of 1 and an intercept of 0, Fig. 6.4.

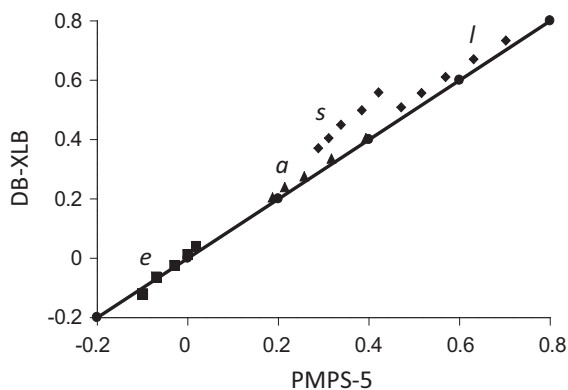


FIGURE 6.4 Correlation plot of the system constants for a typical PMPS-5 and DB-XLB columns over the temperature range 60–140°C. The diagonal represents the plot line for selectivity equivalent columns. The displaced points for the *s* system constant indicate that the DB-XLB column is more dipolar/polarizable than a typical PMPS-5 column.

As Fig. 6.4 demonstrates, the DB-XLB column is significantly more dipolar/polarizable (larger *s* system constant) than a typical PMPS-5 column. This is also the case for carborane-siloxane column CBSO-5, which has similar separation properties to the PMPS-5 stationary phases but is not selectivity equivalent.

The incorporation of 3,3,3-trifluoropropylmethylsiloxane monomers into a poly(dimethylsiloxane) stationary phase results in characteristic changes in selectivity. These stationary phases are significantly more dipolar/polarizable and weaker hydrogen-bond bases than the poly(dimethyldiphenylsiloxane) stationary phases with a similar concentration of polar monomer groups. In addition, electron lone-pair interactions are important and repulsive compared with the poly(dimethyldiphenylsiloxanes).

The incorporation of 3-cyanopropylphenylsiloxane and 3-cyanopropylmethylsiloxane monomers into a poly(dimethylsiloxane) stationary phase, PCPM, PCM, and SACPS in Table 6.4, results in significant changes in selectivity with those stationary phases containing a high incorporation of polar monomer being among the most polar of the stationary phases in Table 6.4. They are cohesive and strongly dipolar/polarizable and hydrogen-bond basic. They have different selectivity to the PMTS stationary phases with a similar incorporation of polar monomer. For the PCPM and PCM stationary phases, the *s/a* system constant ratio is close to 1 and significantly smaller for the PMTS stationary phases. In addition, electron lone-pair interactions are weak for the PCPM and PCM stationary phases but more significant for the PMTS stationary phases. The selectivity of the PCPM and PCM columns are complementary to the PMTS columns as illustrated by the correlation plot for the system constants for PCM-50 and PMTS-50 in Fig. 6.5. The construction of a single line passing through all system constants is impossible in this case and the dispersion of the slopes for individual system constants is a measure of the multiple differences in selectivity and their different temperature dependence. The PCPM and SACPS stationary

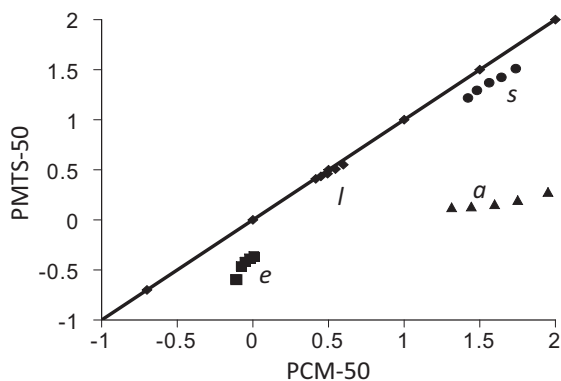


FIGURE 6.5 Correlation plot of the system constants for typical PCM-50 and PMTS-50 columns over the temperature range 60–140°C. The diagonal line represents the hypothetical result if the two columns were selectivity equivalent. The dispersion of the points from this line indicates the extent of selectivity differences and their temperature dependence.

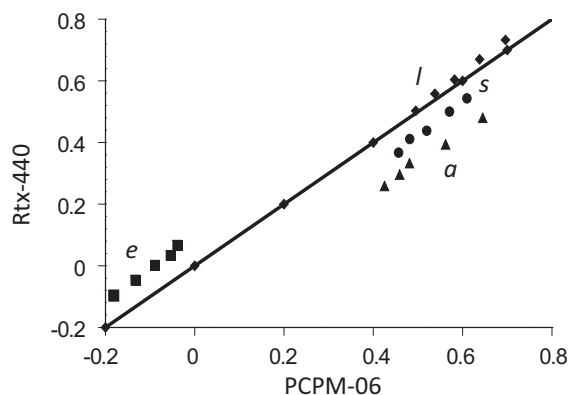


FIGURE 6.6 Correlation plot of the system constants for Rtx-440 and a typical PCPM-06 column over the temperature range 60–140°C. The diagonal line represents the hypothetical result for selectivity equivalent columns. The significant displacement of the *a* system constant from the diagonal indicates the characteristic difference for these columns for the separation of compounds that are strong hydrogen-bond acids.

phases with a high incorporation of polar monomer are among the most cohesive stationary phases in common use with small *l* system constants resulting in low methylene group selectivity. The composition of the Rtx-440 stationary phase is undisclosed but has separation properties similar to PCPM-6 columns for compounds that are weak hydrogen-bond acids, Fig. 6.6. Compounds that are strong hydrogen-bond acids are selectively displaced to shorter retention times on the Rtx-440 column due to the characteristically smaller *a* system constants [41].

Poly(ethylene glycol) stationary phases are more hydrogen-bond basic and nearly as dipolar/polarizable as the SACPS stationary phases in Table 6.4. In addition, they are generally less cohesive, and electron lone-pair interactions, while weak, are more important and of opposite sign. The methods used to stabilize PEG stationary phases employ different chemistries, but the variation in separation properties for all column types in this group is quite small, Table 6.5. Incorporation of propylene oxide into the polymer backbone, PAG column, results in small changes in selectivity. The PAG column is slightly less dipolar/polarizable, cohesive,

and electron lone-pair attractive compared with the PEG stationary phases. It is expected to provide greater separation of members of a homologous series than PEG but poorer separations of compounds that differ mainly in their dipolarity or polarizability.

A notable feature of the ionic liquid stationary phases is their significant hydrogen-bond acidity, a property absent for typical poly(siloxane) and poly(ethylene glycol) stationary phases. Since with the exception of the n-alkanes most other compounds are hydrogen-bond bases to varying extents, this is a significant difference in selectivity. For the other system constants, there is significant overlap between the ionic liquid and conventional polar stationary phases, Table 6.6. Early studies on packed columns demonstrated a connection between the properties of the anion and selectivity for ionic liquids [38]. The limited selection of anions for the commercially available columns, either bis(trifluoromethylsulfonyl)imide or trifluoromethanesulfonate, probably explains some of the dampening of selectivity differences compared

TABLE 6.6 Representative system constants for ionic liquid and polar stationary phases at 120°C.

Column type	System constants				
	<i>e</i>	<i>S</i>	<i>a</i>	<i>b</i>	<i>l</i>
SLB-IL100	0	1.783	1.362	0.528	0.342
SLB-IL76	0.165	1.522	1.584	0.272	0.367
SLB-IL61	0.043	1.446	1.504	0.242	0.407
SLB-IL60	-0.039	1.463	1.157	0.349	0.408
SACPS-90	0.086	1.954	1.816	0	0.387
SACPS-88	0.069	1.716	1.695	0	0.412
PEG	0.237	1.323	1.943	0	0.468
PCM-50	-0.018	1.486	1.444	0	0.450
PCPM-50	-0.017	1.175	1.116	0	0.450
PMTS-50	-0.391	1.287	0.133	0	0.434
PMPS-50	0.117	0.780	0.339	0	0.547

with the broader possibilities for ionic liquids in general [39,42]. A further advantage of the ionic liquids is their higher-temperature operating limits compared with conventional polar stationary phases.

A number of application-specific columns are included in Table 6.4. The stationary-phase compositions for these columns are not generally disclosed, but in several cases can be inferred from a comparison of their system constants with the stationary phases of known composition in the database and confirmed by comparison of retention factors for varied compounds on the stationary phases identified as (near) selectivity equivalent. The proprietary stationary phases identified in this way are summarized in Table 6.7. Several application-specific columns are prepared from stationary phases with conventional compositions and optimized for the specified separation by appropriate selection of the column dimensions and phase ratio. In a

TABLE 6.7 Common application-specific columns and their stationary phase characteristics.

Column identification	Selectivity-equivalent stationary phase
DB-XLB	No selectivity equivalent stationary phase in the database
DB-VRX	PMPS-5
Rtx-Volatiles	PMPS containing about 16% diphenylsiloxane monomer
Rtx-VGC	No selectivity equivalent stationary phase in the database
DB-608	PMPS-50
Rtx-440	No selectivity equivalent stationary phase in the database
Rtx-Dioxin	CBSO-5
Rtx-Dioxin2	Similar to SASO-XLB
Rtx-OPPesticides	Similar to PMTS-35
Rtx-CLPesticides	Similar to PMTS containing between 25% and 30% polar monomer
Rtx-TNT	PMPS-5
Rtx-TNT2	Rtx-OPPesticides

few cases, for example, Rtx-Volatiles, common polymers are used but with a monomer composition that is different to conventional columns. The Rtx-CLPesticides and Rtx-OPPesticides columns have no direct match with the stationary phases in the database. However, the relatively large negative e system constant and characteristic s/a ratio indicate a family resemblance to the PMTS stationary phases. One possibility is that these stationary phases contain additional monomers to the PMTS stationary phases to achieve the extended temperature stability characteristics. These columns might be useful for

other applications as they extend the range of monomer compositions for PMTS stationary phases.

6.2.3 Classification of stationary phases

Principal component analysis of the system constants provides a useful tool to visualize how individual columns occupy the selectivity space, Fig. 6.7. The columns are grouped on the plot according to their monomer chemistry with several columns behaving independently. SPB-Octyl has no close neighbors and is located

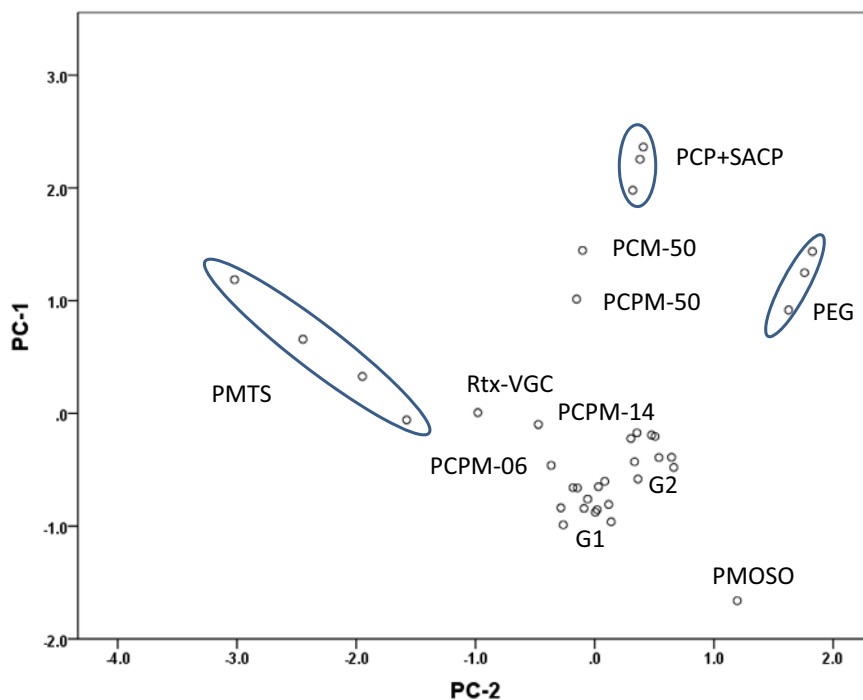


FIGURE 6.7 Score plot for principal component factor analysis (varimax rotation) of the system constants for the temperature range 60–140°C for the nonionic stationary phases in Table 6.4. To simplify the plot, all entries for near selectivity equivalent columns were replaced by a single entry. The first two principal components account for 94.1% of the variance (PC-1 = 63.6% and PC-2 = 30.5%). PC-1 is dominated by variation of the s , a , and l system constants and (PC-2) the e and a system constants. The G1 cluster contains all PDMSO, PMPS stationary phases up to 20% diphenylsiloxane monomer, SASO stationary phases with up to 5% phenyl, CBSO-5, DB-Dioxin, DB-Dioxin2, DB-VRX, DB-XLB, Rtx-Volatiles, and Rtx-440. The group G2 contains PMPS and SASO stationary phases with >20% diphenylsiloxane monomer or equivalent substituents and DB-608.

at the bottom right-hand corner of the plot signaling its low selectivity for polar interactions. The PCPM-06, PCPM-14, PCPM-50, PCM-50, and Rtx-Volatiles columns are located in the central region of the plot representing different blends of selectivity to one another and the other columns in the database. These columns need to be considered individually for selectivity optimization with their position on the plot indicating how they might be used to extend the selectivity of the columns that can be clustered. The PMTS, PCPS and SACPS, and PEG columns are grouped as three separate clusters near the edges of the plot with distinct selectivity characteristics that separate them from the other columns in the database. Note that the Rtx-OPPesticides and Rtx-CLPesticides are clustered in the same group as the PMTS columns and extend the selectivity space enclosed by this cluster. The largest cluster labeled G1 contains the PDMSO, PMPS and SASO stationary phases containing 20% or less diphenylsiloxane monomer or its equivalent, DB-Dioxin, DB-Dioxin2, DB-VRX, DB-XLB, Rtx-Volatiles, and Rtx-440. This large group of 13 column types populates a small area of the selectivity space with few selectivity equivalent stationary phases. Within this cluster there are many possible choices for columns providing a small selectivity difference for a specific separation. The second largest cluster G2 of nine columns contains the PMPS and SASO stationary phases containing more than 20% diphenylsiloxane monomer or equivalent. These are well separated from the columns clustered in G1 but only facilitate relatively small changes in selectivity with few columns indicated as selectivity equivalent. The outstanding feature of Fig. 6.7 is how much of the selectivity space remains empty affording considerable scope for the development of new stationary phases that allow access to the unoccupied regions of the selectivity space.

The selectivity of the ionic liquid stationary phases can be compared with the polar nonionic stationary phases, Fig. 6.8. The ionic liquids

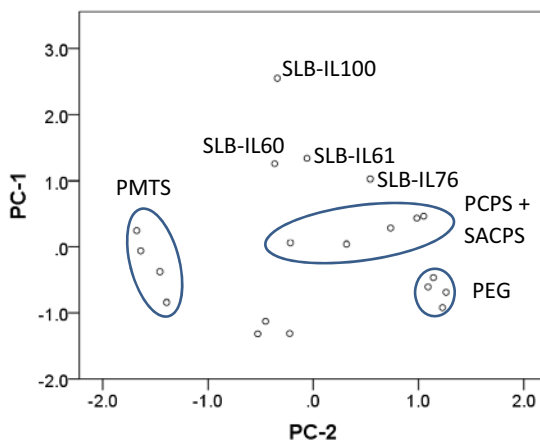


FIGURE 6.8 Score plot for principal component factor analysis (varimax rotation) of the system constants at 140°C for selected polar and ionic liquid stationary phases from Table 6.4. The first two principal components account for 83.2% of the variance (PC-1 = 54.7% and PC-2 = 28.5%). PC-1 is dominated by the variation of l and b system constants and PC-2 by e and a ; s is loaded almost equally on PC-1 and PC-2. See Table 6.4 for column identification.

occupy an otherwise empty region of the selectivity space indicating their complementary separation properties to the polar nonionic stationary phases. Also, the four ionic liquid columns are not clustered into a focused group indicating that they are not selectivity equivalent. The ionic liquid SLB-IL76 is the closest member of these stationary phases to the nonionic stationary phases with properties similar to SACPS-88, but is not selectivity equivalent to the PCPM, PCM, and SACPS stationary phases. The SLB-76 is slightly more cohesive, less dipolar/polarizable, and a weaker hydrogen-bond base than SACPS-88, whereas SLB-IL76 is a weak hydrogen-bond acid, while SACPS-88 has no hydrogen-bond acidity.

A general strategy for method development is to select the minimum number of stationary phases from different selectivity groups that span the selectivity space as evenly as possible (Table 6.8). After trial separations on each column, the region of the selectivity space most useful for the separation can be identified. Further

TABLE 6.8 System constants for columns selected from different selectivity groups at 100°C ($b = 0$ for all column types).

Column type	% Polar monomer	System constants			
		e	s	a	l
Poly(methyloctylsiloxane)		0.185	0.069	0	0.644
Poly(dimethyldiphenylsiloxane)	5	-0.029	0.338	0.257	0.569
Poly(dimethyldiphenylsiloxane)	50	0.083	0.845	0.416	0.593
Poly(methyltrifluoropropylsiloxane)	50	-0.424	1.363	0.156	0.461
Poly(cyanopropylphenyldimethylsiloxane)	50	-0.052	1.318	1.272	0.512
Poly(biscyanopropylsiloxane)	100	0.061	1.853	1.968	0.428
Poly(ethylene glycol)	100	0.228	1.442	2.182	0.514

columns in the same selectivity space are then evaluated to optimize selectivity. In other cases, there may be a great deal of empirical information available for a separation and the decision becomes how to select the best stationary phase from a group of stationary phases considered suitable for a particular application. For example, the separation of volatile organic compounds of regulatory concern can be achieved in most cases using the columns identified in

Fig. 6.9 [43]. These columns have been classified using hierarchical cluster analysis. In choosing stationary phases for this application, the dendrogram indicates the close similarity in properties of three groups of stationary phases (DB-624 and DB-1301; HP-5 and DB-VRX; and Rtx-50 and Rtx-65). These three groups offer different selectivity and to investigate the use of one phase from each group would be more sensible as a screening tool than choosing several

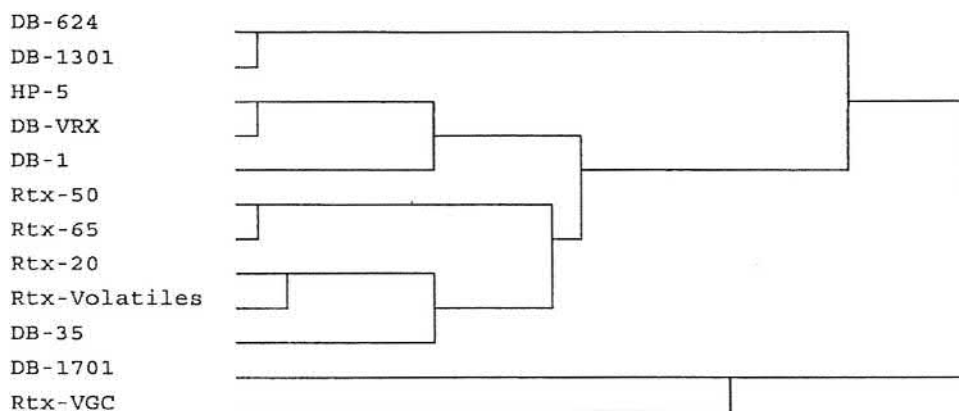


FIGURE 6.9 Dendrogram for the classification of columns for the separation of volatile organic compounds using the near-neighbor agglomeration method for columns identified in Table 6.4. Input data are the system constants for the temperature range 60–140°C. From Ref. C.F. Poole, J. Qian, W. Kiridena, C. DeKay, W.W. Koziol, *Evaluation of the separation characteristics of application specific (volatile organic compounds) open-tubular columns for gas chromatography*, *J. Chromatogr. A* 1134 (2006) 284–290; copyright Elsevier.

phases from a single group. On the other hand, DB-1, Rtx-Volatiles, DB-35, DB-1701, and Rtx-VGC are indicated as stationary phases with significant differences in selectivity and provide complementary separation characteristics for this application. The connections in the dendrogram indicate the degree of similarity and facilitate the selection of stationary phases with a small or relatively large selectivity difference. Empirical and historical information indicates that more polar stationary phases contained in the database are rarely successful for this application and the approach here is to blend established practice with a rationale approach for column selection. Similar selection dendrograms are available for fatty acid methyl esters [44] and pesticides and dioxins [45].

6.2.4 Stationary-phase selectivity tuning

The common approach to method development in gas chromatography is to choose a stationary phase (column) that provides the best separation from a group of available stationary phases. The selected column, however, is simply the best available for the fixed stationary-phase compositions sampled and not necessarily the true optimum composition for the separation. Two general approaches are available for optimizing the stationary-phase composition for a separation: coupling of two or more columns containing different stationary phases in which the residence time is varied in each column to tune the overall selectivity for a separation [46,47] and computer-assisted stationary-phase design using initial experimental data on individual stationary phases of different composition to determine thermodynamic parameters that facilitate the simulation of the separation for different possible stationary-phase compositions to identify an optimum composition for a particular separation [47,48]. The latter approach was used to develop application-specific stationary phases in Table 6.7. Neither approach,

however, is widely used in the current practice of laboratory methods. The emergence and increasing acceptance of comprehensive gas chromatography is an exception.

Comprehensive techniques employ two columns separated by a modulation interface. To achieve a useful increase in peak capacity with respect to a single column, the coupled columns should be of different selectivity. This selectivity difference is usually described in terms of “orthogonality,” but in reality stationary phases differ in the intensity of specific intermolecular interactions, and even the most different stationary phases cannot be stated to be “orthogonal” [49]. Orthogonality is also a useful concept for the selection of separation systems for conventional separations, since the inclusion of systems with the widest possible separation properties ensures adequate sampling of the available separation space. Using the system constants of the solvation parameter model, two scales were used to predict the orthogonality of a large number of stationary phases at 100°C: the Euclidean distance between stationary phases in multidimensional hyperspace (D -parameter) and the angle θ between the linear vectors calculated from the system constants arranged in five-dimensional space. A D -parameter less than about 0.5–0.8 is a good indication that the compared systems are similar in terms of their capability for intermolecular interactions. The closer $\cos \theta$ is to 1, the greater the similarity of the stationary phases. Taking the poly(methyloctylsiloxane) stationary phase as a reference point, since it has the lowest capacity for polar interactions, the orthogonality of a number of common stationary phases is summarized in Table 6.9 [49]. Stationary phases with similar solvation properties are next to each other in the table and those least like the reference stationary phase poly(methyloctylsiloxane) are located at the bottom of the table. These include the SACPS, PEG, PMTS, and ionic liquid stationary phases. The orthogonality represented by $\cos \theta$ corresponds to angles between about 70 and 80

TABLE 6.9 Orthogonality as a basis for column selection with SPB-Octyl (as reference phase) at 100°C.

Column	D-parameter	Cos θ
DB-1	0.348	0.862
PMPS-5	0.401	0.831
DB-5ms	0.436	0.810
DB-XLB	0.498	0.785
Rtx-Volatiles	0.548	0.748
Rtx-440	0.554	0.754
Rtx-20	0.622	0.711
DB-35	0.730	0.656
DB-1301	0.753	0.624
DB-35ms	0.779	0.652
DB-17ms	0.878	0.617
Rtx-50	0.882	0.589
Rtx-CLP	0.908	0.523
Rtx-65	0.937	0.576
Rtx-VGC	0.989	0.501
DB-1701	1.036	0.503
Rtx-OPP	1.103	0.432
DB-200	1.221	0.385
DB-210	1.481	0.296
DB-225	1.851	0.312
SLB-IL100	2.190	0.266
DB-23	2.256	0.266
PEG	2.629	0.258
HP-88	2.641	0.232
SP-2340	2.759	0.223
BPX90	2.787	0.217

degrees for the aforementioned stationary phases. Although orthogonality maximizes the peak capacity, it does not necessarily result in better separations unless the polarity of the

sample covers a sufficiently wide range to spread across the selectivity space. If not, large areas of the retention space remain empty. Many practical separations of complex mixtures of a narrow polarity range, therefore, will require columns with appropriate selectivity differences for the sample type, which do not necessarily correspond to the most orthogonal stationary phases available.

6.3 Structure—retention relationships

Only for the case of a single retention mechanism can a direct connection between a distribution constant and a thermodynamic understanding of solute interactions with the stationary phase be assumed for normal system properties in gas chromatography [50]. Although retention time is both simple to measure and reasonably precise, it is not directly related to the thermodynamic model of the system. For studies of retention models, either the adjusted retention time (or volume) or the retention factor (as a surrogate for the partition constant) is generally required. An accurate value for the column hold-up time (or volume) is required to calculate these terms. Methods to estimate the column hold-up time (or volume) are based on fluid dynamics (Poiseuille' law); deduced from regression models for the semilogarithmic plot of the retention factors for members of a homologous series against their carbon number; as the retention time of a minimally retained marker compound; or from the front of the solvent peak at high temperature [50,51]. Agreement among individual methods is sometimes poor and no single method has gained universal acceptance. Simplicity often dictates that the minimally retained marker compound is the most widely used approach with different compounds utilized to facilitate detector compatibility. It is necessary to have faith in the value obtained since the true value is unknown. Relative retention measurements seem

more attractive, therefore, for the development of shared user retention databases for compound identification. Also, the difficulty of precisely reproducing the system properties in different laboratories results in an unknown uncertainty so that defining a suitable acceptance window for identification purposes is not straightforward.

6.3.1 Isothermal retention index

A general problem in devising a system of relative retention in gas chromatography is that separations are performed over a wide temperature range with stationary phases of different polarity. As a consequence, no single substance can fulfill the role of a universal standard, and in those cases where the retention of the sample and standard are markedly different, accuracy would be impaired. This problem was finally solved by Kovats, who proposed the retention index scale, in which the retention of any substance is expressed with respect to the retention properties of a series of n-alkanes. Each n-alkane is assigned an index of 100 times its carbon number for any stationary phase at any column temperature. For members of a homologous series the logarithm of the adjusted retention time (or retention factor, partition constant) at a given temperature is linearly related, at least approximately to its carbon number, with the possible exception of the first few members of the homologous series. This provides the operational scale for the retention index on which the retention index of any substance is equal to 100 times the carbon number of a hypothetical n-alkane with the same adjusted retention time (retention factor, partition constant, etc.) as the substance of interest, Eq. (6.2)

$$I = 100z + 100[\log t_{R'}(x) - \log t_{R'}(z)] / [\log t_{R'}(z+1) - \log t_{R'}(z)] \quad (6.2)$$

where $t_{R'}$ is the adjusted retention time, z the carbon number of the n-alkane eluting most closely before substance (x), and $z+1$ the carbon number of the n-alkane eluting most closely after substance (x) [50,52]. On a formal basis the isothermal retention index I in Eq. (6.2) is written $I_x^{sp}(T)$ where (x) is the substance, sp the stationary phase, and T the column temperature. Variations of the Kovats retention index scale utilizing different homologous compounds as reference standards have been suggested, for example, fatty acid methyl esters, 2-alkanones, n-alkyl acetates, etc., to improve the repeatability of retention index measurements or to obtain compatibility with element or structure-selective detectors with a weak response to the n-alkanes [53]. If desired, Kovats retention indices can be recovered from these alternative scales from correlation plots of the two sets of reference standards. Numerous retention index databases are available; some for target applications (e.g., fragrance compounds, essential oils, toxicological relevant substances, etc.) while others are broadly based on the types of compounds covered. While some are maintained by individual research groups or professional organizations and usually Internet accessible others are subscription databases. A useful compilation is given in Ref. [54]. The largest is the NIST database with 387,463 records for 82,868 compounds (2014) [55]. The major use of retention index databases is as a filter for removing false-positive mass spectra for automated compound identification using library search software. Most of the available databases, but not all, are literature compilations and consequently somewhat variable in quality. This results in larger retention index acceptance windows than desirable for eliminating false-positive identifications. However, relative elution order is significantly more reliable than individual retention indices and can assist in the identification of compounds with similar mass spectra, for example, isomers. Most

databases contain data reported for only a few stationary phases, typically PDMSO, PMPS-5, and PEG, which limits the use of selectivity optimization for method development if database matching is to be used. The number of known compounds greatly exceeds the number of compounds in current databases and to overcome this limitation some software supports the prediction of retention indices using group contribution or additive schemes, largely for column types indicated earlier [54,56,57]. For compounds of low polarity on nonpolar stationary phases, biparametric models including solute boiling point combined with molar volume or topological indices are commonly used. For polar compounds and/or polar stationary phases additional experimental or theoretical descriptors are required. The effectiveness of these models seems variable and probably depends on molecular complexity, the number and position of functional groups, column polarity, and the similarity to compounds in the database with reliable retention index values. The solvation parameter model has also been used to predict retention factors ($\log k$) from the structure of candidate compounds for nontarget compound analysis [58].

Sources of error in determining retention indices are due to typical system fluctuations (temperature and flow rate), nonideal behavior of the carrier gas, uncertainty in the physical dimensions of the column, the estimation of the column hold-up time, sample size effects, and variations caused by interfacial adsorption and matrix modification of the stationary phase [50,59,60]. For shared databases, temperature variation (differences in set point temperature and oven temperature gradients for different instruments) and matrix modification of the stationary phase (column history) are likely the main sources of variation. Mixed retention mechanisms are an important contribution for polar stationary phases. For compounds of low solubility in polar stationary phases, such as the n-alkanes, adsorption at the gas–liquid

interface can be an important retention mechanism. Both molecular dynamic simulations [61] and experimental results for poly(ethylene glycol) [62], poly(cyanopropylsiloxane) [28], and ionic liquids [63,64] stationary phases point to interfacial adsorption as a component of the general retention mechanism. The impact of a mixed retention mechanism on the interpretation of McReynolds phase constants for stationary phase classification was discussed in Section 6.2.

6.3.2 Temperature-programmed retention and retention indices

For mixtures that span a wide boiling point range (e.g., $>100^{\circ}\text{C}$), isothermal separations are characterized by long separation times, poor separations of early-eluting peaks, and poor detectability of late-eluting peaks due to band broadening. This problem is usually mitigated using temperature-programmed separation conditions.

Column selection for temperature-programmed separations is more challenging than for isothermal separations because selectivity is no longer constant over the temperature range of the separation. The influence of temperature on selectivity can be illustrated by system maps, for example, Fig. 6.2. In a temperature program, each substance interacts with the stationary phase only over the change in temperature while it is resident in the column. Separated substances are associated with different temperature ranges and, therefore, different selectivity ranges. The notion of a column having an assignable selectivity, therefore, has no chemical meaning for temperature-programmed gas chromatography, and there is no general possibility of a column classification system for temperature-programmed conditions. To identify columns thought to offer differences in selectivity throughout a programmed separation, the general characteristics observed

for isothermal separations at an average temperature for the temperature range of the program are used as a guide.

Leaving apart the selection of the stationary phase, many other column operating characteristics can be selected by computer simulation using method translation software (or calculations) [65–67]. System properties that can be optimized by method translation are summarized in Table 6.10. Method translation facilitates the simultaneous optimization of the carrier gas and its flow rate, column dimensions (length and internal diameter), stationary-phase film thickness, system operating pressure (inlet or outlet pressure), and temperature program rate to rescale an obtained separation to a new set of speed-optimized parameters in which the elution order for the original separation is maintained. The basis of method translation is that the column hold-up time can be viewed as a fundamental parameter to express any time-related parameter for a separation. Two methods are usually translatable if they have identical nontranslatable parameters and the same normalized temperature program rate. For translatable methods, the speed gain is given by the ratio of the column hold-up times for the two methods and the change in resolution by the square root of the ratio of the plate number for the two methods. Retention time locking is

based on the method translation approach and is used to minimize differences in retention times with unintentional variation of the operating conditions for the same method using different systems [67,68]. Retention projection provides an alternative approach for standardizing temperature programmed retention times [69–71] or linear retention indices [72] for compound identification. Relative retention in temperature program separations changes with alteration to the program rate, flow rate, column inlet and outlet pressure, column dimensions, and phase ratio through their influence on the effective steepness of the temperature ramp. Retention time locking does not account for nonidealities in the oven temperature profile. Retention projection open-source software allows back calculation of the precise temperature and hold-up time profiles produced by a particular instrument. Transfer of retention data across instrument platforms is based on each system being calibrated with a 25 component n-alkane mixture. This mixture is used to back-calculate temperature and hold-up time profiles to project the retention times of all the n-alkanes for a different instrument compatible with the values obtained for the original data source. The retention projection methodology acts as a hybrid of conventional retention projection and retention indexing, drawing on

TABLE 6.10 Translatable parameters in temperature-programmed gas chromatography.

Translatable (do not affect peak elution patterns)

Column dimensions (length and internal diameter)

Carrier gas (identity of carrier gas)

Pressure conditions (column inlet and outlet pressure, carrier gas flow rate)

Temperature program conditions (proportional changes in the duration of program steps and isothermal plateaus)

Nontranslatable (can effect peak elution patterns)

Stationary-phase type

Column-phase ratio

Set temperatures for isothermal segments of a temperature program

the advantages of both; it properly accounts for a wide range of experimental conditions while accommodating the effects of experimental factors not properly taken into account by nonprojection methods [71,72].

Under temperature program conditions there is an approximate linear relationship between the retention time of the *n*-alkanes and their carbon number, as long as the carbon number range is not too large and can be used to calculate a linear retention index (LRI) for programmed conditions, analogous to the isothermal retention index

$$\text{LRI} = 100z + 100[\text{t}_R(x) - \text{t}_R(z)] / [\text{t}_R(z+1) - \text{t}_R(z)] \quad (6.3)$$

where t_R is the observed retention time during a linear temperature program and the subscripts x , z , and $z + 1$ are as indicated for Eq. (6.2) [73–76]. However, when isothermal steps are included in the temperature program or the rate is changed during the separation, the calculation of the indices is more troublesome. The approximate nature of the linear plot has resulted in several nonlinear models being introduced to fit the retention times for the reference standards. This is in part driven by the desire to improve the precision of temperature-programmed retention indices, which are typically of lower precision than isothermal retention indices. Several other homologous series have been used in place of the *n*-alkane reference compounds, the most common being polycyclic aromatic hydrocarbons in which the ring number is substituted for the carbon number in the retention index calculation (Lee indices).

6.3.3 Quantitative structure–retention relationships

The general goal of quantitative structure–retention relationships (QSRR) is the prediction of retention from molecular structure for such

purposes as to test the reliability of retention data, to predict the retention of compounds unavailable for study, to provide insight into retention mechanisms, or to classify columns for selectivity optimization. The isothermal retention index or linear retention index is the most studied of the possible dependent variables. This topic has generated a great deal of literature over many years and is comprehensively reviewed elsewhere [76–80]. Here we will focus on general approaches with some comments on how these methods fulfill current needs.

QSRR methodology typically employs a mathematical model to correlate experimental retention properties to a group of descriptors that encode properties of the compounds related to their structure or physicochemical properties. There are three general approaches for the assignment of the descriptor values. The theoretical approach starts with the generation of a large number of molecular descriptors using structure-based computational methods, such as DRAGON, SYBYL, ChromGenius, CODESSA (>800 descriptors can be calculated using CODESSA) [81,82]. Statistical tools are then used to reduce the number of descriptors to a more manageable number, typically 5–10. These descriptors are then used as variables in linear or nonlinear models to establish a predictive relationship between the retention and compound properties on one or across several stationary phases. The models used are typically multiple linear regression or partial least squares regression for linear models (most common) [83–85], or genetic algorithms, federation of local models, and support vector regression for linear and nonlinear models [86–89]. A common problem with these methods is that some of the theoretical or topological descriptors may be difficult to interpret and the models may lack obvious chemical sense. The optimized set of selected descriptors for the correlation of retention in any given system is unlikely to be the same as the best set for a different system. A direct comparison of the two systems is then impossible or

at least difficult. The loss of chemical insight results in limited possibilities for further applications to other systems or interpretation of mechanistic details for the studied process.

The aforementioned problems are circumvented by less flexible models that define a small number of descriptors in advance and use the same descriptors to model all systems. The descriptors may be derived from theory [90,91], such as the five COSMOnts (COSMO-RS is a model combining quantum theory, dielectric continuum models, and statistical thermodynamics) or experimentally derived parameters, such as descriptors used in Abraham's solvation parameter model. The solvation parameter model was the method employed in this chapter for column characterization and provides both insight into retention mechanisms and the prediction of retention on any calibrated system (systems with known system constants) [22–24].

Hybrid methods, such as fragmentation methods, afford a middle ground between purely computational and experimental methods [56,92,93]. These methods involve breaking the molecular structure into a series of fragments, each with an assignable descriptor value. These fragments values are then summed to provide an estimate of the descriptors for new molecules built up from the defined fragments. The initial assignment of descriptor values to fragments requires a large training set of experimental values for varied compounds. Fragmentation methods may produce poor descriptor values for multifunctional compounds on account of the problem of generalizing the variation in intramolecular interactions accompanying changes in structure. They cannot be used at all for compounds whose fragments are unavailable in the database of fragment constants.

There are many QSRR papers where it is unclear how to proceed from an algebraic model that fits a specific data set to more general prediction of retention for further diverse compounds. Herberger offers sage advice on validating QSRR models and determining their predictive capability [78,94]. It is too early to state that efforts in this field are entirely

successful, and from a practical point of view there is currently limited application of QSAR models to assist in the identification of unknown compounds simply based on retention or as a filter for misidentification in shared mass spectral databases.

References

- [1] C.F. Poole, *The essence of chromatography*, Elsevier, Amsterdam, 2003.
- [2] C. Cruz-Hernandez, F. Destailates, Recent advances in fast gas chromatography: application to the separation of fatty acid methyl esters, *J. Liq. Chromatogr. Relat. Technol.* 82 (2009) 1672–1688.
- [3] S.K. Poole, C.F. Poole, Experimental protocol for the assessment of solvent strength and selectivity of liquid phases used in gas chromatography, *J. Chromatogr.* 500 (1990) 329–348.
- [4] M.H. Abraham, C.F. Poole, S.K. Poole, Classification of stationary phases and other materials by gas chromatography, *J. Chromatogr. A* 842 (1999) 79–114.
- [5] C.F. Poole, S.K. Poole, Characterization of the solvent properties of gas chromatographic liquid phases, *Chem. Rev.* 89 (1989) 377–395.
- [6] C.F. Poole, S.K. Poole, Separation characteristics of wall-coated open-tubular columns for gas chromatography, *J. Chromatogr. A* 1184 (2008) 254–280.
- [7] K. Heberger, Evaluation of polarity indicators and stationary phases by principal component analysis in gas-liquid chromatography, *Chemometr. Intell. Lab. Syst.* 47 (1999) 41–49.
- [8] C.F. Poole, T.O. Kollie, S.K. Poole, Recent advances in solvation models for stationary phase characterization and the prediction of retention in gas chromatography, *Chromatographia* 34 (1992) 281–302.
- [9] H. Rotzsche, *Stationary Phases for Gas Chromatography*, Elsevier, Amsterdam, 1991.
- [10] L. Rohrschneider, Characterization of GC stationary phases in multilinear retention model, *Chromatographia* 48 (1998) 728–738.
- [11] W.O. McReynolds, Characterization of some liquid phases, *J. Chromatogr. Sci.* 8 (1970) 685–691.
- [12] A.R. Johnson, M.F. Vitha, Chromatographic selectivity triangles, *J. Chromatogr. A* 1218 (2011) 556–586.
- [13] E. Chong, B. de Bricero, G. Miller, S.J. Hawkes, Spectroscopy and the classification of liquid stationary phases in gas chromatography, *Chromatographia* 20 (1985) 293–302.
- [14] E. Fernandez Sanchez, A. Fernandez Torres, J.A. Garcia Dominguez, E.L. Debias, Thermodynamic characterization of Superox 20 M by inverse gas chromatography, *J. Chromatogr. A* 655 (1993) 11–20.

- [15] P. Laffort, Solvation parameters part 5: physicochemical interpretation of experimental of experimental solvent values for stationary phases of gas-liquid chromatography, *J. Chromatogr. A* 1218 (2011) 4025–4033.
- [16] R.V. Golovnya, R.M. Polanuer, Comparison of methods for the determination of polarity and selectivity of stationary phases in gas chromatography from a thermodynamic point of view, *J. Chromatogr.* 517 (1990) 51–66.
- [17] T.O. Kollie, C.F. Poole, Influence of solute size and the nonpolar interaction term on the selection of test solutes for the classification of stationary phase selectivity in gas chromatography, *J. Chromatogr.* 556 (1991) 457–484.
- [18] M.H. Abraham, G.S. Whiting, R.M. Doherty, W.J. Shuely, Hydrogen bonding 13. A new method for the characterization of GC stationary phases – the Laffort data set, *J. Chem. Soc. Perkin Trans. 2* (1990) 1451–1460.
- [19] M.H. Abraham, Scales of solute hydrogen bonding: their construction and application to physicochemical and biochemical processes, *Chem. Soc. Chem. Rev.* 221 (1993) 73–83.
- [20] B.R. Kersten, C.F. Poole, K.G. Furton, Ambiguities in the determination of McReynolds stationary phase constants, *J. Chromatogr.* 411 (1987) 43–59.
- [21] M. Vitha, P.W. Carr, The chemical interpretation and practice of linear solvation energy relationships in chromatography, *J. Chromatogr. A* 1126 (2006) 143–194.
- [22] M.H. Abraham, A. Ibrahim, A.M. Zissimos, Determination of sets of solute descriptors from chromatographic measurements, *J. Chromatogr. A* 1037 (2004) 29–47.
- [23] C.F. Poole, S.N. Atapattu, S.K. Poole, A.K. Bell, Determination of solute descriptors by chromatographic methods, *Anal. Chim. Acta* 652 (2009) 32–53.
- [24] C.F. Poole, T.C. Ariyasena, N. Lenca, Estimation of the environmental properties of compounds from chromatographic measurements and the solvation parameter model, *J. Chromatogr. A* 1317 (2013) 85–104.
- [25] C.F. Poole, Wayne state university experimental descriptor database for use with the solvation parameter model, *J. Chromatogr. A* 1617 (2020), 460841.
- [26] ADME Suite 5.0, Advanced Chemistry Development, Toronto, Ontario, Canada.
- [27] N. Ulrich, S. Endo, T.N. Brown, N. Watanabe, C. Bronner, M.H. Abraham, K.-H. Goss, UFZ-LSER Database V. 3.2.1 [internet], Available from Helmholtz Centre for Environmental Research-UFZ, 2017. Leipzig, Germany, <http://www.ufz.de/lserd>.
- [28] C.F. Poole, Gas chromatography system constant database for 52 wall-coated open-tubular columns covering the temperature range 60–140°C, *J. Chromatogr. A* 1604 (2019) 4604482.
- [29] S.N. Atapattu, C.F. Poole, Solute descriptors for characterizing retention properties of open-tubular columns of different selectivity in gas chromatography at intermediate temperatures, *J. Chromatogr. A* 1195 (2008) 136–145.
- [30] S.N. Atapattu, C.F. Poole, Selectivity equivalence of two poly(methylphenylsiloxane) open-tubular columns prepared with different deactivation techniques for gas chromatography, *J. Chromatogr. A* 1185 (2008) 305–309.
- [31] S.N. Atapattu, K. Eggers, C.F. Poole, W. Kiridena, W.W. Koziol, Extension of the system constants database for open-tubular columns: system maps at low and intermediate temperatures for four new columns, *J. Chromatogr. A* 1216 (2009) 1640–1649.
- [32] C.F. Poole, Gas chromatography system constant database over an extended temperature range for nine open-tubular columns, *J. Chromatogr. A* 1590 (2019) 130–145.
- [33] N. Lenca, C.F. Poole, A system map for the ionic liquid stationary phase 1,9-di(3-vinylimidazolium)nonane bis(trifluoromethylsulfonyl)imide, *Chromatographia* 78 (2014) 240–254.
- [34] N. Lenca, C.F. Poole, System map for the ionic liquid stationary phase tri(triethylphosphoniumhexanamido)triethylamine bis(trifluoromethylsulfonyl)imide for gas chromatography, *J. Chromatogr. A* 1524 (2017) 210–214.
- [35] N. Lenca, C.F. Poole, A system map for the ionic liquid stationary phase 1,12-di(triethylphosphonium) dodecane bi(trifluoromethylsulfonyl)imide for gas chromatography, *J. Chromatogr. A* 1525 (2017) 138–144.
- [36] N. Lenca, C.F. Poole, A system map for the ionic liquid stationary phase 1,12-di(triethylphosphonium) dodecane bis(trifluoromethylsulfonyl)imide trifluoromethanesulfonate for gas chromatography, *J. Chromatogr. A* 1559 (2018) 164–169.
- [37] S.D. Martin, C.F. Poole, M.H. Abraham, Synthesis and gas chromatographic evaluation of a high-temperature hydrogen-bond acid stationary phase, *J. Chromatogr. A* 805 (1998) 217–235.
- [38] C.F. Poole, S.K. Poole, Ionic liquid stationary phases for gas chromatography, *J. Chromatogr. Sci.* 34 (2011) 888–900.
- [39] C.F. Poole, N. Lenca, Gas chromatography on wall-coated open-tubular columns with ionic liquid stationary phases, *J. Chromatogr. A* 1357 (2014) 87–109.

- [40] W. Kiridena, C.C. Patchett, W.W. Koziol, H. Ahmed, C.F. Poole, Separation characteristics of phenyl-containing stationary phases for gas chromatography based on silarylene-siloxane copolymer chemistries, *J. Sep. Sci.* 29 (2008) 211–217.
- [41] W. Kiridena, C.C. Patchett, W.W. Koziol, C.F. Poole, System constants for the bis(cyanopropylsiloxane)-*co*-methylsilarylene HP-88 and poly(siloxane) Rtx-440 stationary phases, *J. Chromatogr. A* 1081 (2005) 248–254.
- [42] C. Yao, J.L. Anderson, Retention characteristics of organic compounds on molten salts and ionic liquid-based gas chromatography stationary phases, *J. Chromatogr. A* 1216 (2009) 1658–1712.
- [43] C.F. Poole, J. Qian, W. Kiridena, C. DeKay, W.W. Koziol, Evaluation of the separation characteristics of application specific (volatile organic compounds) open-tubular columns for gas chromatography, *J. Chromatogr. A* 1134 (2006) 284–290.
- [44] W. Kiridena, J. Qian, W.W. Koziol, C.F. Poole, Evaluation of the separation characteristics of application-specific (fatty acid methyl esters) open-tubular columns for gas chromatography, *J. Separ. Sci.* 30 (2007) 740–745.
- [45] W. Kiridena, C. DeKay, C.C. Patchett, W.W. Koziol, J. Qian, C.F. Poole, Evaluation of the separation characteristics of application-specific (pesticides and dioxin) open-tubular columns for gas chromatography, *J. Chromatogr. A* 1128 (2006) 228–235.
- [46] R. Sacks, C. Coutant, A. Grall, Advancing the science of column selectivity, *Anal. Chem.* 72 (2000) 524A–533A.
- [47] F.L. Dorman, P.D. Schettler, L.A. Vogt, J.W. Cochran, Using computer modeling to predict and optimize separations for comprehensive two-dimensional gas chromatography, *J. Chromatogr. A* 1186 (2008) 196–201.
- [48] F.L. Dorman, P.D. Schettler, C.M. English, D.V. Patwardhan, Predicting gas chromatographic separation and stationary-phase selectivity using computer modeling, *Anal. Chem.* 74 (2002) 2133–2138.
- [49] S.K. Poole, C.F. Poole, The orthogonal character of stationary phases for gas chromatography, *J. Sep. Sci.* 31 (2008) 1118–1123.
- [50] C.F. Poole, S.K. Poole, Foundations of retention in partition chromatography, *J. Chromatogr. A* 1216 (2009) 1530–1550.
- [51] L. Wu, M. Chen, Y. Chen, Q.X. Li, Determination and evaluation of gas hold-up time with the quadratic equation model and comparison with non-linear models for isothermal gas chromatography, *J. Chromatogr. A* 1297 (2013) 196–203.
- [52] G. Tarjan, S. nyiredy, M. Gyor, F.R. Lombosi, M.V. Budahegyi, S.Y. Meszaros, J.M. Takacs, 31 st Anniversary of the retention index according to Kovats in gas-liquid chromatography, *J. Chromatogr.* 472 (1989) 1–92.
- [53] G. Castello, Retention index systems: alternatives to the n-alkanes as calibration standards, *J. Chromatogr. A* 842 (1999) 51–64.
- [54] V.I. Babushok, Chromatographic retention indices in identification of chemical compounds, *Trends Anal. Chem.* 69 (2015) 98–104.
- [55] NIST, 2014 GC Method and Retention Index Database, Wiley, 2014.
- [56] C.T. Peng, Retrieval of structure information from retention index, *J. Chromatogr. A* 678 (1994) 189–200.
- [57] B. Karolat, J. Harynyuk, Prediction of gas chromatographic retention time via an additive thermodynamic model, *J. Chromatogr. A* 1217 (2010) 4862–4867.
- [58] N. Ulrich, J. Muhlenberg, H. retzbach, G. Schuurmann, W. Brack, Linear solvation energy relationship as classifiers in non-target analysis – a gas chromatographic approach, *J. Chromatogr. A* 1264 (2012) 95–103.
- [59] A.A. Pavlovskii, K. Heberger, I.G. Zenkevich, Anomalous temperature dependence of gas chromatographic retention indices of polar compounds on non-polar stationary phases, *J. Chromatogr. A* 1445 (2016) 126–134.
- [60] J.M. Santiuste, J.E. Quintanilla-Lopez, K. Bacerra, R. Lebron-Aguilar, On the influence of column temperature on the isothermal retention indices of structurally different solutes on a poly(dimethylsiloxane) capillary column, *J. Chromatogr. A* 1365 (2014) 204–211.
- [61] C.D. Wick, J.I. Siepmann, M.R. Schure, Molecular simulation of concurrent gas-liquid interfacial adsorption and partitioning in gas-liquid chromatography, *Anal. Chem.* 74 (2002) 3518–3524.
- [62] F.R. Gonzales, R.C. Castells, A.M. Nardillo, Behavior of n-alkanes on poly(oxyethylene) capillary columns – evaluation of interfacial effects, *J. Chromatogr. A* 927 (2001) 111–120.
- [63] N.R. Ronco, M.F. Fiorella, L.M. Romero, C.B. Castells, Determination of gas-liquid partition coefficients of several organic solutes in tris(tetradecyl)phosphonium bromide using capillary gas chromatography columns, *J. Chromatogr. A* 1501 (2017) 134–141.
- [64] N.R. Ronco, M.F. Fiorella, L.M. Romero, C.B. Castells, Determination of gas-liquid partition coefficients of several organic solutes in tris(tetradecyl)phosphonium dicyanamide using capillary gas chromatography columns, *J. Chromatogr. A* 1584 (2019) 179–186.
- [65] L.M. Blumberg, Temperature-programmed Gas Chromatography, Wiley-VCH, Weinheim, Germany, 2010.

- [66] M.S. Klee, L.M. Blumberg, Theoretical and practical aspects of fast gas chromatography and method translation, *J. Chromatogr. Sci.* 40 (2002) 234–247.
- [67] L.M. Blumberg, M.S. Klee, Method translation and retention time locking in partition GC, *Anal. Chem.* 70 (1998) 3828–3838.
- [68] N. Etxebarria, O. Zuloaga, M. Olivares, L.J. Bartolome, P. Navarro, Retention-time locked methods in gas chromatography, *J. Chromatogr. A* 1216 (2009) 1624–1629.
- [69] B.B. Barnes, M.B. Wilson, P.W. Carr, M.F. Vitha, C.D. Broeckling, A. Heuberger, J. Prenni, G.C. Janis, H. Corcoran, N.H. Snow, S. Chopra, R. Dhandapani, A. Tawfall, L.W. Sumner, P.G. Boswell, “Retention projection” enables reliable use of shared gas chromatographic retention data across laboratories, instruments and methods, *Anal. Chem.* 85 (2013) 11650–11657.
- [70] B.J. Peng, M.Y. Kuo, P.H. Yang, J.T. Hewitt, P.G. Boswell, A practical methodology to measure unbiased gas chromatographic retention factor vs. temperature relationships, *J. Chromatogr.* 1374 (2014) 207–215.
- [71] M.B. Wilson, B.B. Barnes, P.G. Boswell, What experimental factors influence the accuracy of retention projections in gas chromatography-mass spectrometry, *J. Chromatogr. A* 1373 (2014) 179–189.
- [72] P.G. Boswell, P.W. Carr, J.D. Cohen, A.D. Hageman, Easy and accurate calculation of programmed temperature gas chromatographic retention times by back-calculation of temperature and hold-up time profiles, *J. Chromatogr. A* 1263 (2012) 179–188.
- [73] Y.L. Sun, R.Y. Zhang, Q.Q. Wang, B.J. Xu, programmed-temperature gas-chromatographic retention index, *J. Chromatogr. A* 657 (1993) 1–15.
- [74] B.D. Zeliner, B. d’Acampora, C. Bicchi, P. Dugo, P. Rubiolo, G. Dugo, L. Mondello, Linear retention indices in gas chromatographic analysis: a review, *Flavour Fragrance J.* 23 (2008) 297–314.
- [75] G. Castello, P. Moretti, S. Vezzani, Retention models for programmed gas chromatography, *J. Chromatogr. A* 1216 (2009) 1607–1623.
- [76] J. Yan, X.B. Liu, W.W. Zhu, X. Zhong, Q. Sun, Y.Z. Liang, Retention indices for identification of aroma compounds by GC: development and application of a retention index database, *Chromatographia* 78 (2015) 89–108.
- [77] R. Kalisz, *Structure and Retention in Chromatography. A Chemometric Approach*, Harwood Academic, Amsterdam, 1977.
- [78] K. Heberger, Quantitative structure-(chromatographic) retention relationships, *J. Chromatogr. A* 1158 (2007) 273–305.
- [79] K. Heberger, Quantitative structure-retention relationships, in: C.F. Poole (Ed.), *Gas Chromatography*, Elsevier, Amsterdam, 2012, pp. 451–494.
- [80] A.K. Zhokhov, A.Y. Loskutov, I.V. Rybal’chenko, Methodological approaches to the calculation and prediction of retention indices in capillary gas chromatography, *J. Anal. Chem.* 73 (2018) 207–220.
- [81] A.R. Katritsky, U. Maran, V.S. Lobonov, M. Karelson, Structurally diverse quantitative structure-relationship correlations of technologically relevant physical properties, *J. Chem. Inf. Comput. Sci.* 40 (2000) 1–18.
- [82] A.M. Heiguera, R.D. Combes, M.P. Gonzalez, M.N.D.S. Corderio, Applications of 2D descriptors in drug design: a DRAGON tale, *Curr. Top. Med. Chem.* 8 (2008) 1628–1655.
- [83] J. Yan, D.S. Cao, F.Q. Guo, L.X. Zhang, M. He, J.H. Huang, Q.S. Xu, Y.Z. Liang, Comparison of quantitative structure-retention relationship models on four stationary phases with different polarity for a diverse set of flavor compounds, *J. Chromatogr. A* 1223 (2012) 118–125.
- [84] C. Veensas, A. Linusson, P. Haglund, Retention-time prediction in comprehensive two-dimensional gas chromatography to aid identification of unknown contaminants, *Anal. Bioanal. Chem.* 410 (2018) 7931–7941.
- [85] A.A. D’Archivio, A. Giannitto, Characterization of gas-chromatographic poly(siloxane) stationary phases by theoretical molecular descriptors and prediction of McReynolds constants, *J. Mol. Sci.* 20 (2019) 2120.
- [86] Q.Q. Shen, W.W. Tao, Y.J. Guo, S.J. Wang, Y.F. Wang, E.M. Zheng, Z.X. Chen, K. Chen, Quantitative structure-retention relationships of the chromatographic retentions of phthalic acid ester contaminants in foods, *J. Sep. Sci.* 42 (2019) 2771–2778.
- [87] F. Qiu, Z.T. Lei, L.W. Sumner, MetExpert: an expert system to enhance gas chromatography-mass spectrometry-based metabolite identifications, *Anal. Chim. Acta* 1037 (2018) 316–326.
- [88] J. Zhang, C.H. Zheng, Y. Xia, B. Wang, P. Chen, Optimization enhanced genetic algorithm-support vector regression for the prediction of compound retention indices in gas chromatography, *Neurocomputing* 240 (2017) 183–190.
- [89] P. Goel, S. Bapat, R. Vyas, A. Tambe, S.S. Tambe, Genetic programming based quantitative structure-retention relationships for the prediction of Kovats retention indices, *J. Chromatogr. A* 1420 (2015) 98–109.
- [90] A.M. Zissmos, M.H. Abraham, A. Klamt, J. Eckert, J. Wood, A comparison between two general set of linear free energy descriptors of Abraham and Klamt, *J. Chem. Inf. Comput. Sci.* 42 (2002) 1320–1331.

- [91] G.R. Famini, L.Y. Wilson, Linear free energy relationships using quantum mechanical descriptors, *Rev. Comput. Chem.* 18 (2002) 211–255.
- [92] S.H. Hilal, S.W. Karickhoff, L.A. Carreira, Prediction of the solubility, activity coefficient, and liquid/liquid partition coefficients of organic compounds, *QSAR Comb. Sci.* 23 (2004) 709–720.
- [93] J.A. Platts, D. Butina, M.H. Abraham, A. Hersey, Estimation of molecular linear free energy relation descriptors using a group contribution approach, *J. Chem. Inf. Comput. Sci.* 39 (1999) 835–845.
- [94] K. Heberger, Sum of ranking differences compares methods or models fairly, *Trends Anal. Chem.* 29 (2010) 101–109.

Multidimensional and comprehensive gas chromatography

John V. Seeley

Oakland University, Department of Chemistry, Rochester, MI, United States

7.1 Introduction

A modern gas chromatograph equipped with a split/splitless inlet, a capillary column, and a fairly universal detector (e.g., a flame ionization detector (FID)) can be used to generate high-resolution separations of a wide range of samples. Unfortunately, experience and theory [1] have shown that complex samples, such as petroleum-based fuels or environmental extracts, produce chromatograms with significant peak overlap. The limited ability of single-column gas chromatography (GC) to isolate analytes in complex mixtures has led to the adoption of selective detectors such as the electron-capture detector or scanning detectors such as the mass spectrometer. Such detectors supply additional resolving power but decrease generality and increase cost. It is also possible to improve performance by increasing the resolving power of the chromatographic separation. Changing stationary phases can separate a critical pair of components, but it frequently leads to the creation of new overlapping pairs. Switching to a longer or

narrower column can generate more theoretical plates, but this also increases separation time or decreases sample capacity.

Introducing an additional chromatographic stage is an effective approach for increasing the resolving power of a separation. This chapter examines methods that employ two sequential GC separations. Such analyses fall into the category of two-dimensional gas chromatography (2D GC). In addition to increasing peak capacity, obtaining retention information on two different stationary phases can help distinguish functional classes of components. This effect can be observed by examining the retention indices of components on two different stationary phases. For example, the Kovats retention indices of alkyl esters and aliphatic alcohols [2] are interspersed on both the DB-5 and DB-Wax stationary phases (see Fig. 7.1A and B). However, when a 2D plot of DB-Wax and DB-5 retention indices is constructed, the alkyl esters are fully resolved from the aliphatic alcohols (see Fig. 7.1C). Combining two separations has the potential to increase the resolution and

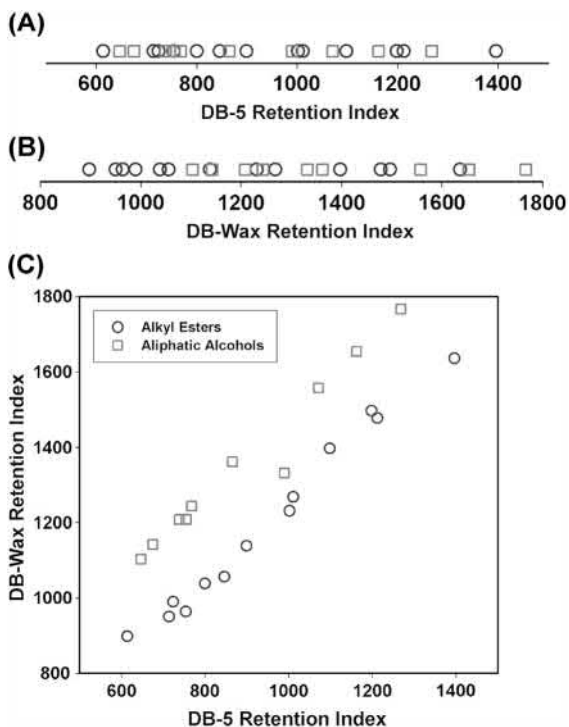


FIGURE 7.1 Kovats retention indices of C_4 – C_{12} alkyl esters (circles) and C_4 – C_{10} aliphatic alcohols (squares) on the DB-5 and DB-Wax stationary phases. (A) DB-5 retention indices. (B) DB-Wax retention indices. (C) A 2D plot of DB-5 and DB-Wax retention indices.

information provided by GC analyses, but the challenge is to develop practical laboratory methods capable of exploiting this potential.

2D GC was first reported over 60 years ago [3], and numerous improvements have been made since. This chapter focuses on the chromatographic characteristics required for an effective 2D GC separation and examines the basic instrument designs that are currently in use, including heartcutting 2D GC and comprehensive 2D GC (GC \times GC). For a more in-depth account of the development of multidimensional GC, the reader is referred to the numerous review articles and book chapters published over the past three decades [4–9].

Many 2D separation techniques, such as 2D gel electrophoresis and 2D thin-layer chromatography, use a planar separation medium. In contrast, 2D GC is performed using two capillary columns containing different stationary phases. The majority of the instrument components associated with 2D GC are identical to those used for conventional GC. However, 2D GC analyses require a device for coupling the columns and in some cases special software for analyzing the resulting data. A schematic of a basic gas chromatograph capable of performing a 2D separation is shown in Fig. 7.2. The sample is injected through an inlet located at the head of the primary column. The mixture components pass through the primary column until they reach an interface that controls transfer from the primary column to the secondary column. Depending on the mode of operation, the interface may send the component to an exhaust line, temporarily accumulate the component in a storage region, or send the component to the head of the secondary column. Components that enter the secondary column are transported down its length until they reach a detector.

2D GC separations combine three time-dependent processes: transport through the primary column, transport through the interface, and transport through the secondary column. As such, there are more degrees of freedom present in 2D GC than conventional GC. This increased flexibility provides the opportunity to tune separations for a specific set of analytes, but it also introduces more sources of error. Successful separations require precise control of many parameters including carrier gas flow rates, temperatures of heated zones, and the timing of interfacial events. Fortunately, GC instruments are now equipped with high-precision electronic pneumatics, multiple independently heated regions, and programmable electronic outputs. Stationary-phase selection is a critical part of the development of a successful

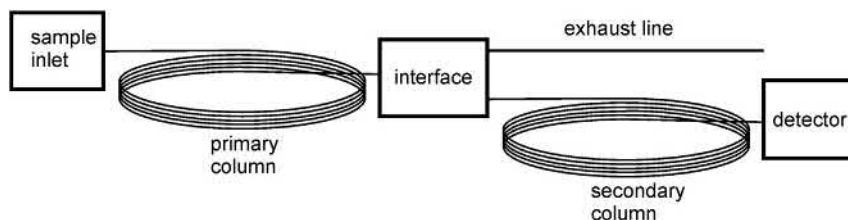


FIGURE 7.2 The basic construction of a 2D GC instrument. Samples are injected through a standard inlet and separated by the primary column. Upon eluting from the primary column, components pass through an interface that controls entry into a secondary column. Components are detected as they elute from the secondary column.

2D GC analysis. The primary and secondary stationary phases should have complementary selectivities that maximize the contrast between the analytes and the sample matrix components. The ease of identifying promising stationary-phase pairs has been improved with the introduction of simple models for quantitatively predicting chromatographic retention [10].

7.2 A graphical representation of 2D GC separations

Component transports in the primary column, interface, and secondary column all occur simultaneously in a 2D GC separation. In this chapter, a graphical approach will be used to represent these concurrent processes. Fig. 7.3 is a plot that represents the retention of a single component in a coupled-column separation. In this hypothetical case, the component enters the primary column at $t = 0$ min, exits the primary column with a primary retention time $t_1 = 12$ min, quickly passes through the interface into the secondary column, and then exits the secondary column 8 min later with a cumulative retention time of $t_c = 20$ min. The chromatogram produced by the primary column is shown along the top edge of Fig. 7.3, whereas the chromatogram observed at the end of the

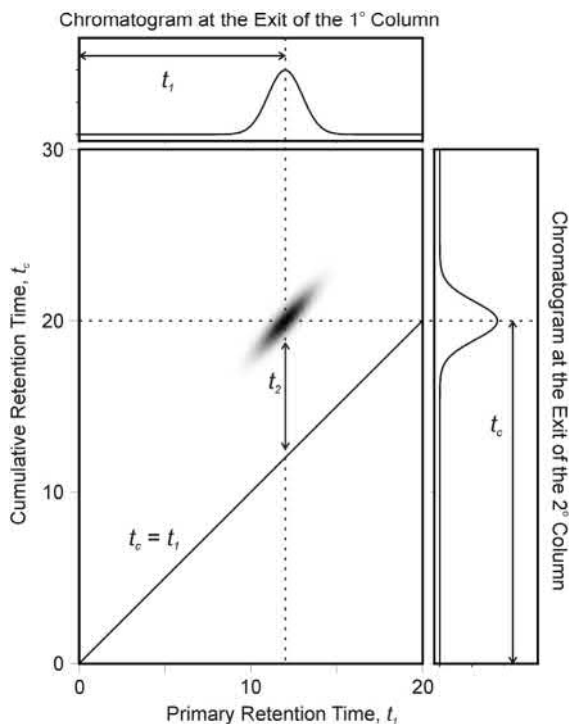


FIGURE 7.3 A graphical representation of a 2D GC separation. The primary retention time t_1 of a component is represented by its horizontal position, and the cumulative retention time t_c (i.e., the sum of t_1 and the secondary retention time t_2) is represented by its vertical position. The chromatogram produced by the primary column is shown along the top edge of Fig. 7.3, whereas the chromatogram observed at the end of the

secondary column is shown along the right edge of Fig. 7.3. Both of these chromatograms could be obtained by monitoring the component concentration exiting the primary and secondary columns.

The 2D plot shown at the center of Fig. 7.3 resembles the separations generated with planar media (e.g., 2D thin layer chromatography, 2D gel electrophoresis, etc.). Unfortunately, coupled-column separations do not directly yield a 2D chromatogram like that shown in the center of Fig. 7.3. Throughout this chapter, 2D retention plots will be used to visualize the factors that are critical for designing an effective coupled-column separation. The 2D plot represents the probability distribution that a component will have a primary retention time t_1 and a cumulative retention time t_c (i.e., the sum of the primary and secondary retention times). Horizontal position represents the primary retention time and vertical position represents the cumulative retention time. Secondary retention time t_2 can be determined by the difference of the cumulative retention time and the primary retention time ($t_2 = t_c - t_1$). Graphically, this corresponds to the vertical distance between the 2D peak and the diagonal line representing $t_c = t_1$. The chromatogram obtained at the exit of the primary column is equivalent to the integral of the 2D plot in the vertical direction, whereas the chromatogram obtained at exit of the secondary column is equivalent to the integral of the 2D plot in the horizontal direction. The width of a vertical slice of the 2D peak is proportional to the standard deviation of the secondary retention time. For example, if the peaks broaden on the primary column but do not broaden appreciably on the secondary column, the 2D peak will appear as a slender diagonal ellipse.

A 2D retention plot can be used to demonstrate why simply connecting two different GC columns in a serial fashion does not generate a 2D separation. Fig. 7.4 shows a simulation for the case of 20 components analyzed with the

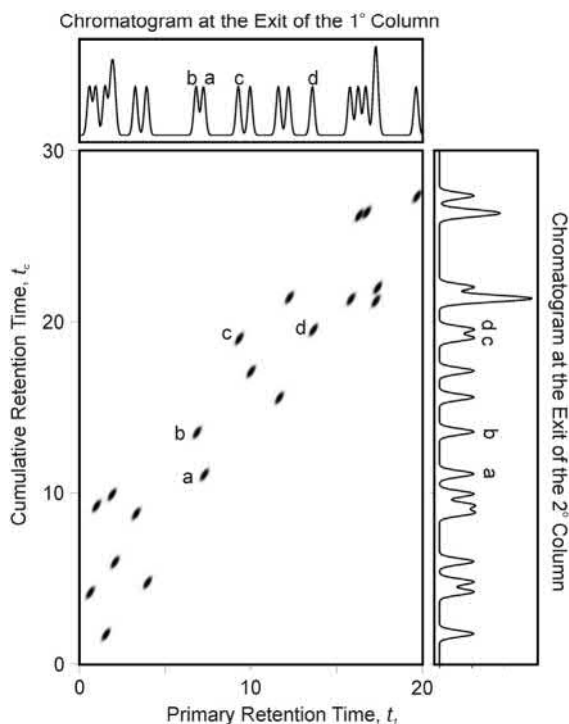


FIGURE 7.4 Simulation of a coupled-column separation of 20 components. All of the components are allowed to pass directly from the primary column to the secondary column. The chromatogram at the top of the figure shows that eight of the 20 components are separated at the end of the primary column. The chromatogram on the right shows that seven of the 20 components are separated at the end of the secondary column.

coupled-column apparatus shown in Fig. 7.2. In this case, the interface is a simple butt connector (i.e., primary effluent flows uninterrupted into the head of the secondary column). The simulation was conducted by assigning each component a random primary retention time within the range of 0–20 min and a random secondary retention time within the range of 0–10 min (thus, the cumulative retention time ranged from 0 to 30 min). The primary column chromatogram is shown at the top of Fig. 7.4. A total of eight of the 20 components are resolved from their neighboring peaks (i.e., $R > 1$ on both sides). The chromatogram at the

end of the secondary column is shown on the right edge of Fig. 7.4. Only seven of the 20 components are fully isolated. One might have predicted that the chromatogram obtained at the end of the secondary column would have more isolated components because of the additional resolving power of the secondary column. The secondary column does help resolve some components that coeluted from the primary column. For example, components a and b in Fig. 7.4 coelute on the primary column, but they are separated when they reach the end of the secondary column because component b experiences much greater secondary retention than component a. Unfortunately, the secondary column can also recombine components that were separated by the primary column. For example, components c and d are separated on the primary column with component d more strongly retained. However, component c has much greater secondary retention causing the pair to recombine as they pass down the secondary column. This simple simulation demonstrates an important point: In the absence of judicious action taken at the interface between the columns, the mere addition of a secondary column does not significantly increase resolution.

A much greater level of separation is observed in the 2D plot shown in the center of Fig. 7.4 than in 1D chromatogram. Within the 2D plot, 18 of the 20 components are isolated. The 2D plot exhibits enhanced resolving power because components that are separated in the primary column (i.e., those with different horizontal positions) remain separated no matter what happens in the secondary column, and components that coelute from the primary column (i.e., those with same horizontal position) can potentially be separated if they have different levels of retention in the secondary column.

One of the design goals of 2D GC is to in effect transfer the resolution of the theoretical 2D retention plot to the chromatogram that is observable at the end of the secondary column. This capability largely boils down to devising

ways to add a secondary separation without diminishing the separation already produced by the primary column. This goal can be achieved through the action of the interface (which was absent in the example shown in Fig. 7.4) along with carefully controlled retention in the secondary column. The remainder of this chapter will examine the main forms of 2D GC currently being employed with particular attention paid to the conditions that produce successful 2D GC separations.

7.3 Backflushing 2D GC

Backflushing 2D GC is the simplest form of 2D GC. It allows a class of analytes to be fully resolved from sample matrix components when the analytes are fairly volatile and possess a significantly different polarity than the matrix components.

7.3.1 Basic mode of operation

A common implementation of backflushing 2D GC is shown in Fig. 7.5. In this case, the interface is a tee union that introduces an auxiliary flow of carrier gas to the junction between the primary and secondary columns. The apparatus can be placed in two different states: foreflush and backflush. In the foreflush state (Fig. 7.5A), the carrier gas flows from the sample inlet through the primary column to the tee union. A small auxiliary flow mixes with the primary column effluent in the tee union and the combined stream moves through the secondary column toward the detector. In the backflush state (Fig. 7.5B), the pressure in the sample inlet is reduced significantly while the pressure in the tee union is maintained at its original value. This causes the auxiliary carrier flow entering the tee union to increase. A portion of the auxiliary flow maintains the flow in the secondary column, while the remainder of the auxiliary flow enters the primary column reversing the flow direction toward the sample inlet.

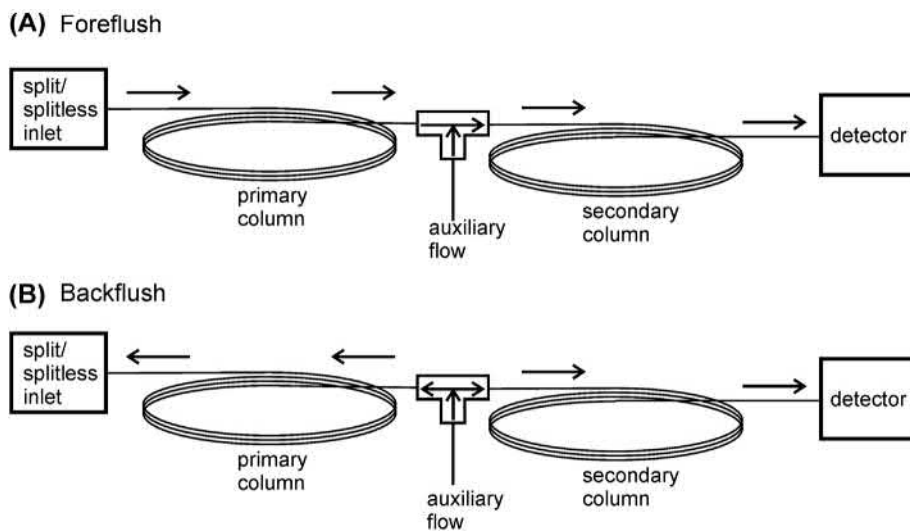


FIGURE 7.5 A backflushing 2D GC apparatus. (A) The instrument is initially in the foreflush state where the sample passes from the inlet through the primary column toward the interface. (B) After the last analyte enters the secondary column, the instrument is placed in the backflush state where the sample matrix components that are still in the primary column are backflushed out of the split vent and thereby prevented from reaching the secondary column.

A backflushing 2D GC analysis involves a single switch from the foreflush state to the backflush state. The apparatus is initially in the foreflush state when the sample is injected through the split/splitless inlet. Compounds that are weakly retained on the primary column pass through the tee and reach the secondary column. Just after the last analyte reaches the secondary column, the apparatus is placed in the backflush state. This reverses the flow in the primary column and causes any sample matrix components that are still in the primary column to be backflushed out of the split vent, while the components in the secondary column continue traveling toward the detector.

The retention characteristics and timing required for an effective backflushing 2D GC analysis are demonstrated in the simulation shown in Fig. 7.6. A primary column stationary phase is chosen that weakly retains analytes while strongly retaining most matrix components, and a secondary column stationary phase is chosen that strongly retains analytes while

weakly retaining most matrix components. The analytes are encircled in the 2D retention plot and the remainder of the peaks represent sample matrix components.

Fig. 7.6A considers the situation when a backflush is not implemented. In this case, the chromatogram produced by the primary column (see the top of Fig. 7.6A) contains analyte peaks confined to low retention times while sample matrix peaks are scattered over a wide range of retention times. The analyte peaks overlap with matrix components weakly retained by the primary column (i.e., those left of the *dotted line*). Upon entering the secondary column, the analytes experience greater retention than the sample matrix components. This causes the analyte peaks to reach the end of the secondary column later than the matrix components that were weakly retained by the primary column. Unfortunately, the analyte peaks now overlap with matrix components that were strongly retained by the primary column (i.e., those right of the *dotted line*). The

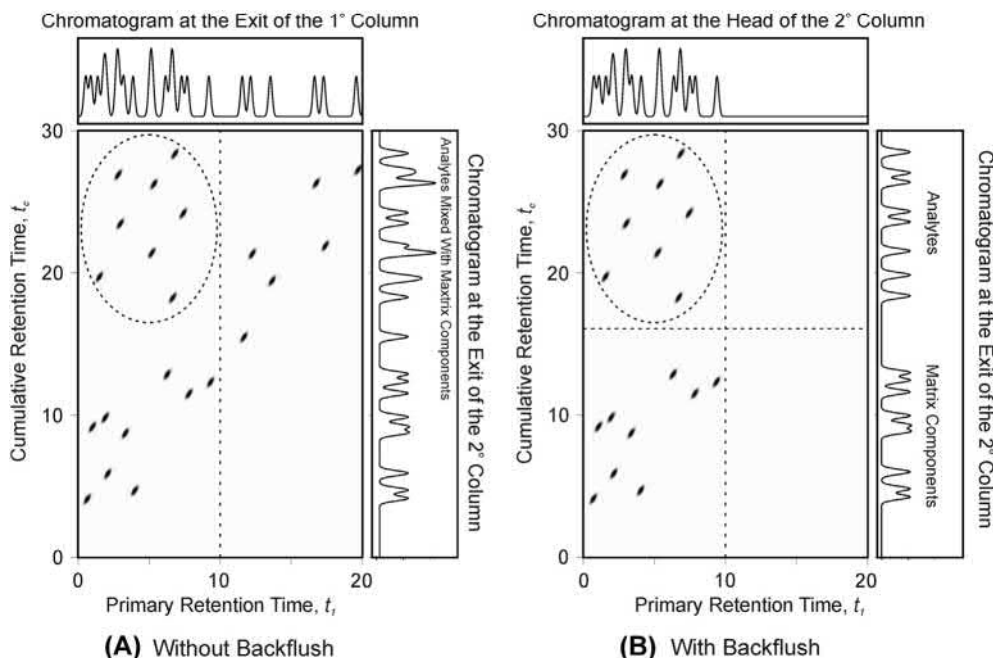


FIGURE 7.6 2D plots of a simulated backflushing 2D analysis. (A) Without backflushing, the analytes (circled in the 2D plot) coelute with sample matrix components at the end of the primary column and at the end of the secondary column. (B) Backflushing prevents the components that elute from the primary column after the dashed vertical line from entering the secondary column. This causes the analytes to be fully separated from the sample matrix components at the end of the secondary column.

chromatogram at the end of the secondary column (see right edge of Fig. 7.6A) shows that the analyte peaks are shifted to higher retention times while the matrix components are still scattered over the full range of retention times. Thus, neither the chromatogram generated at the end of the primary column nor the chromatogram generated at the end of the secondary column fully isolates the analytes from the matrix.

Fig. 7.6B considers the situation when the backflush event is introduced shortly after the last analyte has exited the primary column and entered the secondary column (shown with the vertical dotted line). The backflush prevents matrix components strongly retained by the primary column from entering the secondary column. Thus, the secondary column separates the analytes from the matrix components that

were weakly retained by the primary column (i.e., those left of the vertical backflush line), and the backflush removes the matrix components that were strongly retained by the primary column (i.e., those right of the vertical backflush line). Full isolation of the analytes is observed in the chromatogram obtained at the end of the primary column when the backflush is employed.

7.3.2 An example of backflushing 2D GC: the analysis of oxygenates in gasoline

The separation of oxygenates from gasoline hydrocarbons is a common application of backflushing 2D GC. Gasoline contains hundreds of hydrocarbons with carbon numbers ranging from C₅ to C₁₂. Gasoline can also contain oxygenated compounds. The most prevalent oxygenates

are C₁–C₅ aliphatic alcohols and C₅–C₆ aliphatic ethers. The concentrations of many oxygenates are at parts per million (ppm) levels or below; however, ethanol and methyl tert-butyl ether (MTBE) can be present at levels above 10%. The main analytical goal is to separate the entire oxygenate class from the hydrocarbons. Unfortunately, there is no single capillary column that can generate such a separation. This is because oxygenates overlap with the low-molecular-weight hydrocarbons on nonpolar columns and oxygenates overlap with the high-molecular-weight hydrocarbons on polar columns. However, backflushing 2D GC with a poly(dimethylsiloxane) primary column and a CP-Lowox secondary column can fully separate the oxygenates from the hydrocarbons.

An example of an instrument used for separating oxygenates from gasoline is shown in Fig. 7.7. This particular configuration, developed by Andrew Tipler of PerkinElmer, Inc., employs a miniature column-coupling device known as an S-Swafer [11]. The S-Swafer has minimal unswept volume, low thermal mass, and provides leak-free connections for the primary

column, secondary column, and auxiliary flow. Fig. 7.7 also shows a flow restrictor that leads to an additional detector that allows a chromatogram of the components eluting from the primary column to also be obtained. The chromatogram of gasoline eluting from the primary column without backflushing is shown in Fig. 7.8A. The oxygenates elute between 1.0 and 1.5 min and, when present in low concentrations, are obscured by the hydrocarbons. Under normal conditions, backflushing is initiated at 1.52 min, which is just after the last oxygenate, tert-amyl methyl ether (TAME), has entered the secondary column. All compounds with retention times on poly(dimethylsiloxane) greater than that of TAME are not transferred to the CP-Lowox secondary column and are backflushed out of the split inlet. The chromatogram observed at the end of the CP-Lowox secondary column when backflushing is employed is shown in Fig. 7.8B. The high affinity of the CP-Lowox stationary phase for oxygenates causes the ethers and alcohols to have significantly higher cumulative retention times than the hydrocarbons. A complete separation of

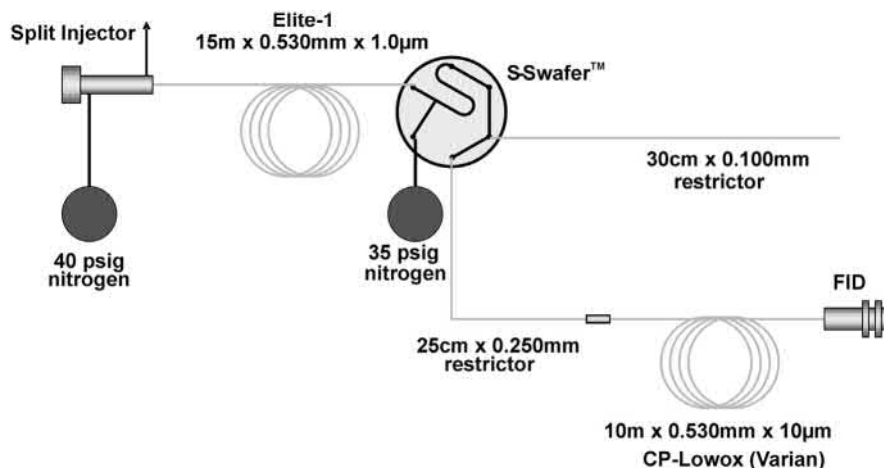


FIGURE 7.7 Backflushing 2D GC apparatus used to analyze oxygenates in gasoline. Reprinted with permission from Ref. A. Tipler, Application Note: Determination of Low-Level Oxygenated Compounds in Gasoline Using the Clarus 680 GC with S-Swafer Micro-channel Flow Technology, 2010; Copyright 2010, PerkinElmer, Inc.

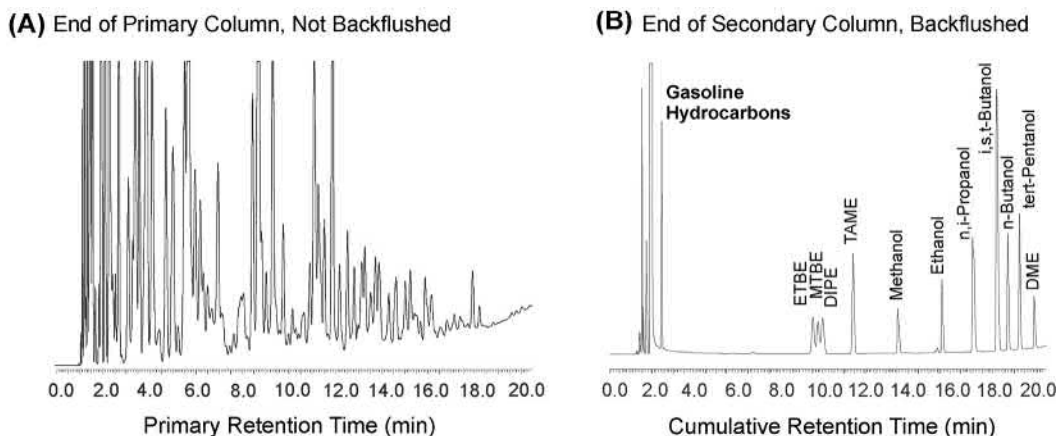


FIGURE 7.8 (A) Gasoline chromatogram obtained on the nonpolar primary column. The oxygenates elute between 1.0 and 1.5 min along with numerous hydrocarbons. (B) Chromatogram obtained at the end of the CP-Lowox secondary column for gasoline containing percent levels of oxygenates. When the primary column is backflushed at 1.52 min, the chromatogram obtained at the end of the secondary column fully separates the oxygenates from the hydrocarbons. The names of the alcohols are listed in the figure. The names of the ethers are abbreviated: *DIPE*, diisopropyl ether; *DME*, 1,2-dimethoxyethane; *ETBE*, ethyl tert-butyl ether; *MTBE*, methyl tert-butyl ether; *TAME*, tert-amyl methyl ether. Reprinted with permission from Ref. A. Tipler, *Application Note: Determination of Low-Level Oxygenated Compounds in Gasoline Using the Clarus 680 GC with S-Swafer Micro-channel Flow Technology*, 2010; Copyright 2010, PerkinElmer, Inc.

the oxygenate class from gasoline hydrocarbons is achieved. The high resolution of this method allows ppm levels of oxygenates to be accurately quantified. Backflushing improves the speed of the analysis as the run can be concluded shortly after the last oxygenate elutes from the secondary column, and there is no need to wait for the low-volatility hydrocarbons to elute from the secondary column because they have been backflushed off the primary column. Another advantage of backflushing is that it protects the high-polarity CP-Lowox secondary column from being exposed to low-volatility hydrocarbons that could otherwise lead to contamination.

Backflushing 2D GC analyses can also be performed with multiport rotary valves in place of the coupling tee union. While such valves are generally considered more appropriate for packed-column analyses, they can generate a more diverse set of flow patterns than fluidic devices. For example, ASTM method D 4815 [12] analyzes oxygenates in petroleum-based fuels

using a micropacked primary column containing 1,2,3-tris-(2-cyanoethoxy)propane (TCEP) followed by a poly(dimethylsiloxane) secondary column. The sample is initially injected into the TCEP column where the oxygenates and heavy hydrocarbons are strongly retained while the light hydrocarbons are only weakly retained. The rotary valve is initially in a position that causes the light hydrocarbons to be directed to an exhaust line as they elute from the primary column. When all of the light hydrocarbons have fully eluted from the TCEP column, the valve is rotated and the trapped oxygenates and heavy hydrocarbons are backflushed onto the poly(dimethylsiloxane) secondary column. The oxygenates elute individually from the secondary column and are detected with an FID, while most of the heavy hydrocarbons are strongly retained at the head of the nonpolar secondary column. The rotary valve is actuated back to its original position, and the heavy hydrocarbons are backflushed out of the secondary column to the FID.

While these two methods for analyzing oxygenates employ different hardware and different polar stationary phases, they exploit the same fundamental principle found in all backflushing 2D GC analyses: A precisely timed change in flow direction in the primary column removes sample matrix components that would otherwise coelute with the analytes at the exit of the secondary column.

7.4 Heartcutting 2D GC

Heartcutting 2D GC is a simple approach for isolating a few selected analytes from a large number of sample matrix components. Within the field of analytical chemistry, the generic term “two-dimensional gas chromatography” is often used to denote what will be called heartcutting 2D GC in this chapter.

7.4.1 Basic mode of operation

Heartcutting 2D GC divides the primary column effluent into a series of fractions. Fractions that contain the targeted analyte components along with any coeluting sample matrix components are directed to the secondary column, whereas fractions that contain only sample matrix components are directed to an exhaust flow restrictor. The general schematic of a 2D GC instrument shown in Fig. 7.2 can also serve as a schematic for a heartcutting 2D GC instrument. The interface is normally in a bypass state where the primary column effluent is directed to an exhaust flow restrictor. The interface is switched from the bypass state to an inject state immediately before an analyte elutes from the primary column. In the inject state, the primary effluent is directed to the head of the secondary column. As soon as the analyte has been loaded onto the secondary column, the interface is switched back to the bypass state.

Fig. 7.9 shows a simulation that demonstrates the key retention features associated with a

successful heartcutting 2D GC analysis of two analytes in a mixture containing 21 sample matrix components. The analytes are circled in the 2D plot shown in the center of Fig. 7.9. In the absence of heartcutting (see Fig. 7.9A), the analytes coelute with sample matrix components at the exit of the primary column and the exit of the secondary column (see the top and right of Fig. 7.9A). Fortunately, the matrix components overlapping with the analytes on the primary column are different than the matrix components that overlap on the secondary column. In such a case, heartcutting can isolate the analytes. The beginning and end of the two heartcuts in the simulation are shown in Fig. 7.9A with the dashed vertical lines. The effective 2D retention plane after performing two heartcuts is shown in Fig. 7.9B. Heartcutting removes all of the sample matrix components that were successfully separated from the analytes by the primary column. The secondary column only needs to separate the analytes from matrix components that coeluted on the primary column. In this simulation, the analytes are fully isolated by the time they exit the secondary column (see the chromatogram on the right side of Fig. 7.9B). Heartcutting 2D GC applies the full resolving power of a genuine two-dimensional separation, but only to a small number of analytes.

There are numerous interfaces that can be used to execute heartcuts. Multiport valves have been used extensively in the past, but many current methods employ a Deans' switch. The Deans' switch is a fluidic device introduced over 50 years ago [13] that uses an auxiliary flow to control the direction of the primary column effluent. A Deans' switch is constructed from a two-way, three-port solenoid valve and an assembly of tee junctions. A schematic of a simple Deans' switch is shown in Fig. 7.10. The exit of the primary column is connected to the center tee junction, while the secondary column and an exhaust flow restrictor are connected to the peripheral tee junctions. The auxiliary flow passes through the solenoid valve and then to

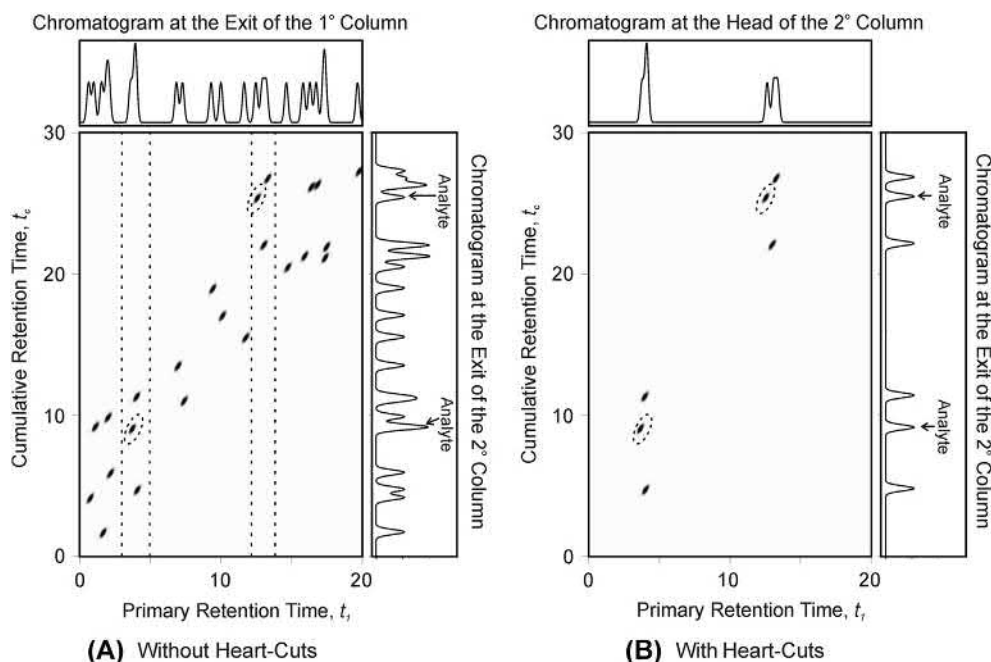


FIGURE 7.9 2D plots of a simulated heartcutting analysis. (A) Without heartcutting, the analytes (circled in the 2D plot) coelute with sample matrix components at the end of the primary column and at the end of the secondary column. (B) Two separate heartcuts are performed to prevent numerous sample matrix components from entering the secondary column. This allows the analytes to be fully separated from the sample matrix components at the end of the secondary column.

one of the two peripheral tee junctions. The bypass state is generated by having the solenoid valve introduce the auxiliary flow to the tee junction connected to the secondary column (see the left part of Fig. 7.10). The majority of the auxiliary flow goes to the secondary column while a smaller portion moves toward the center tee junction where it directs the incoming primary

column effluent to the exhaust flow restrictor. The inject state is generated by having the solenoid valve introduce the auxiliary flow to the tee junction connected to the exhaust restrictor (see the right part of Fig. 7.10). A small portion of the auxiliary flow goes to the center tee junction where it directs the primary column effluent to the secondary column.

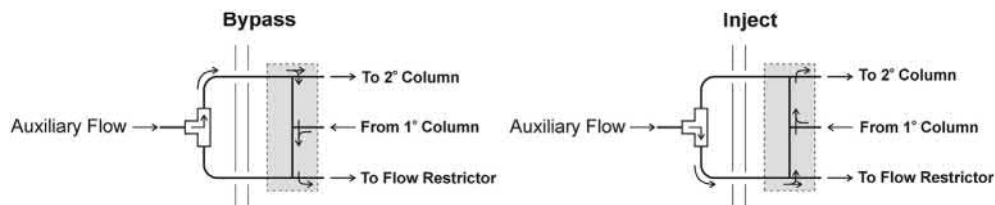


FIGURE 7.10 A simple Deans' switch. A Deans' switch is constructed from a solenoid valve placed outside the oven and an assembly of tee junctions placed inside the oven. The left side of the figure shows the Deans' switch in the "bypass" state where the primary column effluent is directed away from the secondary column and into the flow restrictor. The right side shows the switch in the "inject" state where the primary column effluent is directed into the secondary column.

Deans' switches have several advantages over multiport valves. The only moving part of the Deans' switch, the solenoid valve, is not in the sample path; thus, it can be placed outside of the oven. The portion of the device that contacts the sample, the tee junction assembly, is a static device that can be assembled from inert materials that are capable of operating over a broad range of temperatures. Tee junction assemblies can be constructed by combining three individual tee unions, but now several manufacturers make assemblies that integrate all of the necessary flow paths and connections into a single device [14]. This reduces dead volume within the device and decreases the likelihood of leaks. Transitioning a Deans' switch between the bypass and inject state does not significantly disturb the flow in the primary or secondary columns. Thus, heartcuts can be performed without affecting the primary retention times of later-eluting analytes. This allows multiple heartcuts to be made with high precision. In contrast, multiport valves require mechanical activation and cause brief but significant disturbances to the primary and secondary flows.

7.4.2 An example of heartcutting 2D GC: the analysis of 4,6-DMDBT in diesel fuel

The analysis of trace levels of 4,6-dimethyldibenzothiophene (4,6-DMDBT) in diesel fuel serves as a good example of a simple heartcutting 2D GC analysis. Diesel fuel contains thousands of hydrocarbon components and numerous sulfur compounds including 4,6-DMDBT. The concentration of sulfur compounds must be reduced to ppm levels to meet regulatory requirements. Refiners determine the efficacy of their sulfur mitigation strategies by monitoring the levels of 4,6-DMDBT because it is one of the most difficult compounds to remove. The analysis is normally done with GC and a sulfur-selective detector; however, McCurry and Quimby [15] have demonstrated

that heartcutting 2D GC with FID detection is also a viable strategy. They used a 15 m × 0.25 mm × 0.25 μm HP-5MS primary column followed by a 30 m × 0.25 mm × 0.25 μm Innowax secondary column. Preliminary studies with high levels of 4,6-DMDBT spiked into diesel fuel showed that 4,6-DMDBT had a primary retention time near 6.5 min. Thus, low levels of 4,6-DMDBT in diesel fuel were analyzed by using a Deans' switch to heartcut the components eluting from the primary column between 6.40 and 6.65 min (see Fig. 7.11A). The Innowax secondary column was selected because it retained 4,6-DMDBT more than the hydrocarbons that coeluted on the HP-5MS primary column (see Fig. 7.11B). The 4,6-DMDBT is fully isolated from the diesel fuel hydrocarbons, and the quantitative result is in excellent agreement with GC results obtained with an atomic emission detector. This method was found to be capable of accurately measuring 4,6-DMDBT levels down to 2 ppm.

7.4.3 Advanced applications: multiple heartcuts and independent column heating

The current generation of heartcutting 2D GC instruments is capable of making numerous, precisely timed heartcuts. For example, Gras et al. [16] have shown that a polyethylene glycol primary column coupled to a CP-PoraBonD Q column can be used to analyze alkyl mercaptans in natural gas. Four heartcuts were used to individually isolate the C₁ through C₄ mercaptans. Sciarrone et al. [17] have described the use of 13 heartcuts to evaluate the quality of Australian tea tree oil. A 5% diphenyl/95% dimethyl polysiloxane primary column was coupled to a polyethylene glycol secondary column. A mass spectrometer was used to monitor the secondary column effluent. With this approach, they were able to isolate and identify 18 critical components within the complex mixture.

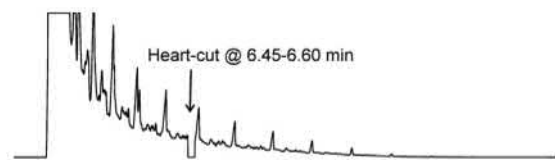
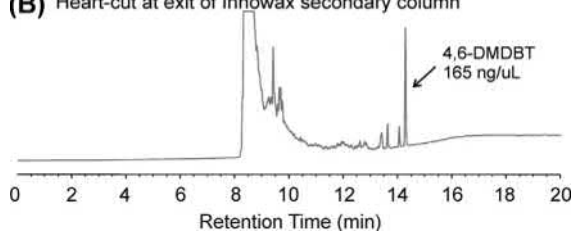
(A) Diesel fuel on HP-5 primary column**(B)** Heart-cut at exit of Innowax secondary column

FIGURE 7.11 Heartcutting 2D GC analysis of 4,6-DMDBT in diesel fuel. (A) The chromatogram obtained at the end of the primary column. A heartcut is performed from 6.40 to 6.65 min to direct the 4,6-DMDBT to the secondary column. (B) Chromatogram of the heartcut obtained at the end of the secondary column. The 4,6-DMDBT is fully separated from the hydrocarbons that coeluted on the primary column. Reprinted with permission from Ref. J.D. McCurry, B.D. Quimby, *Two-dimensional gas chromatography analysis of components in fuel and fuel additives using a simplified heart-cutting GC system*, *J. Chromatogr. Sci.* 41 (2003) 524–527. <http://www.ingentaconnect.com/content/pres/jcs/2003/00000041/00000010/art00003>; Copyright 2003, Preston Publications.

It is important to note that if multiple heartcuts are performed, care must be taken to ensure that the peaks from the adjacent fractions do not remix on the secondary column. This can be prevented by keeping the range of secondary retention times within each fraction less than the time between heartcuts. This measure ensures that a slow-moving component from a prior heartcut does not recombine with a fast-moving component from a subsequent heartcut. Thus, multiple heartcutting 2D GC requires that additional attention be paid to the chromatographic conditions including the column dimensions, carrier gas flow rates, and the column temperatures. Fortunately, GC instrumentation is constantly improving, and new technologies

are giving analysts unprecedented control. For example, direct heating of the capillary columns [18] allows the analyst to run independent temperature programs on the primary and secondary columns. This ability provides greater control over the range of secondary retention times and allows complicated heartcutting strategies to be successfully implemented.

7.5 Comprehensive 2D GC

Heartcutting 2D GC is effective for isolating a few important components, but much less effective for a broad-based characterization of sample composition. Comprehensive 2D gas chromatography ($GC \times GC$), a technique introduced nearly 30 years ago by John B. Phillips and Zaiyou Liu [19], is the only 2D GC method suited for a complete analysis of the sample composition. In contrast to backflushing and heartcutting, $GC \times GC$ passes each sample component through both the primary and secondary columns. The principles and applications of $GC \times GC$ have been the subject of numerous reviews [7–9,20–24].

7.5.1 Basic mode of operation

$GC \times GC$ analysis combines a standard GC separation in the primary column with a continuous repetition of separations in the secondary column. A $GC \times GC$ analysis is essentially an extreme version of heartcutting 2D GC with heartcuts being repeated at a rapid rate. The interface between the primary and secondary columns is called a modulator. The modulator transfers samples of primary column effluent to the secondary column at a constant interval called the modulation period. Each modulation event introduces primary effluent to the head of the secondary column as a narrow pulse. These narrow pulses are separated on the secondary column and passed on to the detector. One of the goals of all 2D GC analyses is to perform

secondary separations without significantly diminishing the separation produced by the primary column. GC \times GC achieves this goal by (1) operating with a modulation period that is less than the width of the peaks emerging from the primary column and (2) by keeping the range of secondary retention times less than the modulation period. These two measures require the individual secondary separations to be conducted on a timescale of seconds while the primary separation is often on the timescale of tens of minutes. The high speeds of the secondary separations are achieved by using a short narrow-bore column (e.g., 1 m \times 0.10 mm \times 0.10 μ m) or a high carrier gas flow.

The retention characteristics required for a successful GC \times GC analysis are demonstrated

in Fig. 7.12 for a three-component mixture. Due to the huge difference in the timescales of the primary and secondary separation, this simulation highlights a small portion of the primary separation. The components are assumed to have primary retention times between 60 and 80 s with primary widths of 10 s and secondary retention times between 0 and 3 s. Fig. 7.12A shows the case where the modulator allows primary column effluent to flow uninterrupted to the secondary column (i.e., the modulator is “turned off”). Due to the short secondary retention times and the high efficiency of the secondary column, the peaks in the 2D retention plot appear as a series of long, narrow, diagonal streaks situated very close to the $t_c = t_1$ line. The chromatograms generated at the end of the primary column (see the top of Fig. 7.12A) and

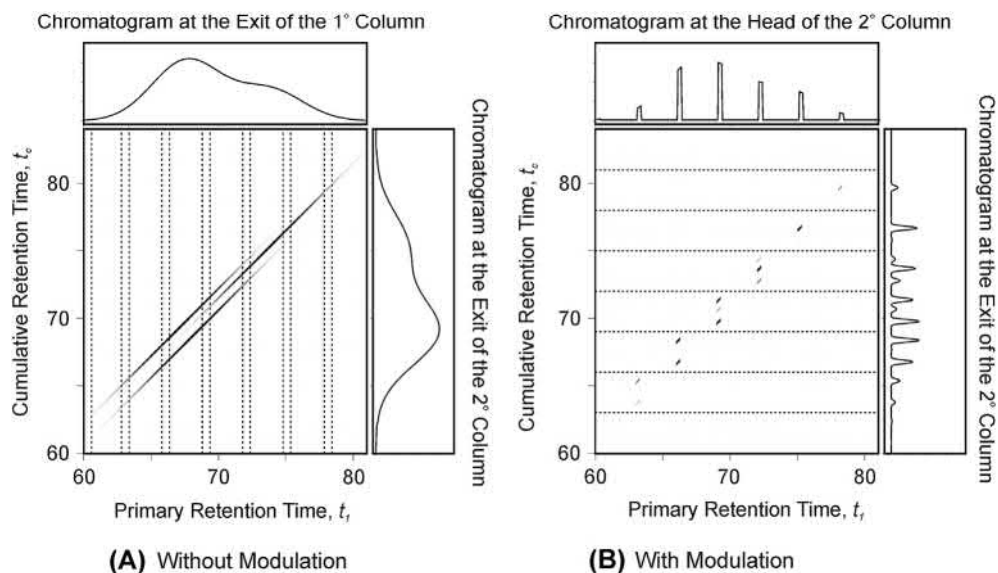


FIGURE 7.12 2D plots of a simulated GC \times GC analysis of three components. (A) Without modulation, the components appear as diagonal streaks in the 2D plot. This is because the short, highly efficient secondary column leads to secondary retention times that are less than the widths of the peaks along the primary dimension. The sampled sections of the 2D retention plot when modulation is performed are shown with the vertical *dashed lines*. (B) With modulation, the broad component peaks are replaced by a series of narrow pulses that enter the secondary column at the beginning of each modulation period (see the 1D chromatogram at the top of Fig. 7.12B) and exit the secondary column as a series of separated peaks (see the 1D chromatogram at the right of Fig. 7.12B).

at the end of the secondary column (see the right of Fig. 7.12A) look very similar in the absence of modulation due to the small retention time shifts generated by the short secondary column.

The modulated 2D plot is shown in Fig. 7.12B. In order to simulate modulation, it was assumed that the primary column effluent enters the secondary column for the first 10% of each 3.0 s modulation period. The primary column effluent is sent to an exhaust vent for the remaining 90% of the modulation period. Thus, the modulator essentially performs a 0.3 s heartcut every 3 s. The sampled slices of primary effluent are shown between the vertical dashed lines in Fig. 7.12A. The act of modulation causes a series of 0.3 s pulses to enter the secondary column every 3.0 s (see the top of Fig. 7.12B). The secondary separation is conducted within the baseline spaces between these input pulses. The components are retained to varying degrees in the secondary column and reach the detector as numerous individual peaks (see the right side of Fig. 7.12B). The high efficiency of the secondary column allows the peaks to retain much of the sharpness of the original input pulses.

When the range of secondary retention times is kept below the modulation period, the components injected in a particular modulation cycle do not overlap with components from previous or subsequent modulation cycles. This is demonstrated in the 2D graph in Fig. 7.12B by the absence of horizontal overlap between the groups of peaks resulting from individual modulation cycles. Under such conditions, the chromatogram obtained at the end of the secondary column is composed of segments that map directly to discrete regions of the 2D retention plane. This allows a 2D chromatogram to be constructed from the 1D chromatogram. This process is shown in Fig. 7.13. The first step is to divide the modulated chromatogram into a series of segments that have the length of the modulation period (see the top of Fig. 7.13). These segments are then rotated 90 degrees and stacked side by side to generate a 2D

chromatogram (see middle of Fig. 7.13). In practice, the 2D chromatograms generated by GC \times GC are usually displayed as a linearly interpolated contour plot (see bottom of Fig. 7.13). The primary retention time is displayed on the horizontal axis and the secondary retention time is displayed on the vertical axis. The construction of 2D chromatograms requires software that is normally not included with the software used to operate conventional gas chromatographs.

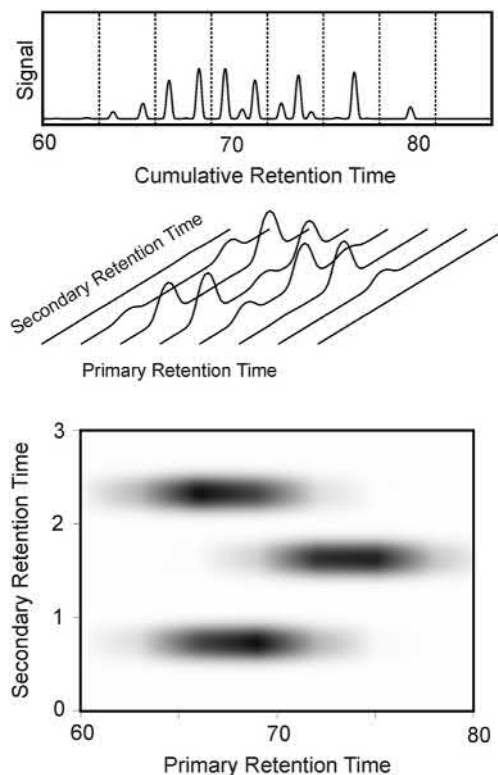


FIGURE 7.13 The process of converting the signal array into a 2D chromatogram. The signal array is first divided into segments with widths given by the modulation period (see top graph). The individual segments are stacked side by side to generate a 2D chromatogram (see middle graph). 2D chromatograms are most often displayed as a contour plot (see bottom graph).

If the range of secondary retention times exceeds the modulation period, then an unambiguous construction of the 2D chromatogram cannot be produced from the 1D chromatogram. In practice, it is common for a few components to experience high secondary retention and to fall outside the preferred range. Such components appear to be “wrapped around” in the 2D chromatogram. As long as only a few components are wrapped around, the resulting 2D chromatograms are still useful.

7.5.2 GC × GC modulators

The modulator is a piece of hardware that is unique to GC × GC, and it plays a critical role in the resolution produced by a GC × GC separation. The development of GC × GC modulators continues to this day. Numerous reviews have described the operating principles and relative merits of the modulator technology introduced over the past three decades [9,23,25]. Two classes of modulators have been developed: valve-based modulators and thermal modulators. Valve-based modulation strategies will be considered first in this chapter as they have much in common with the flow switching technology used in backflushing and heartcutting 2D GC. However, it should be kept in mind that thermal modulation has been used more frequently than valve-based modulation.

Valve-based modulation was introduced by Bruckner et al. [26] 7 years after the original GC × GC work of Phillips and Liu. Bruckner et al. used a high-speed diaphragm valve to produce a series of pulses at the head of the secondary column. Their modulator transferred only a small fraction of the primary column effluent to the secondary column and thus is classified as a low-duty-cycle modulator. The study of Bruckner et al. showed that a modulator constructed with off-the-shelf components could be combined with a standard GC to create an effective, high-speed GC × GC instrument. Several other

low-duty-cycle modulators have been introduced [27–30] since the original work of Bruckner et al.

Low quantitative precision is possible when employing a low-duty-cycle modulator. If the modulation period is too long, then the total amount of the component transferred to the secondary column depends on the position of the primary peak within the sequence of modulation events [31]. For example, if the modulation period is substantially larger than the width of the peak emerging from the primary column, then the entire peak would be missed if it eluted between injections into the secondary column. The ratio of the primary peak width (4σ) to the modulation period is known as the modulation ratio [32]. Theoretical and experimental studies [29,31,33] have shown that when the modulation ratio is kept above 3.0, the fraction of effluent transferred to the secondary column is essentially constant. This means that if the modulation produces three or more significant pulses per primary peak, then the quantitative precision is not diminished by employing a low-duty-cycle modulator.

While low-duty-cycle modulators can produce precise quantitative measurements, they are not optimized for high sensitivity as most of the primary effluent does not reach the detector. The majority of GC × GC separations have been performed with modulators that transfer 100% of the primary column effluent to the secondary column (i.e., they have duty cycles of 1). These modulators work by accumulating the primary effluent throughout the modulation period and then introducing the effluent as a pulse at the end of the modulation period. Full transfer modulators are well suited for analyses requiring high sensitivity. In addition, these devices do not cause a decrease in quantitative precision when operated at a large modulation ratio; however, large modulation ratios lead to diminished chromatographic resolution along the primary axis [34]. Two classes of full transfer modulators have been developed: differential flow modulators and thermal modulators.

Differential flow modulation is a valve-based technique first demonstrated by Seeley et al. [35] using a diaphragm valve fitted with a sample loop. The primary effluent is collected in the sample loop. Near the end of the modulation period, the valve is actuated and the loop contents are flushed into the secondary column. The flow rate of carrier gas is much higher in the secondary column than in the primary column (e.g., 15 mL min^{-1} secondary flow and 1 mL min^{-1} primary flow). Thus, the time required to flush the loop is much less than the time required to fill the loop. Alternating between the fill and flush states of the valve leads to a series of high-intensity pulses from each primary peak. Several designs of differential flow modulators have been introduced including simple fluidic devices that sample all of the primary column effluent [36,37].

The main limitations of differential flow modulation are caused by the high secondary flow rate. High carrier gas velocities in the secondary column lead to increased plate heights. Fortunately, longer secondary columns can be used to partially offset the loss in secondary resolution [35]. Narrow-bore columns (i.e., diameter $<0.25 \text{ mm}$) are rarely used in differential flow modulation GC \times GC because of the extremely high head pressures that would be required to generate high flow rates. Perhaps the biggest drawback of differential flow modulation is that the high flows do not allow the secondary column to be directly coupled to a mass spectrometer. However, Poliak et al. [38] have shown that mass spectrometers with differentially pumped vacuum chambers are compatible with differential flow modulation.

Thermal modulators are the most commonly used GC \times GC modulators. They employ precisely timed temperature changes to convert primary peaks into concentrated pulses. The original GC \times GC modulator of Liu and Phillips [19] was a thermal modulator that accumulated components in a thick-film capillary column situated between the primary and secondary

column. Concentrated pulses were generated by the two-stage heating of the trapping capillary. In 1998, Marriot and Kinghorn [39] introduced the longitudinally modulated cryogenic system. This system employs a cryogenic fluid to cool a capillary joining the primary and secondary columns. Components eluting from the primary column condense inside the capillary at the location of the cooled region. Precise movement of the cooled region along the length of the capillary segment produces extremely sharp pulses of primary effluent.

Today, most commercially produced thermal modulators are two-stage devices that use jets of gas to cool and heat two small sections of a capillary joining the primary and secondary columns [40–42]. Fig. 7.14 shows the cryogenic modulator developed and marketed by Zoex Corporation [43]. The modulator is situated inside the main GC column oven. A jet of cold nitrogen is sprayed onto a capillary loop. The looped configuration causes the cold jet to hit the capillary in two places. Primary column effluent accumulates in the cold spots. A jet of hot gas is pulsed in a precise manner to heat the cold spots to release the accumulated components.

The basic mechanism for two-stage thermal modulation is illustrated in Fig. 7.15. The plots represent the spatial concentration profile of a component as it moves down the length of the

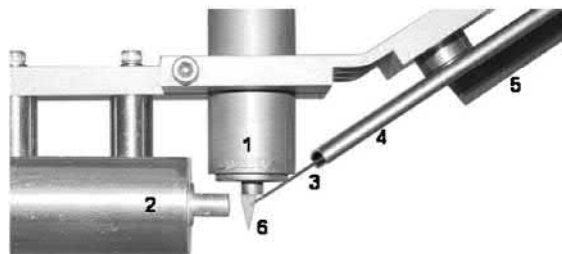


FIGURE 7.14 The cryogenic loop modulator from Zoex: (1) cold jet assembly; (2) hot jet assembly; (3) capillary loop; (4) loop clip; (5) loop retainer; (6) cold jet. Copyright Zoex Corporation.

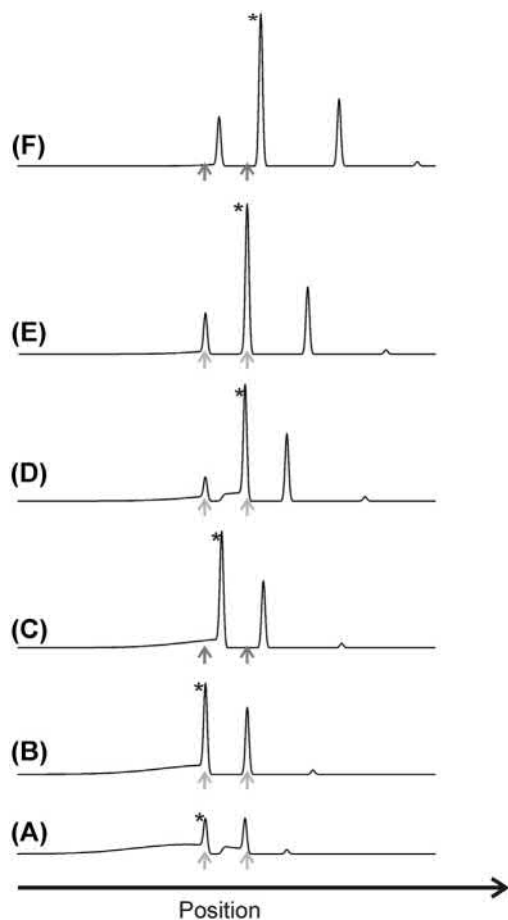


FIGURE 7.15 Two-stage thermal modulation. The carrier gas moves from left to right bringing a single component from the exit of the primary column into the modulator. The positions of the two heating/cooling spots are designated with arrows. This analysis follows the formation of a single pulse designated with the star: (A) A portion of a component emerging from the primary column is accumulated in the upstream cold spot. (B) The amount of collected material increases with time. (C) The hot jets heat the capillary column and cause the focused material to be released. (D) The hot jets are turned off and the pulse moves into the downstream cold spot where it is focused further. (E) The pulse is fully focused with no tail. (F) The hot jets heat the capillary column to release a sharp pulse into the carrier stream that heads to the secondary column.

capillary joining the primary and secondary columns. The capillary is cooled in an upstream location and a downstream location. Both locations are shown with arrows in Fig. 7.15. The sequence of events leading to the formation of a single pulse is described further: As a component elutes from the primary column, it moves through the capillary from left to right. Fig. 7.15A shows the central portion of the primary peak as it encounters the upstream cold spot shown with the left arrow. The low temperature condenses the component and forms the concentration pulse highlighted with a star. The component continues to flow into the upstream cold spot causing the pulse amplitude to grow as shown in Fig. 7.15B. At a specified time, the cooling is replaced by heating as shown in Fig. 7.15C. The rapid increase in temperature causes the accumulated pulse to be released into the carrier gas and then move downstream (i.e., to the right in Fig. 7.15C). During this brief heating period, unfocused material passes through the upstream zone producing a tail on the left side of the focused pulse. After a brief period, the cold jet is reapplied as shown in Fig. 7.15D, while the pulse and shoulder move downstream. The pulse and shoulder enter the downstream cold spot where they are focused further into a single pulse as shown in Fig. 7.15E. Finally, a sharp symmetric pulse is released to the secondary column by heating the downstream cold spot as shown in Fig. 7.15F. This entire sequence is repeated throughout the chromatographic run and, in the process, converts primary column peaks into a series of highly focused pulses that enter the secondary column for further separation. Two-stage thermal modulation can produce pulses with widths less than 50 ms and concentrations that are increased by nearly two orders of magnitude [41].

In terms of chromatographic performance, thermal modulation is superior to valve-based strategies. However, thermal modulation GC \times GC is more expensive to implement. Most thermal modulators use large amounts of liquid cryogen and working fluid. This represents a substantial increase in consumable costs when compared to conventional GC and mostly limits thermal modulation GC \times GC to well-funded R&D laboratories. However, several research groups have recently developed thermal modulators that do not require liquid cryogen [9,25,44,45]. It remains to be seen if these low-resource modulators can match the outstanding performance of cryogenic modulators.

7.5.3 Detection and quantitation in GC \times GC separations

The peaks exiting the secondary column in a GC \times GC analysis often have widths on the order of 100 ms. Thus, it is imperative that the detector has a fast response time, low internal volume, and 50 Hz or greater sampling rates. To date, the FID has been the most common GC \times GC detector. The stable, fairly uniform response of the FID makes it particularly well suited for the comprehensive analysis of complex organic mixtures. Studies have also been performed with several selective detectors such as the electron-capture detector and the sulfur chemiluminescence detector [46].

Mass spectrometry (MS) is an especially effective GC \times GC detector and has been the subject of review articles [47,48]. Numerous studies have been performed with quadrupole mass spectrometers, but the scanning rates of these analyzers (<20 Hz) make them incompatible for GC \times GC separations that generate especially narrow peaks. Time-of-flight mass spectrometers (TOFMS) are ideally suited for GC \times GC analysis as they can easily generate full scans at a rate \geq 100 Hz. Several companies now market fully integrated GC \times GC–TOFMS systems.

Quantitation in GC \times GC is complicated by the fact that a single component produces several 1D peaks. However, software is available that automatically groups the peaks according to their position in the 2D plane and provides precision that matches that of conventional single-column GC [49]. Furthermore, the detection limits of GC \times GC are often better than those of GC because peak overlap is greatly reduced and peak intensities are increased when thermal modulators or differential flow modulators are used. Chemometric data analysis strategies can often greatly increase the resolution and sensitivity of GC \times GC. Several reviews of developments in the application of chemometrics to GC \times GC have been published [8,50,51].

7.5.4 Example GC \times GC application I: the aromatic composition of gasoline

GC \times GC is particularly well suited to analyze the composition of complex petrochemical mixtures. Seeley et al. [29] used a GC \times GC instrument equipped with a Deans' switch modulator (see Fig. 7.16) to determine the aromatic composition of gasoline. A 15 m \times 0.25 mm \times 0.50 μ m poly(dimethylsiloxane) primary column was coupled to a 2.5 m \times 0.25 mm \times 0.25 μ m polyethylene glycol secondary column. A modulation period of 1.0 s was employed with the modulator in the inject state for 0.07 s at the beginning of each modulation period. Thus, only 7% of each component was passed from the primary column to the secondary column. A typical GC \times GC chromatogram of gasoline is shown in Fig. 7.17. The primary retention times ranged from 60 to 500 s and the secondary retention times ranged from 1.2 to 2.2 s. Individual peaks were observed to have 100 ms widths along the secondary axis.

Adding modulation and a secondary separation greatly increased the peak capacity of the analysis. This can be observed in Fig. 7.17 by

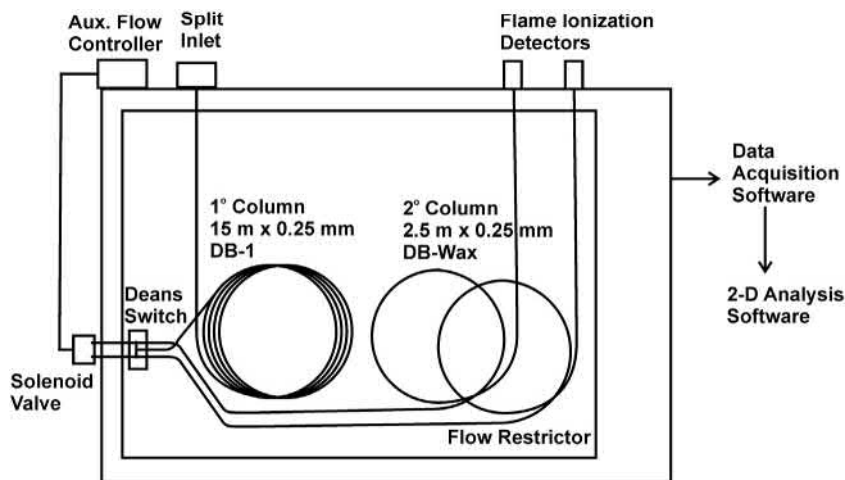


FIGURE 7.16 GC \times GC apparatus employing a Deans' switch modulator. Gasoline samples were injected into a split inlet and then passed through a nonpolar primary column. A Deans' switch was used to transfer the primary column effluent as a series of pulses to the polyethylene glycol secondary column. Gasoline components were detected with an FID. Reprinted with permission from Ref. J.V. Seeley, N.J. Micyus, S.V. Bandurski, S.K. Seeley, J.D. McCurry, *Microfluidic Deans switch for comprehensive two-dimensional gas chromatography*, *Anal. Chem.* 79 (2007) 1840–1847, <http://doi.org/10.1021/ac061881g>; Copyright 2007, American Chemical Society.

noting the number of peaks that share the same primary retention time but are separated in the secondary dimension. In addition to greater peak capacity, GC \times GC analysis often produces

“structured” chromatograms. This is demonstrated in the gasoline chromatogram by the formation of peak clusters representing specific compound classes. Saturated hydrocarbons

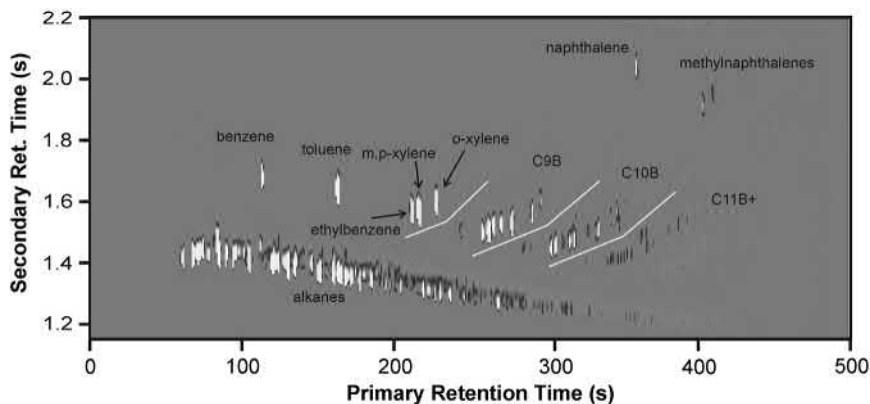


FIGURE 7.17 Deans' switching GC \times GC analysis of gasoline. Compound classes were observed to form distinct peak clusters in the chromatogram. The alkybenzene classes are highlighted in the chromatogram. Reprinted with permission from Ref. J.V. Seeley, N.J. Micyus, S.V. Bandurski, S.K. Seeley, J.D. McCurry, *Microfluidic Deans switch for comprehensive two-dimensional gas chromatography*, *Anal. Chem.* 79 (2007) 1840–1847, <http://doi.org/10.1021/ac061881g>; Copyright 2007, American Chemical Society.

form a narrow band with low secondary retention running horizontally across the base of the 2D chromatogram. The alkylbenzenes form a series of “roof-tile” bands with moderate secondary retention. Each roof tile corresponds to a group of alkylbenzene isomers having the same number of carbon atoms. The diaromatic compounds (i.e., naphthalene and methylnaphthalene) have a large primary and secondary retention and are located in the upper-right corner of the chromatogram. Seeley et al. determined the concentration of each compound class from the total peak areas within each group. Excellent agreement was observed between the concentrations determined with Deans’ switching GC \times GC and GC-MS.

7.5.5 Example GC \times GC application II: GC \times GC-MS analysis of yeast extracts

GC \times GC–TOFMS was used by Mohler et al. [52] to identify chemical differences in the metabolite extracts of yeast cells. The extracts were methoximated and trimethylsilylated prior to analysis. Mohler et al. used a GC \times GC instrument equipped with a quad-jet cryogenic modulator and a TOFMS that were both manufactured by Leco (see Fig. 7.18). A 20 m \times 0.25 mm \times 0.50 μ m 5% phenyl/95% dimethyl polysiloxane primary column was coupled to a 2.0 m \times 0.18 mm \times 0.20 μ m poly(trifluoropropylmethylsiloxane) secondary column. Extracts were analyzed with a 1.5 s modulation period and a total run time of 37.75 min. The mass spectrometer produced 100 spectra/s with a mass range of 40–600 m/z .

A typical 2D chromatogram of a sample extract is shown in Fig. 7.19A. This particular chromatogram was obtained for a mass channel, $m/z = 73$, that represents the trimethylsilyl functional group. Over 2500 individual peaks can be observed in the chromatogram.

Fig. 7.19B is a zoomed-in portion of the 2D chromatogram that demonstrates the high resolution and complexity of the chromatogram. The mass spectra produced by the instrument allowed full 2D chromatograms to be generated for each mass channel. This provides the ability to produce 2D chromatograms that are selective for a particular compound class. For example, the $m/z = 205$ mass fragment is known to be indicative of trimethylsilyl derivatives of carbohydrates. Thus, the 2D chromatogram of this channel (see Fig. 7.19C) is representative of carbohydrate composition. Similarly, the 2D chromatogram obtained at $m/z = 387$ (see Fig. 7.19D) represents the trimethylsilyl derivatives of sugar phosphates. The key point is that “real world” samples such as yeast metabolite extracts produce extremely complex chromatograms even when GC \times GC is used. The resolution gained by adding time-of-flight mass spectrometry can both greatly reduce the complexity of the 2D chromatograms and greatly increase the amount and quality of information produced.

7.6 Conclusions

This chapter has described several basic approaches for combining two GC separations. Backflushing 2D GC separates an entire class of analyte components from the sample matrix by employing a single change in primary-column flow direction. To be successful, the polarity difference between the analyte class and the sample matrix must be quite large. Heartcutting 2D GC separates targeted analytes from the sample matrix. Subtle retention differences can be exploited to fully resolve individual analytes. GC \times GC combines a standard GC separation with a series of high-speed secondary separations. GC \times GC can be used for the comprehensive analysis of the sample

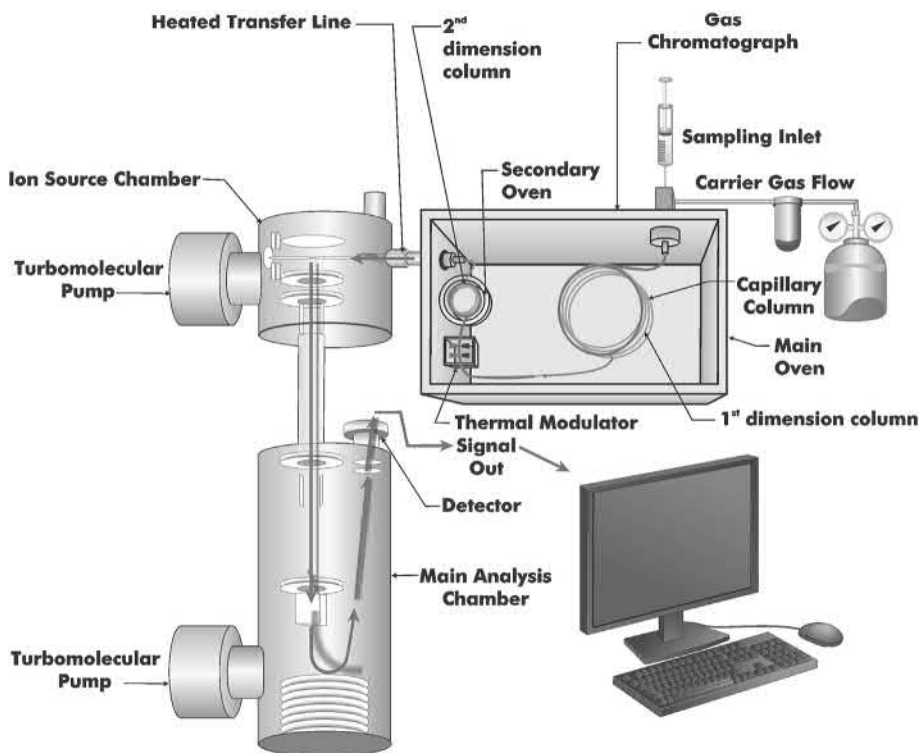


FIGURE 7.18 Leco GC \times GC-TOFMS system. This system uses a quad-jet thermal modulator and a high speed time-of-flight mass spectrometer. Copyright Leco.

composition, and it is also effective at class separations and monitoring individual analytes. All three of these 2D GC approaches have been successfully applied to the analysis of complex mixtures such as petroleum-based fuels, flavors and fragrances, and environmental samples.

It is important to note that the individual forms of 2D GC separations examined in this chapter can be combined. For example, Maikhunthod et al. [53] constructed an apparatus that can perform both GC \times GC and heartcutting 2D GC analyses. An overview of sample composition is first obtained

with GC \times GC and then heartcutting 2D GC is used to isolate a few particularly important analytes. Several groups have also shown that additional GC stages can be added to generate multidimensional GC separations. For example, Watson et al. [54] reported the successful implementation of comprehensive three-dimensional gas chromatography (GC³). A third dimension of separation is added by injecting the secondary effluent into a tertiary column every 200 ms. It is clear that future research efforts will continue to discover effective ways of exploiting the benefits of combining GC separations.

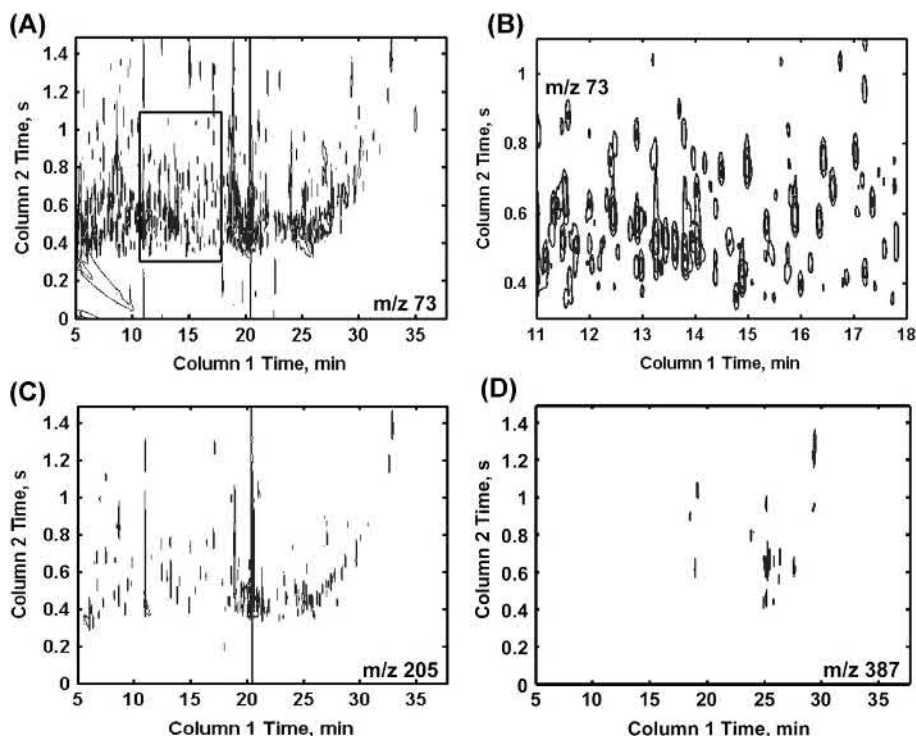


FIGURE 7.19 GC \times GC–TOFMS chromatograms of yeast metabolite extract. (A) Chromatogram obtained at $m/z = 73$ indicative of trimethylsilyl derivatives. (B) Zoomed-in version of the chromatogram shown in panel A. (C) Chromatogram obtained at $m/z = 205$ indicative of carbohydrates. (D) Chromatogram obtained at $m/z = 387$ indicative of sugar phosphates. Reprinted with permission from Ref. R.E. Mohler, K.M. Dombek, J.C. Hoggard, E.T. Young, R.E. Synovec, *Comprehensive two-dimensional gas chromatography time-of-flight mass spectrometry analysis of metabolites in fermenting and respiring yeast cells*, *Anal. Chem.* 78 (2006) 2700–2709, <http://doi.org/10.1021/ac052106o>; Copyright 2006, American Chemical Society.

References

- [1] J.M. Davis, J.C. Giddings, Statistical theory of component overlap in multicomponent chromatograms, *Anal. Chem.* 55 (1983) 418–424, <https://doi.org/10.1021/ac00254a003>.
- [2] K.L. Goodner, Practical retention index models of OV-101, DB-1, DB-5, and DB-Wax for flavor and fragrance compounds, *LWT - Food Sci. Technol.* 41 (2008) 951–958. <http://www.sciencedirect.com/science/article/pii/S0023643807002605>.
- [3] M.C. Simmons, L.R. Snyder, Two-stage gas-liquid chromatography, *Anal. Chem.* 30 (1958) 32–35, <https://doi.org/10.1021/ac60133a007>.
- [4] J.C. Giddings, Use of multiple dimensions in analytical separations, in: H.J. Cortes (Ed.), *Multidimens. Chromatogr. Techniques Appl.*, M. Dekker, New York, 1990, pp. 1–27.
- [5] W. Bertsch, Two-dimensional gas chromatography. Concepts, instrumentation, and applications – Part 1: fundamentals, conventional two-dimensional gas chromatography, selected applications, *J. High Resolut. Chromatogr.* 22 (1999) 647–665, [https://doi.org/10.1002/\(sici\)1521-4168\(19991201\)22:12<647::aid-jhrc647>3.0.co;2-v](https://doi.org/10.1002/(sici)1521-4168(19991201)22:12<647::aid-jhrc647>3.0.co;2-v).
- [6] W. Bertsch, Two-dimensional gas chromatography. Concepts, instrumentation, and applications – Part 2: comprehensive two-dimensional gas chromatography,

- J. High Resolut. Chromatogr. 23 (2000) 167–181, [https://doi.org/10.1002/\(sici\)1521-4168\(20000301\)23:3<167::aid-jhrc167>3.0.co;2-2](https://doi.org/10.1002/(sici)1521-4168(20000301)23:3<167::aid-jhrc167>3.0.co;2-2).
- [7] J.V. Seeley, S.K. Seeley, Multidimensional gas chromatography: fundamental advances and new applications, *Anal. Chem.* 85 (2013) 557–578, <https://doi.org/10.1021/ac303195u>.
- [8] S.E. Prebitalo, K.L. Berrier, C.E. Freye, H.D. Bahaghighat, N.R. Moore, D.K. Pinkerton, R.E. Synovec, Multidimensional gas chromatography: advances in instrumentation, chemometrics, and applications, *Anal. Chem.* 90 (2018) 505–532, <https://doi.org/10.1021/acs.analchem.7b04226>.
- [9] M.S.S. Amaral, Y. Nolvachai, P.J. Marriott, Comprehensive two-dimensional gas chromatography advances in technology and applications: biennial update, *Anal. Chem.* (2020), <https://doi.org/10.1021/acs.analchem.9b05412>.
- [10] C.F. Poole, S.K. Poole, Separation characteristics of wall-coated open-tubular columns for gas chromatography, *J. Chromatogr. A.* 1184 (2008) 254–280, <https://doi.org/10.1016/j.chroma.2007.07.028>.
- [11] A. Tipler, Application Note: Determination of Low-Level Oxygenated Compounds in Gasoline Using the Clarus 680 GC with S-Swafer Micro-channel Flow Technology, 2010.
- [12] Standard Test Method D4815 for Determination of MTBE, ETBE, TAME, DIPE, Tertiary-Amyl Alcohol and C1 to C4 Alcohols in Gasoline by Gas Chromatography, 2009.
- [13] D.R. Deans, A new technique for heart cutting in gas chromatography, *Chromatographia* 1 (1968) 18–22.
- [14] B.D. Quimby, J.D. McCurry, W.M. Norman, Capillary Flow Technology for Gas Chromatography: Reinvigorating a Mature Analytical Discipline, LCGC Peak, 2007, pp. 7–15.
- [15] J.D. McCurry, B.D. Quimby, Two-dimensional gas chromatography analysis of components in fuel and fuel additives using a simplified heart-cutting GC Ssystem, *J. Chromatogr. Sci.* 41 (2003) 524–527. <http://www.ingentaconnect.com/content/pres/jcs/2003/00000041/00000010/art00003>.
- [16] R. Gras, J. Luong, V. Carter, L. Sieben, H. Cortes, Practical method for the measurement of Alkyl mercaptans in natural gas by multi-dimensional gas chromatography, capillary flow technology, and flame ionization detection, *J. Chromatogr. A.* 1216 (2009) 2776–2782. <http://www.sciencedirect.com/science/article/pii/S0021967308015021>.
- [17] D. Sciarrone, C. Ragonese, C. Carnovale, A. Piperno, P. Dugo, G. Dugo, L. Mondello, Evaluation of tea tree oil quality and ascaridole: a deep study by means of chiral and multi heart-cuts multidimensional gas chromatography system coupled to mass spectrometry detection, *J. Chromatogr. A.* 1217 (2010) 6422–6427. <http://www.sciencedirect.com/science/article/pii/S002196731001071X>.
- [18] J. Luong, R. Gras, G. Yang, H. Cortes, R. Mustachich, Multidimensional gas chromatography with capillary flow technology and LTM-GC, *J. Separ. Sci.* 31 (2008) 3385–3394, <https://doi.org/10.1002/jssc.200800163>.
- [19] Z. Liu, J.B. Phillips, Comprehensive two-dimensional gas chromatography using an on-column thermal modulator interface, *J. Chromatogr. Sci.* 29 (1991) 227–231, <https://doi.org/10.1093/chromsci/29.6.227>.
- [20] A.M. Muscalu, T. Górecki, Comprehensive two-dimensional gas chromatography in environmental analysis, *TrAC Trends Anal. Chem. (Reference Ed.)* 106 (2018) 225–245, <https://doi.org/10.1016/j.trac.2018.07.001>.
- [21] B. Gruber, B.A. Weggler, R. Jaramillo, K.A. Murrell, P.K. Piotrowski, F.L. Dorman, Comprehensive two-dimensional gas chromatography in forensic science: a critical review of recent trends, *TrAC Trends Anal. Chem.* 105 (2018) 292–301, <https://doi.org/10.1016/j.trac.2018.05.017>.
- [22] B.J. Pollo, G.L. Alexandrino, F. Augusto, L.W. Hantao, The impact of comprehensive two-dimensional gas chromatography on oil & gas analysis: recent advances and applications in petroleum industry, *TrAC Trends Anal. Chem.* 105 (2018) 202–217, <https://doi.org/10.1016/j.trac.2018.05.007>.
- [23] P.Q. Tranchida, Comprehensive two-dimensional gas chromatography: a perspective on processes of modulation, *J. Chromatogr. A.* 1536 (2018) 2–5, <https://doi.org/10.1016/j.chroma.2017.04.039>.
- [24] L. Lebanov, L. Tedone, M. Kaykhaai, M.R. Linford, B. Paull, Multidimensional gas chromatography in essential oil analysis. Part 1: technical developments, *Chromatographia* 82 (2019) 377–398, <https://doi.org/10.1007/s10337-018-3649-3>.
- [25] H.D. Bahaghighat, C.E. Freye, R.E. Synovec, Recent advances in modulator technology for comprehensive two dimensional gas chromatography, *TrAC Trends Anal. Chem.* 113 (2019) 379–391, <https://doi.org/10.1016/j.trac.2018.04.016>.
- [26] C.A. Bruckner, B.J. Prazen, R.E. Synovec, Comprehensive two dimensional high-speed gas chromatography with chemometric analysis, *Anal. Chem.* 70 (1998) 2796–2804.
- [27] J.F. Hamilton, A.C. Lewis, K.D. Bartle, Peak amplitude and resolution in comprehensive gas chromatography using valve modulation, *J. Separ. Sci.* 26 (2003) 578–584.

- [28] A.E. Sinha, B.J. Prazen, C.G. Fraga, R.E. Synovec, Valve-based comprehensive two-dimensional gas chromatography with time-of-flight mass spectrometric detection: instrumentation and figures-of-merit, *J. Chromatogr. A*. 1019 (2003) 79–87, <https://doi.org/10.1016/j.chroma.2003.08.047>.
- [29] J.V. Seeley, N.J. Micyus, S.V. Bandurski, S.K. Seeley, J.D. McCurry, Microfluidic Deans switch for comprehensive two-dimensional gas chromatography, *Anal. Chem.* 79 (2007) 1840–1847, <https://doi.org/10.1021/ac061881g>.
- [30] A. Ghosh, C.T. Bates, S.K. Seeley, J.V. Seeley, High speed Deans switch for low duty cycle comprehensive two-dimensional gas chromatography, *J. Chromatogr. A*. 1291 (2013) 146–154, <https://doi.org/10.1016/j.chroma.2013.04.003>.
- [31] J.V. Seeley, Theoretical study of incomplete sampling of the first dimension in comprehensive two-dimensional chromatography, *J. Chromatogr. A*. 962 (2002) 21–27.
- [32] W. Khummueng, J. Harynuk, P.J. Marriott, Modulation ratio in comprehensive two-dimensional gas chromatography, *Anal. Chem.* 78 (2006) 4578–4587, <https://doi.org/10.1021/ac052270b>.
- [33] W.C. Siegler, B.D. Fitz, J.C. Hoggard, R.E. Synovec, Experimental study of the quantitative precision for valve-based comprehensive two-dimensional gas chromatography, *Anal. Chem.* 83 (2011) 5190–5196, <https://doi.org/10.1021/ac200302b>.
- [34] R.E. Murphy, M.R. Schure, J.P. Foley, Effect of sampling rate on resolution in comprehensive two-dimensional liquid chromatography, *Anal. Chem.* 70 (1998) 1585–1594.
- [35] J.V. Seeley, F. Kramp, C.J. Hicks, Comprehensive two-dimensional gas chromatography via differential flow modulation, *Anal. Chem.* 72 (2000) 4346–4352.
- [36] J.V. Seeley, N.J. Micyus, J.D. McCurry, S.K. Seeley, Comprehensive two-dimensional gas chromatography with a simple fluidic modulator, *Am. Lab. News*. 38 (2006) 24.
- [37] J.F. Griffith, W.L. Winniford, K. Sun, R. Edam, J.C. Luong, A reversed-flow differential flow modulator for comprehensive two-dimensional gas chromatography, *J. Chromatogr. A*. 1226 (2012) 116–123, <https://doi.org/10.1016/j.chroma.2011.11.036>.
- [38] M. Poliak, A.B. Fialkov, A. Amirav, Pulsed flow modulation two-dimensional comprehensive gas chromatography-tandem mass spectrometry with supersonic molecular beams, *J. Chromatogr. A*. 1210 (2008) 108–114, <https://doi.org/10.1016/j.chroma.2008.09.039>.
- [39] P.J. Marriott, R.M. Kinghorn, Longitudinally modulated cryogenic system. A generally applicable approach to solute trapping and mobilization in gas chromatography, *Anal. Chem.* 69 (1997) 2582–2588, <https://doi.org/10.1021/ac961310w>.
- [40] E.B. Ledford Jr., C.A. Billesbach, J.R. Termaat, *Transverse Thermal Modulation*, 2003.
- [41] J. Beens, M. Adahchour, R.J.J. Vreuls, K. van Altena, U.A.T. Brinkman, Simple, non-moving modulation interface for comprehensive two-dimensional gas chromatography, *J. Chromatogr. A*. 919 (2001) 127–132. <http://www.sciencedirect.com/science/article/pii/S0021967301007853>.
- [42] J. Harynuk, T. Górecki, New liquid nitrogen cryogenic modulator for comprehensive two-dimensional gas chromatography, *J. Chromatogr. A*. 1019 (2003) 53–63. <http://www.sciencedirect.com/science/article/pii/S0021967303016479>.
- [43] E.B. Ledford Jr., *Method and Apparatus for Measuring Velocity of Chromatographic Pulse*, 2007.
- [44] M. Libardoni, J.H. Waite, R. Sacks, Electrically heated, air-cooled thermal modulator and at-column heating for comprehensive two-dimensional gas chromatography, *Anal. Chem.* 77 (2005) 2786–2794, <https://doi.org/10.1021/ac040161b>.
- [45] O. Panić, T. Górecki, C. McNeish, A.H. Goldstein, B.J. Williams, D.R. Worton, S. V. Hering, N.M. Kreisberg, Development of a new consumable-free thermal modulator for comprehensive two-dimensional gas chromatography, *J. Chromatogr. A*. 1218 (2011) 3070–3079, <https://doi.org/10.1016/j.chroma.2011.03.024>.
- [46] M. Adahchour, J. Beens, U.A.T. Brinkman, Recent developments in the application of comprehensive two-dimensional gas chromatography, *J. Chromatogr. A*. 1186 (2008) 67–108. <http://www.sciencedirect.com/science/article/pii/S0021967308000216>.
- [47] L. Mondello, P.Q. Tranchida, P. Dugo, G. Dugo, Comprehensive two-dimensional gas chromatography-mass spectrometry: a review, *Mass Spectrom. Rev.* 27 (2008) 101–124, <https://doi.org/10.1002/mas.20158>.
- [48] P.Q. Tranchida, I. Aloisi, B. Giocastro, L. Mondello, Current state of comprehensive two-dimensional gas chromatography-mass spectrometry with focus on processes of ionization, *TrAC Trends Anal. Chem.* 105 (2018) 360–366, <https://doi.org/10.1016/j.trac.2018.05.016>.
- [49] S.E. Reichenbach, M. Ni, V. Kottapalli, A. Visvanathan, Information technologies for comprehensive two-dimensional gas chromatography, *Chemometr. Intell. Lab. Syst.* 71 (2004) 107–120. <http://www.sciencedirect.com/science/article/pii/S0169743903002375>.
- [50] R.E. Synovec, J.C. Hoggard, Chemometric approaches, in: L. Ramos (Ed.), *Compr. Two Dimens. Gas Chromatogr.*, Elsevier, Amsterdam, 2009, pp. 3–14.

- [51] Z.-D. Zeng, H. Hugel, P. Marriott, Chemometrics in comprehensive multidimensional separations, *Anal. Bioanal. Chem.* (2011) 1–14, <https://doi.org/10.1007/s00216-011-5139-4>.
- [52] R.E. Mohler, K.M. Dombek, J.C. Hoggard, E.T. Young, R.E. Synovec, Comprehensive two-dimensional gas chromatography time-of-flight mass spectrometry analysis of metabolites in fermenting and respiring yeast cells, *Anal. Chem.* 78 (2006) 2700–2709, <https://doi.org/10.1021/ac052106o>.
- [53] B. Maikhunthod, P.D. Morrison, D.M. Small, P.J. Marriott, Development of a switchable multidimensional/comprehensive two-dimensional gas chromatographic analytical system, *J. Chromatogr. A* 1217 (2010) 1522–1529. <http://www.sciencedirect.com/science/article/pii/S0021967309019281>.
- [54] N.E. Watson, W.C. Siegler, J.C. Hoggard, R.E. Synovec, Comprehensive three-dimensional gas chromatography with parallel factor analysis, *Anal. Chem.* 79 (2007) 8270–8280, <https://doi.org/10.1021/ac070829x>.

Sample introduction methods*

Andrew Tipler

PerkinElmer Inc., Shelton, CT, United States

8.1 Introduction

The means of introducing samples into a gas chromatograph (GC) remains one of the processes most critical to its successful operation. It does not matter how good the rest of the system is (column, oven, detector, etc.); if the sample cannot be introduced into the system reliably, then the results are not going to be reliable either. The old computer software adage “garbage in, garbage out” is particularly relevant within this context.

So, what do we mean by a “good sample introduction technique” within the field of gas chromatography?

In simple terms, we want the analytical results we get from whatever is introduced into the GC to be representative of the original sample.

In practice, we want the following:

- narrow symmetrical peaks to be able to fully exploit the efficiency of the GC column,
- good-sized peaks to be able to discern them from the background (noise) signal,

- no losses of analytes due to adsorption or chemical breakdown,
- good quantitative repeatability to provide confidence in results,
- easy to understand and use, and
- compatible with autosampler injection for throughput and performance.

Typical GC columns and GC detectors are really only suited to handle a few micrograms of a particular sample component at the most; hence, rarely do we introduce the whole sample into the system.

Many samples exist in the liquid form—either as a solution in a suitable solvent (for example, a plant extract) or because they are naturally liquid (for instance, gasoline). For such samples, it is convenient to use a microliter syringe to take a small amount of the sample and introduce it into a device called a “*liquid injector*.” This liquid injector provides the interface between the sample in the syringe and the GC column. There are several different types of liquid injector,

* This chapter is reprinted from the first edition of Gas Chromatography. The editor has updated and expanded the bibliography.

which may cause confusion to the novice gas chromatographer. Each injector has its place; each has its advantages and idiosyncrasies that will make it particularly suited to certain types of sample and column.

This chapter focuses mainly on the design and operation of liquid injectors; however, we will also discuss the use of gas and liquid mechanical valves in making sample introductions of gases and pressurized liquids.

There are also more specialized sample introduction systems such as those for headspace sampling, thermal desorption, and pyrolysis sampling that are covered elsewhere in this book (see Chapters 9–11).

8.2 Choosing a sample introduction system

In this section, we summarize the various injection devices and techniques discussed in this chapter and suggest how they may be used. These are intended to be just guidelines—one of the advantages of gas chromatography is learning how to bend the rules for a particular need or application.

In this table, we classify the injectors into two groups:

- Vaporizing—the sample is injected into a hot zone so that vaporization starts immediately. Typically, this will be set to 25–50°C above the maximum programmed column temperature.
- Nonvaporizing—the sample is injected into a cold zone where it remains as a liquid until the temperature is increased at some point after the injection. Typically, this will be set to 10–20°C below the boiling point of the solvent.

Table 8.1 summarizes the injector types, their modes of operation, and guidelines on their application.

8.3 Supporting devices

Before we discuss the injectors and injection techniques, it would be useful to consider some of the other technologies needed to support the injectors.

8.3.1 Syringes

A microliter syringe is usually used to make liquid sample injections into GC injectors. For most applications, the injection volume is in the range 0.1–10.0 μL . The needle is normally fabricated from hypodermic stainless-steel capillary tubing and the body from glass. The plunger will normally be stainless steel and may have a PTFE tip for better sealing. The length of the needle needs to be compatible with the type and design of injector being used. The outer diameter is normally 0.63 mm, although a smaller diameter (of 0.47 mm) will be needed for on-column injection into 0.53-mm tubing. The tip of the needle may have a variety of geometries, conical, tapered, flat, etc., to suit different injector seals and septa.

Two types of syringe are available:

- Plunger in barrel—this is the most familiar type of syringe in which the tip of the plunger resides inside the visible barrel of the syringe. This is the type normally used for samples of 1 μL or above. For large-volume injection (LVI) applications (see [Section 8.7.5](#)), the syringe capacity may be 50 μL or even more.
- Plunger in needle—in this type of syringe, the plunger extends down into the needle itself. This is suitable for small-volume injections of 0.5 μL or less.

The two types of syringe are illustrated in [Fig. 8.1](#).

A larger-capacity, gastight syringe may be used to inject gas samples either directly into a liquid injector or into a gas sampling valve. It

TABLE 8.1 Summary of injectors and injection techniques covered in this chapter.

Injector	Technique	Type	Column type	Concentrated samples	Dilute samples	Trace samples	Labile components	Volatile compounds	Heavy compounds	Gases	Pressurized liquids
Cold on column	Cold on-column	Nonvaporizing	Capillary	Poor	Best	Good ^a	Best	Poor	Best	Poor	Poor
Flash vaporization	Flash injection	Vaporizing	Packed and 0.53 mm capillary ^b	Good ^c	Fair ^c	Poor	Poor	Fair ^c	Fair	Fair ^c	Fair ^d
	Hot on-column	Vaporizing	Packed	Poor	Fair	Poor	Poor	Poor	Fair	Poor	Poor
Split/splitless	Classical split	Vaporizing	Capillary	Good	Poor	Very poor	Poor	Good	Fair	Fair	Fair ^d
	Classical splitless	Vaporizing	Capillary	Poor	Good	Fair ^a	Poor	Poor	Fair	Poor	Poor
Programmable split/splitless	Programmed split	Nonvaporizing	Capillary	Best	Poor	Very poor	Good	Good	Good	Fair	Fair ^d
	Programmed splitless	Nonvaporizing	Capillary	Poor	Good	Fair ^a	Good	Poor	Good	Poor	Poor
	Vaporizing split	Vaporizing	Capillary	Fair	Poor	Very poor	Poor	Good	Fair	Fair	Poor
	Vaporizing splitless	Vaporizing	Capillary	Poor	Fair	Fair ^a	Poor	Poor	Fair	Poor	Poor
	Cold on-column	Nonvaporizing	Capillary	Poor	Best	Good	Best	Poor	Best	Poor	Poor
	Hot on-column	Vaporizing	Capillary	Poor	Fair	Poor	Poor	Poor	Fair	Poor	Poor
	Large volume injection	Nonvaporizing	Capillary	Poor	Good	Best	Good	Poor	Good	Poor	Poor
Gas sampling valve	Gas loop injection	Not applicable	Packed and capillary ^e	Good ^c	Good ^c	Fair ^c	Poor	Best	Poor	Best	Poor
Liquid sampling valve	Pressurized liquid injection	Nonvaporizing	Packed and capillary ^e	Good ^c	Good ^c	Poor	Poor	Best	Poor	Poor	Best

^a With a retention gap.

^b At high flow rates.

^c With packed columns.

^d With valved syringe.

^e With splitter at column inlet.

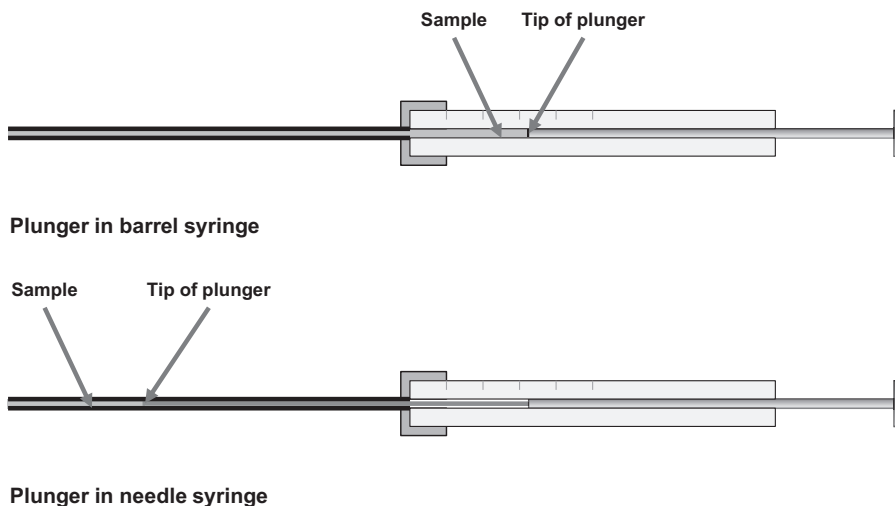


FIGURE 8.1 Types of syringe used for liquid injections.

is normally made from glass and has a gastight plunger to prevent sample leakage when the needle is inserted into a pressurized injector. Some syringe designs have a sealing valve at the point where the needle joins the barrel. This effectively prevents sample vapors from escaping from the syringe barrel or ambient air entering the syringe while it is being handled prior to injection.

Smaller-capacity syringes with a sealing valve may be used to sample and inject pressurized liquids such as aerosol propellants or liquid petroleum gases into a liquid injector.

8.3.2 Liners

Most liquid injectors use some form of liner into which the sample is injected by syringe. These are normally fabricated from glass or quartz tubing. For some injectors, the liner may need to be packed with glass or quartz wool. It is usual to deactivate the liner with a suitable chemical agent to prevent breakdown or adsorption of sensitive analytes particularly at low concentrations.

The geometry of the liner depends on the type of injector and the injection technique, which will be discussed further in the sections on injectors.

For vaporizing injectors, it is important that the internal capacity of the liner is sufficient to hold the volume of vapor generated after a liquid sample injection. This will depend on the following factors:

- volume of sample injected,
- number of moles in the injected sample,
- the liner temperature,
- the carrier gas pressure inside the liner, and
- the injection speed.

The potential vapor volume from a given solvent can be calculated using a variant of the ideal gas law given in Eq. (8.1):

$$V_v = \frac{V_l \cdot \rho \cdot R \cdot T_v}{M \cdot P_v} \quad (8.1)$$

where V_v is the potential volume of solvent vapor generated in the liner (μL), V_l is the volume of liquid solvent injected (μL), ρ is the density of the liquid solvent (g mL^{-1}), R is the ideal gas constant ($8314 \text{ mL kPa K}^{-1} \text{ mol}^{-1}$), T_v is the absolute temperature of the solvent vapor

inside the liner (K), M is the molar mass (molecular weight) (g), and P_v is the absolute pressure of the solvent vapor inside the liner (kPa) (1 psi is equivalent to 6.894 kPa).

The potential vapor volumes for typical solvents used in GC are given in Table 8.2. This table also contains boiling-point information, which is discussed later in this chapter.

Table 8.2 clearly shows that liner capacity will be more of a concern for polar solvents such as water and alcohols and less of a concern with higher hydrocarbons. The solvent with the lowest potential vapor volume in this list is

isooctane (and so has greater tolerance for larger-volume liquid injections). This is a popular solvent for many applications.

8.3.3 Septa

There have been many developments to seal the syringe inlet of liquid injectors and yet facilitate the introduction of the needle into the liner below. None has yet surpassed the simplicity and ruggedness of a simple rubber septum. Most injectors still make use of this type of seal—it is cheap, reliable, easy to replace, and generally gives good performance. The advent of modern silicone polymers has improved their performance significantly—they last much longer than earlier versions, and issues with septum bleed have been largely addressed.

TABLE 8.2 Boiling points and vapor volumes of common solvents used in GC.

Solvent	Normal boiling point (°C)	Vapor volume from 1 μ L of liquid injected at 250°C and 15 psig (μ L)
Acetone	56	290
Carbon disulfide	46	352
Chloroform	61	265
Cyclohexane	81	197
Dichloromethane	40	332
Ethanol	78	364
Ethyl acetate	77	217
Isooctane	99	124
Isopropanol	82	278
Methanol	65	526
n-Pentane	36	185
n-Hexane	69	162
n-Heptane	98	145
n-Octane	126	131
n-Nonane	151	119
n-Decane	174	109
Toluene	111	200
Water	100	1180

8.3.4 Autosampler

Modern autosamplers automate the process of syringe injection. They save time for the operator as they will function continuously even at times when the operator is not present. The other great advantage is the precision of the injection process. Every setting in the autosampler method is executed with high repeatability, giving excellent precision in the chromatography. With a good manual injection technique, the expected quantitative precision of an analysis will be in the order of 2%–4% relative standard deviation; with an autosampler this should improve to 1% or even lower.

Purchase of an injector autosampler is a highly recommended option for any GC—it will quickly repay the initial investment with much higher sample throughput, better quality data, and give operators more time for other duties.

8.3.5 Pneumatic systems

The design of carrier gas control systems is a complex subject and difficult to cover as part of

a single chapter in a general book on GC such as this. However, pneumatic system design and configuration are critical parts of GC injector operation and so we will cover the basics here.

Several types of pneumatic components may be used to control GC carrier gases:

- Forward pressure regulator—this is a pressure-reducing device that adjusts a variable restrictor to maintain a constant pressure at its outlet.
- Backpressure regulator—this is a pressure-reducing device that adjusts a variable restrictor to maintain a constant pressure at its inlet.
- Mass flow controller—this device adjusts a variable restrictor to maintain a constant mass flow rate of gas through it.
- Needle valve—this device is a variable restrictor.
- Pressure gauge or transducer—a device that displays or reads the pressure at a given point.
- Flow transducer—a device that reads the mass flow rate through a given point.

In the early days of GC, all the controllers were mechanical devices that required the user to turn a rotary knob until the required pressure or flow rate was achieved. These days, most GCs use microprocessor-controlled electromechanical modules to perform these functions. These devices offer significant advantages over their mechanical counterparts. They not only make method setup easier and more precise but also enable flow rates and pressures to be dynamically programmed during the course of an analysis. Some modes of injection are not possible without this pneumatic programmability.

Details of specific pneumatic requirements for each injector will be made in the following sections, but one topic that will be covered here concerns the control of the carrier gas flow rate through open-tubular capillary columns.

Many capillary injectors have multiple gas outlets. These may include the column, septum purge, and split vent. Traditional mass flow controllers will regulate the flow rate of carrier gas going *into* the injector. As often only a small fraction of this gas will make it into the column, the flow rate of carrier gas through the column cannot be controlled directly in this way.

Most programmable pneumatic systems control the carrier gas flow rate through the column by applying a carrier gas *pressure* calculated to give the required flow rate through the column. In this way, the column flow rate is completely unaffected by septum purge, splitting, or even gas leaks.

The calculation used for this purpose is usually based on a variant of the Hagen–Poiseuille relationship [1] developed in the mid-19th century and modified here for calculations with compressible gases and is shown in Eq. (8.2):

$$F_o = \frac{\pi \cdot d_c^4 \cdot (p_i^2 - p_o^2)}{256 \cdot L \cdot p_o \cdot \eta} \quad (8.2)$$

where F_o is the flow rate at the column outlet at the temperature and pressure at the outlet ($\text{mL} \cdot \text{min}^{-1}$), d_c is the internal diameter of the column (cm), L is the length of the column (cm), p_i is the absolute carrier gas pressure at the column inlet (kPa), p_o is the absolute carrier gas pressure at the column outlet (kPa), and η is the dynamic viscosity of the carrier gas, which varies with column temperature (kPa s).

If the pneumatic control system has knowledge of the column geometry and type of carrier gas (which would be entered by the user), it can adjust the column inlet pressure, p_i , to deliver a set flow rate, F_o , at any set column temperature.

It is important when using carrier gas flow control to understand what the pressure will be inside the injector. Some of the advanced injection techniques discussed in this chapter rely on pressure changes.

8.4 The cold on-column injector

The cold on-column injection (COCI) technique is, in concept, the simplest injection technique in capillary GC and yet it is probably the least used.

Essentially, it involves the deposition of a liquid sample directly into the inlet of the capillary column at a low temperature as shown in Fig. 8.2. The syringe needle is withdrawn and the sample in the column is heated and vaporized during the column oven temperature program [2,3]. In this way, once it has left the syringe, the sample only makes contact with the surface of the capillary column as it makes its way to the detector. Because the injection takes place at a low temperature, there is low risk of thermolysis of labile compounds on a hot metallic syringe needle and almost no risk of the analyte mass discrimination from preinjection or postinjection vaporization effects such as those seen with vaporizing injectors [4,5].

If applied correctly, COCI will outperform all other injection techniques. It is a technique not suited to all samples, however (especially for concentrated or very volatile analytes), and care must be taken in choosing the conditions in the analytical method.

The main challenge to the user is the need to insert the syringe needle directly into the column inlet. When such injectors were first introduced, this was achieved by using syringes with a fine delicate length of fused-silica tubing that was

manually threaded through a guide and complex seal inside the injector and directly into column inlets down to 0.25 mm in internal diameter. This was not for the fainthearted.

The advent of retention gaps (see Section 8.4.3) enabled the use of syringes with more robust metal needles that could also be driven by a standard autosampler and make use of a standard septum as a seal. Although this has made the prospect of COCI more approachable to many users, there is still an element of skill and uncertainty in the installation and alignment of the column within the injector. Many users prefer to opt for the higher robustness of the classical split/splitless or the programmable-temperature vaporizing (PTV) injection systems.

8.4.1 Sample considerations

Because the whole sample injection is made directly into the column, care must be taken not to overload the column with too much analyte. Overloaded peaks cause characteristic “fronting” peaks on columns as shown in Fig. 8.3. Overloaded peaks are no taller than regular peaks but they are much broader and may give apparent changes in retention time and so should be avoided if possible.

The amount of analyte that will overload a capillary column will depend on the geometry of that column, the stationary-phase thickness, and the applied conditions, but a value of 50–100 ng would be fairly typical. For COIC, a

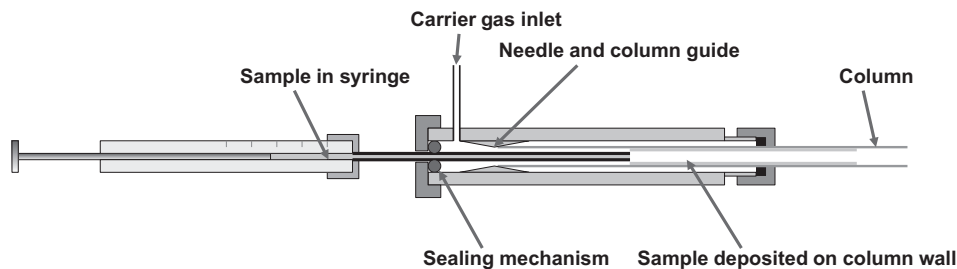


FIGURE 8.2 The basics of cold on-column injection.

typical injection volume would be 1–5 μL , and so maximum analyte concentrations would need to be in the order of 10–100 $\mu\text{g mL}^{-1}$. Thus, COCI is only suited to very dilute liquid samples and, in most applications, a suitable solvent must be added to ensure that analyte concentrations are compatible with the column being used.

Another point that should be considered is that because the sample is being deposited directly into the column, any involatile or reactive components will also be introduced into that column. Over a period of time, there may be sufficient buildup of residue or attack of the stationary phase to cause significant degradation of the column. This may need the removal of a short section of the column from the inlet (or

exchange of the retention gap) but a better solution would be to ensure that such materials are not present in the sample at all. To be robust, COCI needs samples to be reasonably clean. If this is not possible, then an injection technique that uses a replaceable liner may be preferable.

8.4.2 Role of the solvent

In order for COCI to work, the sample must essentially remain in the liquid state before, during, and after injection. This requires careful consideration of the sample solvent and the temperature of the GC column during injection. Generally, the column oven temperature is chosen to be approximately 10–20°C lower than the boiling point of the solvent at the

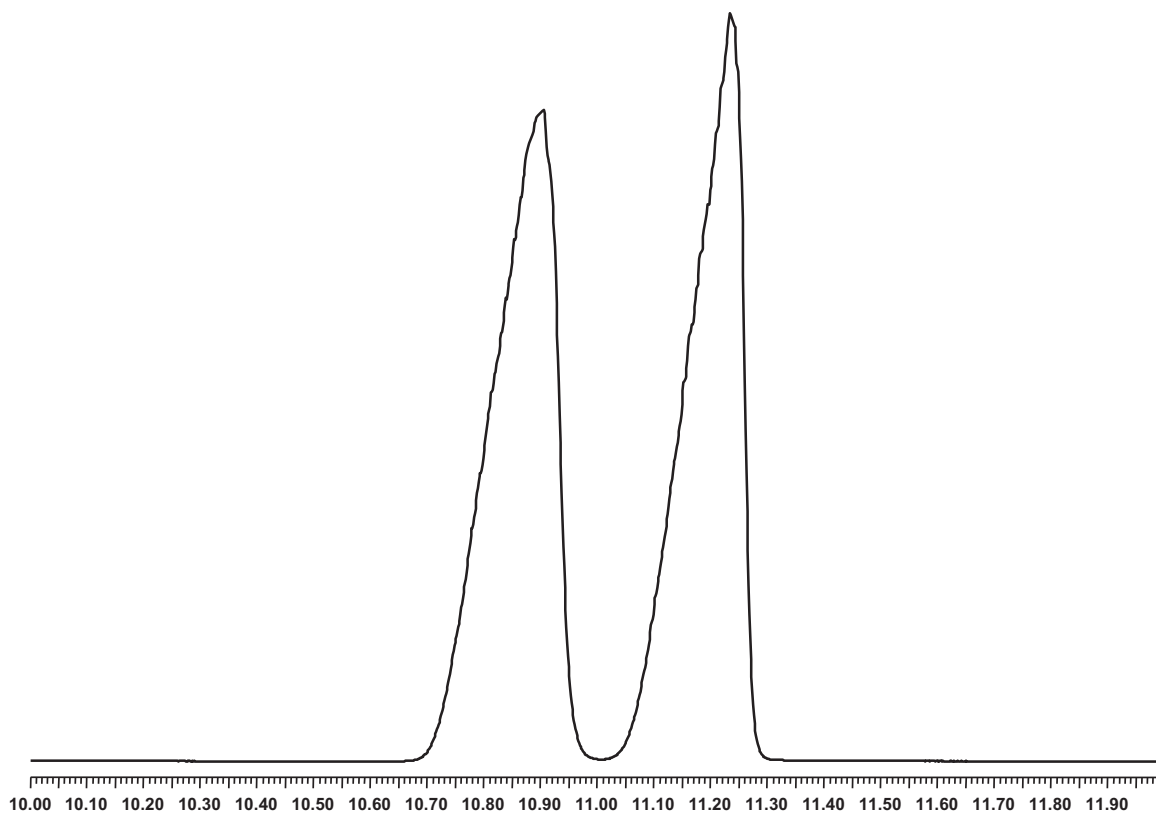


FIGURE 8.3 Example of overloaded peaks.

column inlet pressure. If the temperature is too high, the solvent will boil within the confined space within the column causing “flashback,” leading to poor chromatography, poor quantitative performance, and a high risk of system contamination. Table 8.2 lists the normal boiling points for some of the most common solvents used in GC. Note that, because the column inlet is at an elevated pressure because of the applied carrier gas, the solvent boiling points will also be elevated.

The solvent itself may play an active part in obtaining good chromatographic peak shapes especially for the early-eluting peaks. In COIC, it is normally (but not exclusively) assumed that the solvent will be the first component that will elute from the column. At the point of injection, the solvent should distribute itself as a liquid layer on the inside of the column walls near the inlet. This “pseudo” stationary phase serves to refocus the analyte vapors that follow it out of the injector and so concentrate them as a narrow band at the column inlet. The column oven is then temperature-programmed to first vaporize the solvent and

then the refocused analytes. This ensures that the early-eluting peaks are sharp and symmetrical. This effect is termed the “solvent effect” [6] and requires the careful choice of a solvent that will both adhere to the walls of the column (wettability) and have an affinity (partitioning) for the analytes.

If the solvent does not adhere to the walls of the column, then it will form droplets of the solvent that will absorb analyte vapors. These droplets are easily driven down the column sometimes for a significant distance by the carrier gas, which has a velocity normally in the range of 20–50 cm s⁻¹. As the droplets travel along the column, they will slowly evaporate. This has the effect of depositing patches of analytes randomly along the column. When temperature programming is initiated and these analytes vaporize, the chromatographic peaks may become highly distorted, as the molecules for each analyte will have different distances to travel through the column. This “solvent flooding effect” [7] is usually seen with midrange-volatility components. An example of a severe case is given in Fig. 8.4.

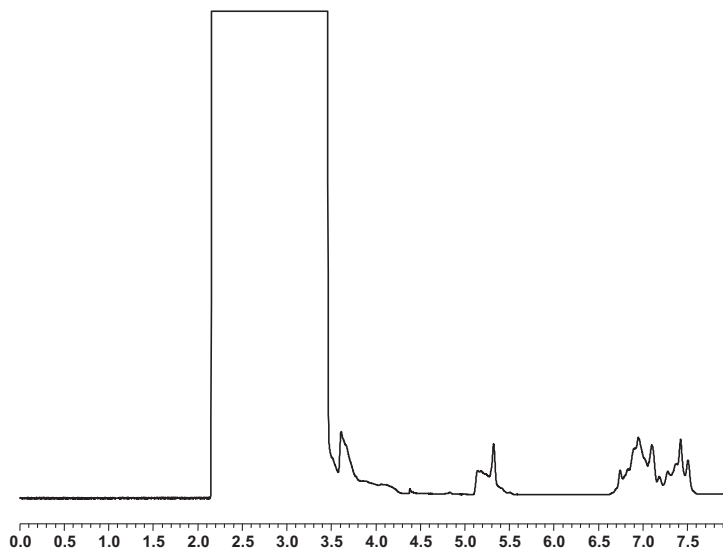


FIGURE 8.4 Example of the solvent flooding effect caused by using methanol as a solvent with a thin-film nonpolar column.

If the analytes do not sufficiently partition into liquid solvent, then there will be no focusing effect and so the early peaks may be broad or even tailing.

If analytes precede the solvent as it passes from the injector and through the column, they may undergo what is known as the “reverse solvent effect” [8]. In such instances, the solvent may actually displace the analyte molecules from the stationary phase and so undermine the whole chromatographic process and the resultant peaks may be broad and poorly separated (Fig. 8.5).

As should now be apparent, choosing a suitable solvent is one of the most critical decisions when developing a COCI method. Fig. 8.6 shows an example of good chromatography obtained with COCI.

Although the solvent effect is an important technique for volatile analytes in a sample, it may not be needed for heavier (semivolatile) components (although these will still be at risk from the solvent flooding effect). The heavier components will tend to sit as a narrow band

on the column at the point that they were initially deposited during injection. The solvent will be long gone before they start to vaporize during a temperature program. They will vaporize as a narrow plug of vapor and generally give narrow and symmetrical peaks.

8.4.3 Using a retention gap

In many instances, choosing a suitable solvent is not easy and compromises must be made. The use of a technique called the “retention gap” [9,10] enables COCI to be far more forgiving of the solvent being used.

A retention gap is simply a length of uncoated and inert tubing connected between the injector and the column. It is normally made from chemically deactivated fused-silica tubing. It may be of a wider internal diameter than the column itself and the length is chosen to suit the solvent being used and the injection volume. Many modern columns may be purchased with a retention gap prebonded by the vendor to the column inlet.

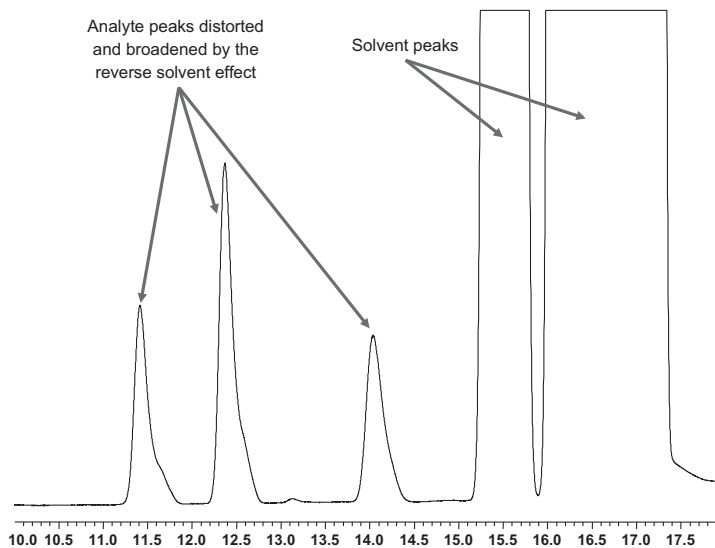


FIGURE 8.5 Example of the reverse solvent effect caused by using a less volatile solvent (hexane isomer mixture) to chromatograph light hydrocarbons.

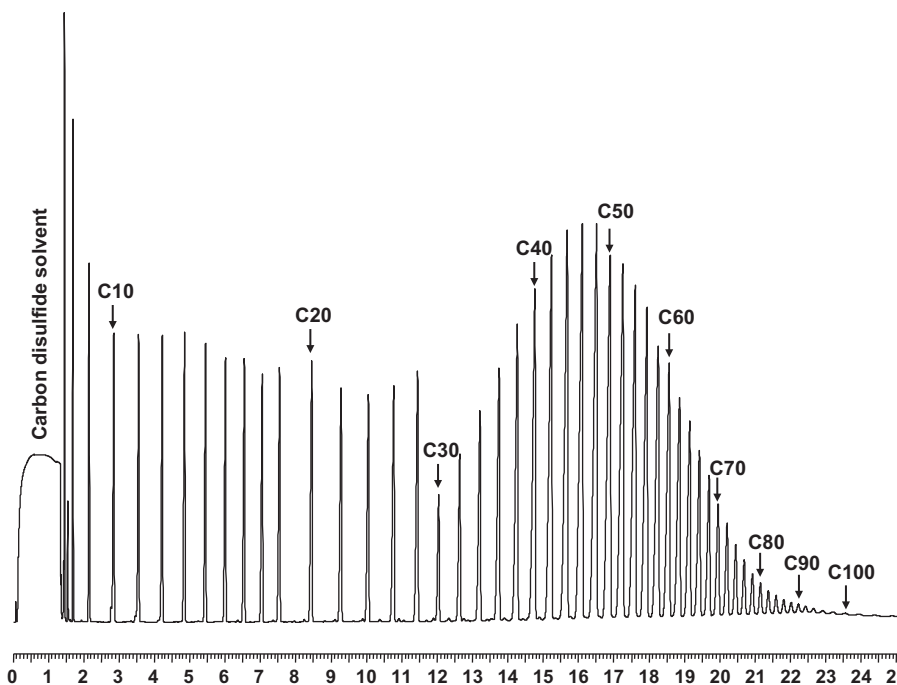


FIGURE 8.6 Example of a chromatography obtained with cold on-column injection. This is an injection of a high-temperature simulated distillation calibration mixture containing hydrocarbons up to 100 carbon atoms. The column was a $10\text{ m} \times 0.53\text{ mm} \times 0.1\text{ }\mu\text{m}$ methyl silicone high-temperature metallic column and the solvent was carbon disulfide. The temperature program was -20 to 425°C at $20^\circ\text{C min}^{-1}$ and held for 4 min.

The main function of the retention gap and the reason why it is so named are to act as an unretentive buffer between the injector and the column. The length of the retention gap should be sufficient to ensure that all the liquid solvent is retained within it and only enters the separation column as vapor. The solvent effect is effectively reduced but, more importantly, so is the solvent flooding effect. This enables selection from a wider range of solvents that would not normally work with COCI. The loss of the solvent effect, which would have helped keep the chromatographic peaks sharp, is compensated by another effect. The stationary-phase gradient that is created at the union between the retention gap and the column acts as an analyte focusing point as illustrated in Fig. 8.7.

A retention gap provides several other benefits besides improving the chromatographic

peak shape. It is such a powerful technique that many experienced chromatographers will insist on its use with most columns.

Because the retention gap is normally removable and replaceable, it can be seen as a guard column to protect the main (and much more expensive) separation column from dirty or reactive samples. When the chromatography degrades, it is a relatively simple matter to replace the retention gap and return to the original chromatography.

One of the main reasons a retention gap is popular is because, with the wider internal diameter normally used, it is possible to insert a robust metal syringe needle directly into it. This enables a regular autosampler to automate COCI.

Finally, as mentioned earlier, the retention gap is able to overcome the solvent flooding effect that would otherwise cause severe peak

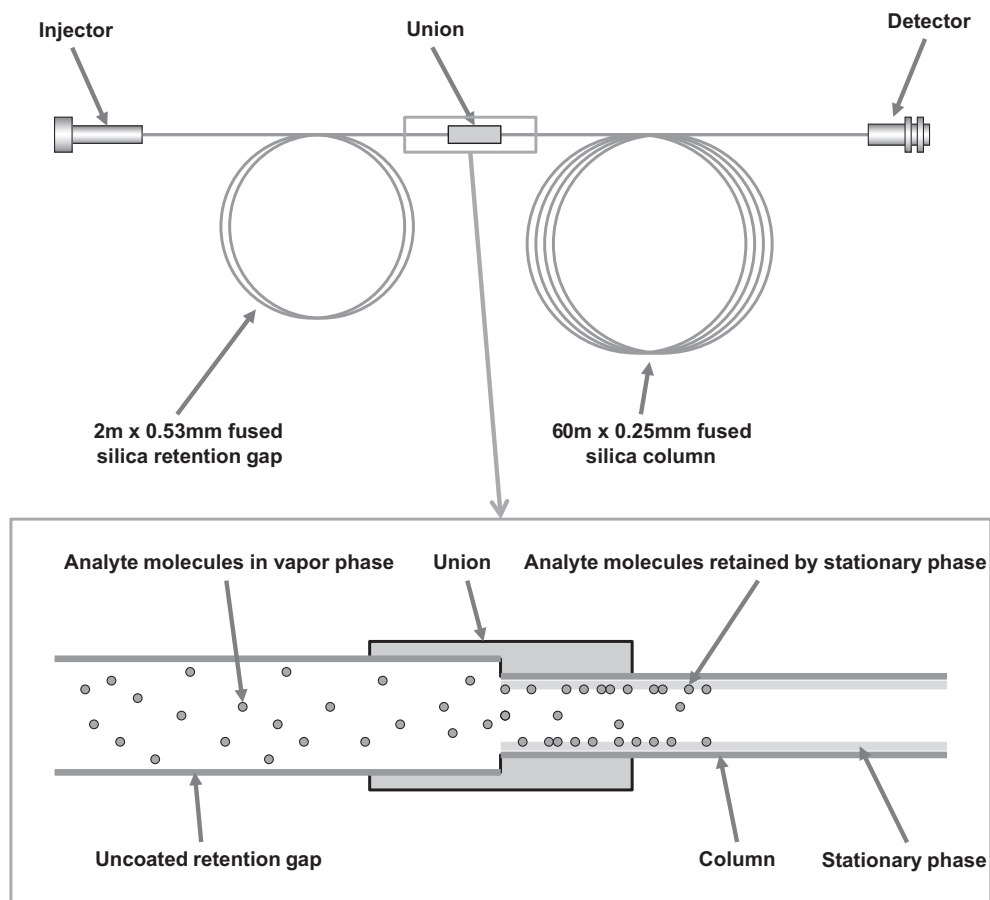


FIGURE 8.7 The retention gap principle.

distortion. By using a long retention gap, large sample volumes may be injected. As a general rule, approximately 0.2–0.5 m of 0.53-mm internal-diameter retention gap is required for each μL of sample injected, although this will depend on the potential vapor volume of the solvent as indicated in Table 8.2. Some workers have demonstrated liquid sample injections of 1 mL using a 100-m retention gap. These injection volumes generate a lot of solvent vapor to move through a capillary column at a typical carrier gas flow rate and so this is often not a very practical technique.

One variant of the retention gap technique that overcomes the problems of venting large volumes of solvent vapor through a capillary column is the “vented retention gap” technique [11] as shown in Fig. 8.8. In this case, a split line is opened for a short time after injection to vent the solvent. The split vent is closed and a column temperature program is initiated. This keeps the bulk of the solvent out of the column and so helps to protect it and minimizes the time that would otherwise be required to vent the solvent vapor through the column.

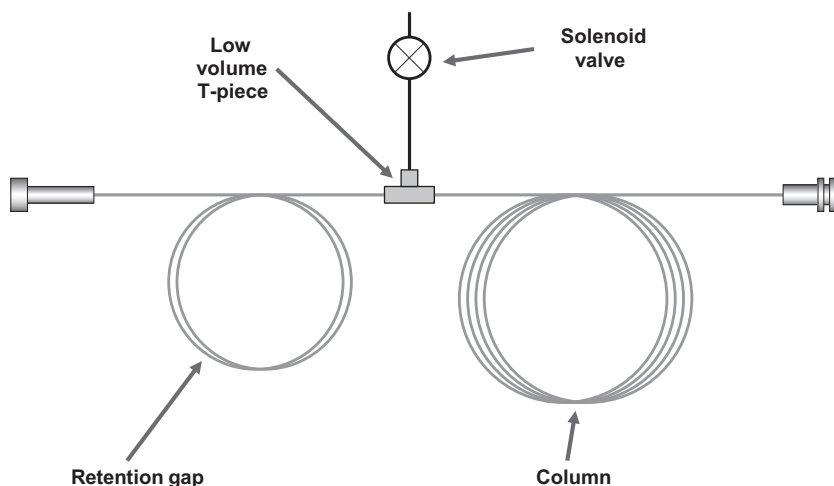


FIGURE 8.8 The vented retention gap technique.

Although the use of a long retention gap and a vented retention gap has facilitated large-volume sample injections, the use of a PTV injector (see Section 8.7) for this purpose is usually more robust and easier to set up and operate.

8.5 The flash vaporization injector

This is perhaps the simplest and most robust means of injecting liquid samples into a GC column [12]. Sample is injected into a heated (normally) glass liner, and it is vaporized and carrier gas carries it into the GC column. Method development is very straightforward: the liner temperature must be high enough to vaporize the whole sample. Fig. 8.9 illustrates the basics of flash vaporization injection.

Unfortunately, despite its simplicity, flash vaporization does suffer from some significant disadvantages. The liner capacity has to be sufficient to retain the volume of sample vapor generated, as the sample is injected and vaporized. An injection volume of 1 μL may generate as much as 0.5 mL of vapor with some solvents as shown in Table 8.2 and so require a liner with a capacity

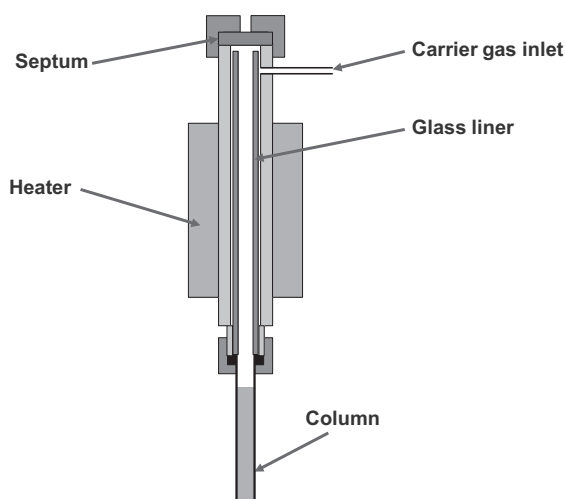


FIGURE 8.9 The flash vaporization injector.

of between 0.5 and 1 mL. For a capillary column with a carrier gas flow rate of, say, 1 mL min^{-1} , it would take over 5 min to sweep the sample vapor into the GC column. Thus, the chromatography would start with a very broad tailing solvent peak. An example of this is shown in Fig. 8.10.

For this reason, the flash vaporization technique is normally restricted to packed columns

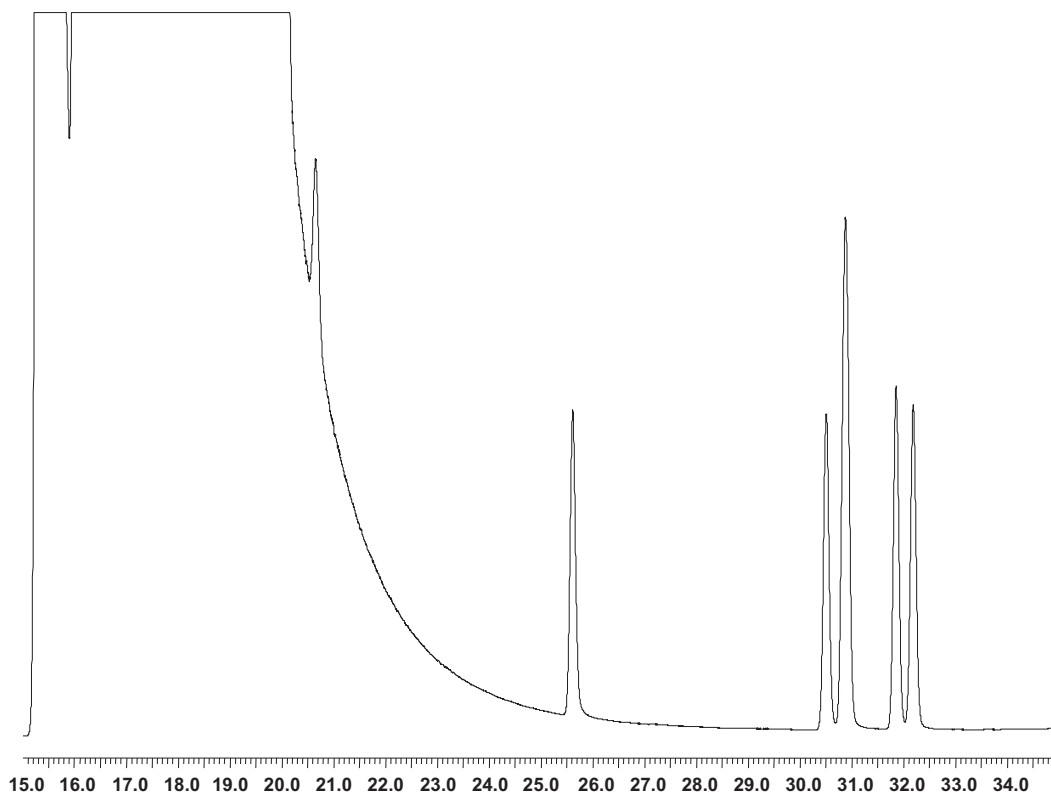


FIGURE 8.10 Result of using the flash vaporization injection technique with a narrow-bore capillary column. This is an injection of 1 μL of a 1% mixture of benzene, toluene, ethyl benzene, xylenes, and styrene in hexane into a flash vaporization injector connected to a 30 m \times 0.32 mm \times 5.0 μm 5% phenyl/methyl silicone column.

where the much higher carrier gas flow rates are more efficient at sweeping the sample vapor from the liner. For packed columns, the flash vaporization injection technique performs very well.

One exception to the rule that says that this technique is unsuitable for capillary columns is in the case of 0.53-mm internal-diameter (wide-bore) capillary columns at high carrier gas flow rates (e.g., 10–20 mL min^{-1}) and especially those with thick stationary-phase coatings. Although this will not be using the column at its optimum chromatographic efficiency, it will allow the use of a simple flash vaporizing injector as shown in Fig. 8.11.

Some flash vaporization injector designs will support the technique of “hot on-column injection.” This was popular in the days of mainly packed-column chromatography as injecting a sample directly into the packing of a glass packed column appeared to be more inert than injecting into a liner. To use this technique, the liner would be removed and the inlet end of a specially designed glass packed column with an extended inlet would be pushed right up through the injector until it was immediately below the injector septum. These days, if inertness is sought, then a suitable fused-silica capillary column is nearly always a better option.

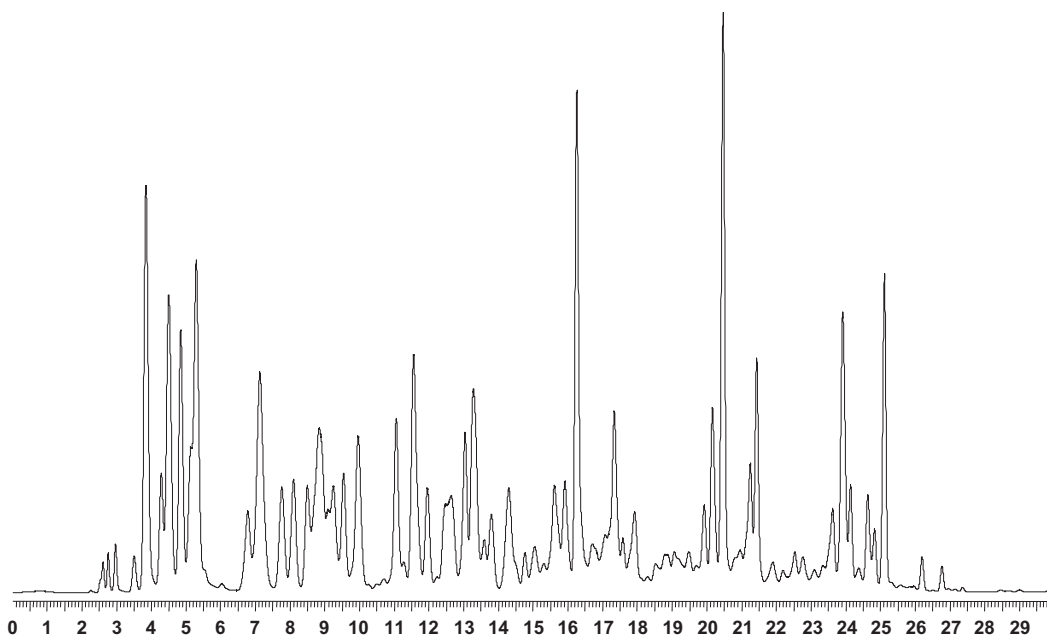


FIGURE 8.11 Flash vaporization injection of a gasoline sample with a $30 \text{ m} \times 0.53 \text{ mm} \times 5.0 \text{ }\mu\text{m}$ methyl silicone capillary column. The helium carrier gas flow rate was 12 mL min^{-1} and the temperature program was 35°C for 5 min, then 5°C min^{-1} to 160°C .

Hot on-column injection may also be used with 0.53-mm i.d. capillary columns. The inlet end of the column is inserted into a special adapter that is installed in the injector and guides the syringe needle directly into the column. The injection site is within the heated injector and so there is rapid vaporization within a confined space. Because of this, the technique is really only suitable for a small injection volume of $0.5 \text{ }\mu\text{L}$ or less. This is very inferior to the other capillary column injection techniques, but it does retain the robustness and simplicity offered by the flash vaporization injector.

8.6 The split/splitless injector

The classical split/splitless injector is the most popular GC injector currently in use. It is

reasonably rugged as well as being easy to use, and there are hundreds of papers describing its operation and application [13,14]. It is normally operated in one of two modes: split injection or splitless injection. These two “classical” injection modes are possible with a single design of injector as shown in Fig. 8.12.

The injector comprises a stainless-steel body that is heated to an isothermal temperature by a surrounding heater block. A glass (or quartz) liner resides inside the heated area and is sealed around its outer circumference to ensure that gas only passes through the center of the liner and not between it and the body. Carrier gas enters the top of the liner and exits into the column and, optionally, a split vent at the bottom. The split vent is enabled by activating a solenoid valve. A septum is used to seal the interior at the top of the injector and enables

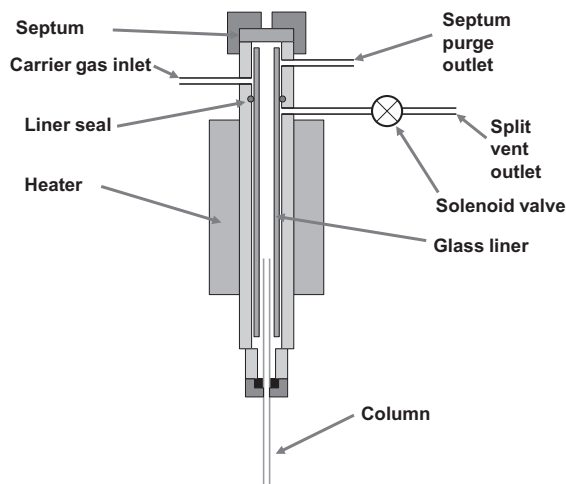


FIGURE 8.12 The split/splitless injector.

liquid sample injection by syringe into the liner. A septum purge is provided to prevent materials outgassing from the septum or sample deposited onto the septum during injection from finding their way into the sample stream and causing contamination peaks in the chromatography.

We will consider the two injection modes separately here.

8.6.1 Classical split injection

The sample is injected into a heated liner where it undergoes rapid vaporization. A high flow rate of carrier gas is applied through the liner during injection (typically $25\text{--}500\text{ mL min}^{-1}$). The flow rate through the column is much less and is chosen to suit that column. The excess carrier gas is vented from the injector through the split vent. This technique achieves two things: first, it reduces the sample vapor residence time in the liner and delivers a sharp plug of vapor to the column inlet, and second, it delivers only a small

fraction of the injected sample to the column inlet. In summary, split injection gives very sharp peaks but is only suitable for samples with high concentrations of analytes; it is not suitable for trace-level analyses.

Split injection has a wide tolerance for different solvents—they can elute before or after the analytes without significantly affecting chromatographic performance. It is even possible to inject some samples without the use of an added solvent, for example, in the analysis of gasoline.

Almost any column oven temperature (isothermal or programmed) may be used with split injection. The injector liner temperature, however, must be sufficiently high to vaporize efficiently the whole sample.

Although split injection is conceptually simple, the dynamics occurring inside the heated liner during the injection are very complex and there are a number of considerations that must be taken into account when developing methods.

8.6.1.1 The role of the syringe

To make an injection, the syringe needle must first be inserted into the heated liner. Thus, the needle heats up before the syringe plunger is depressed. Any sample that resides inside the needle at this point is going to become vaporized and will enter the GC column prematurely. This “preinjection effect” may cause apparent peak distortion or even splitting especially with early-eluting components and may degrade the quantitative performance. This effect would be more apparent with plunger in-needle style syringes.

Similarly, after the plunger is depressed to inject the sample, the residual sample left in the needle may become vaporized and enter the GC column. This “post-injection effect” may give rise to peak distortion again and cause an effect called mass discrimination, where more of

the volatile sample components will enter the GC column than they should. This effect would be more apparent with plunger in-barrel style syringes.

Fig. 8.13 shows an example of poor syringe technique. In this instance, care was not taken in the way the syringe needle was inserted or withdrawn. The peaks are larger and broader than they should be and the earlier peak has become split.

One of the most successful ways of overcoming preinjection and postinjection effects is to use a fast injection technique [15]. This requires an autosampler designed to support

this, as it would be almost impossible to perform this manually because of the speeds involved. The autosampler inserts the syringe needle into the injector liner, depresses the plunger to effect the sample injection, and then withdraws the needle from the injector. This complete process takes 100 ms or even less. The syringe needle is within the injector liner for such a short time that it does not really have the chance to heat up to produce either the preinjection or postinjection effects. A plug of glass wool is needed within the liner to wipe the syringe needle during its withdrawal or else it is likely that some of the liquid sample may be pulled back

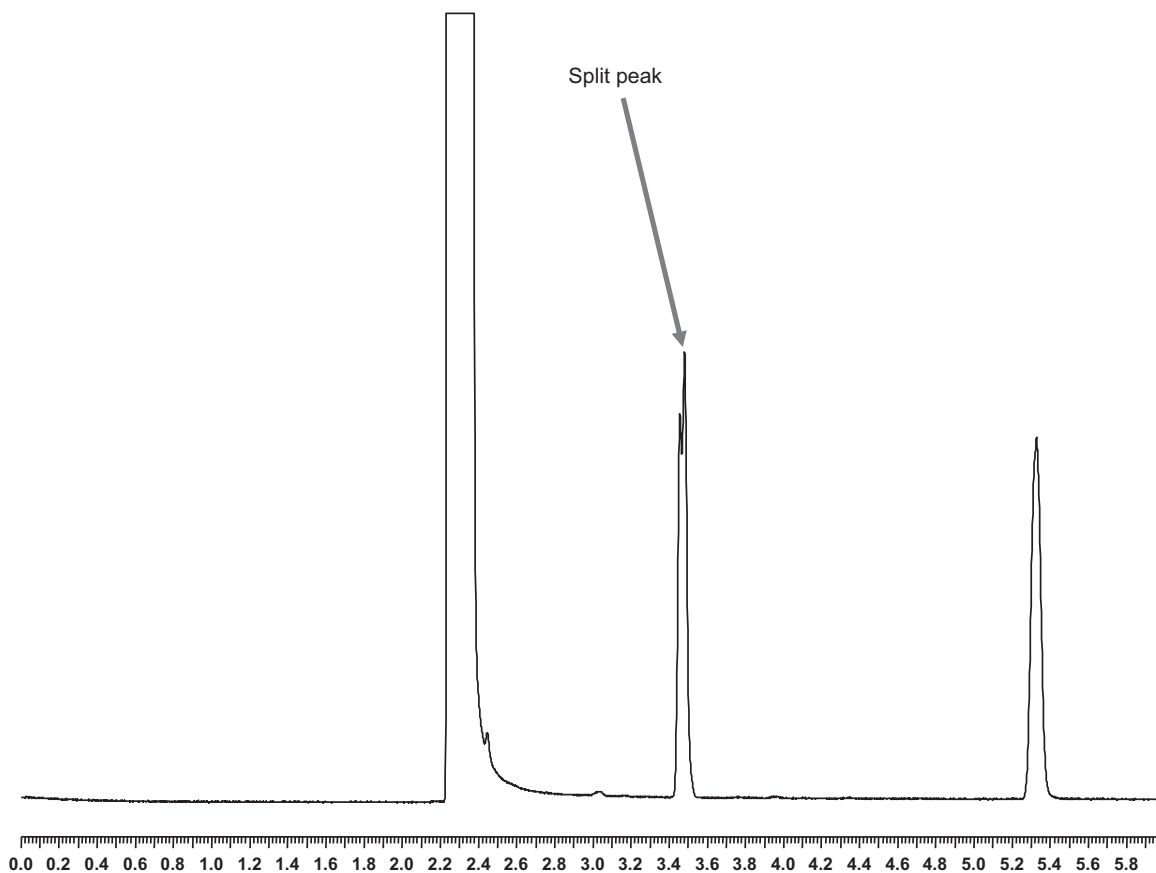


FIGURE 8.13 Example of syringe needle effects.

onto the base of the septum and lost from the analysis. Fast injection will provide more accurate injection volumes, sharp peaks, and low mass discrimination of wide-volatility-range samples. Fig. 8.14 shows how fast injection can improve the chromatography. Compare this chromatogram against Fig. 8.14 that was from the same sample run under identical chromatographic conditions and plotted with the same scaling.

Another approach to overcome preinjection effects with a plunger in barrel syringe is to pull back the plunger prior to injection so that all sample is withdrawn from the needle. It does not work with plunger in-needle syringes.

The postinjection effects may be addressed on a plunger in-barrel syringe by using either the "air plug" or the "solvent plug" technique. Prior to taking up sample into the syringe, a fixed volume of air or solvent is loaded into the syringe. The required volume of sample is then drawn into the syringe. The plunger may then be further withdrawn to empty the needle as described earlier. A small volume of air or solvent now sits between the sample and the end of the syringe plunger. When the syringe needle is inserted into the heated liner and the plunger is depressed, the air or solvent plug sweeps the whole sample out of the needle so that there is no sample in the needle at the end

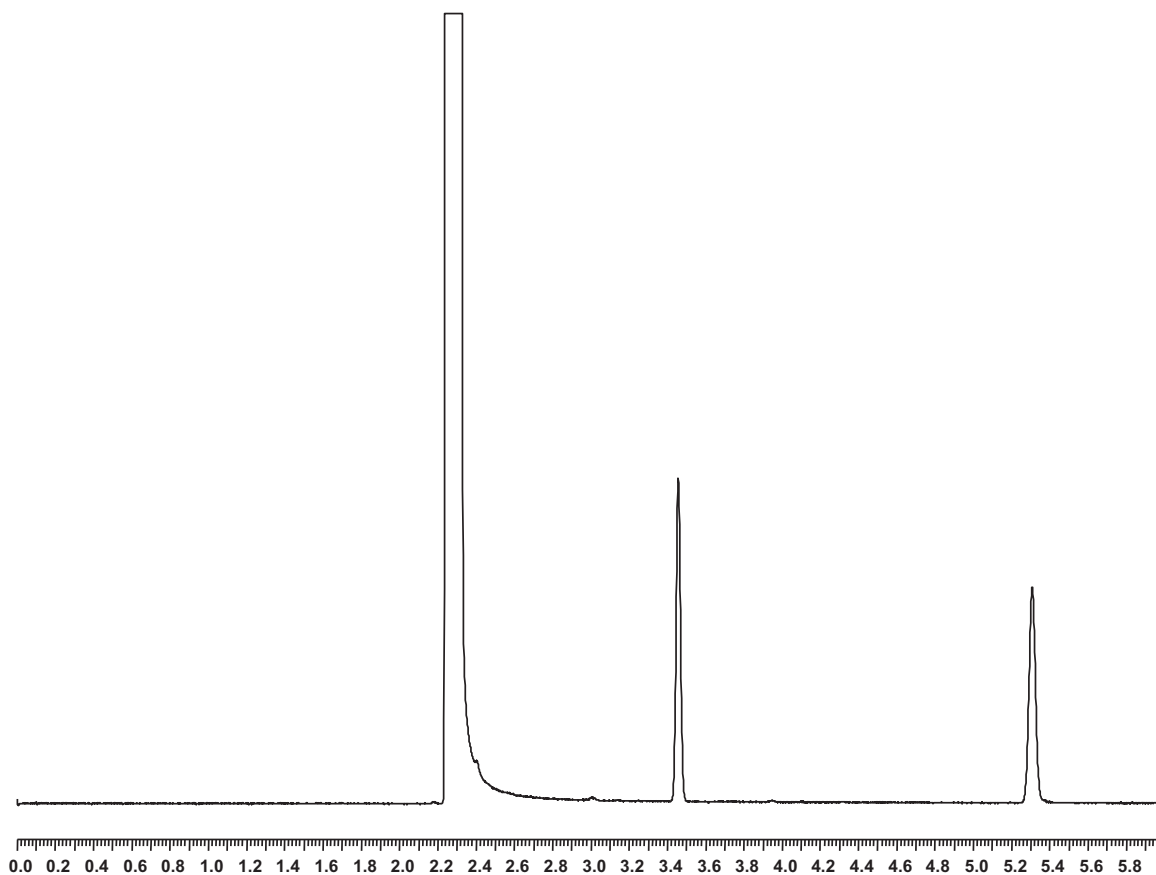


FIGURE 8.14 Overcoming preinjection and postinjection effects by using a fast injection technique.

of the injection. This effectively eliminates the postinjection effects. This technique may be used with manual injection and some modern autosamplers will automate the technique.

8.6.1.2 The role of the injector liner

The geometry of the injector liner is a critical factor with classical split injection. The role of the liner is twofold. First, it is to keep the sample vapor within the confines of the liner and deliver a fraction of the sample into the column that is truly representative of the sample injected. Second, it is to do this in a repeatable manner. This is what makes a split injector the most difficult injector of all to design to get good chromatographic performance.

In practice, there are many variables that conspire to affect performance and so make the liner choice difficult. Different manufacturers will give apparently conflicting advice and different users seem to have very different opinions as to what liner is best; there is possibly an element of black magic, too, in getting the best out of a given liner. In reality, there is probably no liner design that is good for all applications.

The following is a list of some of the liner attributes that affect performance:

- Internal diameter—a narrow liner has a low vapor capacity and will have a high carrier gas velocity flowing through it. This will limit the volume of sample injected and reduce the time available for sample vaporization and homogeneous mixing with the carrier gas before it reaches the column inlet. Conversely, a wide-bore liner will be able to accept larger sample injections and have more time for the vapor to homogenize with the carrier gas. However, the sample vapor will have more time to diffuse into the carrier gas inside the liner and give rise to broader and likely tailing peaks. A liner with a $1/4$ " (6 mm) internal diameter is typical for split injection.
- Sample size—the sample injection volume must be kept sufficiently low to prevent the generated vapor from escaping from the sample liner (see [Section 8.3.2](#)). Typically, 2 μL is the maximum sample volume that should be injected with split injection.
- Thermal mass—as the injected sample vaporizes, the energy needed for this vaporization will be drawn from the immediate surroundings, in this case the walls of the liner. If these walls are thin, then this would cause a significant temperature drop causing inconsistent vaporization and possible mass discrimination in the chromatography of wide-volatility-range samples.
- Packing—most split injector liner designs require some form of packing material to be present. Normally this will comprise a plug of glass or quartz wool. This provides a suitable bed on which the sample may be initially deposited so that it is ideally exposed to the carrier gas flowing through it and aids the vaporization process. It also assists with the mixing of the sample vapor with the carrier gas so that a homogeneous mixture is presented to the column inlet. Finally, with high-speed injection (see [Section 8.6.1.2](#)), the packing will wipe the end of the syringe needle and help prevent unevaporated liquid sample from being pulled back (and effectively lost) on the outside of the needle and be deposited on the underside of the septum.
- Internal geometry—although a plug of packing material will greatly assist with sample vapor homogenization, the flow path of sample vapor and carrier gas through the liner will also have a significant impact on performance. Liners have been developed with sophisticated internal geometry such as the Jennings inverted cup and various baffles.
- Inertness—for many applications, the liner should be chemically deactivated. Different types of samples will need different types of deactivation chemistries. The most important part of the deactivation process is to ensure

that any glass or quartz wool plug is fully deactivated—this is the material in closest contact with the sample during injection. Liner deactivation is a complex process and many users will purchase liners that have already been fully deactivated from vendors.

8.6.1.3 The split ratio

An important factor in split injection is the split ratio, which may be calculated for a given set of conditions from Eq. (8.3). The two flow rates apply to movement of the sample vapor in the carrier gas at the split point (i.e., the end of the column in the injector). In practice, the flow rates are measured (or calculated) at the split vent and at the end of the column where the temperature and pressure are at ambient conditions. As long as the two measurements are made under the same conditions of temperature and pressure, the result should remain the same:

$$\text{Split ratio} = \frac{\text{Flow ratio into split line} + \text{Flow ratio into column}}{\text{Flow ratio into column}} \quad (8.3)$$

The split ratio is used as a measure of how much of the sample injected into the injector liner actually enters the capillary column. A small ratio will place more sample in the column, whereas a large ratio will reduce it.

There are practical limits on the split ratio for any split injector; at low ratios, peaks become broad and tailing and, at high ratios, insufficient time for mixing may occur.

8.6.1.4 Pneumatics

The design of the pneumatics system is critical to split injection performance. The flows and pressures must be carefully controlled to deliver a stable split ratio and hence good quantitative performance and to retain the sample vapors

within the liner during a fairly explosive injection process as liquid sample hits a hot liner.

There are essentially two approaches to the pneumatic system that are discussed in the following:

Forward pressure regulation as shown in Fig. 8.15 is the traditional design. This may be implemented using mechanical or programmable electronic controllers. The pressure (or flow rate) of carrier gas into the column is set by the pressure regulator and the split flow rate is set by the needle valve or mass flow controller on the split line. The solenoid valve is normally left on during split injection although with programmable electronic pneumatics, the split flow rate may be later reduced to conserve carrier gas. The main disadvantage with this approach is that the pressure is controlled upstream of the injector and so any pressure drop through the plumbing or through the liner will cause a

reduction in flow rate through the GC column affecting retention times and split ratios.

A better approach is to use backpressure regulation as shown in Fig. 8.16. At first, this looks similar to forward pressure regulation but it is fundamentally different. Carrier gas is supplied to the injector by means of a mass flow controller. This controls the total flow into the injector. A backpressure regulator maintains the pressure inside the injector by regulating the passage of carrier gas through it until the set pressure is attained. Some of the carrier gas will flow into the column, some will exit from the septum purge vent, and the rest will be released through the split vent. Because the pressure is regulated downstream of the liner, the

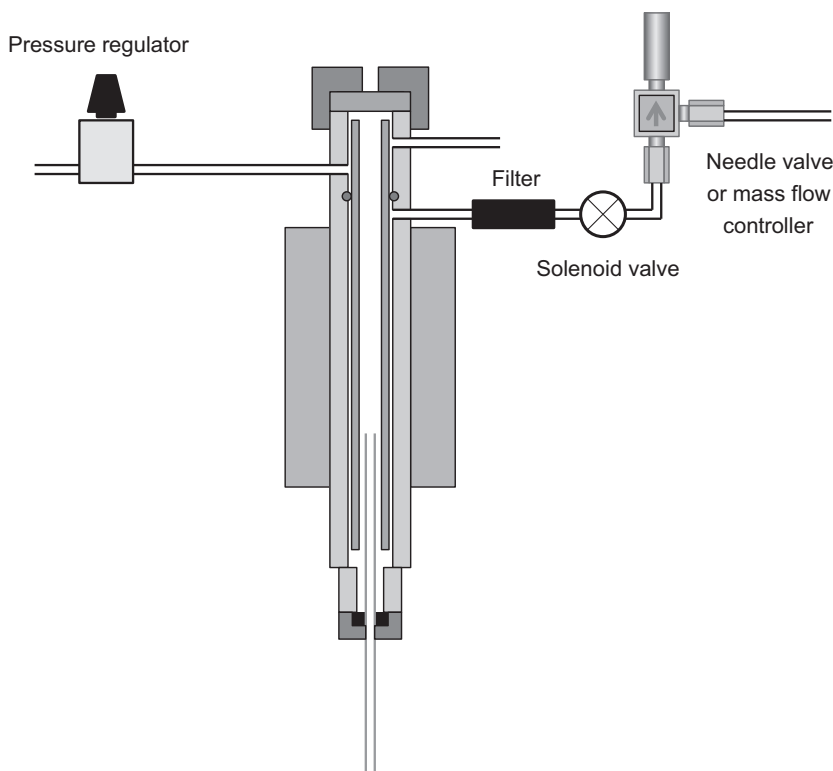


FIGURE 8.15 Forward pressure regulation in split injection.

pressure applied to the head of the column is more tightly controlled and better retention time repeatability and split ratio linearity are observed.

Backpressure regulation is the approach adopted in most modern GCs and especially those with programmable electronic controllers.

8.6.2 Splitless injection

Classical splitless injection [13–15] must be the most difficult of all the liquid injection techniques to master. There are so many critical variables that affect performance that a good understanding of the principles is essential before embarking on method development using this technique. Yet, it remains one of the most popular injection techniques—mainly because

of its robustness and because the same injector can usually be used for split injection too (see [Section 8.6.1](#)).

The aim of splitless injection is to allow sample injection into a glass or quartz liner and then transfer the whole sample into the GC column. The use of a liner overcomes several of the key concerns with COCI (see [Section 8.3](#)) but raises the question of how to get several hundred microliters of sample vapor into a narrow-bore capillary column and still get sharp peaks.

Like COCI, the key to successful splitless injection lies with the solvent.

In splitless injection, the sample is injected into a heated liner where it is immediately vaporized. There is no split applied at this stage, so the carrier gas will exit the liner through the column alone. The flow rate through the column

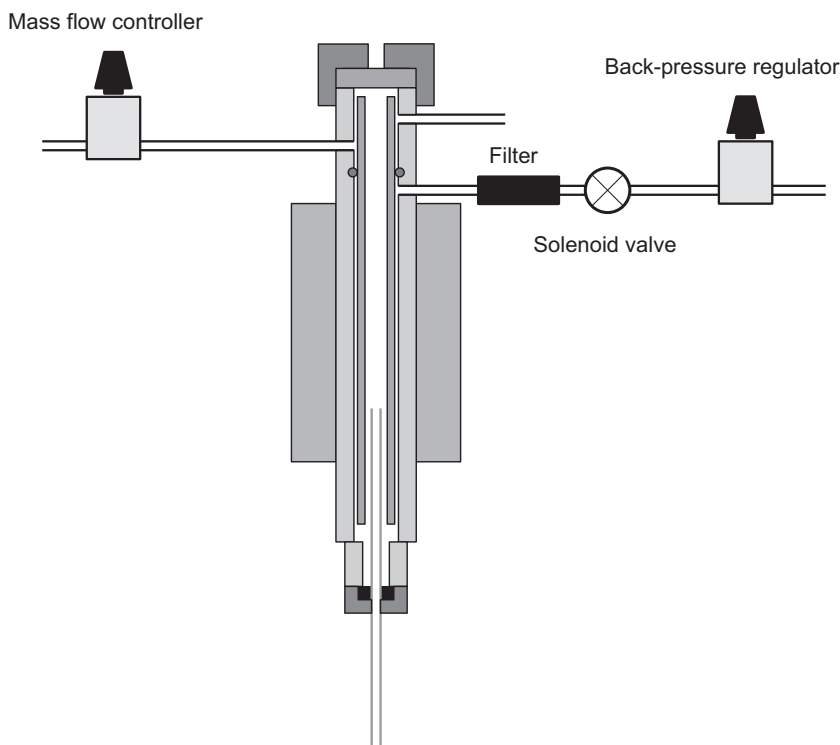


FIGURE 8.16 Backpressure regulation in split injection.

will be low (perhaps only 1.0 mL min^{-1}) and so it will take several minutes for the sample to be fully purged into the column (and so produce peaks several minutes wide at the start of the chromatography). However, if the column is held at a temperature that is less than the boiling point of the solvent, then most of the solvent will recondense in the column. This condensation induces a rapid drop in pressure within the column inlet and serves to pull the rest of the sample vapor out of the liner and into the column. In this way, a very rapid transfer of the sample into the column as a narrow band can be achieved.

Once in the column, the recondensed liquid sample is in a very similar state to that of COCI, and so the discussion on solvent effect, solvent flooding, and retention gaps applies

here too (see [Section 8.3.3](#)). It also means that splitless injection normally requires a column temperature program to be effective.

At some point after injection (normally about 30 s), the split vent is opened to flush out any remaining sample residue from the liner (and any other parts of the injector into which it may have diffused); this creates a small but unavoidable loss of the sample from the column. The benefit of doing this is that it cleans up the solvent peaks and sharpens many of the early-eluting peaks in the chromatography. The split flow is set to typically 25 mL min^{-1} . At the point that the split vent is opened, there will be a momentary drop in pressure inside the liner, which will serve to backflush any sample close to the end of the column—this will help to remove any peak tailing.

8.6.2.1 The role of the syringe

Classical splitless injection is, like its split equivalent, a vaporizing injection technique. A syringe deposits the liquid sample into a heated liner. It will have the same issues and solutions with the syringe technique that have already been discussed for split injection (see [Section 8.6.1.1](#)).

The volume of liquid sample that may be injected is much greater with splitless injection than with split injection. There are two things to consider:

- The injection rate—this should not be greater than the rate of recondensation in the capillary column or else vapor will exit the liner in other ways than into the column. The rate at which the syringe plunger is depressed will control this effect. A typical rate for LVI is $0.5\text{--}1.0\ \mu\text{L s}^{-1}$. This technique has been termed “*total concurrent vaporization*” [16].
- The buildup of liquid in the column—like cold on-column, too much solvent causes problems with solvent flooding. The use of a retention gap is recommended for LVIs.

Although some methods do use classical splitless injection for large sample volumes, the use of a PTV is often a better option as there is dynamic control of the liner temperature (see [Section 8.7.5](#)).

8.6.2.2 The role of the injector liner

Unlike split injection, splitless injection does not need to concern itself about homogeneous mixing of the sample vapor with the carrier gas in the liner; it just needs to get the whole sample into the column as efficiently as possible. Because of the solvent recondensation effect, the splitless liner can be much narrower than that used for split injection; a 2-mm-internal-diameter liner is typical. It is likely that much of the sample is not fully vaporized as it enters the column—this would improve transfer efficiency. The exotic baffles that are used in some

split injector liners have no place in splitless injection.

For the same reason, packing the liner with glass or quartz wool is normally not required except to wipe the liquid sample off the end of the syringe needle during high-speed liquid autosampler injection.

Liner deactivation is much more critical with splitless injection because of the much lower analyte concentrations in the samples and because the residency time in the liner will be greater.

8.6.2.3 Pneumatics

The split injection mode pneumatics are normally also deployed with the splitless injection technique.

With forward pressure regulation (see [Fig. 8.15](#)), the solenoid valve on the split line is simply closed during injection and opened later in the run.

With backpressure regulation (see [Fig. 8.16](#)), matters are more complicated because a high flow rate is still needed for the mass flow controller and backpressure regulator to function. Either the system should revert to forward pressure regulation (which is possible with programmable electronic controllers) or the flow from the flow controller should bypass the injector and be fed directly to the backpressure regulator.

8.6.2.4 Pressure-pulsed injection

Although a good splitless injector and method will get most of the sample into a capillary column, it will not get it all. Compounds will be lost through adsorption or diffusion into other parts of the injector.

Clearly, the flow rate of the carrier gas that is passing through the liner into the column at the point of injection is going to have a very direct effect on the transfer efficiency. Temporarily increasing this flow rate during the injection can have a significant effect on the peak size in the resultant chromatography. This technique has been termed “*pressure-pulsed injection*”

[17,18] and is normally only possible with a GC that has a programmable electronic pneumatic system. Fig. 8.17 shows a typical carrier gas pressure program for pressure-pulsed injection. The value of pressure-pulsed injection will depend on the application and the design of the injector being used.

8.7 The programmable-temperature vaporizing (PTV) injector

This injector is the most versatile of all the GC liquid injection systems. It has the convenience of a classical split/splitless injector and yet approaches the performance of a cold on-column injector. It also is able to offer a number of additional techniques that are not possible with any other injector type.

The PTV may be called different names by different instrument vendors: the temperature vaporizing injector (TPI), the programmable splitless injector (PSS), the septum-equipped temperature-programmable capillary injector (SPI), the brightly enhanced sample transfer (BEST) injector, and the OPTIC.

Despite the confusing array of acronyms, all these injectors essentially perform the same basic functions.

A PTV injector differs from other injectors in that the injector liner inside the injector is able to be programmatically heated and cooled [19]. Fig. 8.18 shows a typical PTV design in which the heater block has fins to enable fast cooling from a fan directed at it. The body of the injector will normally be narrower and lighter than its vaporizing equivalent to facilitate rapid heating and cooling. Normally there is a split vent to enable both split and splitless modes of injection.

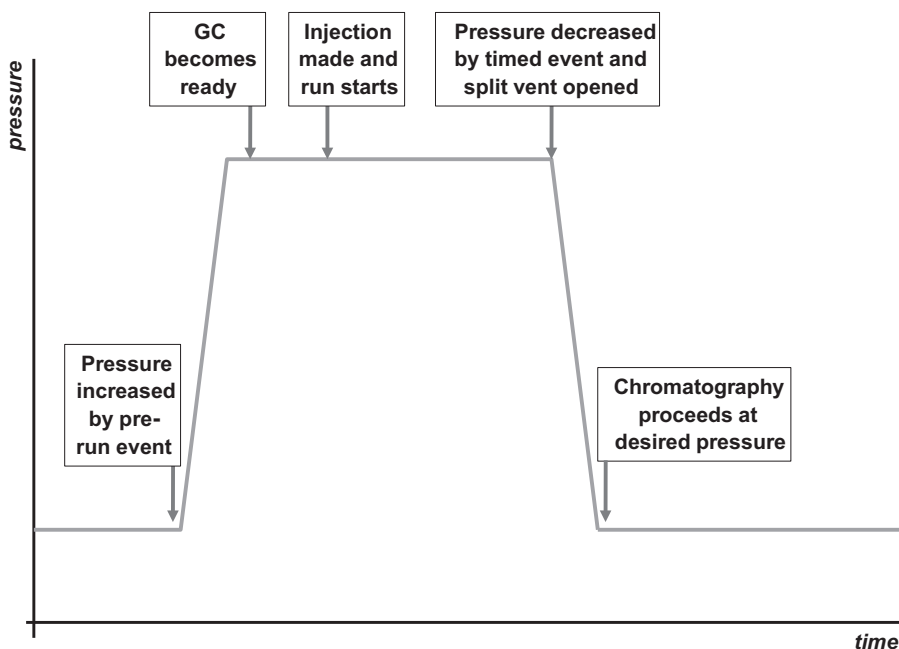


FIGURE 8.17 The principle of pressure-pulsed injection.

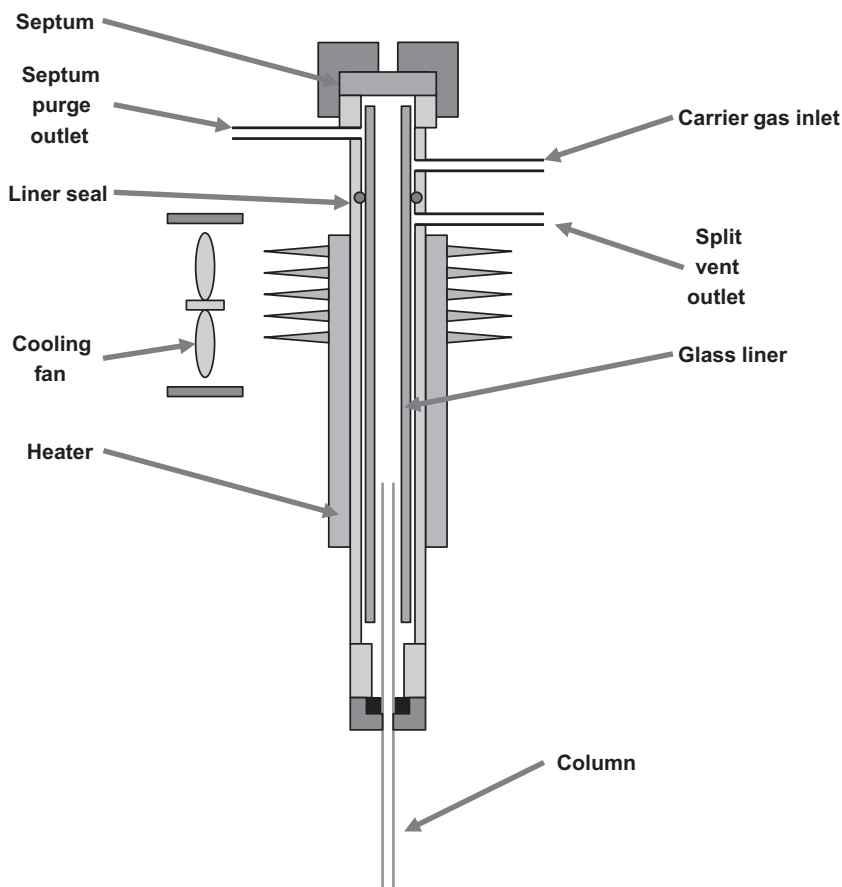


FIGURE 8.18 The programmable-temperature vaporizing injector.

Table 8.3 shows the various injection modes achievable from this injector.

TABLE 8.3 Injection modes that may be supported by a PTV injector.

8.7.1 Programmed split injection

This mode is very similar to the split injection technique described earlier (see Section 8.6.1). The main difference is that the sample is injected by syringe into a cooled liner. The syringe needle is then withdrawn and only then is the liner heated to vaporize the sample and transfer the vapors to the GC column.

Mode
Programmed split
Programmed splitless
Vaporizing split
Vaporizing splitless
Cold on-column
Hot on-column
Large-volume injection

This two-step injection technique provides several advantages over traditional heated liner injection:

- The sample largely remains as a liquid as it is deposited into the liner. This eliminates the explosive vaporization of the sample solvent seen with heated vaporizing injection, which can cause the sample to be expelled from the liner resulting in an apparent loss of sensitivity, discrimination effects, and possible cross-contamination between samples. With PTV injection, the solvent vaporization occurs at a more gradual rate as the liner temperature is increased, which helps keep vapors within the confines of the liner.
- The (normally) metal syringe needle is not exposed to high temperatures while in contact with the sample. Such contact with hot metal may promote the chemical breakdown of sensitive components. Injection into a cold liner ensures that there is no hot metal present during sample vaporization, so breakdown of sample components is much less likely.
- The syringe needle is not exposed to heat and so the preinjection and postinjection effects experienced with heated injectors are not seen.
- Each sample component, as soon as it is vaporized as the liner temperature is increased, will be swept out of the liner by carrier gas into the column and out through the split vent. Thus, no component should stay in the liner long enough to be exposed to any temperatures higher than necessary for its vaporization. This is one of the key reasons why PTV injection is so suited for the injection of samples containing thermally labile compounds.
- Once the sample components of interest have vaporized, the liner may be increased to a much higher temperature than would be used in methods with other injectors. This serves to

bake-out traces of less volatile sample residue, which would otherwise build up in the liner. The PTV liner is much easier to keep clean than with other injectors.

The injector liner is normally narrower (typically 2-mm internal diameter) than for classical split injection because there is no longer the explosive vaporization that occurs with that technique during sample injection. The lower-capacity liner assists in getting the sample out of the liner and into the column, as the temperature is increased. The walls of the liner tend to be much thinner to aid heat transfer from the heater into the liner interior. The liner is usually a simple glass or quartz cylinder. Because this is a nonvaporizing injection technique and the sample will be deposited as a liquid into the liner, it is important to have a plug of glass or quartz wool to wipe traces of liquid sample off the syringe needle during injection to prevent being pulled back onto the septum.

Despite the apparent complexity of a PTV injector, it is a much more straightforward prospect to design than a classical split/splitless injector because the dynamics of rapid sample vaporization no longer have to be considered.

Because of the narrower liner there will be a significant pressure drop across it at high split flow rates. This pressure drop will increase as the liner is temperature-programmed due to the viscosity of the carrier gas increasing. This will have the effect of changing the split ratio during the liner program, giving rise to significant mass discrimination effects. Fortunately, by using backpressure regulation (see [Section 8.6.2.3](#)), the effect is largely eliminated.

8.7.2 Programmed splitless injection

The principle of programmed splitless injection is very similar to programmed split injection: the sample is injected into a cooled liner; the syringe needle is removed and only then

is the liner heated to affect controlled sample vaporization. All the benefits of programmed split injection apply to programmed splitless injection too.

As with classical splitless injection, the split vent is opened shortly after injection to purge out residual traces of sample from the injector. This should only be done after the liner has reached its final temperature or else loss of heavier components may result. Typically, the vent will be opened with a flow rate of, say, 25 mL min^{-1} 0.5–1.0 min after the liner has reached its top temperature.

For programmed splitless injection, the liner may be very narrow (down to 1.0 mm) to ensure rapid transfer of the desorbed vapors into the GC column during temperature programming of the liner.

8.7.3 Vaporizing split and splitless injection

These are essentially the same techniques as those described for classical split and splitless injection (as described in Sections 8.6.1 and 8.6.2). The main difference is that the liners for the PTV techniques are usually smaller and of lower mass than those used in their vaporizing injector counterparts. This may mean that the maximum volume of sample that can be handled will be much less. For a 2-mm liner, this may limit the sample volume to 0.3 or even 0.2 μL .

It is not possible to design an injector that is optimized for both vaporizing and nonvaporizing injection techniques without making compromises in the performance or application. However, a good PTV design is as close as it can get.

8.7.4 Cold and hot on-column injection

A PTV injector may be easily adapted for on-column injection. A special liner may be installed

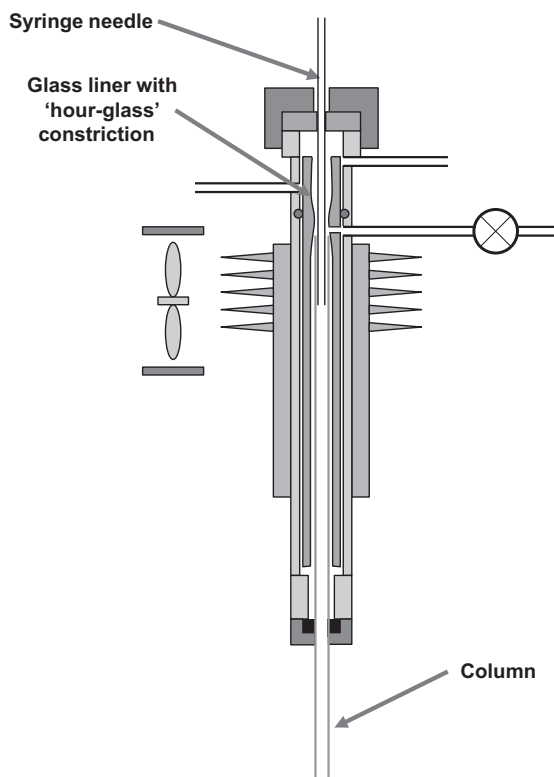


FIGURE 8.19 Cold on-column injection with a PTV injector.

as shown in Fig. 8.19 The end of a 0.53-mm column or retention gap is pushed right up into this liner until it is located within the hourglass constriction in the liner. The other side of the hourglass constrictor acts as a guide for a metal syringe needle, which can now be fully inserted into the end of the 0.53-mm tubing. A small hole may be required in the side of the liner for coupling to pneumatic components in the split line.

The sample is injected into the column or retention gap with the liner set to a low temperature that is just below the boiling point of the solvent. After the needle is withdrawn, the liner may be rapidly heated to a high temperature or programmed to track the temperature of the

column during a temperature program. In other respects, the cold on-column and hot on-column techniques are as described in Sections 8.3 and 8.5, respectively.

8.7.5 Large-volume injection

For some samples, lower detection limits are needed that can only be achieved by injecting more sample into the column [20]. The possibility of using cold on-column or splitless injection techniques to do this has been discussed earlier. None of these is very easy or practical as some effective way of dealing with large volumes of sample liquid and vapor is needed.

The PTV injector allows a mode of operation that simplifies LVI and yet addresses the issues with the large solvent volume.

The LVI technique may be viewed as a combination of both split and splitless techniques applied to the same sample injection at different temperatures. Fig. 8.20 illustrates the principle. A suitable syringe injects a large volume (typically 50–100 μL) of sample into a cold PTV injector liner. The split vent is open and the carrier gas flow rate will be set to 100 mL min^{-1} or above. The injector is left under these conditions for a few minutes. During this time, the solvent will become vaporized and be carried out of the liner through the split vent. A small amount

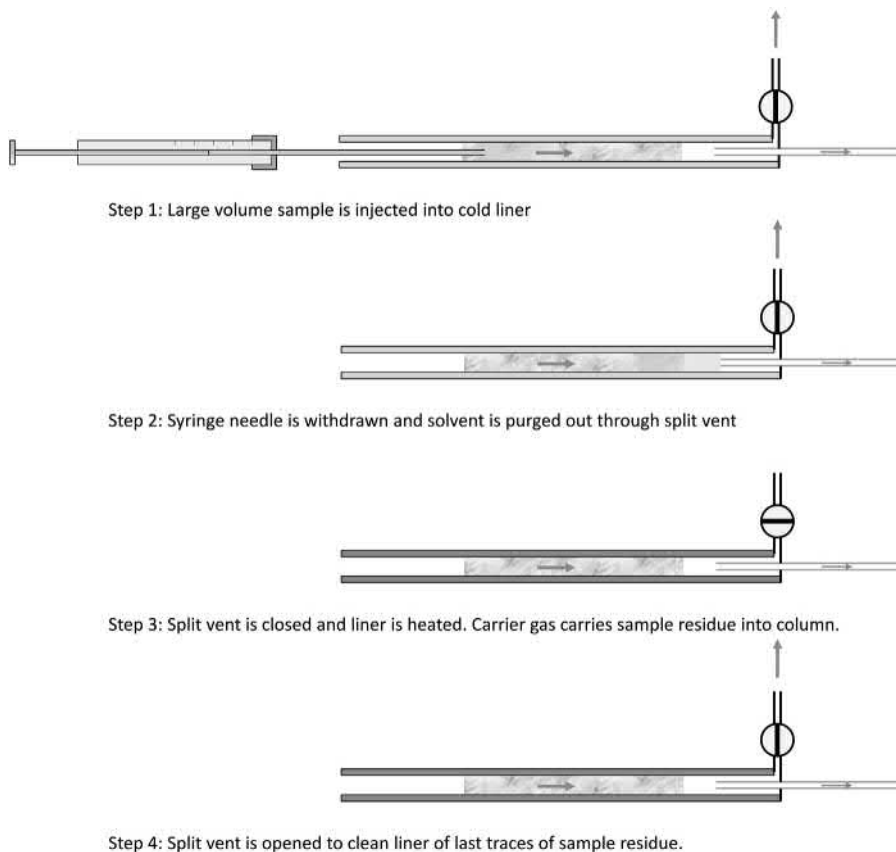


FIGURE 8.20 Large-volume injection with a PTV injector.

of the solvent vapor will enter the column. At the end of this “solvent purge” process, the less volatile components in the original sample should still remain in the liner. The split vent is then closed and the liner temperature is raised to effect the vaporization of the sample residue and its splitless transfer by carrier gas into the GC column.

For this technique to work, there must be a sufficient difference between the volatility of the solvent and the analytes. For n-alkane solvents, this normally means a 4-carbon number difference or a boiling-point difference of 100°C. The liner must be able to retain the large volume of liquid without it spilling over into the column or into the far recesses of the injector interior. A tight plug of glass or quartz wool will help with the liquid retention. Some liners have an etched surface to help with the liquid retention. Fig. 8.21 shows an example of a chromatogram produced using this technique with a chlorinated solvent on an electron capture detector.

A 2 × 50 mm liner bed will have a maximum volumetric capacity of just 160 μL (leaving no space for carrier gas); so such a liner would comfortably handle injection volumes of 50 μL but 100 μL would be too much.

For larger volumes, there are two approaches that could be considered:

- Multiple injections—for example, a 50-μL injection could be made and then solvent purged and then further injection/purge cycles could be applied until the desired volume is reached. After the final cycle, the split vent is closed and the liner temperature is increased to affect the injection.
- Partial concurrent vaporization [21–23]—the liner temperature is set to a value that is found to vaporize the sample solvent at a reasonable rate. A large syringe injects the sample at a slow rate so that the total volume of liquid inside the liner at any time does not exceed its capacity. This needs some trial and error to establish satisfactory conditions.

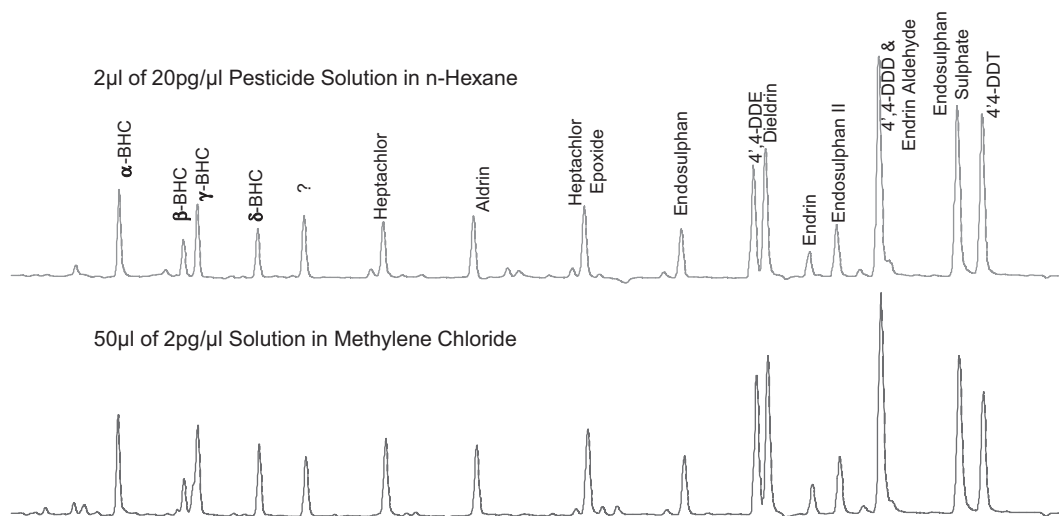


FIGURE 8.21 Example of a large-volume injection with a PTV injector. This compares the chromatography obtained on an electron capture detector from a solution of pesticides in a regular solvent like n-hexane against a dilute solution of the same compounds in methylene chloride using the LVI technique.

8.8 The gas sampling valve

The previous injectors discussed are primarily designed for liquid injection. It is possible to use some of these injectors with a gastight syringe to make injections of gas samples; however, this is a very manual process and subject to errors resulting mainly from temperature and pressure changes occurring inside the syringe during sample loading and injection.

In most instances, much better performance will be obtained through the use of a gas sampling valve. Although there is not real scope to cover this topic in detail in this section, the basics will be discussed.

A gas sampling valve is a mechanical device comprising a rotor with etched channels in it rotating between a series of ports that connect it to other components in a GC. There are a variety of valve designs with different numbers of ports in them that may be configured either independently or with other valves in a large number of ways for many different applications.

For injecting a gas sample into a GC column, we will just consider the classic 6-port valve configuration given in Fig. 8.22.

The principle of operation is straightforward. Prior to injection, sample gas flows through a valve loop as shown in Fig. 8.22. This stream may be flowing from a pressurized source, it may be introduced by a gas syringe, or it may be drawn through by a vacuum pump. Although the loop will have a fixed and normally calibrated capacity, the amount of sample injected

into the column will also be directly dependent on the temperature and pressure of the sample in the loop at the point of injection. For all gas analyses to be accurate, the samples and the calibration standard mixtures must all use the same loop and at the same temperature and pressure. If these requirements are met, a GSV is capable of producing the highest precision of any injection technique in GC.

To ensure that the temperature is consistent, the valve loop is often located inside the GC oven where it is effectively thermostated to the same temperature for each analysis. For most applications, the loop is held in a semisealed location so that it is effectively insulated from changes in the temperature of the ambient air.

For consistent sample pressure inside the loop, two approaches may be considered:

- using a backpressure regulator on the valve sample vent or
- turning off the sample supply (or reduce the flow rate) immediately prior to injection to allow the pressure inside the loop to decay to atmospheric pressure.

Because of the internal dead volumes of valves, their relatively high thermal mass, and the potential chemical activity of their internal surfaces, they are usually used with packed columns. Generally, this is not a problem as most gas analyses will require packed columns anyway to get the necessary retention and dynamic range.

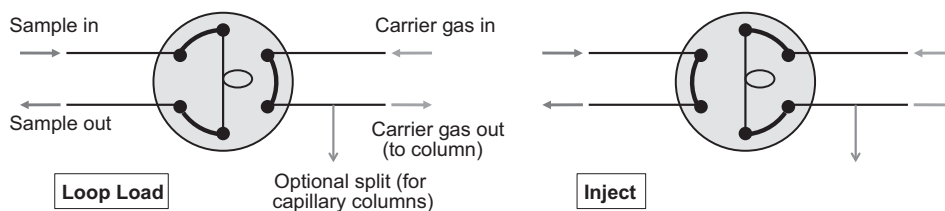


FIGURE 8.22 Example of a gas sampling valve configured for injection of gas samples into a GC column.

There are methods, however, that use capillary columns especially with some of the modern porous layer open-tubular (PLOT) columns. In such instances, a splitter is often deployed between the valve and column to get the peak widths sufficiently sharp for good chromatography.

An example of a gas analysis using GSV injection is given in Fig. 8.23.

8.9 The liquid sampling valve

Like the GSV, the liquid sampling valve (LSV) is a mechanical rotary valve with a fixed sample

capacity. It is used to inject a pressurized liquid into a GC column. Instead of an external loop that is connected to ports on the valve, the sample is loaded into a cavity on the rotor that is typically just a few microliters in capacity. The sample is fed, under pressure into the valve—a restrictor on the vent port maintains the sample in the liquid state within the valve.

Once the sample is loaded, the rotor rotates and the pressurized liquid rapidly vaporizes and it is carried to the column by a flow of carrier gas. A schematic diagram of a typical LSV installation is given in Fig. 8.24 and an example application is given in Fig. 8.25.

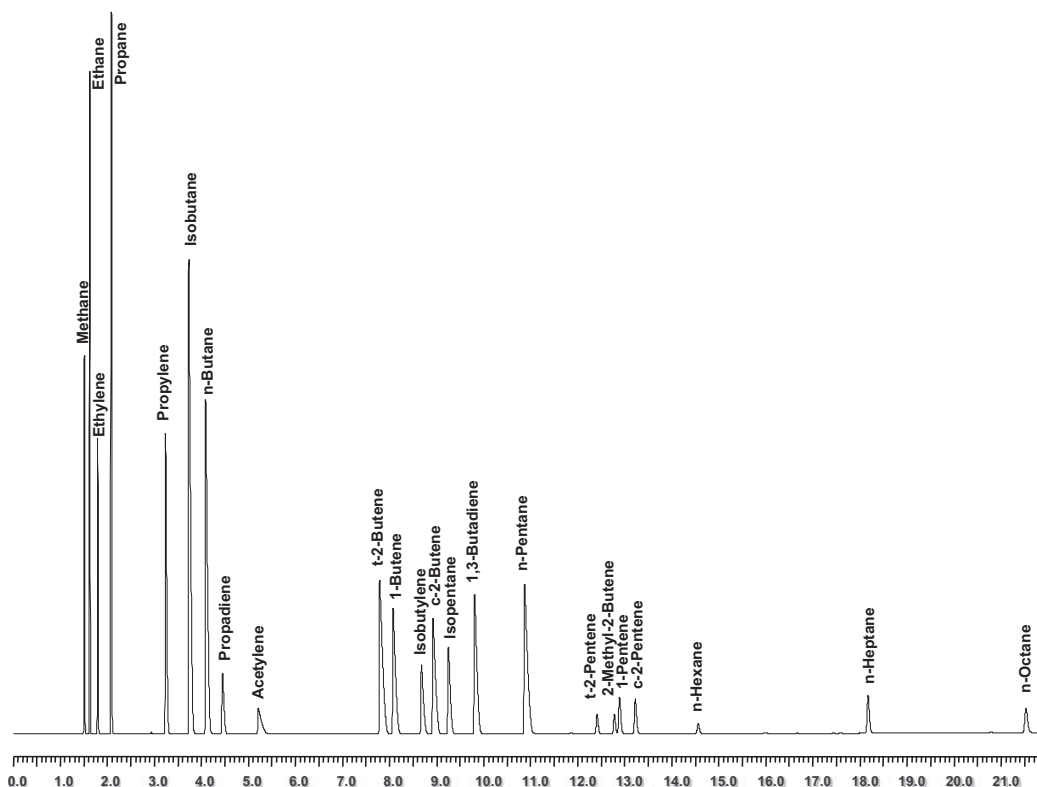


FIGURE 8.23 Example of a chromatogram on an alumina capillary porous layer open-tubular (PLOT) column using a gas sampling valve for injection of a refinery gas standard mixture.

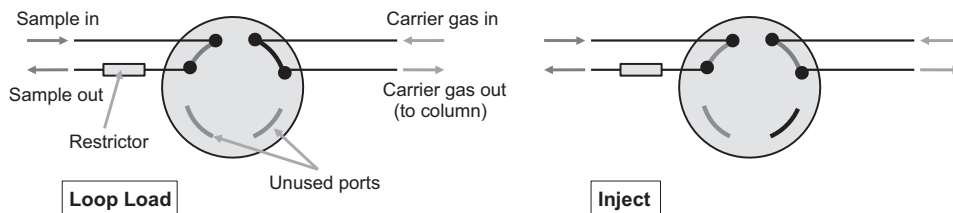


FIGURE 8.24 Example of a liquid sampling valve with internal loop built into rotor for injection of liquid samples into a GC column.

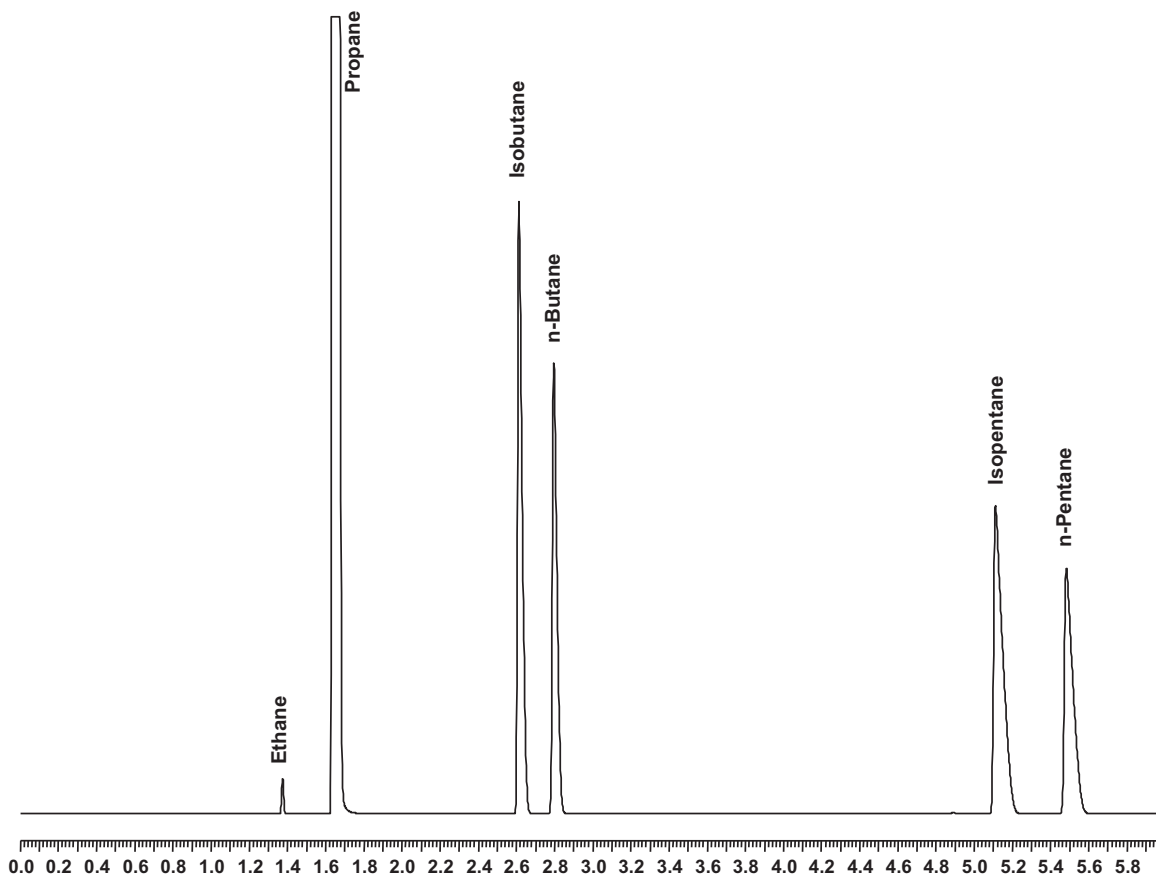


FIGURE 8.25 Example of a chromatogram using a liquid sampling valve for injection of a liquid petroleum gas standard mixture into an adsorbent packed column.

Acknowledgments

The author would like to thank PerkinElmer for its support in the writing of this chapter and colleagues who were so forthcoming with their help and advice.

References

- [1] S.P. Sutera, R. Skalak, The history of Poiseuille Law, *Annu. Rev. Fluid Mech.* 25 (1993) 1–19.
- [2] K. Grob, K. Grob, On-column injection on to glass capillary columns, *J. Chromatogr.* 151 (1978) 311–320.
- [3] K. Grob, On-column Injection in Capillary Gas Chromatography, Huethig, Heidelberg, 1987.
- [4] M. Buchgraber, F. Ulberth, E. Anklam, Interlaboratory evaluation of injection techniques for triglyceride analysis of cocoa butter by capillary gas chromatography, *J. Chromatogr. A* 1036 (2004) 197–203.
- [5] S. Ucles, E. Hawkme, C. Ferrer, A.R. Fernandez-Alba, Analysis of thermally labile pesticides by on-column injection gas chromatography in fruit and vegetables, *Anal. Bioanal. Chem.* 410 (2018) 6861–6871.
- [6] K. Grob, Solvent effects in capillary gas chromatography, *J. Chromatogr.* 279 (1983) 225–232.
- [7] K. Grob, Peak broadening or splitting caused by solvent flooding after splitless or cold on-column injection in capillary gas chromatography, *J. Chromatogr. A* 213 (1981) 3–14.
- [8] K. Grob, Broadening of peaks eluted before the solvent in capillary GC. 1 the role of solvent trapping, *Chromatographia* 17 (1983) 357–360.
- [9] K. Grob, G. Karrer, M.L. Riekkola, On-column injection of large sample volumes using the retention gap technique in capillary gas chromatography, *J. Chromatogr.* 334 (1985) 129–155.
- [10] K. Grob, Band broadening in space and the retention gap in capillary gas chromatography, *J. Chromatogr.* 237 (1982) 15–23.
- [11] K. Grob, H.-G. Schmarr, A. Mosandl, Early solvent vapor exit in GC for coupled LC-GC involving concurrent solvent evaporation, *J. High Resolut. Chromatogr.* 12 (1989) 375–382.
- [12] J.I. Cacho, N. Campillo, P. Vinas, M. Hernandez-Cordoba, Direct sample introduction gas chromatography and mass spectrometry for the determination of phthalate esters in cleaning products, *J. Chromatogr. A* 1380 (2015) 156–161.
- [13] K. Grob, K. Grob Jr., Splitless injection on capillary columns, 1. Basic technique – steroid analysis as an example, *J. Chromatogr. Sci.* 7 (1969) 584–586.
- [14] K. Grob, Split and Splitless Injection for Quantitative Gas Chromatography: Concepts, Processes, Practical Guidelines and Sources of Error, Wiley-VCH, Weinheim, 2007.
- [15] S. Bieri, P. Christen, M. Biedermann, K. Grob, Inability of unpacked gooseneck liners to stop the sample liquid after injection with band formation (fast autosampler) into hot GC injectors, *Anal. Chem.* 76 (2004) 1696–1701.
- [16] E. Boselli, K. Grob, G. Lercker, Solvent trapping during large volume injection with an early vapor exit – part 3: the main cause of volatile component loss during partially concurrent evaporation, *J. High Resolut. Chromatogr.* 22 (1999) 327–334.
- [17] P.L. Wylie, R.J. Phillips, K.J. Klein, M.Q. Thomas, B.W. Hermann, Improving splitless injection with electronic pressure control, *J. High Resolut. Chromatogr.* 14 (1991) 649–655.
- [18] J. Zrostikova, J. Hajslova, M. Godula, K. Mastovska, Performance of programmed temperature vaporizer, pulsed splitless and on-column injection techniques in analysis of pesticide residues in plant matrices, *J. Chromatogr. A* 937 (2001) 73–86.
- [19] F.S. Poy, F. Visani, F. Terrosi, Automatic injection in high-resolution gas chromatography: a programmed temperature vaporizer as a general purpose injection system, *J. Chromatogr.* 217 (1981) 81–90.
- [20] E. Hoh, K. Mastovska, Large volume injection techniques in capillary gas chromatography, *J. Chromatogr. A* 1186 (2008) 2–15.
- [21] W. Vogt, K. Jacob, A.B. Ohnesorge, H.W. Obwexer, Capillary gas chromatographic injection system for large sample volumes, *J. Chromatogr.* 186 (1979) 197–205.
- [22] W. Vogt, K. Jacob, H.W. Obwexer, Sampling method in capillary column gas-liquid chromatography allowing injections of up to 250 μ l, *J. Chromatogr.* 174 (1982) 437–439.
- [23] F. Munari, A. Trisciani, G. Mapelli, S. Trestianu, K. Grob Jr., J.M. Colin, Analysis of petroleum fractions by online micro HPLC-HRGC coupling, involving increased efficiency in using retention gaps by partially concurrent solvent evaporation, *J. High Resolut. Chromatogr.* 8 (1985) 601–606.

Headspace gas chromatography

Michael J. Sithersingh¹, Nicholas H. Snow²

¹KR Consultants, Parsippany, NJ, United States; ²Chemistry and Biochemistry, Seton Hall University, South Orange, NJ, United States

9.1 Introduction

The term “headspace” in gas chromatography (GC) denotes the vapor phase within a sealed container also containing a liquid or solid. Usually, the vapor is above the liquid or solid, at the top of the container, hence the term “headspace.” Headspace extraction refers to the collection and analysis of the vapor phase in the container. There are two modes of headspace extraction: static and dynamic. In static headspace extraction (SHE), which is more common, the vapors are sampled from a system that is brought to equilibrium prior to the sampling, typically in a sealed vial or container. In dynamic headspace extraction (DHE), a gas flows through or over the sample moving sample vapors to a sorbent for collection. DHE is commonly referred to as “purge and trap”.

In a typical SHE, a liquid or solid sample is placed in a sealed vial and heated to a predetermined temperature until equilibrium is reached, providing a constant composition mixture of gases in the vapor phase. An aliquot of this vapor-phase mixture is withdrawn from the container and transferred to a gas chromatograph for separation and analysis of the components. Since a defined amount of the equilibrium

vapor is taken and carried to the column in the gas chromatograph for the analysis, only volatile substances reach the gas chromatographic column, with nonvolatile matrix components remaining in the sample container. Complex sample matrices, especially those that include volatile analyte(s) in a less volatile matrix, which would otherwise require sample extraction or preparation, or be difficult to analyze directly, are ideal candidates for headspace extraction, since they can be placed directly in a vial with little or no preparation.

Table 9.1 provides a quick overview of headspace extraction techniques and a summary of sample matrices and concentration levels amenable to each. Today, SHE includes a family of techniques, which can be as simple as using a gas-tight syringe to collect a sample of the vapor from a vial or as complex as using multiple sorbents to extract analytes from a vapor phase. An equilibrium technique that generally does not extract all of the analyte from the sample, SHE can be used for analyte concentrations ranging from percent to part per billion. Multiple headspace extraction (MHE) is a variant of SHE that can be used to analyze lower concentrations by performing multiple extractions. DHE is most often used for lower concentration samples,

TABLE 9.1 Summary of Headspace Extraction Techniques. Selected Concentration Levels are General Guidelines.

	Sample matrix			Analyte concentration			
	Solid	Liquid	Gas	High	ppm	ppb	Sub-ppb
Static headspace extraction—gas-tight syringe (SHE)	X	X	X	X	X		
Static headspace extraction—loop and pressure-balanced (SHE)	X	X			X	X	
Dynamic headspace extraction (DHE) (purge and trap)		X				X	X
Multiple headspace extraction (MHE)	X	X			X	X	
Sorptive extractions (SPME/SBSE/SDME)	X	X	X		X	X	X

ppb or lower, as it provides strong analyte concentration and can be an exhaustive extraction technique. Techniques such as DHE and the sorptive methods, which may add instrumental complexity and allow concentration of the headspace vapors, are preferred for the lowest concentration analytes, while simpler, inexpensive methods such as a gas-tight syringe inserted into a vial may be effective for higher analyte concentrations. The traditional instrumental SHE techniques using pressure-balanced or loop-type systems can be used for a broad range of samples, usually ranging in the ppm to ppb concentration levels. Detector sensitivity and detection limits also play roles in the choice of technique. A more sensitive detector may allow simpler instrumentation or less sample concentrating.

9.1.1 History

The precise origin of the idea that analyzing the headspace above a sample in a sealed container would provide useful information about the composition of the sample is unclear. Some early non-GC-related applications of “aerometric analysis” date to the 1930s [1,2]. The use of headspace extraction with GC is almost as old as GC itself, dating to the 1950s. Early work in the late 1950s and early 1960s included analysis of nontraditional samples, such as food in flexible packaging, soda in cans, and ethanol in blood and breath, and led to the introduction of the first automated instrument for headspace GC in the late 1960s. In 2002,

Ettre provided an excellent and concise history of the early days of headspace extraction for GC [3].

The popularity of headspace GC has grown over the past 50 years due to automation of the instruments and the seeming fundamental simplicity of the technique [4–10]. Some common fields of application include analysis of polymers [11], volatile components in drinks and foodstuffs [12,13], forensics and blood alcohol [14,15], water and environmental analysis [16], and fragrances in perfumes and cosmetics [17]. In the pharmaceutical industry, headspace GC is widely used to determine residual solvents in active pharmaceutical ingredients (APIs) and drug substances [18,19]. The United States Pharmacopeia (USP), harmonized with the International Conference on Harmonization (ICH), incorporated the technique into its General Chapter <467> “Residual Solvents” to determine the most common residual solvents in drug substances using headspace GC [20–22].

9.1.2 Print and online resources

There is a large literature of headspace GC applications, although it can be difficult to access as specific headspace symposia, books, journals, and reviews are relatively few. The theory and practice of SHE are thoroughly described in three texts, by Kolb and Ettre, Ioffe and Vitenberg, and Hachenberg and Schmidt [23–25]. Headspace extraction in its various forms is often covered as a chapter or as part of the sample preparation chapter in general textbooks about GC [26,27].

Hinshaw's two-part discussion of headspace GC principles and instrumentation is freely available online [28,29]. When searching literature databases, such as SciFinder or Science Direct, care should be taken to be as specific as possible about the use of keywords, as general keywords, such as "headspace and water," can produce thousands of references. Instrument vendor websites and general chromatography websites may also provide information and application notes to assist in developing headspace-based methods [30]. As a general resource for SHE, the text by Kolb and Ettre, mentioned earlier, is the best starting point.

9.2 Fundamentals of headspace extraction

There are several means by which the vapor component in a sealed container may be collected and transferred to a gas chromatograph. In SHE, analyte vapors may be transferred using a gas-tight syringe, a capillary, or a sample loop placed between the vial and the gas chromatographic inlet, or vapors may be trapped on a sorbent followed by desorption into the gas chromatograph. In DHE (purge and trap), a gas is passed through the liquid phase, evaporating analytes, which are then collected on a sorbent and transferred to the gas chromatograph. While the solution–vapor-phase equilibrium upon which headspace extraction is based is generally straightforward, there are subtleties in both theory and instrumentation that make headspace extraction similar to the game of chess: easy to learn, yet challenging to master.

9.2.1 Static headspace extraction (SHE)

Fig. 9.1 shows a schematic representation of a vial containing the sample phase in equilibrium with the headspace of the vial, gaseous phase. The sample phase contains the analytes and

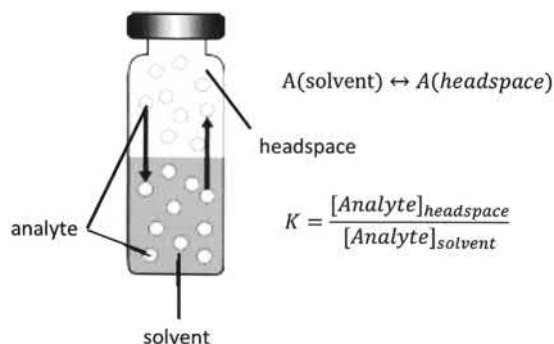


FIGURE 9.1 Schematic of the system for static headspace extraction inside a sealed vial with equilibrium constant expressions.

matrix. The volatile analytes, originally present in the sample phase, are distributed between the two phases at equilibrium. Most extraction and chromatographic theory assumes that the system is at equilibrium. Failure to bring the system to equilibrium is one of the most common causes of problems with reproducibility in extractions.

The chemical equation and equilibrium constant expression leading from this configuration are given in Eqs. (9.1) and (9.2), which describe the phase transfer of an analyte from the sample phase in the bottom of the vial into the vapor phase above it:



$$K = \frac{[A(\text{headspace})]}{[A(\text{sample})]} \quad (9.2)$$

In their text, Kolb and Ettre use mass balance to derive an expression relating the chromatographic peak area (A) in SHE-GC to the analyte concentration in the vapor phase (C_G), the initial analyte concentration of a liquid sample (C_0), the analyte's solution–vapor partition constant (K), and the phase ratio (β) in the sealed vial. This

is the fundamental relationship in SHE that provides the basis for related techniques:

$$A \propto C_G = \frac{C_0}{K + \beta} \quad (9.3)$$

It is interesting to note that the partition constant in Eq. (9.3) is for the reverse of the system shown in Eqs. (9.1) and (9.2), so most partition constants determined in SHE systems are expressed with the larger values favoring the condensed phase. This keeps this partition constant consistent with GC, in which the analyte concentration in the stationary phase is in the numerator of the equilibrium constant expression. The fundamental importance of β and K is described subsequently. Also note that by itself, this expression does not account for matrix effects, which would alter the sample–vapor partition coefficient, K .

9.2.1.1 Phase ratio (β)

The phase ratio is defined as the ratio of the volume of gaseous phase, V_G , to the volume of the sample liquid phase, V_S , in a vial of total volume V_V . It allows definition of the mass balance of the distribution of a dissolved analyte between the two phases in the vial:

$$\beta = \frac{V_G}{V_S} \text{ and } V_V = V_G + V_S \quad (9.4)$$

A known, reproducible sample volume (careful delivery of the sample into the vial) and reproducible vial volume are both necessary for effective quantitative analysis. Although the vial is usually heated following sample delivery, the change in volume of the sample phase upon heating is generally insignificant. Since the vial is a closed system, the vapor moving from the sample phase to the gaseous phase does not change the vapor-phase volume although it can change the pressure. Therefore, the initial volume of the sample added to the headspace vial remains the same after equilibrating the vial to the desired condition.

9.2.1.2 Partition coefficient

The partition coefficient or distribution constant is the equilibrium constant of an analyte partitioning between two phases at equilibrium as described in Eqs. (9.1) and (9.2). In this chapter, K is defined as described by Kolb and Ettre: the ratio of the concentration of the analyte in the sample phase (C_S) to that of the analyte in the gaseous phase (C_G) at equilibrium, the inverse of Eq. (9.2):

$$K = \frac{C_S}{C_G} \quad (9.5)$$

The sensitivity of an analysis in headspace GC depends on the partition constant of the analyte. A lower partition constant indicates a higher concentration of the analyte in the vapor phase and higher sensitivity. Method development efforts such as increasing the vial temperature, salting out, and adjusting the pH are often geared toward reducing the partition constant. K is related to more than the vapor pressure and enthalpy of vaporization of the analyte; its solubility in the sample phase is also important. Lower solubility can assist in driving the analyte into the vapor phase. This can be thought of as being similar to the idea of activity versus concentration. These ideas will be discussed later in this chapter, in the section on method development.

As seen in the denominator of Eq. (9.3), the relative magnitude of the partition constant and phase ratio is a critical aspect of method development, discussed in detail in Section 9.4. The measured chromatographic peak area is further directly proportional to the concentration of the analyte in the gas phase, through instrument response–related factors such as injection technique and detector response. These factors account for the use of a proportionality symbol rather than an equal sign in Eq. (9.3).

SHE is an equilibrium-based technique. Generally, the analyte is not exhaustively removed from the sample matrix. Rather, a portion of the

total amount of the analyte, based on the partition constant and factors in the discussion earlier, is collected and analyzed. This can be problematic, as much method development time and effort involve defeating the problem of reaching equilibrium in the sample vial, with a reproducible partition constant, even as the matrix may change from sample to sample. If the reproducibility of a final method is not satisfactory, it is likely that equilibrium in the sample vial has not been achieved prior to sampling or the sampling method itself alters the equilibrium position in the vial.

9.2.1.3 Multiple headspace extraction

In MHE, analytes are extracted multiple times from the sample vial, providing the possibility for exhaustive extraction or derivation of the instrument response that exhaustive extraction would provide. MHE is analogous to extracting the compounds of interest from a sample multiple times using a separatory funnel with fresh aliquots of solvent each time and combining the extracts. After several extraction steps, the analytes of interest may be exhaustively extracted from the original sample.

Using the same instrumentation as SHE, the concentrations of the analytes are determined at each extracted step. After each extraction, the analytes in the headspace vial are reequilibrated between the sample phase and the gaseous phase. The decrease in concentration of the compound in subsequent extraction steps follows a first-order exponential decay with the time variable being the number of extractions and the exponential term k being determined experimentally in the same fashion as a first-order rate constant:

$$C = C_0 e^{-kt} \quad (9.6)$$

In order to be useful experimentally, it is convenient to express Eq. (9.6) in terms of the chromatographic peak area, replacing the time t with the number of extraction steps performed,

n . The initial concentration C_0 is replaced with the peak area A_1 from the first extraction step, which occurs at $n-1$:

$$A_n = A_1 e^{-k^*(n-1)} \quad (9.7)$$

A_n is the peak area of the analyte at the number of extraction steps, n , and k^* is the new constant obtained by including instrument parameters. The parameters may be obtained by expressing Eq. (9.7) in a linear form and plotting the natural logarithm of the obtained peak areas versus the number of extractions, shown in Eq. (9.8):

$$\ln A_n = -k^*(n-1) + \ln A_1 \quad (9.8)$$

By summing the peak areas from each extraction step, the total peak area of any volatile analyte in the sample can be determined as seen in Eq. (9.9):

$$\sum A_n = \frac{A_1}{(1 - e^{-k^*})} \quad (9.9)$$

An extrapolated total peak area, which corresponds to the total amount of the analyte present in the sample, can be obtained by applying the values determined using regression analysis, with Eqs. (9.8) and (9.9). MHE allows exhaustive extraction using the same instrumentation as SHE; although with multiple extraction steps, it can be time-consuming.

9.2.2 Sorptive extraction

Many SHE techniques involve the addition of a sorbent to trap analytes for transfer to the GC rather than the direct transfer of the vapor phase. A sorbent may be placed directly into the sample vial, as in headspace solid-phase microextraction (HS-SPME) [31,32], stir-bar sorptive extraction (SBSE) [33], or single-drop microextraction (HS-SDME, HS-LPME) [34], in which a liquid drop is placed in the headspace, or the sorbent can be placed directly in the transfer line (HS-trap) [35].

HS-SPME is the most developed of these techniques, so it is discussed in more detail here; the other methods rely on similar principles.

Fig. 9.2 gives a schematic presentation of an HS-SPME sampling system. Note the similarity to Fig. 9.1 except that the system now includes the SPME fiber, exposed to the headspace. This generates a second equilibrium, besides the sample–vapor-phase equilibrium that must be considered: the vapor-phase–fiber equilibrium. By manipulating both equilibrium constants, HS-SPME has proven highly sensitive and versatile.

In HS-SPME, the analytes are partitioned between three phases, liquid phase, gaseous phase, and the fiber phase, so the mass balance is more complex. The liquid phase and the fiber coating are connected by the gaseous phase. The amount of a volatile analyte distributed between these three phases is shown in Eqs. (9.10) and (9.11):

$$C_0 + V_S = (C_S \times V_S) + (C_G \times V_G) + (C_F \times V_F) \quad (9.10)$$

$$A(\text{sample}) \leftrightarrow A(\text{headspace}) \leftrightarrow A(\text{fiber}) \quad (9.11)$$

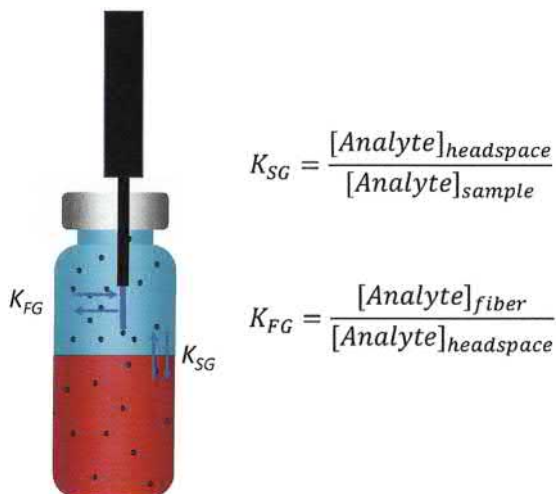


FIGURE 9.2 Schematic of the system for static headspace extraction inside a sealed vial with a sorbent, an SPME fiber in this example, collecting analyte vapors from the headspace. Note the presence of two equilibria.

where C_0 is the concentration of the analyte in the original sample with volume V_S and C_S , C_G , and C_F are the concentrations of the analyte at equilibrium in liquid phase, gaseous phase, and fiber with volumes V_S , V_G , and V_F , respectively. As seen earlier, there are two sets of equilibrium constants, $K_{G/S}$ and $K_{F/G}$, which are involved in this system and can be written as follows:

$$K_{G/S} = \frac{C_G}{C_S} \text{ or } C_S = \frac{C_G}{K_{G/S}} \quad (9.12)$$

$$K_{F/G} = \frac{C_F}{C_G} \text{ or } C_G = \frac{C_F}{K_{F/G}} \quad (9.13)$$

Eqs. (9.10)–(9.13) can be combined and rearranged to give the mass of analyte extracted into the fiber, shown in Eq. (9.14):

$$W_F = \frac{(C_0 V_S V_F K_{F/G} K_{G/S})}{\left[(K_{F/G} K_{G/S} V_F) + (K_{G/S} V_G) + V_G \right]} \quad (9.14)$$

The mass of the analyte extracted into the fiber, which is then injected into the GC, is a function of nearly all variables that may occur in the vial. If the small fiber volume along with possible cases of $K_{G/S}$ is considered, Eq. (9.14) simplifies to two cases:

$$K_{G/S} \ll 1: W_F = C_0 \left(\frac{1}{\beta} \right) V_F K_{F/G} K_{G/S} \quad (9.15)$$

$$K_{G/S} \gg 1: W_F = C_0 \left(\frac{1}{\beta} \right) V_F K_{F/G} \quad (9.16)$$

When $K_{G/S}$ is large (low volatility or semivolatile analytes), the mass extracted is essentially related to the vapor–fiber partition constant, which is likely to also be large; when $K_{G/S}$ is small (volatile analytes), the mass is related to both partition constants. For example, heating the vial may drive more analyte into the vapor phase from the sample, but reduce extraction from the vapor to the fiber. In any event, both

equilibria should be considered during method development. Following the extraction, the sorbent is transferred to the inlet of a gas chromatograph and desorbed into the column. This presents an additional process that also must be optimized during method development.

The other sorbent-based techniques work on the same principles. HS-SBSE is essentially the same as HS-SPME except that the stir-bar coating has a much larger volume than the SPME fiber (although still much smaller than the sample and vapor volumes), allowing a larger mass of analyte to be extracted, although with slower kinetics. In HS-SDME and HS-LPME, a small drop of liquid is suspended in the headspace phase; therefore, extraction theory is almost exactly the same as for SPME, except that the liquid solvent is less viscous and has lower surface tension than the polymeric phases used in SPME, allowing for possibly faster equilibration. In HS-trap systems, analyte vapor is trapped on a sorbent following extraction in a manner similar to purge and trap, described next.

9.2.3 Dynamic headspace extraction (purge and trap)

DHE, also called “purge and trap,” provides a means for exhaustive extraction of the analyte from the matrix. An inert gas is bubbled through a liquid sample, continuously evaporating and removing volatile analyte(s) from the less volatile solvent. This system does not reach equilibrium in the sample vial, as the evaporation process is continuous; however, Le Chatelier's Principle, the drive toward equilibrium generated by removing the vapor-phase analyte(s) and continuously refreshing the gas stream with fresh gas, enables exhaustive extraction. The ability and time required to extract analytes are dependent on the equilibrium constant, diffusion kinetics, and the volume of gas passed through the sample. Following extraction, the flowing gas containing extracted analyte(s) is

passed over a sorbent trap to collect them. They are subsequently desorbed into the inlet of a gas chromatograph.

As in SHE with a sorbent trap, purge and trap involves three steps driven by their equilibrium constants. In the purge step, an inert gas is passed through the sample to evaporate and carry volatile analytes into the vapor phase. In the second step, the gas is passed over a sorbent trap that extracts the analytes from the vapor phase. In the third step, analytes adsorbed on the trap are desorbed back into a flowing gas stream and into the inlet of the GC. Most fundamental developments in purge and trap have focused on developing trapping sorbents that can extract a variety of volatile analytes from the vapor phase. Often, a multilayer sorbent that consists of a combination of weak, moderate, and strong materials, such as Tenax, silica gel, and charcoal, respectively, is used.

9.3 Instrumentation and practice

The basic principle underlying all instrumentation for headspace GC is that an aliquot of the analyte from the vapor phase above a liquid or solid sample in a sealed vial or container must be reproducibly and effectively transferred to the inlet of a gas chromatograph. There are several means for accomplishing this, including: gas-tight syringe, transfer line, sample loop, and collection on a sorbent. The most important challenges are to ensure that the sample composition that reaches the gas chromatograph is truly representative of the composition of the headspace vapor in the vial and that the headspace vapor is representative of the composition of the original sample. Fundamentals of each approach are described in the following sections.

Table 9.2 provides a summary of systems offered by major instrument vendors and the modes of headspace extraction for each, found by searching World Wide Web sites in spring, 2020. Most systems employing a simple

TABLE 9.2 Major Headspace Vendors and Instruments 2020.

Vendor/Unit	Type	SHE	SHE/Trap	MHE	DHE	Sorbent
Agilent 7697A	Loop	X	X	X		
Agilent G1888	Loop	X		X		
CDS Purge and Trap	P+T				X	
CTC PAL (multiple versions and vendors)	Syr		X	X	X	X
Dani Master SHS	Loop	X	X	X		
EST Purge and Trap	P+T				X	
PerkinElmer Turbo Matrix	PB	X	X	X		
Shimadzu HS-20	Loop	X	X	X		
Tekmar Purge and Trap	P+T				X	
Thermo Scientific tri-plus 500	Loop	X	X	X		

DHE, dynamic headspace extraction; *MHE*, multiple headspace extraction; *SHE*, static headspace extraction; *SHE/Trap*, static headspace extraction with sorbent trap; *Sorbent*, sorbent headspace extraction (SPME/SBSE/SDME); Type, sampling type (Loop, P+T (purge and trap), Syr (gas-tight syringe), PB (pressure-balanced)).

gas-tight syringe are now automated using CTC PAL rail-based autosamplers. Note that most GC vendors also include their own versions of rail-based systems as an option. Most systems today are based on loop injection for sample transfer, with PerkinElmer the main vendor employing pressure-balanced sampling. Most also include a trapping capability to allow multiple static extractions followed by trapping and combining the aliquots on a sorbent, followed by transfer to the GC. Purge and trap can also be performed online with nearly any capillary GC system. Choosing a headspace instrument to add to a GC is a lot like customizing a car. Consider capability along with ease of interfacing and vendor support. Mixing vendors is often difficult.

9.3.1 Gas-tight syringe

Classically and most simply, headspace may be sampled using a gas-tight syringe of appropriate volume. This is also the most convenient and inexpensive method for sampling vapors from nontraditional containers such as cans or bags. The syringe is inserted into the headspace

and an aliquot of appropriate volume is removed. Modern rail-type autosamplers can easily accommodate a heated gas-tight syringe and a vial oven allowing automation of this procedure. Although seemingly simple, there are several challenges associated with this method:

- If the syringe volume is similar to the headspace volume, equilibrium in the vial may be disrupted. In effect, insertion of the syringe and withdrawal of the syringe plunger result in an increase in the vapor-phase volume, disrupting equilibrium.
- If the syringe is at a lower temperature than the vial, analyte(s) or matrix components may condense in the syringe.
- The syringe volume and concentration of analytes may necessitate significant optimization of the injection conditions for GC.
- The syringe may require cleaning or purging with inert gas between each analysis.

Heated and/or purged syringes are available to reduce these challenges. Although reproducibility may be difficult to obtain, even using an

automated system, a gas-tight syringe is the least expensive and simplest way to begin using or to test the feasibility of a proposed SHE method.

9.3.2 Transfer-line-based systems

The most common method for directly transferring an aliquot of the headspace within a vial to a gas chromatograph is by using a capillary transfer line. Both pressure-balanced and loop-based systems use a heated transfer line to move the sample from the vial or sorbent trap to the inlet of the GC. Because the gas chromatographic inlet is pressurized, the vial must be pressurized to a pressure higher than the inlet prior to sampling. The pressure drop from the vial to the inlet, the sampling time, and the transfer-line dimensions determine the amount of vapor that is transferred from the vial to the inlet. This also means that there are several steps in a transfer-line-based analysis that must be optimized during method development. A schematic diagram of these steps for a pressure-balanced system is shown in Fig. 9.3. The same gas flow is used both for pressurizing the vial and as a carrier gas for the GC.

9.3.2.1 Thermostating and pressurizing

During the thermostating phase, the sampling needle is in the upper position. The carrier gas flows through the solenoid valve V1 to the column; at the same time, the needle cylinder is purged by a small cross-flow vented through solenoid/needle valve V2. After thermostating, the two phases attain equilibrium. At this stage, the sampling needle pierces the septum and the tip of the needle is positioned in the headspace of the vial. The carrier gas flows into the vial headspace, pressurizing the vial for a preset time, usually a few minutes, to achieve homogenization of the volatile analyte and the incoming carrier gas in the headspace of the vial.

9.3.2.2 Injection

After pressurization of the vial, the solenoid valves are closed, stopping the carrier gas flow from the headspace sampler. Now, the needle inside the headspace vial is opened up to the injection port of the GC system via the transfer line. The pressurized gas expands and flows into the injection port through the transfer line and then to the column for a preselected injection time.

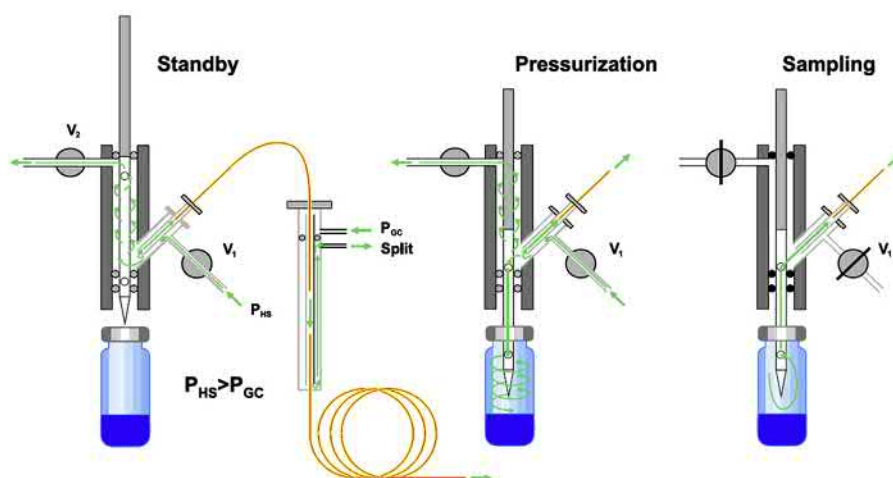


FIGURE 9.3 Steps in static headspace extraction with a transfer-line-based system. First the vial is heated with no connection to the inlet (standby). Second, the vial is pressurized with carrier gas (pressurization). Third, the pressurized vial is opened to the transfer line and inlet (sampling). Courtesy PerkinElmer Instruments.

At the end of the injection time, the solenoid valves are opened, preventing any of the vial headspace from being additionally transferred through the needle.

Pressure-balanced sampling is highly reproducible and uses the injection time and pressure to determine the volume of the sample transferred to the GC, so these are generally electronically controlled. It should be noted that when the headspace vial is pressurized during the pressurization mode, the volatile analyte in the gaseous phase is diluted by the addition of the carrier gas and also the equilibration achieved after thermostating the vial is disturbed. It is possible that a small amount of analyte might move back to the liquid phase, but the effects on quantitation are negligible, since these factors are constant throughout multiple injections. Since pressurization of the vial following equilibration may disrupt the equilibrium, pressure-balanced SHE is not the best technique for determining physical constants, such as partition constants, for example.

9.3.3 Sample-loop system

The sample-loop system is another injection mode used in SHE and MHE, depicted in Fig. 9.4 and offered by several vendors in their systems. This system encompasses a sample loop connected to the headspace vial and transfer line to the GC system through a six-port valve. The headspace sample vial is pressurized to a preset value after thermostating the vial. The vial is then opened to the loop for a short time. The sample thus collected in the loop is swept by the carrier gas to GC injection port through a transfer line. Fig. 9.4A–D depict the various modes in the loop sampling system.

During pressurization, the heated needle pierces through the septum of the headspace vial and is positioned in the headspace of the vial. The vial is pressurized using the carrier gas for a preset time in order to obtain a uniform mixture of volatile components in the headspace. After pressurization, the headspace of the vial is opened through the needle to the heated sample

loop through the six-port valve. The sample from the headspace of the vial moves into the sample loop and purges the loop. The sample loop is opened to the atmosphere during filling and then closed to allow it to reach equilibrium. During injection, the sample collected in the loop is swept into the inlet through the heated transfer line for a preset time. After the injection time, the system goes back to a standby condition in which the carrier gas bypasses the loop and flows to the inlet through the transfer line.

9.3.4 Purge and trap

Like SHE, purge and trap relies on the volatility of the analytes to achieve extraction and release from the matrix. However, the volatile analytes and matrix are not allowed to reach a state of equilibrium. This is accomplished by continually sweeping the carrier gas through the sample or across the headspace of the sample matrix, thus providing a continuous concentration gradient, which aids in the more exhaustive extraction of the analytes by the Le Chatelier's principle. Once in the carrier gas, the analytes are swept from the vial and trapped on a sorbent prior to analytical analysis.

Fig. 9.5 shows a schematic representation of a typical purge-and-trap system. In Step 1, the purge gas, usually helium or the same gas as the carrier gas for the GC, is passed through the sample in a vial and is vented to the trap using a six-port valve, as seen on the green (white in printed version) lines in the figure. The red (black in printed version) lines show carrier gas flowing directly to the GC. The valve is then switched to desorb the trap into the GC. In Step 2, injection, the carrier gas now passes through the trap and into the GC, as seen in the green (white in printed version) lines and the red (black in printed version) lines show the sample vial being vented to waste. This allows control over variables such as the time and flow rate of the gas. Note that this is a multistep process: first analytes are evaporated from the matrix and adsorbed on the trapping material and finally desorbed into the gas chromatograph.

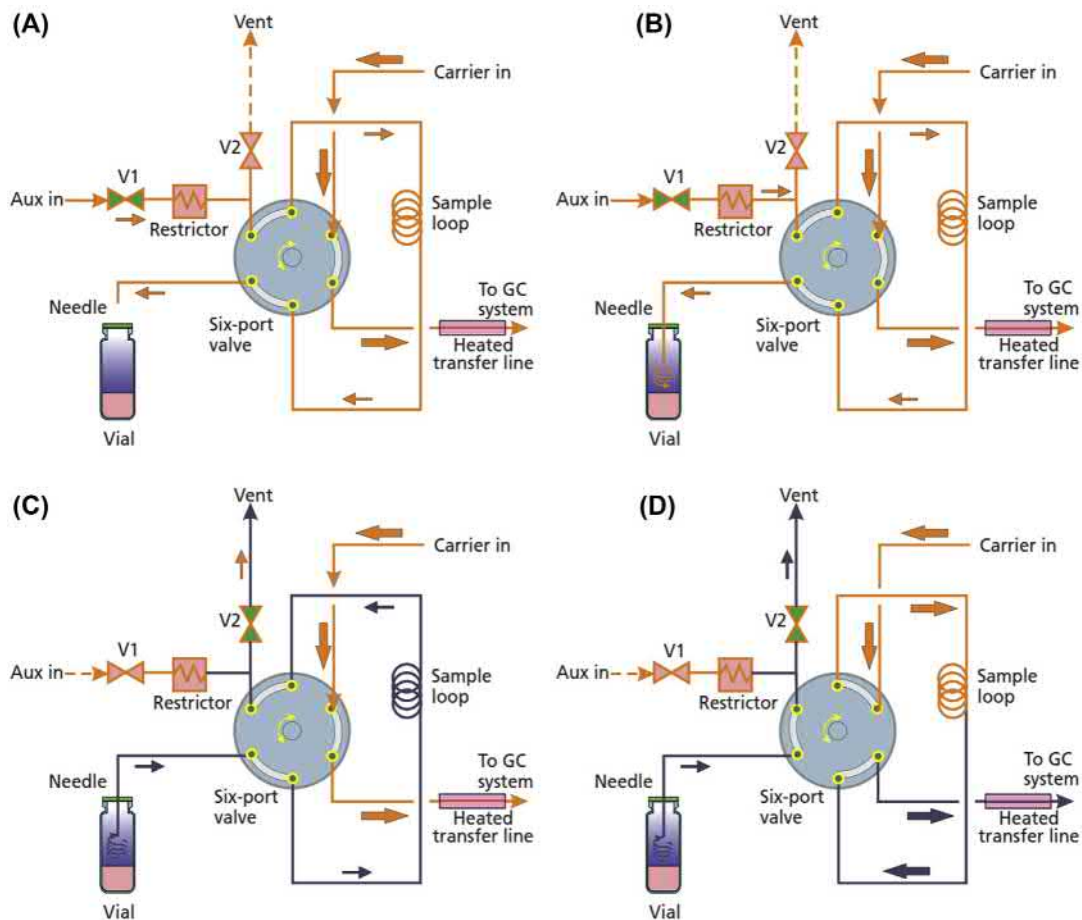


FIGURE 9.4 Steps in static headspace extraction with a sample loop-based system. (A) standby; (B) pressurization; (C) loop filling; and (D) injection. Orange (White in print version) connecting lines denote inert gas flows; blue (black in print version) lines denote sample gas. Reprinted with permission of the author from reference [29].

There are several methods of analyte trapping: cryogenic, sorbent, and column focusing. Each of these methods has advantages and disadvantages. In general, the trap should do the following: retain the analytes of interest, not introduce impurities, and allow rapid injection of the analytes to the column. Once the analytes are sorbed on the trap, they must be desorbed into the gas chromatograph. This is most often accomplished by passing the carrier gas over the trap, combined with heating to facilitate desorption.

9.3.5 Solid-phase microextraction, stir-bar sorptive extraction, and single-drop microextraction

The instrumentation for SPME, SBSE, and SDME is straightforward. In SPME, a coated fused-silica fiber is contained within a syringe needle as seen in Fig. 9.2. The fiber is retracted into the needle for storage and transport and is extended from the needle for extraction in a vial and desorption into a gas chromatograph. SPME can be performed in both manual and

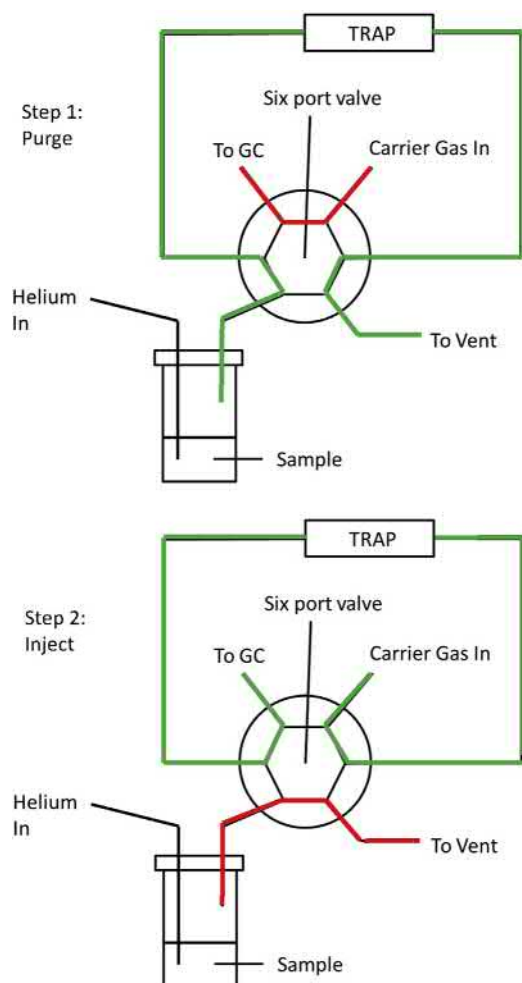


FIGURE 9.5 Schematic of a purge-and-trap system. (A) First, gas is passed through a liquid sample in a sealed vial and passed over the trap (green [white in print version] lines) and the carrier gas passes directly to the GC (red [black in print version] lines). (B) Second, the six port valve is moved and the carrier gas passes through the trap and into the GC (green [white in print version] lines) and the vial is connected to waste (red [black in print version] lines).

automated instruments. In SBSE, the coated stir bar is suspended in the headspace, while in SDME, a liquid drop is suspended from the tip of a standard microsyringe needle, as seen in Fig. 9.6, which shows a schematic of an HS-SDME setup with a drop of 1-octanol suspended in the headspace of a glass vial [36,37].

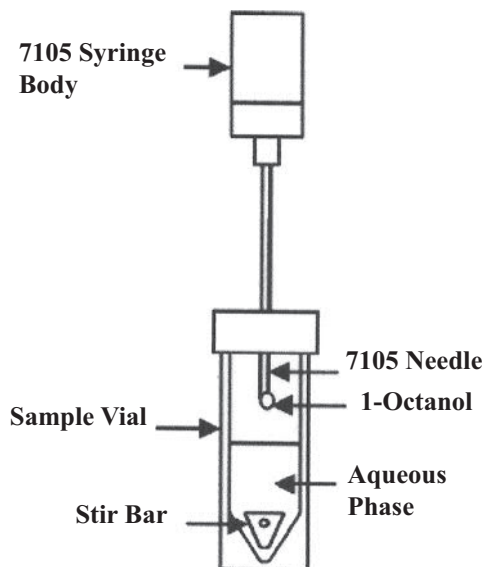


FIGURE 9.6 Schematic of a headspace SDME system with the liquid drop suspended in the headspace of the vial. The drop would be retracted into the needle for transfer to the gas chromatograph. *Reproduced with permission from H. Hachenberg, A.P. Schmidt, Gas Chromatographic Headspace Analysis, Hayden and Son, 1977. (Translated by D. Verdin). Copyright 2001, American Chemical Society.*

9.4 Method development considerations

Method development for headspace extractions is based on similar considerations for all analytical methods. There are compromises between sensitivity, resolution, and ease of use that must be made. In all cases, the mass of the analyte that can be extracted is governed by the initial concentration in the original sample, the partition constant, and the phase ratio, as shown in Eq. (9.3). As discussed under instrumentation, the simplest instruments, such as a gas-tight syringe, may be the most difficult to obtain acceptable figures of merit, such as adequate reproducibility and a sufficient linear range. In each case, method development efforts focus on driving analytes into the vapor phase within a sealed vial, as seen in Figs. 9.1 and 9.2.

9.4.1 Effect of vial temperature

In general, the relationship between the solution–vapor equilibrium constant and temperature is given by classical thermodynamics, with K increasing exponentially with temperature. However, as written in Eq. (9.5) for SHE, K decreases with temperature. According to Eq. (9.3), the effect of a change in temperature on the sensitivity of an analyte depends on the sum of the partition constant (K) and phase ratio (β). This generates three cases relevant to developing methods:

- $K \ll \beta$: In this case, a change in K has little effect on Eq. (9.3); therefore a change in T has little effect.
- $K = \beta$: In this case, a change in K will be somewhat offset by not changing β , but there will be an effect from changing T . Increased T will lower K and increase A .
- $K \gg \beta$: In this case, a change in T may have a dramatic effect on sensitivity. Increased T will lower K and increase A .

9.4.2 Effect of sample volume

Changing the sample volume would result in change in the phase ratio (β). Again, the combination of phase ratio and equilibrium constant determines the effect of changing sample volume and phase ratio. As in the effect of temperature, the effect of sample volume can be illustrated by three cases:

- $K \ll \beta$: In this case, the change in β dominates; more sample means lower β and higher sensitivity.
- $K = \beta$: In this case, more sample will generate higher sensitivity, but not as dramatically.
- $K \gg \beta$: In this case, additional sample volume has little effect.

9.4.3 Effect of sample solvent

Selecting the right solvent or solvent mixture can be a challenge for method development. The ideal solvent would dissolve the analytes and matrix components but not with such high solubility that it hinders vaporization. It also should be nonvolatile and not react with sample components. These requirements often lead to unusual solvent choices, such as the use of dimethyl sulfoxide, *N,N*-dimethyl acetamide, and water in pharmaceutical headspace methods. For example, ethanol has a partition constant (K) of ~ 7000 at room temperature in water, but benzene, which is not soluble in water, has a partition constant (K) of only 7 in water, although the boiling points are similar. It is important to know as much as possible about the solubility of analytes and matrix components in the solvent. In addition to traditional solvents, there has been recent interest in the use of room-temperature ionic liquids as diluents for SHE [38,39]. Many ionic liquids can dissolve a wide range of materials and have very low vapor pressure, making them ideal solvents for SHE.

Beyond the solvent choice, there are several additional methods for reducing K and therefore increasing the amount of analyte in the vapor phase. Temperature increases, as discussed earlier, should be used carefully, as increasing the temperature close to or above the boiling point of the solvent increases the amount of solvent vapor in the headspace of the vial, which in turn can flood the inlet with solvent. This is one reason for the use of dimethyl sulfoxide and *N,N*-dimethyl acetamide, mentioned earlier, with boiling points of 189 and 165°C, respectively. By using solvents with higher boiling points, the thermostating temperature can be increased without generating significant vapor pressure from the solvent and the sensitivity of the analytes may be increased. One drawback

of using these solvents at elevated temperature is that any residual volatile impurities present in these solvents will also be detected and may interfere with the chromatography.

Salting out is also commonly used to assist in driving analytes into the vapor phase. This is the addition of a large (often 1 M or more) concentration of a common salt, such as sodium or potassium chloride to the samples. Addition of the salt is believed to disrupt hydration of the analytes by the solvent, making them more available to vaporize and reducing *K*. There are many examples of salting out being used in the literature, but there is little systematic information on how to use it with specific analyte and solvent combinations. Salting-out conditions must be studied experimentally.

Acknowledgments

The authors gratefully acknowledge Dr. Thomas M. and Sylvia Tencza for providing an endowed professorship. This chapter is dedicated to the memory of Dr. Leslie S. Ettre, who may be considered as the father of modern headspace extraction and analysis. His insight, dedication, and humor reflect a spirit that we may hope to continue.

References

- [1] R.N. Harger, E.G. Bridwell, B.B. Raney, An aerometric method for rapid determination of alcohol in water and body fluids, *J. Biol. Chem.* 128 (1939) xxxvii–xxxix.
- [2] R.N. Harger, B.B. Raney, E.G. Bridwell, M.F. Kitchel, The partition ratio of alcohol between air and water, urine and blood; estimation and identification of alcohol in these liquids from analysis of air equilibrated with them, *J. Biol. Chem.* 183 (1950) 197–213.
- [3] L.S. Ettre, The beginnings of headspace analysis, *LC-GC N. Am.* 20 (12) (2002) 1120–1129.
- [4] N.H. Snow, G.C. Slack, Headspace analysis in modern gas chromatography, *TrAC Trends Anal. Chem.* 21 (2002) 608–617.
- [5] S. Mitra (Ed.), *Sample Preparation in Analytical Chemistry*, John Wiley and Sons, 2003.
- [6] B. Kolb, *Chromatography: Gas: Headspace Gas Chromatography*, *Encyclopedia of Separation Science*, Elsevier, 2007, pp. 489–496.
- [7] J.D. Green, *Headspace Analysis: Static*, *Encyclopedia of Analytical Science*, Elsevier, 2005, pp. 229–236.
- [8] N.H. Snow, G. Bullock, Novel techniques for enhancing sensitivity in static headspace extraction gas chromatography, *J. Chromatogr. A* 1217 (2010) 2726–2735.
- [9] I. San Roman, M.L. Alonso, L. Bartolome, R.M. Alonso, Headspace gas chromatography methods and their potential industrial applications, *Curr. Chromatogr.* 1 (2) (2014) 100–121.
- [10] Z.E. Penton, *Headspace gas chromatography*, in: J. Pawliszyn, H. Lord (Eds.), *Handbook of Sample Preparation*, John Wiley and Sons, 2010, pp. 25–37.
- [11] N. Delaunay-Bertoncini, F.W.M. van der Wielen, P. de Voogt, B. Erlandsson, P.J. Schoenmakers, Analysis of low-molar-mass materials in commercial rubber samples by soxhlet and headspace extractions followed by GC–MS analysis, *J. Chromatogr. A* 35 (2004) 1059–1073.
- [12] M. Mestres, O. Busto, J. Guasch, Chromatographic analysis of volatile sulphur compounds in wines using the static headspace technique with flame photometric detection, *J. Chromatogr. A* 773 (1997) 261–269.
- [13] C. Munoz-Gonzalez, J.J. Rodriguez-Bencomo, M.V. Moreno-Arribas, M.A. Pozo-Bayon, Beyond the characterization of wine aroma compounds: looking for analytical approaches in trying to understand aroma perception during wine consumption, *Anal. Bioanal. Chem.* 401 (5) (2011) 1501–1516.
- [14] E. Bernal, Determination of volatile substances in forensic samples by static headspace gas chromatography, in: B. Salih, O. Celikbicak (Eds.), *Gas Chromatography in Plant Science, Wine Technology, Toxicology and Some Specific Applications*, Intech Open Access, 2012, pp. 197–224.
- [15] R.G. Gullberg, Alcohol: Breath Alcohol Analysis, *Encyclopedia of Forensic and Legal Medicine*, Elsevier, 2005, pp. 21–29.
- [16] H. van der Jagt, H.F. Reijnders, Water Analysis: Overview. *Encyclopedia of Analytical Science*, Elsevier, 2005, pp. 233–252.
- [17] F. Augusto, A.L. Lopes, C. Zini, Sampling and sample preparation for analysis of aromas and fragrances, *TrAC Trends Anal. Chem.* 22 (2003) 160–169.
- [18] S. Countryman, Analysis of residual solvents by head space gas chromatography, in: J.V. Bonilla, G.S. Srivatsa (Eds.), *Handbook of Analysis of Oligonucleotides and Related Products*, CRC Press, 2011, pp. 331–350.
- [19] A. Datar, J. Kelkar, Headspace gas chromatography for residual solvent analysis for pharmaceutical industry, *Indian Pharmacist (New Delhi, India)* 10 (5) (2011) 29–32, 35–36.
- [20] General chapter <467> residual solvents, USP 43-NF 38, United States Pharmacopeia, Interim Revision Announcement November 1, 2019; Official December 1, 2020.

- [21] ICH Harmonised Guideline, Impurities: Guideline for Residual Solvents (Q3C-R6), Final Version Adopted October 20, 2016.
- [22] M.W. Dong, L. Dai, A.C. Quiroga, N.P. Chetwyn, K. Zhang, H.B. Runes, K. Mistry, D.T. Yazzie, A generic headspace GC method for residual solvents in pharmaceutical: benefits, rationale, and adaptations for new chemical entities, *LC-GC N. Am.* 28 (2010) 54–66.
- [23] B. Kolb, L.S. Ettre, *Static Headspace-Gas Chromatography Theory and Practice*, second ed., John Wiley and Sons, 2006.
- [24] B.V. Ioffe, A.G. Vitenberg, *Headspace Analysis and Related Methods in Gas Chromatography*, John Wiley and Sons, 1984 (Translated by I.A. Mamantov).
- [25] H. Hachenberg, A.P. Schmidt, *Gas Chromatographic Headspace Analysis*, Hayden and Son, 1977 (Translated by D. Verdin).
- [26] R.L. Grob, E.F. Barry (Eds.), *Modern Practice of Gas Chromatography*, fourth ed., John Wiley and Sons, 2003.
- [27] H.M. McNair, J.M. Miller, N.H. Snow, *Basic Gas Chromatography*, third ed., John Wiley and Sons, 2019.
- [28] J.V. Hinshaw, Headspace sampling, *LC-GC Europe* 24 (10) (2011), 538, 540, 542, 544, 546.
- [29] J.V. Hinshaw, Headspace sampling, Part II: instrumentation, *LC-GC N. Am.* 30 (1) (2012), 42, 45–46, 48–50.
- [30] CHROMacademy, <https://www.chromacademy.com/>. (Accessed June 2020).
- [31] D.A. Lambropoulou, I.K. Konstantinou, T.A. Albanis, Recent developments in headspace microextraction techniques for the analysis of environmental contaminants in different matrices, *J. Chromatogr. A* 1152 (2007) 70–96.
- [32] J. Pawliszyn, *Handbook of Solid Phase Microextraction*, Elsevier, 2011.
- [33] F. David, P. Sandra, Stir bar sorptive extraction for trace analysis, *J. Chromatogr. A* 1152 (2007) 54–69.
- [34] M.A. Jeannot, A. Przyjaznyb, J.M. Kokosac, Single drop microextraction—development, applications and future trends, *J. Chromatogr. A* 1217 (2010) 2326–2336.
- [35] K. Schulz, J. Dreßler, E. Sohnius, D.W. Lachenmeier, Determination of volatile constituents in spirits using headspace trap technology, *J. Chromatogr. A* 1145 (2007) 204–209.
- [36] A.L. Theis, A.J. Waldack, S.M. Hansen, M.A. Jeannot, Headspace solvent microextraction, *Anal. Chem.* 73 (2001) 5651–5654.
- [37] M.R.A. Mogaddam, A. Mohebbi, A. Pazhohan, F. Khodadadeian, M.A. Farajzadeh, Headspace mode of liquid phase microextraction: a review, *TrAC Trends Anal. Chem.* 110 (2019) 8–14.
- [38] G. Laus, M. Andreb, G. Bentivoglio, H. Schottenberger, Ionic liquids as superior solvents for headspace gas chromatography of residual solvents with very low vapor pressure, relevant for pharmaceutical final dosage forms, *J. Chromatogr. A* 1216 (2009) 6020.
- [39] J. Feng, H.M. Loussala, S. Han, X. Ji, C. Li, M. Sun, Recent advances of ionic liquids in sample preparation, *TrAC Trends Anal. Chem.* 125 (2020) 115833.

Thermal desorption gas chromatography

Elizabeth Woolfenden

Markes International Limited, 1000 Central Park, Western Avenue, Bridgend, United Kingdom

10.1 General introduction to thermal desorption

Thermal desorption (TD) is arguably the most powerful and versatile of all sample introduction technologies for gas chromatography (GC). It combines aspects of sampling and sample preparation/extraction with selective analyte focusing and efficient GC injection and packages them all into one fully automated operation. Overall, target compounds can be selectively concentrated by factors up to 10^6 .

TD is used primarily for monitoring trace levels of vapor-phase organics in air, gas, or sample headspace (HS) and is available in either off-line (laboratory) configurations or for continuous online air/gas monitoring at site or in mobile laboratories. It may also be integrated with other GC sampling technologies such as purge and trap (as widely used for volatile organics in drinking water) and is increasingly combined with solid-phase microextraction (SPME), HS and sorptive extraction technologies to enhance the sensitivity and selectivity of test methods for volatile and semivolatile organic compounds

(VOCs and SVOCs) in challenging liquid and solid matrices.

TD is generally, but not exclusively, used with GC or GC/mass spectrometer (GC-MS) technology. Alternative analyzers that can be combined with TD include real-time mass spectrometry and sensors (“eNose” technology).

The development of TD was initially driven by the limitations and complexity of conventional GC sample preparation methods—liquid extraction, steam distillation, etc. It held the promise of an alternative high-sensitivity/solvent-free gas extraction process that could be fully automated.

10.1.1 General principles

In its simplest form, TD is a straightforward extension of GC. It involves heating sample materials or sorbents in a flow of inert “carrier” gas, such that retained organic volatiles and semivolatiles are “desorbed” directly into the vapor phase and transferred or injected into the GC column in the carrier gas stream. As in GC, key method parameters include temperature, carrier

gas flow rate, desorption time, and sorbent (stationary phase) selection.

Though simple in concept, the selective concentration (enrichment) power and potential of TD expand significantly when it is applied in multiple steps and/or in combination with complementary sampling techniques. It is possible, for example, to configure a system such that analytes are repeatedly extracted and reconcentrated into smaller and smaller volumes of gas, thus optimizing sensitivity/detection limits. By way of example, Fig. 10.1 illustrates a relatively conventional monitoring procedure whereby 100 L of air or sample gas is pumped through a sorbent sampling tube over a period of say

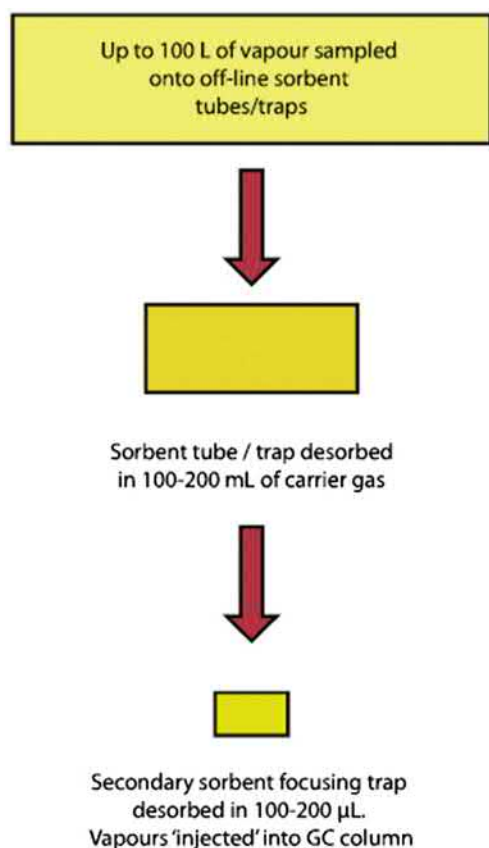


FIGURE 10.1 An illustration of the concentration potential of multistage thermal desorption.

12 h. Retained organic vapors are then desorbed in approximately 100 mL of carrier gas and subsequently refocused on a smaller ("cold") sorbent trap. Depending on trap design and parameter selection, this in turn can be quantitatively desorbed, with the analytes eluting in as little as 100 μL of gas, thus providing a millionfold enhancement in vapor concentration overall.

The selectivity of TD is another major advantage. Even very volatile and polar organic compounds, such as methyl chloride and methanol, can be retained on sorbent tubes or traps while unwanted interferences, such as water and permanent gases, are selectively purged to vent before desorption and analysis. This allows the signal for trace target compounds to be optimized while background interference levels are simultaneously reduced, thus greatly improving signal-to-noise ratios and detection limits. Selectively eliminating air and water also improves analytical stability and extends the operating life of capillary columns and the entire GC system.

10.1.2 Comparing thermal desorption with solvent extraction for air monitoring

Routine TD was originally developed for workplace and environmental air monitoring. Up to that time, occupational hygienists usually pumped air samples through one-use glass tubes packed with charcoal (so-called "NIOSH tubes"), which were subsequently "desorbed" or extracted with one or 2 mL of solvent (typically CS_2), 1–2 μL of which was then injected into a GC.

The new TD approach offered a number of significant advantages:

Enhanced automation: In comparison to solvent extraction, TD was much less labor-intensive, requiring little or nothing in the way of manual sample preparation.

Greatly enhanced sensitivity: Thermal desorption allowed 100% transfer of retained analytes to the GC column versus the conventional μL

injections of milliliter extracts. This, on its own, equated to a thousandfold increase in sensitivity.

Enhanced desorption efficiency: Most TD standard methods demand at least 95% desorption efficiency [1] from the sorbent sampling tube, and in practice, complete extraction/desorption and transfer of target analytes to the GC in a single cycle are invariably straightforward. This is because TD is a dynamic process, with gas continually purging compounds away from the sorbent or sample matrix as soon as they are released into the vapor phase by the rising temperature. In contrast, typical solvent extraction procedures are static, with analytes partitioning, in equilibrium, between the sorbent, solvent, and vapor (HS) phases. Standard solvent extraction methods therefore typically require only 75% recovery [2] and even this can be challenging to achieve reliably in practice (see next point).

Reliable extraction efficiency: The efficiency of solvent extraction can also be compromised by variability depending on the presence of interferences. For example, desorption efficiencies as low as 20 or 30% have been reported when charcoal tubes and CS₂ extraction are used for polar compounds in the presence of water [3]. This uncertainty is particularly problematic for air monitoring, as the analyst may not be aware of field/sample conditions such as high humidity, and poor recovery may lead to underreporting.

Reduced analytical interference: Solvent interference can be a major consideration for liquid extraction methods. One of the reasons CS₂ was originally selected as the preferred solvent for charcoal-based air sampling methods is that it gives little or no signal on a GC flame ionization detector (FID). However, nowadays, with the preference for MS detection, this advantage no longer holds. Common solvent interference issues include masking of peaks of interest, signal quenching (for components coeluting with the solvent), and baseline disturbances. All these make peak integration difficult and more prone to error. TD is inherently free of solvent interference.

Selective elimination of interferences: Depending on the sample matrix and compounds of interest, TD procedures can generally be optimized to selectively purge volatile interferences while target species are retained and enriched/concentrated. Applications as diverse as monitoring (S) VOC emissions from paint and characterizing the aroma of whisky benefit from the selection of sorbents that quantitatively retain compounds of interest while allowing water, and in the latter case, ethanol, to purge to vent. Selectivity is usually only possible for solvent extraction procedures when there is a very significant volatility difference between the compounds of interest and the interferences.

Reduced exposure risk: Many common extraction solvents, such as CS₂, are toxic, odorous, and present a potential health and safety hazard. TD is inherently safer in this respect. TD-GC(MS) systems can generally be installed in the laboratory without fume hoods or other extraction equipment, provided all outlet points, including sample split lines, are configured with appropriate filters. In TD operation, wet chemistry procedures are confined to the preparation of liquid standards for spiking tubes when gas standards aren't available—see notes on calibration in [Appendix A](#).

Reusable samplers and lower cost per analysis: Traditional charcoal air monitoring tubes for solvent extraction can only be used once and require extensive manual sample preparation between sampling and analysis. Although prepacked TD tubes typically cost around 10 times more than charcoal tubes, they can be reused at least a 100 times as long as sorbent maximum temperatures are not exceeded [4]. They also require no manual preparation or consumables (solvents, etc.) and are automatically reconditioned by the analytical process. Even taking into account the higher initial capital costs of an automated thermal desorber (compared to a regular liquid autosampler + fume hood), this means that TD methods are usually significantly less expensive per sample than solvent extraction.

10.1.2.1 The “one-shot” limitation of TD

Traditionally, the only advantage offered by solvent extraction to offset all of the aforementioned drawbacks was repeat analysis—generally speaking, liquid extracts can be reinjected if anything goes wrong in the initial run, whereas target volatiles are usually completely stripped from a substrate during TD, leaving no sample behind to retest.

Despite the fact that early TD systems had no means of overcoming this issue, use of TD continued to expand rapidly because of the sensitivity and other advantages it offered and because carbon disulfide extracts were themselves notoriously unstable, meaning that in practice, repeat analysis was unreliable.

10.2 Brief history of thermal desorption—essential functions and performance characteristics

The history of TD can be traced back to the mid-1970s. Scientists struggling with the limitations of conventional GC sample preparation and extraction techniques began to experiment by packing conventional GC injector liners with sorbent material. These sorbent-packed injector liners were used to sample a fixed volume of air or gas and were then quickly inserted back into the GC inlet for desorption and transfer of analytes to the analytical column. The limitations of these primitive adaptations of conventional GC injectors are many and obvious (air ingress, volatile losses, variability, contamination from handling the outer surfaces of the liner, single stage, etc.), but the fact that it was attempted at all is testament to the fundamental need for this technology.

Another early incarnation of TD was incorporated into purge-and-trap systems. The US Environmental Protection Agency (EPA) rushed to develop purge-and-trap/GC-based test methods to measure VOCs in drinking water in the late 1970s in response to serious environmental incidents such as the Love Canal tragedy. Love Canal refers to an area of housing in Niagara

City in New York State, which had been developed on land contaminated by the chemical industry in the 1940 and 1950s. Work to develop test methods began in earnest after an unusually high incidence of serious birth defects was reported for the neighborhood. Ultimately, it was found that underground chemical waste had been seeping into the drinking water supply and impacting the health of residents. The 500-series test methods, produced by the US EPA in response to this and similar issues, relied on volatiles being purged/sparged from water samples in a stream of pure nitrogen and trapped on a tube packed with sorbents. This was subsequently heated in a reverse stream of carrier gas to thermally desorb the organic chemicals of interest and transfer them to a packed GC column in a single-stage TD-type procedure.

The first early commercial configurations of dedicated thermal desorbers were based around desorption of a single tube or badge. The “Coker cooker,” designed by Environmental Monitoring Systems Ltd. (UK) in the mid-1970s [5], was a popular example and accommodated samples or sorbents contained in $\frac{1}{4}$ -inch O.D. tubes. These early systems were very primitive by modern standards, typically offering only single-stage desorption and without any of the functions that would now be regarded as standard, such as leak testing or prepurging of air from the tube. However, they usually operated sufficiently well, within specific constraints (e.g., packed column only, stable compounds only, narrow concentration, and volatility ranges) to provide a useful tool for straightforward applications such as workplace air monitoring in the petrochemical industry [5].

Perhaps the most important early technical advances in thermal desorption came from “Working Group 5” (WG5) of the UK Health and Safety Executive’s (HSE) “Committee on Analytical Requirements” (CAR). HSE/CAR WG5 began with a chance meeting at a UK conference on workplace air monitoring in the late 1970s. Scientists from the UK chemical industry and British Health and Safety Executive (HSE), including Dr. Kevin Saunders, Dr. Richard

Brown, Jack Charlton, and Brian Miller, found that they had a common interest in both diffusive (passive) sampling and TD.

This group believed that passive sampling would allow quantitative air monitoring without the complications and expense of personal sampling pumps [6]. At a series of meetings over the next couple of years, various other experts joined the team including Peter Hollingdale-Smith of the UK Chemical Defence establishment at Porton Down [7], David Coker of Exxon, and Nico van den Hoed of Shell in The Netherlands. Between them, the working group evaluated the available forms of diffusive monitors and homed in on the axial tube-form samplers based on the $1/4$ -inch O.D. sorbent tubes used in the “Coker cooker.” These were identified as a practical size, being least susceptible to air speed limitations [6,8] and having the most flexibility (notably they are suitable for both passive and pumped sampling).

WG5 saw thermal desorption as an enabling technology for passive sampling because the huge sensitivity enhancement it offered (~ 1000 times) was more than enough to offset the relatively slow sampling (uptake) rate of axial-form diffusive samplers (typically around 1 mL min^{-1}). They also realized that TD overcame the toxicity and variability issues inherent with the standard charcoal/ CS_2 extraction methods in use at that time. As soon as consensus was reached on the sampler dimensions, WG5 set about outlining a specification for the world's first automated thermal desorber to accommodate them. The functionality requirements that

came out of these discussions in the late 1970s are still relevant today. They include two-stage desorption, the necessity of certain predesorption checks (leak testing, prepurging of air to vent), and automation.

10.2.1 Two-stage desorption

With standard sampling tubes containing 200 mg to 1 g sorbent (depending on density), WG5 realized that single-stage TD (Fig. 10.2) was inherently limited because tens of milliliters of gas are required for complete compound extraction. “Injection”/transfer volumes like these are not compatible with capillary chromatography and would compromise analytical resolution/sensitivity even with packed GC columns. Some form of refocusing would therefore be needed between the sorbent tube and the GC column.

Initial attempts to address this utilized capillary cryofocusing, either on-column or in cooled GC inlets such as “programmable temperature vaporisers” (PTVs). In this case, analytes desorbed from the primary sorbent tube were refocused/concentrated in a short length of capillary or narrow-bore tubing (typically $< 1 \text{ mm}$ internal diameter) cooled with liquid cryogen. Heat was then applied to release the compounds into the analytical system in a small volume of carrier gas (see Fig. 10.3).

Early TD configurations that harnessed capillary cryofocusing included the Chrompack CTC unit designed in the Netherlands. The peak shape produced by this system was excellent even during splitless capillary GC operation, and it

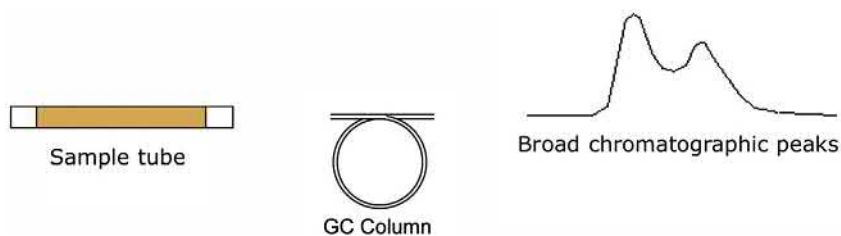


FIGURE 10.2 Single-stage thermal desorption.

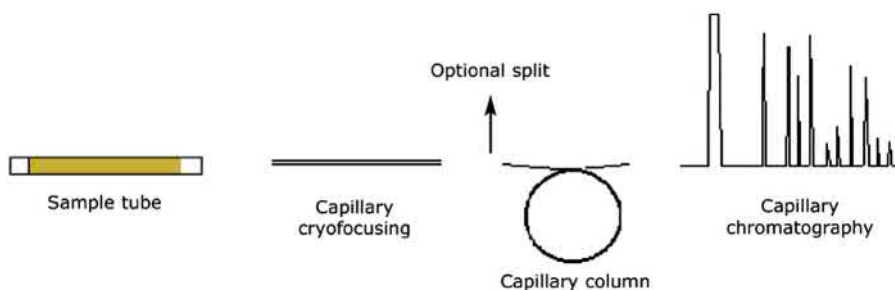


FIGURE 10.3 Two-stage thermal desorption incorporating capillary cryofocusing.

therefore offered exceptional sensitivity, but there were several major limitations. Key concerns included ice blockage, incomplete retention of very volatile compounds [9], loss of high boilers due to aerosol formation [10], and high running costs (systems consumed up to 6 L of liquid nitrogen per hour in operation [11]). Another major issue was that, because the cryofocusing devices were permanently connected to the GC column, they couldn't be isolated to implement the essential predesorption functions specified by WG5—leak test, purge of air to vent, etc.

Ultimately, the PerkinElmer ATD 50 unit, developed around the WG5 specification, addressed all these concerns. Designed by Dr. Peter Higham and introduced in 1981, the ATD 50 incorporated a small, Peltier-(electrically) cooled, sorbent-packed focusing trap (see Fig. 10.4). The

combination of sorbent packing and modest focusing temperatures (minimum: -30°C) was a real breakthrough. It offered quantitative retention of a wide range of compounds, including very volatile species such as the lightest gasoline components [12], SF_6 and N_2O [13], without the cost and inconvenience of liquid cryogen. The steel focusing trap also had a wide enough internal diameter (~ 3 mm) to prevent ice plug formation yet could be heated at rates approaching $60^{\circ}\text{C s}^{-1}$ to allow rapid (capillary-compatible) desorption/injection with minimal split and good sensitivity. Another breakthrough was the inclusion of a rotary valve in the flow path of the desorber (see Fig. 10.4). This isolated the sorbent tube from the GC, allowing both stringent “stop-flow” leak testing and prepurging of air to vent prior to desorption of every tube.

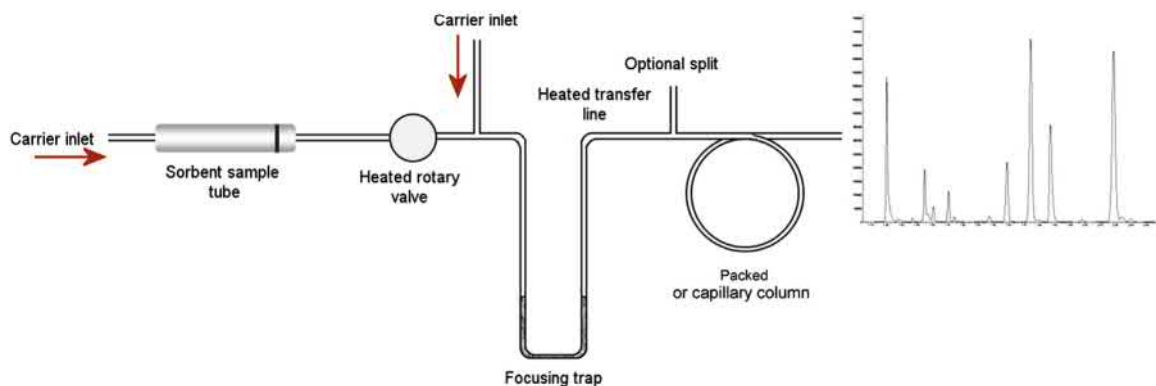


FIGURE 10.4 Two-stage thermal desorption incorporating sorbent focusing trap and heated valve.

10.2.2 Automation

Automating TD requires sample tubes to be sealed both before and after desorption to minimize risk of artifact ingress from laboratory air and to prevent loss of analytes over periods of at least 2–3 days (for weekend operation). Caps are essential because sample losses from poorly sealed tubes can be significant. In the end, this issue was addressed on the ATD 50 by using stainless steel end caps that incorporated a ball valve. They weren't ideal, involving several o-rings in direct contact with the sample flow path, but they could remain on the tubes throughout an entire sequence (no uncapping/recapping required) and provided a robust mechanical solution for the time.

Introduction of the ATD 50 led to a rapid expansion of TD-GC applications. Over and above personal exposure assessment [12–14], these included residual solvents in drugs [15] and ambient air monitoring [16–18].

10.2.3 Double splitting

Sample splitting before and after focusing (“double splitting”) was not part of the original WG5 specification but was introduced as an enhancement to the ATD 50 in around 1985 (Figs. 10.5 and 10.6). It allowed the transfer of analytes from the tube to the trap to be carried

out split or splitless and likewise the subsequent injection of analytes from the secondary (focusing) trap to the GC analytical column.

Double splitting brought immediate benefits in terms of application versatility. Overall split ratios as high as 10,000:1 could be readily and reproducibly achieved, accommodating samples containing milligrams of individual analytes while ng or pg level samples could still be analyzed with negligible split or no split at all.

While it might seem strange to want to implement such a high split ratio for TD applications, it must be remembered that sensitivity is not the only advantage that thermal desorption offers—many laboratories simply preferred to use TD because it eliminated the hazard of CS₂, was more reliable and less labor-intensive. Moreover, a surprising number of workplace air or industrial emission monitoring applications using TD benefit from (or even require) a significant split ratio. For example, sampling ~5 ppm levels of compound X (nominal molecular weight 100) at 50 mL min⁻¹ over a full 8-h shift means pumping ~24 L of air through a tube and collecting ~500 μg of X. An overall split ratio of at least 1000:1 would be advisable in this case in order to prevent overload of high-resolution capillary GC columns and detectors.

Over and above application flexibility, the introduction of double splitting has also allowed

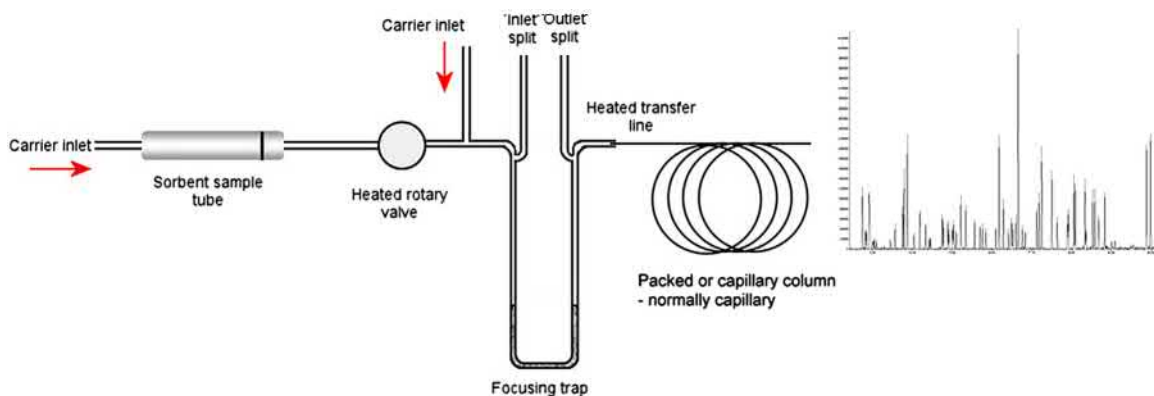


FIGURE 10.5 Two-stage thermal desorption, as shown in Fig. 10.4, but incorporating double splitting capability.

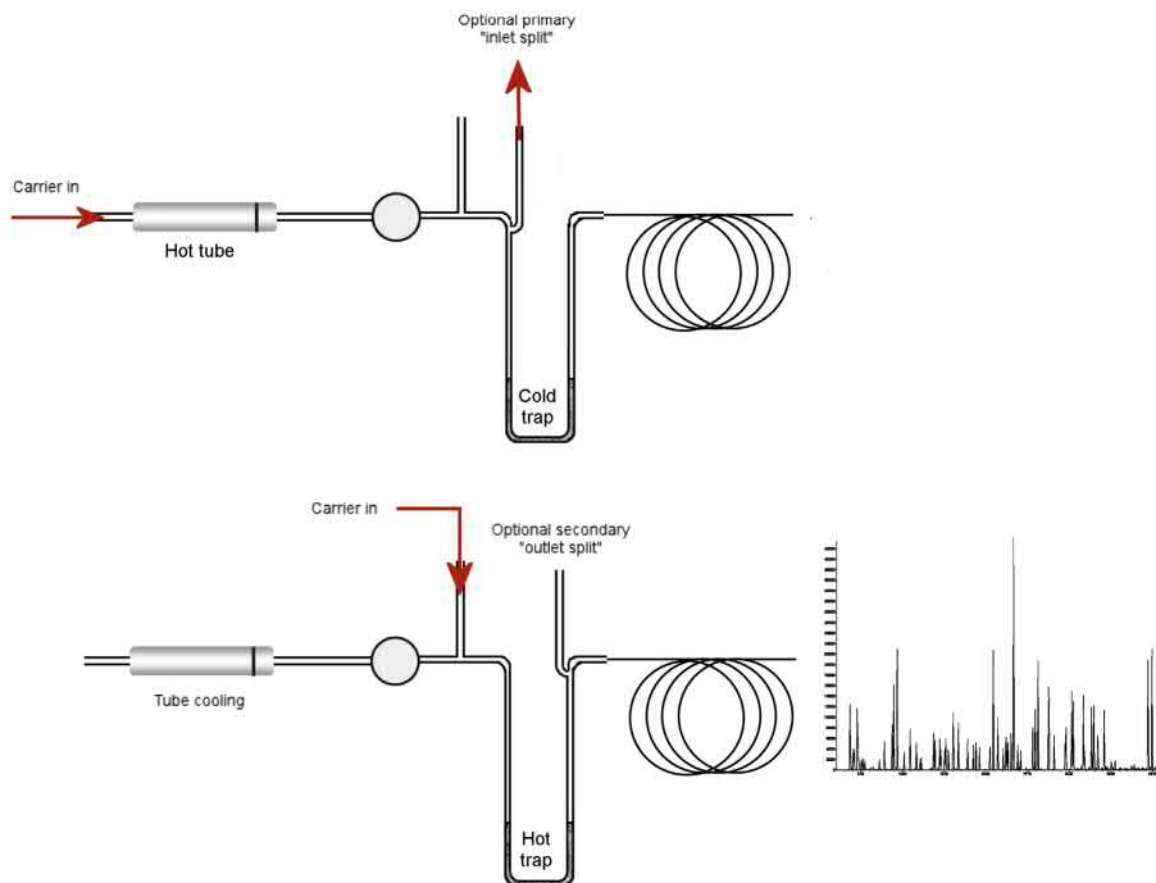


FIGURE 10.6 An illustration of gas flow during two stages of desorption with double splitting.

the process of two-stage TD to be enhanced, improving method performance. Analytical objectives during primary (tube) desorption are usually: (a) complete removal (extraction) of target compounds from the sample tube combined with (b) quantitative trapping of the compounds of interest on the secondary (focusing) trap. If the sample is sufficiently large to allow implementation of a split during primary desorption, this benefits both objectives—it allows a high carrier gas flow to be applied to the hot sample tube during primary desorption (enhancing and speeding up extraction) while a low flow is maintained through the cold

focusing trap to aid analyte retention. Application of a second split during subsequent trap desorption then increases the gas flow through the trap during secondary (trap) desorption, speeding up GC injection (Fig. 10.6). See Appendix A for more information.

Implementation of double splitting enabled the first serious expansion of TD into direct desorption of material samples weighed into empty tubes (Fig. 10.7). Relevant application examples include solvents in paint, residual monomers in polymers, essential oils, and volatiles in dried vegetable products such as tobacco or spices [15,19,20] (Fig. 10.8).

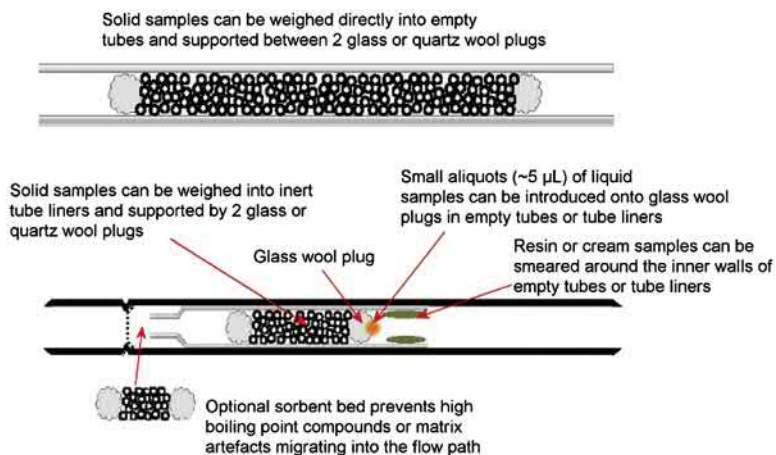


FIGURE 10.7 An illustration of sample preparation for direct desorption of materials.

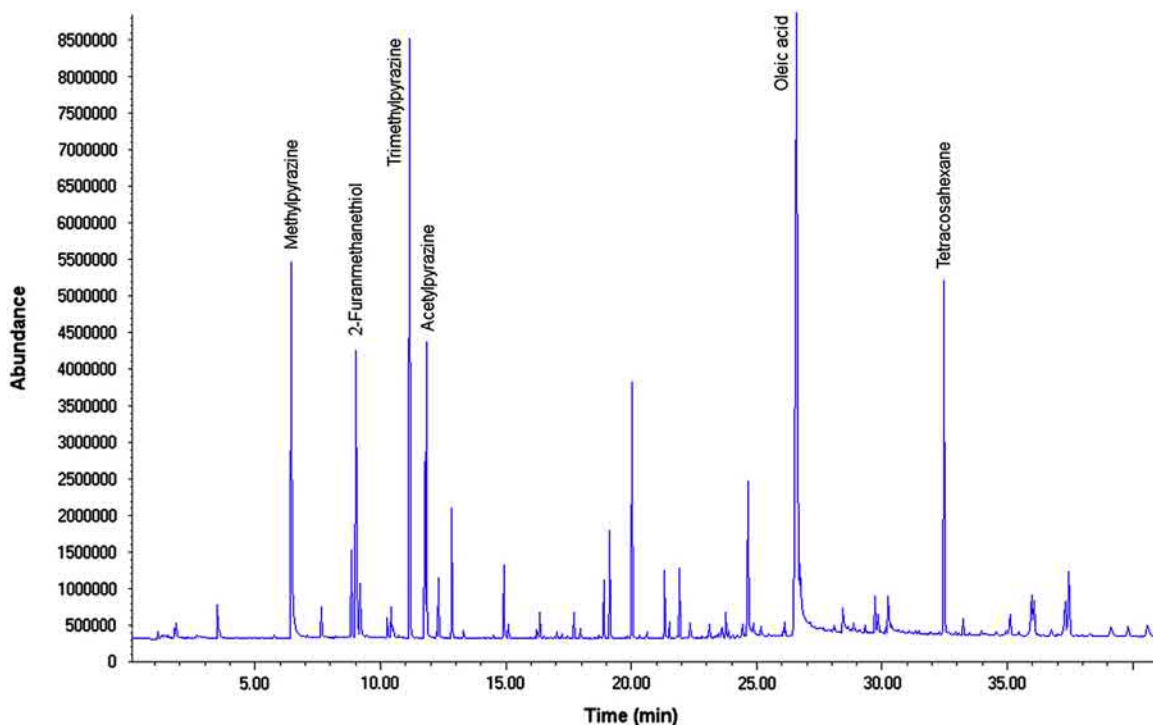


FIGURE 10.8 Direct thermal desorption with GC-MS analysis of aroma constituents from powdered dry mushroom. Experimental conditions: TD-100 automated thermal desorber (Markes International Ltd., UK) combined with a 7890-5975 GC-MS system (Agilent Technologies). Desorption: 5 min at 50°C into a multisorbent (“air toxics”) trap at 0°C. Trap desorption: 300°C with 25 mL min^{-1} split flow. Flow path: 140°C. Column: 30 m \times 0.25 mm I.D. \times 0.25 μm film HP-Innowax. GC oven: 50 to 220°C at 3°C min^{-1} . Scan range: 35–300 amu.

10.3 The evolution of TD technology—important milestones

10.3.1 The limitations of early systems

While the ATD 50 represented state-of-the-art for TD instrumentation in its day, new application requirements began to emerge, which highlighted the limitations of this first-generation technology. Key concerns included:

- *Volatility range:* The ATD 50's use of forward-flow trap desorption meant all analytes had to pass through the entire focusing trap en route to the GC column. This reduced the volatility range of components that could be analyzed simultaneously.
- *Recovery of high-boiling semivolatiles:* The ATD 50 operated with a flow path maximum of 150°C and maximum desorption temperatures of 250°C and 300°C for the tube and focusing trap, respectively. This was hot enough to allow complete recovery of compounds up to n-C₂₆ (b.p. ~400°C) [21]. However, interest was already growing in measuring the vapor concentration of even higher-boiling semivolatiles such as polychlorinated biphenyls (PCBs), phthalates, and multiring polycyclic aromatic hydrocarbons (PAHs).
- *Inertness:* The predominantly stainless steel flow path of early systems, such as the ATD 50, caused degradation of the most reactive organic species.
- *Internal standard (IS) addition:* Internal standard addition had become an accepted part of automated GC procedures generally, and TD users were beginning to demand this option.
- *Automated dry purging:* The introduction of stronger, less hydrophobic sorbents meant tubes could retain as much as tens of milligrams of water under some atmospheric conditions. In these cases, it is necessary to selectively eliminate water by dry-purging

tubes in the sampling direction before desorption to prevent analytical interference.

- *Whole air sampling of ultravolatile organics:* There was increasing interest in ultravolatile compounds such as C₂ hydrocarbons, which cannot be quantitatively retained by conventional sorbent tubes at ambient temperatures. Demand was also growing for semicontinuous, near-real-time monitoring of urban air pollutants with known adverse health effects—specifically C₂–C₉ hydrocarbons originating primarily from vehicle exhaust emissions [22,23]—the so-called “ozone precursors.” This led to TD technology being adapted for online field operation and the controlled introduction of whole air or gas samples directly into the cooled focusing trap [24].

To address these limitations and respond to the new demands, TD technology began to evolve rapidly from the early 1990s. The most significant changes were made in the following areas:

10.3.2 Optimization of the focusing trap

While electrically cooled/sorbent-packed focusing traps remain the most robust and versatile platform for two-stage TD, the technology has been refined considerably since 1981. Modern traps are typically constructed of inert materials such as quartz, have a reduced internal diameter (typically ~2 mm), can be heated at rates up to 100°C s⁻¹, and are desorbed efficiently at flows down to 1.5 mL min⁻¹ to allow splitless or low-flow operation to optimize sensitivity. They are also invariably configured in “backflush” mode, such that analytes enter and leave the trap from the same end (see Fig. 10.9)—to maximize the compatible analyte volatility range [8]. This combination of functions and features enhances the flexibility of modern desorbors (relative to older, forward-flow designs) facilitating both routine (target) and research

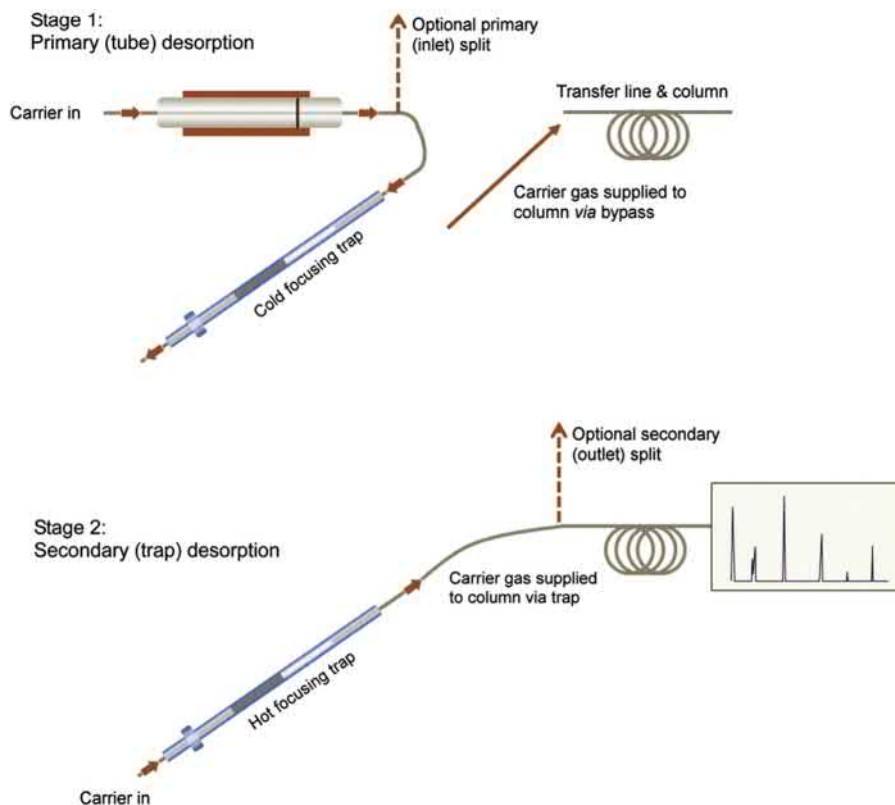


FIGURE 10.9 Illustration of two-stage thermal desorption, incorporating backflush of the focusing trap.

(nontarget) applications on the same system. Examples of the analytical performance that can be routinely obtained for air monitoring using the latest TD trapping technology are presented in Figs. 10.10 and 10.11. Even ultravolatile organics can now be retained from useful air/gas volumes without resorting to liquid cryogen cooling (see Fig. 10.12 and Table 10.1).

10.3.3 The evolution of heated valve technology for thermal desorption

The fundamental functions of leak testing and prepurging of air to vent, plus the more recent requirements for backflush trap desorption, automated dry purging (of tubes and traps), and internal standard addition (to the sampling

end of the tube), have all confirmed the need for valving in the TD sample flow path. Rotary valves are still widely used in commercial thermal desorbers, but cold spots and temperature limitations have also led to the development of inert, low-volume TD-specific valving that enables recovery of both high-boiling semivolatiles (e.g., up to $n\text{-C}_{44}$ —see Fig. 10.13) and temperature-sensitive species on the same TD platform. Thiols and CS gas (tear gas), for example, work best with TD flow path temperatures at or below 125°C [25].

10.3.4 Tube sealing for automation

Early attempts to overcome the sorption and artifact limitations of the original ATD 50 analytical tube seals involved caps that were removed

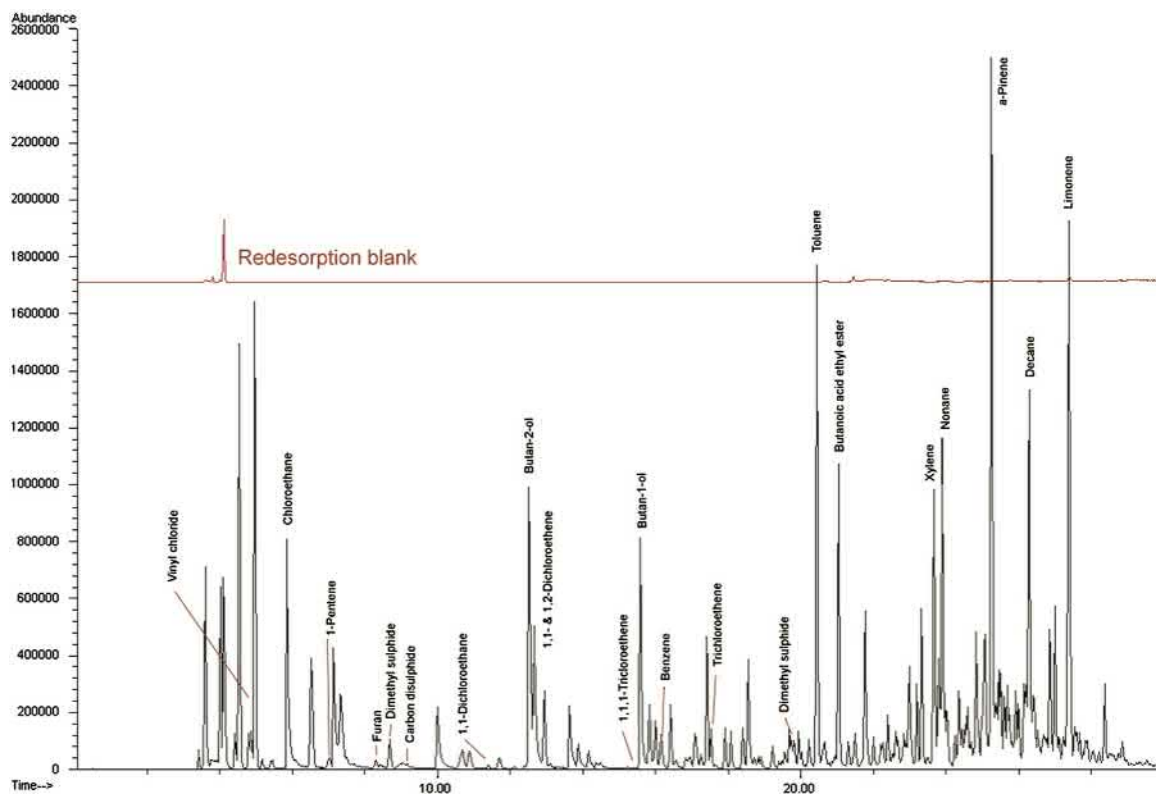


FIGURE 10.10 100 mL landfill gas with trace target analytes and many major components. Experimental conditions: ULTRA-UNITY automated thermal desorber (Markes International Ltd., UK) combined with a 6890-5975 GC-MS system (Agilent Technologies). Silcosteel tube packed with Tenax/Unicarb. Tube desorption: 5 min at 200°C into a multisorbent (“sulfur”) trap at -15°C, split 20 mL min⁻¹:20 mL min⁻¹. Trap desorption: 220°C with 80 mL min⁻¹ split flow. Flow path: 120°C. Column: 60 m × 0.25 mm I.D. × 1.4 μm film DB VRX (Agilent Technologies). GC oven: 40 to 225°C at 10°C min⁻¹. Scan range: 35–260 amu.

and replaced by the thermal desorber during automatic operation. These incorporated PTFE-coated o-rings to reduce friction and make robotic uncapping/recapping processes as reliable as possible. However, while a major step forward, these caps were found to allow significant loss of volatiles over time [26]. A more robust later solution was the development of caps that incorporated a long, narrow gas flow path through the cap. Such “diffusion-locking” mechanisms reduced analyte loss and artifact ingress to negligible levels, even over extended periods (e.g., a week), but still allowed gas to flow

unimpeded when pressure was applied. This meant that the integrity of sampled and clean (desorbed) tubes could be rigorously maintained without complicating the TD automation process, i.e., without the need to uncap/recap tubes.

10.3.5 Recollection of split flow

An inherent drawback of all early thermal desorption systems was that the technique was “one-shot”—if anything went wrong during the analytical procedure, no sample remained to repeat the test. Quantitative re-collection

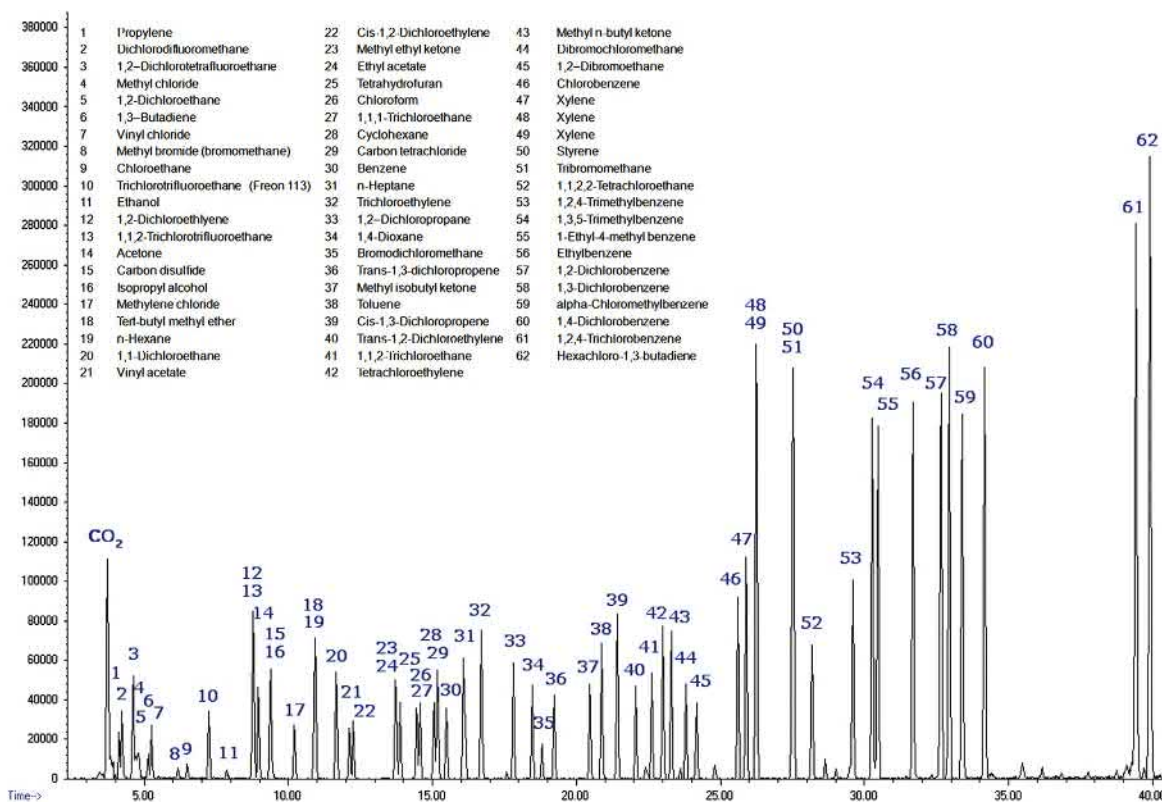


FIGURE 10.11 Splitless analysis of 1 L × 1 ppb 62-component air toxics standard in a canister. Experimental conditions: UNITY-CIA system (Markes International Ltd., UK) combined with a 7890-5975 GC-MS system (Agilent Technologies). Multisorbent (“air toxics”) trap at 25°C. Trap desorption: 40°C s⁻¹ to 320°C. Flow path: 140°C. Column: 60 m × 0.32 mm I.D. × 1.8 μm film DB-624 (Agilent Technologies). GC oven: 40 to 230°C at 5°C min⁻¹. Scan range: 35–300 amu.

of TD sample split flow was first reported by Dr. Jan Kristensson in 1987 and 1988 [14,27]. His initial implementation involved adapting a standard TD system of the time and was therefore unavoidably cumbersome. Nevertheless, it showed the potential of split flow re-collection for overcoming the one-shot limitation of traditional TD technology and for confirming analyte recovery and test results.

The first commercial implementation of quantitative split flow re-collection for TD was developed in 1998 by a team led by Dr. Peter Higham, then lead mechanical engineer at Markes International. Harnessing a new

TD-specific heated valve (pioneered a few months earlier by the same team), the TD flow path was configured such that both primary tube desorption (“inlet”) split flow and secondary trap desorption (“outlet”) split flow were directed to the same re-collection tube (Fig. 10.14). This overcame the one-shot limitation of TD for the vast majority of applications. Furthermore, because re-collection involved analytes passing through an extended version of the TD flow path, repeating the analysis of a single standard allowed selective losses of one or more analytes (relative to split ratio or to other more stable/volatile compounds in the mix) to be readily identified.

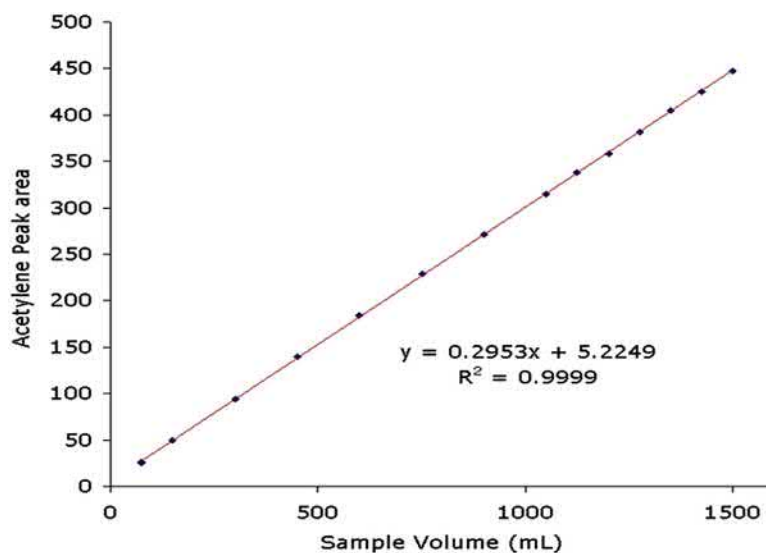


FIGURE 10.12 Cryogenic-free retention of ultravolatile analytes from large volumes of air/gas. Illustration with acetylene.

TABLE 10.1 Sampling and detection limit data, determined in SIM mode, for low concentration standards of potent greenhouse gases in nitrogen and real air.

Compound	Sample volume (mL)	Sampling flow (mL min ⁻¹)	Lowest measured concentration (std) (ppt)	RMS S:N (std)	Estimated minimum detection limit (std) (ppt)	Lowest measured concentration (air) (ppt)	RMS S:N (air)	Estimated minimum detection limit (air) (ppt)
CF ₄	25	10	70	40:1	<10	300	20:1	50
C ₂ F ₆	1000	50	6	80:1	0.2	100	2000:1	0.2
SF ₆	1000	50	1.5	80:1	0.05	100	5500:1	0.05

Quantitative sample re-collection has now been automated and implemented on several different commercial systems, and this functionality is fast becoming accepted as a standard or recommended approach to validate analyte recovery [28,29].

10.3.6 Electronic control of flows and pressures

While GC systems with conventional liquid injectors have benefitted from electronic pneumatic control of carrier gas and split flow for many years, two-stage TD presents a more difficult technical challenge to carrier gas flow

and pressure regulation. This is because the route (flow path) by which carrier gas is supplied to the column changes depending on the phase of operation. For example, at the start of trap desorption, the flow to the column switches from a simple bypass line to pass through the very different impedance of a sorbent focusing trap. The trap then heats, thus changing the impedance once again. Maintaining a stable electronically controlled carrier gas pressure or flow to the head of the GC column under these circumstances requires rapid and robust closed-loop feedback.

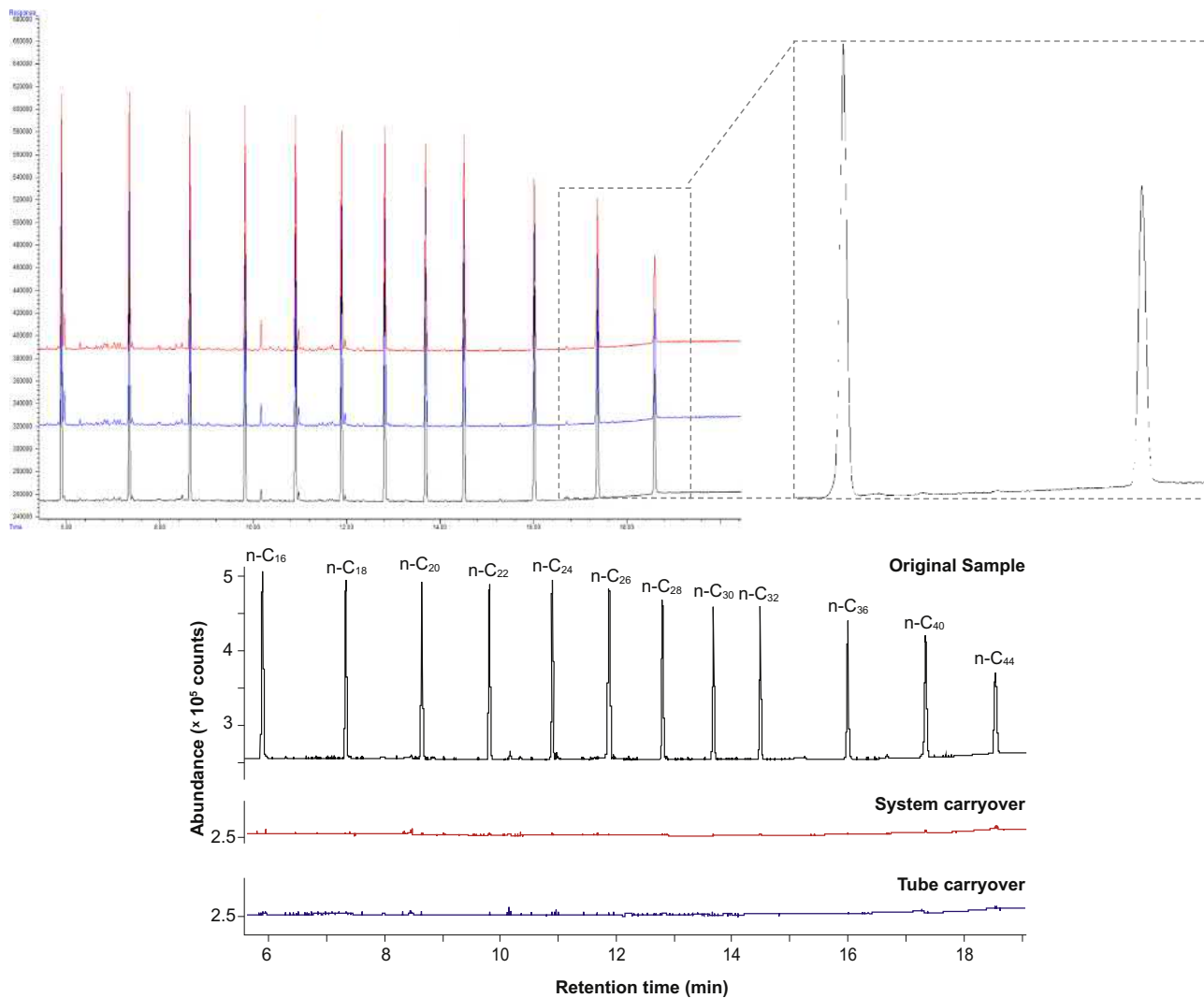


FIGURE 10.13 Analysis of a sorbent tube loaded with 1 mL of n-C₁₆–n-C₄₄ hydrocarbons (100 ng per compounds on tube) using two-stage thermal desorption via a TD-specific heated valve and with trap desorption in backflush mode. Experimental conditions: TD100-xr thermal desorber combined with Agilent 7890 GC/FID. Stainless steel tube packed with quartz wool and Tenax TA. Tube desorption 15 min at 320°C with 50 mL min⁻¹ flow onto multibed sorbent trap (quartz wool/graphitized carbon black) at 25°C. Trap desorption 350°C for 10 min with an outlet split ratio of 17.6:1. Main figure shows minimal carryover for both the system and a re-desorption of the sample tube. **Inset:** Original n-C₁₆ to n-C₄₄ sample and two subsequent re-collections showing >95% recovery for even the least volatile n-C₄₄ hydrocarbon. (See [Section 10.3.5](#)). The left hand inset shows all 3 full chromatograms off-set. The right hand inset shows a close up of the three repeat analyses of n-C₄₀ and n-C₄₄ overlaid.

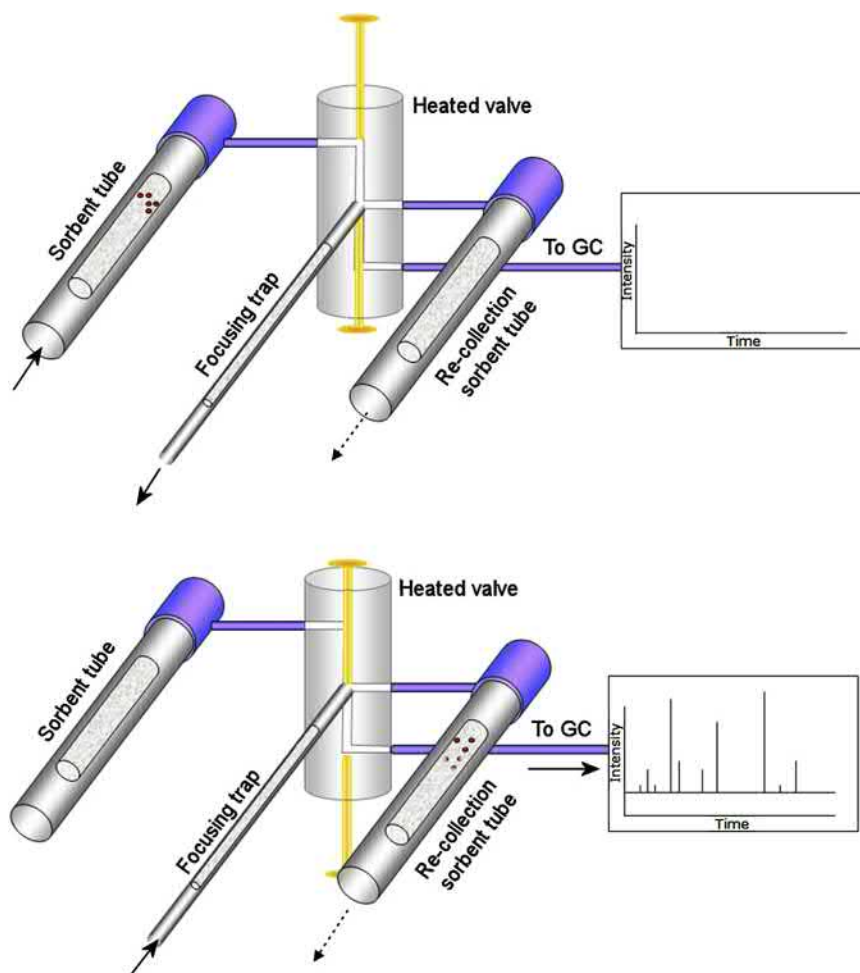


FIGURE 10.14 Operation of two-stage thermal desorber with integrated capability to re-collect primary and/or secondary split flow.

Despite this complexity, several modern TD systems have now implemented both precise electronic pneumatic control of carrier gas flow/pressure (either via the attached GC or via independent TD pneumatic modules) and electronic mass flow control of desorption and split flows. This enhances complex analyses by stabilizing peak retention times independent of split flow, trap impedance, etc. (Fig. 10.15).

10.3.7 TD innovations for whole air/gas sampling (canisters/bags and online monitoring)

The first important canister-based standard for air monitoring required cryofocusing and was published by the US EPA in 1991 to target “air toxics” (predominantly volatile halogenated hydrocarbons) in urban and industrial air [30]. Since then, manufacturers have prioritized two

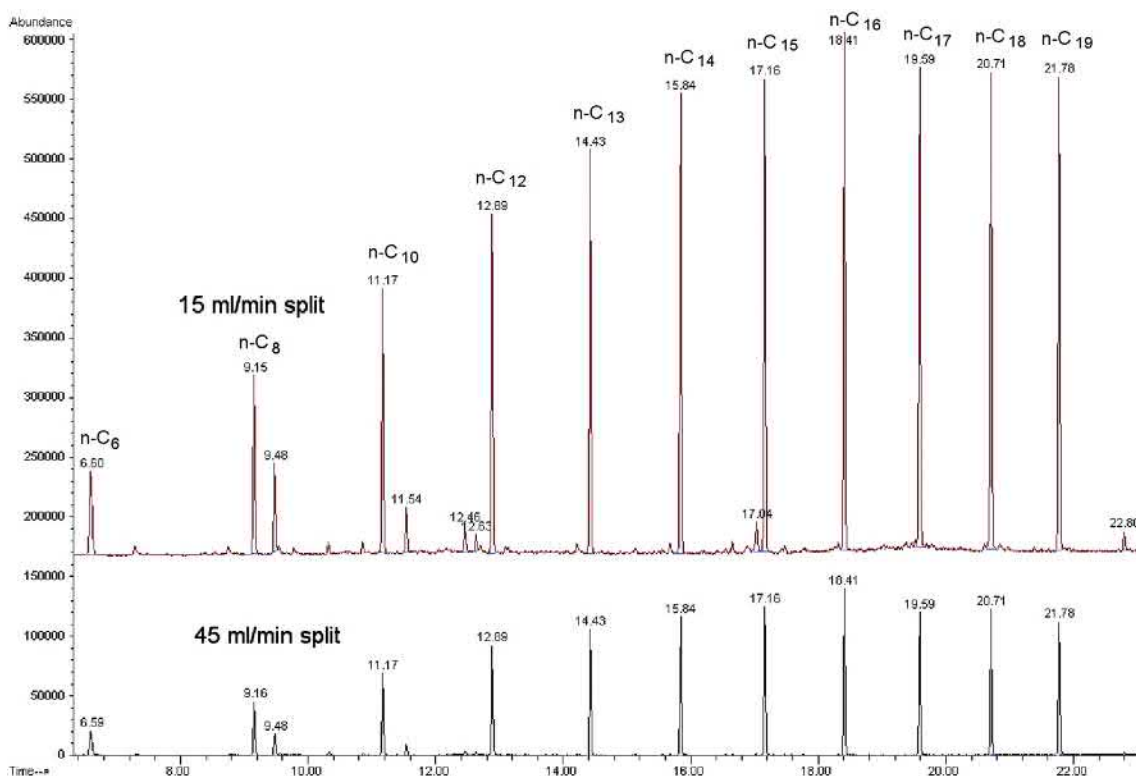


FIGURE 10.15 Using electronic carrier gas control to stabilize TD-GC(MS) retention times.

areas of system development: (a) cryogen-free focusing technology offering quantitative retention of the most volatile compounds of interest from large enough volumes of canister air to meet detection limits [31,32] and (b) improved systems for selectively removing water without losses of oxygenated and polar VOCs [33]. Practical features such as enhanced purging of sample lines have also been implemented to reduce carryover [34] and make modern canister auto-samplers more versatile and productive than their predecessors.

The TD technology improvements made for canister analysis also benefitted online air/gas installations. Online air/gas monitoring is usually deployed in or around major industrial plants/sites or in field monitoring stations and is typically expected to produce data fully

automatically, around the clock for weeks at a time without user intervention. Data sets are typically generated hourly and transmitted electronically to a central hub for qualification and reporting. High liquid cryogen consumption was a real problem for the earliest online TD-GC systems [11], but this was addressed as soon as the first Peltier-cooled focusing systems became available [24]. The most challenging online TD applications now include ultralight perfluorinated “greenhouse gases” (see Table 10.1) and methods specifying an extended suite of target compounds. Several of the recently released Chinese environmental standards, for example, push the analytical systems to their limits with complex and varied target lists. One such method targets 117 individual organics [35] including traditional “ozone precursors,”

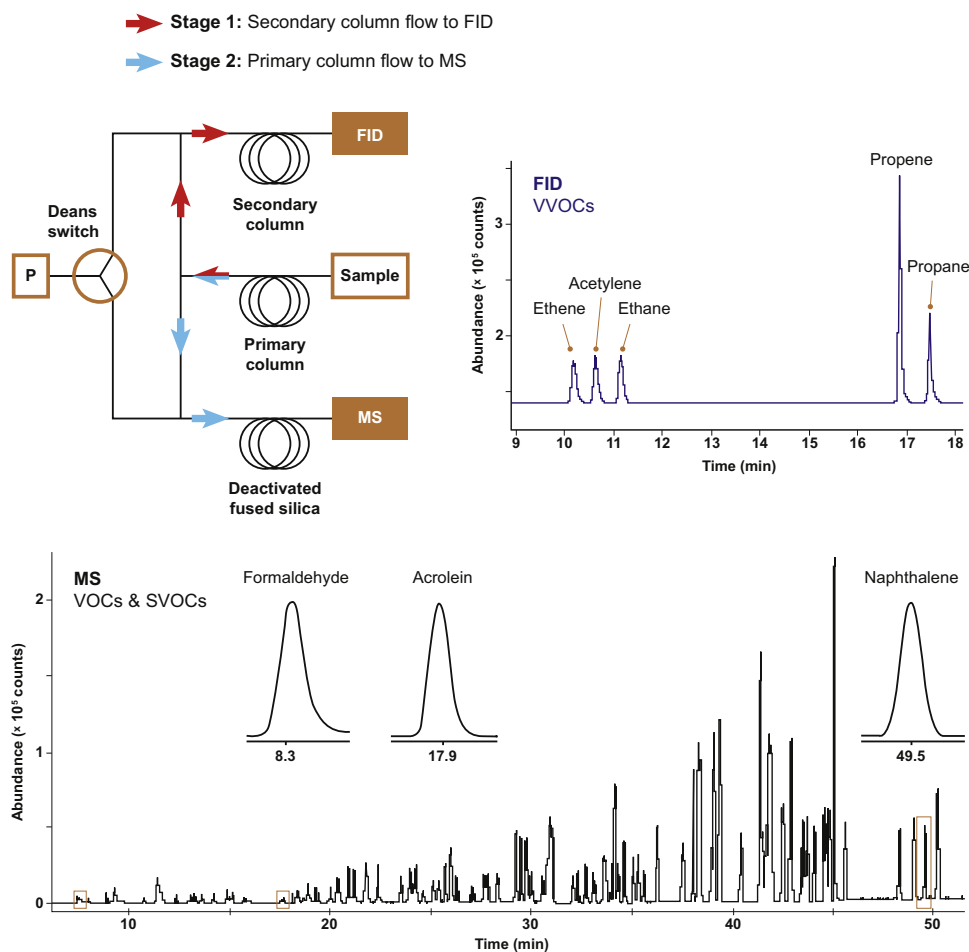


FIGURE 10.16 400 mL of a 10 ppb, 100% relative humidity standard containing ozone precursors, air toxics, oxygenated VOCs, and formaldehyde in a single analysis. Experimental conditions: UNITY–CIA *Advantage*–Kori-xr, sampling flow rate of 50 mL min^{-1} , trap low temperature -30°C , focusing trap materials Tenax TA, graphitized carbon black, and carbonized molecular sieve. Trap desorption 250°C for 2 min with an outlet split ratio of 2.5:1. Separation and detection using Agilent 7890 GC fitted with a Deans' switch, flame ionization detector, and 5977A single quadrupole mass spectrometer.

common "air toxics," and formaldehyde (Fig. 10.16)—all in a single sampling and analysis cycle.

10.3.8 Formaldehyde

A benefit of online monitoring is that it provides one of the few viable sampling options for GC-(MS) analysis of reactive air pollutants such as formaldehyde without the need for derivatization. Formaldehyde is ubiquitous in

ambient air and commonly emitted by wood-based and other materials into the indoor environment. It can present a serious risk to human health [36]. However, the tendency of formaldehyde to react with atmospheric humidity during sample storage makes it very difficult to store using conventional off-line samplers such as sorbent tubes, bags, or canisters. Instead, most relevant reference methods specify use of Dinitrophenylhydrazine (DNPH) sampling cartridges to derivatize and stabilize formaldehyde

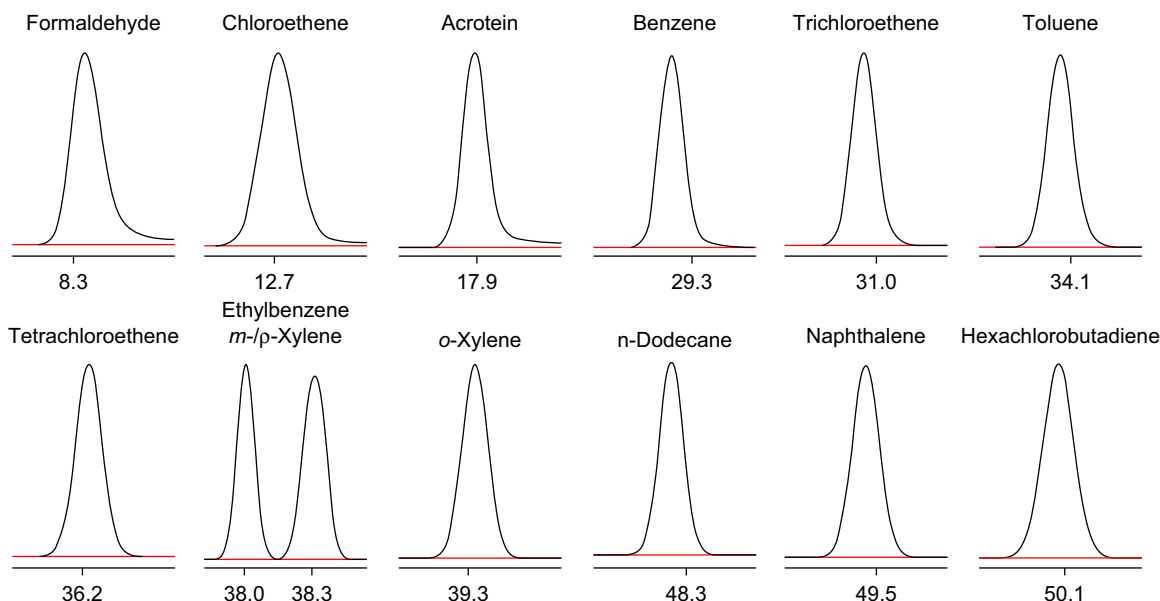


FIGURE 10.17 Identification of compounds covering the polarity and volatility range of the target list without the use of liquid cryogen: 10 replicate analyses of a 10 ppb standard at 100% RH overlay perfectly for all compounds. Canister sampling: Instrument: CIA *Advantage*-xr (Markes International); Sample purge: 4 min at 50 mL min⁻¹; Sample flow: 50 mL min⁻¹; Sample volume: 50–600 mL; Postsample purge: 5 min at 50 mL min⁻¹. Water removal: Instrument: Kori-xr (Markes International); Trap temperatures: -30/300°C. TD: Instrument: UNITY-xr (Markes International); Focusing trap: Part no. U-T22117-2S; Flow path: 120°C; Trap purge: 2 min at 50 mL min⁻¹; Trap low: -30°C; Trap high: 250°C for 2 min; Outlet split: 3 mL min⁻¹. GC: Carrier gas: Helium, constant flow; Column flow: Primary column 2 mL min⁻¹; Oven temperature: 35°C (10 min), then 6°C min⁻¹ to 240°C (0 min), then 20°C min⁻¹ to 270°C (6 min); Run time: 52 min.

during sampling [37,38]. The downside of this is that the sampled DNPH cartridges require subsequent analysis by HPLC not GC-MS. If applicable, online TD-GC-MS configurations therefore offer labs a unique opportunity to monitor formaldehyde and other VOCs simultaneously without needing to invest in a separate analytical system (Fig. 10.17).

10.3.9 Continuous online monitoring

Reciprocally operated twin-trap TD systems are also available nowadays for truly continuous online air sampling. Continuous monitoring is needed for some particularly sensitive applications—for example, counterterrorism, controlling hazardous chemical processes, and

general kinetic studies—examples are included in the applications section.

10.4 Using thermal desorption to enhance analysis of complex liquid and solid samples

Historically, most GC analyses of liquids and solids have fallen outside the scope of TD. Twenty years ago, the only exceptions to this were the purge-and-trap methods described at the start of this chapter and direct TD of homogeneous materials (adhesives, powdered spice, polymer beads/fibers, soap powder, drug powders, etc.). Complex liquid and solid samples have always been more commonly processed by traditional liquid extraction methods or alternative gas extraction systems, such as HS, with or without SPME.

However, with recent improvements in water management, modern TD focusing traps are increasingly being applied to improve HS and SPME-HS methods by selectively focusing extracted analytes before final injection/transfer into the GC. This enables the HS transfer and/or SPME-fiber extraction processes to be separated from the GC injection so that each phase of the process can be optimized independently. For example, it allows the volume of HS gas transferred to be increased without swamping the capillary column. Similarly, carrier gas flows above 10 mL min^{-1} can be used to optimize the desorption of SPME fibers without necessitating a split. Use of a focusing trap also selectively concentrates the organic vapors, injecting them into the GC in a narrow band of vapor. This peak

sharpening increases sensitivity while, at the same time, water and other interferents may be selectively purged out of the focusing trap and away from the system, thus reducing system background.

This combination of enhancements—maximizing sample volumes, eliminating split, sharpening peaks, and reducing background—significantly improves detection limits compared to equivalent conventional methods. The latest commercial systems also facilitate multistep enrichment, allowing several HS or SPME-HS extracts from the same or multiple samples to be transferred sequentially onto the focusing trap before final desorption and GC injection [39] (see Fig. 10.18). Techniques such as these maximize sensitivity for research applications,

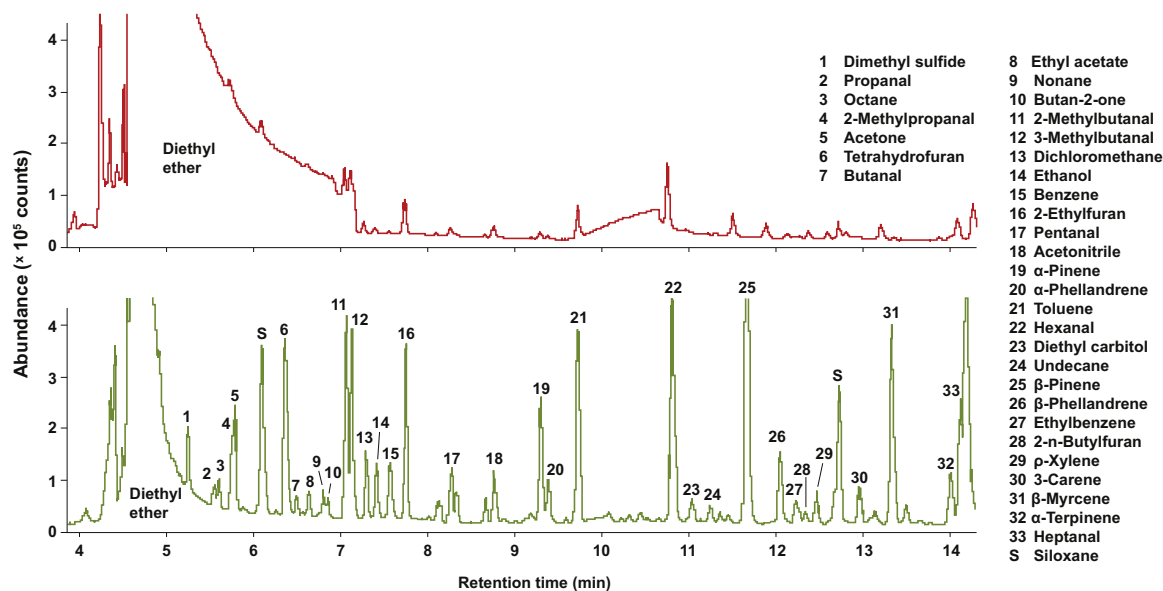


FIGURE 10.18 A comparison of direct SPME (top) and SPME-trap with multistep enrichment (bottom) with analysis by GC-MS for the determination of aroma constituents in a dried tea sample. Sample preparation: Each sample vial was identically prepared: 1 g of dried tea placed into a 20 mL vial. Addition of 10 mL HPLC grade water and 10 μL of a halophenol mix (nine compounds) in diethyl ether solvent. Experimental conditions: Centri sample extraction and enrichment platform (Markes International Ltd., UK) combined with 7890–5977 system (Agilent Technologies). Extraction: 15 min at 60°C using a multiphase fiber (DVB/CAR/PDMS, Supelco). Fiber desorption via the Centri inlet direct to the GC (direct SPME) or to the multisorbent-bed focusing trap (SPME-trap with multistep enrichment) 3 min at 250°C . Enrichment: 2 further rounds of the extraction–desorption procedure using the same sample vial and SPME fiber. Focusing trap: “Material emissions,” held at 25°C during fiber desorption. Trap desorption: 290°C for 3 min with a 5 mL min^{-1} split flow (split ratio 6:1). Flow path: 180°C . Column: $60 \text{ m} \times 0.25 \text{ mm} \times 0.25 \mu\text{m}$, DB-WAX Ultra Inert (Agilent Technologies). GC oven: 40°C (3 min), then $30^\circ\text{C min}^{-1}$ to 60°C , then 3°C min^{-1} to 230°C (15 min). Scan range: m/z^{-1} 35–300.



FIGURE 10.19 Sorptive devices compatible with direct immersive sampling. Clockwise from top left: HiSorb, thin-film SPME and SPE-tD.

allowing detection at levels approaching those of purge and trap but without the associated issues of foaming and aerosol formation [40].

While HS methods (regular or sorptive) are convenient for analyzing volatiles in solids and liquids, immersive sorptive extraction techniques have also been developed. These are particularly appropriate for the measurement of semivolatile and polar compounds that don't readily partition into the vapor phase. SPME fibers are generally too fragile for reliable immersive sampling, but various forms of robust higher-capacity sorbent samplers are now coming onto the market¹ (Fig. 10.19). Once sampled, washed, and dried, these devices are analyzed by TD, with the extracted analytes from one or multiple samples being concentrated on the focusing trap before GC(MS) injection.

The main advantages of immersive sorbent extraction are that it typically reduces the amount of sample preparation required (e.g., salting, buffering) and simplifies the extraction process itself. While analyte masses collected during sorptive sampling of HS depend on two equilibria (the first between the liquid sample and the HS, the second between the HS and the sorptive medium), immersive methods are only subject to one—target organics partition directly between the liquid and the sorptive phase. This reduces the numbers of variables and associated measurement uncertainty.

The only barrier to wider adoption of immersive sorptive extraction methods until now has been lack of automation, with manual intervention traditionally required to remove the sorptive device from the sample, wash it, dry

¹ Commercial implementations of sorptive extraction technology for TD-GC include coated fibers from Sigma-Aldrich Inc., PDMS-coated stir bars (Gerstel-Twister—Gerstel GmbH and Co. KG), SPE-tD cartridges from Japan, and HiSorb probes (Markes International Ltd., UK).

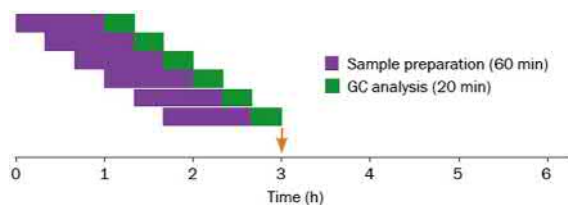


FIGURE 10.20 Illustration of the automation of sorptive extraction using Centri (Markes International Ltd., UK). Using this system, multiple sorptive sampling probes are typically deployed in an overlapping sequence to minimize analytical cycle time.

it, and transfer it to the desorption system [41]. However, new fully automated and robust platforms are now becoming commercially available and should allow immersive sorptive extraction methods to be adopted for routine work—food quality testing, water quality monitoring, targeted screening of biological fluids, etc.—see Fig. 10.20. Note that some of these automated platforms also enable multistep enrichment [39], providing the same benefits for immersive sampling as described for HS methods.

10.5 Sampling options for thermal desorption

The range of TD sampling options has expanded significantly over recent years to support and exploit the advances in TD analytical technology. Sorbent tubes (pumped and passively sampled) are still widely used alongside whole air containers (bags, canisters) and online air or gas manifolds. Solid and liquid samples are accommodated using empty tubes (for direct desorption/dynamic HS), traditional 10- or 20-mL vials, or on/off-line purge-and-trap sample vessels.

Several specialist “stand-alone” sampling devices have also been introduced for TD over time [42] to further expand the application range. Prominent examples include alveolar breath

samplers [43,44], a variety of material emission testing equipment [45–47], and soil probes [48,49]. Relevant applications are described in reference 42 and toward the end of this chapter.

The broad scope of TD and the roles it now plays in sampling and sample introduction for GC-MS may be summarized diagrammatically—see Fig. 10.21.

10.6 An introduction to thermal desorption applications

Before diving headlong into the wonderful world of TD applications and the analytical potential delivered by this powerful technique, it is important to clarify the limitations—the following areas are not generally suited to TD:

- Measurement of trace inorganic gases such as O_2/O_3 , N_2 , CO_2 , NO_x , SO_x , and NH_3 . (Exceptions include N_2O , H_2S , and SF_6 , which can all be conveniently monitored using TD methods.)
- Methane monitoring: This is hard to trap quantitatively, even on the most efficiently cooled sorbent traps. Moreover, it is often present in such abundance (relative to other organic vapors) that it can usually be monitored without preconcentration, e.g., using portable FIDs.
- Organic compounds that aren't stable enough for analysis by conventional GC.
- Nonvolatiles, i.e., compounds less volatile than $n-C_{44}$, dodecyl phthalate, or six-ring PAHs.

Outside these few exceptions, TD has the versatility to benefit a wide spectrum of GC work, especially those samples that present a challenge to conventional liquid injection technology. Compatible analyte concentrations range from as high as percent levels to subparts per trillion.

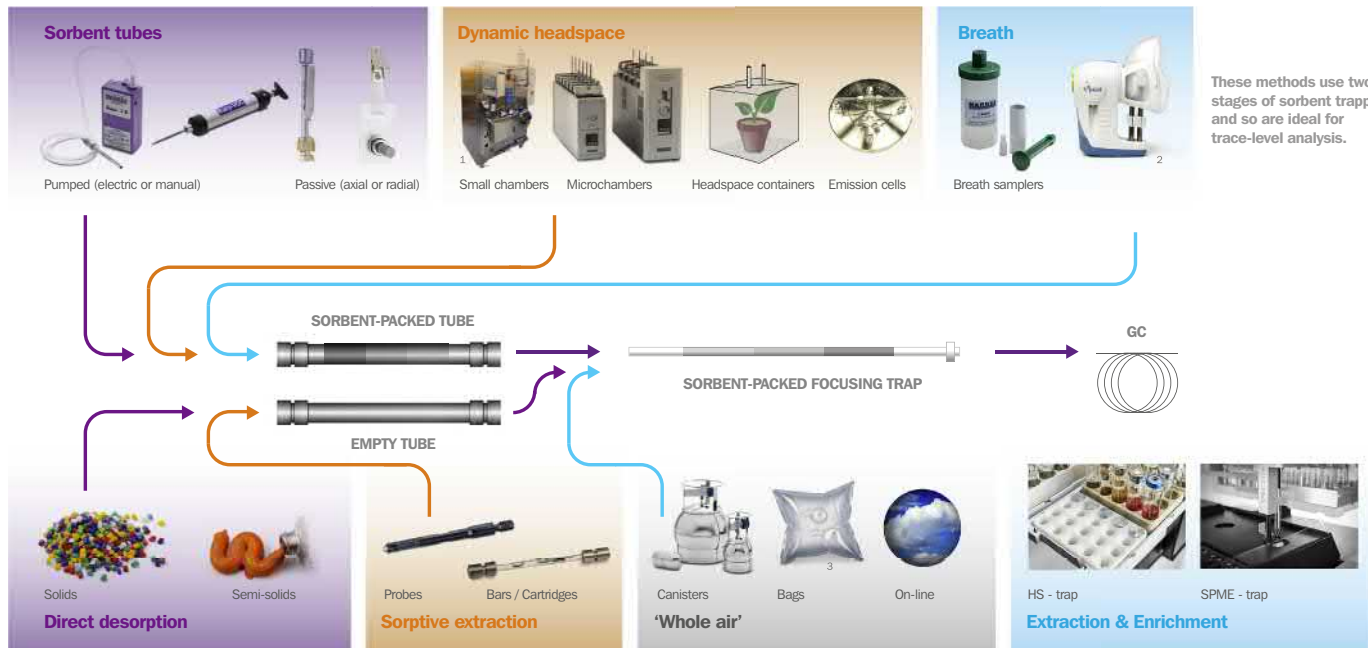


FIGURE 10.21 GC(MS) sample introduction options supported by thermal desorption.

10.7 Breath monitoring

One of the most topical areas of research involving TD-GC-MS currently is the study of VOC profiles in breath. Vapor-phase organics in the alveolar or “end-tidal” air, deep in the lungs, are in equilibrium with blood concentrations and thus provide a valuable insight into the status of metabolic processes or contamination levels of an individual.

Breath testing is one approach to biological monitoring: i.e., the process of evaluating an individual's total or overall chemical exposure (workplace and/or environmental). Chemicals enter the body via inhalation but can also be ingested or absorbed through the skin. Traditional air monitoring methods only monitor the inhalation route so biological monitoring is a necessary complement for some industries and processes [43,50,51]. The advantage of breath sampling in this case is that it is noninvasive and much more convenient than the alternatives of blood or urine testing, which both require trained medical personnel [43]. With sufficient data, guideline “acceptable breath concentration” levels can be set for specific processes or tasks. However, results are more typically interpreted in relative terms, e.g., for checking that mean exposure levels aren't increasing over time or for identifying anomalies across a group of workers all ostensibly doing the same job. Guidance notes are available to help interpret breath monitoring data for some common skin-absorbed compounds [52].

Breath analysis is also of increasing interest in clinical research. Many biological processes and medical conditions generate specific indicative VOCs or patterns of VOCs (so-called biomarkers), which are exhaled in alveolar air. If biomarkers can be found that reliably allow patients to be distinguished from controls, within the normal complexity and variability of breath profiles, they provide a valuable and low-cost diagnostic tool [53]. Interest in this area has accelerated recently with improvements to TD

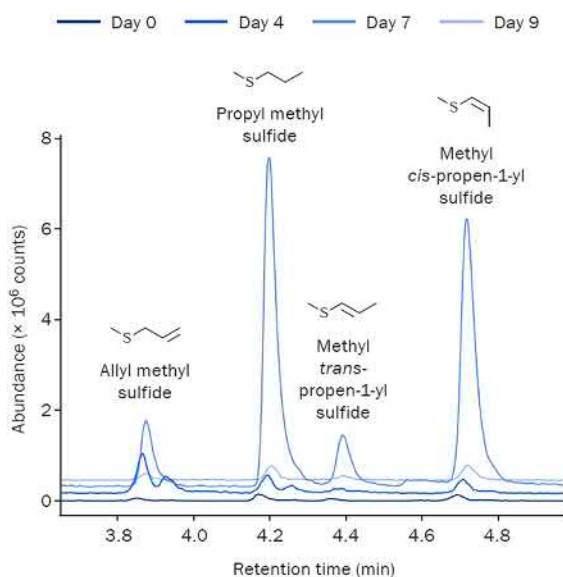


FIGURE 10.22 Detail of a typical breath profile of a malaria patient. The study found four thioethers with concentrations that increased to a maximum when blood parasite levels were highest (day 7) and which subsequently decreased rapidly following drug treatment (day 9). This behavior strongly suggests these compounds would be ideal biomarkers of malarial infection in humans. Traces have been horizontally and vertically offset for clarity. Breath sampling: Breath was collected each morning, before which individuals fasted. 1 L breath samples were collected and transferred onto “Odour/Sulfur” inert-coated stainless steel tubes (Markes International part no. C2-CAXX-5314). These are packed with an inert combination of sorbents specially designed for monitoring sulfur compounds. TD: Instrument: UNITY 2 (Markes International); Tube desorb: 250°C (10 min) at 20 mL min⁻¹; Focusing trap: “Sulfur/labile” (part no. U-T6SUL-2S); Trap low: 30°C; Trap desorb: 300°C; Trap outlet split flow: 5 mL min⁻¹; Flow path: 120°C. GC: Column: ZB-5MS (Phenomenex), 30 m × 0.25 mm × 0.25 μm; Oven: 35°C (5 min), then 5°C min⁻¹ to 250°C (2 min); Column flow: Helium, 0.8 mL min⁻¹. Quadrupole MS: Scan mode: m/z⁻¹ 35–350.

hardware and complementary advances in GC separation, MS detection, and data analysis technologies all enabling more, and better qualified, information to be “mined” from every sample. The extensive range of disease conditions being investigated includes lung cancer, TB, malaria (Fig. 10.22), diabetes, and various gastrointestinal disorders [53–59].

Other important breath monitoring applications include studies of halitosis or breath odor [60] and the reliable identification of smokers [61,62].

10.8 Air monitoring

Air monitoring is the application everyone first thinks of in connection with TD, but it is a broad field in its own right and can be subdivided into several interesting and distinct areas [8,42].

10.8.1 Industrial (occupational) hygiene or workplace air monitoring

Monitoring personal (inhalation) exposure to toxic chemicals for compliance with workplace health and safety regulations was one of the very first applications of TD. Samples are typically collected using pumped or diffusive (passive) sorbent tubes according to various national and international standard methods [28,63–66]. Time-weighted average measurements, e.g., over an 8-h shift, are then assessed against threshold limit values (TLVs), sometimes called occupational exposure limits (OELs), to check compliance with relevant regulations. While vast improvements in workplace health and safety have been implemented in most industrialized countries over recent years, the developing world still struggles to keep workplace personal exposure levels below safe limits. Additional information on chemical toxicity has also led to the continued reevaluation and reduction of many limit levels, thus driving the ongoing need to monitor personal exposure at lower concentrations.

There are many excellent publications reporting on the use of analytical TD for occupational hygiene [67,68]. One point of note is that best practice typically requires average (mean) monitoring results to be well below prescribed limit levels (e.g., one-tenth). This is because differences in behavior between individuals

generate results that vary by as much as 1 or even 2 orders of magnitude, even for a group of people all supposedly doing the same job [1]. Therefore, it is only when the average falls well below the OEL that it is safe to assume that no individual workers are being exposed to unsafe levels.

10.8.2 Monitoring ambient outdoor air and indoor air quality (IAQ)

TD-GC-MS has been the analytical method of choice for environmental outdoor and indoor air monitoring applications for at least three decades. A wide variety of sampling options are applied to this field, depending on monitoring objectives. Online/near-real-time monitoring systems are used for round-the-clock monitoring of key pollutants such as ozone precursors in urban air [22–24,69,70] (Fig. 10.23), pollution from industrial areas [35] (Fig. 10.16), and odorous sulfur compounds (hydrogen sulfide, methane thiol, dimethyl sulfide, dimethyl disulfide) near landfill sites and sewage treatment works [71,72]. Off-line sampling options include both sorbent tubes (pumped and diffusive) [73–76] (Fig. 10.10) and whole air sampling into canisters [77] (Fig. 10.11). Applications for whole air sampling options such as canisters include the more volatile “air toxic” [78] species and ultravolatile trace greenhouse gases—CF₄, C₂F₆, SF₆, etc. [79]. Generally speaking, most indoor and outdoor air monitoring applications are more conveniently sampled using pumped sorbent tubes [18,28,75,78,80–83]. Some detailed surveys of indoor air quality in homes and schools [17,84] and pollution hot spots in major metropolitan areas have also been carried out using diffusive (passive) sampling—with both axial sorbent tubes [73,85] and radial diffusive cartridges [84,86]. The low cost of passive (diffusive) sampling and ease of deployment facilitate the collection of large numbers of samples, allowing accurate mapping of pollution isopleths and hot spots—see Fig. 10.24 [85].

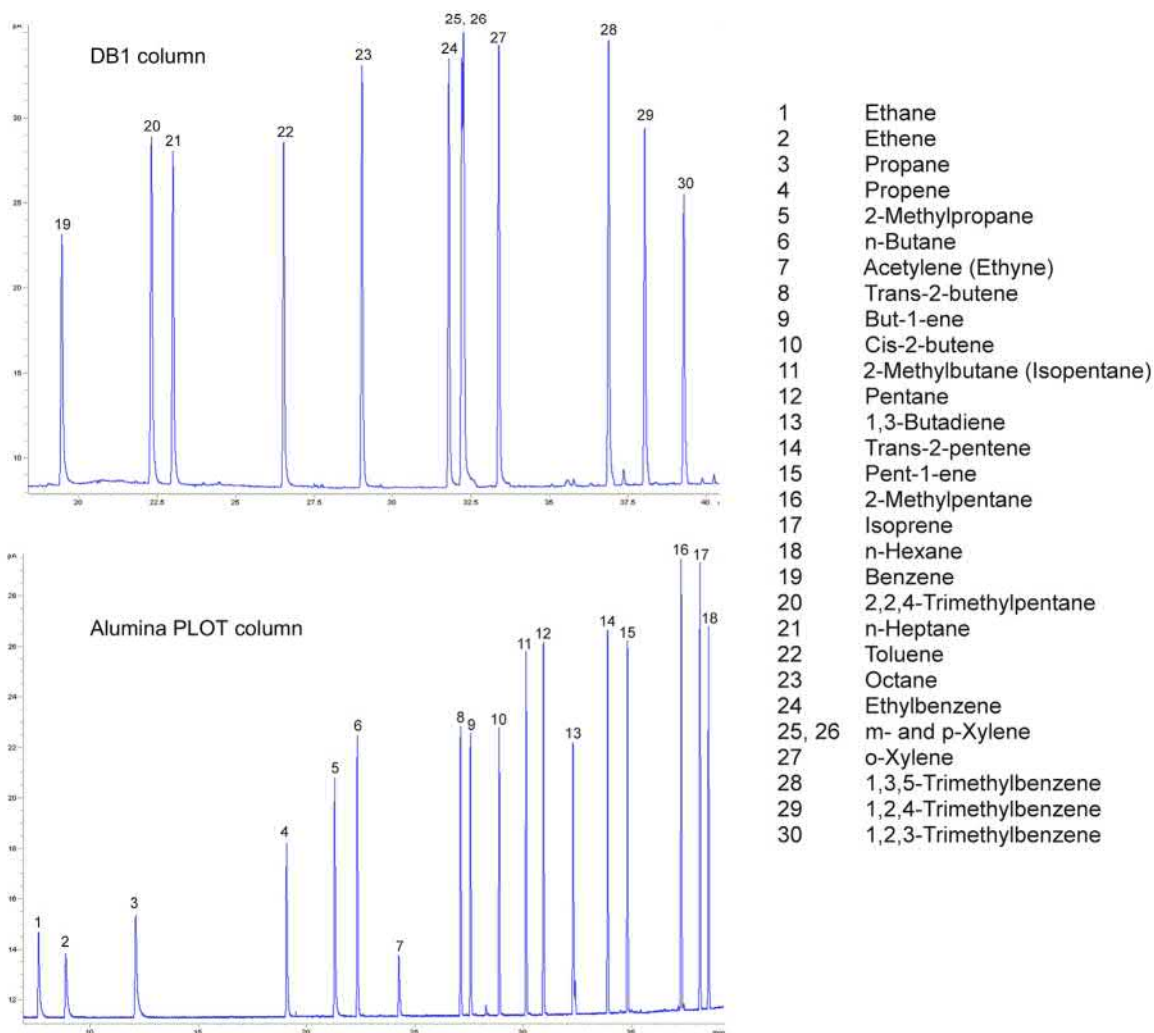


FIGURE 10.23 On-line monitoring of “ozone precursors”— C_2 – C_9 hydrocarbons—using TD-GC with dual column/Deans’ switch configuration and dual FID. Experimental conditions: UNITY-Air Server online thermal desorption system (Markes International Ltd., UK) combined with a 7890 GC configured with Deans’ switch, “Micro-fluidics” (Agilent Technologies). Multisorbent (“ozone precursor”) trap at -30°C . Trap desorption: 40°C s^{-1} to 325°C . Flow path: 80°C . Columns: $60\text{ m} \times 0.25\text{ mm I.D.} \times 1.0\ \mu\text{m}$ film DB1 and $50\text{ m} \times 0.32\text{ mm} \times 8\ \mu\text{m}$ Alumina PLOT (Na_2SO_4 wash) (Agilent Technologies). GC oven: 30°C (12 min) 5°C min^{-1} to 170°C then $15^\circ\text{C min}^{-1}$ to 200°C . Deans’ switch at 17.5 min.

10.8.3 Monitoring vehicle interior air quality (VIAQ)

Many people spend a significant proportion of time in their own vehicle or on public

transport, and public awareness of cabin air quality (cars, trucks, aircraft, etc.) and its potential impact on human health and comfort is growing. The Chinese authorities have blazed a trail in this area with regulations controlling

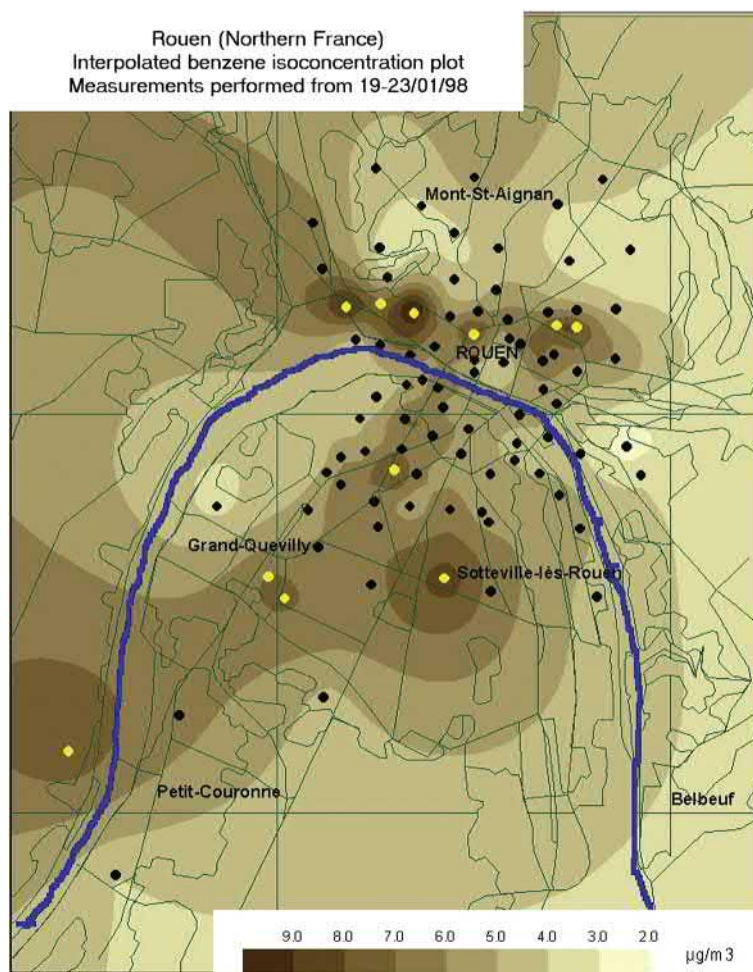


FIGURE 10.24 Mapping criteria pollutants in urban air using diffusive sampling.

VIAQ levels of target VOCs in new cars [87] and stimulating renewed international efforts to harmonize test standards. Methods typically require pumped sampling onto sorbent tubes with TD-GC-MS analysis [29,88]. Near-real-time monitoring technologies combining online TD with fast GC-MS or real-time mass spectrometers are also sometimes applied but are often unable to resolve all compounds of interest and potential interferences satisfactorily in the absence of GC separation.

10.8.4 Industrial (fugitive) emissions—stack (flue) gases and perimeter monitoring

TD-based methods have always been popular for monitoring around the perimeter of industrial plants as a check on industrial emissions and their dispersion. The simplicity of diffusive monitoring lends itself to this application. It enables multiple samplers to be cost-effectively deployed around a site, allowing accurate mapping of

pollution/contamination levels under different wind and weather conditions [76,89].

While most bulk organic vapor measurements in industrial (stationary source) emissions are made using sensors (continuous emission monitoring (CEM) technology), trace-level toxic compounds are often collected on sorbent tubes with subsequent analysis by TD-GC(-MS). Relevant test methods include EPA Methods 0030, 0031 and 5041A in the United States, EN TS 13649 in Europe [90], and HJ 734 in China [91].

Several important new monitoring methods have also been developed recently by Chinese agencies for monitoring air pollution around chemical and industrial parks and in nearby urban areas [92]. Some of these are among the most challenging modern TD applications, targeting as many as 117 target compounds in one run, including both VOCs and formaldehyde [35]—see Fig. 10.16.

10.8.5 Atmospheric research

The impact of air pollution on climate and other finely balanced natural systems, such as the stratospheric ozone layer, has been studied in multiple national and international research projects. Studies have included global background pollution levels (monitoring some of the cleanest atmospheres on earth [93,94]), long-distance migration or transport of air pollution, biogenic emissions/atmospheric chemistry [95,96], and measurements of air–seawater interactions [97].

These studies typically involve vapor concentration measurements at ppt or even ppq concentrations, requiring the best available TD-GC technology coupled with high-sensitivity MS detection (negative-ion chemical ionization (NCI), time-of-flight (TOF), etc.). Preferred sampling options include pumped sorbent tubes or canisters [94], depending on target analyte range.

10.8.6 Soil gas and vapor intrusion into buildings

As the human population continues to expand, there is increasing pressure to redevelop disused industrial land rather than build on “greenfield” sites. However, as in the case of the infamous Love Canal incident mentioned earlier, there is always concern that the residue from chemical processes originally carried out on a site, or from disused chemical/fuel storage tanks, may remain in the soil. Redevelopment of industrial land therefore requires a detailed risk assessment, plus monitoring and remediation of any identified contamination. Even after remediation (cleanup), long-term monitoring of soil gas, or air from inside buildings constructed on the site, may also be required to make sure that the risk from any residual pollution remains low. Occasionally, it is necessary to adapt building methods to minimize risk of vapor intrusion, for example, by installing impermeable membranes in the basement.

The United States has led the way in this field, and many related monitoring methods are now under development, for example, within ASTM. Cited soil gas (or “under slab”) sampling approaches include using canisters (limited to compounds more volatile than $n\text{-C}_{9/10}$) and sampling onto sorbent tubes (compatible with a wider volatility range.) Analysis is by thermal desorption in either case [8,98,99].

10.8.7 Monitoring tracer gases (for example, in studies of building ventilation)

Tracer gases typically comprise perfluorinated compounds (sulfur hexafluoride or perfluoromethylcyclohexane), which don't occur naturally and are readily detected at low levels by GC methods (e.g., by using electron capture detection or GC-MS in NCI mode.) Sources of

tracer gases are placed in various locations in buildings or vehicles. On- or off-line TD-GC methods are then used to monitor the concentrations as they change over time, thus allowing ventilation efficiency to be evaluated. Both passive and active sampling methods have been applied [100,101].

In one interesting aside, halogenated organic compounds are now known to play a key role in ozone depletion (i.e., damaging the ozone layer) and to have very high global warming potential (5000–10,000 times more than that of CO₂). They also have a long half-life in the atmosphere. SF₆, for example, can now be detected around the planet at ~6 ppt and Freon 113 at ~75 ppt—see Fig. 10.25. While these levels do not present any immediate or significant environmental risk, scientists are nevertheless concerned to make sure their research does not contribute to global pollution levels. Use of tracer gases has therefore been minimized over recent years.

10.9 Chemical emissions from everyday products to indoor and in-vehicle air

Fears relating to global warming have also driven new regulations relating to the energy performance of buildings in many parts of the world (for example [102]). Unfortunately, this well-intentioned legislation has had the unwanted side effect of significantly reducing building ventilation levels and consequently having a negative impact on indoor air quality. While ventilation rates in traditional Northern European and US housing stock were in the order of 1 or 2 air changes per hour, levels of 0.2 or even 0.1 air changes per hour are not uncommon in some new apartments and offices [103,104]. Reports of adverse health effects have therefore led to an increased focus on controlling the sources of indoor pollutants, including

chemical emissions from the wide range of products used indoors [105]. Construction products, decorative materials, car interior trim components, furniture, and cleaning products have all come under scrutiny. Even natural materials that have been used in homes for centuries may compromise air quality when installed in modern, air-tight dwellings.

New regulations [106], test protocols [107–109], and analytical methods [110–113] have been developed to address these concerns. Those relating to vapor-phase organic chemicals predominantly specify the use of sorbent tubes with subsequent TD-GC-MS analysis [29,110–113].

Reference methods for material emission testing generally specify small environmental chambers (typically 20–1000 L volume) or test cells, both of which can be used to evaluate chemical emissions from products and materials under simulated “real-use” conditions and for extended periods. Samples are usually prepared such that only the surface exposed to the indoor environment in real use is exposed in the test chamber or cell. Pure humidified air is then driven into the chamber under controlled conditions of temperature, humidity, time, etc. After a given period, the exhaust air is sampled and analyzed as described earlier to measure the area-, mass-, or product-specific chemical emission rate. Tests are usually carried out over an extended period—typically 3, 7, 14, or 28 days—to simulate airborne concentrations soon after product installation or building occupation.

Faster emission screening methods using microchambers have also been developed [114,115] to complement long-term reference tests and to provide manufacturers with a practical tool for routine in-house product quality control testing. Microchambers are typically used in combination with sorbent tubes and TD-GC-MS to measure emitted organic vapors—see Fig. 10.26.

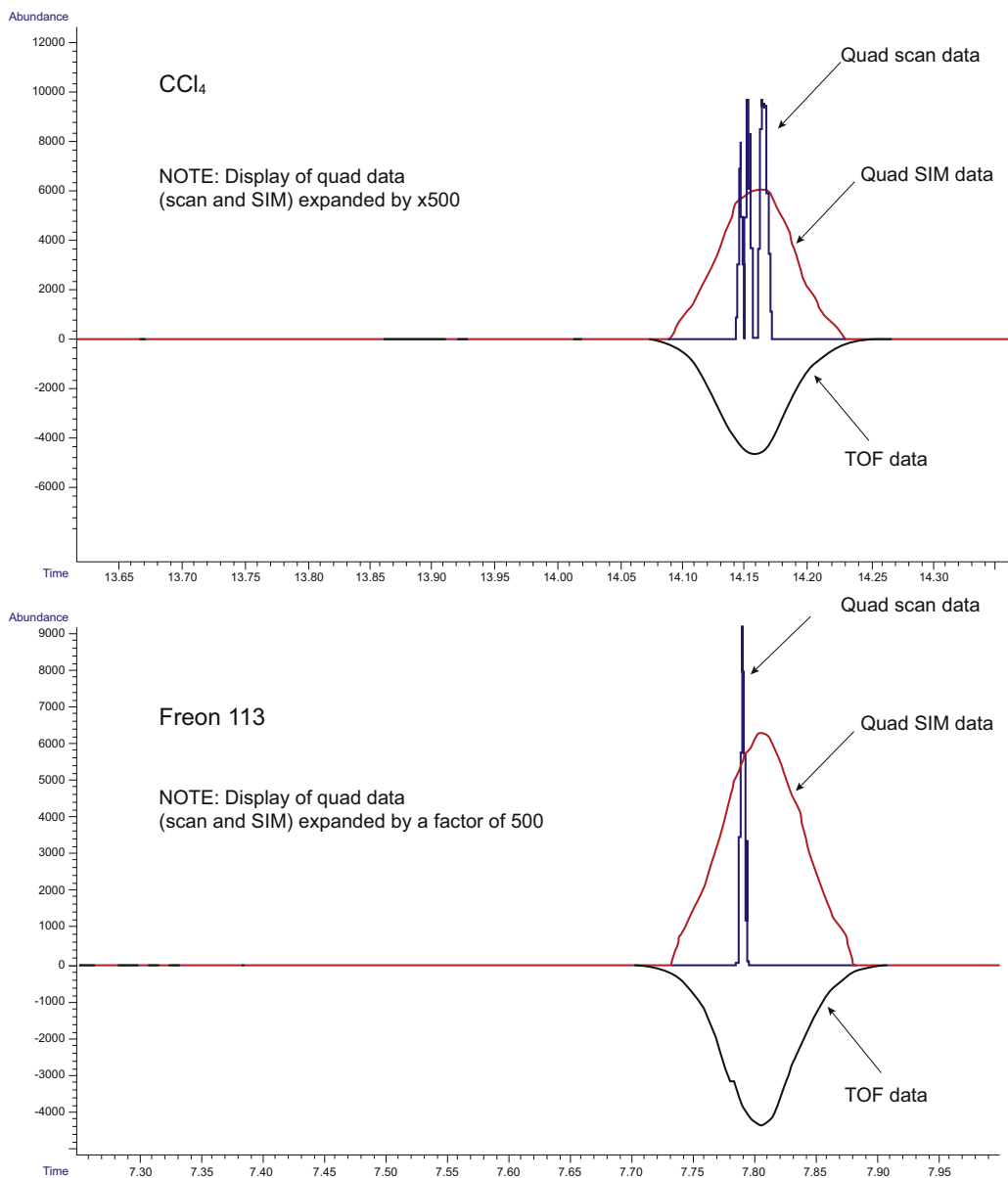


FIGURE 10.25 Comparing TD-GC-MS (quad) with TD-GC-MS (TOF) results for the analysis of carbon tetrachloride and Freon 113 in 200 mL forest air. Experimental conditions: TD-100 (Markes International Ltd., UK) linked to a 7890-5975 GC-MS system (Agilent Technologies) and a 7890 GC with a BenchTOF-dx system (SepSolve Analytical Ltd.). Stainless steel tube packed with carbon black and carbon molecular sieve. Tube desorption: 10 min at 320°C into a multisorbent (“air toxics”) trap at +25°C. Trap desorption: 320°C at 40°C s⁻¹ with 5 mL min⁻¹ split. Flow path: 140°C. Column: 60 m × 0.32 mm I.D. × 1.8 μm film DB 624 (Agilent Technologies). GC oven: 35 to 230°C at 5°C min⁻¹. Quad MS: 20–300 amu (scan) and SIM groups: (1) 56, 67, 93, 151; (2) 57, 78, 106; (3) 58, 91, 117. Masses acquired using TOF MS: 20–300 amu. TOF data (black), quad scan data (white), quad SIM data (black). NOTE: Display of SIM and SCAN data from quad MS expanded by factor of 500 relative to TOF data.

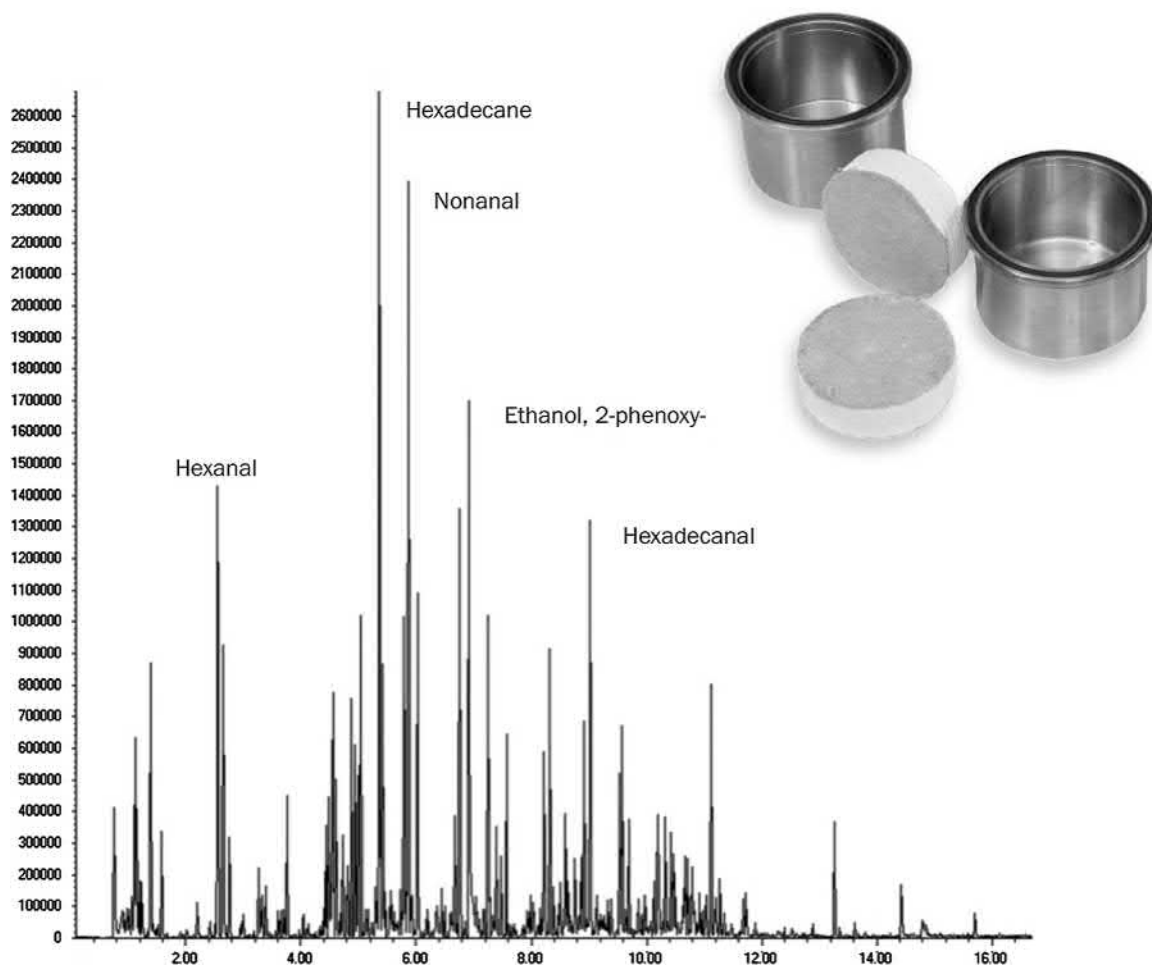


FIGURE 10.26 Screening chemical emissions from plasterboard (dry wall) using test chambers/microchambers or emission cells with sorbent tubes and TD-GC-MS. Experimental conditions: Micro-Chamber/Thermal Extractor (Markes International Ltd., UK) set at 50°C with a flow of 100 mL min⁻¹ dry air. Equilibration time: 20 min, vapor sampling time: 15 min. Sampling onto stainless steel tube packed with Tenax TA. TD-100 automated thermal desorber (Markes International Ltd., UK) combined with a 7890-5975 GC-MS system (Agilent Technologies). Tube desorption: 5 min at 280°C into a multisorbent qtz/Tenax/Carbograph 5 TD trap at +25°C. Trap desorption: 300°C with 30 mL min⁻¹ split flow. Flow path: 150°C. Column: 60 m × 0.25 mm I.D. × 0.5 μm film DB5 (Agilent Technologies). GC oven: 40 to 225°C at 10°C min⁻¹. Scan range: 35–300 amu.

There are numerous publications and reports describing emission tests from construction products and car trim [116,117]. Other everyday products that are commonly checked for chemical release include furniture, furnishings, air fresheners, electronic components, medical devices, and toys—see Fig. 10.27. Note that, even

though the toy emission profiles shown in Fig. 10.27 were obtained at relatively low temperatures (40 and 90°C, respectively), they still show significant emission levels. Several phthalates, for example, are now designated “Substances of Very High Concern” under REACH (the European regulation on the registration,

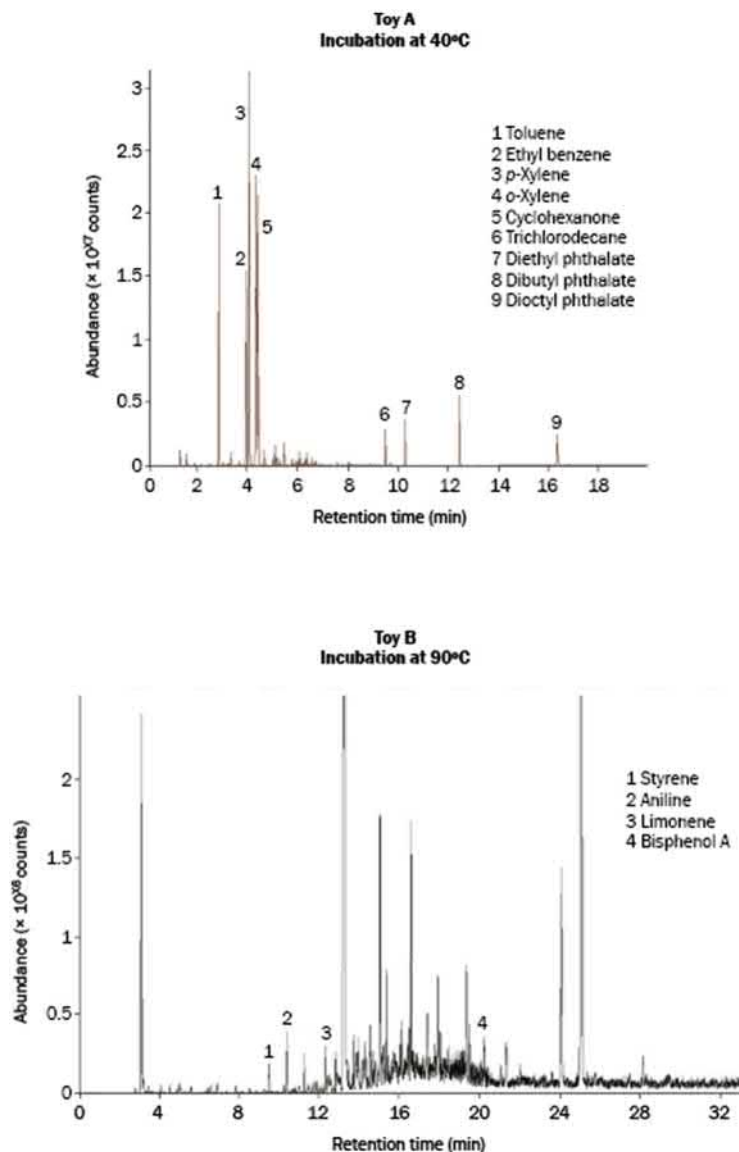


FIGURE 10.27 Screening volatile and semivolatile chemical emissions from children's toys. Experimental conditions: Micro-Chamber/Thermal Extractor (Markes International Ltd., UK) set at 40°C and 100 mL min⁻¹ flow (top chromatogram) or 90°C/50 mL min⁻¹ flow (bottom chromatogram). Equilibration time: 20 min, vapor sampling time: 15 min in each case. Similar analytical conditions to Fig. 10.26.

evaluation, authorization and restriction of chemicals), and bisphenol A is a known endocrine disruptor.

Chemical release/emission testing is now being implemented more widely within manufacturing industry in the interests of consumer safety and to take advantage of market demand for low-emission products. It can also be used in R&D for assessing prototype “low-emission” product ranges, checking the quality and authenticity of incoming raw materials, and comparing products against best-in-class competitors.

10.10 Toxic chemical agents and civil defense

While in many ways a simple extension of air monitoring, use of TD for detection of extremely toxic compounds, such as chemical warfare agents, is usually considered a field in its own right. Relevant example applications include:

- Battlefield protection—using sorbent tubes with TD-GC(MS) to evaluate protective equipment, e.g., monitoring the permeation of agent through masks and clothing.
- First responders—teams equipped with mobile laboratories and trained to be first on the scene in the event of a major chemical incident.
- Monitoring agent storage and destruction facilities—to ensure the safety of personnel and protect the nearby environment.
- Studies of decontamination technology and protective coatings, e.g., paints designed to prevent agent from penetrating into the fabric of buildings or machinery to simplify decontamination in the event of a chemical attack.
- Continuous monitoring of critical civilian locations—transport hubs, key government buildings, etc.

Many of the most dangerous chemical warfare agents present a significant analytical challenge because of their extreme toxicity and the low detection limits required. The “general

population” exposure limit level for the nerve agent VX, for example, is only $0.0006 \mu\text{g m}^{-3}$. Early TD technology was not compatible with many of the highest boiling or most reactive CW agents. VX, for example, was traditionally monitored by sampling the air through silver fluoride pads to derivatize it to the more volatile “G-analogue” [118]. However, this conversion process was rarely 100% efficient and the performance tended to diminish as the pads aged, leading to the risk of underreporting. The latest on- and off-line thermal desorption technology is compatible with free VX even at the lowest levels (Fig. 10.28), thus removing the need for derivatization and reducing analytical uncertainty.

Much of the impetus for developing twin-trap TD configurations came from this field. Twin-trap systems allow air or gas streams to be sampled continuously, thus generating near-real-time data without any unsampled time or “blind spots.” While air is being drawn into trap A, trap B is desorbed and analyzed. Once trap B has cooled, it can be switched to sampling, thus allowing trap A to be desorbed. Data shown in Fig. 10.29 illustrates continuous monitoring of the chemical agent Sarin (GB) using one such system. Typical applications for this kind of technology include continuous monitoring of government buildings against terrorist attack and process monitoring at agent destruction (“demil”) facilities to ensure the safety of site personnel.

10.11 Direct thermal desorption of residual volatiles

Direct TD is also now widely applied for measuring residual volatiles and the VOC content of homogeneous materials. Samples are weighed or pipetted into empty sample tubes or tube liners (Fig. 10.7) for what is effectively a gas extraction or dynamic HS procedure. When operated in this mode, the thermal desorber combines sample preparation/extraction and GC injection into one fully automated process.

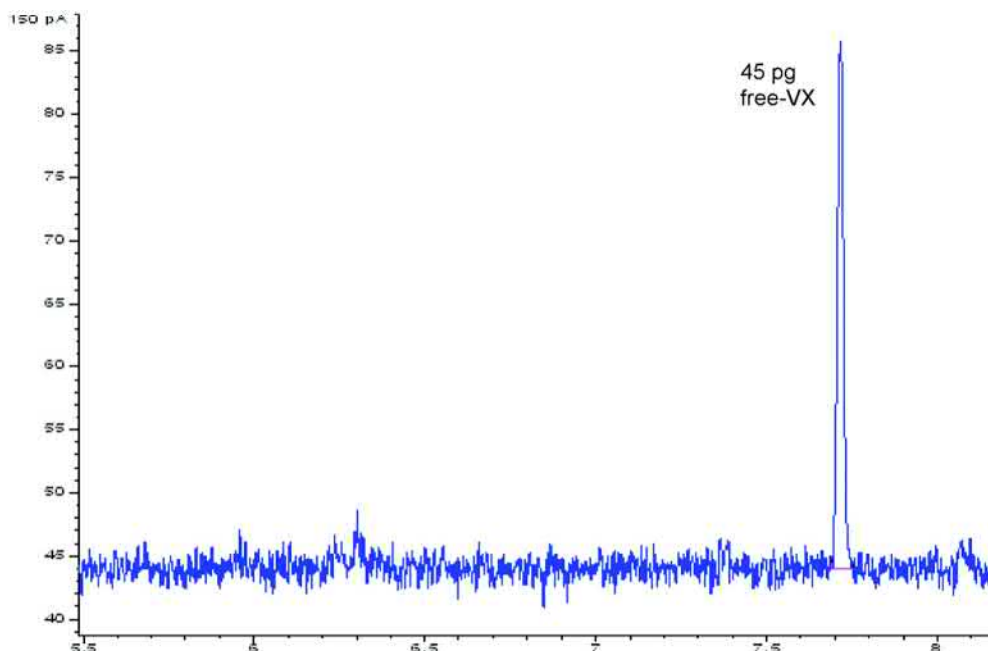


FIGURE 10.28 TD-GC-FPD analysis of free VX at 45 pg level on tube. Experimental conditions: Silcosteel tube packed with Tenax TA. UNITY 2 thermal desorber (Markes International Ltd., UK) combined with a 6890 GC/FPD system (Agilent Technologies). Tube desorption: 8 min at 300°C into a multisorbent qtz/Tenax trap at +20°C. Trap desorption: 300°C splitless. Flow path: 200°C. Column: 30 m × 0.25 mm I.D. × 0.5 μm film HP-5 (Agilent Technologies). GC oven: 60 to 250°C at 20°C min⁻¹. FPD: 250°C, H₂ 150 mL min⁻¹, Air 110 mL min⁻¹, N₂ 55 mL min⁻¹.

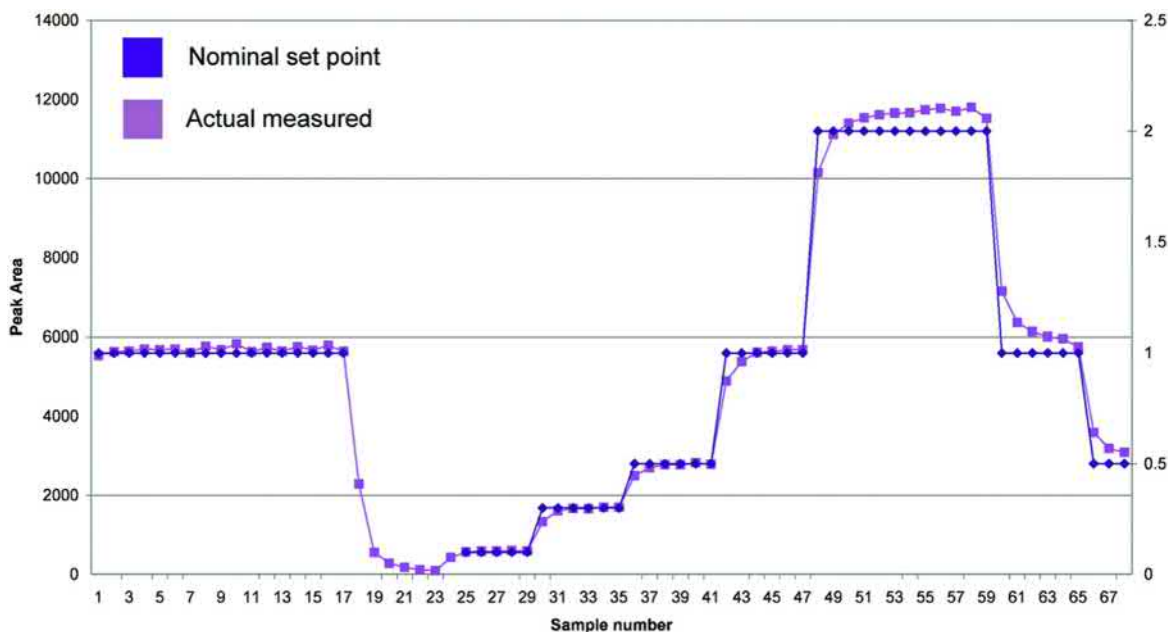


FIGURE 10.29 Using twin-trap thermal desorption equipment for continuous, near-real-time monitoring of the chemical warfare agent GB (Sarin) in a dynamically generated standard atmosphere (see Ref. [153]).

The technique works best if solid samples present a high surface area to mass ratio (e.g., powders, granules, fibers, or thin films) or if small (e.g., 5 μL) aliquots of sample liquids/emulsions are introduced reproducibly onto glass wool. The power and simplicity of direct TD relative to conventional static (equilibrium) HS methods are that no additional dissolution or salting-out steps are required and that it does not rely on partition coefficients or equilibria. Moreover, complete (or nearly complete) extraction is often possible in one run, thus simplifying calibration. Direct TD can also be applied to much smaller sample sizes (e.g., 2 or 3 mg) rather than the 2 or 3 g often required for conventional HS, which suits applications with a limited supply of sample material.

Applications for direct desorption range from manufacturing QA/QC to forensic investigations and examples include:

- Residual solvents and active ingredients in powdered drugs and ointments—see Fig. 10.30 [15].
- Quality control of fragranced products such as soap powder (see further).
- Quality control of textiles and treated leather—see Fig. 10.31.
- The chemical content of paints and adhesives [119].
- Residual monomer or other volatiles in polymers [15,120].
- Packaging materials [121].
- Analysis of house dust [122].

10.12 Odor/fragrance profiling and VOC “fingerprinting”

With the expansion of focusing and TD technology into the broad area of sample extraction and enrichment (see Fig. 10.21), fragrance, aroma, and odor profiling has become one of the fastest growing TD application areas. Researchers can now automatically apply multiple complementary extraction and enrichment

approaches—e.g., HS-trap, SPME-trap, TD, and immersive sorptive extraction—to every sample, maximizing the information obtained. This is especially true when used in conjunction with other advanced GC-MS technologies such as multidimensional GC and/or tandem ionization (see Fig. 10.32 and Appendix B). Relevant applications include wine, beer, fruit, vegetables, drinking water (Fig. 10.33), dairy products, tea, tobacco, cannabis, and extracts of fresh and prepared foods [39,40,123–129].

Maximizing the quality and quantity of data obtained from each sample is important for research work, and the comprehensive odor/fragrance profiles thus generated facilitate identification of key marker compounds (that is, components that allow sample types to be reliably differentiated and categorized.) Following this discovery phase, fast routine methods, focusing on these compounds, can then be developed to reliably classify samples as required, for example, by source/brand, pass or fail, diseased or normal, authentic or fake, natural or synthetic.

Direct TD may also provide a convenient approach for profiling homogeneous materials such as spice, instant coffee, cocoa powder, tobacco, soap powder, etc. In this case, the intention is not to get complete extraction of volatiles but to obtain a representative profile or fingerprint of the odor, aroma, or fragrance. Desorption temperatures are typically kept low in these applications to prevent denaturing the sample.

Direct TD (dynamic HS) fulfills a slightly different role to conventional HS. While static HS selectively concentrates the most volatile constituents, TD allows a wider, more representative profile to be dynamically extracted, covering both volatile and less volatile components. The technique is also very sensitive to changes in sample composition, accentuating even minor variations—5% less of a given ingredient, 10% more of another—thus allowing very precise quality control.

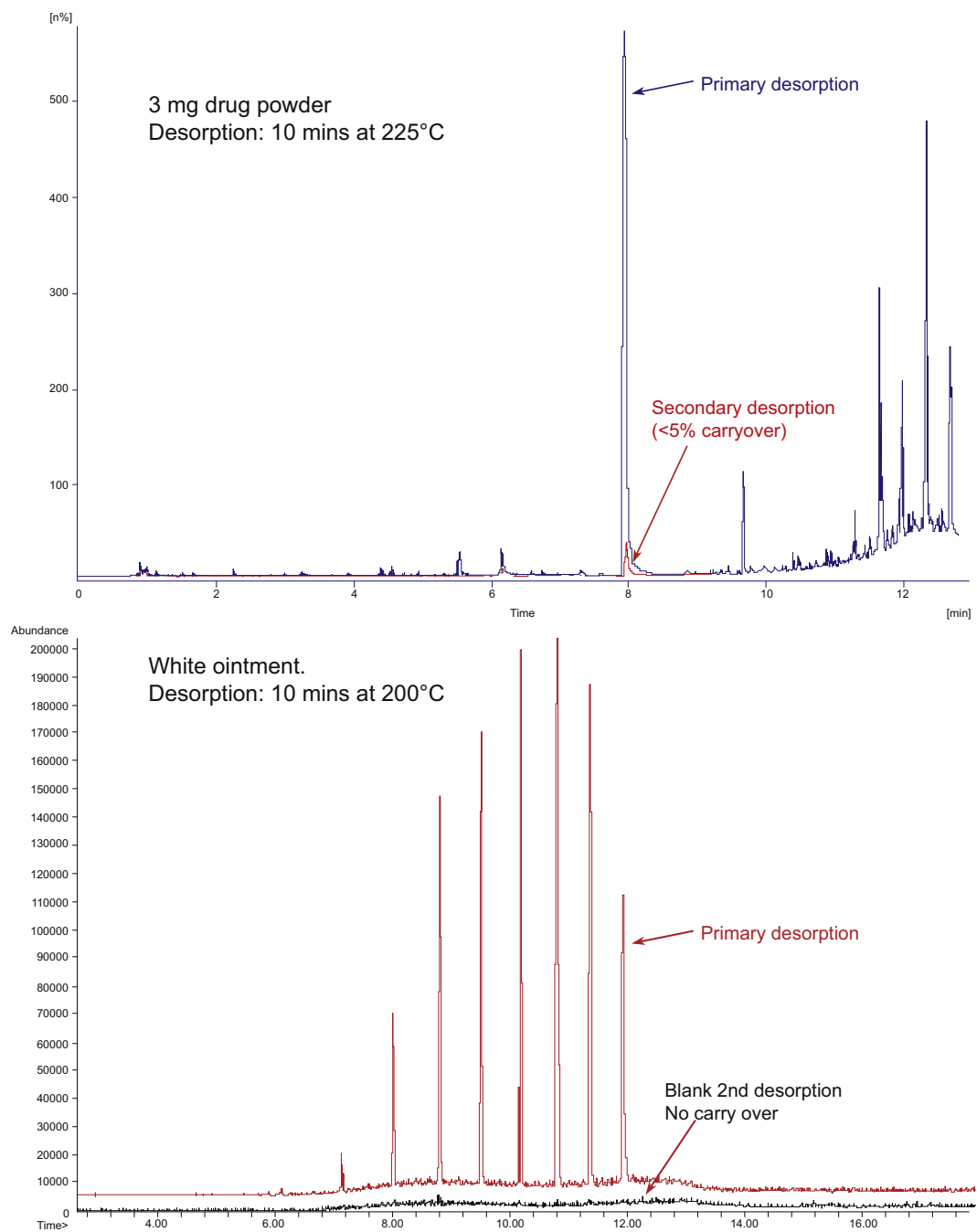


FIGURE 10.30 Direct desorption of residual solvents and/or active ingredients from pharmaceutical preparations.

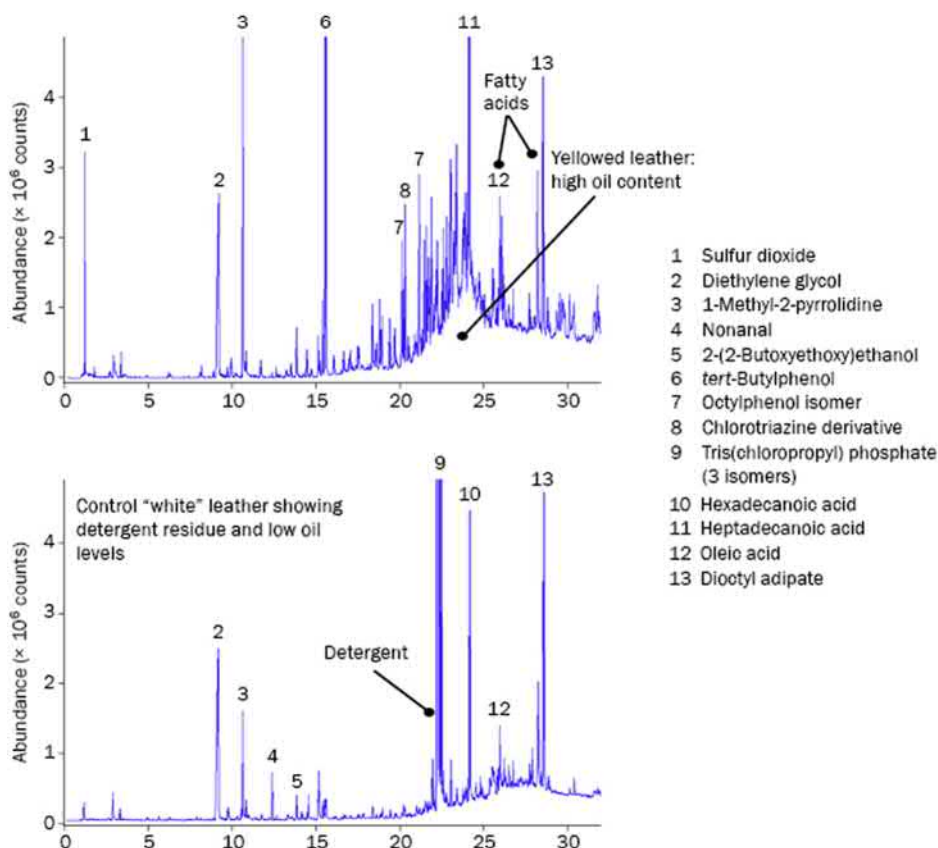


FIGURE 10.31 Direct desorption of discolored and control samples of white leather. The control sample shows detergent residue and much lower levels of natural oils. Experimental conditions: 1.5×10 mm sections of control and discolored leather were desorbed at 150°C for 5 min in a flow of 60 mL min^{-1} carrier gas (split 50:50). Trap: packed with Tenax/Carbograph 1 held at -10°C . Trap desorption: 300°C with 30 mL min^{-1} split flow and 2 mL min^{-1} column flow. Flow path: 200°C . Column: $30 \text{ m} \times 0.32 \text{ mm I.D.} \times 1.0 \mu\text{m}$ film DB 1 (Agilent Technologies). GC oven: 60°C (5 min hold) to 280°C at $10^\circ\text{C min}^{-1}$. Scan: 45–350 amu.

Overall, this is a growing field with many interesting applications and research opportunities. Highlights include:

- Accelerated food shelf-life studies—sometimes using similar microchamber technology to that applied to material emission testing [130].
- The composition of fragrance profiles and the kinetics of fragrance decay.
- Identification of crop emissions, plant species, and plant health [124,128,131–133].
- Monitoring flavor/aroma quality in genetically modified foods [131].
- Studies of insect interactions with plants and other species—pheromones, etc. [134,135].
- Identifying molds, fungi, and bacteria [136].
- Tracking sources of taint and off-odor in meat [137].
- Studies of human body odor and bad breath [60,138].
- Automated analysis of ppt-level odors in drinking water (geosmin, methylisoborneol, and trichloroanisoles) using sorptive extraction and HS-trap [139]—see Fig. 10.33.
- Characterizing soil quality [140]—see Fig. 10.34.

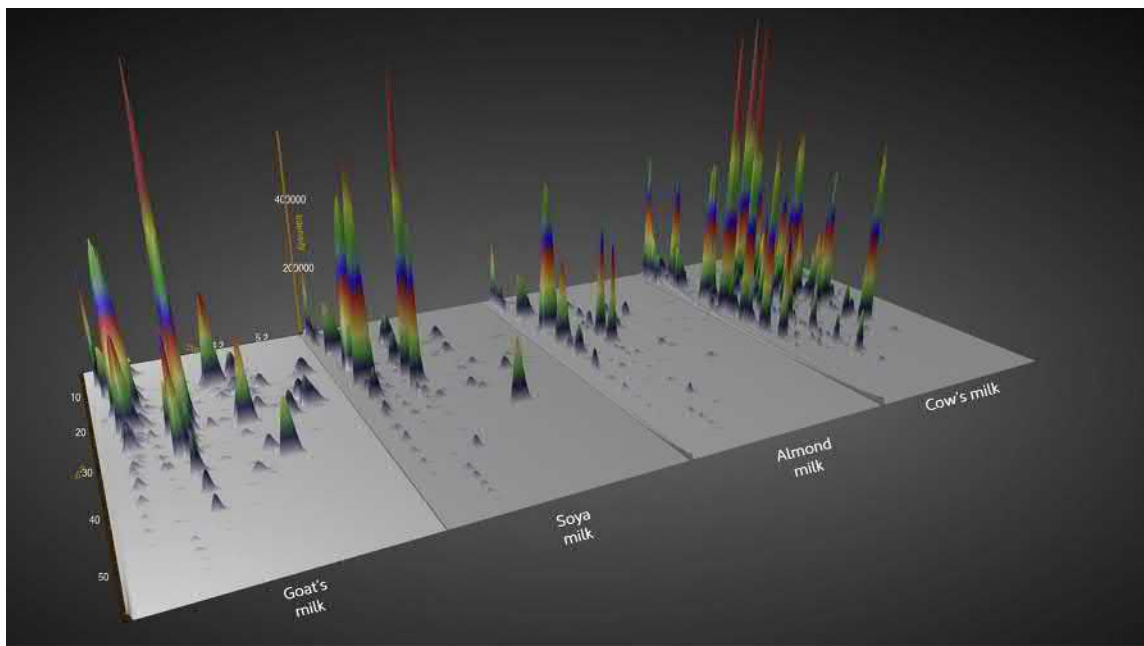


FIGURE 10.32 GC \times GC–TOF MS surface plots of goat's milk, soya milk, almond milk, and cow's milk. Sample preparation: 10 mL of each sample was placed in a 20 mL headspace vial with 2 g of NaCl. Immersive sorptive extraction: PDMS sampler: Inert HiSorb probe (Markes International); Time: 60 min; Temperature: 35°C. TD: Instrument: TD100-xr (Markes International); Focusing trap: “General-purpose.” HiSorb probes were inserted into empty inert-coated stainless-steel TD tubes. GC \times GC: Flow modulator: INSIGHT (SepSolve Analytical). PM: 5.0 s. TOF MS: Instrument: BenchTOF-Select; Tandem Ionization: Simultaneous acquisition of 70 and 12 eV data; Mass range: m/z 35–500.

Linearity over five concentration levels from 1–20 ppt					
Compound	IPMP	IBMP	2-MIB	2,4,6-TCA	Geosmin
r^2	0.996	0.995	0.992	0.994	0.992

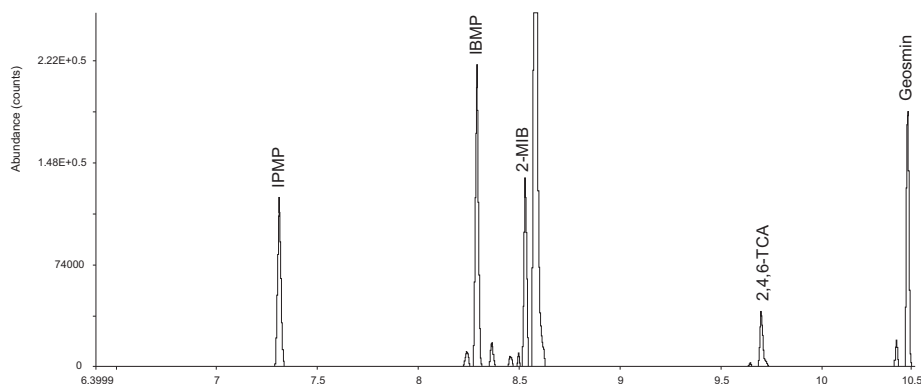


FIGURE 10.33 5 ppt level odorants in water analyzed by immersive sorbent extraction and GC-MS (SIM). Abbreviations: 2,4,6-TCA, 2,4,6-trichloroanisole; 2-MIB, 2-methylisoborneol; IBMP, 2-isobutyl-3-methoxypyrazine; IPMP, 2-isopropyl-3-methoxypyrazine. Experimental conditions: Centri extraction and enrichment platform (Markes International Ltd., UK) combined with Trace1310-ISQLT GC-MS system (Thermo Scientific). Sorbent extraction with HiSorb standard-length inert-coated probes (Markes International Ltd., UK) immersed in a 19 mL sample. Extraction for 60 min at 65°C Multisorbent (“material emissions”) trap at 20°C. 3 min trap purge. Trap desorption: 50°C s^{-1} to 260°C. Flow path: 180°C. Column: 30 m \times 0.25 mm I.D. \times 0.25 μ M film MEGA-5 HT (MEGA S.r.l.). GC oven: 60°C (2 min), 10°C min^{-1} to 100°C then 20°C min^{-1} to 190°C (4.5 min) SIM ions: 95, 112, 124, 137, 195. Inset: Results of a linearity experiment using 5 calibration levels from 1 to 20 ppt, experimental conditions as described for 5 ppt.

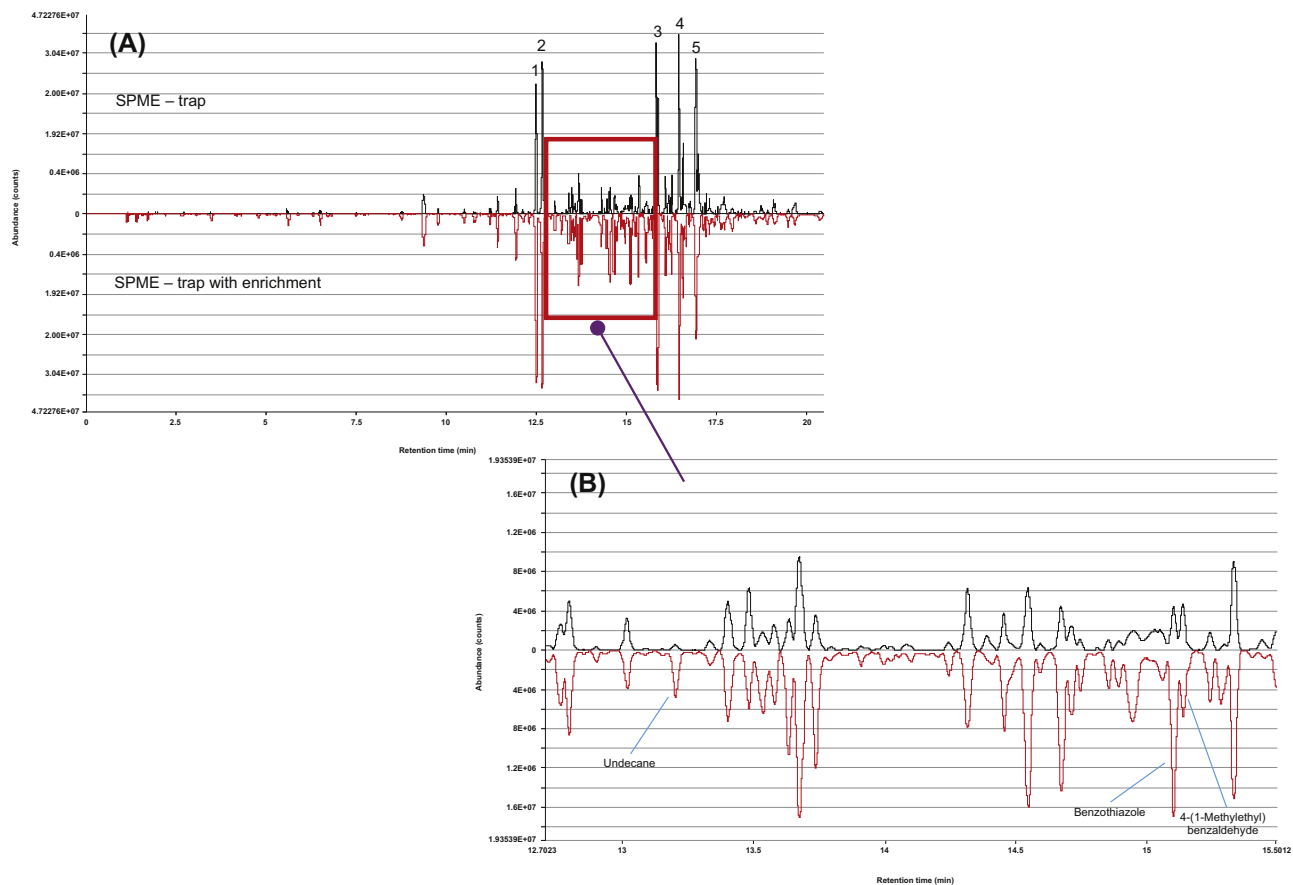


FIGURE 10.34 (A) Total VOC profile for a soil sample using SPME–trap and SPME–trap with enrichment (3×). The most prominent compounds identified in the sample were (1) benzaldehyde, (2) n-octanal, (3) cyclosativene, (4) calarene, and (5) 4,9-muroladiene. (B) The chromatogram between 12.7 and 15.5 min is highlighted, detailing the increase in sensitivity from SPME–trap to SPME–trap with enrichment and indicating excellent peak shapes for the VOCs. Undecane, benzothiazole, and 4-(1-methylethyl)benzaldehyde show a significant increase in response when extracted multiple times. 2 g of soil was agitated at 90°C for 15 min (3× for SPME–trap with enrichment), desorbed to trap at 260°C for 3 min, and desorbed from trap at 280°C for 5 min. For all analyses, a multiphase, 20 mm long, 50/30 μm d_r DVB/CAR/PDMS SPME-fiber was used. GC-MS: Column: MEGA-624, 30 m × 0.25 mm × 1.4 μm. Constant flow: Helium, 2.0 mL min⁻¹. Oven program: 35°C (3 min), then 10°C min⁻¹ to 100°C, then 20°C min⁻¹ to 220°C (5 min). Transfer line: 230°C Ion source: 230°C Quad: 150°C Mass range: m z⁻¹ 35–350.

10.13 Forensic applications

One of the major advantages of TD in forensic science is that it eliminates a lot of manual sample preparation, meaning less risk of data being compromised and of evidence being challenged in court. Relevant application examples are as follows:

10.13.1 Accelerants in fire debris

TD is often used to determine the presence or absence of “accelerants” (i.e., fuels such as gasoline or kerosene) in burnt residue from the scene of suspected cases of arson [141]. Typically, the fire debris is collected in inert containers such as metal cans or nylon bags. Pumps or large gas syringes are then used to draw the HS vapors through well-conditioned sorbent tubes. The volume of vapor sampled varies considerably because the only objective in this case is to confirm or exclude the presence of accelerants. Small volumes (20–50 mL) are sufficient if the sample smells of fuel.

TD offers several advantages over conventional static HS methods for this application. Firstly, it is not limited to specific container sizes, e.g., HS vials. Thus, it allows larger, more

representative samples of the fire debris to be analyzed, giving enhanced sensitivity and better reliability. Moreover, the presence of large quantities of liquid water in many fire residue samples can present a challenge to the detection of trace levels of higher-boiling accelerants using conventional HS. In comparison, the dynamic sampling process of TD allows both selective elimination of water and enhanced detection of less volatile compounds.

10.13.2 Drugs of abuse

Many drug-related applications benefit from the versatility of thermal desorption. Examples include direct desorption of house dust from the scene of a crime (Fig. 10.35), direct desorption of bank notes [142], and detection of amphetamine “factories” by monitoring the air nearby for indicative solvents. The example shown in Fig. 10.35 is interesting, not only because the levels of drugs were so high in this case (the dust was found to be nearly 3% heroin/cocaine) but also because phenobarbital—an antiepileptic treatment for dogs—was identified at the same time. Presumably, the police were able to use this finding to narrow their investigations to dealers who'd recently visited the local vet?!

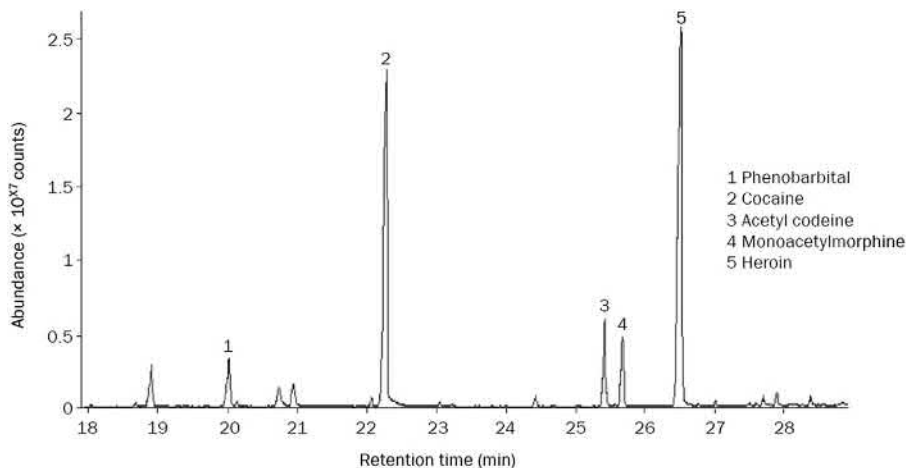


FIGURE 10.35 Direct desorption of proscribed drugs in house dust. Experimental conditions: ~5 mg dust weighed into empty glass tubes supported by quartz wool plugs. Desorption: 150°C for 10 min in a flow of 50 mL min⁻¹ carrier gas. Trap: packed with quartz/Tenax held at +20°C. Trap desorption: 40°C s⁻¹ to 250°C with 30 mL min⁻¹ split flow and 2 mL min⁻¹ column flow. Flow path: 150°C.

Further, sorptive extraction with TD provides a convenient analytical approach for detecting GC-compatible proscribed substances in biological fluids [143].

10.13.3 Explosives and shotgun propellant residues

Explosive vapors present a significant challenge, even to conventional GC analysis. These highly reactive compounds are very sensitive to any slight deterioration in system

performance, for example, injector activity, column age, and detector contamination. It is therefore a testament to the quality of modern TD technology that two-stage TD of trace-level DNT and TNT is now considered routine and that even more challenging compounds such as RDX and PETN can be analyzed quantitatively—see Fig. 10.36. Detection and characterization (“fingerprinting”) of residual propellant on spent shotgun cartridges using TD-GC-MS have also been reported and could be applied to link individual cartridges or weapons to specific crimes.

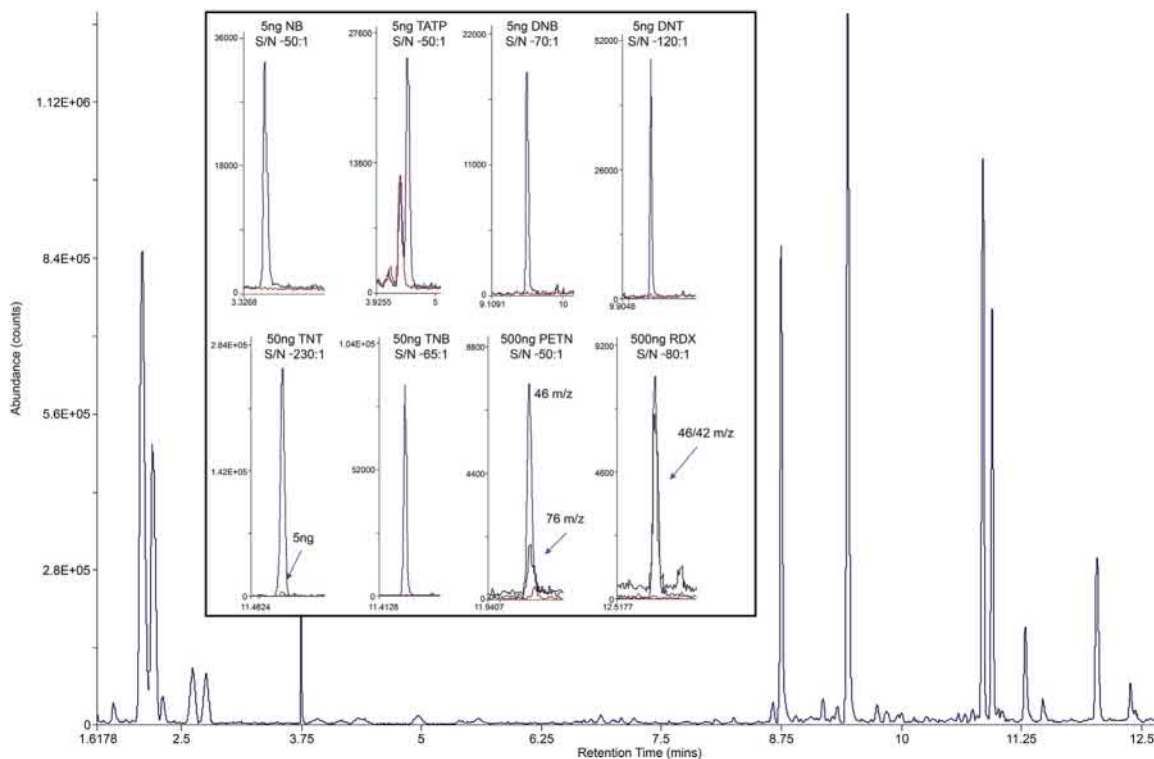


FIGURE 10.36 Using TD and immersive sorptive extraction with GC-MS to analyze explosives. Abbreviations: *DNT*, dinitrotoluene; *NB*, nitrobenzene; *PETN*, pentaerythritol tetranitrate; *TATP*, triacetone triperoxide; *TNB*, trinitrobenzene; *TNT*, trinitrotoluene. RDX a.k.a. cyclonite. **Main image:** Explosives at 50 ng each introduced to a Silcosteel tube packed with quartz wool and Tenax TA. TD performed with Centri extraction and enrichment platform (Markes International Ltd., UK) combined with 7890B-5977A GC-MS system (Agilent Technologies). Tube desorption: 3 min at 180°C followed by 2 min at 210°C into a multisorbent phase quartz/Tenax trap at -10°C. Trap desorption: 25°C s⁻¹ to 190°C 18 mL min⁻¹ split flow and 3 mL min⁻¹ column flow (7:1 split). Flow path: 150°C. Column: 15 m × 0.25 mm I.D. × 0.25 μm film MEGA-5MS (MEGA S.r.l). Scan range: 35–300 m z⁻¹. Total ion chromatogram shown. **Inset:** Explosives at masses as indicated introduced to 20 μL water. Sorbent extraction with HiSorb standard-length inert-coated probes (Markes International Ltd., UK) suspended above sample for 20 min at 65°C. Trap and GC-MS settings as already described. Black/white trace: Explosives sample EIC (major ion). Black trace: Distilled water EIC (major ion). Black trace: Explosive sample EIC (ion as indicated).

10.13.4 Forensication (characterization) of inks, paper, and other materials

Many other materials can also be reliably characterized from their VOC profiles. Key examples include paper, ink, and natural materials

such as plants and their fossilized derivatives [131,144].

Fig. 10.37 shows direct desorption of organic volatiles/semivolatiles from paper with and without writing. Investigations like this may be used to link the document to a particular paper

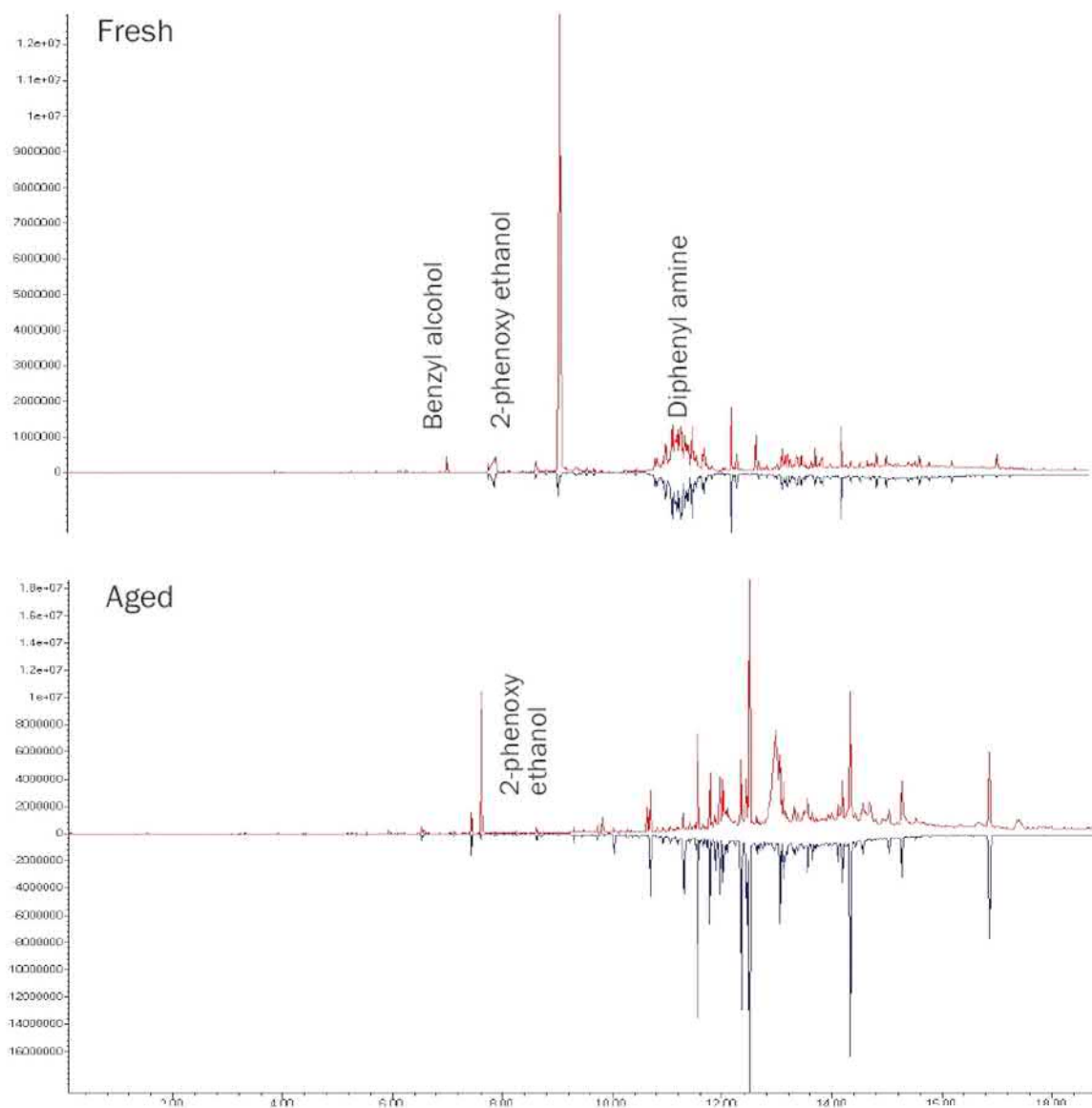


FIGURE 10.37 Direct desorption of documents for forensic characterization of paper and inks. Experimental conditions: Direct desorption of $\sim 2 \times 20$ mm sections of paper (with and without ink) at 100°C for 5 min in a flow of 30 mL min^{-1} carrier gas. Trap: packed with Tenax/Carbograph 1 held at $+25^\circ\text{C}$. Trap desorption: 300°C with 20 mL min^{-1} split flow. Flow path: 200°C . Column: $30\text{ m} \times 0.32\text{ mm I.D.} \times 1.0\text{ }\mu\text{m}$ film DB 1 (Agilent Technologies). GC oven: 60°C (5 min hold) to 280°C at $10^\circ\text{C}/\text{min}$. Scan: 45–350 amu.

source and specific ink/pen. The extent of selective losses of the most volatile constituents in the ink can also be useful in estimating the age of a document.

10.14 Monitoring manufacturing and other industrial chemical processes

The concentrating power of thermal desorption makes it invaluable for detecting leaks in dangerous industrial chemical processes. Key examples include chemical agent destruction facilities and monitoring chemical syntheses that generate lethal by-products such as bis(chloromethyl) ether [145]. In each case, continuous or very regular monitoring is necessary to ensure the safety of plant personnel.

TD-GC-MS systems are also increasingly used for routine product quality control and development of low-emission materials—see aforementioned.

Other examples of TD implementation for industrial/process applications include:

- Monitoring trace impurities in CO₂ supplying the food and beverage industries.
- Monitoring tracer gases for leak detection in critical fuel pipes or lines.
- Control of monoethylene glycol (MEG) and other additives to domestic fuel gas supplies [146].

When used to monitor trace organic impurities in process gas streams such as CO₂, TD may sometimes be coupled directly to real-time detectors such as process mass spectrometers. The GC can be eliminated in these cases, provided the process gas stream is well characterized and as long as the range of failure modes and potential contaminants are well known. Elimination of the GC, where applicable,

minimizes cycle times and allows rapid detection/notification of any contaminants exceeding control levels.

Appendix A

10.A Thermal desorption method development, optimization, and calibration

Detailed information on TD method development and optimization should be provided by system manufacturers, but the following general points are included here as a guide.

10.A.1 Sampling considerations for successful analysis

Sample collection is a critical part of any analytical procedure. Considerations for optimizing sorbent selection for initial sampling (if applicable) and for analyte focusing have been well documented [8,42]. While the selected sorbents must be strong enough to prevent breakthrough and loss of any target compounds, they must also be weak enough to allow quantitative recovery of all the analytes of interest at safe temperatures during the desorption phase, i.e., at temperatures that don't exceed the stability limits for the sorbent or compounds of interest. It is also an advantage if retention of interfering compounds, such as permanent gases and water, can be minimized during the sampling and/or focusing process, e.g., by selecting hydrophobic sorbents when sampling humid air or gas. Similarly, use of canisters, bags, or unheated online air/gas manifolds must be restricted to vapors that can be recovered from ambient-temperature containers or streams, without condensing on internal surfaces. This typically means compounds more volatile than n-C_{9/10}.

Sampling conditions for direct TD of materials, HS-TD, and sorptive extraction are application-specific. They are described in the literature [15,147] and in relevant application notes from system manufacturers.

10.A.2 Optimizing the analytical procedure

General considerations: As described in the main text, thermal desorption is essentially an extension of gas chromatography with key variables (parameters) including temperature, gas flow, desorption time, and choice of sorbent (stationary phase). While TD parameters vary widely from application to application, it is possible to apply general guidelines that aid method development.

It is best to consider the two stages of TD separately and understand what needs to be achieved during each part of the process. It is also important to understand the expected concentration and volatility range of the compounds of interest, the temperature limits of the sample matrix or sorbent (if relevant), and what, if any, split is required to prevent overloading the GC system without compromising required method detection limits.

In the case of sorbent tubes, the process of primary (tube) desorption is usually (but not always) intended to strip everything that has been trapped/collected on the tube so that it is left clean and ready for immediate reuse. The other objective during tube desorption is to selectively retain all the compounds of interest on the focusing trap while (if possible) allowing unwanted interferences (CO₂, water, or ethanol, for example) to be purged to vent.

Once primary desorption is complete, the objective of secondary (trap) desorption is invariably to completely desorb everything retained by the trap during stage 1 and transfer it to the GC analytical column in as small a band (injection volume) of carrier gas as possible. This is the GC injection.

Temperature: Selection of the right desorption and flow path temperatures is usually straightforward, taking into account both the volatility and thermal stability of the compounds of interest and the temperature limits of the tube and/or trap sorbents concerned. Note that the energy required to break the sorbent–sorbate bond and release retained analytes into the gas stream is much higher than that required to keep analytes in the vapor phase as they pass through the empty, narrow-bore tubing that comprises the rest of the TD system flow path. In fact, provided the rest of the TD flow path is uniformly heated (inert and narrow-bore), desorbed compounds will remain comfortably in the vapor phase at temperatures much below those required for tube or trap desorption. This is intuitive to most gas chromatographers. Just as analytes would be expected to elute from a 30-m coated capillary column at temperatures well below their boiling point, so compounds will elute very readily from the short, uncoated, narrow-bore flow path of a thermal desorber at surprisingly moderate temperatures. For example, re-collection and repeat analysis (Fig. 10.14) were used to validate recovery of the hydrocarbon standard shown in Fig. 10.13 through an automated TD system. The experiment was carried out with the TD flow path and transfer line set at 210°C. Results demonstrate negligible losses of n-C₄₄ (b.p. ~550°C) and are shown in Fig. 10.38 [148,149]. This is important to understand because it allows moderate flow path and transfer line temperatures to be applied for most applications, thus optimizing recovery of thermally labile species [25] without compromising recovery of high boilers.

Flow and split ratio selection: The power of gas flow to enhance TD is also often underestimated. Increasing flow can be a very useful alternative to increasing temperatures—for example, when analyzing reactive compounds such as explosives and/or to minimize artifacts when using

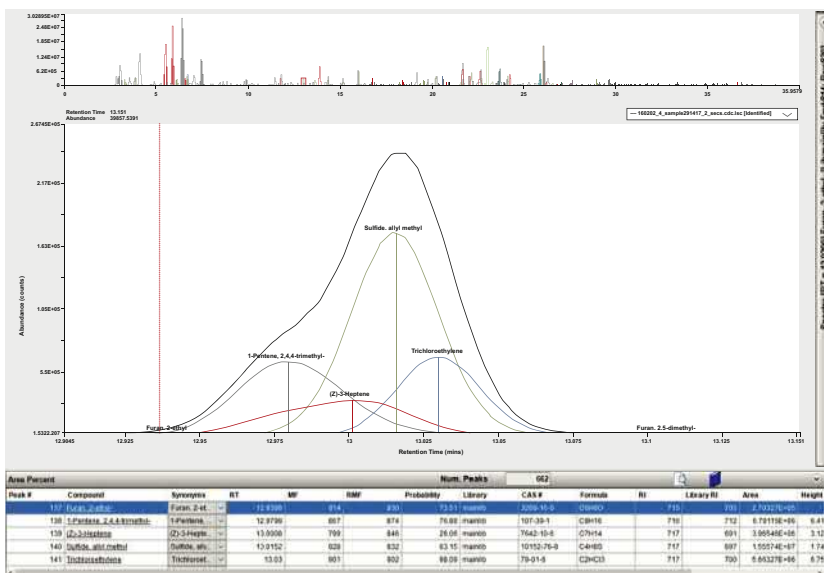


FIGURE 10.38 Deconvolution applied to a TD-GC-TOF MS chromatogram for two successive 129 mL samples of end-tidal breath transferred onto the same sorbent tube. Sampling: A disposable Bio-VOC sampler (Markes International) was used to collect two successive 129 mL samples of end-tidal breath onto the same sorbent tube (Markes International), for each of three participants. TD: Instrument: TD100-xr (Markes International); Tube desorb: 270°C (8 min); Trap flow: 30 mL min⁻¹ (no split); Focusing trap: “Material emissions” (Markes International part no. U-T12ME-2S); Outlet split: 5 mL min⁻¹. TOF MS: Instrument: BenchTOF-Select (SepSolve Analytical Ltd); Mass range: m z⁻¹ 40–400. Software: Instrument control and data processing by TOF-DS.

less stable porous polymer sorbents. As a general rule, doubling the desorption flow halves the desorption time.

Typical TD flow rates are in the following ranges:

- During primary (tube) desorption: 20–200 mL min⁻¹ through the tube and 2–50 mL min⁻¹ through the focusing trap.
- Through the focusing trap during secondary (trap) desorption: 2–100 mL min⁻¹.
- Whole air sampling rates, directed straight to the focusing trap, are typically in the range 5–100 mL min⁻¹.

As described in the main text, implementation of sample splitting can also often be used to enhance the TD process by allowing tube and/

or trap desorption flows to be set higher than (and independently of) the trap flow during focusing or the GC column flow.

Minimizing interferences: As discussed, common volatile interferences (e.g., permanent gases, water, and calibration solvents) can often be selectively eliminated or reduced during the sampling and/or focusing stages by appropriate choice of sorbents and trapping temperatures. Likewise, dry purging or prepurging of samples/standards (in the sampling direction) prior to primary or secondary desorption (with gas flowing in the sampling direction) can reduce residual water and solvents effectively. Selective purging of water is more difficult when analyzing very volatile compounds such as Freons or “ozone precursors” from online air or

canisters. In these cases, selective purging can be replaced or supplemented by dryers placed in the sample flow path before the focusing trap [33,150].

10.A.3 Special considerations for the analysis of nontube-form sorptive samplers

Empty TD sample tubes can also be used to house two alternative forms of sorptive sampler during analysis:

1. Absorptive probes or cartridges used for HS or immersive extraction of VOCs and SVOCs from liquid samples or extracts.
2. Adsorptive cartridges used for radial-form diffusive (passive) sampling [84,86].

All sorptive devices need to be positioned carefully within the central, heated zone of the empty TD tube for analysis and any devices used for immersive sampling of liquids must be carefully washed and dried before desorption. As always, care must be taken not to exceed the maximum temperature of any sorbent materials present and to ensure that the carrier tube isn't completely blocked by the sampling device—carrier gas must still be able to flow unimpeded. Fast desorption flows ($>50 \text{ mL min}^{-1}$) can be used if necessary to compensate for moderate desorption temperatures. Note that radial passive sampling cartridges may require more stringent desorption conditions than their axial tube counterparts, because of the strong carbon sorbents that are generally used and because analytes are sampled across the entire length of the cartridge, meaning complete desorption can take longer than expected.

10.A.4 Method development considerations for the direct desorption of materials

As described in the text, TD is also widely used for the direct gas extraction of volatile and semivolatile organics from material samples

weighed directly into empty thermal desorption tubes or tube liners. In this case, TD becomes a form of dynamic HS with extracted vapors transferred to the focusing trap in a stream of carrier gas before GC injection. There are, broadly, two ways in which direct desorption methods are applied to material samples:

1. Complete ($>95\%$) extraction of (semi-)volatile residues in a single run.
2. Extraction of a representative profile or fingerprint of vapors that can be used to characterize and categorize samples.

The former is suited to quantitative applications such as measuring the levels of residual solvents or monomers in drugs, plastics, or other materials. The latter harnesses low-temperature desorption conditions to obtain a consistent and representative profile of volatiles that can be used to compare and characterize scented or odorous samples versus controls.

Materials or products suitable for direct TD are generally homogeneous—such that the mass weighed into a standard TD tube or liner is representative. Other considerations include:

- Matrix stability under required desorption conditions.
- High surface-to-mass ratio—speeding up desorption.
- Ensuring the flow path through the tube is not blocked by sample material such that carrier gas can still flow through unimpeded.
- Ensuring the sample material is positioned securely in the central, heated portion of the sample tube, not in the relatively cooler zones at either end of the tube.
- Understanding the nature of the sample matrix—maximum temperature, water content, etc.

A major advantage of this form of direct TD or dynamic HS is that it can be applied to much

smaller quantities of sample than conventional headspace—milligrams rather than grams of material. This makes it ideal for applications with limited amounts of sample such as forensic residues or prototype pharmaceuticals. The process of direct TD is a wonderfully simple form of GC automation for many otherwise challenging sample matrices including ointments, paints with high solid content (e.g., for sheet metal), drug powders, dried spices, etc. It eliminates complex sample preparation, protects the GC from contamination by the sample matrix, and excludes water and other interfering volatiles, all in a single automated step. Example applications are presented in the main text.

10.A.5 Calibration of thermal desorption methods

Once optimized, TD procedures are typically calibrated using external standards with the optional addition of a gas-phase internal standard such as deuterated toluene or bromofluorobenzene to the sampling end of the tube.

Theoretically, gas-phase standards should be used for calibrating all vapor-monitoring applications, but they can be expensive and/or difficult to obtain at appropriate concentrations. Certified cylinders of ppb-level hydrocarbons for calibrating ozone precursor systems, for example, retail at upward of US\$ 3000.

Reliable gas standards are also notoriously difficult to generate. Static standard atmospheres are prone to analyte losses through surface sorption, condensation, and dissolution into any liquid water present inside the container—even the thinnest surface film. Dynamic methods of standard-atmosphere generation are much more reliable and are described in several papers [151–153]. However, few laboratories around the world have sufficiently sophisticated apparatus, including independent monitoring equipment, to produce low-concentration (ppb-level) standard atmospheres that are reliably traceable to primary standards.

For these reasons, the most important international standard methods for TD allow calibration using liquid solutions (e.g. Refs. [28,29,63,75]) as well as gas standards. Standard solutions are prepared such that when a small (typically 0.2–1 μL) volume is introduced to the sampling end of a sorbent tube, the masses of analytes retained will be in the same order as those collected (or loaded) during sampling. The preferred injection method involves introducing the liquid standards through what is essentially a simple unheated GC injector connected to the sampling end of a conditioned sorbent tube as if it was the injector end of a $1/4$ -inch packed column. Carrier gas flows are typically set to something in the order of 100 mL min^{-1} , and the syringe is usually inserted through the septum and into the injector such that the tip of the syringe just touches the sorbent-retaining material—gauze, frit, quartz/glass wool, etc. After the aliquot of standard has been introduced in this way, tubes are typically left in situ with the carrier gas flowing for 5 or 10 min to allow selective purging of solvent (typically methanol) if applicable. Calibration of very volatile components is similar but involves gas standards and gas syringes. If multiple standards are required to cover a wide range, liquid solutions of higher-boiling stable components are introduced first with gas standards of the lighter compounds being loaded last.

Note that with two-stage TD, it is not always essential to load standards onto tubes packed with exactly the same sorbents that will be used for vapor sampling. This is because the critical “analytical” injection is desorption of the secondary (focusing) trap. It is more important to make sure the calibration is simple and robust and that selective purging is used wherever possible to minimize the mass of carrier solvent allowed to reach the focusing trap.

For obvious practical reasons, if the nature of the analytes means it is not possible to use a solvent that can be selectively purged prior to

analysis, it is usually best to minimize injection volumes ($<0.5 \mu\text{L}$) and choose a solvent that gives a sharp, well-resolved peak under the GC conditions selected.

10.A.6 Validation of analyte recovery during thermal desorption

Traditional methods for validating analyte recovery through a TD system were complex and tedious. Users were generally advised to carry out a multilevel calibration using the TD-GC(MS) and then set up an equivalent liquid injection method (same column flow, replicating the split ratio, etc.) and repeat the process. Aside from the time required, it is difficult to exactly match column and split flows for two such different GC injection systems. The latest international standard methods for TD have therefore begun to recommend the use of quantitative sample re-collection and subsequent repeat analysis as an alternative means of validating analyte recovery—see [Figs. 10.13 and 10.14](#).

Appendix B

10.B New GC-related technology developments that complement TD applications

The concentrating power and application range of thermal desorption are complemented by recent advances in other GC-related technologies. Some of the most useful examples are summarized here.

10.B.1 Innovations in MS detection

Advanced mass spectrometric detectors for GC complement TD operation and methods. Triple quadrupole mass spectrometers, for example, would be well suited to TD applications targeting specific, ultratrace-level compounds. However, as TD is so often used for uncharacterized samples and/or for screening

large numbers of compounds (see general references), the development of GC-compatible TOF mass spectrometers, which offer a combination of both high sensitivity and full spectral information, is particularly exciting.

Sensitivity: As TOF technology does not involve scanning, it theoretically offers 2 or 3 orders of magnitude more sensitivity than conventional quadrupole MS detectors operating in SCAN mode (depending on mass range). Actual GC-TOF sensitivity varies significantly from instrument to instrument, but some modern systems do live up to their billing and are able to provide full spectral information at levels approaching single-ion (SIM) detection limits on a regular quad-MS system—see [Fig. 10.25](#). This aids identification and quantitation of toxic or odorous analytes at the lowest possible levels and, from a TD perspective, is an obvious advantage for screening/characterizing unknown samples and for research applications such as the discovery of biomarkers of disease [57], evaluating food quality [127], and identification of trace odorants [137].

Using high-sensitivity triple quad or TOF detectors can also benefit routine applications by allowing collection of smaller samples without compromising method detection limits. For example, in atmospheric monitoring, 100 mL of air may provide as much data as 10 L of air analyzed using a conventional quad-MS-based system. Quick/easy low-volume “grab” sampling options [154] and short-term diffusive monitoring can both significantly simplify large-scale air monitoring projects if high-sensitivity TD-GC-MS systems are used [155].

Speed: Another particular advantage of TOF MS is that its inherent speed facilitates implementation of more robust and TD-relevant configurations of comprehensive two-dimensional GC (GC \times GC). While the immense resolving power of GC \times GC has already been usefully applied to particularly complex thermal desorption applications such as breath profiling, aroma

characterization, atmospheric research, and vehicle exhaust emissions [58,96,123,156], most system configurations have, until recently, been based on thermally modulated GC \times GC technology. This uses intermittent cooling and heating to achieve the modulation necessary for two-dimensional separation [157]. On the other hand, flow modulators use precise control of carrier and auxiliary gas flows to fill and flush a sampling channel or loop [158]. Depending on the target compound range, flow-modulated GC \times GC is often better suited to TD because it is compatible with very volatile compounds. For example, the technology has already been combined for monitoring subtle changes in VOCs from blood to aid forensic investigations and human rescue [159]. Here, an additional layer of information is added to the analysis by acquiring data from both hard and soft ionization simultaneously using a technique called tandem ionization. Developed specifically for GC-MS, tandem ionization allows conventional 70 eV spectra to be obtained in parallel with high-sensitivity soft ionization spectra, e.g., at 12 eV. The lower-energy ionization generates a different, but equally repeatable, spectrum for each compound, which is typically richer in the larger mass fragments than that obtained at 70 eV and subject to lower noise (Fig. 10.38). The beauty of this approach is that it improves both quantitative and qualitative data, leveraging the second independent spectrum to both enhance peak deconvolution and confirm the identity of each peak found—great for characterization of unknown samples and for distinguishing between isomers.

TOF is the preferred MS technology for fast GC and GC \times GC operation because it generates in the order of 10,000 full spectra per second (typically from 10 to 1500 amu and above) without scanning and without spectral “skew.” This in turn improves spectral matching and allows more efficient application of “data mining” algorithms such as spectral deconvolution, which are increasingly important for complex

applications. For example, in the detection of airborne chemical warfare agents, speed and sensitivity are vitally important in order to confidently identify such hazardous compounds as quickly as possible [160].

10.B.2 Advanced data mining and data processing software for GC-MS

Many TD applications generate extremely complex organic profiles—see Fig. 10.26—with odorous or toxic compounds of interest frequently comprising the smallest peaks in a “busy” chromatogram. Advanced MS technologies, such as TOF, can help as described; however, without the benefit of advanced/automated processing functionality, such as spectral deconvolution and automated chromatographic comparison, data analysis remains a skilled and time-consuming task.

Powerful and automated “data mining” software packages are now available commercially and can be applied to enhance TD-GC-MS data analysis post-run. Key examples include spectral deconvolution algorithms that “separate” (deconvolve) coeluting compounds by evaluating the rate of change of individual mass ions. This allows the software to identify the numbers of components present in a single chromatographic peak and accurately assign the various individual mass ions to respective constituents. One of the original and most widely used spectral deconvolution packages for GC-MS was originally developed by NIST in the United States and is now available free of charge under the tradename AMDIS (Automated Mass Spectral Deconvolution and Identification System). Other more automated options have since become available that combine AMDIS-type or proprietary spectral deconvolution algorithms with additional screening parameters such as peak alignment (accommodating RT drift over months years⁻¹) and automated comparison of multiple complex chromatographic data sets Fig. 10.39.

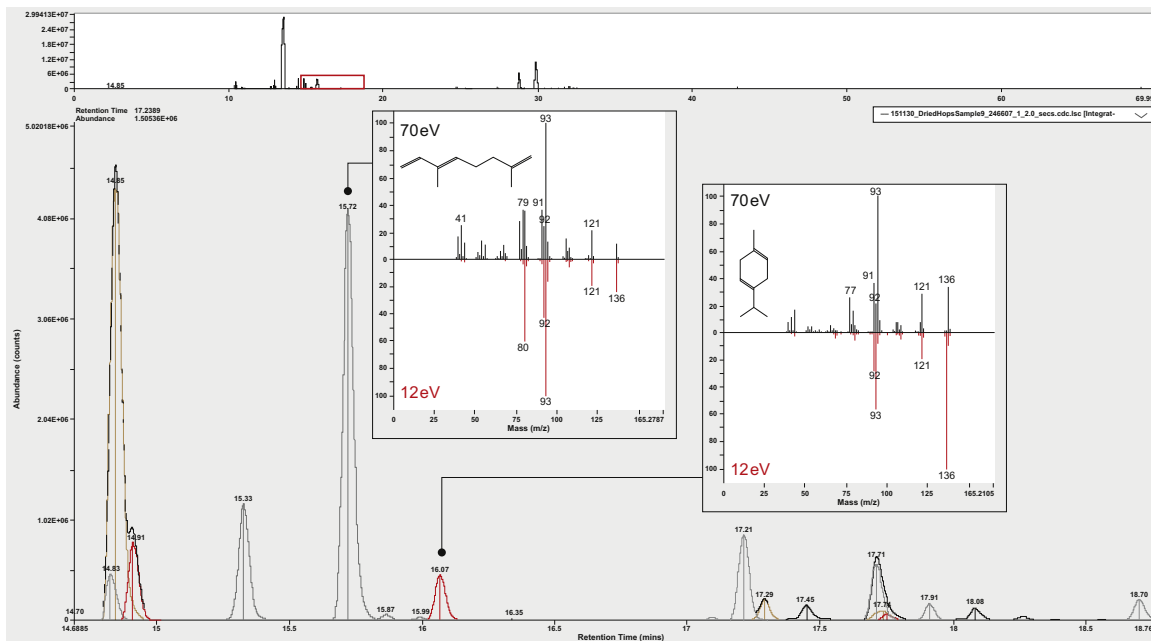


FIGURE 10.39 Dynamic headspace sampling of VOCs from 1 g hops onto a Tenax TA sorbent tube. TD-GC-TOF MS chromatogram (TIC, top) with Tandem Ionization showing distinctive soft ionization (12 eV) spectra for two monoterpenes. Dynamic headspace sampling was performed for three varieties of hops (“Fuggle,” “Goldings,” and “Target”) using the μ -CTE (Markes International). Hops (~1 g) were placed in individually sealed and temperature-controlled pots within the μ -CTE. Volatiles were then extracted by a dynamic headspace process for a period of 30 min at 30°C and collected onto an inert-coated stainless steel sorbent tube packed with Tenax TA. Tubes were then analyzed by TD-GC-TOF MS. TD: Instrument: UNITY-ULTRA-xr (Markes International); Tube desorb: 10 min at 280°C and 50 mL min⁻¹ trap flow; Focusing trap: Tenax TA; Split flow: 150 mL min⁻¹, collected onto a clean Tenax TA sorbent tube. TOF MS: Instrument: BenchTOF-Select; Mass range: m/z⁻¹ 35–500.

This type of advanced data mining has successfully been applied in TD-GC-MS applications, such as the identification of food quality markers [161], decomposition rates [162], and profiling of e-cigarette aerosol [163].

References

- [1] E.A. Woolfenden, Ch. 5: practical aspects of monitoring volatile organics in air, in: *Quality Assurance in Environmental Monitoring: Instrumental Methods*. Edit: G. Subramanian, Published by VCH, 1995.
- [2] ISO 16200-1 Workplace Air Quality – Sampling and Analysis of Volatile Organic Compounds by Solvent Desorption/Gas Chromatography. Part 1: Pumped Sampling Method.
- [3] B. Callan, K. Walsh, P. Dowding, Industrial hygiene VOC measurement interference, *Chem. Ind.* 5 (April) (1993) 250–252.
- [4] M. Wood, The use of the Perkin-Elmer passive sampler and ATD 50 automatic thermal desorber in the measurement of atmospheric concentrations of organic nitriles, *Ann. Occup. Hyg.* 29 (1985) 339–413.
- [5] D. Coker, Personal monitoring techniques for gases and vapours, *Int. Environ. Safe. J.* (1979) 43–44.
- [6] Annual Report of the UK Health and Safety Executive, 1978, ISBN 0-11-883285-9.
- [7] P.A. Hollingdale-Smith, A. Bailey, Passive sampling and dosimetry. In *Trace-organic Sample Handling*. Volume 10 of *Methodological Surveys (A): Analysis*. Published by Ellis Horwood Ltd, UK, Distributed by Halstead Press a division of John Wiley & Sons.
- [8] E.A. Woolfenden, A review of sorbent-based sampling methods for volatile and semi-volatile organic

- compounds in air. Part 1 – sorbent-based air monitoring options, *J. Chromatogr.* 1217 (2010) 2674–2684.
- [9] J. Manura, Selection of GC guard columns for use with GC cryo-trap, *Sci. Inst. Ser. Inc., Appli. Note* 24a (1999).
- [10] B. Kolb, *J. Chromatogr.* 842 (1–2) (1999) 163.
- [11] M.W. Holdren, D.L. Smith, Performance of automated gas chromatographs used in the 1990 Atlanta ozone study, *Proc. 1991 US EPA/AWMA Int. Symp., Measure. Toxic Relat. Air Pollut.; Air Waste Manage. Assoc.* (1991) (Pittsburgh, USA).
- [12] D.T. Coker, N. van den Hoed, K.J. Saunders, P.E. Tindle, A monitoring method for gasoline vapour giving detailed composition, *Ann. Occup. Hyg.* 33 (1) (1989) 15–26.
- [13] J. Kristensson, M. Widen, Development and evaluation of a diffusive sampler for measurements of anaesthetic gases, in: A. Berlin, R.H. Brown, K.J. Saunders (Eds.), *Diffusive Sampling – an Alternative Approach to Workplace Air Monitoring*, RSC Publication, 1987, pp. 423–426.
- [14] J. Kristensson, *Diffusive Sampling and GC Analysis of Volatile Compounds*, PhD Thesis, Dept. of Analytical Chemistry, Arrhenius Laboratory, Stockholm University, 1987.
- [15] E.A. Woolfenden, A novel approach to the determination of volatile organics in pharmaceuticals, polymers and food stuffs, *Proc. Pittsburgh Conf.*, New York (1990).
- [16] A.P. Bianchi, M.S. Varney, Sampling and analysis of volatile organic compounds in estuarine air by gas chromatography and mass spectrometry, *J. Chromatogr.* 643 (1993) 11–23.
- [17] V.M. Brown, D.R. Crump, D. Gardiner, Measurement of volatile organic compounds in indoor air by a passive technique, *Environ. Technol.* 13 (1992) 367–375.
- [18] R. Janson, J. Kristensson, Sampling and Analysis of Atmospheric Monoterpenes, Report CN-79, Dept. of Meteorology, Stockholm University, 1991.
- [19] PerkinElmer Thermal Desorption Application Note No. 20: The Determination of Residual Freon 11 in Dried Vegetable Matter. Published by PerkinElmer Corp. USA.
- [20] PerkinElmer Thermal Desorption Application Note No. 26: The Thermal Desorption of Volatiles from Food Packaging Film. Published by PerkinElmer Corp. USA.
- [21] E.A. Woolfenden, G.M. Broadway, An overview of sampling strategies for organic pollutants in ambient air, *LC GC Int.* 5 (Issue 12) (1986) 28–35.
- [22] L. Purdue, Technical Assistance Document for Sampling and Analysis of Ozone Precursors, US Environmental Protection Agency, 1991. EPA/600-8-91/215.
- [23] D. Kotzias, J. Hjorth, M. Duane, J.V. Eijk, Sampling and Analysis of Selected Volatile Organic Compounds (VOC) Relevant for the Formation of Photochemical Oxidants. Proceedings of the Conference: 'Reactivite Chimique De l'Atmosphere Et Measure Des Polluants Atmospheriques' Grenoble, France, 1990.
- [24] J. Gibich, L. Ogle, P. Radenheimer, Analysis of ozone precursor compounds in Houston, Texas using automated, continuous gas chromatographs, *Proc. AWMA Confer.: 'Measur. Toxic Relat. Air Pollut.'*, US (1994) 164–191.
- [25] R. Muir, W.A. Carrick, D.B. Cooper, Application of central composite design in the optimisation of thermal desorption parameters for the trace level determination of the chemical warfare agent chloropicrin, *Analyst* 127 (2002) 1198–1202.
- [26] P. Perez-Ballesta, Losses from ATD-400. 'The Diffusive Monitor, vol. 9, 1997. Issued by HSE/CAR WG5.
- [27] J. Kristensson, Repeat Analysis. The Diffusive Monitor, vol. 1, 1988, p. 3. Published by UK HSE/CAR WG5.
- [28] ASTM D6196, Standard Practice for Choosing Sorbents, Sampling Parameters and Thermal Desorption Analytical Conditions for Monitoring Volatile Organic Chemicals in Air, 2015.
- [29] ISO 16000-6, Indoor Air – Part 6: Determination of Vapour-phase Organic Compounds in Indoor and Test Chamber Air by Active Sampling on Sorbent Tubes, Thermal Desorption and Gas Chromatography Using MS or MS-FID, 2011.
- [30] US EPA Compendium Method TO-14, The Determination of Volatile Organic Compounds in Ambient Air Using Summa Passivated Canister Sampling and Gas Chromatographic Analysis, 1988.
- [31] US EPA Compendium Method TO-15, Determination of Volatile Organic Compounds in Air Collected in Specially-Prepared Canisters and Analyzed by Gas Chromatography/Mass Spectrometry, 1999.
- [32] ASTM D5466: Standard Test Method for Determination of Volatile Organic Chemicals in Atmospheres (Canister Sampling Methodology).
- [33] U.S. Environmental Protection Agency, Method TO-15A, Determination of Volatile Organic Compounds (VOCs) in Air Collected in Specially Prepared Canisters and Analyzed by Gas Chromatography–Mass Spectrometry (GC-MS), 2020.

- [34] S. Davies, M. Bates, D. Wevill, L. Kelly, K. Thaxton, One system for trace and high level air monitoring. The future of ambient air and soil gas analysis, Proc. Pittcon (2011).
- [35] Chinese Environmental Protection Agency Report, Ambient Air VOC monitoring program in key areas, Appendix 1 (2018).
- [36] US Centers for Disease Control and Prevention, Final Report on Formaldehyde Levels in FEMA-Supplied Travel Trailers, Park Models, and Mobile Homes, July 2, 2008 (Amended December 15th, 2010).
- [37] ISO 16000-3. Indoor Air - Part 3: Determination of Formaldehyde and Other Carbonyl Compounds in Indoor Air and Test Chamber Air — Active Sampling Method.
- [38] ASTM D5197 Test Method for Determination of Formaldehyde and Other Carbonyl Compounds in Air (Active Sampler Methodology).
- [39] S. Mascrez, G. Purcaro, Exploring multiple-cumulative trapping solid-phase microextraction for olive oil aroma profiling, *J. Separ. Sci.* (2020) 1–8. www.jss-journal.com.
- [40] L. Kelly, E.A. Woolfenden, Enhanced GC-MS aroma profiling using thermal desorption technologies, *Separ. Sci.* 1 (2008) 16–23.
- [41] A. Prieto, O. Basauri, R. Rodil, A. Usobiaga, L.A. Fernandez, N. Etxebarria, O. Zuloaga, Stir-bar sorptive extraction: a view on method optimization, novel applications, limitations and potential solutions, *J. Chromatogr., A* 1217 (2010) 2642–2666.
- [42] E.A. Woolfenden, A review of sorbent-based sampling methods for volatile and semi-volatile organic compounds in air. Part 2 – sorbent selection and other aspects of optimizing air monitoring methods, *J. Chromatogr.* 1217 (2010) 2685–2694.
- [43] D. Dyne, J. Cocker, H.K. Wilson, A novel device for capturing breath samples for solvent analysis, *Sci. Total Environ.* 199 (1997) 83–89.
- [44] S.L.F. Doran, A. Romano, G.B. Hanna, Optimisation of sampling parameters for standardised exhaled breath sampling, *J. Breath Res.* 12 (2018) 016007, <https://doi.org/10.1088/1752-7163/aa8a46>.
- [45] L. Gunnarsen, P.A. Nielsen, P. Wolkoff, Design and characterization of the CLIMPAQ chamber for laboratory investigations of materials, pollution and air quality, *Indoor Air* 4 (1994) 56–62.
- [46] P. Wolkoff, An emission cell for measurement of volatile organic compounds emitted from building materials for indoor use - the field and lab, *Emission cell. Gefahrstoffe-Reinhaltung der Luft* 56 (1996) 151–157.
- [47] T. Schripp, B. Nachtwey, J. Toelke, T. Salthammer, E. Uhde, M. Wensing, M. Bahadir, A microscale device for measuring emissions from materials for indoor use, *Anal. Bioanal. Chem.* 387 (5) (2007) 1907–1919.
- [48] K.J. Saunders, *Air Monitoring Goes Underground*, the Diffusive Monitor, vol. 3, 1989. Published by HSE/CAR WG5.
- [49] J. Kristensson, Soil-probe. The Diffusive Monitor, vol. 4, 1991. Published by HSE/CAR WG5.
- [50] K. Jones, J. Cocker, L.J. Dood, I. Fraser, Factors affecting the extent of dermal absorption of solvent vapours: a human volunteer study, *Ann. Occup. Hyg.* 47 (2) (2003) 145–150.
- [51] S.M. Gordon, L.A. Wallace, P.J. Callahan, D.V. Kenny, M.C. Brinkman, Effect of water temperature on dermal exposure to chloroform, *J. of the National Ins. Of Environ. Health Sci.* 106 (6) (1998) 337–345.
- [52] UK Health and Safety Laboratory, Illustrative Laboratory Guidance Notes for Biological Monitoring via Breath, 2002. <https://www.hsl.gov.uk/online-ordering/analytical-services-and-assays/biological-monitoring/breath-sampling-for-solvents/tetrachloroethene>.
- [53] S.M. Gordon, J.P. Szidon, B.K. Krotoszynski, R.D. Gibbons, H.J. O'Neill, Volatile organic compounds in exhaled air from patients with lung cancer, *Clin. Chem.* 31 (8) (1985) 1278–1282.
- [54] J.W. Dallinga, C.M.H.H.T. Robroeks, J.J.B.N. van Berkel, E.J.C. Moonen, R.W.L. Godschalk, Q. Jöbssis, E. Dompeling, E.F.M. Wouters, F.J. van Schooten, Volatile organic compounds in exhaled breath as a diagnostic tool for asthma in children, *Clin. Exp. Allergy* 40 (2010) 68–76.
- [55] M. Phillips, R.N. Cataneo, R. Condos, G.A.R. Erickson, J. Greenberg, V.L. Bombardi, M.I. Munawar, O. Tietje, Volatile biomarkers of pulmonary tuberculosis in the breath, *Tuberculosis* 87 (2007) 44–52.
- [56] J.J.B.N. van Berkel, J.W. Dallinga, G.M. Möller, R.W.L. Godschalk, E. Moonen, E.F.M. Wouters, F.J. Van Schooten, A profile of volatile organic compounds in breath discriminates COPD patients from controls, *Respir. Med.* 104 (2010) 557–563.
- [57] A.Z. Berna, J.S. McCarthy, R.X. Wang, K.J. Saliba, F.G. Bravo, J. Cassells, B. Padovan, S.C. Trowell, Analysis of breath specimens for biomarkers of plasmidium falciparum infection, *J. Infect. Dis.* 212 (2015) 1120–1128.
- [58] M.J. Wilde, R.L. Cordell, D. Salman, B. Zhao, W. Ibrahim, L. Bryant, D. Ruszkiewicz, A. Singapuri, R.C. Free, E.A. Gaillard, C. Beardsmore, C.L. P

- Thomas, C.E. Brightling, S. Siddiqui, P.S. Monks, Breath analysis by two-dimensional gas chromatography with dual flame ionisation and mass spectrometric detection – method optimisation and integration within a large-scale clinical study, *J. Chromatogr. A* 1594 (2019) 160–172.
- [59] S.R. Markar, B. Brodie, S.-T. Chin, A. Romano, D. Spalding, G.B. Hanna, Profile of exhaled-breath volatile organic compounds to diagnose pancreatic cancer, *BJS* 105 (2018) 1493–1500.
- [60] S. van den Velde, M. Quirynen, P. van Hee, D. van Steenberghe, Halitosis associated volatiles in breath of healthy subjects, *J. Chromatogr. B* 853 (2007) 54–61.
- [61] S.M. Gordon, Identification of exposure markers in smokers' breath, *J. Chromatogr.* 511 (1990) 291–302.
- [62] S.M. Gordon, Application of continuous breath sampling to determine VOC dose and body burden: some VOC Markers of ETS Exposure, EPA Contract: 68-D4-0023 (1998).
- [63] EN ISO 16017. Air Quality - Sampling and Analysis of Volatile Organic Compounds in Ambient Air, Indoor Air and Workplace Air by Sorbent Tube/thermal Desorption/capillary Gas Chromatography. (Part 1: Pumped Sampling, Part 2: Diffusive sampling.).
- [64] NIOSH 2549 Volatile Organic Compounds - (Screening) Using Multibed Sorbent Tubes, Thermal Desorption, Gas Chromatography and Mass Spectrometry.
- [65] MDHS 72 Volatile organic compounds in air, Laboratory Method Using Pumped Solid Sorbent Tubes, Thermal Desorption and Gas Chromatography, February 1992.
- [66] MDHS 80 Volatile organic compounds in air, Laboratory Method Using Diffusive Solid Sorbent Tubes, Thermal Desorption and Gas Chromatography, August 1995.
- [67] R.H. Brown, M. Curtis, K.J. Saunders, S. Vandendriessche, Clean air at work: new trends in assessment and measurement for the 1990s, in: Organized by the Health and Safety Directorate of the European Commission, Proceedings of the Luxembourg Symposium, Sept, vol. 108, RSC Publication No, 1991, ISBN 0-85186-217-9.
- [68] A.A. Grote, E.R. Kennedy, Workplace monitoring for VOCs using thermal desorption-GC-MS, *J. Environ. Monit.* 4 (2002) 679–684.
- [69] J. Roukos, H. Plaisance, T. Leonardis, M. Bates, N. Locoge, Development and validation of an automated monitoring system for oxygenated volatile organic compounds and nitrile compounds in ambient air, *J. Chromatogr. A* (2009) 8642–8651.
- [70] H.T. Nguyen, K.-H. Kim, M.-Y. Kim, Volatile organic compounds at an urban monitoring station in Korea, *J. Hazard Mater.* 161 (2009) 163–174.
- [71] K.-H. Kim, Some insights into the gas chromatographic determination of reduced sulfur compounds (RSCs) in air, *Environ. Sci. Technol.* 39 (2005) 6755–6769.
- [72] K.-P. Song, J.-S. Han, M.-D. Lee, D.-W. Ju, M.-S. Im, T.-H. Kim, H.-I. Song, M.-J. Lee, W.-S. Kwack, J.-S. Yun, S.-Y. Moon, S.-R. Jo, A Study of quality assurance/quality control between institutions for reduced sulfur compounds in the ambient air using cryofocusing thermal desorber with GC/PFPD, *Kor. J. Odor Res. Eng.* 6 (1) (2007) 33–39.
- [73] N.T. Plant, M.D. Wright, European diffusive sampling initiative: world survey for BTX by diffusive sampling, UK Health safe. lab. Rpt: IACS 97/16 (1998).
- [74] M.R. Ras, R.M. Marcé, F. Borrull, Characterization of ozone precursor volatile organic compounds in urban atmospheres and around the petrochemical industry in the Tarragona region, *Sci. Total Environ.* 487 (2009) 4312–4319.
- [75] US EPA Compendium Method TO-17: Determination of Volatile Organic Compounds in Ambient Air Using Active Sampling onto Sorbent Tubes, 1999.
- [76] Method 325—volatile organic compounds from fugitive and area sources Part A: sampler deployment and VOC sample collection and and Part B: sampler preparation and analysis, US EPA: Fed. Regist. 79 (No. 125) (2014).
- [77] S.A. Batterman, G.-Z. Zhang, M. Baumann, Analysis and stability of aldehydes and terpenes in electropolished canisters, *Atmos. Environ.* 32 (10) (1998) 1647–1655.
- [78] E.H. Daughtrey, K.D. Oliver, J.R. Adams, K.G. Kronmiller, W.A. Lonneman, W.A. McClenny, A comparison of sampling and analysis methods for low-ppbC levels of volatile organic compounds in ambient air, *J. Environ. Monit.* 3 (2001) 166–174.
- [79] D. Wevill, The Use of a Thermal Desorption System as a Cryogen-free Method for the Monitoring of Trace Greenhouse Gases in Air. Labmate UK, September, 2009.
- [80] M.D. Wright, N.T. Plant, R.H. Brown, Storage Stability Study of TO-14 Compounds on Single and Multi-bed Carbon Thermal Desorption Tubes. UK Health and Safety Laboratory Rpt: IACS 98/02, 1999.
- [81] S. Baek, Y. Kim, R. Perry, Indoor Air quality in homes, offices and restaurants in Korean urban areas-Indoor/Outdoor relationships, *Atmos. Environ.* 31 (4) (1997) 529–544.
- [82] V.M. Brown, S.K.D. Coward, D.R. Crump, J.W. Llewellyn, H.S. Mann, G.J. Raw, Indoor air quality

- in English homes – VOCs, *Proc.: Indoor Air* (2002) 477–482.
- [83] P.A. Clausen, P. Wolkoff, Evaluation of automatic thermal desorption - capillary GC for determination of semivolatile organic compounds in indoor air, *J. High Resolut. Chromatogr.* 20 (1997) 99–108.
- [84] P. Pérez Ballesta, R.A. Field, R. Fernández-Patier, D. Galàn Madruga, R. Connolly, A. Baeza Caracena, E. De Saeger, An approach for the evaluation of exposure patterns of urban populations to air pollution, *Atmos. Environ.* 42 (2008) 5350–5364, <https://doi.org/10.1016/j.atmosenv.2008.02.047>.
- [85] E. De Saeger, P. Perez-Ballesta, BTX monitoring campaign in Brussels, *Diff. Monit.* 7 (1995) 7–8. Published by HSE/CAR WG5.
- [86] P. Pérez Ballesta, et al., Validation and modelling of a novel diffusive sampler for determination of Volatile organic compounds in air, *Anal. Chim. Acta* 908 (2016) 102–112, <https://doi.org/10.1016/j.aca.2015.12.032>. Epub 2016 Jan 5.
- [87] GB/T 27630-2011, Guideline for Air Quality Assessment of Passenger Car, 01 March 2012.
- [88] ISO 12219-1, Interior Air of Road Vehicles Part 1: Whole Vehicle Test Chamber — Specification and Method for the Determination of Volatile Organic Compounds in Cabin Interiors, 2012.
- [89] Energy Institute, Protocol for the Determination of the Speciation of Hydrocarbon Emissions from Oil Refineries New ISBN 9780852934050 Old, 2004, ISBN 085293405X.
- [90] EN TS 13649 Stationary Source Emissions – Determination of the Mass Concentration of Individual Gaseous Organic Compounds, 2011.
- [91] Chinese Environmental Protection Agency Standard, HJ734 - Stationary Source Emissions. Determination of Volatile Organic Compounds. Sorbent Adsorption and Thermal Desorption Gas Chromatography Mass Spectrometry Method, 2014.
- [92] Chinese Environmental Protection Agency Standard, HJ759 Ambient Air. Determination of Volatile Organic Compounds with Canister Sampling and GC/MS, 2015.
- [93] P. Ciccioli, E. Brancaleoni, A. Cecinato, R. Sparapani, Identification and determination of biogenic and anthropogenic volatile organic compounds in forest areas of Northern and Southern Europe and a remote site of the Himalaya region by high-resolution gas chromatography-mass spectroscopy, *J. Chromatogr.* 643 (1993) 55–69.
- [94] N. Schmidbauer, M. Oehme, Comparison of solid adsorbent and stainless steel canister sampling for very low ppt-concentrations of aromatic compounds (>C6) in ambient air from remote areas, *Fresenius Z. Anal. Chem.* 331 (1988) 14–19.
- [95] D. Helmig, Air analysis by gas chromatography, *J. Chromatogr., A* 843 (1999) 129–146.
- [96] X. Xu, L.L.P. van Stee, J. Williams, J. Beens, M. Adahchour, R.J.J. Vreuls, U.A.T. Brinkman, J. Lelieveld, Comprehensive two-dimensional gas chromatography (GC x GC) measurements of volatile organic compounds in the atmosphere, *Atmos. Chem. Phys.* 3 (2003) 665–682.
- [97] R. Chance, A.R. Baker, F.C. Küpper, C. Hughes, B. Kloareg, G. Malin, Release and transformations of inorganic iodine by marine microalgae, *Estuar. Coast Shelf Sci.* 82 (3) (2009) 406–414.
- [98] H. Hayes, D.J. Benton, S. Grewal, N. Khan, Evaluation of sorbent methodology for petroleum-impacted site investigations, A WMA Confer.: "Vapour Intrus.: Learn. Challenge. (2007). September 26-28, Providence, RI, USA.
- [99] ASTM D7648: Standard Practice for Active Soil Gas Sampling for Direct-Push or Manual-Driven Hand Sampling Equipment.
- [100] H.J.T. Bloemen, T.T.M. Balvers, A.P. Verhoeff, J.H. Van Wijnen, P. Van der Torn, E. Knol, Ventilation Rate and Exchange of Air in Dwellings -Development of a Test Method and Pilot Study. Report, 1992.
- [101] D. Helmig, L. Vierling, Water adsorption capacity of the solid adsorbents tenax TA, tenax GR, carbotrap, carbotrap C, carbosieve SIII, and carboxen 569 and water management techniques for the atmospheric sampling of volatile organic tracer gases, *Anal. Chem.* 67 (23) (1995) 4380–4386.
- [102] EC Directive on Energy Performance of Buildings (EPBD) [2002/91/EC].
- [103] California Air Resources Board, Ventilation and Indoor Air Quality in New Homes. CEC-500-2009-085, 2009.
- [104] P. Wargocki, J. Sundell, W. Bischoff, G. Brundrett, P.O. Fanger, F. Gyntelberg, S.O. Hansen, P. Harrison, A. Pickering, O. Seppanen, P. Wouters, Ventilation and health in non-industrial indoor environments: report from a European, multi-disciplinary scientific consensus meeting (EUROVEN), *Indoor Air* 12 (2002) 113–128.
- [105] M. Larson, J. Sundell, B. Kolarik, L. Hagerhed-Engman, C.-G. Bornehag, The Use of PVC Flooring Material and the Development of Airway Symptoms Among Young Children in Sweden, 2008. Proceedings of Indoor Air '08, Copenhagen, Denmark. Paper 862.
- [106] European Construction Product Regulation, EC 305/2011.
- [107] International Green Construction Code, ANSI/ASHRAE/ICC/USGBC/IES 189, 2018.

- [108] Japanese Ministry of health Labour and Welfare – Recommendations of the Committee on Sick House Syndrome.
- [109] Deutsches Institut Fur Bautechnik, AgBB: Health-Related Evaluation of Emissions of Volatile Organic Compounds (VOC, VOC and SVOC) from Building Products, 2018.
- [110] ANSI/BIFMA M7, 1 FES Test Method Standard Test Method for Determining VOC Emissions From Office Furniture Systems, Components and Seating, 2011. Revised 2016.
- [111] Japanese Industrial Standard A 1901: Determination of the Emission of Volatile Organic Compounds and Aldehydes for Building Products – Small Chamber Method, 2003.
- [112] California Department of Public Health, Standard Method for the Testing and Evaluation of Volatile Organic Chemical Emissions from Indoor Sources Using Environmental Chambers, 2017, Version 1.2. www.cdph.ca.gov/Programs/CCDC/DCDC/DEOD/EAH/Pages/VOC.aspx.
- [113] EN 16516 Construction Products – Assessment of Emissions of Regulated Dangerous Substances – Determination of Emissions into Indoor Air, 2017.
- [114] ASTM D7706 Standard Practice for Rapid Screening of VOC Emissions from Products Using Micro-scale Chambers.
- [115] ISO 12219-3 Indoor Air of Road Vehicles – Screening Method for the Determination of the Emissions of VOCs from Vehicle Interior Parts and Materials – Micro-scale Chamber Method, 2012.
- [116] M. Lor, K. Vause, K. Dinne, E. Goelen, F. Maes, J. Nicolas, A.-C. Romain, C. Degrave, Final Report - Horizontal Evaluation Method for the Implementation of the Construction Products Directive HEM-ICPD, Belgium. Final Report, 2010.
- [117] M. Pharaoh, Final Report: Work on the Correlation between the VDA 276 Test and Micro-chamber Testing. PARD Extension Report: Warwick Manufacturing Group, University of Warwick, 2009.
- [118] R.M. Black, B. Muir, Derivatisation reactions in the chromatographic analysis of chemical warfare agents and their degradation products, *J. Chromatogr. A* 1000 (2003) 253–281.
- [119] Markes International Thermal Desorption Technical Support Note No. 57: Characterisation of Paint Samples by Direct Thermal Desorption with GC/MS. Markes International Ltd, UK.
- [120] SepSolve White Paper 030, Comprehensive Screening of Volatile Emissions from Plastics, SepSolve Analytics, UK, 2020.
- [121] M. Ezrin, G. Lavigne, Analysis of organic compounds in recycled dairy-grade HDPE by thermal desorption with GC/MS, SPE Recycl. Division 2nd Ann. Recycl. Confer. (1995) 104–110.
- [122] P. Wolkoff, C.K. Wilkins, Indoor VOCs from household floor dust: comparison of headspace with desorbed VOCs; method for VOC release determination, *Indoor Air* 4 (1994) 248–254.
- [123] R. Preston, L. McGregor, D. Barden, Combining sorptive extraction with two-dimensional gas chromatography for the flavour profiling of milk, *LC GC* 14 (9) (2018) 11–18. <http://www.chromatographyonline.com/combining-sorptive-extraction-two-dimensional-gas-chromatography-flavour-profiling-milk>.
- [124] S. Eri, B.K. Khoo, J. Lech, T.G. Hartman, Direct TD-GC and GC/MS profiling of hop (*Humulus lupulus* L) essential oils in support of varietal characterisation, *J. Agric. Food Chem.* 48 (4) (2000) 1140–1149.
- [125] Y. Yang, M. Zhang, H. Yin, Y. Deng, Y. Jiang, H. Yuan, C. Dong, J. Li, J. Hua, J. Wang, Rapid profiling of volatile compounds in green teas using Micro-Chamber/Thermal Extractor combined with thermal desorption coupled to gaschromatography-mass spectrometry followed by multivariate statistical analysis, *LWT-Food Sci. Technol.* 96 (2018) 42–50.
- [126] N.D. Spadafora, G. Cocetta, A. Ferrante, R.J. Herbert, S. Dimitrova, D. Davoli, M. Fernández, V. Patterson, T. Vozel, C. Amarysti, H.J. Rogers, C.T. Müller, Short-term post-harvest stress that affects profiles of volatile organic compounds and gene expression in rocket salad during early post-harvest senescence, *Plants* 9 (4) (2020), <https://doi.org/10.3390/plants9010004>.
- [127] N.D. Spadafora, G. Cocetta, M. Cavaiuolo, R. Bulgari, R. Dhorajiwala, A. Ferrante, A. Spinardi, H.J. Rogers, C.T. Müller, A Complex Interaction between Pre-harvest and Postharvest Factors Determines Fresh-Cut Melon Taste and Aroma, February 2019. www.nature.com/scientificreports.
- [128] C.-T. Wang, C. Wiedinmyer, K. Ashworth, P.C. Harley, J. Ortega, W. Vizuete, Leaf enclosure measurements for determining VOC emission capacity from Cannabis spp, *Atmos. Environ.* 199 (2019) 80–87.
- [129] H.-S. Lee, H.J. Lee, H.J. Yu, D.W. Ju, Y. Kim, C.-T. Kim, C.-J. Kim, Y.-J. Cho, N. Kim, S.-Y. Choi, H.J. Suh, A comparison between high hydrostatic pressure extraction and heat extraction of ginsenosides from ginseng, *J. Sci. Food Agric.* 91 (2011) 1466–1473.
- [130] Markes International Thermal Desorption Technical Support Note No. 95: Food Decomposition Analysis Using the Micro-chamber/Thermal Extractor with TD-GCMS. Markes International Ltd, UK.
- [131] G.W. Robertson, D.W. Griffiths, W. MacFarlane Smith, R.D. Butcher, The application of thermal desorption-gas chromatography-mass spectrometry to the analyses of flower volatiles from five varieties of oilseed rape (*Brassica naous* spp. Oleifera), *Photochem. Anal.* 4 (1993) 152–157.

- [132] R.M.C. Jansen, J.W. Hofstee, J. Wildt, F.W.A. Verstappen, H.J. Bouwmeester, M.A. Posthumus, E.J. van Henten, Health monitoring of plants by their emitted volatiles: trichome damage and cell membrane damage are detectable at greenhouse scale, *Ann. Appl. Biol.* (2009) 1–12 (ISSN 0003-4746).
- [133] N.D. Spadafora, A. Amaro, M.J. Valle Pereira, C.T. Muller, M. Pintado, H.J. Rogers, Multi-trait analysis of post-harvest storage in rocket salad (*Diplomatix tenuifolia*) links sensorial, volatile and nutritional data, *Food Chem.* 04 (2016) 107.
- [134] D.W. Griffiths, G.W. Robertson, A.N.E. Birch, R.M. Brennan, Evaluation of thermal desorption and solvent elution combined with polymer entrainment for the analysis of volatiles released by leaves from midge (*Dasineura tetensi*) resistant and susceptible blackcurrant (*Ribes Nigrum* L.) cultivars, *Phytochem. Anal.* 10 (1999) 328–334.
- [135] A. Kessler, I.T. Baldwin, Defensive function of herbivore-induced plant volatile emissions in nature, *Science* 291 (2001) 2141–2144.
- [136] K. Wilkins, K. Larsen, M. Simkus, Volatile metabolites from mould growth on building materials and synthetic media, *Chemosphere* 41 (2000) 437–446.
- [137] J. Fischer, T. Haas, J. Leppert, P. Schulze Lammers, G. Horner, M. Wüst, P. Boeker, Fast and solvent-free quantitation of boar taint odorants in pig fat by stable isotope dilution analysis–dynamic headspace–thermal desorption–gas chromatography/time-of-flight mass spectrometry, *Food Chem.* 158 (2014) 345–350, <https://doi.org/10.1016/j.foodchem.2014.02.113>.
- [138] S.K. Pandey, K.-H. Kim, Human body-odor components and their determination, *Trends Anal. Chem.* 30 (2010) 784–796.
- [139] Markes International Application Note 255, Quantifying Trace Odorants in Water by GC–MS with Trap-Based Preconcentration: Assessing SPME-Trap and High-Capacity Sorptive Extraction, Markes International Ltd, UK, 2019.
- [140] J. Peñuelas, D. Asensio, D. Tholl, K. Wenke, M. Rosenkranz, B. Piechulla, J.P. Schnitzler, Biogenic volatile emissions from the soil, *Plant Cell Environ.* 37 (2014) 1866–1891.
- [141] G.P. Jones, Evaluation of a fully automated thermal desorption device for the headspace screening of fire debris, *Sci. Miscell. Forensic Fillips* (1986) 141–148.
- [142] J.F. Carter, R. Sleeman, J. Parry, The distribution of controlled drugs on banknotes via counting machines, *Forensic Sci. Int.* 132 (2003) 106–112.
- [143] B. Tienpont, F. David, A. Stopforth, P. Sandra, Comprehensive profiling of drugs of abuse in biological fluids by stir-bar sorptive extraction–thermal desorption–capillary GCMS, LC–GC Eur. (2003) 2–10. December.
- [144] M. Virgolici, C. Ponta, M. Manea, D. Negut, M. Cutrubinis, I. Moise, R. Ş uvăila, E. Teodor, C. Sârbu, A. Medvedovici, Thermal desorption/gas chromatography/mass spectrometry approach for characterization of the volatile fraction from amber specimens: a possibility of tracking geological origins, *J. Chromatogr. A* 1217 (2010) 1977–1987.
- [145] R.P. Galvin, M. House, Atmospheric monitoring of bischloromethylether at low ppb levels using an automated system, *Environ. Technol. Lett.* 9 (1988) 563–570.
- [146] Markes International Thermal Desorption Technical Support Note No. 43: Large-scale Monitoring of Mono-Ethylene Glycol Vapour in Natural Gas Using Pumped Sampling onto Tenax Tubes Followed by TD–GC Analysis. Markes International Ltd, UK.
- [147] Thermal Desorption Analysis of Organic Emissions for the Characterization of Non-Metallic Materials for Automobiles Verband Der Automobilindustrie (VDA) Method 278, 2011.
- [148] E. Wauters, P. Van Caeter, G. Desmet, F. David, C. Devos, P. Sandra, Improved accuracy in the determination of polycyclic aromatic hydrocarbons in air using 24 h sampling on a mixed bed followed by thermal desorption capillary gas chromatography–mass spectrometry, *J. Chromatogr. A* 1190 (2008) 286–293.
- [149] B. Lazarov, R. Swinnen, M. Spruyt, E. Goelen, M. Stranger, G. Desmet, E. Wauters, Optimisation steps of an innovative air sampling method for semi-volatile organic compounds, *Atmos. Environ.* 79 (2013) 780–786.
- [150] A. Tipler, Water management in capillary gas chromatographic air monitoring systems, *Proc. AWMA Confer.:* ‘Measur. toxic and related air pollut.’, US (1994) 624–630. May.
- [151] UK Health and Safety Executive, Methods for the Determination of Hazardous Substances No. 4: Generation of Test Atmospheres of Organic Vapours by the Permeation Tube Method, Apparatus for laboratory use, 1981.
- [152] T. Hafkenscheid, F. Langellan, Dynamically Generated Standard Atmospheres: A Support for Air Monitoring, *Proceedings of Conference ‘Measuring Air Pollution by Diffusive Sampling’*, Montpellier, 2001.
- [153] J.H. Buchanan, L.C. Buettner, A.B. Butrow, D.E. Tevault, Vapor Pressure of VX (Research and

- Technology Directorate). Edgewood Chemical Biological Center: Report No. ECBC-TR-068, 1999.
- [154] N. Watson, Making Sorbent Tube Sampling Easier; the Development of a New Type of 'Grab' Sampler', Proceedings of the Air & Waste Management Association Conference, beyond All Borders, June 2011.
- [155] Y.-H. Kim, K.-H. Kim, Ultimate detectability of volatile organic compounds: how much further can we reduce their ambient air sample volumes for analysis? *Anal. Chem.* 84 (2012) 8284–8293, <https://doi.org/10.1021/ac301792x>.
- [156] M.S. Alam, S. Zeraati-Rezaei, C.P. Stark, Z. Liang, H. Xu, R.M. Harrison, The characterisation of diesel exhaust particles – composition, size distribution and partitioning, *Faraday Discuss* 189 (2016) 69–84, <https://doi.org/10.1039/c5fd00185d>.
- [157] R.B. Gaines, G.S. Frysinger, Temperature requirements for thermal modulation in comprehensive two-dimensional gas chromatography, *J. Separ. Sci.* 27 (2004) 380–388.
- [158] J.F. Griffith, W.L. Winniford, K. Sun, R. Edam, J.C. Luong, A reversed-flow differential flow modulator for comprehensive two-dimensional gas chromatography, *J. Chromatogr. A* 1226 (2012) 116–123, <https://doi.org/10.1016/j.chroma.2011.11.036>.
- [159] L.M. Dubois, K.A. Perrault, P.-H. Stefanuto, S. Koschinski, M. Edwards, L. McGregor, J.-F. Focant, Thermal desorption comprehensive two-dimensional gas chromatography coupled to variable-energy electron ionization time-of-flight mass spectrometry for monitoring subtle changes in volatile organic compound profiles of human blood, *J. Chromatogr. A* 1501 (2017) 117–127, <https://doi.org/10.1016/j.chroma.2017.04.026>.
- [160] J. Leppert, G. Horner, F. Rietz, J. Ringer, P. Schulze Lammers, P. Boeker, Near real time detection of hazardous airborne substances, *Talanta* 101 (2012) 440–446, <https://doi.org/10.1016/j.talanta.2012.09.056>.
- [161] L. Bell, N.D. Spadafora, C.T. Müller, C. Wagstaff, H.J. Rogers, Use of TD-GC–TOF-MS to assess volatile composition during post-harvest storage in seven accessions of rocket salad (*Eruca sativa*), *Food Chem.* 194 (2016) 626–636, <https://doi.org/10.1016/j.foodchem.2015.08.043>.
- [162] J. O'Leary, J. Hiscox, D.C. Eastwood, M. Savoury, A. Langley, S.W. McDowell, H.J. Rogers, L. Boddy, C.T. Müller, The whiff of decay: linking volatile production and extracellular enzymes to outcomes of fungal interactions at different temperatures, *Fungal Ecol.* 39 (2019) 336–348, <https://doi.org/10.1016/j.funeco.2019.03.006>. ISSN 1754-5048.
- [163] C. Rawlinson, S. Martin, J. Frosina, C. Wright, Chemical characterisation of aerosols emitted by electronic cigarettes using thermal desorption - gas chromatography - time of flight mass spectrometry, *J. Chromatogr. A* (2017) 1497, <https://doi.org/10.1016/j.chroma.2017.02.050>.

Pyrolysis-gas chromatography

Karen D. Sam

Applications Lab, CDS Analytical, Oxford, PA, United States

11.1 Introduction

The principle behind all thermal sample preparation methods for gas chromatography (GC) is that the volatile analytes are delivered to the GC column by controlling the sample temperature rather than by injecting them in a solvent [1]. Since there is no large solvent peak at the beginning of the GC run, these techniques are both sensitive and ideal for determining the presence of trace levels of solvents in products. In many cases, the volatile organics are first adsorbed onto a trapping material and then thermally desorbed in a GC carrier. However, whether desorbed from a sorbent or directly from a solid or liquid sample, the volatiles that constitute the GC analysis are compounds that are isolated from the matrix and transported to the GC intact. This is more a physical technique in that the analytes have not been chemically altered; hence, the identification of a particular compound as a peak in the chromatogram means the compound was present in the sample originally. Typical applications of this kind of thermal sampling include the determination of residual solvents and monomers in polymers, air quality monitoring using sorbent tubes, the identification of aroma compounds in foods, and the identification of plasticizers.

11.1.1 Pyrolysis

Analytical pyrolysis-GC differs from other thermal techniques in one important way: the temperatures used are intentionally high enough to cause chemical changes to the sample [2]. This is specifically avoided in thermal desorption techniques, where the temperature is carefully controlled to prevent chemically altering the analytes. At low temperatures, the intention is to demonstrate that the peaks identified in the chromatogram are the exact compounds present in the sample before processing. The purpose of pyrolysis, however, is to create smaller, volatile molecules from a large molecule so that GC may be used to study the macromolecule [3], with the understanding that it is a destructive technique. The result resembles mass spectrometry in that a large molecule is intentionally fragmented and information about the original molecule is inferred from the identity of the fragments made. It is therefore important to understand the chemistry involved when large molecules are thermally fragmented in interpreting the results of pyrolysis-GC and Py-GC-MS. The reactions include dehydration, decarboxylation, and, to a large extent, bond dissociation to form free radicals, with the typical reactions and rearrangements of such entities.

11.2 Molecular theory

Analytical pyrolysis is, strictly speaking, the study of chemical changes that occur to a molecule at high temperatures under vacuum or in an inert atmosphere. Although these reactions are also involved in processes such as hydrogenation and oxidation, which may also be performed with pyrolysis instruments, the theory here will assume that the sample is simply heated in an inert gas, typically helium at relatively low pressure (about 1 atmosphere). The reactions involved can be categorized into several schemes, including depolymerization, random scission, and side-group elimination, but for practical purposes, it is convenient to limit consideration to just two cases: those reactions that make oligomers and those that do not.

11.2.1 Bond dissociation and free radicals

The fragmentation caused by pyrolysis—and the ultimate products formed and identified in the analysis—depends on the relative strengths of the bonds in the molecule and how the free radicals formed when the bonds dissociate react to form products. As the sample is heated, the weakest bonds break first. In the case of most polymers, there is a molecular chain with additional atoms, or groups attached to the chain, which make one chain different from another. For the purpose of GC, the most favorable case is that the chain bonds are broken first, since this reduces the size of the molecule, eventually to a point where the fragments are small enough to be volatile and compatible with separation by GC. On the other hand, if the side groups are attached with bonds that are weaker than the chain bonds, they will be removed from the chain, which generally then becomes unsaturated before degrading.

Once the free radicals are formed by bond dissociation, they behave in normal fashion.

Primary free radicals are more energetic, and tertiary ones are more stable. Primary free radicals will stabilize through reactions that result in the formation of secondary or tertiary free radicals, including rearrangements, especially the transfer of a hydrogen atom from four carbon atoms removed from the free radical (a 1–5 hydrogen shift). In general, molecules in which the chain bonds are the weakest break apart to form oligomers, including monomers, and polymers while weakly attached side groups do not.

11.2.2 Oligomer formation

Many synthetic polymers are essentially carbon–carbon chains with side groups attached similar to scheme 1 in Fig. 11.1. Here, two adjacent carbons each have two side groups, shown as R1–R4. If all four R groups are hydrogens, then the polymer is polyethylene. If one is a methyl group, it is polypropylene. If one is benzene, the polymer is polystyrene, and so on. Carbon–hydrogen bonds are stronger than carbon–carbon bonds; hence, these polymers generally fragment by chain-bond dissociation, producing two free radicals. If R1 and R2 are both hydrogens, then the resulting free radical is primary and very reactive. If one of the R groups is not hydrogen, then it is a secondary free radical, and if neither R1 nor R2 is hydrogen, the result is a tertiary free radical.

Line 2 of Fig. 11.1 illustrates the bond between the two chain carbon atoms dissociating to make the free radicals. One path is available for the free radical to take a hydrogen atom from another molecule, forming a saturated end. This may or may not make a volatile product, depending on the size of the rest of the molecule. Another mechanism is β -scission, illustrated in line 3 of Fig. 11.1. In this case, the unpaired electron and one of the electrons from the bond between the second and third carbon atoms in the chain form a bond, making a double bond between the first two carbons

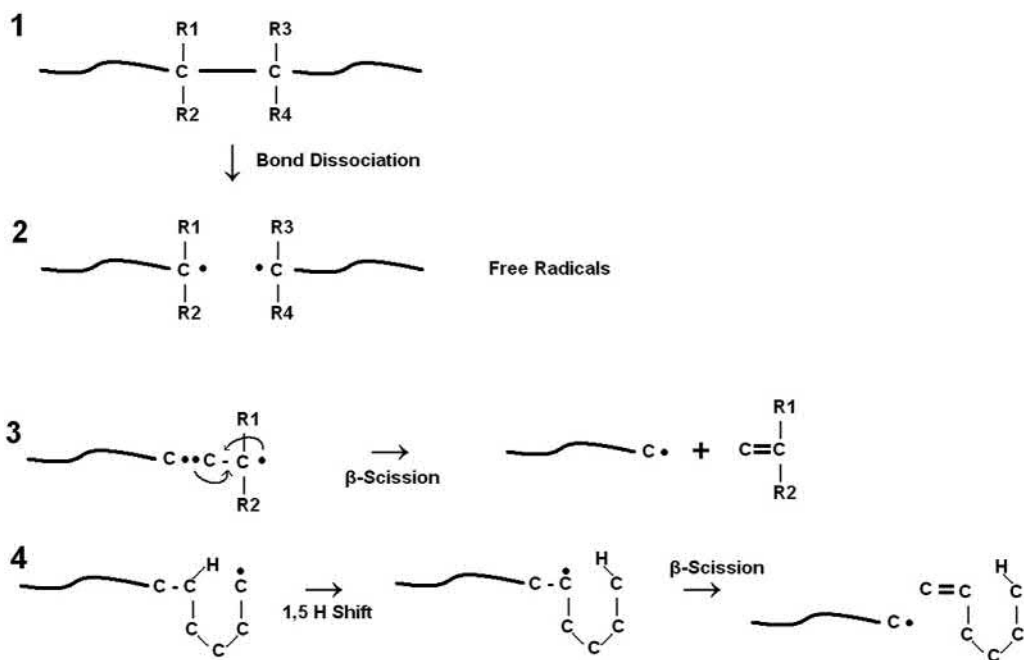


FIGURE 11.1 Free radical generation with production of monomer and trimer.

and breaking the bond to the rest of the molecule. This produces a new free radical and a stable product with two carbon atoms with R1 and R2 still attached. This product is frequently a molecule of the monomer of the polymer and may be the primary degradation pathway, that is, a molecule of the monomer is split off, creating a new free radical, which undergoes β -scission again, eventually unzipping the whole polymer chain. Methacrylate polymers and polytetrafluoroethylene are examples of polymers that essentially unzip to monomer through pyrolysis.

If the free radical is primary or secondary, as illustrated in line 4 of Fig. 11.1, it can become more stable after rearrangement. By forming a six-membered ring, with five carbon atoms and a hydrogen atom, the hydrogen can be transferred from the fifth carbon atom to the first. The unpaired electron is now on the fifth carbon; therefore, the free radical is secondary or tertiary.

This free radical can now undergo β -scission, again making a new, terminal free radical and a stable product. However, this product is a six-carbon fragment of the polymer, with the six carbon atoms still connected to each other as they were originally. This makes it a trimer molecule (an oligomer with three monomers), retaining significant microstructural information. The sequence of bond dissociation, and then a 1,5 hydrogen transfer to make a more stable free radical, and then β -scission to make a trimer is an important pathway for many polymers. In some cases, it produces the largest peak in the pyrogram, and the information it contains is useful for distinguishing between polymers of similar structure.

Some polymers, especially polyolefins, produce a variety of oligomers when pyrolyzed, including molecules with 35 or more carbon atoms. Oligomers beyond the trimer generally result from breaking bonds at two different

places in the molecule. If the section between the bond-breaking sites is sufficiently volatile, it becomes part of the pyrogram. The free radical at each end may abstract a hydrogen atom, producing a saturated end to the fragment, or the end may be unsaturated. Polyethylene, for example, generates fragments that may have a double bond at each end, only one double bond, or no double bonds; hence, the oligomers consist of alkanes, alkenes, and dienes (see Section 11.4.3).

11.2.3 No oligomers

For some polymers, the bonds to side groups are weaker than the bonds holding the chain together; hence, during pyrolysis, the weaker bonds break first and the side groups are removed. In this case, it is not possible to expel

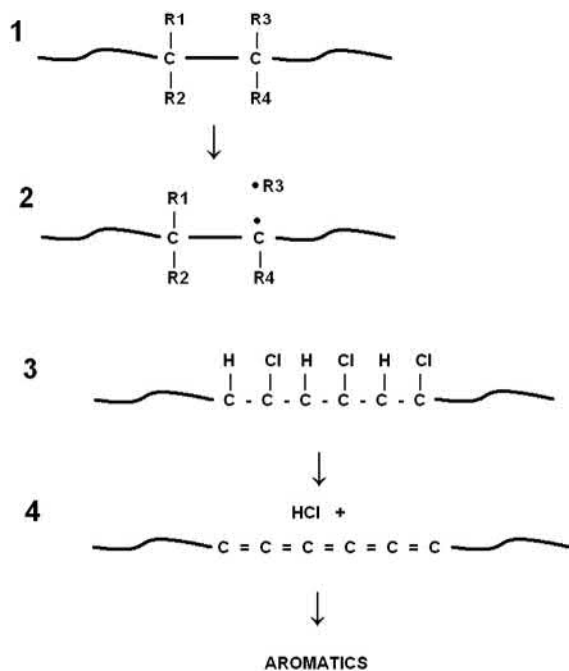


FIGURE 11.2 Side group elimination with production of aromatics.

monomers since the identity of the polymer chain has been altered. Instead, small molecules from the side groups are created, and then the remaining chain is fragmented. As an example, this is illustrated in Fig. 11.2 for polyvinyl chloride. The C–Cl bond is weaker than either the C–C or the C–H bonds; hence, at a relatively low temperature the C–Cl bond breaks. The chlorine radical abstracts a hydrogen atom from a neighboring carbon atom forming HCl, leaving behind a chain with many double bonds. At higher temperatures, this chain fragments further, forming aromatics, including benzene, toluene, and naphthalene. No vinyl chloride is formed, but the pyrogram, which includes HCl and the aromatics, is characteristic of the polymer and suitable for its identification (see Section 11.4.4).

11.2.4 Copolymers

In practice, it is more likely that a sample is a mixture, blend, or copolymer than a pure, single polymer. Copolymers are typically classified as random or block copolymers. In block copolymers and in blends, mixtures, laminates, and layered materials, there are discrete regions formed by the individual polymers. In random copolymers, the various monomers are bound to each other in a random manner. Therefore, a section of a block copolymer of monomers A and B can be represented like this:

---A-A-A-A-A-A-A-A-A-A-A-A-A-A-A-A-A-A-A-B-B-B-B-B-B-B-B-B-B-B-B-B-B-B-B-BB---

and a section of a random copolymer like this:

---A-A-B-A-B-B-A-B-A-B-B-A-A-B-A-B-A-B-B-A-B-A-A-B-B-A-B-A-B-A-B-A---

resulting in two very different polymer molecules. If the polymers form oligomers, then the block sample (or a blend or mixture) will make oligomers of just A and just B, including the trimers A-A-A and B-B-B. The random copolymer will make additional mixed trimers, such as A-B-A, A-A-B, B-A-B, B-B-A, and so on; hence, the pyrograms

will be substantially different. The relative concentrations of A and B will also create differences, as well as the actual degree of randomness in the sample thought to be completely random.

11.3 Instrumentation

For typical pyrolysis-GC and pyrolysis-GC-MS, the sample is placed in the carrier gas stream of the GC and heated to a high temperature—usually 600–800°C—rapidly, transferring the volatile fragments formed directly to the GC column. Sample size is dictated by the capacity of the chromatographic system but is generally about 10–100 µg. This is the equivalent of injecting 1 µL of a standard containing 1%–10% analyte. Since there is no solvent used in pyrolysis, the sample contains only analytes, and even if the pyrogram contains 100 peaks, each one will still represent about 1 µg. Even with such a small sample, split ratios of 50:1 or higher are typical. Dead volume should be as small as possible so that the resolution of peaks is not affected. Cold spots are of concern since many polymers produce oligomers that are large and likely to condense on cool surfaces, producing contamination peaks in later runs.

Although many pyrolysis-GC runs consist of just a single, high-temperature analysis, the technique and the instrumentation used have expanded to include slow, programmed runs, multiple-step analyses taking samples to sequentially higher temperatures, and analyses performed in reactive atmospheres, including hydrogen and air.

11.3.1 Pulse pyrolysis

The ideal for a pulse pyrolysis is to take a small sample to a high temperature instantaneously. In this way, it will degrade all at once and the resulting peaks will be sharp and well resolved. Commercially available pyrolyzers for pulse pyrolysis come close to achieving this

ideal. With heating rates in the tens of degrees per millisecond, they reach a final temperature in less than a second, producing very rapid pyrolysis. There are basically three types of instruments designed for pulse pyrolysis, Curie point, microfurnace, and heated filament. Each has its own specific characteristics, but all can produce a satisfactory pyrogram in a way that is well controlled and reproducible [4]. The ways in which they differ involve how the sample is introduced and how the heating is applied.

11.3.1.1 Curie-point pyrolyzer

In a Curie-point pyrolyzer, a ferromagnetic wire or foil is heated inductively by placing it into a high-frequency coil. The wires are made of various combinations of nickel, cobalt, and iron. The current induced in the wire causes it to heat to a point at which it is no longer ferromagnetic—the Curie point—at which the temperature stabilizes. Each alloy has a different Curie point; hence, the temperature is controlled by the choice of alloy rather than by a setpoint on the instrument. The heating is very fast, and the sample, usually applied directly to the wire or foil, pyrolyzes quickly.

Curie-point systems are simple, heat quickly, and the temperature is reproducible within a given batch of alloy. Although the final pyrolysis time is selectable, the heating rate is always ballistic; hence, programmed heating is not an option. The choice of temperature depends on the alloys that are available. Most instruments supply a range of 10–20 different alloys and therefore temperatures to choose from.

11.3.1.2 Microfurnace pyrolyzers

Microfurnaces are generally used isothermally, inserting the sample into a preheated pyrolysis zone. The temperature is usually selectable in 1°C increments to about 900°C. Samples may be placed into small cups, which are dropped into the furnace, or inserted using a special syringe that can accommodate powders and fibers. Some furnaces have a separate,

lower-temperature zone that permits analysis of the sample initially at a desorption temperature followed by a second run for pyrolysis.

In addition to isothermal operation, a micro-furnace can usually be programmed to heat in °C/min for time- or temperature-resolved methods. Because of the difficulty in loading volatile samples onto a filament or Curie-point wire, microfurnaces are preferred for the pyrolysis of such samples. Since a microfurnace generally has a larger heated surface area than a filament or Curie-point system, secondary pyrolysis reactions are a concern, and it is typical to operate them at lower temperatures to compensate for this.

11.3.1.3 Heated filament pyrolyzers

In a resistively heated filament pyrolyzer, the sample is placed either onto the surface of a cool filament or into a small quartz tube, which is then fitted into a coil of heating wire. The filament is usually platinum, and the temperature is controlled by the voltage applied across the wire or strip. The filament mass is very small, and it heats up quickly, but can also be heated at slow or programmed rates. Temperature selection is generally in 1°C increments to about 1400°C. Programmed operation may include an initial temperature, heating rate, and final temperature and time.

Since the filament temperature is controlled by the instrument setpoint, it is easier to perform multistep sequences, unlike a Curie-point system, which requires a different wire for each temperature. Sample heating is very fast when the sample is placed directly onto the filament, but slower if the sample is contained inside a quartz tube.

11.3.2 Programmed pyrolysis

Rapid heating for a short time is preferred for a simple pyrolysis-GC analysis since the quick production of volatiles insures narrow peaks

and good resolution. There are, however, other analyses that require slower or programmed heating. These may involve interfacing the pyrolyzer directly to a mass spectrometer, reproducing thermogravimetric programs, or simulating industrial processes. If the sample is to be heated slowly, but the analysis is conducted using GC, the evolved products must be trapped before introduction into the GC. This is done using either a sorbent or a cryogenic trap so that the sample introduction to the GC is rapid even if the analyte production extended over a period of several minutes or longer. Programmed heating is usually not possible with a Curie-point pyrolyzer, but microfurnaces may be programmed to heat in degrees per minute, and filaments, because of their small mass, may be programmed to heat in degrees per minute, second, or millisecond.

11.4 Applications

Pyrolysis-GC has been used for decades for the analysis of rubber [5], forensic samples [6,7], coatings [8], artwork [9,10], and other kinds of solid materials. The applications compiled in this section were chosen to illustrate the range of materials analyzed by pyrolysis-GC and to illustrate the chemical behaviors described in the theory section. Most examples are for “real world” samples and consequently are not pure polymers but blends, copolymers, and composite materials such as paints, adhesives, textiles, and so on.

11.4.1 Polystyrene

As shown in lines 3 and 4 of Fig. 11.1, if a polymer structure has a hydrogen atom on the fifth carbon from the bond breaking, it can rearrange and make significant trimer in addition to monomer. This is true of the acrylates (as opposed to the methacrylates) and for other polymers, including polystyrene.

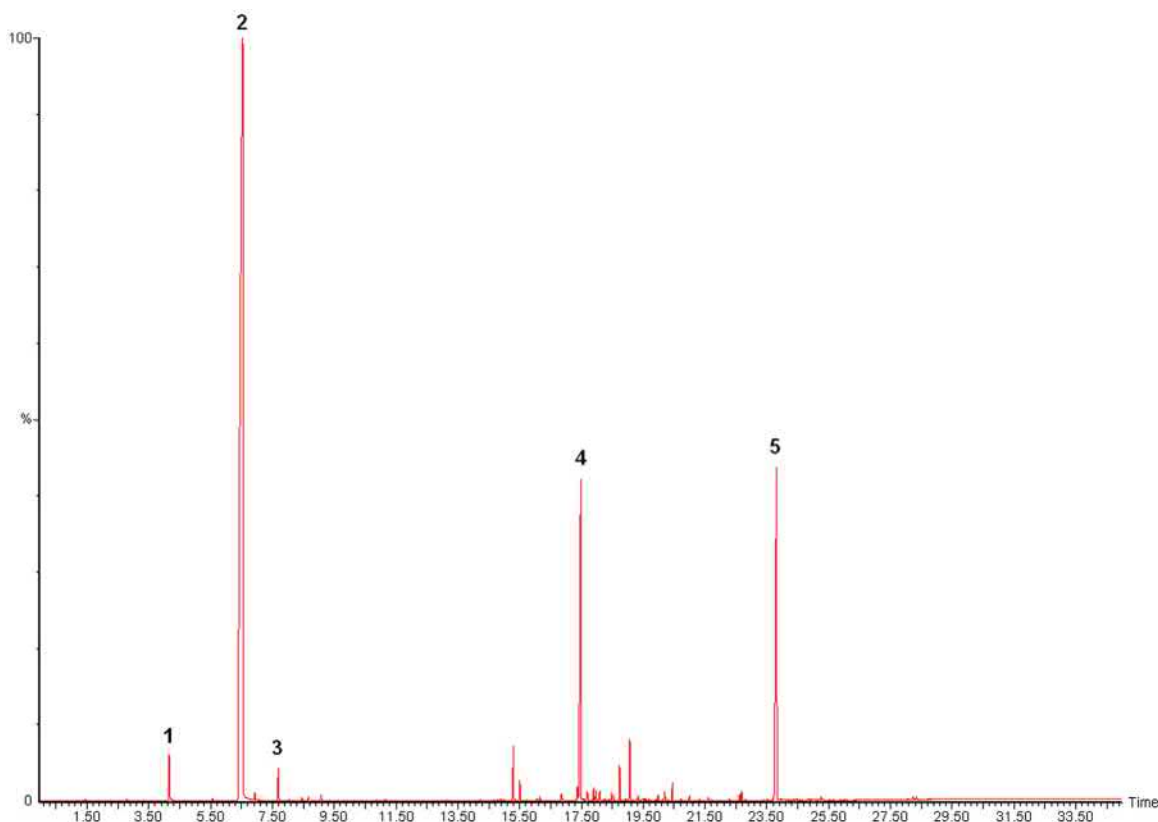


FIGURE 11.3 Pyrolysis of polystyrene at 750°C. Peak #1, toluene; #2, styrene; #3, alpha methyl styrene; #4, styrene dimer; and #5, styrene trimer.

Fig. 11.3 shows a pyrogram of polystyrene at 750°C, in which about 70% of the pyrolysate is comprised of the monomer, styrene (peak 2). There is also considerable dimer (peak 4) and trimer (peak 5). The relative amount of the trimer is sensitive to the temperature, so that at lower temperatures the trimer peak is larger, and at higher temperatures it decreases. Small peaks are also observed for toluene and alpha-methylstyrene, which are generally present in the pyrolysis of polystyrene.

11.4.2 Acrylics

Acrylic polymers include the acrylates such as ethyl acrylate and butyl acrylate and the

methacrylates, such as methyl methacrylate and butyl methacrylate. Looking at line 1 in Fig. 11.1, for acrylates, R1, R3, and R4 are all hydrogen, and R2 is the ester group. This means that there is a hydrogen atom on the fifth carbon from the bond breaking that can be transferred; hence, the trimer can be formed by the mechanism shown in line 4, Fig. 11.1. For methacrylates, R1 is a methyl group; therefore, the bond breaking makes a tertiary free radical. There is also a methyl group on the fifth carbon; hence, there is no hydrogen to transfer, and the polymer simply unzips to monomer.

The acrylic material shown in Fig. 11.4 contains both acrylic and methacrylic monomers, specifically methyl methacrylate, butyl

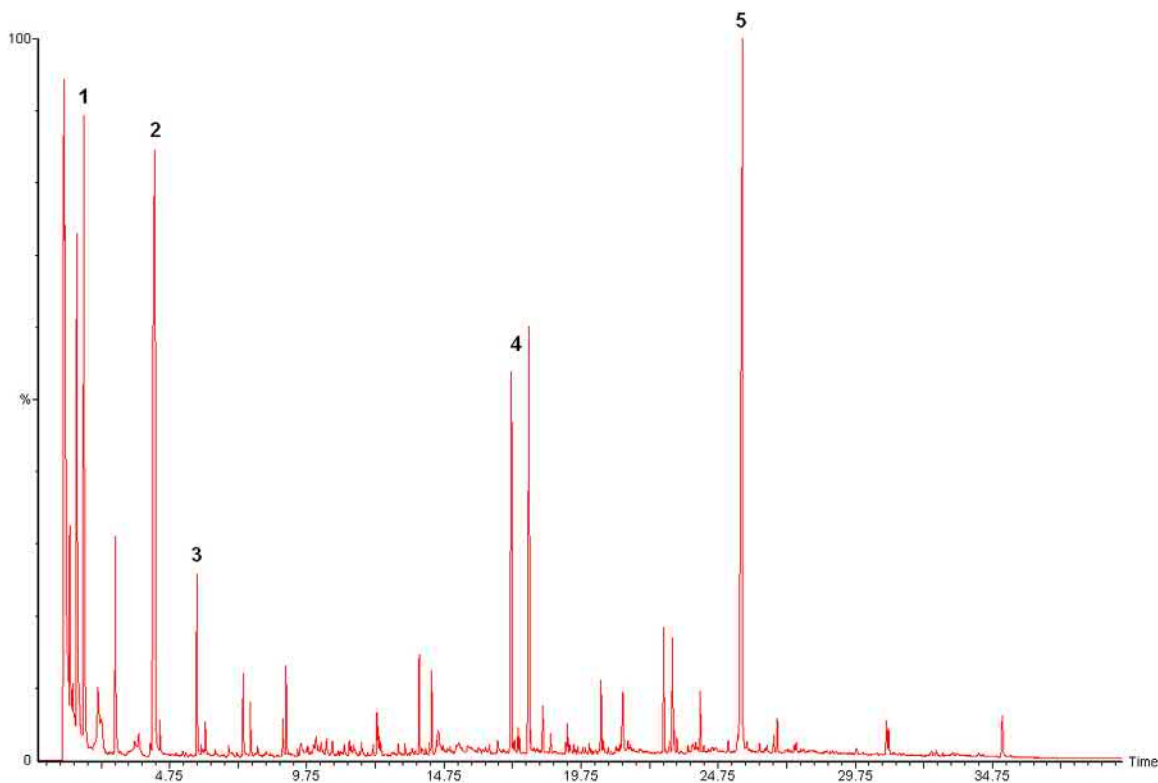


FIGURE 11.4 Pyrolysis of an acrylic copolymer at 750°C. Peak #1, Methyl methacrylate; 2, Butyl acrylate; 3, Butyl methacrylate; 4, Butyl acrylate dimers; 5, Butyl acrylate trimer.

methacrylate, and butyl acrylate. Consequently, there is a large peak for methyl methacrylate monomer (peak 1) and a peak for butyl methacrylate (peak 3). There is also a considerable amount of butyl acrylate, which appears as the monomer, dimer, and trimer (peaks 2, 4, and 5). The trimer peak is the largest, which is typical, and there are two dimer peaks, also typical for acrylics. The relative sizes of the monomers (and other oligomers) are reflective of their abundance in the original copolymer [11]; hence, Py-GC-MS may be used to quantitate the monomer ratios in copolymers like these.

11.4.3 Polyolefins

Polyolefins, including polyethylene, polypropylene, polyisobutylene, and polybutene, form many fragments when pyrolyzed, making pyrograms with many—frequently hundreds of—peaks. In general, it takes two bond scissions to create a pyrolysis fragment for the polyolefins; hence, one bond breaks, and then another, maybe 10 or 20 carbons away breaks so that a piece of the polymer is snipped out. These pieces range from small and volatile to those too large for separation by GC. In each case, a series of pyrolysis products is formed with a specific

pattern characteristic of the polyolefin pyrolyzed. Polypropylene produces a series of oligomers with each group of peaks having three more carbon atoms than the one that eluted previously. For polyisobutylene, the groups contain four more carbon atoms. For polyethylene, the groups of peaks increase by one carbon atom; hence, hydrocarbons of each carbon number are present. In all cases, the end of the pyrolysate molecule (where the bond broke) may be a double bond or may be saturated; therefore, there are opportunities for products with two double bonds, or just one, or none.

In addition to random scission of the macromolecule, once the free radical has been formed, it may still rearrange as in Fig. 11.1 line 4; hence, there is a second pathway for some of the products, especially the trimer.

All the aforementioned is demonstrated in the pyrolysis of polyethylene, such as a piece of a plastic bag, in Fig. 11.5. The overall result is a chromatogram of a series of triplet peaks, all normal hydrocarbons. The group with peak 1 (hexene) has six carbon atoms and is followed by groups with seven, then eight carbon atoms, and so on. The group with 27 carbon atoms is expanded to

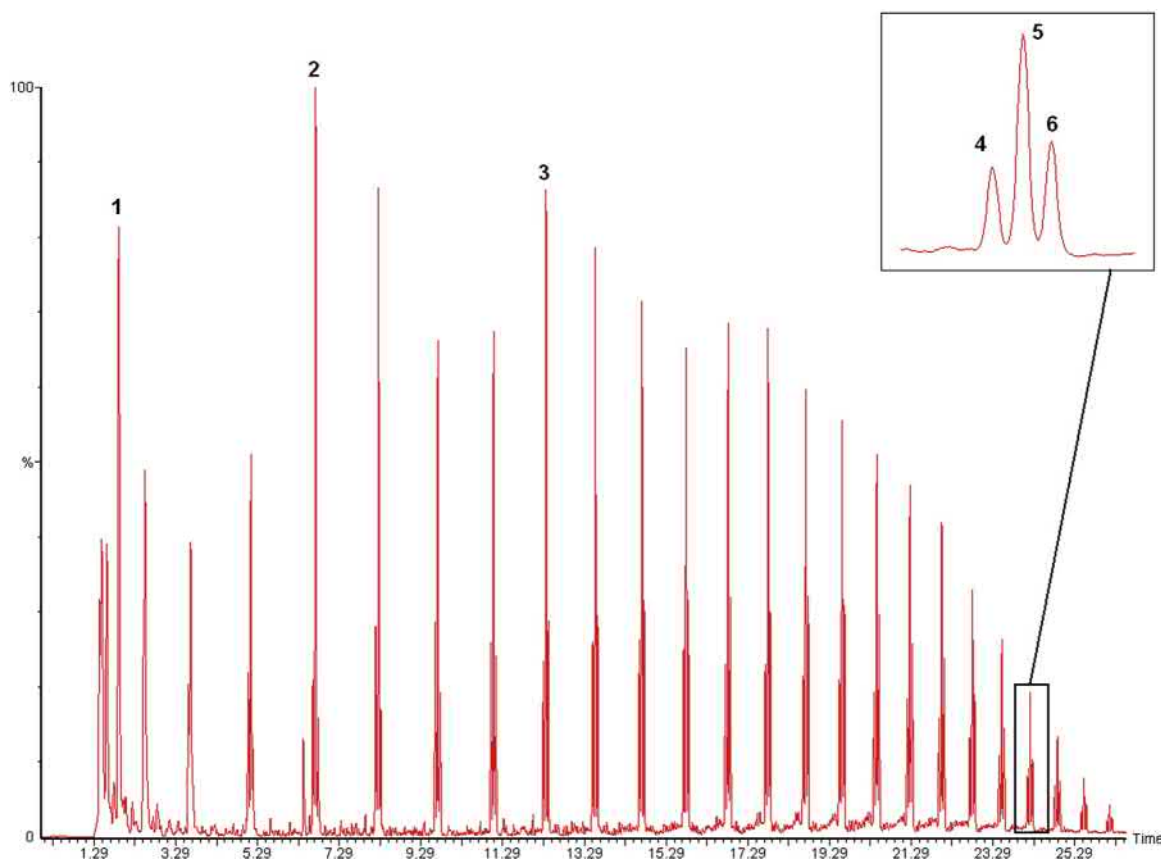


FIGURE 11.5 Pyrolysis of polyethylene at 750°C. Peak #1, hexene; #2, decene; #3, tetradecene; #4, C27 diolefin; #5, olefin; and #6, paraffin.

show the triplets, first the diene, with double bonds at both ends, then the olefin, and finally the paraffin. Peak 1 (hexene) is produced by breaking two bonds six carbon atoms apart, and by the 1–5 hydrogen shift free radical rearrangement that makes the trimer. Consequently, there are more of the C6 compounds than of the C5 or C7. This rearrangement can take place more than once. A second shift moves the unpaired electron to carbon 9, and β -scission produces decene. A third shift produces tetradecene. These are marked as peaks 2 and 3 in the pyrogram, each of which is present at greater abundance than the neighboring compounds because of the rearrangement. In general, for polyolefins, the trimer is the largest peak—for example, with polypropylene, this is dimethylheptene.

11.4.4 Vinyl polymers

Fig. 11.2 shows the degradation scheme for polymers containing a side-group bond weaker than the carbon chain bonds. In these cases, the side group is removed first, and then the chain fragments to form smaller molecules, but not monomer. Polyvinylchloride (PVC) and polyvinylacetate (PVA) both behave in this way. In each case, the side group breaks off, producing acetic acid from PVA and HCl from PVC and leaving a polyunsaturated chain, which then forms many aromatics.

Fig. 11.6 shows a program for a polymer packaging material that is largely PVC but contains other polymers as well. Peaks 1 through 8 all result from pyrolysis of the PVC portion of the

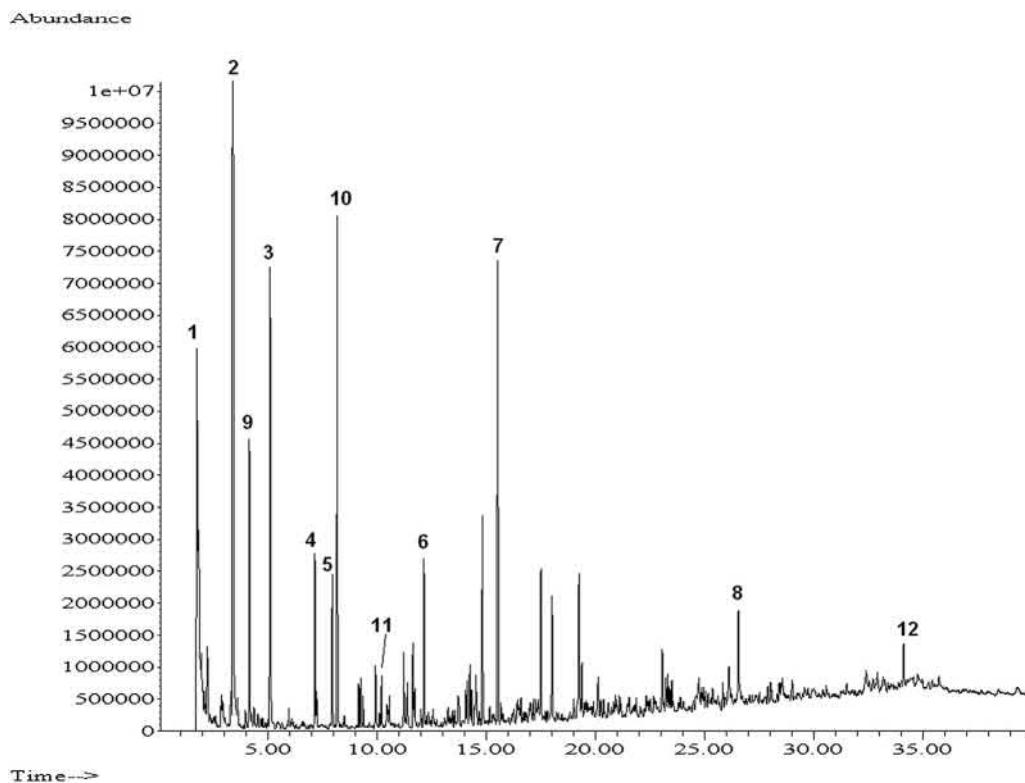


FIGURE 11.6 Pyrolysis of PVC with polystyrene and acrylic at 750°C. Peak #1, HCl; #2, benzene; #3, toluene; #4, ethyl benzene; #5, xylene; #6, indene; #7, naphthalene; #8, anthracene; #9, methyl methacrylate; #10, styrene; #11, alpha methyl styrene; and #12, styrene trimer.

material. Peak 1 is HCl, and the aromatics benzene (2) and naphthalene (7) are significant in the pyrogram. There is also a large peak for methyl methacrylate (9) and for styrene (10). As with most polymers, the presence of several materials being pyrolyzed at the same time does not necessarily confuse things. The peaks 1–8 for PVC would look the same if the sample was pure PVC with no other compounds present. The styrene and methyl methacrylate productions are likewise not affected by the products from PVC. This means that it is unlikely that the pyrolysis products from one material react with those from other materials to form new compounds. This is especially important when considering copolymers. Mixed dimers and trimers in random copolymers are not the result of monomers reacting with each other after pyrolysis, but rather indicate the original structure of the molecule before pyrolysis. In this example, there is a small peak for styrene trimer, which confirms the presence of polystyrene.

11.4.5 Polyurethanes

Polyurethanes are one of the easiest group of polymers to recognize by Py-GC-MS. They are formed by reaction of a diisocyanate and a polyol. The polyol may be a polyester or a polyether. The diisocyanates are regenerated and generally identified by mass spectrometry. In addition, fragments from the polyols are generally simple and indicative of the type used. Many consumer products called polyurethanes, especially paints, contain only a small amount of polyurethane, with other, less expensive ingredients. However, even if the polyurethane content is small, the characteristic peaks are present and identifiable.

Fig. 11.7 illustrates an interesting example of polyurethane made from two different diisocyanates. Peak 3 is a double peak for toluene diisocyanate (TDI), which exists as two isomers,

both of which appear in commercial products. Isophorone diisocyanate also exists as two isomers, marked in the pyrogram as peaks 4 and 5. The identity of the diisocyanate isomers is not altered by pyrolysis; hence, the isomers reappear in the pyrogram in the relative abundance they had in the polymer. That is, if only one isomer is used, only one peak will be observed in the chromatogram, and if two are present in a specific ratio in the polymer, that ratio is preserved in the chromatogram.

Peaks 1 and 2 are small ether compounds, indicating that the polyol part of the polyurethane was a polyether. Polyester polyols frequently use adipic acid (also used in some polyamides and other condensation polymers), which produces cyclopentanone when pyrolyzed. Consequently, it is usually possible to determine the diisocyanate and the type of polyol used in a polyurethane from the identity of just a few peaks in the pyrogram.

11.4.6 Polyamides

Condensation polymers, including nylons [12], have been extensively studied using PY-GC-MS. Nylons are made either from a single monomer, with the acid group at one end and the amine at the other, or from two monomers, one a diacid and the other a diamine. The most used are Nylon 6, which is polycaprolactam, and Nylon 6.6, which combines a six-carbon diacid (adipic acid) and hexanediamine. Although similar in molecular structure, Nylon 6 and Nylon 6.6 are easily discriminated by PY-GC. Nylon 6 essentially reverts to monomer; hence, the pyrogram has a large peak for caprolactam, while Nylon 6.6 produces many fragments, of which one of the most abundant peaks (and any polymer made with adipic acid) is cyclopentanone.

Fig. 11.8 was produced from carpet fibers, which contained mostly Nylon 6.6. The cyclopentanone peak (1) is prominent, but there are

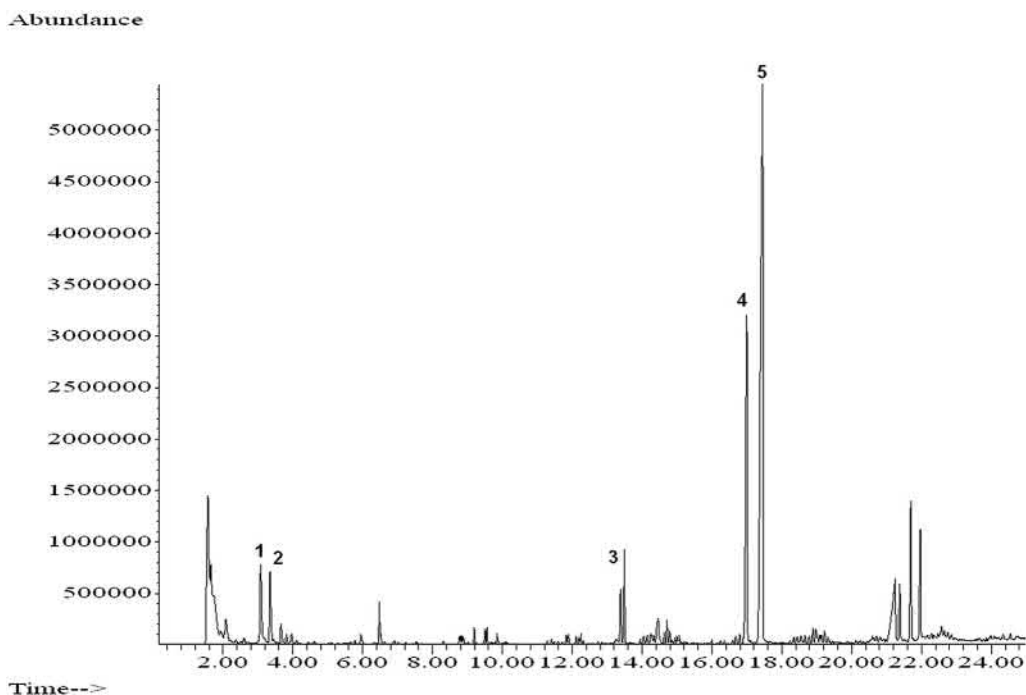


FIGURE 11.7 Pyrolysis of a polyurethane at 750°C. Peak #1, 2-ethoxypropane; #2, 1-(1-methylethoxy)propane; #3, toluene diisocyanate; #4 and 5, isophorone diisocyanate.

also peaks from the hexanediamine, including hexanenitrile (2) and hexanedinitrile (3). There is also a small peak for caprolactam (4), which is the major product from Nylon 6. There are larger fragments of the molecule eluting later in the pyrogram as well.

11.4.7 Epoxies

Epoxies are generally formulated using bisphenol A and once compounded seem so rugged that chemical analysis would be difficult. They are, however, organic polymers and simple to analyze by pyrolysis. Epoxies are increasingly used in coatings in the form of powdercoats. These can be pure epoxy or hybrids using epoxies and other polymers.

The pyrogram in Fig. 11.9 was produced by pyrolyzing the powdercoat finish used on a

metal hook. It is a simple epoxy finish, with no other polymers; hence, it is typical of epoxy materials. The large peak (6) at about 25 min is bisphenol A, which is generally present in epoxies but not specific for epoxies since polycarbonates also use, and produce, bisphenol A.

Hybrid powdercoats incorporating polyesters or polyurethanes, for example, contain the same distribution of phenolic compounds seen for a pure epoxy, as well as the specific pyrolysis products (benzoic acid and diisocyanates) from the additional polymers.

11.4.8 Biomass

Most plant materials, including wood, grasses, and leaves, are lignocellulosic [13], meaning that they are comprised of two biopolymers—lignin and cellulose. Lignin is a

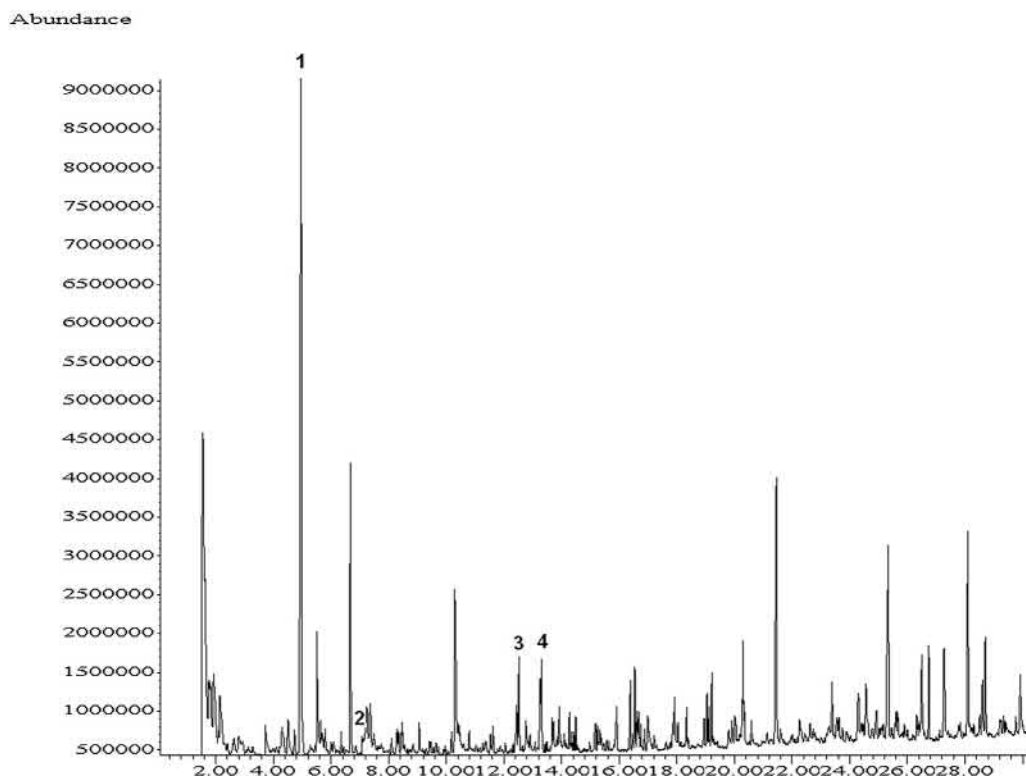


FIGURE 11.8 Pyrolysis of nylon carpet fiber at 800°C. Peak #1, cyclopentanone; #2, hexanenitrile; #3, hexanedinitrile; and #4, caprolactam.

phenolic polymer, and cellulose is a polymer of glucose; hence, their structures, and consequently their pyrolysis products, are quite different. When pyrolyzed, cellulose makes considerable water and carbon dioxide and organics that are suited to GC analysis. These include many furans, alcohols, acetic acid, and levoglucosan. Different plants make different lignins, but they are all phenolic and produce substituted phenols when pyrolyzed.

Like other copolymer systems, if a plant material contains both lignin and cellulose, the resulting pyrogram will contain compounds from each of the individual polymers. Fig. 11.10 illustrates

the pyrogram from a sample of wood. Peaks 1, 2, and 10 (acetic acid, furancarboxaldehyde, and levoglucosan) as a group are characteristic of cellulose pyrolysis. Just after peak 3 at about 9 min is a small peak for phenol, but the more characteristic methoxyphenols, such as peaks 4 and 5, are both larger and more informative of the type and structure of the lignin involved.

11.4.9 Advanced applications

In addition to traditional pulse pyrolysis applications for GC, pyrolysis instruments can be used for a variety of more complex sample

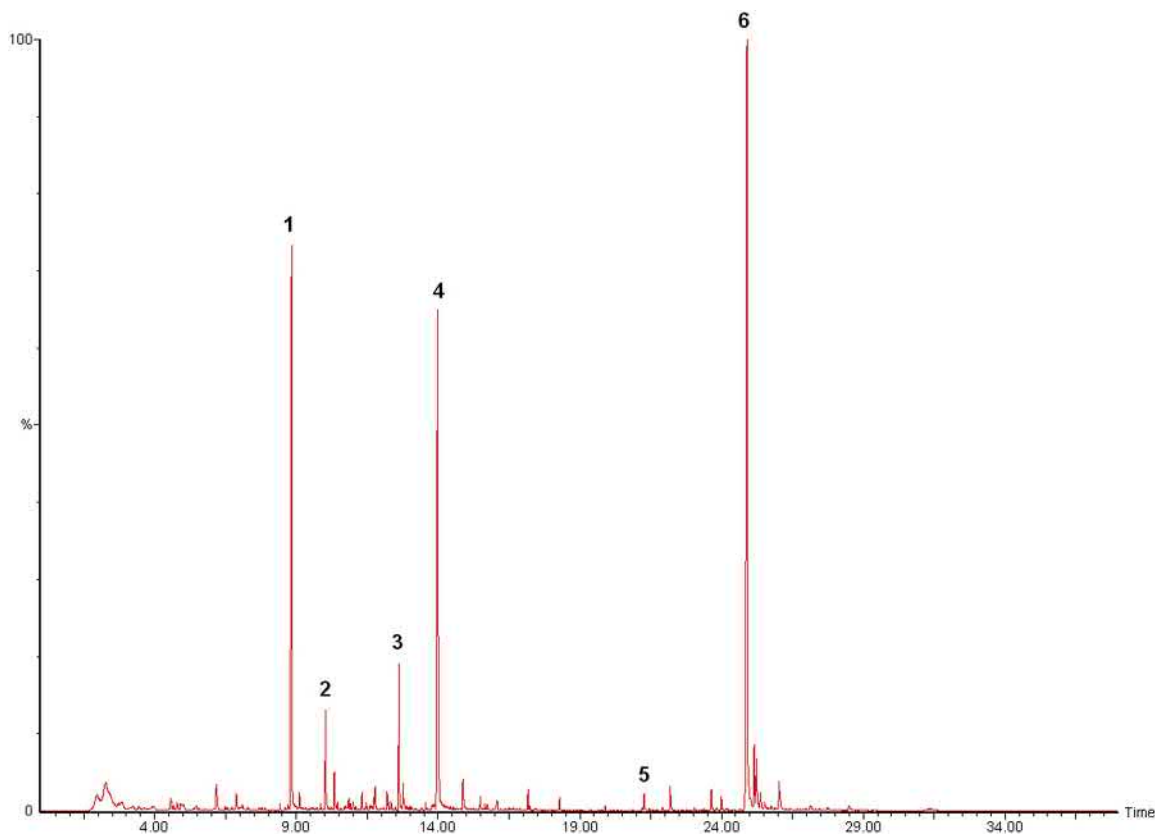


FIGURE 11.9 Pyrolysis of an epoxy powdercoat at 750°C. Peak #1, phenol; #2, methylphenol; 3, 4-(1-methylethyl)-phenol; #4, p-isopropenylphenol; #5, 4-(1-methyl-1-phenylethyl)phenol; and #6, bisphenol A.

treatments. Simultaneous derivatization with a methylating [14] or silylating [15] agent is applied to many samples, especially those that form polar products, particularly free fatty acids. By adding a methylating agent, such as tetramethylammonium hydroxide (TMAH), directly to the sample before pyrolysis, the polar compounds produced are methylated, improving the chromatography. This is a frequently used technique for the analysis of condensation polymers. With the help of TMAH at elevated temperatures, e.g., 500°C, ester linkages are hydrolyzed, and the

active hydrogen replaced with a methyl group. Fig. 11.11 illustrates a standard pyrogram of poly(ethylene terephthalate) and one that underwent thermally assisted hydrolysis and methylation (TMAH). PET under pyrolysis conditions produces acid and ester fragments, representative of the original polymer, while PET under TMAH mostly produces a methylated version of the terephthalate monomer, resulting in a cleaner, simpler chromatogram.

The ability to perform multiple temperature steps on a single sample is useful, as different

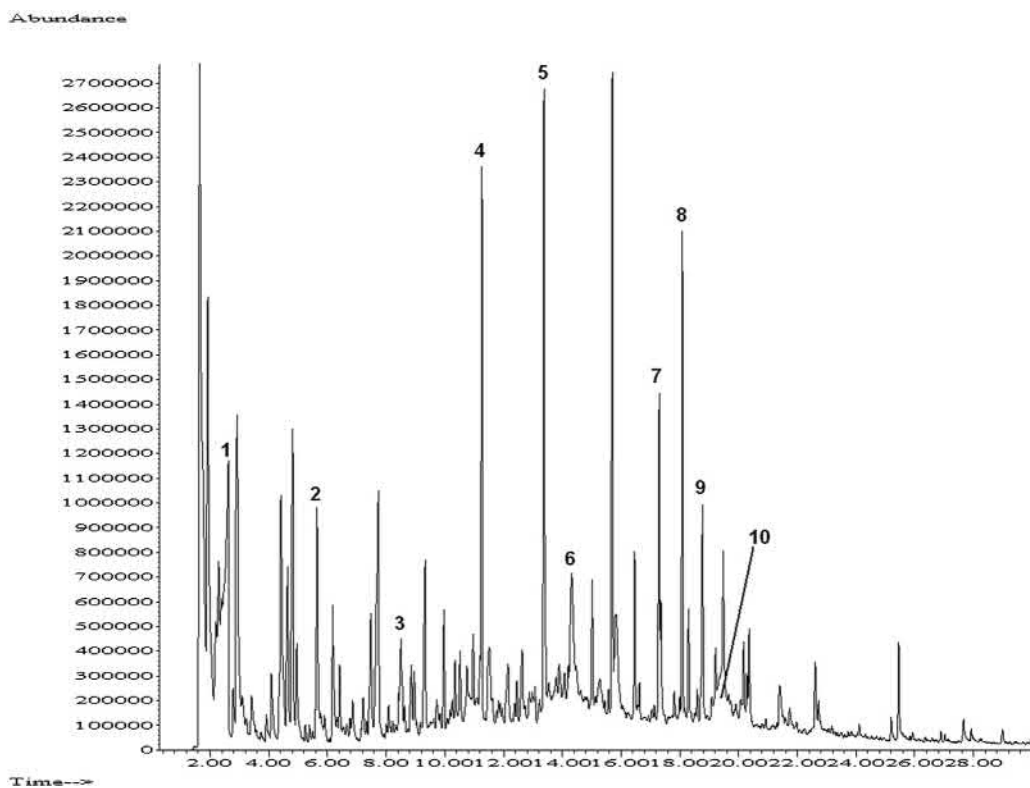


FIGURE 11.10 Pyrolysis of wood at 600°C. Peak #1, acetic acid; #2, 2-furancarboxaldehyde; #3, 5-methyl-2-furancarboxaldehyde; #4, 2-methoxyphenol; #5, 2-methoxy-4-methylphenol; #6, 5-(hydroxymethyl)-2-furancarboxaldehyde; #7, vanillin; #8, eugenol; #9, 1-(4-hydroxy-3-methoxyphenyl)ethanone; and #10, levoglucosan.

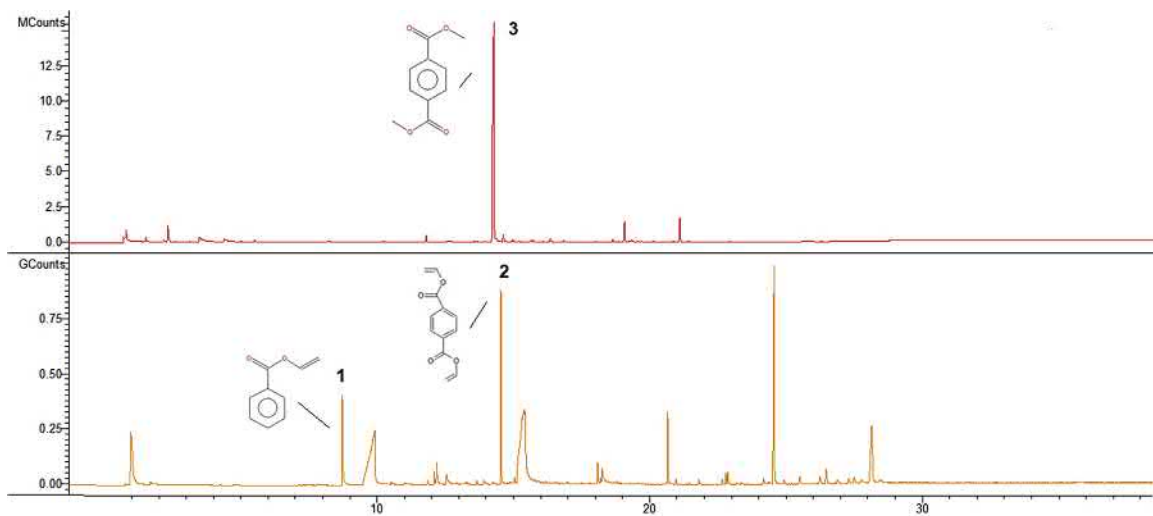


FIGURE 11.11 Polyethylene(terephthalate): Pyrolysis, 700°C (bottom), TMAH, 500°C (top) Peak #1, vinyl benzoate, Peak #2 divinyl terephthalate, Peak #3, dimethyl terephthalate.

components may have different decomposition temperatures [17]. Thermal desorption products, such as additives, can be separated from the polymer, and even polymers with different decomposition temperatures can be separated from each other. Fig. 11.12 is an example of thermal paper heated to three sequential temperatures; at each temperature, a GC separation is performed. At 300°C, desorption products, such as additives, are seen, at 400°C cellulose in the paper pyrolyzes,

and finally at 550°C, only the polystyrene coating on the paper remains.

Samples may also be processed at low temperatures or using slow heating rates over a protracted time, with the collection of the products on a trap before transfer to the GC for analysis. The use of a trap also permits heating in a reactive atmosphere such as air or oxygen [16] to study oxygenation without introducing air into the GC system. Fig. 11.13 illustrates this technique with a filament pyrolyzer.

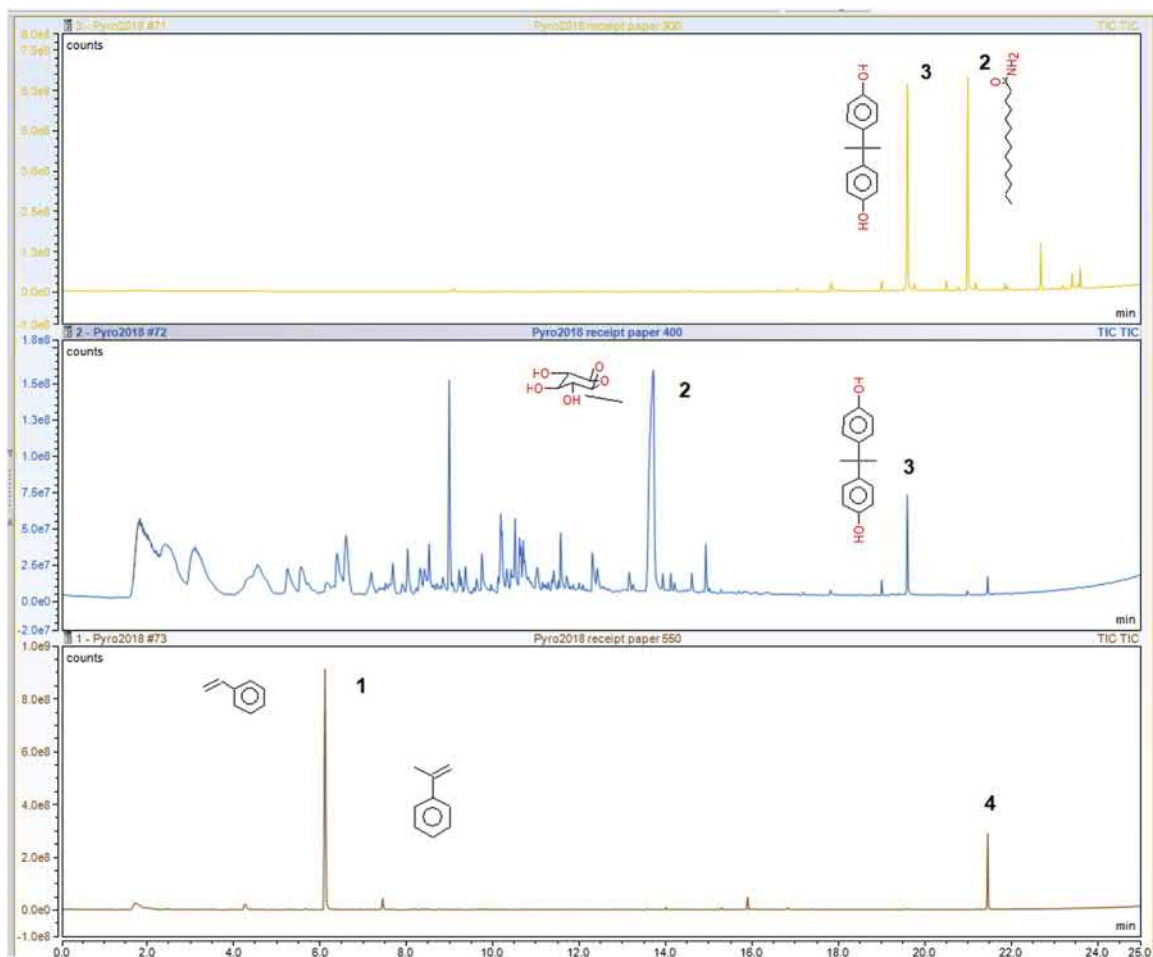


FIGURE 11.12 Thermal paper heated first at 300°C (top), 400°C (center), then 550°C (bottom) Peak #1, styrene, Peak #2, levoglucosan, Peak #3, bisphenol A, Peak #4, styrene trimer.

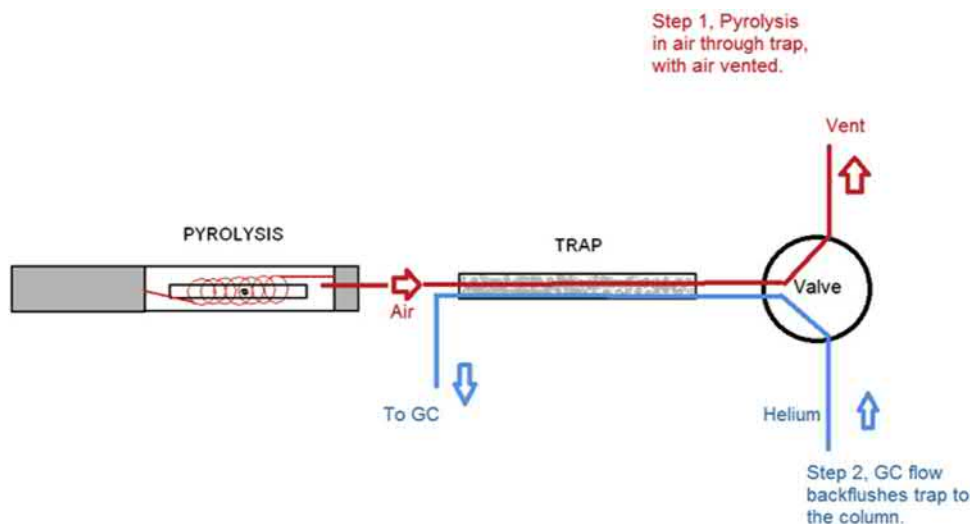


FIGURE 11.13 Illustration of pyrolysis in reactant gas.

After the pyrolysis step, the sorbent trap can be backflushed with carrier gas for analysis. As shown in Fig. 11.14, when polyethylene is pyrolyzed in air, in addition to the triplicate peak pattern from random scission, alcohols and aldehydes emerge, as the oxygen in the

air reacts with the free radicals formed during pyrolysis (oxidation).

Some systems have incorporated catalytic reactors [18] to process the pyrolysate and modify it after pyrolysis, to permit reforming or hydrogenation.

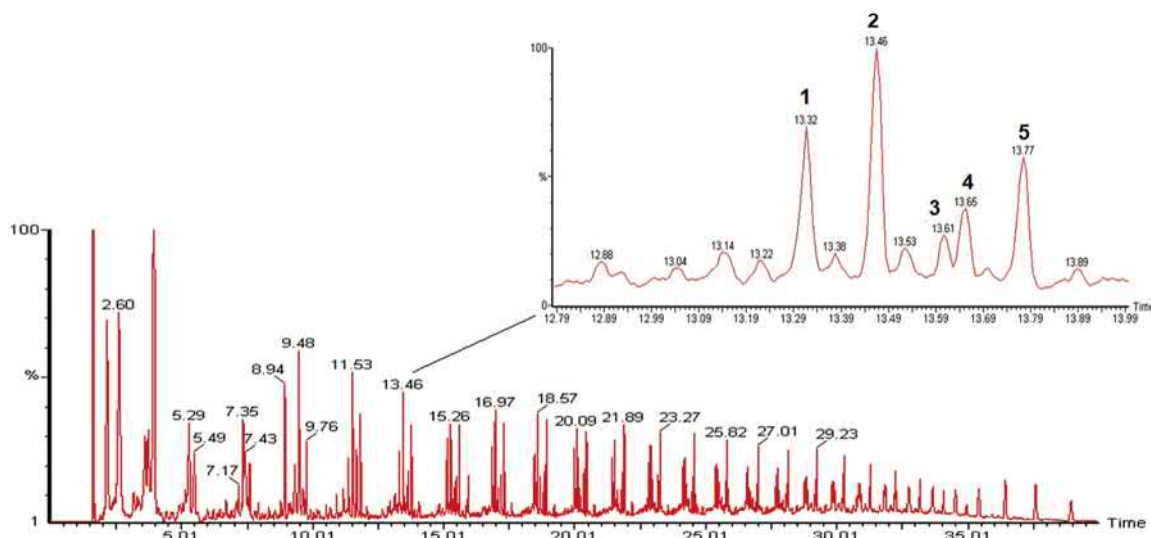


FIGURE 11.14 Pyrolysis of polyethylene in Air at 750°C Peak #1, dodecadiene, Peak #2, dodecane, Peak#3, dodecane, Peak #4, decanol, Peak #5, decanal.

References

- [1] T.P. Wampler, Temperature as a sample preparation tool in the analysis of materials by GC-MS, *LC GC* 17 (2S) (1999) 14–17.
- [2] I. Ericsson, Pyrolysis nomenclature, *J. Anal. Appl. Pyrolysis* 14 (1989) 219–221.
- [3] S. Tsuge, H. Ohtani, Structural characterization of polymeric material by pyrolysis-GC/MS, *Polym. Degrad. Stabil.* 58 (1–2) (1997) 109–130.
- [4] B.A. Stankiewicz, P.F. van Bergen, M.B. Smith, J.F. Carter, D.E.G. Briggs, R.P. Evershed, Comparison of the analytical performance of filament and curie-point pyrolysis devices, *J. Anal. Appl. Pyrolysis* 45 (1998) 133–151.
- [5] T.P. Wampler, *Pyrolysis Techniques in the Analysis of Polymers and Rubbers*, Encyclopedia of Analytical Chemistry, John Wiley & Sons, 2000.
- [6] B.K. Kochanowski, S.L. Morgan, Forensic discrimination of automotive paint samples using pyrolysis-GC/MS with multivariate statistics, *J. Chromatogr. Sci.* 38 (3) (2000) 100–108.
- [7] L. Gueissaz, G. Massonnet, Study on the discrimination of tires using chemical profiles obtained by Py-GC/MS, *J. Anal. Appl. Pyrolysis* 124 (2017) 704–718.
- [8] K.D. Jansson, T.P. Wampler, C.P. Zawodny, Analysis of coatings using pyrolysis-GC/MS, *Paint Coat Ind. Mag.* 25 (2) (2009) 42–46.
- [9] T. Learner, The analysis of synthetic paints by Py-GC/MS, *Stud. Conserv.* 46 (4) (2001) 225–241.
- [10] G. Chiavari, S. Prati, Analytical pyrolysis as a diagnostic tool in the investigation of works of art, *Chromatographia* 58 (2003) 543–554.
- [11] H. Matsubara, A. Yoshida, H. Ohtani, S. Tsuge, Compositional analysis of UV-cured acrylic ester resins by pyrolysis-gas chromatography in the presence of organic alkali, *J. Anal. Appl. Pyrolysis* 64 (2) (2002) 159–175.
- [12] R.S. Lehrle, I.W. Parsons, M. Rollinson, Thermal degradation mechanisms of nylon 6 deduced from kinetic studies by pyrolysis-GC, *Polym. Degrad. Stabil.* 67 (1) (2000) 21–33.
- [13] D. Meier, I. Fortmann, J. Odermatt, O. Faix, Discrimination of genetically modified poplar clones by analytical pyrolysis-gas chromatography and principal component analysis, *J. Anal. Appl. Pyrolysis* 74 (2005) 129–137.
- [14] J.M. Challinor, Review: the development and applications of thermally assisted hydrolysis and methylation reactions, *J. Anal. Appl. Pyrolysis* 61 (2001) 3–34.
- [15] L. Osete-Cortina, M.T. Domenech-Carbo, Characterization of acrylic resins used for restoration of artworks by pyrolysis-silylation-gas chromatography/mass spectrometry with hexamethyldisilazane, *J. Chromatogr. A* 1127 (1–2) (2006) 228–236.
- [16] T.P. Wampler, E.J. Levy, Effect of heating rate on oxidative degradation of polymeric materials, *J. Anal. Appl. Pyrolysis* 8 (1985) 153–161.
- [17] T.P. Wampler, C.P. Zawodny, K.D. Jansson, Multistep thermal characterization of polymers using GC-MS, *Am. Lab.* 39 (6) (2007) 16–19.
- [18] D.A. Gunawardena, S.D. Fernando, Deoxygenation of methanol over ZSM-5 in a high-pressure catalytic pyroprobe, *Chem. Eng. Technol.* 34 (2) (2011) 173–178.

Conventional detectors for gas chromatography

Colin F. Poole

Department of Chemistry, Wayne State University, Detroit, MI, United States

12.1 Introduction

Numerous methods have been proposed for the detection of compounds separated by gas chromatography. Some of these have become commercially available and meet the general needs for typical problems. They can be conveniently grouped into ionization, bulk physical property, optical and electrochemical detectors based on the principle of the detection mechanism [1–3]. These detectors are rugged, require minimal maintenance and training, and are simply expected to work on demand. These detectors are the basis of this chapter. Detectors still at a research stage and those instrumentally more sophisticated for identification and/or quantification are described in the chapters that follow (Chapters 13–16).

Gas chromatography is typically used for the separation of volatile organic compounds. Salts are rarely analyzed directly and inorganic compounds, except for a few organometallic compounds, are usually handled by other techniques. Detection requirements are largely limited, therefore, to compounds containing the elements carbon, hydrogen, oxygen, nitrogen,

sulfur, phosphorous, and the halogens. These elements form a large number of diverse compounds that may present separation difficulties but simplify general requirement for detection. This is true for element-selective detectors and also justifies their development for gas chromatography, since the total number of detectors required is manageable compared to the larger number of elements in the periodic table.

Gas chromatographic detectors can be classified in different ways according to their characteristic properties, Table 12.1 [2,4]. By application they can be grouped into universal, selective, or specific and by response type, as mass or concentration-dependent. Universal detectors are able to detect all compounds (or most compounds) that elute from the column. Selective detectors respond only to specific compounds based on some molecular, elemental, or physical property. Specificity refers to the capability of a detector to respond to a certain atom or functional group to the exclusion of all others.

A concentration-sensitive detector will generate a response proportional to the amount of a compound in the carrier gas expressed in concentration units (e.g., ng mL^{-1}). They are

TABLE 12.1 Classification terms for conventional gas chromatographic detectors.

Term	Description
Response type	Universal, selective, specific, reaction-based
Response	Mass- or concentration-dependent
Sensitivity	The signal output per unit concentration or mass of test substance in the carrier gas
Minimum detectability (Minimum detection limit)	Amount of test substance that produces a detector signal equal to twice (or three times) the noise Mass detector = $(2 \times \text{noise} \times \text{mass on column/area}) \text{ units} = \text{mass/time}$ (e.g., pg s^{-1}) Concentration detector = $(2 \times \text{noise} \times \text{mass on column/area} \times \text{total gas flow through detector})$ units = mass/volume (e.g., pg ml^{-1})
Dynamic range	The range for the amount of test substance over which a change in amount produces a change in the detector signal
Linear range	Range over which the detector response per sample amount injected is constant to within $\pm 5\%$ as determined from a linearity plot
Noise	The amplitude of the baseline envelope, which includes all random variations of the detector signal of a frequency $\geq 1 \text{ cycle min}^{-1}$
Selectivity	Relative response of the detector for one compound type (or element) versus another compound (or element). Element-selective (defined atom identity). Structure-selective (defined arrangement of atoms in a portion of a molecule)
Specific	A selective detector with a very high degree of selectivity

typically nondestructive and can be coupled in series with other detectors [5]. Mass-sensitive detectors respond to the mass of compound passing through the detector in a given time expressed in units of mass per unit time (e.g., pg s^{-1}). Adding makeup gas at the end of the column does not alter the response of a mass-sensitive detector while for a concentration-sensitive detector its response is proportional to the volume of makeup gas added. For both mass-sensitive and concentration-sensitive detectors, narrower peaks yield better detection limits because both mass/time and concentration are higher.

One metric used to compare detectors is the limit of detection or simply the detection limit. This is the minimum amount of substance

that can be distinguished from the signal background. This is expressed as an instrument detection limit and should be distinguished from method detection limits. It is evaluated as the amount (concentration or mass per unit time) of a compound that can be detected with a specified signal-to-noise ratio (S/N) of typically 2 or 3. The greater the S/N for a given compound and set of conditions, the better the detector is suited for the detection of minute amounts of that compound.

The detector output contains signal associated with the detector response to the compound and noise originating from the interactions of the detector with its environment and from its electronic circuitry [6]. All detectors have a characteristic noise associated with random and/or

systematic events in the detection process, electronic circuitry, and fluctuations in temperature, vibration, and pressure. Some of this high-frequency noise can be minimized by analog and/or digital filters. Compromises are made to balance detector response time and noise suppression. For most real analyses the major source of noise is chemical noise that manifests itself as low-frequency noise. Typical sources are impurities in the carrier gas, stationary-phase bleed, and carryover from earlier sample injections. These result in rolling baselines, exaggerated baseline rise with an increase in column temperature, ghost peaks, and a general elevated overall background.

The usable (operating) range over which a detector generates a signal that varies with the amount of a compound is called the dynamic range. The low end of this range is established by the limit of detection and the upper end by detector saturation. In the saturation region the detector response is no longer a function of the amount of compound in the carrier gas stream. The linear range refers to the portion of the dynamic range over which the change in detector signal increases linearly with the amount (mass or concentration) of the compound. It should be noted that not all detectors have a linear response mechanism and the absence of a suitable linear dynamic range is not in itself a problem. Modern data systems can easily deal with nonlinear calibration. Nevertheless, a large linear dynamic range simplifies calibration procedures and data reduction, and therefore it is still a useful attribute for a detector to have.

For element- and structure-selective detectors their capability to detect the compound type of interest while ignoring everything else is important. In this regard selectivity is determined as the ratio of the amount of a nontarget compound that generates an equivalent signal to the target compound(s). The larger the amount of nontarget species that meets this criterion, the more selective the detector response is to the target species. For example, selectivity might be expressed as $10^6 \text{ g C} / \text{g S}$ indicating that for

any carbon-containing compound without sulfur in an amount smaller than 10^6 times the amount of sulfur-containing compound, the detector will not register a response. Selective detectors usually provide better detection limits for target compounds because they are able to reject more chemical noise than a universal detector.

The sensitivity of a detector is the change in response per change in sample amount or concentration. A detector of higher sensitivity is one that can better differentiate between small changes in compound amounts and for a linear response detector is the slope of the calibration curve. It is not a surrogate for differences in the limit of detection but is often incorrectly used in this sense.

12.2 Ionization-based detectors

For typical separation conditions the carrier gases commonly used in gas chromatography behave as perfect insulators. This allows any mechanism that results in the production of ions to be an effective detection mechanism [4]. The fact that ions can be generated from neutral compounds by several processes provides a range of options for the design of detectors. In addition, any gas-phase element-selective or structure-selective ionization process can afford a mechanism for the design of detectors with low detection limits and high discrimination against compounds poorly ionized under the same conditions. In all cases, the quantitative basis of detector operation corresponds to changes in the observed ion current as an organic vapor is transported through the detector in an inert carrier gas.

12.2.1 Flame ionization detector

The flame ionization detector (FID) is the most widely used general-purpose detector for gas chromatography. It provides a near universal (unit carbon) response to organic compounds,

low detection limits, long-term stability, low dead volume, a fast response, and an exceptional linear response range. Typical performance characteristics are summarized in Table 12.2. Only the fixed gases (e.g., He, Ar, Ne, Xe, H₂, N₂, O₂), certain nitrogen oxides (N₂O, NO, etc.), compounds containing a single carbon atom bonded to oxygen or sulfur (e.g., CO₂, CS₂, COS, etc.), inorganic gases (e.g., NH₃, SO₂, etc.), water, formamide, and formic acid provide a weak or insignificant detector response. For other compounds its near unit carbon response means that the response of the FID is reasonably independent of compound structure for moderate and high-mass compounds with a limited number of heteroatoms. This allows a single compound to be used for the calibration of complex mixtures and percent composition reports for mixtures to be obtained with reasonable

accuracy directly from the sum of the detector response for all observed peaks. The influence of structure on the detector response is discussed subsequently. The early history of the development of the FID is described by Ettre [7].

A schematic diagram of an FID is shown in Fig. 12.1 [1–4,8,9]. The detector response results from the combustion of organic compounds in a small hydrogen–air diffusion flame. The carrier gas at the column exit is mixed with hydrogen (combustion gas) and possibly makeup gas at the narrow-orifice flame jet and burned gas at the jet in a chamber through which excess air is flowing. A glow plug engaged momentarily at start up serves as an igniter. A cylindrical electrode located a short distance above the flame collects the charged particles by application of a voltage (200–300 V) between the jet tip and the collector electrode. The potential is of sufficient

TABLE 12.2 Typical performance characteristics for the flame ionization and thermionic ionization detectors.

Parameter	Response characteristics	
<i>Flame ionization detector</i>		
Type	Carbon-selective detector	
Response mechanism	Mass dependent	
Minimum detection limit	$2 \times 10^{-12} \text{ g C s}^{-1}$	
Linear range	$10^6\text{--}10^7$	
<i>Thermionic ionization detector</i>		
	NP-mode	P-mode
Type	Element-selective detector	
Response mechanism	Mass dependent	
Minimum detection limit	$5 \times 10^{-14} - 5 \times 10^{-13} \text{ g N s}^{-1}$	
	$1 \times 10^{-14} - 2 \times 10^{-13} \text{ g P s}^{-1}$	$5 \times 10^{-14} \text{ g P s}^{-1}$
Linear range	10^5	10^5
Selectivity	Nitrogen and phosphorous	Phosphorous
	$10^4\text{--}10^5 \text{ g C/g N}$	
	$10^4\text{--}10^5 \text{ g C/g P}$	10^6 g C/g P
	$0.1\text{--}0.5 \text{ g P/g N}$	

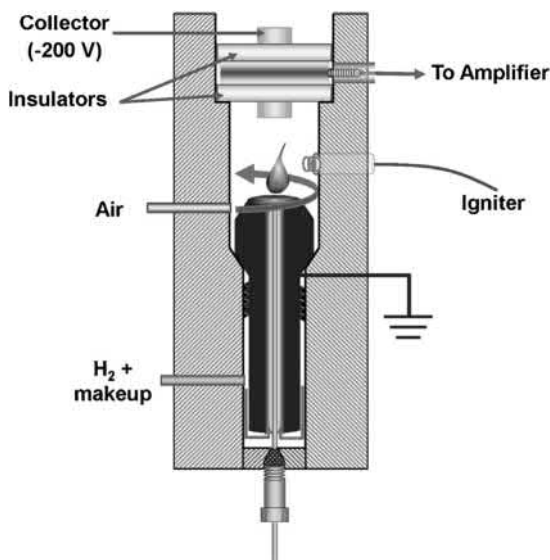


FIGURE 12.1 Schematic diagram of a flame ionization detector. From Ref. M.S. Klee, *Detectors*, in C.F. Poole (Ed.), *Gas Chromatography*, Elsevier, Amsterdam, 2012. p. 307–347; copyright Elsevier.

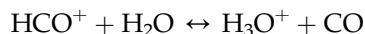
magnitude to ensure complete collection of the charged particles. Either the jet tip or collector electrode is usually grounded. Depending on the detector design, either electrons or positive ions are collected. The small ion currents (picoamps) are converted to a voltage and amplified by a precision electrometer. The limit of the detector response is largely the result of thermal noise and the upper end of the response range by the flame size, the bias voltage at the collector electrode, and detector geometry. The negligible unswept internal volume combined with fast transduction of the chemical signal ensures that the detector imposes minimal detector-based band broadening on the chromatographic signal for the most demanding separations. A data acquisition rate of 10 Hz is adequate for typical open-tubular column separations but for comprehensive two-dimensional and fast gas chromatography (peak widths at half height < 1 s), data acquisition rates higher than 50 Hz may be required [10].

Detector performance is influenced primarily by the ratio of the carrier gas to hydrogen to air flow rates and detector geometry (size of the jet tip orifice and position of the collector electrode) [9,10]. Less influential is the choice of carrier gas and detector temperature. The optimum response plateau is typically fairly broad, allowing operation over a reasonable range of gas flow rates without a large penalty in detector performance [1,3,5]. Generally, there is little benefit from selecting conditions different to those recommended by the manufacturer so long as these conditions have been optimized correctly.

The dominant reaction of carbon-containing compounds in a hydrogen–air diffusion flame is their combustion to carbon dioxide and water. The production of ions is a minor reaction pathway, perhaps a few ions per million carbon-containing molecules entering the flame, which contributes to the difficulty of studying the ion-production mechanism [11,12]. In addition, the temperature and chemical composition of the flame are not uniform. The base of the flame is hydrogen-rich and contains partially fragmented compounds, which are thought to approach complete combustion as they migrate toward the flame tip. At the flame periphery oxygen diffuses into the flame creating an oxygen-rich mantle depleted by combustion in the direction of the flame center. The flame also contains a large concentration of radicals (H^\bullet , O^\bullet , and OH^\bullet , etc). In the hottest part of the flame, a temperature of about 1500–2000°C is reached but is too low to explain the production of ions. It is assumed that ion formation results from chemical ionization of CHO^* produced by reaction of O^\bullet and CH^\bullet



The parent CHO^+ ion then rapidly reacts further to produce H_3O^+ ions and other secondary hydrocarbon ions



The ionization process is expected to be a first-order reaction, explaining the linear detector response. Two steps are thought to be important in the aforementioned process: radical formation, requiring the absence of oxygen, and chemical ionization of radicals by reaction with atomic or molecular oxygen in excited states. Organic compounds are most likely degraded in the hydrogen–air diffusion flame by attack by hydrogen atoms causing fission of carbon–carbon bonds. One point of view is that the hydrocarbon radicals produced by fission are unstable and undergo a cascade of fast fractionation and hydrogenation reactions with all carbon atoms eventually converted to methane [11]. The alternative point of view is less specific concerning the final product of the cascade of fast fractionation and fission reactions. These reactions result in a pool of kinetically coupled radicals (e.g., CH^\bullet , CH_2^\bullet , $\text{C}_2\text{O}^\bullet$, etc.) indistinguishable in their subsequent fast reactions [12]. The linear relationship with the effective carbon number stems from their presence in the same pool of connected reactions. Both reaction mechanisms can explain the near uniform response of the FID to carbon-containing compounds and the effect of heteroatoms in the hydrocarbon structure on the detector response.

The FID response is the highest for hydrocarbons, being proportional to the number of carbon atoms, while substances containing oxygen, nitrogen, sulfur, or halogens yield a lower response, depending on the characteristics of the carbon–heteroatom bond and the electron affinity of the combustion products [8,13]. The lower response is due to competition between hydrogenation of the carbon–heteroatom bond and hydrogen abstraction with formation of neutral species (e.g., CO, HCN), which are poorly ionized in the flame.

The effective carbon number concept was developed in the 1960s to account for the lower detector response for compounds containing heteroatom functional groups [4,13,14]. The

effective carbon number is defined as the number of equivalent alkane carbon atoms that would produce the same detector response as the compound of interest. The presence of oxygen in a ketone, aldehyde, or ether functional group reduces the apparent carbon number by one. The C=O structure is retained in the combustion process preventing the carbon atom from entering into the flame radical chemistry. Ethers behave in a similar manner to carbonyl groups. Oxygen in an alcohol group behaves differently and the availability of the carbon atom to participate in the combustion process depends on the type of alcohol group. Information for other fragments is summarized in Table 12.3 and can be interpreted in a similar way. Bond strengths are known to depend on structure as the capability of atoms to share electron density depends on the identity of their nearest neighbors and their connectivity. Thus, the information in Table 12.3 should be considered general and qualitatively useful. If accurate response factors are required for calibration purposes for small molecules with an unfavorable ratio of carbon atoms to heteroatoms, these should be determined experimentally.

12.2.2 Thermionic ionization detector

Contemporary versions of the thermionic ionization detector (TID) evolved out of earlier studies of alkali-metal-doped FIDs [4,15]. Adding an alkali metal salt to a flame enhanced the response of the FID to compounds containing certain elements, such as N, P, S, B, and some metals. In early detector designs, however, the response was unreliable and critically dependent on experimental parameters. All modern versions of the TID detector are related in one way or another to a general design proposed by Kolb and Bischoff in 1974 [16].

A schematic diagram of a modern TID is shown in Fig. 12.2 [2,4]. The detector employs a

TABLE 12.3 Approximate contributions of molecular fragments to the response of the flame ionization detector determined as the effective carbon number.

Atom	Type	Effective carbon number
C	Aliphatic	1.0
C	Aromatic	1.0
C	Olefinic	0.95
C	Acetylenic	1.30
C	Carbonyl	0
C	Carboxyl	0
C	Ester	-0.50
C	Nitrile	0.3
O	Ether	-1.0
O	Primary alcohol	-0.5
O	Secondary alcohol	-0.75
O	Tertiary alcohol	-0.25
N	In amines	Similar to O in alcohols
Cl	On an olefinic C	0.05
Cl	On an aliphatic C	-0.14
Cl	Two or more on aliphatic C	-0.12 per Cl
Br	On an aliphatic C	-0.25
I	On an aliphatic C	-0.14

solid surface, composed of a ceramic or glass matrix doped with an alkali metal (usually rubidium or cesium) salt, in the form of a bead or cylinder, molded onto an electrical heater wire as the thermionic source. A current applied to the wire controls the source temperature, which is typically set to 400–800°C. The carrier gas is combined with hydrogen at the detector base and flows through a jet where it is mixed with air. The flow of detector gases is insufficient for combustion, in contrast to the FID, and a

plasma is formed in the immediate vicinity of the heated thermionic source. The thermionic source is located just above the jet tip and the cylindrical collector electrode either surrounds the source or is located just above it. A potential of a few hundred volts is set between the collector electrode and jet tip for collection of (usually) negative ions and the ion current is measured by an electrometer. The detector response is fast and the detector is suitable for use in comprehensive and fast gas chromatography [10,17]. All versions of the TID exhibit some loss of sensitivity and selectivity in use necessitating periodic source replacement and routine checks on calibration. Some solvents, particularly chlorinated solvents and excess silylating reagents, should be avoided or vented from the detector to maintain detector stability and extend source lifetime.

The dilute mixture of hydrogen in air forms a plasma (or boundary layer) localized at the surface of the hot thermionic source. The source is responsible for dissociation of hydrogen molecules into reactive hydrogen radicals and the formation of a reactive chemical environment containing hydrogen, oxygen, and hydroxyl radicals, water, and the original detector gases. A hydrogen-rich plasma is used for nitrogen and phosphorous detection (NP-mode) and an oxidizing plasma for higher selectivity toward phosphorous (P-mode). Compounds entering the hot reactive boundary layer are efficiently decomposed into fragments. Those of high electronegativity, e.g., NO_2^\bullet , CN^\bullet , and PO_2^\bullet are thought to be of particular importance in explaining the selectivity of the detector response [18,19]. They act as precursor species for the negative ion products CN^- , PO^- , PO_2^- , and PO_3^- responsible for the enhanced detector response for nitrogen- and phosphorous-containing compounds. However, the detailed mechanism whereby these decomposition products become selectively ionized is less clear [4]. The two dominant theories differ in whether the interaction between the alkali metal atoms

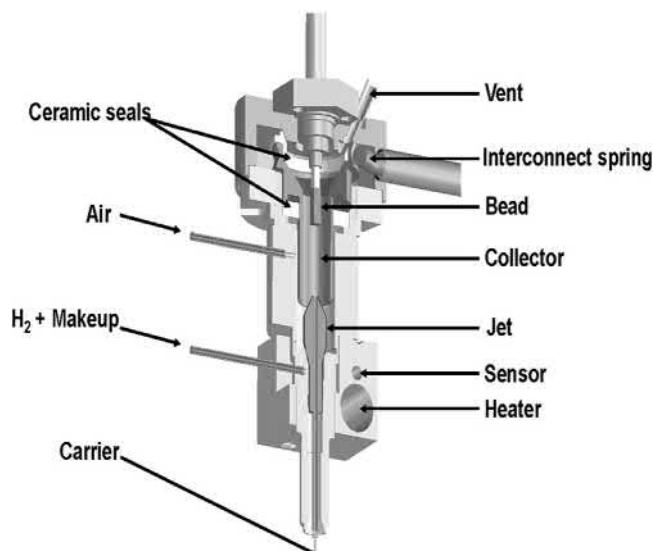


FIGURE 12.2 Schematic diagram of a thermionic ionization detector. From Ref. M.S. Klee, *Detectors*, in C.F. Poole (Ed.), *Gas Chromatography*, Elsevier, Amsterdam, 2012. p. 307–347; copyright Elsevier.

and organic fragments occurs as a homogeneous reaction in the gas phase or is purely a surface phenomenon.

Although the TID requires more attention than an FID, it is not particularly difficult to operate. Discrimination against nitrogen in the P-mode is good, but discrimination against phosphorous in the NP-mode for the determination of nitrogen compounds is poor. Typical detector response characteristics are summarized in Table 12.2.

The surface chemistry of the TID can be modified to allow positive-ion surface ionization for the detection of compounds with different functional groups [20]. In these applications the surface ionization detector is operated without a plasma source, and as a consequence, the detector response is proportional to the ionization potential for each compound. When configured as a reaction detector, the surface TID can be operated as a halogen-selective detector [21]. The column effluent is mixed with air and passed through a short tubular reactor at about 1000°C. Compounds are efficiently converted into their

oxidation products with halogen-containing compounds producing halide ions, free halogen atoms, and halogen molecules. The reactor products are swept into the ionization zone consisting of a heated platinum coil wrapped around an alkali-doped ceramic rod with a platinum bead attached to the end of the rod and held at a negative potential. The halogens are adsorbed onto the alkali-activated cathode and desorbed as either halogen atoms, halide ions, or alkali halide molecules. The halide ions (mainly) are then detected downstream of the thermionic source and are (largely) responsible for the detector signal. The detector has high selectivity ($\approx 10^4$ g C / g Cl), low detection limits ($\approx 1 \times 10^{-12}$ g Cl s⁻¹), and a more uniform and predictable response to halogen-containing compounds than the electron-capture detector (ECD).

12.2.3 Electron-capture detector

The ECD is a structure-selective detector with a response to organic compounds that covers about seven orders of magnitude [4,8,22].

Compounds containing halogen atoms or nitro groups, some organometallic compounds, and certain conjugated compounds have a strong detector response and in favorable cases can be detected at trace concentrations (5×10^{-14} g mL⁻¹). On the other hand, compounds of low electron affinity, for example, hydrocarbons, alcohols, phenols, amines, and aliphatic aldehydes, ketones, ethers, and esters barely register a response at normal concentrations, facilitating the selective detection of target compounds in complex matrices. The response of the ECD to halogen-containing compounds decreases in the order I > Br > Cl >> F and increases synergistically with multiple substitutions on the same or neighboring carbon atoms. Compounds containing reactive functional groups can be derivatized with a wide range of general and functional-group specific reagents to introduce a suitable electrophore to extend the scope of electron-capture detection to additional compounds of specific interest [23]. The ECD is the second most popular ionization-based detector for gas chromatography and owes this popularity to its unsurpassed sensitivity to a wide range of environmentally important and biologically active compounds. Characteristic detector properties for favorable compounds are summarized in Table 12.4.

The ECD is available in two general designs that differ in the method used to generate the population of thermal electrons responsible for the operating characteristics of the detector. From early times high-energy beta electrons generated by the decay of a radioisotope have been used as the primary source of ionizing radiation [4]. These particles produce a large number of secondary electrons through multiple collisions with carrier gas molecules forming a plasma of thermal electrons (mean energies 0.02–0.05 eV), radicals, and positive ions. Radioisotope-based detectors are subject to compliance with national regulations concerning storage, use, and transport of radioactive materials. Non-radioisotope-based detectors employ

TABLE 12.4 Typical performance characteristics for popular structure-selective detectors.

Parameter	Response characteristics
<i>(i) Electron-capture detector</i>	
Type	Structure-selective detector
Response mechanism	Concentration dependent
Minimum detectable level	5×10^{-14} g mL ⁻¹
Linear range	10^4 – 10^5
Selectivity	Variable (see text)
<i>(ii) Photoionization detector</i>	
Type	Structure-selective detector
Response mechanism	Concentration dependent
Minimum detectable level	10^{-11} g mL ⁻¹
Linear range	10^6
Selectivity	Depends on the photon source
<i>(iii) Helium ionization detector</i>	
Type	Universal
Response mechanism	Concentration dependent
Minimum detectable level	10^{-11} – 10^{-13} g mL ⁻¹
Linear range	10^5
Selectivity	Depends on the dopant gas

high-energy photons from a pulsed discharge in pure helium to ionize a support gas added downstream of the discharge [24]. A plasma of thermal electrons and positive ions is formed in the ionization chamber with properties similar to the radioisotope-based detector.

The majority of radioisotope-based detectors use nickel-63 as a source of β -electrons on account of its high thermal stability (to 400°C) and its operational and practical convenience. Although many general detector designs have been proposed over the years, those typically in use today are related in one way or another to either the coaxial cylinder or asymmetric configurations shown in Fig. 12.3. The radioisotope source is plated on the inside wall of a

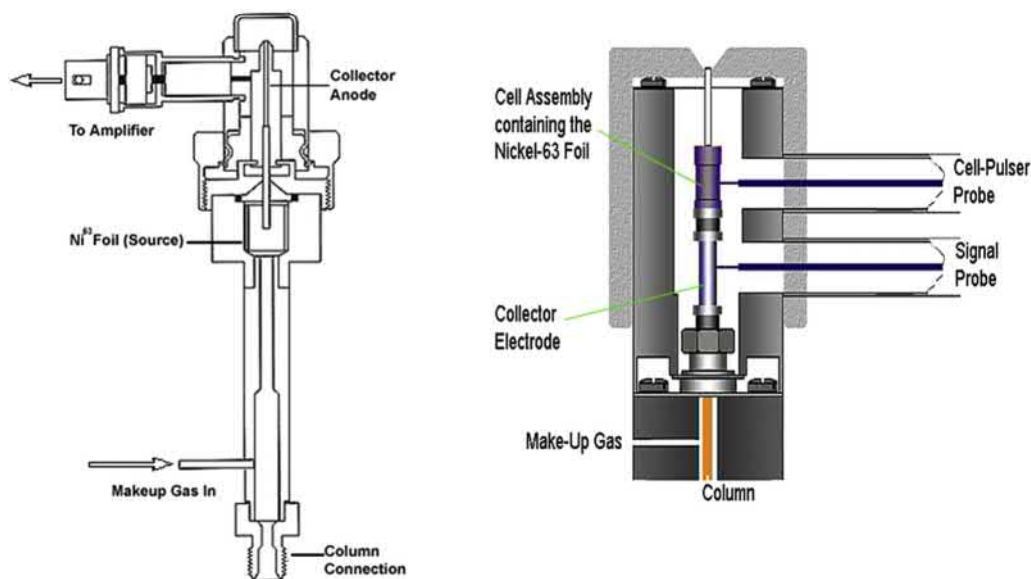


FIGURE 12.3 Schematic diagram of a radioisotope-based coaxial-cylinder (left) and asymmetrical (right) electron-capture detector. From Ref. C.F. Poole, *Ionization-based detectors for gas chromatography*, *J. Chromatogr. A* 1421 (2015) 137–153; copyright Elsevier.

flow-through ionization chamber. The low specific activity of the nickel-63 source requires a relatively large source area to obtain the desired background current and is more easily accommodated in the coaxial cylinder design. On the other hand, this configuration results in a relatively large ionization chamber volume (typically ≥ 1.5 mL). In the asymmetric design, locating the anode entirely upstream from the ionized gas volume minimizes the collection of long-range beta particles and facilitates a more compact design with an effective detector volume between 0.15 and 1.0 mL [10,25]. In addition, the direction of gas flow minimizes diffusion and convection of electrons to the anode. These relatively large detector volumes are not ideal for fast separations using open-tubular columns of narrow internal diameter. Makeup gas is typically added at the column exit to reduce the effective detector dead volume to preserve column efficiency at the expense of sample dilution and a reduced detector response. High-purity

hydrogen and helium are typically used as carrier gases, with argon containing 5%–10% methane or nitrogen as the makeup gas to minimize other interactions (e.g., Penning reaction) besides those occurring by electron capture. Application of a square-wave potential to the ionization chamber allows collection of the thermal electrons and establishes a steady-state (or baseline) detector current. When an electron-capturing compound enters the ionization chamber, thermal electrons are removed by formation of negative ions. Owing to their relatively slow velocity and more favorable neutralization by positive ions, these negative ions do not reach the collector electrode. Thus, in the presence of electron-capturing compounds, the population of thermal electrons is reduced and the detector current is smaller compared with the steady-state current in the absence of electron-capturing compounds. This decrease in the detector standing current within the dynamic operational range of the detector is linearly

proportional to the concentration of the electron-capturing compound passing through the ionization chamber. In practice, virtually all detectors are operated in the constant current mode, in which the pulse frequency of the applied voltage is varied throughout the separation to maintain the detector current at a reference value [26]. The detector signal is a voltage proportional to the pulse frequency. This has the advantage of increasing the linear response range and reduces detector disturbance from column contamination. For a few compounds with ultrafast electron attachment rate constants, a nonlinear response is observed, but these compounds are the exception [27].

The ECD is a concentration-dependent detector and its response depends on the flow rate and purity of the carrier and makeup gases, as well as specific detector design and operating characteristics (including detector temperature), and the contribution of background contamination from the column and chromatographic system [28]. For compounds that undergo dissociative electron capture with bond breaking (e.g., halogen-containing compounds), the highest detector response is usually obtained at the maximum detector operating temperature. For compounds that undergo nondissociative capture (electron attachment with the preservation of bond order), the highest response typically corresponds to the lowest practical detector operating temperature, but not less than the highest column temperature used for the separation.

The pulsed discharge electron-capture detector (PDECD) generates thermal electrons by photoionization of an additive gas (dopant) downstream of the discharge zone where a small bias potential allows isolation of the thermal electrons and their interaction with the column effluent [24,29]. A schematic diagram of the PDECD is shown in Fig. 12.4 [4]. A pulsed discharge in pure helium is used to generate high-energy photons to ionize a dopant gas, usually methane or xenon (1%–5% v/v) in helium,

added downstream of the discharge. The helium discharge gas is introduced at the top of the detector and flows through the discharge region and into the ionization region. The flow is strong enough to minimize diffusion of the dopant gas and column effluent into the discharge region. The dopant gas is ionized producing electrons, which are reduced to thermal energies by inelastic collision and attracted into the electron-capture region by a small bias voltage. The column effluent is introduced at the detector base close to the collector electrode. The PDECD uses a variable dc bias to maintain a constant direct current. The increase in bias voltage is proportional to the concentration of electron-capturing compound entering the detector and provides the detector signal. Operation in the constant-current mode extends the linear range of the detector and simplifies detector operation.

In general, the response mechanisms of the PDECD and radioisotope-based ECD are identical and result in similar detection limits. The PDECD has no specific regulatory compliance issues similar to those associated with radioisotope-based detectors. On the other hand, the detector requires a constant supply of ultrahigh-purity helium (about 30 mL min⁻¹), which is becoming increasingly expensive as helium production declines.

A general understanding of the ECD response is based on the kinetic model of Wentworth and coworkers and applies equally well to the radioisotope-based and pulsed discharge ECDs [22,24,30]. In this model the ionization chamber is treated as a homogeneous reactor into which electrons are continuously introduced at a constant rate and electron-capturing compounds are added at a variable rate in a constant flow of carrier and makeup gases. The major consumption of electrons is via electron capture and recombination with positive ions. The model can be expanded to allow for the presence of electron-capturing contaminants and the formation of excited-state negative ions. The kinetic model provides a reasonable explanation of the

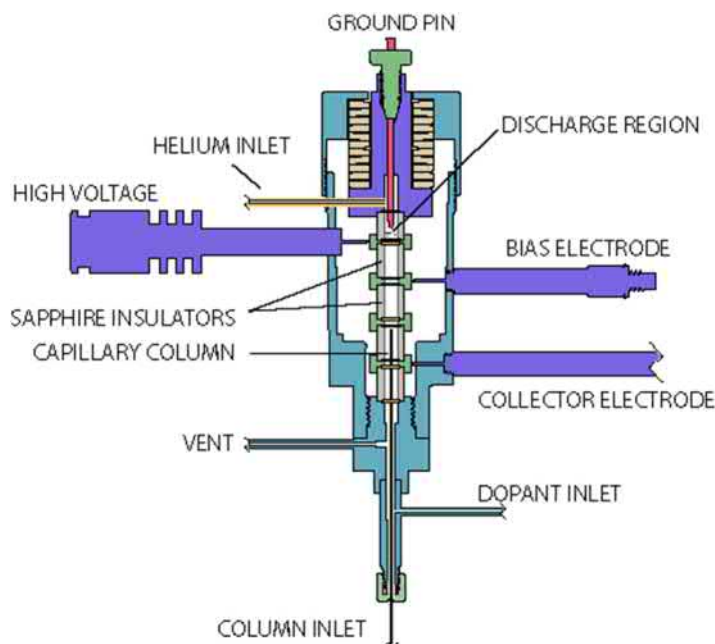


FIGURE 12.4 Schematic diagram of a pulsed discharge electron-capture detector. From Ref. C.F. Poole, *Ionization-based detectors for gas chromatography*, *J. Chromatogr. A* 1421 (2015) 137–153; copyright Elsevier.

detector response in the constant-current mode and the temperature dependence of the detector response. Exactly calculated solutions, however, are uncommon. This is because the necessary rate constants are usually unavailable, and the identity and relative concentration of all species present in the detector are uncertain.

12.2.4 Photoionization detector

For typical organic compounds, photons with energies between 5 and 20 eV are required for ionization usually resulting in the formation of molecular ions without further fragmentation. The first commercially successful PID detectors appeared in the early 1970s and employed a detector design that separated the photon source from the ionization chamber by a photon-transparent window material [2,8,31]. This facilitated the independent optimization of photon

production and ion collection compared with early open source designs. Photoionization using typical gas discharge sources is an inefficient process (<0.1% ionization), and this together with the neutralization of ions at the collector electrode supports its classification as a nondestructive detector suitable for series coupling with other, generally destructive, detectors [5]. The detector is easily miniaturized and is a popular choice for portable gas chromatographs [32].

A schematic diagram of a typical photoionization detector is shown in Fig. 12.5 [4]. The photon source is a compact low-pressure gas-discharge lamp emitting a line spectrum of specific energies that depends on the choice of fill gases and window material. Typical fill gases and their emission energies are summarized in Table 12.5 [31]. An optically transparent window made of a metal fluoride or sapphire, Table 12.6, separates the discharge compartment from the ionization chamber. The window material also acts

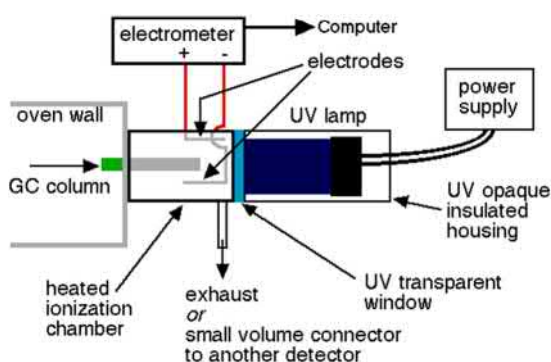


FIGURE 12.5 Schematic diagram of a photoionization detector. From Ref. C.F. Poole, *Ionization-based detectors for gas chromatography*, *J. Chromatogr. A* 1421 (2015) 137–153; copyright Elsevier.

as a cutoff filter and the combination of discharge gas and window material dictates the nominal output energy of the source. The highest energy emission line that can pass through the window without significant attenuation is usually designated as the nominal energy of the source. Sources of different nominal energies (8.3, 9.5, 10.2, 10.9, and 11.7 eV) provide for the selective ionization of organic compounds based on their ionization potential and

discrimination of matrix components with higher ionization potentials. The column effluent passes through the thermostatted ionization chamber and between two annular electrodes separated by an insulator. Shielding the electrodes from the photon flux is important to minimize the background effect generated by the photoelectron effect at electrode surfaces. An electric field of a few hundred volts is applied between the electrodes to collect ions and electrons and the current amplified by an electrometer.

An alternative detector design employs a pulsed gas discharge with an open source configuration [33,34]. Photons are generated by a high-voltage atmospheric pressure discharge in helium doped with auxiliary gases to provide a range of photon energies. Photons produced in the helium discharge are then consumed in the ionization of the dopant gases. In the presence of argon the main photon emission occurs as a broad band between 9.2 and 10.3 eV with resonance line emission at 11.6 and 11.8 eV. In the presence of krypton the main photon emission occurs as a broad band between 8.1 and 8.8 eV with resonance line emission at 10.1 and 10.6 eV. The detector is constructed from a

TABLE 12.5 Typical line spectra for low-pressure gas discharge sources for photoionization detection.

Lamp type	Fill gas	Wavelength(nm)	Energy(eV)	Relative intensity (%)	Common applications
8.3	Xe	147	8.44	100	Polycyclic aromatic compounds
9.5 ^a	Xe	119.3	10.40	0.18	Simple aromatics, mercaptans, hydrogen sulfide, and amines
		139.6	9.57	2.1	
		147	8.41	97.6	
10.2	Kr	116.6	10.64	17.1	Most compounds except for permanent gases, C ₁ –C ₄ alkanes, methanol, acetonitrile, and chloromethanes
		123.6	10.03	82.9	
11.7	Ar	104.9	11.82	26.2	Formaldehyde, chloromethanes, ethane, and acetylene
		106.6	11.62	71.8	

^a Also produces minor emissions at 114 nm (10.88 eV, 0.03%); 117.2 nm (10.58 eV, 0.01%); and 125 nm (9.92 eV, 0.05%).

TABLE 12.6 Typical window materials used for the separation of the photon source and ionization chamber and their effective wavelength cutoff limit.

Window material	Cutoff limits ^a	
	Wavelength (nm)	Energy (eV)
LiF	104	11.9
MgF ₂	112	11.1
CaF ₂	122	10.3
NaF	132	9.4
BaF ₂	134	9.2
Sapphire	143	8.7

^a Window material will attenuate all energies higher than the cutoff limit.

quartz tube divided into two zones with electrodes located at the end flanges and middle section.

The minimum detection level of the PID may be 5–50 times better than the FID for favorable compounds, while in other cases, it may not respond at all or respond poorly, as determined by the ionization potential of the compound and the detector photon energy and flux. Since response factors are structure dependent and vary over a wide range, calibration for each compound of interest is required. Characteristic detector properties for favorable compounds are summarized in Table 12.4.

12.2.5 Helium ionization detector

The helium ionization detector (HID) is a universal and ultrasensitive detector used primarily for the analysis of compounds with a poor response to the FID and present at too low a concentration for detection with a thermal conductivity detector. Representative examples include the analysis of permanent gases (H₂, O₂, N₂, Ar, Kr) as well as some volatile organic (CH₂O, CS₂, CH₄, CCl₄, CH₃Cl) and inorganic [CO, CO₂, (C₂H₅Pb), (C₄H₉)Sn] compounds. The

HID is capable of ionizing all compounds with an ionization potential <19.8 eV. This includes all known compounds of general interest for gas chromatography. The two general designs of the HID employ either a radioisotope [4,8] or gas discharge [29,35] as a source of ionizing radiation. The gas discharge detector, with separate regions for the generation of photons and ionization of compounds, results in a more stable and robust detector, overcoming many of the difficulties associated with radioisotope-based detectors. The latter had a reputation of being difficult to use requiring operation under stringent conditions with respect to contamination from carrier gas impurities, the ingress of air, and column bleed. Ultra-high-purity helium is required for all version of the detector and is a significant contribution to operating costs.

The pulsed-discharge HID (PDHID) is available in three forms: a stand-alone helium ionization detector; a detector configuration that can be unobtrusively switched between electron-capture and helium ionization detection; and a miniaturized HID. A schematic diagram of a stand-alone HID is shown in Fig. 12.6. The detector body is a single cylindrical chamber divided into a separate discharge region (top) and reaction region (bottom) without a physical barrier. Separation of the two regions is established by the gas flow and bias voltages applied to the single or multiple ring electrodes. The helium support gas is introduced at the top of the detector while the carrier gas enters from the opposite end in a counterflow configuration. The discharge electrodes are located at the top of the detector. A pulsed high-voltage discharge is maintained between the electrodes sustaining the photon emission from the dissociation of diatomic helium as a broadband emission from 11.3 to 20.7 eV. The photons have unimpeded access to the reaction region while the strong counterflow of support gas (typically about 30 mL min⁻¹) prevents compounds in the column effluent from entering the discharge region. Compounds in the reaction region are ionized by

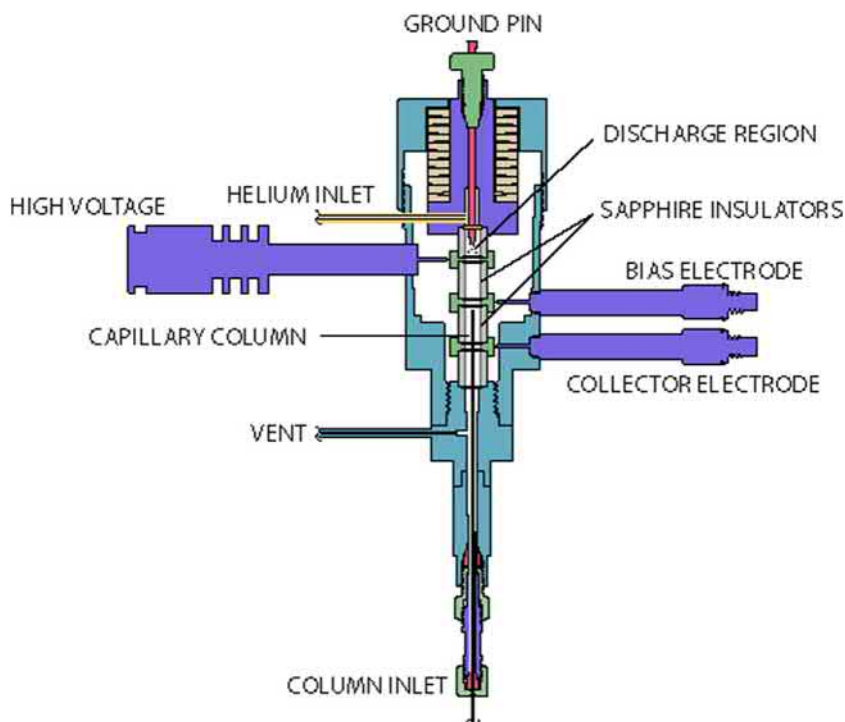


FIGURE 12.6 Schematic diagram of a stand-alone pulsed discharge helium ionization detector. From Ref. C.F. Poole, *Ionization-based detectors for gas chromatography*, *J. Chromatogr. A* 1421 (2015) 137–153; copyright Elsevier.

the photon flux and (usually) the electrons generated migrate to the collector electrode driven by the electric field set between the bias electrode and the collector electrode. Typical detector performance characteristics are summarized in Table 12.4.

12.2.6 Barrier-discharge ionization detector

The barrier-discharge ionization detector (BID) is a recent development that uses a low-temperature helium plasma generated by an electric discharge between two electrodes, at least one of which is coated with a dielectric material [36,37]. The detector consists of a plasma generator in the form of a quartz tube with a central ring electrode and two auxiliary grounded

electrodes and a charge collector downstream of the plasma generator, Fig. 12.7. The discharge is initiated by a high-voltage alternating current and is self-limiting on account of the dielectric barrier at the electrode surface. The discharge produces metastable helium species and photons responsible for ionizing compounds entering the detector at the charge collector region. Ions are produced by interaction of compounds with the metastable helium particles and photons and the ion current subsequently detected. The detector is designed to minimize sample dilution and to provide a fast response. The detector response is strongly influenced by background contamination (both column bleed and helium support gas), makeup gas flow rate, and the detector temperature. Typical applications are the detection of low-molecular-mass compounds containing heteroatoms with a weak or modest

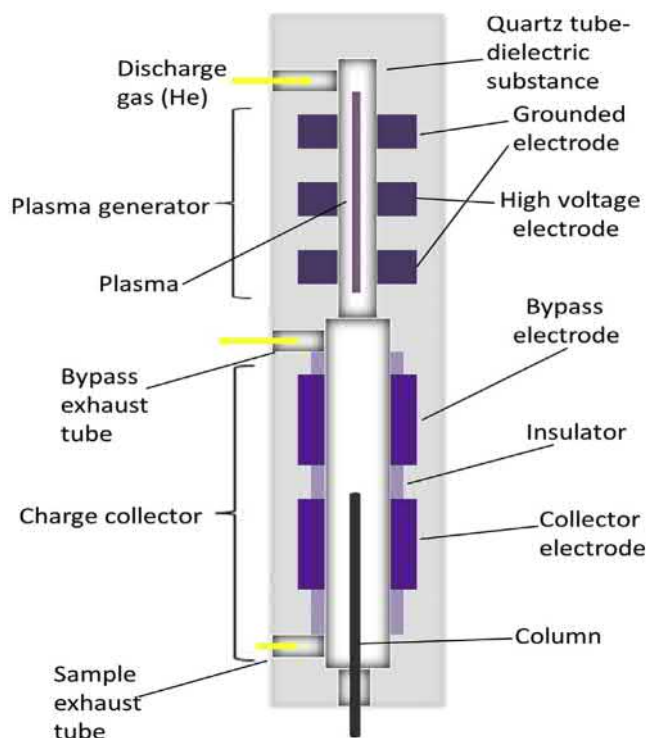


FIGURE 12.7 Schematic diagram of a barrier-discharge ionization detector. From Ref. M. Antoniadou, G.A. Zachariadis, E. Rosenberg, *Investigating the performance characteristics of the barrier discharge ionization detector and comparison to the flame ionization detector for the gas chromatographic analysis of volatile and semivolatile organic compounds*, *Anal. Letts.* 52 (2019) 2822–2839; copyright Taylor and Francis.

response to the FID where it easily outperforms the FID. This advantage is gradually lost with increasing mass as BID ionization results in mainly singularly charged ions compared with the extensive fragmentation and generation of multiple charge species in the FID.

12.3 Bulk physical property detectors

Bulk physical property detectors respond to some difference in the properties of the carrier gas due to the presence of another substance. Typically a large signal for the characteristic carrier gas property is desirable to provide a reasonable dynamic range for the detector response and a significant difference in the characteristic

property for the compounds eluted from the column to obtain a reasonable minimum detection level. Ultimately, for the detection of low compound concentrations, bulk physical property detectors are noise limited and their response tends to be poor compared with ionization-based detectors. The most important of the bulk physical property detectors are the thermal conductivity detector, gas density balance, and the ultrasonic detector. Of these, only the thermal conductivity detector (TCD) is widely used.

12.3.1 Thermal conductivity detector

The TCD is a universal, nondestructive, concentration-dependent detector with a linear

response range $\approx 10^4$ – 10^5 and a modest response (minimum detection level 10^{-6} – 10^{-8} g per peak or about 4×10^{-10} g mL $^{-1}$ in favorable cases). It is generally used to detect compounds with a poor response to the FID, which is otherwise the preferred detector for general laboratory use. Typical applications overlap with the helium ionization and barrier discharge detectors, which have better detection limits but are more demanding to operate. TCDs are also found in micromachined and field portable instruments favored by their low power consumption and lack of auxiliary gases as well as ease of downsizing [38].

There are numerous detector designs generally based on flow through, semidiffusion, or diffusion cell principles in which the carrier gas flows through a heated thermostatted cavity containing a sensing element, either a heated metal wire or thermistor [2,39]. With only carrier gas flowing through the cavity, heat loss from the sensor depends only on the thermal conductivity of the carrier gas. In the presence of a mixture of carrier gas and sample, a change in thermal conductivity for the mixture is observed

as a resultant change in temperature of the sensor. A common arrangement combines the TCD with a simple Wheatstone bridge circuit to measure the change in resistance of a heated filament as sample passes over it. In the simplest design, Fig. 12.8, there are two heated filaments, but more common is a four filament design (two sample and two reference cells). A constant voltage or current is applied to the circuit and the balanced current or voltage between opposite legs of the Wheatstone bridge is monitored. The main function of the reference side of the TCD is to minimize drift due to temperature and flow variation within the cell and flow rate changes of the carrier gas. TCDs are more sensitive to temperature variations than most other detectors used in gas chromatography. The TCD is typically set at a temperature that matches the isothermal column temperature or the highest column temperature in programmed separations in order to minimize sample condensation, detector contamination, and peak tailing due to sample interaction with the filament and/or flow path surfaces. Excessive temperatures should be avoided since the TCD is less sensitive at higher temperatures. To maximize

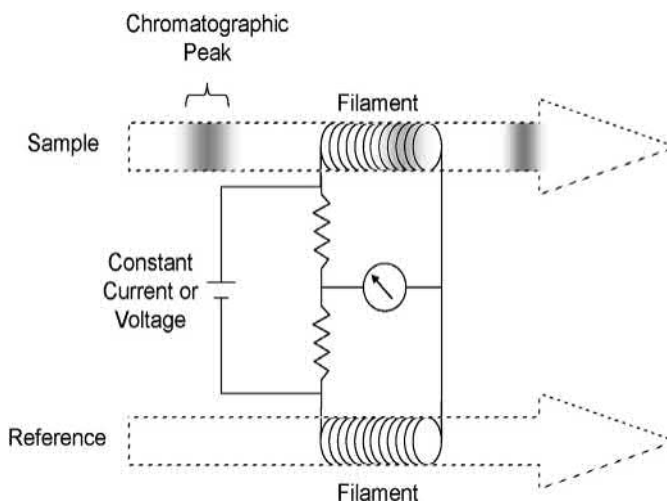


FIGURE 12.8 Schematic diagram of a dual-cell thermal conductivity detector in a Wheatstone bridge network. From Ref. M.S. Klee, *Detectors*, in C.F. Poole (Ed.), *Gas Chromatography*, Elsevier, Amsterdam, 2012. p. 307–347; copyright Elsevier.

the response of the TCD, the choice of carrier gas is important. Its thermal conductivity should be as different as possible to the sample. Generally, only hydrogen, helium, nitrogen, and perhaps argon are used as a carrier gas, but as these gases differ in their thermal conductivity, it is not possible to specify a single gas for all applications (more so as the TCD is often used for the detection of fixed gases with a similar thermal conductivity to the common carrier gases). The thermal conductivity of volatile organic compounds does not vary as much as simple gases resulting in similar response factors that may allow calibration for each compound to be dispensed with if lower accuracy can be tolerated.

TCD filaments have a finite lifetime somewhat related to temperature (higher temperature decreases lifetime), reactivity of samples, and exposure to vibration/shock. The filament should never be left on without a flow of carrier gas as this is guaranteed to reduce filament lifetime. In most detector designs, the sample passes directly over the filament. Some polar or reactive compounds interact with filaments (usually tungsten), causing peak tailing. Acidic compounds are notorious in this regard. To counteract this problem, filaments are typically coated to reduce interaction with the bare filament. Over time, the protective coating can wear, exposing the filament to sample. Most TCD designs allow filaments to be easily replaced.

An alternative detector design uses flow modulation to switch the carrier gas between two channels, Fig. 12.9, one of which contains a single filament [2,40]. Every 100 ms a switching valve fills the filament channel alternately with carrier gas and column effluent. Detector electronics gate detection of the signal and reference flows synchronously with the switch time (incorporating an appropriate delay to allow the cell to be cleared and filled with the switched gas). Although this provides a stable response, it works best at flow rates compatible with packed

or wide-bore, open-tubular columns ($>20 \text{ mL min}^{-1}$), and a makeup gas flow is required for other column types resulting in a diminished response.

12.4 Optical detectors

Flames are suitable atom reservoirs for elemental analysis using emission spectroscopy. The hydrogen–air diffusion flames used in gas chromatography are weak excitation sources and the principal emission lines for most nonmetallic elements occur in the ultraviolet region where flame background contributions are troublesome. Microwave-induced helium plasmas are more efficient atom reservoirs for gas chromatographic applications but require complex instrumentation for element-selective detection. The important optical emission detectors for gas chromatography are element-selective detectors based on chemiluminescence in flames or the gas-phase for sulfur-, phosphorous-, and nitrogen-containing compounds.

12.4.1 Flame photometric detector

The flame photometric detector (FPD) is an element-selective detector commonly used for the detection of volatile sulfur- and phosphorous-containing compounds and sometimes tin-containing compounds. The detector uses a hydrogen-diffusion flame to fragment compounds and then excite them to a higher electronic state. The principal burner designs include single-flame, dual-flame, and pulsed-flame designs [2,8,41–43]. In the single-flame design the carrier gas and air are mixed, conveyed to the flame tip, and combusted in an atmosphere of hydrogen. With this burner and flow configuration interfering emissions from hydrocarbons occur mainly in the oxygen-rich flame region close to the burner tip, whereas sulfur and phosphorous emissions occur in the diffuse hydrogen-rich upper portions of the

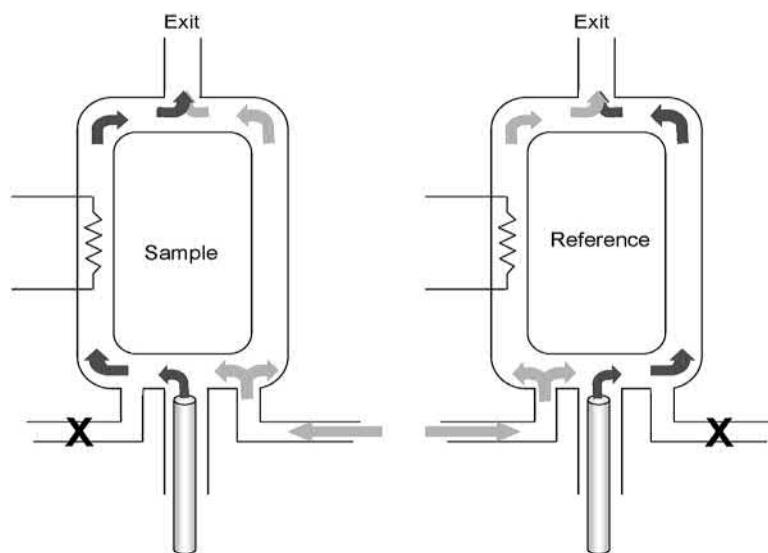


FIGURE 12.9 Schematic diagram of the flow path through a single filament thermal conductivity detector. Sample and reference streams are alternately switched across the single filament by a microfluidic switch. From Ref. M.S. Klee, *Detectors*, in C.F. Poole (Ed.), *Gas Chromatography*, Elsevier, Amsterdam, 2012. p. 307–347; copyright Elsevier.

flame. Problems with solvent flame out, hydrocarbon quenching of the detector response, and structure-response variations for different sulfur- and phosphorous-containing compounds led to the development of dual-flame and pulsed-flame designs, although single-flame

detectors remain in production. A typical arrangement for a single or dual-flame detector is shown in Fig. 12.10 [41]. In the dual-flame design two series-separated flames are used. The lower flame is typically hydrogen-rich and functions as a matrix normalization reactor.

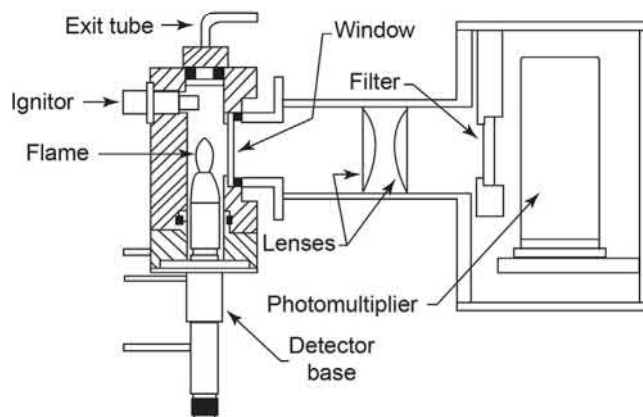


FIGURE 12.10 Schematic diagram of a flame photometric detector with a continuous flame source. From Ref. P.L. Patterson, R.L. Howe, A. Abushumays, *Dual-flame photometric detector for sulfur and phosphorous-compounds in gas chromatograph effluents*, *Anal. Chem.* 50 (1978) 339–344; copyright American Chemical Society.

The products of combustion from the bottom flame are swept into a second longitudinally separated flame optimized to enhance the desired emission. The pulsed-flame detector employs combustion gas flow rates too low to sustain a continuous flame. The air and hydrogen combustion gases are mixed in a small chamber and flow toward a heated wire igniter. The ignited flame then propagates back to the gas source and is self-terminating once all the combustion gases in the chamber are consumed. The continuous flow of combustion gases removes the products of combustion and creates additional ignition in a periodic fashion. The selectivity of the pulsed-flame detector is enhanced by time resolution of the various luminescent species by setting a variable gate delay and gate width for each element [42,44]. The emission from carbon species is rapidly depleted after ignition. The phosphorous emission peaks approximately 5 ms after ignition while sulfur emission occurs over a wide time range from about 5 to 25 ms after ignition. By gating detection of sulfur and phosphorous emissions after that of carbon, most of the spectral interference from carbon is eliminated. Since the pulse frequency is dependent on flow conditions, the range of applications for this detector is narrower than for detectors employing a continuous flame source [2]. For any given burner design, the detector response is critically dependent on the hydrogen-to-air ratio, the flow rates of combustion and carrier gases, the type of carrier gas, and detector temperature. Different conditions are usually required for optimum sulfur and phosphorous detection, for detectors with different burner designs, and generally also for different compound types. Dual-detector designs with separate photomultiplier and filter assemblies are available for the simultaneously detection of sulfur and phosphorous.

In the relatively low-temperature and hydrogen-rich flame, sulfur-containing compounds are decomposed to species such as H_2S , HS , S , S_2 , SO , and SO_2 in relative proportions

that depend on the flame chemistry. Excited state species are formed from these primary species, mainly S_2^* in low yield by several two- or three-body collision reactions. The relaxation results in broadband emission over the wavelength range from 320 to 460 nm with a maximum emission at 394 nm. The response for sulfur is inherently nonlinear and proportional to the mass of sulfur entering the flame ($[\text{S}]^n$). The theoretical value for n is 2, but in practice, values between 1.6 and 2.2 are typically observed. Nonoptimized flame conditions, compound-dependent decomposition, hydrocarbon quenching, and competing flame reactions that lead to deexcitation all contribute to the deviation of n from its theoretical value. The decoupling of the compound decomposition process from the excitation process results in a more truly quadratic response for the multiple-flame and pulsed-flame detectors. In the case of phosphorus, phosphorus-containing compounds are first decomposed to PO molecules and finally to electronically excited HPO^* species in three-body collisions. A linear relationship between detector response and the mass of phosphorus atoms entering the flame is expected for phosphorus-containing compounds, at least for low sample concentrations. Typical performance characteristics for the FPD are summarized in Table 12.7, although there is considerable variation among the different detector designs [45].

A general problem for all FPD designs is matrix suppression of the detector response, referred to as quenching [46,47]. A significant reason for choosing the FPD is its capability to perform as an element-selective detector under conditions where coelution of matrix components is expected. Although the exact mechanism of quenching is unknown, it appears that both the change in flame temperature and flame chemistry that occur when a large amount of matrix components are introduced into the flame play a role. Quenching is generally more important for sulfur-containing compounds and a likely major contributing factor is nonradiative

TABLE 12.7 Typical performance characteristics of optical detectors.

Parameter	Response characteristics	
<i>(i) Flame photometric detector</i>		
	P-mode	S-mode
Type	Element-selective detector	
Response mechanism	Mass dependent	
Minimum detectable level	$5 \times 10^{-13} - 1 \times 10^{-14} \text{ g P s}^{-1}$	$10^{-12} - 10^{-14} \text{ g S s}^{-1}$
Linear response range	10^5	Nonlinear
Selectivity	$5 \times 10^5 \text{ g C/g P}$	$10^4 - 10^7 \text{ g C/g S}$
<i>(ii) Chemiluminescence detector</i>		
	N-mode	S-mode
Type	Element-selective detector	
Response mechanism	Mass dependent	
Minimum detectable level	$10^{-12} \text{ g N s}^{-1}$	$10^{-12} \text{ g S s}^{-1}$
Linear range	10^5	10^5
Selectivity	10^7 g C/g N	$10^7 - 10^8 \text{ g C/g S}$
<i>(iii) Atomic emission detector</i>		
Type	Element-selectable detector	
Response mechanism	Mass dependent	
Minimum detectable level ^a	$1 - 400 \times 10^{-13} \text{ g X s}^{-1}$	
Linear response range ^a	$10^3 - 10^5$	
Selectivity ^a	$10^3 - 10^6 \text{ g C/g X}$	

^a Depends on the identity of element X.

collisional deactivation of S_2^* by matrix combustion products. More specifically, Kalonterov et al. identified the reaction between carbon monoxide and sulfur forming COS as the main source of quenching of the sulfur emission [47]. Mitrevski et al. [48] noted a 10-fold improvement in detection limits for sulfur compounds in shale oil using comprehensive two-dimensional gas chromatography due to the efficient removal of the hydrocarbon background from the elution window for the sulfur compounds. The dual-flame and pulsed-flame detector designs are

less affected by quenching compared with the single-flame detector.

12.4.2 Gas-phase chemiluminescence detector

The chemiluminescent detector (CLD) is an element-selective detector for sulfur-containing (SCD) and nitrogen-containing (NCD) compounds and nitrosamines (NCD). Even though the detection processes are similar for nitrogen and sulfur, the hardware and optimized

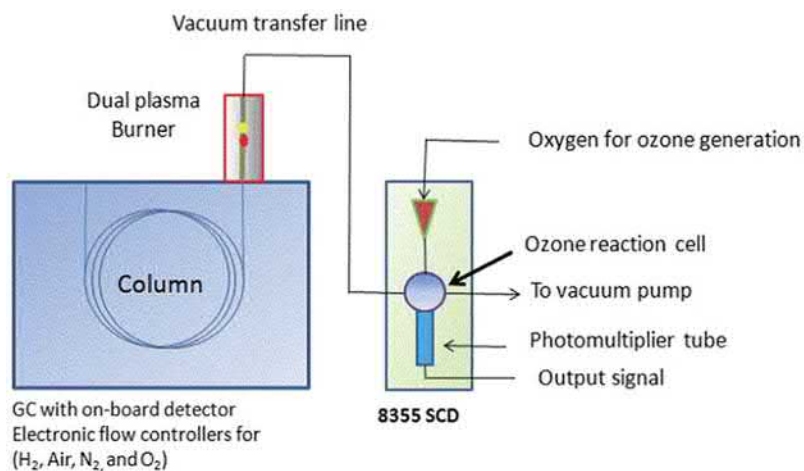


FIGURE 12.11 Schematic diagram illustrating the relationship between the main components of a gas-phase chemiluminescence detector. From Ref. J. Luong, R. Gras, M. Hawryluk, R. Shearer, *A brief history of recent advances in ozone induced chemiluminescence detection for the determination of sulfur compounds by gas chromatography*, *Anal. Methods* 8 (2016) 7014–7024; copyright Royal Society of Chemistry.

operating conditions are sufficiently different that the NCD and SCD can be considered separate detectors. The SCD is the preferred detector for sulfur compounds in complex matrices on account of its equimolar and linear response and high selectivity. Its operation and maintenance, however, are more complex than typical ionization-based and FPDs.

A typical gas-phase CLD consists of coupled thermal and ozone reaction chambers, Fig. 12.11 [2,49–51]. A dual-plasma burner functions as a catalytic reactor for the conversion of nitrogen- and sulfur-containing compounds into nitric oxide and sulfur monoxide, respectively, which are the precursor species for the chemiluminescent reaction with ozone. The burner employs an oxygen-rich plasma to decompose nitrogen- and sulfur-containing compounds into various heteroatom fragments and carbon-containing compounds to noninterfering species, such as carbon dioxide and water. The second longitudinally separated plasma and heated ceramic tube provide the specific condition for conversion of the products from the first plasma to the chemiluminescent precursor

species. For nitrogen-containing compounds oxidative pyrolysis at 800–1000°C is used to generate nitric oxide. The selective detection of nitrosamines is based on the facile low-temperature (275–300°C) catalytic pyrolysis with release of nitric oxide. For sulfur-containing compounds, a counterflow of hydrogen is mixed with the products from the first plasma and exits the dual plasma burner through a heated ceramic tube at about 800°C in which highly oxidized sulfur compounds are selectively reduced to predominantly sulfur monoxide. The products from the reaction chamber flow into the ozone chamber, maintained at a pressure of a few torr. An ozone generator provides a continuous flow of ozone to the reaction chamber by a separate connection. Nitric oxide reacts with ozone in the gas phase forming electronically excited nitrogen dioxide, which returns to the ground state with broadband near-infrared emission centered at 1200 nm. Sulfur monoxide reacts with ozone in the gas phase forming electronically excited sulfur dioxide, which returns to the ground state with emission of light of 280–460 nm centered at 360 nm. The

chemiluminescence emission is isolated by appropriate optical filters and detected by a photomultiplier tube optimized for detection of the characteristic emission. By maintaining an excess of ozone in the ozone reaction chamber, the reaction becomes pseudo first order for the heteroatom precursor species, providing the linear response mechanism for the detector. Reduced pressure operation of the ozone reaction chamber has three advantages: it enhances the detector response by diminishing collisional deactivation of the excited-state reaction products; it prevents condensation of water in the reaction chamber; and it reduces the effective detector dead volume maintaining compatibility with open-tubular columns. The characteristic properties of the CLD are summarized in Table 12.7.

12.4.3 Atomic emission detector

The atomic emission detector (AED) is an element-selectable detector capable of detecting any of the elements typically of interest in gas chromatography. It is uniquely suited to the

detection of metallic elements in organometallic compounds. The AED is a relatively complex and expensive instrument with significant maintenance and operating costs. These features have conspired to limit its general use outside of laboratories that have a specific need for the analysis of organometallic compounds.

The AED is a complex detector and its operation is described in outline only here [37,52–54]. Coupling of the separation column to the thermostatted microwave cavity is made through a heated transfer line. The plasma is produced in a thin-walled silica discharge tube within a microwave “reentrant” cavity, Fig. 12.12 [52]. Power is supplied by a magnetron and coupled to the plasma through a waveguide. The exit of the cavity is closed with a fused-silica window and purged with helium to prevent back-diffusion of air into the cavity and to allow flow reversal so that the solvent peak can be vented in front of the cavity to minimize carbon buildup. The plasma is generated in an atmospheric pressure flow of helium, carrier gas, and makeup flow as required. Depending on the elements being determined, low concentrations of various scavenger gases (e.g., O_2 , H_2 ,

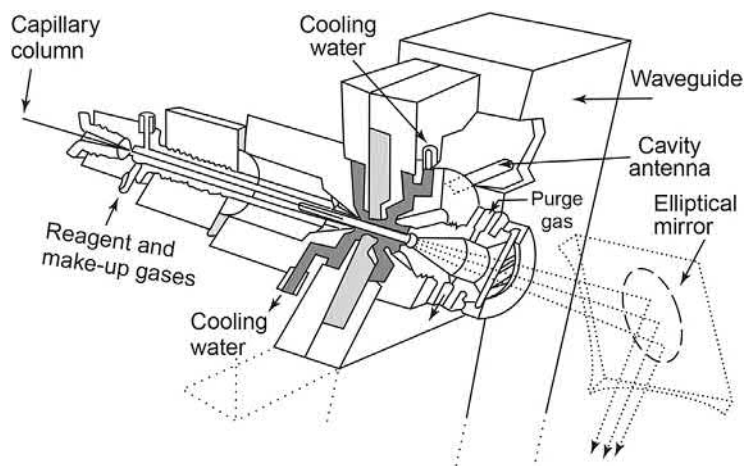


FIGURE 12.12 Cross-sectional view of the cavity block of an atomic emission detector. From Ref. P.L. Wylie, B.D. Quimby, *Applications of gas-chromatography with atomic emission detector*, *J. High Resolut. Chromatogr.* 12 (1989) 813–818; copyright John Wiley and Sons.

TABLE 12.8 Response characteristics of the atomic emission detector for different elements.

Element	Wavelength	Minimum detection	Selectivity	Linear
(X)	(nm)	Level (pg s^{-1})	(g X/g C)	Range
C	193.1	2.6	2×10^4	
H	486.1	2.2	6×10^3	
Cl	479.5	39	2.5×10^4	2×10^4
Br	470.5	10	1.1×10^4	1×10^3
F	685.6	40	3.0×10^4	2×10^3
S	180.7	1	3.5×10^4	1×10^4
P	177.5	1	5.0×10^3	1×10^3
N	174.2	15	2.0×10^3	4×10^3
O	777.2	50	3.0×10^4	3×10^3
Sn	303.1	0.5	3.0×10^4	1×10^3
Se	196.1	4	5.0×10^4	1×10^3
Hg	253.7	0.1	3.0×10^6	1×10^3

and CH_4) are added as needed to enhance response or improve selectivity. An elliptical mirror collects emissions from inside the end of the discharge tube. The emission sensor consists of a flat focal-plane spectrometer with a movable photodiode array detector capable of monitoring emission from about 150 to 800 nm. However, the size of the photodiode array detector limits the elements that can be determined simultaneously to an emission range of about 25 nm (the selected elements must also be compatible with the scavenger gases doped into the plasma). Typically, up to four elements can be determined simultaneously and displayed as element-specific chromatograms at the same time. These may not be the only elements, or the four or fewer elements of interest, in which case multiple analyses of the same sample are required. Typical performance characteristics of the AED are summarized in Table 12.7. The variation of response to different elements is quite wide but

for an individual element reasonably independent of compound structure. Some further specific details of element detection are summarized in Table 12.8.

In theory, it should be possible to determine the empirical formula for each compound in the chromatogram from the ratio of the AED response to the individual elements or to use a single compound as an internal standard to quantify other compounds present in the sample [55–57]. Both require stable interelement response factors independent of structure. A lack of plasma stability, incomplete compound destruction, and deviations from linearity of the individual element responses, however, limit the accuracy of such measurements. The atomization efficiency of the relatively low-power helium plasma may fail to destroy all molecular fragments resulting in broad emission bands, which interfere with the elemental atomic lines being monitored. Accurate formula values for oxygen and nitrogen can be particularly difficult to determine due to entrainment of atmospheric gases into the plasma. Numerous factors affect the response of the AED at any particular wavelength. Among these the type and concentration of reagent gas, the flow rate of makeup gas, and the presence of excess matrix compounds are among the most important. On account of these problems, it is not always possible to use a single compound internal standard for quantification with the desired accuracy.

12.5 Electrochemical detectors

There are two general problems with electrochemical detection in the gas phase. First, few electrochemical detectors are gas-phase sensing devices, and therefore the separated sample components must be transferred into solution for detection. Second, the majority of organic compounds separated by gas chromatography are neither electrochemically active nor conducting. The electrolytic conductivity detector

(ELCD) solves both of these problems by decomposing the gas-phase sample into small inorganic molecules, which are detected by their conductivity in a support solvent [8,58–60]. The ELCD is a mass-sensitive, element-selective detector used primarily for the detection of halogen-, sulfur-, and nitrogen-containing compounds. The carrier gas is mixed with a reagent gas and then passed through a small diameter nickel tube at 850–1000°C. The nickel tube acts as catalyst for the decomposition reaction. With hydrogen as the reagent gas, halogen-containing compounds are converted to hydrogen halides (HCl, HBr) and nitrogen-containing compounds to ammonia. Sulfur-containing compounds are reacted with air to produce sulfur dioxide with a small amount of sulfur trioxide. A chemical scrubber mounted at the exit of the reaction tube is used, if needed, to enhance the specificity of the detection process. For example, silver wire is used to remove hydrogen halides or hydrogen sulfide and potassium hydroxide supported on quartz fibers to remove acidic species. The reaction products from the furnace are swept into a gas–liquid contactor where they are mixed with an appropriate solvent. The support solvent is selected to promote ionization of the reaction species over ionization of interfering compounds. This solvent is usually circulated through a closed system containing beds of ion exchange resins to purify and condition the solvent for reuse. From the gas–liquid contactor the support solvent flows to the conductivity cell, where detection takes place, either after separation of the liquid from insoluble gases, or as a mixed phase, depending on the detector design. Each detection mode requires a specific combination of reactor conditions, resin cartridges, and choice of the support solvent. Common practical problems include the loss of response, excessive noise, poor linearity, and poor peak shapes. The ELCD is capable of high sensitivity and selectivity with detection limits of about 10^{-12} g of N or $S s^{-1}$ and 5×10^{-13} g $Cl s^{-1}$

with a linear range of 10^3 – 10^5 . Selectivity varies with the heteroatom detected and detector operating conditions with values of 10^4 – 10^9 g/C g N, S, or Cl possible. In recent years there has been a sharp decline in the use of the ELCD due to competition from more user-friendly and rugged ionization-based and gas-phase chemiluminescence optical detectors as well as mass spectrometric detection.

References

- [1] C.F. Poole, *The essence of chromatography*, Elsevier, Amsterdam, 2003.
- [2] M.S. Klee, *Detectors*, in: C.F. Poole (Ed.), *Gas Chromatography*, Elsevier, Amsterdam, 2012, pp. 307–347.
- [3] K. Dettmer-Wilde, W. Engelwald (Eds.), *Practical Gas Chromatography: A Comprehensive Reference*, Springer, Berlin, 2014.
- [4] C.F. Poole, Ionization-based detectors for gas chromatography, *J. Chromatogr. A* 1421 (2015) 137–153.
- [5] L. Dabrowski, Multidetector systems in gas chromatography, *Trends Anal. Chem.* 102 (2018) 185–193.
- [6] A. Felinger, *Data Analysis and Signal Processing in Chromatography*, Elsevier, Amsterdam, 1998.
- [7] L.S. Ettre, The invention, development and triumph of the flame ionization detector, *LC-GC Eur.* 15 (2002) 364–371.
- [8] D.G. McMinn, H.H. Hill, *Detectors for Capillary Gas Chromatography*, Wiley, New York, 1992.
- [9] J.V. Hinshaw, The flame ionization detector, *LC-GC N. Am.* 23 (2005) 1262–1269.
- [10] C. von Muhlen, W. Khummueng, C.A. Zini, E.B. Caramao, P.J. Marriott, Detector technologies for comprehensive two-dimensional gas chromatography, *J. Sep. Sci.* 29 (2006) 1909–1921.
- [11] T. Holm, Aspects of the mechanism of the flame ionization detector, *J. Chromatogr. A* 842 (1999) 221–227.
- [12] K. Schofield, The enigmatic mechanism of the flame ionization detector: its overlooked implications for fossil fuel combustion modeling, *Prog. Energy Combust. Sci.* 34 (2008) 330–350.
- [13] C.L. Faiola, M.H. Erickson, V.L. Fricaud, B.T. Johnson, T.M. VanReken, Quantification of biogenic volatile compounds with the flame ionization detector using the effective carbon number concept, *Atmos. Meas. Tech.* 5 (2012) 1911–1923.

- [14] H.Y. Tong, F.W. Karasek, Flame ionization detector response factors for compound classes in quantitative analysis of complex organic mixtures, *Anal. Chem.* 56 (1984) 2124–2128.
- [15] P.L. Patterson, Recent advances in thermionic ionization detection for gas chromatography, *J. Chromatogr. Sci.* 24 (1986) 41–52.
- [16] B. Kolb, J. Bischoff, New design of a thermionic nitrogen and phosphorous detector for GC, *J. Chromatogr. Sci.* 12 (1974) 625–629.
- [17] D. Ryan, P.J. Marriott, Studies on thermionic detection in comprehensive two-dimensional gas chromatography, *J. Sep. Sci.* 29 (2006) 2375–2380.
- [18] D.D. Bombick, J. Allison, Investigation into the response mechanism of the gas chromatographic thermionic ionization detector, *J. Chromatogr. Sci.* 27 (1989) 612–619.
- [19] H. Carlsson, G. Robertsson, A. Colmsjo, Response mechanisms of thermionic ionization detectors with enhanced nitrogen selectivity, *Anal. Chem.* 73 (2001) 5698–5700.
- [20] H. Kishi, T. Fujii, G. Sato, Surface ionization detector with supersonic free jet for gas chromatography. Some applications, *J. Chromatogr. A* 750 (1996) 335–340.
- [21] W.S. Zhang, A.B. McCague, D.W. Reeve, J.H. Carey, Evaluation of a halogen-specific detector (XSD™) for trace analysis of chlorinated fatty acids in fish, *Instrum. Sci. Technol.* 33 (2005) 481–507.
- [22] A. Zlatkis, C.F. Poole (Eds.), *Electron Capture: Theory and Practice in Chromatography*, Elsevier, Amsterdam, 1981.
- [23] C.F. Poole, Derivatization reactions for use with the electron-capture detector, *J. Chromatogr. A* 1296 (2013) 15–24.
- [24] W.E. Wentworth, J. Huang, K. Sun, Y. Zhang, L. Rao, H. Cao, S.D. Stearns, Non-radioactive electron-capture detector, *J. Chromatogr. A* 842 (1999) 229–266.
- [25] M.S. Klee, M.D. Williams, L. Chang, J. Murphy, Superior ECD performance through design and application, *J. High Resolut. Chromatogr.* 22 (1999) 24–30.
- [26] R.J. Maggs, P.L. Joynes, A.J. Davies, J.E. Lovelock, Electron-capture detector – a new mode of operation, *Anal. Chem.* 43 (1971) 1966–1970.
- [27] P. Rotocki, B. Drozdowicz, Non-linearity of constant-current electron-capture detection, *Chromatographia* 27 (1989) 71–76.
- [28] C.F. Poole, Temperature dependence of the electron-capture detector response, *J. Chromatogr.* 118 (1976) 280–281.
- [29] H.M. Cai, S.D. Stearns, W.E. Wentworth, Pulsed-discharge electron-capture detector operating in the constant-current mode by means of feedback dc bias voltage, *Anal. Chem.* 70 (1998) 3770–3780.
- [30] E.C.M. Chen, E.S. Chen, Molecular electron affinities and the calculation of the temperature dependence of the electron capture response, *J. Chromatogr. A* 1037 (2004) 83–106.
- [31] J.N. Davenport, E.R. Adlard, Photoionization detectors for gas chromatography, *J. Chromatogr.* 290 (1984) 13–22.
- [32] J.H. Sun, F.Y. Guan, D.F. Cui, X. Chen, L.I. Zhang, J. Chen, An improved photoionization detector with a micro gas chromatography column for portable rapid gas chromatography, *Sens. Actuators, B* 188 (2013) 513–518.
- [33] D.J. Dojahn, W.E. Wentworth, S.N. Deming, S.D. Stearns, Determination of percent composition of a mixture by gas chromatography – comparison of a helium pulsed-discharge photoionization detector with a flame ionization detector, *J. Chromatogr. A* 917 (2001) 187–204.
- [34] D.S. Forsyth, Pulsed discharge detector: theory and applications, *J. Chromatogr. A* 1050 (2004) 63–68.
- [35] H. Cai, S.D. Stearns, Pulsed discharge helium ionization detector with multiple combined bias/collecting electrodes for gas chromatography, *J. Chromatogr. A* 1284 (2013) 163–173.
- [36] M. Antoniadou, G.A. Zachariadis, E. Rosenberg, Investigating the performance characteristics of the barrier discharge ionization detector and comparison to the flame ionization detector for the gas chromatographic analysis of volatile and semivolatile organic compounds, *Anal. Lett.* 52 (2019) 2822–2839.
- [37] C. Li, Z. Long, X. Jiang, P. Wu, X. Hou, Atomic spectrometric detectors for gas chromatography, *Trends Anal. Chem.* 77 (2016) 139–155.
- [38] R. Gras, J. Luong, R.A. Shellie, Miniaturized micromachined gas chromatography with universal and selective detectors for targeted volatile compounds, *J. Chromatogr. A* 1573 (2018) 151–155.
- [39] G. Wells, P. Simon, Thermal conductivity detector: theory and numerical model, *J. Chromatogr.* 256 (1983) 1–15.
- [40] Y. Weijun, Analytical accuracy of hydrogen measurement using gas chromatography with a thermal conductivity detector, *J. Sep. Sci.* 38 (2015) 2640–2646.
- [41] P.L. Patterson, R.L. Howe, A. Abushumays, Dual-flame photometric detector for sulfur and phosphorous-compounds in gas chromatograph effluents, *Anal. Chem.* 50 (1978) 339–344.
- [42] H.W. Jiang, A. Amirav, Pulsed-flame photometric detector – a step towards universal heteroatom selective detection, *J. Chromatogr. A* 805 (1998) 177–213.

- [43] A.G. Clark, K.D. Thurbide, An improved multiple flame photometric detector for gas chromatography, *J. Chromatogr. A* 1421 (2015) 154–161.
- [44] J.P. Le Harle, B. Bellier, Optimization of the selectivity of a pulsed-flame photometric detector for unknown compound screening, *J. Chromatogr. A* 1087 (2005) 124–130.
- [45] L.J.J. Catalan, V. Liang, C.Q. Jia, Comparison of various detection limit estimates for volatile sulfur compounds by gas chromatography with flame photometric detection, *J. Chromatogr. A* 1136 (2006) 89–98.
- [46] W.A. Aue, X.Y. Sun, Quenching in the flame photometric detector, *J. Chromatogr.* 641 (1993) 291–299.
- [47] L. Kalonterov, H.W. Jung, A. Amirav, Mechanism of sulfur emission quenching in flame photometric detectors, *J. Chromatogr. A* 696 (1995) 245–256.
- [48] B. Mitrevski, M.W. Amer, A.L. Chaffee, P.J. Marriott, Evaluation of comprehensive two-dimensional gas chromatography with flame photometric detection: potential application for sulfur speciation in shale oil, *Anal. Chim. Acta* 803 (2013) 174–180.
- [49] X.W. Yan, Detection by ozone-induced chemiluminescence in chromatography, *J. Chromatogr. A* 842 (1999) 267–308.
- [50] X. Yan, Unique selective detectors for gas chromatography: nitrogen and sulfur chemiluminescence detectors, *J. Sep. Sci.* 29 (2006) 1931–1945.
- [51] J. Luong, R. Gras, M. Hawryluk, R. Shearer, A brief history of recent advances in ozone induced chemiluminescence detection for the determination of sulfur compounds by gas chromatography, *Anal. Method* 8 (2016) 7014–7024.
- [52] P.L. Wylie, B.D. Quimby, Applications of gas chromatography with atomic emission detector, *J. High Resolut. Chromatogr.* 12 (1989) 813–818.
- [53] B.D. Quimby, J.J. Sullivan, Evaluation of a microwave cavity discharge tube, and gas flow system for combined gas chromatography-atomic emission detection, *Anal. Chem.* 62 (1990) 1027–1034.
- [54] L.L.P. van Slee, U.A.T. Brinkman, Developments in the application of gas chromatography with atomic emission (plus mass spectrometric) detection, *J. Chromatogr. A* 1186 (2008) 109–122.
- [55] G. Li, D. Wu, W. Xie, X. Zhang, B. Liu, Evaluation of compound-independent calibration using gas chromatography with atomic emission detector, *Talanta* 95 (2012) 36–41.
- [56] J.T. Andersson, Some unique properties of gas chromatography coupled with atomic-emission detection, *Anal. Bioanal. Chem.* 373 (2002) 344–355.
- [57] E.S. Chernetsova, A.I. Revetsky, D. Durst, T.G. Sobolevsky, Improving the accuracy of carbon-to-hydrogen ratio determination for P, N, S, O, Cl, and Br-containing organic compounds using atomic emission detection, *Anal. Bioanal. Chem.* 382 (2005) 448–451.
- [58] D.E. Pape, D.H. Rodgers, T.C. Flynn, The electrolytic conductivity detector as an element-selective gas chromatography detector, *J. Chromatogr.* 134 (1977) 1–24.
- [59] H.L. Mu, C. Wesen, I. Odenbrand, K.G. Wahlund, Response factors of organochlorine compounds in the electrolytic conductivity detector, *J. Chromatogr. A* 849 (1999) 285–292.
- [60] N.V. Fehring, D.M. Gilvydis, S.M. Walters, C.F. Poole, Optimization of an electrolytic conductivity detector for determination of toxic nitrogen-containing food contaminants separated by open-tubular column gas chromatography, *J. High Resolut. Chromatogr.* 15 (1992) 124–127.

Molecular spectroscopic detectors for gas chromatography

Ariel M. O'Brien, Kevin A. Schug

Department of Chemistry & Biochemistry, The University of Texas, Arlington, TX, United States

13.1 Introduction

Classical molecular spectroscopy methods have been coupled to gas chromatography (GC) as detectors, including dispersive infrared (IR), Fourier transform infrared (FTIR), ultraviolet (UV), and vacuum ultraviolet (VUV) absorption spectroscopic detection. These techniques predominantly measure absorbance of source light by gas-phase compounds, which exhibit specific chromophores and absorb light at specific energies (or wavelengths) of light. Ultimately, signal attenuation can result from various different processes, including reflection, scattering, absorption, and interferences [1]. The transmitted light is then converted into an electrical signal [2]. Absorption spectra are generated based on the measured wavelength dependence of light absorption; ideally, the absorption of individual pure components from a sample containing many components is measured in a time-resolved fashion following high-efficiency GC separations. These compounds can then be identified and quantified based on their detector response.

Nearly all molecules absorb electromagnetic radiation between the far-IR and far-UV wavelength regions. As such, GC-VUV and GC-FTIR are considered to be both universal and selective detection methods [3]. (As a note, we refer primarily here to GC-IR systems in the context of GC-FTIR as the predominant GC-IR technique.) For systems that measure broadband absorption, near universality can be achieved by monitoring broadband absorption across a wide wavelength range. In contrast, selectivity for compounds that possess specific chromophores (e.g., aromatic compounds) can be attained by monitoring more discrete wavelength ranges where, ideally, only those compounds absorb. In gas-phase absorbance, a “cross-section” is a molecule’s wavelength-dependent probability of photon absorption [4]. An absorption cross section for a molecule is akin, and proportional to, its molar absorptivity. Within limits, absorbance is proportional to the concentration of the analyte. Ideally, molecular spectroscopy detection should have a wide wavelength range, high spectral resolution, high sensitivity, low noise,

linear calibration response, high-speed acquisition, and low sample consumption [2].

Table 13.1 summarizes conversions between wavelength, wavenumber, and photon energy over the relevant ranges used in spectroscopic GC detection. IR and FTIR spectroscopies tend to detect mid-IR spectra between the wavenumbers 40000 and 600 cm^{-1} [5]. Visible light has a wavelength range of 400–800 nm [2]. Yet, only colored compounds can be viewed in the visible range. The UV region has a wavelength range of 190–380 nm [1]. In this range, primarily molecules exhibiting pi-bond characteristics can typically be viewed in the mid-to-near UV region. However, nearly all compounds show absorption between 120 and 240 nm [3]. The VUV or far-UV region has a wavelength range of 10–200 nm or photon energies of 6.2–124 eV. In the far-UV region, sensitivity increases by an order of magnitude [6]. Today, two commercial VUV detectors are available: the VGA-100 (VUV Analytics, Inc.), which has a wavelength range of 120–240 nm; and the VGA-101, which has a wavelength range of 120–430 nm. These VUV detectors rapidly collect full wavelength range absorption spectra and are readily coupled to GC [4]. There are currently limited commercial offerings for GC-FTIR and GC-UV technologies.

In 2018, Zavahir et al. compared GC molecular spectroscopy techniques, including FTIR and VUV [1]. Herein, GC-FTIR, followed by GC-VUV are discussed in terms of instrumentation, development, and performance characteristics, as well as data analysis, interpretation, and treatment. GC-FTIR and GC-VUV are also compared in terms of their performance characteristics and applications.

13.2 Milestones

It is important to note that IR preceded FTIR. Techniques such as matrix isolation (MI) were coupled to IR spectroscopy early on [7]. In 1958, double-beam interferometry was introduced [8]. In the early 1960s, the first GC-IR papers were published [9–11]. In 1964, Cooley & Tukey introduced the fast Fourier transform (FFT) algorithm, which made GC-FTIR possible [12]. The first GC-FTIR was coupled to a packed column GC and its interface consisted of a heated flow-through gas cell [13]. Just as packed column GC separations were quickly replaced by capillary GC, the heated flow cell was quickly replaced by a gold-coated light pipe (LP) interface [14,15]. The gold-coated LP was refined in the early 1970s and coupled to capillary GC in

TABLE 13.1 Conversion between wavenumber (cm^{-1}), wavelength (nm), and photon energy (eV).

Approximate range	Wavenumber (cm^{-1})	Wavelength (nm)	Photon energy (eV)
Far-infrared	400–20	25000–500000	0.05–0.002
Mid-infrared	4000–400	2500–25000	0.5–0.05
Near-infrared	14000–4000	700–2500	1.8–0.5
Visible	25000–14000	400–700	3.1–1.8
Near-ultraviolet	30000–25000	300–400	4.1–3.1
Mid-ultraviolet	50000–30000	200–300	6.2–4.1
Far-ultraviolet	50000–1,000,000	10–200	124–6.2

1974 [16]. In 1977, Nicolet made its first commercial GC-FTIR. By 1979, FTIR spectrometers were manufactured by Bruker, MIDAC Corp, Digilab, and Nicolet, while Digilab and Nicolet manufactured commercial GC-FTIR accessories [9]. De Haseth and Isenhour contributed to the empirical determination of the optimum interferogram segment position for the Gram–Schmidt Orthogonalization (GSO) technique [17]. In 1979, MI interfaces were first developed by Gerald T. Reedy [18]. In 1984, the Cryolect (Mattson Instruments) MI interface became commercially available [16,19]. Today, method difficulties, poor reliability, and lack of a support system for maintenance and upgrades have caused many to abandon GC-FTIR [1].

Initially, VUV spectroscopy was limited to synchrotron light sources to compensate for significant background absorption and single-wavelength photodiodes [20,21]. A vacuum was necessary to reduce background absorption from moisture and air, as residual water and oxygen absorb strongly in the VUV region [3]. When a far-UV detector (FUVD) was first coupled to GC in 1988, it was limited to an essentially single-wavelength light source at 122 nm (10.2 eV) and did not provide qualitative data [22]. Lagesson published the first work using broadband (168–330 nm) GC-VUV/UV in 1998. These early light sources had difficulty transmitting light at wavelengths less than 168 nm [23,24]. Prior attempts to couple VUV/UV molecular spectroscopy to GC were limited. Use of the first commercial GC-VUV was first published in 2014 [25] by Schug and coworkers. The broadband VUV/UV GC detector technology was developed by Dale Harrison and associates at VUV Analytics, Inc. The GC-VUV, based on the initial VGA-100 model, is capable of simultaneous acquisition of gas-phase absorption from 120 to 240 nm at an acquisition speed of up to 100 Hz. Following significant development of GC-VUV applications, in recent years, GC-VUV has been applied to comprehensive two-dimensional (2D) GC \times GC separations [26], as well as to dual-

detection GC-VUV/ mass spectrometry (MS) systems [27]. A second-generation model VGA-101 was released in 2018; it provides for collection of an increased wavelength range (120–420 nm), can be operated up to 420°C, and provides a significant sensitivity increase over the VGA-100 in some cases.

In 2015, Luong and Shellie et al. also reported investigation of GC-UV detectors beginning with a single-wavelength (254 nm) [28] HPLC detector and evolving to coupling of a diode-array detector (DAD) in line with both flame ionization detection (FID) [29] and MS [30], even for miniaturized GC instruments [31]. Fig. 13.1 illustrates the major developments in the use of molecular spectroscopy detection techniques for GC over the last 70 years.

13.3 Gas chromatography Fourier transform infrared spectroscopy

FTIR spectroscopy was developed to overcome the limitations of dispersive IR [32]. Dispersive IR was more time-consuming and lacked the sensitivity necessary for coupling to GC [9]. Dispersive IR was rapidly replaced by FTIR. First, dispersive IR required multiple moving parts, which are susceptible to mechanical wear. In FTIR, only the mirror moves during an experiment. Second, in dispersive IR, calibration against a reference spectrum was required to accurately measure frequency. Dispersive IR had an extremely slow scanning speed because only radiation of a narrow frequency falls on the detector at one time. In FTIR, use of a laser radiation source provides high-frequency spectral acquisition and a rapid scan rate. Third, dispersive IR was highly susceptible to thermal effects from the focused IR beam falling onto the sample. The focused beam spanned a wide range of radiation energies, thus exciting the sample while only measuring a small band of wavenumbers at a time [32]. In FTIR, the sample is not subjected to thermal effects from the IR beam;

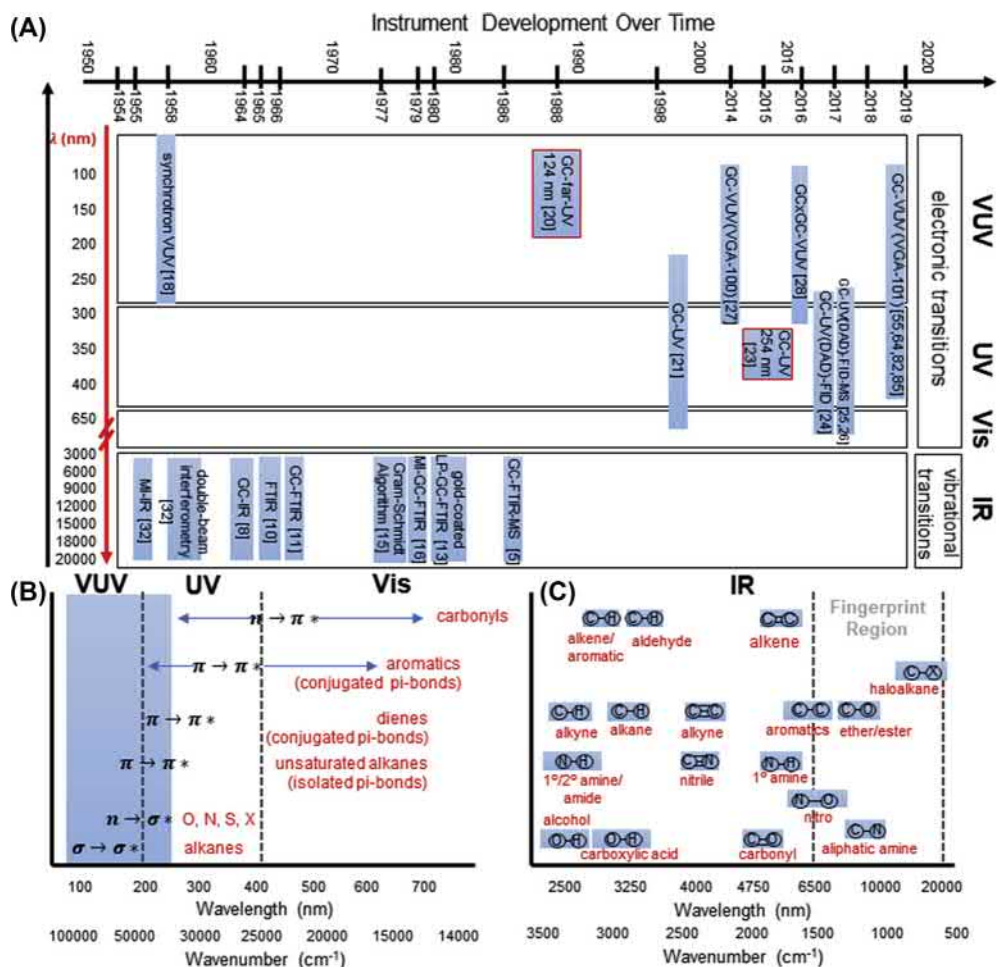


FIGURE 13.1 (A) Timeline of major developments in GC molecular spectroscopy. (B) Electronic transitions of molecules in the near-, mid-, and far-ultraviolet regions. (C) Vibrational transitions of molecules in the mid-infrared region.

rather, all frequencies of radiation fall on the detector simultaneously. FTIR thus has higher sensitivity, a faster scan rate, better precision, and higher throughput than dispersive IR [9,32]. Additionally, the FTIR instrument is fast enough to achieve several scans over a chromatographic peak such that all peaks of a chromatogram are observed, and multicomponent peaks can be deconvoluted [9]. The instrumentation and applications of GC-FTIR have been reviewed numerous times [9,16,32].

13.3.1 Instrumentation

GC-FTIR interfacing requires a makeup/matrix gas and an interface to couple the GC instrument to an FTIR detector. Interfaces, marketed as GC-FTIR accessories, include flow cell and sample storage interfaces. Gold-coated LP interfaces allow online detection, while sample storage devices allow unlimited signal averaging. A comparison of GC-FTIR interfaces has been published [33]. With LP interfaces, considerations

of makeup gas flow, temperature, and volume must be made [32,34]. Alternatively, sample storage devices utilize an inert matrix gas and are operated at low temperatures [18,35]. The FTIR instrument consists of a Michelson interferometer, an IR light source, IR-transparent windows, a mercury–cadmium–tellurium (HgCdTe; MCT) detector, and software. Fig. 13.2 illustrates the instrumental setup of GC-FTIR with various interfaces and data processing [1].

Nitrogen (N_2) is typically used as the makeup gas for the LP interface, to simplify the instrumental setup. The GC-FTIR instrument must be purged to remove carbon dioxide and water, which absorb strongly in the IR region [32]. For this reason, an initial background scan must be performed before runs to ensure N_2 is flowing briskly enough to remove background atmospheric interferences from the measurement [16]. It is convenient that most GC carrier gases are transparent in the IR region [32]. Makeup flow is added either at the junction of the column and transfer line or at the LP entrance. A baseplate optically aligns the interface and detector during installation. The addition of the makeup gas increases the mean velocity of the analyte in the LP, thus reducing its residence time. Additionally, the makeup gas further dilutes the analyte in the carrier gas [34].

In GC-FTIR, unmodulated radiation emitted from the LP oven contributes to detector saturation [16]. This means that the IR throughput of the LP is degraded at high temperatures; this leads to poorer detection limits for compounds of low volatility [16]. However, the LP and transfer lines must be heated to prevent condensation of compounds eluting from the GC column. This means the material used to fabricate the LP must withstand high temperatures, up to at least 300°C [9]. Not only the material used in the fabrication of an LP needs to be inert, as many compounds are labile and may decompose on an active surface, but the material must also be highly reflective. The reflectivity of the LP surface, windows, and gas entry and exit ports must be considered. Gold is highly reflective, inert, and thermally stable; thus, a gold-coated borosilicate glass capillary is typically used [9]. Potassium bromide (KBr) windows, which are transparent to IR light, are placed at the ends of the gold-coated LP [9,32]. When choosing an LP interface, one must consider geometry, reflectivity, and the fabrication methods used in the manufacturing of the LP [9,16]. The LP dimensions must be such that the IR radiation from the source is transmitted with minimum signal loss. To keep the flow laminar and prevent mixing, the length-to-diameter ratio must be as high

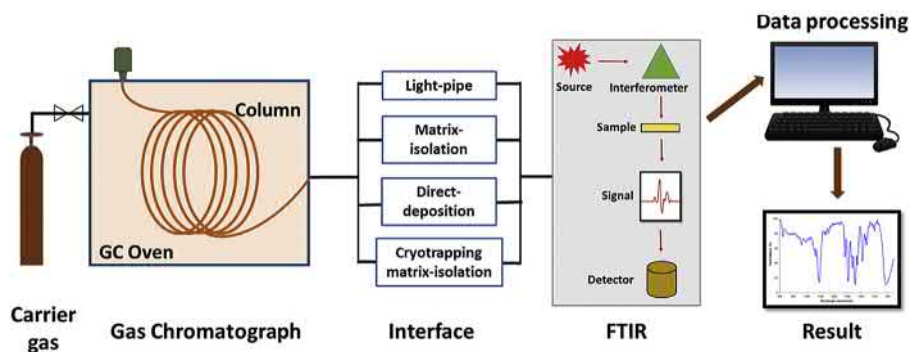


FIGURE 13.2 Schematic diagram illustrating the GC-FTIR setup with various interfaces and data processing. Figure was reproduced with permission from Elsevier (copyright, 2018) Zavahir JS, Nolvachai Y, Marriott PJ. *Molecular spectroscopy: information rich detection for gas chromatography*. *TrAC Trend Anal. Chem.* 2018;99(1):47–65.

as possible. A gold-coated LP has optimized dimensions ($L/D = 120$). In general, LP volumes should be equal to 76% of the total elution volume.

Sample-storage GC-FTIR interfacing offers sensitivities three orders of magnitude lower than LP interfaces [33]. The effluent is concentrated, the mobile phase is eliminated, and the separated analytes are immobilized on a trapping medium within a matrix of inert gas [1,32]. The high specificity of sample-storage techniques allows straightforward discrimination between closely related chemical compounds and provides enhanced ability to differentiate isomers. Because these methods utilize cryogenic "freezing" of molecules, temperatures in the separation have no effect on the IR spectra unlike conventional LP interfaces [18].

The hardware for MI requires precise construction and operating parameters, which affect sample collection and must be carefully defined and controlled [18]. The Cryolect is an MI interface for GC-FTIR that was initially manufactured by Cryolect Scientific Corporation, led by Gerald T. Reedy. This interface requires a turbopump, an expensive stepper motor, a remote MCT detector, and a cryogenic refrigerator [19]. In the design of an MI interface, volume and surface area of the matrix perpendicular to the spectrometer light beam must be considered. While the absorbance measured by FTIR is directly proportional to the mass of the compound, absorbance is inversely proportional to the surface area of the matrix. Thus, it is advantageous to minimize the surface area of the matrix [18]. In MI-GC-FTIR, a helium (He) effluent with 1%–5% argon (Ar) is typically utilized [18,19]. The GC effluent and Ar matrix gas are directed under vacuum and codeposited on the edge of a reflective four-inch diameter gold-coated collection disk or cylinder, which is slowly rotated during GC separation. Eluent is deposited as a thin band on the surface of the disk and is cryogenically frozen at 12 K [16,19,32]. FTIR spectra are recorded

postseparation [16,32]. After the chromatographic run is complete, the operator selects the peaks of interest and positions the Cryolect cylinder so that the peak can be detected by FTIR [19]. MI obtains the IR spectrum in reflectance mode meaning the IR beam is then reflected through the deposited eluent and focused on an MCT detector [5,16]. The low-temperature Ar matrix partially isolates individual molecules yielding a high level of IR spectral absorbance per nanogram of sample [18]. Thus, spectra exhibit sharp features due to reduction of intermolecular interactions and elimination of rotational and vibrational band broadening [19,32]. Detailed discussions of MI GC-FTIR have been published [18,19].

Direct deposition (DD), sometimes referred to as cryo-trapping, is a subambient GC-FTIR trapping interface [16] that positions an IR microscope very close to the deposition site of the GC effluent [1]. DD is most commonly used for the analysis of high-volatility substances by cooling to subambient temperatures and trapping the effluent on a zinc selenide (ZnSe) window using a thermoelectric cooler [16]. The sample is cryogenically frozen onto the N₂-cooled IR-transparent ZnSe substrate window for analysis [1,32]. While subambient trapping concentrates the effluent, it does not achieve molecular isolation [16]. However, spectra produced are similar, if not identical, to the spectra produced through the use of KBr windows.

FTIR measures all frequencies simultaneously, rather than individually as in the case of dispersive IR instruments [32]. As an alternative to using a monochromator grating, an interferometric spectrometer requires only that the radiant energy passes through the interferometer [9]. The interferometer is an optical device that causes two beams of light to travel different distances. A Michelson interferometer performs double-beam interferometry. A single-beam interferometer collects only one beam, while the other beam returns to the IR source [16]; in a Michelson interferometer, both beams exiting the interferometer are utilized [9]. The Michelson

interferometer incorporates moving and stationary cube corner mirrors to generate two modulated beams, which are 180 degrees out of phase with each other [16]. The stationary mirror is used so that parallel beams of IR radiation from the source are passed onto the mirrors through a beam splitter at a 45 degrees angle from the initial position of the moving mirror. The beam splitter splits the beam of incoming radiation into two paths, which reach the detector at different path lengths. The beam splitter is a thin film of Mylar sandwiched between two plates of a solid with a refractive index of 1. For typical experiments within the mid-IR range, a thin film of germanium deposited on KBr is required. The detector measures the intensity of the variation between beams as a function of path length changes. As each frequency comes in and out of phase at a characteristic optical path difference, the superposition of all frequencies produces the observed interferogram. The interferogram measured is the resulting optical path difference resulting from constructive and destructive interference [32]. The recombined beam from the interferometer may be in phase (constructive) or out of phase (destructive) depending on the optical path [9]. In double-beam interferometry, beam recombination produces a nulled interferogram with a significantly lower dynamic range than single beam detection [16].

The use of tunable IR lasers is appealing due to the increased sensitivity, which results from an increased source intensity [9]. Often a gas laser, consisting of 10:1 He:Ne, inside a small bore capillary tube is used. The laser is powered by a DC electrical charge and creates the driving voltage for the moving mirror. Additionally, the laser itself is used as an internal reference [32]. Because IR radiation produced by a laser is monochromatic, no interferometer or monochromatic grating is required. Instead, the laser output is "scanned" through an IR region, the

beam passes through the sample, and the intensity is measured by the detector. However, the major disadvantage of using a laser source is its limited spectral range in the IR region. A laser optoacoustic detector operates over four discontinuous regions between 900 and 1100 cm^{-1} . This detector has a detection limit of 20 pg or as low as 0.2 pg s^{-1} [9]. The electronically temperature controlled (ETC) EverGlo Global source is made of an efficient ceramic refractory composite that rapidly rises to operating temperatures. ETC EverGlo is thermally insulated to maintain constant operating temperature and provides strong, stable, reliable energy over the 50–7400 cm^{-1} region. Alternatively, the Nernst Glower source is a hollow rod made of zirconium, yttrium, and thorium. When heated to 1000–1800 K using an electrical source, the Nernst Glower produces IR radiation, which can reach temperatures of 1300 K. The major disadvantage of this source is that it produces UV and visible radiation, as well, and it tends to have a high failure rate. Finally, the mercury arc consists of a quartz jacketed tube containing mercury vapor at a pressure of 1 Pa and provides continuous radiation in the far-IR (20–400 cm^{-1}) region [32].

Nearly all GC-FTIR systems use MCT mid-IR detectors [16]. These detectors allow for rapid data acquisition [1]. Liquid N_2 -cooled MCT detector response times enable operation at data acquisition rates greater than 1 MHz. Notably, the GC-FTIR marketed by Thermo Scientific Nicolet utilizes an MCT-A "smart" detector. This detector is equipped with a patented mechanism to prevent the formation of ice on the detector element during the 18-h liquid-hold time. The disadvantages of an MCT detector are its reported ease of saturation and a nonlinear response caused by preamplifiers, which can result in spectral artifacts. By using small-area MCT detectors and microsampling applications, background noise can be reduced [16].

13.3.2 Performance characteristics

The efficient utilization of GC-FTIR depends upon optimization of the interfacing between the GC and the FTIR detector [34]. The Digilab LP-GC-FTIR system was the first to provide the speed necessary to conduct FT computations in 700 ms for 8 cm^{-1} spectral resolution [36]. MI interfaces can achieve spectral resolution as low as 4 cm^{-1} [33]. While FTIR spectroscopy has improved the degree of precision at the frequency scale of the output spectrum to 0.01 cm^{-1} , the requirements of GC-FTIR chromatography are temporal and volumetric [9]. GC-FTIR requires a sample bandwidth in time, which ensures one or more FTIR scans can be taken for each component band. The goal is to achieve the maximum vapor-phase concentration for each eluted band [34]. Theoretically, the sensitivity of MCT detectors increases with acquisition speed, but little dependence of sensitivity on acquisition rate is observed [16]. The sample gas volume in GC is typically in the microliter range. In GC, volume can be approximated as a volume equal to the full width at half maxima (FWHM) of peaks emerging from a common capillary column. It is difficult to achieve a sufficient absorption path length with an incoherent light source in a small gas volume [1,37].

The number of spectral scans performed on each eluting component is a function of the sample peak width, flow rate through the LP, and the acquisition rate of the FTIR spectrometer [5]. Rapid scan interferometry is necessary to avoid temporal chromatographic resolution "degradation." Eluent concentration changes can cause IR distortions if the acquisition rate is too slow [16]. LP-GC-FTIR easily achieves acquisition rates of 5 Hz but increasing resolution will result in a lower acquisition rate [5]. Volumetric resolution between each eluted band must be greater than the LP volume, such that each spectrum for each component band is recorded separately. For an LP of fixed volume

scanned at a predetermined rate, the concentration of the sample in the LP flow cell is dependent on GC column efficiency and decreases as flow rate is increased [34]. The number of scans possible per peak for an LP interface is restricted by the flow rate and is therefore of low resolution [16]. Thus, LP-GC-FTIR is a concentration-sensitive detector [3]. Samples move through the LP very quickly resulting in certain sensitivity issues [19]. The gold-coated LP-GC-FTIR achieves limits of detection as low as 10 ng and routinely operates to reliably detect quantities of 100–1000 ng on column [9]. While permitting analysis of trace components, the LP is the least sensitive GC-FTIR interface with limits of detection in the nanogram range [1]. Improvements in sensitivity for LP interfaces require discrimination between modulated IR radiation passing through the LP and unmodulated IR radiation from the GC oven [16].

Sample-storage interfacing techniques, which are mass-sensitive rather than concentration-sensitive, are much more sensitive than LP interfaces [9,16]. DD-GC-FTIR has mid-range 500 pg detection limits, which is competitive with MI-GC-FTIR [16]. In MI-GC-FTIR, the absorbance measured is directly proportional to the mass of the compound [35]. Because MI freezes molecules in a single rotational state, the IR spectra recorded from MI-GC-FTIR is characterized by sharp absorption bands due to minimal intermolecular interaction and absence of rotational band broadening [16,19]. Rotational states are unpopulated in the cryogenic effluent, so vibrational absorbance transitions begin from ground states rather than excited states. Additionally, a large number of vibrational absorptions not resolved in gas-phase spectra collected by LP-GC-FTIR are resolved in absorbance–reflectance spectra collected using MI [16]. By freezing molecules in a single rotational state, MI results in an increased signal-to-noise ratio and reduced band broadening compared to LP interfaces [16,18,19]. MI has

detection limits in the low picogram range, due to a more concentrated effluent on the collection disk than would flow through an LP, as well as due to unrestricted signal averaging capabilities [16,35]. Because the low-temperature matrix freezes the entire chromatogram onto the cylinder until it is warmed back up, signal averaging can be used to improve sensitivity [19]. To improve MI sensitivities further would involve decreasing the surface area of the gold-coated cylinder while maintaining optical throughput [35]. The performance characteristics of MI-GC-FTIR [35] and DD-GC-FTIR [38] have been evaluated in detail.

13.3.3 Data analysis and interpretation

The absorption value determined by a spectrometer depends on the absorptivity of the compound at the chosen wavelength, the number of absorbing molecules per cross-sectional area of the spectrometer beam, and the assumption that the absorptivity of a molecule is independent of sample state [35]. FTIR spectroscopy has the ability to provide a wealth of vibrational and fine structure information [1]. Thus, FTIR spectroscopy is adept at detecting functional groups and characterizing covalent bonds [32]. The absorption of IR radiation leads to vibrational excitations within molecules. Due to varied bond lengths, bond strengths, and vibrational modes between atoms in a molecule, the frequency of radiation absorption varies. IR absorbances are specific to stretches, wagging, rocking, and other excitations dependent on the functional units present; therefore, the IR signal fingerprint can be directly predicted using quantum chemical methods [1]. Mid-IR interfaces have small absorption cross sections leading to inferior sensitivity, but fingerprint spectral selectivity remains high [6]. Because every molecule has a unique IR spectrum, FTIR spectroscopy can differentiate between aromatic substitutions, *cis*- and *trans*-isomers, ring isomers, aliphatic chains, and functional groups [9,32]. In

MI-GC-FTIR, the band broadening and shifting observed due to intermolecular bonding, rotational absorption, and vibrations of molecules are absent within the fingerprint region, and this results in higher resolution spectra [1,19]. The absorptivities from liquid and gas-phase spectra can be referenced in MI-GC-FTIR, unlike with LP interfaces, which require gas-phase reference spectra [35]. Additionally, there is a larger spectral library available for DD-GC-FTIR than for reflection-absorbance (used for MI applications) or vapor-phase spectra (used for LP applications) [32]. A database of standard reference gas-phase spectra has been published [39]. Fig. 13.1 illustrates some vibrational transitions of molecules in the mid-IR region.

Library-search methods are used extensively in GC-FTIR. Initial GC-FTIR library search methods were based on absorbance spectral comparisons. However, in order to avoid time-consuming FFT, search techniques based on time-domain interferogram comparisons were developed. Ordered libraries and the development of prefilters limit searching to a portion of the library, which is most appropriate for the target spectrum. Library comparisons are made using squared differences, absolute differences, or match factors. The squared differences metric computes the sums of the squared differences (residuals) between digitized library intensities and corresponding target spectral intensities. The absolute difference metric is the unsquared sum of differences between target/library intensities. Finally, match factors are a derivative metric that are less susceptible to sloping baselines. Typically, match factors are calculated for each target/library comparison, and the library spectrum with the lowest match factor is the most similar to the target [16].

Deconvolution is possible because high accuracy in measured frequencies allows for precise subtraction of data. Peaks are deconvolved using the same spectral subtraction and curve-fitting programs used for routine FTIR. Deconvolution is achieved by subtracting a known spectrum

from an unknown mixture or by fitting Gaussian or Lorentzian curves to spectral bands of the unknown mixture to synthesize a spectrum representing a single component of the unknown mixture. One can deconvolute the spectra of overlapping peaks by deriving the positions, intensities, widths, and relative areas for individual lines [9].

13.3.4 Data treatment

Manual interpretation of GC-FTIR spectra is time-consuming and requires significant expertise; therefore, computerized methods have been developed to aid in mixture component identification. Interpretive methods use pattern recognition techniques to predict the presence or absence of specific functional groups [16]. Interpretative software provides rapid class information using pattern recognition algorithms generally performed after FFT. Additionally, interpretations have been demonstrated using interferometric data and a cross-correlational procedure [5]. Detailed discussions of the different algorithms for the reconstruction of gas chromatograms in GC-FTIR have been published [36,40]. FFT and GSO are the most common methods used to generate chromatograms in GC-FTIR [16,40]. While FFT provides greater specificity than GSO, it is computationally inefficient [36]. The GSO algorithm was developed in response to a need for a method, which is fast enough computationally to be performed online during data collection [19]. Today, improvements in the computational efficiency of data processing systems have allowed for the facile application of online FFT to GC-FTIR.

FFT is an automated data reduction technique, which makes it less necessary for the user to manually intervene. However, as automated data reduction techniques are often fallible, intermediate data formats should be intelligible to the user [36]. FFT is a mathematical process that converts a time-domain GC-FTIR

interferogram into an IR spectrum [16]. FFT transforms the interferometric data and sums the absorbance values over the mid-IR frequency range [5]. Measurement of IR absorbance from a GC-FTIR time domain requires that for each acquired interferogram, an IR spectrum must be computed during the chromatographic separation [16]. It is important to keep post-run processing to less than the time necessary for the GC temperature to recycle. Time-consuming calculations are overlapped with data analysis to minimize data reduction time [36]. Chromatographic resolution is sacrificed if the FFT is not performed quickly [16]. By saving absorbance spectra rather than interferograms, the interferometer essentially becomes a spectrometer. Data volume is reduced because component spectra are derived from coadded spectra rather than coadded interferograms [36]. Absorbance integration after FFT can be used to generate functional group chromatograms with a greater signal-to-noise ratio than a GSO method [16].

The functional group specific regional reconstruction technique works with absorbance spectra [36]; therefore, it is typically applied post-FFT. In fact, this technique requires the rapid capabilities of the Cooley–Tukey FFT [16]. Regional reconstruction normally disregards spectral frequencies with low signal to noise and selects for only certain absorbance frequencies but will detect all shapes of absorbance bands within those frequencies [36]. The concept of “functional group regional reconstruction” is analogous to mass chromatograms produced by GC-MS [16]. Synthesized functional group interferograms can be mathematically cross-correlated with GC-FTIR interferograms to produce functional group specific chromatograms by selectively monitoring associated absorption bands [5,16]. Although it is not as computationally efficient as the GSO technique, this technique provides more information than a GSO trace if regions are adequately selected [36]. Essentially, more specific information regarding

the structures of separated compounds can be obtained post-FFT [16]. An example of functional group regional reconstruction compared to the GSO reconstruction is shown in Fig. 13.3 [41,42].

Alternative to FFT, chromatograms can be generated from interferograms directly by monitoring slight changes in the digitized waveforms [16,36]. The GSO algorithm calculates chromatograms directly from the absorbance information

in the interferograms [5,17]. GSO chromatogram generation is a vector orthogonalization process in which each sample scan interferogram is orthogonalized with respect to a basis set derived from background interferograms [9]. Twice as sensitive as other obsolete non-FFT-based techniques, the GSO method is more computationally efficient than methods applying FFT as it requires fewer “floating-point operations” [16,36]. It is feasible to compute low-resolution

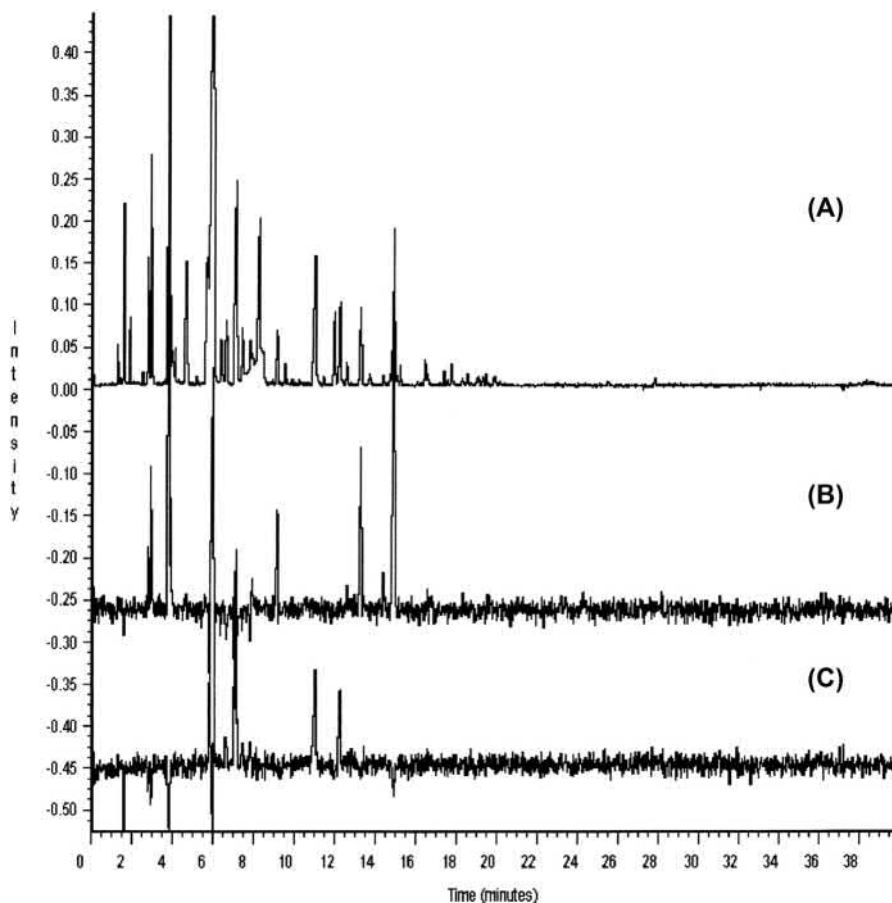


FIGURE 13.3 GC-FTIR profiling of the aroma from *F. ananassa* cv. Oso Grande on a DB-Wax capillary by purge-and-trap sampling: (A) total Gram–Schmidt reconstruction; (B) selected wavelength chromatogram within the range $1250\text{--}1210\text{ cm}^{-1}$ (esters); (C) selected wavelength chromatogram within the range $1200\text{--}1150\text{ cm}^{-1}$ (acetates). Figure was reproduced with permission from American Chemical Society (copyright, 1999) Gomes da Silva MD, Chaves das Neves HJ. Complementary use of hyphenated purge-and-trap gas chromatography techniques and sensory analysis in the aroma profiling of strawberries (*Fragaria ananassa*). *J. Agric. Food Chem.* 1999;47(11):4568–4573.

IR spectra using the GSO maximum absorbance algorithm. Digilab's FTS-GCS software uses this maximum absorbance algorithm for the automatic identification of chromatographic peaks [36]. GSO reconstruction is used to locate eluting compounds in the GC data and pattern recognition techniques may be used to classify separated compounds [43]. However, the GSO reconstruct is nonselective and therefore not truly comparable to regional reconstruction methods. This is because the GSO reconstruct only looks at absorbance bands of specific widths, rather than specific frequencies. The spatial features selected are the differences between two spectra produced by different interferometric resolutions. Low spatial frequency–baseline features are subtracted out, while high spatial frequency–narrow line bands cause attenuated ringing and tend to cancel each other out [36]. An online class-specific GC-FTIR reconstruction from interferometric data has been described [44].

13.4 Gas chromatography vacuum ultraviolet spectroscopy

In 2019, Lelevic et al. published a review of GC-VUV instrumentation and applications [6]. An earlier publication by Santos and Schug discussed advances in GC-VUV research and development through 2016. The term “vacuum” refers to the historical need for a vacuum to reduce background absorption from air and moisture; thus, VUV refers to an operation that would normally require a vacuum and a synchrotron light source [3]. However, benchtop GC-VUV does not require a vacuum. Instead, the VUV detector utilizes an inert gas to purge the VUV system and remove air and moisture. VUV detection for GC is preferable to UV detection because most volatile compounds exhibit limited absorption in the UV-Vis region but tend to exhibit strong absorption in the VUV region, ultimately resulting in a highly featured gas-phase absorption spectra

[1]. Fig. 13.1B illustrates the electronic transitions of molecules probed by VUV absorption spectrophotometry.

13.4.1 Instrumentation

GC-VUV interfacing requires makeup gas, a heated transfer line, a flow cell, a light source, optical housings, windows, mirrors (reflective optics), a diffractometer, a charge-coupled device (CCD) detector, and software [1,2]. Fig. 13.4 illustrates the instrumental setup for GC-VUV (not to scale) [25]. The VUV detector for GC does not require a vacuum to operate. Instead, the optical path is purged by an inert gas to reduce background absorption from water and oxygen. The effluent from the transfer line is mixed with a makeup gas before entering the flow cell. The makeup gas is typically N₂ or Ar, but He is also used [3]. When high-purity N₂ (99.999%) is compared to high-purity He (99.999%), no optical gas-dependent spectral differences are observed [45]. It is convenient that GC carrier gases have relatively low absorptivity and can be easily subtracted from the background. Therefore, using the same GC carrier gas and VUV makeup gas can simplify the instrumental setup. The makeup gas flow rate can be varied to control residence time of the analyte peaks within the flow cell. A longer residence time in the flow cell reduces noise due to repeated measurements. However, this also increases band broadening. Increasing the makeup gas flow rate reduces band broadening [3].

In GC-VUV, there are three temperature-controlled thermal zones. The first is the GC oven and the second is a heated transfer line connecting the GC to the VUV detector. From the GC column, eluted analytes are carried through a heated transfer line to the detector [3]. The heated transfer line is typically an uncoated, deactivated stainless steel capillary held at 275°C (maximum 300°C for VGA-100 and 420°C for VGA-101) [25]. The heated transfer line is temperature-controlled to avoid

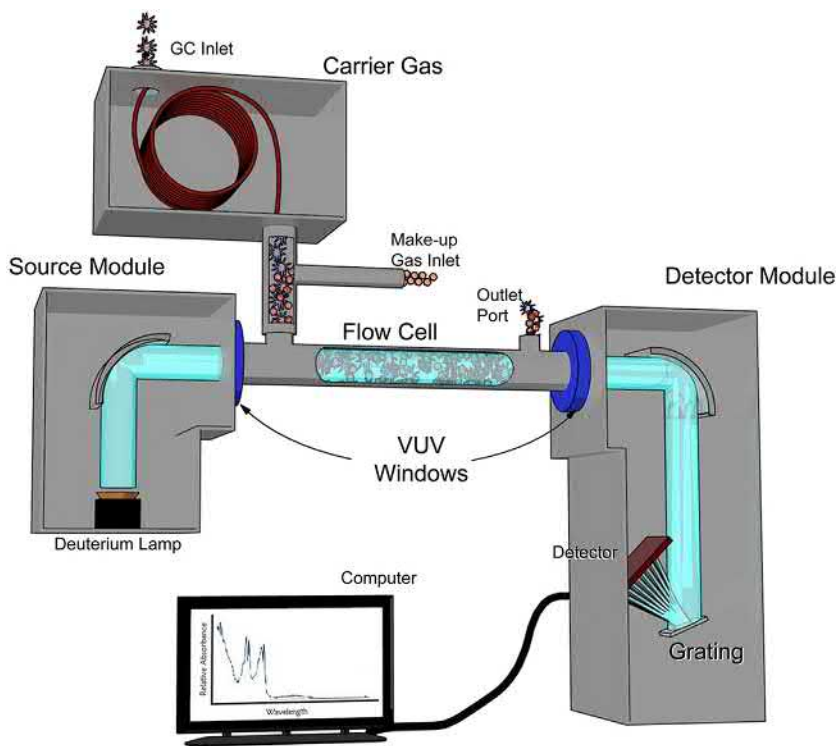


FIGURE 13.4 Schematic of a gas chromatography vacuum ultraviolet spectroscopy instrument. *Figure was reproduced with permission from ACS Publications (copyright, 2014) Schug KA, Sawicki I, Carlton Jr DD, Fan H, McNair HM, Nimmo JP, Kroll P, Smuts J, Walsh P, Harrison D. Vacuum ultraviolet detector for gas chromatography. Anal. Chem. 2014;86(1):8329–8335.*

condensation of the effluent before it can reach the detector [1]. The third thermal zone consists of an internal VUV transfer line and the detection flow cell. This thermal zone is held dozens of degrees higher than the final temperature of the GC separation or of the first thermal zone. The flow cell is maintained at a temperature high enough to avoid condensation of high-boiling constituents, which would result in analyte loss and/or fouling of the instrument [6]. The VUV detector thermal zones can be heated up to 300°C (for the VGA-100; up to 420°C for the VGA-101) [3]. The elevated temperature increases flow rate and pressure through the flow cell compared to the first thermal zone. At high flow rates, this may affect quantitation. Additionally, the larger the size of the flow cell, the

more significant the peak dispersion, especially for lower molecular weight species. However, a smaller flow cell volume does not require a marked increase in makeup gas pressure and thus maintains higher sensitivity [6]. Both the VGA-100 and the VGA-101 detectors have a path length of 10 cm, but, the VGA-101, with an internal flow cell volume of 40 μL , results in superior peak shape compared to the VGA-100, which has an internal volume of 80 μL [3]. The VGA-101 is also capable of operating at temperatures up to 420°C, in order to accommodate high-temperature GC analysis.

Broadband UV/VUV detection requires a broadband deuterium, tungsten, and/or xenon source lamp. A typical deuterium discharge lamp produces wavelengths between 190 and

380 nm for detection, while a tungsten lamp produces longer wavelengths for UV/Vis detection [1]. Single-wavelength light sources have also been used [22]. A modified deuterium lamp (equipped with MgF windows) is used in the VGA-100 and VGA-101. It is able to deliver shorter wavelengths, down to 120 nm, essentially the bandpass cutoff for MgF₂ materials. MgF₂ windows are required for VUV detection as this is one of the few materials that will allow such high-energy photons to pass [3]. Reflective optics focus the VUV/UV light to the flow cell, which is capped by MgF₂ windows and diffracted by the holographic grating onto the CCD detector. The use of specially coated reflective optics and a back-thinned CCD allows for the collection of high-quality VUV spectra between 120 and 240 nm for the VGA-100 and between 120 and 420 nm for the VGA-101 detector [25].

Typically, VUV detection is achieved using a CCD. CCD uses a silicon chip to convert light into an electrical signal by absorbing a photon and subsequently releasing an electron. The released electrons are held in an array of wells or pixels by electrodes and a charge is built up corresponding to the pattern of incident light. The advantages of CCD include a low dark count rate, low read noise, and high quantum efficiency [2]. The CCD is capable of acquisition rates up to 77 Hz and records all wavelengths simultaneously [3].

The instrumental setup for GC-UV detection is very similar to GC-VUV. GC-UV detection, as reported by Luong and Shellie, is achieved with a DAD traditionally used for UV detection of liquid samples by high-performance liquid chromatography (HPLC). A downside to this GC-UV is thus the lack of high-temperature capabilities necessary to volatilize samples. Also, because a smaller range of compounds are visible in the mid-to-near UV range, GC-UV does not have the large range of applications offered by GC-VUV detection [28–31]. That said, a traditional repurposed

UV detector is relatively inexpensive relative to the commercial VUV detector.

13.4.2 Performance characteristics

The VUV is not a mass-sensitive detector but can appear to exhibit a mass-dependent response due to the minimal influence of GC effluent and makeup gas on analyte concentration in the flow cell. GC-VUV is often not considered a concentration-sensitive detector, because increasing the flow rate does not significantly reduce the signal; however, significant experimentation has been performed to technically define the VUV as a concentration-sensitive detector [6,46]. VUV detectors have high signal averaging capabilities and are capable of fast acquisition rates up to 100 Hz, making VUV detection amenable to “fast” GC separations [1,6]. However, elevated acquisition frequencies can induce significant noise, while lower acquisition frequencies can improve signal average and result in a smoother baseline [6]. For example, a “tolerable” acquisition rate of 4.5 Hz yields a reasonably noiseless signal and enough points across a typical chromatographic peak [27]. Increased residence time of the analyte in the flow cell allows for greater signal averaging and reduction of noise [1].

While GC-UV has detection limits in the nanogram-on-column range, GC-VUV has superior detection limits in the picogram-on-column range [1]. VUV detection has sufficient linear range (2–3 orders of magnitude) and good sensitivity. The overall sensitivity for different molecule classes does not vary by more than two orders of magnitude [6]. Spectral filters (applied digitally following data acquisition) allow for the selective identification of classes of molecules and improve sensitivity, detection limits, and noise observed within a spectrum [1,6]. Currently, while GC-VUV is the most sensitive molecular absorption detector (and essentially the only detector widely commercially available), its limits of detection are often worse

than flame ionization and MS detection. A comprehensive evaluation of the detection limits offered by the newest VGA-101 GC-VUV detector for a wide range of compounds has not been reported so far.

13.4.3 Data analysis and interpretation

GC-amenable compounds that absorb in the UV wavelength range are few, but in the VUV range, virtually all molecules absorb and have unique absorption signatures [6]. A chromophore is some functionality on a molecule that is amenable to absorption of certain energies of light [2]. Different molecules possess different chromophores based on their structures and thus have different sensitivities [3]. VUV detection probes ground electronic state to excited electronic state transitions of chromophores [6]. The shape of the VUV spectra acquired is heavily dependent on the electronic structure of the analyte. Vibrational bands cause some spectral feature broadening and additional spectral fine structure [3]. Functional groups have different absorptivity, produce different sensitivities, and result in different absorption maxima such that unique spectral fingerprints exist for all compound classes in VUV [1]. Group-specific selectivity and quantification are thus possible. For example, Rydberg transitions can be explored for a range of alkanes resulting in unique spectra. Additionally, bathochromic shifts, which shift absorbance maxima toward longer wavelengths, indicate an increase in the number of aromatic rings or double bonds, as shown in Fig. 13.5 for fatty acid methyl esters [6]. VUV can differentiate between isomers by deconvolution of coeluting peaks [3]. Because VUV has high specificity, isomers, isobaric, small, and labile compounds difficult to distinguish with other detection methods often can be distinguished [25].

The shape of the absorbance spectra is dependent on the electronic and vibrational structure of the analyte, not on the amount of analyte, which allows for spectral deconvolution based

on molecular structure [3]. Absolute quantitation of the amount of analyte present within the flow cell without chemical interferences is possible [25]. The absorption cross section for an analyte can be determined by correlating a “reference” spectrum to a specific amount of analyte using a scaling factor. This method is considered “absolute” when it is used to determine the amount of analyte directly at the detector. In principle, the “absolute” cross section of an analyte can be determined by measuring a known concentration of standard analyte and calculating the mass-on-column using concentration, injection volume, and split ratio values. Peak area is dependent upon the amount of analyte, its absorption cross section over the given wavelength range, total flow rate of the GC carrier gas and the makeup gas, and the geometry of the flow cell in terms of length and volume [4]. It is important to note that instrumental settings for parameters, such as injection volume or split ratio, may not be accurate and subject to systematic error.

13.4.4 Data treatment

The VUV software (VUV-Analyze, VUVision) allows continuous monitoring of data in a three-dimensional (3D) plot of retention time, wavelength, and absorbance. Thus, simultaneous analyte and product decomposition can be detected [1]. When recording VUV spectra, dark and reference spectra are automatically measured prior to each run [27]. First, a “dark” spectrum is collected at the beginning of each run for subtraction of the makeup/carrier gas [3] by integrating 100 spectra over 11 ms in the absence of UV/VUV light. The “reference” spectrum is then collected by integrating 100 spectra over 11 ms in the presence of UV/VUV light. Finally, a series of absorption spectra are measured using 20 scans of 11 ms and corrected against the background “dark” and “reference” spectra [27]. Integration of analyte absorbance over a wavelength interval converts

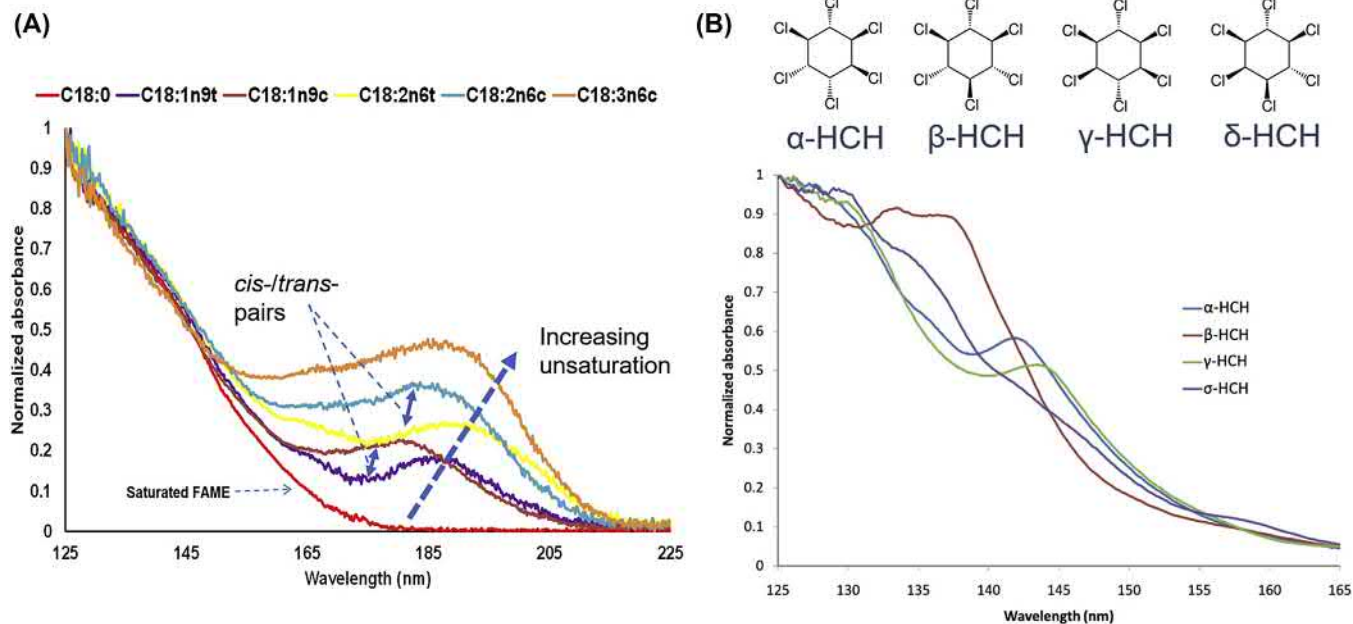


FIGURE 13.5 Some examples of VUV absorption spectra for (A) saturated and multiple unsaturated fatty acid methyl esters and for (B) hexachlorohexane isomers, of which lindane (γ -HCH) is a pesticide. In (A) is demonstrated how spectra shift with increasing unsaturation and how cis-/trans-isomers are often well distinguished. Stereochemical and conformational effects clearly alter VUV absorption as shown in (B). *Figures were reproduced with permission from Elsevier (copyright, 2015; 2016) (A) Fan H, Smuts J, Bai L, Walsh P, Armstrong DW, Schug KA. Gas chromatography–vacuum ultraviolet spectroscopy for analysis of fatty acid methyl esters. Food Chem. 2016;194:265–271. (B) Fan H, Smuts J, Walsh P, Harrison D, Schug KA. Gas chromatography–vacuum ultraviolet spectroscopy for multiclass pesticide identification. J. Chromatogr. A 2015;1389:120–127.*

the absorbance spectrum to a single-value chromatographic response. Any integration procedure can be used as long as the same procedure is used for all spectra in the analysis [4].

The VUV software provides the ability to deconvolute individual analyte contributions to coeluting peaks. Spectral deconvolution reduces the need for special column chemistries to separate compounds not easily discriminated by other detectors. Deconvolution is based on an additive absorption concept as applied for classification and speciation of complex mixtures. Additive absorption is a property of Beer's Law and only fails when absorption saturation occurs; this is typically when absorption exceeds 1.1 - 1.2 absorption units, or when 95% of the light is absorbed. Additivity also assumes there is no physical interaction between multiple species present simultaneously in the flow cell, but this is easily accommodated by the dilute nature of the analytes that pass through the flow cell volume. The VUV absorbance fitting algorithm is based on wavelength and molar absorptivity, which is directly related to the absorption cross section by Avogadro's constant. The algorithm utilizes fitting coefficients based on the amount of analyte contributing to the total absorbance value relative to the amount of analyte contributing to the reference absorbance at each wavelength. Each absorbance scan is fit resulting in a distinct set of fitting coefficients. A single reference absorbance spectrum can be used to determine the absorbance. If both compounds are known, and their pure reference spectra are available in the VUV library, it is possible to determine the individual contribution of each compound [3].

The ability to deconvolute coeluting compounds allows chromatographic resolution to be sacrificed for faster separations without losing the ability to distinguish compounds of different classes. Compounds with similar absorption spectra are more difficult to deconvolve; thus, there are greater limitations to the relative abundances of co-eluting compounds of the same

class, which can be deconvolved. The sum of the squared residuals (SSR) indicates the ability to distinguish between two similar absorbance spectra. Smaller SSR values indicate that deconvolution will be more difficult to perform and can only be performed for analytes having limited disparity in abundance. For pairwise overlapping isomers of dimethylnaphthalenes, relative abundance can be estimated up to two orders of magnitude (99:1); covariance calculations estimate detection limits in the high picogram range for coeluting isomers [3]. For compounds with a low SSR (<0.25), the relative abundance that can be estimated is lower (50:1). Sufficient spectral dissimilarity ($SSR > 1$) is needed to estimate relative abundances of species in concentrations as low as 10:1 [6].

Although there is a scarcity of reference spectra in the far-UV range, the VUV spectral databases are being constantly augmented and refined [6]. A database of gaseous VUV/UV/Vis spectra can be found [47]. Theoretical spectra can be calculated using semiempirical methods, time-dependent density functional theory (TDDFT), inexpensive parametric approaches such as ZINDO/S, and sophisticated post-Hartree-Fock methods offered in software packages, such as Gaussian. However, the applicability of highly accurate theoretical spectral calculations is limited by the size of the molecule; here, simple and inexpensive methods are often sufficient. TDDFT, using for example a PBE0 aug-cc-pVDZ functional and a B3LYP/6-31+G** basis set, has been shown to provide good prediction power for limited computational cost [49,54]. Theoretical VUV spectra assume discrete transitions between discrete energy levels, yet simultaneous excitation of a number of electronic and vibrational modes using a broadband light source complicates the absorbance profile. Distinct features seen in theoretical spectra of isomers and other related compounds do not always translate to experimental spectra [25]. The theoretical spectral lines have to be artificially broadened using Gaussian

functions, in order to more closely align with experimental spectra. Fig. 13.6 illustrates experimental and theoretical spectra calculated for an isobaric set of designer drugs using TDDFT.

TDDFT can be used to model theoretical VUV spectra for sets of compounds (e.g., isomers) without preexisting library reference spectra and/or limited standard availability. Following computation of spectra by TDDFT, an SSR is calculated between theoretical and experimental spectra [6]. In an investigation of the potential for deconvolution by replacing actual spectra with theoretical spectra, important features of the experimental spectra were reproduced in the theoretical spectra. In TDDFT, when the relative abundance of two coeluting peaks is comparable (1:1 to 3:1), deconvolution gives reasonable results, but when one component is in significant excess, the deconvolution exaggerates the ratio of the other component significantly [1]. TDDFT has been applied to modeling the spectra [48] of alkanes [49], designer drugs [50], dimethylnaphthalenes [51], isotopologues [52]; oxidation of polycyclic aromatic hydrocarbons [53]; paraffin, iso-paraffin, olefin, naphthalene, and aromatic (PIONA)-class molecules [54], and nitrate ester explosives [55].

Time interval deconvolution (TID) is a process whereby automated deconvolution and classification of peaks and coeluting peaks across an entire chromatogram can be performed. Compared to conventional methods that take 2–3 h for data analysis, TID takes approximately 30 s to run deconvolution and analysis on a 30-min chromatographic run [3]. TID is considered a “supervised approach” because this spectral mixture estimation algorithm is based on estimating a linear combination of known spectra in the given retention window where known compounds elute. Thus, TID requires known reference spectra, retention indices, and relative response factors (RRFs) [6]. The data set is divided into time interval slices and each slice is analyzed using the general least squares regression procedure. Time intervals are constrained by a user-

defined retention index window. After all time intervals are analyzed, the total response for classes of compounds speciated is converted to percent mass contributions using RRFs [3]. Estimation of RRF based on mass percent has been demonstrated [6]. Finally, TID can break down bulk content into subcategories such as carbon distribution [3,56]. TID has been applied to the analysis of petroleum chemicals [57–59] and polychlorinated biphenyls [60].

For practical purposes, internal standard-based pseudoabsolute quantification is an approach where RRFs are computed for unknown coeluting compounds [6]. While an “absolute” method is based on a functional relationship between physical constants and universal quantities [4], this method referred to as “pseudo-absolute” because an internal standard is used to account for systematic errors acquired during injection [3]. The conversion of the detected amount of analyte to the amount of analyte present during sample preparation is dependent upon the efficiency of the sample preparation and injection. Thus, this method can be used for system diagnosis and potentially calibrationless quantification [4]. Use of an internal standard normalizes systematic errors, because the internal standard encounters the same systematic errors as the analyte. Using this method, the total number of on-column molecules registering an absorption event can be determined when the absorbance cross section, detector scan rate, flow cell volume, path length, and carrier gas flow rate are known. While this method reduces the need for extensive calibration procedures, rigorous method validation should be considered best practice. Researchers should report linearity, limits of detection, and accuracy/precision even when using internal standard-based pseudoabsolute quantification [3]. The use of pseudoabsolute quantification was discussed in detail by Bai et al., [4]. Pseudoabsolute quantification was applied to GC × GC-VUV analysis of complex fatty acid methyl ester mixtures [61].

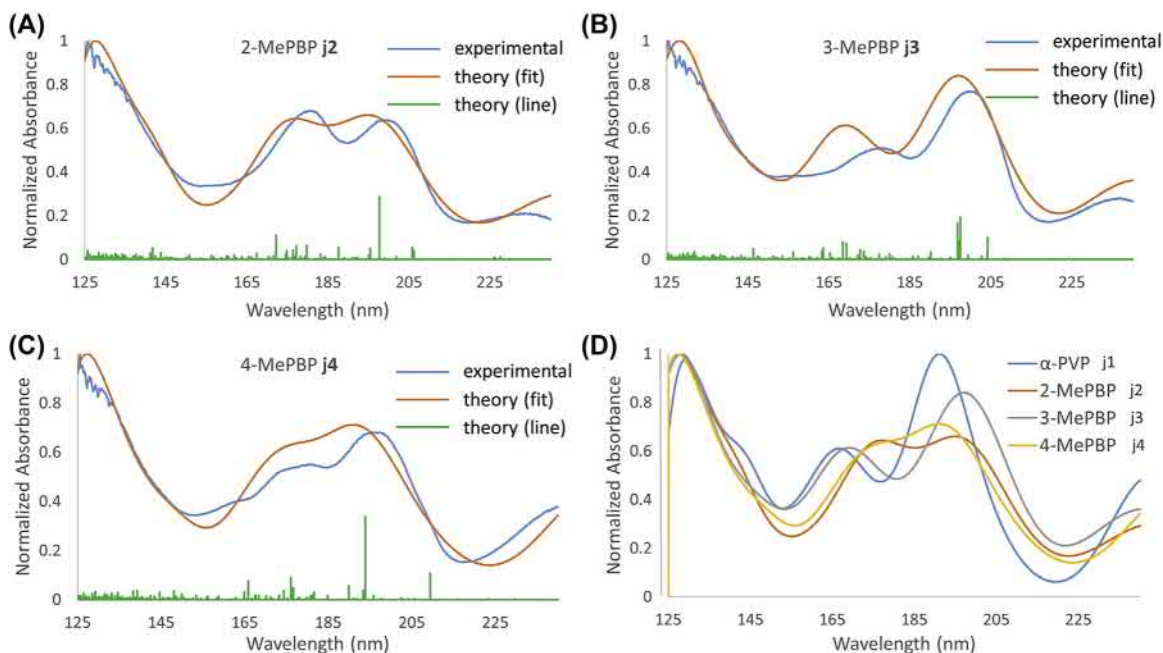


FIGURE 13.6 The experimental and theoretical VUV spectra for molecules from an isobaric set. The green (black in print version) stick diagram shows the excitation energies/oscillator strengths from TDDFT calculation using B3LYP functional and 6-31 + G(d,p) basis set. The theoretical spectrum is simulated with full-width-at-half-maximum (FWHM) of 0.07 eV and peak shifting factor of 0.99. From panel D, one could see although they are isomers, the computed spectra are distinct and differentiable. Figure was reproduced with permission from Elsevier (copyright, 2017) Skultety L, Fryczak P, Qiu C, Smuts J, Shear-Laude L, Lemr K, Mao JX, Kroll P, Schug KA, Szewczak A, Vaught C. Resolution of isomeric new designer stimulants using gas chromatography–Vacuum ultraviolet spectroscopy and theoretical computations. *Anal. Chim. Acta* 2017;971:55–67.

Nonnegative matrix factorization (NMF) allows for an entirely “unsupervised approach” to mixture estimation for compounds, which are unknown without retention indices or a spectral library entry. However, the number of compounds present in coeluting peaks must be known. NMF can only separate compound maxima, which have less than 33% overlap. Using this method for pairwise overlapping mixtures, relative abundance can only be estimated for ratios of 10:1 or smaller [6]. NMF has been applied to the analysis of drug and explosive precursors [62].

13.5 Comparison of techniques

In principle, LP-GC-FTIR and GC-VUV have similar instrumental setups. However, VUV detection is unaffected by high temperatures, while FTIR detection is easily saturated and often possesses significant baseline noise due to unmodulated radiation from the high-temperature GC separation. GC-VUV has greater sensitivity than GC-FTIR. MI freezes a molecule in a single rotational state increasing the signal-to-noise ratio, achieving picogram detection limits, and allowing for unlimited spectral averaging. LP-GC-FTIR is concentration-sensitive utilizing a flow-through gold-coated LP and achieving only nanogram detection limits [16]. Both VUV and FTIR molecular spectroscopies have high specificity and can provide both quantitative and, in particular, qualitative information. GC-FTIR and GC-VUV can elucidate structure-specific information not gathered by other detectors [3,16]. Additionally, because there is no ionization needed, VUV and FTIR molecular spectroscopy can analyze labile compounds. Finally, discrimination of isomers and deconvolution of coeluting peaks are easily achieved for both VUV [3] and FTIR spectra [9]. Today, GC-VUV is more heavily used over GC-FTIR, as GC-VUV can achieve low picogram detection limits and full spectral acquisition in real time, even when performing

fast GC [3]. A comparison of performance characteristics for GC-VUV and GC-FTIR can be found in Table 13.2.

13.5.1 Applications

Both GC-VUV and GC-FTIR have a wide range of applications in different fields, including: oil and gas; foods, flavors, and fragrances; life sciences; forensics; environmental analyses; pharmaceutical development; and others [6,32]. The applications of GC-VUV and GC-FTIR are compared in Table 13.3. These detectors are essentially applicable anywhere GC is applicable for analysis of volatile and semivolatile compounds. Applications of GC-FTIR [1,9,16,32] and GC-VUV [1,3,6] are summarized in a series of reviews. Interfacing molecular spectroscopy to MS provides complementary information, such that molecules that give poor or nearly identical fragmentation in MS can often be differentiated [1]. VUV is nondestructive [27] and does not alter the spectral features of downstream EI-MS fragmentation patterns if the detectors are placed in tandem [45]. VUV absorption does not result in any significant analyte photodissociation or modification in any manner to prevent successful MS identification [27]. The same can be assumed when coupling GC-FTIR to MS. FTIR can provide functional group identification, but often cannot distinguish between members of a homologous series. MS provides molecular weight and can distinguish between homologues, but often cannot differentiate between isomers [32]. Software such as Resolutions Pro and EZChrom Elite were used to analyze GC-FTIR-MS data [14/16]. GC-FTIR has been compared to GC-MS for the analysis of petroleum hydrocarbons and biomarkers [63], mineral oils [64], high-temperature degradation products [65]. GC-FTIR-MS was applied to the analysis of *cis-/trans*-FAMES isomers [66] and polychlorinated biphenyls [67].

TABLE 13.2 Comparison of the performance characteristics for GC-FTIR and GC-VUV.

Performance characteristics	GC-FTIR		GC-VUV		# Citations
	Light pipe	Matrix isolation /Cryo-trapping	VGA-100	VGA-101	
Light source	Mercury Arc/Nernst Glower/ETC Global/tunable laser-based light source		broadband deuterium/tungsten/xenon lamp		[6,32]
Wavelength/wavenumber	20–400/600–4000/50–7400/90–1100 cm ⁻¹		120–240 nm	120–430 nm	
Molar absorptivity			100–3000 Lmol ⁻¹ cm ⁻¹		[6]
Absorbance cross section	2 × 10 ⁻¹⁹ cm ² /molecule		1.00 × 10 ⁻¹⁷ –5.00 × 10 ⁻¹⁶ cm ² /molecule		[3,72]
Transfer line	Uncoated deactivated stainless steel capillary		Uncoated deactivated stainless steel capillary		[18,42]
Transfer line dimensions			610 × 0.25 mm		[37,56]
Analog-to-digital converter	110–200 kHz (16 bit-32 bit)				[10]
Instrument dimensions	41 × 67 × 334 cm (12 kg)		76.2 × 33 × 43.2 cm		[37,56,72]
Power input	120 V, 20 A, 60 Hz/240 V, 10 A, 50 Hz		120/240 V		
Power consumption	<1650 Watts		<700 VA		
Detector	MCT (18-h nitrogen hold time)		CCD		[1]
Universal detection	Concentration-sensitive; non-destructive		“Mass-sensitive”; nondestructive		[1,3,32]
Acquisition frequency	5–7 Hz		77 Hz		[1,5,6,19]
Data collection interval	700 ms	10 s	11 ms		[18,19]
Mirror velocity	6 cm s ⁻¹				[9]
Number of data points	2048/120–320		2068		[44]
Noise			4 × 10 ⁻⁵ cm ² g ⁻¹		[35]
Sensitivity			10–5000 cm ² g ⁻¹		
Signal-to-noise ratio	Nanogram	picogram	picogram		[1,3,16]
Limit of detection	10–100 ng	50–500 ng	20–60 pg	15–250 pg	[9,16,37,56]

Continued

TABLE 13.2 Comparison of the performance characteristics for GC-FTIR and GC-VUV.—cont'd

Performance characteristics	GC-FTIR		GC-VUV		#
	Light pipe	Matrix isolation /Cryo-trapping	VGA-100	VGA-101	Citations
Linear dynamic range	2–3 orders of magnitude		3–4 orders of magnitude		[41]
Pressure/vacuum	Atmospheric/ambient				[3,32]
Makeup gas pressure			0.25 psi/0.35–0.5 psi		[3]
Makeup gas flow	0.2 mL min ⁻¹ /3.3–10 mL min ⁻¹		3.4 mL min ⁻¹ (optimal)		[34]
Does not detect	N ₂ , Ar, He		H ₂ , He, Ar, N ₂		[3,32]
Strongly absorbing	CO ₂ , H ₂ O		H ₂ O, O ₂		
Carrier gases	N ₂ , Ar, He		H ₂ , He, Ar, N ₂		[3]
Makeup/matrix gas	N ₂ (carrier gas)	He (1%–5% Ar)	He, Ar, N ₂		[3,15,32,37,56]
Maximum temperature	300–325°C		300°C	430°C	[9,37,42,56]
Minimum temperature	24 K > lowest b.p.	12 K			[6,9,15]
Specificity	High spectral differentiation capabilities				[1]
Wavelength accuracy	0.01 cm ⁻¹ (1 cm ⁻¹ band width)		± 0.2 nm		[9,37,56]
Wavelength reproducibility	0.2 cm ⁻¹		0.05 nm		
Wavelength resolution	8 cm ⁻¹	4 cm ⁻¹	0.5 nm		[3,16,33]
Path length /Sampling area	10–20 cm	0.3 mm	10 cm		[3,18,32]
Flow-cell internal diameter/size of matrix	0.1–1.0 mm i.d.	1.5–2 mm diameter 0.02 cm ²			[32,35]
Flow-cell volume	48–120 μL			80 μL 40 μL	[5,16,32]
Flow-cell windows	KBr, ZnSe		MgF ₂		[3,32]
Flow-cell material	Gold-coated		deactivated stainless steel		[32]
Flow-cell dimensions	22" × 19.3" × 8.3" 0.3 cm i.d. × 42 cm 10 cm × 0.01–1.0 cm		10 cm length		[42]

TABLE 13.3 Comparison of the applications for GC-FTIR and GC-VUV.

Applications	GC-FTIR	GC-VUV
Oil and gas	Petroleum hydrocarbons and biomarkers bearing information of the geographic source (diamondoids, adamantanes, terpanes) [63], oxygenates in gasoline [73]	Paraffins, isoparaffins, olefins, naphthalenes, aromatics (PIONA) [54,57], dimethylnaphthalene (DMN) isomers in jet and diesel fuel sample [51], diesel fuel and weathered diesel fuel [58,71], methane, ethane, carbon monoxide and carbon dioxide, liquid hydrocarbon streams [59], alkanes [61], hydrocarbons [49]
Foods, flavors, and fragrances	cis/trans fatty acid methyl esters (FAMES) [66], organic volatiles [64], terpenes [74,75]	Terpenes, fatty acid methyl esters (FAMES) [76], ink photoinitiators [77], aromatic hydrocarbons [78]
Life sciences	Saturated and unsaturated fatty acid methyl ester degradation products [65]	Glucocorticoids—steroidal hormones, saccharides [79], fatty acids in blood plasma [80], cannabinoids and their metabolites [81]
Forensics	Nerve agents (isopropyl methylphosphonofluoridate, pinacol methylphosphonofluoridate) [82], amphetamine isomers [83]	Nitrate ester explosives [55], designer drugs [50], drug and explosive precursors [62], chemical warfare agent simulants, phenethylamines [84], fentanyl analogues [69], opiates [85]
Environmental	Nitrated polycyclic aromatic hydrocarbons [86], pesticides [87], polychlorinated biphenyl congeners [67],	Pesticides [88], polychlorinated biphenyl congeners [60], fatty acids methyl esters (FAMES) for bacterial identification and discrimination [89], formaldehyde leachates from proppants [68]
Pharmaceutical	Volatile organics in blood [90], drug development, amphetamine isomers [83]	Drug isomers [70], trace level water content and impurity profiling and stability investigation of 4-Ethoxy-1,1,1-trifluoro-3-buten-2-one (ETFBO) [91]
Other Applications	Cis- and trans-configurations of disubstituted piperidines and pyrrolidines [92]	Polycyclic aromatic hydrocarbons [53], permanent gases [93], isotopologues [52]

Complementary information derived from multiple detection methods can aid in the deconvolution of coeluting peaks [16]. UV, FID, and MS can be coupled in series to GC [30]. Similarly, VUV detection is orthogonal to GC separation, whereas MS detection is typically parallel [6]. This means VUV and MS library searches are orthogonal. Matches made with the VUV library have a 69.3% success rate, while matches made with the MS library have an 88.5% success rate. Utilizing both VUV and MS libraries can help avoid false assignments [27]. Headspace (HS) GC-VUV has been compared to HS-GC-MS revealing the orthogonality of the two techniques [68].

GC-VUV-MS data was analyzed utilizing match factors and correlation coefficients [27,45]. Using GC-VUV-MS, researchers have analyzed fentanyl analogues [69] and other drug isomers [70]. GC \times GC-VUV was utilized in the analysis of diesel fuels [71], liquid hydrocarbon streams [59], and complex mixtures [61]. Currently, GC Image is the only software supporting direct import of GC \times GC-VUV data for 2D visualization. However, GC image does not allow spectral filtering or specific processing of data. Free Open Access im! software (<https://www.plugin.fr/>) offers 3D visualization, spectral profile extraction, and spectral filtering of GC \times GC-VUV data [6].

13.6 Conclusions and future outlook

GC-VUV and GC-FTIR detections provide a wealth of qualitative information. Due to the orthogonality of VUV and FTIR to MS detection, the addition of molecular spectroscopy to GC-MS can aid in the identification of unknown species and facile deconvolution of coeluting compounds, even those that are of similar structure. In general, GC-VUV has superior sensitivity compared to GC-UV and GC-FTIR. VUV detection has a fast acquisition speed, making it amenable to fast GC separations and ultimately comprehensive 2D GC \times GC-VUV. Theoretical calculations of spectra can be performed for both GC-VUV and GC-FTIR using available software. However, for commercial GC-FTIR to regain popularity, it would require new instrument designs and major improvement in sensitivity. The development of commercial GC-VUV instrumentation has spurred recent experimentation. Further developments will likely include a move toward simplified, portable, and cheaper detection platforms, which sample only a few wavelengths (without full-wavelength range collection), to potentially improve sensitivity. Spectroscopic detection is also amenable to miniaturization.

References

- [1] J.S. Zavahir, Y. Nolvachai, P.J. Marriott, Molecular spectroscopy: information rich detection for gas chromatography, *TrAC Trend Anal. Chem.* 99 (1) (2018) 47–65.
- [2] M.L. Passos, M.L.M. Saraiva, Detection in UV-visible spectrophotometry: detectors, detection systems, and detection strategies, *Measurement* 135 (1) (2018) 896–904.
- [3] I.C. Santos, K.A. Schug, Recent advances and applications of gas chromatography vacuum ultraviolet spectroscopy, *J. Sep. Sci.* 40 (1) (2017) 138–151.
- [4] L. Bai, J. Smuts, P. Walsh, C. Qiu, H.M. McNair, K.A. Schug, Pseudo-absolute quantitative analysis using gas chromatography – vacuum ultraviolet spectroscopy: a tutorial, *Anal. Chim. Acta* 953 (1) (2017) 10–22.
- [5] S.L. Smith, Coupled systems – capillary GC/MS and capillary GC/FTIR, *J. Chromatogr. Sci.* 22 (1) (1984) 143–148.
- [6] A. Lelevic, V. Souchon, M. Moreaud, C. Lorentz, C. Geantet, Gas chromatography vacuum ultraviolet spectroscopy: a review, *J. Sep. Sci.* 43 (1) (2019) 1–65.
- [7] E. Whittle, D.A. Dows, G.C. Pimentel, Matrix isolation method for the experimental study of unstable species, *J. Chem. Phys.* 22 (11) (1954) 1943–1944.
- [8] P. Fellgett, Les principes généraux des méthodes nouvelles en spectroscopie interférentielle – a propos de la théorie du spectromètre interférentiel multiplex, *J. Phys. Radium* 19 (3) (1958) 187–191.
- [9] M.D. Erickson, Gas chromatography/Fourier transform infrared spectroscopy applications, *Appl. Spec. Rev.* 15 (1) (1979) 261–298.
- [10] M.S. Flett, J. Hughes, The application of a long-path infra-red cell in gas chromatography, *J. Chromatogr. A.* 11 (1963) 434–439.
- [11] D. Welti, R. Stephany, Some comments on the infrared spectra of vapor, *Appl. Spec.* 22 (6) (1968) 678–688.
- [12] J.W. Cooley, J.W. Tukey, An algorithm for the machine calculation of complex Fourier series, *Math. Comput.* 19 (90) (1965) 297–301.
- [13] M.J. Low, Rapid infrared analysis of gas-chromatography peaks, *Chem. Commun. (London)* 12 (1966) 371–372.
- [14] P.A. Wilks, R.A. Brown, Construction and performance of an infrared chromatographic fraction analyzer, *Anal. Chem.* 36 (10) (1964) 1896–1899.
- [15] L.V. Azarraga, Gold coating of glass tubes for gas chromatography/Fourier transform infrared spectroscopy “light-pipe” gas cells, *Appl. Spec.* 34 (2) (1980) 224–225.
- [16] R.L. White, Gas chromatography-Fourier transform infrared spectrometry, *Appl. Spec. Rev.* 23 (1) (1987) 165–245.
- [17] J.A. De Haseth, T.L. Isenhour, Reconstruction of gas chromatograms from interferometric gas chromatography/infrared spectrometry data, *Anal. Chem.* 49 (13) (1977) 1977–1981.
- [18] G.T. Reedy, D.G. Ettinger, J.F. Schneider, S. Bourne, High-resolution gas chromatography/matrix isolation infrared spectrometry, *Anal. Chem.* 57 (1) (1985) 1602–1609.
- [19] S.A. Barman, Matrix isolation for GC-FTIR, *Anal. Chem.* 56 (8) (1984) 936–938.
- [20] E.C.Y. Inn, Vacuum ultraviolet spectroscopy, *Spectrochim. Acta* 7 (1955) 65–87.
- [21] M.A. Wickramaaratchi, E.T. Premuzic, M. Lin, P.A. Snyder, Circular dichroism detection of optically active compounds in gas chromatography using vacuum ultraviolet synchrotron radiation, *J. Chromatogr. A* 390 (1987) 413–420.

- [22] J.N. Driscoll, M. Duffy, S. Pappas, Capillary gas chromatographic analysis with the far-UV absorbance detector, *J. Chromatogr. A* 441 (1) (1988) 63–71.
- [23] L. Lagesson-Andrasko, V. Lagesson, J. Andrasko, The use of gas-phase UV spectra in the 168–330-nm wavelength region for analytical purposes. Qualitative measurements, *Anal. Chem.* 70 (5) (1998) 819–826.
- [24] V. Lagesson, L. Lagesson-Andrasko, J. Andrasko, F. Baco, Identification of compounds and specific functional groups in the wavelength region 168–330 nm using gas chromatography with UV detection, *J. Chromatogr. A* 867 (1–2) (2000) 187–206.
- [25] K.A. Schug, I. Sawicki, D.D. Carlton Jr., H. Fan, H.M. McNair, J.P. Nimmo, P. Kroll, J. Smuts, P. Walsh, D. Harrison, Vacuum ultraviolet detector for gas chromatography, *Anal. Chem.* 86 (1) (2014) 8329–8335.
- [26] T. Gröger, B. Gruber, D. Harrison, M. Saraji-Bozorgzad, M. Mthembu, A. Sutherland, R. Zimmermann, A vacuum ultraviolet absorption array spectrometer as a selective detector for comprehensive two-dimensional gas chromatography: concept and first results, *Anal. Chem.* 88 (6) (2016) 3031–3039.
- [27] I.G.M. Anthony, M.R. Brantley, C.A. Gaw, A.R. Floyd, T. Solouki, Vacuum ultraviolet spectroscopy and mass spectrometry: a tandem detection approach for improved identification of gas chromatography-eluting compounds, *Anal. Chem.* 90 (1) (2018) 4878–4885.
- [28] R. Gras, J. Luong, R.A. Shellie, Direct measurement of trace elemental mercury in hydrocarbon matrices by gas chromatography with ultraviolet photometric detection, *Anal. Chem.* 87 (22) (2015) 11429–11432.
- [29] R. Gras, J. Luong, R.A. Shellie, Gas chromatography with diode array detection in series with flame ionization detection, *J. Chromatogr. A* 1500 (2017) 153–159.
- [30] R. Gras, J. Luong, P.R. Haddad, R.A. Shellie, Gas chromatography with simultaneous detection: ultraviolet spectroscopy, flame ionization, and mass spectrometry, *J. Chromatogr. A* 1563 (2018) 171–179.
- [31] R. Gras, J. Luong, R.A. Shellie, Miniaturized micromachined gas chromatography with universal and selective detectors for targeted volatile compounds analysis, *J. Chromatogr. A* 1573 (2018) 151–155.
- [32] K.B. Sri, B. Bhairavi, R. Swethasri, Gas chromatography-FTIR spectroscopy: a review, *J. Gujarat Res. Soc.* 21 (1) (2019) 226–237.
- [33] T. Visser, M.J. Vredenburgt, P. Jackson, G. Dent, D. Carter, D. Schofield, J.M. Chalmers, Comparison of light pipe, matrix isolation, and cryotrapping GC-FTIR, *Proc. SPIE* 2089 (1) (1994) 184–185.
- [34] M.A. Ford, R.A. Hurrell, An integrated approach to GC-FTIR, *Proc. SPIE* 553 (1985) 312–314.
- [35] S. Bourne, G.T. Reedy, P.T. Cunningham, Gas chromatography/matrix isolation/infrared spectroscopy: an evaluation of the performance potential, *J. Chromatogr. Sci.* 17 (1979) 460–463.
- [36] S.C. Simonoff, M.L. Olson, D. Kuehl, R.B. Turner, Algorithms and techniques for gas chromatography/Fourier transform infrared spectroscopy (GC/FTIR): the nitty-gritty, *Proc. SPIE* 289 (1981) 135–139.
- [37] P.R. Griffiths, D.A. Heaps, P.R. Breyne, The gas chromatography/infrared interface: past, present, and future, *Appl. Spectrosc.* 62 (10) (2008) 259A–270A.
- [38] S. Bourne, A.M. Haefner, K.L. Norton, P.R. Griffiths, Performance characteristics of a real-time direct deposition gas chromatography/Fourier transform infrared spectrometry system, *Anal. Chem.* 62 (22) (1990) 2448–2452.
- [39] S. Johnson, NIST Standard Reference Database 35, NIST, 2018.
- [40] R.L. White, G.N. Giss, G.M. Brissey, C.L. Wilkins, Comparison of methods for reconstruction of gas chromatograms from interferometric gas chromatography/infrared spectrometry data, *Anal. Chem.* 53 (12) (1981) 1778–1782.
- [41] T. Visser, FT-IR detection in gas chromatography, *Trends Anal. Chem.* 21 (9–10) (2002) 627–636.
- [42] M.D. Gomes da Silva, H.J. Chaves das Neves, Complementary use of hyphenated purge-and-trap gas chromatography techniques and sensory analysis in the aroma profiling of strawberries (*Fragaria ananassa*), *J. Agric. Food Chem.* 47 (11) (1999) 4568–4573.
- [43] B.A. Hohne, G. Hangac, G.W. Small, T.L. Isenhour, An online-class specific GC-FTIR reconstruction from interferometric data, *J. Chromatogr. Sci.* 19 (6) (1981) 283–289.
- [44] G.W. Small, G.T. Rasmussen, T.L. Isenhour, An infrared search system based on direct comparison of interferograms, *Appl. Spec.* 33 (1979) 444–450.
- [45] I.G. Anthony, M.R. Brantley, A.R. Floyd, C.A. Gaw, T. Solouki, Improving accuracy and confidence of chemical identification by gas chromatography/vacuum ultraviolet spectroscopy-mass spectrometry: parallel gas chromatography, vacuum ultraviolet, and mass spectrometry library searches, *Anal. Chem.* 90 (1) (2018) 12307–12313.
- [46] H. Liu, G. Raffin, G. Trutt, J. Randon, Is vacuum ultraviolet detector a concentration or a mass dependent detector? *J. Chromatogr. A* 1530 (2017) 171–175.
- [47] H. Keller-Rudek, G.K. Moortgat, R. Sander, R. Sörensen, The MPI-Mainz UV/VIS spectral atlas of gaseous molecules of atmospheric interest, *Earth Syst. Sci. Data* 5 (2013) 365–373.

- [48] M. Oakley, M. Klobukowski, Computing UV–vis spectra of 1-bromo-1-propene: a comparison of model core potential and all-electron basis sets, *Can. J. Chem.* 95 (5) (2017) 627–631.
- [49] J.X. Mao, P. Kroll, K.A. Schug, Vacuum ultraviolet absorbance of alkanes: an experimental and theoretical investigation, *Struct. Chem.* 30 (6) (2019) 2217–2224.
- [50] L. Skultety, P. Frycak, C. Qiu, J. Smuts, L. Shear-Lauade, K. Lemr, J.X. Mao, P. Kroll, K.A. Schug, A. Szewczak, C. Vaught, Resolution of isomeric new designer stimulants using gas chromatography–vacuum ultraviolet spectroscopy and theoretical computations, *Anal. Chim. Acta* 971 (2017) 55–67.
- [51] J. Schenk, J.X. Mao, J. Smuts, P. Walsh, P. Kroll, K.A. Schug, Analysis and deconvolution of dimethylnaphthalene isomers using gas chromatography vacuum ultraviolet spectroscopy and theoretical computations, *Anal. Chim. Acta* 945 (2016) 1–8.
- [52] C. Weston, J. Smuts, J.X. Mao, K.A. Schug, Investigation of gas phase absorption spectral similarity for stable-isotopically labeled compounds in the 125–240 nm wavelength range, *Talanta* 177 (2018) 41–46.
- [53] T.T. Ponduru, C. Qiu, J.X. Mao, A. Leghissa, J. Smuts, K.A. Schug, H.R. Dias, Copper (i)-based oxidation of polycyclic aromatic hydrocarbons and product elucidation using vacuum ultraviolet spectroscopy and theoretical spectral calculations, *New J. Chem.* 42 (24) (2018) 19442–19449.
- [54] J.X. Mao, P. Walsh, P. Kroll, K.A. Schug, Simulation of vacuum ultraviolet absorption spectra: paraffin, isoparaffin, olefin, naphthene, and aromatic hydrocarbon class compounds, *Appl. Spec.* 74 (1) (2020) 72–80.
- [55] C.A. Cruse, J.V. Goodpaster, Generating highly specific spectra and identifying thermal decomposition products via gas chromatography/vacuum ultraviolet spectroscopy (GC/VUV): application to nitrate ester explosives, *Talanta* 195 (2019) 580–586.
- [56] ASTM D8071-19, Standard Test Method for Determination of Hydrocarbon Group Types and Select Hydrocarbon and Oxygenate Compounds in Automotive Spark-Ignition Engine Fuel Using Gas Chromatography with Vacuum Ultraviolet Absorption Spectroscopy Detection (GC-VUV), ASTM International, West Conshohocken, PA, 2019.
- [57] P. Walsh, M. Garbalena, K.A. Schug, Rapid analysis and time interval deconvolution for comprehensive fuel compound group classification and speciation using gas chromatography–vacuum ultraviolet spectroscopy, *Anal. Chem.* 88 (22) (2016) 11130–11138.
- [58] L. Bai, J. Smuts, J. Schenk, J. Cochran, K.A. Schug, Comparison of GC-VUV, GC-FID, and comprehensive two-dimensional GC–MS for the characterization of weathered and unweathered diesel fuels, *Fuel* 214 (2018) 521–527.
- [59] M.N. Dunkle, P. Pijcke, B. Winniford, G. Bellos, Quantification of the composition of liquid hydrocarbon streams: comparing the GC-VUV to DHA and GCxGC, *J. Chromatogr. A* 1587 (2019) 239–246.
- [60] C. Qiu, J. Cochran, J. Smuts, P. Walsh, K.A. Schug, Gas chromatography–vacuum ultraviolet detection for classification and speciation of polychlorinated biphenyls in industrial mixtures, *J. Chromatogr. A* 1490 (2017) 191–200.
- [61] M. Zoccali, K.A. Schug, P. Walsh, J. Smuts, L. Mondello, Flow-modulated comprehensive two-dimensional gas chromatography combined with a vacuum ultraviolet detector for the analysis of complex mixtures, *J. Chromatogr. A* 1497 (2017) 135–143.
- [62] R. Reiss, B. Gruber, S. Klingbeil, T. Gröger, S. Ehlert, R. Zimmermann, Evaluation and application of gas chromatography–vacuum ultraviolet spectroscopy for drug- and explosive precursors and examination of non-negative matrix factorization for deconvolution, *Spectrochim. Acta* 219 (2019) 129–134.
- [63] K. Sharma, S.P. Sharma, S.C. Lahiri, Characterization and identification of petroleum hydrocarbons and biomarkers by GC-FTIR and GC-MS, *Petrol. Sci. Technol.* 27 (11) (2009) 1209–1226.
- [64] L. Jirovetz, W. Jaeger, G. Remberg, J. Espinosa-Gonzalez, R. Morales, A. Woidich, A. Nikiforov, Analysis of the volatiles in the seed oil of *Hibiscus sabdariffa* (Malvaceae) by means of GC-MS and GC-FTIR, *J. Agric. Food Chem.* 40 (7) (1999) 1186–1187.
- [65] O. Berdeaux, S. Fontagné, E. Sémon, J. Velasco, J.L. Sébédio, C. Dobarganes, A detailed identification study on high-temperature degradation products of oleic and linoleic acid methyl esters by GC–MS and GC–FTIR, *Chem. Phys. Lipids* 165 (3) (2012) 338–347.
- [66] H.G. Wahl, S.Y. Habel, N. Schmieder, H.M. Liebich, Identification of cis/trans isomers of methyl ester and oxazoline derivatives of unsaturated fatty acids using GC–FTIR–MS, *J. High Resolut. Chromatogr.* 17 (7) (1994) 543–548.
- [67] D.M. Hembree, N.R. Smyrl, W.E. Davis, D.M. Williams, Isomeric characterization of polychlorinated biphenyls using gas chromatography–Fourier transform infrared/gas chromatography–mass spectrometry, *Analyst* 118 (3) (1993) 249–252.
- [68] J. Schenk, D.D. Carlton, J. Smuts, J. Cochran, L. Shear, T. Hanna, D. Durham, C. Cooper, K.A. Schug, Lab-simulated downhole leaching of formaldehyde from proppants by high performance liquid chromatography (HPLC), headspace gas chromatography–vacuum ultraviolet (HS-GC-VUV) spectroscopy, and headspace gas chromatography–mass spectrometry (HS-GC-MS), *Environ. Sci. Process. Impacts* 21 (2) (2019) 214–223.

- [69] S. Buchalter, I. Marginean, J. Yohannan, I.S. Lurie, Gas chromatography with tandem cold electron ionization mass spectrometric detection and vacuum ultraviolet detection for the comprehensive analysis of fentanyl analogues, *J. Chromatogr. A* 1596 (2019) 183–193.
- [70] R.F. Kranenburg, A.R. García-Cicourel, C. Kukurin, H.G. Janssen, P.J. Schoenmakers, A.C. van Asten, Distinguishing drug isomers in the forensic laboratory: GC–VUV in addition to GC–MS for orthogonal selectivity and the use of library match scores as a new source of information, *Forensic Sci. Int.* 302 (2019) 1–14.
- [71] F.C. Wang, GC×GC VUV Study of diesel: a two-dimensional separation approach, *Energy Fuel*. 34 (2) (2020) 1432–1437.
- [72] E.T. Es-sebbar, Y. Benilan, A. Farooq, Temperature-dependent absorption cross-section measurements of 1-butene (1-C₄H₈) in VUV and IR, *J. Quant. Spectrosc. Radiat. Transf.* 115 (2013) 1–2.
- [73] B.M. Weber, P. Walsh, J.J. Harynyuk, Determination of hydrocarbon group-type of diesel fuels by gas chromatography with vacuum ultraviolet detection, *Anal. Chem.* 88 (11) (2016) 5809–5817.
- [74] V.F. Kalasinsky, J.T. McDonald Jr., GC/FTIR spectra of terpenes, *J. Chromatogr. Sci.* 21 (5) (1983) 193–200.
- [75] V.F. Kalasinsky, S. Pechsiri, K.S. Kalasinsky, Analysis of terpenes by capillary gas chromatography/Fourier transform infrared spectroscopy (GC/FTIR), *J. Chromatogr. Sci.* 24 (12) (1986) 543–548.
- [76] H. Fan, J. Smuts, L. Bai, P. Walsh, D.W. Armstrong, K.A. Schug, Gas chromatography–vacuum ultraviolet spectroscopy for analysis of fatty acid methyl esters, *Food Chem.* 194 (2016) 265–271.
- [77] R. Pechancová, C. Qiu, J. Smuts, K. Lemr, K.A. Schug, Comparative study of ink photoinitiators in food packages using gas chromatography with vacuum ultraviolet detection and gas chromatography with mass spectrometry, *J. Sep. Sci.* 42 (2) (2019) 556–565.
- [78] A.R. García-Cicourel, H.G. Janssen, Direct analysis of aromatic hydrocarbons in purified mineral oils for foods and cosmetics applications using gas chromatography with vacuum ultraviolet detection, *J. Chromatogr. A* 1590 (2019) 113–120.
- [79] J. Schenk, G. Nagy, N.L. Pohl, A. Leghissa, J. Smuts, K.A. Schug, Identification and deconvolution of carbohydrates with gas chromatography–vacuum ultraviolet spectroscopy, *J. Chromatogr. A* 1513 (2017) 210–221.
- [80] I.C. Santos, J. Smuts, M.L. Crawford, R.P. Grant, K.A. Schug, Large-volume injection gas chromatography–vacuum ultraviolet spectroscopy for the qualitative and quantitative analysis of fatty acids in blood plasma, *Anal. Chim. Acta* 1053 (2019) 169–177.
- [81] A. Leghissa, J. Smuts, C. Qiu, Z.L. Hildenbrand, K.A. Schug, Detection of cannabinoids and cannabinoid metabolites using gas chromatography with vacuum ultraviolet spectroscopy, *Sep. Sci. Plus.* 1 (1) (2018) 37–42.
- [82] M.T. Söderström, R.A. Ketola, Identification of nerve agents and their homologues and dialkyl methylphosphonates by gas chromatography/Fourier transform infrared spectrometry (GC-FTIR), *Fresenius J. Anal. Chem.* 350 (3) (1994) 162–167.
- [83] S. Gosav, M. Praisler, J. Van Bocxlaer, A.P. De Leenheer, D.L. Massart, Class identity assignment for amphetamines using neural networks and GC–FTIR data, *Spectrochim. Acta* 64 (5) (2006) 1110–1117.
- [84] Z.R. Roberson, J.V. Goodpaster, Differentiation of structurally similar phenethylamines via gas chromatography–vacuum ultraviolet spectroscopy (GC–VUV), *Forensic Chem.* 15 (2019) 1–7.
- [85] Z.R. Roberson, H.C. Gordon, J.V. Goodpaster, Instrumental and chemometric analysis of opiates via gas chromatography–vacuum ultraviolet spectrophotometry (GC–VUV), *Anal. Bioanal.* 412 (2020) 1–6.
- [86] V.F. Kalasinsky, C. Saiwan, K.G. Whitehead, GC/FTIR study of nitrated polycyclic aromatic hydrocarbons, *J. Chromatogr. Sci.* 26 (11) (1988) 584–587.
- [87] K.S. Kalasinsky, GC/FTIR Applications in pesticide chemistry, *J. Chromatogr. Sci.* 21 (6) (1983) 246–253.
- [88] H. Fan, J. Smuts, P. Walsh, D. Harrison, K.A. Schug, Gas chromatography–vacuum ultraviolet spectroscopy for multiclass pesticide identification, *J. Chromatogr. A* 1389 (2015) 120–127.
- [89] I.C. Santos, J. Smuts, W.S. Choi, Y. Kim, S.B. Kim, K.A. Schug, Analysis of bacterial FAMES using gas chromatography–vacuum ultraviolet spectroscopy for the identification and discrimination of bacteria, *Talanta* 182 (2018) 536–543.
- [90] I. Ojanperä, K. Pihlainen, E. Vuori, Identification limits for volatile organic compounds in the blood by purge-and-trap GC-FTIR, *J. Anal. Toxicol.* 22 (4) (1998) 290–295.
- [91] J. Zheng, C. Huang, S. Wang, Challenging pharmaceutical analyses by gas chromatography with vacuum ultraviolet detection, *J. Chromatogr. A* 1567 (2018) 185–190.
- [92] H.M. Garraffo, L.D. Simon, J.W. Daly, T.F. Spande, T.H. Jones, Cis-and trans-configurations of α , α' -disubstituted piperidines and pyrrolidines by GC-FTIR; application to decahydroquinoline stereochemistry, *Tetrahedron* 50 (39) (1994) 11329–11338.
- [93] L. Bai, J. Smuts, P. Walsh, H. Fan, Z. Hildenbrand, D. Wong, D. Wetz, K.A. Schug, Permanent gas analysis using gas chromatography with vacuum ultraviolet detection, *J. Chromatogr. A* 1388 (2015) 244–250.

Mass spectrometric detectors for gas chromatography

David J. Harvey

Target Discovery Institute, Nuffield Department of Medicine, University of Oxford, Oxford, United Kingdom

14.1 Introduction

The combination of mass spectrometry (MS) with gas-liquid chromatography (GLC) provides one of the most powerful analytical methods for many organic and inorganic compounds and has major application in several fields such as environmental monitoring [1,2], drug monitoring in patients and athletes [3], clinical chemistry [4], law enforcement by narcotics detection, horse-racing, safety of foods and beverages [5], structural confirmation of the products of organic synthesis, and potential detection of life forms on other planets and moons. Many types of mass spectrometer and ionization methods are available, each providing optimal instrumentation for particular applications. This chapter briefly describes the main systems and their application, with references directing the reader to further information. Much relevant information can, of course, be found in standard textbooks and reviews on MS (e.g., Ref. [6–8]) and combined gas-chromatography/mass spectrometry (GC/MS) [9–13].

Sample concentrations are generally compatible between GLC and MS but the gas flow, particularly from packed columns can cause problems when attached to the vacuum system of the mass spectrometer. Contemporary GC/MS almost invariably uses capillary columns with low gas flows (1 mL min^{-1} or less) and mass spectrometers with fast pumping allowing capillary columns to be attached directly. However, the problem was acute with packed columns leading to the development of several flow-reducing interfaces. Obviously, simply splitting the column effluent provides a solution but at the expense of sensitivity and is not a practical solution. Some systems, most of which concentrate the analyte, are outlined further [14].

14.2 Gas chromatography—mass spectrometry interfaces

Because of the high outlet temperature of the effluent from GC columns, GC/MS interfaces and any transfer lines between the column and

the mass spectrometer must be maintained at least at the highest temperature of the effluent. Ideally, a slight positive gradient should be maintained between the column and the mass spectrometer to avoid condensation problems. Also, dead volumes should be avoided or minimized to retain column resolution.

14.2.1 Open split interface

The GC column enters a small chamber through which passes helium buffer gas (Fig. 14.1). The outlet of the chamber is a narrow capillary, which restricts the flow of gas into the mass spectrometer such that this is constant. Dilution of the column effluent is controlled by

the flow of helium through the device. The interface offers several advantages for GC coupling: The column is maintained at atmospheric pressure, thus avoiding distortions that would be caused with an exit at the vacuum of the mass spectrometer and the column can be changed without disturbing the vacuum system.

14.2.2 Jet molecular separator

The jet, or Ryhage, separator (Fig. 14.2) works on the principal of relative rates of diffusion of compounds with different masses. The column effluent exits through a small jet located in a vacuum chamber and spaced close to and aligned with a second orifice leading to the mass

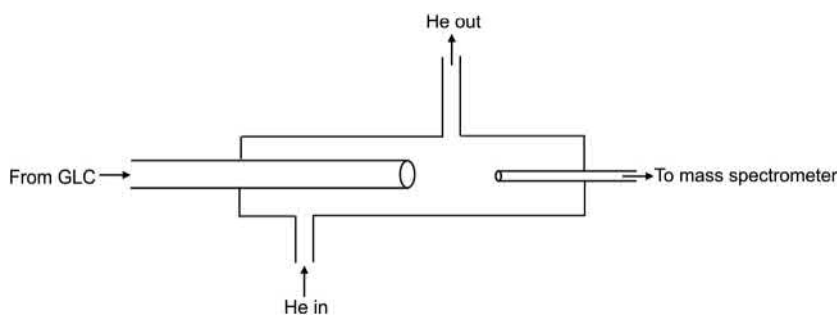


FIGURE 14.1 Open split interface.

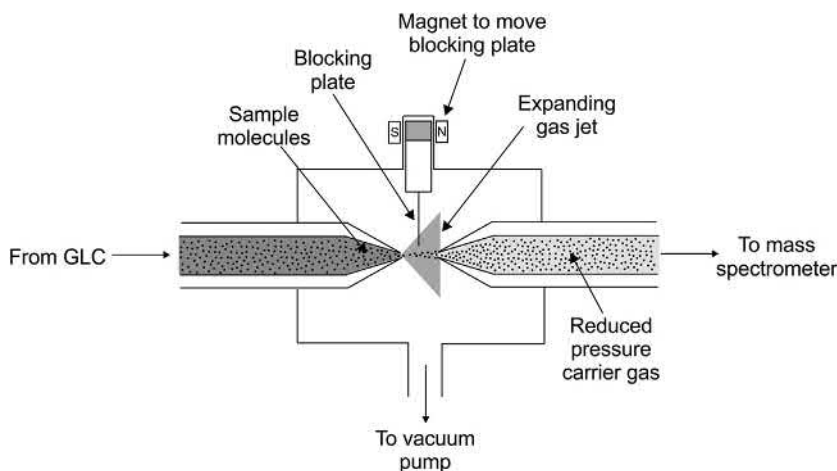


FIGURE 14.2 Jet molecular separator.

spectrometer. To prevent condensation of the analyte, the chamber is maintained at above the highest temperature of the column. The gas exiting the GC column expands as a high-velocity jet with the lighter components (carrier gas) diffusing sideways faster than the heavier molecules (the analyte), which preferentially enter the second orifice and mass spectrometer. Helium is usually used as the carrier gas because of its low mass and consequently high diffusion coefficient. Enrichments of 40–86 have been reported. A two-stage separator was used in the early commercial GC/MS instruments with a valve placed afterward that could be used to prevent the GC solvent from entering the mass spectrometer. Some later single jets had a metal plate operated by a magnet from outside the vacuum system, which could be positioned between the orifices to serve the same purpose.

Patent issues associated with the jet separator sparked the invention of several other devices, none of which appeared to work as well.

14.2.3 Effusion or Watson–Biemann separator

This separator consists of a porous tube made of ultrafine sintered glass, ceramic, stainless steel, or silver through which the column effluent passes (Fig. 14.3). The carrier gas diffuses through the sinter and is pumped away leaving the enriched effluent to enter the mass spectrometer. The separator only works well within a narrow range of gas flow and there can be problems with decomposition or adsorption on the walls of the sinter, particularly if this is metal. Also, lower mass compounds tend to be lost.

14.2.4 Lipsky–Horvath separator

The little used Lipsky–Horvath separator consists of a thin (0.12 mm wall thickness) Teflon capillary tube (approx. 2 m × 0.5 mm) through which the helium carrier gas diffuses and which is maintained at about 280°C (Fig. 14.4). It presents a very low dead volume with enrichments

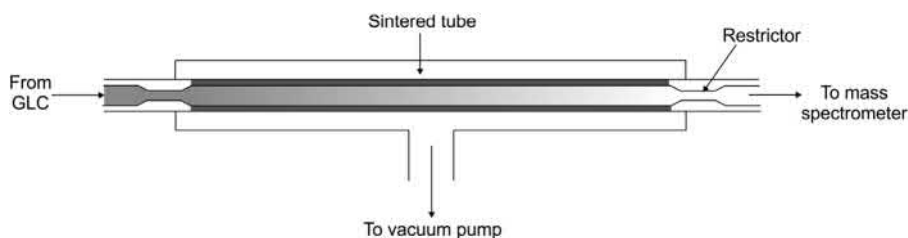


FIGURE 14.3 Watson–Biemann effusion separator.

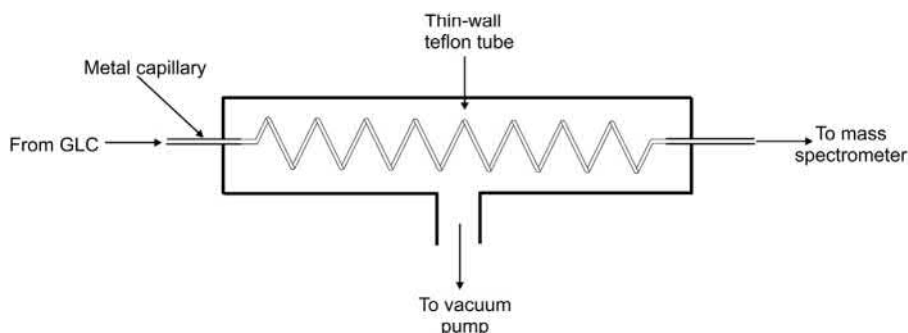


FIGURE 14.4 Lipsky–Horvath separator.

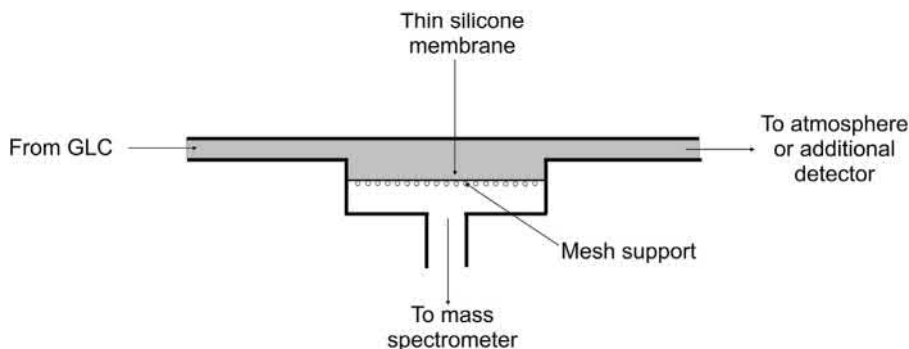


FIGURE 14.5 Membrane separator.

of the order of 200 being reported. However, it has several disadvantages: (a) There is a time lag of about 20–30 s between the appearance of a peak in the chromatograph and the mass spectrometer, (b) the maximum useable flow rate is approximately 15 mL min^{-1} , and (c) the operating temperature is limited to the range 280–330°C.

14.2.5 Membrane separator

The membrane separator (Fig. 14.5) consists of a thin (0.025 mm) silicone rubber membrane stretched across a metal mesh or sintered glass screen on the side connected to the mass spectrometer. Organic compounds can pass through the membrane, which is impermeable to the helium carrier gas that can be vented to atmosphere or to an additional detector because only about 60% of the sample molecules pass through the membrane. The membrane separates the GC column from the mass spectrometer vacuum meaning that the column exit is maintained at atmospheric pressure.

14.3 Ionization techniques

Two methods dominate ion production for GC/MS, namely electron ionization (EI) (sometimes known as electron-impact ionization) and chemical ionization.

14.3.1 Electron ionization (EI)

EI involves bombarding the sample molecules with electrons, which transfer energy causing them to ionize. The EI ion source (Fig. 14.6) consists of a small (~10 mm across) heated chamber located within the vacuum system of the mass spectrometer into which the column effluent passes. A beam of electrons, generated from a heated tungsten or rhenium filament, passes through the chamber at right angles to the

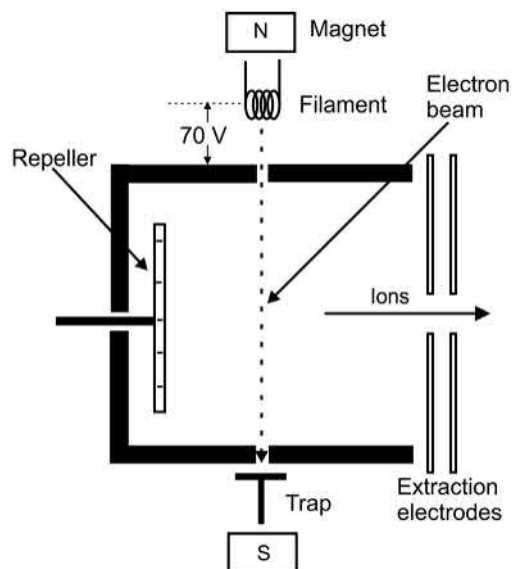


FIGURE 14.6 EI ion source.

column effluent to a second electrode, known as the trap. The voltage difference between the filament and the ion block governs the energy of the electrons and is usually set at some value above the ionization potential of the sample molecules, typically 70 eV. Small permanent magnets positioned in line with the electron beam cause it to execute a spiral path in order to increase the path length and maximize collisions with the sample molecules. Ions are ejected from the ion source and focused into a beam by the combined use of a positive potential on a repeller plate positioned at the back of the ion source and a high potential, of the order of 5–10 kV at the front of the source. The beam then enters the analyzer section of the instrument for mass separation.

Collision between the electrons and the sample molecules transfers energy to the sample causing ionization by release of an electron to give a positively charged ion:



This ion is termed an odd-electron molecular ion and is written in the form $M^{+\bullet}$ where the dot denotes the free, unpaired electron. Most ions are, thus, singly charged and are denoted by m/z where m is the mass and z the charge (m/e in the older literature). Although the ionization efficiency is low, with only about 1 in 10^3 sample molecules producing ions, the high sensitivity of the mass spectrometer is more than adequate to produce a strong spectrum. The extent to which a molecule ionizes is related to its structure; molecules containing heteroatoms, such as nitrogen, with lone pairs of electrons ionize well by loss of one electron from a lone pair, whereas molecules such as saturated hydrocarbons are difficult to ionize as all electrons are involved in sigma bond formation.

Because the energy imparted to the molecules during ionization considerably exceeds the ionization potential, the odd-electron molecular ions are generally unstable and decompose,

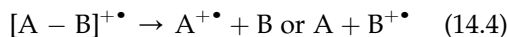
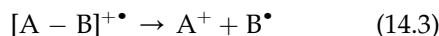
mainly rapidly within the ion source but, sometimes more slowly during transit through the instrument. Fragmentation within the ion source produces sharp, well-defined mass spectra, whereas ions fragmenting after the ion source and before the mass analyzer can produce broad peaks known as metastable ions. The relationship between the masses of the metastable, parent and its product ion is given by Eq. (14.2):

$$m^* = \frac{m_2^2}{m_1} \quad (14.2)$$

Where m^* is the mass of the metastable ion and m_1 and m_2 are the masses of the parent and product ions, respectively. Observation of appropriate metastable ions is invaluable in confirming fragmentation pathways.

Fragmentation usually involves several consecutive and competing reactions to give the fragmentation spectra consisting of a display of the ions' m/z values and relative abundance expressed as a percentage of the most abundant ion. A typical spectrum is shown in Fig. 14.7.

Such spectra are very reproducible for a given electron beam energy, 70 eV, which is well above the ionization potential of organic compounds, being chosen as a value that produces negligible changes in the spectrum for small changes in electron energy. Typical fragmentation pathways include elimination of a radical to give an even-electron ion (14.3), elimination of a neutral molecule to give another odd-electron ion (14.4), which often fragments further, or fragmentation by rearrangement, often involving hydrogen migrations.



In Fig. 14.7, elimination of a methyl group from the molecular ion gives the fragment at m/z 341 (Eq. 14.3) and the ion at m/z 132 is a rearrangement ion formed by hydrogen migration from the hydrocarbon chain to the carbonyl

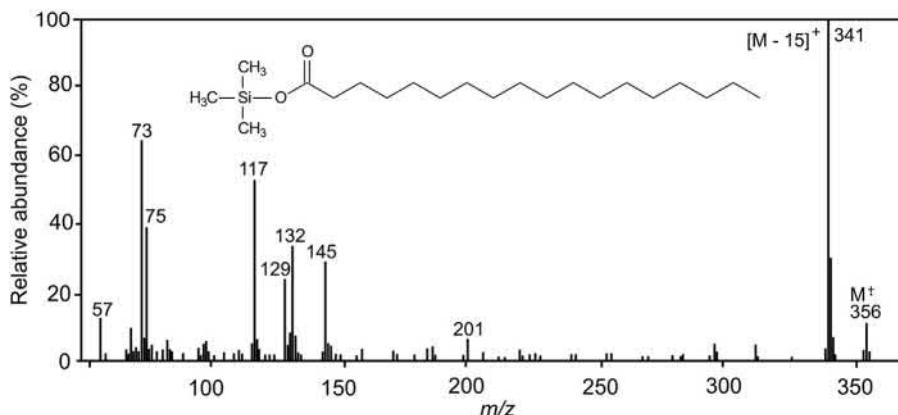


FIGURE 14.7 Positive ion EI mass spectrum of the TMS derivative of a fatty acid.

oxygen (Scheme 14.1), known as a McLafferty rearrangement. Further loss of a methyl radical from this odd-electron ion yields m/z 117.

An enormous amount of published material exists on the chemistry of these fragmentation mechanisms see, e.g., Refs. [6,15,16]; most reactions are unimolecular although some ion–molecule reactions have been reported for selected compounds. Only the ions, not the neutral species, appear in the spectra.

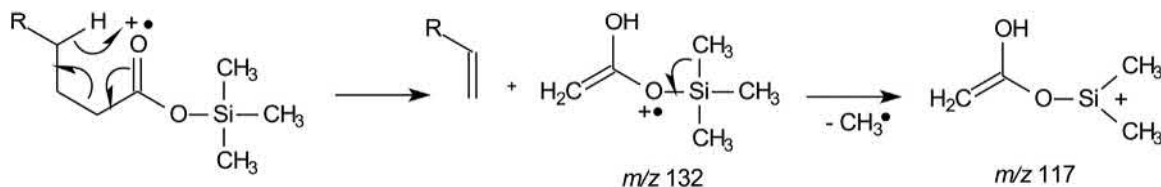
Because the molecules are ionized in the vapor phase, they must be stable at the temperatures needed to vaporize them. Many molecules, such as the fatty acid shown in Fig. 14.7, do not fulfill these requirements but can be stabilized and made more volatile by derivatization. The acid in Fig. 14.7 is derivatized as its trimethylsilyl (TMS) ester. More information on derivatization can be found in textbooks [17,18]

and reviews [16,19,20]. However, even with derivatization and heated ion sources, the technique is only applicable to molecules with masses less than ~ 1000 .

The instability of odd-electron ions formed by EI together with their relatively high internal energy frequently results in spectra in which the molecular ion, arguably the most important ion in the spectrum, is absent because none of the ions survive long enough to exit the ion source. Two techniques, cold EI and chemical ionization (CI), are available to overcome this problem.

14.3.2 Cold EI

This technique aims to reduce the internal energy of the ions enabling more of the molecular ions to survive by using supersonic molecular beams. Helium makeup gas is added to the



SCHEME 14.1 McLafferty rearrangement yielding fragment ions at m/z 132 and 117 in the EI mass spectrum of the TMS derivatives of fatty acids.

column effluent and the mixture is introduced into the ion source through a small pinhole. Sample molecules are accelerated to the velocity of the helium and collisions during the supersonic expansion cause vibrational cooling of the sample molecules. Subsequent EI produces spectra with considerably enhanced abundance of the molecular ion and a very low background [21]. Three changes to the original system, increasing the helium makeup gas flow rate, reduced electron energy and an increase in the nozzle–skinner distance has further improved the relative abundance of the molecular ions and prompted the authors of the technique to name it Soft Cold EI [22]. A standard 70 eV EI spectrum of the hydrocarbon $n\text{-C}_{28}\text{H}_{58}$ is shown in Fig. 14.8C together with the corresponding cold EI and soft cold EI spectra.

14.3.3 Chemical ionization (CI)

14.3.3.1 Positive ion CI

CI is a much “softer” ionization technique than EI and involves reaction of the sample molecules with an ionized “reagent gas” within the ion source to form mainly even-electron adducts. The ion source is constructed in a similar manner to the EI source but with a much smaller exit slit, thus making it much more gas-tight, allowing pressures of 0.1–1 Torr to be achieved inside. A reagent gas is introduced into the source chamber and ionized by the electron beam as in EI. Although many suitable gases have been reported, methane, *iso*-butane, and ammonia are the most common. Once ionized, the gases undergo a series of ion–molecule reactions to form species such as CH_5^+ (from methane) and NH_4^+ (from ammonia). These reactant ions collide with, and bind to, the sample molecules present at partial pressures of ~0.01% of the reagent gas

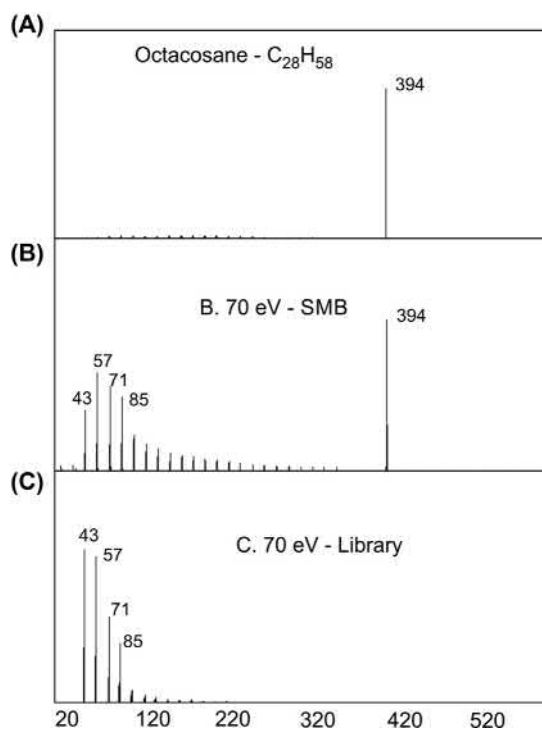
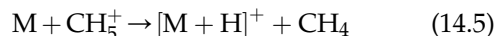


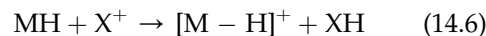
FIGURE 14.8 (A) Soft cold EI, (B) cold EI, and (C) 70 eV EI spectra of the n -hydrocarbon $n\text{-C}_{28}\text{H}_{58}$. Reproduced from S. Dagan, A. Amirav, *Electron impact mass spectrometry of alkanes in supersonic molecular beams*, *J. Am. Soc. Mass Spectrom.* 6 (1995)120–131 with permission from the American Chemical Society. [34]

pressure, with a variety of outcomes, five of which are outlined further:

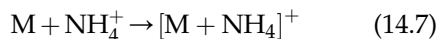
- (i) Proton transfer, typically from hydrocarbon reagent gases and ammonia



- (ii) Hydride ion extraction



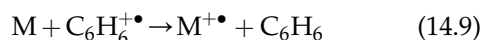
(iii) Electrophilic addition (from ammonia)



(iv) Anion abstraction as with nitric oxide



(v) Charge exchange from, for example, benzene to give an odd-electron ion



Of these reactions, the formation of $[M + \text{H}]^+$ is the most common.

These ionization reactions involve transfer of much less energy to the sample molecules than EI, and consequently, there is much less fragmentation. In addition, the $[M + X]^+$ or $[M - X]^+$ species do not contain unpaired electrons, i.e., they are even-electron ions. Consequently, they are much more stable than the odd-electron ions and show very little fragmentation (Fig. 14.9).

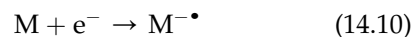
EI and CI are, thus, complementary ionization techniques for the same types of volatile

molecule and have been combined into a single ion source in a technique termed ACE (alternate CI/EI). Essentially, a CI spectrum of the sample is acquired to produce a strong molecular ion, after which the CI reagent gas is removed and an EI spectrum is acquired to record the fragments. The reagent gas is then pulsed back and the process is repeated. A downside of CI, however, is an estimated reduced sensitivity of about two orders of magnitude compared with EI.

14.3.3.2 Negative ion CI

Many ionization processes, such as CI, produce both positive and negative ions, sometimes favoring the latter. Several reactions, such as those shown further, are recognized:

(i) Electron capture from thermal electrons



(ii) Proton abstraction

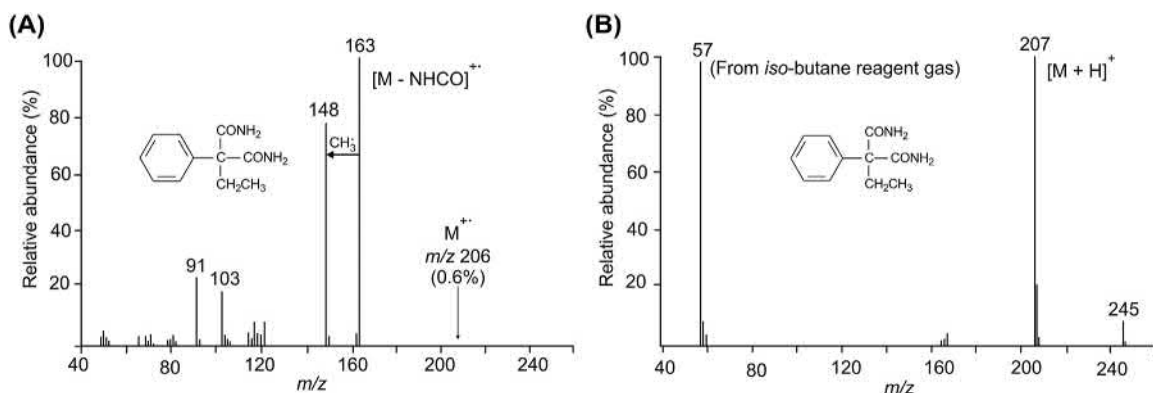
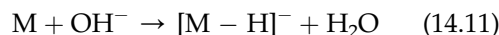
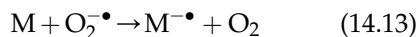


FIGURE 14.9 (A) EI spectrum of a drug molecule exhibiting no molecular ion. (B) CI mass spectrum of the same compound with *iso*-butane as the reagent gas. The ion at m/z 57 is from the reagent. Redrawn from *Encyclopedia of Analytical Science*, third edition with permission from Elsevier.

(iii) Nucleophilic addition from, for example, chlorine produced from methylene dichloride



(iv) Charge exchange

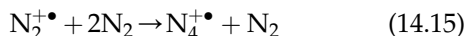
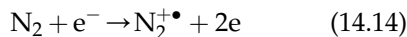


Capture of electrons that have been thermalized to 0–2 eV can be a very efficient process with suitable compounds and can, thus, often produce greater sensitivity than EI. Many molecules that are not efficiently ionized by this technique can be derivatized with electron-capturing reagents such as fluorocarbon esters or fluorinated silyl compounds in order to increase their susceptibility. This technique is often used for trace analysis, particularly as the derivatization reaction can be compound-specific.

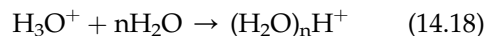
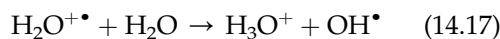
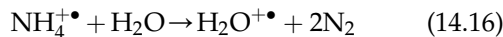
14.3.4 Atmospheric pressure chemical ionization (APCI)

This technique was first developed by Evan Horning's group in 1973, but the technique has not been used extensively for GC/MS systems although it has been more widely implemented for LC/MS. In Horning's system, the analyte, in a stream of dry nitrogen, enters the reaction chamber where it was irradiated by a 12.5-mCi nickel-63 (on gold foil) radiation source. Ions enter the mass spectrometer through a 25 μ pinhole aperture. Ionization is by charge exchange, protonation (positive ion), or proton abstraction (negative ion).

In modern systems, the radioactive source has been replaced by a corona-discharge needle providing a potential of 2–3 kV, which ionizes the dry nitrogen gas sheath gas surrounding the GC inlet.



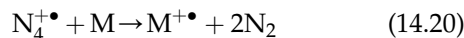
The N_4^+ then reacts with traces of water to form H_2O^+ and water clusters:



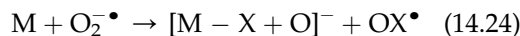
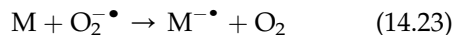
These clusters can protonate the analyte:



If the ionization potential of the analyte is lower than the ionization potential of N_4 , a charge-transfer reaction can occur:



In negative mode, the major negative ions formed at atmospheric pressure are the result of both electron capture and clustering processes.



For more information, see the review by Li et al. [23].

14.3.5 Field ionization

Field ionization is an old, soft ionization technique dating back to the work of Beckey in the 1960s [25]. It has not been widely used for GC/MS but has proved useful for analysis of petroleum mixtures. Samples are deposited on fine carbon microneedles coating the emitter and exposed to a high potential (10–20 kV) between the emitter (at ground potential) and the two-rod cathode (Fig. 14.10A). This potential induces a gradient of -10^7 to -10^8 v cm^{-1} around the tips of the needles causing electron tunneling to produce M^+ ions with little or no fragmentation. $[M + H]^+$ ions can be formed from a few

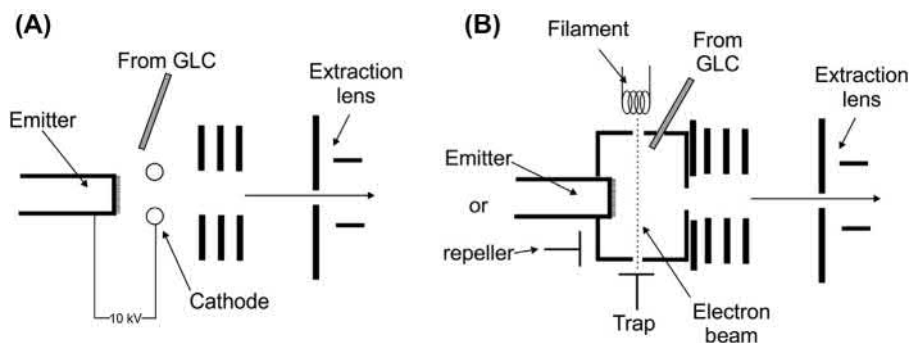


FIGURE 14.10 (A) Field ionization (FI) ion source and (B) combined EI/FI ion source. After K. Miyamoto, S. Fujimaki, Y. Ueda, *Development of a new electron ionization/field ionization ion source for gas chromatography/time-of-flight mass spectrometry*, *Rapid Commun. Mass Spectrom.* 23 (2009) 3350–3354. [24]

molecules with heteroatoms. Ionization efficiencies are generally low.

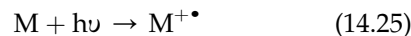
Like the combined EI/CI ion source, a similar EI/FI source has been developed (Fig. 14.10B). The ionization modes can be changed from EI mode to FI or vice versa by exchanging two types of probes, i.e., a repeller probe for the EI mode and an emitter probe for FI mode. A repeller electrode to extract ions is installed on the repeller probe, while an FI emitter is mounted on the emitter probe. Therefore, the ionization mode can be changed without breaking the ion source vacuum. The ion source is operated at a high temperature (250°C) to suppress contamination and the GC effluent is introduced through a heated interface up to 350°C.

14.3.6 Photoionization

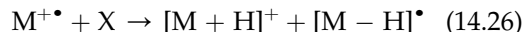
Ionization can be also produced photochemically. Thus, the output of a GC column is irradiated with light from a UV lamp at atmospheric pressure, placed at a 45 degrees angle to the column effluent and the resulting ions transferred directly to the mass spectrometer. The UV lamps that are generally used provide photons at higher energy than the ionization potentials of the analytes but lower than those of the carrier

or other makeup gases allowing selective production of ions from the analytes without ionizing the gases.

The initial ionization event is production of an odd-electron radical cation as in EI:



Collisions with various molecules (X) in the air produce hydrogen abstractions yielding $[M + H]^+$, which may coexist with the $M^{+\bullet}$ ions:



In negative ion mode, molecular ions are produced by charge exchange or by electron capture if they have a sufficient electron affinity. Formation of $[M - H]^-$ ions is also possible for analytes with high gas-phase acidity. Ionization efficiency can be improved considerably if a photoionizable dopant is added in relatively large amounts relative to the analyte. Ionization of this dopant subsequently ionizes the analyte by charge exchange or proton transfer.

Lasers can also be used to produce more selective ionization. Thus, resonance enhanced multiphoton ionization (REMPI), which involves absorption of two photons, produces particularly strong signals from polycyclic aromatic hydrocarbons. For more information, see [26].

14.4 Methods of mass separation

14.4.1 Magnetic sector instruments

Although magnetic sector instruments were once the most frequently used type of mass analyzers for GC/MS applications, they are now rarely encountered except for some specific applications. Magnetic sectors (Fig. 14.11A) deflect the trajectories of ions into circular paths of radii that depend on the strength of the magnetic field and the momentum-to-charge ratios (effectively m/z because the velocity component is in the same direction as the ion beam) of the ions. Ions with large momentum-to-charge ratios follow paths of larger radius than ions with smaller values and are, thus, dispersed in space. By changing the ion trajectories by variations of the magnetic field strength, ions with different momentum-to-charge ratios can be focused onto a point detector. The output is a plot of ion abundance against time. The time component is converted to m/z with the aid of a suitable calibration file. Resolution, which is related to the width of the ion peaks, is limited by peak broadening caused by ions with the same m/z value having slightly different velocities. The resolution can be improved by use of an additional electric sector (ESA) to produce energy focusing, arranged in such a way that ions are brought to a point focus after traversing both the magnetic (B) and

electric (E) fields; hence the term “double focusing sector instrument” The electric sector can be positioned either before (forward, or Nier–Johnson geometry, Fig. 14.11B) or after (reverse geometry) the magnet. Such instruments can achieve resolutions well in excess of 10,000 (defined as the mass at which the overlap of peaks one unit apart, which broaden with increasing mass, is 10% above the baseline). Additional configurations such as instruments that focus the ions into a focal plane (Mattauch–Herzog geometry) or those with two ESAs have also been produced. Obvious disadvantages with magnetic sector instruments are their large size and weight, relatively slow scan speeds, and difficulties in controlling the magnetic fields with a computer.

14.4.2 Quadrupole (Q) mass filters

Quadrupole mass filters are the most commonly encountered types of mass analyzers found in GC/MS instruments today because of their fast scanning capabilities and relative simplicity compared with magnetic sector instruments.

14.4.2.1 Linear quadrupole mass filters

Linear quadrupole (Q) mass filters (Fig. 14.12) consist of four parallel rods extending in the direction of the ion beam. Opposing rods are

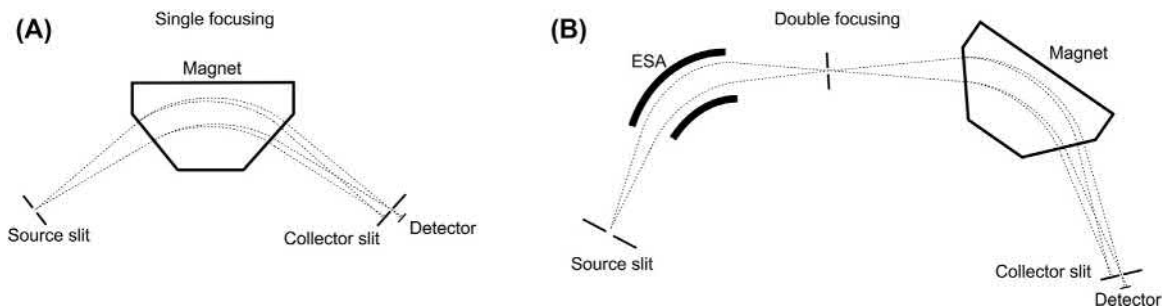


FIGURE 14.11 (A) Single-focusing magnetic sector instrument. (B) Double-focusing magnetic sector instrument. Broken lines indicate the position of the ion beams.

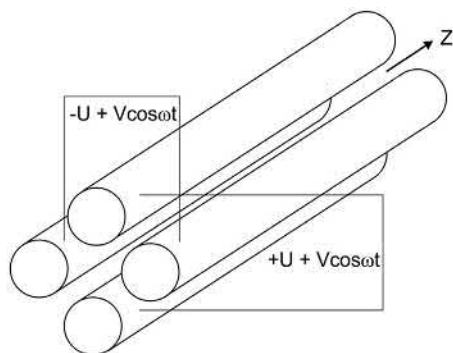


FIGURE 14.12 Linear quadrupole filter.

connected and are supplied with both DC (U) and AC fields (V). Ions oscillate between the rods and, depending on the combination of fields, ions with a given m/z ratio are stable and can pass through the rod assembly. Scanning is accomplished by changing the field strengths so that U/V is constant. Quadrupole mass spectrometers, although providing lower resolution than double-focusing magnetic instruments, can be scanned rapidly because only voltage scanning is involved. In addition, they are less costly and weigh much less than sector instruments. Consequently, they are ideally suited for use in combination with chromatographic inlet systems and are frequently found in tandem instruments consisting of serially connected quadrupoles interspersed with a collision cell for fragmentation studies (see further).

14.4.2.2 Quadrupole ion traps

Quadrupole ion trap (QIT) spectrometers (Fig. 14.13), sometimes known as Paul trap spectrometers after the inventor, Wolfgang Paul, consist of a ring electrode with hyperbolic inner surfaces with two end caps, often at ground potential to trap the ions. Ions are pulsed into or formed within the trap by pulsed EI as a small packet and a buffer gas within the trap reduces the ions energy by collisional cooling. An RF field is applied to the ring electrode causing

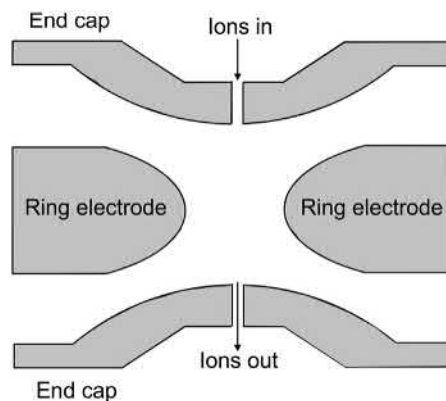


FIGURE 14.13 Paul-type quadrupole ion trap.

ions to circulate within the trap. The amplitude of the RF potential is varied to expel ions from the trap through the end caps and create the spectrum. The device offers high sensitivity because about 50% of ions expelled from the trap (m/z varies with time) reach the detector, unlike the case with sector instruments where ions are dispersed in space and only a small fraction of a given m/z is sampled during a magnetic scan. Consequently, these devices have enjoyed considerable popularity as GC/MS detectors. Another advantage for GC/MS is that because all ions within the mass range of the instrument are sampled simultaneously, there is no spectral skewing caused by changes in ionic concentration across the mass range as with scanned instruments as the result of the dynamic nature of the GC peak. A disadvantage, however, is that collisions of analyte ions with the buffer gas can result in some CI and/or collision-induced dissociation (CID) in what should be a pure EI spectrum. However, this feature can be used to advantage if CI spectra are required. Other disadvantages are a comparatively low resolution and a limited mass range (maximum about 6000), neither of which poses major problems for GC/MS applications.

A major difference that these instruments have over scanned analyzers is that the ions can be stored for subsequent experiments and

analysis. For example, all ions except those of a chosen m/z ratio can be ejected from the trap and the remaining ions caused to fragment to produce an MS/MS or MS² spectrum. This process can be repeated with selected fragment ions to yield MS³ spectra with considerable use for structural determination. The process can continue until too few ions to be detected remain. This technique is known as MSⁿ. Its main disadvantage is that ions in the lower third of the mass range are unstable and are not recorded in the spectrum. Many analytes, such as peptides and carbohydrates, require the observation of ions in this region for structural studies. For more information on ion traps, see Ref. [27].

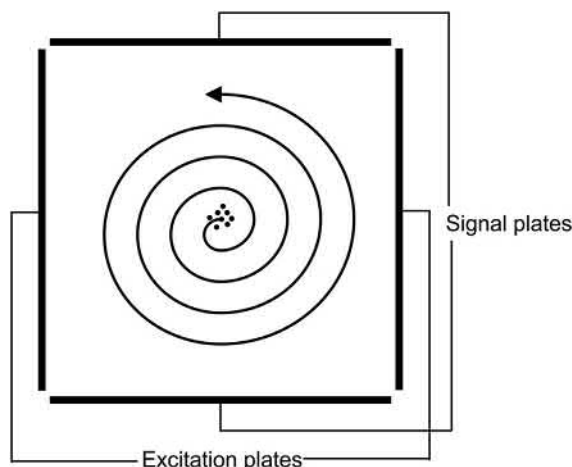


FIGURE 14.14 FT-ICR mass spectrometer.

14.4.2.3 Linear ion traps

Reducing the DC voltage on a quadrupole mass filter to zero, combined with collisional cooling of the ions and incorporation of end caps, converts a quadrupole instrument into a linear (RF-only) ion trap capable of storing ions covering the total mass range. Such devices are frequently used as collision cells for CID experiments but, again, suffer with the absence of ions in the low mass region. Hexapole or octopole devices are also common and provide similar functionality.

14.4.3 Fourier transform—ion cyclotron resonance (FT-ICR) mass spectrometers

Fourier transform mass spectrometers (Fig. 14.14) represent another type of trapping instruments. They offer very high resolution (10^5 – 10^6) and mass accuracy but their high cost and maintenance requirements have restricted their use for GC/MS studies to only a few specific applications. In these instruments, ions are trapped electrostatically within a cubical cell in a constant high superconducting magnetic field where they cycle in an orbit whose frequency is inversely proportional to the ion's

m/z ratio. An RF pulse is applied across the exciter (or emitter) plates placed on opposing sides of the cell in the x-axis. If the RF frequency resonates with an ion's orbital motion, the ions absorb energy and their radius of rotation increases so that a packet of such ions moves nearer to the signal plates (y axis) and induces a signal. In operation a "chirp" of a wide range of frequencies is applied so that all ions in a chosen mass range are excited. The output signal, therefore, consists of a complicated waveform containing contributions of all the various resonant frequencies whose amplitude is proportional to the number of ions having that m/z value. The signal is amplified and all the frequency components are extracted using a Fourier transform, yielding the mass spectrum. Since the pressure in the cell is very low, the ion orbital motion can be maintained over many cycles and the frequency, and consequently, the mass can be measured with very high precision. FT-ICR instruments can, therefore, be used to generate exceptionally high-resolution spectra with great mass accuracy. However, resolution falls rapidly with increasing mass and the longer acquisition times, possibly a few seconds, required are not ideal for GC/MS applications.

14.4.4 Orbitrap mass spectrometers

Yet another trapping analyzer is the Orbitrap (Fig. 14.15), found as an analyzer in more complex instruments. It consists of a cylinder (barrel electrode) with concave inner surfaces surrounding a central spindle such that the space between the center of the spindle is greater toward the center of the device. A fixed DC potential is applied between the spindle and barrel electrodes creating an inhomogeneous electric field. Ions are injected at right angles to the z -axis at a point away from the center of the device and circle the central electrode. The increasing electric field remote from the center of the Orbitrap repels the ions and causes them to oscillate in an m/z -dependent linear motion along the z -axis. This motion induces a current in the two halves of the barrel electrode. These simple

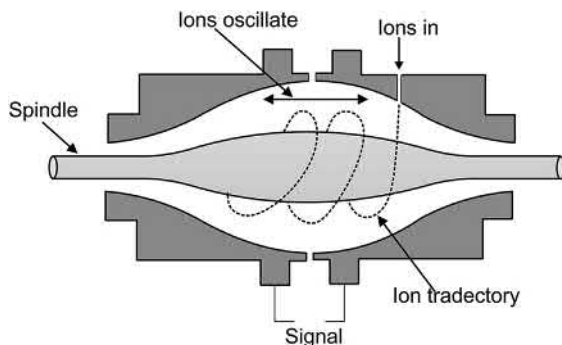


FIGURE 14.15 Orbitrap mass spectrometer.

analyzers can achieve very high resolutions for a very small size and are favorite devices for mass spectrometers used in proteomics experiments.

14.4.5 Time-of-flight (TOF) mass spectrometers

TOF mass analyzers (Fig. 14.16) separate ions by virtue of their different m/z -dependent flight times over a known distance in a field-free flight tube. The ion's velocity is inversely proportional to the square root of mass. The instruments have the advantages of high acquisition speed, high sensitivity because all ions are recorded, a theoretical unlimited mass range, and low cost. Unfortunately, resolution is low (in the order of a few hundred) because of the small velocity differences between ions with the same m/z ratio, which causes peak broadening. This effect can be rectified by use of a reflectron, which can increase the resolution to match that of sector instruments. The reflectron presents an increasing electric field to the ions traversing the flight tube such that they are reflected back to a detector. Ions with a higher velocity penetrate the field further than the slower ions and the resulting longer path length can be used to compensate for the velocity difference and to focus the ions at the detector. Other methods for increasing resolution include multiturn or multireflectron instruments but with the disadvantage of increasing price. Although normally associated with laser

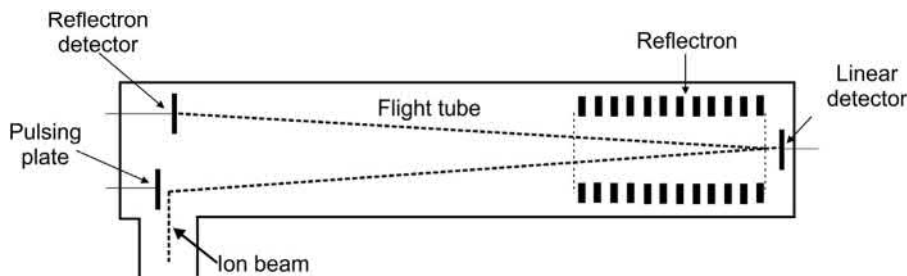


FIGURE 14.16 Time-of-flight mass spectrometer.

ionization, which naturally produces bursts of ions, TOF analyzers can be adapted to beam instruments by pulsing packets of ions orthogonally into the flight tube. Consequently, this configuration is suitable for GC/MS work where its speed is appropriate for separations with high-resolution columns. See the review by Gröger et al. [28] for more information.

14.4.6 Tandem mass spectrometers

14.4.6.1 Triple quadrupole instruments

Few instruments today consist of a single analyzer. Most contain two or three. One of the most common configurations used for GC/MS work is the “triple quadrupole” (QqQ) instrument consisting, as its name suggests, of three quadrupoles arranged in series. The central quadrupole (hexapole or octopole) operates in an RF-only mode as a collision cell containing a collision gas such as argon at a higher pressure than the surrounding vacuum such that ions hitting the gas molecules acquire sufficient

energy to fragment and are analyzed by the third quadrupole.

These instruments can be operated in several modes: The first quadrupole can be set to transmit ions of a single m/z value into the collision cell and the resulting fragments can be analyzed by scanning the third quadrupole to give a “product ion spectrum” (formerly known as a “daughter ion spectrum,” Fig. 14.17A). Alternatively, the first quadrupole can scan the entire spectrum with the third quadrupole set to transmit only ions of a single m/z ratio (Fig. 14.17B). A signal will be detected only when a precursor ion fragments to form the product ion that is being monitored. This technique, known as “precursor” or parent ion scanning, is often used to screen for compounds of related structure, such as the metabolites of a known drug. In a third method, known as constant neutral loss scanning, the first and third quadrupoles are scanned simultaneously but with an offset corresponding to the difference in mass between the precursor and product ions (Fig. 14.17C). A signal only appears when a precursor ion yields a product ion

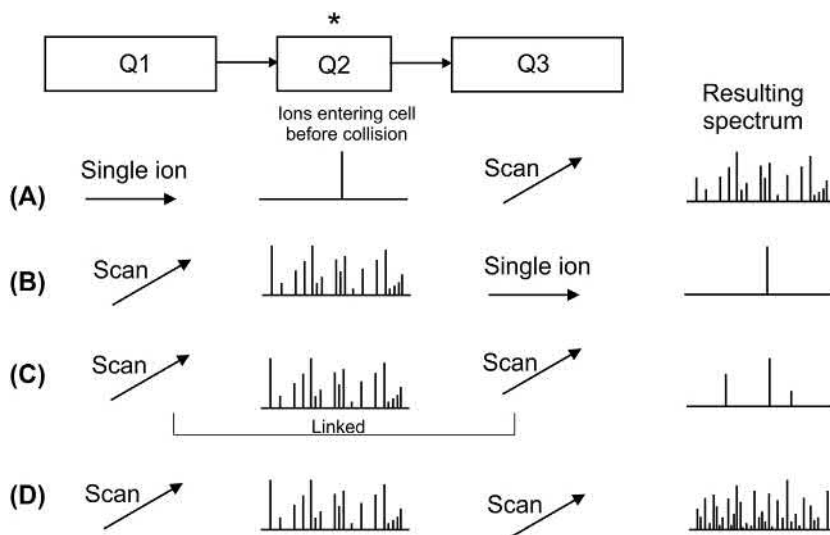


FIGURE 14.17 Triple quadrupole mass spectrometer with fragmentation in Q2. Scans: (A) Product ion from selected precursor, (B) selected ion from scanned spectrum, (C) single ion transmission with selected product ion in Q3, (D) fragmentation spectra from all precursors, deconvolution by time alignment.

with the mass difference that has been selected. This technique can be used to screen for compounds that contain a specific structural feature that yield a common fragmentation process. Fourthly, both quadrupoles can be set to scan resulting in complex spectra containing all fragment ions from all precursors (Fig. 14.17D). However, the spectra can be deconvoluted by time-aligning parent and product ions.

14.4.6.2 Other tandem configurations

Another popular combination of tandem instruments is the quadrupole-collision cell–TOF (Q-TOF) instrument. It provides high resolution, especially with a reflectron-TOF and high scan speeds suitable for GC/MS. In MS/MS mode, these instruments produce product ion spectra but parent ion scanning is difficult. TOF instruments have also been coupled to ion traps as in the ion trap–TOF instrument produced by Shimadzu. The TOF analyzer overcomes the limited resolution properties of the ion trap. Instruments consisting of two TOF analyzers can produce rapid scanning and have the ability to acquire high-energy CID spectra. However, none of these combinations enjoys wide application for GC/MS.

14.5 Modes of operation

14.5.1 Full scan spectra

The mass spectrometer cycles across the mass range continuously, spectra are accumulated by the data system for postprocessing as described further. It is important to obtain sufficient scans across a GC peak for the data system to reconstruct the peak without distortion. An optimum of about 10 spectra per peak is usually sufficient, which, with a 1 s wide GC peak, requires spectra to be acquired in less than 100 ms. If isothermal conditions are employed, the scan speed can be decreased during later stages of an analysis to accommodate the resulting broader peaks. One

problem inherent in spectra acquired from chromatographic columns is spectral skewing. Because the spectrum recorded with a scanning instrument takes time, the concentration of sample entering the mass spectrometer changes during the scan. Thus, with a low-to-high mass scan recorded on the leading edge of the peak, the spectrum will be biased toward the high mass end and vice versa. The least biased spectrum, but one that is biased toward its center, is that obtained at the top of the peak (Fig. 14.18). Before the advent of data systems, it was quite a skill watching the GC peak on a pen recorder and acquiring a single spectrum just at the top of the peak to be recorded on expensive paper from a UV recorder. Data systems can now average all spectra acquired across a peak and produce what approximates to an unbiased spectrum.

14.5.2 Selected ion monitoring

Selected ion monitoring is a major application for GC/MS and allows the instrument to be used in its most sensitive mode for quantitative measurements. The technique was introduced in the 1960s by Hammar and coworkers under the name mass fragmentography and has acquired a number of other names over the years. Several modes of operation are available; single ion monitoring (SIM), multiple ion monitoring, and single or multiple reaction monitoring.

14.5.2.1 Single ion monitoring (SIM)

For SIM, the instrument is set to transmit only a single ion. Consequently, all of the current from this ion is captured, whereas, if the mass spectrometer was scanned, only a small fraction of the ions at this m/z value would be acquired. Sensitivity can be improved further by derivatization of the sample such that its spectrum contains mainly a single fragment of high abundance. *t*-Butyldimethylsilyl (TBDMS) derivatives

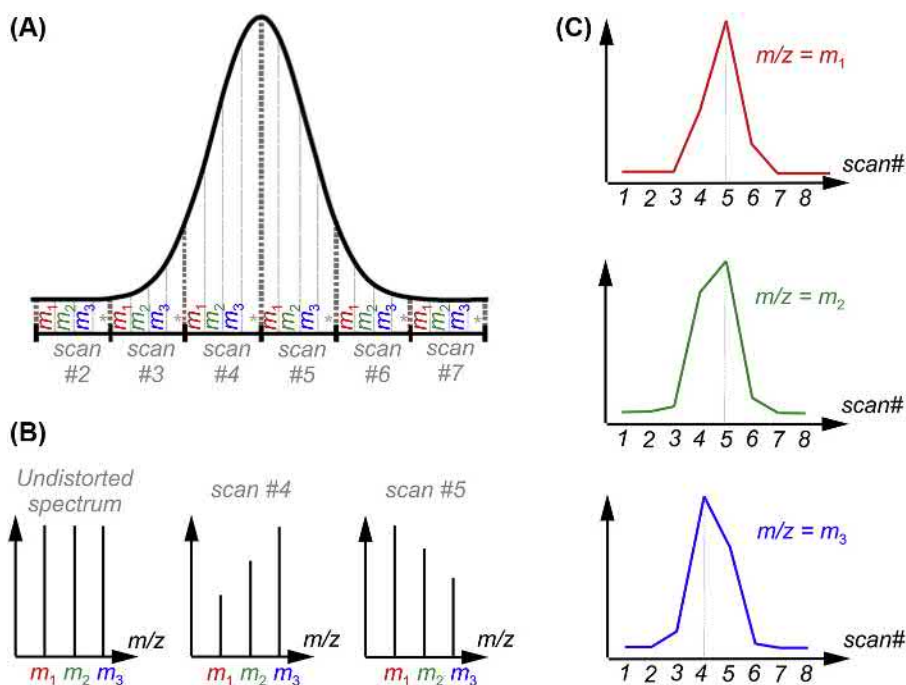


FIGURE 14.18 Skewing of spectra across a GLC peak. (A) Hypothetical GLC peak, (B) the first spectrum of three peaks should be the undistorted spectrum, The second spectrum shows the spectrum recorder from scan 4 shown in (A) displaying abundance skewing toward the high mass peaks. The third spectrum is taken at scan 5 showing the opposite effect. The reconstructed chromatograms in panel (C) show the effect of skewing on their peak shape. From A. Samokhin, *Spectral skewing in gas chromatography-mass spectrometry: Misconceptions and realities.* *J Chromatogr A.* 1576 (2018) 113–119 [29] with permission from Elsevier.

are a favorite in this context; they fragment by loss of the *t*-butyl group to yield a very abundant $[M - t\text{-Bu}]^+$ ion [16] (Fig. 14.19).

High sensitivity, as used in trace analysis, often requires the use of high resolution to separate ions of the same nominal mass but different ionic compositions. A good example of this is in dioxin analysis where several other chlorinated aromatic compounds have the same nominal but different accurate masses. By monitoring only at the absolute mass of the dioxin molecule (m/z 321.8936), usually with a sector instrument, the interfering compounds can be rejected.

14.5.2.2 Multiple ion monitoring

By monitoring only a single ion, SIM suffers from the disadvantage of reduced selectivity

compared with that of scanning the whole spectrum. Selectivity can be partially restored by continually jumping between several significant ions, recording their ion current for a few ms, and then reconstructing the ion profiles. This mode of operation is used for quantitative studies where the analyte or analytes are monitored on one or more channels and the internal standard(s) on others. This assumes, of course, that there is a mass difference between the ions. Reference compounds are frequently labeled with stable isotopes and it is important to achieve a large enough mass difference between their masses and that of the analytes so that the natural isotope peaks of the latter do not interfere with the standard. Where interference is experienced, nonlinear calibration

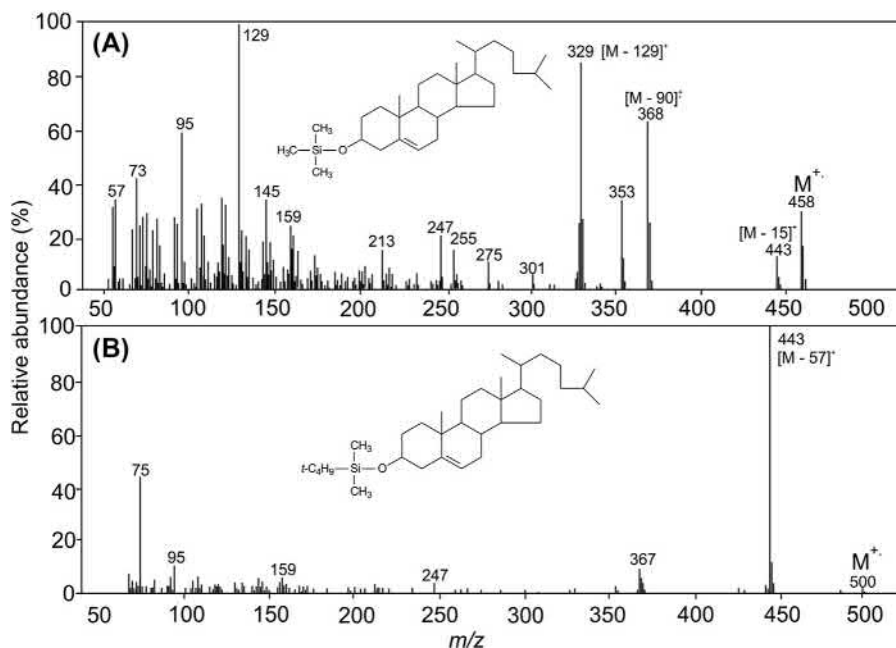


FIGURE 14.19 EI mass spectra of (A) the TMS and (B) the TBDMS derivative of cholesterol. Fragmentation of the TBDMS derivative is characterized by a prominent loss of the *t*-butyl group ($[M - 57]^+$ ion), which therefore, contains much of the ion current.

curves are obtained, which require special treatment to restore accuracy. Several such methods have been described in the literature but none appears to be universally valid. For more information on quantitation, see [30]: (unfortunately out of print but, at the time of writing, used copies are available on e.g., Amazon) [31,32]. Quantification by SIM can also be accomplished using nonlabeled standards if a chromatographic separation exists between standard and analyte provided they both yield the same ion for monitoring allowing both of them to be monitored on the same channel.

The technique is most conveniently implemented with a quadrupole or ion trap instruments because mass changes can be accomplished very rapidly. Such channel switching with magnetic sector instruments is very slow and impractical by changing the magnetic field and difficult to control because of magnetic hysteresis

effects. Consequently, with these instruments, channel switching can be achieved rapidly by altering the accelerating voltage but at the expense of a reduction in sensitivity for ions with higher m/z values and some defocusing of the ion source.

14.5.2.3 Multiple reaction monitoring (MRM)

For the highest selectivity and sensitivity, multiple reaction monitoring can be employed. In this technique, an ion from the spectrum is selected, fragmented, and a single fragment ion is monitored (Fig. 14.17C). Although the absolute sensitivity is reduced because of the reduced ion count, the effective sensitivity is usually considerably greater because of the reduction in background, usually chemical, noise because the monitored fragment ion must have arisen from a specific precursor. Such experiments are conveniently implemented on tandem instruments, particularly triple quadrupoles.

Several complex methods allowing several analytes to be monitored simultaneously have been introduced recently, mainly for LC/MS but which could also be adapted for GC/MS. These methods involve using several isobaric derivatives labeled with multiple stable isotopes such that, upon fragmentation, each derivative fragments to yield ions of a different mass. The single chromatographic peak can, therefore, represent multiple, detectible components. On a more sophisticated level, even the fragments have the same nominal mass but differ in their absolute masses requiring very high resolution for successful monitoring.

14.6 Data analysis

14.6.1 Definitions of mass and their uses

Before the advent of data systems, mass spectra were recorded on UV chart paper with no mass or intensity scales. Processing was done by hand and spectra consisting of histograms of m/z against normalized relative abundance (now often called “stick” spectra) were drawn manually. Accurate masses, which were the providence of high-resolution instruments, whose scan speeds were too slow for GC/MS work, were ignored and m/z values were presented as “nominal” masses (C = 12.00, H = 1.00, O = 16.00, etc.). Early computer systems basically duplicated this approach with manually measured values entered onto IBM computer cards from which the computer reproduced the spectra. With the development of faster computers with extensive storage, it was possible to record total peak profiles of the ions, perform accurate peak centering, which yielded accurate masses from which elemental compositions could be calculated. With isotopic resolution, these masses are known as “monoisotopic” masses as compared with the average or chemical masses produced by gravimetric instruments or mass spectrometers incapable of

isotopic resolution. Recognition of these three mass types becomes increasingly important as masses rise because they can differ by several units at higher masses (Fig. 14.20).

Another use of accurate masses is for compound-type identification in a spectrum containing ions from several compounds. Compounds with different combinations of atoms giving similar m/z values will fall on different lines in graphs such as those shown in Fig. 14.20. Thus, for example, hydrocarbons with masses in the region of m/z 500 will have fractional masses of around +0.58 Da, whereas the figure for carbohydrates is only +0.16 Da, numbers that are easily identified in the spectra.

14.6.2 Computer processing of spectra

The initial function of the GC/MS data system in acquisition mode is to digitize the analogue output from the mass spectrometer detector and to perform a time-to-mass conversion or Fourier transform analysis to produce the mass spectrum. The digitization rate for the signal should give about 10–20 samples over each ion peak in the spectrum so as to preserve its profile. A centroid calculation can then be applied to determine the accurate m/z ratio. Various filters can be set to remove noise, set the base line, and accommodate multiplet ion peaks. Spectra can then be presented in stick or full-scan format. However, depending on how the various filters are applied, broad metastable ions can be filtered out in the stick format (e.g., too many sample points). These data can then be further processed to produce various reconstructed chromatograms or to perform library searches.

14.6.2.1 Spectrum addition and subtraction

Spectral addition, such as from those acquired across a single GC peak, overcomes the spectrum bias present in a single spectrum, as described earlier, and improves the total signal strength. Spectral subtraction can also be used, either to

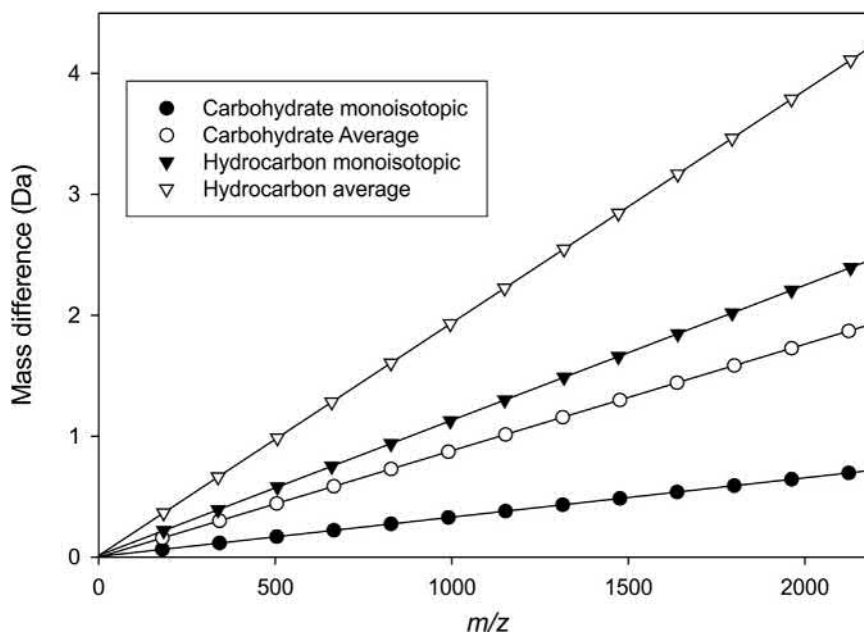


FIGURE 14.20 Graph showing how monoisotopic and average masses differ with increasing mass for carbohydrates ($(C_6H_{10}O_5)_n + H_2O$) (with mass deficient oxygen) and hydrocarbons ($(CH_2)_n + H_2$).

remove background or to subtract ions from a given compound from a mixed spectrum. Most data systems now allow an almost unlimited selection of peaks to be either added to or subtracted from each other.

14.6.2.2 Ion chromatograms

14.6.2.2.1 Total ion chromatograms (TIC)

A plot of total ion current in each spectrum against time (or scan number) gives a chromatogram comparable with that obtained by GC using a conventional detector (Fig. 14.21, top trace). However, the TIC peak abundance can vary from that shown in the GC chromatogram for compounds of different structure because of their different ionization efficiencies. For example, under EI conditions, the signal recorded for hydrocarbons is much weaker relative to that from many other compounds recorded with a

flame ionization detector, because hydrocarbons are more difficult to ionize than compounds with, for example, free electron pairs.

14.6.2.2.2 Single ion chromatograms

The plot of the intensity of the m/z value of a single ion with time provides a single ion chromatogram and a method for locating specific compounds in the TIC, particularly when they occur as components of an unresolved GC peak (Fig. 14.21). It must, however, be borne in mind that false positives are possible. These can occur, for example, from the presence of an ion at the selected mass formed from a different fragmentation pathway or from an ion present as an isotopic peak from an ion at a lower m/z value. Although the output resembles that of a SIM trace as described earlier, it should not be confused as such because it lacks the increase in sensitivity

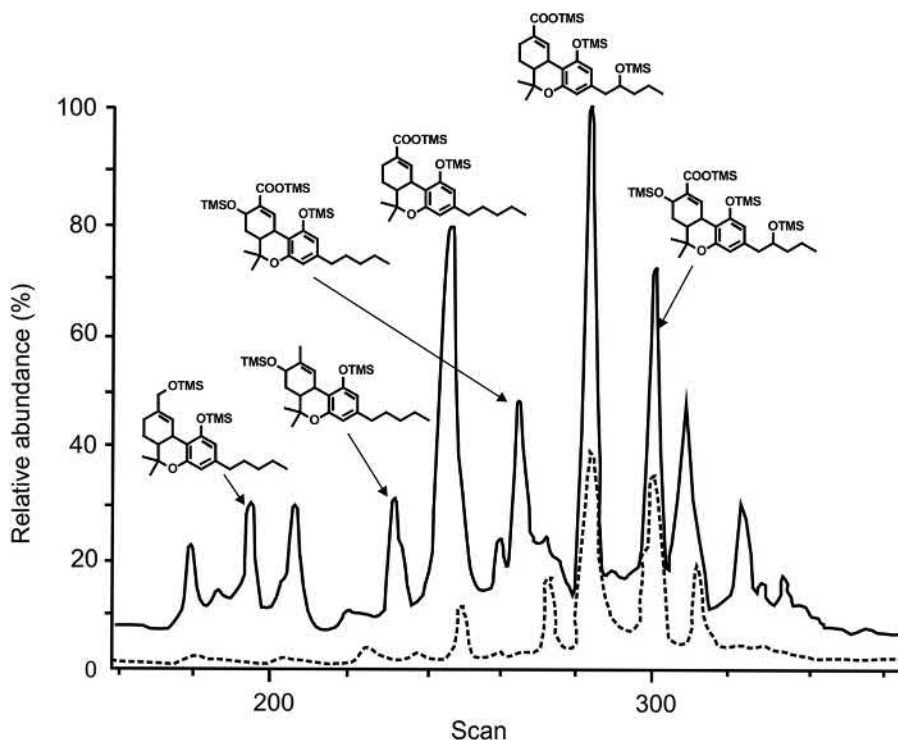


FIGURE 14.21 Top trace—TIC of metabolites of TMS derivatives of Δ^9 -tetrahydrocannabinol (Δ^9 -THC) from mouse liver (packed SE30 column). Lower trace, single ion plot of the ion at m/z 145 ($[\text{TMSO}=\text{CH}_2\text{-CH}_2\text{-CH}_2\text{-CH}_3]^+$) diagnostic for substitution in the 2'' position of the C_5 side chain.

provided by monitoring the entire ion current. It does allow, however, for retrospective ion plotting from stored data.

14.6.2.2.3 Multiple ion chromatograms

Chromatograms derived from combinations of several ions may also be plotted. These ions may be from a single compound thus adding confidence to the assignment of structure, or they can be common to a group of compounds with similar structures. Ions that are characteristic of the presence of a given isotopic profile such as those given by chlorine-containing compounds can also be plotted to quickly identify such compounds in a mixture. Another technique is to use only ions above a given mass for compounds that produce ions mainly in the

upper mass range. In this way, many of the undiagnostic, low mass ions leading to high backgrounds in the chromatograms may be removed.

14.6.2.3 Library searching

Library searching is invaluable for the rapid identification of sample constituents and can often give clues to the identity of unknown compounds. Several commercial libraries are available containing many tens of thousands of spectra. Among the largest is the NIST-17 library (2017) with 306,623 spectra and the Wiley Registry of Mass Spectral Data 11th Edition, (2016) with 775,818 spectra. Many smaller ones exist, such as the SWGDRUG Mass Spectral Library (2019) with 3160 spectra and collections

provided by some mass spectrometer manufacturers. Several search algorithms are available, of which the so-called reverse search involving finding the peaks from the library spectrum in the spectrum of interest is probably the most useful. Best-fit spectra are usually presented to the analyst, together with a goodness of fit factor for evaluation. However, it is important to realize that the best library match may not be the correct molecular identity. More confidence in a correct match can be gained by making use of the compound's GC retention index, another parameter that can be incorporated into databases.

14.7 Sample preparation

Needless to say, solvents and reagents used for sample preparation should be as pure as possible and plastic apparatus (sample tubes, etc.) should be avoided because of the danger of extracting compounds such as plasticizers (common phthalate plasticizers yield major ions at m/z 149 and 167). Glass conical vials are more suitable; these can be treated with silanizing reagents to limit surface adsorption of analytes. Polyethylene glycol is another common contaminant (characterized by a series of ions 44 mass units apart). Column bleed from silicon-containing GC phases yields ions at m/z 73, 75, 207, 281 and 355.

14.7.1 Derivatives

For successful GC/MS analysis, the sample must be both volatile and thermally stable. Few organic compounds fulfill these criteria because they possess polar or reactive functional groups. Protecting these functional groups by derivatization is the normal method for conferring good GC/MS behavior. Such derivatives should be easy to prepare in a quantitative manner and not cause degradation of the analytes. Suitable derivatives are listed in [Table 14.1](#).

In addition to stabilizing compounds for GC/MS analysis, these can be tailored to confer specific advantages for MS such as the preparation of TBDMS derivatives for quantitative work outlined earlier. A large number of other substituted silyl derivatives have been prepared for different purposes. Of particular use are the [$^2\text{H}_9$]-TMS reagents, which provide invaluable information on the pathways of fragmentation of these derivatives, some of which involve extensive rearrangements. A recent review discusses many of these in detail [16].

Other derivatives can specifically direct fragmentation into structure-revealing pathways. A good example are derivatives prepared from 3-substituted pyridines. As noted in [Table 14.1](#), TMS and methyl derivatives do not yield much information on the structure of the alkyl chains of long-chain fatty acids or alcohols (see [Fig. 14.7](#)). However, the pyridine-containing derivatives (prepared from 3-pyridyl carbinol from fatty acids and 3-carboxypyridine (nicotinic acid)) yield abundant radical-induced ions from the chain as the result of hydrogen abstraction by the charged pyridine ring after ionization. Structural features such as the position of unsaturation, methyl groups, or rings are clearly visible in the spectra ([Fig. 14.22](#)).

14.8 Conclusions

This chapter has summarized the mass spectrometric instrumentation used in combined GC/MS together with examples of its use. The technique is one of the most powerful available for mixture analysis providing that the analytes are volatile or can be made so by derivatization. Although the technique is 50 years old and generally regarded as "mature," it is still the most appropriate for the analysis of many compounds such as derivatized fatty acids. Faster analysis times could be an area for advancement in the future and the incorporation of ion mobility, recently implemented on commercial

TABLE 14.1 Derivatives suitable for GC/MS.

Functional group	Derivative	Comments
Hydroxyl	TMS ether	Easy to prepare, good GC and MS properties
	[² H ₉]-TMS derivatives	Provide mass shifts for determination of fragmentation pathways
	TBDMS ether	Produce abundant [M – 57] ⁺ ion for high sensitivity. Longer retention time than TMS
	Higher alkyl silyl derivatives (e.g., tri-ethylsilyl)	Used as GLC shift reagents (reagents used to alter the retention time of selected compounds). MS spectra can contain abundant [M – R] ⁺ ions
	Methyl ether	Not as easy to prepare or purify as TMS but provide good GC and MS properties
Acetyl	Acetyl	Easy to prepare, sometimes relatively large increases in GC retention time
	Cyclic alkane boronate	Low mass increment (particularly Me-boronates). Derivatized compounds identified by ¹⁰ B/ ¹¹ B-isotopic ratio.
cis-diol	Acetonide	Easy to prepare from acetone
	TMS	Large increase in molecular weight. Spectra can contain multiple ions produced by TMS migrations
Poly-ols, carbohydrates	Per-methyl	Good derivatives but high-pH conditions necessary for preparation
	Per-methylated alditol acetates (PMAA derivatives)	Multistage derivatization. Used for constituent monosaccharide and linkage determination by GC/MS
	Methyl ester	Good GC performance, relatively poor MS fragmentation (little information on alkyl chain unsaturation or branching)
Carboxylic acid	TMS ester	Slightly acid labile. Again relatively poor MS fragmentation of alkyl chain
	Nitrogen-containing e.g., 3-pyridylcarbinol	Good for structural studies (unsaturation, Me-branching) of long-chain compounds
	Acyl	Very stable
Amine	Various fluorinated acyl e.g., heptafluorobutyryl (HFB)	Short retention times, very sensitive CI detection
	Schiff bases	Very easy preparation from carbonyl compounds. Many examples
	TMS	Less stable than TMS ethers of alcohols. Primary amines can yield mono- or di-TMS derivatives
	Schiff bases	Many suitable amines available
Carbonyl	Alkylloxime	Can give two GC peaks (<i>syn</i> and <i>anti</i>)
	Ring-opening reaction with TMS-Cl	Chlorine isotopes effectively label the product for MS detection
Epoxide	TMS	Spectra contain many rearrangement ions, e.g., <i>m/z</i> 299
	Methyl ester	More stable than TMS derivatives
Phosphate	Unstable	Usually detected by replacement following derivatization of other functional groups to give mixed derivative such as TMS/Acetyl
Sulfate		

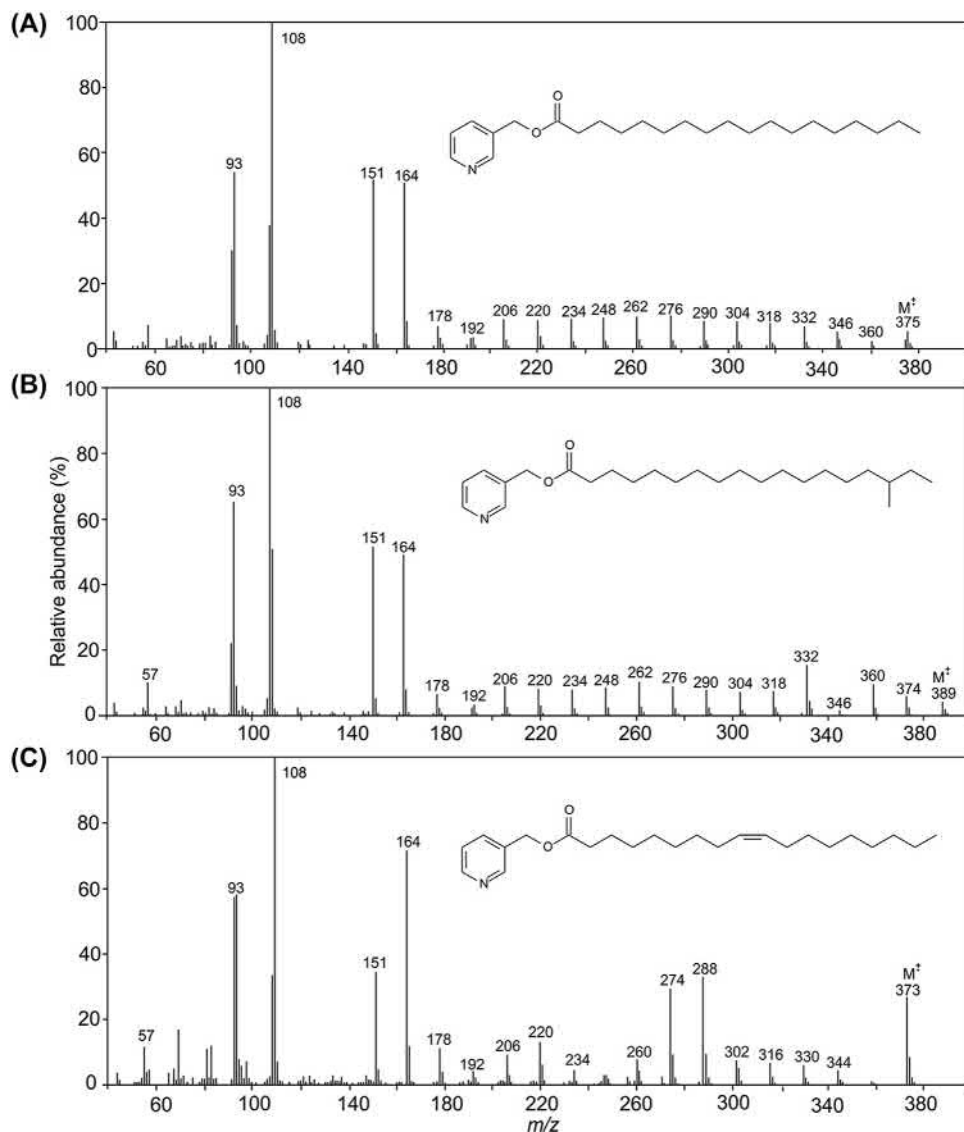


FIGURE 14.22 3-Pyridyl carbinol derivative of (A) stearic acid (18:0), (B) Anteiso-19:0, and (C) Oleic acid (Δ^9 -18:1). The branch point of the derivatized acid shown in spectrum (B) is defined by the very low abundance of the ion at m/z 346 and the increased relative abundance of the flanking ions at m/z 332 and 260. In spectrum (C), the double bond position is revealed by the virtual absence of m/z 248 (cleavage through the double bond), the 26 rather than 28 mass unit difference between the ions at m/z 234 and 260, and the high abundances of m/z 274 and 288. Mechanisms for the formation of these ions are given in Ref. [33].

instruments, could see the technique acquiring another dimension to help with structural analysis.

References

- [1] I. Ferrer, E.M. Thurman, *Advanced Techniques in Gas Chromatography–Mass Spectrometry (GC–MS–MS and GC–TOF–MS) for Environmental Chemistry*, Elsevier, Kidlington, UK, Amsterdam, 2013.
- [2] K.J. Bisceglia, G. Kroening, B. Subedi, *GC-MS Methods for monitoring illicit drug biomarkers in wastewater: a critical review*, *ACS Symp. Ser.* 1319 (2019) 51–77.
- [3] H.H. Maurer, Screening of drugs in body fluids by GC/MS, in: J. Yinon (Ed.), *Advances in Forensic Applications of Mass Spectrometry*, CRC Press, Boca Raton, 2003, pp. 1–62.
- [4] P. Gerhards, U. Bons, J. Sawazki, J. Szigan, A. Wertmann, *GC/MS in Clinical Chemistry*, Wiley-VCH, Weinheim, 1999. Online 2007.
- [5] L. Mondello, P.Q. Tranchida, P. Dugo, *Advances in GC–MS for food analysis*, *LC GC May* (2012) 25–30.
- [6] J.H. Gross, *Fragmentation of Organic Ions and Interpretation of Mass Spectra*. *Mass Spectrometry, A Textbook*, third ed., Springer Nature, Cham, Switzerland, 2017, pp. 325–438.
- [7] E. de Hoffmann, V. Stroobant, *Mass Spectrometry. Principles and Applications*, third ed., John Wiley and Sons, Chichester, UK, 2007.
- [8] J.T. Watson, O.D. Sparkman, *Introduction to Mass Spectrometry: Instrumentation, Applications, and Strategies of Data Interpretation*, fourth ed., John Wiley and Sons, Chichester, UK, 2008, p. 862.
- [9] M.C. McMaster, *GC/MS, A Practical User's Guide*, second ed., Wiley, Hoboken, 2008.
- [10] H.-J. Hübschmann, *Handbook of GC/MS: Fundamentals and Applications*, third ed., Wiley-VCH, Weinheim, 2015.
- [11] S. Bouchonnet, *Introduction to GC-MS Coupling*, CRC Press, 2013.
- [12] B. Gruber, F. David, P. Sandra, *Capillary gas chromatography-mass spectrometry: current trends and perspectives*, *Trends Anal. Chem.* 124 (2020). Article 115475.
- [13] M. Zoccali, P.Q. Tranchida, L. Mondello, *Fast gas chromatography-mass spectrometry: a review of the last decade*, *Trends Anal. Chem.* 118 (2019) 444–452.
- [14] C.F. Simpson, C.F. Gough, *Gas chromatography - mass spectrometry interfacial systems*, *Crit. Rev. Anal. Chem.* 3 (1) (1972) 1–40.
- [15] F.W. McLafferty, F. Tureček, *Interpretation of Mass Spectra*, fourth ed., University Science Books, Sausalito, CA, 1993.
- [16] D.J. Harvey, P. Vouros, *Mass spectrometric fragmentation of trimethylsilyl and related alkylsilyl derivatives*, *Mass Spectrom. Rev.* 39 (2020) 105–211.
- [17] K. Blau, J. Halket, *Handbook of Derivatives for Chromatography*, second ed., Wiley, Chichester, 1993.
- [18] D.R. Knapp, *Handbook of Analytical Derivatization Reactions*, Wiley Interscience, New York, 1979.
- [19] J.M. Halket, V.G. Zaikin, *Derivatization in mass spectrometry - 1. Silylation*, *Eur. J. Mass Spectrom.* 9 (1) (2003) 1–21.
- [20] J.M. Halket, V.G. Zaikin, *Derivatization in mass spectrometry - 5. Specific derivatization of monofunctional compounds*, *Eur. J. Mass Spectrom.* 11 (2005) 127–160.
- [21] A. Amirav, A. Gordin, M. Poliak, A.B. Fialkov, *Gas chromatography-mass spectrometry with supersonic molecular beams*, *J. Mass Spectrom.* 43 (2008) 141–163.
- [22] A. Amirav, U. Keshet, A. Danon, *Soft Cold EI - approaching molecular ion only with electron ionization*, *Rapid Commun. Mass Spectrom.* 29 (2015) 1954–1960.
- [23] D.-X. Li, L. Gan, A. Bronja, O.J. Schmitz, *Gas chromatography coupled to atmospheric pressure ionization mass spectrometry (GC-API-MS): review*, *Anal. Chim. Acta* 891 (2015) 43–61.
- [24] K. Miyamoto, S. Fujimaki, Y. Ueda, *Development of a new electron ionization/field ionization ion source for gas chromatography/time-of-flight mass spectrometry*, *Rapid Commun. Mass Spectrom.* 23 (2009) 3350–3354.
- [25] H.D. Beckey, *Determination of the structures of organic molecules and quantitative analyses with the field ionization mass spectrometer*, *Angew. Chem. Int. Ed.* 8 (9) (1969) 623–688.
- [26] R. Zimmermann, W. Welthagen, T. Gröger, *Photoionisation mass spectrometry as detection method for gas chromatography. Optical selectivity and multidimensional comprehensive separations*, *J. Chromatogr. A* 1184 (2008) 296–308.

- [27] R.E. March, J.F.J. Todd, *Practical Aspects of Ion Trap Mass Spectrometry*, CRC Press, Boca Raton, New York, London, Tokyo, 1995.
- [28] T.M. Gröger, U. Käfer, R. Zimmermann, Gas chromatography in combination with fast high-resolution time-of-flight mass spectrometry: technical overview and perspectives for data visualization, *Trends Anal. Chem.* 122 (2019) 115677.
- [29] A. Samokhin, Spectral skewing in gas chromatography-mass spectrometry: misconceptions and realities, *J. Chromatogr. A* 1576 (2018) 113–119.
- [30] B.J. Millard, *Quantitative Mass Spectrometry*, Heyden, London, 1978.
- [31] M.W. Duncan, P.J. Gale, A.L. Yergey, *The Principles of Quantitative Mass Spectrometry*, Rockpool Publications, Denver, CO, 2006.
- [32] I. Lavagnini, F. Magno, R. Seraglia, P. Traldi, *Quantitative Applications of Mass Spectrometry*, John Wiley and Sons Ltd., Chichester, UK, 2006.
- [33] D.J. Harvey, Picolinyl esters as derivatives for the structural determination of long-chain branched and unsaturated fatty acids, *Biomed. Mass Spectrom.* 9 (1982) 33–38.
- [34] S. Dagan, A. Amirav, Electron impact mass spectrometry of alkanes in supersonic molecular beams, *J. Am. Soc. Mass Spectrom.* 6 (1995) 120–131.

Ion mobility detectors for gas chromatography

Maria Jose Cardador, Natividad Jurado-Campos, Lourdes Arce

Department of Analytical Chemistry, University of Córdoba, Institute of Fine Chemistry and Nanochemistry, Córdoba, Spain

15.1 Introduction

Intensive work on ion mobility spectrometry (IMS) started about half a century ago. These initial works were focused on the development of the fundamentals of the measurement technique, which allowed detection of various chemical compounds present in air [1]. The first IMS devices were not developed until the 1970s by Karasek and Keller [2], who employed the term “plasma chromatography” to refer to what is currently known as ion mobility spectrometry. Gas chromatography (GC) has been coupled to ion mobility spectrometers as detectors since the 1970s [2–5]. However, the spectacular success of IMS was related to the use of detectors without any additional elements for separating the sample components. Since ion mobility spectrometers were small, light, and not very complex, it was possible to build portable analyzers [1]. From that moment, the development of IMS devices has risen exponentially in order to overcome problems encountered in monitoring vapors at ambient pressure. Improvements in analytical properties such as high sensitivity (low detection

limits), low price, speed, robustness, and simplicity were achieved [6].

Nowadays, IMS is considered as a vanguard analytical technique, which could be used to acquire data in an analytical process providing fast and low-cost results with very low detection limits. Also, little or any sample preparation is required when using IMS devices [7]. Other remarkable advantages of IMS devices are working at atmospheric pressure, gas-phase ion separation, and that IMS methods are environmentally friendly, since solventless measurements are carried out. In addition, IMS has an important application in understanding the chemistry of ion–molecule reactions [8], especially at atmospheric pressures. Unlike mass spectrometry (MS) that operates in vacuum, IMS works at atmospheric pressure promoting numerous collisions between ions and neutral species. This makes the results of the experiments more similar to those of the natural world, since ion–molecule reactions in nature typically occur at atmospheric pressure conditions [9].

Despite its advantages, sometimes the stand-alone IMS instrument is insufficient for the

identification of all target compounds when complex samples are analyzed on account of the low resolving power of IMS devices. Therefore, hyphenated techniques are employed to overcome this problem. Nowadays, the coupling of GC to ion mobility spectrometers (GC-IMS) is easily achieved. Preseparation by GC avoids clustering in the ionization region, improving selectivity, and the retention time obtained from this setup can be used as an additional parameter for the identification of the detected compounds.

15.2 IMS operation

IMS is based on the movement of swarms, defined as ensembles of gaseous ions, in an electric field through a supporting gas [6]. Gaseous ions in an electric field at atmospheric pressure are accelerated and through multiple collisions acquire a constant velocity over macroscopic distances [10]. The ion velocity is directly proportional to the electric field through a magnitude named ion mobility, as shown in Eq. (15.1):

$$v = K \cdot E \quad (15.1)$$

where v is ion velocity, K the ion mobility coefficient, and E the electric field.

The separation of ions on the basis of mobility differences is the principle of IMS operation. It depends on the mass, charge, size, and shape of the ions. Mobility values are characteristic of each ion and K is a qualitative parameter for their identification in IMS separations. Also, the ion velocities in IMS are determined from the time that they need to traverse the distance between the ion shutter and detector or, in other words, the drift tube length as shown in Eq. (15.2):

$$v = \frac{L}{D_t} \quad (15.2)$$

where L is the drift tube length and D_t the drift time. The drift time is characteristic for the analyte ion. Eqs. (15.1) and (15.2) can be combined to obtain Eq. (15.3), which allows K for an

analyte to be calculated from experimental parameters:

$$K = \frac{L}{D_t \cdot E} \quad (15.3)$$

K values are typically normalized to standard conditions ($T_0 = 273.15$ K and $P_0 = 760$ Torr) as a reduced mobility constant (K_0), Eq. (15.4). The reduced mobility constant facilitates comparisons between IMS devices since both pressure and temperature influence the density of molecules, and accordingly, their mobility:

$$K_0 = K \cdot \frac{P}{P_0} \cdot \frac{T_0}{T} \quad (15.4)$$

However, calculated K_0 values do vary for data reported by different groups. These differences are attributed to instrumental variables such as inhomogeneities in temperature and electric field or contamination of buffer gas with moisture or other volatile compounds [11]. The analysis of standard compounds or simultaneous mass measurements can be used to assist in identification when using IMS [12]. Karpas suggested the use of standard compounds to correct K_0 values. 2,4-Lutidine was selected on account of its high proton affinity and because it produces a single peak at the studied conditions. The K_0 value reported for 2,4-lutidine was $1.95 \text{ cm}^2 \text{ V}^{-1} \text{ s}^{-1}$ [13]. Also, 2,6-di-*t*-butylpyridine (2,6-DtBP) was used as a calibrant by Eiceman et al. [14] based on its stability and reduced tendency for hydration, which leads to a roughly temperature-independent K_0 value ($1.42 \text{ cm}^2 \text{ V}^{-1} \text{ s}^{-1}$). Later, this value was updated to $1.46 \text{ cm}^2 \text{ V}^{-1} \text{ s}^{-1}$, with slight changes depending on the drift field [15]. Using an accepted standard, K_0 values can be calculated from measured mobility values by Eq. (15.5) as follows:

$$\frac{K_0(\text{unknown})}{K_0(\text{standard})} = \frac{D_t(\text{standard})}{D_t(\text{unknown})} \quad (15.5)$$

The mobility of an ion is also related to its collision cross section (Ω) and number density (N , the number of molecules per unit volume) according to the Mason–Schamp equation, Eq. (15.6) [16]:

$$K = \frac{3 \cdot q}{16 \cdot N} \cdot \left(\frac{2\pi}{\mu \cdot k_B \cdot T} \right)^{1/2} \cdot \frac{1}{\Omega} \quad (15.6)$$

where q is the ion charge, $\mu = mM/(m^{-1} + M)$ is the reduced mass of the pair of diffusing ions (m) and carrier gas molecule (M), k_B is the Boltzmann constant ($1.38065 \times 10^{-23} \text{ J K}^{-1}$), and T is the gas temperature.

Both, mobility and the collision cross section (CCS) are suitable for ion identification, although the fundamental meaning of the IMS as a structural measurement technique is better reflected in the CCS values [17]. The CCS represents the average of all geometric orientations and interactions of an ion that depend on its size and shape during the measurement. Not only does the CCS of the analyte influence its empirical CCS but also contributions from the drift gas (momentum transfer and gas polarization effects) and also from the ion mobility experiment (temperature and magnitude of the electric field) [18,19]. In any case, CCS is preferred parameter for comparison across different instrument platforms, and in recent

years, several CCS databases have been built in an attempt to use CCS as a qualitative parameter in IMS [17,20].

In addition, the number of detected ions in IMS is a measure of the analyte concentration. Normally, this information is amplified and transduced as a voltage. Typically, IMS data is represented as a mobility spectrum, which includes ion peaks for the separated ions. Each peak is defined by its drift time as a qualitative parameter and a voltage as a quantitative parameter as shown in Fig. 15.1.

15.3 IMS device components

An ion mobility instrument is composed of three main parts: the ionization region (ion source); drift tube; and a detector, as shown in Fig. 15.2.

15.3.1 Ionization sources

Neutral compounds require ionization since measurements are based on the separation of ions in an electric field. Ionization typically occurs at ambient pressure. Common ion sources employ radioisotopes, photoionization (photodischarge lamps and lasers), corona discharge (CD), or electrospray ionization (ESI).

15.3.1.1 Radioisotope sources

Radioisotope sources are preferred due to their stability and reliability. They do not require a power source but special permits to ensure safe use are required, which can be difficult to obtain. The most widely used radioisotope sources is nickel (^{63}Ni) although tritium (^3H) and americium (^{241}Am) are also used. Sample ionization results from the electrons emitted from ^{63}Ni producing ions and secondary electrons by collision with the supporting gas and its impurities, such as N_2 , H_2O , or O_2 generating either positive or negative ions. These ions are called reactant ions and produce a signal named as the reactant

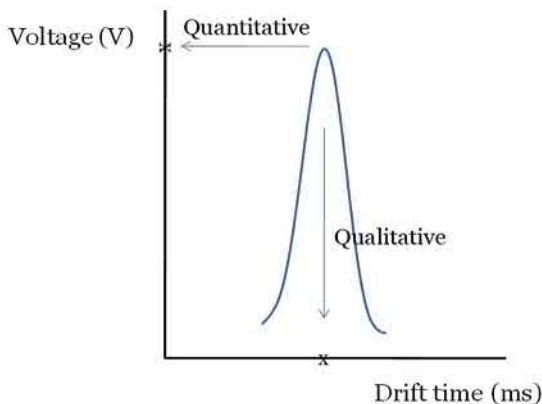


FIGURE 15.1 Synthetic ion mobility spectrum.

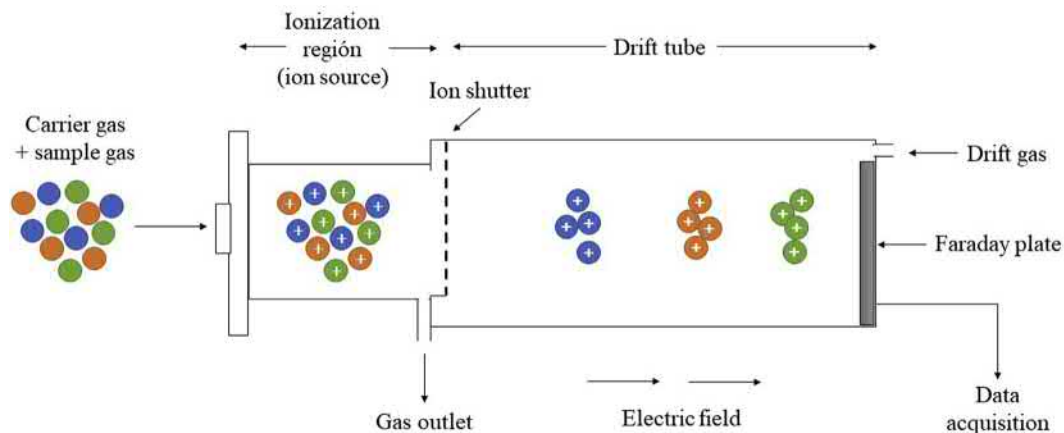
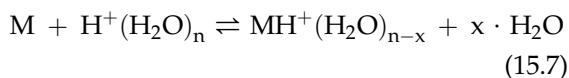


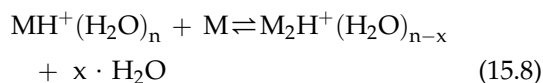
FIGURE 15.2 Basic scheme of the main components of a generic IMS device.

ion peak (RIP). These reactant ions are used to ionize neutral compounds prior to their introduction into the drift tube. The identity of these ions is $\text{H}^+(\text{H}_2\text{O})_n$, called a hydrated proton, in positive polarity and $\text{O}_2^-(\text{H}_2\text{O})_n$ in negative polarity. These reactant ions transfer their charge to sample molecules (M) with greater proton affinity (in positive mode) or electronegativity (in negative mode). When reactant ions are exhausted, the upper limit of ionization is reached [21]. The ions generated by collision of reactant ions and M are named product ions, which are stabilized through displacement of water molecules as shown in Eq. (15.7) for the positive ion mode:



Sample + Hydrated proton \rightarrow Protonated monomer + Water.

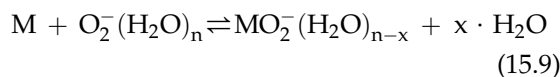
Moisture levels and temperature govern the magnitude of n and proton-bound dimers (M_2H^+) may be formed with increased [M] as shown in Eq. (15.8):



Protonated monomer + Sample \rightarrow Proton-bound dimer + Water.

Ion peaks for proton-bound trimers or higher-order clusters are seldom observed in mobility spectra. However, these product ions have been observed in some applications [22].

Separately, the formation of product ion in the negative ionization mode is shown in Eq. (15.9):



Sample + Negative reactan ion \rightarrow Protonated monomer + Water.

15.3.1.2 Photoionization sources

The photoionization of neutral molecules in air at ambient pressure is possible using photodischarge lamps or lasers. When a photodischarge lamp is used, charge transfer does not take place, unlike for radioisotope sources. In this case, positive ions are formed from photons emitted by the electrical excitation of the fill gases contained in the lamp [23] as shown by Eq. (15.10):



where $h \cdot \nu$ is the photon energy and M is a neutral molecule. The energy of commercial

photodischarge lamps is 9.5, 10.2, 10.6, and 11.7 eV. The main advantage of photodischarge sources is the selectivity provided by wavelength selection. However, these lamps require an external power supply and require periodic replacement due to their finite lifetimes.

Lasers can be used for photoionization of samples in the ultraviolet to infrared wavelength range. However, only a handful of studies have employed lasers with IMS [24].

15.3.1.3 Corona discharge sources

Basically, a CD source consists of a sharp needle or thin wire and a metal plate or discharge electrode. These are separated by between 2 and 8 mm and a voltage difference of 1–3 kV is applied. In the gap between needle and electrode, an electric discharge generates ions similar to those observed for ^{63}Ni radioisotope sources. Different source designs have been developed for IMS [25–28]. One disadvantage of this ionization source in the negative mode is interference from impurities of high electronegativity in the support gas, such as oxygen and ozone, in the general ionization scheme. To overcome this issue, increasing the distance between electrodes [29] or reversing the airflow past the corona needle [27] has been used. This type of source has the value of simplicity, high ion currents, no radioactivity, and an expanded range of applications, such as the direct analysis of liquid samples. However, corrosion of the needle causes instability, which together with the formation of corrosive vapors (NO_x and ozone) requires periodic source maintenance. Also, an external power supply is required.

15.3.1.4 Electrospray sources

Electrospray is an aerosol generated from the liquid samples formed between a needle tip and a grid or plate in a strong electric field. The liquid effluent passes through the needle tip and the charged droplets are evaporated producing gas-phase ions. If an analyte is dissolved in the effluent, it will receive some of this charge and

become a gas-phase ion [30]. Two mechanisms have been proposed for ion formation: the ion evaporation model [31] and the charged radius model [32]. A number of innovative ion sources based on ESI have been developed, including secondary electrospray ionization (SESI) [33], desorption electrospray ionization (DESI) [34], and nanoelectrospray ionization (nESI) [35]. An advantage of ESI sources is their capability to combine the operations of liquid sample introduction and sample ionization in a single step. Moreover, molecular ion information is not lost during ionization since it is a soft process. Memory effects, however, require long rinsing times between samples for IMS.

15.3.1.5 Other ionization sources

Other ionization sources have also been employed with IMS technology but are less common, such as MALDI [36], surface ionization sources [37], flames [38], plasma-based ion sources [39], or glow discharge ion source [40]. Among these, one of the most important in MALDI which is a laser-based source suitable for the analysis of solid samples. In this case, the sample is incorporated in a crystal matrix and vaporized and ionized without significant fragmentation by absorption of the laser energy by the crystal matrix. Some of the aforementioned sources are universal while others are limited with respect to sample types or by cost.

15.3.2 Drift tube and important parameters for ion separation

The separation of ions is carried out in a drift tube at ambient pressure in an electric field. Typically, an ion gate or shutter is positioned before the drift region. These are formed from wire grids and mediate the entrance of ions to the drift region. Ions pass when a brief pulse (between 10 and 1000 μs) is applied, called the grid pulse width. This parameter influences the peak shape and width in mobility spectra. A high grid

pulse width value yields an increase in sensitivity at the expense of resolution [41].

The drift tube consists of drift rings stacked or arranged alternately with insulating rings in a tubular geometry connected by a resistor chain. The construction of drift tubes is expensive and laborious due to need for accurate assembly of the many parts. An electric field is established using a voltage divider to separate ions between the ion shutter and the detector. Ions are separated based on their size and shape mediated by collisions with the particles of the drift gas, which flows countercurrent to the sample flow. Smaller ions move faster than larger ions through the drift tube to the detector.

The critical parameters that affect ion separations are temperature, purity, and composition of the supporting gas atmosphere, the electric field, and drift tube length. Firstly, drift temperature influences the mobility of ions according to Eq. (15.6). Also, the drift temperature affects the degree of ion clustering. At low temperature, neutral water molecules are available to attach to ions in the drift region, which influences sensitivity, resolving power, and reduces ion mobility. Conversely, increasing the drift tube temperature causes declustering of water-containing ions minimizing changes in ion mobility. Also, the mobility of ions is higher at higher drift tube temperatures. However, operating at a high temperature is unfavorable with respect to power consumption and may promote reactivity or fragmentation of ions [42].

Another important parameter is the purity and composition of the carrier and drift gases. The carrier gas in the drift tube is used to transport sample molecules from the inlet into the reaction region and provide the supporting atmosphere for ionization to occur. The drift gas is intended to maintain a clean gas environment in the drift region, free of unwanted impurities. If ambient air is used as a carrier or drift gas, it should be dried with a molecular sieve filter to remove moisture or reduce its content, as well as other volatile impurities to avoid

undesirable reactions in IMS devices. In fact, clean air is the most widely used gas, but the same precautions should be taken with other gases, such as nitrogen, helium, etc. The accuracy of ion mobility measurements should not be affected when nitrogen and synthetic clean air are used as drift gases [43,44]. It can be concluded that no significant differences in mobility values in nitrogen and air are likely for most compounds given that the polarizability constants and masses of nitrogen and oxygen and their corresponding abundances in air are similar. Other gases such as carbon dioxide provide unique ion mobility separation patterns resulting from its higher polarizability compared with nitrogen or air [45]. Also, increasing the field strength applied to the drift region improves resolving power [46]. Finally, resolution can be improved using an IMS analyzer with a longer drift tube. Cluster formation and fragmentation reactions are minimized in longer drift tubes [47].

15.3.3 Detector

Ions are typically detected at ambient pressure by a Faraday plate detector, which can be easily interfaced to an IMS. Ions that impinge on the detector are converted into current by neutralization on a collector electrode. The amplified ion current versus time results in an ion mobility spectrum [6]. A mass spectrometer positioned after an IMS device provides additional qualitative information unavailable with a Faraday plate detector [48].

15.4 Types of IMS instruments

Apart from the classical configuration of drift time IMS, other types of IMS instruments are: high-field asymmetric waveform IMS (FAIMS), differential mobility spectrometer (DMS), traveling-wave IMS (TWIMS), trapped IMS (TIMS), open-loop IMS (OLIMS), transversal modulation IMS (TMIMS), and overtone mobility

spectrometers (OMS) [49]. Only drift time IMS, FAIMS, and DMS have been coupled to GC.

15.4.1 Principle of operation of DMS/FAIMS

Both DMS and FAIMS are based on the same principle of operation and differ mainly in the cell geometry. FAIMS cells are curved, whereas DMS cells have a planar geometry, which can lead to different analytical properties [50]. DMS and FAIMS instruments are operated at high electric fields ($>7500 \text{ V cm}^{-1}$). For normal conditions a conventional drift time IMS with a 10 cm long drift region operated at 200 kV would correspond to a field strength of 20000 V cm^{-1} . Such high field strengths can be avoided using asymmetric waveforms and parallel plates or cylinders, for DMS and FAIMS, respectively [51].

In DMS and FAIMS, ion identification is based on the difference in the mobility coefficient of a compound at both high and low electric field strengths. Fig. 15.3 illustrates the operating principle of a planar DMS system, consisting of an ionization region, a tunable ion filter, and two parallel planar electrodes separated by a gap. The lower plate is maintained at ground potential while the upper plate has an asymmetric waveform, $V(t)$, applied to it. Ions formed in the ionization region are transported by a stream

of carrier gas perpendicular to the electric field through the ion filter region containing the two planar electrodes. The asymmetric radiofrequency (RF) electric field applied to the electrodes causes the ions to oscillate in a perpendicular direction to the carrier gas flow. Ions with different mobility differentials are displaced to unique positions in the y-direction for a given residence time. Both positive and negative ions can be filtered simultaneously and detected by the corresponding detector electrodes. Ion filtering is produced by the superposition of two electric fields, a high-frequency $\sim 1.2\text{-MHz}$ RF field with an associated variable voltage from -500 to 1500 V , and a compensation voltage. The DMS spectrum (ion current intensity vs. compensation voltage) for the ions in the gas sample is obtained by ramping or sweeping the compensation voltage, which is characteristic of the ion species. In the cylindrical version (FAIMS), the sample is ionized and travels with the carrier gas between two concentric tubes (the inner and outer electrodes). The asymmetric electric field is applied between these electrodes. Thus, DMS and FAIMS are a space-dispersive IMS since the ion mobility spectrum is represented as intensity versus the sweeping compensation voltage [49].

DMS and FAIMS offer a greatly simplified drift tube design over conventional mobility

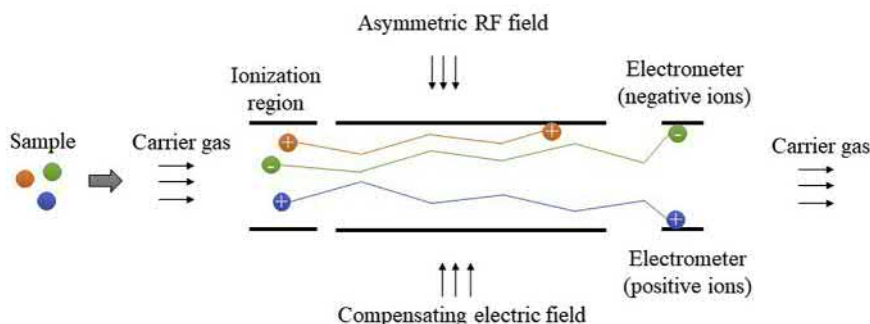


FIGURE 15.3 Schematic of a gas chromatograph coupled with a drift tube ion mobility spectrometer.

spectrometers. The drift tube does not require ion-shutters, voltage dividers, and aperture grids typical of conventional IMS instruments. Another advantage is that positive and negative ions are detected simultaneously [52]. The main disadvantage of DMS and FAIMS is lower selectivity compared with conventional IMS instruments. Therefore, GC-IMS is preferred when analyzing samples containing unknown components.

15.5 Limitations of IMS

One of the main limitations of IMS instruments is their low selectivity on account of their low resolving power. In addition, the identification of analytes represents a challenge due to the presence of several ions generated from the same neutral compound or additional intermediate products that depends on the sample concentration. The selectivity of IMS methods can be improved in different ways. Firstly, choosing a suitable ionization source can suppress the ionization of interferences and/or favor the ionization of target compounds. Also, the choice of polarity mode allows some interferences to be avoided. In general, compounds of high electronegativity, such as explosives, are more favorably detected as negative ions, whereas electropositive compounds, such as drugs and other amines, are better detected as positive ions. Furthermore, the selection of a proper electric field strength and drift tube length can improve selectivity. A higher electric field results in a higher resolving power [48] while a longer drift tube produces narrower peaks [47]. Also, preseparation by GC enhances both selectivity and the identification capability for real samples when using IMS as detector.

Moreover, charge and exchange reactions and competitive ionization, which happen in IMS analyzers, yield narrow dynamic quantification ranges. If more of one chemical enters in the ionization chamber simultaneously, the competition

for charge available or any kind of ionization reinforces the problem of the narrow dynamic response of IMS. This problem is also largely mitigated by GC preseparation prior to IMS measurement.

15.6 Fundamentals of GC-IMS

IMS belongs to the group of ionization detectors for GC [42]. When IMS is operated in the positive ion mode to monitor reactant ions, it affords a response similar to a flame ionization detector (FID), although typically with higher sensitivity. When operated in the negative ion mode, it behaves similar to an electron-capture detector (ECD). However, due to ion losses in the drift section, the sensitivity of the ECD is typically two or three orders of magnitude higher [6]. As an advantage, the IMS detector is capable of providing qualitative sample identification information based on the measurement of mobility while typical GC ionization-based detectors cannot [1].

The GC-IMS coupling can mitigate or eliminate the main limitations of the stand-alone IMS [6]. Using GC as a preseparation step can decrease the competitive ionization effects in the IMS device since analytes enter the ionization region sequentially. This results in an improvement in sensitivity. Also, a dual separation takes place, which allows the separation of some compounds in the preseparation step when the resolving power of the IMS is insufficient. Moreover, an easier identification of compounds is possible since an additional qualitative parameter, chromatographic retention, is obtained. Garrido-Delgado et al. [53] used both stand-alone IMS and GC-IMS to classify 49 Spanish olive oils in their three categories (extra virgin, virgin, and pomace olive oil). The classification rates for validation of GC-IMS data (100%) were higher than that for stand-alone IMS (86.1%), demonstrating the potential of GC-IMS for olive oil classification. Nevertheless, while

an IMS measurement can be conducted in milliseconds, longer times are required in methods employing a preseparation.

An IMS can be interfaced directly to the exit of a GC column as a selective detector. As both GC and IMS operate at near atmospheric pressure, their coupling need not involve elaborate pumping systems and the GC-IMS interface is simple and low-cost [6]. In addition, because ion mobility spectra are obtained at a frequency of 20–50 Hz, many IMS spectra can be obtained for each chromatographic peak. However, attention to some technical details is required to reduce memory effects. This mainly concerns the proper positioning of the column end in the IMS and the use of a makeup gas stream to transport the analytes from the GC column to the ionization source.

15.6.1 GC columns

As well as conventional open-tubular columns, short multicapillary columns (MCC) are often coupled to IMS to achieve a better match of flow rates for good chromatographic resolution [6,52]. Garrido-Delgado et al. [54] demonstrated an improvement in the classification of different olive oil categories using an open-tubular column (92%) compared with a short multicapillary column (87%) but the latter provided a faster analysis.

Isothermal separations predominated in the first commercial GC-IMS instruments because of the emphasis on portable instruments [52]. The FlavourSpec, the most widely used portable GC-IMS device, has a maximum temperature operating limit of 80°C due to the incompatibility of the interface and drift tube with higher temperatures. However, some of the advantages of a temperature-programmable GC oven can be simulated by gas flow programming [52]. Nowadays, IMS devices support higher operating temperatures and can be coupled to conventional

GC ovens, allowing the use of temperature-programmed separations [55,56].

15.6.2 IMS detection modes

For conventional IMS, only either positive or negative ions can be detected at one time while simultaneous detection of both positive and negative ions has advantages for some applications. Both positive and negative ions can be measured by two sequential measurements after the switching polarity of the high voltage power supply or simultaneously by using two drift tubes with different polarity [52]. An alternative solution, the dual IMS, enables the simultaneous detection of positive and negative ions from a single sample. In this setup, sample introduction and ionization occur at the middle of the drift tube with detection of positive and negative ions at opposite ends of the drift tube [57]. Other approaches for simultaneous detection include rapid switching of the electric field during a measurement [52].

15.7 Types of IMS coupled to GC

The choice of the IMS technology as detector for GC depends on the type of target analytes, the purpose of the intended application, and economic factors [1,58]. The majority of commercially IMS detectors for GC are based on the conventional drift tube ion mobility spectrometer. These devices are more selective and sensitive than DMS and FAIMS instruments. In fact, DMS and FAIMS act as signal filters controlled by the selected compensation voltage with loss of sample information because the number of detected compounds is limited. On the other hand, the IMS design is the most complicated, which influences the size of the detector, its adoption for field use, and price. Analyzers based on the DMS and FAIMS principle are simpler and easily miniaturized.

Another important aspect is the selection of the ionization source, which depends on the sample type and target compounds. CD and ^{63}Ni ionization sources are the preferred choice for halogenated compounds while photoionization sources are better for aromatic compounds. Also, ^3H sources are recommended for compounds with a high proton affinity in the positive ion mode [6].

15.7.1 GC drift tube IMS coupling

Fig. 15.4 shows the principal components and operation of a GC coupled to an IMS detector. The sample is vaporized in the GC injector and separated into individual components by the column. Individual compounds are then transported into the ionization region of the IMS where they are ionized. The ionization process can lead to protonated monomer and sometimes dimer or even trimer ions. Ions formed in the ionization region are injected into the drift region of the IMS separated in time eliminating the competition problems with IMS.

15.7.2 GC-DMS or GC-FAIMS coupling

Fast GC in which relatively simple mixtures are separated in less than a few seconds provides a rapid separation-and-introduction method for

DMS [59]. One advantage is that DMS and FAIMS allow both positive and negative ions to be monitored simultaneously [60]. Fig. 15.5 shows a schematic of a typical GC-DMS instrument. After separation, the DMS gas flow is mixed with the GC carrier gas to produce the total flow through the DMS. At the entrance to the DMS, the sample is ionized by either a radioisotope or photoionization source. The ability to deconvolute analytes that overlap in GC provides GC-DMS with high specificity and reproducibly [6].

DMS and FAIMS are both extensively used as GC detectors. Sampling is usually carried out using solid-phase microextraction (SPME). For example, Eiceman et al. [61] described the analysis of VOCs in smoke by SPME-GC-FAIMS, and Telgheder et al. [62] described VOCs from aqueous samples by SPME-GC-DMS. SPME-GC-FAIMS was used to distinguish between treated and untreated wood by detecting volatile organic preservatives [63] and SPME-GC-FAIMS to determine formaldehyde released from wood-based panels [64].

15.8 Data obtained from GC-IMS instruments

The data obtained directly by a stand-alone drift time IMS is current or intensity (mV) versus drift time. Fig. 15.6 shows a conventional

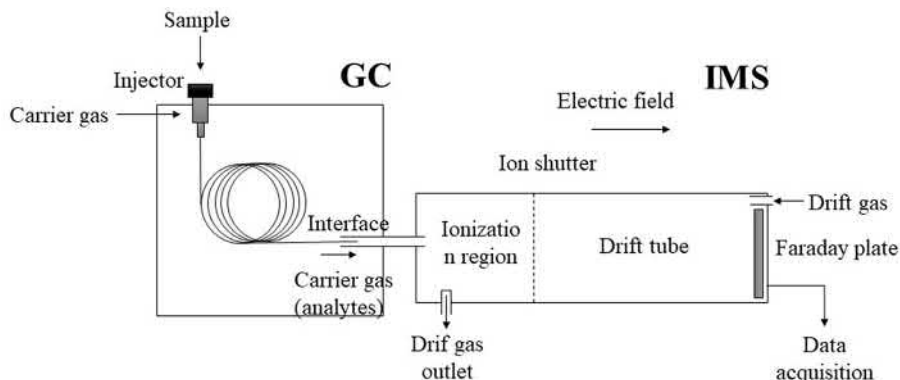


FIGURE 15.4 Schematic of the differential mobility spectrometer.

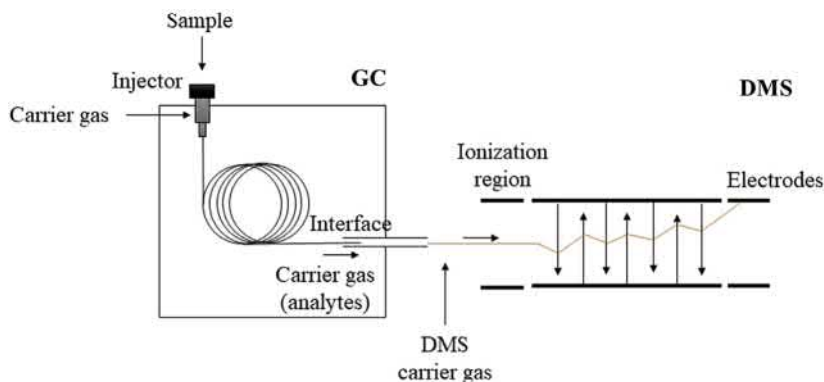


FIGURE 15.5 Experimental setup for GC-DMS system.

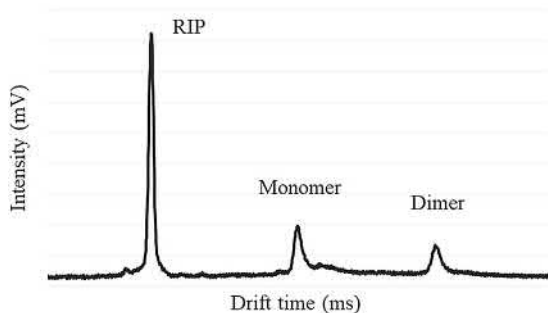


FIGURE 15.6 Example of a typical IMS spectrum showing the reactant ion peak (RIP), one monomer, and one dimer.

IMS spectrum showing the RIP, a monomer, and a dimer. However, GC-IMS data include an additional separation dimension providing both retention time and drift time of the analytes, which increases the confidence in their identification. The data represent a tridimensional map, in which each point is characterized by the retention time (s), the drift time (ms), and the signal intensity (mV) (Fig. 15.7A). The data can be represented by a topographic plot, in which the drift time and retention time are set along the x-axis and y-axis, respectively. Signal intensity is indicated by color (Fig. 15.7B). Because GC separation times are on a minute to second timescale and IMS on a millisecond timescale, multiple IMS spectra can

be obtained for each chromatographic peak [42]. Thus, a single IMS spectrum can be obtained at each retention time in the topographic plot. Also note that one compound can result in more than one signal (monomer and dimer or even trimer) depending on their concentration [65]. As an example, Fig. 15.8 shows the topographic plot of 2-heptanone (Fig. 15.8A) and two single IMS spectra (Fig. 15.8B and C) at different retention times. Notice that each peak from the 2-heptanone in the IMS spectrum corresponding to $t_R = 372$ s is represented by a spot on the topographic plot. However, when compounds are not detected on the topographic plot (e.g., $t_R = 359$ s), only the RIP signal appears on the IMS spectrum (Fig. 15.8C). Moreover, the RIP intensity changes over time after the introduction of the sample into the ionization region [9]. The intensity of the RIP signal decreases as the intensity of the analyte peak increases, the RIP signal recovering its original height in the absence of analyte.

15.9 Treatment of IMS data

At its beginnings, progress in IMS was hindered by the variation in observed signals between instruments and operators. Recent advances in multidimensional coupling of IMS to GC has created additional challenges for

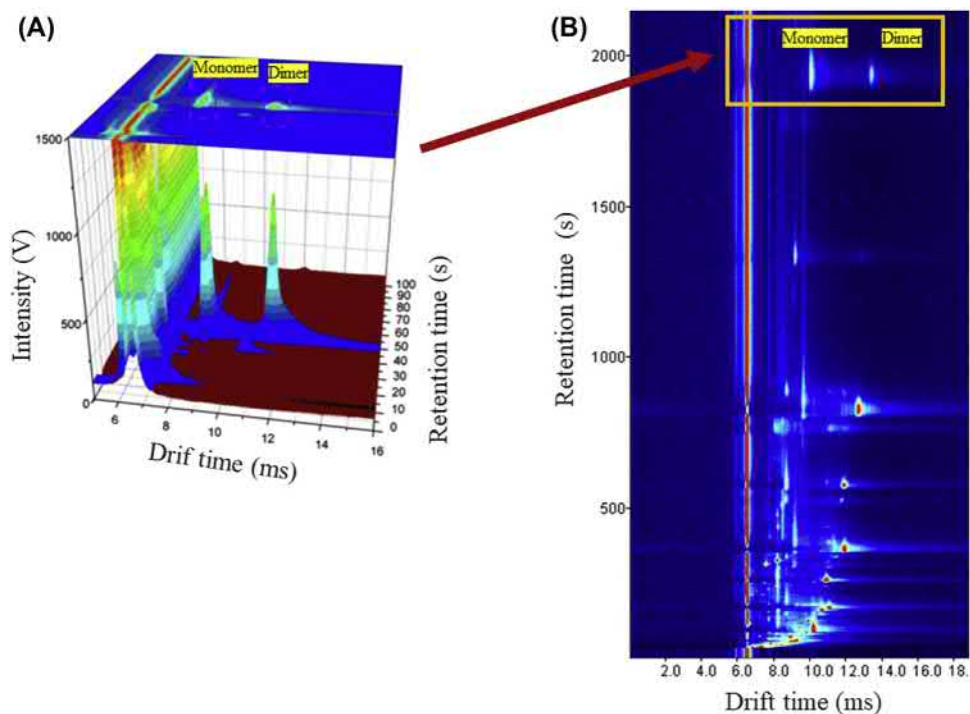


FIGURE 15.7 Example of a typical topographic plot (A) and 3D plot of the detail area marked on the topographic plot (B).

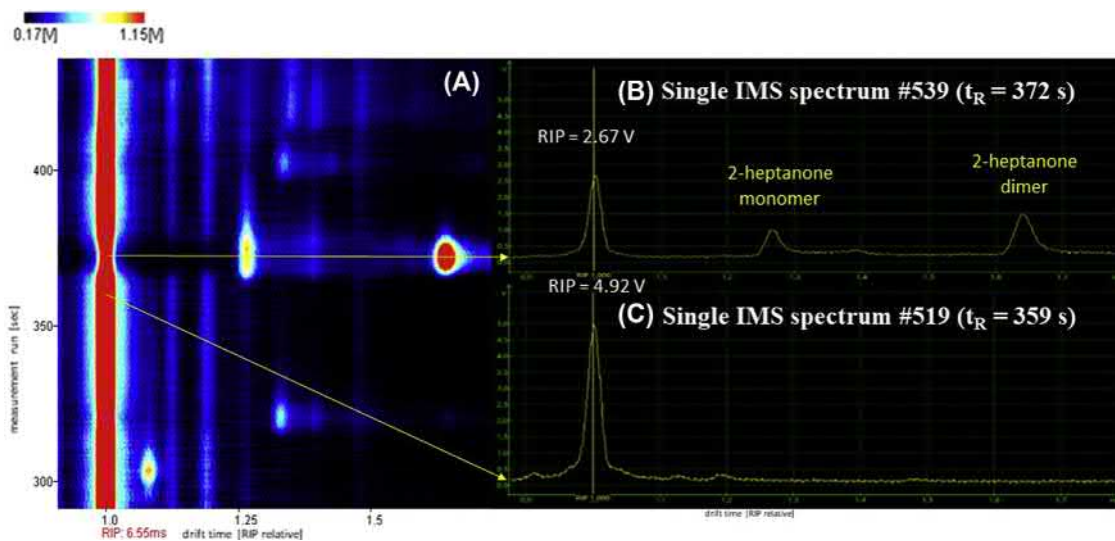


FIGURE 15.8 Topographic plot of 2-heptanone (0.75 mg L^{-1}) (A), single IMS spectrum #539 ($t_R = 372$ s) (B), and single IMS spectrum #519 ($t_R = 359$ s) (C).

data processing, yielding high-dimensional data sets. This has triggered the development of chemometric techniques to analyze the precious information content of ion mobility spectra. Data treatment approaches for GC-IMS are designed according to the selected strategy, being slightly different between targeted and untargeted analysis.

Normally, data analysis is subdivided into two steps: data preprocessing and pattern recognition or statistical analysis. The first step is usually time-consuming and crucial for subsequent data treatment. A general workflow for IMS data analysis is shown in Fig. 15.9. Note that peak picking applies only to targeted analysis and RIP detailing when radioisotope sources are used [66].

15.9.1 Data pretreatment

Data pretreatment is the first step of the workflow that attempts to prepare raw data for statistical analysis. IMS data pretreatment

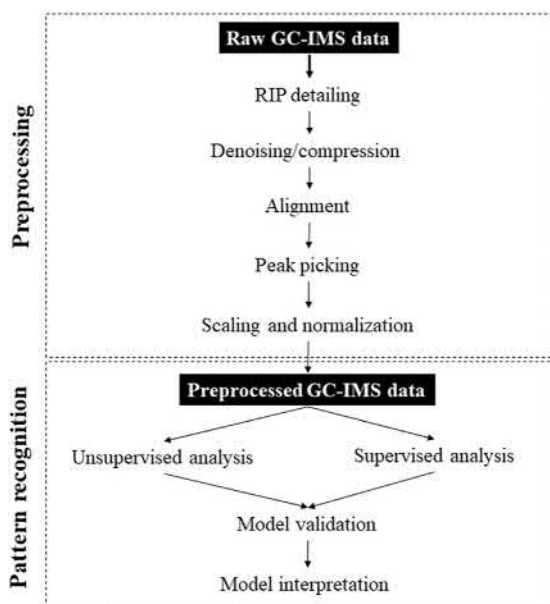


FIGURE 15.9 General workflow for IMS data analysis.

encompasses several preprocessing steps crucial for data quality and interpretation of the results.

For the two dimensional GC-IMS data, analyte peaks are composed of several points grouped in circle or oval-shaped spots depending on the instrument setup. The preprocessing of GC-IMS data can be divided into separate steps: peak picking [67,68], RIP detailing [69,70], denoising and compression [71,72], baseline correction [70,73,74], alignment [72,75–78], and data scaling and normalization [70,79–81].

15.9.2 Statistical analysis

When the aim of the measurements is qualitative analysis, statistical procedures are usually employed for sample classification, discrimination, and marker detection. Conversely, calibrations are commonly used when the purpose is a quantitative analysis. Also, univariate or multivariate statistical techniques can be employed. Univariate techniques focus on one variable at a time, e.g., analysis of variance (ANOVA), while multivariate techniques analyze all variables simultaneously.

Typically, pattern recognition procedures start with an exploratory analysis using unsupervised chemometric techniques. Later, supervised chemometric techniques, which employ sample information such as their classes, are applied. Finally, the results are validated to confirm a correct interpretation [66].

15.9.2.1 Exploratory analysis by unsupervised analysis

Unsupervised learning refers to those techniques for data analysis where a measured or defined outcome (response) is not of primary concern [82]. Unsupervised learning uses procedures that attempt to find the natural patterns in a data set to facilitate an understanding of the relationship between the samples and to highlight the variables that are responsible for these relationships. The most widely used technique

in IMS is principal component analysis (PCA). PCA is an orthogonal transformation of multivariate data that extracts and displays its systematic variations [82]. PCA attempts to describe the maximal variance of the data and is a useful tool for displaying purposes as it provides a low-dimension projection of the data (i.e., a window into the original K-dimensional space) by transformation into a new coordinate system [83].

15.9.2.2 Classification by supervised multivariate analysis

Supervised learning uses labeled data to classify samples or objects according to an observed response that generally includes several variables [83]. This classification aims at producing general hypotheses based on samples assigned to existing classes. For IMS data partial least squares discriminant analysis (PLS-DA), sparse-PLS-DA, linear discriminant analysis (LDA), recursive supporting vector machine (r-SVM), random forests, genetic algorithms (GA), k-nearest neighbor (KNN), principal component regression (PCR), partial least squares regression (PLSR), and n-way-PLSR are the most popular techniques. PLS-DA is commonly employed in metabolomics studies and in food screening. Regression techniques (PCR, PLSR, and n-way-PLSR) are routinely used in food quality and safety, environmental and monitoring analyses [66].

15.9.2.2.1 Validation and interpretation

The validation of the data treatment procedure can be carried out by internal and/or external approaches. GC-IMS data set should be split into a training set (used to train the classification or calibration model), a validation set (employed to optimize the model parameters (internal validation)), and an independent test set employed to assess the predictive power of the model (external validation). Currently, the most common validation methods are leave-one-out cross-validation, double cross-validation, bootstrapping, and permutation tests

[66]. Validation results can be expressed as a number of misclassifications, accuracy, sensitivity, specificity, area under ROC curve (AUROC), or root mean square error of prediction (RMSEP) [84,85].

15.10 Advantages and disadvantages of GC-IMS analysis

GC-IMS is a powerful analytical technique for the determination of compounds in complex samples. There are many advantages to use of IMS as a selective GC detector as well as some drawbacks.

15.10.1 Advantages of GC-IMS

- GC-IMS instruments provide an added dimension of separation that improves selectivity and resolution. Moreover, since the compounds are previously separated by GC, they arrive individually at the IMS ion source and cross-sensitivity/charge competition effects are eliminated. DMS provides further information in the form of the compensation voltage.
- Multiple IMS spectra are obtained for each chromatographic peak.
- Incorporating GC as a sample introduction system for IMS can help reduce humidity effects, which can be problematic for IMS analysis at ppb levels.
- IMS is an extremely sensitive detector for GC (ppb or ppt levels) without previous sample preconcentration steps.
- IMS is a versatile detector for GC, which can operate in the positive or negative ion mode, or simultaneously for positive and negative ion detection in the dual IMS configuration. Moreover, DMS and FAIMS can operate simultaneously in both modes without change to their configuration.

- Reduced mobility measurements are absolute and related directly to the structure of a compound.
- The coupling of portable GC instruments with IMS provides analytical methods for field analyses.
- Ion mobility spectrometers are less expensive than mass spectrometers with comparable analytical performance.

15.10.2 Disadvantages of GC-IMS

- IMS as detector has a short linear range, about 1–2 orders of magnitude.
- There is no general compound database available. A suitable database needs to be developed for each instrument due to slight deviations in the experimental setup.
- GC preseparation (minutes) is longer than that for a stand-alone IMS (seconds)

15.11 Applications

The stand-alone IMS instrumentation has historically been applied for chemical measurements of warfare agents in military preparedness [1,86], explosives or illicit drugs in commercial aviation security [87], and in human spaceflight [88]. In recent years, GC-IMS has expanded the application areas of IMS technology through the analysis of complex samples, such as pharmaceutical, food, environmental, biological, and medical samples. This coupling enhances the identification of target compounds in complex mixtures impossible using stand-alone IMS instruments. The total number of publications related to GC-IMS in the last 20 years are summarized in Fig. 15.10A. From 1991 to 2014, the total number of publications related to GC-IMS was 52. However, in the last 5 years alone (from 2015 until 2019), this number rose by 65. Fig. 15.10B illustrates the increase in the number of citations in the last 20 years. A summary of the publications related to GC-IMS in different application fields up to 2020 is included

in Fig. 15.11. Currently, food applications are the most important, especially applications related to food authentication.

15.11.1 Food analysis

Most applications describe the determination of known compounds through targeted or semi-targeted analysis. However, an increase in non-targeted approaches is expected, such as in food fingerprinting [89].

Olive oil labeling in its three categories (extra virgin, virgin, and lampante) represents a large number of publications related to food authentication [90]. Classification rates between 87% and 100% were obtained using PCA, LDA, and kNN [53,54,91]. Moreover, a database of volatile compounds in olive oils was constructed containing retention and ion mobility information. A total of 26 volatile compounds were identified by GC-IMS (including aldehydes, alcohols, ketones, and esters), some of which showed marked differences in content between the three olive oil categories [54]. GC-IMS was used to establish the geographical origins of olive oil [55,56]. GC-IMS and chemometric analysis were also used to detect the adulteration of other vegetable oils such as canola oil [92] and palm oil [93]. Chen et al. [94] reported 100% classification accuracy for characterizing three categories of vegetable oil by headspace (HS)-GC-IMS. Further work used GC-IMS to differentiate refined grades of rapeseed oils [95].

A rapidly evolving application for GC-IMS is the detection of agricultural food adulteration by determining the flavor fingerprints of a specific food. Arroyo-Manzanares et al. [65] used this approach to distinguish feed-fed and acorn-fed Iberian hams with a 100% classification accuracy. A nondestructive sampling method using GC-IMS was proposed to detect labeling fraud in Iberian cured ham [96]. Aheto et al. [97] observed differences between fresh, cured, and commercial dry-cured pork belly by using GC-IMS without chemometric processing.

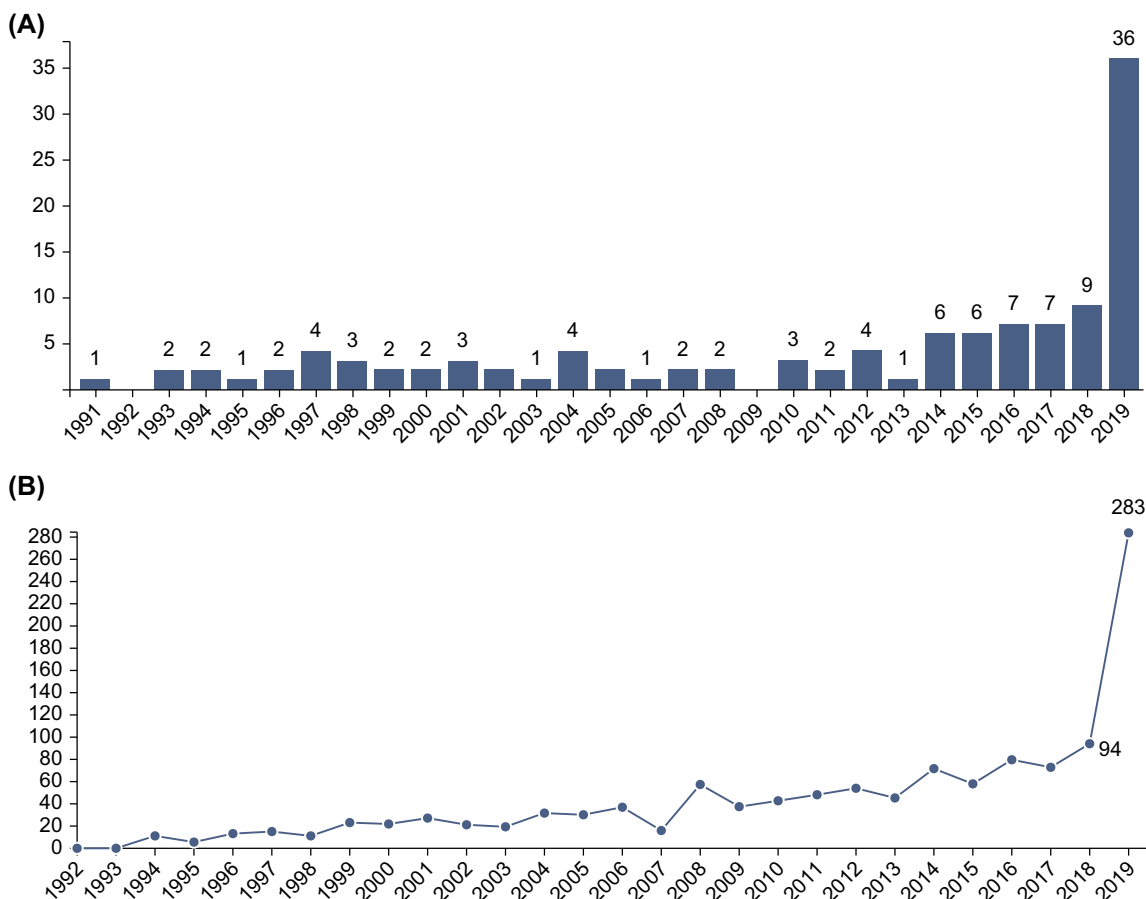


FIGURE 15.10 Total of publications (A) and citations (B) related to GC-IMS from 1991 to 2019 in the database "ISI Web of Knowledge."

The authentication of the botanical origins of honey was performed using GC-IMS and chemometric techniques [98]. HS-GC-IMS was a cost-efficient, faster, and more robust method to assign the botanical origin of honey than an established NMR-based screening method. The potential of GC-IMS to detect mislabeling of honey was further demonstrated in Refs. [99,100].

Snyder et al. [101] introduced a handheld GC-IMS device for detecting certain volatile amines related to the deterioration of fish products. Recent research demonstrated the possibility of determining the freshness of eggs using GC-

IMS [102]. Additionally, some volatile chemical markers (butyl acetate, 1-heptanol, dimethyl disulfide, dimethyl trisulfide, and 1-butanol) associated with the thermal degradation of eggs were identified using SPME-GC-IMS. GC-IMS was used to monitor volatile metabolites during food processing, such as beer fermentation [103] and cheese ripening [104]. HS-GC-IMS allowed samples of fresh and dry mushrooms to be differentiated [105]. A total of 25 target compounds were used as markers to investigate different parts (lower stipe, upper stipe, and pileus) of fresh and dried samples of *Tricholoma*

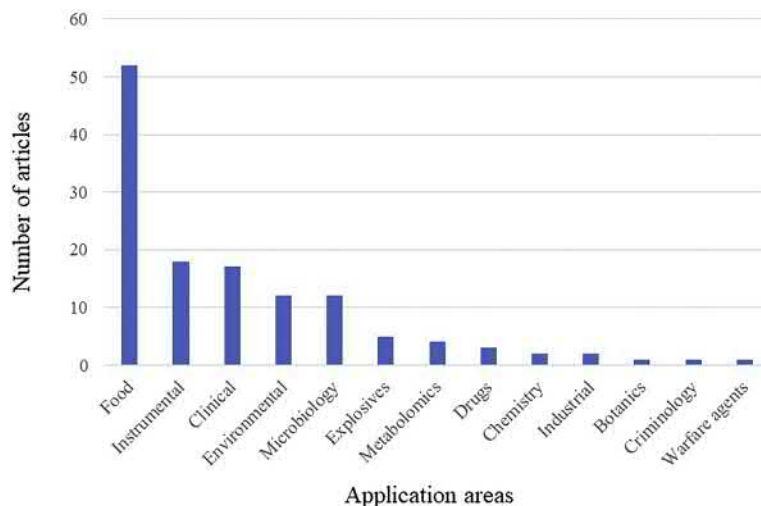


FIGURE 15.11 Summary of the number of articles concerning GC-IMS categorized by field of application in the database “ISI Web of Knowledge” (from 1991 until June 2020).

matsutake singer [106]. In addition, GC-IMS was employed in several applications for food safety to screen a wide range of residues and contaminants. The analysis of pesticides in vegetables (i.e., apples, tomatoes, cucumbers, etc.), oils, animal feed, juices, and water is a typical example [89].

15.11.2 Clinical applications and metabolomics

Tiele et al. [107] used a commercial breath analyzer for volatile organic compounds, a GC-IMS, to distinguish between mild cognitive impairment, Alzheimer's disease, and controls. This methodology was shown to be a fast and real-time diagnostic tool for detecting Alzheimer's disease. Moreover, six biomarkers were tentatively identified (acetone, 2-propanol, 2-butanone, hexanal, heptanal, and 1-butanol), which play a crucial role in distinguishing between diagnostic groups. A similar approach was used for the diagnosis of inflammatory bowel disease [108] and chronic obstructive pulmonary disorder [109]. GC-IMS was used to

supplement information obtained by GC-MS for faster diagnosis of Alzheimer's disease thorough the analysis of VOCs in urine and feces of mice [110]. The detection of infected wounds was investigated by the analysis of odors emanating from infected wounds and colonized wound dressings after surgery [111]. Although only 19 samples were tested, the results were promising with a specificity of 88%. Detection of colorectal cancer and adenomas using urinary VOC markers within a screening population was demonstrated using FAIMS and GC-IMS [112].

Finally, GC-DMS has been widely used in a clinical setting for the identification of various bacterial species and strains via their growth-associated metabolites [113] or pyrolysis-associated breakdown products [70,114,115] and viruses [116].

15.11.3 Environmental applications

Environmental analysis using GC-IMS is focused on the determination of contaminants in water and aerosols [117,118]. Some examples for aqueous environmental samples include the

determination of volatile halogenated compounds by HS–single-drop microextraction prior to GC-IMS [119] and HS-SPME and MCC-UV-IMS [120].

15.11.4 Explosives

IMS instruments are widely used for the detection of explosives due to the need for sensitive, noninvasive, and rapid technology to identify acts of terrorism at control points, international borders, and airports [6]. However, stand-alone IMS devices have limitations on account of their low resolution. Stand-alone devices are prone to inaccurate detection and false-positive responses when samples contain chemical interferences. Moreover, sample size must be carefully controlled to prevent saturation or a nonlinear response [121]. GC-IMS can overcome these limitations in explosives detection [122]. GC-IMS showed a significant reduction in the number of false-positive results. However, the number of false-negative results was the same for both GC-IMS and IMS. The number of false-negative responses in GC-IMS could be reduced by using a sample preconcentrator with a higher affinity for the target compounds. In conclusion, GC-IMS could be used only as an intermediate screening tool for validating IMS positive responses for explosive compounds among airport passengers and baggage, cargo shipping containers, buildings, or improvised explosive devices. A tandem ion mobility spectrometer built from two differential mobility spectrometers coupled to a thermal desorber provided a more robust detector [123]. This GC-DMS-F-DMS configuration provided orthogonal separations, within a total separation time of 3 min, and parts per quadrillion detection limits.

References

- [1] J. Puton, J. Namies'nik, Ion mobility spectrometry: current status and application for chemical warfare agents detection, *Trends Anal. Chem.* 85 (2016) 10–20.
- [2] F.W. Karasek, R.A. Keller, Gas chromatograph/plasma chromatograph interface and its performance in the detection of musk ambrette, *J. Chromatogr. Sci.* 10 (1972) 626–628.
- [3] M.A. Baim, H.H. Hill, Tunable selective detection for capillary gas chromatography by ion mobility monitoring, *Anal. Chem.* 54 (1982) 38–43.
- [4] M.A. Baim, R.L. Eatherton, H.H. Hill, Ion mobility detector for gas chromatography with a direct photoionization source, *Anal. Chem.* 55 (1983) 1761–1766.
- [5] A.P. Snyder, W.M. Maswadeh, J.A. Parsons, A. Tripathi, H.L.C. Meuzelaar, J.P. Dworzanski, M.-G. Kim, Field detection of bacillus spore aerosols with stand-alone pyrolysis gas chromatography/ion mobility spectrometry, *Field Anal. Chem. Technol.* 3 (4–5) (1999) 315–326.
- [6] G.A. Eiceman, Z. Karpas, H.H. Hill Jr., *Ion Mobility Spectrometry*, third ed., CRC Press, United States, 2013.
- [7] M. Valcárcel, S. Cárdenas, Vanguard-rearguard analytical strategies, *Trac. Trends Anal. Chem.* 24 (2005) 67–74.
- [8] A.J. Bell, K. Giles, S. Moody, P. Watts, Studies on gas-phase positive ion-molecule reactions of relevance to ion mobility spectrometry the reactions of 2-methyl-2-propanol (t-butyl alcohol) with protonated water clusters in an ion mobility system, *Int. J. Mass Spectrom. Ion Process.* 173 (1998) 65–70.
- [9] M. Tozihi, H. Bahrami, B. Farajmand, M. Tabrizchi, Ion mobility spectrometry and theoretical study for investigation of thermal decomposition, chemical ionization, and dimer formation of proline, *Int. J. Mass Spectrom.* 448 (2020) 116272.
- [10] H.H. Hill, W.F. Siems, R.H. Louis, D.G. Mc Minn, Ion mobility spectrometry, *Anal. Chem.* 62 (1990) 1201–1209.
- [11] R. Fernandez-Maestre, C.S. Harden, R.G. Ewing, C.L. Crawford, H.H. Hill Jr., Chemical standards in ion mobility spectrometry, *Analyst* 135 (2010) 1433–1442.
- [12] M. Maurer, G.C. Donohoe, S.J. Valentine, Advances in ion mobility-mass spectrometry instrumentation and techniques for characterizing structural heterogeneity, *Analyst* 20 (2015) 6782–6798.

- [13] Z. Karpas, Ion mobility spectrometry of aliphatic and aromatic amines, *Anal. Chem.* 61 (1989) 684–689.
- [14] G.A. Eiceman, E.G. Nazarov, J.A. Stone, Chemical standards in ion mobility spectrometry, *Anal. Chim. Acta* 493 (2003) 185–194.
- [15] B.C. Hauck, W.F. Siems, C.S. Harden, V.M. McHugh, H.H. Hill Jr., Determination of E/N influence on K_0 values within the low field region of ion mobility spectrometry, *J. Phys. Chem. A* 121 (2017) 2274–2281.
- [16] E.A. Mason, E.W. McDaniel, *Transport Properties of Ions in Gases*, John Wiley & Sons Inc., New York, 1988.
- [17] J.C. May, C.B. Morris, J.A. McLean, Ion mobility collision cross section compendium, *Anal. Chem.* 89 (2017) 1032–1044.
- [18] E.W. McDaniel, *Collision Phenomena in Ionized Gases*, Wiley, New York, 1964.
- [19] W.F. Siems, L.A. Viehland, H.H. Hill, Improved momentum-transfer theory for ion mobility. 1. Derivation of the fundamental equation, *Anal. Chem.* 84 (2012) 9782–9791.
- [20] J.A. Picache, B.S. Rose, A. Balinski, K.L. Leaprot, S.D. Sherrod, J.C. May, J.A. McLean, Collision cross section compendium to annotate and predict multi-omic compound identities, *Chem. Sci.* 10 (2019) 983–993.
- [21] C.S. Creaser, J.R. Griffiths, C.J. Bramwell, S. Noreen, C.A. Hill, C.L.P. Thomas, Ion mobility spectrometry: a review. Part 1. Structural analysis by mobility measurement, *Analyst* 129 (2004) 984–994.
- [22] N. Jurado-Campos, R. Garrido-Delgado, B. Martínez-Haya, G.A. Eiceman, L. Arce, Stability of proton-bound clusters of alkyl alcohols, aldehydes and ketones in ion mobility spectrometry, *Talanta* 185 (2018) 299–308.
- [23] J.N. Driscoll, Evaluation of a new photoionization detector for organic compounds, *J. Chromatogr. A* 134 (1977) 49–55.
- [24] D.M. Lubman, M.N. Kronick, Plasma chromatography with laser-produced ions, *Anal. Chem.* 54 (1982) 1546–1551.
- [25] M. Tabrizchi, T. Khayamian, N. Taj, Design and optimization of a corona discharge ionization source for ion mobility spectrometry, *Rev. Sci. Instrum.* 7 (2000) 2321–2328.
- [26] M. Tabrizchi, A. Abedi, A novel electron source for negative-ion mobility spectrometry, *Int. J. Mass Spectrom.* 218 (2002) 75–85.
- [27] A.J. Bell, S.K. Ross, Reverse flow continuous corona discharge ionization, *Int. J. Ion Mobil. Spectrom* 5 (2002) 95–99.
- [28] C.A. Hill, C.L.P. Thomas, A pulsed corona discharge switchable high resolution ion mobility spectrometer-mass spectrometer, *Analyst* 128 (2003) 55–60.
- [29] G.A. Eiceman, J.H. Kremer, A.P. Snyder, J.K. Tofferi, Quantitative assessment of a corona discharge ion source in atmospheric pressure ionization-mass spectrometry for ambient air monitoring, *Int. J. Environ. Anal. Chem.* 33 (1988) 161–183.
- [30] C. Shumate, Electrospray ion mobility spectrometry, *trac-trend*, *Anal. Chem.* 13 (1994) 104–109.
- [31] P. Kebarle, L. Tang, From ions in solution to ions in the gas phase, *Anal. Chem.* 65 (1993) 972–986A.
- [32] J.V. Iribarne, B.A. Thomson, On the evaporation of small ions from charged droplets, *J. Chem. Phys.* 64 (1976) 2287–2294.
- [33] Y.H. Chen, H.H. Hill Jr., D.P. Wittmer, Analytical merit of electrospray ion mobility spectrometry as a chromatographic detector, *J. Microcol.* (September 6, 1994) 515–524.
- [34] C. Wu, W.F. Siems, H.H. Hill Jr., Secondary electrospray ionization ion mobility spectrometry - mass spectrometry of illicit drugs, *Anal. Chem.* 72 (2000) 396–403.
- [35] Z. Takats, J.M. Wiseman, B. Gologan, R.G. Cooks, Mass spectrometry sampling under ambient conditions with desorption electrospray ionization, *Science* 306 (2004) 471–473.
- [36] J.M. Koomen, B.T. Ruotolo, K.J. Gillig, J.A. Mclean, D.H. Russell, M.J. Kang, K.R. Dunbar, K. Fuhrer, M. Gonin, J.A. Schultz, Oligonucleotide analysis with MALDI-ion-mobility-TOFMS, *Anal. Bioanal. Chem.* 373 (2002) 612–617.
- [37] C. Wu, H.H. Hill, U.K. Rasulev, E.G. Nazarov, Surface-ionization ion mobility spectrometry, *Anal. Chem.* 71 (1999) 273–278.
- [38] H.C. Bolton, J. Grant, I.G. McWilliam, A.J.C. Nicholson, D.L. Swingler, Ionization in flames. II. Mass-spectrometric and mobility analyses for the flame ionization detector, *Proc. R. Soc. London A Math. Phys. Eng. Sci.* 360 (1978) 265–277.
- [39] M.J. Waltman, P. Dwivedi, H.H. Hill, W.C. Blanchard, R.G. Ewing, Characterization of a distributed plasma ionization source (DPIS) for ion mobility spectrometry and mass spectrometry, *Talanta* 77 (2008) 249–255.
- [40] Q. Zhao, M.W. Soyk, G.M. Schieffer, K. Fuhrer, M.M. Gonin, R.S. Houk, E.R. Badman, An ion trap-ion mobility-time of flight mass spectrometer with three ion sources for ion/ion reactions, *J. Am. Soc. Mass Spectrom.* 20 (2009) 1549–1561.

- [41] P.V. Johnson, L.W. Beegle, H.I. Kim, G.A. Eiceman, I. Kanik, Ion mobility spectrometry in espace exploration, *Int. J. Mass Spectrom.* 262 (2007) 1–15.
- [42] A.B. Kanu, H.H. Hill Jr., Ion mobility spectrometry detection for gas chromatography, *J. Chromatogr. A* 1177 (2008) 12–27.
- [43] F. Gunzer, Comparison of experimental and calculated ion mobilities of small molecules in air, *J. Anal. Methods Chem.* 2016 (2016) 6246415.
- [44] A.T. Kirk, C.R. Raddatz, S. Zimmermann, Separation of isotopologues in ultra-high-resolution ion mobility spectrometry, *Anal. Chem.* 89 (2017) 1509–1515.
- [45] K.L. Davidson, M.F. Bush, Effects of drift gas selection on the ambient-temperature, ion mobility mass spectrometry analysis of amino acids, *Anal. Chem.* 89 (2017) 2017–2023.
- [46] C. Wu, W.F. Siems, G.R. Asbury, H.H. Hill Jr., Electrospray ionization high-resolution ion mobility spectrometry-mass spectrometry, *Anal. Chem.* 70 (1998) 4929–4938.
- [47] S. Sielemann, J.I. Baumbach, H. Schmidt, P. Pilzecker, Quantitative analysis of benzene, toluene, and m-xylene with the use of a UV-ion mobility spectrometer, *Field Anal. Chem. Technol.* 4 (2000) 157–169.
- [48] D.C. Collins, M.L. Lee, Developments in ion mobility spectrometry-mass spectrometry, *Anal. Bioanal. Chem.* 372 (2002) 66–73.
- [49] R. Cumeras, E. Figueras, C.E. Davis, J.I. Baumbach, I. Gràcia, Review on ion mobility spectrometry. Part 1: current instrumentation, *Analyst* 140 (2014) 1376–1390.
- [50] B.B. Schneider, E.G. Nazarov, F. Londry, P. Vouros, T.R. Covey, Differential mobility spectrometry/mass spectrometry history, theory, design optimization, simulations, and applications, *Mass Spectrom. Rev.* 35 (2016) 687–737.
- [51] I.A. Buryakov, E.V. Krylov, E.G. Nazarov, U.K. Rasulev, A new method of separation of multi-atomic ions by mobility at atmospheric pressure using a high-frequency amplitude-asymmetric strong electric field, *Int. J. Mass Spectrom. Ion Proc.* 128 (1993) 143–148.
- [52] W. Vautz, J. Franzke, S. Zampolli, I. Elmi, S. Liedtke, On the potential of ion mobility spectrometry coupled to GC pre-separation – a tutorial, *Anal. Chim. Acta* 1024 (2018) 52–64.
- [53] R. Garrido-Delgado, L. Arce, M. Valcárcel, Multi-capillary column-ion mobility spectrometry: a potential screening system to differentiate virgin olive oils, *Anal. Bioanal. Chem.* 402 (2012) 489–498.
- [54] R. Garrido-Delgado, M.M. Dobao-Prieto, L. Arce, M. Valcárcel, Determination of volatile compounds by GC-IMS to assign the quality of virgin olive oil, *Food Chem.* 187 (2015) 572–579.
- [55] R. Garrido-Delgado, L. Arce, M. Valcárcel, Multi-capillary column-ion mobility spectrometry: a potential screening system to differentiate virgin olive oils, *Anal. Bioanal. Chem.* 402 (2012) 489–498.
- [56] N. Gerhardt, S. Schwolow, S. Rohn, P.R. Pérez-Cacho, H. Galán-Soldevilla, L. Arce, P. Weller, Quality assessment of olive oils based on temperature-ramped HS-GC-IMS and sensory evaluation: comparison of different processing approaches by LDA, kNN, and SVM, *Food Chem.* 278 (2019) 720–728.
- [57] Patent DE102009008266 (A1) - Binary Ion Mobility Spectrometer for Detecting e.g. Positive Ion in Gaseous Chemical Substance, has Ionization Device Comprising Two Different Ionization Sources that are Independently Activatable, n.d.
- [58] G.A. Eiceman, J. Gardea-Torresday, E. Overton, K. Carney, F. Dorman, Gas chromatography, *Anal. Chem.* 76 (2004) 3387–3394.
- [59] A. Cagan, H. Schmidt, J.E. Rodriguez, G.A. Eiceman, Fast gas chromatography differential mobility spectrometry of explosives from TATP to tetryl without gas atmosphere modifiers, *Int. J. Ion Mobil. Spectrom* 13 (2010) 157–165.
- [60] M. Hernández-Mesa, D. Ropartz, A.M. García-Campaña, H. Rogniaux, G. Dervilly-Pinel, B. Le Bizec, Ion mobility spectrometry in food analysis: principles, current applications and future trends, *Molecules* 24 (2019) 2706.
- [61] G.A. Eiceman, A. Tarassov, P.A. Funk, S.E. Hughes, E.G. Nazarov, R.A. Miller, Discrimination of combustion fuel sources using gas chromatography-planar field asymmetric-waveform ion mobility spectrometry, *J. Separ. Sci.* 26 (2003) 585–593.
- [62] U. Telgheder, M. Malinowski, M. Jochmann, Determination of volatile organic compounds by solid-phase microextraction – gas chromatography-differential mobility spectrometry, *Int. J. Ion Mobil. Spectrom* 12 (2009) 123–130.
- [63] D. Mauruschat, A. Schumann, P. Meinschmidt, J. Gunschera, T. Salthammer, Application of gas chromatography – field asymmetric ionmobility spectrometry (GC-FAIMS) for the detection of organic preservatives in wood, *Int. J. Ion Mobil. Spectrom* 17 (2014) 1–9.
- [64] S. Himmel, C. Mai, A. Schumann, J. Hasener, V. Steckel, C. Length, Determination of formaldehyde release from wood-based panels using SPME-GC-FAIMS, *Int. J. Ion Mobil. Spec.* 17 (2014) 55–67.
- [65] N. Arroyo-Manzanares, A. Martín-Gómez, N. Jurado-Campos, R. Garrido-Delgado, C. Arce, L. Arce, Target vs spectral fingerprint data analysis of Iberian

- ham samples for avoiding labelling fraud using headspace – gas chromatography–ion mobility spectrometry, *Food Chem.* 246 (2018) 65–73.
- [66] E. Szymańska, A.N. Davies, L.M.C. Buydens, Chemometrics for ion mobility spectrometry data: recent advances and future prospects, *Analyst* 141 (2016) 5689–5708.
- [67] A.-C. Hauschild, T. Schneider, J. Pauling, K. Rupp, M. Jang, J.I. Baumbach, J. Baumbach, Computational methods for metabolomic data analysis of ion mobility spectrometry data—reviewing the state of the art, *Metabolites* 2 (2012) 733–755.
- [68] A. Smolinska, A.-C. Hauschild, R.R.R. Fijten, J.W. Dallinga, J. Baumbach, F.J. Van Schooten, Current breathomics—a review on data pre-processing techniques and machine learning in metabolomics breath analysis, *J. Breath Res.* 8 (2014) 27105.
- [69] S. Bader, W. Urfer, J.I. Baumbach, Preprocessing of ion mobility spectra by lognormal detailing and wavelet transform, *Int. J. Ion Mobil. Spectrom* 11 (2008) 43–49.
- [70] W. Cheung, Y. Xu, C.L.P. Thomas, R. Goodacre, Discrimination of bacteria using pyrolysis-gas chromatography-differential mobility spectrometry (Py-GC-DMS) and chemometrics, *Analyst* 134 (2009) 557–563.
- [71] A.A. Urbas, P.B. Harrington, Two-dimensional wavelet compression of ion mobility spectra, *Anal. Chim. Acta* 446 (2001) 391–410.
- [72] E. Szymańska, E. Brodrick, M. Williams, A.N. Davies, H.-J. van Manen, L.M.C. Buydens, Data size reduction strategy for the classification of breath and air samples using multicapillary column-ion mobility spectrometry, *Anal. Chem.* 87 (2015) 869–875.
- [73] E. Szymańska, G.H. Tinnevelt, E. Brodrick, M. Williams, A.N. Davies, H.-J. van Manen, L.M.C. Buydens, Increasing conclusiveness of clinical breath analysis by improved baseline correction of multi capillary column-ion mobility spectrometry (MCC-IMS) data, *J. Pharmaceut. Biomed. Anal.* 127 (2016) 170–175.
- [74] M. Westhoff, P. Litterst, L. Freitag, W. Urfer, S. Bader, J.I. Baumbach, Ion mobility spectrometry for the detection of volatile organic compounds in exhaled breath of patients with lung cancer: results of a pilot study, *Thorax* 64 (2009) 744–748.
- [75] G. Kaur-Atwal, G. O'Connor, A.A. Aksenov, V. Bocos-Bintintan, C.L.P. Thomas, C.S. Creaser, Chemical standards for ion mobility spectrometry: a review, *Int. J. Ion Mobil. Spectrom* 12 (2009) 1–14.
- [76] T. Khayamian, S.M. Sajjadi, S. Mirmahdih, A. Mardihallaj, Z. Hashemian, Simultaneous analysis of bifenthrin and tetramethrin using corona discharge ion mobility spectrometry and Tucker 3 model, *Chemometr. Intell. Lab. Syst.* 118 (2012) 88–96.
- [77] T. Perl, B. Bödeker, M. Jünger, J. Nolte, W. Vautz, Alignment of retention time obtained from multicapillary column gas chromatography used for VOC analysis with ion mobility spectrometry, *Anal. Bioanal. Chem.* 397 (2010) 2385–2394.
- [78] E. Szymańska, M.J. Markuszewski, X. Capron, A.-M. van Nederkassel, Y. Vander Heyden, M. Markuszewski, K. Krajka, R. Kaliszan, Evaluation of different warping methods for the analysis of CE profiles of urinary nucleosides, *Electrophoresis* 28 (2007) 2861–2873.
- [79] D. Isailovic, M.D. Plasencia, M.M. Gaye, S.T. Stokes, R.T. Kurulugama, V. Pungpapong, M. Zhang, Z. Kyselova, R. Goldman, Y. Mechref, M.V. Novotny, D.E. Clemmer, Delineating diseases by IMS-MS profiling of serum N-linked glycans, *J. Proteome Res.* 11 (2012) 576–585.
- [80] R.A. van den Berg, H.C.J. Hoefsloot, J.A. Westerhuis, A.K. Smilde, M.J. van der Werf, Centering, scaling, and transformations: improving the biological information content of metabolomics data, *BMC Genom.* 7 (2006) 142.
- [81] L. Zhang, Q. Shuai, P. Li, Q. Zhang, F. Ma, W. Zhang, X. Ding, Ion mobility spectrometry fingerprints: a rapid detection technology for adulteration of sesame oil, *Food Chem.* 192 (2016) 60–66.
- [82] J. Bible, S. Datta, S. Datta, Cluster analysis: finding groups in data, in: *Informatics for Materials Science and Engineering*, Elsevier, 2013, pp. 53–70.
- [83] M. Calderón-Santiago, Mass Spectrometry for the Identification and Quantitation of Metabolomic Biomarkers in Clinical Analysis, Doctoral Thesis, University of Córdoba, Spain, 2014.
- [84] D. Szöllösi, D.L. Dénes, F. Firtha, Z. Kovács, A. Fekete, Comparison of six multiclass classifiers by the use of different classification performance indicators, *J. Chemom.* 26 (2012) 76–84.
- [85] E. Szymańska, E. Saccenti, A.K. Smilde, J.A. Westerhuis, Double-check: validation of diagnostic statistics for PLS-DA models in metabolomics studies, *Metabolomics* 8 (2012) 3–16.
- [86] Z. Karpas, Ion mobility spectrometry: a tool in the war against terror, *Bull. Isr. Chem. Soc.* 24 (2009) 26–31.
- [87] D. Martinak, A. Rudolph, Explosives detection using an ion mobility spectrometer for airport security, in: *Proc. IEEE 31st Annu. 1997 Int. Carnahan Conf. Secur. Technol.*, 1997, pp. 188–189.
- [88] G.A. Eiceman, M.R. Salazar, M.R. Rodriguez, T.F. Limero, S.W. Beck, J.H. Cross, R. Young, J.T. James, Ion mobility spectrometry of hydrazine, monomethylhydrazine, and ammonia in air with

- 5-nonanone reagent gas, *Anal. Chem.* 65 (1993) 1696–1702.
- [89] M. Hernández-Mesa, A. Escourrou, F. Monteau, B. Le Bizec, G. Dervilly-Pinel, Current applications and perspectives of ion mobility spectrometry to answer chemical food safety issues, *TrAC Trends Anal. Chem.* 94 (2017) 39–53.
- [90] S. Wang, H. Chen, B. Sun, Recent progress in food flavor analysis using gas chromatography–ion mobility spectrometry (GC–IMS), *Food Chem.* 315 (2020) 126158.
- [91] N. Gerhardt, M. Birkenmeier, D. Sanders, S. Rohn, P. Weller, Resolution optimized headspace gas chromatography-ion mobility spectrometry (HS-GC–IMS) for non-targeted olive oil profiling, *Anal. Bioanal. Chem.* 409 (2017) 3933–3942.
- [92] T. Chen, X. Chen, D. Lu, B. Chen, Detection of adulteration in canola oil by using GC–IMS and chemometric analysis, *Int. J. Anal. Chem.* 2018 (2018) 3160265.
- [93] A. Othman, K.A. Goggin, N.I. Tahir, E. Brodrick, R. Singh, R. Sambanthamurthi, et al., Use of headspace–gas chromatography–ion mobility spectrometry to detect volatile fingerprints of palm fibre oil and sludge palm oil in samples of crude palm oil, *BMC Res. Notes* 12 (2019) 229.
- [94] T. Chen, X. Qi, D. Lu, B. Chen, Gas chromatography-ion mobility spectrometric classification of vegetable oils based on digital image processing, *J. Food Meas. Charact.* 13 (2019) 1973–1979.
- [95] T. Chen, X. Qi, M. Chen, B. Chen, Gas chromatography-ion mobility spectrometry detection of odor fingerprint as markers of rapeseed oil refined grade, *J. Anal. Methods Chem.* 2019 (2019), 3163204.
- [96] A. Martín-Gómez, N. Arroyo-Manzanares, V. Rodríguez-Estévez, L. Arce, Use of a non-destructive sampling method for characterization of Iberian cured ham breed and feeding regime using GC–IMS, *Meat Sci.* 152 (2019) 146–154.
- [97] J.H. Aheto, X. Huang, X. Tian, R. Lv, C. Dai, E. Bonah, X. Chang, Evaluation of lipid oxidation and volatile compounds of traditional dry-cured pork belly: the hyperspectral imaging and multi-gas-sensory approaches, *J. Food Process. Eng.* 43 (2019) 13092.
- [98] N. Gerhardt, M. Birkenmeier, S. Schwolow, S. Rohn, P. Weller, Volatile compound fingerprinting by headspace-gas-chromatography ion-mobility spectrometry (HS-GC–IMS) as a benchtop alternative to ¹H NMR profiling for assessment of the authenticity of honey, *Anal. Chem.* 90 (2018) 1777–1785.
- [99] N. Arroyo-Manzanares, M. García-Nicolás, A. Castell, N. Campillo, P. Viñas, I. López-García, M. Hernández-Córdoba, Untargeted headspace gas chromatography–ion mobility spectrometry analysis for detection of adulterated honey, *Talanta* 205 (2019) 120123.
- [100] X. Wang, S. Yang, J. He, L. Chen, J. Zhang, Y. Jin, J. Zhou, Y. Zhang, A green triplelocked strategy based on volatile-compound imaging, chemometrics, and markers to discriminate winter honey and sapium honey using headspace gas chromatography ion mobility spectrometry, *Food Res. Int.* 119 (2019) 960–967.
- [101] A.P. Snyder, C.S. Harden, D.M. Davis, D.B. Shoff, W.M. Maswadeh, Hand-portable gas chromatography-ion mobility spectrometer for the determination of the freshness of fish, in: Conference Paper of the Third International Workshop on Ion Mobility Spectrometry, April 1995, pp. 146–166.
- [102] D. Cavanna, S. Zanardi, C. Dall’Asta, M. Suman, Ion mobility spectrometry coupled to gas chromatography: a rapid tool to assess eggs freshness, *Food Chem.* 271 (2019) 691–696.
- [103] W. Vautz, J.I. Baumbach, J. Jung, Continuous monitoring of the fermentation of beer by ion mobility spectrometry, *Int. J. Ion Mobil. Spectrom* 7 (2004) 3–5.
- [104] J. Gallegos, C. Arce, R. Jordano, L. Arce, L.M. Medina, Target identification of volatile metabolites to allow the differentiation of lactic acid bacteria by gas chromatography-ion mobility spectrometry, *Food Chem.* 220 (2017) 362–370.
- [105] Y. Guo, D. Chen, Y. Dong, H. Ju, C. Wu, S. Lin, Characteristic volatiles fingerprints and changes of volatile compounds in fresh and dried *Tricholoma matsutake* singer by HS-GC–IMS and HS-SPME-GC–MS, *J. Chromatogr. B* 1099 (2018) 46–55.
- [106] M. Li, R. Yang, H. Zhang, S. Wang, D. Chen, S. Lin, Development of a flavor fingerprint by HS-GC–IMS with PCA for volatile compounds of *Tricholoma matsutake* singer, *Food Chem.* 290 (2019) 32–39.
- [107] A. Tiele, A. Wicaksono, E. Daulton, E. Ifeachor, V. Eyre, S. Clarke, L. Timings, S. Pearson, J.A. Covington, X. Li, Breath-based non-invasive diagnosis of Alzheimer’s disease: a pilot study, *J. Breath Res.* 14 (2020) 026003.
- [108] A. Tiele, A. Wicaksono, J. Kansara, R.P. Arasaradnam, J.A. Covington, Breath analysis using eNose and ion mobility technology to diagnose inflammatory bowel disease - a pilot study, *Biosensors* 9 (2019) 55.
- [109] M. Allers, J. Langejuergen, A. Gaida, H.S. Schuchardt, J.M. Hohlfeld, S. Zimmermann, Measurement of exhaled volatile organic compounds from patients with chronic obstructive pulmonary disease (COPD) using closed gas loop GC-IMS and GC-APCI-MS, *J. Breath Res.* 10 (2016) 026004.
- [110] H. Tian, S. Li, H. Wen, X. Zhang, J. Li, Volatile organic compounds fingerprinting in faeces and urine of

- Alzheimer's disease model SAMP8 mice by headspace-gas chromatography-ion mobility spectrometry and headspace-solid phase microextraction-gas chromatography-mass spectrometry, *J. Chromatogr. A* 1614 (2020) 460717.
- [111] D. Daulton, A. Wicaksono, J. Bechar, J.A. Covington, J. Hardwicke, The detection of wound infection by ion mobility chemical analysis, *Biosensors* 10 (2020) 19.
- [112] E. Mozdiak, A.N. Wicaksono, J.A. Covington, R.P. Arasaradnam, Colorectal cancer and adenoma screening using urinary volatile organic compound (VOC) detection: early results from a single-centre bowel screening population (UK BCSP), *Tech. Colo-proctol.* 23 (2019) 343–351.
- [113] M. Shnayderman, B. Mansfield, P. Yip, H.A. Clark, M.D. Krebs, S.J. Cohen, J.E. Zeskind, E.T. Ryan, H.L. Dorkin, M.V. Callahan, T.O. Stair, J.A. Gelfand, C.J. Gill, B. Hitt, C.E. Davis, Species-specific bacteria identification using differential mobility spectrometry and bioinformatics pattern recognition, *Anal. Chem.* 77 (2005) 5930–5937.
- [114] H. Schmidt, F. Tadjimukhamedov, I.V. Mohrenz, G.B. Smith, G.A. Eiceman, Microfabricated differential mobility spectrometry with pyrolysis gas chromatography for chemical characterization of bacteria, *Anal. Chem.* 76 (2004) 5208–5217.
- [115] M.D. Krebs, B. Mansfield, P. Yip, S.J. Cohen, A.L. Sonenshein, B.A. Hitt, C.E. Davis, Novel technology for rapid species-specific detection of *Bacillus spores*, *Biomol. Eng.* 23 (2006) 119–127.
- [116] S. Ayer, W.X. Zhao, C.E. Davis, Differentiation of proteins and viruses using pyrolysis gas chromatography differential mobility spectrometry (PY/GC/DMS) and pattern recognition, *IEEE Sens. J.* 8 (2008) 1586–1592.
- [117] H. Ren, J. Jensen, W. Loerop, Pyrolysis gas-chromatography ion-mobility spectrometry data analysis for chemical detection in water monitoring, in: J. Arthur, Sedlacek III, S.D. Christesen, R. Colton, T. Vo-Dinh (Eds.), *Chemical and Biological Point Sensors for Homeland Defense*, 2004.
- [118] A.P. Snyder, W.M. Maswadeh, A. Tripathi, J. Eversole, J. Hod, M. Spence, Orthogonal analysis of mass and spectral based technologies for the field detection of bioaerosols, *Anal. Chim. Acta* 513 (2004) 365–377.
- [119] E. Aguilera-Herrador, R. Lucena, S. Cárdenas, M. Valcárcel, Ionic liquid-based single drop microextraction and room-temperature gas chromatography for on-site ion mobility spectrometric analysis, *J. Chromatogr. A* 1216 (2009) 5580–5587.
- [120] G. Walendzik, J.I. Baumbach, D. Klockow, Coupling of SPME with MCC/UV-IMS as a tool for rapid on-site detection of groundwater and surface water contamination, *Anal. Bioanal. Chem.* 382 (2005) 1842–1847.
- [121] G.A. Eiceman, Z. Karpas, *Ion Mobility Spectrometry*, second Rev, Taylor and Francis, Boca Rotan, FL, 2005.
- [122] G.W. Cook, P.T. LaPuma, G.L. Hook, B.A. Eckenrode, Using gas chromatography with ion mobility spectrometry to resolve explosive compounds in the presence of interferences, *J. Forensic Sci.* 55 (2010) 1582–1591.
- [123] M. Amo-Gonzalez, S. Perez, R. Delgado, G. Arranz, I. Carnicero, Tandem ion mobility spectrometry for the detection of traces of explosives in cargo at concentrations of parts per quadrillion, *Anal. Chem.* 91 (2019) 14009–14018.

Speciation and element-selective detection by gas chromatography

Qilin Chan, Joseph A. Caruso[†]

University of Cincinnati, Cincinnati, OH, United States

16.1 Introduction to plasma-based detectors

Plasma is a state of matter, other than solids, liquids, or gases, containing positive ions and negative electrons. A gas can be turned into plasma when losing or gaining an electron ionizes the gaseous molecules. The presence of high electron density and positive ions makes plasma a good ionization source. Their capability to fully or partially ionize is related to their electron density of ca. 10^{15} cm^{-3} . There are three major plasma-based ionization sources, inductively coupled plasma (ICP), microwave-induced plasma (MIP), and glow discharge (GD). More recently, additional intriguing plasma sources have been introduced, but these have not yet received the popularity for GC detection and are not included in this chapter.

ICP is created by igniting plasma gas, typically argon, with a spark, and the plasma is sustained under a high radio frequency electromagnetic field. ICP temperatures range between

6000 and 10,000 K [1]. The samples introduced to ICP are instantly dried, vaporized, atomized, and finally ionized by the plasma. ICP was first used as an excitation source for atomic emission spectroscopy in the 1960s [2], but commercial inductively coupled plasma–atomic emission spectrometry (ICP-AES) instrumentation was not available until 10 years later. Inductively coupled plasma–mass spectrometry (ICPMS) emerged commercially in the 1980s and has been growing rapidly. With the unmatched advantages of producing singly charged positive ions for most elements in the periodic table, ICP-AES and ICPMS quickly surpassed other techniques of elemental detection, such as atomic absorption spectrometry, and have become the dominant techniques for trace-level elemental analysis.

Both ICP-AES and ICPMS have been used as atomic detectors for gas chromatography (GC) since the 1980s. However, ICPMS has been the first choice when an online atomic detection is needed for GC, because of the advantages of

[†] Author J.A. Caruso is deceased.

ICPMS over ICP-AES, such as higher sensitivity, lower detection limits, higher selectivity, and the ability for multiisotope detection. The development of GC-ICPMS has been ascribed to the continuous growth of interest in elemental speciation. In addition to GC-ICPMS, the emergent needs of elemental speciation also drive the growth of other hyphenated techniques, such as HPLC-ICPMS [3,4] and capillary electrophoresis (CE-ICPMS) [5].

MIP, an alternative plasma-based ionization source, uses microwaves produced from a magnetron (a microwave generator) to oscillate the electrons in the plasma gas. The oscillating electrons collide with atoms in the flowing plasma gas to create and maintain a high-temperature plasma. MIP typically uses helium (He) as a plasma gas, which leads to one advantage of MIP over the ICP, namely the capability to ionize all elements in the periodic table with an ionization potential of 24.5 eV, which is significantly higher than Ar at 15.7 eV. Therefore, MIP can easily excite nonmetals, which are poorly ionized in Ar plasma. However, it is worth noting that electron densities and electron energies are typically lower in the analytical MIP—important parameters for efficient ionization. Another benefit of using He is that it reduces isobaric interferences since monoisotopic ^4He forms fewer polyatomic ions than multiisotopic Ar. Despite the advantages of MIP, ICP is the dominant plasma source on the market. The main drawbacks of MIP include difficulties with plasma ignition and sustainment as well as sample desolvation and atomization due to its limited thermal energy. Therefore, the amount of sample introduced into MIP may be limited. However, this is not an issue for the hyphenated technique GC-MIP-AES/MS because GC is also a great matrix removal technique allowing the plasma more energy to excite or ionize particular analyte ions.

GD, another type of plasma, is developed in a cell with two separate electrodes with a potential difference from a few hundreds to thousands of volts [6]. The plasma gas, argon, or helium typically fills the cell and is excited by electrons from the cathode. The generated positive ions are accelerated toward the cathode, and secondary electrons are released at the electrode. The first and secondary electrons make GD a self-sustained plasma. For surface analytical applications, the cathode is the subject of analysis, but for GC, it is the plasma (GD) that is the compartment of interest. GD is typically powered by direct current (dc) and radio frequency (rf). The dc-GD has been the most commonly used, but the rf-GD is increasingly popular due to its capability of ionizing nonconductive cathode materials. GD has been used in glow discharge—atomic emission spectrometry (GD-AES) and glow discharge—mass spectrometry (GD-MS), which are widely used for bulk solids analysis and depth profiling of solid conducting materials as discussed by Marcus [6]. However, Olson et al. were first to show the power of the GD as a GC detector, illustrating both soft and hard ionization by coupling GC to dc-GD and rf-GD [7,8]. In addition to inorganic analysis, a versatile GD capable of both atomic and molecular ionization has been developed [9].

Increasingly strong interest in elemental speciation has been driving fast growth of hyphenated techniques, which enable online atomic detection for various separation approaches. Fig. 16.1 shows the comparison among the three major GC-hyphenated atomic detections, GC-ICP, GC-MIP, and GC-GD. All three were actively studied in the 1990s, but GC-ICP was clearly the most studied. GC-ICP has become the dominant online atomic detection for GC since 2000, and over 90% of the GC-ICP

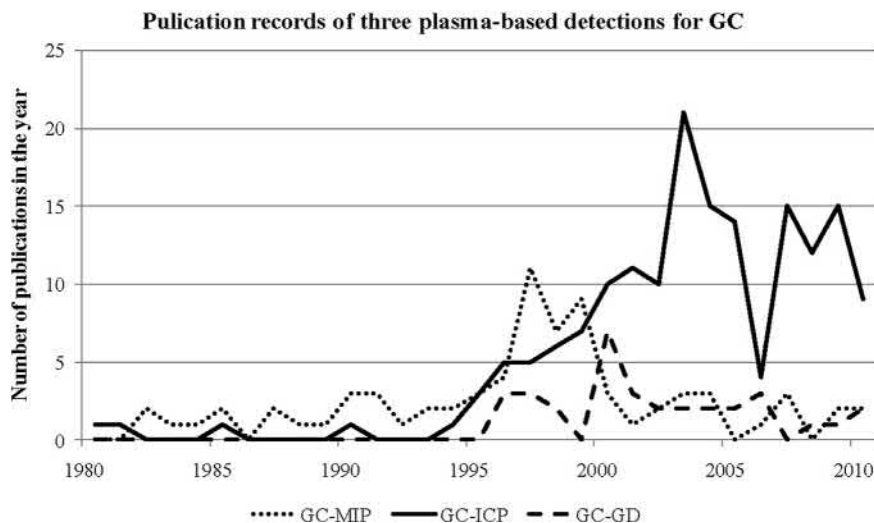


FIGURE 16.1 This graph shows the abundance of publications on each of the three plasma-based detections for GC in an individual year since the first online plasma-based atomic detection for GC in 1980. Above 90% of the GC-ICP publications are from GC-ICPMS. The data were obtained from Scopus by searching the corresponding keywords. The graph is for a trend analysis of these hyphenated techniques, rather than an accurate representation of their actual number of publications.

applications are performed on GC-ICPMS. ICPMS is the most favorable atomic detector for GC in the last 10 years.

16.2 GC-ICPMS

16.2.1 Brief introduction to ICPMS

ICPMS is currently one of the most powerful and popular multielement atomic detectors. The first ICPMS, an ICP source coupled to a quadrupole-based mass analyzer, was introduced by Houk et al. in 1980 in the United States while British scientists Gray and Date were making excellent progress [10]. The introduction of collision/reaction cells in 2001 increased the potential of ICPMS for high matrix samples [11,12]. In the ensuing years, ICPMS has become one of the most important techniques for the detection of more than 70% of the elements in the periodic table. Since the development of laser ablation (LA) and LA-ICPMS [13], ICPMS has been a versatile tool for any type of samples, gaseous,

liquid, and solid. In addition to total concentration measurement, it is also a useful online detection tool for common separation techniques, GC, LC, and CE. More than 5000 ICPMS instruments have been installed in various institutions, academic labs, companies, and government agencies all over the world [1].

ICPMS is typically made of six compartments: sample introduction, ICP, ion extraction, ion optics, mass analyzer, and detector (Fig. 16.2). Liquid samples are usually introduced into the sample introduction system in which the nebulizer/spray chamber and high-pressure gas (Ar) convert liquid into fine aerosol. The sample is then carried through the ICP torch and enters the center of the plasma, about 6000–8000 K temperature. The liquid sample is instantly dried, vaporized, atomized, and finally ionized in the plasma. The ions are extracted by sampler and skimmer cones and accelerated and focused by the ion optics. If a collision/reaction cell (usually octopole or hexapole between ion optics and mass analyzer) is installed, the collision/reaction

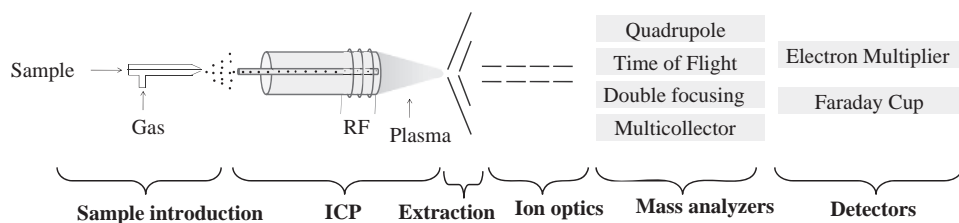


FIGURE 16.2 A simplified schematic of ICPMS.

gas can be introduced in the cell to minimize or eliminate the polyatomic interference ions by collision, reaction, or energy discrimination. The mass analyzer and detector collect the ions of different m/z values in rapid sequence (essentially simultaneously). There are four types of commercially available mass analyzers for ICPMS: quadrupole, time of flight, double-focusing sector field, and multicollector, which are nicely reviewed by Becker [1]. For the detector, an electron multiplier is usually used for quadrupole and time-of-flight mass analyzers.

16.2.2 Advantages and limitations of ICPMS detection

As a “hard” ion source, ICP breaks down most molecules to atoms or atomic ions, making ICPMS a robust elemental detection technique for complex matrices. The atoms of the same element share the same ionization energy and the difference of their ionization efficiency is negligible; hence, ICPMS is also an exceptional tool for elemental quantification. On the other hand, the ionization efficiency of molecular MS heavily depends on the specific structure of the analytes and the matrix. A slight modification of the structure, for example, replacing a hydroxyl group with an ether group, can cause substantial alteration of ionization potential in ESI-MS,

even if the elemental composition remains unchanged. The differences in ionization efficiency make quantification problematic although it is done. ICPMS has been proposed as a complementary tool for molecular MS when both identification and quantification are necessary and is known as a metallomics approach. This has been done by introducing an ICPMS-sensitive element such as Eu through derivatization or simply using a “natural” elemental label or tag, such as P.

Another advantage of ICPMS is the accurate measurement of the abundance of a single isotope, which cannot be achieved by atomic emission. Due to this capability, GC-ICPMS with postcolumn isotope dilution can be used for species-unspecific quantification when the standard is not available. An isotope-enriched elemental standard is introduced to ICPMS as a spike to the eluent coming from a GC column [14,15]. The concentration and isotopic abundance of the element are usually known and the sample's concentration depends on the ratio of the two isotopes used for calculation. Postcolumn isotope dilution has also been used widely for species-specific quantification, in which the isotope-enriched specific compound was spiked. Isotope dilution is considered as the most accurate method of quantification because the analytes and spikes share the same matrix and interferences.

One of the major limitations of ICPMS is that it is not capable of molecular structure characterization, because molecular structures are destroyed in plasma due to the harsh ionization conditions. In order to obtain structural information, molecular MS as a complementary technique for ICPMS is more and more often used in elemental speciation and now has become associated with “metallomics studies.” Recently, scientists have started thinking of a versatile MS that is capable of both atomic and molecular MS. The first mass spectrometry of “dual-source,” ICP and ESI, was designed, constructed, and characterized by the Hieftje group [16,17]. Another strategy to achieve both atomic and molecular detection was initially developed by the Sanz-Medel group by utilizing a versatile ionization source, microsecond-pulsed direct current GD [9,18]. Both of these two designs were able to provide element-specific detection and molecular structural identification simultaneously or close to simultaneously, suggesting that the study of elemental speciation in the absence of standards has a promising future.

16.2.3 Interfacing GC to ICPMS

An interface from GC to ICPMS needs to efficiently transport the effluent from the end of the GC column to the inlet of the ICP torch. There have been a few interface designs and they have been comprehensively reviewed by Lobinski et al. [19] and Caruso et al. [20]. The main challenge of these designs is to avoid condensation, which causes sensitivity loss or peak broadening. Two strategies have been commonly adopted in an interface design. One is isothermal heating of the transfer line to eliminate hot or cold spots and the other is introducing a flow of makeup carrier gas at the end of the GC column, which effectively dilutes the analyte and better transports it to the plasma. With the exceptional detection limits of ICPMS, this dilution is not a problem, for there is the great advantage with GC of gaseous sample introduction and matrix removal. Further, the plasma prefers a gaseous sample, thereby eliminating the energy it must provide for desolvation, vaporization, and atomization, resulting in far better analyte ionization. As shown in Fig. 16.3,

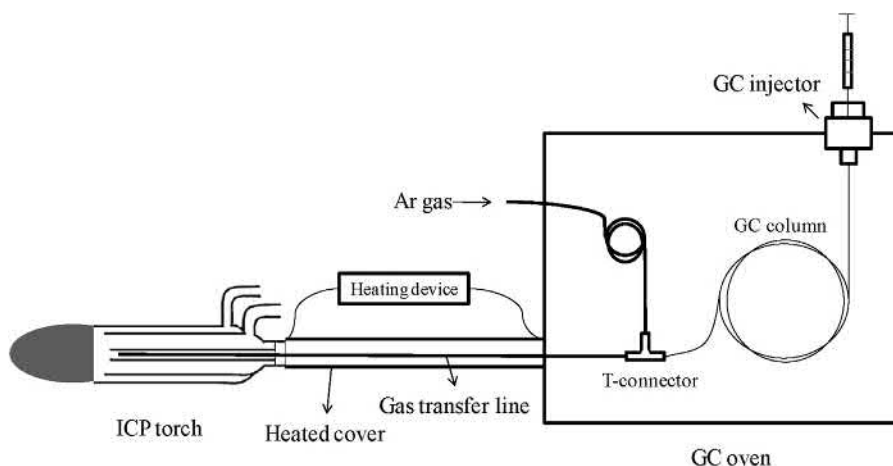


FIGURE 16.3 Schematic representation of the GC-ICPMS interface. The effluent from a GC column is mixed with preheated Ar gas at the T-connector, and the Ar gas carries the effluent through the heated transfer line till the center of plasma.

the current GC-ICPMS interfaces integrate both the strategies and offer very efficient analyte transfer at temperatures up to 325°C (some commercial vendors indicate even higher temperatures are possible). Interfacing of MIP and GD to GC is similar to that of ICPMS—all use heated transfer lines to direct GC eluent to the plasma.

16.2.4 ICPMS as a detector for GC

GC-ICPMS is a very effective hyphenated system for speciation analysis. Its extraordinary sensitivity of attogram (10^{-18}) to femtogram (10^{-15} g) levels of detection for Hg, Sn, Pb, Se, etc., is because of the superb sensitivity of both GC and ICPMS enhanced by avoiding condensed mobile phase. GC-ICPMS also has very good separation efficiency due to the high resolving power of GC capillary columns. Therefore, GC-ICPMS is the most sensitive speciation technique. However, GC-ICPMS usage is limited solely for volatile and thermally stable species or for some compounds that can be converted to thermally stable species by derivatization. Macromolecules or certain nonvolatile compounds are best suited to other techniques, such as HPLC-ICPMS or CE-ICPMS.

The extraordinary sensitivity of ICPMS is enhanced when it is used as a detector for GC. First, GC introduces relatively “clean” sample to the plasma compared to direct aspiration or LC. Second, the gas-phase compounds consume less energy from ICP with the benefit of higher ionization efficiency. Third, the sample is totally consumed with 100% loaded onto a GC column carried to the ICP, rather than the 2% with a standard nebulizer/spray chamber. GC-ICPMS has been established for about 30 elements, including the ones of most common interests in elemental speciation, such as Hg, Se, and As [Table 16.1](#) lists the elements that have been studied by GC-ICPMS post-2001.

Isotope dilution analysis, an alternative to standard quantification with calibration curves,

is used frequently in GC-ICPMS. About 24% of the total GC-ICPMS studies involve isotope dilution techniques, and the percentage is still increasing. Species-specific isotope dilution with GC-ICPMS has been markedly increasing since 2003 and accounts for more than half of the total isotope dilution studies. Species of Hg, Sn, Se, and S are accurately quantified with this technique from a variety of matrices, such as soil, water, petroleum, and biological tissues. Researchers also have started developing methods for multiisotope GC-ICPMS detection using multiple spikes. Double spike and triple spike have been reported for simultaneous detection of Sn [\[21\]](#).

16.3 GC-MIP and GC-GD

16.3.1 GC-MIP-AES

GC-MIP-AES has been a well-established technique since the 1990s [\[22\]](#). The widespread of GC-MIP-AES is due to its low cost as well as relatively high performance. The cost of an ICPMS is much higher than an MIP-AES. Although GC-MIP-AES is not as sensitive as GC-ICPMS, it offers lower detection limits than GC-ICP-AES, for nonmetals. The advantage of high sensitivity for nonmetals is because He is used as a plasma gas instead of Ar. However, GC as sample introduction is favored by MIP-AES because the low load produced from gaseous samples enhances plasma performance as noted years ago by the Cincinnati group [\[23\]](#). Elemental speciation studies using GC-MIP-AES are summarized in [Table 16.2](#).

16.3.2 GC-GD-MS and GC-GD-AES

The versatility and stability of GD make it a constantly attractive ionization source. The primary application of GD is for direct analysis

TABLE 16.1 The list of elements analyzed by GC-ICPMS since 2001.

Element	No. of publications	Species determined	Sample matrices	Detection limits (ng L ⁻¹ or ng kg ⁻¹)	Sample treatment/comment	Representative references
Sn	32	MBT, DBT, TBT, TPhT, and DPhT	Sediment and water	0.18–0.25 [21]	Isotope dilution with single or multiple spikes was well developed for organotin quantification.	[50,69]
Hg	5	Inorganic Hg, methylmercury, ethylmercury, and Hg–S compounds	Seafood, water, blood, plant, and sediment	4 [70]	Isotope dilution has been often used.	[64,71–73]
Se	14	DMSe, DMDSe, DEtSe, SeMet, SeEt, SeCys, and Se–S compounds	Urine, breath, plant, microbe, and cell	7–300 [29]	SPME has been often used for sampling. Selenoamino acids need to be derivatized [74].	[60,75]
S	8	Thiophene derivatives, pesticides, and sulfur gases	Petroleum, water, breath, and landfill gas emission	800–3300 [76]		[77–79]
P	8	Pesticides, nerve agents, other organophosphates, and phosphine	Water, blood, flame retardant, and industrial gas	0.09–143 [46]	SPME or derivatization [36] is often needed.	[46,53,80]
Br	8	PBDE and brominated volatile organic compounds	Flame retardant, blood, soil, and water	15.2–40.5 [81]		[82,83]
As	6	MAs, TMAs, TPhAs, TEtAs, DMA, MMA, and TMAO	Soil, natural gas, and gas condensate	2–10 [84]	Hydride generation is needed for DMA, MMA, and TMAO [84].	[32,85]
Pb	4	Trimethyl-lead, PbEt ₄	Standard solution	60 [86]		[86]
Sb	4	SbH ₃ , monomethyl-, dimethyl-, and trimethylantimony	Sediment	310 [87]	Hydride generation was used for sampling.	[88,89]
I	3	Iodinated phenols and iodinated volatile organic compounds	Water and air	0.07–0.12 [90]	SPME was used for sampling.	[83,90]

TABLE 16.2 The list of elements analyzed by GC-MIP-AES.

Element	No. of publications	Species determined	Sample matrices	Detection limits	Sample treatment/ comment	Representative references
F	2	Fluoroethers, 2-(Heptadecafluorooctyl)ethanol	Rat blood plasma	0.82 ng [91]		[91]
Br and Cl	4	CH _x Br _y Cl _z	Seawater, motor car exhaust gas	0.01–0.12 ng [47]		[47,92]
I	2	CH _x I _y and iodopropane	Seawater	11–257 pg for molecules [47]		[47,93]
Hg	13	MeHg, Me ₂ Hg, EtHg, PhHg, MePhHg, Ph ₂ Hg, Hg ²⁺	Seafood, water, and sediment	0.8–1.1 ng L ⁻¹ [94]		[94–99]
Pb	5	Me _x Pb, Et _x Pb	Water, sediment, and gasoline	43–83 pg [100]	Derivatization	[94,101–103]
Se	2	Me ₂ Se, Me ₂ Se ₂ , Et ₂ Se, and selenite	Plants	0.19–0.57 μg L ⁻¹	SPME, derivatization (selenite)	[97,104]
Sn	7	MBT, DBT, TBT, MPhT, TPhT, and DPhT	Sediment, seawater, seafood, fresh water, and urine	0.4–0.6 ng L ⁻¹ [94]		[43,96,99,105–107]
Mn	1	Cyclopentadienylmanganese tricarbonyl and (methylcyclopentadienyl) manganese tricarbonyl	Sediment and seawater	0.62–0.65 pg L ⁻¹ [108]		[108]
As	1	Arsenic-containing hydrocarbons	Seafood	0.05–0.13 ng μL ⁻¹ for molecules [109]	Parallel analysis with GC-ICPMS	[109]

of solid samples, both conductive and nonconductive [6]. However, GD has been used for gaseous analytes, and it has been combined with GC for elemental speciation since the 1990s [7,8]. The system construction cost is less for GC-GD-AES than for GC-MIP-AES, as well as lower consumption of plasma gas, but higher sensitivity by GC-GD-AES was reported for mercury [24]. However, the applications of GC-GD-AES are limited; only a few elements have been studied by this technique so far. GD-MS has been coupled to GC for elemental speciation studies as well [25].

As an online atomic detection for GC, either GD-AES or GD-MS plays a minor role compared to ICPMS and MIP-AES. In addition GC-GD-MS has been used for elemental speciation with both atomic and molecular detections, which occur virtually simultaneously [9]. This unique feature gives GC-GD-MS possible future advantages over the other hyphenated techniques.

16.4 Sample preparation for GC–plasma spectroscopy

Gaseous analytes are often at ultratrace levels in the ambient environment. Although the detection limits of GC-ICPMS can go as low as 0.01 ng L^{-1} , a preconcentration step is sometimes required. For volatile or semivolatile species, the preconcentration is typically done with extraction or cryotrapping. There are many different types of extraction methods for GC-ICPMS, such as solid-phase microextraction (SPME) [26], stir bar sorptive extraction (SBME) [27], and single-drop liquid-phase microextraction (SDME) [28]. SPME has been the most popular one because of its advantages such as small sample size, low cost, solventless nature (although it can be used being immersed in solvent), and full automation of the entire process. The in-needle fiber can be directly inserted into the GC injection port [29]. The applications of SPME in elemental speciation

were comprehensively reviewed by Diez et al. [30]. In cryogenic trapping, another option for preconcentration in GC-ICPMS, the volatile analytes are trapped just by condensation at very low temperatures followed by instantaneous evaporation [31]. Cryotrapping using chromatographic packing followed by thermal desorption into GC-ICPMS was studied by Feldmann et al. [32–34].

Because most organometallic species lack volatility, a derivatization step is often mandatory prior to the extraction. With derivatization, the analytes are converted to volatile or semivolatile compounds in alkylation and hydride-forming reactions. It has been applied to elemental speciation for tin [35], phosphorus [36], mercury [37], lead [30], etc. Hydride generation has been employed to convert nonvolatile species of Se, As, and Sb to gas-phase hydride followed by a cryotrapping step [38].

16.5 Advances in applications of GC–plasma spectroscopy

GC–plasma spectroscopy is one of the most powerful tools for elemental speciation because of its unmatched advantages of high-resolution separation and sensitive detection. This hyphenated technique has been employed for numerous applications in a variety of fields. In this book chapter, the most recent and significant applications of GC-ICPMS are presented in the following two main categories, environmental and biological applications.

16.5.1 Environmental applications

16.5.1.1 Water

Elemental speciation has been a critical field for environmental studies since many elements are of high environmental concern [39]. Water pollution is a major problem in local and global contexts. It has been suggested that water pollution is the leading worldwide cause of deaths

and diseases and that it accounts for thousands of deaths daily [40]. In order to evaluate water safety, many studies of elemental speciation have been carried out for all types of water samples, including wastewater, drinking water, seawater, and groundwater.

Some species of interest in water are at an ultratrace level that often requires excellent sensitivity and detection capabilities for the speciation methods. The sensitivity can be increased by a preconcentration step such as SPME or an enhanced detection such as hydride generation (HG)-ICPMS. Due to the widespread use of tributyltin (TBT)-based paints on all vessel types since the 1970s, organotins are priority substances (Decision 2455/2001/EC) [41] that have to be taken into account, in evaluating water chemical pollution according to the European Water Framework Directive 2000/60/EC. A rapid and sensitive determination was achieved for mono-, di-, and tributyltin (MBT, DBT, and TBT) in seawater by GC-ICPMS with ^{119}Sn species-specific isotope dilution [42]. The detection limits are in the range of 0.04–0.27 ng L^{-1} for Sn. The ultralow detection limits for organotins were also achieved by GC-MIP-AES [43]. The method was applied to various organotin species in urine samples, and the detection limits were reported as 0.42–0.67 $\mu\text{g L}^{-1}$ for tin.

Organotins are usually derivatized before they are extracted and analyzed by GC-ICPMS. Xiao et al. determined butyltin compounds in seawater with GC-ICPMS [44]. The organotins were derivatized by adding sodium tetraethylborate (NaBEt_4) and sodium tetrahydroborate (NaBH_4) and the products, volatile tin species, were extracted by single-drop microextraction (SDME). In SDME, a microdrop of solvent suspended at a syringe needle tip was exposed to the headspace of the sample vial, in which the derivatized butyltins were extracted into the microdrop. SDME is a simple, fast, inexpensive, and effective method of extraction, but its application in elemental speciation is rare. The LODs

were 1.4 ng L^{-1} for MBT, 1.8 ng L^{-1} for DBT, and 0.8 ng L^{-1} for TBT, and relative standard deviations (RSDs) were in the range of 1.1%–5.3% ($c = 1 \mu\text{g L}^{-1}$, $n = 3$).

Mercury contamination in water, sediment, and seafood raises many concerns for human health. GC-ICPMS and GC-MIP-AES are primary techniques for mercury speciation. Methylmercury is the primary species of interest. The sensitivity, accuracy, and precision of the analytical method for measuring methylmercury have been significantly improved by innovative methods such as isotope dilution. Jackson et al. reported a GC-ICPMS method offering excellent figures of merit for methylmercury quantification in Lake Champlain, VT, in the United States [45]. The analysis utilized species-specific isotope dilution, purge-and-trap GC-ICPMS. The instrument detection limit was about 0.3 fmolar (0.06 pg L^{-1}), and the method detection limit was 15 fmolar (0.003 ng L^{-1}). The method was accurate even at low concentrations of 0.025 ng L^{-1} . This combination of precision, accuracy, and sensitivity allows for quantification of significant differences in methylmercury concentration between different locations and over time, within the same spot. GC-ICPMS is also a good choice for characterizing organophosphorus in water samples. A few studies were carried out to evaluate the water contamination caused by usage of organophosphorus pesticides. Fidalgo et al. developed an SPME-GC-ICPMS method to measure these in river water samples [46]. In this study, the experimental conditions for SPME of organophosphorus pesticides, such as type of fiber, extraction mode, extraction time, extraction temperature, salt additives, and pH, were optimized.

With the advantage of better excitation efficiency on nonmetals, GC-MIP-AES has been often used for speciation of F, Cl, Br, I, Se, etc. Halogenated compounds in seawater were well characterized by GC-MIP-AES [47]. Br and Cl were monitored for the volatile halogenated

compounds such as CH_2BrCl and CH_2Br_2 . The detection limits was 0.01–0.04 ng for bromine and 0.03–0.12 ng for chlorine.

16.5.1.2 Soil

Soil contamination is another big threat to the environment, food safety, and sustainable agriculture. The leachate of the contaminated area can cause cross-contamination of water within and underlying it, and the emission from the soil can cause cross-contamination of the surrounding atmosphere. Elemental speciation in soil is as important as that in water, but it is a more challenging task. The complexity of the matrix and variation from sample to sample in soil make the sample preparation for speciation a difficult step. It often requires a complex sequential extraction procedure to recover analytes from the soil sample. Microwave extraction was employed to increase the speed and efficiency of extraction [48]. GC-ICPMS and GC-MIP-AES are extensively used for elemental speciation in soil. The elements of interest include arsenic, mercury, tin, antimony, selenium, tellurium, chromium, iodine, etc.

Tin, mercury, arsenic, and antimony in soil are frequently speciated by GC-ICPMS. The use of TBT as a marine antifouling agent has led to its near-global dispersal, and it is still prominent in coastal seawaters. The sediment is a good indicator for environmental changes in water, and thus TBT and its degradation products, DBT and MBT, in sediment are often analyzed by GC-ICPMS to evaluate TBT pollution in the water environment. Extracting organotins from sediments with high recovery and low degradation is not a simple task. Kumar et al. evaluated five extraction protocols and two derivatization methods [49]. The recovery rate varied significantly from one tin species to another. Microwave and ultrasonic radiation were introduced to enhance the extraction [50]. Different SPME procedures were also evaluated, and the best results were obtained by using the divinylbenzene/Carboxen/polydimethylsiloxane 2 cm

50/30 μm fiber with the optimal extraction conditions as the following: $T = 30^\circ\text{C}$, $t = 40$ min, and $\text{pH} = 4$ [51]. Isotope dilution has been well established for accurate GC-ICPMS analysis of organotins, including species-specific isotope dilution with a single spike solution of ^{118}Sn -enriched butyltins [52], as well as a triple spike solution containing each butyltin species enriched with a different tin isotope [30]. The results demonstrated that multiple spikes could provide information on possible extraction-derived rearrangement reactions when optimizing and selecting the always-critical solid-liquid extraction procedure of the species from a solid sample. Once it has been demonstrated that the selected extraction procedure provides quantitative extraction without promoting degradation of the species, less sophisticated single isotope spikes can be routinely applied for the determination of the amount of butyltin in a given matrix.

16.5.1.3 Air

Indoor air pollution and urban air quality have been listed as two of the world's worst pollution problems. Some volatile metal(loid) compounds are very toxic; hence, their species and concentration in air can be of high concern. The gas-phase analytes are collected by either absorbing stationary phases such as SPME fibers [31] or cryotrapping with liquid nitrogen [21]. A cryosampling system together with a low temperature GC-ICPMS method was developed for the determination of phosphine emission from a tobacco factory [53]. CO_2 was eliminated by a cartridge filled with NaOH during the analytical desorption step. Phosphine recovery was above 98%, and its concentration in ambient air was about 1 ng m^{-3} .

To enhance the sensitivity and accuracy of gas characterization, a GC-ICPMS method based on species-specific isotope dilution in combination with online derivatization was developed for the simultaneous determination of volatile organometallic compounds and reactive gaseous

mercury-related species, such as Hg^0 , $(\text{CH}_3)_2\text{Hg}$, CH_3HgX , and HgX_2 ($X =$ counter ions), in gaseous samples [54]. Elevated concentrations of these mercury compounds have been found in, for example, emissions from contaminated sediments, landfills, and sewage treatment plants. In this work, a mixture of developing Hg species and isotope-enriched standards was derivatized by 1% sodium tetraethylborate solution, and the derivatives were collected with Tenax TA and Au–Pt tubes. After preheating the Tenax TA tube to 250°C for 45 s, it was purged with 100 mL min^{-1} of He for 5 s, allowing efficient injection of the vapor enriched with Hg species from the Tenax TA tubes to the GC for separation. Determination of Hg^0 in natural samples based on collection on Au–Pt tubes in series with Tenax TA provided a detection limit of 0.8 ng m^{-3} , which is about two times lower than the reported atmospheric background concentrations of total gaseous mercury. The developed method was successfully applied for measuring gaseous mercury in the emission from sediment samples.

16.5.2 Biological applications

16.5.2.1 Plants and microbes

Plants and microbes have been very popular materials for analysis in the field of elemental speciation. A number of studies have been devoted to elucidating the biotransformation of various elements whose species are of great interest in toxicology, nutrition, biology, and environmental science [55]. Furthermore, plants and microbes are relatively easy to grow and the growth conditions can be readily manipulated. For instance, nutrient supplementation in the soil of plants is a common strategy for making certain element-enriched samples.

Selenium speciation in plants and yeast has been a popular topic since the 1990s when Se was suggested as a chemopreventive agent because of Se supplementation reducing cancer incidence in a clinical trial [56]. Although Se's

anticancer effect is not totally understood, the study of Se biotransformation in plants and yeasts has been well established. Previous studies have shown that plants and microbes are able to make volatile Se species, selenoamino acids, selenopeptides, and some high-molecular-weight selenium from inorganic selenium supplementation [57]. GC-ICPMS has been a common technique for studying selenium transformation in plants and microbes. Usually, the samples are grown in Se-enriched media, allowing them to uptake selenium. The selenium species are extracted and then determined by GC or LC-ICPMS. B'Hymer et al. reviewed these studies [58]. Headspace-SPME GC-ICPMS was used for determining volatile selenium compounds (DMSe and DMDSe), whose vapors are emitted from plants such as *Brassica juncea* [59]. The same selenium volatiles were measured in microbes by a cryotrapping cryofocusing GC-ICPMS system (CT-CF-GC-ICPMS) [60]. For nonvolatile selenium metabolites in plants, ion-pairing RP is the dominant separation method and was shown to provide high-resolution separations as well as high sensitivity ($\text{LOQ } 2\text{--}50\text{ }\mu\text{g L}^{-1}$) when coupled to ICPMS [61]. Recently, structural characterization with tandem MS (MS , MS^2 , and MS^3) was achieved for selenium metabolites in plants: selenomethionine (SeMet) in soybean [62] and methylselenocysteine (MeSeCys) in kale [62]. The spectra obtained with ESI-ITMS offered a clear identification, which is essential for analysis of complicated samples such as plant extracts.

16.5.2.2 Body fluids

Speciation of trace elements in body fluids not only facilitates elucidation of their metabolic or detoxification pathways, but also helps in identifying biomarkers or certain proteins that are related to some diseases. For example, the species of Hg and As in blood cause much concern because of their toxicity. On the other hand, glutathione peroxidase (a selenium-containing protein) is important to the functioning of the

immune system and to the inflammatory process, and its level in blood is related to some diseases.

GC-ICPMS has also been applied to blood samples for speciation of elements such as mercury and phosphorus. The blood samples from a group of mercury-exposed workers were analyzed for methylmercury using a combined GC-EI-MS/ICPMS system, allowing the sensitive detection of mercury (ICPMS) and simultaneous structure characterization by EI-MS [63]. Methylmercury was extracted and then derivatized with sodium tetra-*n*-ethylborate solution. The limit of quantification was 300 ng L⁻¹ for ICPMS detection, lower than 500 ng L⁻¹ for EI-MS. Phosphoric acid triesters in human plasma samples were determined by monitoring phosphorous with GC-ICPMS [64]. Alkyl and aryl phosphates were extracted and preconcentrated by direct immersion SPME with 65 μm poly(dimethylsiloxane/divinylbenzene) fiber. The detection limits from blood plasma were 17–240 ng L⁻¹ for tripropyl phosphate, tributyl phosphate, tris(2-chloroethyl) phosphate, and triphenyl phosphate, whose molecular structures were elucidated by GC-TOF-MS.

16.5.2.3 Urine

Many metabolites of trace elements passed through body fluids, such as blood, are finally excreted by urination; hence, determining the elemental species present in urine can provide valuable metabolic information in terms of their toxicity or health benefits. LC-ICPMS has been commonly used for elemental speciation in urine samples.

As an essential element for human health, selenium has caught much attention. Elucidation of selenium metabolism is of high importance to understanding Se's health effects as well as identifying better Se supplementation compounds. Three stable-isotope labeled Se compounds, ⁷⁶Se-selenomethionine (SeMet), ⁷⁷Se-methylselenocysteine (MeSeCys), and ⁸²Se-methylseleninic acid (MSA), were orally

administered to rats, and their metabolites in urine and breath were determined by LC-ICPMS and GC-ICPMS [65]. By comparing the quantity of different isotopes in the metabolites, this study revealed that the three Se species produced similar amount of selenosugars but SeMet generated much less dimethylselenide (DMSe) in breath and trimethyl selenium (TMSe) in urine than the other two. Since DMSe and TMSe are the main metabolites of methylselenol, which is considered to be responsible (at least as a precursor) for the cancer chemopreventive effects of Se, the authors suggest urinary TMSe and exhaled DMSe as biomarkers for production of effective anticancer Se species. The authors were able to distinguish exogenous isotope-enriched Se from endogenous natural Se, and the quantitative speciation of Se was achieved by isotope pattern deconvolution.

16.5.2.4 Food

Many elements are known as essential nutrients while others are considered as toxicants. Regardless of whether an element is nutritional or toxic or both, the actual nutritional value or toxicity highly depends on its specific chemical form(s) because they vary a lot from one species to another. For example, As(III) and As(V) are carcinogens while arsenobetaine (AsB) is relatively nontoxic. Therefore, a proper analysis with elemental speciation is necessary to evaluate food safety or nutritional values. The speciation studies have been carried out with GC-ICPMS, GC-MIP-AES, and other hyphenated techniques.

Seafood provides a prime source of high-quality protein: 14%–16% of the animal protein consumed worldwide; over 1 billion people rely on seafood as their primary source of animal protein. The bioaccumulation of arsenic and mercury in seafood has been a big concern in terms of food safety. Because the toxicity of arsenic and mercury is tightly associated to their particular chemical forms, their speciation in seafood has been a hot topic for decades. The common arsenic species

found in seafood include arsenite (As(III)), arsenate As(V), monomethylarsonate (MMA), dimethylarsinate (DMA), arsenobetaine (AB), and arsenosugars. The primary mercury species include inorganic mercury and methylmercury. The bioaccessibility of the accumulated arsenic and mercury compounds was also evaluated by simulating the digestion in a gastrointestinal environment [66].

GC-ICPMS and GC-MIP-AES offer excellent sensitivity for mercury speciation in fish tissues. The main analytes of interests are the common toxic mercury compounds, methylmercury, and inorganic mercury. Either species-specific or species-unspecific isotope dilution is usually employed to obtain accurate quantification [67]. Yang et al. determined methylmercury in fish tissues using GC-ICPMS with species-specific isotope dilution, in which an in-house synthesized ^{198}Hg -enriched methylmercury was used as the spike [68]. The samples were digested with methanolic potassium hydroxide, derivatized in aqueous solution with sodium tetrapropylborate and headspace sampled with a polydimethylsiloxane-coated, SPME fused-silica fiber. The isotope dilution method was compared with a standard addition method, and it showed nearly fourfold precision enhancement over the other method.

16.6 Conclusions and perspectives

GC and plasma spectroscopy are both well-developed techniques for elemental speciation. They offer unmatched detection limits, as low as ppt level for species of a variety of elements, as well as high-resolution separation. The analytes vary from volatile gases to semivolatile compounds in a wide variety of matrices, such as water, soil, plants, and animals. This chapter has demonstrated the rapid growth of the GC-ICPMS hyphenated technique in the science community. This advancement includes better sensitivity, new sample preparation procedures,

as well as innovative detection methods. Although GC-ICPMS has become a powerful technique for elemental speciation, the new challenges rising from novel applications often require complementary techniques such as molecular MS. GC with both detections of ICPMS and molecular MS, either offline or parallel, has been increasingly popular in modern elemental speciation and is dubbed by some as “a metallo-mics approach.”

References

- [1] J.S. Becker (Ed.), *Inorganic Mass Spectrometry: Principles and Applications*, John Wiley & Sons, Ltd, Chichester, UK, 2007.
- [2] K. Iwasaki, H. Uchida, K. Tanaka, Rapid determination of the alloying elements in titanium alloys by inductively-coupled plasma emission spectrometry, *Anal. Chim. Acta* 135 (2) (1960) 369–372.
- [3] M. Montes-Bayón, K. DeNicola, J.A. Caruso, Liquid chromatography-inductively coupled plasma mass spectrometry, *J. Chromatogr. A* 1000 (1–2) (2003) 457–476.
- [4] K.L. Sutton, J.A. Caruso, Liquid chromatography-inductively coupled plasma mass spectrometry, *J. Chromatogr. A* 856 (1–2) (1999) 243–258.
- [5] S.S. Kannamkumarath, et al., Capillary electrophoresis-inductively coupled plasma-mass spectrometry: an attractive complementary technique for elemental speciation analysis, *J. Chromatogr. A* 975 (2) (2002) 245–266.
- [6] R.K. Marcus, J.A.C. Broekaert (Eds.), *Glow Discharge Plasmas in Analytical Spectroscopy*, John Wiley & Sons Inc., West Sussex, England, 2003.
- [7] L.K. Olson, M. Belkin, J.A. Caruso, Radiofrequency glow discharge mass spectrometry for gas chromatographic detection: a new departure for elemental speciation studies, *J. Anal. At. Spectrom.* 11 (7) (1996) 491–496.
- [8] N.G. Orellana-Velado, R. Pereiro, A. Sanz-Medel, Glow discharge atomic emission spectrometry as a detector in gas chromatography for mercury speciation, *J. Anal. At. Spectrom.* 13 (9) (1998) 905–909.
- [9] A. Solà -Vázquez, et al., Tuneable microsecond-pulsed glow discharge design for the simultaneous acquisition of elemental and molecular chemical information using a time-of-flight mass spectrometer, *Anal. Chem.* 81 (7) (2009) 2591–2599.

- [10] A.L. Gray, A.R. Date, Plasma source mass spectrometry of inorganic samples - recent developments of the technique, *Int. J. Mass Spectrom. Ion Phys.* 46 (1983) 7–10.
- [11] S.F. Boulyga, J.S. Becker, Improvement of abundance sensitivity in a quadrupole-based ICP-MS instrument with a hexapole collision cell, *J. Anal. At. Spectrom.* 17 (9) (2002) 1202–1206.
- [12] S.D. Tanner, V.I. Baranov, D.R. Bandura, Reaction cells and collision cells for ICP-MS: a tutorial review, *Spectrochim. Acta Part B At. Spectrosc.* 57 (9) (2002) 1361–1452.
- [13] B. Hattendorf, C. Latkoczy, D. Günther, Laser ablation-ICPMS, *Anal. Chem.* 75 (15) (2003) 341A–347A.
- [14] J.R. Encinar, J.I. García Alonso, A. Sanz-Medel, Synthesis and application of isotopically labelled dibutyltin for isotope dilution analysis using gas chromatography-ICP-MS, *J. Anal. At. Spectrom.* 15 (9) (2000) 1233–1240.
- [15] J.P. Snell, et al., Species specific isotope dilution calibration for determination of mercury species by gas chromatography coupled to inductively coupled plasma- or furnace atomisation plasma ionisation-mass spectrometry, *J. Anal. At. Spectrom.* 15 (12) (2000) 1540–1545.
- [16] D.A. Rogers, S.J. Ray, G.M. Hieftje, An electrospray/inductively coupled plasma dual-source time-of-flight mass spectrometer for rapid metallomic and speciation analysis: instrument design, *Metallomics* 1 (1) (2009) 67–77.
- [17] D.A. Rogers, S.J. Ray, G.M. Hieftje, An electrospray/inductively coupled plasma dual-source time-of-flight mass spectrometer for rapid metallomic and speciation analysis. Part 1. Molecular channel characterization, *Metallomics* 2 (2010) 271–279.
- [18] A. Sol-Vázquez, et al., Gas chromatography coupled to tunable pulsed glow discharge time-of-flight mass spectrometry for environmental analysis, *Analyst* 135 (5) (2010) 987–993.
- [19] B. Bouysiere, J. Szpunar, R. Lobinski, Gas chromatography with inductively coupled plasma mass spectrometric detection in speciation analysis, *Spectrochim. Acta Part B At. Spectrosc.* 57 (5) (2002) 805–828.
- [20] J.C.A. Wuilloud, et al., Gas chromatography/plasma spectrometry – an important analytical tool for elemental speciation studies, *Spectrochim. Acta Part B At. Spectrosc.* 59 (6) (2004) 755–792.
- [21] G. Centineo, et al., Isotope dilution GC-MS routine method for the determination of butyltin compounds in water, *Anal. Bioanal. Chem.* 384 (4) (2006) 908–914.
- [22] R. Lobinski, F.C. Adams, Recent advances in speciation analysis by capillary gas chromatography-microwave induced plasma atomic emission spectrometry, *Trends Anal. Chem.* 12 (2) (1993) 41–49.
- [23] W. Robbins, J. Caruso, F. Fricke, Determination of Ge, As, Se, Sn, and Sb in complex samples by hydride generation microwave induced plasma atomic emission spectrometry, *Analyst* 104 (1979) 3535.
- [24] N.G. Orellana Velado, R. Pereiro, A. Sanz-Medel, Mercury speciation by capillary gas chromatography with radiofrequency hollow cathode glow discharge atomic emission detection, *J. Anal. At. Spectrom.* 15 (1) (2000) 49–53.
- [25] M.A. Belkin, L.K. Olson, J.A. Caruso, Radiofrequency glow discharge as an ion source for gas chromatography with mass spectrometric detection, *J. Anal. At. Spectrom.* 12 (11) (1997) 1255–1261.
- [26] S. Risticvic, et al., Recent developments in solid-phase microextraction, *Anal. Bioanal. Chem.* 393 (3) (2009) 781–795.
- [27] F. Sánchez-Rojas, C. Bosch-Ojeda, J.M. Cano-Pavón, A review of stir bar sorptive extraction, *Chromatographia* 69 (Suppl. 1) (2009).
- [28] Y. Wang, J. McCaffrey, D.L. Norwood, Recent advances in headspace gas chromatography, *J. Liq. Chromatogr. Relat. Technol.* 31 (11–12) (2008) 1823–1851.
- [29] J. Meija, et al., Monitoring volatile selenium and sulfur species from Se accumulating plants (wild type and genetically modified) by GC-MS and GC-ICP-MS using SPME for sample introduction, *Anal. Chem.* 74 (2002) 5837–5844.
- [30] S. Díez, J.M. Bayona, Trace element determination by combining solid-phase microextraction hyphenated to elemental and molecular detection techniques, *J. Chromatogr. Sci.* 44 (7) (2006) 458–471.
- [31] B. Kolb, Headspace sampling with capillary columns, *J. Chromatogr. A* 842 (1–2) (1999) 163–205.
- [32] E.M. Krupp, et al., Investigation into the determination of trimethylarsine in natural gas and its partitioning into gas and condensate phases using (cryotrapping)/gas chromatography coupled to inductively coupled plasma mass spectrometry and liquid/solid sorption techniques, *Spectrochim. Acta Part B At. Spectrosc.* 62 (9) (2007) 970–977.
- [33] D. Kremer, G. Ilgen, J. Feldmann, GC-ICP-MS determination of dimethylselenide in human breath after ingestion of ⁷⁷Se-enriched selenite: monitoring of in vivo methylation of selenium, *Anal. Bioanal. Chem.* 383 (3) (2005) 509–515.
- [34] S. Wehmeier, A. Raab, J. Feldmann, Investigations into the role of methylcobalamin and glutathione for the methylation of antimony using isotopically enriched antimony(V), *Appl. Organomet. Chem.* 18 (12) (2004) 631–639.
- [35] R. Morabito, P. Massaniso, P. Quevauviller, Derivatization methods for the determination of organotin compounds in environmental samples, *TrAC Trends Anal. Chem.* 19 (2–3) (2000) 113–119.

- [36] D.D. Richardson, J.A. Caruso, Derivatization of organophosphorus nerve agent degradation products for gas chromatography with ICPMS and TOF-MS detection, *Anal. Bioanal. Chem.* 388 (4) (2007) 809–823.
- [37] M. Dzurko, D. Foucher, H. Hintelmann, Determination of compound-specific Hg isotope ratios from transient signals using gas chromatography coupled to multicollector inductively coupled plasma mass spectrometry (MC-ICP/MS), *Anal. Bioanal. Chem.* 393 (1) (2009) 345–355.
- [38] P. Pohl, Hydride generation – recent advances in atomic emission spectrometry, *TrAC Trends Anal. Chem.* 23 (2) (2004) 87–101.
- [39] M. Popp, S. Hann, G. Koellensperger, Environmental application of elemental speciation analysis based on liquid or gas chromatography hyphenated to inductively coupled plasma mass spectrometry—a review, *Anal. Chim. Acta* 668 (2) (2010) 114–129.
- [40] UN, The 2nd United Nations World Water Development Report: Water, a Shared Responsibility, 2006.
- [41] T.F.M. Etty, et al., *Yearbook of European Environmental Law*, vol. 5, Oxford University Press, 2005.
- [42] P. Rodríguez-González, et al., Determination of butyltin compounds in coastal sea-water samples using isotope dilution GC-ICP-MS, *J. Anal. At. Spectrom.* 17 (8) (2002) 824–830.
- [43] G.A. Zachariadis, E. Rosenberg, Speciation of organotin compounds in urine by GC-MIP-AED and GC-MS after ethylation and liquid-liquid extraction, *J. Chromatogr. B Analyt. Technol. Biomed. Life Sci.* 877 (11–12) (2009) 1140–1144.
- [44] Q. Xiao, B. Hu, M. He, Speciation of butyltin compounds in environmental and biological samples using headspace single drop microextraction coupled with gas chromatography-inductively coupled plasma mass spectrometry, *J. Chromatogr. A* 1211 (1–2) (2008) 135–141.
- [45] B. Jackson, et al., Low-level mercury speciation in freshwaters by isotope dilution GC-ICP-MS, *Environ. Sci. Technol.* 43 (7) (2009) 2463–2469.
- [46] N. Fidalgo-Used, et al., Determination of organophosphorus pesticides in spiked river water samples using solid phase microextraction coupled to gas chromatography with EI-MS and ICP-MS detection, *J. Anal. At. Spectrom.* 20 (9) (2005) 876–882.
- [47] S. Slaets, F. Laturus, F.C. Adams, Microwave induced plasma atomic emission spectrometry: a suitable detection system for the determination of volatile halocarbons, *Fresenius' J. Anal. Chem.* 364 (1–2) (1999) 133–140.
- [48] G.M.M. Rahman, H.M. Kingston, Development of a microwave-assisted extraction method and isotopic validation of mercury species in soils and sediments, *J. Anal. At. Spectrom.* 20 (3) (2005) 183–191.
- [49] S.J. Kumar, et al., A simple method for synthesis of organotin species to investigate extraction procedures in sediments by isotope dilution-gas chromatography-inductively coupled plasma mass spectrometry part 2. Phenyltin species, *J. Anal. At. Spectrom.* 19 (3) (2004) 368–372.
- [50] K. Inagaki, et al., Certification of butyltins and phenyltins in marine sediment certified reference material by species-specific isotope-dilution mass spectrometric analysis using synthesized ^{118}Sn -enriched organotin compounds, *Anal. Bioanal. Chem.* 387 (7) (2007) 2325–2334.
- [51] F. Bianchi, et al., Optimization of the solid phase microextraction procedure for the ultra-trace determination of organotin compounds by gas chromatography-inductively coupled plasma-mass spectrometry, *J. Anal. At. Spectrom.* 21 (9) (2006) 970–973.
- [52] K. Inagaki, et al., Species-specific isotope dilution analysis of mono-, di-, and tri-butyltin compounds in sediment using gas chromatography-inductively coupled plasma mass spectrometry with synthesized ^{118}Sn -enriched butyltins, *Analyst* 128 (3) (2003) 265–272.
- [53] M.P. Pavageau, et al., Phosphine emission measurements from a tobacco factory using cryogenic sampling and GC-ICP-MS analysis, *J. Anal. At. Spectrom.* 18 (4) (2003) 323–329.
- [54] T. Larsson, E. Bjorn, W. Frech, Species specific isotope dilution with on line derivatisation for determination of gaseous mercury species, *J. Anal. At. Spectrom.* 20 (11) (2005) 1232–1239.
- [55] S. Husted, et al., Review: the role of atomic spectrometry in plant science, *J. Anal. At. Spectrom.* 26 (1) (2011) 52–79.
- [56] L.C. Clark, et al., Effects of selenium supplementation for cancer prevention in patients with carcinoma of the skin: a randomized controlled trial, *J. Am. Med. Assoc.* 276 (24) (1996) 1957–1963.
- [57] N. Terry, et al., Selenium in higher plants, *Annu. Rev. Plant Physiol. Plant Mol. Biol.* 51 (2000) 401–432.
- [58] C. B'Hymer, J.A. Caruso, Selenium speciation analysis using inductively coupled plasma-mass spectrometry, *J. Chromatogr. A* 1114 (1) (2006) 1–20.
- [59] K.M. Kubachka, et al., Selenium volatiles as proxy to the metabolic pathways of selenium in genetically modified *Brassica juncea*, *Environ. Sci. Technol.* 41 (6) (2007) 1863–1869.
- [60] M. Peitzsch, D. Kremer, M. Kersten, Microfungal alkylation and volatilization of selenium adsorbed by goethite, *Environ. Sci. Technol.* 44 (1) (2010) 129–135.
- [61] M. Kotrebai, et al., Selenium speciation in enriched and natural samples by HPLC-ICP-MS and HPLC-ESI-MS with perfluorinated carboxylic acid ion-pairing agents, *Analyst* 125 (1) (2000) 71–78.

- [62] Q. Chan, S.E. Afton, J.A. Caruso, Selenium speciation profiles in selenite-enriched soybean (*Glycine max*) by HPLC-ICPMS and ESI-ITMS, *Metallomics* 2 (2) (2010) 147–153.
- [63] J. Hippler, et al., Comparative determination of methyl mercury in whole blood samples using GC-ICP-MS and GC-MS techniques, *J Chromatogr B Analyt. Technol. Biomed. Life Sci.* 877 (24) (2009) 2465–2470.
- [64] S. Mounicou, et al., Localization and speciation of selenium and mercury in *Brassica juncea* – implications for Se-Hg antagonism, *J. Anal. At. Spectrom.* 21 (4) (2006) 404–412.
- [65] Y. Ohta, et al., Speciation analysis of selenium metabolites in urine and breath by HPLC- and GC-inductively coupled plasma-MS after administration of selenomethionine and methylselenocysteine to rats, *Chem. Res. Toxicol.* 22 (11) (2009) 1795–1801.
- [66] A.I. Cabañero, Y. Madrid, C. Cámara, Selenium and mercury bioaccessibility in fish samples: an in vitro digestion method, *Anal. Chim. Acta* 526 (1) (2004) 51–61.
- [67] J.I. García Alonso, et al., Determination of butyltin compounds in environmental samples by isotope dilution GC-ICP-MS, *Anal. Bioanal. Chem.* 373 (6) (2002) 432–440.
- [68] L. Yang, Z. Mester, R.E. Sturgeon, Determination of methylmercury in fish tissues by isotope dilution SPME-GC-ICP-MS, *J. Anal. At. Spectrom.* 18 (5) (2003) 431–436.
- [69] P. Rodriguez-Gonzalez, J.I.G. Alonso, A. Sanz-Medel, Development of a triple spike methodology for validation of butyltin compounds speciation analysis by isotope dilution mass spectrometry—Part 2. Study of different extraction procedures for the determination of butyltin compounds in mussel tissue CRM 477, *J. Anal. At. Spectrom.* 19 (6) (2004) 767–772.
- [70] L. Lambertsson, E. Bjorn, Validation of a simplified field-adapted procedure for routine determinations of methyl mercury at trace levels in natural water samples using species-specific isotope dilution mass spectrometry, *Anal. Bioanal. Chem.* 380 (7–8) (2004) 871–875.
- [71] R.C. Rodriguez Martin-Doimeadios, et al., Using speciated isotope dilution with GC-inductively coupled plasma MS to determine and unravel the artificial formation of monomethylmercury in certified reference sediments, *Anal. Chem.* 75 (13) (2003) 3202–3211.
- [72] D. Point, et al., Simultaneous determination of inorganic mercury, methylmercury, and total mercury concentrations in cryogenic fresh-frozen and freeze-dried biological reference materials, *Anal. Bioanal. Chem.* 389 (3) (2007) 787–798.
- [73] T. Karlsson, U. Skyllberg, Bonding of ppb levels of methyl mercury to reduced sulfur groups in soil organic matter, *Environ. Sci. Technol.* 37 (21) (2003) 4912–4918.
- [74] M.V. Pelaez, et al., Comparison of different derivatization approaches for the determination of selenomethionine by GC-ICP-MS, *J. Anal. At. Spectrom.* 15 (9) (2000) 1217–1222.
- [75] H.G. Infante, et al., Investigation of the selenium species distribution in a human B-cell lymphoma line by HPLC- and GC-ICP-MS in combination with HPLC-ESIMS/MS and GC-TOFMS after incubation with methylseleninic acid, *J. Anal. At. Spectrom.* 22 (8) (2007) 888–896.
- [76] J. Rodriguez-Fernandez, et al., Gas chromatography double focusing sector-field ICP-MS as an innovative tool for bad breath research, *J. Anal. At. Spectrom.* 16 (9) (2001) 1051–1056.
- [77] J. Heilmann, K.G. Heumann, Development of a species-specific isotope dilution GC-ICP-MS method for the determination of thiophene derivatives in petroleum products, *Anal. Bioanal. Chem.* 390 (2) (2008) 643–653.
- [78] D. Profrock, et al., Sensitive, simultaneous determination of P, S, Cl, Br and I containing pesticides in environmental samples by GC hyphenated with collision-cell ICP-MS, *J. Anal. At. Spectrom.* 19 (5) (2004) 623–631.
- [79] S. Junyapoon, et al., Analysis of malodorous sulfur gases and volatile organometalloid compounds in landfill gas emissions using capillary gas chromatography with programmed temperature vaporization injection and atomic emission detection, *Int. J. Environ. Anal. Chem.* 82 (2) (2002) 47–59.
- [80] M. Garcia-Lopez, et al., Determination of organophosphate flame retardants and plasticizers in sediment samples using microwave-assisted extraction and gas chromatography with inductively coupled plasma mass spectrometry, *Talanta* 79 (3) (2009) 824–829.
- [81] Q. Xiao, et al., Analysis of PBDEs in soil, dust, spiked lake water, and human serum samples by hollow fiber-liquid phase microextraction combined with GC-ICP-MS, *J. Am. Soc. Mass Spectrom.* 18 (10) (2007) 1740–1748.
- [82] R.F. Swarthout Jr., J.R. Kucklick, W.C. Davis, The determination of polybrominated diphenyl ether congeners by gas chromatography inductively coupled plasma mass spectrometry, *J. Anal. At. Spectrom.* 23 (12) (2008) 1575–1580.
- [83] A. Schwarz, K.G. Heumann, Two-dimensional on-line detection of brominated and iodinated volatile organic compounds by ECD and ICP-MS after GC separation, *Anal. Bioanal. Chem.* 374 (2) (2002) 212–219.

- [84] T. Guerin, et al., Arsenic speciation in some environmental samples: a comparative study of HG-GC-QFAAS and HPLC-ICP-MS methods, *Appl. Organomet. Chem.* 14 (8) (2000) 401–410.
- [85] B. Bouyssiére, et al., Investigation of speciation of arsenic in gas condensates by capillary gas chromatography with ICP-MS detection, *J. Anal. At. Spectrom.* 16 (11) (2001) 1329–1332.
- [86] N. Poperechna, K.G. Heumann, Simultaneous multi-species determination of trimethyllead, monomethylmercury and three butyltin compounds by species-specific isotope dilution GC-ICP-MS in biological samples, *Anal. Bioanal. Chem.* 383 (2) (2005) 153–159.
- [87] Z. Mester, R.E. Sturgeon, J.W. Lam, Sampling and determination of metal hydrides by solid phase microextraction thermal desorption inductively coupled plasma mass spectrometry, *J. Anal. At. Spectrom.* 15 (11) (2000) 1461–1465.
- [88] R. Miravet, et al., Speciation of antimony in environmental matrices by coupled techniques, *TrAC Trends Anal. Chem.* 29 (1) (2010) 28–39.
- [89] S. Wehmeier, J. Feldmann, Investigation into antimony mobility in sewage sludge fermentation, *J. Environ. Monit.* 7 (12) (2005) 1194–1199.
- [90] R.G. Wuilloud, et al., Determination of iodinated phenol species at parts-per-trillion concentration levels in different water samples by solid-phase microextraction/offline GC-ICP-MS, *J. Anal. At. Spectrom.* 18 (9) (2003) 1119–1124.
- [91] D.F. Hagen, J. Belisle, J.S. Marhevska, Capillary GC/helium microwave emission detector characterization of fluorine containing metabolites in blood plasma, *Spectrochim. Acta Part B At. Spectrosc.* 38 (1–2) (1983) 377–385.
- [92] H. Baumann, K.G. Heumann, Analysis of organobromine compounds and HBr in motor car exhaust gases with a GC/microwave plasma system, *Fresenius Z. Anal. Chem.* 327 (2) (1987) 186–192.
- [93] J.P.J. van Dalen, P.A. de Lezenne Coulander, L. de Galan, Optimization of the microwave-induced plasma as an element-selective detector for non-metals, *Anal. Chim. Acta* 94 (1) (1977) 1–19.
- [94] J. Carpinteiro Botana, et al., Fast and simultaneous determination of tin and mercury species using SPME, multicapillary gas chromatography and MIP-AES detection, *J. Anal. At. Spectrom.* 17 (8) (2002) 904–907.
- [95] W. Frech, J.P. Snell, R.E. Sturgeon, Performance comparison between furnace atomisation plasma emission spectrometry and microwave induced plasma-atomic emission spectrometry for the determination of mercury species in gas chromatography effluents, *J. Anal. At. Spectrom.* 13 (12) (1998) 1347–1353.
- [96] S. Tutschku, M.M. Schantz, S.A. Wise, Determination of methylmercury and butyltin compounds in marine biota and sediments using microwave-assisted acid extraction, solid-phase microextraction, and gas chromatography with microwave-induced plasma atomic emission spectrometric detection, *Anal. Chem.* 74 (18) (2002) 4694–4701.
- [97] C. Dietz, et al., Volatile organo-selenium speciation in biological matter by solid phase microextraction-moderate temperature multicapillary gas chromatography with microwave induced plasma atomic emission spectrometry detection, *Anal. Chim. Acta* 501 (2) (2004) 157–167.
- [98] A. Delgado, et al., Production of artifact methylmercury during the analysis of certified reference sediments: use of ionic exchange in the sample treatment step to minimise the problem, *Anal. Chim. Acta* 582 (1) (2007) 109–115.
- [99] M. Zabaljauregui, et al., Fast method for routine simultaneous analysis of methylmercury and butyltins in seafood, *J. Chromatogr. A* 1148 (1) (2007) 78–85.
- [100] M. Heisterkamp, F.C. Adams, Simplified derivatization method for the speciation analysis of organolead compounds in water and peat samples using in-situ butylation with tetrabutylammonium tetrabutylborate and GC-MIP AES, *Fresenius' J. Anal. Chem.* 362 (5) (1998) 489–493.
- [101] I.R. Pereiro, R. Łobiński, Fast species-selective screening for organolead compounds in gasoline by multicapillary gas chromatography with microwave-induced plasma atomic emission detection, *J. Anal. At. Spectrom.* 12 (12) (1997) 1381–1385.
- [102] M. Heisterkamp, F.C. Adams, In situ propylation using sodium tetrapropylborate as a fast and simplified sample preparation for the speciation analysis of organolead compounds using GC-MIP-AES, *J. Anal. At. Spectrom.* 14 (9) (1999) 1307–1311.
- [103] J.R. Baena, et al., Comparison of three coupled gas chromatographic detectors (MS, MIP-AES, ICP-TOFMS) for organolead speciation analysis, *Anal. Chem.* 73 (16) (2001) 3927–3934.
- [104] E. Dimitrakakis, et al., Solid-phase microextraction-capillary gas chromatography combined with microwave-induced plasma atomic-emission spectrometry for selenite determination, *Anal. Bioanal. Chem.* 379 (5–6) (2004) 842–848.
- [105] S. Tutschku, S. Mothes, K. Dittrich, Determination and speciation of organotin compounds by gas chromatography – microwave induced plasma atomic emission spectrometry, *J. Chromatogr. A* 683 (1) (1994) 269–276.

- [106] S. Girousi, et al., Speciation analysis of organotin compounds in Thermaikos Gulf by GC-MIP-AED, *Frese-nius' J. Anal. Chem.* 358 (7–8) (1997) 828–832.
- [107] S. Aguerre, et al., Speciation of organotins in environmental samples by SPME-GC: comparison of four specific detectors: FPD, PFPD, MIP-AES and ICP-MS, *J. Anal. At. Spectrom.* 16 (3) (2001) 263–269.
- [108] N. Campillo, R. Peñalver, M. Hernández-Córdoba, Solid-phase microextraction combined with gas chromatography and atomic emission detection for the determination of cyclopentadienylmanganese tricarbonyl and (methylcyclopentadienyl)manganese tricarbonyl in soils and seawaters, *J. Chromatogr. A* 1173 (1–2) (2007) 139–145.
- [109] U. Arroyo-Abad, et al., Detection of arsenic-containing hydrocarbons in canned cod liver tissue, *Talanta* 82 (1) (2010) 38–43.

Field and portable instruments for gas chromatography

Stanley D. Stearns

Valco Instruments Co. Inc, Houston, TX, United States

17.1 History

Although space instrumentation is discussed in a separate chapter, the history of portable gas chromatography (GC) cannot be discussed without referencing America's pioneering space programs. In 1963, W. F. Wilhite (with acknowledgments to V. I. Oyama of the Jet Propulsion Laboratory, Dr. S. R. Lipsky of Yale University, and Dr. J. E. Lovelock of Baylor University) reported the results of a prototype GC designed to be soft-landed on the surface of the moon as part of the Surveyor scientific payload [1].

Wilhite followed this in 1966 with a subminiaturized GC weighing approximately 100 g, capable of separating gases in a few seconds with a carrier gas flow of 1 mL per minute. This GC was designed to "analyze the atmosphere of Mars in a few seconds during the descent of a landing capsule" [2].

In 1969, Josias, Bowman, and Lovelock applied for a patent on a portable GC using an electron-capture detector [3]. At about the same time, Wilhite founded Aptech, incorporating JPL technologies in the first commercial micro GC. The instrument (Fig. 17.1) used micropacked columns

with an early Valco 10 port valve and a TCD with a 0.0001" straight filament. After the company was sold to a larger firm more interested in older technology, the techniques and components employed in the Aptech GC led, in the early 1970s, to the production of a high-speed in vivo blood gas analyzer, which sampled microliter quantities of gas from an interarterial silicone catheter (Figs. 17.2 and 17.3).

In 1972, a group at the Jet Propulsion Laboratory demonstrated a completely portable, self-contained GC that generated its own H₂ carrier gas from a water supply [4]. But not all of the ongoing research and development was related to the nation's space efforts. Valco Instruments delivered its first portable GC, the Model 1000 Halocarbon Monitor, in 1972 (Fig. 17.4). The Model 1000 measured the concentration of a chlorofluorocarbon (CFC) tracer gas introduced upstream and downstream of a charcoal filter bed in a nuclear reactor facility. A ppm level of the tracer challenged the filter with the downstream flow measured at the ppb level. The linear range of the H₂³ source was extended by sample μL 's upstream and cc's downstream. The same peak height could be found with a 50 ppm

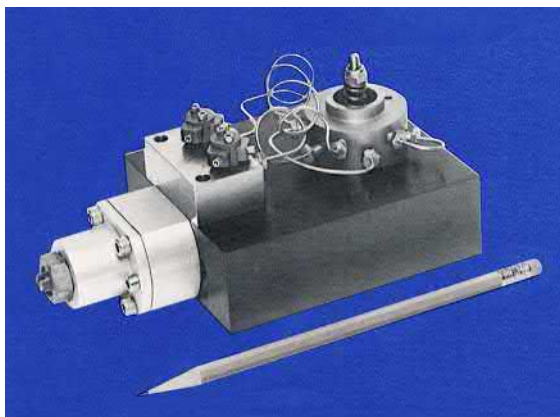


FIGURE 17.1 Aptech micro gas chromatograph. Courtesy of Frank Wilhite.

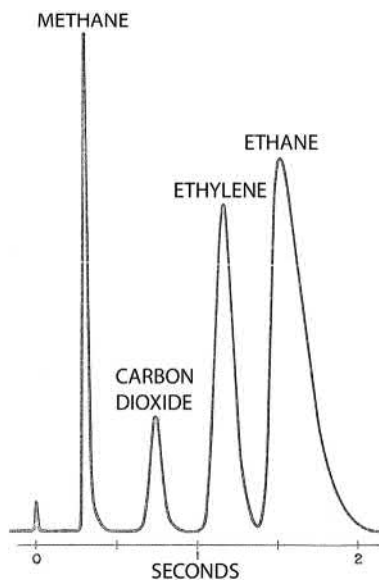


FIGURE 17.2 Aptech micro gas chromatograph analysis of light gases. Column: $3'' \times 0.023''$ ID, $40\text{--}56\ \mu$ Porapak S, ambient temperature; carrier: helium at $6.7\ \text{mL min}^{-1}$; sample size: $1\ \mu\text{L}$. Courtesy of Frank Wilhite.

upstream concentration and 50 ppb downstream concentration.

A 1973 publication cites the Analytical Instrument Development Model 510, featuring an ECD with 5% methane in argon as the carrier gas. The Model 510 had rechargeable batteries sufficient to operate the electrometer and detector

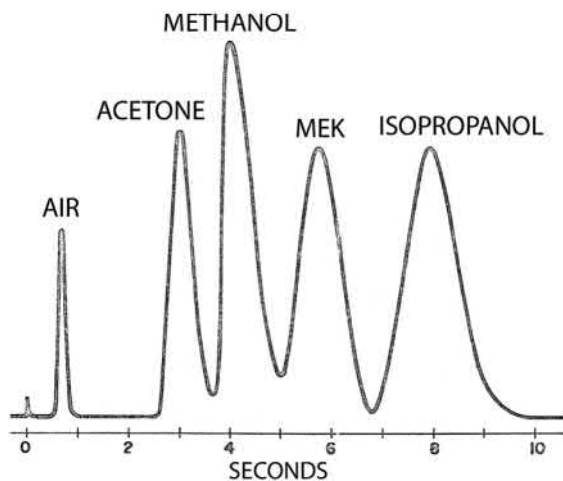


FIGURE 17.3 Aptech micro gas chromatograph analysis of oxygenates. Column: $5'' \times 0.023''$ ID, $36\text{--}75\ \mu$ Porasil 60, 75°C ; carrier: helium; sample size: $1\ \mu\text{L}$ (gas); inlet pressure: 40 psi. Courtesy of Frank Wilhite.

for more than 10 h. Line voltage was required for the Varian 7 port solenoid-actuated sampling valve, Honeywell recorder, and positive-displacement sampling valve [5].

Fig. 17.5 shows Valco's 1975 prototype flyable GC for the detection of stratospheric CFCs and N_2O . The instrument was packaged in a purged enclosure with an absolute pressure regulator. The very low N_2O response with N_2 carrier led to the conclusion that impurities in carrier gas and lab GC system leaks accounted for the N_2O response.

James Morgan patented a portable GC for transformer gas analysis in 1977 [6]. (Fig. 17.6) Polymer tubes isolated dissolved gases from transformer oil, which were then injected into a packed column using air as carrier gas. H_2 was measured with a thermal conductivity detector (TCD). The first commercial version was manufactured for more than 25 years.

Also in the late 1970s, Photovac introduced the first portable GC with a photoionization detector (PID), followed by HNu, whose founder, Jack Driscoll, was the inventor of the lamp-type PID.

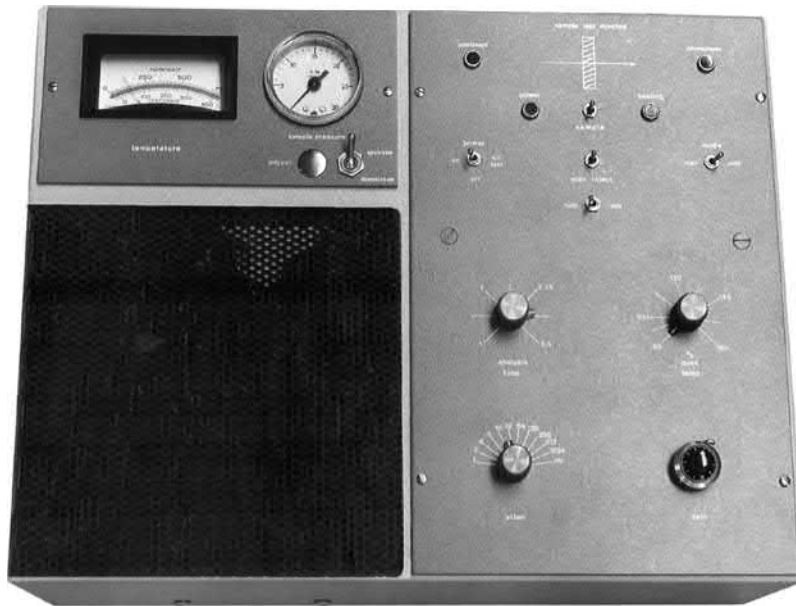


FIGURE 17.4 Valco Instruments Model 1000 Halocarbon Monitor for charcoal filters. *Courtesy of Valco Instruments.*

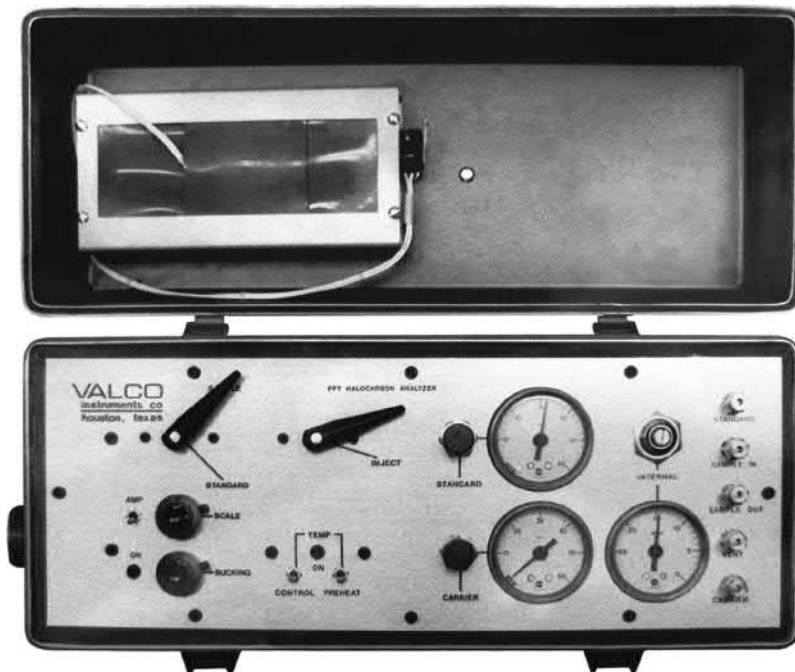


FIGURE 17.5 Valco Instruments prototype flyable CFC and N_2O analyzer, designed for NOAA. *Courtesy of Valco Instruments.*



FIGURE 17.6 Morgan Shaffer model PHA-1000 portable fault gas analyzer. *Courtesy of Morgan Shaffer.*

17.2 Design challenges

One of the major limitations of portable GC is imposed by electrical requirements. To minimize power consumption (and battery size), overhead from control circuitry must be minimal, and heated columns and detectors must have the lowest possible mass.

The second major limitation is carrier gas. Ambient air can be used; however, maximum column temperature is reduced, and the choice of detectors is limited. There is also a trade-off in power consumption, since power is required for air compression and purification. A bottled carrier gas such as He doesn't have these limitations, but again, there is a trade-off—gas bottles and regulators take up a lot of space. Small diameter columns and minimum-flow detectors will allow use of the smallest possible bottle or cartridge, while miniature pressure regulators (Fig. 17.7) are available for the two-stage regulation required for constant flow as the bottle pressure drops.

If a flame ionization detector (FID) is used, hydrogen is required in addition to air, although an FID has been reported that generates both required gases from the electrolysis of water [7].



FIGURE 17.7 Miniature regulators. *Courtesy of Valco Instruments.*

The original “lab on a chip” concept [8] has evolved to include an array of on/off valves, separately heated columns, and an independent thermal conductivity detector. While small size and low power consumption have been achieved, separations are limited to low-molecular-weight compounds.

17.3 Sample introduction

The simplest means of introducing a sample is with a syringe through a septum inlet. For gaseous samples, the inlet can be unheated, but liquid samples may require heat. Field syringe sampling can be of a liquid or of a headspace gas from a sealed container. Purge and trap samplers are also widely used with portable GCs.

A basic sample injection valve can also be used as a liquid or gas inlet. Sample injection valves measure the sample with a slot engraved

on the rotor (four-port internal sample injector) or with an external loop (six-port external loop sample injector). An 8- or 10-port design can perform useful column switching functions as well as sample injection. (See Section 17.3.1).

An alternative sample introduction method uses a silica fiber treated with a bonded phase like those used for coating capillary columns. The fiber is exposed to the air or liquid to be analyzed, then inserted into an inlet, which is heated to desorb the retained compounds [9]. A current version of such a sampling device is the CUSTODION SPME syringe manufactured by PerkinElmer.

17.3.1 Sample introduction and column switching with multiport valves

If an isothermal column is used and the sample contains slowly eluting compounds, two columns in series may be attached to the valve. After the last component of interest has eluted from the first column, returning the valve to the loading position backflushes the late eluting components into the detector or vent (Figs. 17.8 and 17.9). Applications shown with multiport valves can also be done with individual on/off valves and tee fittings, but with greater system complexity.

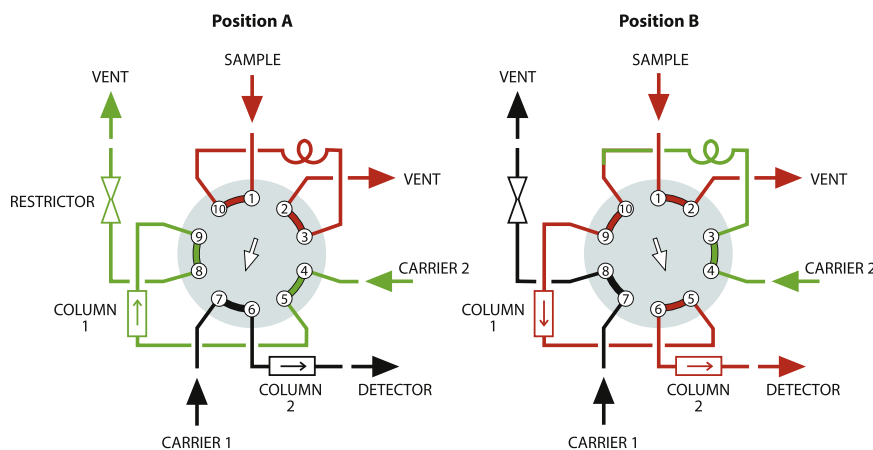


FIGURE 17.8 Loop sampling with backflush of precolumn to vent. *Courtesy of Valco Instruments.*

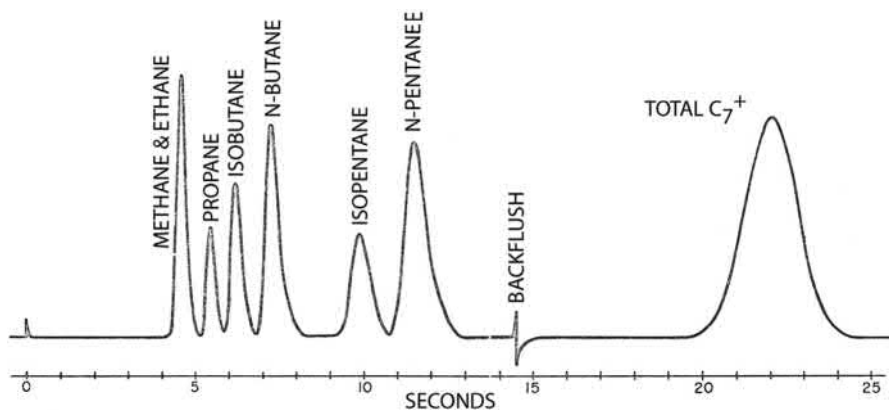


FIGURE 17.9 Light hydrocarbon analysis demonstrating backflush. Column: 30" \times 0.043" ID, 14.4% bis (2-methoxyethyl) adipate on 100–120 mesh chromosorb P, AW, DMCS; column temp: 44.6°C; carrier gas: helium; inlet pressure: 40 psi; sample size: 3 μ L (gas). *Courtesy of Frank Wilhite.*

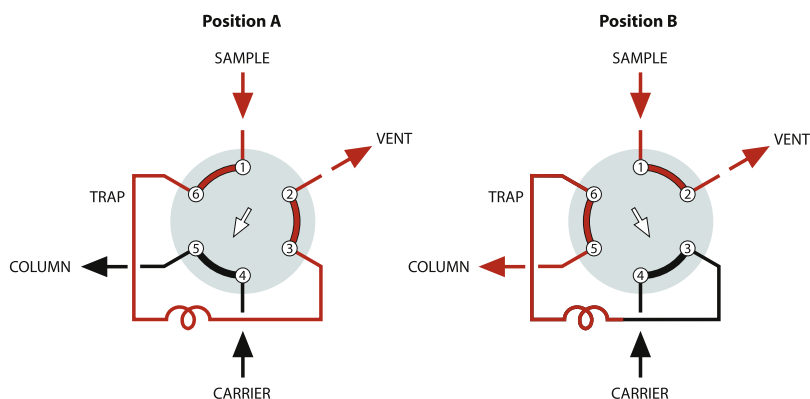


FIGURE 17.10 Six-port valve used to concentrate sample. *Courtesy of Valco Instruments.*

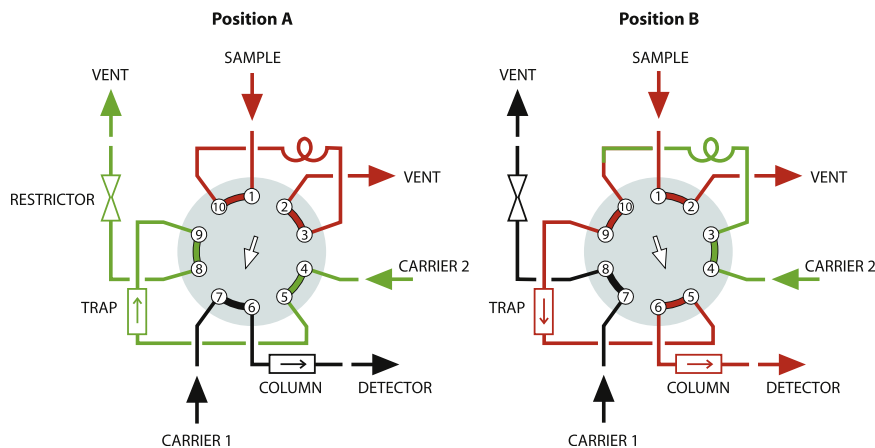


FIGURE 17.11 Volumetric sample injection with concentrating column or trap. *Courtesy of Valco Instruments.*

The use of a trapping or concentrating inlet greatly lowers the minimum detectable level of compounds of interest. If the loop on a standard six-port sample injector is replaced with a trap packed with a porous polymer such as Tenax® or Hayesep® a volume of sample may be pulled through the trap to effect a significant concentration of the sample before the trap is backflushed and heated to transfer the compounds of interest into the separation column (Fig. 17.10).

In the 10-port configuration shown in Fig. 17.8, if Column 1 is replaced with a trap, column switching as described in the previous

paragraph may be used to separate a fraction of interest—early or late eluting—from the bulk of concentrated sample (Fig. 17.11).

17.4 Column configurations

While air bath ovens are the norm for laboratory GCs, their size and power consumption mandate a different approach for portable instruments. Packed columns can be heated by winding them on conductive mandrels and surrounding them with low k factor insulation (Fig. 17.12).



FIGURE 17.12 Column mandrel and insulated enclosure. (Courtesy of Valco Instruments).

17.4.1 Isothermal operation

A micropacked or capillary column is effectively heated by winding the column into a helix and holding it to a polyimide or polyimide film heater by compression or cement.

17.4.2 Temperature programming

The use of conventional packed columns larger than $1/8''$ makes little sense if temperature programming is required; capillary and micropacked columns provide greater efficiency and lower power consumption. Columns can be programmed at $<1000^{\circ}\text{C min}^{-1}$ with low power.

Resistance heating may be accomplished by applying voltage directly to the ends of an electrically insulated column and measuring its temperature with a low mass sensor. Variation

in column temperature will occur if the column is not wound or bundled carefully. This concept is pursued further in Sections 17.7.1 and 17.7.2.

17.4.3 Isothermal packed columns

The application that has done more than any other to stimulate the production of portable GCs is the separation and quantitation of hydrocarbons at the sites of underground storage tanks (UST). The most important compounds, from the perspective of the Environmental Protection Agency (EPA), are the aromatics from gasoline—benzene, toluene ethylbenzene, and xylene (BTEX). These can be separated with a capillary column or a packed column at room temperature or slightly above (75°C for a $6' \times 1/8''$ packed column) and detected by a PID (Fig. 17.13). The presence of higher-molecular-weight compounds may require backflushing or elevating the column temperature periodically. In some instruments, line power is used for the significant increase in column temperature required to elute the high-boiling compounds.

17.4.4 Multiple columns with multiport valves

Many separations, such as the separation of N_2O and CFCs, require more than one column for a complete analysis (Fig. 17.14). Sample is injected into a porous silica column upstream

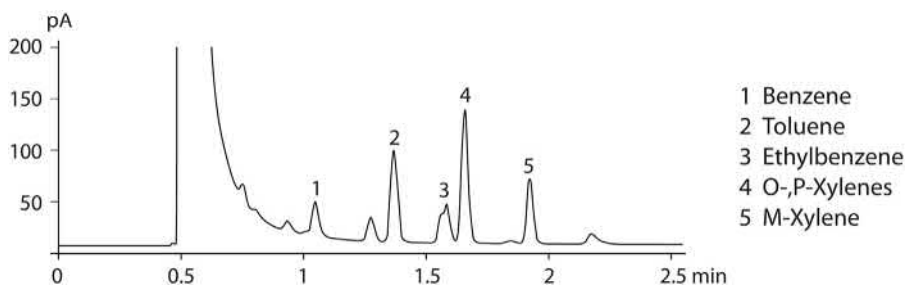


FIGURE 17.13 BTEX chromatogram separated on a packed column. Courtesy of PID Analyzers.

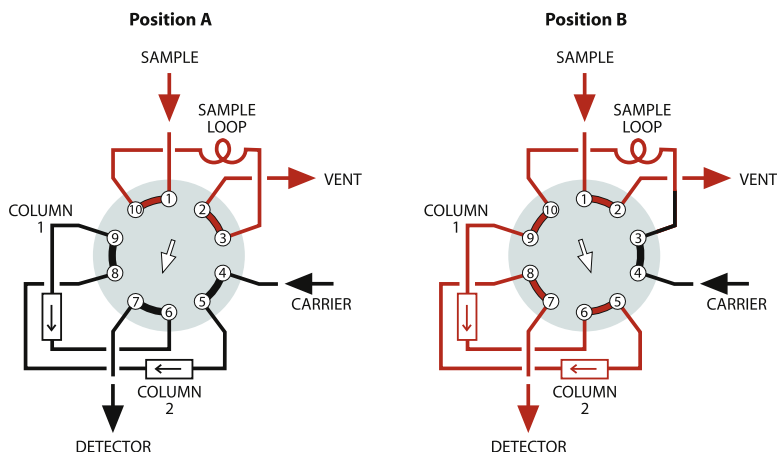


FIGURE 17.14 Loop sampling with two column sequence reversal. Courtesy of Valco Instruments.

of a porous polymer column. After the N_2O enters the porous polymer column, the sequence of the columns is reversed as the valve returns to the load position. The CFCs, which would be retained much longer on the polymer column, elute directly to the detector, while the N_2O makes a second pass through the silica column before detection.

17.4.5 Multiple columns with flow modulation

Flow modulation techniques using tees, three-way (SPDT) and on/off (SPST) valves, and/or flow controllers can be used instead of multipoint valves, possibly reducing costs. However, the technique adds to system complexity.

17.5 Detectors

17.5.1 Photoionization detector (PID)

While generally any detector used in a laboratory GC can be used in a portable GC, some types are used more often than others. The PID, with its insensitivity to air and its parts-

per-billion sensitivity to important pollutants, is an excellent detector for field instrumentation. The selectivity of the PID can be enhanced by the choice of lamps.

17.5.2 Pulsed-discharge photoionization detector (PDD)

The PDD is a universally responsive helium photoionization detector with a high ionization efficiency. In Ar-, Kr-, or Xe-doped modes it responds similarly to a PID, but with less selectivity since there is no window to exclude the high energy emissions from He. Compared to a PID, it requires higher-purity carrier gas, but functions at much lower flow ($<5 \text{ cc min}^{-1}$ for mini and micro versions).

17.5.3 Electron capture detectors (ECD and PDECD)

The electron capture detector is useful for portable chromatography, as it has unparalleled sensitivity to strongly electronegative compounds. ECDs require high-purity gases— N_2 or Ar/5% CH_4 for radioactive source

detectors and He for pulsed-discharge photoionization detectors. Both the ECD and PDECD have drawbacks. Radioactive ECDs—which have a Ni^{63} or H^3 source—require licensing, and there may be restrictions on transport. The nonradioactive PDECD requires very high-purity He for carrier and discharge gases; however, a small, low-power active-metal purifier is available for portable use.

17.5.4 Flame ionization detector (FID)

The FID is used in portable GCs when universal sensitivity to hydrocarbons is desired. Unlike the lamp-type PID, the FID is sensitive to methane. It is not affected by water or air, so air may be used as a carrier gas. FIDs require H_2 as fuel for the flame, so it must be supplied from a gas bottle or generated within the instrument.

17.5.5 Thermal conductivity detector (TCD)

The TCD is universally responsive, requires little power, and is simple to incorporate. However, its parts-per-million sensitivity may require sample concentration for effective use in portable GCs.

17.5.6 Nitrogen–phosphorus detectors (NPD)

The NPD is a modified FID that has selective response for nitrogen and phosphorus compounds, halogens, and some oxygenates.

17.5.7 Surface acoustic wave detector (SAW)

SAW detectors are piezoelectric crystals with a coating that is selected for response to specific classes of compounds. They may be used alone or in arrays. Their principal use has been the detection of chemical warfare agents [10,11].

17.5.8 Mass spectrometer (MS)

The MS as a detector for portable GC adds considerable complexity, cost, weight, and support requirements, but offers unparalleled power to detect and identify compounds in the field. From the first efforts to construct a space mission GC-MS, advances in design and separation have made possible truly portable systems.

17.5.9 Ion mobility spectrometers (IMS, DMS, and FAIMS)

Ion mobility spectrometers (IMS) in various embodiments including differential (DMS) and field asymmetric (FAIMS) types have been widely studied as a portable option, since they have low power requirement, are tunable, and can function with air as the supply gas. The portable GC-DMS used on the international space station is an example of a successful implementation through years of service [12–14].

17.5.10 Other detectors

Emission detectors using discharge sources can be successfully used in portable instrumentation [15]. Other sensors may be used [16].

17.6 Gas supply

Lecture bottles and similar small pressurized cylinders are convenient sources for portable GCs. For flow stability consistent with maximum content usage, miniature two-stage pressure regulators, two separate regulators, or a combination of a primary pressure regulator and a flow controller can be used. Electronic pressure control (EPC) is used in many current instruments.

When air is the carrier, it may be from a cylinder or from a nonlubricated diaphragm-type miniature air compressor within the analyzer. Although diaphragm compressors are less likely

to add contaminants, most miniature versions are limited to <2 atm. Filtration/purification can eliminate virtually all impurities except methane, which can only be removed with a heated (power-consuming) purifier. Nonheated purifiers can be used with PIDs, since PIDs do not respond to methane.

If air-actuated components are used, actuation pressure comes from the primary-stage regulator, with carrier flow coming from the second-stage regulator.

17.7 Power management

Perhaps the greatest challenge in designing a portable GC is providing adequate electricity for stand-alone, independent operation. If an instrument can be tethered to an auto battery or line supply until the actual time of use, portable use time will be maximized. Establishing a budget for electrical use is often critical.

A wide variety of battery sizes and capacities is available with the most efficient being, not surprisingly, the most expensive.

17.7.1 Column power (isothermal)

Obviously, minimum power is required for column heat if the column(s) can provide the required separation at room temperature. If the sample contains slow-eluting high-boiling

compounds, analyses can be performed until the baseline drifts excessively, at which point extra power is needed to purge the column. As previously described, if the column is connected to a multiport valve or divided into two sections—column and precolumn—regular backflushing or column sequence reversal to vent can discharge the higher-boiling compounds without contaminating the detector and without using extra power for column heat.

A GC that heats columns in an oven is not likely to be considered portable. However, heating capillary or micropacked columns can be accomplished with minimum power by closely associating the column with a low mass heat source, typically with resistance wire or by plating a conductive coating on the column [17,18]. The temperature of the column may be measured for control via the use of a separate sensing wire [19–21], or a single wire can be bundled along the length of the column and serve as both heater and sensor [22]. (Fig. 17.15) Examples of bundled nickel wire columns are shown in Fig. 17.16, with power requirements for various configurations shown in Fig. 17.17.

Plating a fused-silica column with nickel allows the ends of the column to be connected to a common ground with voltage applied to a center electrical tap, allowing even 30 m columns to be heated rapidly with less than 50 V. Efficiencies and repeatability have been

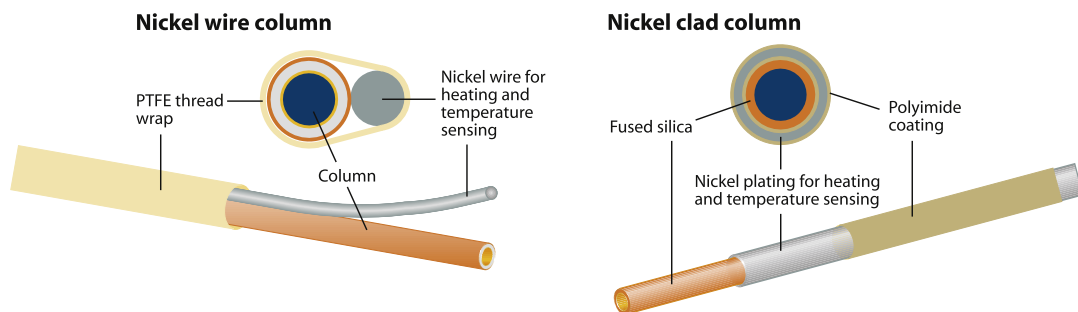


FIGURE 17.15 Resistively heated low mass columns. Column power requirements. *Courtesy of Valco Instruments.*

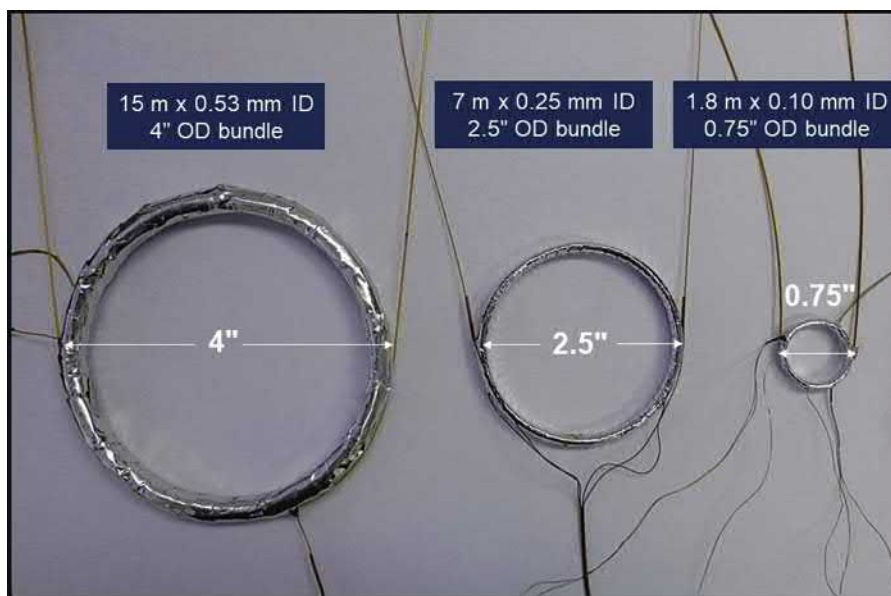
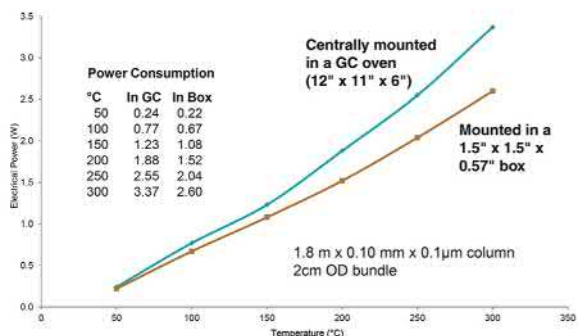


FIGURE 17.16 Examples of insulation-wrapped capillary columns bundled with a single nickel wire, which serves as heater and sensor. *Courtesy of Valco Instruments.*

Power comparison – enclosure size



Power comparison – bundle size

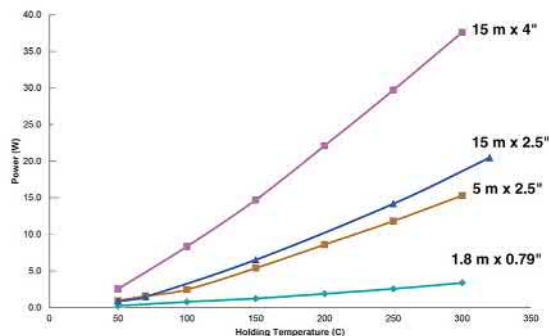


FIGURE 17.17 Column power requirements for bundled columns in isothermal applications. *Courtesy of Valco Instruments.*

measured that approach those of an air bath column oven [23]. (Table 17.1, Figs. 17.18–17.21). To achieve this level of efficiency and repeatability, cold spots in the flow path must be

eliminated. Fused-silica columns have also been heated by jacketing them with stainless-steel tubing [24,25].

TABLE 17.1 Heating efficiency of resistive heating compared to air bath oven heating.

	Isothermal plates loss (%)	Programmed SN loss (%)
Ni wire	4.8	4.1
Ni clad	1.7	1.0
Ni tubing	4.5	6.6

17.7.2 Column power (programmed)

Capillary or micropacked columns bundled with a nickel wire as described earlier are ideal for fast temperature programming with minimum power consumption. Fig. 17.20 shows a high-speed analysis of #2 diesel. The other figures compare this technique versus heating the column in an oven, across various parameters, in isothermal and programmed applications.

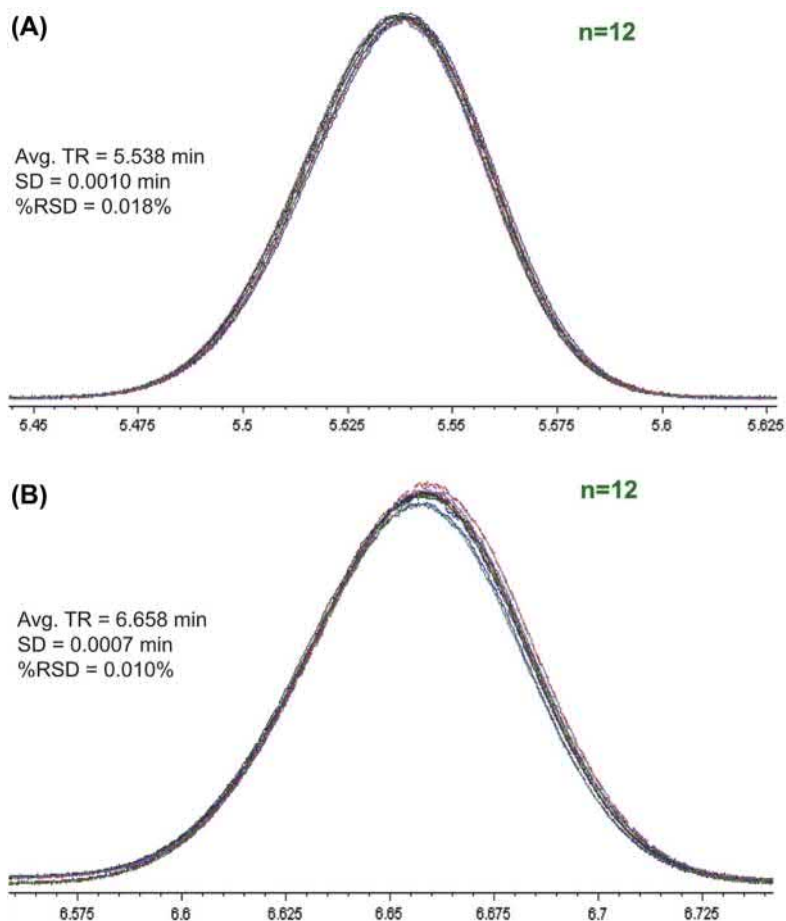


FIGURE 17.18 Repeatability of oven-heated column (A) compared to Ni wire-type resistively heated column (B), isothermal. Column: VB-5, 15 m × 0.25 mm × 0.25 μm at 110°C. Courtesy of Valco Instruments

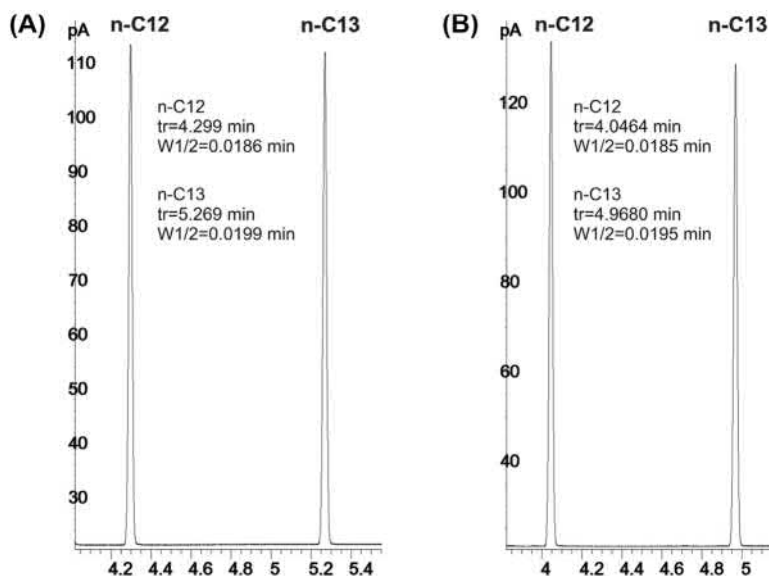


FIGURE 17.19 Heating efficiency of oven-heated column (A) compared to Ni wire-type resistively heated column (B), programmed. Column: VB-5, 15 m \times 0.25 mm \times 0.25 μ m, 70–220°C at 15°C min⁻¹. Courtesy of Valco Instruments.

17.7.3 Pumps—pressure or vacuum

DC low-voltage pumps can deliver up to 24 psi or 20" Hg vacuum at a maximum 6 W.

17.7.4 Additional

Electric precision controllers, which replace mechanical pressure regulators, can operate with less than 3 W. Some applications may also require a heated gas purifier. Miniature models are available, which consume less than 10 W.

17.8 Prototyping

The assembly of a portable GC is basically a matter of connecting components on a panel as closely as possible without causing thermal

zone interference. Transfer lines, injectors, and other components may be heated with high-temperature insulated resistance wire. Polyimide foam or low K factor fiber insulation is helpful in eliminating cold spots and helps reduce power consumption and weight. Fig. 17.23 shows an assembly (covered and uncovered) with a diaphragm sample valve, a resistance heated column, and a micro PDD. In this unit, the valve and detector are heated as well as the column. The chromatogram of chemical weapons surrogates in Fig. 17.22 was done on this platform.

The light gases in Fig. 17.24 were separated on a somewhat cruder arrangement of similar components (Fig. 17.25). At the completion of the analysis, the small fan is turned on to cool the column. As an aid to cooling, the lid of the cardboard box holding the column is blown open by the fan.

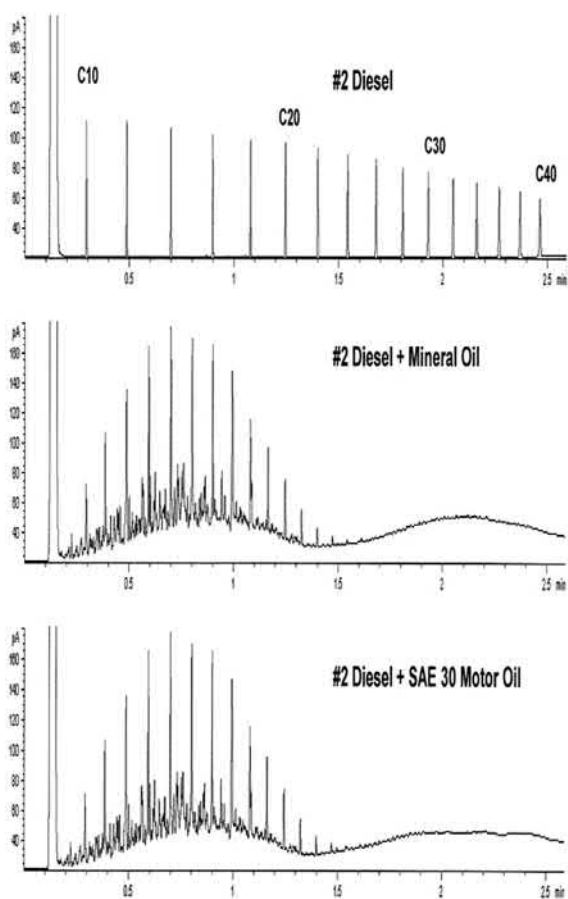
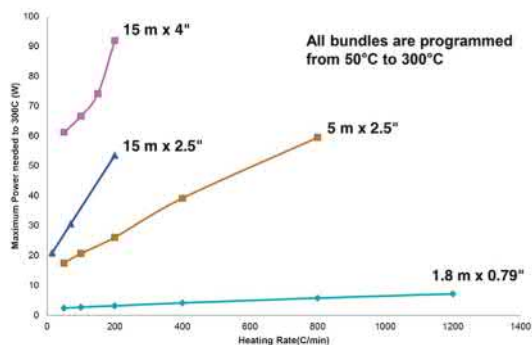


FIGURE 17.20 2.5 min analysis with a temperature-programmed capillary column. Column: VB-5, $5\text{ m} \times 0.10\text{ mm} \times 0.10\text{ }\mu\text{m}$, 3.2 mL min^{-1} ; detector: FID, 330°C ; column heating: $70\text{--}340^\circ\text{C}$ at $120^\circ\text{C min}^{-1}$. Courtesy of Valco Instruments.

Power comparison – bundle size and heating rate



The assembly of a portable GC is basically a matter of connecting components on a panel as closely as possible without causing thermal zone interference. Transfer lines, injectors, and other components may be heated with high-temperature insulated resistance wire. Polyimide foam or low K factor fiber insulation is helpful in eliminating cold spots and helps reduce power consumption and weight. Fig. 15.22 shows an assembly (covered and uncovered) with a diaphragm sample valve, a resistance heated column, and a micro PDD. In this unit, the valve and detector are heated as well as the column. The chromatogram of chemical weapons surrogates in Fig. 15.23 was done on this platform.

17.9 Commercial portable GCs currently available

At the time of publication, portable GCs are offered by ABB, Ametek, Ellutia, Energy Support, Enmet, Nanova Environmental, OI Analytical, PID Analyzers (PNU), Teledyne (Falcon), VICI, and Yamatake.

17.10 Future trends

While the majority of this chapter is dedicated to discussion of practical solutions to field and portable GCs using components that are either

Ending temperature comparison

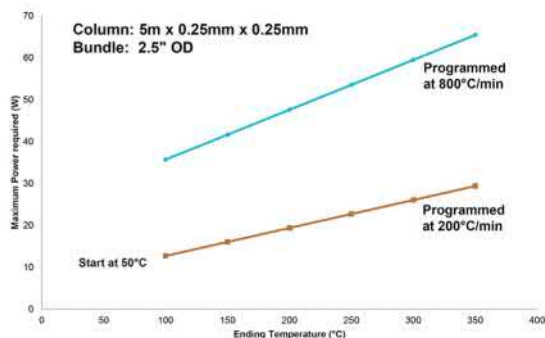


FIGURE 17.21 Heating efficiency of various sizes of column bundles (programmed).

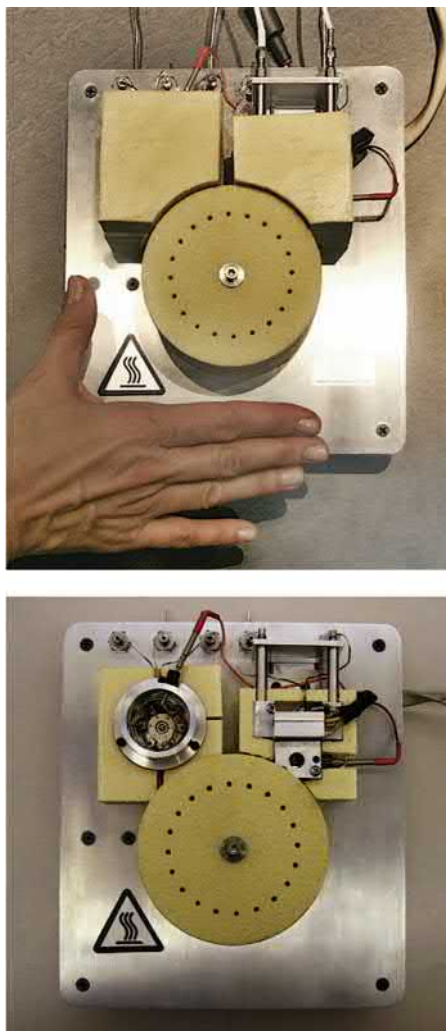


FIGURE 17.22 Prototype portable GC with a diaphragm valve, micro PDD, and resistance heated column. *Courtesy of Valco Instruments.*

readily available or manufacturable, researchers continue to explore the possibility of incorporating semiconductor fabrication techniques and micromachining in the development of compact, low-power, high-speed instruments [26,27].

The original “GC on a chip” became commercial only when the injector, column, and detector were separated. Conventional fused-silica columns simply offer much better performance, even considering the difficulty of intracomponent connections.

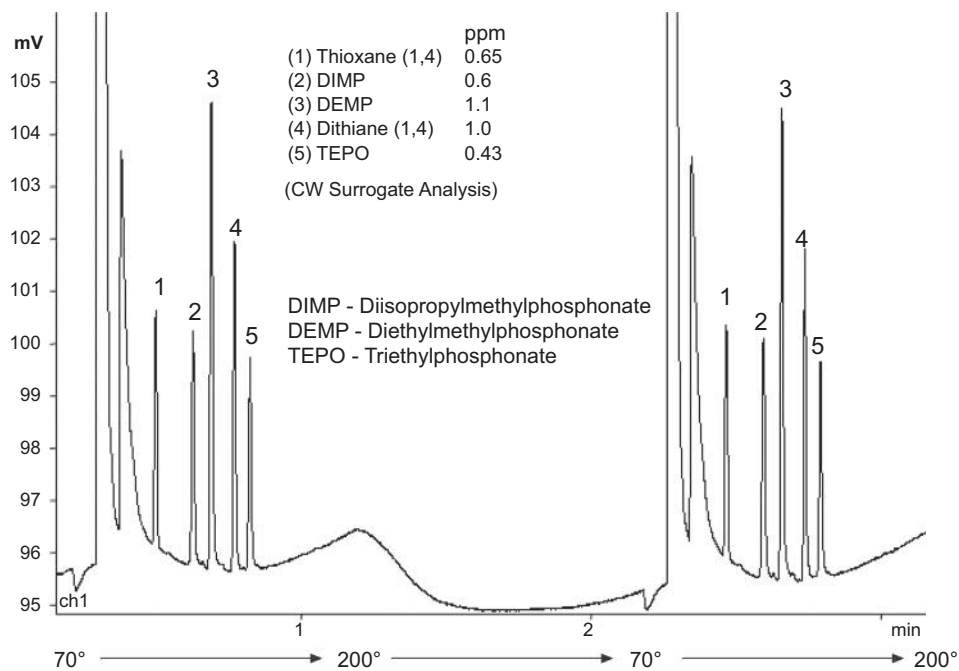


FIGURE 17.23 < 1 min analysis of chemical weapons surrogate. *Courtesy of Valco Instruments.*

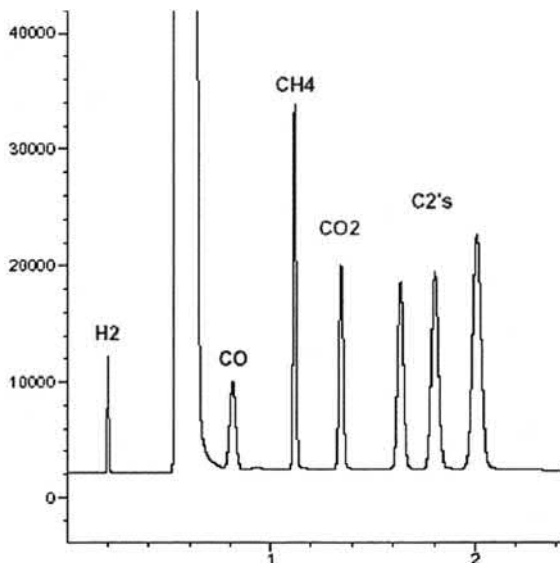


FIGURE 17.24 2 min gas mixture analysis with a temperature-programmed micropacked column. Column: ShinCarbon column, 8 mL min^{-1} ; column heating: 30°C (0.9 min) to 230°C at $500^\circ\text{C min}^{-1}$, 1 min cooling time. *Courtesy of Valco Instruments.*



FIGURE 17.25 A second prototype portable GC with a diaphragm valve, micro PDD, and resistance heated column. Courtesy of Valco Instruments.

There are now manufacturers of micromachined injectors and detectors, making the assembly of micro GCs feasible for specific applications. Currently, the GC/MS instruments from INFICON, Griffin/FLIR, and Torion allow a user to bring virtually an entire laboratory to the field, offering a balance of power and performance.

Acknowledgments

Thanks to W. F. Wilhite for providing early portable GC data, to Dr. Huamin Cai of Valco Instruments for demonstrating separation with minimal complexity, and to Dr. John Driscoll of PID Analyzers for providing crucial insights and data. Thanks also to David Salge, recently retired from VICI Gig Harbor Group, without whose efforts in layout and editing this chapter would not have been completed.

References

- [1] W. F. Wilhite, The Development of the Surveyor Gas Chromatograph, Technical Report No. 32-425, Jet Propulsion Laboratory, California Institute of Technology, 15.05.1963.
- [2] W.F. Wilhite, Subminiaturized gas chromatograph gives fast, efficient analysis, NASA Tech. Brief 66-10182 (May 1966).
- [3] C.S. Josias, L.D. Bowman, J.E. Lovelock, Gas detector and analyzer, US Patent 3 (714) (1973) 421, filed May 29, 1969, and issued. (Accessed 30 January 1973).
- [4] M.R. Stevens, C.E. Giffin, G.R. Shoemake, P.G. Simmonds, A portable self-contained gas chromatograph, Rev. Sci. Instrum. 43 (Issue 10) (October 1972) 1530.
- [5] R.N. Dietz, E.A. Cote, Tracing atmospheric pollutants by gas chromatographic determination of sulfur hexafluoride, Environ. Sci. Technol. 7 (4) (1973) 338-342.

- [6] J.E. Morgan, Transformer fault detection, US Patent 4 (112) (1978) 737, filed April 27, 1977, and issued. (Accessed 12 September 1978).
- [7] N. Tzanani, A. Amirov, Electrolyzer powered flame ionization detector, *Anal. Chem.* 69 (1997) 1218–1255.
- [8] J.B. Angell, J.H. Jerman, S.C. Terry, Soheil Saadat, Prototype Gas Analysis System Using a Miniature Gas Chromatograph, Interagency Energy/Environment R&D Program Report, NIOSH/EPA, December, 1980.
- [9] C.L. Arthur, J. Pawliszyn, Solid phase microextraction with thermal desorption using fused silica optical fibers, *Anal. Chem.* 62 (19) (1990) 2145–2148.
- [10] C.J. Lu, C. Jin, E.T. Zellers, Chamber evaluation of a portable GC with tunable retention and microsensor-array detection for indoor air quality monitoring, *J. Environ. Monit.* 8 (2006) 270–278.
- [11] Q. Zhong, W.H. Steinecker, E.T. Zellers, Characterization of a high-performance portable GC with a chemiresistor array detector, *Analyst* 2 (2009).
- [12] W.T. Wallace, T.F. Limero, L.J. Loh, P.D. Mudgett, D.B. Gazda, Monitoring of the atmosphere on the international space station with the air quality monitor, NTRS, Presented at the 47th International Conference on Environmental Systems, 16–20, 07, 2017.
- [13] W.T. Wallace, T.F. Limero, K.W. Clark, A.V. Macatangay, P.D. Mudgett, D.B. Gazda, Enhanced AQM: development of an exploration compatible air quality monitor, Presented at the 49th International Conference on Environmental Systems, 7–11, 07, 2019.
- [14] T. Limero, Volatile organic analyzer (VOA) in 2006: repair, revalidation, and restart of elektron event, NTRS, Presented at 16th International Conference on Lon Mobility, 22–26, 07, 2007.
- [15] W. Wentworth, K. Sun, D. Zhang, J. Madabushi, S. Stearns, Pulsed discharge emission detector: an element-selective detector for gas chromatography, *J. Chromatogr., A* 872 (1–2) (2000) 119–140.
- [16] L. Spinelle, M. Gerboles, G. Kok, S. Persijn, T. Sauerwald, Review of portable and low-cost sensors for the ambient air monitoring of benzene and other volatile organic compounds, *Sensors* 17 (7) (July 2017).
- [17] R.A. Yost, M.E. Hall, Compact gas chromatograph probe for gas chromatography/mass spectrometry utilizing resistively heated aluminum-clad capillary columns, *Anal. Chem.* 61 (21) (1989) 2410–2416.
- [18] R.A. Yost, M.E. Hall, Direct resistive heating and temperature measurement of metal-clad capillary columns in gas chromatography and related separation techniques, US Patent 5 (114) (1992) 439, filed September 25, 1990, and issued. (Accessed 19 May 1992).
- [19] R.V. Mustacich, Gas chromatography column assembly temperature control system, US Patent 5 (1998) 782–964, filed January 27, 1997, and issued. (Accessed 21 July 1998).
- [20] R.V. Mustacich, J.F. Everson, Reduced power consumption gas chromatograph system, US Patent 6 (2001) 217–829, filed January 27, 1997, and issued. (Accessed 17 April 2001).
- [21] R.V. Mustacich, J.F. Everson, Reduced power consumption gas chromatograph system, US Patent 6 (2004) 682–699, filed March 2, 2001, and issued. (Accessed 27 January 2004).
- [22] S.D. Stearns, Huamin Cai, J. Art Koehn, Martin Brisbin, Chris Cowles, and Chris Bishop, Direct Resistively Heated Columns for Fast and Portable Gas Chromatography, Pittcon Oral Session vols. 1130–1133, 4,03. 2008.
- [23] *ibid* Stearns, Cai, K., Brisbin, C., and Bishop.
- [24] D.P. Rounbehler, E. Hainsworth, Selective detection with high speed gas chromatography, US Patent 5 (099) (1992) 743, filed July 8, 1987, and issued. (Accessed 31 March 1992).
- [25] W.A. Rubey, Gas chromatography methods and apparatus, US Patent 5 (028) (1991) 243, filed March 5, 1990, and issued. (Accessed 2 July 1991).
- [26] A. Peters, M. Klemp, L. Puig, C. Rankin, R. Sacks, Instrumentation and strategies for high speed gas chromatography, *Analyst* 116 (1991) 1313–1320.
- [27] V. Reid, M. Stadermann, O. Bakajin, R. Synovec, High-speed temperature programmable gas chromatography utilizing a microfabricated chip with an improved carbon nanotube stationary phase, *Talanta* 77 (4) (2009) 1420–1425.

Preparative gas chromatography

*Leesun Kim*¹, *Philip J. Marriott*²

¹Ulsan National Institute of Science and Technology, Ulsan, South Korea; ²School of Chemistry Monash University, Clayton, VIC, Australia

18.1 Introduction

Preparative gas chromatography (prep-GC) has a rich and well-established history. This ranges from the use of GC as a bulk isolation method for compounds in mixtures that are well known, but simply cannot be otherwise separated from mixture components in large-scale amounts, to applications where much smaller quantities of compounds require more substantial structure elucidation than available with classical GC detectors.

The characterization of trace components, unknown analytes, and complex mixtures of components has always been a challenge in organic analytical chemistry, such as in the flavor/fragrance [1], pheromone [2], environmental [3], pharmaceutical [4], metabolomics [5], and petrochemical areas [6]. As modern techniques or technical innovations in analysis methods increasingly deal with trace compounds, often this simply pushes the boundary of sample characterization to focus on components at even lower abundance. This is well demonstrated in the field of metabolomics, where there is a continual demand for lower detection limits and a corresponding need to accurately characterize more compounds at trace levels in order

to cover a wider scope of the metabolome [7]. There are many strategies for the reliable measurement of components at a low level. Samples can be concentrated using prior sample preparation for the subsequent analytical measurement. A large volume of sample can be applied to the analytical instrumental step (e.g., large-volume sample introduction; LVSI) in GC [8,9], or a chromatographic preparative step can be an integral part of the analysis method. It is also possible to remove, reduce, or eliminate matrix in a sampling step, so that the sensitivity of target analytes can be increased in the detection step and a concomitant reduction of unwanted or potentially interfering material can be excluded for the “analytical finish.”

Prep-GC includes the elegant approach of incorporating a sample preparative step as an integral part of the analysis step, allowing the component of interest to be isolated from complex matrices and then to be collected after GC analysis. As a result of this operation, the analytes can be characterized further to provide improved identification. This allows an expanded range of spectroscopic detection techniques, which are not normally available as hyphenated chromatographic methods. Thus, the components collected can be studied by

other analysis techniques, to be more suitably characterized using mass spectrometry (MS), Fourier transform infrared spectroscopy (FTIR), nuclear magnetic resonance (NMR) spectroscopy, X-ray, accelerator MS (AMS), or other spectroscopic tools [10–13]. Traditionally, GC hyphenated with MS has been essential to identify compounds from a variety of matrices [14]. However, significant problems exist when some compounds cannot be identified from their mass spectra and retention data alone. This is due to high similarities between isomeric compounds and the lack of specificity of the derived mass spectrum for similar compounds or lack of specific fragmentation patterns. The (over-)reliance of many researchers on the mass spectrum to deduce the molecular structure can often cause erroneous identification.

In consequence, prep-GC may play an important role, when compounds either need to be enhanced in abundance (enriched) or need to be isolated due to inadequate elucidation of structure with available online detection methods. Prep-GC can conveniently be classified as a large-scale or analytical-scale methodology, depending on the sample and component properties and the purpose of using this technique. This chapter will use the following differentiation between these two goals, outlined in [Section 18.2](#).

18.2 Application scale of preparative gas chromatography

Prep-GC can range from large-scale prep-GC methods capable of producing kg h^{-1} of substance to the analytical scale preparatory method, where it is only necessary to isolate sufficient material for subsequent characterization techniques e.g., off-line spectroscopic or micro-scale reaction methods.

18.2.1 Large-scale preparative GC

We may define large-scale prep-GC as a technique that is used as a purification step for a compound, often synthetic, but sometimes natural, that is needed for either large-scale commercial production or subsequent synthesis reaction [15]. Generally, this means that the target component is well characterized and therefore is a known compound and just needs to be produced in large amounts of pure compound. The scale can therefore be in the kg or greater quantity, and GC may be suitably scaled up to provide the necessary purity of the compounds. In this case, it is simply the act of recovering the compound in a large amount that is the goal of the prep-GC step.

This can be summarized as follows: Known synthetic or natural sample \rightarrow large-scale prep-GC \rightarrow pure compound in large amount.

The present review will not consider this role of prep-GC here, as it has been the focus of recent publications, such as the book by Schmidt-Traube [15]. As this citation illustrates, scaling up of the prep-GC method operates according to well-established physical and chemical separation principles, and the reader is directed to this and other references for further information.

18.2.2 Analytical-scale prep-GC

Prep-GC on the analytical scale plays a significant role, when it is difficult to identify a molecule by using just the retention time or retention index, or by correspondence of retention with a coinjected authentic compound, or when MS is not sufficient to provide adequate characterization of the structure of the compound. Under these circumstances, alternative methods for compound identity are needed—above and beyond that available from classical GC detectors. This requires a collection method to isolate and transport the compound to other

detector(s) or techniques. The standard proof of identity relied on by chemists includes techniques such as UV, NMR, and FTIR, and, where possible, X-ray analysis; so it is useful to apply this knowledge and this degree of identification for separated/collected GC peaks where necessary.

In the analytical-scale process, prep-GC has been utilized for a wide range of applications, including compounds such as sex pheromones, essential oil compounds, environmental residues, polycyclic aromatic hydrocarbons, petroleum components, and chiral drugs. These applications can be categorized into the following situations (note that some of these target individual compounds and others target zones of compounds or indeed the full range of volatile compounds):

1. Analytes in complex samples
 - a. Natural products such as pheromones [16–19] and essential oils [20].
 - b. Synthetic products such as nonylphenol (NP) [3,21].
2. “Simple” samples but with impurities that require precise structural characterization [10].
3. Samples with trace-level compounds requiring further concentration or enrichment in order to meet the needs of the detection limits for quantitative and qualitative analysis.

The general need and justification for analytical-scale prep-GC therefore can be readily articulated, but there is still scope for improvement in systematic approaches to the general problem of enhancing the identification of components at trace levels and in complex sample matrices. The following section briefly highlights various separation and collection strategies that illustrate approaches to analytical prep-GC taken by researchers, in order to provide elucidation of the structure of components in a variety of sample types. Discussion in [Section 18.4](#) focuses on case studies of selected applications.

18.3 Experimental techniques for analytical-scale prep-GC

18.3.1 1D GC

The implementation of prep-GC with a single packed column format is the most productive [22–24] in terms of recovering a large mass of compound with few injections. However, it does not provide the best separation for a complex sample with many potentially interfering peaks. Many applications will require a higher-resolution separation method. In this case, higher-resolution capillary columns, which may be “mega-bore” dimensions—0.53 mm i.d.—or narrower bore 0.25–0.32 mm i.d. may be used. In all cases, a smaller phase ratio will reduce the effect of peak broadening due to overloading effects if larger amounts of analyte are injected. A typical schematic of a prep-GC instrument is shown in [Fig. 18.1A](#). The method incorporates a suitable collection or trapping device T, which often may be operated at subambient or cold temperature by using a cooling system. A detector and a switching system are also incorporated here to monitor the progress of the GC analysis. The switching device, which is directed to the detector in normal operation, allows selection of the component(s) to be transferred to the trapping system by switching the flow to the trapping channel. The trap may also be an adsorbent cartridge, a phase-coated capillary trap, or a solvent-filled collector, which will be described further in [Section 18.3.3](#).

18.3.2 Capillary multidimensional gas chromatography (MDGC)

Since multidimensional gas chromatography (MDGC) was first proposed by Simmonds and Snyder in 1958 [25], it has been mostly implemented using a wide range of switching devices and/or valves. Multidimensional chromatography (MDC) can be defined as the coupling of two (or more) different separation stages, with

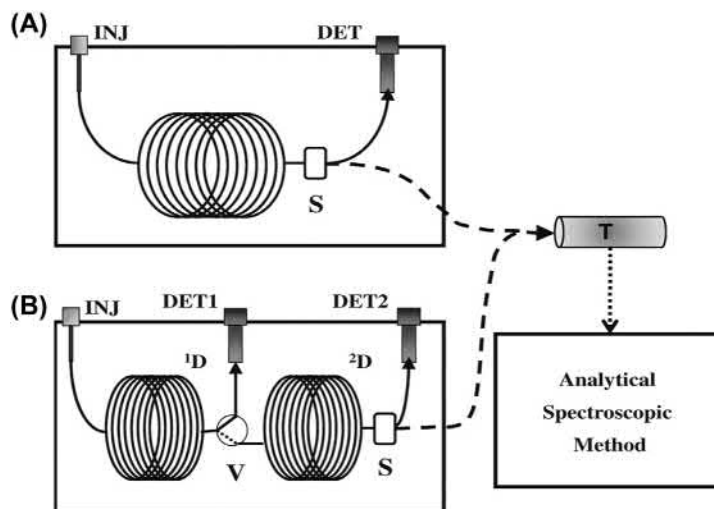


FIGURE 18.1 Schematic arrangements of one-dimensional (A) and multidimensional (B) separation systems, comprising online detector(s) with switching to a preparative sample collection system followed by off-line detection. The switching device (S) directs flow either to the detector or to collection. The trapping system (T) can be any mode of collection used for the prep-GC fractions. For MDGC, a valve or interface (V) is used for the heart-cutting process to transfer compounds to the ^2D column.

independent elution through each stage. Therefore, it is imperative that the chromatographic dimensions not only should be connected directly (e.g., two GC columns) but there also should be an interface, such as a valve or switching system between dimensions. The valve or switching system allows a small zone of effluent from the first dimension (^1D) to be directed into the second dimension (^2D) by changing the flow of gas from the detector channel to the ^2D channel as shown in Fig. 18.1B. In this way, improved resolution in the ^2D column can be achieved by MDGC, which can benefit a wide range of applications areas already alluded to such as petroleum, environmental pollutants, and essential oil components, all of which demonstrate a degree of complexity that often precludes separation of individual peaks on a single column [26,27].

18.3.3 Trapping systems

Trapping systems are critical to the success of the prep-GC method. Most studies using prep-GC have utilized preparative fraction collection into dedicated collection devices or capillary tubes as a trapping method. Both systems can incorporate an additional cooling system, which can increase the recovery efficiency of the semi-volatile or volatile target components [11,17,28]. Sorbent traps are alternatives to the aforementioned, and liquid traps are also described.

18.3.3.1 Gerstel preparative fraction collector

The Gerstel preparative fraction collector (PFC) has been used in various studies using prep-GC [19,29,30]. This sample collection system, equipped with six sample traps and one waste trap, automatically collects individual

compounds, a series of compounds, or specific classes of compounds after GC separation. Trap tubes are available in 1 or 100 μL volumes. To increase recovery efficiency, PFC can be equipped with optional N_2 (liq) or cryostatic trap cooling systems. Microprocessor control allows the trap switching times to be selected to within 0.01 min, which permits reliable collection of individual compounds that are closely resolved. The reliability and reproducibility of the system make it possible to trap compounds over the course of hundreds of injections [10,31]. This allows further analyses of the fractions by techniques requiring larger sample mass such as NMR or IR. In order to overcome the technical limitation to only six collectable fractions, Meinert et al. [28] introduced a new technique combining two PFCs through a special zero-dead volume effluent splitter, shown in Fig. 18.2. The same group [31] optimized the performance of the prep-GC system by identifying the best operating parameters for the two PFC system using six environmentally significant target analytes: phenol, naphthalene, acenaphthene, methyl parathion, methoxychlor, and benzo[a]pyrene. Solvent-filled traps were used instead of temperature-controlled trapping. Dichloromethane (DCM) proved to be the most suitable solvent for a large range of compounds. Recoveries were in the range of 50%–70% for all compounds apart from benzo[a]pyrene with a recovery of 94% using one PFC (not two PFCs) and DCM-filled traps at a trapping temperature of -10°C . Transfer line and PFC switch temperatures of 300°C for phenol, 400°C for benzo[a]pyrene, and 320°C for the rest of the analytes gave the best results. Highly heat-tolerant capillaries for the transfer line were used in order to prevent significant capillary porosity and breakdown [31].

18.3.3.2 Capillary trapping

Eyres et al. [11,12] and Rühle et al. [32,33] used an Agilent G2855B microfluidic Deans' switch (DS) to isolate the peak of interest eluting from the outlet of the column, directing the flow to either a detector (flame ionization detector (FID)), or the external trapping assembly (xTA) via deactivated fused silica (DFS) transfer lines. A length of megabore DFS tubing (trapping capillary) was used within a cryotrap cooled with liquid CO_2 to collect the transferred (heart-cut) peak. The simple heart-cutting procedure is shown in Fig. 18.3. After multiple injections, the capillary was removed from the cryotrap and eluted with an appropriate solvent for characterization using spectroscopic techniques including NMR or X-ray.

In a series of prep-GC studies, Nojima et al. [13,17,18,34] described the use of a short collection tube attached to the end of the analytical capillary column. The tube was pulled through a heated exit and passed out of the GC just before the elution time window of the target solute, to collect only the component of interest. A sheath that generated a cooling zone was attached to the tube and assisted sample trapping. After the sample collection, the sheath was removed and the collection tube was withdrawn from the analytical column, with collected compound eluted and taken for NMR analysis. This method is described in Fig. 18.4. Nojima et al. [34] investigated the performance of various types of capillary column traps (deactivated, methyl polysiloxane, and polyethylene glycol) using the prep-GC technique and under various collection conditions. The model compounds were C_4 – C_{20} normal alkanes, esters, and alcohols. Above a critical Kovat's index, recovery efficiencies of traps with methyl polysiloxane films were 80%–100% for a wide range of injected sample mass.

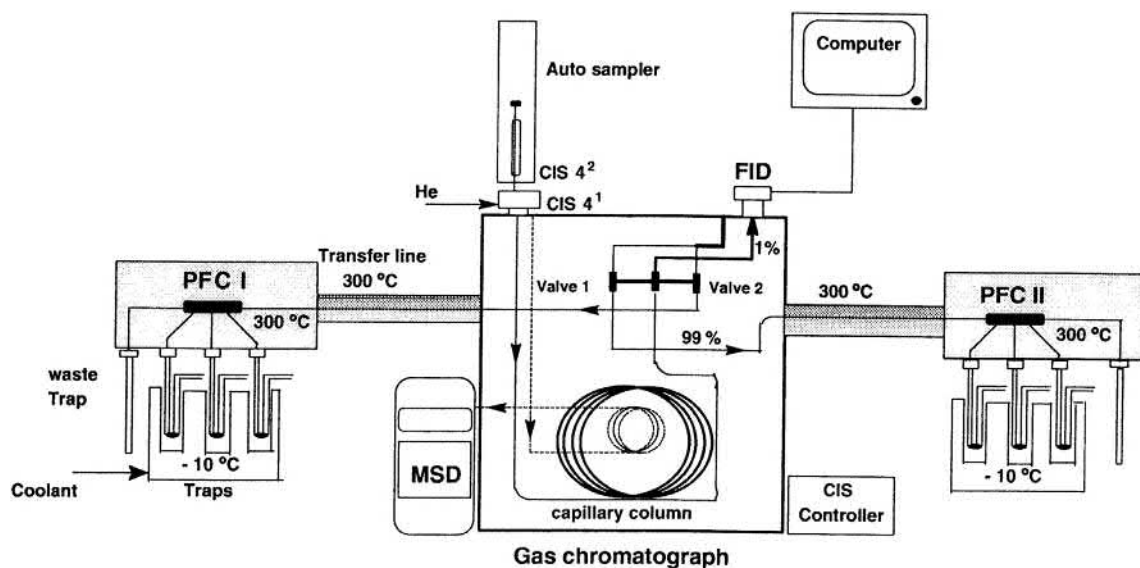


FIGURE 18.2 Schematic illustration of an analytical scale prep-GC system consisting of two prep-fraction collectors (PFC I and PFCII) modules and a waste trap, as described for the Gerstel system in Ref. [28]. Used with Permission of the Copyright Holder.

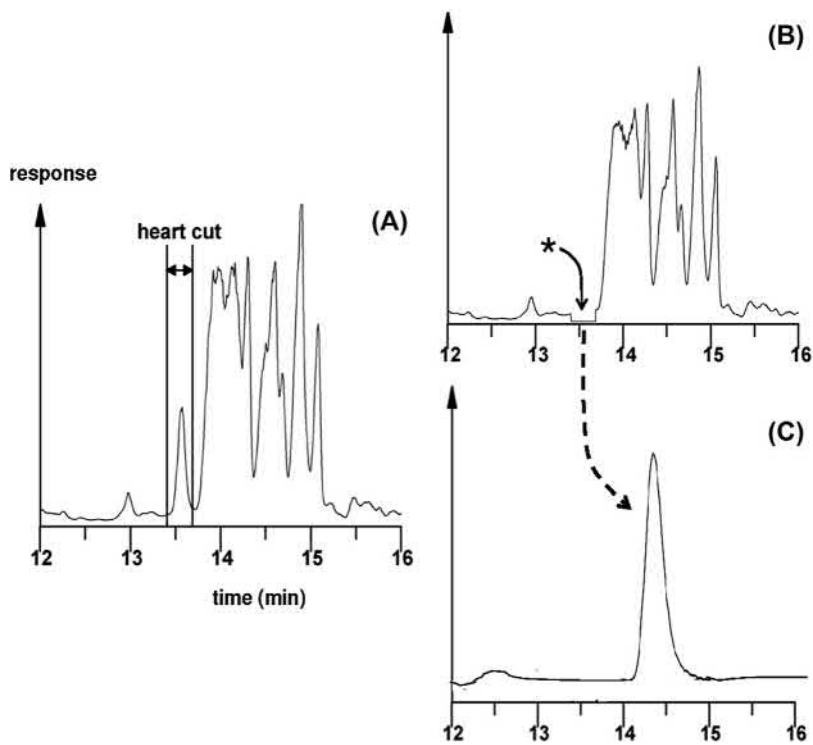


FIGURE 18.3 Demonstration of the heart-cutting procedure using a Deans' switch (A) before heart-cutting and (B) after heart-cutting of a target compound— here, a nonylphenol isomer of a polyethoxylate sample. (C) The subsequent GC analysis of the single isolated component peak.

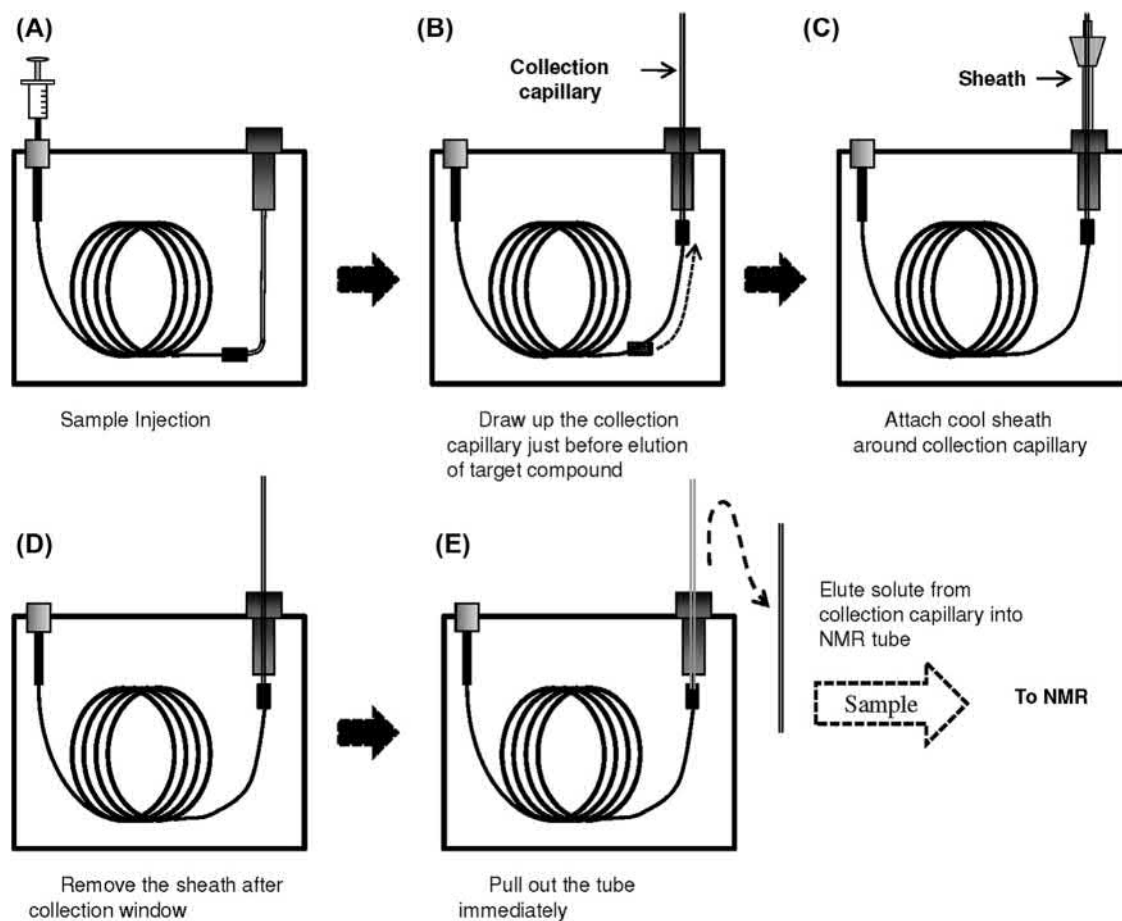


FIGURE 18.4 Sample collection procedure using prep-GC with a trapping capillary method adopted by Nojima. Adapted from S. Nojima, C. Apperson, C. Schal, *A simple, convenient, and efficient preparative GC system that uses a short megabore capillary column as a trap*, *J. Chem. Ecol.* 34 (3) (2008) 418–428.

18.3.3.3 Sorbent trapping method

In order to enrich many key odor compounds that can occur at a very low level in a complex sample such as wine, Ochiai et al. [35] introduced a single PFC module consisting of a heated transfer line, an additional heater, an adsorbent packed tube (e.g., Tenax tube), and a PFC pneumatic box, shown in Fig. 18.5. The adsorbent packed tube was used to enrich the target components from multiple injections. The trapped and enriched compounds were thermally desorbed and subsequently analyzed by GC-olfactometry (GC-O)/MS for identification. Stir-bar sorptive extraction

(SBSE) was used to extract components from white wine (Sauvignon Blanc and Chardonnay) and placed in a glass thermal desorption liner. Subsequently, the glass liner was placed in the thermal desorption unit. More than 30 extractions could be performed with the same bar, which allowed enriching the target components into the adsorbent packed tube. They evaluated PFC recovery of a single injection of the 15 model flavor compounds at 10 ng each, including alcohols, aldehydes, esters, lactones, and phenol. Recovery in the range of 85%–98% was obtained [35]. This application is typical of the general sorbent-trapping procedure.

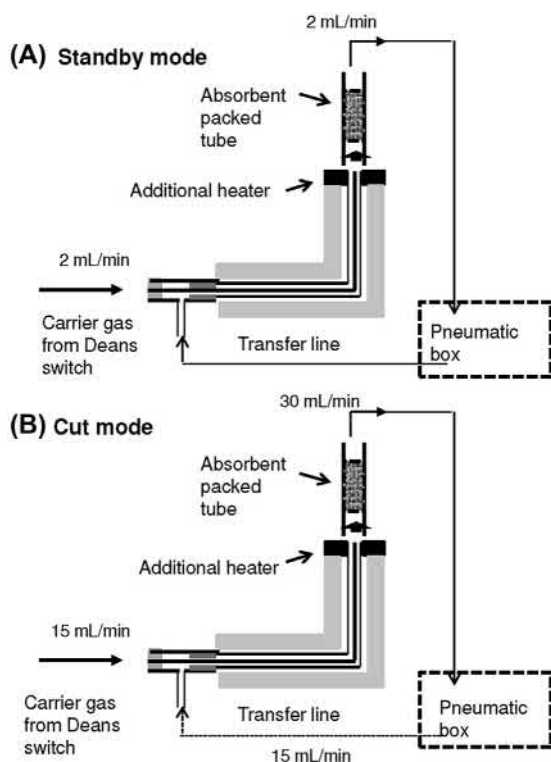


FIGURE 18.5 Sorbent-trapping method introduced by Ochiai and Sasamoto [35] for a switchable 1D–2D GC method. (A) Standby mode; (B) cut mode. The absorbent packed tube (Tenax TA) after trapping and enriching the target components can be thermally desorbed using thermal desorption (TD)-GC-O/MS for identification. *Diagram redrawn based on N. Ochiai, K. Sasamoto, Selectable one-dimensional or two-dimensional gas chromatography-olfactometry/mass spectrometry with preparative fraction collection for analysis of ultra-trace amounts of odor compounds, J. Chromatogr. A 1218 (21) (2011) 3180–3185.*

18.3.4 Spectroscopic methods for use with prep-GC

Once the target compound(s) is (are) trapped in adequate amount, it can be taken—usually manually—to any spectroscopic instrument for subsequent study. This is limited only by either the needs or availability of the appropriate technique or the ingenuity of the researcher to devise suitable analytical approaches for identification. Generally, this constitutes off-line hyphenation (denoted by the double-forward slash mark

chromatography//spectroscopy), where the collected fraction is remote from the subsequent molecular characterization tool. With fraction in hand, therefore, any tool can be used to provide identification, subject to sensitivity requirements and physical or chemical considerations. This section is not intended to provide an exhaustive survey of the various techniques, which have been employed as the “//spectroscopy” component of the system, but, rather, in conjunction with the applications outlined Table 18.1 and those covered in Section 18.4, will illustrate a selection of typical (mainly recent) studies that have been conducted with prep-GC.

18.4 Case studies: applications

Many studies, which have been recently carried out using prep-GC, are summarized in Table 18.1. Some of these will be discussed further further.

18.4.1 Natural products: pheromones

Many pheromones, which often are multi-component mixtures and present in nanogram or picogram amounts, require structure elucidation for a variety of purposes such as pest control. Nojima et al. [17] developed a simple and inexpensive approach to submicro-scale prep-GC of volatile compounds for use with off-line NMR. The recovery efficiency of volatile compounds using cryogenic trapping with a short section of a deactivated megabore capillary tube was >80% with sample sizes of 0.05–0.5 μg . The purity of the collected samples was enough for structure elucidation by high-sensitivity NMR analyses including 2D NMR experiments. Subsequently using the same technique, Nojima et al. [18] described a method to isolate a thermally and chemically unstable sex pheromone from the female German cockroach (*Blattella germanica* (L.)). The gland was collected and extracted, followed by preliminary

TABLE 18.1 Selected reports of analytical prep-scale GC.

Study objective	GC conditions	Trapping method/collected quantity	Analytical methods	References
1 Chiral inhalation anesthetics isoflurane and desflurane	Prep-GC: FID, traps Column: Packed column octakis(2,6-di-0-n-pentyl-3-O-butanoyl)-cyclodextrin in SE-54 (10%, w/w), coated on Chromosorb PAW DMCS (20.3%, w/w)	Collector: Traps cooled with liquid nitrogen	NMRX-ray crystallography	Schurig [24]
2 Degradation product of inhalation anesthetic sevoflurane	Prep-GC: FID, traps Column: Packed column (1 m × 18 mm i.d.)	Collector: Same as case 1	NMRX-ray crystallography	Schmidt [22]
3 Volatile composition of cognac and calvados	Prep-GC: Thermal conductivity detector Column: Packed column (4 m × 5.2 mm i.d.) with a 5% SE-30 (100% dimethylpolysiloxane on Chromosorb PWA 100 mesh)	Collector: Manual collector-connected glass tubes in liquid nitrogen	GC/MS (CI, EI)	Ledauphin [38]
4 Aromatic hydrocarbons from the UCM recovered from a biodegraded crude oil.	Prep-GC: FID, Gerstel PFC Column1: BP-5 (15 m × 0.53 mm i.d. × 1.0 μm d _i) Column2: SolGel-Wax (30 m × 0.25 mm i.d. × 0.25 μm d _i)	Collector: Gerstel PFC	GC/MS	Sutton [37]
5 14 fractions from a commercial nonylphenol (NP)	Prep-GC: FID with PTV-LVI with PFC Column: DB-5 (60 m × 0.25 mm i.d. × 0.25 μm d _i)	Collector: Same as case 4	GC/MS, NMR recombinant yeast screen	Kim [3]
6 Gentsyl quinone isovalerate, sex pheromone of German cockroach, <i>Blattella germanica</i>	Prep-GC: GC-EAD system converted to a prep-GC Column: Nonpolar Equity-1 (5 m × 0.53 mm i.d. × 1.5 μm d _i)	Collector: Injection port modified as a collection port with cryogenic trapping, a detachable sheath with a reservoir for a refrigerant to cool the collection traps	GC/MSNMR	Nojima [18]
7 Fractionation of nonylphenol isomers into 11 fractions	Prep-GC: mps2-Auto-injector, PFC with CIS 4 Column: HP-5MS, 30 m × 0.32 mm i.d., 0.5 μm d _i	Collector: two Gerstel PFC with CIS 4. Recovery: 77–552 μg of isomers after 600 single injections	GC/MSD	Meinert [28]
8 Congeners isolated from several widely produced PCB commercial/technical mixtures	Prep-GC: FID and a 7683 series autoinjector in conjunction with a septumless CIS and Gerstel PFC Column: a VF-5MS “megabore” fused silica capillary column (60 m × 0.53 mm i.d. × 0.5 μm d _i)	Collector: Gerstel PFC with glass traps with CIS was operated in “solvent vent” mode Recovery: Individual PCBs (or coeluting congeners groups) ranged from 90% to 100%	Chlorine isotope analysis, sealed-tube combustion with TIMS	Mandalakis [29]
9 Sex pheromone component of the Japanese mealybug	Prep-GC: PFC with two columns Column1: TC-FFAP (15 m × 0.53 mm i.d. 1 μm d _i) Column2: TC-1 (15 m × 0.53 mm i.d.)	Collector: Gerstel PFC	GC/MSNMR	Sugie [19]

Continued

TABLE 18.1 Selected reports of analytical prep-scale GC.—cont'd

Study objective	GC conditions	Trapping method/collected quantity	Analytical methods	References
10 Investigate capillary column traps under various collection conditions for different compounds	Prep-GC: FID, outlet port assembly Column: Nonpolar EC-5 megabore capillary column (30 m × 0.53 mm i.d. × 1.0 μm d _i) Deactivated column (with a press fit connector): 2 m × 0.53 mm i.d.	Collector: Same as case 6 Collection traps: a DB-1 1.5 μm d _i Recovery: 84% of injected compounds mass with injected sample mass (from 10 to 1000 ng of each)	NMR	Nojima [34]
11 Volatile components (geraniol) from 15 partially coeluting compounds from the first column	Prep-MDGC: two columns in an oven, FID1, 2, a three-channel EPC module, DS and LMCS. 1D column: DB-5 (15 m × 0.32 mm i.d. × 1 μm d _i) 2D column: DB-Wax (15 m × 0.32 i.d. × 0.5 μm d _i)	Collector: External trapping assembly (xTA), trapping capillary (100 × 0.53 mm i.d.) in a cryotrap (xCT) recovery: From 10 (8.6 μg) and 100 injections (77.6 μg; purity >99%) 12.3 μg mL ⁻¹ (10 injections) for proton and gCOSY 110.8 μg mL ⁻¹ (100 injections) gHSQC and gHMBC	2D NMRgCOSY NMRgHSQC and gHMBC NMR	Eyres [11]
12 Isolation of 1,4-dimethoxybenzene from an essential oil, isomers of methylnaphthalene from a crude oil	Prep-MDGC: Same as case 10 1D column: Same as case 10 2D column: Same as case 10	Collector: Same as case 11 Recovery: 1,4-Dimethoxybenzene (5.2 μg, 10 injections) 1- and 2-methylnaphthalene (3.1 μg, 38 injections and 5.0 μg, 35 injections)	¹ H-NMR	Eyres [12]
13 Characterization of menthol, linalyl acetate, carvone and geraniol from essential oil	Prep-MDGC: Same as case 10 1D column: Same as case 10 2D column: Same as case 10	Collector, DFS transfer lines: Same as case 10 Recovery:	MSNMR	Rühle [32]
14 Identification of (<i>E,E</i>)-2,4-undecadienal from coriander	Prep-GC: FID Column: Supelco-wax (60 m × 0.75 mm i.d.)	Collector: Short capillary column (25 cm × 0.53 mm i.d. × 2.0 μm d _i)	GC/MS	Ikeura [40]
15 Multidimensional method to assess quality of pure tea tree oil and presence of allergenic agents	Prep-GC: FID with a fractionation system View Prep Station (VPS278) Column: A wide bore non-polar (30 m × 0.53 mm i.d. × 5.0 μm d _i)	Collector: VPS278 through software, VPS control. Seven microtubes (5°C) (six × collection, one × waste) An additional gas flow (He) was used, with reversed gas flow to avoid cross-contamination inside collection tubes	GC/MS ¹ H-NMR	Sciarrone [20]
16 Potentially mutagenic components	Prep-GC: Same as case 7 Column: Same as case 7	Collector: Same as case 7 Auto-sampler mps2 (Gerstel) and a speed of injection: 100 μL s ⁻¹	GC/MS	Meinert [30]
17 Best parameters for PFC using six test analytes with different physicochemical properties	Prep-GC: Zero-dead volume effluent splitter to FID, two Gerstel PFC with CIS 4. Column: HP-5MS (30 m × 0.32 mm i.d. × 0.5 μm d _i)	Collector: two Gerstel PFC with CIS 4. Two columns: 0.87 m × 0.32 mm i.d. Deactivated FS-Phenyl-Sil column: 0.5 m × 0.1 mm i.d. (for effluent splitter)	GC/MS	Meinert [31]

18	Reaction of phenylacetylene with para-substituted aryl-iodides	Prep-GC: FID, xTA with cryotrap Column: a DB-5 (15 m × 0.32 mm i.d. × 1 μm d _f)	Recovery: 50%–70% for all compounds except benzo[a]pyrene (94%) Collector: Same as case 10 DFS transfer lines: 2 m × 0.18 mm i.d.	GC/MSNMRX-ray	Rühle [33]
19	Volatile impurities at major and minor percentage levels in a pharmaceutical matrix by NMR and MS	Prep-GC: FID, a CIS 4 PTV and Gerstel PFC Column: a DB-5 (30 m × 0.53 mm i.d. × 5 μm d _f) PTV: At 20°C for the injection	Collector: Gerstel PFC with traps containing 200 μL of methanol-d ₄ and a small (1.7 mm) cryogenic probe Conditions: Trapping optimized using liquid sorbents Recovery: Total amount of one of the isolated impurities <60 nmol	GC-APCI-TOF MS1D NMR2D NMR-COSYHSQC, HMBCDQF, CASE	Codina [10]
20	Selectable 1D or 2D GC–O/MS with PFC. Off-flavor compounds	1D column: DB-Wax (30 m × 0.25 mm i.d., × 0.25 μm d _f) 2D column: DB-5 (10 m × 0.18 mm i.d. × 0.40 μm d _f)	Collector: Heated transfer line, additional heater, adsorbent packed tube, PFC pneumatic box Selectable 1D/2D GC–Olfactometry/MS with PFC: 1D or 2D GC-MS, DS2, PCM 2, single PFC module. 1D and 2D column outlets (connected to DS2) Transfer capillary: 1 m × 0.32 mm i.d. d _f Recovery: PFC enrichment with 20 injection of 15 model compounds; 500 pg each (98%–116%) SBSE-PFC enrichment efficiency: 71%–78%	2DGC–O/MS	Ochiai [35]
21	Isolation, purification of semiochemicals (i.e., insect pheromones) and NMR analysis of <1 μg of material	Prep-GC: FID, outlet port assembly Column: Either a non-polar EC-5 or polar EC-WAX megabore capillary column, 30 m × 0.53 mm i.d. × 1.0 μm d _f	Collector: Injection port modified as a collection port Collection traps: DB-1 (2 cm × 0.53 mm i.d. × 1 or 5 μm d _f) Recovery: 50 ng of geranyl acetate for NMR 250 ng of geranyl acetate for H–H COSY NMR	¹ H-NMRH-HCOSY NMR	Nojima [13]

high-performance liquid chromatography (HPLC) fractionation in a biological activity-directed isolation step to discern which LC fraction contained the active component. The active fraction was then further separated by analytical-scale GC with antennography, followed by prep-GC of the active region using multiple injection steps to finally isolate the individual active compound of interest. However, it seems that this system is not suitable for sequential fractionation of multiple chemicals with a single GC run.

Nojima et al. [13] described simple off-line integration of prep-GC and capillary NMR analysis to facilitate the identification of minute amounts of small volatile compounds. ^1H -NMR spectra were obtained with 50 ng of geranyl acetate, a model compound, and reasonable H-H COSY NMR spectra were obtained with 250 ng of geranyl acetate. This is a significant development since it pushes the amount required to be isolated by using GC to considerably smaller quantities than in prior work. Thus, either fewer repeat injections are needed or the method can be extended to much smaller abundance components.

18.4.2 Impurities in pharmaceutical samples

Impurity profiling in modern pharmaceutical products analysis is an important but challenging task to improve the quality of drugs as well as the safety and efficacy of drug therapy. In an editorial, Görög [4] described a wide range of techniques for impurity profiling with the dominance of HPLC and GC with MS technologies acknowledged. While many other separation and bulk analysis methods are available, they tend to be less commonly used. Since off-line NMR (both as a bulk analytical method and with fraction collection with LC) provides considerable structural information, its complementary role to MS is valuable. Therefore, the

HPLC/NMR/MS coupled instrument has been attracting increased attention. However, Codina et al. [10] reported prep-GC with fraction collection and NMR precisely for the task of impurity identification. Various computer-aided structural elucidation (CASE) tools for molecular formula assignment supported the task. Three impurities (A, B, and C) were required to be identified in a pharmaceutical matrix with known main compound band (MB). However, the least concentrated sample (impurity D) was identified as well, with sufficient amount collected for 1D and 2D homonuclear (^1H) and possibly heteronuclear (^1H , ^{13}C) NMR experiments. The trapping efficiencies were 63% for MB and 39%, 63%, and 54% for impurities A, B, and C respectively [10]. Their structures are shown in Fig. 18.6. Codina also observed that the prep-GC method saved considerable time and streamlined the analysis procedure for identification of impurities in the drug synthesis they investigated. This was from the perspective of researchers in the pharmaceutical industry.

18.4.3 Environmental pollutant studies

Using a combination of LC fractionation and prep-GC, Kim et al. [3] obtained 14 purified fractions from a commercial nonylphenol (NP). The isomeric structure of the nonyl group was confirmed by GC-MS and NMR analysis. Meinert et al. [28] fractionated technical p-NP into 11 fractions by using prep-GC, with a total of 600 injections made. Being a technical sample, large quantities of sample were available. The collected amounts of fractionated NP isomers ranged from 77 to 552 μg of isomer, which was sufficient to allow subsequent biotesting in the screen assay used. In the absence of pure isolates of each isomer, it is not possible to uniquely allocate the bioactivity associated with each isomer.

Using combined methodologies including genotoxicity testing and reversed-phase liquid chromatography (RP-LC) with prep-GC,

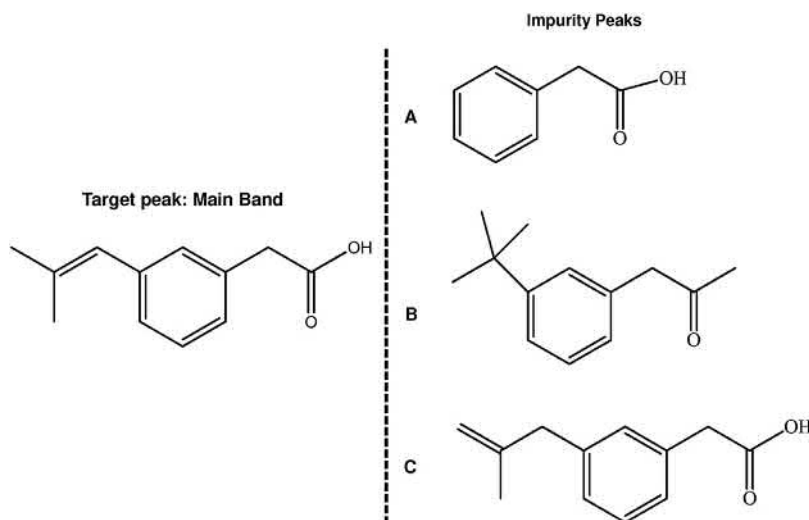


FIGURE 18.6 Main compound and impurity peak structures identified in a pharmaceutical matrix by Codina [10].

Meinert et al. [30] tentatively identified a total of 62 components in genotoxic fractions from a contaminated groundwater. For structure characterization of unknown chemicals, a computer-based structure generation tool called MOLGEN-MS was added to spectral library information from the NIST05 library [30].

In order to study the heterogeneity arising from both ethoxylate and NP groups, Wu et al. [21] fractionated a mixture of nonylphenol polyethoxylate (NPnEO; n = number of ethoxylate groups), nonionic surfactants, using normal-phase liquid chromatography (NPLC). Collected fractions were then analyzed by GC and GC-MS to allow the nonyl isomeric distribution to be displayed. Since mass spectra obtained did not give enough information about the chemical structures of the well-resolved NPnEO isomers, absolute structural identification was not achieved. Therefore, one of the isomers of an NP2EO sample was heart-cut and collected by prep-capillary-scale GC. GC-MS was used to confirm its purity and the structure of the isomer was elucidated by ¹H-NMR spectroscopy.

18.4.4 Chiral studies and X-ray analysis

Schurig et al. [23] reported the preparative enantiomer separation of the inhalation anesthetics, enflurane and isoflurane, in high chemical purity (>99.5%) and enantiomeric purity (>99.9 and 99.4%, respectively). The prep-GC method used a packed column with octakis(2,6-di-O-n-pentyl-3-O-butanoyl)-cyclodextrin dissolved in SE-54 (10% w/w) and coated on Chromosorb P-AW-DMCS (20.3%, w/w). This approach showed the first preparative racemate resolution of both anesthetics by chromatography. Subsequently, Schurig et al. [24] characterized isoflurane and desflurane, which are normally clinically administered as a racemic mixture, by using prep-GC and crystal structure determination.

Schmidt et al. [22] described an experiment in which the enantiomers of an inhalation anesthetic compound were resolved on a chiral packed column in order to isolate the individual isomers of the R and S forms of sevoflurane. The enantiomers were reported to have an unprecedented

high separation factor on the enantioselective phase used, and so this allows considerable overloading without compromising the purity of separation. Not only was sufficient of each of the enantiomers collected to permit NMR analysis, but also crystal structures were possible by careful crystallization of the enantiomers. This provided absolute structural assignment of each isomer.

Marriott and coworkers [33] studied GC separation of a mixture of Sonogashira catalyst products, which could not be separated by classical liquid chromatographic approaches. The products of interest were well separated with one-dimensional GC with a thick-film phase column, but gave equivalent mass spectral data. Therefore, the MS data were not conclusive for structural details. Using prep-GC, up to about 100 μg of pure product was collected, sufficient to conduct NMR and allow crystallization of the bulky aromatic compound. The small crystals were subsequently analyzed by using synchrotron radiation. The first of the peaks had a distinctive NMR result that was similar for all of the different compounds, suggesting a similar structural environment. However, the NMR spectrum of the second isomer was quite different. The primary product was found to be a symmetric tetra-aryl benzene compound.

18.4.5 Petroleum studies

The unresolved complex mixture (UCM) or GC "hump," which is present to various degrees in almost all crude oil samples, has for decades been a difficult task for analysts to identify using one-dimensional GC. Recently, it has been studied by comprehensive two-dimensional gas chromatography ($\text{GC} \times \text{GC}$), which has proved capable of decoding its compositional complexity [36].

Sutton et al. [37] isolated hydrocarbon fractions from a biodegraded crude oil by using prep-GC. This followed a sequence of prep-open column chromatography, prep-HPLC

(using three columns in series), prep-GC on a polar phase into 10 s cuts, and finally prep-GC on a polar phase to recover the final component. They reported a series of C_{26} – C_{28} triaromatic steroids and tentatively identified a novel C_{26} 17-desmethyl triaromatic steroid. They suggested that the UCM might comprise 250,000 compounds, which is a rationale for none of them being resolvable by using a 1D chromatographic analysis. With a novel-capillary MDGC approach, Eyres et al. [12] isolated the isomers of 1- and 2-methylnaphthalene (MN) from a complex crude oil. A total of 3.06 μg 1-MN was collected from 38 injections to give a concentration of 5.07 $\mu\text{g mL}^{-1}$ for NMR analysis. A total of 5.00 μg 2-MN was collected from 35 injections to give a concentration of 8.22 $\mu\text{g mL}^{-1}$ for NMR.

18.4.6 MDGC methods

In addition to the aforementioned study, Eyres et al. [11] had earlier introduced a novel prep-cap MDGC method to resolve geraniol from an essential oil mixture made up of lavender and peppermint oils. Geraniol, a target component, was coeluted with at least six other compounds on the first column. Using a longitudinally modulated cryotrap as a cryogenic storage system, the coeluted zone was completely resolved on the ^2D column. A Deans' switch connected to the end of the second column was used to heart-cut only the geraniol into an external trapping assembly. This system is shown in Fig. 18.7. All other eluted compounds were directed to a monitor FID. From 50 to 100 injections were made to collect sufficient geraniol for 1D and 2D NMR analysis. The 800 MHz NMR instrument provided improved S/N for collected analyte.

In a follow-up study using the same sample matrix as that used by Eyres earlier [11], Ruhle et al. [32] proposed that by targeting a range of different compounds to be heart-cut to an

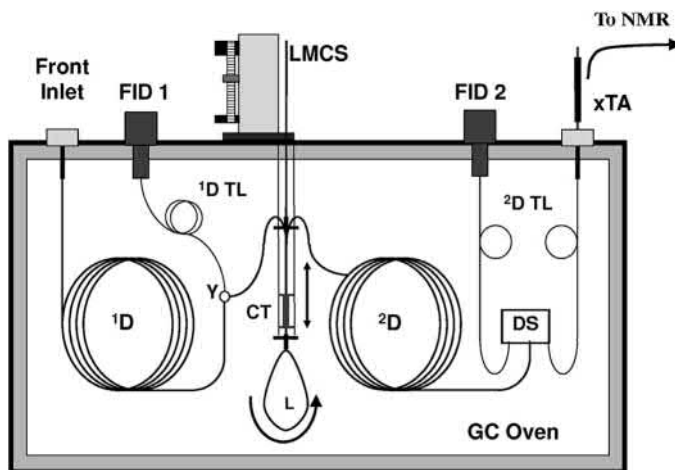


FIGURE 18.7 Preparative capillary MDGC method described by Eyres et al. [11] incorporating a trapping loop segment (L) and cryotrap (CT) that isolates a target region of a ^1D elution and effectively separates it from earlier and later peak regions. Separation of the target region on ^2D yields single peaks that can be heart-cut using a Deans' switch (DS) through a transfer line (TL) into an external trapping assembly (xTA). *Used with Permission of the Copyright Holder.*

external trapping assembly, it would be possible to prepare novel mixtures of compounds from a sample. If this was a natural sample, such as an essential oil, it could theoretically be possible to create a new mixture that is commercially unavailable, or even one that is “impossible” to synthesize due to the natural complexity of some compounds. In the case referred to, various combinations of linalyl acetate, carvone, geraniol, and menthol were collected into mixtures comprising different components, simply as a proof of concept of the method. However, if a specific compound was desired, it could be isolated, and its NMR and mass spectra recorded (and if possible, an X-ray structure obtained) to obtain a pure microquantity reference standard.

18.4.7 Prep-scale enrichment of bulk compounds for further GC analysis

The prep-GC method can be used to enrich bulk volatile compounds from a sample, in order to apply the collected mixture to a further

analysis—and usually this will be by GC/MS. This was used by Ledauphin et al. [38] for cognac and calvados to increase component abundance and achieve greater detectability for many minor components in the samples. In this case, trace compounds present in both spirits were characterized, aided by prep-GC separations. A multiple analytical approach was used to tackle this problem: Initially, groups of compounds were separated by prep-GC, and the fractions were analyzed on a polar stationary phase by GC/MS. Silica gel fractionation was then used to separate prep-extracts by polarity with further GC/MS analysis. A total of 331 compounds were characterized in both freshly distilled cognac and calvados, with 162 considered to be trace compounds, which would have been difficult to identify in the absence of the prep-GC method. Of the trace compounds, the authors reported 39 to be common to both spirits, 30 specific to cognac, and 93 present in calvados but not cognac. Clearly, the prep method proved to be a useful adjunct approach for the discovery process.

18.4.8 Prep-GC via multiple injections with prep-collection in the GC column

By using a cryofocus method and switching devices (e.g., Deans' switch) within one GC oven, it is possible to scale up individual or zones of compounds injected, in order to collect larger amounts of compound at the cryotrap [39]. Elution of the cryotrap then allows the multiple-collected compound(s) to be eluted into a second column (in an MDGC method) or directly to a detector or an external trap to give higher mass of material. This was proposed to be of relevance to give a better response for the compound where the injected sample had a low detection limit, or could give a greater degree of spectral confirmation by increasing mass in a spectroscopic detector, or allow the use of a detector that has a poor detection limit by also increasing the mass delivered to the detector. All of these meet the scope of a prep-GC method, but it is unique in being an online method.

18.5 Conclusions

Analytical-scale prep-GC plays a niche role that is largely associated with the requirement to characterize a compound's structure. This is especially applied to the flavor and fragrance areas, where discovery of new compounds is still directed toward natural products and the perception of desirable characteristics. As this discovery step is pushed to compounds with ever-lower abundance, there remains a need to provide surety of structure. Mass spectrometry does not always provide this level of assurance; so alternative molecular spectroscopic methods are required. This necessitates isolation via prep-GC approaches. NMR has been a mainstay tool for this process and becomes the "gold standard" for characterization. However, in some cases, prep-GC has allowed sufficient material to be collected to permit crystals to be grown, with absolute crystal structure providing unambiguous identity.

As long as there remains a need to fully characterize compounds, where they are present in mixtures such that pure materials cannot be generated by any other means other than by using GC, or where standard GC detectors such as MS are limited in their ability to fully interpret the compound structure, there will be a role to play for analytical-scale prep-GC, as described here.

Acknowledgments

LSK thanks Monash University for the provision of a Dean's International Postgraduate Research Scholarship. This research was supported under Australian Research Council's *Discovery Projects* funding scheme (project number DP1095335). This work was conducted as part of our affiliation with the Australian Centre for Research on Separation Science.

References

- [1] A. Wanikawa, K. Hosoi, T. Kato, K. Nakagawa, Identification of green note compounds in malt whisky using multidimensional gas chromatography, *Flavour Fragrance J.* 17 (3) (2002) 207–211.
- [2] G.R. Jones, N.J. Oldham, Pheromone analysis using capillary gas chromatographic techniques, *J. Chromatogr. A* 843 (1–2) (1999) 199–236.
- [3] Y.S. Kim, T. Katase, M. Makino, T. Uchiyama, Y. Fujimoto, T. Inoue, et al., Separation, structural elucidation and estrogenic activity studies of the structural isomers of 4-nonylphenol by GC-PFC coupled with MS and NMR, *Australas. J. Ecotoxicol.* 11 (3) (2005) 137–148.
- [4] S. Görög, The importance and the challenges of impurity profiling in modern pharmaceutical analysis, *Trac. Trends Anal. Chem.* 25 (8) (2006) 755–757.
- [5] J.R. Idle, F.J. Gonzalez, *Metabolomics, Cell Metab.* 6 (5) (2007) 348–351.
- [6] J. Blomberg, P.J. Schoenmakers, U.A.T. Brinkman, Gas chromatographic methods for oil analysis, *J. Chromatogr. A* 972 (2) (2002) 137–173.
- [7] Y. Li, T. Pang, Y. Li, X. Wang, Q. Li, X. Lu, et al., Gas chromatography-mass spectrometric method for metabolic profiling of tobacco leaves, *J. Separ. Sci.* 34 (12) (2011) 1447–1454.
- [8] J.C. Bosboom, H.-G. Janssen, H.G.J. Mol, C.A. Cramers, Large-volume injection in capillary gas chromatography using a programmed-temperature vaporizing injector in the on-column or solvent-vent injection mode, *J. Chromatogr. A* 724 (1–2) (1996) 384–391.

- [9] K. Grob, M. Biedermann, Vaporising systems for large volume injection or on-line transfer into gas chromatography: classification, critical remarks and suggestions, *J. Chromatogr. A* 750 (1–2) (1996) 11–23.
- [10] A. Codina, R.W. Ryan, R. Joyce, D.S. Richards, Identification of multiple impurities in a pharmaceutical matrix using preparative gas chromatography and computer-assisted structure elucidation, *Anal. Chem.* 82 (21) (2010) 9127–9133.
- [11] G.T. Eyres, S. Urban, P.D. Morrison, J.-P. Dufour, P.J. Marriott, Method for small-molecule discovery based on microscale-preparative multidimensional gas chromatography isolation with nuclear magnetic resonance spectroscopy, *Anal. Chem.* 80 (16) (2008) 6293–6299.
- [12] G.T. Eyres, S. Urban, P.D. Morrison, P.J. Marriott, Application of microscale-preparative multidimensional gas chromatography with nuclear magnetic resonance spectroscopy for identification of pure methyl-naphthalenes from crude oils, *J. Chromatogr. A* 1215 (1–2) (2008) 168–176.
- [13] S. Nojima, D.J. Kiemle, F.X. Webster, C.S. Apperson, C. Schal, Nanogram-scale preparation and NMR analysis for mass-limited small volatile compounds, *PLoS One* 6 (3) (2011) 7.
- [14] N. Ragunathan, K.A. Krock, C. Klawun, T.A. Sasaki, C.L. Wilkins, Gas chromatography with spectroscopic detectors, *J. Chromatogr. A* 856 (1–2) (1999) 349–397.
- [15] H. Schmidt-Traub (Ed.), *Preparative Chromatography of Fine Chemicals and Pharmaceutical Agents*, Wiley-VCH Weinheim, 2005.
- [16] D.A. Carlson, F. Mramba, B.D. Sutton, U.R. Bernier, C.J. Geden, K. Mori, Sex pheromone of the tsetse species, *Glossina austeni*: isolation and identification of natural hydrocarbons, and bioassay of synthesized compounds, *Med. Vet. Entomol.* 19 (4) (2005) 470–479.
- [17] S. Nojima, D.J. Kiemle, F.X. Webster, W.L. Roelofs, Submicro scale NMR sample preparation for volatile chemicals, *J. Chem. Ecol.* 30 (11) (2004) 2153–2161.
- [18] S. Nojima, C. Schal, F.X. Webster, R.G. Santangelo, W.L. Roelofs, Identification of the sex pheromone of the German cockroach, *Blattella germanica*, *Science* 307 (5712) (2005) 1104–1106.
- [19] H. Sugie, M. Teshiba, Y. Narai, T. Tsutsumi, N. Sawamura, J. Tabata, et al., Identification of a sex pheromone component of the Japanese mealybug, *Planococcus kraunhiae* (Kuwana), *Appl. Entomol. Zool.* 43 (3) (2008) 369–375.
- [20] D. Sciarone, C. Ragonese, C. Carnovale, A. Piperno, P. Dugo, G. Dugo, et al., Evaluation of tea tree oil quality and ascaridole: a deep study by means of chiral and multi heart-cuts multidimensional gas chromatography system coupled to mass spectrometry detection, *J. Chromatogr. A* 1217 (41) (2010) 6422–6427.
- [21] Z.Y. Wu, C.P.G. Ruhle, P.J. Marriott, Liquid chromatography fractionation with gas chromatography/mass spectrometry and preparative gas chromatography-nuclear magnetic resonance analysis of selected nonylphenol polyethoxylates, *J. Chromatogr. A* 1218 (26) (2011) 4002–4008.
- [22] R. Schmidt, M. Roeder, O. Oeckler, A. Simon, V. Schurig, Separation and absolute configuration of the enantiomers of a degradation product of the new inhalation anesthetic sevoflurane, *Chirality* 12 (10) (2000) 751–755.
- [23] V. Schurig, H. Grosenick, Preparative enantiomer separation of enflurane and isoflurane by inclusion gas chromatography, *J. Chromatogr. A* 666 (1–2) (1994) 617–625.
- [24] V. Schurig, M. Juza, B.S. Green, J. Horakh, A. Simon, Absolute configurations of the inhalation anesthetics isoflurane and desflurane, *Angew. Chem. Int. Ed.* 35 (15) (1996) 1680–1682.
- [25] M.C. Simmons, L.R. Snyder, Two-stage gas-liquid chromatography, *Anal. Chem.* 30 (1) (1958) 32–35.
- [26] W. Bertsch, Two-dimensional gas chromatography. Concepts, instrumentation, and applications – part 1: fundamentals, conventional two-dimensional gas chromatography, selected applications, *J. High Resolut. Chromatogr.* 22 (12) (1999) 647–665.
- [27] L. Mondello, A.C. Lewis, K.D. Bartle, *Multidimensional Chromatography*, John Wiley & Sons Ltd, Chichester, 2002.
- [28] C. Meinert, M. Moeder, W. Brack, Fractionation of technical *p*-nonylphenol with preparative capillary gas chromatography, *Chemosphere* 70 (2) (2007) 215–223.
- [29] M. Mandalakis, H. Holmstrand, P. Andersson, O. Gustafsson, Compound-specific chlorine isotope analysis of polychlorinated biphenyls isolated from Aroclor and Clophen technical mixtures, *Chemosphere* 71 (2) (2008) 299–305.
- [30] C. Meinert, E. Schymanski, E. Kuster, R. Kuhne, G. Schuurmann, W. Brack, Application of preparative capillary gas chromatography (pcGC), automated structure generation and mutagenicity prediction to improve effect-directed analysis of genotoxicants in a contaminated groundwater, *Environ. Sci. Pollut. Res. Int.* 17 (4) (2010) 885–897.
- [31] C. Meinert, W. Brack, Optimisation of trapping parameters in preparative capillary gas chromatography for the application in effect-directed analysis, *Chemosphere* 78 (4) (2010) 416–422.
- [32] C. Rühle, G.T. Eyres, S. Urban, J.-P. Dufour, P.D. Morrison, P.J. Marriott, Multiple component isolation in preparative multidimensional gas chromatography with characterisation by mass spectrometry and nuclear magnetic resonance spectroscopy, *J. Chromatogr. A* 1216 (30) (2009) 5740–5747.

- [33] C.P.G. Ruhle, J. Niere, P.D. Morrison, R.C. Jones, T. Caradoc-Davies, A.J. Canty, et al., Characterization of tetra-aryl benzene isomers by using preparative gas chromatography with mass spectrometry, nuclear magnetic resonance spectroscopy, and X-ray crystallographic methods, *Anal. Chem.* 82 (11) (2010) 4501–4509.
- [34] S. Nojima, C. Apperson, C. Schal, A simple, convenient, and efficient preparative GC system that uses a short megabore capillary column as a trap, *J. Chem. Ecol.* 34 (3) (2008) 418–428.
- [35] N. Ochiai, K. Sasamoto, Selectable one-dimensional or two-dimensional gas chromatography-olfactometry/mass spectrometry with preparative fraction collection for analysis of ultra-trace amounts of odor compounds, *J. Chromatogr. A* 1218 (21) (2011) 3180–3185.
- [36] T.C. Tran, G.A. Logan, E. Grosjean, D. Ryan, P.J. Marriott, Use of comprehensive two-dimensional gas chromatography/time-of-flight mass spectrometry for the characterization of biodegradation and unresolved complex mixtures in petroleum, *Geochem. Cosmochim. Acta* 74 (22) (2010) 6468–6484.
- [37] P.A. Sutton, C.A. Lewis, S.J. Rowland, Isolation of individual hydrocarbons from the unresolved complex hydrocarbon mixture of a biodegraded crude oil using preparative capillary gas chromatography, *Org. Geochem.* 36 (6) (2005) 963–970.
- [38] J. Ledauphin, J.F. Saint-Clair, O. Lablanquie, H. Guichard, N. Founier, E. Guichard, et al., Identification of trace volatile compounds in freshly distilled calvados and cognac using preparative separations coupled with gas chromatography-mass spectrometry, *J. Agric. Food Chem.* 52 (16) (2004) 5124–5134.
- [39] S.T. Chin, B. Maikhunthod, P.J. Marriott, Universal method for on-line enrichment of target compounds in capillary gas chromatography using in-oven cryotrapping, *Anal. Chem.* 83 (17) (2011) 6485–6492.
- [40] H. Ikeura, K. Kohara, X.X. Li, F. Kobayashi, Y. Hayata, Identification of (E, E)-2,4-undecadienal from coriander (*Coriandrum sativum* L.) as a highly effective deodorant compound against the offensive odor of porcine large intestine, *J. Agric. Food Chem.* 58 (20) (2010) 11014–11017.

Data acquisition and integration

Yuri Kalambet

Ampersand Ltd., Moscow, Russian Federation

19.1 Introduction

Typical problems of data processing are similar for liquid chromatography (LC) and gas chromatography (GC), just that in GC they appeared earlier. GC was the first to meet problems of fast chromatography [1], GC-MS data processing [2], 2D chromatography [3,4], noise reduction in the case of narrow peaks, etc. The same problems later appeared in LC [5]. Every chromatography data system (CDS) can process data from LC and GC devices and algorithms do not differentiate the source of the signal, only terminology sometimes is different (e.g., carrier gas in GC and eluent in LC).

We do not try to review modern CDS from different manufacturers or discuss differences between them; we try to describe how most CDSs work or, sometimes, should work. More detailed reviews of the how CDS works can be found in books [6–10]. Papas provided a good review of the early phase of chromatographic data systems development [11].

Chromatography generates a huge amount of data, which require interpretation; as a result chromatography was one of the technologies that gave birth to a new science—Chemometrics

[12–15]. A significant number of chemometric papers are devoted to chromatography [16].

Tasks of the CDS, discussed in this chapter:

- Control of devices
- Measurement of signals
- Data preprocessing: bunching and smoothing
- Evaluation of peak parameters
- Peak identification
- Quantitative calculations

Some of these themes will be discussed in more detail, for others we will give references to original or review articles. Detailed discussion of the ways CDS works would exceed all reasonable limits—to imagine this one can have to look at the manual for any commercial CDS; they are thousands of pages long. An impressive view of McDowall and Burgess on the demands of an ideal CDS makes a lot of sense [17]. CDS has to obey many rules, from general metrological [18] to legal documents issued by FDA, NIST, ISO, IUPAC, WHO, EURACHEM/CITAC, national regulators, including pharmacopeias, etc. We will focus on mathematical and metrological problems, rather than compliance to legal regulations, paying special attention to the themes that from our view are underestimated.

19.2 Equipment control and signal measurement

Control of chromatographic modules in GC is performed mostly by a small computer, integrated into the GC device itself; the role of the CDS is in sending the working schedule to the device and then receiving back measured data: analytical signal, used to produce qualitative and quantitative results; and auxiliary data, indicating whether the process goes on as expected. CDS exchanges data with the chromatograph in a protected way: making envelopes for each message and protecting messages with checksums. Details of data exchange are hidden from the user, but may be regulated by legal documents.

The function of individual GC devices is discussed in different chapters of this book. The CDS has to send the chromatograph pressure and flow information for gases, temperatures of different modules, and a program of their change in time; switch modules on or off; and set parameters for the detector. Some time ago, every CDS manufacturer had to write software modules for this purpose on their own, duplicating software development and testing efforts many times. A useful initiative by Agilent Technologies, Inc. created a common platform for device control software under Windows, called Instrument Control Framework [19]. Multiple software manufacturers support this platform today.

19.2.1 Measuring chromatographic signals

The signal generated by a conventional detector (analog voltage or current) is converted to a consecutive set of numbers by the chip, called analog-to-digital converter (ADC), in most cases on a time-regular basis. Time between consecutive measurements is called the measurement interval; its inverse is the measurement frequency.

ADC measures the signal during some fraction of the measurement interval (measuring time), this fraction is called the duty cycle. Duty cycle can be expressed as a simple fraction or as percent. Duty cycle of 0.0 (0%) means that measurement corresponds to a voltage or current (signal) at the instant of measurement; duty cycle of 1.0 (100%) means that the signal is integrated; and the result produced by the ADC is proportional to integral of signal during the measurement time. An ADC with a duty cycle 1.0 is called an integrating ADC. An intermediate duty cycle means that the ADC integrates the signal during part of the time and then is busy with another job (e.g., measuring another signal). The duty cycle can be very small for a scanning MS detector and large for conventional GC detectors if the signal is measured by an integrating sigma-delta ADC [20–22]. The idea of the duty cycle can be extended to sample transfer in 2D chromatography [23].

ADCs in chromatography can have very high resolution, up to 32 bit with 26 bit RMS accuracy (2^{26} informative steps per e.g., 5V measurement range, one informative step corresponds to $\approx 0.075 \mu\text{V}$) [20,22]. High resolution has its drawbacks—a lot of interference signals can be detected. Most electrical interference signals are periodic with a frequency the same as the power line network (mains frequency). These signals are generated by the power supply of the device itself and by other devices available in the laboratory. Manufacturers of ADC chips incorporate digital filters that try to suppress 50 and/or 60 Hz frequencies. It is easy to model mains interference by a sine wave with the period of the mains and unknown amplitude, added to the analytical signal. The best way to suppress this interference is to select a measuring time and interval equal to or multiples of the mains period. If the interval is selected poorly, a large part of the interference is left in the chromatogram and has to be suppressed by data bunching or smoothing (Fig. 19.1).

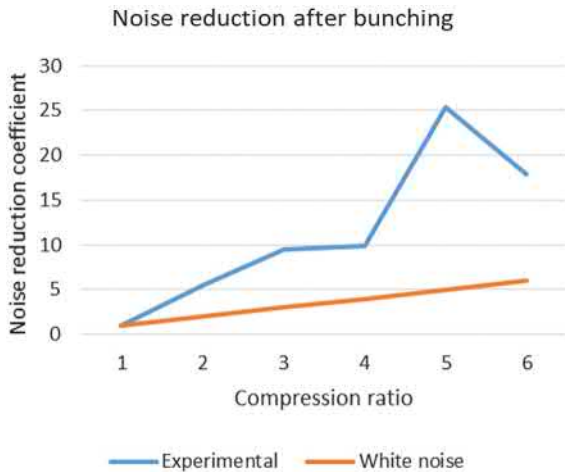


FIGURE 19.1 Baseline noise suppression of the detector signal measured by an integrating ADC at 100 Hz, in a country in which the mains frequency is 60 Hz, by compression (bunching). Every “compression ratio” points of the baseline signal are averaged and form single measurement. Before and after bunching, noise dispersion of the selected baseline region is calculated. Graphs demonstrate the dependence of the noise reduction coefficient for measured data (Experimental) and expected ratio for white noise (White noise) on the compression ratio. Noise reduction coefficient equals ratio of noise dispersion before compression to noise dispersion after compression. Evidence of mains interference: 1) noise reduction coefficient is higher than the expected coefficient for white noise; 2) maximum noise reduction happens at a compression ratio of 5, where the integration period is equal to triple the mains period: $5 \cdot 10 \text{ ms} = 3 \cdot 16.7 \text{ ms} = 50 \text{ ms}$. Similar graphs can be made for any type of weighted average smoothing, but only for the arithmetic mean, it is easy to calculate an optimal window size in advance.

Preferable measurement frequencies depend on the continent: they are {50, 25, 16.7, 12.5, 10 Hz, ...} in Europe with a 50 Hz mains frequency and {60, 30, 20, 15, 12, 10 Hz, ...} in the United States with a 60 Hz mains frequency. The first common frequency in these two lists is 10 Hz; that is why it is used as the default frequency for data acquisition in many devices. The best mains interference suppression happens when the duty cycle equals 1.0. Note that the real frequency of the mains network at any moment is slightly different from nominal,

allowed limits for the EU are $50 \pm 0.2 \text{ Hz}$, so some small amount of mains interference may be unsuppressed.

Measurement frequencies higher than the mains frequency are required for fast chromatography. In this case, one cannot avoid measuring the mains interference and there is a need to suppress it electronically and by digital filters. Electronic noise suppression requires special attention to the construction of the power supply and detector unit—with on-board ADC, shielding, and galvanic isolation. Nevertheless, it is rather difficult to suppress mains interference completely. The proper selection of measurement frequency may simplify digital filter construction. For example, a measurement frequency of 80 Hz in the presence of mains interference in the United States (60 Hz mains frequency) may induce $80 - 60 = 20 \text{ Hz}$ periodic interference in a Fourier spectrum, whereas 120 or 180 Hz measuring frequency will reveal only “pure” 60 Hz mains interference and no lower frequency signals. To avoid spreading of the mains interference power to low frequencies, it is preferable to keep the measurement frequency a multiple of the mains frequency.

So, “rule of thumb” for working with conventional detectors at high and low frequencies—keep the measurement frequency or period a multiple of the mains frequency.

19.2.2 Constant and variable data rates

The need for variable data rate measurements is very seldom, but there are some detectors that produce such data. In this case, time, when the measurement was born, cannot be indicated by a point index, but only by a “time stamp” generated by the detector or CDS. Most CDSs process data with a constant data rate model, which assumes that all measurements are made with the same measurement interval. Irregular data from the detector have to be converted to regular data for integration. It is preferable that this conversion is made not inside the detector, but

inside the CDS. Every CDS should keep raw data (measured value + time of birth) and report them, so the user has a chance to verify that the CDS algorithm converts irregular data to regular, whereas conversion in the detector hides "true" raw data forever. Time stamps are also useful in the case of a constant measuring interval for detection of missing measurements and device malfunctions.

19.3 Peak search

"Integration" is a very general term, the meaning of which differs significantly in mathematics and in chromatography data processing [24]. In mathematics, it's just a calculation of functions integrals; in chromatography it includes smoothing, peak detection, baseline construction, calculation of peak parameters, and peak identification. We will differentiate between them so, that "integration" is used in a mathematical sense, and "chromatographic integration" will be used for a more general chromatographic term.

We intentionally omit a deep investigation of peak search algorithms, as different manufacturers implement them in slightly different ways, and a comparison leads us to a comparison of CDSs, which we should avoid. Many new algorithms are emerging (e.g., Ref. [25]). What is common between algorithms is the result required by the user:

Peak is a reconstructed bell-shaped concentration profile of the substance of interest, converted to a chromatographic detector response profile and visualized along with measurements.

Baseline is a reconstructed imaginative profile of detector signal provided all substances of interest are eliminated from the analyzed mixture.

Our definition of the peak differs from that in the pharmacopeia, but is more convenient for use. Some CDS manufacturers also prefer this definition [26]. The benefit is that a peak is

associated with the substance and not with some shape of the curve. One bell-shaped detector response curve may describe one peak or several overlapping peaks, depending on how many substances correspond to this curve. The detector response for two different masses corresponds to one peak, despite the fact that there are two curves and so on.

19.3.1 Statistical moments of the peak

Zeroth peak moment is peak area

$$M0 = \int_{-\infty}^{\infty} f(x)dx \approx h \cdot \sum_{i=0}^N f(x_i) \quad (19.1)$$

First moment is the average retention time (unfortunately, it is rarely used in chromatography)

$$M1 = \frac{1}{M0} \int_{-\infty}^{\infty} x \cdot f(x)dx \approx \frac{h}{M0} \sum_{i=0}^N (x_i \cdot f(x_i)) \quad (19.2)$$

Second central moment is a dispersion of the peak (standard deviation σ is a square root of dispersion):

$$M2 = \sigma^2 = \frac{1}{M0} \int_{-\infty}^{\infty} (x - M1)^2 \cdot f(x)dx \quad (19.3)$$

$$\approx \frac{h}{M0} \sum_{i=0}^N ((x_i - M1)^2 \cdot f(x_i))$$

Other moments usually are presented not only central, but also normalized to σ^n .

$$Mn = \frac{1}{M0 \cdot \sigma^n} \int_{-\infty}^{\infty} (x - M1)^n \cdot f(x)dx \quad (19.4)$$

$$\approx \frac{h}{M0 \cdot \sigma^n} \sum_{i=0}^N ((x_i - M1)^n \cdot f(x_i))$$

19.3.2 Convolution and moving weighted average

Convolution of two functions $f(x)$ and $g(x)$ is a function

$$(\mathbf{f} * \mathbf{g})(x) = \int_{-\infty}^{\infty} \mathbf{f}(y)\mathbf{g}(x-y)dy \quad (19.5)$$

Moving weighted average smoother is a discrete analog of convolution, where integration is replaced by summation:

$$Y_k = \sum_{i=-n}^n w_i y_{k-i} \quad (19.6)$$

where Y_k stays for smoothed value for the k -th point of the data array, w_i —weight of the point with index $(k-i)$, $y_{(k-i)}$ —unsmoothed (“raw”) signal value. Usually sum of weights equals 1, and $w_i = w_{-i}$. Smoothing window size N_f in these notations equals $N_f = 2n+1$.

19.3.3 Peak shape

The analytical signal, corresponding to the concentration profile of eluted components, is generated by the detector. The signal is typically bell-shaped and approximately Gaussian

$$G(t) = h_G \cdot \exp\left(-(\mu_G - t)^2/2\sigma_G^2\right)$$

In many practical cases, the difference from a true Gaussian shape can be modeled by convolution of Gaussian with an exponent $E(t) = \exp(-t/\tau)/\tau$, called an exponentially modified Gaussian (EMG) [27–30] and can be written as a formula in several different ways:

$$F(t) = \frac{h_G \cdot \sigma_G}{\tau} \sqrt{\frac{\pi}{2}} \cdot e^{\left(\frac{\sigma_G^2}{2\tau^2} \cdot \frac{t-\mu_G}{\tau}\right)} \cdot \left(1 - \operatorname{erf}\left(\frac{1}{\sqrt{2}} \left(\frac{\mu_G - t}{\sigma_G} + \frac{\sigma_G}{\tau}\right)\right)\right) \quad (19.7)$$

$$F(t) = h_G \cdot e^{-\frac{-(\mu_G - t)^2}{2\sigma_G^2}} \cdot \frac{\sigma_G}{\tau} \sqrt{\frac{\pi}{2}} \cdot \operatorname{erfcx}\left(\frac{1}{\sqrt{2}} \left(\frac{\mu_G - t}{\sigma_G} + \frac{\sigma_G}{\tau}\right)\right), \quad (19.8)$$

$$F(t) \approx \frac{h_G \cdot e^{-\frac{-(\mu_G - t)^2}{\sigma_G^2}}}{\left(1 + \frac{(\mu_G - t) \cdot \tau}{\sigma_G^2}\right)} \quad (19.9)$$

where h_G —height, μ_G —apex position, σ_G —standard deviation of the unmodified Gaussian; τ —time constant of the modifying exponent; $\operatorname{erfcx}()$ —scaled complementary error function [31]. The way the peak is calculated is selected in such a way that computation operations do not create overflow of data type *double*; depending on t different parts of EMG with the same σ and τ may be calculated by different formulas [30]. Statistical moments of EMG: $M1 = \mu_G + \tau$; $M2 = \sigma^2 + \tau^2$; $M3 = 2\tau^3$.

In many cases, peak shape is neither Gaussian nor EMG, and CDS has to compute several parameters that chromatographers agree to use for peak description. These include peak position, area, height, width, asymmetry, resolution, plate number count, retention factor, etc. There are differences in how these parameters should be calculated in different countries, reflected in national pharmacopeia documents [32–34]. Every CDS has to calculate these parameters by all possible ways. Parameters are calculated from digitized data stored in the computer.

19.3.4 Peak parameters

The aim of chromatographic integration is the calculation of peak parameters. We should take a stop to look at the formulas used for their calculation. Let us assume that peaks are already

detected at the proper position and a baseline is constructed and subtracted. An asterisk * marks the pharmacopeia way of calculating parameters.

Area A

- * M_0 = zeroth moment

Height (Maximum) H

- *Response of peak apex

Retention T_r

- *Retention of peak apex
- M_1 = first moment
- Position of peak median (the point on retention axis when half of the component has eluted; corresponds to the vertical line, splitting a peak into two parts with the same area).

Width(s) (Fig. 19.2)

- Standard deviation $\sigma = \sqrt{M_2}$ (M_2 = second statistical moment). For EMG $M_2 = \sigma_G^2 + \tau^2$.

- * $FWHM = F_{BL} + T_{BL}$, full width at half maximum, for Gaussian $FWHM \approx 2.355\sigma$ (Fig. 19.2)
- Full width at 0.607 of maximum, for Gaussian $w_{607} \approx 2 \cdot \sigma$
- *Base width (BLW), obtained by intersecting tangents through the inflection points with the baseline. For Gaussian $BLW = 4\sigma$ Asymmetry (Fig. 19.3)
- *(USP) tailing factor, (EP) symmetry factor $S = (WF_{05} + WT_{05}) / (2 \cdot WF_{05})$
- Asymmetry factor $S_a = WT_{10} / WF_{10}$
- τ or τ/σ_G using peak moments. Can be a valuable alternative to traditional methods for very narrow peaks

Void time T_0

- *Retention time of an unretained component. Can be entered manually, from the peak of an unretained component or from void volume and flow rate (LC).

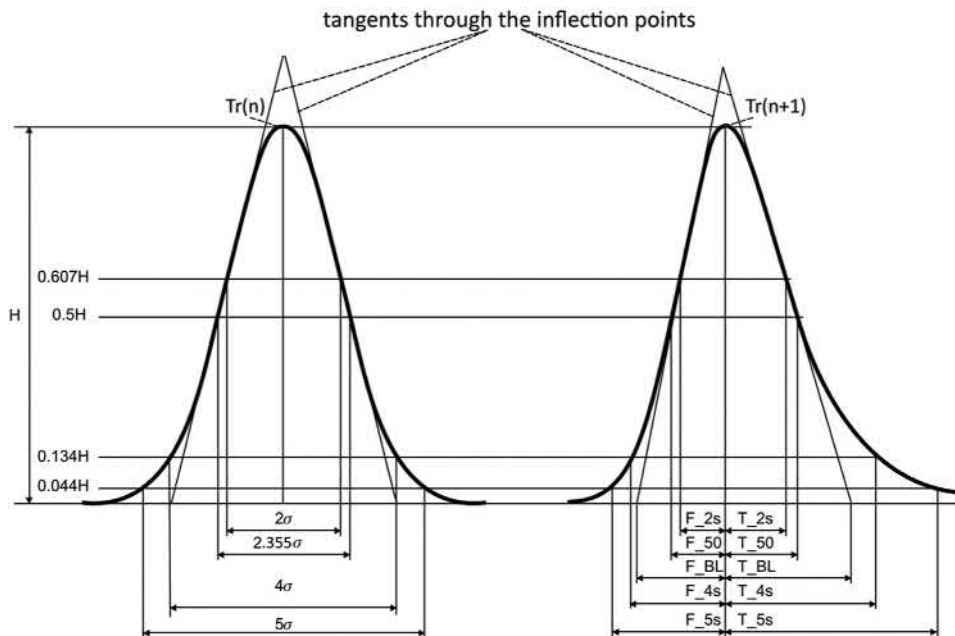


FIGURE 19.2 Peak features, used to calculate parameters.

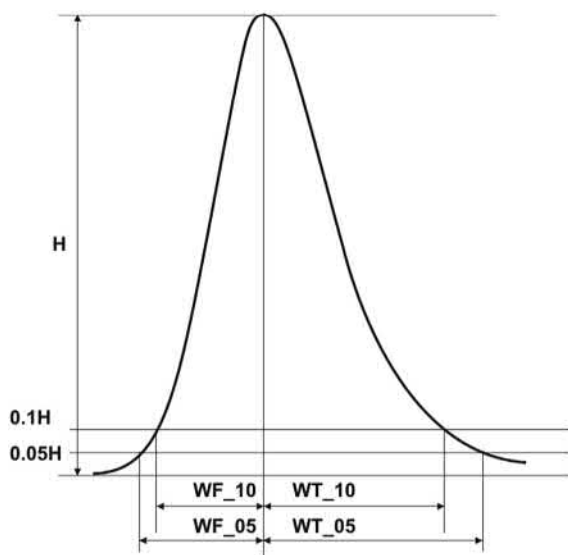


FIGURE 19.3 Illustration of (a) symmetry and tailing factor calculation.

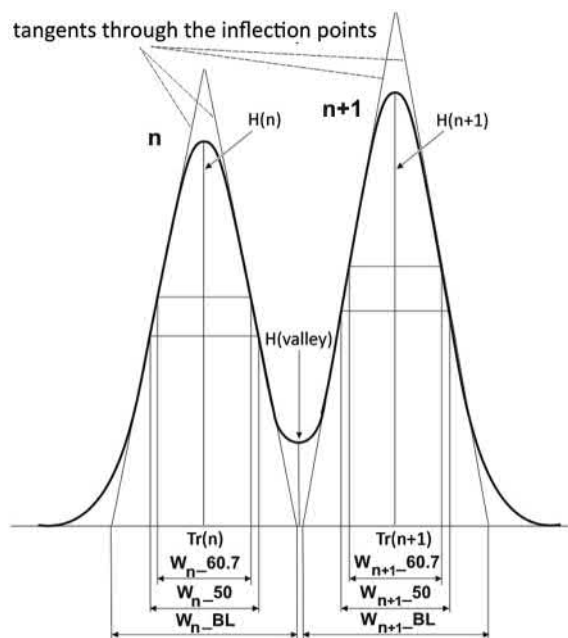


FIGURE 19.4 Peak resolution features.

Resolution (Fig. 19.4)

- * $R = 2 \cdot (T_r(n+1) - T_r(n)) / (BLW_{n+1} + BLW_n)$
- * $R = (2.355/2) \cdot (T_r(n+1) - T_r(n)) / (FWHM_{n+1} + FWHM_n)$
- * $R = (T_r(n+1) - T_r(n)) / (w_{.607}(n+1) + w_{.607}(n))$
- *Peak-to-valley ratio. The peak-to-valley ratio (p/v) is a measure of the quality indicating how well the peak is separated from other substance peaks. Applies to perpendicular drop-separated peaks.
 $p/v = H(n) / H(\text{valley})$

Number of theoretical plates per column

- * $N = 16 \cdot T_r^2 / BLW^2$
- * $N = 5.54 \cdot T_r^2 / FWHM^2$
- * $N = M1^2 / M2$, useful formula for very narrow peaks
- * $N = 2 \cdot \pi \cdot (T_r \cdot H / A)^2$, useful formula, rarely used, that gives reasonable results for insufficiently separated peaks

retention factor (capacity ratio)

- * $k = (T_r - T_0) / T_0$

Noise

- *Peak-to-peak (Fig. 19.5)
- *6·SD (SD = standard deviation of linear regression through peak-free chromatogram region, Fig. 19.5)
- *ASTM (ASTM E685-93, Fig. 19.6)

Signal/Noise ratio

- * $S/N = 2 H / \text{Noise}$
- *Response (area or height) divided by the confidence interval (CI) for this response from the calibration curve

Peak purity

- *Peak purity measures are popular in LC with diode array detectors. GC-MS systems have much more powerful tools to separate peaks due to the high resolution of MS/MS detectors and do not use this measure.

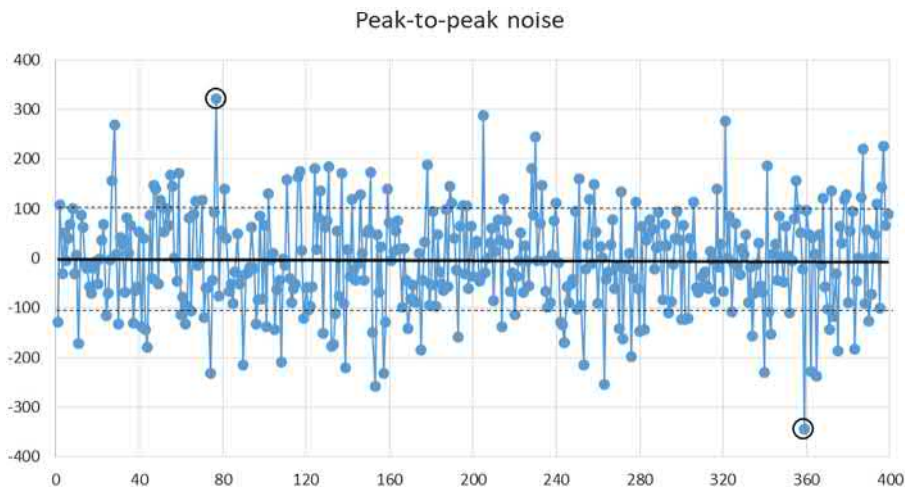


FIGURE 19.5 Peak-to-peak and standard deviation calculations. Fragment of model chromatogram with normal noise, standard deviation equals 100.0. Maximum positive and maximum negative deviation points are circled. Trend line is black solid, plus/minus standard deviations are drawn by dashed line.

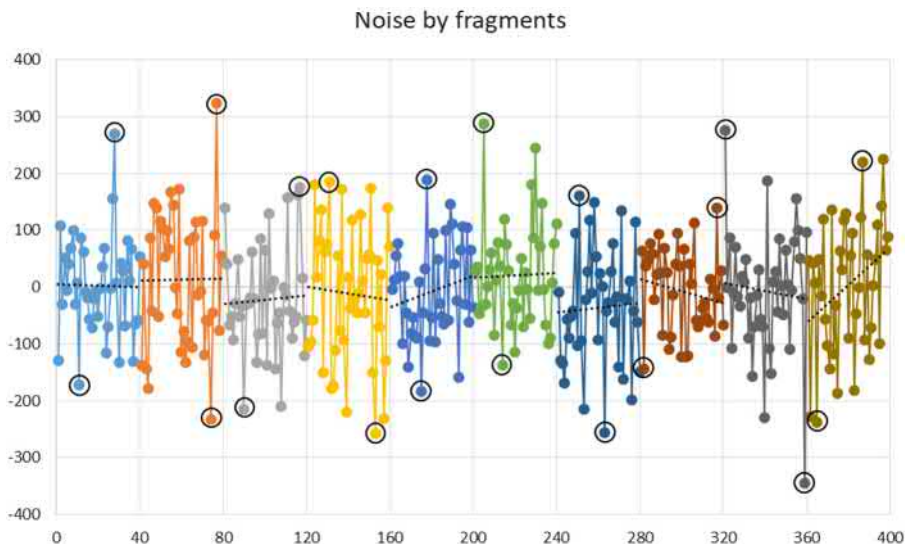


FIGURE 19.6 The same data as for Fig. 19.5, fragmented according to ASTM E685-93; fragments are colored differently. Maximum positive and maximum negative deviation points are circled for every fragment. Trend lines for every fragment are black.

19.4 Errors caused by discretization (data rate) and conversion (bit price value)

Data rate in this chapter is expressed normalized to BLW as $BLWN = 4\sigma / (\text{measuring time interval})$, in data points. The major metrological

peak parameter is area (zeroth peak moment). There are different ways (“rules”) to calculate area, the most important being trapezoidal and Simpson's rules [35]. The long-standing discussion on the number of data points required to integrate a chromatographic peak ([36–38] and

references herein) seems to be closed by the paper of Kalambet et al. [39]. This paper illustrates that all integration rules in the case of peak-like functions have extraordinary high efficiency and:

- Narrow peaks are suitable for quantitative analysis by the trapezoidal rule integration at very low data rates; minimal BLWN for 1% accuracy of the area vary from 2.1 to 5.1 depending on the peak shape;
- Simpson's rule requires a 1.8 times higher data rate to achieve the same efficiency provided by the trapezoidal rule;
- Peak moments for exponentially decaying peaks, such as Gaussian or exponentially modified Gaussian functions are also peak functions and can be efficiently evaluated using the trapezoidal rule.

The calculation of the zeroth peak moment is the only way to calculate its area. Peak height cannot be evaluated by moments; retention, width, and τ , calculated using moments, may be used for most chromatographic calculations, since they have errors caused by discretization close to or below 1% of peak σ . In practice, it may cause problems, since they are not included in any pharmacopeia. Moments are rather sensitive to noise and baseline construction errors [40,41], but there is no alternative in the case of narrow peaks.

Therefore, each parameter requires a different data rate depending on how it is calculated and the required accuracy. The least demanding are measures based on moments. Parameters calculated from peak approximations by polynomials: time/response position of peak apex, FWHM, asymmetry or tailing factors, resolution, typically require higher data rates, $BLWN \geq 25$.

For proper measurement of the signal, an ADC uncertainty should be lower than the detector noise. If the least significant bit for ADC is three or more times smaller than the detector noise, the ADC conversion error can be neglected. The lack of random noise on the

unsmoothed chromatogram means that either the detector sensitivity can be increased by using an ADC with a higher resolution, or that random noise is aggressively suppressed within the detector, giving the illusion of very low noise and hindering proper data processing by the CDS. Digital smoothing of the signal by the detector should be considered as a harmful feature of the detector firmware and should be avoided.

It is very important to evaluate reliability of the analytical results [42]. One of the demands postulated in legal documents is the signal/noise ratio. The basic part here is how to evaluate baseline noise. Pharmacopeias define noise as so-called peak-to-peak noise (Fig. 19.5), calculated as the sum of distances for maximum positive and maximum negative deviations from a trend line. Alternative, offered by all CDS, is six times the standard deviation of the noise distribution. The ASTM definition of detector noise is based on the peak-to-peak noise obtained by dividing the baseline region of the chromatogram into short segments (Fig. 19.6) and calculates an average peak-to-peak noise for all segments. Peak-to-peak noise is a poor statistical measure of noise. Fig. 19.7 shows the dependence of the peak-to-peak noise on the number of data points in the segment.

This problem has practical significance. The minimal number of measurements required for evaluation of peak parameters by peak approximation is about 15 per FWHM. The size of the baseline region required for noise evaluation according to USP [43] equals $5 \cdot FWHM \approx 11.2\sigma_p$ or 75 points. The noise estimate in this case is about $4.7\sigma_n$ or at least 20% less than the unbiased estimate using the $6 \cdot SD$ formula. The situation for very narrow peaks is even worse, as the formal baseline noise region can be decreased to 6 ... 15 measurements, which correspond to an underestimation of the noise by at least twofold. The only benefit of peak-to-peak noise is that it can be measured by a ruler, using a chromatogram drawn on the chart paper of a strip chart recorder.

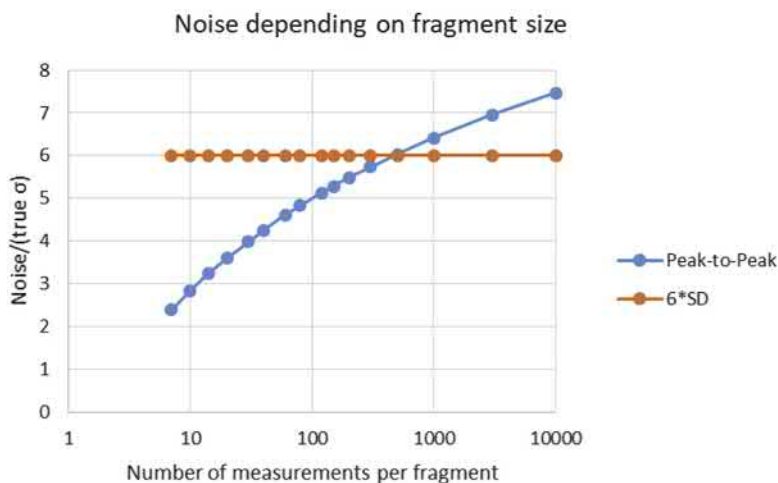


FIGURE 19.7 Processing of the baseline with 120,000 measurements simulated as normal noise with a standard deviation σ_n . The data array was divided into segments with an equal number of measurements (abscissa axis); average peak-to-peak noise for the segments was calculated and divided by σ_n (ordinate axis). It is easy to see that the peak-to-peak detector noise definition provides a biased estimate of the noise level: an unbiased estimate cannot depend on the number of measurements. The 6*SD method provides an unbiased estimate: noise level does not depend on segment size.

19.5 Smoothing

Each measurement can be represented as a sum of the original signal, random noise, and systematic error. Noise and errors are produced by electronic parts of an instrument, variations in environmental conditions, and chemical noise, etc. Enke et al. stated that “Least-squares smoothing is of cosmetic value only. Smoothed data do not contain any additional information” [44]. This statement is very close to reality for all smoothing methods. The aim of smoothing is not to add-in some information, but to eliminate excessive information, not relevant to chromatographic data interpretation.

The aim of smoothing is:

- Maximization of signal/noise ratio, required by formal documents
- Improved precision of figures of merit (area, height, asymmetry, peak width, etc.)
- Simplified peak detection

Smoothing may be explicit or implicit. Explicit smoothing is the application of some smoothing algorithm to the data and conversion of the raw data array into a processed data array for reprocessing and visualization to the user. Implicit smoothing is the application of approximation techniques for evaluation of peak parameters. In all cases, when the least-squares approximation is used for evaluation of some value, implicit smoothing is applied. A typical example of implicit smoothing is a routine that calculates retention time and peak height by approximation of the apex region by a parabola, if the number of points used to construct the parabola is more than three; or evaluation of full peak width at half height using least-squares approximation of peak slopes. Implicit smoothing can help to solve the last two tasks, but maximization of the S/N ratio requires explicit smoothing. In some cases implicit smoothing requires too many computations, in which case, it is better to use explicit smoothing to decrease reprocessing time.

Linear filters. Smoothing operator $S()$ is linear, if the following rules are satisfied:

$$S(a + b) = S(a) + S(b)$$

and

$$S(k' \cdot a) = k' \cdot S(a)$$

where a and b are data arrays of signal and noise, k' is a scalar constant. Otherwise, the smoothing operator is nonlinear. All methods based on a moving weighted average are linear, as well as Fourier [9,45–47] and wavelet [48,49] filters. A median filter is an example of a nonlinear method.

Moving weighted average has many names depending on the weight distribution within the smoothing window. The smoothed value is calculated as a sum

$$Y_j = \sum_{i=-n}^n w_i y_{j-i} \quad (19.10)$$

where i and j are indices, Y_j is a smoothed value, y_{j-i} is a measured value (raw data), and w_i is a weight; set of weights $\mathbf{w} = \{w_{-n}, w_{-n+1}, \dots, w_{n-1}, w_n\}$ is called a kernel. Weight distribution for several kernels is illustrated in Fig. 19.8. Random noise reduction coefficient K can be calculated as

$$K = \text{Var}(y_j) / \text{Var}(Y_j) = 1 / \sum w_i^2.$$

The noise amplitude after smoothing decreases by \sqrt{K} times.

Smoothing by moving weighted average may change statistical moments of the chromatographic peak:

$M0(Y) = M0(y) \cdot M0(\mathbf{w})$, smoothing weights always sum up to 1, so $M0(w) = 1.0$ and $M0(Y) = M0(y)$;

$M1(Y) = M1(y) + M1(\mathbf{w})$, simplest way to set $M1(\mathbf{w}) = 0$ is to make weights symmetric, $w_{-i} = w_i$;

$M2(Y) = M2(y) + M2(\mathbf{w})$, for most weight distributions all weights are positive and chromatographic peak becomes wider and lower.

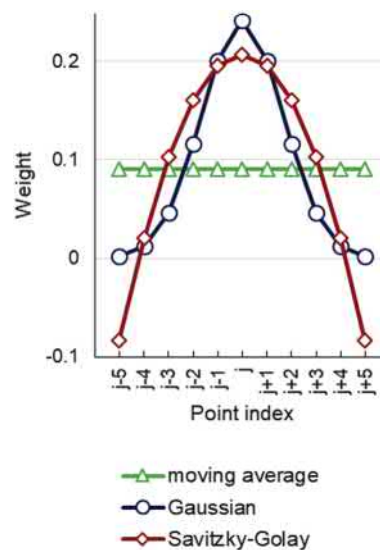


FIGURE 19.8 Weight distribution for three popular kernels, window of size 11, $n = 5$. Savitzky–Golay weights correspond to polynomials of degrees 2 and 3.

Moving average is the simplest noise filtering technique. In this method, all weights are equal, $w_i = 1/(2n + 1)$. The moving average has the highest possible noise reduction coefficient $K = 2n + 1$ for windows with a width $(2n + 1)$.

Bunching (substitution of several consecutive points by one average) can be considered as a special case of the moving average. Bunching is useful when acquisition frequency is too high. Reasonable bunching retains the accuracy, however, processing time and memory requirements are decreased. Bunching is a reasonable first step to convert raw data to processed data.

Multiple smoothing by kernel with nonnegative coefficients starting from 5... 10 passes (depending on the kernel) is equivalent to a single-pass smoothing with weights, distributed according to a normal distribution (*Gaussian smoothing*).

Savitzky–Golay filter. Savitzky and Golay proposed a noise filtering technique based on ordinary least squares [50] implemented as a weighted average. A polynomial of degree m is

fitted to $2n + 1$ consecutive points. The value of the polynomial at the central point is considered as a smoothed value. The Savitzky–Golay smoothing window has weights (Fig. 19.8), which are positive at the center and negative at the edges. Polynomials of degrees $2m$ and $2m + 1$ give the same kernel. The second moment of Savitzky–Golay smoothing for degrees higher than 2 equals 0. The price for that are valleys before and after the peak being smoothed.

Median filter. In this nonlinear method, a median of $2n + 1$ points is calculated. Abscissa of the smoothed value corresponds to the central point of the window. The median filter is robust, because it effectively rejects outliers. However, a median filter can cause area and height distortion. In the presence of outliers, a three-point median filter in combination with some other smoothing technique might provide a favorable result.

Adaptive smoothing is rather not a smoother, but a way to compare different least-square smoothers [51,52]. Each smoother can be used to calculate a smoothed value and a confidence interval (CI) for the smoothed value as well. Adaptive smoothing calculates CIs of different solutions and selects the solution with the lowest CI for every point of the data array. The process of adaptive smoothing starts from the evaluation of the variance of the measurement using the whole data array (chromatogram) and then applies multiple models to approximate data. In the simplest case, these models are just polynomial. Wavelet and Fourier set of basic functions can be used instead or in addition. Result of smoothing consists of two numbers: the smoothed value and CI for this value. Adaptive smoothing is nonlinear, as the optimal smoother for the given measurement depends on the signal profile.

Adaptive smoothing differs from the well-known approach of Kolmogorov–Wiener [45,46]: it does not try to construct an optimal model for the whole data array, it looks for an optimal model for every point, this filter is

optimal locally. The smoother has variable noise reduction; at the baseline it is higher than within the peak region. As evaluation of the measurement variance is an essential part of adaptive smoothing, it cannot be applied to data smoothed in the detector to such an extent that random noise disappears. The best idea is to leave smoothing to the CDS and cancel it in the detector.

19.5.1 Smoother comparison

After smoothing the signal changes, it has a reduced random error, and there appears a systematic error, generated by the smoother. It is possible to compare these errors for the model, consisting of the sum of noise-free (true) signal, close to the signal to be smoothed and the modeled experimental noise. The summary signal is smoothed and compared with the true signal. Making this operation many (e.g., 100) times with different noise implementations, it is possible to separate the residual random and systematic errors for a particular smoother [52]. The peak shape is considered unmodified if the systematic error for every peak point is lower than residual random error. The lower the baseline noise suppression provided that the peak shape is not modified, the better the smoother.

In the case of the moving weighted average, it is possible to predict results without digital modeling: the noise variance will decrease K times and the systematic error can be obtained by subtracting the true signal from the smoothed true signal. The rather complicated scheme described earlier is required for comparisons that include nonlinear smoothers only.

19.5.2 Influence of smoothing on area and height

A major quantitative measure of a peak is its area. Area error consists of the error of the integral (summation) and the error of the baseline. Most filters do not change the sum of

measurements, thus only baseline error can be decreased [53]. The only way to improve the area estimate is to improve the baseline. Results of formal S/N tests based on height also depend on baseline noise suppression. The lower the baseline noise, the better is the S/N ratio.

In the case of a dropped requirement of conserved peak shape, the optimal (minimum of relative error for height and area) noise reduction for most linear filters exists, and for a Gaussian peak and smoother this happens when the second moment M2 of the filter equals M2 of the peak (matched filter) [53]. Other filters with nonnegative weights have similar properties. Savitzky–Golay filter is an exception, as the second moment of this filter equals 0 due to the negative coefficients. It has a further drawback: negative pits around the peak.

Adaptive noise reduction provides the relative random error achieved by an optimal linear filter. Relative random height variations in this case are larger than for an optimal linear filter, but systematic height changes are less (Fig. 19.9).

19.6 Peak identification

A component is an element of the calibration table describing properties of one of the separated substances (components). Its properties

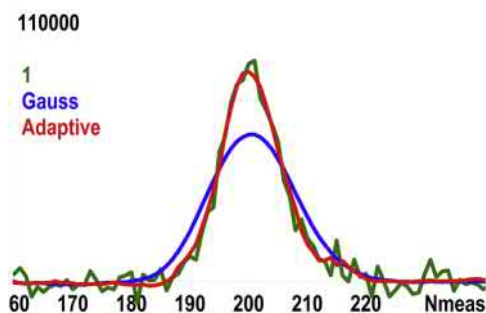


FIGURE 19.9 Model Gaussian peak with normal noise, $S/N \approx 10$ (green: light gray in printed version), smoothed by optimal Gaussian (blue line: dark gray line in printed version) and an adaptive polynomial (red line: gray line in printed version) smoothers.

include name, expected retention time, tolerance interval for the deviation of the experimental and expected retention times (window), type, calibration function coefficients, and spectrum (when applicable). Identification (linking a peak to the component record) is made according to retention time, peak spectrum, or their combination. In the case of identification according to retention, their type—reference and regular components, divides the components in two groups. Every component has its tolerance interval for retention. Reference components are identified before regular components by a link to the highest peak in their window. After that, expected retention time of all regular components is corrected, and every yet unidentified component establishes a link to the peak with a retention time closest to the corrected retention of the components.

Identification of regular peaks can be made by retention index instead of retention time. Retention index appeared as a mean to transfer results of identification between columns or separation conditions. Chromatograms of hydrocarbons typically have very large peaks for n-alkanes, which can be used as reference peaks, and these peaks are assigned retention index values equal to the number of carbon atoms multiplied by 100: methane—100, ethane—200, propane—300, etc. Peaks between the n-alkanes are assigned intermediate retention indices. The relationship for the increase in the index with time can be either logarithmic [54,55] for isothermal separation or piecewise linear for a temperature program [55].

Identification of a peak using its spectrum compares the spectrum of the measured peak with the library spectra [56]. The measures of spectra similarity (score) are specific to the CDS or library search engine [57]. The most common spectral detector for GC is mass spectrometer. If the detector scans a spectrum during a time comparable to a peak width, different measurements within one spectrum correspond to different concentrations of analyte, which leads to spectrum distortion. Integral or average spectra of stand-alone peaks may be correct for quite low

data rates, as area is properly measured with a very small number of points [39]. Recalculation of spectra to one concentration can significantly improve the similarity of spectra within a homogeneous peak [58].

19.6.1 Handling of overlapped peaks

There is a big difference in handling overlapped peaks for multichannel (MS) and conventional detectors. MS detectors can easily separate peaks (if they are not stereoisomers) by difference in their m/z values for molecular or fragment ions. Even if chromatographic peaks are overlapped, there are unique m/z values, which can be used for quantification. Anyway, a set of chemometric tools can be a good addition to CDS algorithms [59].

In the case of conventional detectors the situation is more complicated, as only peak shape can be taken into account. There are several ways to attribute area to each of the overlapped peaks. If peaks are close in size, a drop line from the valley position is used. There are also several ways of skimming a smaller (child, rider) peak from a bigger (parent, horse) peak: linear, exponential, and Gaussian. All these methods are simplified implicit ways of peak shape modeling [60,61]. Explicit peak fitting routines [8,30,62–65] can provide more reliable results. The best solution for CDS is to have a peak fitting routine integrated into the software.

19.7 Quantification

Quantification in chromatography is based on the calibration procedure [66]. Two common methods of calibration are called External standard and Internal standard calibrations. Calibration involves the separation of a number of samples with known analyte concentrations and the construction of a calibration function using a least squares procedure. The internal standard method [66–69] is used to improve the

accuracy of calculations in the case of an unstable detector response, variable sample introduction volumes, and substance loss during sample preparation. These methods are included in many formal documents; the definitions in most cases are close to those found in the European Pharmacopoeia [33]:

“External standard method. The concentration of the component(s) to be analyzed is determined by comparing the response(s) (peak(s)) obtained with the test solution to the response(s) (peak(s)) obtained with a reference solution.

Internal standard method. Equal amount of a component that is resolved from the substance to be examined (the internal standard) is introduced into the test solution and a reference solution. The internal standard should not react with the substance to be examined; it must be stable and must not contain impurities with a retention time similar to that of the substance to be examined. The concentration of the substance to be examined is determined by comparing the ratio of the peak areas or peak heights due to the substance to be examined and the internal standard in the test solution with the ratio of the peak areas or peak heights due to the substance to be examined and the internal standard in the reference solution.

Calibration procedure. The relationship between the measured or evaluated signal (y) and the amount (concentration, mass, etc.) of substance (x) is determined and the calibration function is calculated. The analytical results are calculated from the measured signal or evaluated signal of the analyte by means of the inverse function.”

In other words, the obligatory part of internal standard calibration is using the response (the area or height) ratio of the substance of interest (let us call it the analyte) and the internal standard component (let us call it the standard). The internal standard technique was initially implemented as a one-point calculation [67,68]. The monograph by Yost et al. [69] is the first publication that we could find where the multipoint

internal standard method was explicitly formulated. The modern implementation of this method is such that according to Yost et al. [69], most CDSs construct the internal standard calibration function in the response ratio/concentration ratio coordinates. We will further refer to this as the “traditional ISTD” approach.

19.7.1 External standard calculations

Let us introduce the following notations: R is the analytical signal (response), standing for the peak height or area in chromatography; C is the concentration of the component in the sample; V is the injection volume; Q is the quantity (mass) of the component being analyzed, $Q = C \cdot V$. We are using quantity, not concentration, similar to Ref. [69] as it is a proper model for a measuring system in chromatography: the chromatographic peak response is proportional to the product of the concentration of the component in the sample and the injection volume, i.e., mass (quantity) of the injected component. The subscript a stands for analyte; s , for the standard; e , for the external standard method; i , for the traditional internal standard method; and r , for relative calculations.

The calibration function of the external standard method

$$R_a = F_{ea}(Q_a) \quad (19.11)$$

shows how the response R_a depends on the injected quantity Q_a . The evaluation function

$$W_{ea}(R_a) = Q_a \quad (19.12)$$

allows one to solve an inverse task and evaluate the injected quantity using the peak response. $W()$ is the inverse of $F()$. The quantity Q is converted into the external standard concentration using the relationship

$$C = Q_a/V = W_{ea}(R_a)/V. \quad (19.13)$$

The calibration function is a functional relationship between the detector response and the amount of analyte [70]. The limit of detection

(LOD) [71–76] is based on the statistical verification of the hypothesis that the concentration of analyte equals 0. The limit of quantification (LOQ) corresponds to the expected signal for the analyte content, which varies within preset limits; typically, it is three to five times higher than the LOD. The confidence interval [77] formally applies to a specific measured or predicted value only. The notion is generalized as the calibration band by assigning a CI to each calibration point. Note that there are several confidence bands varying in their meaning (Fig. 19.10).

The confidence band (the region containing the calibration curve at a specified probability level) depends on the accuracy of the calibration function parameters. A prediction band confines the region at a given probability that contains the new measurement of known analyte content if the accuracy of the new measurement does not differ from that of the calibration measurements. The CI for the content prediction, reconstituting the analyte content from the detector response, can be constructed from the prediction band of the calibration graph by crossing it with a horizontal line; it is not symmetrical with respect to the analyte content predicted and could be calculated in most cases only by computer. Equations for the prediction CI calculated as a prediction band divided by a proportionality coefficient (see, for instance Ref. [70]) are deemed

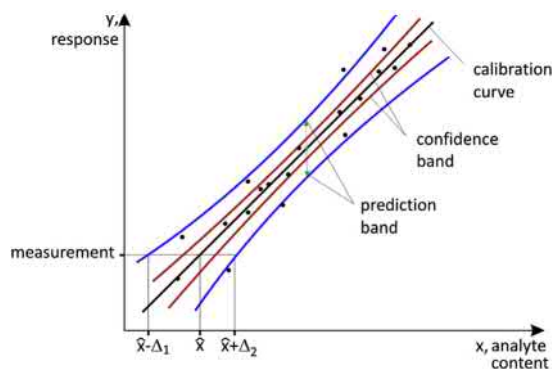


FIGURE 19.10 Calibration and confidence bands.

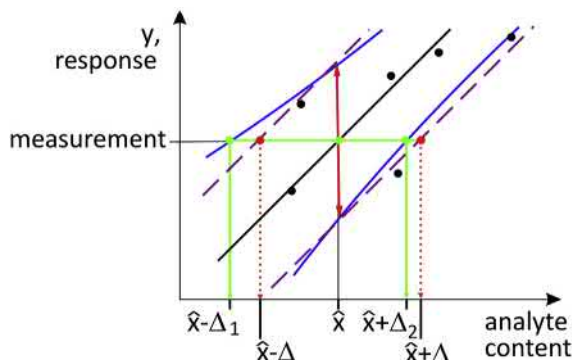


FIGURE 19.11 \hat{x} —predicted analyte content for the analysis; $\hat{x} - \Delta$, $\hat{x} + \Delta$ —traditional (approximate) CI estimate; $\hat{x} - \Delta_1$, $\hat{x} + \Delta_2$ —correct CI estimate.

to be rough and result from lines parallel to the calibration as shown on Fig. 19.11.

There is a possibility to reduce the signal-to-noise value, detection, and quantification limits calculated in this way, by accepting the hypothesis of heteroscedastic error, i.e., assuming that dispersion of the response depends on the response [70,78,79]. As usual, the error increases with increasing area, the confidence interval at the beginning of the calibration curve, where response is small, may become less, than in the case of assumed homoscedastic error.

To average or not to average?

Let the term “level” designate an outcome for averaging the analytical response for all measurements (points) with equal analyte content. The number of points for each level is required to be equal; let it be m . There are two ways to construct a calibration function: using all of the points measured or using the levels. The coefficients of the regression function calculated by points would precisely match the coefficients calculated by levels. The major difference is in the confidence bands, in particular, the prediction band, and in the procedure for outlier rejection. While construction of a level-based calibration function requires that an appropriate calibration level is completely eliminated, or a calibration point has to be rebuilt. A point-based

calibration function does not require that the number of measurements for each analyte content is exactly m , so one point can be easily eliminated from the set, used to build the calibration function.

19.7.2 Internal standard calculations

Traditional internal standard calibration calculates the calibration function:

$$R_a/R_s = F_{ia}(Q_a/Q_s). \quad (19.14)$$

The ratios of quantities and concentrations are equal, $Q_a/Q_s = C_a/C_s$, as the volume is the same for the standard and the analyte. The inverse task is solved by equations

$$Q_{ia} = Q_s \cdot W_{ia}(R_a/R_s). \quad (19.15)$$

or

$$C_{ia} = C_s \cdot W_{ia}(R_a/R_s). \quad (19.16)$$

In the case of traditional ISTD approach, the calibration and evaluation functions of the standard component do not exist.

19.7.2.1 Relative concentration

Relative concentration is an alternative way to implement the internal standard procedure [80], utilizing the knowledge for the concentration of one of the components (the standard) and concerns about the injected amount. Having the calibration $R_s = F_{es}(Q_s)$ and evaluation $Q_s = W_{es}(R_s)$ functions for the standard and additional information for concentration C_s of the standard in the injected sample, the injection volume can be calculated:

$$V = Q_s/C_s = W_{es}(R_s)/C_s. \quad (19.17)$$

This volume can be applied to calculate the relative concentration of the analyte:

$$C_{ra} = W_{ea}(R_a)/V = C_s \cdot W_{ea}(R_a)/W_{es}(R_s). \quad (19.18)$$

The calibration and evaluation functions are constructed by the external standard method. Any component with known concentration can

be used as an internal standard component. Relative concentration is the concentration of the analyte calculated with the assumption that the concentration of the standard is known a priori.

19.7.2.2 Relative calibration

The aim of relative internal standard calibration is to compensate for the different behavior of the standard and analyte during sample preparation. The trick used to construct the relative concentration can be repeated to construct a calibration curve. It is assumed that the standard component must have the *external standard*-type calibration function constructed in advance. The metrological features of the measuring system depend on the accuracy of this calibration. The calibration function of the analyte is constructed assuming the known calibration function of the standard. During the calibration procedure, a sample containing the standard and analyte undergoes all sample preparation procedures, and the resulting responses and concentrations of the standard and analyte for j th calibration point are processed as follows. The calibration function of the standard is treated as external information. The points (Q_{aj}, R_{aj}) are plotted to construct the calibration function of the analyte, where Q_{aj} is calculated as

$$Q_{aj} = C_{aj}V_j = W_{es}(R_{sj}) \cdot C_{aj}/C_{sj}. \quad (19.19)$$

These points are used to construct the calibration function $R_{a}=F_{ra}(Q_a)$ and the inverse of this function $Q_a = W_{ra}(R_a)$.

The constructed calibration function is essentially similar to the external standard calibration function. When there is no sample preparation, they can be considered almost identical. Besides, during sample preparation and different behavior of the standard and analyte, the relative internal standard calibration can account for some differences (e.g., in the extraction coefficients of analyte and standard), similar to the traditional ISTD approach. In the case of directly proportional calibrations, it is possible to

implement relative calibration, called simple relative calibration [80], which is almost indistinguishable from the traditional approach.

References

- [1] J.C. Giddings, Theory of minimum time operation in gas chromatography, *Anal. Chem.* 34 (1962) 314–319, <https://doi.org/10.1021/ac60183a005>.
- [2] B.S. Finkle, D.M. Taylor, E.J. Bonelli, A gc/ms reference data system for the identification of drugs of abuse, *J. Chromatogr. Sci.* 10 (1972) 312–333, <https://doi.org/10.1093/chromsci/10.5.312>.
- [3] J. Dallüge, J. Beens, U.A.T. Brinkman, Comprehensive two-dimensional gas chromatography: a powerful and versatile analytical tool, *J. Chromatogr. A* 1000 (2003) 69–108, [https://doi.org/10.1016/S0021-9673\(03\)00242-5](https://doi.org/10.1016/S0021-9673(03)00242-5).
- [4] O. Amador-Muñoz, P.J. Marriott, Quantification in comprehensive two-dimensional gas chromatography and a model of quantification based on selected summed modulated peaks, *J. Chromatogr. A* 1184 (2008) 323–340, <https://doi.org/10.1016/j.chroma.2007.10.041>.
- [5] A.S. Kaplitz, G.A. Kresge, B. Selover, L. Horvat, E.G. Franklin, J.M. Godinho, K.M. Grinias, S.W. Foster, J.J. Davis, J.P. Grinias, High-throughput and ultrafast liquid chromatography, *Anal. Chem.* 92 (1) (2020) 67–84, <https://doi.org/10.1021/acs.anal-chem.9b04713>. Publication Date: October 22, 2019.
- [6] N. Dyson, *Chromatographic Integration Methods*, second ed., RSC, 1988.
- [7] H. Kuss, S. Kromidas (Eds.), *Quantification in LC and GC: A Practical Guide to Good Chromatographic Data*, Wiley-VCH Verlag GmbH & Co., 2009.
- [8] T. O'Haver, *A Pragmatic Introduction to Signal Processing with applications in scientific measurement*, May 2020. (Accessed 10 November 2020). <http://bit.ly/1NLOILR>.
- [9] A. Felinger, *Data Analysis and Signal Processing in Chromatography*, Elsevier, 1998.
- [10] P.D. Wentzell, C.D. Brown, Signal processing in analytical chemistry, in: *Encycl. Anal. Chem.*, John Wiley & Sons, Ltd, Chichester, UK, 2000, pp. 9764–9800, <https://doi.org/10.1002/9780470027318.a5207>.
- [11] A.N. Papas, Chromatographic data systems: a critical review, *CRC Crit. Rev. Anal. Chem.* 20 (1989) 359–404, <https://doi.org/10.1080/10408348908050072>.
- [12] E.R. Malinowski, *Factor Analysis in Chemistry*, third ed., Wiley, 2002. <https://www.wiley.com/en-us/Factor+Analysis+in+Chemistry%2C+3rd+Edition-p-9780471134794>.

- [13] D.L. Massart, B.G.M. Vandeginste, J.M.C. Buydens, S. de Jong, P.J. Lewi, J. Smeyers-Verberke, L.M.C. Buydens, S. De Jong, J. Smeyers-Verbeke, Handbook of Chemometrics and Qualimetrics, 1997, [https://doi.org/10.1016/S0922-3487\(97\)80056-1](https://doi.org/10.1016/S0922-3487(97)80056-1).
- [14] R.G. Brereton, J. Jansen, J. Lopes, F. Marini, A. Pomerantsev, O. Rodionova, J.M. Roger, B. Walczak, R. Tauler, Chemometrics in analytical chemistry—part I: history, experimental design and data analysis tools, *Anal. Bioanal. Chem.* 409 (2017) 5891–5899, <https://doi.org/10.1007/s00216-017-0517-1>.
- [15] R.G. Brereton, J. Jansen, J. Lopes, F. Marini, A. Pomerantsev, O. Rodionova, Chemometrics in Analytical Chemistry — Part II: Modeling, Validation, and Applications, 2018.
- [16] T.S. Bos, W.C. Knol, S.R.A. Molenaar, L.E. Niezen, P.J. Schoenmakers, G.W. Somsen, B.W.J. Pirok, Recent applications of chemometrics in one- and two-dimensional chromatography, *J. Separ. Sci.* (2020) 1–50, <https://doi.org/10.1002/jssc.202000011>.
- [17] R.D. McDowall, C. Burgess, The Ideal Chromatography Data System for a Regulated Laboratory, LCGC, 2016, pp. 1–34.
- [18] A.C. Olivieri, Practical guidelines for reporting results in single- and multi-component analytical calibration: a tutorial, *Anal. Chim. Acta* 868 (2015) 10–22, <https://doi.org/10.1016/j.aca.2015.01.017>.
- [19] Instrument Control Framework (ICF), 2018. <https://www.agilent.com/en-us/products/liquid-chromatography/icf>.
- [20] T. Instruments, ADS126x 32-Bit, Precision, 38-kSPS, Analog-To-Digital Converter (ADC) with Programmable Gain Amplifier (PGA) and Voltage Reference, Dallas, 2015. www.ti.com.
- [21] L. Tan, J. Jiang, Digital Signal Processing: Fundamentals and Applications, third ed., Elsevier, 2019.
- [22] AD7177-2 32-Bit, 10 kSPS, Sigma-Delta ADC with 100 μ s Settling and True Rail-To-Rail Buffers, 2016, p. 60. <https://www.analog.com/media/en/technical-documentation/data-sheets/AD7177-2.pdf>.
- [23] J.V. Seeley, Theoretical study of incomplete sampling of the first dimension in comprehensive two-dimensional chromatography, *J. Chromatogr. A* 962 (2002) 21–27, [https://doi.org/10.1016/S0021-9673\(02\)00461-2](https://doi.org/10.1016/S0021-9673(02)00461-2).
- [24] J. V Hinshaw, Data handling for fast chromatography – peak integration, LCGC North Am. 20 (2002) 34–38.
- [25] L.G. Johnsen, T. Skov, U. Houlberg, R. Bro, An automated method for baseline correction, peak finding and peak grouping in chromatographic data, *Analyst* 138 (2013) 3502–3511, <https://doi.org/10.1039/c3an36276k>.
- [26] Waters, Bands, Peaks and Band Spreading, 2020. https://www.waters.com/waters/en_US/Chromatographic-Bands%2C-Peaks-and-Band-Spreading/nav.htm?cid=134803614&changedCountry=Y&lset=1&locale=en_US. (Accessed 21 April 2020).
- [27] J.C. Sternberg, Extracolumn contributions to chromatographic band broadening, in: J.C. Giddings, R.A. Keller (Eds.), *Adv. Chromatogr.*, vol. 2, Marcel Dekker, New York, 1966, pp. 205–270.
- [28] E. Grushka, Characterization of exponentially modified Gaussian peaks in chromatography, *Anal. Chem.* 44 (1972) 1733–1738, <https://doi.org/10.1021/ac60319a011>.
- [29] R. Delley, Series for the exponentially modified Gaussian peak shape, *Anal. Chem.* 57 (1985), <https://doi.org/10.1021/ac00279a094>, 388–388.
- [30] Y.A. Kalambet, Y.P. Kozmin, K.V. Mikhailova, I.Y. Nagaev, P.N. Tikhonov, Reconstruction of chromatographic peaks using the exponentially modified Gaussian function, *J. Chemom.* 25 (2011), <https://doi.org/10.1002/cem.1343>.
- [31] W.J. Cody, Rational Chebyshev approximations for the error function, *Math. Comput.* 23 (1969), <https://doi.org/10.1090/S0025-5718-1969-0247736-4>, 631–631.
- [32] United States Pharmacopeia, General Notices and Requirements, United States Pharmacop. 37 (USP 37), 2013.
- [33] European Pharmacopoeia, European Directorate for the Quality of Medicines, Strasbourg, 2014. www.edqm.eu.
- [34] Государственная фармакошея Российской Федерации, XIII издание, Федеральная электронная медицинская библиотека, 2015. <http://femb.ru/feml>.
- [35] F.W.J. Olver, A.B. Olde Daalhuis, D.W. Lozier, B.I. Schneider, R.F. Boisvert, W. Clark, B.R. Miller, B.V. Saunders, H.S. Cohl, M.A. McClain, [DLMF] NIST Digital Library of Mathematical Functions, 2016. <http://dlmf.nist.gov/>. Release 1.0.28 of 2020-0c9-15.
- [36] G. Guiochon, M. Sepaniak, Exchange of comments on data acquisition for chromatographic peaks, *Anal. Chem.* 63 (1991) 73–75, <https://doi.org/10.1021/ac00001a014>.
- [37] N. Dyson, Peak distortion, data sampling errors and the integrator in the measurement of very narrow chromatographic peaks, *J. Chromatogr. A* 842 (1999) 321–340, [https://doi.org/10.1016/S0021-9673\(99\)00299-X](https://doi.org/10.1016/S0021-9673(99)00299-X).
- [38] M.F. Wahab, P.K. Dasgupta, A.F. Kadjo, D.W. Armstrong, Sampling frequency, response times and embedded signal filtration in fast, high efficiency liquid chromatography: a tutorial, *Anal. Chim. Acta* 907 (2016) 31–44, <https://doi.org/10.1016/j.aca.2015.11.043>.

- [39] Y. Kalambet, Y. Kozmin, A. Samokhin, Comparison of integration rules in the case of very narrow chromatographic peaks, *Chemometr. Intell. Lab. Syst.* 179 (2018) 22–30, <https://doi.org/10.1016/j.chemolab.2018.06.001>.
- [40] S.N. Chesler, S.P. Cram, Effect of peak sensing and random noise on the precision and accuracy of statistical moment analyses from digital chromatographic data, *Anal. Chem.* 43 (1971) 1922–1933, <https://doi.org/10.1021/ac60308a005>.
- [41] D.J. Anderson, R.R. Walters, Effect of baseline errors on the calculation of statistical moments of tailed chromatographic peaks, *J. Chromatogr. Sci.* 22 (1984) 353–359.
- [42] J.W. Dolan, The role of the signal-to-noise ratio in precision and accuracy, *LCGC North Am.* 23 (2005) 1256–1260.
- [43] The United States Pharmacopeia—National Formulary. www.usp.org.
- [44] C.G. Enke, T.A. Nieman, Signal-to-noise ratio enhancement by least-squares polynomial smoothing, *Anal. Chem.* 48 (1976) 705A–712A, <https://doi.org/10.1021/ac50002a007>.
- [45] А.Н. КолмоГоров, ИнтегрШолирование и экстраШолирование стационарных случайных Последовательностей, *Изв. АН СССР. Сер. Матем.* 5 (1941) 3–14.
- [46] N. Wiener, *The Extrapolation, Interpolation and Smoothing of Stationary Time Series*, Wiley, New York, 1949.
- [47] A. Felinger, A. Kilar, B. Boros, The myth of data acquisition rate, *Anal. Chim. Acta* 854 (2015) 178–182, <https://doi.org/10.1016/j.aca.2014.11.014>.
- [48] C. Torrence, G.P. Compo, A practical guide to wavelet analysis, *Bams* 79 (1998) 61–78, [https://doi.org/10.1175/1520-0477\(1998\)079<0061:APGTWA>2.0.CO;2](https://doi.org/10.1175/1520-0477(1998)079<0061:APGTWA>2.0.CO;2).
- [49] X. Shao, A.K.-M. Leung, F.-T. Chau, Wavelet: a new trend in chemistry, *Acc. Chem. Res.* 36 (2003) 276–283, <https://doi.org/10.1021/ar990163w>.
- [50] A. Savitzky, M.J.E. Golay, Smoothing and differentiation of data by simplified least squares procedures, *Anal. Chem.* 36 (1964) 1627–1639, <https://doi.org/10.1021/ac60214a047>.
- [51] Y.A. Kalambet, S.A. Maltsev, Y.P. Kozmin, Noise filtering. Final solution of the problem (in Russian), *Analitika 1* (2011) 50–55.
- [52] Y.A. Kalambet, Y.P. Kozmin, A.S. Samokhin, Noise filtering. Comparative analysis of methods, *Analytica* (2017) 88–101, <https://doi.org/10.22184/2227-572X.2017.36.5.88.101>.
- [53] Y.A. Kalambet, Optimization of parameters of linear smoothing applied to chromatographic peaks, *Nauchnoe Prib.* 29 (2019) 51–65.
- [54] E. Kovats, Characterization of organic compounds by gas chromatography. Part 1. Retention indices of aliphatic halides, alcohols, aldehydes and ketones, *Helv. Chim. Acta* 41 (1958) 1915–1932.
- [55] IUPAC, *Compendium of Chemical Terminology, The “Gold Book”*, second ed., Blackwell Sci. Publ., Oxford, 2014, p. 1670, <https://doi.org/10.1351/goldbook.I03352>.
- [56] NIST/EPA/NIH Mass Spectral Library (NIST 14) and NIST Mass Spectral Search Program (Version 2.2), 2014th ed., National Institute of Standards and Technology, Gaithersburg, MD 20899, 2014. <http://www.nist.gov/srd/>.
- [57] A. Samokhin, K. Sotnezova, V. Lashin, I. Revelsky, Evaluation of mass spectral library search algorithms implemented in commercial software, *J. Mass Spectrom.* 50 (2015) 820–825, <https://doi.org/10.1002/jms.3591>.
- [58] A. Samokhin, Spectral skewing in gas chromatography—mass spectrometry: misconceptions and realities, *J. Chromatogr. A* 1576 (2018) 113–119, <https://doi.org/10.1016/j.chroma.2018.09.033>.
- [59] T. Skov, R. Bro, Solving fundamental problems in chromatographic analysis, *Anal. Bioanal. Chem.* 390 (2008) 281–285, <https://doi.org/10.1007/s00216-007-1618-z>.
- [60] M.K.L. Bicking, Integration errors in chromatographic analysis, part I: peaks of approximately equal size, *LCGC North Am.* 24 (2006) 402–414.
- [61] M.K.L. Bicking, Integration errors in chromatographic analysis, part II: large peak size ratios, *LCGC North Am.* 24 (2006) 604–616.
- [62] S.N. Chesler, S.P. Cram, Iterative curve fitting of chromatographic peaks, *Anal. Chem.* 45 (1973) 1354–1359, <https://doi.org/10.1021/ac60330a031>.
- [63] J.P. Foley, Equations for chromatographic peak modeling and calculation of peak area, *Anal. Chem.* 59 (1987) 1984–1987, <https://doi.org/10.1021/ac00142a019>.
- [64] V.B. Di Marco, G.G. Bombi, Mathematical functions for the representation of chromatographic peaks, *J. Chromatogr. A* 931 (2001) 1–30, [https://doi.org/10.1016/S0021-9673\(01\)01136-0](https://doi.org/10.1016/S0021-9673(01)01136-0).
- [65] A. Felinger, Deconvolution of overlapping Skewed peaks, *Anal. Chem.* 66 (1994) 3066–3072, <https://doi.org/10.1021/ac00091a013>.
- [66] L. Cuadros-Rodríguez, M.G. Bagur-González, M. Sánchez-Viñas, A. González-Casado, A.M. Gómez-Sáez, Principles of analytical calibration/quantification for the separation sciences, *J. Chromatogr. A* 1158 (2007) 33–46, <https://doi.org/10.1016/j.chroma.2007.03.030>.
- [67] N.H. Ray, Gas chromatography. I. The separation and estimation of volatile organic compounds by gas-liquid partition chromatography, *J. Appl. Chem.* 4 (1954) 21–25.
- [68] D.E. Willis, Internal standard method calculations, *Chromatographia* 5 (1972) 42–43.
- [69] R.W. Yost, L.S. Ettre, R.D. Conlon, *Practical Liquid Chromatography: An Introduction*, Perkin-Elmer Corporation, Norwalk, CT, U.S.A., 1980.

- [70] K. Danzer, L.A. Currie, Guidelines for calibration in analytical chemistry. Part I. Fundamentals and single component calibration (IUPAC Recommendations 1998), *Pure Appl. Chem.* 70 (1998) 993–1014, <https://doi.org/10.1351/pac199870040993>.
- [71] L.A. Currie, Detection: international update, and some emerging di-lemmas involving calibration, the blank, and multiple detection decisions, *Chemometr. Intell. Lab. Syst.* 37 (1997) 151–181, [https://doi.org/10.1016/S0169-7439\(97\)00009-9](https://doi.org/10.1016/S0169-7439(97)00009-9).
- [72] E. Voigtman, Limits of detection and decision. Part 1, *Spectrochim. Acta B At. Spectrosc.* 63 (2008) 115–128, <https://doi.org/10.1016/j.sab.2007.11.015>.
- [73] E. Voigtman, Limits of detection and decision. Part 2, *Spectrochim. Acta B At. Spectrosc.* 63 (2008) 129–141, <https://doi.org/10.1016/j.sab.2007.11.018>.
- [74] E. Voigtman, Limits of detection and decision. Part 3, *Spectrochim. Acta B At. Spectrosc.* 63 (2008) 142–153, <https://doi.org/10.1016/j.sab.2007.11.012>.
- [75] E. Voigtman, Limits of detection and decision. Part 4, *Spectrochim. Acta B At. Spectrosc.* 63 (2008) 154–165, <https://doi.org/10.1016/j.sab.2007.11.014>.
- [76] H. Evard, A. Kruve, I. Leito, Tutorial on estimating the limit of detection using LC-MS analysis, part I: theoretical review, *Anal. Chim. Acta* 942 (2016) 23–39, <https://doi.org/10.1016/j.aca.2016.08.043>.
- [77] G.A.F. Seber, A.J. Lee, *Linear Regression Analysis*, second ed., John Wiley & Sons, Inc., Hoboken, NJ, USA, 2003 <https://doi.org/10.1002/9780471722199>.
- [78] K. Danzer, M. Otto, L.A. Currie, Guidelines for calibration in analytical chemistry part 2. Multispecies calibration (IUPAC technical report), *Pure Appl. Chem.* 76 (2004) 1215–1225, <https://doi.org/10.1351/pac200476061215>.
- [79] Y.A. Kalambet, S.A. Maltsev, Y.P. Kozmin, Confidence interval of weighted least squares method and calibration strategy, *Ind. Lab. Diagnostics Mater.* 81 (2015) 69–76.
- [80] Y. Kalambet, Y. Kozmin, Internal standard arithmetic implemented as relative concentration/relative calibration, *J. Chemom.* 33 (2019) 1–10, <https://doi.org/10.1002/cem.3106>.

Data analysis methods for gas chromatography

*Karisa M. Pierce*¹, *Timothy J. Trinklein*², *Jeremy S. Nadeau*²,
*Robert E. Synovec*²

¹Department of Chemistry and Biochemistry, Seattle Pacific University, Seattle, WA, United States;

²Department of Chemistry, University of Washington, Seattle, WA, United States

Data analysis methods are essential to transform chromatographic data into useful information. There is an ongoing evolution of data analysis methods as increasingly challenging applications need to be addressed, instrumentation advances occur, separation speeds increase, data dimensionality increases, and growing volumes of data are collected. As the traditional data analysis methods have been covered in prior chapters, this chapter focuses primarily on advanced data analysis methods known as chemometrics. Chemometrics are mathematical methods that glean useful information from large volumes of complex chemical data that are not amenable to manual or traditional analysis. Chemometrics fill several analytical roles. First, the ability to identify and quantify analytes at extremely low chromatographic resolution can be provided. Second, pattern recognition and classification are often implemented by treating chromatograms as a chemical fingerprint. Third, groups of compounds may be simultaneously quantified using chemometric methods. Finally, another area of broad interest

is predicting retention times to optimize separation parameters.

20.1 Introduction

In chromatography, the detected signal of a resolved analyte is usually directly proportional to the concentration of the analyte. Analyte quantification is traditionally achieved by either using the internal standard method and analyzing either peak height or pseudointegrated chromatographic peak areas/volumes [1,2]. Pseudointegration is generally achieved by baseline correcting and automatically summing the signals of a peak (at the raw resolution data point level, i.e., the pixel level) often while using Gaussian statistics to define the retention time limits of each peak. According to legend, prior to automated peak integration, quantification by peak area was generally achieved by manually cutting out peaks from a chart recording and observing the mass of each cutout peak. Since those days of old, sources of manual variation have been greatly reduced as

automated analysis methods have evolved from simple integration to powerful chemometric analysis of massive volumes of multidimensional chromatographic data. Massart [3], Brereton [4], Beebe et al. [5], and Sharaf et al. [6] have written excellent textbooks about chemometrics related generally to spectroscopy and chromatography. This chapter focuses on chemometric advances for chromatography, often coupled with mass spectrometry, and loosely categorizes chemometric methods into the following four procedural categories: preprocessing, pattern recognition, calibration, and experimental method optimization.

The analyst's chemometric options are defined and limited by the dimensions of the data; so within each of the four chemometric categories, this chapter will categorize the chemometric methods based on the data dimensionality. Data of a variety of dimensions are depicted in Fig. 20.1. One-dimensional (1D) gas chromatography (GC) coupled to a univariate detector such as a flame ionization detector (GC-FID) continually records detector signal as a function of time, yielding a 1D data vector as shown in Fig. 20.1A. Likewise, a univariate detector coupled to comprehensive two-dimensional (2D) gas chromatography (GC \times GC-FID) continually records detector signal as a function of time, again yielding a 1D data vector as shown in Fig. 20.1B. However, this vector is composed of consecutive second-dimension separations defined by the modulation period that can be reshaped or *folded* into a 2D matrix as shown in Fig. 20.1C to match the physical process of the modulator in a GC \times GC separation. In this 2D matrix, the peak modulations ("slices") of a single chemical component will exhibit a similar first-dimension retention time and identical second-dimension retention time. Thus, it is necessary to combine multiple 1D peak modulations into a single 2D peak that ideally has an integrated signal volume that is proportional to analyte concentration. These 2D chromatograms are frequently depicted either as a surface plot (Fig. 20.1D) or as a contour plot (Fig. 20.1E), where the contours represent signal magnitude.

Thus, for GC \times GC data, chemometric options are related to whether or not the data have been folded into a 2D matrix. When multiple 2D chromatograms are combined into a single three-way array, then a new sample dimension is added to the data (Fig. 20.1F). Again, this added dimensionality affects chemometric options.

While an instrument with two separation dimensions and a univariate detector will generate 2D data, comprehensive 2D GC coupled to a multivariate detector, such as a time-of-flight mass spectrometer (GC \times GC-TOFMS), will generate three-dimensional (3D) data. When multiple 3D chromatograms are combined into a single four-way array, then a fourth dimension (the sample dimension) is added and the data are 4D. Fig. 20.2 depicts the data structures that are most common in GC. Fig. 20.2 shows how analysts often combine multiple chromatograms into a higher-order array to increase dimensionality and use chemometric methods that are available for high-order data structures. Fig. 20.2 also depicts how analysts often *unfold* data and purposely decrease dimensionality in order to use chemometric methods that are only available for lower-order data structures. Some chromatographers choose to analyze "peak-level" data (tables of peak data often provided by native instrument software) rather than "pixel-level" data (raw data points of signal values gathered at the resolution of the original data acquisition rate). The dimensions of peak-level data are generally lower than the dimensions of pixel-level data. If appropriate preprocessing is applied and if data integrity is maintained when raw data in its native file format are converted into a compatible format, then analyzing entire chromatograms at the pixel level should return results that are equally as accurate as analyzing comprehensive peak-level data. However, when the analyst has access to pixel-level data, then this opens up new opportunities to advance the field of novel data analysis software development. Often when data are output at the peak level, many important data analysis decisions have been made by the native instrument software that can impact

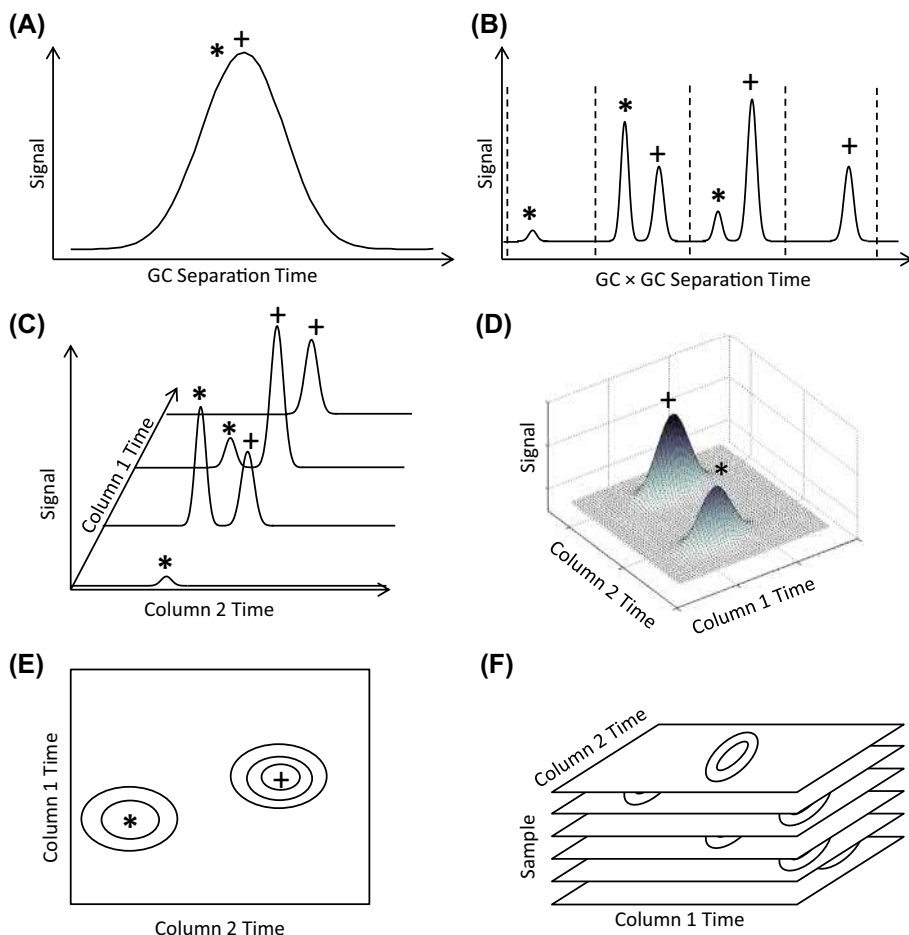


FIGURE 20.1 (A) A univariate detector on a 1D chromatographic instrument collects a 1D data vector as a function of time. (B) A univariate detector on a 2D chromatographic instrument collects a 1D data vector composed of consecutive second-dimension separations that (C) can then be reshaped into a 2D matrix where the peak modulations (“slices”) that elute at a similar column 1 retention time and identical column 2 retention time are considered to be a single compound. Thus, multiple 1D peak modulations are actually a single analyte peak with an integrated signal volume that is proportional to analyte concentration. (D) These 2D chromatograms are frequently depicted as surface plots or (E) as a contour plot where the contours represent signal magnitude. Two chemical components represented by an asterisk or cross are shown in these figures. (F) When multiple 2D chromatograms are combined into a single three-way array, then another dimension (the sample dimension) is added to the data.

analytical results. This can be an advantage if the analyst is satisfied with the peak-level outputs. However, this can be a disadvantage if the analyst feels the peak-level outputs exhibit shortcomings for particular applications.

20.2 Preprocessing

Interesting chemical variations that reveal important information in chromatographic data are often obscured by chemically irrelevant

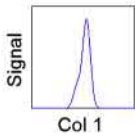
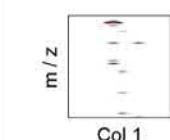
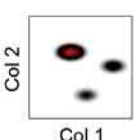
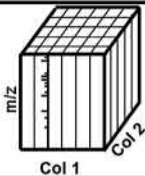
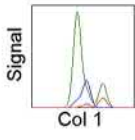
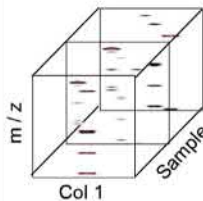
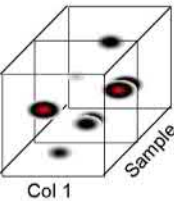
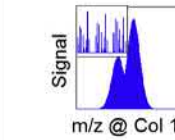
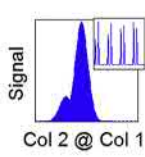
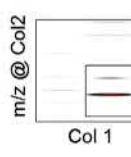
	1D Data (GC-FID)	2D Data (GC-MS)	2D Data (GCxGC-FID)	3D Data (GCxGC/TOF-MS)
ND Data for a Single Sample				
(N+1)D Data by Combining Samples				4D Data Structure
(N-1)D Data by Unfolding a Sample				

FIGURE 20.2 The analyst's chemometric options are defined by the dimensionality of the data set. If it is appropriate, multiple pixel-level 1D chromatograms can be combined into a 2D matrix that is suitable for certain chemometric methods. Likewise, multiple pixel-level 2D chromatograms can be combined into a 3D array, and 3D chromatograms can be combined into a 4D array, thus increasing dimensionality in order to use desired chemometric methods that are only available for high-order data structures. Analysts can also *unfold* a pixel-level chromatogram and purposely decrease dimensionality in order to use desired chemometric methods that are only available for lower-order data structures.

variations. Preprocessing chromatographic data reduces chemically irrelevant variations and improves results of qualitative and quantitative analyses. The major data preprocessing steps that may be required are baseline correction, noise reduction, normalization, and retention time alignment.

20.2.1 Baseline correction

In chromatographic data analysis at the pixel level, baseline correction is typically the first preprocessing step. Baseline-correction procedures are designed to correct drifting baselines and

reduce low-frequency baseline signal variations that arise due to uncontrollable column bleeding, background ionization, and low-frequency detector variations. Fig. 20.3 shows GC chromatograms of a diesel fuel before and after submission to three different baseline-correction procedures. The raw chromatogram is shown in Fig. 20.3A. The simplest baseline-correction procedure is to subtract a “blank” chromatogram from the sample chromatogram, as shown in Fig. 20.3B. The next simplest baseline-correction procedure is to identify the regions of noise in a sample chromatogram, fit a line through that noise, and subtract that

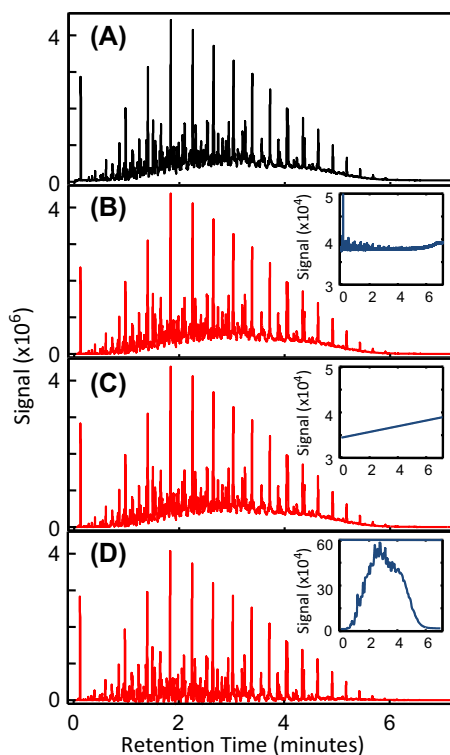


FIGURE 20.3 A single diesel fuel chromatogram is baseline-corrected using various baseline-correction procedures. The raw chromatogram in (A) is baseline-corrected in (B) using blank run subtraction and in (C) using linear fit subtraction. Both techniques produce almost identical results in this example, while in (D) the higher-order baseline subtraction algorithm removes much of the chemical information. The calculated baselines are shown in the insets.

best-fit line from the sample chromatogram as shown in Fig. 20.3C. In Fig. 20.3C, the beginning and end of the chromatogram were the fitted noise regions. More complex baseline-correction procedures exist to correct more severe variations [7]. One approach is to subtract the least-squares fit of a high-order polynomial from the sample chromatogram. Another approach is to directly fit a collection of points calculated from the actual chromatogram using a piecewise cubic Hermite interpolation, as shown in Fig. 20.3D [7]. In this case, the parameters for piecewise cubic Hermite interpolation

were not optimized for the diesel chromatogram, and the high-order baseline was overfit. This illustrates that choosing an inappropriate baseline-correction procedure that overfits the data could remove important chemical variations. The baselines calculated by the different algorithms are shown as insets in Fig. 20.3B–D. It is important to understand the chemical nature of the samples and the extent of chromatographic resolution when choosing a baseline-correction procedure because inadvertently fitting a baseline to unresolved chemical signals rather than the targeted baseline signal will remove important chemical variations along with the baseline variations. Similar baseline-correction procedures can be used with GC \times GC and GC-MS chromatograms. These first three baseline-correction procedures perform well for correcting drifting baselines and low-frequency noise, but other noise-reducing procedures are necessary to reduce high-frequency variations.

20.2.2 Noise reduction

For chromatographic data analysis at the pixel level, several approaches exist to improve the signal-to-noise ratio (S/N). Noise-reduction procedures are designed to reduce uncontrollable instrumental noise and high-frequency noise that may result from flow variations, particulates, or stationary phase escaping the column, external frequencies entering into the electronic signals, and thermal noise. Fig. 20.4A shows a raw chromatogram from an isothermal GC separation of a 10-component sample. The end of the raw chromatogram has a very low S/N , which should be improved upon submission to noise-reduction algorithms. A popular noise-reduction procedure is boxcar filtering, which replaces each data point with the average of a certain number of data points surrounding and including that data point [1,2]. The analyst chooses the number of data points that are averaged

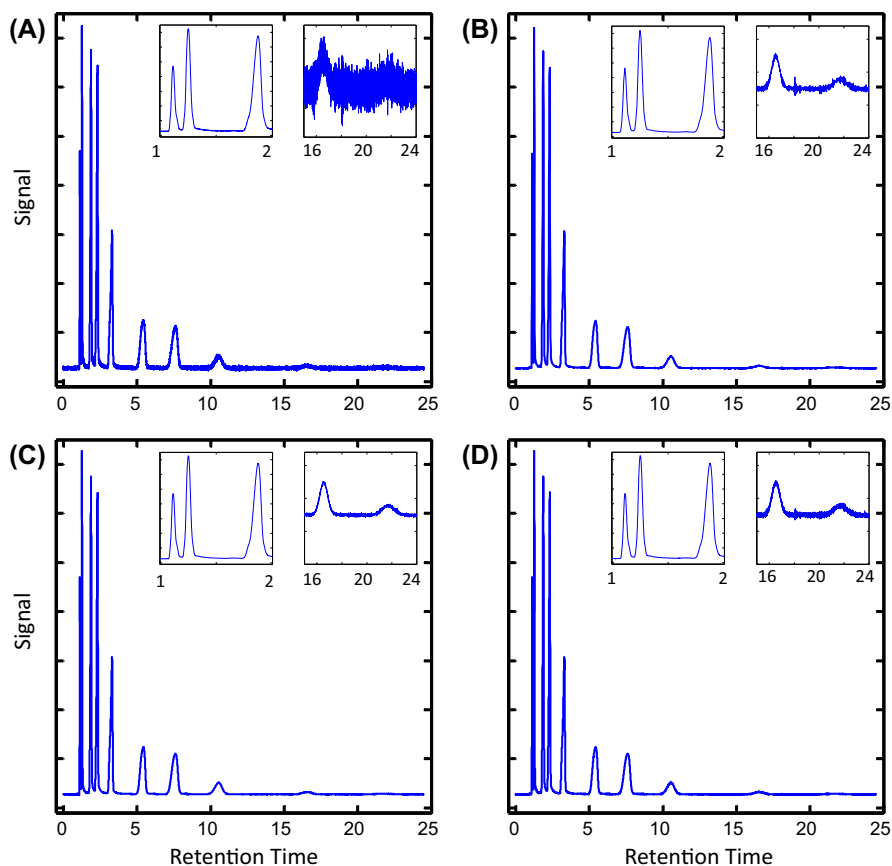


FIGURE 20.4 Different noise-reduction procedures are applied to an isothermal separation. (A) The raw data are (B) boxcar filtered, (C) low-pass filtered with a fast Fourier transform (FFT), and (D) filtered with a Savitsky–Golay smoothing algorithm. The window size for the boxcar filter was 9, the low-pass filter was set to 59 Hz, and the window for the Savitsky–Golay smoothing algorithm was 25.

(boxcar window size), and it is important to choose an appropriate boxcar size that is sufficiently smaller than the number of data points per peak so that noise is minimized while preserving the chemical information present in analyte peaks. The result of boxcar filtering a raw chromatogram is shown in Fig. 20.4B, and the S/N is improved. Median filtering is complementary to boxcar filtering if any outlier signals exist in a chromatogram because the mean is influenced significantly by the outlier itself, while the median is not [8]. The next degree of complexity

in noise reduction is using a low-pass filter. This takes advantage of analyte peaks that have a lower-frequency-signal content relative to much of the detected noise. For example, after submitting the chromatogram to the fast Fourier transform (FFT) function, the analyte peaks with 50 ms width-at-base are located well below 60 Hz in the frequency domain. The signal content defined at frequencies greater than about 60 Hz can be eliminated by replacing the values with zeroes in the frequency domain. The zero-filled frequency-domain chromatographic data

are then submitted to the inverse fast Fourier transform (IFFT) function to convert the chromatogram back into the time domain. This significantly improves the S/N of a raw chromatogram shown in Fig. 20.4C.

Savitzky–Golay smoothing is another popular noise-reduction algorithm that replaces each data point with a polynomial fit to a certain number of data points surrounding the central point within a given window [9]. Again, as with all noise-reduction procedures, the analyst must choose an appropriate window size. Fig. 20.4D shows the chromatogram after being filtered by the Savitzky–Golay function using a second-order polynomial fit using an appropriate window size of 25. Care must be taken to not overly smooth the data and hence adversely impact peak shapes and/or chromatographic resolution. In the example presented in Fig. 20.4, the resolution has not been compromised at the front end of the isothermal chromatogram, while the noise-reduction procedures improved S/N for the wider peaks at the end of the chromatogram. Other noise-reduction procedures include applying power functions or wavelets to model and eliminate noise. In all of the noise-reduction procedures, the analyst must pick a boxcar size or window that is small enough to preserve the original peak shape and peak area, but large enough to reduce chemically irrelevant noise. Boxcar averaging is the simplest and provides sufficiently improved S/N ; hence it is the most commonly applied noise-reduction procedure.

20.2.3 Normalization

During data analysis, chromatograms often need to be normalized to correct for variation introduced during the injection process and to correct variations inadvertently introduced during manual sample preparation procedures. The two major forms of normalization are normalizing to an internal standard or, in appropriate

cases, using the sum-normalization method. For the simplest internal standard normalization procedure, the analyst adds a constant amount of one or more nonnative standard(s) to every sample. Every sample is then chromatographically separated, ensuring that the internal standard is completely resolved. Each data point in each chromatogram is then divided by the signal of the internal standard in that particular chromatogram. The division causes all the normalized chromatograms in the data set to have equal internal standard signals, thus minimizing variations due to injection volume variations between samples and allowing chemical variations among samples to be less obscured. However, new problems may arise such as undetected coelution with a native component, difficulty in choosing a nonnative standard that is completely resolved from all other components of complex unknown samples, and ensuring that the nonnative chemical is inert and will not react with components of unknown samples. Another potential shortcoming of the internal standard method is that variation introduced by the additional sample handling could be worse than the variation in the injection process. For instance, it is difficult to precisely manipulate small volumes of viscous or volatile standards. When it is not practical to use the internal standard method, some analysts use the sum-normalization method. The sum-normalization method uses the total sum of all baseline-corrected signals as the normalization factor, so each data point in a chromatogram is divided by the total sum of all the data points in that chromatogram, and thus all chromatograms in a sum-normalized data set would sum to unity [10,11]. The major assumption here is that within the constraints of the instrumental error, the samples are sufficiently similar such that equal volumes of the samples should have “sufficiently” equal total signals at the detector. Indeed, different chemicals have different response factors, and so the major assumption is not strictly true; however, if there is less variation in total response factors than the variation introduced by injector volume

discrepancies, then the sum-normalization method can be supported and applied with confidence.

20.2.4 Retention time alignment

Retention time variation obscures important chemical variations when comparing one chromatogram to the next; therefore, retention time alignment is a critical preprocessing step for nearly all chemometric methods. Retention time alignment algorithms shift peak positions, so each peak has an accurate retention time. These algorithms should also preserve the accuracy of peak areas or peak volumes. Alignment algorithms can be classified into four major categories: simple scalar shift, alignment to select target peaks, local alignment algorithms, and globally optimized alignment algorithms. The simplest alignment algorithms apply a scalar shift to the entire sample chromatogram. Scalar shift algorithms quickly use a cross-correlation coefficient (or other similarity metric) to calculate the shift that minimizes the difference between the sample and target chromatograms. The problem is that the similarity metrics are usually heavily influenced by the largest peak in the chromatogram. For more complex shifting, more sophisticated alignment algorithms can align selected standard peaks in a sample chromatogram to the same standard peaks in a target chromatogram. However, if the samples are complex and shifting is present, it is difficult to algorithmically identify the standard peaks without manual intervention. For cases when selected standard peaks are not available, and reducing manual intervention is necessary, local alignment algorithms are useful. Local alignment algorithms iteratively shift subregions of the sample chromatogram across the target chromatogram until a matching metric is maximized, thus yielding the shift correction that is applied to each subregion [12–15]. The most sophisticated, robust, and powerful alignment

algorithms are globally optimized alignment algorithms that can handle severe and dynamic shifting [16–18]. The globally optimized algorithms can make use of dynamic programming to find the locally and globally optimized shift for every window in the chromatogram. The correlation optimized warping (COW) algorithm is the most popular alignment method produced for globally optimized alignment. The algorithm was introduced in 1998 by Nielsen et al. [16]. It has been improved by various chemometricians to be applied to GC-FID [16,17], GC-MS [19], GC × GC-TOFMS [20], and LC with diode array detection (LC-DAD) [16], but all of the algorithms are very similar. The chromatograms are separated into windows, sometimes called segments, and each window is shifted and warped until the maximum correlation between the sample window and the target is determined, yielding the locally optimized shift. Dynamic programming is used to find the globally optimized shift. Starting at one end of the chromatogram, the locally optimized correlation paths are added together until the opposite end of the chromatogram is reached. At this point, the globally optimized shifts are the maximum values for each of the locally optimized shifts creating one globally optimized path for all the shifts for each window. This is clearly outlined by Nielsen et al. [16] and also in Massart's insightful comparison of alignment algorithms [21]. The piecewise alignment (PWA) algorithm also uses correlations between windows of a sample chromatogram and a target chromatogram to calculate optimal shifts for a window [18]. By using the locally optimized shifts and comparing the correlations of surrounding windows, a globally optimized path can be calculated in a similar way to the COW algorithms. Data alignment using PWA is much faster than the COW algorithms because there is no warping of the data. Because the window sizes for the globally optimized PWA algorithm and the segment sizes for COW are approximately the size of a peak width, both algorithms accurately align

chromatograms as well as accurately preserve peak areas [18]. By combining a fast cross-correlation coefficient algorithm with the COW algorithm, the ChromAlign software reduces the number of iterative calculations required by the COW algorithm and yields a fast alignment algorithm for GC-MS chromatograms [22]. For the local alignment algorithms and globally optimized alignment algorithms, one must optimize certain parameters such as window length, selecting a target chromatogram, and sometimes even selecting a maximum shift. Analysts typically want parameter optimization to be objective, automated, and require minimal manual intervention [23–25]. Overall, alignment algorithms are designed to reinterpolate signals along the retention time axis so the retention time of a given analyte matches from one chromatogram to the next and the accuracy of the peak signal area should be preserved during alignment. During reinterpolation, alignment algorithms do involve the risk of introducing distortions in peak shapes and areas. The analyst must ensure that the algorithm correctly aligned peaks and did not cause mismatches to occur.

20.2.5 Software platforms

In order to apply preprocessing procedures and advanced chemometric methods, the analyst must be able to import pixel-level or peak-level data into user-friendly data analysis platforms. Commercially available software is critical in this regard. Common data analysis platforms are MATLAB (Mathworks), Excel (Microsoft), and SAS (SAS Cary, NC). These platforms can process both pixel-level and peak-level data, and they allow the analyst to develop algorithms and visualize their data. Some common software packages that provide pixel-level visualization are ChromaTOF (LECO), ChemStation (Agilent, Santa Clara, CA, USA), GC Solution or GCMS Solution from Shimadzu (Columbia, MD, USA), Xcalibur from Thermo Fisher Scientific

(Waltham, MA, USA), and the Reichenbach et al. GC Image GC \times GC Software for 3D chromatographic data (<http://www.gcimage.com>) [26]. ChromaTOF and ChemStation software programs provide easily exportable peak-level data with preprocessing, calibration, and/or pattern recognition capabilities. GC Image software provides pixel-level analysis options such as baseline correction, alignment, blob detection, and differential analysis, and it converts the data into easily exportable formats. Some common chemometrics software packages for processing pixel-level or peak-level data are the PLS Toolbox (Eigenvector Research, Inc), Pirouette (Infometrix), Statistica (Statsoft Inc), and SIMCA (Umetrics, Umea, Sweden).

20.3 Pattern recognition

Pattern recognition is a very important chromatographic data analysis tool for studying complex samples when it is impractical or insufficient to identify, resolve, and quantify all of the peaks present. Pattern recognition generally takes advantage of the reproducible “chemical fingerprint” provided by a sample in a chromatographic context. Chemometric pattern recognition methods can be categorized as either unsupervised or supervised. Unsupervised pattern recognition methods are helpful when the analyst desires to discover the class membership of a sample. Supervised pattern recognition methods are helpful when the analyst desires to discover the chemical components that distinguish sample classes, so the algorithm requires class information to be input by the analyst. Mathematical resolution (decomposition and/or deconvolution) of unresolved chromatographic peaks is also a form of a pattern recognition method that can be either supervised or unsupervised. Resolution algorithms are expected to recognize typical peak shapes and sometimes specific spectral profiles; so in this

chapter resolution algorithms are categorized as pattern recognition algorithms.

20.3.1 Hierarchical cluster analysis

Hierarchical cluster analysis (HCA) is one of many clustering algorithms that belongs in the category of unsupervised pattern recognition methods. HCA functions by calculating the distance between samples in the original independent variable space, where distance can be defined as the Euclidean distance or Mahalanobis distance among all samples from the centroid or origin. Classification is achieved by assuming close samples are chemically similar to each other while distant samples are chemically different from each other. Fig. 20.5 illustrates how a chromatogram can be thought of as a single point in independent variable space. A pixel-level chromatogram that may contain thousands of data points is described by a single vector endpoint that is positioned by the chromatographic signal (dependent variable) at each retention time data point (independent variable) in independent variable space where each independent variable has its own axis. Dendrograms are often the graphical output containing the distance in independent variable space among the samples. HCA is applicable to multiple pixel-level or peak-level 1D chromatograms that are combined into a 2D matrix. HCA can be applied to multiple pixel-level 2D or 3D chromatograms if the 2D or 3D chromatograms are each unfolded into 1D data vectors and then combined into a single 2D matrix, as shown in Fig. 20.2. HCA has been applied to the classification of seized drug samples [27] and fuels for regulatory bodies [28] as just two of many examples.

20.3.2 Principal component analysis

Principal component analysis (PCA) is a common unsupervised pattern recognition method.

Just as in HCA, the first step in PCA is to plot each mean-centered 1D data vector in independent variable space, so each chromatogram is represented by a single vector endpoint. Then, a line of finite length called a principal component (PC) is fit so that it captures the greatest variance in those vector endpoints. A second principal component (PC 2) that is orthogonal to the first PC (PC 1) is fit such that it captures the next greatest variance in those vector endpoints. More orthogonal PCs are fit and ordered based on percent variance captured until 100% of the variance is captured. This allows the analyst to see the vector endpoints in PC space, rather than in the original independent variable space. Since the PCs are ordered and nested, the analyst can truncate the later PCs and focus on the vector endpoints projected onto the primary PCs that captured the most variation (i.e., the most useful information), generally PC 1 and PC 2. The distance between each vector endpoint and each PC is called a score. Samples that are similar to each other will have vector endpoints that cluster together in PC space. Samples that are different from each other will have vector endpoints that are further apart in PC space. Independent variables (retention time data points) that have the most influence on clustering will be the most positively loaded and most negatively loaded variables because the loadings for each variable are the cosine of the angle between each PC and each original independent-variable axis. If a retention time data point has a substantial amount of signal variation over the data set, then it will be highly loaded (very negatively or very positively for mean-centered data) in the primary PCs. Chemical similarities (or differences) among samples can be deduced from the clustering in the scores plot and by identifying the retention time data points that are highly loaded in the loadings plots for each PC. Noise, which may have obscured important chemical information in the raw data, is removed when the scores are visualized in the truncated PC space.

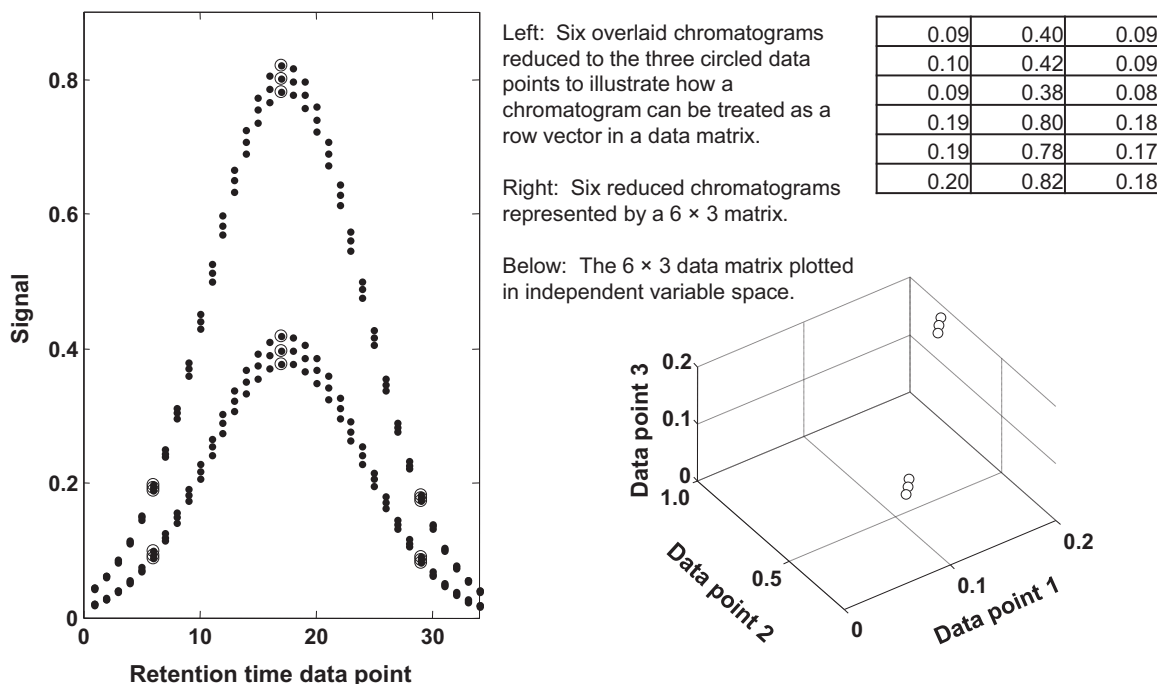


FIGURE 20.5 Illustration of how a chromatogram can be thought of as a single point in independent variable space. A 1D pixel-level chromatogram is described by a single vector endpoint that is positioned by the chromatographic signal (dependent variable) at each retention time data point (independent variable) in independent variable space wherein each data point has its own axis. Chemically similar chromatograms will cluster together in independent variable space. This example shows two clusters, so two classes of samples must be present in the original data set of six chromatograms. This simple data set can be manually classified by visual observation of the overlaid chromatograms, but the same idea applies to large data sets of complex chromatograms where visually observing the chromatograms is not effective.

Chemometric texts provide detailed explanations of the linear algebra behind all the chemometrics described in this chapter [3–6,29]. Data are usually mean-centered and sometimes auto-scaled prior to PCA. Binning can also be applied to improve classification by enhancing the S/N [30]. Fig. 20.6 illustrates PCA applied to 18 simulated chromatograms containing thousands of data points. The 18 overlaid chromatograms in Fig. 20.6A are actually six replicates of three classes of samples. For this simple example, manual intervention such as offsetting overlaid chromatograms allows the analyst to determine how many classes there are in the data set and which chromatograms belong to each class.

However, for truly complex sample analysis, manual observation and manual intervention generally do not yield class information. To provide class information, PCA fits PC 1 and PC 2 to capture the greatest variations of the 18 vector endpoints in variable space, and the projections of these endpoints onto the PCs are the scores on PC 1 and PC 2. The scores plot is shown in Fig. 20.6B where clustering indicates that there are indeed three classes of samples, each with six replicates. The highly loaded variables on PC 1 are shown in Fig. 20.6C, where it is apparent that the earliest eluting component peak and the latest eluting component peak were responsible for distinguishing two of the

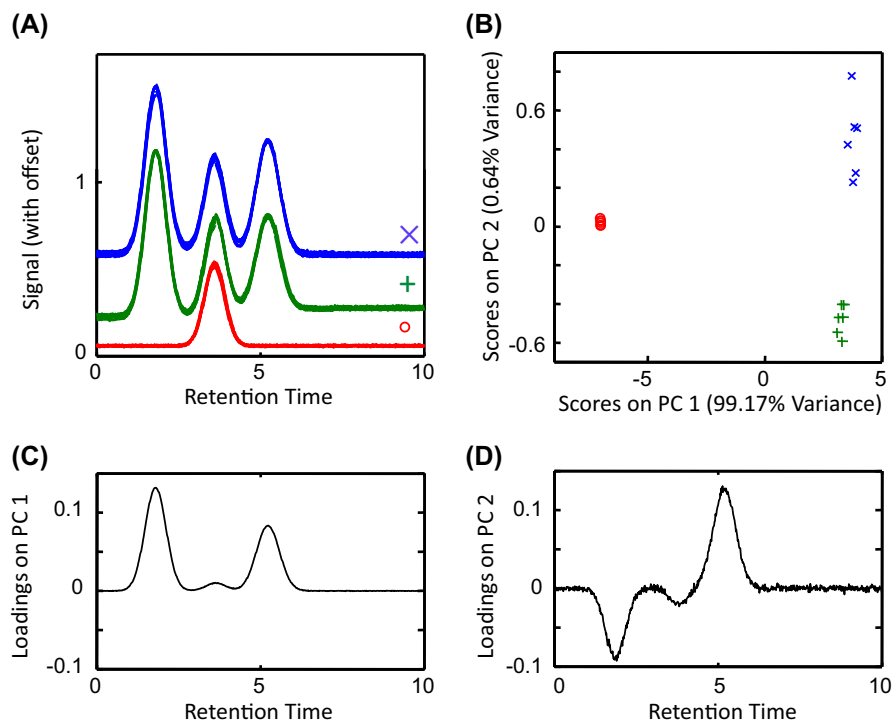


FIGURE 20.6 Illustration of PCA applied to 18 simulated chromatograms. (A) The overlaid and offset chromatograms are 6 replicates of 3 classes of samples. (B) Scores on PC 1 and PC 2 cluster into groups that distinguish the three classes of samples (symbolized by \times , $+$, and o). (C) The most highly loaded variables on PC 1 are the retention times of the earliest eluting peak and the latest eluting peak which represent chemicals that are present in two of the classes (\times and $+$) and absent in the third class (o). Indeed, PC 1 separates the \times and $+$ classes from the o class. (D) The most positively and most negatively loaded variables on PC 2 represent the chemical differences that distinguish the \times class from the $+$ class.

classes (symbolized by \times and $+$) from the third class (symbolized by o). The variables with little to zero loadings on PC 1 are also shown in Fig. 20.6C, indicating that the component with the middle elution time did not differentiate the samples significantly, and the noise regions in the chromatograms did not play a role in differentiating the components at all. The variables with largest loadings on PC 2 are shown in Fig. 20.6D, indicating that the latest eluting component was responsible for differentiating the two classes that PC 1 did not previously differentiate (symbolized by \times and $+$). PCA is applicable to 1D chromatograms that are combined into a 2D matrix. PCA can be applied to multiple pixel-level 2D or 3D chromatograms if the multiple 2D or 3D chromatograms are each

unfolded into 1D vectors and then combined into a single 2D matrix, as shown in Fig. 20.2. PCA is applicable to peak-level data as long as the 1D data vectors for samples are combined into a 2D matrix. PCA is a widely employed chemical analysis tool, for example, with the classification of oil spill samples and oil source samples [31] and volatile components in wine [32,33].

20.3.3 Discriminant analysis

Partial least squares–discriminant analysis (PLS-DA) is a common supervised pattern recognition method. In contrast to a PCA model, where the PCs (latent variables) are defined by the signals that vary the most in a data set,

with a PLS-DA model the latent variables are defined by the signals that both vary and correlate (i.e., covary) with given quantitative information about each sample class. The analyst can inspect PLS-DA loading plots of primary latent variables to discover chemicals that covary with the given quantitative information [34,35]. Fig. 20.7 illustrates how PLS-DA models are based on covariations between given quantitative information and chromatographic data. Three simulated chromatograms with given quantitative values (90, 60, and 30 units) are shown. PLS loadings for latent variable 1 would positively load the middle chromatographic peak because its signal variations positively correlate with the given quantitative values. PLS would negatively load the latest eluting peak because its signal variations negatively correlate with the given quantitative values. The PLS loadings for the earliest peak would

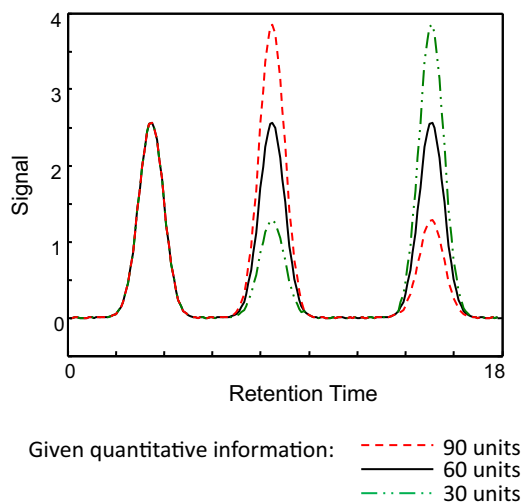


FIGURE 20.7 Illustration of how PLS-DA models show covariation between given quantitative information and chromatographic peaks for three simulated chromatograms. A PLS-DA loading plot would have positive loadings for the middle peak, negative loadings for the last peak, and little to zero loadings for the regions that have little to no correlation with the given quantitative information (first peak and noise regions).

be zero because there is no correlation between the signals for that peak and the given quantitative values. Likewise, noise regions in the chromatograms would have little to no correlation, so zero loadings are observed for the regions of noise in these chromatograms. PLS-DA can be applied to 2D or 3D chromatograms as long as the chromatograms are unfolded and combined into a single 2D matrix and as long as retention time precision is adequate. PLS-DA has been widely used, with just a few interesting applications provided here: identification of biomarkers for certain cancers [36], identification of sources of fuel adulteration [37], and classification of fuels by octane rating after ion filtering [38].

Supervised pattern recognition methods such as PLS-DA require an experimental design where sample class membership is known, sufficient replicates are obtained, and important sources of variation are modeled. In this regard, the Fisher criterion is a statistic that can be employed for supervised methods. The Fisher ratio (F-ratio) calculates the ratio of class-to-class signal variance (information) relative to the within-class signal variance (noise), as a function of an independent variable (such as data point index for pixel-level analysis or peak retention time for peak-level analysis) [3,39]. A variety of supervised algorithms exist that use the F-ratio criterion (or another discriminatory criterion) to do a point-by-point comparison in a data set of multiple chromatograms [40–45]. Chromatographic features with large F-ratios (or other discrimination metric) reveal the chemicals that significantly differentiate the sample classes. This is sometimes called supervised feature selection. Algorithms based on this sort of point-by-point comparison are applicable to 2D, 3D, or 4D data as long as retention time precision is adequate. The point-by-point comparison basically means the method is univariate. Linear discriminant analysis (LDA) is a multivariate algorithm that uses the Fisher criterion to seek linear combinations of variables that distinguish classes if the classes are normally distributed

[43]. Whether univariate or multivariate, feature selection algorithms can greatly reduce data density by filtering out retention time data points that do not contain relevant chemical information if retention time precision is adequate. Orthogonal signal correction (OSC) is another supervised feature selection method that identifies variations in the chromatographic data that are orthogonal to given quantitative information and then removes irrelevant signals causing the important chemical variations to be captured and modeled by primary latent variables. For the same purpose, some analysts use unsupervised pattern recognition algorithms such as PCA to filter interesting chromatographic features from noise prior to submission to other chemometric methods [46]. A useful “tiling” method was developed to discriminate samples and avoid the shortcomings of alignment algorithms for GC \times GC-TOFMS data sets [47–49]. In this approach, the sample class chromatograms are strategically binned into four tiling schemes, such that a given 2D peak is optimally captured in one of the four tiling grids. The F-ratio is calculated for every m/z between all tiles of the sample chromatograms. The tile size is carefully selected to mitigate retention time shifting without capturing multiple peaks or extraneous noise. The original raw data does not need to be reinterpolated to create an aligned chromatogram so peak shapes are not distorted by warping. The output of the tile-based F-ratio software is a hit list, which contains the locations of analyte features, ordered from highest to lowest F-ratio. An analyst can then “mine” the hit list, top-down, to further investigate these class-distinguishing analytes. A “pin-and-cluster” step in the algorithm automatically removes redundant hits prior to outputting the hit list, which may have arisen from overlapping tiles. Tile-based Fisher ratio analysis has been applied to identify statistically significant compositional differences between acid-treated and -untreated diesel fuel samples [49]

and to discover metabolites that discriminate between respiring and fermenting yeast cells [50].

20.3.4 Resolution methods

Mathematical resolution methods are able to resolve overlapping peaks in a chromatogram. In this chapter, mathematical resolution methods are loosely classified as pattern recognition methods because they are often expected to recognize particular peak shapes or spectral profiles. Multivariate curve resolution (MCR) and the generalized rank annihilation method (GRAM) are mathematical resolution methods applicable to 2D chromatograms. GRAM requires that the GC \times GC data be bilinear, while MCR does not require bilinearity. The definition of bilinearity means the chromatographic profile of the pure compound can theoretically be defined by the outer product of two vectors, in this case the chromatographic peak profile on each dimension. Bilinearity is instrumentally achieved if retention time and peak shape reproducibility are adequate along the second dimension and if signals of coeluting components are linearly additive. MCR uses chemically selective portions of a chromatogram where there is only one component to obtain the correct shapes of each fully resolved peak. Then shape is used as a constraint along with a nonnegativity constraint to linearly combine estimated pure profiles until the calculated chromatogram approximates the given unresolved chromatogram via alternating least squares fitting. This reveals the pure resolved peak profiles and peak area information [51]. GRAM requires that both a sample chromatogram and a standard chromatogram be augmented together to form a single matrix [52]. As such, in addition to being a preprocessing resolution algorithm, GRAM is also used as a single-point external standard calibration method. Many analysts use rank minimization prior to GRAM in order to improve data structure bilinearity and retention time precision. The rank minimization algorithm seeks to

maximize the information content in the lower singular values using singular value decomposition (SVD) to calculate loadings for the original independent variables that are consistent with the previous description of PCA loadings. An interesting application of GRAM was reported to mathematically resolve subregions of GC \times GC-FID separations containing overlapping alkyl benzenes [53]. This demonstrated the ability to accurately quantify low concentrations of overlapping analytes even in regions with a higher concentration of interfering compounds.

Parallel factor analysis (PARAFAC), trilinear decomposition (TLD), as well as MCR, are mathematical resolution methods that are applicable to either a single 3D chromatogram (such as GC \times GC-TOFMS) or multiple 2D chromatograms that have been combined into a 3D matrix as shown in Fig. 20.2. To implement PARAFAC successfully, the 3D data must exhibit a sufficiently trilinear structure. This means that the signal for a pure compound can theoretically be defined by the outer product of three vectors and this is instrumentally achieved if retention time precision is adequate and if signals of coeluting components are linearly additive. PARAFAC back-calculates the outer product of the three vectors and predicts pure component concentrations, pure spectral profiles, and pure chromatographic peak profiles for analyte signals that were originally overlapping using alternating least squares with unimodality and nonnegativity constraints to converge upon a best fit. PARAFAC greatly improves *S/N* by removing noise as an independent component separate from the chemical signals present [54]. TLD estimates the profiles of each component by eigenvector decomposition and then estimates the component concentrations by least squares fitting [55,56]. As long as the data are sufficiently trilinear and there is adequate selectivity for each of the coeluting components on two of the three dimensions, then PARAFAC and TLD can resolve overlapping peaks [57,58]. GC \times GC-TOFMS is generally capable of

providing that trilinearity and selectivity. PARAFAC has also been applied to comprehensive three-dimensional gas chromatography data (GC³) with both FID and TOFMS detection [59–61]. PARAFAC and TLD algorithms are usually only applicable to manually selected chromatographic subregions where a maximum of about 6–7 chemical compounds are present in the subregion and even smaller ranks are preferred. However, to avoid the step of selecting a subregion, a version of PARAFAC that automatically resolves all peaks in an *entire* GC \times GC-TOFMS chromatogram has been reported [62]. The key to this was an algorithm that automatically selects an appropriate number of factors for PARAFAC modeling (i.e., automated rank determination), thus reducing the number of required analyst inputs and reducing the extent of required manual intervention [63,64]. A derivative of PARAFAC called PARAFAC2 was developed for data that severely deviate from trilinearity due to insufficient retention time precision or a drifting retention time in the second dimension of GC \times GC [65–67]. PARAFAC2 can improve trilinearity of appropriate data structures, thus improving resolution results. However, the unique constraints in PARAFAC2 make the model more likely to incur quantitative inaccuracy relative to PARAFAC and MCR [68]. The interested reader is referred to several excellent reports and reviews on the use of MCR-ALS and PARAFAC [69–72].

Nontargeted algorithms are a commonly applied tool for the analyst to gain a foothold into identifying chromatographic peaks using mass spectral data. Such nontargeted algorithms can also be categorized as pattern recognition algorithms because they are expected to recognize similarities between observed spectra of chromatographic peaks and library mass spectra. The publicly available US National Institute of Standards and Technology (NIST) MS Search for electron ionization spectra allows analysts to input observed mass spectra and then the algorithm outputs best matches to identify

analytes. Many instrument manufacturers have incorporated the NIST MS search algorithm as a data processing option in their native instrument software. The automated mass spectral purification and identification system (AMDIS) also matches observed mass spectra with library mass spectra for identification, and it also has a mathematical resolution capability [73]. Both the MS Search and AMDIS algorithms can be applied to mass spectra from GC-MS or GC \times GC-MS chromatograms.

20.4 Calibration

Calibration methods are used to predict a quantitative property of interest for an unknown sample by modeling known samples. A training set composed of chromatograms with known quantitative property values is used to build the regression model. Models are generally evaluated using an independent test set or by a leave-one-out cross-validation procedure. Classical least squares (CLS) is a calibration method that is used to mathematically resolve and quantify chromatographic peaks since chromatographic instruments are generally designed to produce component signals that are additive and linearly related to concentration [74,75]. To construct a CLS model, pixel-level 1D chromatograms of pure standards must be available for the algorithm to calculate a standard mixture chromatogram that is the linear combination of the pure component peaks with known concentration coefficients. An unknown sample chromatogram is regressed onto this model by least squares fitting, yielding the pure resolved profiles of each component that is present in the unknown sample. A shortcoming of CLS is its inability to detect the presence of unresolved interfering components. An interesting application of CLS was reported to resolve mass spectra of overlapping GC \times GC-TOFMS peaks that were initially a combination of a spiked ^{13}C -labeled analyte peak and the unlabeled analyte peak

[74]. CLS predicted the pure mass spectra, the $^{12}\text{C}/^{13}\text{C}$ ratio, and the absolute amounts of ^{12}C and ^{13}C in the unknown samples.

20.4.1 Partial least squares regression

PLS is a calibration method that highly loads chromatographic features that covary with given quantitative information [75,76]. The loadings are linearly combined into latent variables, with the most highly loaded independent variables (retention time data points) captured in the primary latent variables. The analyst chooses a subset of the latent variables to build the calibration model. The PLS algorithm then estimates the quantitative property for an unknown chromatogram by regression. Prior to applying PLS, the matrix of chromatograms and the quantitative properties are both usually mean-centered. PLS is designed for multiple 1D chromatograms combined into a 2D matrix. It is also applicable to data sets of 2D or 3D chromatograms as long as they are unfolded into 1D chromatograms and combined into a single 2D matrix. However, keeping data in their original structure without unfolding may improve accuracy. Thus N-PLS was developed and extends PLS to higher dimensions of data [77]. N-PLS can accept an ND matrix composed of multiple (N - 1)D chromatograms. PLS has been applied to quantify naphthalenes in jet fuels with GC \times GC-FID data [78] and predict flavor profiles of coffee with SPME-GC-FID [79], for example.

20.4.2 Principal component regression

Principal component regression (PCR) is a calibration method that functions by building a model that regresses given quantitative values onto the PCA scores for a training set, and then the scores for an unknown chromatogram are submitted to that model to quantify the unknown. Mean centering and sometimes autoscaling the data are common procedural steps prior to PCR. An interesting application of PCR was

reported to model and classify food packaging materials according to the array of volatile chemicals that were emitted from the wrappers [80].

Overall, calibration models perform best when future samples are similar to the samples that were in the training set. All calibration models decline when forced to extrapolate beyond the range of the variations in the modeled training set. Therefore, all calibration models should be evaluated by checking the accuracy of predicted values for an independent test set, or if the size of the data set is limited, then by using the leave-one-out cross-validation technique. Leave-one-out cross-validation is a traditional method whereby, one at a time, each chromatogram is pulled out of the training set, the model is built with the remaining chromatograms, and then that left-out chromatogram is submitted to the model to predict that sample's quantitative property. This is repeated for every chromatogram in the training set and yields a leave-one-out cross-validation plot of predicted quantity versus known quantity (typically obtained from a benchmark method). The calibration model is evaluated based on the slope, R^2 , and relative root-mean-squared-error of cross-validation (RMSECV) values of this plot. When the model is robust and useful, the covariations between quantitative property and chromatographic signal are strong, the slope = 1.00, ideal R^2 values are close to 1.0, and the ideal RMSECV value approaches 0. Such a robust model will then yield reliable quantitative predictions for unknown samples. The underlying assumption is that the benchmark method to provide the known quantity information is sufficiently accurate and precise for modeling purposes. A typical application of this approach is to provide a fast predictive modeling method to replace a slow (often more traditional) method used for benchmarking.

20.5 Experimental method optimization

Chromatographic method development often requires that a large number of parameters be considered and optimized: choice of stationary phase(s), column dimensions, flow rate, temperatures, run time, detector settings, types of replicates, numbers of replicates, and a host of sample preparation options. Optimization of these parameters can be determined by assessing a variety of properties: resolution of key analytes, S/N , response factors, magnitude of variance, sources of variance, use of the separation space, and 2D separation orthogonality. Statistical experimental design methods provide mathematical optimization of combinations of these continuous experimental variables. The classic statistical designs are factorial designs, response surface designs, mixture designs, and simplex optimization [4,81]. Classic chemometric texts provide additional information about each of these statistical designs [4]. It is likely that industrial researchers who are doing large-scale and/or long-term research applications are using the classic statistical designs to make intelligent decisions about efficient sampling options, instrumental options, and data analysis methods, all to improve analytical performance, to save time, and to lower expenses. Less commonly, individual analysts doing individual research will apply classic statistical design strategies, but individual analysts do monitor experimental response as a function of experimental conditions, and they do carefully consider obtaining appropriate replicates, using appropriate calibration methods, and modeling appropriate sources of variation, all in order to have a good experimental design and properly support their results. There are generally two approaches that individual researchers use to seek optimal parameters: methods that assess experimentally obtained chromatographic data and output the

optimal parameters [82,83] or methods that use given parameter ranges to simulate chromatograms and then assess the simulated chromatograms to determine the optimal parameters [84,85]. Experimental design techniques are becoming increasingly useful for GC \times GC practitioners due to the complexity of method optimization relative to 1D GC [86,87]. An interesting method that uses experimental chromatographic data is a closed-loop machine-learning program that repeatedly runs samples on a GC \times GC-TOFMS, iteratively analyzes the collected data, and adjusts instrument parameters until the separations are at an optimum based on assessments of resolution, S/N , and run time [82]. Experimentally obtained chromatographic data were also used to thoroughly and definitively optimize the experimental design for extraction and GC-MS analysis of human blood plasma metabolites based on PLS results [88].

20.6 Conclusion

This chapter introduced basic chemometric methods for chromatographic data analysis while loosely categorizing them as preprocessing, pattern recognition, calibration, or experimental optimization methods. There are many derivatives of these chemometric techniques that were not mentioned. Some of these derivatives actually cause the chemometric method to shift categories. For instance, when PCA is used as a noise-reduction method prior to other chemometrics, it could fit in the preprocessing category instead of the pattern recognition category. Another example is TLD applied prior to PARAFAC to improve trilinearity, so this method could fit in the preprocessing category as well as the pattern recognition category [58]. Some of the derivatives allow the algorithms to relax their requirements and still yield accurate results, such as tiling approaches or fuzzy methods that are robust against shifting and

also indirect classical least squares (ICLS) that does not require given standards (as CLS requires) to resolve overlapping peaks. We could also consider all of the nonlinear chemometric methods that remove the assumption of linearity in its signal response. For information about these and more, the classic chemometric textbooks are excellent resources [3–6]. In this chapter, we also refrained from explaining the linear algebra driving the chemometrics. For descriptions of the math behind the chemometrics, the classic chemometric textbooks and the PLS Toolbox user's manual are excellent resources [29]. For information about recent developments in chemometrics, review articles that comprehensively cover chemometrics applicable to gas or liquid chromatography are good sources [89–94]. Overall, it is indeed exciting to see how the field of GC is being advanced by the emergence, acceptance, and application of chemometric data analysis methods.

References

- [1] D.A. Skoog, F.J. Holler, T.A. Nieman, Principles of Instrumental Analysis, vol. 5, Sanders College Publishing, San Francisco, 1998.
- [2] D.C. Harris, Quantitative Chemical Analysis, vol. 8, Freeman and Company, New York, 2010.
- [3] D.L. Massart, Chemometrics: A Textbook, Elsevier Sciences Ltd., New York, 1988.
- [4] R.G. Brereton, Chemometrics: Data Analysis for the Laboratory and Chemical Plant, Wiley, New York, 2003.
- [5] K.R. Beebe, R.J. Pell, M.B. Seasholtz, Chemometrics: A Practical Guide, Wiley-Interscience, New York, 1998.
- [6] M.A. Sharaf, D.L. Illman, B.R. Kowalski, Chemometrics, John Wiley & Sons, New York, 1986.
- [7] L. Zhu, R.G. Brereton, D.R. Thompson, P.L. Hopkins, R.E.A. Escott, On-line HPLC combined with multivariate statistical process control for the monitoring of reactions, *Anal. Chim. Acta* 584 (2007) 370–378.
- [8] S.C. Wang, S.M. Chiang, C.M. Huang, Parametric studies of matched filters to enhance the signal-to-noise ratios of LC-MS-MS peaks, *Anal. Chim. Acta* 556 (2006) 201–207.
- [9] A. Savitzky, M.J. E Golay, Smoothing and differentiation of data by simplified least squares procedures, *Anal. Chem.* 36 (1964) 1627–1639.

- [10] K. Robards, P.R. Hadad, P.E. Jackson, *Principles and Practice of Modern Chromatographic Methods*, Academic Press, New York, 1994.
- [11] M.L. Lee, F.J. Yang, K.D. Bartle, *Open Tubular Column Gas Chromatography*, John Wiley & Sons, New York, 1984.
- [12] C.G. Fraga, B.J. Prazen, R.E. Synovec, Comprehensive two-dimensional gas chromatography and chemometrics for the high-speed quantitative analysis of aromatic isomers in a jet fuel using the standard addition method and an objective retention time alignment algorithm, *Anal. Chem.* 72 (2000) 4154–4162.
- [13] C.G. Fraga, B.J. Prazen, R.E. Synovec, Objective data alignment and chemometric analysis of comprehensive two-dimensional separations with run-to-run peak shifting on both dimensions, *Anal. Chem.* 73 (2001) 5833–5840.
- [14] K.S. Booksh, B.R. Kowalski, Y. Wang, M.J. Lysaght, Standardization of second-order chromatographic/spectroscopic data for optimum chemical analysis, *Anal. Chem.* 70 (1998) 218–225.
- [15] K.J. Johnson, B.W. Wright, K.H. Jarman, R.E. Synovec, High-speed peak matching algorithm for retention time alignment of gas chromatographic data for chemometric analysis, *J. Chromatogr. A* 996 (2003) 141–155.
- [16] N.-P. Vest Nielsen, J.M. Carstensen, J. Smedsgaard, Aligning of single and multiple wavelength chromatographic profiles for chemometric data analysis using correlation optimised warping, *J. Chromatogr. A* 805 (1998) 17–35.
- [17] G. Tomasi, F. Van Den Berg, C. Andersson, Correlation optimized warping and dynamic time warping as pre-processing methods for chromatographic data, *J. Chemometr.* 18 (2004) 231–241.
- [18] J.S. Nadeau, B.W. Wright, R.E. Synovec, Chemometric analysis of gas chromatography-mass spectrometry data using fast retention time alignment via a total ion current shift function, *Talanta* 81 (2010) 120–128.
- [19] M. Chae, R.J. Shmookler Reis, J.J. Thaden, An iterative block-shifting approach to retention time alignment that preserves the shape and area of gas chromatography-mass spectrometry peaks, *BMC Bioinf.* 9 (Suppl. 9) (2008) S15.
- [20] D. Zhang, X. Huang, F.E. Regnier, M. Zhang, Two-dimensional correlation optimized warping algorithm for aligning GC \times GC-MS data, *Anal. Chem.* 80 (2008) 2664–2671.
- [21] V. Pravdova, B. Walczak, D.L. Massart, A comparison of two algorithms for warping of analytical signals, *Anal. Chim. Acta* 456 (2002) 77–92.
- [22] R.G. Sadygov, F.M. Maroto, A.F.R. Hühner, ChromAlign: a two-step algorithmic procedure for time alignment of three-dimensional LC-MS chromatographic surfaces, *Anal. Chem.* 78 (2006) 8207–8217.
- [23] K.M. Pierce, B.W. Wright, R.E. Synovec, Unsupervised parameter optimization for automated retention time alignment of severely shifted gas chromatographic data using the piecewise alignment algorithm, *J. Chromatogr. A* 1141 (2007) 106–116.
- [24] T.I. Dearing, J.S. Nadeau, B.G. Rohrbach, L.S. Ramos, R.E. Synovec, Real-time target selection optimization to enhance alignment of gas chromatograms, *Talanta* 83 (2011) 738–743.
- [25] T. Skov, F. Van Den Berg, G. Tomasi, R. Bro, Automated alignment of chromatographic data, *J. Chemometr.* 20 (2006) 484–497.
- [26] S.E. Reichenbach, X. Tian, Q. Tao, E.B. Ledford, Z. Wu, O. Fiehn, Informatics for cross-sample analysis with comprehensive two-dimensional gas chromatography and high-resolution mass spectrometry (GC \times GC-HRMS), *Talanta* 83 (2011) 1279–1288.
- [27] T. Gröger, M. Schäffer, M. Pütz, B. Ahrens, K. Drew, M. Eschner, R. Zimmermann, Application of two-dimensional gas chromatography combined with pixel-based chemometric processing for the chemical profiling of illicit drug samples, *J. Chromatogr. A* 1200 (2008) 8–16.
- [28] L.R. Zano, B.C. Diniz Brito Dos Santos, R. Sequinel, D.L. Flumignan, J.E. De Oliveira, Prediction of relative density, distillation temperatures, flash point, and octane number of S500 diesel oil using multivariate calibration of gas chromatographic profiles, *Energy Fuels* 32 (2018) 8108–8114.
- [29] B.M. Wise, N.B. Gallagher, R. Bro, J.M. Shaver, W. Windig, S.R. Koch, *PLS Toolbox 3.5 for Use with Matlab™*, 2004. ISBN:0-97611840-8.
- [30] P.E. Sudol, D.V. Gough, S.E. Prebihalo, R.E. Synovec, Impact of data bin size on the classification of diesel fuels using comprehensive two-dimensional gas chromatography with principal component analysis, *Talanta* 206 (2020) 120239.
- [31] J.H. Christensen, G. Tomasi, A.B. Hansen, Chemical fingerprinting of petroleum biomarkers using time warping and PCA, *Environ. Sci. Technol.* 39 (2005) 255–260.
- [32] J.E. Welke, M. Zanusi, M. Lazzarotto, F.H. Pulgati, C.A. Zini, Main differences between volatiles of sparkling and base wines accessed through comprehensive two dimensional gas chromatography with time-of-flight mass spectrometric detection and chemometric tools, *Food Chem.* 164 (2014) 427–437.

- [33] J.E. Welke, V. Manfroi, M. Zanusi, M. Lazarotto, C. Alcaraz Zini, Characterization of the volatile profile of Brazilian Merlot wines through comprehensive two dimensional gas chromatography time-of-flight mass spectrometric detection, *J. Chromatogr. A* 1226 (2012) 124–139.
- [34] D.J. Crockford, J.C. Lindon, O. Cloarec, R.S. Plumb, S.J. Bruce, S. Zirah, et al., Statistical search space reduction and two-dimensional data display approaches for UPLC-MS in biomarker discovery and pathway analysis, *Anal. Chem.* 78 (2006) 4398–4408.
- [35] S.J. Dixon, Y. Xu, R.G. Brereton, H.A. Soini, M.V. Novotny, E. Oberzaucher, K. Grammer, D.J. Penn, Pattern recognition of gas chromatography mass spectrometry of human volatiles in sweat to distinguish the sex of subjects and determine potential discriminatory marker peaks, *Chemom. Intell. Lab. Syst.* 87 (2007) 161–172.
- [36] H.M. Woo, K.M. Kim, M.H. Choi, B.H. Jung, J. Lee, G. Kong, S.J. Nam, S. Kim, S.W. Bai, B.C. Chung, Mass spectrometry based metabolomic approaches in urinary biomarker study of women's cancers, *Clin. Chim. Acta* 400 (2009) 63–69.
- [37] M.G. Nespeca, J.F.V.L. Munhoz, D.L. Flumignan, J.E. de Oliveira, Rapid and sensitive method for detecting adulterants in gasoline using ultra-fast gas chromatography and Partial Least Square Discriminant Analysis, *Fuel* 215 (2018) 204–211.
- [38] L.A. Adutwum, J.J. Harynyuk, Unique ion filter: a data reduction tool for GC/MS data preprocessing prior to chemometric analysis, *Anal. Chem.* 86 (2014) 7726–7733.
- [39] R.O. Duda, P.E. Hart, *Pattern Classifications and Scene Analysis*, vol. 1, Wiley, New York, 1973.
- [40] K.J. Johnson, R.E. Synovec, Pattern recognition of jet fuels: comprehensive GC \times GC with ANOVA-based feature selection and principal component analysis, *Chemometr. Intell. Lab. Syst.* 60 (2002) 225–237.
- [41] K.M. Pierce, J.C. Hoggard, J.L. Hope, P.M. Rainey, A.N. Hoofnagle, R.M. Jack, B.W. Wright, R.E. Synovec, Fisher ratio method applied to third-order separation data to identify significant chemical components of metabolite extracts, *Anal. Chem.* 78 (2006) 5068–5075.
- [42] T. Kind, V. Tolstikov, O. Fiehn, R.H. Weiss, A comprehensive urinary metabolomic approach for identifying kidney cancer, *Anal. Biochem.* 363 (2007) 185–195.
- [43] D.R. Burgard, J.T. Kuznicki, *Chemometrics: Chemical and Sensory Data*, CRC Press, Boca Raton, 1990.
- [44] H.D. Bean, J.E. Hill, J.M.D. Dimandja, Improving the quality of biomarker candidates in untargeted metabolomics via peak table-based alignment of comprehensive two-dimensional gas chromatography-mass spectrometry data, *J. Chromatogr. A* 1394 (2015) 111–117.
- [45] C.E. Freye, P.R. Bowden, M.T. Greenfield, B.C. Tappan, Non-targeted discovery-based analysis for gas chromatography with mass spectrometry: a comparison of peak table, tile, and pixel-based Fisher ratio analysis, *Talanta* 211 (2020) 120668.
- [46] M. Jalali-Heravi, A. Kyani, Use of computer-assisted methods for the modeling of the retention time of a variety of volatile organic compounds: a PCA-MLR-ANN approach, *J. Chem. Inf. Comput. Sci.* 44 (2004) 1328–1335.
- [47] L.C. Marney, W. Christopher Siegler, B.A. Parsons, J.C. Hoggard, B.W. Wright, R.E. Synovec, Tile-based Fisher-ratio software for improved feature selection analysis of comprehensive two-dimensional gas chromatography-time-of-flight mass spectrometry data, *Talanta* 115 (2013) 887–895.
- [48] B.A. Parsons, L.C. Marney, W.C. Siegler, J.C. Hoggard, B.W. Wright, R.E. Synovec, Tile-based Fisher ratio analysis of comprehensive two-dimensional gas chromatography time-of-flight mass spectrometry (GC \times GC-TOFMS) data using a null distribution approach, *Anal. Chem.* 87 (2015) 3812–3819.
- [49] B.A. Parsons, D.K. Pinkerton, B.W. Wright, R.E. Synovec, Chemical characterization of the acid alteration of diesel fuel: non-targeted analysis by two-dimensional gas chromatography coupled with time-of-flight mass spectrometry with tile-based Fisher ratio and combinatorial threshold determination, *J. Chromatogr. A* 1440 (2016) 179–190.
- [50] N.E. Watson, B.A. Parsons, R.E. Synovec, Performance evaluation of tile-based Fisher Ratio analysis using a benchmark yeast metabolome dataset, *J. Chromatogr. A* 1459 (2016) 101–111.
- [51] R. Gargallo, R. Tauler, F. Cuesta-Sgncnez, D.L. Massart, Validation of alternating least-squares multivariate curve resolution for chromatographic resolution and quantitation, *Trends Anal. Chem.* 15 (1996) 279–286.
- [52] L.S. Ramos, E. Sanchez, B.R. Kowalski, Generalized rank annihilation method II. Analysis of bimodal chromatographic data, *J. Chromatogr.* 385 (1987) 165–180.
- [53] C.G. Fraga, B.J. Prazen, R.E. Synovec, Enhancing the limit of detection for comprehensive two-dimensional gas chromatography (GC \times GC) using bilinear chemometric analysis, *J. High Resolut. Chromatogr.* 23 (2000) 215–224.
- [54] J.C. Hoggard, J.H. Wahl, R.E. Synovec, G.M. Mong, C.G. Fraga, Impurity profiling of a chemical weapon precursor for possible forensic signatures by comprehensive two-dimensional gas chromatography/mass spectrometry and chemometrics, *Anal. Chem.* 82 (2010) 689–698.

- [55] E. Sanchez, B.R. Kowalski, Tensorial resolution: a direct trilinear decomposition, *J. Chemometr.* 4 (1) (1990) 29–45.
- [56] K.S. Booksh, Z. Lin, Z. Wang, B.R. Kowalski, Extension of trilinear decomposition method with an application to the flow probe sensor, *Anal. Chem.* 66 (1994) 2561–2569.
- [57] P. Hindmarch, K. Kavianpour, R.G. Brereton, Evaluation of parallel factor analysis for the resolution of kinetic data by diode-array high-performance liquid chromatography, *The Analyst* 122 (1997) 871–877.
- [58] A.E. Sinha, C.G. Fraga, B.J. Prazen, R.E. Synovec, Trilinear chemometric analysis of two-dimensional comprehensive gas chromatography-time-of-flight mass spectrometry data, *J. Chromatogr. A* 1027 (1–2) (2004) 269–277.
- [59] N.E. Watson, W.C. Siegler, J.C. Hoggard, R.E. Synovec, Comprehensive three-dimensional gas chromatography with parallel factor analysis, *Anal. Chem.* 79 (2007) 8270–8280.
- [60] N.E. Watson, S.E. Prebihalo, R.E. Synovec, Targeted analyte deconvolution and identification by four-way parallel factor analysis using three-dimensional gas chromatography with mass spectrometry data, *Anal. Chim. Acta* 983 (2017) 67–75.
- [61] V.H.C. Ferreira, L.W. Hantao, R.J. Poppi, Consumable-free comprehensive three-dimensional gas chromatography and PARAFAC for determination of allergens in perfumes, *Chromatographia* 83 (2020) 581–592.
- [62] J.C. Hoggard, W.C. Siegler, R.E. Synovec, Toward automated peak resolution in complete GC × GC-TOFMS chromatograms by PARAFAC, *J. Chemometr.* 23 (2009) 421–431.
- [63] J.C. Hoggard, R.E. Synovec, Parallel factor analysis (PARAFAC) of target analytes in GC × GC-TOFMS data: automated selection of a model with an appropriate number of factors, *Anal. Chem.* 79 (2007) 1611–1619.
- [64] J.C. Hoggard, R.E. Synovec, Automated resolution of nontarget analyte signals in GC × GC-TOFMS data using parallel factor analysis, *Anal. Chem.* 80 (2008) 6677–6688.
- [65] T. Skov, J.C. Hoggard, R. Bro, R.E. Synovec, Handling within run retention time shifts in two-dimensional chromatography data using shift correction and modeling, *J. Chromatogr. A* 1216 (2009) 4020–4029.
- [66] R. Bro, C.A. Andersson, H.A.L. Kiers, PARAFAC2 - Part II. Modeling chromatographic data with retention time shifts, *J. Chemometr.* 13 (1999) 295–309.
- [67] K. Tian, L. Wu, S. Min, R. Bro, Geometric search: a new approach for fitting PARAFAC2 models on GC-MS data, *Talanta* 185 (2018) 378–386.
- [68] M.B. Anzardi, J.A. Arancibia, A.C. Olivieri, Interpretation of matrix chromatographic-spectral data modeling with parallel factor analysis 2 and multivariate curve resolution, *J. Chromatogr. A* 1604 (2019) 60502.
- [69] H. Parastar, J.R. Radović, M. Jalali-Heravi, S. Diez, J.M. Bayona, R. Tauler, Resolution and quantification of complex mixtures of polycyclic aromatic hydrocarbons in heavy fuel oil sample by means of GC × GC-TOFMS combined to multivariate curve resolution, *Anal. Chem.* 83 (2011) 9289–9297.
- [70] H. Parastar, R. Tauler, Multivariate curve resolution of hyphenated and multidimensional chromatographic measurements: a new insight to address current chromatographic challenges, *Anal. Chem.* 86 (2014) 286–297.
- [71] G.M. Escandar, A.C. Olivieri, Multi-way chromatographic calibration—a review, *J. Chromatogr. A* 1587 (2019) 2–13.
- [72] L.W. Hantao, H.G. Aleme, M.P. Pedroso, G.P. Sabin, R.J. Poppi, F. Augusto, Multivariate curve resolution combined with gas chromatography to enhance analytical separation in complex samples: a review, *Anal. Chim. Acta* 731 (2012) 11–23.
- [73] J.M. Halket, A. Przyborowska, S.E. Stein, W.G. Mallard, S. Down, R.A. Chalmers, Deconvolution gas chromatography/mass spectrometry of urinary organic acids-potential for pattern recognition and automated identification of metabolic disorders, *Rapid Commun. Mass Spectrom.* 13 (1999) 279–284.
- [74] E.M. Humston, J.C. Hoggard, R.E. Synovec, Utilizing the third order advantage with isotope dilution mass spectrometry, *Anal. Chem.* 82 (2010) 41–43.
- [75] D.M. Haaland, E.V. Thomas, Partial least-squares methods for spectral analyses. 1. Relation to other quantitative calibration methods and the extraction of quantitative information, *Anal. Chem.* 60 (1988) 1193–1202.
- [76] P. Geladi, B.R. Kowalski, Partial least-squares regression: a tutorial, *Anal. Chim. Acta* 185 (1986) 1–17.
- [77] R. Bro, Multiway calibration. Multiway PLS, *J. Chemometr.* 10 (1996) 47–61.
- [78] K.J. Johnson, B.J. Prazen, D.C. Young, R.E. Synovec, Quantification of naphthalenes in jet fuel with GC × GC/Tri-PLS and windowed rank minimization retention time alignment, *J. Separ. Sci.* 27 (5–6) (2004) 410–441.
- [79] J.S. Ribeiro, F. Augusto, T.J.G. Salva, R.A. Thomaziello, M.M.C. Ferreira, Prediction of sensory properties of Brazilian Arabica roasted coffees by headspace solid phase microextraction-gas chromatography and partial least squares, *Anal. Chim. Acta* 634 (2009) 172–179.

- [80] M. Frank, H. Ulmer, J. Ruiz, P. Visani, U. Weimar, Complementary analytical measurements based upon gas chromatography-mass spectrometry, sensor system and human sensory panel; a case study dealing with packaging materials, *Anal. Chim. Acta* 431 (2001) 11–29.
- [81] S.L.C. Ferreira, R.E. Bruns, E. Galvão, P.d. Silva, W.N.L.d. Santos, C.M. Quintella, et al., Statistical designs and response surface techniques for the optimization of chromatographic systems, *J. Chromatogr. A* 1158 (2007) 2–14.
- [82] S. O'Hagan, W.B. Dunn, J.D. Knowles, D. Broadhurst, R. Williams, J.J. Ashworth, et al., Closed-loop, multiobjective optimization of two-dimensional gas chromatography/mass spectrometry for serum metabolomics, *Anal. Chem.* 79 (2007) 464–476.
- [83] V.M. Morris, J.G. Hughes, P.J. Marriott, Examination of a new chromatographic function, based on an exponential resolution term, for use in optimization strategies: application to capillary gas chromatography separation of phenols, *J. Chromatogr. A* 755 (1996) 235–243.
- [84] J. Beens, H.-G. Janssen, M. Adahchour, U.A.T. Brinkman, Flow regime at ambient outlet pressure and its influence in comprehensive two-dimensional gas chromatography, *J. Chromatogr. A* 1086 (1–2) (2005) 141–150.
- [85] D. Ryan, P. Morrison, P. Marriott, Orthogonality considerations in comprehensive two-dimensional gas chromatography, *J. Chromatogr. A* 1071 (1.2) (2005) 47–53.
- [86] J. Omar, I. Alonso, M. Olivares, A. Vallejo, N. Etxebarria, Optimization of comprehensive two-dimensional gas-chromatography (GC × GC) mass spectrometry for the determination of essential oils, *Talanta* 88 (2012) 145–151.
- [87] M. Brokl, L. Bishop, C.G. Wright, C. Liu, K. McAdam, J.F. Focant, Multivariate analysis of mainstream tobacco smoke particulate phase by headspace solid-phase micro extraction coupled with comprehensive two-dimensional gas chromatography-time-of-flight mass spectrometry, *J. Chromatogr. A* 1370 (2014) 216–229.
- [88] A. Jiye, J. Trygg, J. Gullberg, A.I. Johansson, P. Jonsson, H. Antti, S.L. Marklund, T. Moritz, Extraction and GC/MS analysis of the human blood plasma metabolome, *Anal. Chem.* 77 (2005) 8086–8094.
- [89] R.E. Synovec, B.J. Prazen, K.J. Johnson, C.G. Fraga, C.A. Bruckner, *Advances in Chromatography*, Marcel Dekker, Inc., New York, 2003.
- [90] J.M. Amigo, T. Skov, R. Bro, ChroMATHography: solving chromatographic issues with mathematical models and intuitive graphics, *Chem. Rev.* 110 (2010) 4582–4605.
- [91] K. Pierce, J. Hoggard, R. Mohler, R. Synovec, Recent advancements in comprehensive two-dimensional separations with chemometrics, *J. Chromatogr. A* 1184 (2008) 341–352.
- [92] H.J. Cortes, B. Winniford, J. Luong, M. Pursch, Comprehensive two-dimensional gas chromatography review, *J. Separ. Sci.* 32 (2009) 883–904.
- [93] O. Amador-Muñoz, P.J. Marriott, Quantification in comprehensive two-dimensional gas chromatography and a model of quantification based on selected summed modulated peaks, *J. Chromatogr. A* 1184 (2008) 323–340.
- [94] M. Navarro-Reig, C. Bedia, R. Tauler, J. Jaumot, Chemometric strategies for peak detection and profiling from multidimensional chromatography, *Proteomics* 18 (2018) 1700327.

Validation of gas chromatographic methods

Bieke Dejaegher, Johanna Smeyers-Verbeke, Yvan Vander Heyden

Department of Analytical Chemistry, Applied Chemometrics and Molecular Modelling, Vrije Universiteit Brussel (VUB), Brussels, Belgium

21.1 Introduction

Method validation is the last step in the development of an analytical method (Fig. 21.1), for example, a gas chromatographic method [1]. During method development, a method is selected, e.g., based on information from the literature or on an already known method. This method is then optimized for the intended application. This can, for example, be necessary because the matrix is different from that analyzed in the original method (e.g., blood vs. urine), because another but similar component is determined (e.g., propranolol vs. alprenolol in blood), or because the chromatographic column is not present in the laboratory and another but similar column will be used. After optimization of the analytical conditions and selection of the calibration scheme, a candidate method is obtained, which is expected to comply with the requirements set for the method.

This candidate method should then be validated to ensure its suitability for the intended purpose(s). The method validation should indicate that the candidate method complies with

the requirements, i.e., that the method is able to measure a given component with a suitable precision, trueness, detection limit, etc.

After validation, there are two possible outcomes (Fig. 21.1). A first is that the method performs acceptably and can be used routinely. Such a method is then regularly submitted to a quality control, to verify whether the method keeps performing acceptably in routine analysis. A second outcome is that the validation indicates that the method does not perform acceptably well. Then either the method is reoptimized or another method is selected. The aforementioned steps (Fig. 21.1) are then repeated until validation indicates that the new candidate method performs acceptably well.

During validation, some performance criteria are evaluated and documented. The requirements for these criteria are specified and then experimentally verified [1]. The characteristics possibly tested are the linearity, precision, trueness, detection limit, quantification limit, range, specificity, and robustness.

There are three golden rules for method validation, i.e., validate the whole method,

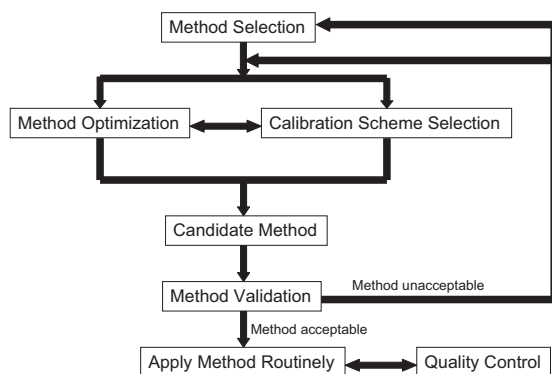


FIGURE 21.1 Different steps in the lifetime of an analytical method.

validate it over the range of concentrations, and validate it over the range of matrices [1].

In this chapter, first, some regulatory aspects concerning method validation are overviewed. Then, the different method validation items are discussed and illustrated with some examples. Finally, the application of an accuracy profile is discussed shortly.

21.2 Regulatory aspects

During validation, it is examined whether the method provides acceptable analytical results when measuring samples in the expected concentration range and matrices. For instance, drug substance, drug product, blood, plasma, urine, food, water, soil, organs, and air samples are possible matrices. Method validation is most elaborated and the requirements are most strict in pharmaceutical analysis, as can be seen further.

Different guidelines on validation, describing the requirements for analytical methods, for example, guidelines from the International Conference on Harmonisation of Technical Requirements for the Registration of Pharmaceuticals for Human Use (ICH) [2], the United States Food and Drug Administration (FDA) [3,4], Eurachem [5], the International Union of Pure and Applied Chemistry (IUPAC) [6,7], the European

Medicines Agency (EMA) [8], the International Organization for Standardization (ISO) [9], the Association of Official Analytical Chemists (AOAC) [10,11], the Société Française des Sciences et Techniques Pharmaceutiques (SFSTP) [12], and the European Commission [13] are available. These guidelines indicate which validation characteristics should be evaluated, e.g., linearity, precision (repeatability and time-different intermediate precision), trueness, specificity, limits of detection (LOD) and quantification (LOQ), range, and/or robustness, for a given type of method (see further). The requirements may slightly vary depending on the guideline considered. The FDA, for instance, recommends also evaluating the sample stability.

According to the ICH guidelines [2], which are adopted by the EMA [8], drug analysis methods can be divided into identification tests (qualitative methods), assays (quantitative methods), or tests for impurities (quantitative methods or limit tests) (Table 21.1a). The FDA [3,4] added specific test methods for the drug substance, excipient, or drug product, for instance, methods as particle size analysis, droplet distribution, spray pattern, and dissolution. Depending on the type of method, a number of characteristics need to be validated.

The AOAC guideline [10,11] divides the methods into identification tests, qualitative methods, and limit tests and quantitative methods for components with either a low or a high concentration (Table 21.1b).

21.3 Method validation items

As mentioned in the Introduction, one of the golden rules of method validation is to perform the validation over the entire concentration range. This means that the validation items, such as linearity, precision, accuracy and/or trueness, should be evaluated in that range. In this section, each item is briefly discussed and illustrated with some examples from the literature.

TABLE 21.1 Recommended (+) validation characteristics for different types of analytical methods, specified by: (a) different guidelines [2–4,8], and (b) the AOAC guidelines [10,11].

Type of analytical method					
(a) Validation characteristic	Identification test	Assay, dissolution, Content/Potency	Testing for impurities		
			Limit test	Quantitative method	Specific test
Linearity		+		+	
Precision					
Repeatability		+		+	(+)
Time-different intermediate precision		+		+	(+)
Accuracy		+		+	(+)
Specificity	+	+	+	+	(+)
Detection limit			+	(+)	
Quantification limit				+	
Range		+		+	
Robustness		+	(+)	+	(+)

Type of analytical method					
(b) Validation characteristic	Identification test or qualitative test	Component with a low concentration		Component with a high concentration	
		Limit test	Quantitative method	Limit test	Quantitative method
Linearity			+		+
Precision					
Repeatability			+	+	+
Time-different intermediate precision			+	+	+
Accuracy/Trueness			+	+	+
Specificity	+	+	+	+	+
Detection limit		+	+		(+)
Quantification limit			+		(+)
Range			+		+
Robustness			+		+

The examples discuss the validation of assays for finasteride in tablets [14] and antidepressants in pharmaceutical preparations [15] and in human urine [16]. Furthermore, validation is discussed for GC assays to determine 3,4-methylenedioxymethamphetamine and its metabolites in plasma and urine [17], estrogens and testosterone in human urine [18], free and total bisphenol A and B in human urine [19], sterol oxidation products in serum [20], cocaine and its metabolites in human primary cultured renal cells [21] and in hair [22], amphetamine-type stimulants and their metabolites in human urine [23], benzene in urine [24], the insecticide lufenuron in wheat flour [25], flumethrin in honey [26], pesticide residues in food samples [27], acrylamide in heat-processed starchy foods [28], phthalates in wine [29], and pesticides in vegetables [30,31], fruits [31], and baby food [31]. However, this list is not exhaustive.

Some reports [16,20,21] follow the ICH guidelines, one [23] the FDA guidelines, one [22] the SFSTP guidelines, one [27] the European Commission guidelines, and one [30] the Eurachem guidelines. Most reports, however, do not refer to any guideline.

21.3.1 Linearity

In different guidelines, **linearity** is defined as “a method’s ability to obtain test results proportional to the concentration of analyte in a sample” [2,5] and most often refers to the linearity of the calibration line. Most analytical techniques use some type of calibration scheme to estimate the (unknown) concentration of a given compound in a sample. Most often, a straight-line relationship between response and concentration is aimed at. Sometimes, a mathematical transformation is needed to obtain a linear relation [1]. After determining a straight-line model, its adequacy should be evaluated.

Commonly, calibration approaches are the classic calibration with or without internal standard (IS) and the standard addition, also with

or without IS. These approaches are discussed further. In GC, often the classic calibration with IS is used [14–23,29]. In Ref. [24], a classic approach with IS to quantify benzene in urine was compared with a standard addition approach with IS, and the latter was preferred because it allows compensation for differences in urinary matrices. Some publications [27,30] describe also the application of standard addition with IS as calibration scheme to correct for matrix effects. Rarely, classic [25,26] or standard addition calibration [28,31] without IS is applied in GC. These different approaches to assess linearity are discussed further.

21.3.1.1 Classic calibration

The simplest calibration procedure is the classic approach, in which a calibration line is constructed with standards of different concentrations. For each standard, a GC chromatogram is recorded and least-squares regression is used to establish a linear model between the dependent variable, the response, y , and the independent variable, the concentration, x , of a given compound [1]. Usually, the considered response in GC methods is the peak area of the component, $\text{Area}_{\text{component}}$. When sharp symmetrical Gaussian peaks are obtained, the peak height, $H_{\text{component}}$ might also be considered as a response.

However, most often in GC an IS is added to each standard and sample in order to correct for random errors, such as the variability in injection volume. The IS is added in a constant concentration at the start of the sample-pretreatment procedure. Consequently, the IS is subject to the same treatments as the component to be determined. The IS preferably should fulfill some requirements: have a structure similar to the component to be determined, not interfere with the component, be well separated from the other peaks, and have a signal of the same order of magnitude as the calibration standards. For each solution, a chromatogram is recorded and least-squares regression is used to estimate the linear model between the response, here the ratio

of the peak area of the component, $\text{Area}_{\text{component}}$ to that of the IS, Area_{IS} , i.e., $\text{Area}_{\text{component}}/\text{Area}_{\text{IS}}$, and the concentration of the given compound.

The true linear relation between the x and y variables is given by

$$\eta = \beta_0 + \beta_1 x \quad (21.1)$$

where η is the real dependent variable of which y is an estimate, and β_0 and β_1 are the unknown true intercept and slope of the calibration line. They are estimated by the intercept b_0 and the slope b_1 of the calibration line. The least-squares regression model of the calibration line is given as follows:

$$\hat{y} = b_0 + b_1 x \quad (21.2)$$

where \hat{y} is the response predicted by the model. The least-squares line minimizes the sum of the squared residuals, $\min \sum e_i^2$ [1]. For each point i of the calibration line, the residual e_i is

$$e_i = y_i - \hat{y} \quad (21.3)$$

where y_i is the measured response and \hat{y} the response predicted by the model.

For the sample(s), from the response y_{sample} , i.e., either $\text{Area}_{\text{component}}/\text{Area}_{\text{IS}}$ or $\text{Area}_{\text{component}}$ depending on whether or not an IS is used, and the estimated calibration line, the concentration of the component in the sample x_{sample} is determined as

$$x_{\text{sample}} = \frac{y_{\text{sample}} - b_0}{b_1} \quad (21.4)$$

21.3.1.2 Standard addition

In the standard addition method, the concentration of a component in a sample is determined by adding to aliquots of the sample, several known quantities of the component (C_{standard}). C_{standard} represents the added concentrations without taking into account the dilution. For example, the different standard addition solutions are prepared by adding to each “ s ” mL of the sample, each time “ t ” mL of a standard with a different concentration, C_{standard} .

The response for the different solutions is then measured and the standard addition calibration line calculated using least-squares regression. For GC, the response can again be either $\text{Area}_{\text{component}}/\text{Area}_{\text{IS}}$ or $\text{Area}_{\text{component}}$.

The response plotted as a function of C_{standard} is given in Fig. 21.2.

The concentration of the sample is then estimated as

$$C_{\text{sample}} = \frac{b_0}{b_1} \times \frac{V_{\text{standard}}}{V_{\text{sample}}} \quad (21.5)$$

Standard addition approaches are often used in spectroscopic methods to correct for matrix interferences. In GC methods, they are applied to correct for matrix-induced response enhancement [32]. This enhancement occurs when the chromatographic response of a compound in a matrix is larger than that of the same compound with the same concentration in a matrix-free solution. Matrix-induced response enhancement often occurs, for instance, in the analysis of pesticide residues. Ref. [32] provides a table with compounds typically susceptible to matrix enhancement. Different correction methods, including standard addition, are suggested [32]. Standard addition will usually be applied when only a few samples are to be analyzed, because of its elaborate and time-consuming procedure for each individual sample.

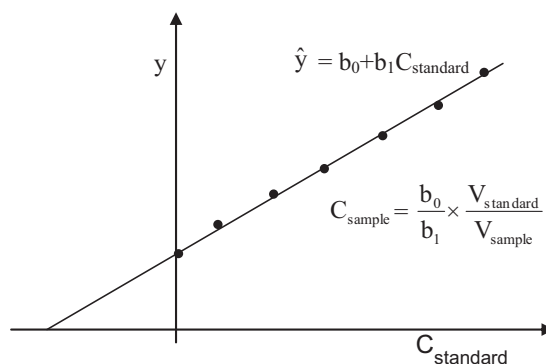


FIGURE 21.2 Standard addition approach.

21.3.1.3 Assessment of linearity

To assess the linearity of the calibration line, i.e., to evaluate whether a straight line model fits the experimental results, a number of standards, usually at least 5 [2] or 6 [5,6], covering the expected concentration range, are prepared. After determining the signal for each standard, the calibration line (intercept and slope) is estimated with least-squares regression. In order to properly apply least-squares modeling, two requirements should be fulfilled: (i) the x values are exactly known, i.e., errors in x are considered negligible, and errors occur only in the responses, and (ii) the measurements are homoscedastic, i.e., the responses at the different concentrations have a constant variance, independent of x . The latter can be verified statistically using a Cochran's test or graphically by evaluating a residual plot [1]. A Cochran's test compares n variances s_i^2 , each based on n_k replicates, by calculating $C = \frac{s_{\max}^2}{\sum_{i=1}^n s_i^2}$, with s_{\max}^2 being the maximal variance, and comparing C to a tabulated value $C_{\text{tab}}(\alpha, n_k, n)$ at a given significance level α , usually $\alpha = 0.05$. When $C > C_{\text{tab}}$, the variances are considered heteroscedastic, otherwise homoscedastic.

A residual plot shows the residuals of the calibration standards, e_i , as a function of their concentrations, x_i . For homoscedastic data, the residuals are randomly distributed, while for heteroscedastic data, they show a trend, i.e., they increase in absolute value with increasing concentration. For heteroscedastic data, either a data transformation (e.g., a square root or log transformation)

can be applied to obtain constant variances or weighted least-squares regression can be used to estimate the coefficients of the calibration line [1]. In the latter regression, a higher weight is assigned to the standards with a small variance and a lower weight to those with a high variance.

To assess linearity, the data are plotted and their linearity is first inspected visually to check for outliers or a deviation from the straight-line behaviour. Outliers may also be observed graphically by evaluating a residual plot. They further can be detected with statistical diagnostics, such as the evaluation of the standardized residuals, Cook's squared distance, the Mahalanobis distance, or the leverage measure, or with robust methods, such as the single median method, the repeated median method, or the least median of squares method [1].

The adequacy of the straight-line model can be verified statistically using either an analysis of variance (ANOVA) lack-of-fit (LOF) test or a test for the significance of the quadratic coefficient b_2 in a second-order model fitted to the data [1,6]. The LOF test requires replicate measurements. The total residual sum of squares (SS), SS_R , is split into the SS due to LOF to the applied model, SS_{LOF} , and the SS due to the pure experimental error, SS_{PE} (Table 21.2). By dividing these SS values by their corresponding number of degrees of freedom (df), the corresponding mean squares (MS) are obtained, MS_{LOF} and MS_{PE} . The LOF test is a one-sided F -test at significance level α , often $\alpha = 0.05$, to compare MS_{LOF} and MS_{PE} , i.e., $F = \frac{MS_{\text{LOF}}}{MS_{\text{PE}}} \leftrightarrow F_{\text{tab}}(\alpha; df_{\text{LOF}}, df_{\text{PE}})$.

TABLE 21.2 ANOVA lack-of fit test.

Source of variation	Sum of squares (SS)	Degrees of freedom (df)	Mean squares (MS)	F-value
Residual	$SS_R = SS_{\text{LOF}} + SS_{\text{PE}}$	$n_{\text{Tot}} - 2$	$MS_R = \frac{SS_R}{df_R}$	
Lack of fit	$SS_{\text{LOF}} = \sum_i^k n_i (\bar{y}_i - \hat{y}_i)^2$	$k - 2$	$MS_{\text{LOF}} = \frac{SS_{\text{LOF}}}{df_{\text{LOF}}}$	$F = \frac{MS_{\text{LOF}}}{MS_{\text{PE}}}$
Pure error	$SS_{\text{PE}} = \sum_i^k \sum_j^{n_i} (y_{ij} - \bar{y}_i)^2$	$n_{\text{Tot}} - k$	$MS_{\text{PE}} = \frac{SS_{\text{PE}}}{df_{\text{PE}}}$	

y_{ij} = one of the n_i replicate measurements at x_i , $\sum_{i=1}^k n_i = n_{\text{Tot}}$ = total number of observations, k = number of different x values (including the blank), \bar{y}_i = average of the replicates y_{ij} at x_i , \hat{y}_i = predicted value of y at x_i , and \bar{y} = average of all observations [1].

If the variance (MS) due to LOF is found to be significantly larger than that due to experimental error, the straight-line model is considered to be inadequate to describe the data. If the variance due to LOF is not significantly larger, the straight-line model is considered adequate.

An alternative approach to verify linearity of the data, for example, when no replicate measurements are available, is to fit a second-order polynomial model, $y = b_0 + b_1x + b_2x^2$, to the data and to test the significance of the quadratic coefficient b_2 by means of the 95% two-sided confidence interval (CI) around β_2 (Eq. 21.6) or by means of a two-sided t -test (Eq. 21.7) [6].

$$95\%CI_{\beta_2} = b_2 \pm t_{\text{tab}(\alpha, \text{df} = n-3)} s_{b_2} \quad (21.6)$$

$$|t| = \frac{|b_2|}{|s_{b_2}|} \leftrightarrow t_{\text{tab}(\alpha, \text{df} = n-3)} \quad (21.7)$$

Where s_{b_2} is the standard deviation of b_2 (and obtained from the variance–covariance matrix of the regression coefficients) and t_{tab} the tabulated t -value, at the significance level α , usually $\alpha = 0.05$, and the number of degrees of freedom, $n - 3$, with n being the number of calibration standards, including the blank. When zero is not included in the 95% CI or when $|t| \geq t_{\text{tab}}$, then b_2 is significantly different from zero and the linear model is considered inadequate. Otherwise, the linear model is considered appropriate. However, this latter conclusion is not always correct. Indeed, a quadratic coefficient that is not significantly different from zero means that the quadratic model does not fit the data better than the straight line. However, this does not imply that there is no LOF from the straight-line model.

In the literature, linearity is often verified visually [14–31]. The statistical ANOVA LOF test was used in Refs. [26,27]. Although the correlation or determination coefficient is not appropriate to evaluate linearity [1,6], many authors still report it as a proof of linearity.

The **range**, i.e., the concentration interval in which the method possesses acceptable linearity, precision, and trueness [2–4], was determined in Ref. [14–31].

21.3.2 Limits of detection and quantification

The **limit of detection (LOD)** of an analytical procedure is defined by the ICH as “the lowest amount of analyte in a sample that can be detected but not necessarily quantitated as an exact value” [2]. ICH also states that the **limit of quantification (LOQ)** of an analytical procedure is “the lowest amount of analyte in a sample which can be quantitatively determined with suitable precision and accuracy” [2]. In fact, this definition corresponds to the lower limit of quantification (LLOQ). Besides LLOQ, also an upper limit of quantification (ULOQ) exists, which can be defined as the highest concentration of a compound that can be quantified with an acceptable precision and accuracy, applying the calibration line. According to the ICH and IUPAC guidelines [2,6,7], the LOD and LOQ can be determined from the standard deviation of replicated measurements of the blank and the slope of the calibration line:

$$L_d = \mu_{\text{bl}} + k'_d \sigma_{\text{bl}} \text{ with } k'_d = k_c + k_d \quad (21.8)$$

$$X_d = (L_d - \mu_{\text{bl}})/b_1 = k'_d \sigma_{\text{bl}}/b_1 \quad (21.9)$$

$$L_q = (\mu_{\text{bl}}) + k_q \sigma_{\text{bl}} \quad (21.10)$$

$$X_q = (L_q - \mu_{\text{bl}})/b_1 = k_q \sigma_{\text{bl}}/b_1 \quad (21.11)$$

where L_d and X_d are the LOD, expressed as response/signal and as concentration, respectively. L_q and X_q are the corresponding limits of quantification. μ_{bl} and σ_{bl} are the true response and the standard deviation of the blank, and b_1 is the slope of the calibration line. μ_{bl} and σ_{bl} are estimated experimentally as \bar{y}_{bl} and s_{bl} , respectively, often determined from 6 [6] or 10 [5] blank measurements (see further).

The multiplication factors k_c , k_d , k'_d , and k_q are constants and their values determine the risk of making a wrong decision. Two types of wrong decisions are distinguished, i.e., false-positive decisions related to the type I or α -error and false-negative decisions related to the type II or β -error. For $\alpha = \beta = 5\%$, $k_c = k_d = 1.645$, and $k'_d = 3.29$. With $k_q = 10$, one expects at the quantification limit a precision, expressed as relative error, of 10% [7].

To ensure realistic LOD and LOQ estimates, it is of the utmost importance to select an appropriate blank [1]. For example, an analytical blank, containing all reagents and analyzed in the same way as the samples, can be considered appropriate. Ideally, a matrix blank, having exactly the same composition as the sample except for the compound to be analyzed, is used. In the absence of an appropriate blank, a standard with a low concentration near the expected LOD can also be used. Alternatively, the residual standard deviation of the calibration

line, $s_e = \sqrt{\frac{\sum (y_i - \hat{y}_i)^2}{n-2}}$, or the standard deviation

of the intercept of the calibration line, $s_{b_0} = s_e \sqrt{\frac{\sum x_i^2}{n \sum (x_i - \bar{x})^2}}$, can also be used as estimates of

σ_{bl} in the estimation of LOD and LOQ. The average blank response, \bar{y}_{bl} , is then replaced by the intercept of the calibration line. The aforementioned approach (Eqs. 21.8–21.11) was used in GC to estimate LOD in Ref. [15,16,29] and LOQ in Ref. [15,16].

The SFSTP guidelines [12] suggest an alternative approach to estimate LOD and LOQ for chromatographic methods. A matrix blank is injected and the maximum amplitude, h_{max} , in the chromatogram is determined over a distance equal to 20 times the width at half height of the peak of the compound, around its retention time. LOD is then defined equal to $3 h_{max}R$ and LOQ to $10 h_{max}R$, with R the response factor, i.e., the component concentration/peak height (C/H) ratio.

LOD and LOQ can also be determined based on the signal-to-noise ratio, $S/N = \frac{2H}{h_{max}}$, where

H is the height of a low concentration standard [2,33,34]. A concentration corresponding to an S/N ratio of 3 is then considered the LOD, and one with an S/N ratio of 10 the LOQ. The thus-obtained LOD and LOQ values are half of those estimated according to the SFSTP guidelines and are therefore more optimistic estimations. The estimated LOD and, certainly, LOQ values need to be confirmed experimentally.

However, these latter approaches can only be applied to analytical procedures that exhibit baseline noise, such as chromatographic methods. Moreover, this approach is only appropriate when the baseline noise is obtained from the injection of an appropriate blank sample, for example, a matrix blank. If the baseline noise is determined in a region where no peaks elute from the injection of a standard or a sample (which often is done), it is assumed and should be verified that the baseline noise is constant over the entire chromatogram.

No GC example that applied the SFSTP procedure was found. The S/N ratio procedure was used in Refs. [14,17,21,26,28,30] to estimate both LOD and LOQ and in Refs. [18,19,22,25,29] for LOD. However, none of the papers specified how the baseline noise was estimated.

In [22,23,25], LOQ was determined as the lowest point of the calibration line with adequate precision (e.g., %RSD_{repeatability} <15% [22] or <20% [23], and %RSD_{intermediate precision} <25% [22]) and trueness (e.g., %recovery = 100% ± 20% [22,23]).

21.3.3 Precision

The **precision** of an analytical method “expresses the closeness of agreement (degree of scatter) between a series of measurements obtained from multiple sampling of the same homogeneous sample under the prescribed conditions” [2]. Precision is related to random errors [1]. According to the ICH, FDA, Eurachem, ISO, and AOAC guidelines [2–5,9,11], precision comprises repeatability, intermediate precision, and reproducibility,

depending on the conditions for the repeated experiments. Repeatability is the precision estimated under the most optimal operating conditions (same testing material, same laboratory, same analyst, same instrument, and short time interval, e.g., same day). Reproducibility is the precision estimate obtained under the most diverse operating conditions (same testing material, different laboratories, different analysts, different instruments, and different days) and is only to be determined when different laboratories are involved in the routine analysis. Between both extreme operating conditions, intermediate precision conditions may be considered. These result in the precision estimated in the same laboratory, but where larger time intervals (different days), different analysts, and/or different instruments are considered. The M -factor intermediate precision is defined by ISO [9], where M refers to the number of factors (time, analyst, or equipment) that differs ($M = 1, 2, \text{ or } 3$). It is recommended to estimate always the time-different intermediate precision.

The precision can be expressed as a standard deviation s , variance s^2 , or percentage relative standard deviation %RSD. It was reported as s in Ref. [14,17,18,21,25] and as %RSD in Refs. [14–27]. To estimate the repeatability, time-different intermediate precision, or reproducibility, a number of samples covering the entire range of concentrations and matrices are replicatedly measured under the specified circumstances. Repeatability was assessed in Ref. [14–30] and time-different intermediate precision in Ref. [14–24,26,28,29]. When possible, the samples should be real homogeneous samples. If this is not possible, artificial samples can be used [2]. The precision is estimated for each concentration and then it is evaluated whether a mathematical relation exists between the standard deviation (as precision estimate) and the concentration. Such relation allows estimating the precision for concentrations intermediate to those tested [9].

The ICH guidelines advise using an experimental design approach (full-factorial design) to simultaneously determine the repeatability and time-different intermediate precision [2]. In this approach, n replicates (e.g., $n = 2$) are analyzed during P days (e.g., $P = 6$, often $5 \leq P \leq 8$) at each concentration level [1]. Then, ANOVA is used to estimate the variance components, i.e., the repeatability, s_r , and the between-days variance, s_{between}^2 , at each concentration level. The time-different intermediate precision is then estimated as $s_{\text{I(t)}}^2 = s_r^2 + s_{\text{between}}^2$. However, no GC examples were found applying this approach.

21.3.4 Trueness

The **trueness** is “the closeness of agreement between an average value from a number of test results and the accepted reference value” and is only related to systematic errors [5–9,11]. Two types of systematic errors can be distinguished. The first type is a constant or absolute systematic error, which does not depend on the reference value. The second type is a proportional or relative systematic error, which is proportional to the reference value. To evaluate trueness, parameters, such as $\text{bias} = \bar{x} - \mu_0$, $\% \text{bias} = \frac{\bar{x} - \mu_0}{\mu_0} \times 100\%$, and $\% \text{recovery} = \frac{\bar{x}}{\mu_0} \times 100\%$, can be used, with \bar{x} the average value and μ_0 the accepted reference value.

To estimate the trueness, different setups can be applied, depending on the concentration range to be evaluated, on the availability of reference material, on the availability of blank material that can be spiked with the compound to be determined, on the possibility to reconstitute the sample, or on the possibility to add the compound in a representative way to the sample [1].

When blank matrix, which can be spiked with known amounts of the compound, is available or when the sample can be reconstituted, the following approaches may be used. In the examined concentration range, a number of replicates

is measured at each concentration tested. At each level, a t -test is performed to compare the average measured concentration, \bar{x} , with the true concentration, μ_0 . This procedure can be applied when at the most 3 or 4 levels are evaluated [1]. When more levels are examined, two options are possible: either the multiple t -tests with the Bonferroni correction (i.e., a correction where α and thus t_{tab} are adapted depending on the number of t -tests considered) are performed or a regression analysis relating the measured to the known concentrations is performed, where equality of slope to 1 and of intercept to 0 are tested [1].

For GC analysis, to evaluate the trueness, spiking of placebos of pharmaceutical formulations [15], urine [16–18,23,24], plasma [17], renal cells [21], hair [22], wheat flour [25], blank honey [26], and synthetic wine [29], with different concentrations of the compound(s) to be analyzed, was performed. In none of the studies t -tests or a regression approach was applied to statistically evaluate the trueness. The trueness was simply evaluated by calculating and reporting the parameters %bias [18,23,24] and %recovery [14–17,21–23,25,26,29].

When a blank matrix is not available, but when representative addition of the compound to the sample is possible, one can proceed as follows. In the evaluated concentration range, a one-point standard addition is performed at each concentration level. At each level, a t -test is performed to compare the absolute difference between the average concentrations measured after and before the addition, $|\bar{x}_2 - \bar{x}_1|$, with the known added concentration. This procedure may be applied, provided that at the most 3 or 4 levels are considered [1]. With more levels, the two aforementioned options again are possible: the t -tests with the Bonferroni correction or a regression analysis [1].

In [28], the trueness was evaluated using a one-point standard addition at only one concentration level for each of four food matrices, and the parameter %recovery was reported.

21.3.5 Specificity

The **specificity** is “the ability of a method to assess unequivocally the analyte in the presence of components which may be expected to be present, such as e.g., impurities, degradants, matrix, etc” [2]. If one analytical method is insufficient to indicate method specificity, the lack of specificity may be illustrated using other supporting analytical methods [1–5].

Specificity in GC was evaluated in Refs. [14,15,17,18,20,21,23,25,26] by analyzing possible interfering substances, potentially occurring in blank plasma or urine or in the sample matrix in general. In fact, the compound(s) to be determined should not coelute or overlap with other substances occurring in the samples.

21.3.6 Robustness

Robustness is sometimes also called **ruggedness**. Several definitions are available. Some only use the term ruggedness [10], some distinguish between robustness and ruggedness [34], while others consider them synonyms [2–4]. Youden and Steiner [10] used the term **ruggedness** test for a setup in which the influences of minor but deliberate and controlled changes in the method parameters or factors are evaluated, applying an experimental design, in order to detect nonrobust factors. In the United States Pharmacopeia (USP) [34], ruggedness is defined as “The **ruggedness** of an analytical method is the degree of reproducibility of test results obtained by the analysis of the same sample under a variety of normal test conditions, such as different laboratories, different analysts, different instruments, different lots of reagents, different elapsed assay times, different assay temperatures, different days, etc.” In this approach, no deliberate changes in method parameters are introduced and the method is executed under different test conditions. This definition is equivalent to that of intermediate precision or reproducibility, depending on

whether or not the test is performed in one laboratory. Detailed ISO guidelines exist for these precision estimates [9].

The USP definition of robustness is the same as that of the ICH [2], i.e., “*The robustness of an analytical procedure is a measure of its capacity to remain unaffected by small, but deliberate variations in method parameters and provides an indication of its reliability during normal usage*”. This definition is most widely applied for robustness and similar to the “older” ruggedness definition of [10].

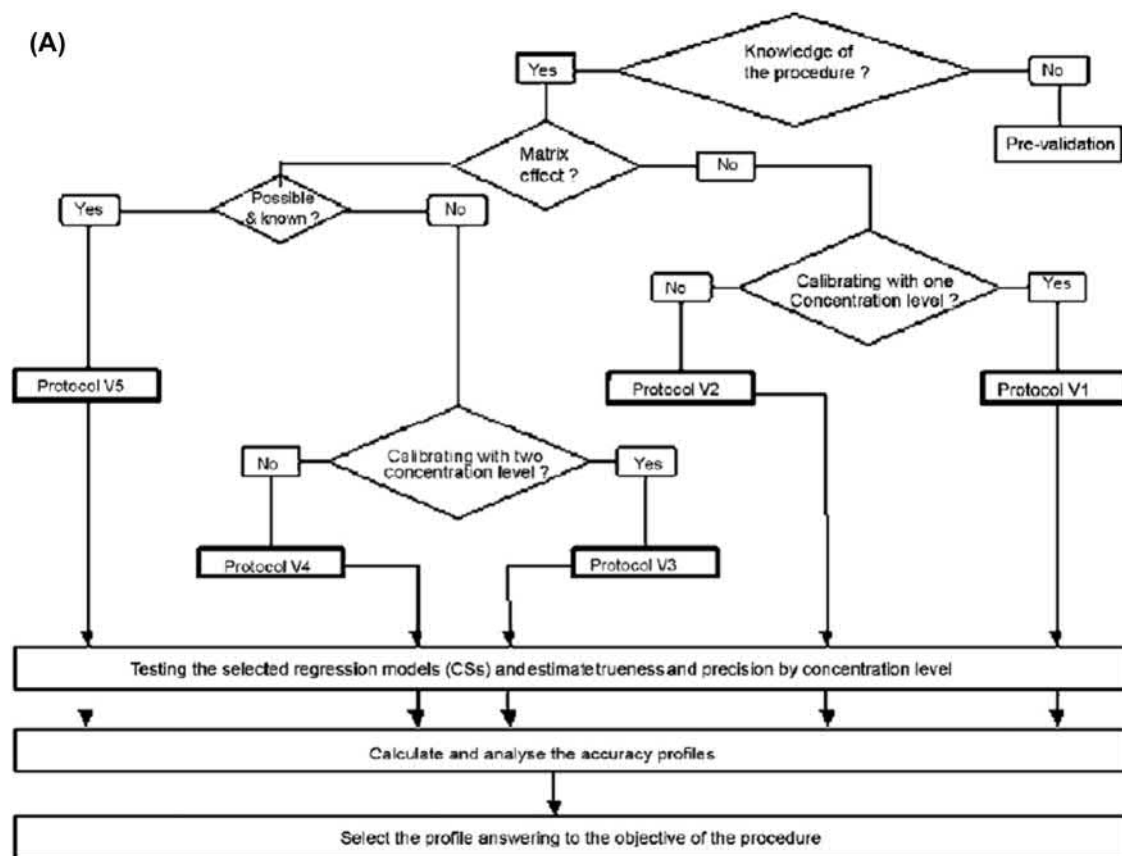
A robustness test is an experimental setup applied to evaluate the robustness of the method. It is an intralaboratory approach, simulating the potential changes in factors when a method is transferred to different instruments or different laboratories, to evaluate their effects on the responses of the method. Although robustness tests are not mandatory in the ICH guidelines [2], they are demanded by the FDA for the registration of drugs in the United States of America [3,4]. Robustness can be evaluated using a one-variable-at-a-time (OVAT) approach. In Ref. [14], an OVAT procedure in GC analysis was used to examine the effects of injector-, detector-, initial oven-, and final oven temperatures and injection volume on the finasteride concentration in tablets. No significant effect was found on the results, and the method was considered robust. However, an OVAT approach is not recommended [35,36].

More appropriate is to apply a multivariate approach, i.e., by using an experimental design. Such robustness tests were performed on GC assays to determine antidepressants in pharmaceutical preparations [15] or in human urine [16]. Examined factors were column head pressure, injector temperature, time and temperature of the splitless step, detector temperature, oven temperature programs, voltage of the MS detector, steps of the SPE procedure, SPE cartridge lots, time (days), and analysts. Examined responses were peak resolutions, efficacy (expressed as plate count N), and relative peak areas of compounds. However, the most

important responses to examine should be related to the content or concentration of the compound(s), since one is dealing with method validation. In Ref. [15], a reflected two-level Plackett–Burman (PB) design was executed to examine the effects of seven factors at three levels in 15 experiments. The significance of factor effects was determined by comparing, for each response, the main factor effects with an error estimate, according to the procedure described in Ref. [10]. Graphically, bar plots were drawn. In Ref. [16], a PB design was executed to examine the effects of 11 factors at two levels in 12 experiments. Graphically, plots of the ranked factor effects were drawn.

21.3.7 Sample stability

Some GC assays [15,17,18,23,24,26,27] also examine the sample **stability**, which is required by the FDA [3,4]. In Refs. [15], the stability of standard solutions and of spiked placebo solutions stored in darkness at 4°C was verified over time by comparing the response factors or relative peak areas, respectively, with those of the corresponding freshly prepared solutions. In Ref. [17], the stability of spiked matrix solutions at 4°C was evaluated as a function of time. In another report [18], the stability of the composition of a mixture of standard compounds was tested by measuring the mixture before and after the urinary work-up and comparing the results. A freeze–thaw (freezing during 24 h at –20°C and thawing at room temperature), a short-term (8 h at room temperature), and a long-term (3–6 months at –20°C) stability study of spiked samples was performed in Ref. [23]. The influence of freezing and thawing on the stability of spiked samples was also evaluated in Ref. [24]. Zhou et al. [26] evaluated the stability of stock solutions after 12 h at room temperature, after 4 weeks at 4°C, and after 2 months at –18°C. A long-term stability study was also performed in Ref. [27] to evaluate the stability of the calibration solutions.



(B)

Standards	Concentration levels	PROTOCOL				
		V1	V2	V3	V4	V5
CSs without matrix	Low		2		2	
	Mid	2	(2) ^a		(2) ^a	
	High	(2) ^b	2	(2) ^b	2	
CSs within matrix	Low				2	2
	Mid				(2) ^a	(2) ^a
	High			(2) ^b	2	2
	Additional					(2) ^c
VSs within matrix	Low	3	3	3	3	3
	Mid	3	3	3	3	3
	High	3	3	3	3	3
Minimum number of series		3	3	3	3	3
Total number of experiments (minimum)		33	45	39	63	45

^a Considering the regression model selected (ex.: simple regression line), the possible suppression of the mid range concentration level depending on the regression model considered to express the response function (for example: model as the simple regression line). In this case, there are 39 experiments for the protocols V2 (without matrix) and V5 (within matrix). There are 51 experiments for the protocol V4.

^b Selection of a concentration level higher than the target concentration in order to calibrate (for example: 120% of target concentration).

^c Addition of a concentration level for a more complex response function (for example: 4-parameter logistic regression).

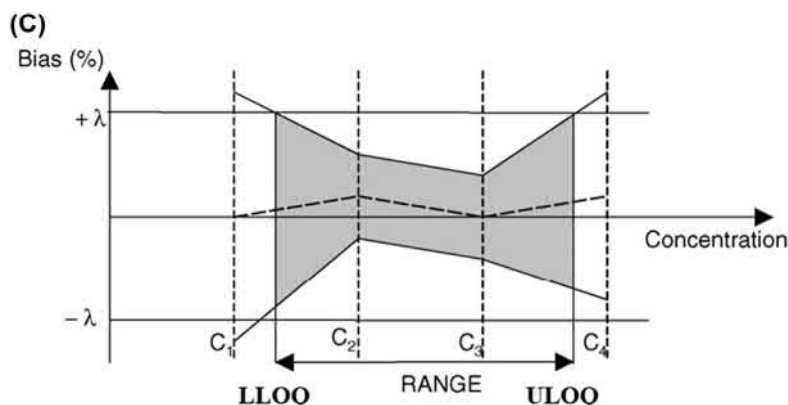


FIGURE 21.3 Determining accuracy profiles: (A) decision tree to select a validation protocol, (B) validation protocols, and (C) accuracy profile (grey area describing the range in which the procedure is able to quantify with a known accuracy and a risk a priori fixed by the analyst). λ = acceptance limit, LLOQ = lower limit of quantification, and ULOQ = upper limit of quantification. Reproduced with permission from Ref. [37,38].

21.4 Accuracy profiles

Method validation is most often performed as described in Section 21.3. However, the parameters and approaches described there are used for a diagnostic purpose, e.g., the trueness and precision parameters are individually estimated and evaluated.

An alternative approach consists of determining accuracy profiles. An accuracy profile is a visualization that allows determining the **method capability**. Such profiles are based on two-sided β -expectation tolerance intervals of validation standards for the measurement of the total error, i.e., including both bias and precision. They are developed in Refs. [37–39]. This statistical tool is used for decision purposes. The use of this approach reduces the risks of accepting an unsuitable assay or to reject a suitable one. In Ref. [37], method validation is critically reviewed in order to develop a more harmonized approach. In Ref. [38], several experimental protocols are proposed, presenting the types of calibration and validation standards, the concentration levels to use, the number of replicates, and the number of series to be performed. A decision tree (Fig. 21.3A) is presented to allow

selecting a suitable protocol (Fig. 21.3B) needed to obtain all required information to demonstrate the reliability of the method. In Ref. [39], the statistical methodology used to produce the accuracy profiles (Fig. 21.3C) is described.

References

- [1] D.L. Massart, B.G.M. Vandeginste, L.M.C. Buydens, S. De Jong, P.J. Lewi, J. Smeyers-Verbeke, *Handbook of Chemometrics and Qualimetrics: Part A*, Elsevier, Amsterdam, 1997.
- [2] Guidelines Prepared within the International Conference on Harmonisation of Technical Requirements for the Registration of Pharmaceuticals for Human Use (ICH), *Validation of Analytical Procedures: Text and Methodology, Q2(R1)*, 2005, pp. 1–13. <http://www.ich.org/>. (Accessed 18 May 2020).
- [3] Food and Drug Administration (FDA), Department of health and human services. *Analytical Procedures and Methods Validation for Drugs and Biologics, Guidance for Industry*, 2015. <http://www.fda.gov/>. (Accessed 18 May 2020).
- [4] Food and Drug Administration (FDA), Department of health and human services, *bioanalytical method validation, Guidance for Industry*, 2018. <http://www.fda.gov/>. (Accessed 18 May 2020).
- [5] Eurachem, *The Fitness for Purpose of Analytical Methods: A Laboratory Guide to Method Validation and Related Topics*, Second Edition, 2014. (Accessed 18 May 2020).

- [6] M. Thompson, S.L.R. Ellison, R. Wood, Harmonized guidelines for single laboratory validation of methods of analysis, *International Union of Pure and Applied Chemistry (IUPAC), Pure Appl. Chem.* 74 (2002) 835–855.
- [7] L.A. Currie, Nomenclature in evaluation of analytical methods including detection and quantification capabilities, *Pure Appl. Chem.* 67 (1995) 1699–1723.
- [8] The European Medicines Agency, Note for Guidance on Validation of Analytical Procedures: Text and Methodology, 1995. CPMP/ICH/381/95, <http://www.ema.europa.eu/>. (Accessed 18 May 2020).
- [9] International Organization for Standardization (ISO), Statistical methods for quality control. vol. 2, fourth ed., Accuracy (trueness and precision) of measurement methods and results – part 1–6, ISO 1994(E), 5725 – 1 till 6, <http://www.iso.org/> accessed on 18. 05. 2020.
- [10] W.J. Youden, E.H. Steiner, *Statistical Manual of the Association of Official Analytical Chemists*, The Association of Official Analytical Chemists, Arlington, 1975.
- [11] Association of Official Analytical Chemists, How to Meet ISO 17025 Requirements for Method Verification, 2007, pp. 1–18. <http://www.aoc.org/>. (Accessed 18 May 2020).
- [12] Commission Société Française des Sciences, et al., Techniques Pharmaceutiques (SFSTP), Guide de validation analytique, Rapport d'une commission SFSTP I Méthodologie, *STP Pharma Prat.* 2 (1992) 205–226.
- [13] European Commission, Guidance Document on Analytical Quality Control and Method Validation Procedures for Pesticide Residues and Analysis in Food and Feed, 2017. SANTE/11813/2017, https://ec.europa.eu/food/sites/food/files/plant/docs/pesticides_mrl_guidelines_wrkdoc_2017-11813.pdf. (Accessed 18 May 2020).
- [14] S. Sağlık, S. Tatar Ulu, *Anal. Biochem.* 352 (2006) 260–264.
- [15] J.J. Berzas, C. Guiberteau, M.J. Villaseñor, V. Rodríguez, *Anal. Chim. Acta* 519 (2004) 219–230.
- [16] J.J. Berzas Nevado, M.J. Villaseñor Llerena, C. Guiberteau Cabanillas, V. Rodríguez Robledo, *J. Chromatogr. A* 1123 (2006) 130–133.
- [17] D. Gomes da Silva, P. Guedes de Pinho, H. Pontes, L. Ferreira, P. Branco, F. Remião, et al., *J. Chromatogr. B* 878 (2010) 815–822.
- [18] P. Hoffmann, M.F. Hartmann, T. Remer, K.-P. Zimmer, S.A. Wudy, *Steroids* 75 (2010) 1067–1074.
- [19] S.C. Cunha, J.O. Fernandes, *Talanta* 83 (2010) 117–125.
- [20] M. Menéndez-Carreño, C. García-Herreros, I. Astiasarán, D. Ansorena, *J. Chromatogr. B* 864 (2008) 61–68.
- [21] M. João Valente, F. Carvalho, M. Lourdes Bastos, M. Carvalho, P. Guedes de Pinho, *J. Chromatogr. B* 878 (2010) 3083–3088.
- [22] E. Cognard, S. Rudaz, S. Bouchonnet, C. Staub, *J. Chromatogr. B* 826 (2005) 17–25.
- [23] W.A. Wan Raihana, S.H. Gan, S.C. Tan, *J. Chromatogr. B* 879 (2011) 8–16.
- [24] P. Basilicata, N. Miraglia, M. Pieri, A. Acampora, L. Soleo, N. Sannolo, *J. Chromatogr. B* 818 (2005) 293–299.
- [25] K.C. Ahire, M.S. Arora, S.N. Mukherjee, *J. Chromatogr. B* 861 (2008) 16–21.
- [26] J. Zhou, X. Xue, Y. Li, J. Zhang, L. Wu, L. Chen, J. Zhao, *J. Separ. Sci.* 30 (2007) 1912–1919.
- [27] A. Garrido Frenich, J.L. Martínez Vidal, J.L. Fernández Moreno, R. Romero-González, *J. Chromatogr. A* 1216 (2009) 4798–4808.
- [28] Y. Zhu, G. Li, Y. Duan, S. Chen, C. Zhang, Y. Li, *Food Chem.* 109 (2008) 899–908.
- [29] J.D. Carrillo, M.P. Martínez, M.T. Tena, *J. Chromatogr. A* 1181 (2008) 125–130.
- [30] A. Garrido Frenich, M.J. González-Rodríguez, F.J. Arrebola, J.L. Martínez Vidal, *Anal. Chem.* 77 (2005) 4640–4648.
- [31] P. Sandra, B. Tienpont, F. David, *J. Chromatogr. A* 1000 (2003) 299–309.
- [32] C.F. Poole, *J. Chromatogr. A* 1158 (2007) 241–250.
- [33] *European Pharmacopoeia 6.2*, Council of Europe, Strasbourg, France, 2008.
- [34] *United States Pharmacopoeia 30*, National Formulary 25, General Chapter 1225, Validation of Compendial Methods, The United States Pharmacopoeial Convention, Rockville, Maryland, USA, 2007.
- [35] B. Dejaegher, Y. Vander Heyden, *J. Chromatogr. A* 1158 (2007) 138–157.
- [36] B. Dejaegher, A. Durand, Y. Vander Heyden, Experimental design in method optimization and robustness testing, in: G. Hanrahan, F.A. Gomez (Eds.), *Chemometric Methods in Capillary Electrophoresis*, Chapter 2, John Wiley & Sons, New Jersey, 2010, pp. 11–74.
- [37] P. Hubert, J.-J. Nguyen-Huu, B. Boulanger, E. Chapuzet, P. Chiap, N. Cohen, et al., *J. Pharmaceut. Biomed. Anal.* 36 (2004) 579–586.
- [38] P. Hubert, J.J. Nguyen-Huu, B. Boulanger, E. Chapuzet, P. Chiap, N. Cohen, et al., *J. Pharmaceut. Biomed. Anal.* 45 (2007) 70–81.
- [39] P. Hubert, J.-J. Nguyen-Huu, B. Boulanger, E. Chapuzet, N. Cohen, P.-A. Compagnon, et al., *J. Pharmaceut. Biomed. Anal.* 45 (2007) 82–96.

Physicochemical measurements (inverse gas chromatography)

Adam Voelkel

Institute of Chemical Technology and Engineering, Poznan University of Technology, Poznań, Poland

22.1 Introduction

During last 40–50 years, inverse gas chromatography (IGC) has become widely used, popular, and a fruitful technique for physicochemical characterization of various materials, as well as the description of interactions between components in various systems. Several reviews of the theoretical background, parameters, interpretation of experimental data, and application are available [1–8]. Therefore, the basic information of IGC “standard” parameters will be reduced here to the necessary minimum. The author intends to focus on the interpretation of the most often used characteristics, error analysis, comparison of IGC results with those achieved using other techniques, as well as the most interesting applications.

The newcomers to this field will learn that IGC “was born” in the early stage of the gas chromatography. The first published papers were connected with activity of catalysts and various adsorbents [9–11]. These activities were soon called inverse gas chromatography and then extended to the examination of polymers, polymer blends, minerals, and other materials.

The characteristic feature of an IGC experiment is the location of the examined material in the column. It performs the role of the stationary phase. Its properties influence the retention of carefully selected test solutes. Retention data (retention time, net retention volume, specific retention volume) are further converted into the parameters describing the required property of the examined substance.

At the end of the second decade of 21st century, two statements concerning IGC should be noted: i) it is possible to work at finite concentration of test solutes—FC-IGC or in the region of infinite dilution ID-IGC; and ii) retention of the test solute may be the result of a pure adsorption equilibrium or mixed retention mechanism, e.g., bulk sorption and adsorption on existing interfaces. The first mechanism is obvious during the examination of solid materials (adsorbents, fibers, polymers below T_g), while the second might be important when polymer (above T_g), polymer blends, or oils are characterized.

IGC experiments can also be carried out using pulse or frontal techniques. In the pulse mode, a given amount of the test solute is injected into the stream of carrier gas (mobile phase) and

transported through a column filled with the stationary phase (examined material). In the frontal technique the test solute is continuously added to the mobile phase, leading to the formation of a breakthrough curve. The use of the pulse technique is suggested for systems where the equilibrium is quickly established. This is common when interactions between the test solute and examined material are relatively weak. For systems of "slow" equilibrium the frontal mode is generally used [4].

The first important step in the development of an IGC investigation is to establish the experimental conditions: temperature, carrier gas flow rate, humidity of the carrier gas, sample amount (examined material), sample preparation. The temperature of the IGC experiment might be imposed either by the interest of the researcher or by the properties of the examined material. During the investigation of polymer systems, it is not unusual for a phase transition to occur within the temperature range of the IGC experiment [12]. In such a case, the $\log V_g$ vs. $1/T$ plot will include the region of the phase transition. The researcher should carefully adopt the appropriate model for transformation of the experimental data (retention parameter of the test solutes) into the required physicochemical parameter. An inappropriate model will lead, of course, to vague values of the characteristic parameter and inconclusive results. The carrier gas flow rate should be individually established and optimized by using the van Deemter equation [4]. If the flow rate is too low, the time required for the experiment will increase, broad peaks are obtained, and the retention data will be less precise. Too high a flow rate may prevent the establishment of local equilibrium assumed in IGC theory; it may also lead to erroneous results. As already mentioned, the method of choice for systems with "slow" equilibrium is frontal analysis [4].

22.2 Gas–solid inverse gas chromatography

22.2.1 Nonspecific interactions

The dispersive component of the surface free energy, γ_s^D , is most often used to characterize the surface layer of the examined material by means of IGC. Two popular procedures were proposed by Dorris and Gray [12] and Schultz et al. [13,14], for its calculation.

The dispersive properties of the examined material are calculated from retention data of test solutes determined at infinite dilution in the Henry's law region [2,12]. It is also assumed that interactions between the adsorbed molecules are negligible.

In the infinite dilution regime the net retention volume V_N of adsorbing test solute

$$V_N = j \cdot t'_R \cdot F \quad (22.1)$$

where: j —James–Martin compressibility factor, F —carrier gas flow rate [$\text{cm}^3 \text{min}^{-1}$]

is related to the slope of its adsorption isotherm (K):

$$V_N = K \cdot A_{TOT} \quad (22.2)$$

where: A_{TOT} is the total area of the examined material in the column. As K is related to the standard free energy of adsorption and

$$-\Delta G_A = RT \ln V_N + C \quad (22.3)$$

where R —gas constant, T —absolute temperature, C —constant, leading to

$$RT \ln V_N = 2a_{mol} (\sigma_s^{LW} \sigma_L^{LW})^{1/2} + C \quad (22.4)$$

where σ_s^{LW} denotes the Lifshitz–van der Waals component of the solid (examined material) surface tension, σ_L^{LW} is the LW component of the test solute liquid surface tension, a_{mol} is the molar area occupied by the adsorbing molecule, and C is constant dependent on the reference state applied.

The σ_s^{LW} value can be determined by plotting $RT \ln V_N$ against $a_{mol} \cdot (\sigma_L^{LW})^{1/2}$. Sun and Berg [15] applied this model to examine the moisture effect on the surface free energy and acid–base properties of mineral oxides. They calculated a_{mol} assuming a spherical molecular shape and hexagonal packing for the polar test solutes

$$a_{mol} = 1.33N^{1/3}v_{mol}^{2/3} \quad (22.5)$$

with v_{mol} being the liquid molar volume and N is the Avogadro number.

a_{mol} of nonpolar species were calculated according to the procedure of Dorris and Gray [12].

An equation similar to Eq. (22.4) can be developed by considering the concept of the work of adhesion. For nonpolar probes, only dispersive interactions (Lifshitz–van der Waals) influence their retention. The free energy of adsorption is related to the work of adhesion by the following equation:

$$-\Delta G_A = aNW_a \quad (22.6)$$

The work of adhesion is described as $W_a = \gamma\gamma$

$$W_a = W_a^{LW} = 2(\gamma_S^{LW}\gamma_L^{LW})^{1/2} \quad (22.7)$$

Eqs. (22.3, 22.6, and 22.7) combined lead to Eq. (22.8)

$$RT \ln V_N = 2N \left((\gamma_S^{LW})^{1/2} a (\gamma_L^{LW})^{1/2} \right) + C \quad (22.8)$$

In the IGC literature, this relationship is commonly presented in the form introduced by Schultz and Lavielle [13,14]:

$$R \cdot T \cdot \ln V_N = 2 \cdot N \cdot a_p \cdot \sqrt{\gamma_S^D \cdot \gamma_L^D} + C \quad (22.9)$$

where the symbol γ_S^D is used instead of γ_S^{LW} and denotes the dispersive component of the surface free energy of the solid; the symbol γ_L^D is used instead of γ_L^{LW} and denotes the dispersive component of the surface free energy of the test solute; and the symbol a_p is used instead of a and denotes the area occupied by the adsorbing molecule.

Dorris and Gray calculated γ_S^D according to the equation:

$$\gamma_S^D = \frac{-R^2 \cdot T^2 \cdot \left[\ln \left[\frac{V_N^{(C_{n+1}H_{2n+4})}}{V_N^{(C_nH_{2n+2})}} \right] \right]^2}{4 \cdot N^2 \cdot (a_{CH_2})^2 \cdot \gamma_{(CH_2)}} \quad (22.10)$$

where $a_{(CH_2)}$ is the surface area of a methylene group, and the value of this parameter is assumed to be equal to 6 \AA^2 but sometimes is taken as 5.2 or 5.5 \AA^2 ; variation of these quantities is high, e.g., 3.1 \AA^2 calculated from a spherical model [16] while values up to 7.7 \AA^2 have been observed by scanning tunneling microscopy (STM) [17]; N is the Avogadro's number ($6.023 \cdot 10^{23} \text{ [mol}^{-1}\text{]}$); $V_N^{(C_{n+1}H_{2n+4})}$ is the net retention volume of an alkane $C_{n+1}H_{2n+4}$; $V_N^{(C_nH_{2n+2})}$ is the net retention volume of the alkane C_nH_{2n+2} ; and $\gamma_{(CH_2)}$ is the surface energy of the polyethylene-type polymers with a finite molecular weight $[\text{mJ m}^{-2}]$. The value $\gamma_{(CH_2)}$ is calculated according to the following equation:

$$\gamma_{(CH_2)} = 34.0 - 0.058 \cdot t \quad (22.11)$$

or

$$\gamma_{(CH_2)} = 35.6 + 0.058(293 - T) \quad (22.12)$$

t is the temperature in $^\circ\text{C}$ and T is the temperature in K.

Hamieh [18] summarized the problem of uncertainty concerning the “ a ” value. This might be calculated by using various models. The additional limitation is the fact that the “ a ” value for a given test solute varies with the nature of the examined solid, the temperature, and surface coverage [19]. It should be noted that the most uncertain value is a_p and may be determined with a large error margin, depending on adsorbent properties, temperature, and reference substance. Although the assumption that a_p is constant is most comfortable, under IGC conditions the most realistic approach is to treat the test solute as an ideal gas [20]. Hamieh [18]

also pointed out that γ_L^D values are not always available from the literature for the required temperature range.

Schultz et al. [13,14] applied the Fowkes model for the determination of γ_s^D . The van Oss et al. [21] approach is often used in the surface free energy determination by means of contact angle experiments [22] and references cited therein:

$$(1 + \cos \theta)\gamma^{TOT} = 2 \left(\sqrt{\gamma_s^{LW} + \gamma_L^{LW}} + \sqrt{\gamma_s^+ \gamma_L^-} + \sqrt{\gamma_s^- \gamma_L^+} \right) \quad (22.13)$$

where surface free energy γ^{TOT} is the sum of nonpolar (LW, Lifshitz–van der Waals; γ_s^{LW} for solid; γ_L^{LW} for liquid) and polar (AB, acid–base; γ_s^+ , γ_s^- for solid; γ_L^+ , γ_L^- for liquid) components.

Shi et al. [23] compared γ_s^D values obtained using the Dorris–Gray and Shultz et al. methods. They found that the ratio defined by the following equation,

$$\frac{\gamma_{s,Dorris-Gray}^D}{\gamma_{s,Schultz}^D} = \frac{(a_{n+1}\gamma_{L,n+1}^{0.5} - a_n\gamma_{L,n}^{0.5})^2}{\gamma_{CH_2} \cdot a_{(CH_2)}^2} \quad (22.14)$$

is always higher than 1. It means that the value of γ_s^D will be larger when calculated by the Dorris–Gray procedure. The ratio slightly increases with the temperature of the IGC experiment. Karaoglan and Sakar [25] reached a similar conclusion.

Comparison of γ_s^D values found from contact angle and IGC experiments indicated that the IGC data are higher. Garnier and Glasser [21] suggested that the differences arise from the changes of the “*a*” value in different states, while others indicated [26,27] that IGC evaluates, primarily, high-energy surface sites. The dispersive component of the surface free energy is often used to characterize various materials [25–36]. However, it is impossible to cite all such work in this section.

22.2.2 Influence of the humidity on IGC parameters

Thielmann emphasized the importance of carrier gas purity and its dryness [4]. It is clear that any impurity, including moisture, will affect the experimental results. However, it is well known that there is a group of materials containing a “natural” amount of water, which influences their stability, activity, etc. In such a case, the use of standard, i.e., dry, carrier gas during the IGC examination will cause progressive loss of the water and, finally, the “demolition” of the examined substance. This group of materials may consist of cellulose wooden pulp, natural fibers, dental cements, etc. Therefore, the justified use of a wet carrier gas and the influence of the carrier gas humidity on the estimated parameters will be shortly discussed here.

Comte et al. [37] examined the influence of carrier gas relative humidity (RH) on surface properties of low specific surface area glass beads. The specific retention volume and free enthalpy of adsorption of apolar molecules decreased with an increase of the RH of the carrier gas. Progressive coverage of the glass beads by water molecules masks high-energy sites and the retention times of alkanes decreased. When the whole surfaces of the glass beads are covered, the alkanes adsorbed on a film of water (Fig. 22.1). The specific retention value of the test solute became constant. This effect was achieved at $p/p_0 = 0.15$. The same result, i.e., the value of “critical” RH, was found when changes of the free enthalpy of adsorption with RH were taken into account. Enthalpy and entropy of adsorption also varied with the RH. The authors [24] found that the entropy term went through minima at $p/p_0 = 0.06$ for octane and nonane and $p/p_0 = 0.03$ for decane. Comte et al. explained this by nonrandom adsorption due to orientation of the molecules at the surface. With an increase of the RH the free, nonwetted zones of the bead surface decrease, which

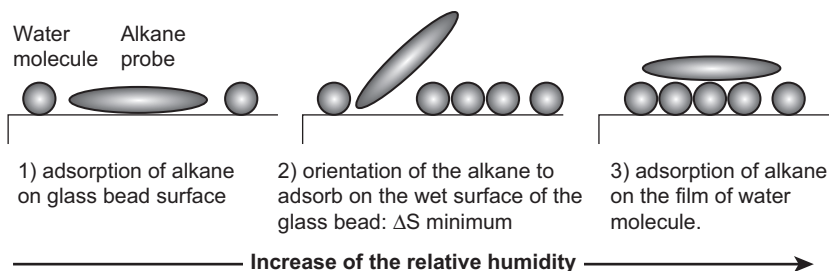


FIGURE 22.1 Representation of the adsorption of alkane probes at different relative humidity. From S. Comte, R. Calvet, A. Dodds, H. Balard, *Powder Technol.* 157 (2005) 39 with permission.

imposes orientation of the test solute molecules to reach nonwetted part of the

surface. After formation of a water film, the test solute molecules gain a few degrees of freedom. The decrease of the retention of the test solutes with an increase in RH was also reported by Garcia-Herruzo et al. [38]. for the sorption of hydrocarbons on soil.

The adsorption of polar probes shows that ΔG_A decrease occurs in two stages [16,37]. The decrease of ΔG_A was attributed to progressive masking of acidic and basic surface groups by water molecules. Stable ΔG_A values indicated the coverage of the surface by water film. The parameter exhibiting surface ability to acidic (K_A) and basic (K_B) interactions decreased when the RH increased.

Sun and Berg [16] indicated that many mineral oxide surfaces adsorb water and their surface properties correspond to a clean surface covered by hydroxyl groups and water. Although these are not the characteristics of a pure surface, from a practical point of view, "they are a fair representation of the surfaces of everyday use materials."

Boutboul et al. [39]. examined the interactions between aroma compounds and native corn starch under humid and dry conditions. Selective interactions between the system components result from an adsorption phenomenon involving hydrogen bonding prevailing when dried starch (4.5% water content) was examined. The increase of RH enabled the diffusion of more

hydrophilic test solutes into the native starch matrix. The partial change of the retention mechanism is probably an explanation of the increase of the retention volume of the polar test solutes used in IGC experiments.

The effect of moisture on the transport properties of various test solutes across different polymer matrices has been investigated [40–43]. The sorption of water by these materials, used as stationary phases, caused an increase in the partition and diffusion coefficients of alcohol with an EVOH (ethylene oxide–vinyl alcohol) copolymer.

Sunkersett et al. [44] studied the influence of carrier gas humidity on the dispersive component of the surface free energy (γ_s^D) for two pharmacologically active powders, i.e., carbamazepine and paracetamol. They found that γ_s^D values do not vary significantly with an increase of RH. However, the specific component of the free energy of adsorption ($-\Delta G_A$) remained constant or decreased by up to 10%. The authors interpreted this as an indication of the decrease of surface activity of these materials. This finding agrees with the findings of Sun and Berg [16] as well as Comte et al. [37]. It is important to note that Sunkersett et al. [31] supported their IGC findings by the GRID analysis of preferential interaction sites of the test solutes around paracetamol. They found that the decrease in the adsorption of the test solute might be the result of a competitive sharing of the same chemical site by the test solutes and water molecules.

Das et al. [45] found that the influence of humidity on the surface energetics of various powders is unclear. Further reports found that a decrease in the dispersive component of the surface free energy with increasing RH was observed [46–48] or remained constant [44,49]. Das et al. [45] concluded that there is no general relationship between the specific surface energy and the RH of the environment. They found that for salmeterol xinafoate (SX) and α -lactose monohydrate samples, the total surface energies increased after the storage at high RH (75%). This increase was attributed to the adsorption of water during storage. The authors pointed out that examination of only the dispersive part of the surface energy would result in misleading interpretation of the results. The dispersive component of surface energy of SX decreased after storage, as reported by other research groups. The determination of the total surface energy, including the nonspecific and specific contribution, allowed one to properly interpret the changes in the “community” of functional groups onto the powder surface. Das et al. interpreted this as an artifact of shielding by moisture adsorbed at polar sites [37]. However, it is important to note the differences between the influence of storage at high RH and carrying out the experiments with the use of wet carrier gas.

Kim et al. [50] used IGC for the estimation of thermodynamic characteristics for sorption of water onto three polymer surfaces. Similar values of the molar enthalpy of sorption were found for polystyrene (PS) and poly(methyl methacrylate) (PMMA), while lower values were observed for the poly(2-hydroxyethyl methacrylate) PHEMA surface. A larger amount of protein was adsorbed on PS and PMMA in comparison to PHEMA. The strength of water–polymer interactions is an important factor for controlling the amount of nonspecifically adsorbed protein. This finding might be extremely important for evaluation of various polymeric biomaterials where proteins deposition may lead to adverse biological consequences such as biofouling and/or activation of the immune system.

Slimane et al. [51] examined the wetting behavior of materials by polypyrrole. The authors stressed the advantage of IGC over the XPS technique. The analysis depth of XPS is 10 nm (several monolayers), while IGC supplies information on atoms and functional groups at the outermost layers of the material.

22.2.3 Specific surface properties

The ability of the examined surface for specific interactions by means of IGC might be determined by the interaction of polar probes of known characteristics with the surface and the collection of their retention data. The difficulties connected with this approach were presented by Papirer and Balard [52]: (i) a polar test solute will interact with a polar surface through both dispersive and specific interactions; and (ii) the investigator collects only one chromatographic peak and its parameters result from both types of interactions. One has to separate and evaluate both contributions. The term “specific interactions” denotes all types of interactions except for London forces, i.e., bipolar, H-bond type, acid–base, metallic, magnetic, and hydrophobic. Such intermolecular forces are known to dominate over dispersion and dipole–dipole interactions [53]. In the absence of electrostatic, magnetic, or metallic interactions, acid–base interactions prevail over dispersive interactions. Therefore, the special attention was focused on the evaluation of procedures enabling the determination of the acid–base characteristics of the examined surfaces [20].

Acidity and basicity of solid surface are deduced from the behavior of polar compounds being injected onto the chromatographic column filled with the studied material [5,54–57]. The capability of the solid surface to interact as a base or acid is expressed in different ways. However, the Gutmann’s scale seems to be the most frequently used in IGC procedures. It should be noted that AN^* and DN numbers of the test solutes express their capability to act as electron

acceptor and electron donor, respectively. Therefore, the final result should be discussed in term of Lewis acid–base interactions. An interesting discussion of physicochemical aspects of “Gutmann’s model” was presented by Hamieh [58]. He raised the problem of direct transposition of bulk quantities (AN , AN^* and DN) to interfacial interactions. The main contradiction “lies in the discontinuity in the symmetry of the local interactions involving the molecules, when transferring them from the bulk to the rigid surface.” Hamieh stated that the dependence of the reference bulk quantities on the nature of interacting species, the local coordination, and physical constraints are properly corrected by the modification of equations used in the evaluation of the specific interaction parameters. This important finding is carefully verified and discussed in the following paragraphs.

The ability of the examined surface to cause specific interactions is determined by the procedure consisting of the determination of the specific component of the adsorption energy ΔG_A^s , then the specific component of the enthalpy of adsorption ΔH_A^s followed by the solution of the relationship between ΔH_A^s and parameters characterizing the examined material. ΔG_A^s is determined as the difference between the adsorption energy of the polar compound, $\Delta G_{A,polar}$ and the adsorption energy of a hypothetical alkane, $\Delta G_{A,ref}$ Eq. (20.15), having the same selected property as the polar test solute (e.g., vapor pressure in Papirer method [52,59–62] or $a \cdot \sqrt{\gamma_L^D}$ value in Schultz and Lavielle method:

$$\Delta G_A^s = \Delta G_{A,polar} - \Delta G_{A,ref} \quad (22.15)$$

where

$$\Delta G_{A,polar} = -RT \ln V_{N_{polar}} + C \text{ and}$$

$$\Delta G_{A,ref} = -RT \ln V_{N_{refr}} + C$$

Chehimi and Pigois-Landureau [63] compared six methods of evaluating ΔG^s where $RT \ln V_N$ was related to the abscissa coordinates labeled as

follows: I, ΔH_{vap}^d (dispersive component of enthalpy of evaporation); II, ΔH_{vap} (enthalpy of evaporation); III, T_b (boiling point); IV - $\log P^o$ (saturated vapor pressure); V, $a_p (\gamma_L^D)^{1/2}$ (area occupied by adsorbing molecule and the dispersive component of the liquid solute surface tension, respectively); VI, $(h\nu)^{1/2} \alpha$ (molecular polarizability). Chehimi and Pigois-Landureau suggested the use of the ΔH_{vap}^d parameter for the description of the reference state to demonstrate the self-association character of polar test solutes as postulated by Fowkes [64].

ΔH_A^s is calculated from the dependence of ΔG_A^s on temperature:

$$\Delta G_A^s = \Delta H_A^s - T \cdot \Delta S_A^s \quad (22.16)$$

where ΔG_A^s —specific component of the free adsorption energy; ΔS_A^s —specific component of the free adsorption entropy of polar compound onto the surface of investigated solid.

Plotting $\Delta G_A^s/T$ against $1/T$ yields a straight line with the slope of ΔH_A^s . ΔH_A^s should be determined for at least four test compounds, and ΔG_A^s should be determined at at least three temperatures. However, calculation of K_A and K_D parameters from ΔH_A^s is time-consuming. The estimation of ΔH_A^s from Eq. (20.16) might be the source of the largest error in the determination of the specific characteristics of the examined material. Moreover, this procedure might be “dangerous” for labile materials at the elevated temperatures making the determination of ΔH_A^s impossible.

Specific component of enthalpy of adsorption of the polar compound, ΔH_A^s , is related to acceptor and donor numbers describing the electron acceptor (AN^*) and electron donor (DN) properties of the test compound:

$$\Delta H_A^s = DN \cdot K_A + AN^* \cdot K_D \quad (22.17)$$

K_A and K_D parameters express the ability of the examined material to act as an electron acceptor and electron donor, respectively.

Plotting $\Delta H_A^s/AN^*$ against DN/AN^* ,

$$\frac{\Delta H_A^s}{AN^*} = \frac{DN}{AN^*} \cdot K_A + K_D \quad (22.18)$$

one obtains the straight line with the slope of K_A . As the estimation of K_D from the intercept of (Eq. (22.18)) may lead to significant error [65], one should determine this value as the slope of the following relationship:

$$\frac{\Delta H_A^s}{DN} = \frac{AN^*}{DN} \cdot K_D + K_A \quad (22.19)$$

Parameters K_A and K_D were also calculated by using ΔG_A^s [3,59,60,66] instead of ΔH_A^s . This method of determination of K_A and K_D leads to the temperature-dependent values containing also entropic factors [5,66].

Hamieh et al. [58,67] proved that the relationship (Eq. (22.18)) is, in general, not verified in the case of some metallic oxides. They suggested the use of a corrected version,

$$\begin{aligned} \Delta H_A^s &= K_A \cdot DN + K_D \cdot AN - K(K_A, K_D)AN \cdot DN \\ &= w(K_A \cdot DN + K_D \cdot AN) \end{aligned} \quad (22.20)$$

where w is a parameter expressing a weighting factor for the interactions between the adsorbed molecules and the solid substrate ($0 \leq w \leq 1$). $K(K_A, K_D)$ is a constant depending on K_A and K_D and describing the amphoteric nature of the solid substrate.

The paper presented by Hamieh [58] is interesting and provides a concise summary of earlier papers [67–73]. However, the proposal expressed by Eq. (22.20) is problematic from a chemometric and mathematical perspective. It is also known [74,75] that parameters, “constants” used therein must be independent and free of “intercorrelation.” The approach proposed by Hamieh et al. enhanced, of course, the statistics of ΔH_A^s versus K_A, K_D relationship, but the meaning of K and/or w parameters is obscure. The authors showed the existing relationships between K and K_A, K_D (see Eq. (20.18)

and Table 20.11 in Ref. [44]). Hopefully, R^2 (regression coefficient) values given therein are relatively low. In my opinion, the deviations in the properties of metallic oxides and other examined materials from those predicted by Eq. (22.17) should be explained not by overbuilding the appropriate relationships but by looking for another (from Gutmann’s) model. Despite any doubts this model was used several times for the characterization of various materials [76–79].

The influence of RH on both the dispersive and specific surface properties of various excipients and active materials important for drug delivery has been discussed [39,47,49,79–86]. The IGC-derived parameters supported by those determined by other techniques (e.g., XPS, DSC, TGA, DVS) were used to estimate the batch-to-batch variation in the manufacturing of the pharmaceutical materials. Various carbohydrates were characterized using dispersive and specific IGC parameters [87–96]. The role of IGC in the characterization of drug delivery systems increases [44,97–107]. Tran et al. [102] examined the flow properties of blends of two common pharmaceutical excipients and colloidal silica to study the mechanism of colloidal silica glidant action. The authors stated that the dynamic nature of the processes of glidant aggregate breakage, glidant attachment to host particles, and spreading the glidant over the host particle surface is the main obstruction preventing the straightforward utilization of surface energy measurements, which was successfully utilized elsewhere. It is worth noting the examination of chitin and its N-deacetylation derivative [108] by means of IGC. Influence of the nature and treatment of starch on aroma–starch interactions were examined by Boutboul et al. [31,109]. Various minerals, silicas, modified silicas, talc, modified talc, and other materials are often characterized by IGC and became an accepted standard [110–129]. Surface energy characteristics of toner articles, ink fillers, printing ink pigments, and components used in

coil-coating primers were also achieved using the methods and procedures of IGC [129–133]. It should be noted that IGC has been successfully applied to the characterization of various zeolites [134–142]. Both surface properties and solubility parameters were determined for two different chewing-gum bases [143]. Chehimi et al. presented a series of reports on the characterization of cement components, cements pastes, and the interactions between structural adhesive components with cement pastes [144–147]. The key role of IGC in the determination of interactions between components of polymeric systems was reviewed by Santos and Guthrie [148,149].

Natural (also vegetable) and synthetic fibers were also characterized by means of IGC [96,150–166]. An important contribution of IGC to the present-day fiber technology.

Carbons, activated carbons were the next groups of materials characterized by this technique [167–173]. The influence of measurement conditions on the elution peaks of the test solutes was discussed by Wu et al. [169]. The first papers of Kiselev [9–11] were devoted to the examination of catalysts. This remains a current trend in IGC [174].

22.3 Bulk properties of polymers and polymers blends

IGC has been used for examination of the bulk properties of polymers and their blends, as well as complex systems consisting of organic and organic components (polymer–filler compositions).

The Flory–Huggins interaction parameter (χ) reflects the interaction between low-molecular-weight solvent and high-molecular-weight polymer and has been considered as a Gibbs free energy parameter. According to such an assumption, the interaction parameter χ can be divided into enthalpy χ_H and entropy χ_S components [175]:

$$\chi = \chi_H + \chi_S \quad (22.21)$$

It was found that χ_S is positive and usually between 0.2 and 0.6. This term is also sometimes related to the reciprocal of the coordination number in the polymer solution. It has been assumed that in some cases it is between 0.3 and 0.4 limit [176]. For complete miscibility between polymer and solvent, the interaction parameter χ should be less than 0.5. Also, the entropy term is about 0.3; therefore enthalpy term χ_H must be very small to meet the miscibility's criterion [175].

At infinite dilution of the probe and for high molecular weight of the stationary phase, the Flory–Huggins interaction parameter can be determined from Ref. [177,178]:

$$\begin{aligned} \chi_{12}^{\infty} = & \ln\left(\frac{273.15 \cdot R}{p_1^o \cdot V_g \cdot M_1}\right) - \frac{p_1^o}{R \cdot T} \cdot (B_{11} - V_1^o) \\ & + \ln\left(\frac{\rho_1}{\rho_2}\right) - \left(1 - \frac{V_1^o}{V_2^o}\right) \end{aligned} \quad (22.22)$$

V_g is the specific retention volume, 1 denotes the solute and 2 denotes examined material, M_1 is the molecular weight of the solute, p_1^o is the saturated vapor pressure of the solute, B_{11} is the second virial coefficient of the solute, V_i^o is the molar volume, ρ_i is the density, R is the gas constant.

The simplified form of Eq. (22.22) is also found in the literature [20,179,180]:

$$\chi_{12}^{\infty} = \ln\left(\frac{273.15 \cdot R \cdot v_2}{p_1^o \cdot V_g \cdot V_1^o}\right) - \frac{p_1^o}{R \cdot T} \cdot (B_{11} - V_1^o) - 1 \quad (22.23)$$

where v_2 is the specific volume of the polymer.

Deshpande et al. [181] first suggested the use of IGC for studying polymer blends. Starting from the Flory–Huggins expression for the change of free enthalpy of mixing ΔG_{mix} extended to three-component systems, they proposed a method to elaborate IGC data collected for polymer blends leading to the polymer–polymer interaction coefficient.

When a mixture of components is used as a stationary phase in a chromatographic column,

subscripts 2 and 3 are used to represent the first and second mixtures' component, respectively:

$$\begin{aligned} \chi_{1m}^{\infty} = & \ln\left(\frac{273.15 \cdot R}{p_1^{\circ} \cdot V_g \cdot M_1}\right) - \frac{p_1^{\circ}}{R \cdot T} \cdot (B_{11} - V_1^{\circ}) \\ & + \ln\left(\frac{\rho_1}{\rho m}\right) - \left(1 - \frac{V_1^{\circ}}{V_2^{\circ}}\right) \cdot \phi_2 - \left(1 - \frac{V_1^{\circ}}{V_3^{\circ}}\right) \cdot \phi_3 \end{aligned} \quad (22.24)$$

where ϕ_2 and ϕ_3 are the volume fractions of components [175].

The problem of availability and credibility of physical data used in Eqs. (20.22)–(20.24) was discussed earlier [20,179]. However, it is worth repeating here that due to the uncertainty of the basic physicochemical data, one should take into account the possible error of estimation of IGC parameter, which may, in several cases, exceed 10%.

Applying the Flory–Huggins equation of polymer solutions to a ternary system with two polymers and one probe, the interaction parameter χ_{1m}^{∞} is related to the probe–polymer interaction parameters and the polymer–polymer interaction parameter by the following equation:

$$\chi_{1m}^{\infty} = \phi_2 \cdot \chi_{12}^{\infty} + \phi_3 \cdot \chi_{13}^{\infty} - \phi_2 \cdot \phi_3 \cdot \chi'_{23} \quad (22.25)$$

where ϕ_2 and ϕ_3 are the volume fractions of the polymers.

The magnitude of the interactions between the two components of the polymer blend is expressed in terms of χ'_{23} . Large positive values of χ'_{23} indicate the absence or negligible interactions between components, a low value indicates favorable interactions, while a negative value indicates strong interactions (the polymer pair is miscible).

The interaction parameter χ'_{23} can be calculated from equation [182,183]:

$$\begin{aligned} \chi'_{23} = & \frac{\chi_{23}^{\infty} \cdot V_1^{\circ}}{V_2^{\circ}} = \frac{1}{\phi_2 \cdot \phi_3} \cdot \left(\ln \frac{V_{g,m}}{W_2 \cdot \nu_2 + W_3 \cdot \nu_3} \right. \\ & \left. - \phi_2 \cdot \ln \frac{V_{g,2}}{\nu_2} - \phi_3 \cdot \ln \frac{V_{g,3}}{\nu_3} \right) \end{aligned} \quad (22.26)$$

Here, the second subscript of V_g identifies the nature of the column:

$$\chi'_{23} = \frac{1}{\phi_2 \cdot \phi_3} \cdot (\chi_{12}^{\infty} \cdot \phi_2 + \chi_{13}^{\infty} \cdot \phi_3 - \chi_{1m}^{\infty}) \quad (22.27)$$

Values of Flory–Huggins χ'_{23} parameter depend on the chemical structure of the solute [184,185]. It has been interpreted as arising from preferential interaction with one of two types of components. Hsu and Prausnitz [186] as well as Su and coworkers [187,188] suggested that the compatibility of polymeric components should reflect not only the interaction between the components themselves, i.e., χ'_{23} , but also the difference in strength of the polymer–probe interactions, i.e., $\Delta\chi = |\chi_{12} - \chi_{13}|$. They called it the $\Delta\chi$ effect, and a large $\Delta\chi$ in addition to a high χ'_{23} value leads to incompatibility. Accordingly, one must select probes that give $\chi_{12}^{\infty} = \chi_{13}^{\infty}$ for studying the blend.

Farooque and Deshpande [185] rearranged (Eq. (22.25)) to the following form:

$$\frac{\chi_{1(23)}^{\infty} - \chi_{13}^{\infty}}{V_1} = \phi_2 \cdot \frac{\chi_{12}^{\infty} - \chi_{13}^{\infty}}{V_1} - \phi_2 \cdot \phi_3 \cdot \frac{\chi'_{23}}{V_2} \quad (22.28)$$

By plotting the left-hand side of Eq. (22.28) versus $\phi_2 \cdot \frac{\chi_{12}^{\infty} - \chi_{13}^{\infty}}{V_1}$ the interaction parameter can be obtained from the intercept. Although this method gives reliable χ'_{23} values, they are affected by large errors. To reduce the uncertainty in the χ'_{23} values, a possible alternative is an adequate selection of the probes. However, the slopes deviated from their theoretical values.

Huang [188–190] proposed to rearrange (Eq. (22.28)) as follows:

$$\frac{\chi_{1(23)}^{\infty}}{V_1} = \frac{\phi_2 \cdot \chi_{12}^{\infty} + \phi_3 \cdot \chi_{13}^{\infty}}{V_1} - \phi_2 \cdot \phi_3 \cdot \frac{\chi'_{23}}{V_2} \quad (22.29)$$

A linear plot can be obtained from the left-hand side versus $(\phi_2 \cdot \chi_{12}^{\infty} + \phi_3 \cdot \chi_{13}^{\infty})/V_1$. The polymer–polymer interaction term can be determined from the intercept at $(\phi_2 \cdot \chi_{12}^{\infty} + \phi_3 \cdot \chi_{13}^{\infty})/V_1 = 0$. A

physical meaning of this procedure is that when $(\varphi_2 \cdot \chi_{12}^\infty + \varphi_3 \cdot \chi_{13}^\infty)/V_1 = 0$, the probe is experiencing a similar environment in the blend compared to the probe liquid. The disturbance of liquid polymer structure is expected to be minimal.

Several other papers where IGC was used to examine polymer blends should be mentioned here [191–193]. Benabdelghani et al. [193] studied the miscibility of poly(styrene-*co*-methacrylic acid) (PSMA-12) blends containing 12% of methacrylic acid with poly(2,6-dimethyl-1,4-phenylene oxide) (PPO). They rearranged (Eq. (22.28)) as follows:

$$\frac{1}{V_1} \ln \left(\frac{V_{g,m}}{\nu_m} \right) = \left[\frac{1}{V_1} \cdot \left(\varphi_2 \ln \left(\frac{V_{g,2}}{\nu_2} \right) + \varphi_3 \ln \left(\frac{V_{g,3}}{\nu_3} \right) \right) \right] + \varphi_2 \varphi_3 \frac{\chi'_{23}}{V_2} \quad (22.30)$$

The plot of the left-hand side term as a function of the expression between brackets of the right-hand side term of Eq. (22.30) allows the true value of $\frac{V_{g,m}}{\nu_m}$ to be calculated from the intercept. They found that χ'_{23} values are in the good agreement with T_g data from DSC measurements.

Zhao and Choi [194] used nonrandom partitioning of solutes in binary polyolefin blends to test whether solutes may cause the solute dependence of the Flory–Huggins parameter χ'_{23} observed in IGC experiments. They concluded that the nonrandom partitioning behavior of solutes is not the real reason for the probe dependence problem. This is mainly attributed to the improper use of the reference volume in calculations of the solute–stationary phase interaction parameters (χ_{1i}^∞). The authors suggested using a single common reference volume (V_o) instead of individual molar volumes of the solutes used in IGC experiments for the calculations of the χ_{12}^∞ parameter. In the reference volume, Zhao and Choi proposed to use molar volume

of repeated unit of polymer at the experimental temperature [194]:

$$\chi_{1m}^\infty = \frac{V_0}{V_1} \cdot \left(\ln \frac{273.15 \cdot R \cdot (W_2 \cdot \nu_2 + W_3 \cdot \nu_3)}{V_g \cdot V_1 \cdot p_1^0} - 1 + \frac{V_1}{M_2 \cdot \nu_2} + \frac{V_1}{M_3 \cdot \nu_3} - \frac{(B_{11} - V_1)}{R \cdot T} p_1^0 \right) \quad (22.31)$$

Milczewska and Voelkel [195,196] used procedures proposed by Farooque and Deshpande, Zhao and Choi, and Huang to calculate values of χ'_{23} parameters independent from the solute type. The results (values of χ'_{23}) obtained from those procedures minimized $\Delta\chi$ effect. For the system PU-N2 (a system containing polyetherurethane filled with carbonate–silicate filler modified with octylsilane and stearic acid), they obtained low, negative values, which indicated strong interactions between the polymer and the N2 filler [195,196].

Diffusivity of solvents in polymers, gel permeation parameters, and other transport properties as well as interaction parameters between system components were determined for a series of polymeric systems [197–209]. Studies of miscibility of components of polymer blends were presented by several research groups [210–213].

Composite materials were extensively examined by means of IGC [214–225] including mucoadhesive polymers [219], silicone membranes [220] as well as metal–organic frameworks [222,223]. It is worth to distinguish the attempt of examination of tacticity of PMMA by IGC tools [218]. The authors tried to compare the results obtained from IGC experiments with those collected by other techniques, i.e., immersion calorimetry [221,222] or dynamic mechanical–thermal analysis [224]. This technique (IGC) was also applied in the

examination of chemical changes in cured phenol-formaldehyde resins during storage [225].

22.3.1 Solubility parameter

Strong interactions between molecules exist in condensed phases (liquids, solutions, solid materials), resulting in considerable (negative) potential energy in each molecule. This energy is called the *molar cohesive energy* ($-E$) [226]. Cohesive energy related to a molar volume is called *cohesive energy density* c :

$$c = \frac{-E}{V} \quad (22.32)$$

and the square root of the cohesive energy density is called *solubility parameter* δ . This term proposed by Hildebrand for nonpolar systems and used as a measure of intermolecular forces of different solvents is related to the enthalpy of evaporation ΔH_w :

$$\delta = \sqrt{c} = \sqrt{\frac{E_{coh}}{V}} = \sqrt{\left(\frac{\Delta H_w - RT}{V}\right)} \quad (22.33)$$

where δ is the solubility parameter, E_{coh} is the cohesive energy, V the molar volume of a pure liquid, R the gas constant, T the temperature. The solubility parameter expressed by the relationship in Eq. (22.32) is called the Hildebrand solubility parameter.

The solubility parameter reflects van der Waals interactions between molecules, forming a liquid. However, such a definition could not be used for other systems where, besides dispersive forces, polar forces need to be taken into account.

The most widely accepted concept of solubility parameter (total solubility parameter) related to more complex systems has been proposed by Hansen:

$$\delta_T^2 = \delta_d^2 + \delta_p^2 + \delta_h^2 \quad (22.34)$$

where δ_d , δ_p , and δ_h denote dispersive, polar, and hydrogen bonding contribution, respectively.

The determination of the solubility parameter and Hansen's solubility parameters (HSPs) by means of IGC was discussed earlier [20]. The author wishes to focus readers' attention on Hansen's book [227] and the third edition of the e-book on practical applications of HSP [228] (also including IGC).

The procedure proposed by Ito and Guillet [229] was applied by Price [230,231] for the estimation of solubility parameter values for low-molecular-weight compounds [230] and liquid crystalline systems [231]. Price reported that the experimental relationship between the left-hand side of Eq. (22.35) and solubility parameters of test solutes is different from the linear relationship. Significant curvature of the relationship shown further was observed:

$$\frac{\delta_{1i}^2}{RT} - \frac{\chi_{(12)i}^\infty}{V_{1i}} = \frac{2\delta_2}{RT}\delta_{1i} - \left(\frac{\delta_2^2}{RT} + \frac{\chi_s^\infty}{V_{1i}}\right) \quad (22.35)$$

The downward curvature for alkanes and an upward curvature for other compounds were found. Therefore, the tendency for alkanes leads to underestimation of δ_2 while tendency for polar compounds may cause the overestimation of δ_2 values.

According to the three-component solubility parameter theory of Hansen, Price assumed that different types of intermolecular interactions between the examined material and test solutes will influence the value of the solubility parameter. Price proposed to estimate the solubility parameter as the sum of two terms:

$$\delta_T^2 = \delta_d^2 + \delta_a^2 \quad (22.36)$$

resulting from dispersive and polar intermolecular interactions.

However, in complex systems, additional hydrogen bonding interaction should be considered. The extension of Price's concept, enabling calculation of all components of the total solubility parameter, is the procedure proposed by Voelkel and Janas [232]. They increased the number of test solutes by addition of solutes

representing hydrogen bonding interactions. However, the problem of test solute selection might be the reason for the relatively large error in HSPs determinations.

Adamska et al. [233] proposed to calculate HSP data by using the model proposed by Lindvig et al. [234], combining experimental data of the Flory–Huggins interaction parameter χ_{12}^{∞} with components of the solubility parameter for the material:

$$\chi_{12}^{\infty} = \alpha \frac{V_1}{RT} \left((\delta_{1,d} - \delta_{2,d})^2 + 0,25(\delta_{1,p} - \delta_{2,p})^2 + 0,25(\delta_{1,h} - \delta_{2,h})^2 \right) \quad (22.37)$$

where α , V_1 , R , T are a corrective coefficient, molar volume of the test solute, gas constant, and the measurement temperature, respectively. In this relationship known, values for components of different test solutes ($\delta_{1,d}$, $\delta_{1,p}$, $\delta_{1,h}$) and solubility parameter of material

($\delta_{2,d}$, $\delta_{2,p}$, $\delta_{2,h}$) are used to estimate the Flory–Huggins interaction parameter. Experimentally obtained χ_{12}^{∞} values can be used for the determination of the HSP for examined material by applying the aforementioned relationship (Eq. (22.37)) [233].

Choi [235] proposed to calculate the critical value of interaction parameters by using the following relationship:

$$\chi_{crit} = \frac{1}{2} \left(1 + \sqrt{\frac{V_1}{V_2}} \right)^2 \quad (22.38)$$

where V_1 a molar volume of the test solute and V_2 the molar volume of polymer. Test solutes for which

$$\chi < \chi_{crit} \quad (22.39)$$

are further used in the calculation of the solubility parameter. Their ($\delta_{1,d}$, $\delta_{1,p}$, $\delta_{1,h}$) values are used to calculate the components of the solubility parameter of the examined material as the average of the respective values for all selected

solutes. Therefore, all data for “disqualified” test solutes are omitted and are not taken into consideration. In the author’s opinion, one should take into account all interactions between the examined material and test solutes.

The solubility parameter was used to characterize various materials [180,236–239]. HSPs were successfully applied to express the properties of, e.g., ibuprofen [240], alkali lignin/acrylonitrile-butadiene–styrene blends [241], polyethylene glycols [242,243] or to assist with oral delivery of poorly water-soluble drugs [244]. Mutelet et al. [245] have shown that IGC data might be used for the direct calculation of solubility parameters of ionic liquids. They found that the solubility parameter of 1 butyl-3-methylimidazolium hexafluorophosphate determined by IGC agreed well with the value obtained by Monte Carlo simulation.

Regretfully, the limited space available resulted in the omission of the problem of FC-IGC. However, the interested readers should consult the review of Charmas and Leboda [246] and additional reports referring to the DVS technique [247–249]. The authors also recommend reviews and papers on reversed-flow gas chromatography [20,250–260].

In conclusion, it is worth to cite the final sentence from Santos and Guthrie review [148]: “All these approaches have valuable advantages and relevant drawbacks. Thus, it is recommended the simultaneous use of several alternative approaches in order to corroborate the experimental results, analyses and theoretical predictions.”

References

- [1] D.R. Lloyd, T.S. Ward, H.P. Schreiber (Eds.), ACS Symp. Series, Inverse Gas Chromatography of Polymers and Other Materials, vol. 391, American Chemical Society, Washington DC, 1989.
- [2] M.N. Belgacem, A. Gandini, IGC as a tool to characterize dispersive and acid-base properties of the surface of fibers and powders, in: E. Pefferkorn (Ed.), Interfacial Phenomena in Chromatography, Marcel Dekker, New York, 1999, p. 41.

- [3] A. Voelkel, *Crit. Rev. Anal. Chem.* 22 (1991) 411.
- [4] F. Thielmann, *J. Chromatogr. A* 1037 (2004) 115.
- [5] A. Voelkel, Inverse gas chromatography in examination of acid-base and some other properties of solids, in: A. Dąbrowski, V.A. Tertykh (Eds.), *Adsorption on New and Modified Inorganic*, Elsevier, Amsterdam, 1996, p. 465.
- [6] C. Sun, J.C. Berg, *Adv. Colloid Interface Sci.* 105 (2003) 151.
- [7] A. Voelkel, B. Strzemieska, K. Adamska, K. Milczewska, K. Batko, Surface and bulk characteristics of polymers by means of inverse gas chromatography, in: A. Nastasovic, S. Jovanovic (Eds.), *Polymeric Materials, Research Signpost*, 2009, pp. 71–102.
- [8] R. Wu, D. Que, Z.Y. Al-Saigh, *J. Chromatogr. A* 1146 (2007) 93.
- [9] A.V. Kiselev, V.V. Kulichenko, *Dokl. Akad. Nauk SSSR* 93 (1953) 101.
- [10] A.V. Kiselev, B.A. Frolov, *Kinet. Catal.* 3 (1962) 667.
- [11] A.V. Kiselev, B.A. Frolov, *Kinet. Catal.* 3 (1962) 672.
- [12] A.B. Nastasović, A.E. Onjia, *J. Chromatogr. A* 1195 (2008) 1.
- [13] G.M. Dorris, P. Gray, *J. Colloid Interface Sci.* 77 (1980) 353.
- [14] J. Schultz, L. Lavielle, C.J. Martin, *Adhesion* 23 (1987) 45.
- [15] J. Schultz, L. Lavielle, Interfacial properties of carbon fibre – epoxy resin matrix composites, in: D.R. Lloyd, T.S. Ward, H.P. Schreiber (Eds.), *Inverse Gas Chromatography of Polymers and Other Materials*, ACS Symp. Series 391, American Chemical Society, Washington DS, 1989, pp. 185–202.
- [16] C. Sun, J.C. Berg, *J. Chromatogr. A* 969 (2002) 59.
- [17] P.H. Emmett, R.H. Brunauer, *J. Am. Chem. Soc.* 59 (1937) 155.
- [18] G.C. McGonigal, R.H. Bernhardt, *Appl. Phys. Lett.* 57 (1990) 28.
- [19] T. Hamieh, *Chromatographia* 73 (2011) 705.
- [20] A. Voelkel, B. Strzemieska, K. Adamska, K. Milczewska, *J. Chromatogr. A* 1216 (2009) 1551–1566.
- [21] G. Garnier, W.G. Glasser, *J. Adhes.* 46 (1994) 165.
- [22] C.J. van Oss, R.J. Good, M.K. Chandhury, *Langmuir* 4 (1988) 884.
- [23] O. Planinšek, A. Trojak, S. Srčić, *Int. J. Pharm. (Amst.)* 221 (2001) 211.
- [24] B. Shi, Y. Wang, L. Jia, *J. Chromatogr. A* 1218 (2011) 860.
- [25] G.K. Karaoglan, D. Sakar, *Chromatographia* 73 (2011) 93.
- [26] Y. Matsushita, S. Wada, K. Fukushima, S. Yasuda, *Ind. Crop. Prod.* 23 (2006) 115.
- [27] S.K. Papadoulou, G. Dritsas, I. Karapanagiotis, I. Zuburtikudis, *Eur. Polym. J.* 46 (2010) 202.
- [28] A. Onjia, S.K. Milonjić, N.N. Jovanović, S.M. Jovanović, *React. Funct. Polym.* 43 (2000) 269.
- [29] A.B. Nastasović, A.E. Onjia, S.K. Miljonić, S.M. Jovanović, *Eur. Polym. J.* 41 (2005) 1234.
- [30] F. Dieckmann, C. Klinger, P. Uhlmann, F. Böhme, *Polymer* 42 (2001) 3463.
- [31] A.A. Callhoun, P.D. Nicholson, A.B. Barnes, *Polym. Degrad. Stabil.* 91 (2006) 1964.
- [32] N. Rocha, J.A.F. Gamelas, P.M. Gonçalves, M.H. Gill, J.T. Guthrie, *Eur. Polym. J.* 45 (2009) 3389.
- [33] M.M. Chehimi, E. Abdeljalil, *Synth. Met.* 145 (2004) 15.
- [34] Z.Y. Al-Saigh, *Polymer* 40 (1999) 3479.
- [35] M.K. Kozłowska, U. Domańska, M. Lempert, M. Rogalski, *J. Chromatogr. A* 1068 (2005) 297.
- [36] A. Al-Ghamdi, Z.Y. Al-Saigh, *J. Chromatogr. A* 969 (2002) 229.
- [37] S. Comte, R. Calvet, A. Dodds, H. Balard, *Powder Technol.* 157 (2005) 39.
- [38] F. Gracia-Herruzo, J.M. Rodriguez-Maroto, R.A. Garcia-Delgado, C. Gomez-Lahoz, C. Vereda-Alonso, *Chemosphere* 41 (2000) 1167.
- [39] A. Boutboul, P. Giampaoli, A. Feingenbaum, V. Ducruet, *Food Chem.* 71 (2000) 387.
- [40] D. Cava, J.M. Lagaron, F. Martinez-Gimenez, R. Gavara, *J. Chromatogr. A* 1175 (2007) 267.
- [41] J.M. Lagaron, R. Catala, R. Gavara, *Mater. Sci. Technol. Lond.* 20 (2004) 1.
- [42] G. Lopez-Barballo, D. Cava, J.M. Lagaron, R. Catala, R. Gavara, *J. Agric. Food Chem.* 53 (2005) 7212.
- [43] S. Aucejo, M.J. Pozo, R. Gavara, *J. Appl. Polym. Sci.* 70 (1998) 711.
- [44] M.R. Sunkersett, I.M. Grimsey, S.W. Doughty, J.C. Osborn, P. York, R.C. Rowe, *Eur. J. Pharmaceut. Sci.* 13 (2001) 219.
- [45] S. Das, I. Larson, P. Young, P. Stewart, *Eur. J. Pharmaceut. Sci.* 38 (2009) 347.
- [46] K. Sooben, G. Buckton, J. Newton, *Pharm.Sci. (Suppl. I)* (2000) 2.
- [47] H. Newell, G. Buckton, D. Butler, F. Thielmann, D. Williams, *Int. J. Pharm.* 217 (2001) 45.
- [48] H. Balarad, A. Saada, B. Siffert, E. Papirer, *Clay Clay Miner.* 45 (1997) 489.
- [49] M. Ticehurst, P. York, R. Rowe, S. Dwivedi, *Int. J. Pharm.* 141 (1996) 93.
- [50] J. Kim, W. Qian, Z.Y. Al-Saigh, *Surf. Sci.* 605 (2011) 419.

- [51] A.B. Slimane, K. Boukerma, M. Chabut, M.M. Chehimi, *Colloids Surf., A* 240 (2004) 45.
- [52] E. Papirer, H. Balard, in: E. Pefferkorn (Ed.), *Interfacial Phenomena in Chromatography*, Marcel Dekker, New York, 1999, p. 145.
- [53] J.M.R.C.A. Santos, K. Fagelman, J.T. Guthrie, *J. Chromatogr. A* 969 (2002) 119.
- [54] J.R. Conder, C.L. Young, *Physicochemical Measurements by Gas Chromatography*, Wiley, Chichester, 1979.
- [55] V. Gutmann, *Electrochim. Acta* 21 (1976) 661.
- [56] U. Mayer, V. Gutmann, W. Gerger, *Mh. Chem.* 106 (1975) 1235.
- [57] F.L. Riddle, F.M. Fowkes, *J. Am. Chem. Soc.* 112 (1990) 3259.
- [58] T. Hamieh, *Chromatographia* 73 (2011) 709.
- [59] C.S. Flour, E. Papirer, *Ind. Eng. Chem. Prod. Res. Dev.* 21 (1982) 666.
- [60] C.S. Flour, E. Papirer, *J. Colloid Interface Sci.* 91 (1983) 69.
- [61] E. Papirer, J.M. Perrin, B. Siffert, G. Philipponneau, *J. Colloid Interface Sci.* 144 (1991) 263.
- [62] E. Papirer, J.M. Perrin, B. Siffert, G. Philipponneau, J.M. Lamerant, *J. Colloid Interface Sci.* 156 (1993) 104.
- [63] M.M. Chehimi, E. Pigois-Landureau, *J. Mater. Chem.* 4 (1994) 741.
- [64] F.M. Fowkes, *J. Adhes. Sci. Technol.* 4 (1990) 669.
- [65] B. Shi, Q. Zhang, J. Lina, L. Yang, L. Bin, *J. Chromatogr. A* 1149 (2007) 390.
- [66] E. Fekete, J. Móczó, B. Pukánszky, *J. Colloid Interface Sci.* 269 (2004) 143.
- [67] T. Hamieh, M. Nardin, M. Rageul-Lescouët, H. Haïdara, J. Schultz, *Colloids Surf., A* 125 (1997) 155.
- [68] T. Hamieh, M. Rezzaki, J. Schultz, *J. Therm. Anal.* 51 (2007) 793.
- [69] T. Hamieh, M. Rezzaki, J. Schultz, *J. Colloid Interface Sci.* 233 (2001) 339.
- [70] T. Hamieh, M. Rezzaki, J. Schultz, *J. Colloid Interface Sci.* 233 (2001) 343.
- [71] T. Hamieh, J. Schultz, *J. Chromatogr. A* 969 (2002) 17.
- [72] T. Hamieh, J. Schultz, *J. Chromatogr. A* 969 (2002) 27.
- [73] T. Hamieh, M.B. Falladah, J. Schultz, *J. Chromatogr. A* 969 (2002) 37.
- [74] R. Kaliszan, *Crit. Rev. Anal. Chem.* 16 (1986) 323.
- [75] R. Kaliszan, HPLC as a source of information about chemical structure of solutes, in: P.R. Brown, A.P. Hartwick (Eds.), *High Performance Liquid Chromatography*, Chemical Analysis Series of Monographs, J.D. Winefordner, I.M. Kolthoff, vol. 98, John Wiley&Sons, New York, 1989.
- [76] A. Askin, S.S. Etöz, D.T. Yazıcı, F. Tümsek, *Chromatographia* 73 (2011) 109.
- [77] J.M.R.C.A. Santos, K. Fagelman, J.T. Guthrie, *J. Chromatogr. A* 969 (2002) 111.
- [78] Q.-C. Zou, S.-L. Zhang, Q.-q. Tang, S.-M. Wang, L.-M. Wu, *J. Chromatogr. A* 1110 (2006) 140.
- [79] Y. Wu, Z. Li, H. Xi, *J. Hazard Mater.* B113 (2004) 131.
- [80] G. Buckton, H. Gill, *Adv. Drug Delivery Rev.* 59 (2007) 1474.
- [81] A.V. Ambarkhane, K. Pincott, G. Buckton, *Int. J. Pharm.* 294 (2005) 129.
- [82] M. Ohta, G. Buckton, *Int. J. Pharm.* 289 (2005) 31.
- [83] A. Columbano, G. Buckton, P. Wikeley, *Int. J. Pharm.* 253 (2003) 61.
- [84] M. Ohta, G. Buckton, *Int. J. Pharm.* 272 (2004) 121.
- [85] M. Ohta, G. Buckton, *Int. J. Pharm.* 269 (2004) 81.
- [86] Y. Yokoi, E. Yonemochi, K. Terada, *Int. J. Pharm.* 280 (2004) 67.
- [87] V. Swaminatham, J. Cobb, I. Saracovan, *Int. J. Pharm.* 312 (2006) 158.
- [88] K.V. Kumar, F. Rocha, *J. Chromatogr. A* 1216 (2009) 8528.
- [89] B.A.P. Ass, M.N. Belgacem, E. Frollini, *Carbohydr. Polym.* 63 (2006) 19.
- [90] S. Baumgartner, O. Planinšek, S. Srčić, J. Kristl, *Eur. J. Pharmaceut. Sci.* 27 (2006) 375.
- [91] X. Han, X. Ma, J. Liu, H. Li, *Carbohydr. Polym.* 78 (2009) 533.
- [92] P. Rousset, P. Sellapan, P. Daoud, *J. Chromatogr. A* 969 (2002) 97.
- [93] G. Buchler-Diller, M.K. Inglesby, Y. Wu, *Colloids Surf., A* 260 (2005) 63.
- [94] G. Czeremuszkín, P. Mukhopadhyay, S. Sapiéha, *J. Colloid Interface Sci.* 194 (1997) 127.
- [95] O. Planinšek, J. Zadnik, Š. Rozman, M. Kunaver, R. Dreu, S. Srčić, *Int. J. Pharm.* 256 (2003) 17.
- [96] N. Cordeiro, C. Gouveia, A.G.O. Moraes, S.C. Amico, *Carbohydr. Polym.* 84 (2011) 110.
- [97] N. Shetty, D. Cipolla, H. Park, Q.T. Zhou, *Expet Opin. Drug Deliv.* (2019), <https://doi.org/10.1080/17425247.2020.1702643>.
- [98] I.M. Grimsey, J.C. Feeley, P. York, *J. Pharmacol. Sci.* 91 (2002) 571.
- [99] T. Školáková, L. Souchová, J. Patera, M. Pultar, A. Školáková, P. Zámstný, *Eur. J. Pharmaceut. Sci.* 130 (2019) 247.
- [100] S.C. Das, I.G. Tucker, P.J. Stewart, *Curr. Pharmaceut. Des.* 21 (2015) 3932.
- [101] T. Školáková, J. Patera, P. Zámstný, 8th International Granulation Workshop, At Sheffield, UK, 2017. <https://www.researchgate.net/publication/328043647>.
- [102] D.T. Tran, D. Majerová, M. Veselý, L. Kulaviak, M.C. Ruzicka, P. Zámstný, *Int. J. Pharm.* 556 (2019) 383.
- [103] V. Karde, C. Choroí, *Int. J. Pharmaceutics* 485 (2015) 192.

- [104] M. Težyk, E. Jakubowska, K. Milczewska, B. Milanowski, A. Voelkel, J. Lulek, *Drug Dev. Ind. Pharm.* 43 (2017) 911.
- [105] G. Buckton, H. Gill, *Adv. Drug Deliv. Rev.* 59 (2007) 1474.
- [106] H.E. Newell, G. Buckton, *Pharm. Res.* 21 (2008) 1440.
- [107] S. Maruyama, E. Yonemochi, S. Hasegawa, S. Suzuki, H. Minami, *Int. J. Pharm.* 52 (2017) 118.
- [108] B. Shi, S.Z. hao, L. Jia, L. Wang, *Carbohydr. Polym.* 67 (2007) 398.
- [109] A. Boutboul, F. Lenfant, P. Giampaoli, A. Feigenbaum, V. Ducruet, *J. Chromatogr. A* 969 (2002) 9.
- [110] D.S. Keller, P. Luner, *Colloids Surf., A* 161 (2000) 401.
- [111] M.-P. Comard, R. Calvet, H. Balard, J.A. Dodds, *Colloids Surf., A* 238 (2004) 37.
- [112] M. Rückriem, A. Inayat, D. Enke, R. Gläser, W.-D. Einicke, R. Roskmann, *Colloids Surf., A* 357 (2010) 21.
- [113] C. Sun, J.C. Berg, *J. Colloid Interface Sci.* 260 (2003) 443.
- [114] Y.-C. Yang, S.-B. Jeong, B.-G. Kim, P.-R. Yoon, *Powder Technol.* 191 (2009) 117.
- [115] S.K. Milonjić, *Colloids Surf., A* 149 (1999) 461.
- [116] S. Lazarević, Ž. Radovanović, D. Veljović, A. Onjia, D. Janačković, R. Petrović, *Appl. Clay Sci.* 43 (2009) 41.
- [117] D.M. Ansari, G.J. Price, *Polymer* 45 (2004) 1823.
- [118] J.-B. Donnet, H. Balard, N. Nedjari, B. Hamdi, H. Barthel, T. Gottschalk-Gaudig, *J. Colloid Interface Sci.* 328 (2008) 15.
- [119] M.-P. Comard, R. Calvet, H. Balard, J.A. Dodds, *Colloids Surf., A* 232 (2004) 269.
- [120] M.P. Comard, R. Calvet, J.A. Dodds, H. Balard, *Powder Technol.* 128 (2002) 262.
- [121] S. Hamdi, B. Hamdi, Z. Kessaissia, H. Barthel, H. Balard, J.B. Donnet, *J. Chromatogr. A* 969 (2002) 143.
- [122] S. Mohammadi-Jam, K.E. Waters, *Adv. Colloid Interface Sci.* 212 (2014) 21.
- [123] S. Mohammadi-Jam, K.E. Waters, *Miner. Eng.* 66–68 (2016) 112.
- [124] L.L. Skovbjerg, D.V. Okhrimenko, J. Khoo, K.N. Dalby, T. Hassenkam, E. Makovicky, S.L.S. Stipp, *Energy Fuels* 27 (2013) 3642.
- [125] X.L. Osorio Barajas, M.A. Jochmann, T. Hüffer, B. Schilling, T.C. Schmidt, *J. Separ. Sci.* 40 (2017) 2390.
- [126] B. Mészáros, G. Járvas, L. Hajba, M. Szigeti, A. Dallos, A. Guttman, *Sensor. Actuator. B Chem.* 258 (2018) 1184.
- [127] M. Rudolph, R. Hartmann, *Colloids Surf. A Physicochem. Eng. Asp.* 513 (2017) 380.
- [128] J.F. Gamble, M. Leane, D. Olusanmi, M. Tobyn, E. Supuk, J. Khoo, M. Naderi, *Int. J. Pharm.* 422 (2011) 238.
- [129] L.G.H.J. Segeren, M.E.L. Wouters, M. Bos, J.W.A. van den Berg, G.J. Vancso, *J. Chromatogr. A* 969 (2002) 215.
- [130] M.N. Belgacem, A. Blayo, A. Gandini, *J. Colloid Interface Sci.* 182 (1996) 431.
- [131] C. Castro, G.M. Dorris, C. Daneault, *J. Chromatogr. A* 969 (2002) 313.
- [132] V. Lavaste, J.F. Watts, M.M. Chehimi, C. Lowe, *Int. J. Adhes. Adhes.* 20 (2000) 1.
- [133] B.B. Hole, D.S. Keller, W.M. Burry, J.A. Schwarz, *J. Chromatogr. B* 879 (2011) 1847.
- [134] O. Inel, D. Tapaloglu, A. Askin, F. Tümssek, *Chem. Eng. J.* 88 (2002) 255.
- [135] C. Bilgic, A. Askin, *J. Chromatogr. A* 1006 (2003) 281.
- [136] F. Tümssek, O. Inel, *Chem. Eng. J.* 94 (2003) 57.
- [137] A. Aşkin, C. Bilgiç, *Chem. Eng. J.* 112 (2005) 159.
- [138] E. Diaz, S. Ordonez, A. Vega, J. Coca, *J. Chromatogr. A* 1049 (2004) 139.
- [139] C. Bilgiç, F. Tümssek, *J. Chromatogr. A* 1162 (2007) 83.
- [140] E. Diaz, S. Ordonez, A. Auroux, *J. Chromatogr. A* 1095 (2005) 131.
- [141] E. Diaz, S. Ordonez, A. Vega, J. Coca, *J. Chromatogr. A* 1049 (2004) 161.
- [142] B. Strzemiecka, M. Sandomierski, A. Voelkel, *J. Inorg. Organomet. Polym.* 29 (2019) 1439.
- [143] B. Niederer, A. Le, E. Cantergiani, *J. Chromatogr. A* 996 (2003) 189.
- [144] V. Oliva, B. Mrabet, M.I.B. Neves, M.M. Chehimi, K. Benzarti, *J. Chromatogr. A* 969 (2002) 261.
- [145] I.B. Neves, M. Chabut, C. Perruchot, M.M. Chehimi, K. Benzarti, *Appl. Surf. Sci.* 238 (2004) 523.
- [146] C. Perruchot, M.M. Chehimi, M.-J. Vaulay, K. Benzarti, *Cement Concr. Res.* 36 (2006) 305.
- [147] F. Djouani, C. Connan, M. Delamar, M.M. Chehimi, K. Benzarti, *Constr. Bulid. Mater.* 25 (2011) 411.
- [148] J.M.R.C.A. Santos, J.T. Guthrie, *Mater. Sci. Eng. R* 50 (2005) 79.
- [149] K.E. Fagelman, J.T. Guthrie, *J. Chromatogr. A* 1095 (2005) 145.
- [150] M. Kazayawoko, J.J. Balatincez, M. Romansky, *J. Colloid Interface Sci.* 190 (1997) 408.
- [151] A. van Asten, N. van Veenendaal, S. Koster, *J. Chromatogr. A* 888 (2000) 175.
- [152] E. Cantergiani, D. Benczedi, *J. Chromatogr. A* 969 (2002) 103.
- [153] A. Vega, F.V. Diez, P. Hurtado, J. Coca, *J. Chromatogr. A* 962 (2002) 153.
- [154] P. Jandura, B. Riedl, B.V. Kokta, *J. Chromatogr. A* 969 (2002) 301.

- [155] X. Huang, B. Shi, B. Li, L. Li, X. Zhuang, S. Zhao, *Polym. Test.* 25 (2006) 970.
- [156] N. Riba, M. Nardin, J.-Y. Drean, R. Frydrych, *J. Colloid Interface Sci.* 314 (2007) 373.
- [157] B. Lindsay, M.-L. Abel, J.F. Watts, *Carbon* 45 (2007) 2433.
- [158] N. Cordeiro, C. Gouveia, M.J. John, *Ind. Crop. Prod.* 33 (2011) 108.
- [159] S. Naseri, W.C. Lepry, M.S. Mohammadi, K.E. Waters, S.N. Nazhat, *Biomed. Glas.* 4 (2018) 131.
- [160] R.H. Mills, D.J. Gardner, R. Wimmer, *J. Appl. Polym.* 110 (2008) 3880.
- [161] R.H. Mills, W.T.Y. Tze, D.J. Gardner, A. van Heiningen, *J. Appl. Polym.* 109 (2008) 3519.
- [162] C.S. Barrera, K. Cornish, *J. Compos. Sci.* 3 (2019) 102.
- [163] N. Cordeiro, C. Mendonc, L.A. Pothan, A. Varma, *Carbohydr. Polym.* 88 (2012) 125.
- [164] J.H. Leala, C.M. Moore, A.D. Sutton, T.A. Semelsberger, *Ind. Crop. Prod.* 137 (2019) 628.
- [165] P.N. Jacob, J.C. Berg, *Langmuir* 10 (1994) 3086.
- [166] L. Huber, S.B. Hauser, E. Brendlé, P. Ruch, J. Ammann, R. Hauert, R.N. Widmer, C.J. Ubert, S.K. Matam, S. Yoon, Y. Zhang, M.M. Koebel, *Microporous Mesoporous Mater.* 276 (2019) 239.
- [167] L. Cossaruto, C. Vagner, G. Fiqueneisel, J.V. Weber, T. Zimny, *Appl. Surf. Sci.* 177 (2001) 207.
- [168] C. Vagner, G. Fiqueneisel, T. Zimny, P. Burg, B. Grzyb, J. Machnikowski, J.V. Weber, *Carbon* 41 (2003) 2847.
- [169] Y. Wu, Z. Li, H. Xi, *Carbon* 42 (2004) 3003.
- [170] G.S. Singh, D. Lal, V.S. Tripathi, *J. Chromatogr. A* 1036 (2004) 189.
- [171] E. Diaz, S. Ordonez, A. Vega, J. Coca, *Microporous Mesoporous Mater.* 82 (2005) 173.
- [172] M. Perez-Mendoza, M.C. Almazan-Almazan, L. Mendez-Linan, M. Domingo-Garcia, F.J. Lopez-Garzon, *J. Chromatogr. A* 1214 (2008) 121.
- [173] H. Balard, D. Maafa, A. Santini, J.B. Donnet, *J. Chromatogr. A* 1198–1199 (2008) 173.
- [174] J. Xie, Q. Zhang, K.T. Chuang, *J. Catal.* 191 (2000) 86.
- [175] A.F.M. Barton, *CRC Handbook of Solubility Parameter and Other Cohesion Parameters*, CRC Press, Boca Raton, FL, 2000.
- [176] R.F. Blanks, J.M. Prausnitz, *Ind. Eng. Chem. Fundam.* 3 (1964) 1.
- [177] J.M. Barrales-Rienda, J. Vidal Gancedo, *Macromolecules* 21 (1988) 220.
- [178] J. Fall, K. Milczewska, A. Voelkel, *J. Mater. Chem.* 11 (2001) 1042.
- [179] A. Voelkel, J. Fall, *J. Chromatogr. A* 721 (1995) 139.
- [180] D. Topaloğlu Yazici, A. Aşkin, V. Bütün, *J. Chem. Thermodyn.* 40 (2008) 353.
- [181] D.D. Deshpande, D. Patterson, H.P. Schreiber, C.S. Su, *Macromolecules* 7 (1974) 530.
- [182] Inverse gas chromatography. Characterization of polymers and other materials, in: M.J. El-Hibri, W. Cheng, P. Hattam, P. Munk, D.R. Lloyd, T.C. Ward, H.P. Schreiber (Eds.) 391, ACS Symposium Series, Washington, 1989, p. 121.
- [183] O. Olabisi, *Macromolecules* 8 (1975) 316.
- [184] E. Fernandez-Sanchez, A. Fernandez-Torres, J.A. Garcia-Dominguez, J.M. Santiuste, E. Pertierra-Rimada, *J. Chromatogr.* 457 (1988) 55.
- [185] A.M. Farooque, D.D. Deshpande, *Polymer* 33 (1992) 5005.
- [186] C.C. Hsu, J.M. Prausnitz, *Macromolecules* 7 (1974) 320.
- [187] C.S. Su, D. Patterson, *Macromolecules* 10 (1977) 708.
- [188] J.C. Huang, *J. Appl. Polym. Sci.* 89 (2003) 1242.
- [189] J.C. Huang, *J. Appl. Polym. Sci.* 90 (2003) 671.
- [190] J.C. Huang, *Eur. Polym. J.* 42 (2006) 1000.
- [191] Z. Tan, G.J. Vancso, *Macromol. Theory Simul.* 6 (1997) 467.
- [192] F. Feraz, A.S.H. Hamou, S. Djadoun, *Eur. Polym. J.* 31 (1995) 665.
- [193] Z. Benabdelghani, A. Etxeberria, S. Djadoun, J.J. Iruin, C. Uriarte, *J. Chromatogr. A* 1127 (2006) 237.
- [194] L. Zhao, P. Choi, *Polimery* 43 (2002) 6677.
- [195] K. Milczewska, A. Voelkel, *J. Appl. Polym. Sci.* 107 (2008) 2877.
- [196] K. Milczewska, A. Voelkel, *J. Polym. Sci., Part B: Polym. Phys.* 44 (2006) 1853.
- [197] C. Zhao, J. Li, Z. Jiang, C. Chen, *Eur. Polym. J.* 42 (2006) 615.
- [198] S. Zhang, A. Tsuboi, H. Nakata, T. Ishikawa, *Fluid Phase Equilib* 194–197 (2002) 1179.
- [199] J.R. Galdamez, S.J. Kernion, J.L. Duda, R.P. Danner, *Polymer* 49 (2008) 2873.
- [200] G. Overejo, P. Perez, M.D. Romero, I. Diaz, E. Diez, *Eur. Polym. J.* 45 (2009) 590.
- [201] P.M. Budd, N.B. McKeown, B.S. Ghanem, K.J. Msayib, D. Fritsch, L. St arannikova, N. Belov, O. Sanfirova, Y. Yampolskii, V. Shantarovich, *J. Membr. Sci.* 325 (2008) 851.
- [202] J.V. Scicolone, P.K. Davis, R.P. Danner, J.L. Duda, *Polymer* 47 (2006) 5364.
- [203] R.Y.M. Huang, P. Shao, G. Nawawi, X. Feng, C.M. Burns, *J. Membr. Sci.* 188 (2001) 205.
- [204] H. Eser, F. Tihminlioglu, *Fluid Phase Equil.* 237 (2005) 68.

- [205] F. Tihminlioglu, R.P. Danner, *J. Chromatogr. A* 845 (1999) 93.
- [206] E. sz Kovats, G. Foti, A. Dallos, *J. Chromatogr. A* 1046 (2004) 185.
- [207] C. Etxabarren, M. Iriarte, C. Uriarte, A. Etxeberria, J.J. Iruin, *J. Chromatogr. A* 969 (2002) 245.
- [208] D.M. Ansari, G.J. Price, *Polymer* 45 (2004) 3663.
- [209] J.M.R.C.A. Santos, J.T. Guthrie, *J. Chromatogr. A* 1070 (2005) 147.
- [210] S. Ourdani, F. Amrani, *J. Chromatogr. A* 969 (2002) 287.
- [211] I.M. Shillcock, G.J. Price, *Polymer* 44 (2003) 1027.
- [212] E. Fekete, E. Foldes, B. Pukanszky, *Eur. Polym. J.* 41 (2005) 727.
- [213] Q.-C. Zou, S.-L. Zhang, S.-M. Wang, L.-M. Wu, *J. Chromatogr. A* 1129 (2006) 255.
- [214] A.B. Nastasović, A.E. Onjia, S.K. Milonjić, S.M. Jovanović, *J. Polym. Sci., Polym. Phys. Ed.* 43 (2005) 2524.
- [215] A.B. Nastasović, A.E. Onjia, S.K. Milonjić, Z.M. Vuković, S.M. Jovanović, *Macromol. Mater. Eng.* 290 (2005) 884.
- [216] A.B. Nastasović, N.L. Ignjatović, D.P. Uskoković, D.D. Marković, B.M. Ekmešić, D.D. Maksin, A.E. Onjia, *J. Mater. Sci.* 49 (2014) 5076.
- [217] M. Rajab, T. Hamieh, A. Airoudj, K. Mougin, K. Hariri, W. Rammal, H. Mortada, M. Akil, A. Kassas, J. Toufaily, *J. Res. Updates Polym.* 6 (2017) 76.
- [218] T. Hamieh, J. Toufaily, A.H. Mouneimne, *Chromatographia* 73 (2011) 99.
- [219] M. Rojewska, A. Bartkowiak, B. Strzemiecka, A. Jamrozik, A. Voelkel, K. Prochaska, *Carbohydr. Polym.* 171 (2017) 152.
- [220] L.J. Waters, A.K.M.M.H. Bhuiyan, *Colloids Surf., B* 141 (2016) 553.
- [221] M. Vovk, O. Planinšek, I.G. Ilić, M. Šernek, *J. Adhes. Sci. Technol.* 33 (2019) 2517.
- [222] I. Gutiérrez, E. Díaz, A. Vega, S. Ordóñez, A. Guerrero-Ruiz, E. Castillejos-López, I. Rodríguez-Ramos, *Thermochim. Acta* 602 (2015) 36.
- [223] M. Rieger, P.D. Thesis, Fakultät für Chemie und Pharmazie der Julius-Maximilians-Universität Würzburg, 2018.
- [224] B. Strzemiecka, A. Voelkel, D. Chmielewska, T. Sterzyński, *Int. J. Adhesion Adhes.* 51 (2014) 81.
- [225] B. Strzemiecka, J. Zieba-Palus, A. Voelkel, T. Lachowicz, E. Socha, *J. Chromatogr. A* 1441 (2016) 106.
- [226] A.F.M. Barton, *Chem. Rev.* 75 (1975) 731.
- [227] C.M. Hansen, *Hansen Solubility Parameters: A User's Handbook*, CRC Press, Boca Raton FL, 2007.
- [228] S. Abbott, C.M. Hansen, H. Yamamoto, *HSPiP: Hansen Solubility Parameters in Practice*, 2010, 9780955122026.
- [229] K. Ito, J.E. Guillet, *Macromolecules* 12 (1979) 1163.
- [230] G.J. Price, D.R. Lloyd, T.C. Ward, in: H.P. Schreiber (Ed.), *Inverse Gas Chromatography. Characterization of Polymers and Other Materials*, vol. 391, ACS Symposium Series, Washington, 1989, p. 48.
- [231] G.J. Price, I.M. Shillcock, *J. Chromatogr. A* 964 (2002) 199.
- [232] A. Voelkel, J. Janas, *J. Chromatogr. A* 645 (1993) 141.
- [233] K. Adamska, R. Bellinghausen, A. Voelkel, *J. Chromatogr. A* 1195 (2008) 146.
- [234] T. Lindvig, M.L. Michelsen, G.M. Kontogeorgis, *Fluid Phase Equil.* 203 (2002) 247.
- [235] P. Choi, T. Kavassalis, A. Rudin, *J. Colloid Interface Sci.* 180 (1996) 1.
- [236] F. Tümssek, M. Börekçi, D.T. Yazici, A. Aşkin, *Chromatographia* 73 (2011) 117.
- [237] U. Domańska, Z. Żołek-Tryznowska, *J. Chem. Thermodyn.* 42 (2010) 363.
- [238] N. Scott Bobbitt, J.W. King, *J. Chromatogr. A* 1217 (2010) 7898.
- [239] F. Mutelet, G. Ekulu, M. Rogalski, *J. Chromatogr. A* 969 (2002) 207.
- [240] T. Kitak, A. Dumicić, O. Planinšek, R. Šibanc, S. Srcić, *Molecules* 20 (2015) 21549.
- [241] G. Zhao, H. Ni, L. Jia, S. Ren, G. Fang, *ACS Omega* 3 (2018) 9722.
- [242] K. Adamska, A. Voelkel, *J. Chromatogr. A* 1132 (2006) 260.
- [243] K. Adamska, A. Voelkel, *Int. J. Pharm.* 304 (2005) 11.
- [244] S. Jankovic, G. Tsakiridou, F. Ditzinger, N.J. Koehl, D.J. Price, A.-R. Ilie, L. Kalantzi, K. Kimpe, R. Holm, A. Nair, B. Griffin, C. Saal, M. Kuentz, *J. Pharm. Pharmacol.* (2018), <https://doi.org/10.1111/jphp.12948>.
- [245] F. Mutelet, V. Butet, J.-N. Jaubert, *Ind. Eng. Chem. Res.* 44 (2005) 4120.
- [246] B. Charmas, R. Lebeda, *J. Chromatogr. A* 886 (2000) 133.
- [247] F. Thielmann, D.A. Butler, D.R. Williams, *Colloids Surf., A* 187–188 (2001) 267.
- [248] N.M. Ahfat, G. Buckton, R. Burrows, M.D. Ticehurst, *Eur. J. Pharmaceut. Sci.* 9 (2000) 271.
- [249] C. Tisserand, R. Calvet, S. Patry, L. Galet, J.A. Dodds, *Powder Technol.* 190 (2009) 53.
- [250] N.A. Katsanos, E. Iliopoulou, V. Plagianakos, H. Mangou, *J. Colloid Interface Sci.* 239 (2001) 10.

- [251] A.V. Dremetsika, P.A. Siskos, N.A. Katsanos, J. Hazard Mater. 149 (2007) 603.
- [252] N.A. Katsanos, G. Karaiskakis, Time-resolved Inverse Gas Chromatography and its Applications, HNB Publishing, New York, 2004.
- [253] D. Gavril, K.A. Rashid, G. Karaiskakis, J. Chromatogr. A 919 (2001) 349.
- [254] K.A. Rashid, D. Gavril, N.A. Katsanos, G. Karaiskakis, J. Chromatogr. A 934 (2001) 31.
- [255] N.A. Katsanos, J. Chromatogr. A 969 (2002) 3.
- [256] N.A. Katsanos, D. Gavril, G. Karaiskakis, J. Chromatogr. A 983 (2003) 177.
- [257] N.A. Katsanos, J. Chromatogr. A 1037 (2004) 125.
- [258] G. Karaiskakis, D. Gavril, J. Chromatogr. A 1037 (2004) 147.
- [259] F. Roubani-Kalantzopoulou, J. Chromatogr. A 1037 (2004) 191.
- [260] N.A. Katsanos, J. Kapolos, D. Gavril, N. Bakaoukas, V. Loukopoulos, A. Koliadima, G. Karaiskakis, J. Chromatogr. A 1127 (2006) 221.

Separation of stereoisomers by gas chromatography

Cecilia Cagliero, Barbara Sgorbini, Chiara Cordero, Erica Liberto, Patrizia Rubiolo, Carlo Bicchi

Dipartimento di Scienza e Tecnologia del Farmaco, University of Torino, Torino, Italy

23.1 Introduction

It is well known that the biological interaction is stereospecific and that biological processes in plants or animals are very often stereo-guided, thus usually generating chiral metabolites either pure or in an enantiomeric excess. Three examples of the different biological activities of the enantiomers of randomly chosen chiral volatile compounds are cited here. For instance, in the flavor and fragrance field, the enantiomers of some chiral odorants have different odors. This was first shown by Rienacker and Ohloff in 1961 with β -citronellol, whose (+)-enantiomer typically smells of citronella and whose (–)-enantiomer is reminiscent of geranium [1]. In the following years, different odors were detected for the enantiomers of several other volatile chiral compounds [2,3]. In the environmental field, enantiomers of some chiral synthetic pesticides take different pathways in their enzymatic degradation reactions, as shown for the enantioselective metabolization of the highly chlorinated, chiral hydrocarbon hexachlorocyclohexane, α -HCH in the liver of eider

ducks. Moreover, the use of the most active enantiomer can drastically reduce the amount of chiral pesticide that needs to be applied, thus contributing to sustainable agriculture with an important positive impact on the environment, as is the case for the 2-phenoxypropionic acids, in particular MCPP (4-chloro-2-methylphenoxy) propionic acid, whose (S)-enantiomer is fully inactive [4]. Another topic investigated in depth was the optimization of administered volatile inhalation anesthetics belonging to the haloether group (e.g., enflurane and isoflurane) in surgery. In agreement with theories of anesthetic mechanisms of action, which suggest that anesthesia may result from a specific anesthetic/receptor interaction, enantiomers of the same racemates may have different or improved pharmacological activities. The results with different enantiomers of the same haloether have however not been univocal [5,6].

Enantiomer recognition and enantiomeric excess (ee) and/or ratio (er) determinations of a chiral compound are therefore often mandatory to characterize a living organism and to define the biological activity of its components, in

particular in the pharmaceutical, food, environment, flavor, and fragrance fields.

Enantiomeric recognition has a significant daily-life impact in the quality characterization of matrices for different purposes including, among others:

- (i) to monitor the synthetic process of a compound (e.g., a drug)
- (ii) to define the optimal amount of a drug or a pesticide to administer by choosing the suitable enantiomer
- (iii) to confirm the origin of raw material from where a “natural” product is derived or its geographical origin
- (iv) to provide an additional step in quality control and to detect fraud or adulteration
- (v) to connect the chemical structure of a compound and its biological properties (structure/activity relationship)
- (vi) to define the biosynthetic pathway of a compound (metabolite) in a living matrix.

Two main approaches are available today for the separation of enantiomers by gas chromatography (GC):

- (a) the *indirect* approach that includes the derivatization of the investigated enantiomers to the corresponding diastereomers by reaction with an enantiomerically pure chiral auxiliary to make their separation possible with a conventional achiral or a chiral stationary phase (CSP). The reliability of this approach is mandatorily conditioned by the absence of (i) kinetic resolution and/or racemization of both *reagent* and *substrate* throughout the reaction, (ii) chiral fractionation or rearrangement during sample preparation, and (iii) discriminative detection of diastereomers [7].
- (b) the *direct* approach is based on a noncovalent diastereomeric interaction with a nonracemic CSP. The enantiomers are separated due to the rapid and reversible

formation of diastereomeric association complexes with different stabilities resulting in different retention times [8]. Several chiral selectors of different types, operating on different approaches, have been proposed for chiral recognition in GC [9,10] although most of them have not been commercially marketed for routine application [see paragraph 2–4]. To the best of the author's knowledge, three of them founded on different modes of selector–selectand interaction(s) have been commercialized and are widely used, although to a different extent and for different applications:

- ✓ *Indirect* separation of enantiomers with CSPs based on chiral amino acid (AA) derivatives via hydrogen bonding [11].
- ✓ *Direct* separation of enantiomers with chiral metal chelates as CSPs via complexation [12].
- ✓ *Direct* separation of enantiomers on CSPs based on cyclodextrin (CD) derivatives via host guest interaction and inclusion (inter alia) [13].

Derivatized CDs are now the most commonly used CSPs because of their *direct* enantioselectivity for a large number of chiral compounds with different chemical structures, organic functional groups, and polarity; on the other hand, chiral AA–derived CSPs remain the selectors of choice for the *indirect* GC recognition of chiral AAs.

This chapter is divided into two main parts. The first part describes the three commercially available groups of CSPs and their evolution, including theoretical considerations for enantiomer separation, as well as some aspects involved with routine chiral recognition. In addition, it also provides a short survey of recently introduced chiral selectors of different chemical types whose chiral recognition ability is based on different principles.

The second part deals with the strategy of chiral recognition, comprising enantiomer automatic identification or their excess or ratio

determination in complex mixtures by enantioselective GC (Es-GC) combined with mass spectrometry (Es-GC-MS). This part also includes a discussion of the potential of multidimensional and fast GC in chiral recognition, micropreparative Es-GC, and the development of total analysis systems. All subjects are discussed mainly with a focus on CD CSPs and illustrated with examples of real-world samples from mainly the natural product and food fields based on the authors' daily experience.

23.2 Chiral stationary phases for enantioselective gas chromatography

23.2.1 α -Amino acid derivatives as chiral selectors

The first gas chromatographic (GC) separation of enantiomers on a CSP was carried out by Gil-Av, Feibush, and Charles-Sigler in 1966 [14]. They applied the *indirect* approach to separate (at least partially) the 2-propanol, *n*-butanol, and cyclopentanol esters of N-trifluoroacetylalanine with a glass capillary column coated with N-trifluoroacetyl-L-isoleucine lauryl ester as CSP. The success of these experiments resulted in more extensive studies in this field mainly by Gil-Av and Feibush resulting in the separation of 18 AAs enantiomers as N-trifluoroacetyl- α -AA esters with N-trifluoroacetyl-D- or L-isoleucine lauryl ester and N-trifluoroacetyl-L-phenylalanine cyclohexyl ester as CSPs. They also showed that the L-configured CSP provided the reverse elution of the AAs, i.e., D-enantiomer before the L-enantiomer. Gil-Av's original idea was to transfer to GC the principle of the stereoselective peptide/enzyme interaction in biochemical systems. The separation of the enantiomers was mainly ascribed to hydrogen bonding between NH \cdots O=C- and, to a lesser extent, NH \cdots F functional groups. Moreover, the enantiomer recognition was strongly related to the N-terminal AA in the chiral selector. This finding enabled Feibush to synthesize the

versatile AA diamide selector N-lauroyl-L-valine-*tert*-butylamide [15]. The studies that followed led to the commercial introduction in 1977 of Chirasil-L-Val by Bayer's research group, a CSP consisting of L-valine-*tert*-butylamide condensed into a polysiloxane backbone [originally poly(dimethylsiloxane) and poly-(2-carboxypropyl)-methylsiloxane] obtained via total synthesis [16]. This CSP remains the reference for the *indirect* separation of AAs enantiomers even today. In 1985, the same research group synthesized the mirror-image CSP, Chirasil-D-Val, enabling the reversal of the elution order of the AAs enantiomers [17]. The following studies involved the development of column technology and of the chemistry of the stationary phase (i.e., surface pretreatment, transfer from borosilicate glass to fused-silica columns, immobilization, nature of the supporting polysiloxane(s), spacer between the chiral selector and the polymeric backbone, and its ordered distribution in the polymeric structure). All these aspects together with selectand derivatization procedures were reviewed by Schurig in 2012 [11].

A parallel and fundamental step for the separation of AAs enantiomers and related compounds with hydrogen bonding CSPs is the derivatization process. The well-known reasons for this procedure include the increase in volatility and thermal stability of the analyte(s) and/or the improvement of their separation and detectability, particularly for trace analysis with specific detectors (e.g., electron-capture detector ECD). In addition, with AA chiral recognition, derivatization is specifically adopted to promote the formation of further hydrogen bonds by introducing appropriate functional groups in the selectand(s) and to stabilize their stereochemistry and/or to avoid unwanted racemization [18]. In their early studies, Gil-Av and Feibush used a two-step procedure at room temperature to derivatize α -AAs to the corresponding N-perfluoroacyl-O-alkyl esters [8,14,19] without influence on their stereochemistry [20].

The α -AAs derivatives currently used with Chirasil-Val as CSP are the N-trifluoroacetyl-O-alkyl (methyl, propyl, or pentyl) esters and N-pentafluoropropionyl-O-2-propyl esters. The best N-perfluoroacyl and ester alkyl groups and derivatization conditions for α -AAs on Chirasil-Val were systematically investigated by Liardon [21]. In 1991, Hušek introduced a fast one-step process to derivatize α -AAs to the corresponding N(O)-alkoxycarbonyl alkyl esters with alkyl chloroformates. This one-step derivatization reaction is easy to automate, feasible in aqueous solutions at room temperature, employs commercially available reagents, and produces α -AA derivatives that are easy to isolate [22,23].

Fig. 23.1 illustrates (A) some of the hydrogen-bonding CSPs: (1) N-trifluoroacetyl-L-isoleucine lauryl ester; (2) N-trifluoroacetyl-L-valyl-L-valine cyclohexyl ester; (3) N-Lauroyl-L-valyl-*tert*-butylamide; (4) L-valine-*tert*-butylamide condensed with dimethylsiloxane copolymer (Chirasil-D-Val), and (B) the separation of N(O,S)-TFA-amino acid O-*n*-propyl ester enantiomers by capillary GC with a 20 m \times 0.25 mm glass capillary coated with Chirasil-L-Val 4. The first eluted peak within an AA enantiomeric pair is the D-enantiomer.

23.2.2 Chelates as chiral selectors

After the introduction by Gil-Av et al. of a CSP for chiral recognition operating with a hydrogen-bonding mechanism [14], in the early 1970s, Gil-Av and Schurig sensed the possibilities of abiotic selectors (i.e., chiral metal-organic coordination compounds) as CSPs for enantioselective GC. Gil-Av and Schurig's idea was to extend the π -complexation ability of silver(I) ions in alkene selective separations in argentation chromatography to the study of olefin-rhodium(I) coordination equilibria [25]. The study was focused on the enantiomer separation of racemic olefins using dicarbonyl-

rhodium(I)-3-(trifluoroacetyl)-(1*R*)-camphorate in squalane as CSP [26]. Schurig called this method *complexation gas chromatography* due to the nature of the chiral selector [12,27,28].

This method immediately gave promising results for enantioselective GC, in particular when using chiral selectors with the general formulae metal(II) bis [3-(trifluoroacetyl)-(1*R*)-camphorates] and metal(II) bis[3-(heptafluorobutanoyl)-(1*R*)-camphorates] where central metal atoms were manganese, cobalt, and nickel [29,30]. Further CSPs were also synthesized and evaluated by replacing camphor with other terpenic ketones, such as 3- and 4-pinanone, methylthujone, carvone, pulegone, menthone, and isomenthone [30]. Complexation GC was successfully applied to the separation of the enantiomers of racemates containing nitrogen, oxygen, and sulfur never separated before, such as alkyl-substituted aliphatic aziridines, oxiranes, and thiiranes [29] and oxygenated monoterpenoids [31]. On the other hand, the main limitation of these CSPs in enantioselective GC was the low-temperature stability of columns coated with the metal chelates dissolved in squalane; this limit was partially overcome by cross-linking the selectors to poly(dimethylsiloxane) (Chirasil-Metal) [32]. This method offered important insights into the basic principles of enantioselective GC including: (i) the concept of the retention-increment (chemical retention factor R') of the selectand on the selector to measure the contribution to enantioselectivity of the chiral selector from relative retention; (ii) the calculation of the thermodynamic data related to the molecular association selector/selectand-inert solvent at different temperatures; and (iii) theoretical study on coalescence phenomena and enantiomer interconversion. All these subjects were reviewed by Schurig in 2002 [12]. Fig. 23.2 illustrates the structure of: (1) nickel(II) bis[3-(heptafluorobutanoyl)-10-(ethylidene)-(1*S*)-camphorate] CSP; (2) the chromatogram of a freshly distilled peppermint oil:

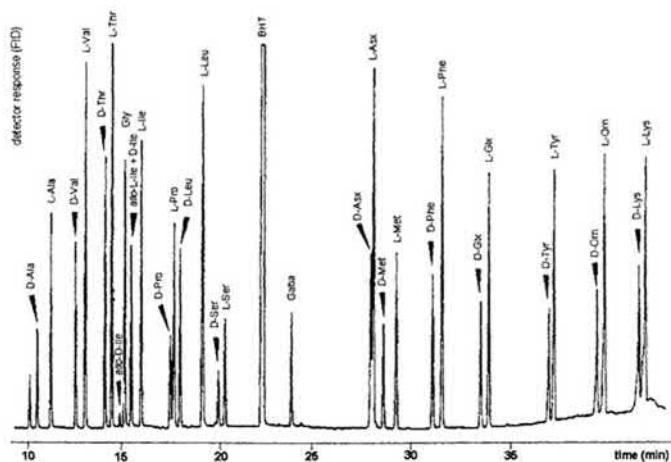
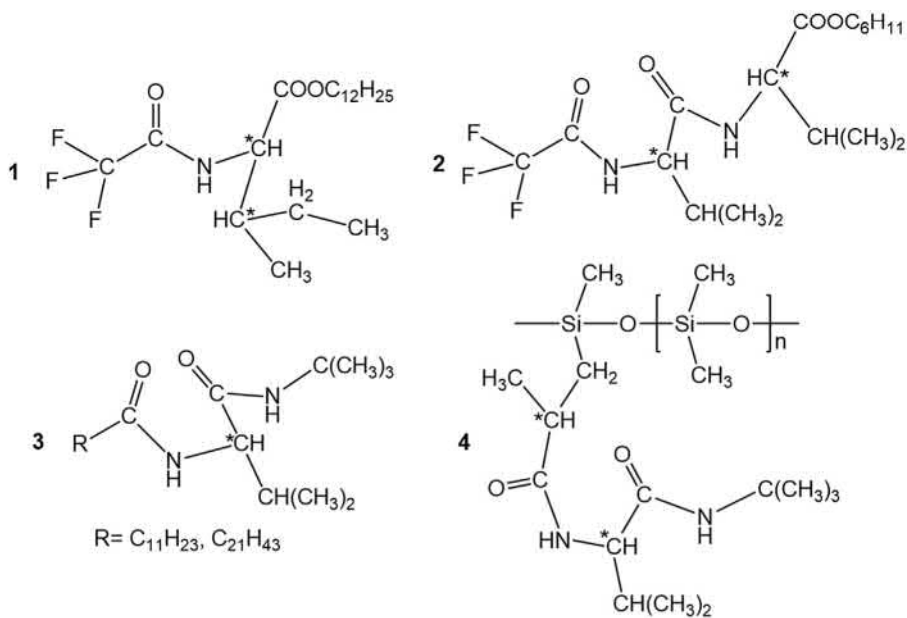


FIGURE 23.1 (A) Hydrogen-bonding CSPs: (1) N-trifluoroacetyl-L-isoleucine lauryl ester; (2) N-trifluoroacetyl-L-valyl-L-valine cyclohexyl ester; (3) N-Lauroyl-L-valyl-*t*-butylamide; (4) L-valine-*t*-butylamide condensed with dimethylsiloxane copolymer (Chirasil-D-Val); (B) enantioseparation of N(O,S)-TFA-amino acid O-*n*-propyl esters by capillary GC with a 20 m × 0.25 mm glass capillary coated with Chirasil-L-Val 4. The first eluted peak within an AA pair is the D-enantiomer. Reproduced from H. Frank, *Gas Chromatography of enantiomers on chiral stationary phases*, in: B. Holmstedt, H. Frank, B. Testa (Eds.), *Chirality and Biological Activity*, 1990, Alan R. Liss, Inc: New York. pp. 33–54 [24]. Permission requested.

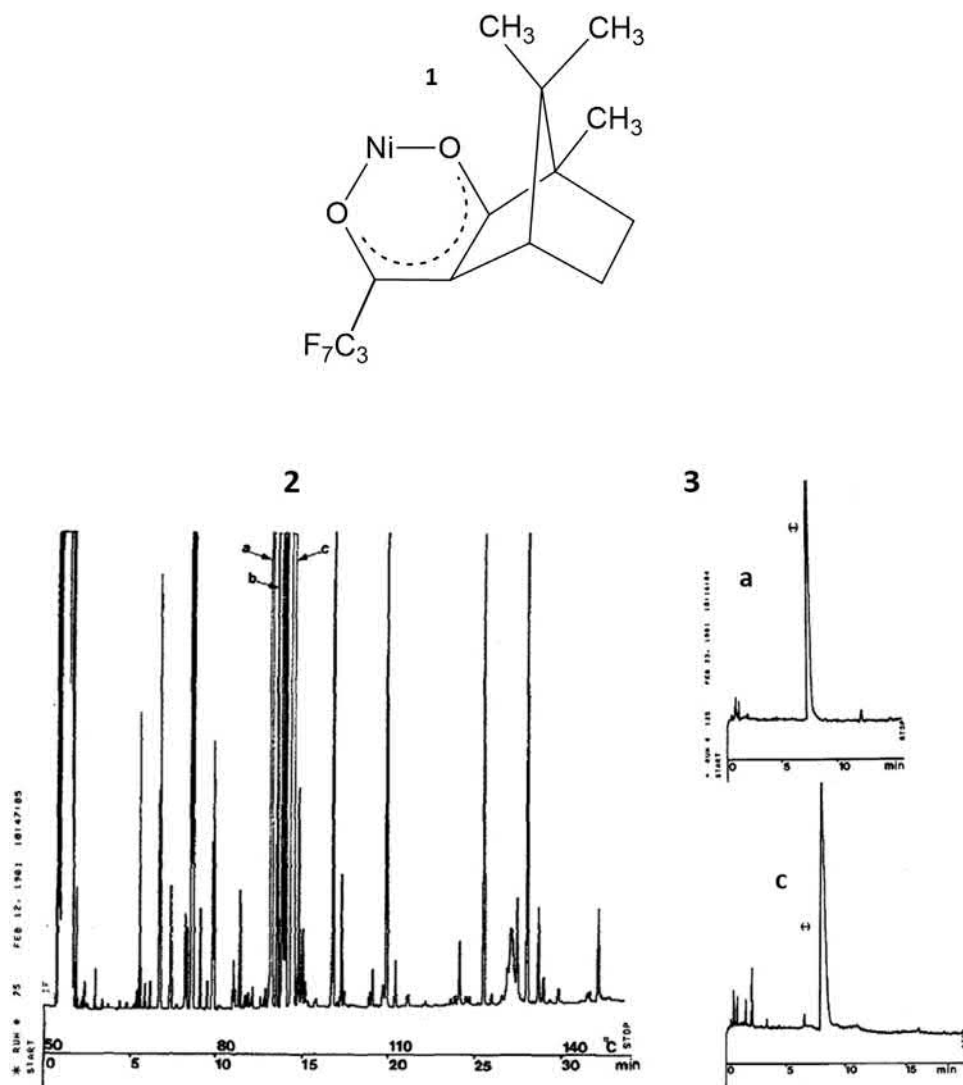


FIGURE 23.2 Complexation gas chromatography: (1) nickel(II) bis[3-(heptafluorobutanoyl)-10-(ethylidene)-(1S)-camphorate]; (2) a chromatogram for a freshly distilled peppermint oil: (a) menthone; (b) isomenthone; (c) menthol. (3) enantiomeric purity of menthone (a) and menthol (c) after heart-cut multidimensional GC (MDGC)-Es-GC of the freshly distilled peppermint essential oil. Analysis conditions: Column combination: first column OV-1 fused-silica open tubular $20\text{ m} \times 0.530\text{ mm} \times 1\text{ }\mu\text{m}$, second column nickel(II) bis[3-(heptafluorobutanoyl)-(1R)-camphorate] [Chira-Metal (I-4)] in SE-54, $12\text{ m} \times 0.22\text{ mm}$ (CC&CC, Kirchentellinsfurt, Germany). Reproduced from C. Bicchi, A. Pisciotto, *Use of two-dimensional gas chromatography in the direct enantiomer separation of chiral essential oil components*, *J. Chromatogr. A* 508 (1990) 341–348. Permission requested.

(a) menthone; (b) isomenthone; (c) menthol; as well as (3) separation of enantiomers of menthone (a) and menthol (c) after heart-cut GC-ES-GC for the same essential oil.

The highly specific enantioselectivity that limits the routine application of a single column to a small number of molecules, along with low column temperature stability and operative inflexibility, has restricted the use of enantioselective complexation GC to specialized laboratories. This has caused a gradual but constant decline of its importance, in particular after the introduction of derivatized CDs as CSPs in the early 1980s.

23.2.3 Derivatized cyclodextrins as chiral selectors

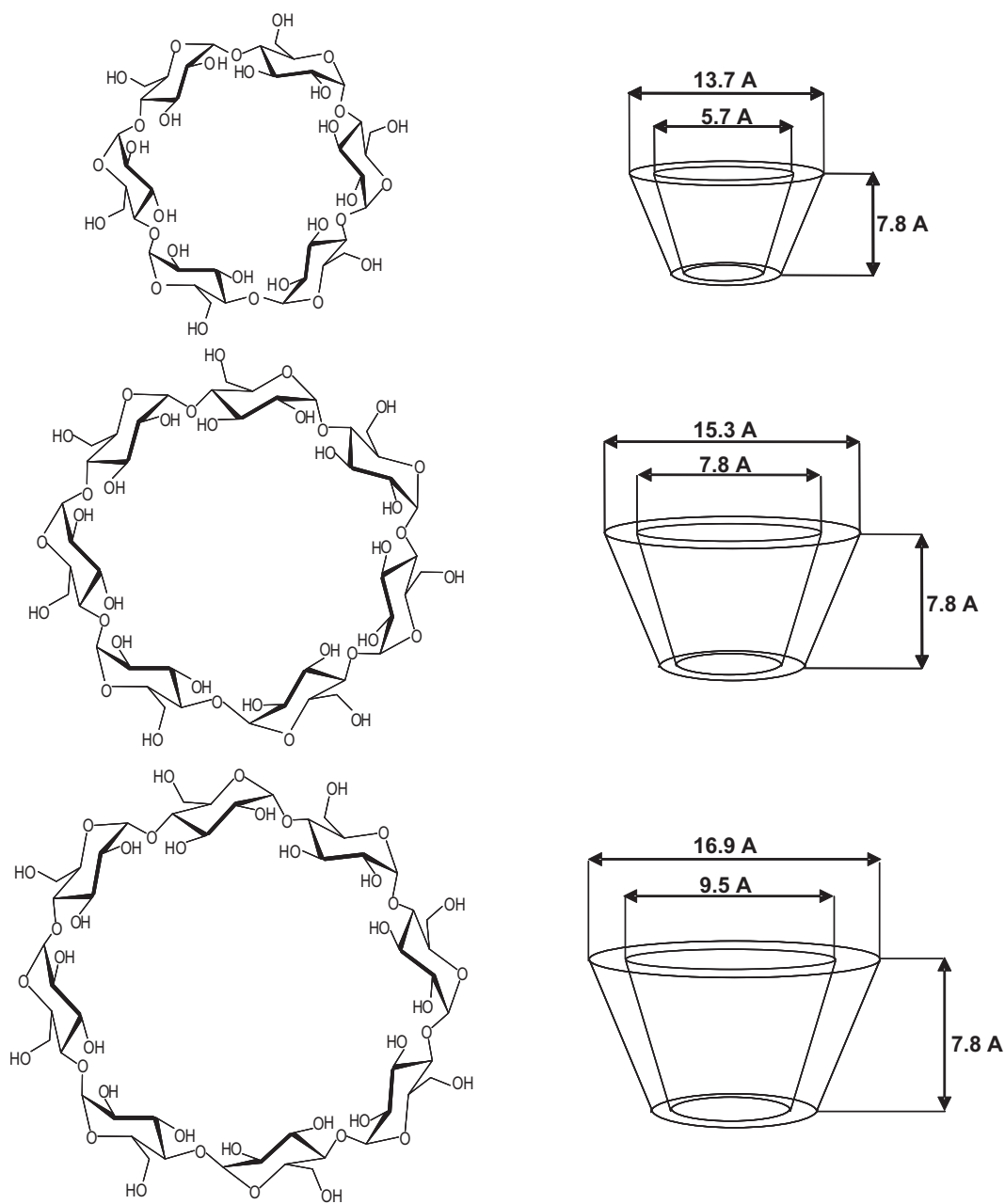
23.2.3.1 General overview of cyclodextrin chemistry

CDs were first isolated as a crystalline substance from starch digested from *Bacillus amylobacter* by Villiers in 1891 and their origin from starch confirmed by Schardinger in 1903 [33,34]. Their chemical and physical properties, inclusion capability, enzymatic production and isolation, and the full elucidation of their structure were the subject of studies over a period of about 30 years, from the 1930s to the late 1960s [35–39]. The three most applied CDs, i.e., α -CDs, β -CDs, and γ -CDs, are crystalline, homogeneous, nonhygroscopic compounds consisting of six, seven, and eight glucopyranose units, respectively, linked through α -1,4-glycosidic linkages. Each glucose unit contains three hydroxyl groups in position 2, 3, and 6. Fig. 23.3 illustrates the structure of α -, β -, and γ -CDs. The CD shape is similar to a hollow truncated cone where the hydroxyl secondary groups at C-2 and C-3 are located at the wide end or “mouth” of the CD and the primary C-6 hydroxyl at the narrow end or “bottom.” The three CDs described earlier have 30 for α -CD, 35 for β -CD, and 40 for γ -CD chiral centers.

23.2.3.2 Chiral stationary phases based on cyclodextrin derivatives

The first CD application in GC was by Schlenk and coworkers, in 1962, who used CD-based packed columns for the separation of achiral polar compounds [40]. Applications in enantioselective GC started at the beginning of the 1980s, with the fundamental studies of Smolkova-Keulemansova and of Koscielski and Sibilska [41–47]. The latter group used columns packed with a mixture of native α -CD in formamide to separate the enantiomers of α - and β -pinene, Δ -3-carene, and their hydrogenated derivatives [41]. The first applications of CDs in capillary GC were carried out almost concurrently by Juvancz et al. in 1987 [48] and Schurig et al. in 1988 [49]. Shortly after, Alexander et al. [50] and Venema and Tolsma [51] demonstrated that undiluted permethylated β -CD was a good chiral selector for separating enantiomers, albeit limited by its high melting point. This drawback was soon overcome by two different approaches:

- (a) Konig and coworkers proposed the use of room-temperature, liquid derivatives, mainly per-*n*-pentylated-, di-*n*-pentylated, or partially pentylated CDs, coated directly on the inner wall of the capillary column. These columns were used successfully to separate the enantiomers of chiral compounds with widely different chemical structures [52–55];
- (b) Schurig and Nowotny utilized a moderately polar polysiloxane (e.g., OV-1701) to dissolve permethylated- β -CD in analogy to Chirasil-Val [49,56]. This approach was immediately successful and nowadays these columns are the most widely used for routine chiral separations, since it combines the high CD enantioselectivity with the favorable GC properties of the poly(siloxanes). More recently, ionic liquids have been proposed as the diluting phase, and this topic is described later in the section dedicated to ionic liquids (Section 23.4.6)

FIGURE 23.3 Structures of α -, β -, and γ -cyclodextrins.

Further studies have been carried out to optimize the quality of the CD-based columns, which now have extended operating temperature ranges (0–240°C) and performances comparable to conventional columns [57,58].

About the same time, Schurig et al. [59] and Fisher et al. [60] permanently linked permethyl- β -CD to a poly(siloxane) backbone, which was then immobilized onto the inner wall of capillary columns by thermal treatment. The CSPs are known as “Chirasil-Dex.” [59,60].

In 2010, Huang et al. developed charged CDs by attaching a cationic pendant group to the CD to improve the chromatographic performance of columns utilizing ionic liquid as the diluting phase, discussed in Section 23.4.6 [61].

The regioselective alkylation and acylation of the three hydroxyl groups in positions 2, 3, and 6 of the CD rim strongly influence the enantioselectivity of the CD derivative. The most used substituents are “small” groups, i.e., mainly acetyl, methyl, or ethyl; their introduction improves the enantioselectivity of the CD, their solubility, and lowers their melting point. An important contribution toward extending the range of CD enantioselectivity and to improve their gas chromatographic performance was the derivatization of the primary C₆-hydroxy group with bulky substituents such as *tert*-butyldimethylsilyl (TBDMS) or *tert*-hexyldimethylsilyl (THDMS) groups [62,63]. These derivatives were first described by Blum and Aichholz [62,64] but they were mainly developed by Mosandl's group [64]. The bulky substituent at the smaller rim affects the CD conformation, avoids blockage of the cavity, and orients the analyte/CD interaction toward the wider rim, where the substituents of the secondary C2–OH and C3–OH groups condition the chiral recognition [63]. These derivatives are considered as a second generation of CD selectors due to their extended enantioselectivity and good chromatographic properties.

Unfortunately, after significant proliferation in the 1990s, the number of new CD derivatives

with higher, wider, or “new” enantioselectivity introduced in the last two decades is relatively low. New derivatives with such characteristics are required to extend the choice of chiral columns when a large number of enantiomers in a single sample need to be separated within “the one column for one problem” approach [65]. In 2010, the authors introduced “fully asymmetrically substituted derivatives” [66], with the term “asymmetric” here indicating different substituents at positions C2–OH, C3–OH, and C6–OH. The enantioselectivity of derivatives with the same group (mainly acetyl, ethyl, or methyl) in the C2–OH and C3–OH and bulky substituents (i.e., *t*-butyldimethylsilyl, TBDMS) in the C6–OH position is frequently complementary. Therefore, CD derivatives with different substituents in positions C2–OH and C3–OH at the wide rim may offer a synergic enantioselectivity useful in routine analysis for the simultaneous separation of several chiral compounds in a single run. This consideration was verified with the asymmetrically substituted methyl/ethyl derivatives (i.e., 6^{I-VII}-O-TBDMS-3^{I-VII}-O-ethyl-2^{I-VII}-O-methyl/3^{I-VII}-O-methyl-2^{I-VII}-O-ethyl- β -cyclodextrin), which were shown to function better than the corresponding symmetrical CDs (i.e., 6^{I-VII}-O-TBDMS-3^{I-VII}-O-methyl-2^{I-VII}-O-methyl/3^{I-VII}-O-ethyl-2^{I-VII}-O-ethyl- β -cyclodextrin), in terms of both the number of chiral compounds separated and the resolution of individual enantiomers [66].

A further option to extend enantioselectivity of CDs and to improve chromatographic performance is to include two or more chiral selectors in a single column. A number of attempts have been made, but the results were not always as good as anticipated. These included:

- (i) mixing two different CDs [67–70]
- (ii) synthetically condensing two CD units
- (iii) mixing two structurally different chiral selectors, for example: (1) by combining amino acid and CD derivatives (a) by simultaneous grafting, (b) by linking to a

poly(siloxane) [71], (c) by covalently linking amino acid derivatives with cyclodextrins [72,73], or (d) by mixing homochiral metal–organic framework (MOFs) with different central elements with permethylated and peramylated CD [74–76] (see Section 23.4.2).

These binary phases have often combined the enantioselective properties of each component extending the enantioselectivity of the resulting chiral selectors.

23.2.3.3 Mechanism of chiral recognition of cyclodextrin-based CSPs

It is rather difficult to rationalize the mechanism of chiral recognition with CD derivatives, since CD-based CSPs have been shown to separate numerous chiral compounds of different chemical types without a logical connection to the molecular shape, size, or functionalities of either the selectand or the selector. This is because the recognition process is multimodal and, *inter alia*, may involve inclusion, hydrogen bonding, dispersion forces, dipole–dipole interactions, electrostatic interactions, and hydrophobic interactions [39,77–79]. The relative retention of enantiomers depends on the steric fit into the CD cavity, controlled by their size and shape, and on their interaction with the substituents on the CD rim. In addition, Schurig's group has shown that the inclusion of a molecule within the CD cavity is not a mandatory requirement for successful chiral recognition, since they observed similar separations of chiral compounds with modified linear dextrans and per-n-pentylated amylose [80–82].

The separation of enantiomers is the result of the synergic occurrence of all the phenomena listed above, which results in differences in the low energy of each selectand (enantiomer)/CD selector diastereomeric association equilibria; the separation of the enantiomers is also favored by the high efficiency of the capillary columns [83]. Schurig and coworkers gave a remarkable

contribution (i) to building up a thermodynamic model to describe enantiomer separations with CD derivatives based on the concept of the retention increase R' (or retention increment) and (ii) to determining the difference in the free enthalpies of formation of the diastereomeric associates [84,85]. An in-depth discussion of this topic is outside the scope of this chapter. These results, however, have strongly influenced routine applications, because they show that the separation of enantiomer is under enthalpy control, thermodynamically driven, and based on fast kinetics and that the separation factor, α , increases as the temperature decreases. Therefore, as a general rule, the optimal separation of enantiomers is achieved at the lowest practical temperature.

23.2.4 Other chiral selectors

A number of other chiral selectors have been developed as CSPs for enantioselective GC, although most of them are not currently used for routine applications. This section is a short survey of these chiral selectors, namely cyclofructans (CFs), MOFs, porous organic cages (POCs) and metal–organic cages (MOCs), chiral mesoporous silicas (CMSs), and chiral ionic liquids. The characteristics and performance of this group of chiral selectors have been reviewed by Armstrong et al. [10] and Sheng-Ming Xie et al. [86].

23.2.4.1 Cyclofructans

CF derivatives as chiral selectors in GC were introduced by Armstrong and coworkers in 2010 [87,88]. CFs or cycloinulohexaoses are cyclic oligosaccharides containing 6–8 fructose units connected by β -(1–2) linkages. The best known are CF6 and CF7, which are made up of six or seven fructose units, respectively. CFs were first obtained by Kawamura et al. in 1989 by fermentation of inulin with an extracellular enzyme *Bacillus circulans* [89]. Fig. 23.4 illustrates their general structure.

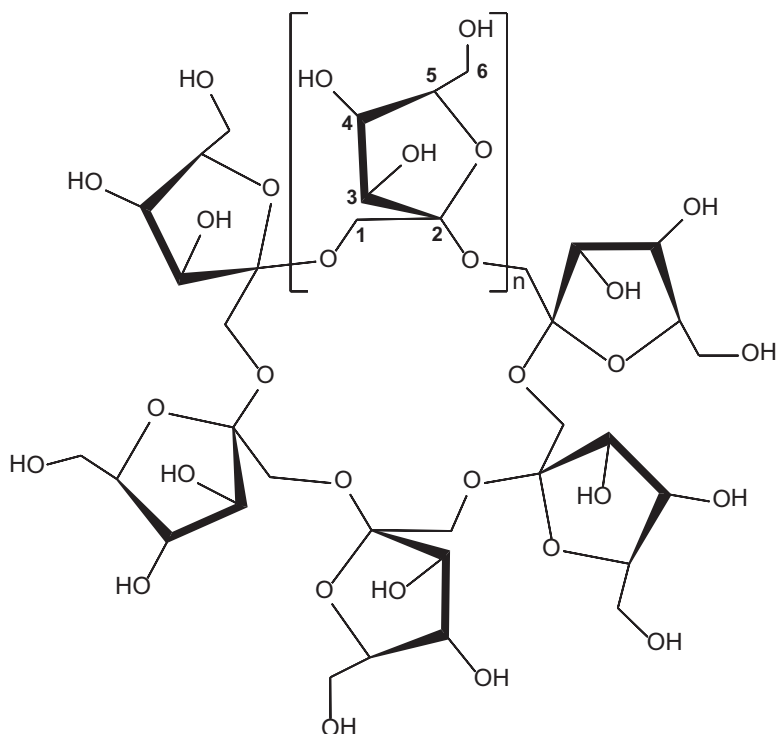


FIGURE 23.4 General structure of cyclofructans.

The separation mechanism of the enantiomers is probably related to hydrogen bonding and dipole–dipole interactions. The CF derivatives evaluated so far have been per-*O*-methylated cycloinulohexaose (PM-CF6, CF-CSP1), per-*O*-methylated cycloinuloheptose (PM-CF7, CF-CSP2), 4,6-di-*O*-pentyl cycloinulohexaose (DP-CF6, CF-CSP3), 4,6-di-*O*-pentyl-3-*O*-trifluoroacetyl cycloinulohexaose (DP-TA-CF6, CFCSP4), and 4,6-di-*O*-pentyl-3-*O*-propionyl cycloinulohexaose (DPPN-CF6, CF-CSP5) [87]. Column coated with the aforementioned CFs, either standalone or diluted in poly(siloxane), has been shown to separate a wide range of racemates, including AA derivatives, alcohols, amines, amino alcohols, β -lactams, tartrates, and esters.

23.2.4.2 Metal–organic frameworks

MOFs are a class of porous hybrid organic–inorganic microcrystalline materials consisting of metal cations or metal oxide clusters coordinated to organic ligands through coordination bonds [90]. MOFs were initially used as packing material for packed column GC [91], while Chen et al. were the first to apply them to capillary columns for the separation of isomeric xylenes and ethylbenzene [92].

Homochiral MOFs for enantiomer separations were first described by Xie et al. in 2010 [93]. They prepared derivatized MOFs with chiral functionalities accessible through open channels or cavities obtained by using single-enantiomer, organic ligands (AAs, organic acids, etc.) [94]. The MOF CSP $[\{\text{Cu}(\text{sala})\}_n]$ is a 3D

chiral channel framework where $H_2sala = N$ -(2-hydroxybenzyl)-L-alanine (MOF-CSP1) [93]. The enantiomer recognition of MOF columns primarily depends on the steric fit between the conformation of the selectand and the chiral channel framework complemented by other interactions, such as dispersion, dipole–dipole, and hydrogen bonding [93]. Chiral MOF $[Cu(sala)_n]$ CSP was used to separate a number of chiral compounds including AAs, alcohols, aldehydes, ketones, and organic acids. Fig. 23.5 demonstrates the separation of racemic amino acids as N-trifluoroacetyl O-isopropyl or O-methyl ester derivatives on MOF-CSP columns.

Several other homochiral MOFs were synthesized from different chiral building blocks and chiral ligands (e.g., D-camphoric acid, L-alanine, L-proline, L-leucine) and metals (Zn, Ni, Cu, Mn, Cd, Co, In, K, etc.). These derivatives afford different coordination geometries that influence the framework of the chiral MOFs. These homochiral MOFs were used to separate various racemates including alcohols, amine, nitriles, esters, and aldehydes [86]. The same group attempted to combine the enantioselectivity of MOFs with Cd, Co, and In as central metals with that of permethylated and peramylated CDs as mixed CSPs obtaining columns with a higher

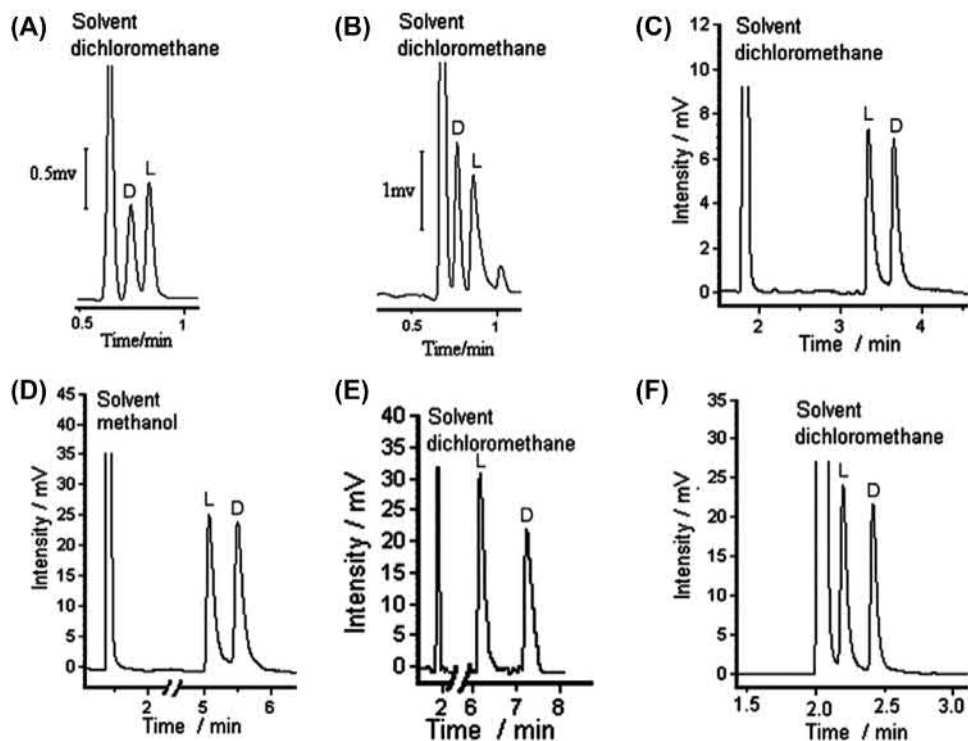


FIGURE 23.5 Separation of racemic isoleucine (A), valine (B), leucine (C), phenylalanine (D), phenylglycine (E), tryptophan (F) AA derivatives on the MOF-CSP1(A, B), CC3-R (or POC-CSP1) (C, D), CC5 (POC-CSP5) (E), and CMS-CSP1 (F) columns, respectively. (A), (B), (E), and (F) are trifluoroacetyl isopropyl ester derivatives; (C) and (D) are methyl ester derivatives. Reproduced from S.-M. Xie, Z.-J. Zhang, Z.-Y. Wang, L.-M. Yuan, *Chiral metal–organic frameworks for high-resolution gas chromatographic separations*, *J. Am. Chem. Soc.* 133 (31) (2011) 11892–11895. Permission requested.

enantioselectivity capability than for the single chiral selectors [74–76].

23.2.4.3 Chiral covalent organic frameworks

Chiral covalent organic frameworks (COFs) are a group of crystalline porous organic frameworks (POFs) obtained by a complex synthetic process from multidentate organic building blocks with strong covalent bonds, such as B–O, C=N, C=N(Ar), C=C, C–N, and B–N [86,95]. They have highly ordered structures, tunable functionalities, and a high chemical and thermal stability. Qian et al. synthesized a group of chiral COFs (CTpPa-1, CTpPa-2, and CTpBD) with which they prepared chiral COF-bound capillary columns and reported the baseline separation of 1-phenylethanol, 1-phenyl-1-propanol, limonene, and methyl lactate enantiomers [96].

23.2.4.4 Porous organic cages and metal–organic cages

POCs and MOCs are discrete crystalline materials with a permanent pore structure created through weak intermolecular interactions [97–100]. The pores in POCs are either intrinsic pores related to the structure of the molecule or extrinsic pores caused by the voids in the molecules formed during crystal piling. POCs are soluble in organic solvents and easily cast as thin porous films that maintain the same crystal structure in both the liquid and solid phases. This characteristic makes them suitable as GC stationary phases. Some POCs for separating enantiomers are now available; the best known and most effective are CC3-R, CC9, and CC10. They are obtained by a one-pot cyclo-amination reaction from 1,3,5-triformylbenzene, tris(4-formylphenyl)amine, and flexible diamines [101]. CC3-R, CC9, and CC10 are chiral structures with a tetrahedral shape with four triangular windows. They differ by how the windows and faces arrange to form a 3D

interconnected pore structure and also because the structure of the cage plays a fundamental role in the chiral recognition process. The chiral selectivity of these POCs is hypothesized to be due to a combination of host–guest inclusion processes, hydrogen-bonding interactions, dispersion forces, dipole–dipole interactions, π – π interactions, chiral steric fits, etc. Columns prepared from POCs showed high enantioselectivity for a large number of racemic compounds without derivatization, including chiral alcohols, diols, amines, alcohol amines, ethers, esters, ketones, halohydrocarbons, organic acids, amino acid methyl esters, and sulfoxides [102]. Fig. 23.5C and D illustrate the separation of racemic leucine and phenylalanine as the corresponding methyl ester on CC3-R (or POC-CSP1) column [102]. Fig. 23.5E illustrates the separation of racemic phenylglycine as the corresponding N-trifluoroacetyl O-isopropyl ester on CC5-R (or POC-CSP5) column [103].

MOCs, also known as metal–organic polygons or polyhedra (MOPs), are a further group of discrete supramolecular cages consisting of coordination-driven assembly by suitable metal ions or metal clusters and polydentate chiral ligands [104]. Xie et al., in 2018, used static coating to prepare a capillary column coated with a chiral MOC [Zn₃L₂] (MOC-CSP1) as a GC stationary phase [105]. A number of other chiral MOCs are available and shown to be useful for the separation of enantiomers [106]. The (MOC-CSP1) column was demonstrated to separate several racemates, including alcohols, diols, epoxides, ethers, halohydrocarbons, and esters. The results also illustrated the primary role of the chiral microenvironment of the cavity of the molecular cages for enantiomer discrimination.

23.2.4.5 Chiral mesoporous silica

Mesoporous materials with highly ordered structures containing organic chiral elements

have been investigated for applications in liquid chromatography, especially [107–110]. The first chiral nematic mesoporous silica (CNMS) (CMS-CSP1) CSP for GC was introduced in 2014 by Zhang et al. [111] and consisted of chiral nematic composite films synthesized by a spontaneous self-assembly of nanocrystalline cellulose (NCC) and tetramethoxysilane (TMOS) and high-temperature calcination. This CSP was able to separate several racemic alcohols, aldehydes, and AA derivatives. Fig. 23.5F illustrates the separation of racemic tryptophan as the corresponding N-trifluoroacetyl O-isopropyl ester derivatives on the CMS-CSP1 column [111].

The same research group explored other derivatives with different chiral anionic surfactants and costructure-directing agents (CSDA) (i.e., CMS-CSP2 [112] and CMS-CSP3 [113]) and an achiral surfactant (sodium dodecyl sulfate SDS) with a chiral amino alcohol ((R)-(–)-phenylglycinol) (CMS-CSP4) [114]. This new CMS-CSP extended the range of chiral compounds with different functional groups separated, to among others, alcohols, alcohol amines, aldehydes, ketones, esters, organic acids, epoxides, halohydrocarbons, alkenes, and AA derivatives [112–114].

23.2.4.6 Chiral ionic liquids

Ionic liquids (ILs) are typically organic salts with a melting point below 100°C, consisting of an organic cation containing N or P (i.e., mainly alkylimidazolium, phosphonium, etc.), and an organic or inorganic anion. Some have found applications as GC stationary phases due to their low volatility, good chromatographic properties, thermal stability, and high selectivity toward specific chemical classes. ILs have been used as achiral diluting phases for chiral selectors and chiral ILs as CSPs for the separation of enantiomers. Chiral ILs as stationary phases for GC were introduced by Armstrong's group in 2004 [115]. They synthesized both enantiomers of several chiral ILs based on ephedrine, in particular (1S,2R)-(+)-N,N-dimethylephedrinium

bis(trifluoromethane-sulfonyl)imide, (1R,2S)-(–)-N,N-dimethylephedrinium bis(trifluoromethanesulfonyl)imide, (1S,2S)-(+)-N,N-dimethyl pseudo-ephedrinium bis(trifluoromethanesulfonyl)imide. The columns prepared with these ILs enabled the separation of 14 chiral compounds and the reversal of the order of elution of the enantiomers when chiral analytes were analyzed with the (1S,2R)- versus the (1R,2S)-IL derivatives. However, a loss of the enantiomeric separation was observed at temperatures above 140°C because the chiral ILs tended to racemize. In 2011, Zhao et al. improved the enantioselectivity and the efficiency of the above columns by pretreating the fused-silica column surface with a dispersion of single-walled carbon nanotubes (SWNTs) prior to coating with the chiral ILs [116]. Fig. 23.6 illustrates the structure of (1S,2R)-(+)-N,N-dimethylephedrinium-bis(-trifluoromethanesulfonyl)imide ionic liquid CSP (A) and the separation of racemic *sec*-phenethyl alcohol, 1-phenyl-1-butanol, and trans-1,2-cyclohexanediol (from left to right) in (B) [115].

In 2001, Berthod et al. used 1-butyl-3-methylimidazolium chloride, an achiral ionic liquid, as a solvent for the dissolution of chiral selectors such as permethylated-β-CD and dimethylated-β-CD [117]. The CD-IL-coated columns were compared to those of similar commercial CD columns with the chiral selector diluted in a moderately polar poly(siloxane). The former resulted in higher efficiency but lower enantioselectivity. In 2010, Huang et al. [61] modified the aforementioned approach by decreasing the accessibility of the IL matrices to the CD cavity through two different approaches: in the first a bulkier dicationic IL was used to avoid obstruction of the CD cavity; and in the second charged CDs were synthesized by attaching a pendant cationic group to the CD to increase the electrostatic repulsion between the IL cation and the CD itself. Fig. 23.6C illustrates the structure of the ionic permethyl-β-CD, where R can be a butyl-3-methylimidazolium or methyltripropylphosphonium cation [61]. The most effective

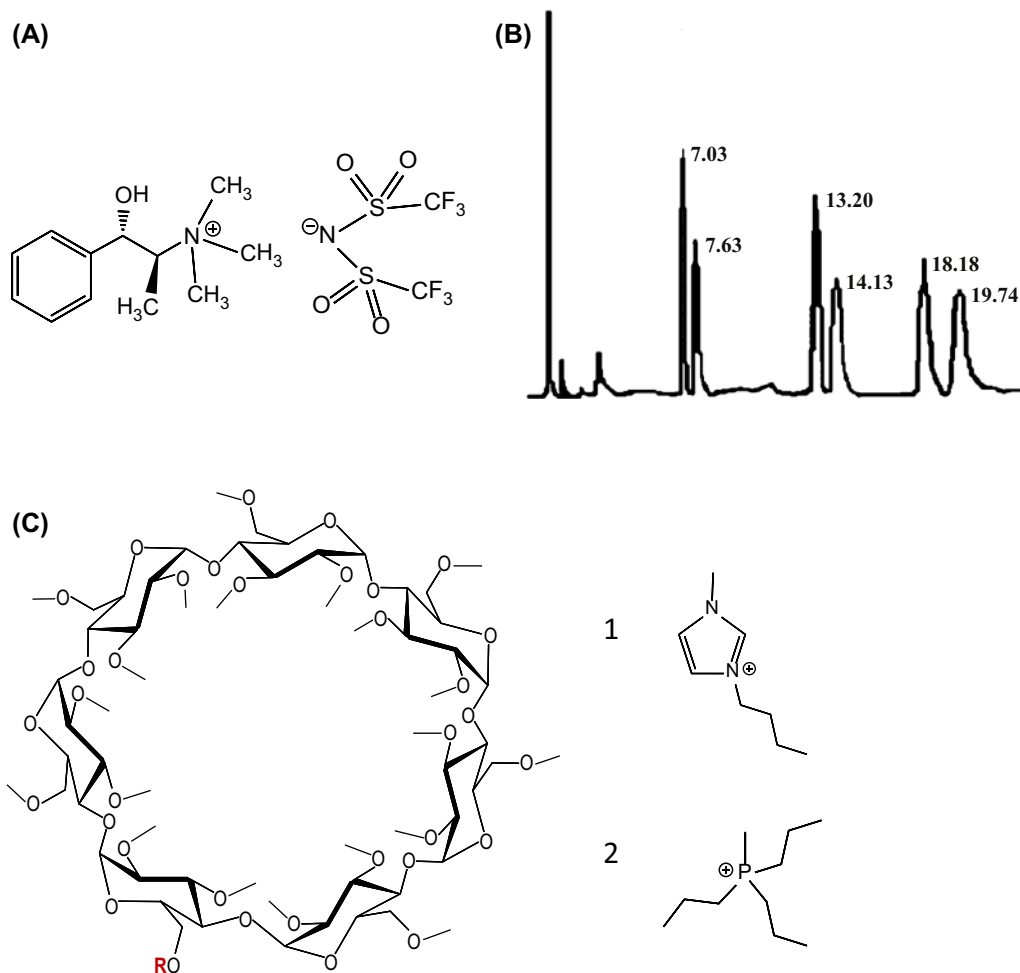


FIGURE 23.6 (A) (1*S*,2*R*)-(+)-*N,N*-dimethylphenhedrinium bis(trifluoromethanesulfonyl)imide; (B) separation of (from left to right) *sec*-phenethyl alcohol, 1-phenyl-1-butanol, and *trans*-1,2-cyclohexanediol. Chromatographic conditions: column: 8 m \times 50 μ m FS column coated with the CSP shown in (A). Structures of ionic permethyl- β -CD in which R is either a 1-butyl-3-methylimidazolium or methyltripropylphosphonium group (C). *Reproduced from K. Huang, X. Zhang, D.W. Armstrong, Ionic cyclodextrins in ionic liquid matrices as chiral stationary phases for gas chromatography, J. Chromatogr. A 1217 (32) (2010) 5261–5273; J. Ding, T. Welton, D.W. Armstrong, Chiral ionic liquids as stationary phases in gas chromatography, Anal. Chem. 76 (22) (2004) 6819–6822. Permission requested.*

charged CD in terms of efficiency and enantioselectivity was the alkylimidazolium-based ionic CD, whose columns were comparable in performance to those coated with the corresponding commercial CD.

23.3 Determination of the enantiomeric distribution

Chiral recognition aims to characterize a matrix by measuring precisely the enantiomer

distribution of one (or more) of its chiral marker(s). Enantiomeric distribution is usually expressed as *enantiomeric excess* (*ee*), *enantiomeric composition* (*ec*), or *enantiomeric ratio* (*er*) [118].

Enantiomeric excess, also known as *enantiomeric purity*, expresses the extra abundance of one enantiomer over the other and is defined as

$$ee = \frac{E_1 - E_2}{E_1 + E_2} \quad (23.1)$$

where E_1 and E_2 are the areas of the enantiomers, E_1 being the major enantiomer; *ee* ranges from 0 for racemic mixture to 1 for pure E_1 . In routine practice, *ee* is often expressed as a percentage

$$\%ee = \frac{E_1 - E_2}{E_1 + E_2} \cdot 100 = \%E_1 - \%E_2 \quad (23.2)$$

Enantiomeric composition (*ec*) is defined as the molar fraction of the major enantiomer x_{E_1} in a mixture:

$$ec = x_{E_1} = \frac{E_1}{E_1 + E_2} \quad (23.3)$$

In this case too, *ec* is generally expressed as a percentage

$$ec\% = x_{E_1} = \frac{E_1}{E_1 + E_2} \cdot 100 \quad (23.4)$$

Lastly, the *enantiomeric ratio*, *er*, is defined as

$$er = \frac{E_1}{E_2} \quad (23.5)$$

where E_1 is the major enantiomer; *er* extends from $ee = 1$, for a racemic mixture, to $ee = \infty$, for pure E_1 . The terms *er* and *ee* are correlated as follows

$$ee = \frac{(er - 1)}{(er + 1)} \quad (23.6)$$

and

$$er = \frac{(1 + ee)}{(1 - ee)} \quad (23.7)$$

In routine analysis, a correct determination of these parameters preferably requires the baseline separation (i.e., $R_s \geq 1.5$) of the two enantiomers.

23.4 Strategy for achieving chiral recognition

The second part of this chapter is devoted to chiral recognition strategies, and it is based on the authors' day-to-day experience. The proposed approach for chiral recognition will, therefore, be illustrated by examples mainly from the flavor and fragrance field using columns coated with CD derivatives as CSPs [13,119,120]. These examples are primarily directed toward the use of chiral recognition in routine quality control by applying "the one column for one problem" approach, developed in the authors' laboratory in the early 1990s. It entails the search for a chiral column specific for a homogeneous group of samples, simultaneously separating all of (or better, most of) the characteristic chiral markers. This approach enables one to overcome the conventional methods based on searching for the optimal enantiomer separation of a single analyte with one specific column to be applied to a set of heterogeneous samples, something that was highly time-consuming and might require several chiral columns for samples with more than one target chiral analyte to monitor [65].

23.4.1 Column efficiency and enantioselectivity

Column efficiency and enantioselectivity must periodically be tested to ensure reliable and consistent performances. In the authors' laboratory two dedicated tests are routinely used: (i) the Grob test to evaluate chromatographic performance of a column over time [121] and (ii) a chiral test mixture to check column enantioselectivity consisting of racemates with different volatilities, structures, and polarities [57]. Fig. 23.7 illustrates the separation of enantiomers

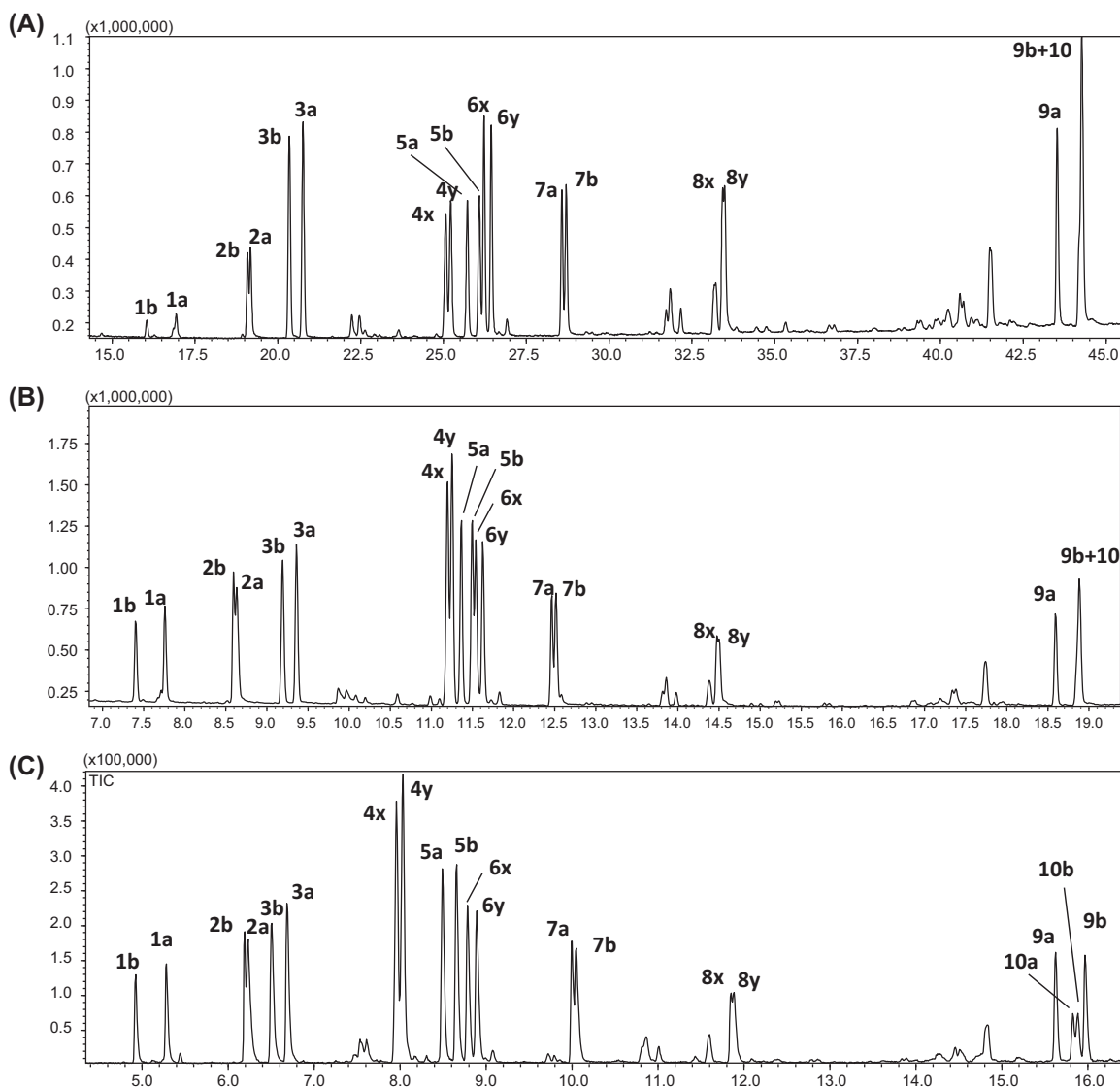


FIGURE 23.7 Chiral test chromatograms on a 30% (w/w) 2,3-di-O-ethyl-6-O-TBDMS-β-CD in PS086: (A) 25 m × 0.25 mm × 0.25 μm; (B) 10 m × 0.10 mm × 0.10 μm; and (C) 5 m × 0.10 mm × 0.10 μm. Peak identification: 1:limonene; 2:2-octanol; 3:camphor; 4:isobornyl acetate; 5:linalyl acetate; 6: cis-2-methyl-(3Z)-hexenyl butyrate; 7:menthol; 8: hydroxycitronellal; 9: γ-decalactone; 10: δ-decalactone; a: (R)-enantiomer; b: (S)-enantiomer; x and y: enantiomer configuration not assigned. Conditions: Injection: split mode with a split ratio 1:20 and temperature 220°C; Detector: FID, at 230°C; temperature program: 50°C/2°C min⁻¹/220°C for (A), 50°C/5°C min⁻¹/220°C for (B) and (C); and flow rate: 1 mL min⁻¹ for (A) and 0.4 mL min⁻¹ for (B) and (C).

(chiral test) developed by the authors on a 30% (w/w) 2,3-di-*O*-ethyl-6-*O*-TBDMS- β -CD in PS086 columns of different dimensions.

23.4.2 Analysis of enantiomers in complex samples

Reliable chiral recognition of markers in complex real-world samples generally requires a two-dimensional approach to avoid possible peak overlap or interferences due to the doubling of the number of chiral analyte peaks. This problem can often be overcome with the introduction of a second dimension either *in separation* (by conventional heart-cut H/C-MDGC or comprehensive 2DGC) (see Section 23.4.2.1) or *in detection*, by coupling GC with MS, or both of these. MS as a *second dimension in detection* for chiral recognition, however, requires a dedicated strategy for enantiomer identification because MS is not a chiral probe (see further).

23.4.2.1 Multidimensional gas chromatography as a second dimension in separation to locate and identify enantiomers in complex samples

Nowadays, two MDGC approaches are used in chiral recognition:

- (i) H/C-MDGC is the technique of choice for *ee* and *er* determination of chiral compounds in complex mixtures, in particular when a limited number of chiral components or simple clusters of peaks elute at different temperatures. With this technique, *the selected chiral components* (peaks) eluting from the first, achiral, column (first dimension-¹D) are online and automatically transferred through a dedicated time-programmable interface to the second, chiral column (second dimension-²D) [122–124]. Fig. 23.8 demonstrates the discrimination afforded by H/C-MDGC-Es-GC-MS for two tea tree essential oils (*Melaleuca alternifolia*) whose origins (i.e., China and Australia) are

indistinguishable by conventional GC [125–128]. The tea tree essential oils are separated on a polydimethylsiloxane-5% phenyl column (Mega 5) in the first dimension and a 30% (w/w) 2,3-di-*O*-ethyl-6-*O*-TBDMS- β -CD/PS086 chiral column for the transferred regions from the first dimension. The origin of the tea tree oils is established by measuring the percentage of enantiomer abundances of limonene, terpinen-4-ol, and α -terpineol.

- (ii) Comprehensive two-dimensional GC (GC \times GC) is used for highly complex matrices with several chiral components to monitor. In GC \times GC *each component* eluting from the first chiral column is online and automatically trapped, refocused, and reinjected into the second column, in a fixed time (4–8 s) by a thermal or valve-based focusing modulator [129]. In GC \times GC, the column coated with CD as CSP must be in the first dimension, because of the high efficiency required for an effective enantiomer separation (Section 23.4.1) Fig. 23.9 illustrates GC \times GC contour plots for lavender essential oil together with the zoom of two critical parts of the GC \times GC separation. Lavender essential oil is characterized by 14 chiral components: the strategy “one chiral selector for one problem” affords the chiral recognition of 13 of them and only the enantiomers of 1-octen-3-ol are not separated [130].

23.4.2.2 Chiral recognition in complex samples by gas chromatography with mass spectrometry as a second dimension in detection

The linear retention index (I^T) of a (chiral) compound is a number representative of the analyte–stationary phase interaction relative to a reference standard mixture (homologous series of n-alkanes or fatty acid methyl or ethyl esters) and is the most effective parameter to identify chiral components from gas chromatographic

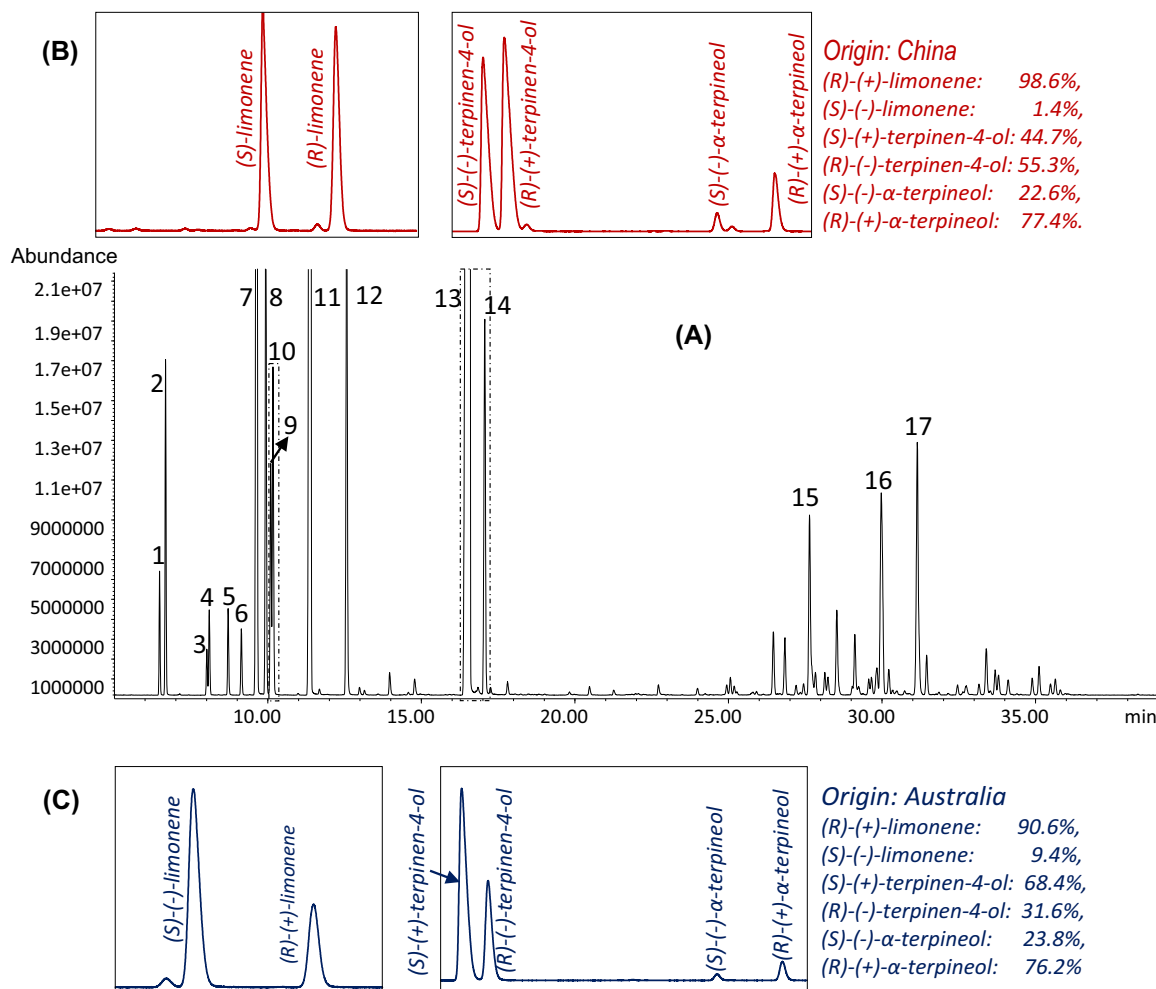


FIGURE 23.8 Discrimination of two tea tree oils from China and Australian by H/C-MDGC-Es-GC-MS. Column 1 Mega 5 (30 m × 0.25 mm × 0.25 μm), injection temperature 220°C, temperature program initially 50°C programmed at 3°C min⁻¹ to 220°C hold 2 min, carrier gas He flow rate 1 mL min⁻¹ and detector FID at 230°C. Column 2 30% (w/w) 2,3-di-O-ethyl-6-O-TBDMS-β-CD/PS086 (25 m × 0.25 mm × 0.25 μm), temperature program initially 50°C programmed at 2°C min⁻¹ to 220°C hold 2 min. Peak order first column: 1. α-thujene; 2. α-pinene; 3. sabinene; 4. β-pinene; 5. myrcene; 6. α-phellandrene; 7. δ-3-carene; 8. *p*-cymene; 9. limonene; 10. 1,8-cineole; 11. γ-terpinene; 12. α-terpinolene; 13. terpine-4-ol; 14. α-terpineol; 15. *trans*-β-caryophyllene; 16. ledene; and 17. δ-cadinene. Second column (B): heart-cut 10.05–10.45 min, limonene, terpine-4-ol (13), and α-terpineol (14) in an essential oil of Chinese origin and enantiomer percent abundances; (C) heart-cut 10.05–10.15 min, limonene, terpine-4-ol (13), and α-terpineol (14) in an essential oil of Australian origin and enantiomer percent abundances.

data because of its specificity, precision, and repeatability. In routine analysis, another reliable method to identify an analyte in a GC chromatogram obtained with a column coated with a specific stationary phase is retention time

locking (RTL) [131,132]. The correct identification and/or elution order within a pair, through chromatographic data, mandatorily requires at least the standard for one of the enantiomers is available, or any number of real-world samples

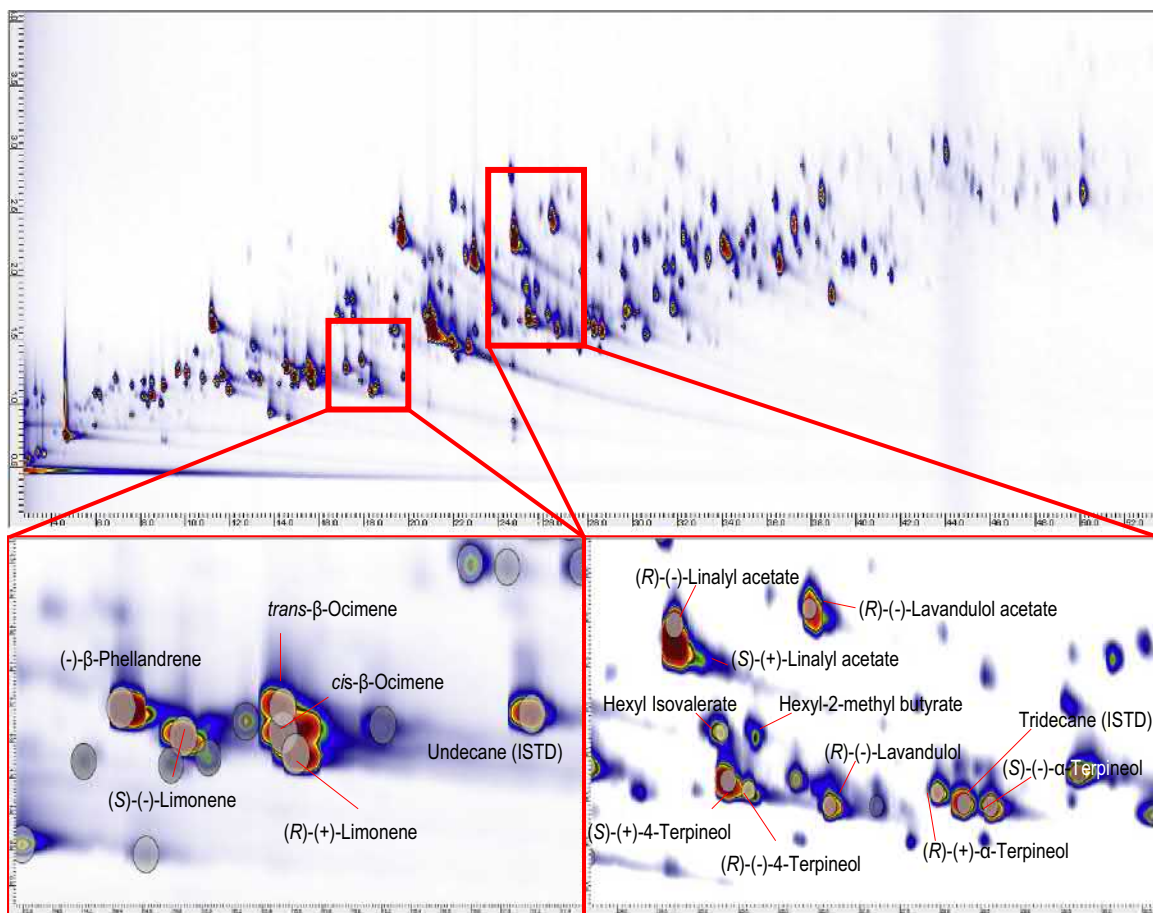


FIGURE 23.9 GC \times GC contour plot of lavender essential oil (*Lavandula angustifolia* P. Mill.). Analysis conditions: GC \times GC-MS system: Agilent 6890 GC and Agilent 5975 MSD (electron impact ionization at 70 eV); transfer line temperature 280°C, scan range m/z 35–250 in the fast scanning mode (12,500 amu/s). GC \times GC interface: KT 2004 loop modulator and modulation time 4 s. Column set: ¹D: 30% (w/w) 2,3-di-*O*-ethyl-6-*O*-TBDMS- β -CD in PS086 (25 m \times 0.25 mm \times 0.25 μm), ²D: OV1701 column (1 m \times 0.10 mm \times 0.10 μm). Modulation loop dimensions: 1 m \times 0.1 mm. Analysis conditions: split injection, ratio 1/20, temperature 250°C; carrier gas helium; Temperature program: 50°C (1 min), programmed at 2°C min^{-1} to 230°C with a 5 min hold. Reproduced from C. Cagliero, B. Sgorbini, C. Cordero, E. Liberto, P. Rubiolo, C. Bicchi, *Enantioselective gas chromatography with derivatized cyclodextrins in the flavour and fragrance field*, *Isr. J. Chem.* 56 (2016) 925–939. Permission requested.

where one reliably identified enantiomer is present either individually, or in a well-known enantiomeric excess. The mass spectra of two enantiomers, however, are indistinguishable because MS is not a chiral probe, making it impossible to identify which enantiomer is present in the investigated sample. The adoption of MS as a second dimension *in detection*

therefore implies that the mass spectrum of a chiral compound, under rigorously standardized analysis conditions, locates correctly each enantiomer in the chromatogram and that its I^T provides its unequivocal identification. I^T 's information is therefore a fundamental second orthogonal tool to identify an enantiomer complementary to its MS spectra. However, the I^T

potential for identification is often underestimated and seldom included in commercial GC-MS software.

In 2008, the authors' research group developed at an interlaboratory level an MS library for the identification of enantiomers in the flavor and fragrance field, where I^T s are an active part of the interactive matching criteria in combination with mass spectra [133–135]. Four different CD chiral selectors were used to ensure the separation of the enantiomers for most of the racemates routinely analyzed in a flavor and fragrance control laboratory:

- (i) 6^{1-VII}-O-methyl-3^{1-VII}-O-pentyl-2^{1-VII}-O-methyl-β-CD (2,6-di-O-methyl3-O-pentyl-β-CD) [136,137].
- (ii) 6^{1-VII}-O-TBDMS-3^{1-VII}-O-methyl-2^{1-VII}-O-methyl-β-CD (2,3-di-O-methyl-6-O-TBDMS-β-CD) [138].
- (iii) 6^{1-VII}-O-TBDMS-3^{1-VII}-O-ethyl-2^{1-VII}-O-ethyl-β-CD (2,3-di-O-ethyl-6-O-TBDMS-β-CD) [139].
- (iv) 6^{1-VII}-O-TBDMS-3^{1-VII}-O-acetyl-2^{1-VII}-O-acetyl-β-CD (2,3-di-O-acetyl-6-O-TBDMS-β-CD) [138].

Each enantiomer was characterized through its MS spectrum and I^T values, which were measured with columns coated with the four chiral selectors. The correct identification of an analyte is further cross-checked against the predetermined range within which its I^T must fall (retention index allowance or RIA) when used with columns with the same characteristics and under the same separation conditions. For the four CSP columns the experimental RIA value ranged between -1 and $+2 I^T$ units.

23.4.3 Evolution of mass spectrometry and reliable chiral recognition

Recent advances in mass spectrometry have enabled the routine use of highly effective soft ionization ion sources in combination with

tandem mass spectrometry (MS/MS or MSⁿ) and have dramatically increased the identification and quantitation power of GC-MS. Available systems include low-resolution triple quadrupole (QqQ—tandem-in-space) and ion trap (IT-MS—tandem-in-time) MS/MS analyzers to the powerful high-resolution MS systems (HRMS), mainly TOF-MS and Orbitrap, either individually or combined with a quadrupole or an ion-trap analyzer (Q-TOF or IT-TOF). The HRMS systems are mainly used for structure elucidation, given their ability to provide the exact mass of molecular ions and/or fragments at an accuracy below 5 ppm.

However, in some cases, enantiomer separation by GC with MS detection is unable to establish the authenticity of a sample, for example, samples of natural origin, as occurs when a chiral compound is present in racemic form, or with matrices deriving from processing and/or storage, or else when adulterated with a synthetic enantiomer. An important contribution to the unequivocal identification of the authenticity of these samples is afforded by combining enantiomer separation by GC with isotope ratio mass spectrometry (IRMS). This technique requires that the analytes eluting from the GC column are online combusted to CO₂ in a dedicated oven interface, from where the combustion product is directly introduced into an IRMS. GC-IRMS provides the ratio for stable isotopes, which for enantiomers from the same natural source is the same (δ -C¹³) even in the presence of partial enantiomer racemization. The diagnostic isotopic ratio is obtained by measuring simultaneously and with high precision (≤ 0.3 ‰) the abundances of 44 (¹²C¹⁶O₂), 45 (¹³C¹⁶O₂, ¹²C¹⁶O¹⁷O₂), and 46 (¹²C¹⁶O¹⁸O) fragments in the nmole range and by comparing the peak areas ratio of the two isotopic peaks to a standard reference value. Two groups, among others, have contributed particularly to the development of GC-IRMS of enantiomers in natural products and foods: (i) Mosandl's group, who applied this technique to chiral recognition

in these fields from the early 1990s, reviewed in Ref. [140]; and (ii) Mondello's group, who more recently investigated multidimensional enantioselective GC combined with combustion IRMS in depth, in order to determine the enantiomeric distribution and the isotopic ratios of the diagnostic markers of several foods, in particular citrus [141–146].

23.4.4 Enantioselective gas chromatography and separation speed

Long separation times are typically necessary for chiral recognition by GC; this is also true with CDs as CSPs because of the small differences in the energy involved with enantiomer recognition, which imposes low temperatures and high chromatographic efficiency (i.e., adoption of long columns). This contrasts with the current trend to increase the number of analyses required in a quality control laboratory, which makes it necessary to adopt high-throughput methods. Fast GC has successfully been applied to chiral recognition with CDs as chiral selectors. Routine fast GC can in general be achieved with short columns [147] with conventional or narrow internal diameter columns. Enantiomer separations with short CD columns were occasionally attempted in the past, resulting in separations in just a few seconds [148–150]. Short columns (and in particular narrow bore columns) not only increase separation speed and analyte detectability, because of peak sharpening [151], but also reduce the enantiomer elution temperature. The lower temperature results in a gain in enantioselectivity compared to columns of a conventional length, with at least a partial compensation for the loss of efficiency caused by shortening the column. This topic was investigated in detail by the authors' group, who proposed two complementary methods to accelerate routine enantiomer separations by GC [152,153]. In the first approach, the separation time is reduced at the expense of excess of resolution provided by columns coated with

the last-generation of CD derivatives for most chiral compounds in a sample (“the one column for one problem” approach) [65]. In other words, it consists of finding the most effective compromise between column length, temperature or temperature program rate, and flow rate enabling a correct *ee* or *er* determination of the chiral compound(s) investigated, even at the expense of the separation of other achiral sample components. MS (second dimension in detection) is here indispensable to overcome possible peak overlap by operating in extract-ion (SIM- or MIM-MS modes) to “focus” on the diagnostic and specific fragments of the separated enantiomers [153]. Fig. 23.10 illustrates the GC enantiomer separation of two pesticides (α -HCH (in black) and metrifonate or trichlorfon (in red: gray in printed version)) on 30% (w/w) 2,3-di-O-ethyl-6-TBDMS- β -CD in OV1701 narrow bore columns of 0.10 mm internal diameter and 0.10 μ m film thickness of different lengths. The separation time changes from about 7 min on a 10 m column to 2.8 min for the 2 m column (i.e., a reduction of about 60%), although a coelution occurs for the enantiomers of the two pesticides. These coelutions on the 2m column can be overcome by extracting the GC patterns of the diagnostic ions of the enantiomers for each of the chiral pesticides, i.e., 79 m/z for α -HCH and 181 m/z for triphosphate. A reduction of the column length from 10 to 5 m not only reduces the separation time by more than 10%, but also reduces the elution temperatures and, thereby, provides a comparable enantioselectivity and similar resolution, increasing from 2.3 to 2.7 for α -HCH and slightly decreasing from 5.2 to 4.9 for metrifonate.

The second approach [152] adopts the opposite strategy, i.e., the separation time is reduced by optimizing the GC conditions to obtain the maximum separation efficiency. Routine analyses are generally performed with a unique standardized method, in which to enable reliable component identification, relative retention times, linear retention indices, or retention time

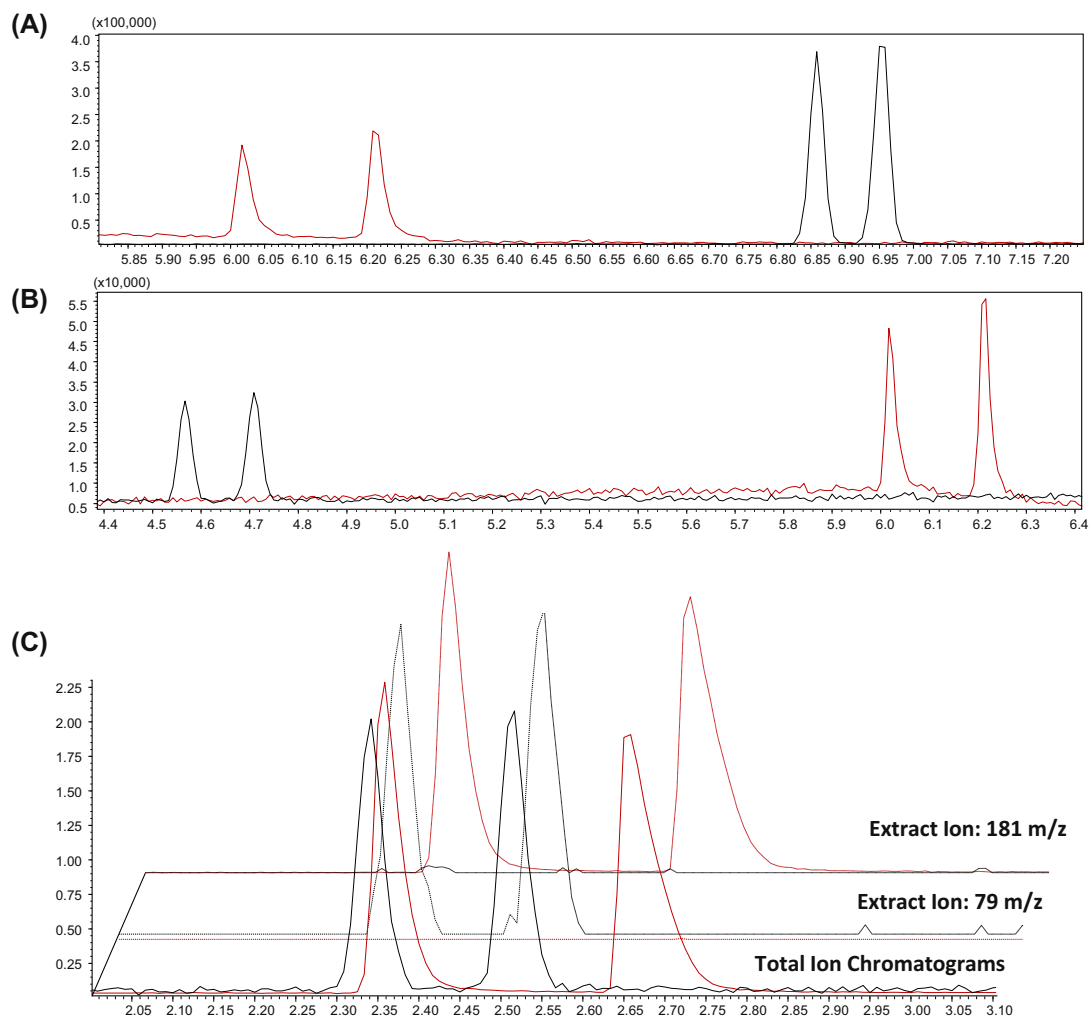


FIGURE 23.10 Enantiomeric separation of α -HCH (black) and metrifonate (in red: gray in printed version) on 30% (w/w) 2,3-di-O-ethyl-6-O-TBDMS- β -CD in OV1701 columns: (A) 10 m \times 0.10 mm \times 0.10 μ m, (B) 5 m \times 0.10 mm \times 0.10 μ m, and (C) 2 m \times 0.10 mm \times 0.10 μ m. For C the total ion chromatogram and the extract ion chromatograms at 181 m/z and 79 m/z are reported. Analysis conditions: Split injection, split ratio 1:20 and temperature 220°C; detector FID temperature 230°C; temperature program 50°C, 10°C min⁻¹ to 220°C; and flow rate 1 mL min⁻¹.

locking is used. These “universal” conditions usually provide satisfactory separations at the expense of longer separation times. Faster separations can be achieved by optimizing the separation conditions for a specific sample (or a group of samples) with a dedicated method for each matrix. On the one hand, this preserves

the enantiomer separation and peak elution order, and on the other, applies the best speed/separation trade-off [154–157]. This method is based on the theoretical and practical studies of Blumberg and coworkers on fast GC [156,157], which resulted in the well-known GC method translation [158,159] and requires the

development of the optimal multirate temperature program for a given sample, from which one can determine either the pressure/flow rate producing the highest efficiency (i.e., the plate number) with a given column (efficiency-optimized flow, EOF) or the flow rate, column dimensions, and carrier gas conditions corresponding to the shortest separation time for a required plate number (speed-optimized flow, SOF [152,156–159]). Fig. 23.11 illustrates the GC-MS profiles of γ -lactones (black) and δ -lactones (red: gray in printed version) with 30% (w/w) 2,3-di-*O*-acetyl-6-*O*-TBDMS- β -CD in PS086 columns: (A) conventional column of 25 m \times 0.25 mm \times 0.25 μ m for standard conditions (He flow rate 1 mL min⁻¹, temperature program 2°C min⁻¹ from 50 to 220°C); (B) the same column under EOF and optimized temperature conditions (He flow rate 1 mL min⁻¹, temperature program rate 3°C min⁻¹ from 90 to 140°C and 7.5°C min⁻¹ to 220°C); (C) the same column under SOF and optimized temperature conditions (He flow rate 1.4 mL min⁻¹, temperature program rate 3.4°C min⁻¹ from 90 to 140°C and 8.6°C min⁻¹ to 220°C); (D) a narrow bore column 10 m \times 0.10 mm \times 0.10 μ m under SOF conditions and translated temperature conditions (He flow rate 0.56 mL min⁻¹, temperature program rate 6.8°C min⁻¹ from 90 to 140°C and 16.9°C min⁻¹ to 220°C with SOF; and (E) a narrow bore column 5 m \times 0.10 mm \times 0.10 μ m under SOF conditions with translated temperature conditions (He flow rate 0.56 mL min⁻¹, temperature program rate 24°C min⁻¹ from 90 to 140°C and 60°C min⁻¹ to 220°C).

The optimization of the separation conditions induced a dramatic drop in the separation time from about 65 min with the 25 m conventional column to about 2.9 min with the 2 m narrow bore column, while maintaining the baseline separations of all enantiomers for each lactone. It is worth noting that the optimization of the GC separation conditions with the same column enables faster separation times of between about 52% with EOF and 64% with SOF.

23.5 Total analysis systems and chiral recognition of complex samples

In a total analysis system (TAS), the three main steps are sample preparation, analysis, and data processing integrated into a single step [160,161]. The development bottleneck for these systems is the sample preparation step, although, when working with volatile compounds or compounds that can be volatilized at low temperature, headspace sampling (HS) fully satisfies the need for TAS development [160,162,163]. HS techniques are solvent-free, fast, simple, reliable, and, above all, easy to automate and to couple online with a GC-MS system. HS sampling can be achieved in at least three modes, including the conventional static (S-HS) or dynamic (D-HS) modes, as well as the so-called high-concentration capacity headspace techniques (HCC-HS) [160,162–164]. These techniques all combine the advantages of S-HS and D-HS where volatiles are isolated on sorbent traps or, less frequently, in liquids (HS-SPME, HSSE, HS-STE, HS-LPME, etc.).

Fig. 23.12 shows an example of TAS for enantiomer separation by GC-MS for the one-step automated analysis of the headspace from a raspberry homogenate sampled by solid-phase microextraction (SPME) with a CAR/PDMS/DVB fiber online desorbed and analyzed with a 5 m narrow bore column coated with 30% (w/w) 2,3-di-*O*-acetyl-6-*O*-TBDMS- β -CD in PS086 to evaluate possible product adulteration [165,166].

23.6 Micropreparative enantioselective gas chromatography

Micropreparative GC is not an adequately investigated subject in enantiomer separations by GC, even though it is often required for the correct identification of stereoisomer responsible for a given biological activity [167,168]. Schurig

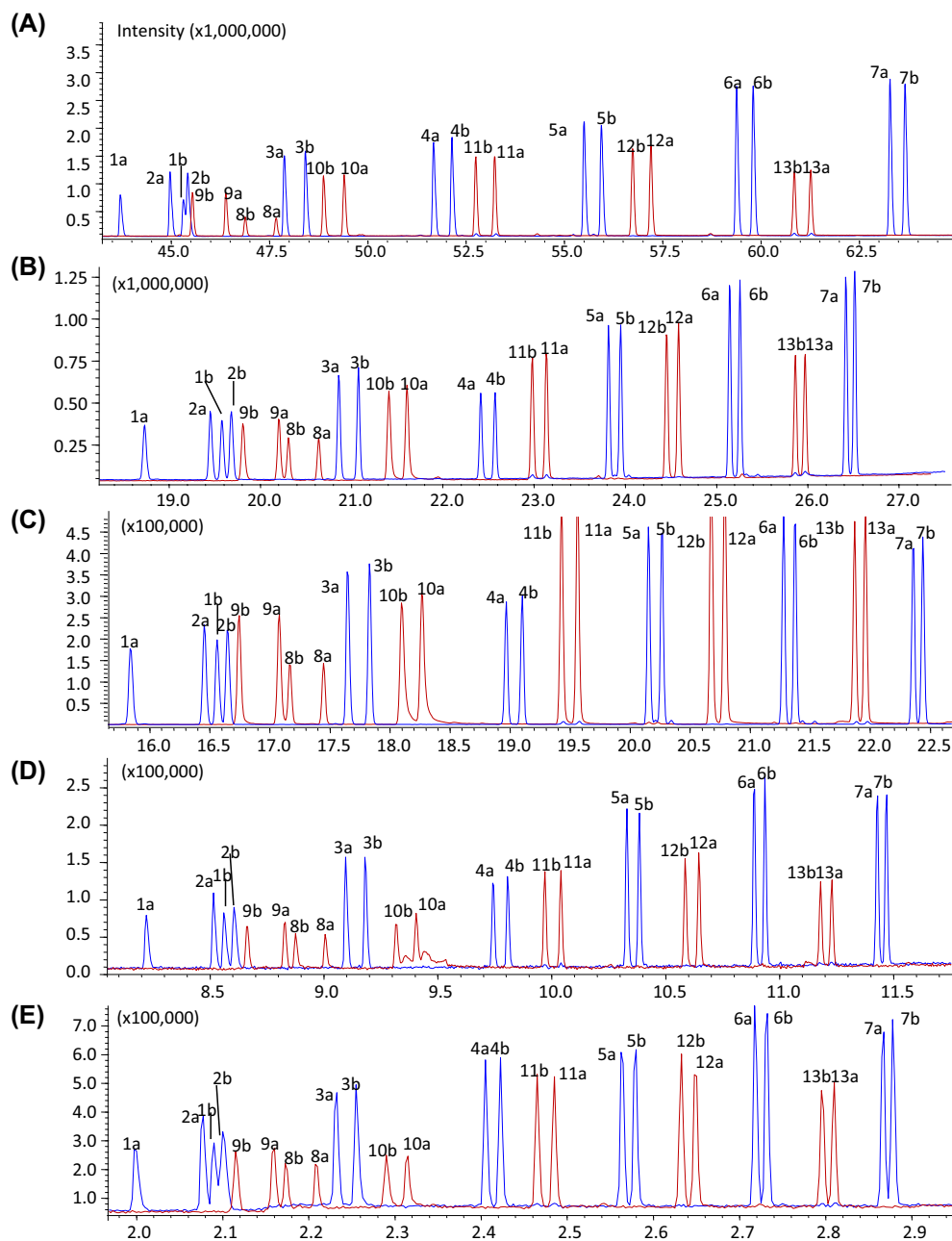


FIGURE 23.11 GC-MS separation of γ -lactones (black) and δ -lactones (red: gray in printed version) with 30% (w/w) 2,3-di-O-acetyl-6-O-TBDMS- β -CD in PS086 columns: (A) 25 m column with conventional conditions; (B) 25 m column with EOF; (C) 25 m column with SOF; (D) 10 m narrow bore column with SOF; and (E) 5 m narrow bore column with SOF. Peak identification: 1 γ -hexalactone, 2 γ -heptalactone, 3 γ -octalactone, 4 γ -nonalactone, 5 γ -decalactone, 6 γ -undecalactone, 7 γ -dodecalactone, 8 δ -hexalactone, 9 δ -octalactone, 10 δ -nonalactone, 11 δ -decalactone, 12 δ -undecalactone, 13 δ -dodecalactone; a: (*R*)-enantiomer, b: (*S*)-enantiomer. For separation conditions, see text.

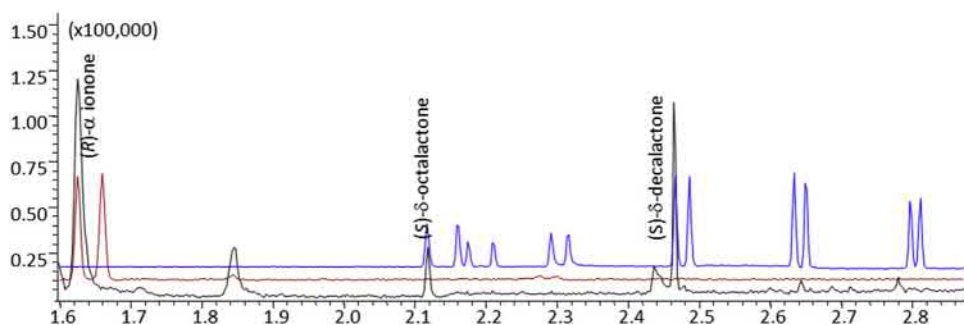


FIGURE 23.12 GC-MS chromatogram of a raspberry homogenate (black), racemic α -ionone (red: light gray in printed version) and δ -lactone standard mixture (blue: gray in printed version) on a 5 m narrow bore 30% (w/w) 2,3-di-*O*-acetyl-6-*O*-TBDMS- β -CD in PS086 column with SOF (He flow rate 0.56 mL min^{-1} , temperature program rate $24^\circ\text{C min}^{-1}$ from 90 to 140°C and $60^\circ\text{C min}^{-1}$ to 220°C).

reviewed this topic in 2004 and 2012 [9,169]. The limit to the use of preparative GC in this field is the low selectivity factor of chiral selectors for racemates, requiring high column efficiency and thin film columns generally, which reduces sample loading. This low value also requires sophisticated automated micropreparative GC systems in combination with multiple injections (up to several dozen) to isolate sufficient amounts of pure enantiomers, for instance, for NMR experiments ($0.5\text{--}1 \text{ mg}$) [167,168]. In addition, aerosol formation seriously affects the recovery of the isolated enantiomers requiring the design of special collection vessels and microcooling systems. Different approaches have been used for the micropreparative isolation of enantiomers, including: (i) Bicchi et al. used moderately thick-film wide-bore columns coated with CD CSPs [167,168], (ii) Schurig et al. applied the simulated moving bed (SMB) technology [170], and (iii) Sciarrone et al. developed a sophisticated but flexible heart-cut three-dimensional GC system enabling the collection of pure analytes after each GC dimension [171,172].

23.7 Conclusions

Enantioselective GC is nowadays a mature technique affording routine chiral recognition thanks to the dramatic improvements of the

robustness of chiral selectors and column technology. CD derivatives remain the most popular CSPs available for enantiomer separations by GC because of their capability to separate many enantiomers without derivatization and also due to the significant number of effective CD derivatives with different enantioselectivity and good chromatographic properties. The ultimate research goal in this field is still the search for new chiral selectors with extensive universal enantioselectivity as well as good chromatographic properties, in particular for chiral recognition without derivatization of highly polar chiral compounds.

References

- [1] R. Rienacker, G. Ohloff, Optisch aktives β -citronellol aus (+)- oder (-)- Pinan, *Angew. Chem.* 73 (1961).
- [2] B. Koppenhoefer, R. Behnisch, U. Epperlein, H. Holzschuh, A. Bernreuther, P. Piras, C. Roussel, Enantiomeric odor differences and gas chromatographic properties of flavors and fragrances, *Perfum. Flavor.* 19 (1994) 1–14.
- [3] C. Geithe, D. Krautwurst, Chirality matters – enantioselective orthologous odorant receptors for related terpenoid structures, in: *Importance of Chirality to Flavor Compounds*, American Chemical Society, 2015, pp. 161–181.
- [4] R. Kallenborn, H. Hühnerfuss, W.A. König, Enantioselective metabolism of (\pm)- α -1,2,3,4,5,6-Hexachlorocyclohexane in organs of the eider duck, *Angew. Chem. Int. Ed.* 30 (3) (1991) 320–321.

- [5] M. Juza, E. Braun, V. Schurig, Preparative enantiomer separation of the inhalation anesthetics enflurane, isoflurane and desflurane by gas chromatography on a derivatized gamma-cyclodextrin stationary phase, *J. Chromatogr. A* 769 (1) (1997) 119–127.
- [6] E.I. Eger 2nd, D.D. Koblin, M.J. Laster, V. Schurig, M. Juza, P. Ionescu, D. Gong, Minimum alveolar anesthetic concentration values for the enantiomers of isoflurane differ minimally, *Anesth. Analg.* 85 (1) (1997) 188–192.
- [7] P. Schreier, A. Bernreuther, M. Huffer, *Analysis of Chiral Organic Molecules: Methodology and Applications*, 2011, pp. 1–334.
- [8] E. Gil-Av, Present status of enantiomeric analysis by gas chromatography, *J. Mol. Evol.* 6 (2) (1975) 131–144.
- [9] V. Schurig, Chapter 21 - separation of enantiomers, in: C.F. Poole (Ed.), *Gas Chromatography*, Elsevier, Amsterdam, 2012, pp. 495–517.
- [10] R.A. Patil, C.A. Weatherly, D.W. Armstrong, Chapter 11 - chiral gas chromatography, in: P.L. Polavarapu (Ed.), *Chiral Analysis*, second ed., Elsevier, 2018, pp. 468–505.
- [11] V. Schurig, Gas chromatographic enantioseparation of derivatized α -amino acids on chiral stationary phases—past and present, *J. Chromatogr. B* 879 (29) (2011) 3122–3140.
- [12] V. Schurig, Practice and theory of enantioselective complexation gas chromatography, *J. Chromatogr. A* 965 (1–2) (2002) 315–356.
- [13] C. Cagliero, B. Sgorbini, C. Cordero, E. Liberto, P. Rubiolo, C. Bicchi, Enantioselective gas chromatography with derivatized cyclodextrins in the flavour and fragrance field, *Isr. J. Chem.* 56 (2016) 925–939.
- [14] E. Gil-Av, B. Feibush, R. Charles-Sigler, Separation of enantiomers by gas liquid chromatography with an optically active stationary phase, *Tetrahedron Lett.* 7 (10) (1966) 1009–1015.
- [15] B. Feibush, Interaction between asymmetric solutes and solvents. N-Lauroyl-L-valyl-t-butylamide as stationary phase in gas liquid partition chromatography, *J. Chem. Soc. D* 11 (1971) 544–545.
- [16] H. Frank, G.J. Nicholson, E. Bayer, Rapid gas chromatographic separation of amino acid enantiomers with a novel chiral stationary phase, *J. Chromatogr. Sci.* 15 (5) (1977) 174–176.
- [17] E. Bayer, H. Allmendinger, G. Enderle, B. Koppenhoefer, Anwendung von D-Chirasil-Val bei der gaschromatographischen Analytik von Enantiomeren, *Fresenius Z. Anal. Chem.* 321 (1985) 321–324.
- [18] W.A. König, *The Practice of Enantiomer Separation by Capillary Gas Chromatography*, Huthig, Heidelberg, 1987.
- [19] E. Gil-Av, B. Feibush, Resolution of enantiomers by gas liquid chromatography with optically active stationary phases. Separation on packed columns, *Tetrahedron Lett.* 8 (35) (1967) 3345–3347.
- [20] W.A. Bonner, M.A. Van Dort, J.J. Flores, Quantitative gas chromatographic analysis of leucine enantiomers. Comparative study, *Anal. Chem.* 46 (14) (1974) 2104–2107.
- [21] R. Liardon, S. Ledermann, GC behaviour of N(O,S)-perfluoroacyl D,L-amino acid alkyl esters on chirasil-val stationary phase, *J. High Resolut. Chromatogr.* 3 (9) (1980) 475–477.
- [22] P. Hušek, Rapid derivatization and gas chromatographic determination of amino acids, *J. Chromatogr. A* 552 (1991) 289–299.
- [23] H. Zahradnicková, P. Husek, P. Simek, GC separation of amino acid enantiomers via derivatization with heptafluorobutyl chloroformate and chirasil-L-Val column, *J. Separ. Sci.* 32 (22) (2009) 3919–3924.
- [24] H. Frank, Gas chromatography of enantiomers on chiral stationary phases, in: B. Holmstedt, H. Frank, B. Testa (Eds.), *Chirality and Biological Activity*, Alan R. Liss, Inc, New York, 1990, pp. 33–54.
- [25] V. Schurig, E. Gil-av, Complexation of olefins with planar rhodium(I) co-ordination compounds, *J. Chem. Soc. D* 12 (1971) 650–651.
- [26] E. Gil-Av, V. Schurig, Gas chromatography of mono-olefins with stationary phases containing rhodium co-ordination compounds, *Anal. Chem.* 43 (14) (1971) 2030–2033.
- [27] F. Mikeš, Thesis: The Resolution of Chiral Compounds by Modern Liquid Chromatography, The Weizmann Institute of Science, Rehovot, 1975.
- [28] V. Schurig, Separation of deuteriated ethylenes $C_2H_4-nD_n$ by complexation chromatography on a rhodium(I) complex, *Angew. Chem. Int. Ed.* 15 (5) (1976) 304–305.
- [29] R. Weber, K. Hintzer, V. Schurig, Enantiomer resolution of spiroketals, *Naturwissenschaften* 67 (9) (1980) 453–456.
- [30] K. Hintzer, R. Weber, V. Schurig, Synthesis of optically active 2s-, and 7s-methyl-1.6-dioxaspiro[4.5]decane, the pheromone components of *Paravespula vulgaris* (L.), from S-ethyl lactate, *Tetrahedron Lett.* 22 (1) (1981) 55–58.
- [31] C. Bicchi, A. Pisciotta, Use of two-dimensional gas chromatography in the direct enantiomer separation of chiral essential oil components, *J. Chromatogr. A* 508 (1990) 341–348.

- [32] V. Schurig, R. Link, Chiral separations, in: Proceedings of the International Meeting on Chromatography, University of Surrey, Guildford: Plenum Press, New York and London, 1987.
- [33] A. Villiers, Sur la fermentation de la fécule par l'action du ferment butyrique, *Compt. Rend. Acad. Sci.* 112 (1891) 536–538.
- [34] F. Schardinger, Über thermophile bakterien aus verschiedenen Speisen und milch, sowie über einige Umsetzungsprodukte derselben in kohlenhydrathaltigen Nährlösungen, darunter kristallisierte polysaccharide (dextrine) aus stärke, *Z. Unters. Nahr. u. Genussm.* 6 (1903) 865–880.
- [35] F. Cramer, *Einschlussverbindungen (Inclusion Compounds)*, Springer-Verlag, Berlin, 1954.
- [36] D. French, The Schardinger dextrins, *Adv. Carbohydr. Chem.* 12 (1957) 189–260.
- [37] K. Freudenberg, G. Blomquist, L. Ewald, K. Soff, Hydrolyse und Acetolyse der Stärke und der Schardinger-Dextrine, *Ber. Dtsch. Chem. Ges.* 69 (1936) 1258–1966.
- [38] H. Pringsheim, *Chemistry of the Saccharides*, McGraw-Hill, New York, 1932, p. 35.
- [39] V. Schurig, H.P. Nowotny, Gas chromatographic separation of enantiomers on optically active metal-complex-free stationary phases. Part 2. Gas chromatographic separation of enantiomers on cyclodextrin derivatives, *Angew. Chem. Int. Ed. Edit.* 29 (9) (1990) 939–957.
- [40] D.M. Sand, H. Schlenk, Acylated cyclodextrins as polar stationary phases for gas-liquid chromatography, *Anal. Chem.* 33 (11) (1961) 1624–1625.
- [41] T. Koscielski, D. Sybilska, J. Jurczak, Separation of α - and β -pinene into enantiomers in gas-liquid chromatography systems via α -cyclodextrin inclusion complexes, *J. Chromatogr.* 280 (1983) 131–134.
- [42] T. Kościelski, D. Sybilska, L. Feltl, E. Smolková-Keulemansová, Comparative studies of the chromatographic properties of α - and β -cyclodextrin in gas-solid and gas-liquid chromatography, *J. Chromatogr. A* 286 (1984) 23–30.
- [43] J. Mráz, L. Feltl, E. Smolková-Keulemansová, Cyclodextrins and methylated cyclodextrins as stationary phases in gas-solid chromatography, *J. Chromatogr. A* 286 (1984) 17–22.
- [44] A. Smolková-Keulemansová, E. Neumannová, L. Feltl, Study of the stereospecific properties of cyclodextrins as gas-solid chromatographic stationary phases, *J. Chromatogr. A* 365 (1986) 279–288, [https://doi.org/10.1016/S0021-9673\(01\)81566-1](https://doi.org/10.1016/S0021-9673(01)81566-1).
- [45] E. Smolková-Keulemansová, Cyclodextrins and their inclusion complexes: by J. Szejtli, *Akadémiai Kiadó, Budapest*, (1982) 296 pp. *J. Chromatogr. A* 253 (1982) 138.
- [46] E. Smolková-Keulemansová, Cyclodextrins as stationary phases in chromatography, *J. Chromatogr. A* 251 (1) (1982) 17–34.
- [47] E. Smolková-Keulemansová, S. Krýsl, Inclusion compounds in chromatography, *J. Chromatogr. A* 184 (3) (1980) 347–361.
- [48] Z. Juvancz, G. Alexander, J. Szejtli, Permethyated b-Cyclodextrin as stationary phase in capillary gas chromatography, *J. High Resolut. Chromatogr.* 10 (1987) 105–107.
- [49] V. Schurig, H.P. Nowotny, Separation of enantiomers on diluted permethylated b-Cyclodextrin by high-resolution gas chromatography, *J. Chromatogr.* 441 (155) (1988) 155–163.
- [50] G. Alexander, Z. Juvancz, J. Szejtli, Cyclodextrins and their derivatives as stationary phases in GC capillary columns, HRC CC, *J. High Resolut. Chromatogr.* 11 (1988) 110–113.
- [51] A. Venema, P.J.A. Tolsma, Enantiomer separation with capillary gas-chromatography columns coated with cyclodextrins .1. Separation of enantiomeric 2-substituted propionic-acid esters and some lower alcohols with permethylated beta-cyclodextrin, *J. High Resolut. Chromatogr.* 12 (1) (1989) 32–34.
- [52] W.A. König, R. Krebber, G. Wenz, Enantioselective capillary gas-chromatography on the basis of host-guest interactions with modified cyclodextrins, *J. High Resolut. Chromatogr.* 12 (10) (1989) 641–644.
- [53] W.A. König, S. Lutz, P. Mischnicklubbecke, B. Brassat, G. Wenz, Cyclodextrins as chiral stationary phases in capillary gas-chromatography 1. Pentylated alpha-cyclodextrin, *J. Chromatogr.* 447 (1) (1988) 193–197.
- [54] W.A. König, S. Lutz, G. Wenz, Modified cyclodextrins - novel, highly enantioselective stationary phases for gas-chromatography, *Angew. Chem. Int. Ed.* 27 (7) (1988) 979–980.
- [55] W.A. König, S. Lutz, G. Wenz, E. Vonderbey, Cyclodextrins as chiral stationary phases in capillary gas-chromatography 2. Heptakis(3-O-Acetyl-2,6-Di-O-Pentyl)-Beta-Cyclodextrin, *J. High Resolut. Chromatogr.* 11 (7) (1988) 506–509.
- [56] V. Schurig, M. Jung, D. Schmalzing, M. Schleimer, J. Duvekot, J.C. Buyten, J.A. Peene, P. Mussche, CGC enantiomer separation on diluted cyclodextrin derivatives coated on fused-silica columns, *J. High Resolut. Chromatogr.* 13 (7) (1990) 470–474.
- [57] C. Bicchì, G. Artuffo, A. D'Amato, V. Manzin, A. Galli, M. Galli, Cyclodextrin derivatives in the GC separation of racemic mixtures of volatile compounds Part VI: the influence of the diluting phase on the enantioselectivity of 2,6-Di-O-Methyl-3-O-Pentyl- β -Cyclodextrin, *J. High Resolut. Chromatogr.* 16 (1993) 209–214.

- [58] C. Bicchi, A. D'Amato, V. Manzin, A. Galli, M. Galli, Cyclodextrin derivatives in GC separation of racemic mixtures of volatiles. 9. The influence of the different polysiloxanes as diluting phase for 2,3-di-*O*-acetyl-6-*O*-*t*-butyldimethylsilyl-beta-cyclodextrin on the separation of some racemates, *J. Microcolumn Sep.* 7 (4) (1995) 327–336.
- [59] V. Schurig, D. Schmalzing, U. Mühleck, M. Jung, M. Schleimer, P. Mussche, C. Duvekot, J.C. Buyten, Gas chromatographic enantiomer separation on polysiloxane-anchored permethyl- β -cyclodextrin (Chirasil-Dex), *J. High Resolut. Chromatogr.* 13 (10) (1990) 713–717.
- [60] P. Fischer, R. Aichholz, U. Bözl, M. Juza, S. Krimmer, Permethyl- β -cyclodextrin, chemically bonded to polysiloxane: a chiral stationary phase with wider application range for enantiomer separation by capillary gas chromatography, *Angew. Chem. Int. Ed.* 29 (4) (1990) 427–429.
- [61] K. Huang, X. Zhang, D.W. Armstrong, Ionic cyclodextrins in ionic liquid matrices as chiral stationary phases for gas chromatography, *J. Chromatogr. A* 1217 (32) (2010) 5261–5273.
- [62] W. Blum, R. Aichholz, Gas-Chromatographic enantiomer separation on tert-butyl dimethylsilylated beta-cyclodextrin diluted in PS-086 - a simple method to prepare enantioselective glass-capillary columns, *J. High Resolut. Chromatogr.* 13 (7) (1990) 515–518.
- [63] F. Kobor, K. Angermund, G. Schomburg, Molecular modeling experiments on chiral recognition in GC with specially derivatized cyclodextrins as selectors, *J. High Resolut. Chromatogr.* 16 (5) (1993) 299–311.
- [64] A. Dietrich, B. Maas, V. Karl, P. Kreis, D. Lehmann, B. Weber, A. Mosandl, Stereoisomeric flavor compounds 55. Stereo differentiation of some chiral volatiles on Heptakis(2,3-di-*O*-Acetyl-6-*O*-Tert-Butyldimethylsilyl)-Beta-Cyclodextrin, *J. High Resolut. Chromatogr.* 15 (3) (1992) 176–179.
- [65] C. Bicchi, A. D'Amato, V. Manzin, Derivatized cyclodextrins in enantiomer GC separation of volatiles, in: K.A.D. Swift (Ed.), *Flavours and Fragrances*, The Royal Society of Chemistry, 1997, pp. 57–69.
- [66] C. Bicchi, C. Cagliero, E. Liberto, B. Sgorbini, K. Martina, G. Cravotto, P. Rubiolo, New asymmetrical per-substituted cyclodextrins (2-*O*-methyl-3-*O*-ethyl- and 2-*O*-ethyl-3-*O*-methyl-6-*O*-*t*-butyldimethylsilyl-beta-derivatives) as chiral selectors for enantioselective gas chromatography in the flavour and fragrance field, *J. Chromatogr. A* 1217 (7) (2010) 1106–1113.
- [67] M. Bayer, A. Mosandl, Improved gas chromatographic stereo differentiation of chiral main constituents from different essential oils using a mixture of chiral stationary phases, *Flavour Fragrance J.* 19 (6) (2004) 515–517.
- [68] M.Y. Nie, L.M. Zhou, Q.H. Wang, D.Q. Zhu, Gas chromatographic enantiomer separation on single and mixed cyclodextrin derivative chiral stationary phases, *Chromatographia* 51 (11–12) (2000) 736–740.
- [69] X.Y. Shi, Y.Q. Zhang, R.N. Fu, Synergistic effects of mixed GC stationary phase consisting of two different cyclodextrin derivatives, *Anal. Chim. Acta* 424 (2) (2000) 271–277.
- [70] S. Tamogami, K. Awano, M. Amaike, Y. Takagi, T. Kitahara, Development of an efficient GLC system with a mixed chiral stationary phase and its application to the separation of optical isomers, *Flavour Fragrance J.* 16 (5) (2001) 349–352.
- [71] P.A. Levkin, A. Levkina, V. Schurig, Combining the enantioselectivities of L-valine diamide and permethylated β -cyclodextrin in one gas chromatographic chiral stationary phase, *Anal. Chem.* 78 (14) (2006) 5143–5148.
- [72] O. Stephany, F. Dron, S. Tisse, A. Martinez, J.-M. Nuzillard, V. Peulon-Agasse, P. Cardinaël, J.-P. Bouillon, (L)- or (D)-Valine tert-butylamide grafted on permethylated β -cyclodextrin derivatives as new mixed binary chiral selectors: versatile tools for capillary gas chromatographic enantioseparation, *J. Chromatogr. A* 1216 (2009) 4051–4062.
- [73] O. Stephany, S. Tisse, G. Coadou, J.P. Bouillon, V. Peulon-Agasse, P. Cardinael, Influence of amino acid moiety accessibility on the chiral recognition of cyclodextrin-amino acid mixed selectors in enantioselective gas chromatography, *J. Chromatogr. A* 1270 (2012) 254–261.
- [74] H. Liu, S.-M. Xie, P. Ai, J.-H. Zhang, M. Zhang, L.-M. Yuan, Metal-organic framework Co(D-Cam)1/2(bdc)1/2(tmdpy) for improved enantioseparations on a chiral cyclodextrin stationary phase in gas chromatography, *ChemPlusChem* 79 (8) (2014) 1103–1108.
- [75] J.-r. Yang, S.-m. Xie, H. Liu, J.-h. Zhang, L.-m. Yuan, Metal-organic framework InH(d-C₁₀H₁₄O₄)₂ for improved enantioseparations on a chiral cyclodextrin stationary phase in GC, *Chromatographia* 78 (7) (2015) 557–564.
- [76] J.-r. Yang, S.-m. Xie, J.-h. Zhang, L. Chen, R.-y. Nong, L.-m. Yuan, Metal-organic framework [Cd(LTP)₂]_n for improved enantioseparations on a chiral cyclodextrin stationary phase in GC, *J. Chromatogr. Sci.* 54 (9) (2016) 1467–1474.

- [77] P. Schreier, A. Bernreuther, M. Huffer, *Analysis of Chiral Organic Molecules*, Walter de Gruyter, Berlin, 1995.
- [78] A. Venema, H. Henderiks, R. Vongeeest, The enantioselectivity of modified cyclodextrins - studies on interaction mechanisms, *J. High Resolut. Chromatogr.* 14 (10) (1991) 676–680.
- [79] A. Berthod, W.Y. Li, D.W. Armstrong, Multiple enantioselective retention mechanisms on derivatized cyclodextrin gas-chromatographic chiral stationary phases, *Anal. Chem.* 64 (8) (1992) 873–879.
- [80] V. Schurig, H.P. Nowotny, M. Schleimer, D. Schmalzing, Gas-chromatographic enantiomer separation on per-N-pentylated amylose, *J. High Resolut. Chromatogr.* 12 (8) (1989) 549–551.
- [81] G. Sicoli, Z. Jiang, L. Jicsinsky, V. Schurig, Modified linear dextrans (acyclodextrins) as new chiral selectors for the gas-chromatographic separation of enantiomers, *Angew. Chem. Int. Ed.* 44 (26) (2005) 4092.
- [82] G. Sicoli, F. Pertici, Z. Jiang, L. Jicsinsky, V. Schurig, Gas-chromatographic approach to probe the absence of molecular inclusion in enantioseparations by carbohydrates. Investigation of linear dextrans (acyclodextrins) as novel chiral stationary phases, *Chirality* 19 (5) (2007) 391–400.
- [83] V. Schurig, Gas chromatographic separation of enantiomers on optically active metal-Complex-free stationary phases, *Angew. Chem. Int. Ed.* 23 (1984) 747–765.
- [84] M. Jung, D. Schmalzing, V. Schurig, Theoretical approach to the gas-chromatographic separation of enantiomers on dissolved cyclodextrin derivatives, *J. Chromatogr.* 552 (1–2) (1991) 43–57.
- [85] V. Schurig, Separation of enantiomers by gas chromatography, *J. Chromatogr. A* 906 (1–2) (2001) 275–299.
- [86] S.-M. Xie, X.-X. Chen, J.-H. Zhang, L.-M. Yuan, Gas chromatographic separation of enantiomers on novel chiral stationary phases, *Trac. Trends Anal. Chem.* 124 (2020) 115808.
- [87] Y. Zhang, D.W. Armstrong, 4,6-Di-O-pentyl-3-O-trifluoroacetyl/propionyl cyclofructan stationary phases for gas chromatographic enantiomeric separations, *Analyst* 136 (14) (2011) 2931–2940.
- [88] Y. Zhang, Z.S. Breitbach, C. Wang, D.W. Armstrong, The use of cyclofructans as novel chiral selectors for gas chromatography, *Analyst* 135 (5) (2010) 1076–1083.
- [89] M. Kawamura, T. Uchiyama, T. Kuramoto, Y. Tamura, K. Mizutani, Formation of a cyclinulooligosaccharide from inulin by an extracellular enzyme of *Bacillus circulans* OKUMZ 31B, *Carbohydr. Res.* 192 (C) (1989) 83–90.
- [90] K. Yusuf, A. Aqel, Z. Alotman, Metal-organic frameworks in chromatography, *J. Chromatogr. A* 1348 (2014) 1–16.
- [91] B. Chen, C. Liang, J. Yang, D.S. Contreras, Y.L. Clancy, E.B. Lobkovsky, O.M. Yaghi, S. Dai, A microporous metal–organic framework for gas-chromatographic separation of alkanes, *Angew. Chem. Int. Ed.* 118 (9) (2006) 1418–1421.
- [92] Z.Y. Gu, X.P. Yan, Metal–organic framework MIL-101 for high-resolution gas-chromatographic separation of xylene isomers and ethylbenzene, *Angew. Chem. Int. Ed.* 49 (2010) 1477–1480.
- [93] S.-M. Xie, Z.-J. Zhang, Z.-Y. Wang, L.-M. Yuan, Chiral metal–organic frameworks for high-resolution gas chromatographic separations, *J. Am. Chem. Soc.* 133 (31) (2011) 11892–11895.
- [94] S.M. Xie, L.M. Yuan, Recent progress of chiral stationary phases for separation of enantiomers in gas chromatography, *J. Separ. Sci.* 40 (1) (2017) 124–137.
- [95] S.Y. Ding, W. Wang, Covalent organic frameworks (COFs): from design to applications, *Chem. Soc. Rev.* 42 (2) (2013) 548–568.
- [96] H.-L. Qian, C.-X. Yang, X.-P. Yan, Bottom-up synthesis of chiral covalent organic frameworks and their bound capillaries for chiral separation, *Nat. Commun.* 7 (1) (2016) 12104.
- [97] J.R. Holst, A. Trewin, A.I. Cooper, Porous organic molecules, *Nat. Chem.* 2 (11) (2010) 915–920.
- [98] T. Tozawa, J.T.A. Jones, S.I. Swamy, S. Jiang, D.J. Adams, S. Shakespeare, R. Clowes, D. Bradshaw, T. Hasell, S.Y. Chong, C. Tang, S. Thompson, J. Parker, A. Trewin, J. Bacsá, A.M.Z. Slawin, A. Steiner, A.I. Cooper, Porous organic cages, *Nat. Mater.* 8 (12) (2009) 973–978.
- [99] A. Kewley, A. Stephenson, L. Chen, M.E. Briggs, T. Hasell, A.I. Cooper, Porous organic cages for gas chromatography separations, *Chem. Mater.* 27 (9) (2015) 3207–3210.
- [100] D.J. Tranchemontagne, Z. Ni, M. O’Keeffe, O.M. Yaghi, Reticular chemistry of metal-organic polyhedra, *Angew. Chem. Int. Ed.* 47 (28) (2008) 5136–5147.
- [101] T. Hasell, X. Wu, J.T.A. Jones, J. Bacsá, A. Steiner, T. Mitra, A. Trewin, D.J. Adams, A.I. Cooper, Triply interlocked covalent organic cages, *Nat. Chem.* 2 (9) (2010) 750–755.
- [102] J.H. Zhang, S.M. Xie, L. Chen, B.J. Wang, P.G. He, L.M. Yuan, Homochiral porous organic cage with high selectivity for the separation of racemates in gas chromatography, *Anal. Chem.* 87 (15) (2015) 7817–7824.
- [103] J.H. Zhang, S.M. Xie, B.J. Wang, P.G. He, L.M. Yuan, A homochiral porous organic cage with large cavity and pore windows for the efficient gas chromatography separation of enantiomers and positional isomers, *J. Separ. Sci.* 41 (6) (2018) 1385–1394.
- [104] L. Chen, Q. Chen, M. Wu, F. Jiang, M. Hong, Controllable coordination-driven self-assembly: from discrete metallocages to infinite cage-based frameworks, *Acc. Chem. Res.* 48 (2) (2015) 201–210.

- [105] S.M. Xie, N. Fu, L. Li, B.Y. Yuan, J.H. Zhang, Y.X. Li, L.M. Yuan, Homochiral metal-organic cage for gas chromatographic separations, *Anal. Chem.* 90 (15) (2018) 9182–9188.
- [106] C. Zhao, Q.-F. Sun, W.M. Hart-Cooper, A.G. DiPasquale, F.D. Toste, R.G. Bergman, K.N. Raymond, Chiral amide directed assembly of a diastereo- and enantiopure supramolecular host and its application to enantioselective catalysis of neutral substrates, *J. Am. Chem. Soc.* 135 (50) (2013) 18802–18805.
- [107] R. Ran, L. You, B. Di, W. Hao, M. Su, F. Yan, L. Huang, A novel chiral mesoporous binaphthylsilicas: preparation, characterization, and application in HPLC, *J. Separ. Sci.* 35 (15) (2012) 1854–1862.
- [108] K.E. Shopsowitz, H. Qi, W.Y. Hamad, M.J. MacLachlan, Free-standing mesoporous silica films with tunable chiral nematic structures, *Nature* 468 (7322) (2010) 422–425.
- [109] M. Silva, D. Pérez-Quintanilla, S. Morante-Zarceo, I. Sierra, M.L. Marina, Z. Aturki, S. Fanali, Ordered mesoporous silica functionalized with β -cyclodextrin derivative for stereoisomer separation of flavanones and flavanone glycosides by nano-liquid chromatography and capillary electrochromatography, *J. Chromatogr. A* 1490 (2017) 166–176.
- [110] G. Zhu, H. Zhong, Q. Yang, C. Li, Chiral mesoporous organosilica spheres: synthesis and chiral separation capacity, *Microporous Mesoporous Mater.* 116 (1–3) (2008) 36–43.
- [111] J.H. Zhang, S.M. Xie, M. Zhang, M. Zi, P.G. He, L.M. Yuan, Novel inorganic mesoporous material with chiral nematic structure derived from nanocrystalline cellulose for high-resolution gas chromatographic separations, *Anal. Chem.* 86 (19) (2014) 9595–9602.
- [112] Y.X. Li, S.G. Fu, J.H. Zhang, S.M. Xie, L. Li, Y.Y. He, M. Zi, L.M. Yuan, A highly ordered chiral inorganic mesoporous material used as stationary phase for high-resolution gas chromatographic separations, *J. Chromatogr. A* 1557 (2018) 99–106.
- [113] Y.Y. He, Q. Pu, J.H. Zhang, S.M. Xie, X.X. Chen, L.M. Yuan, Chiral inorganic mesoporous materials used as the stationary phase in GC, *Sep. Sci. Plus* 2 (2019) 432–439.
- [114] Y.Y. He, J.H. Zhang, Q. Pu, S.M. Xie, Y.X. Li, L. Luo, X.X. Chen, L.M. Yuan, A novel chiral inorganic mesoporous silica used as a stationary phase in GC, *Chirality* 31 (12) (2019) 1053–1059.
- [115] J. Ding, T. Welton, D.W. Armstrong, Chiral ionic liquids as stationary phases in gas chromatography, *Anal. Chem.* 76 (22) (2004) 6819–6822.
- [116] L. Zhao, P. Ai, A.-H. Duan, L.-M. Yuan, Single-walled carbon nanotubes for improved enantioseparations on a chiral ionic liquid stationary phase in GC, *Anal. Bioanal. Chem.* 399 (1) (2011) 143–147.
- [117] A. Berthod, L. He, D.W. Armstrong, Ionic liquids as stationary phase solvents for methylated cyclodextrins in gas chromatography, *Chromatographia* 53 (1–2) (2001) 63–68.
- [118] V. Schurig, Terms for the quantitation of a mixture of stereoisomers, *Enantiomer* 1 (2) (1996) 139–143.
- [119] C. Cagliero, B. Sgorbini, C. Cordero, E. Liberto, P. Rubiolo, C. Bicchi, Enantioselective gas chromatography with cyclodextrin in odorant analysis, in: A. Buettner (Ed.), *Springer Handbook of Odor*, Springer International Publishing, Cham, 2017, pp. 51–52.
- [120] C. Cagliero, B. Sgorbini, C. Cordero, E. Liberto, P. Rubiolo, C. Bicchi, Cyclodextrin derivatives as stationary phases for the GC separation of enantiomers in the flavor and fragrance field, in: *Acs Sym Ser*, American Chemical Society, 2015, pp. 15–34.
- [121] K. Grob, G. Grob, K.J. Grob, Testing capillary gas chromatographic columns, *J. Chromatogr.* 219 (1981) 13–20.
- [122] D.R. Deans, A new technique for heart-cutting in gas chromatography, *Chromatographia* 1 (1968) 18–21.
- [123] L. Mondello, M. Catalfamo, C. Dugo, P. Dugo, Multidimensional tandem capillary gas chromatography system for the analysis of real complex samples. Part I: development of a fully automated tandem gas chromatography system, *J. Chromatogr. Sci.* 36 (4) (1998) 201–209.
- [124] G. Schomburg, H. Husmann, E. Hubinger, W.A. König, Multidimensional capillary gas chromatography - enantiomeric separation of selected cuts using a chiral second column, *J. High Resolut. Chromatogr.* 7 (1984) 404–410.
- [125] Y.F. Wong, N.W. Davies, S.-T. Chin, T. Larkman, P.J. Marriott, Enantiomeric distribution of selected terpenes for authenticity assessment of Australian *Melaleuca alternifolia* oil, *Ind. Crop. Prod.* 67 (2015) 475–483.
- [126] Y.F. Wong, R.N. West, S.-T. Chin, P.J. Marriott, Evaluation of fast enantioselective multidimensional gas chromatography methods for monoterpenic compounds: authenticity control of Australian tea tree oil, *J. Chromatogr. A* 1406 (2015) 307–315.
- [127] N.W. Davies, T. Larkman, P.J. Marriott, I.A. Khan, Determination of enantiomeric distribution of terpenes for quality assessment of Australian tea tree oil, *J. Agric. Food Chem.* 64 (23) (2016) 4817–4819.

- [128] M. Wang, J. Zhao, B. Avula, Y.-H. Wang, A.G. Chittiboyina, J.F. Parcher, I.A. Khan, Quality evaluation of terpinen-4-ol-type Australian tea tree oils and commercial products: an integrated approach using conventional and chiral GC/MS combined with chemometrics, *J. Agric. Food Chem.* 3 (10) (2015) 2674–2682.
- [129] Z.Y. Liu, J.B. Phillips, Comprehensive 2-dimensional gas-chromatography using an on-column thermal modulator interface, *J. Chromatogr. Sci.* 29 (6) (1991).
- [130] B. Sgorbini, C. Cagliero, L. Boggia, E. Liberto, S.E. Reichenbach, P. Rubiolo, C. Cordero, C. Bicchi, Parallel dual secondary-column-dual detection comprehensive two-dimensional gas chromatography: a flexible and reliable analytical tool for essential oils quantitative profiling, *Flavour Fragrance J.* 30 (5) (2015) 366–380.
- [131] L.M. Blumberg, M.S. Klee, Method translation and retention time locking in partition GC, *Anal. Chem.* 70 (18) (1998).
- [132] V. Giarrocco, B. Quimby, M. Klee, Retention time locking: concepts and application, in: *Gas Chromatography Application Note*, Agilent technologies Inc, 1997.
- [133] FFNSC 3 Flavors and Fragrances of Natural and Synthetic Compounds - Mass Spectral Database, Chromaleont, Messina, Italy, 2015.
- [134] R. Costa, M.R. De Fina, M.R. Valentino, P. Dugo, L. Mondello, Reliable identification of terpenoids and related compounds by using linear retention indices interactively with mass spectrometry search, *Nat. Prod. Commun.* 2 (4) (2007) 413–418.
- [135] E. Liberto, C. Cagliero, B. Sgorbini, C. Bicchi, D. Sciarrone, B.D. Zellner, L. Mondello, P. Rubiolo, Enantiomer identification in the flavour and fragrance fields by "interactive" combination of linear retention indices from enantio selective gas chromatography and mass spectrometry, *J. Chromatogr. A* 1195 (1–2) (2008) 117–126.
- [136] C. Bicchi, G. Artuffo, A. D'Amato, V. Manzin, A. Galli, M. Galli, Cyclodextrin derivatives in the GC separation of racemic mixtures of volatile compounds. Part 5 heptakis 2,6-dimethyl-3-pentyl- β -cyclodextrin, *J. High Resolut. Chromatogr.* 15 (11) (1992) 710–714.
- [137] W.A. König, B. Gehrcke, D. Icheln, P. Evers, J. Dönnecke, W.C. Wang, New selectively substituted cyclodextrins as stationary phases for the analysis of chiral constituents of essential oils, *J. High Resolut. Chromatogr.* 15 (6) (1992) 367–372.
- [138] B. Maas, A. Dietrich, D. Bartschat, A. Mosandl, *tert*-Butyldimethylsilylated cyclodextrins: versatile chiral stationary phases in capillary gas chromatography, *J. Chromatogr. Sci.* 33 (5) (1995) 223–228.
- [139] C. Bicchi, A. D'Amato, V. Manzin, A. Galli, M. Galli, Cyclodextrin derivatives in the gas chromatographic separation of racemic mixtures of volatile compounds. Part 10. 2,3-di-*O*-ethyl-6-*O*-*tert*-butyldimethylsilyl- β - and γ -cyclodextrins, *J. Chromatogr. A* 742 (1–2) (1996) 161–173.
- [140] A. Mosandl, Enantioselective capillary gas chromatography and stable isotope ratio mass spectrometry in the authenticity control of flavors and essential oils, *Food Rev. Int.* 11 (4) (1995) 597–664.
- [141] I. Bonaccorsi, D. Sciarrone, L. Schipilliti, P. Dugo, L. Mondello, G. Dugo, Multidimensional enantio gas chromatography/mass spectrometry and gas chromatography-combustion-isotopic ratio mass spectrometry for the authenticity assessment of lime essential oils (*C. aurantifolia* Swingle and *C. latifolia* Tanaka), *J. Chromatogr. A* 1226 (2012) 87–95.
- [142] G. Dugo, I. Bonaccorsi, D. Sciarrone, L. Schipilliti, M. Russo, A. Cotroneo, P. Dugo, L. Mondello, V. Raymo, Characterization of cold-pressed and processed bergamot oils by using GC-FID, GC-MS, GC-C-IRMS, enantio-GC, MDGC, HPLC and HPLC-MS-IT-TOF, *J. Essent. Oil Res.* 24 (2) (2012) 93–117.
- [143] L. Schipilliti, I. Bonaccorsi, D. Sciarrone, L. Dugo, L. Mondello, G. Dugo, Determination of petitgrain oils landmark parameters by using gas chromatography-combustion-isotope ratio mass spectrometry and enantioselective multidimensional gas chromatography, *Anal. Bioanal. Chem.* 405 (2–3) (2013) 679–690.
- [144] L. Schipilliti, P. Dugo, I. Bonaccorsi, L. Mondello, Headspace-solid phase microextraction coupled to gas chromatography-combustion-isotope ratio mass spectrometer and to enantioselective gas chromatography for strawberry flavoured food quality control, *J. Chromatogr. A* 1218 (42) (2011) 7481–7486.
- [145] L. Schipilliti, I. Bonaccorsi, A. Cotroneo, P. Dugo, L. Mondello, Carbon isotope ratios of selected volatiles in *Citrus sinensis* and in orange-flavoured food, *J. Sci. Food Agric.* 95 (14) (2015) 2944–2950.
- [146] L. Schipilliti, I.L. Bonaccorsi, C. Occhiuto, P. Dugo, L. Mondello, Authentication of citrus volatiles based on carbon isotope ratios, *J. Essent. Oil Res.* 30 (1) (2018) 1–15.

- [147] P. Rubiolo, E. Liberto, B. Sgorbini, R. Russo, J.L. Veuthey, C. Bicchi, Fast-GC-conventional quadrupole mass spectrometry in essential oil analysis, *J. Separ. Sci.* 31 (6–7) (2008) 1074–1084.
- [148] C. Bicchi, G. Artuffo, A. Damato, A. Galli, M. Galli, Cyclodextrin derivatives in GC separation of racemic mixtures of volatiles 3, *Chirality* 4 (2) (1992) 125–131.
- [149] H. Grosenick, V. Schurig, J. Costante, A. Collet, Gas-chromatographic enantiomer separation of bromochlorofluoromethane, *Tetrahedron Asymmetry* 6 (1) (1995) 87–88.
- [150] M. Lindstrom, Improved enantiomer separation using very short capillary columns coated with permethylated beta-cyclodextrin, *J. High Resolut. Chromatogr.* 14 (1991) 765–767.
- [151] I. Hardt, W.A. König, Diluted versus undiluted cyclodextrin derivatives in capillary gas-chromatography and the effect of linear carrier gas velocity, column temperature, and length on enantiomer separation, *J. Microcolumn Sep.* 5 (1) (1993) 35–40.
- [152] C. Bicchi, L. Blumberg, C. Cagliero, C. Cordero, P. Rubiolo, E. Liberto, Development of fast enantioselective gas-chromatographic analysis using gas-chromatographic method-translation software in routine essential oil analysis (lavender essential oil), *J. Chromatogr. A* 1217 (9) (2010) 1530–1536.
- [153] C. Bicchi, E. Liberto, C. Cagliero, C. Cordero, B. Sgorbini, P. Rubiolo, Conventional and narrow bore short capillary columns with cyclodextrin derivatives as chiral selectors to speed-up enantioselective gas chromatography and enantioselective gas chromatography-mass spectrometry analyses, *J. Chromatogr. A* 1212 (1–2) (2008) 114–123.
- [154] L.M. Blumberg, Theory of fast capillary gas chromatography Part 2: speed of analysis, *J. High Resolut. Chromatogr.* 20 (12) (1997) 679–687.
- [155] L.M. Blumberg, Theory of fast capillary gas chromatography 1. Column efficiency, *J. High Resolut. Chromatogr.* 20 (11) (1997) 597–604.
- [156] L.M. Blumberg, M.S. Klee, Optimal heating rate in gas chromatography, *J. Microcolumn Sep.* 12 (9) (2000) 508–514.
- [157] M.S. Klee, L.M. Blumberg, Theoretical and practical aspects of fast gas chromatography and method translation, *J. Chromatogr. Sci.* 40 (5) (2002) 234–247.
- [158] <https://www.agilent.com/en/support/gas-chromatography/gcmethodtranslation> (last accessed May, 2020).
- [159] <https://www.restek.com/ezgc-mtfc> (last accessed May, 2020).
- [160] C. Cagliero, B. Sgorbini, C. Cordero, E. Liberto, C. Bicchi, P. Rubiolo, Analytical strategies for multi-purpose studies of a plant volatile fraction, in: K. Hostettmann, et al. (Eds.), *Handbook of Chemical and Biological Plant Analytical Methods*, Wiley, Chichester (UK), 2014.
- [161] A. Manz, N. Graber, H.M. Widmer, Miniaturized total chemical-analysis systems - a novel concept for chemical sensing, *Sensor. Actuator. B Chem.* 1 (1–6) (1990) 244–248.
- [162] C. Bicchi, C. Cordero, E. Liberto, B. Sgorbini, P. Rubiolo, Headspace sampling in flavor and fragrance field, in: J. Pawliszyn (Ed.), *Comprehensive Sampling and Sample Preparation*, Elsevier, Academic Press, Oxford (UK), 2012, pp. 1–25.
- [163] P. Rubiolo, B. Sgorbini, E. Liberto, C. Cordero, C. Bicchi, Analysis of the plant volatile fraction, in: A. Herrmann (Ed.), *The Chemistry and Biology of Volatiles*, Wiley, Chichester (UK), 2010, pp. 50–93.
- [164] C. Bicchi, C. Cordero, P. Rubiolo, A survey on high-concentration-capability headspace sampling techniques in the analysis of flavors and fragrances, *J. Chromatogr. Sci.* 42 (8) (2004) 402–409.
- [165] A. Bernreuther, N. Christoph, P. Schreier, Determination of the enantiomeric composition of γ -lactones in complex natural matrices using multidimensional capillary gas chromatography, *J. Chromatogr. A* 481 (1989) 363–367.
- [166] A. Mosandl, C. Askari, U. Hener, D. Juchelka, D. Lehmann, P. Kreis, C. Motz, U. Palm, H.-G. Schmarr, Chirality evaluation in flavour and essential oil analysis, *Chirality* 4 (1) (1992) 50–55.
- [167] C. Bicchi, C. Balbo, A. D'Amato, V. Manzin, P. Schreier, A. Rozenblum, P. Brunerie, Cyclodextrin derivatives in GC separation of racemic mixtures of volatiles - Part XIV: some applications of thick-film wide-bore columns to enantiomer GC micropreparation, *J. High Resolut. Chromatogr.* 21 (2) (1998) 103–106.
- [168] C. Bicchi, A. D'Amato, V. Manzin, A. Galli, M. Galli, Cyclodextrin derivatives in GC separation of racemic mixtures of volatiles 12. Thick-film wide-bore columns for enantiomer GC preparation, *J. High Resolut. Chromatogr.* 20 (9) (1997) 493–498.
- [169] V. Schurig, Preparative-scale separation of enantiomers on chiral stationary phases by gas chromatography, in: F. Toda (Ed.), *Enantiomer Separation: Fundamentals and Practical Methods*, Springer Netherlands, Dordrecht, 2004, pp. 267–300.

- [170] M. Juza, O. Di Giovanni, G. Biressi, V. Schurig, M. Mazzotti, M. Morbidelli, Continuous enantiomer separation of the volatile inhalation anesthetic enflurane with a gas chromatographic simulated moving bed unit, *J. Chromatogr. A* 813 (1998) 333–347.
- [171] D. Sciarrone, S. Pantò, P. Donato, L. Mondello, Improving the productivity of a multidimensional chromatographic preparative system by collecting pure chemicals after each of three chromatographic dimensions, *J. Chromatogr. A* 1475 (2016) 80–85.
- [172] D. Sciarrone, S. Pantò, C. Ragonese, P. Dugo, L. Mondello, Evolution and status of preparative gas chromatography as a green sample-preparation technique, *Trac. Trends Anal. Chem.* 71 (2015) 65–73.

Sample preparation for gas chromatography

Colin F. Poole

Department of Chemistry, Wayne State University, Detroit, MI, United States

24.1 Introduction

Direct injection is suitable for the analysis of simple mixtures of thermally stable compounds with similar physical and chemical properties and a limited relative concentration range. For most other samples some form of sample preparation is required. Samples that are too dilute require concentration, and perhaps solvent exchange, to a smaller volume to facilitate detection, a common situation for trace analysis. Samples that are too complex, that exceed the peak capacity of the separation system, and those that contain late eluting peaks not of interest for the analysis, require some form of isolation or cleanup step to simplify the sample prior to separation. Also, samples containing involatile components, such as inorganic salts, particulate matter, nonvolatile organic resins, polymeric materials, and compounds that decompose on the column, etc., must be removed prior to separation to avoid deterioration of column performance. Many compounds of poor thermal stability contain polar functional groups and may be rendered suitable for separation by gas chromatography after conversion to

thermally stable derivatives. Derivatization may also be required to enhance the response of target compounds to a particular detector.

A combination of techniques is often required to prepare a complex sample for gas chromatographic analysis. A typical scheme for sample analysis might include one or all of the following steps: preliminary sample fractionation; isolation of the target compounds of interest; and concentration to a level suitable for detection. In this way the sample introduced into the gas chromatograph will be effectively separated with a suitable separation time, with an adequate detector response, and without significant column contamination. Virtually all laboratory-scale separation techniques have been adapted to the needs of sample preparation reflecting the diversity of sample types that can be handled by gas chromatography [1–14]. The selection of a suitable method is usually based on such considerations as the needs of the analysis, the physical and chemical properties of the target compounds, the anticipated concentration of the target compounds, a knowledge of the sample matrix and potential interferences, the time and material costs involved, equipment needs, and

previous experiences with a particular method. For routine methods the ease of automation and possibility of miniaturization may also be important. Many conventional methods of sample preparation are considered labor-intensive and environmentally unsustainable affording scope for the continuous evolution of sample preparation approaches. Added to which, sample preparation is often considered the bottleneck in sample analysis, and new approaches are continually introduced to address the needs for higher sample throughput. All in all, sample preparation for gas chromatography is represented by a breadth of options, a voluminous contemporary literature, and is far from a finished story.

24.2 Isolation and concentration techniques using physical methods

24.2.1 Traditional methods

Here I have made a somewhat arbitrary selection of conventional techniques that have undergone little change since the turn of the century. Although generally mature techniques, they are not dead techniques and are commonly found in official analytical methods for various government bodies and industrial associations. Most are difficult to automate or miniaturize and may seem out of step with contemporary trends in sample preparation but do facilitate batch processes for higher sample throughput.

24.2.1.1 Distillation

Distillation is a suitable technique for the isolation of a narrow-boiling-point fraction from liquid samples or the soluble portion of solid samples [1,7,15,16]. Compounds of low volatility are effectively removed from the isolated fraction and target compounds are isolated in a concentrated form typically suitable for analysis by direct injection. Separations are based on boiling point differences at atmospheric or

reduced pressure. The more volatile components of the sample are found concentrated in the vapor phase, which is collected in one or more fractions after condensation. The most widely used techniques for sample preparation are simple distillation, fractional distillation, vacuum distillation, and steam distillation. Simple distillation refers to the process whereby the composition of the vapor leaving the liquid remains constant as it moves from the bulk liquid to the collected condensed fraction. Equipment requirements are minimal and adaptable to laboratory-scale processes for samples > about 5 mL. Typical applications include stripping a liquid from involatile or solid materials or separation of the sample into a small number of fractions with defined boiling point ranges. For fuels, oils, and spirits the percent distilled in different boiling point ranges can be converted to composition information by analyzing the collected fractions by gas chromatography [16]. Fractional distillation is used when a more efficient separation is required. A fractionation column and a reflux-ratio-controlling device are additional equipment requirements compared with simple distillation. The single-stage concentric tube, rotary-film, climbing-film, and falling-film evaporators operated at atmospheric or reduced pressure are the most useful for isolating organic volatiles, particularly for fragrance and flavor evaluation. Contact times between the target compounds and heated surfaces are short in such devices and concentration increases up to several-hundred-fold can be obtained. However, their major application is the isolation of single-component fractions while simple distillation combined with gas chromatography might provide more information in a shorter time. Steam distillation (hydrodistillation) is the most common distillation sample preparation technique for gas chromatography [4,7,17–19]. Steam distillation is a simple distillation procedure in which vaporization of organic compounds is achieved by either continuously blowing live steam through the sample or by boiling an

aqueous solution/suspension of the sample. Volatile organic compounds are entrained in the steam vapor and carried over into the condenser, leaving nonvolatile fractions and solid residues behind. For efficient isolation (particularly target compounds in low concentration), the product of the vapor pressure and molecular mass of the target compounds should be large compared with the equivalent values for steam. For large sample sizes, phase separation occurs after condensation; however, small or dilute samples require solvent extraction for sample recovery. The Clevenger apparatus is the classical method for the macroscale isolation of essential oils from plant materials by steam distillation. Recent innovations include the incorporation of microwave heating of the sample solution/suspension [20,21]. Steam distillation is often considered an alternative sample preparation method to solvent extraction and gas-phase stripping for the isolation of polar, acidic, and basic compounds from an aqueous sample due to the poor efficiency of water-immiscible organic solvents for the extraction of these compounds and their low volatility and high water solubility, which results in slow transfer to the gas phase in sparging techniques. Since many substances form azeotropes with water of lower boiling point than the parent compound, this helps to extend the mass range of compounds that can be isolated by steam distillation. Salting out, pH adjustment, or the addition of a codistillation solvent may improve the recovery of some difficult compounds.

Likens and Nickerson described an apparatus for combining continuous steam distillation and liquid–liquid extraction that is widely used for the macroscale isolation of volatile compounds from natural products [22]. A small-scale version of this apparatus is better suited for sample preparation for gas chromatography [23–25]. This apparatus can handle 10–100 mL of aqueous solution or 1–20 g of solid as an aqueous

suspension with extraction of the steam distilled compounds into 1 mL of a water-immiscible organic solvent. It is a selective isolation technique since recovery depends on the rate of distillation of the target compounds, their distribution constants for the solvent extraction stage, and the total time of the extraction process.

Sublimation, the direct vaporization and condensation of solid without passing through a liquid phase, is a useful method for purification of compounds that can be sublimed (e.g., polycyclic aromatic hydrocarbons) but is currently less used for sample cleanup [4]. Sweep codistillation (or assisted distillation) for the isolation of pesticides from oily matrices seems to have succumbed to the same fate [26].

24.2.1.2 *Freeze concentration and freeze-drying*

Freeze concentration is a useful technique for the concentration of volatile compounds in aqueous solutions containing thermally labile matrix components [27]. In this case, water is removed as solid ice concentrating the target compounds and matrix components into a small volume of unfrozen water. Artifact formation is uncommon, but sample losses due to occlusion, adsorption, evaporation, and channeling in the ice layer may occur.

Lyophilization (freeze-drying) is a useful technique for concentrating low-volatility organic compounds and for preserving biological samples by vacuum sublimation of ice [28–31]. The bulk of tissue and many food samples is water. Its selective removal considerably reduces the space required for storage. Tissue samples can be ground and sieved to a powder after freeze-drying providing a homogeneous sample for subsequent analysis. High concentration factors can be obtained since large volumes of aqueous samples can be concentrated. Sample losses, particularly of volatile compounds, occur when the bulk of the water has been removed and the temperature rises while the sample remains

under vacuum. There are numerous commercial lyophilizers of different designs, some with external cooling and temperature control of the sample compartment to minimize volatility losses. Inorganic substances are concentrated simultaneously with the target compounds and may require desalting prior to analysis by gas chromatography.

24.2.2 Solvent extraction

Dissolving all or part of a sample by contacting with a solvent is probably the most common sample preparation technique for gases, vapors, liquids, or solids for gas chromatography, Table 24.1 [4,32]. Further separation is possible by distributing the sample between two immiscible solvents in which the target compounds and their matrix have different solubility. It has the following advantages: the availability of a large number of volatile solvents affording a reasonable range of selectivity; simple or minimal equipment requirements; and compatibility of the final extracts with the most common sample introduction methods for gas chromatography. Solvent extractions are usually carried out discontinuously with the attainment of equilibrium or continuously under conditions where equilibrium is not necessarily established. The usefulness of an extraction solvent depends primarily on its relative affinity for the target compounds as measured by a distribution constant, the apparent phase ratio of the extractor (ratio of the extraction solvent and sample volume), and the number of extraction steps. For simple batch-wise extractions using separatory funnels, the distribution constant should be large since there are practical limits to the phase volume and number of extractions before the method becomes tedious and the sample extract very dilute. The difference in the distribution constant for the target compounds and the matrix is a measure of the selectivity of the extraction system.

24.2.2.1 Classical liquid–liquid extraction

Classical liquid–liquid extraction has simple equipment requirements, mostly separation funnels, flasks, and vials suitable for sample volumes from the microliter to liter range. Mixers, shakers, and centrifuges of different types facilitate agitation, settling, and phase separation. Multiwell plates and liquid handlers are used in high-throughput applications employing parallel sample processing [33]. Continuous liquid–liquid extraction is an option to enhance the isolation of target compounds from aqueous solution when the distribution constants are unfavorable, the sample volume is large, or the rate of extraction is slow. Numerous continuous extractors of simple design for lighter-than-water or heavier-than-water solvents have been described [32]. Generally, an immiscible organic solvent is boiled, condensed, and allowed to percolate repetitively through an aqueous sample of fixed volume with transfer to and accumulation of the target compounds in the organic solvent reservoir. Extraction typically takes several hours and can provide concentration factors up to about 10^5 .

24.2.2.2 Countercurrent chromatography

Countercurrent chromatography has emerged as an attractive technique for the preliminary fractionation of complex mixtures by their distribution between two immiscible solvent systems in which one phase is held stationary by use of hydrostatic forces created by either a planetary motion or a centrifugal field while the other phase is pumped through it [32]. On account of dilution there have been few applications for trace analysis but numerous applications for the isolation of main and minor components. The apparatus and its operation are somewhat specialized, which currently limits general applications. Many applications have been described for natural product chemistry and herbal medicines. Target compounds are typically isolated in a solution that is partially

TABLE 24.1 Isolation of organic compounds by solvent extraction.

Sample type	Equipment requirement	Comments
Organic vapors in the gas phase or gas mixtures	Impinger, denuder, gas wash bottle or similar device	<p>Solvent acts as a selective extractant retaining the sample because of its higher affinity for the solvent compared to the gas phase</p> <p>Solutions of a complexing agent may be used to enhance recovery</p> <p>Solubility of the extractants may be adjusted by varying temperature of the extracting solvent</p>
Aqueous or organic solutions	Separatory funnel, continuous extractor, countercurrent apparatus	<p>Sample solution is shaken with a similar volume of an immiscible solvent</p> <p>Restricted to modest sample volumes and target compounds with favorable (large) distribution constants</p> <p>Repetitive extraction required for small distribution constants</p> <p>Addition of salts, pH adjustment, ion-pairing agents can be used to adjust distribution constants</p> <p>Continuous extraction or countercurrent chromatography required for target compounds with small distribution constants and for large sample volumes</p>
Organic liquids	Mixing device	<p>Selective extraction by mixing with a suitable solvent</p> <p>Precipitation or freezing used to remove coextractants</p>
Solid	Homogenizer, Shaker, Soxhlet extractor, Microwave or Ultrasound extractor, Pressurized fluid extractor	<p>Solid sample mechanically shaken with solvent (fixed time)</p> <p>Bulky samples dried, cut, ground, pressed, or milled prior to extraction to promote efficient extraction</p> <p>Tissue samples freeze-dried or homogenized in the presence of a water-miscible organic solvent</p> <p>Recovery of target compounds may be more favorable at higher temperatures or solvent reflux</p> <p>For faster extraction and higher recovery microwave- and ultrasound-assisted extraction is utilized</p> <p>Samples that are difficult to extract efficiently using a few solvent exchanges can be extracted continuously at the boiling point of the solvent in a Soxhlet extractor or at higher temperatures in a pressurized fluid extractor</p>

aqueous and may also contain salts. Thus, solvent exchange may be required for gas chromatographic analysis. Solvent extraction is also possible in the form of liquid–liquid chromatography using a physically adsorbed solvent on a porous support as a stationary phase and equipment similar to classical liquid chromatography or potentially high-pressure liquid chromatography. Currently, this approach is not widely used as attention at present is focused on small-scale sample preparation methods.

24.2.2.3 *Salting-out-assisted liquid–liquid extraction*

Salting-out-assisted liquid–liquid extraction is a form of homogeneous liquid–liquid extraction based on the salting-out effect of a water-miscible organic solvent by the addition of a substance capable of inducing phase separation from an aqueous solution [32,34–36]. It employs the spontaneous formation of a biphasic system and simultaneous extraction of target compounds into a separated organic solvent-rich phase suitable for gas chromatography sometimes following additional sample cleanup and/or desiccation. The high salt and organic solvent concentrations typically employed effectively precipitate proteins in biological fluids and less solvent is generally required compared with classical liquid–liquid extraction. It is particularly well suited to the analysis of polar compounds (but not exclusively) inefficiently extracted by typical water-immiscible organic solvents. Common organic solvents used in this technique include acetonitrile, acetone, ethanol, and tetrahydrofuran and inorganic salts containing small multiply charged anions (potassium or magnesium sulfate, phosphate, carbonate, etc.) or sucrose as additives for phase separation. Salting-out-assisted liquid–liquid extraction is the enabling technique incorporated in the QuEChERS method for the multiresidue analysis of contaminants in food and environmental samples.

24.2.2.4 *Solvent selection*

General rubrics for solvent selection for extraction are reviewed elsewhere [32,37,38]. The choice of solvent is of paramount importance for controlling selectivity along with additives to optimize distribution constants for polar and ionizable compounds. To expand the selectivity space for solvent extraction as well as complying with the goals of green chemistry, room-temperature ionic liquids and deep eutectic solvents have attracted attention as environmentally friendly replacements for volatile organic solvents, at least for research purposes, as there are few current routine uses [32,39–41]. These solvents provide a blend of physical properties complementary to conventional organic solvents as well as being good solvents for a wide variety of compounds in which they behave as polar solvents. They can form biphasic systems with water or low-polarity organic solvents depending on their structure. Some properties attractive from the green chemistry perspective are disadvantages for gas chromatographic analysis. Their general high viscosity compared with typical organic solvents makes manipulation during extraction and injection by microliter syringes difficult. The absence of vapor pressure prevents their evaporation in typical injectors for gas chromatography. This results in contamination of the inlet, unstable baselines, and possibly unstable column flow rates. Direct injection is possible using modified inlets to retain the involatile solvents or by thermal desorption from a solid support. These options are not as convenient as sample introduction for volatile organic solvents.

24.2.2.5 *Applications of classical liquid–liquid extraction*

Most practical examples of liquid–liquid distribution for the isolation of target compounds utilize water as the main component of one phase of biphasic systems. Water forms the largest number of biphasic systems with organic

solvents than any other solvent [37]. Also, water is a ubiquitous component of most biological and environmental samples and a common component among food and industrial products. Thus samples containing water as a major component are common and favor extraction techniques that are compatible with water. On the other hand, water is the most cohesive and polar of common laboratory solvents, and any solvent competitive with water for polar interactions is almost certainly miscible with water. This limits the possible selectivity space available for water-containing biphasic systems. Totally organic biphasic systems provide complementary and more varied distribution properties compared with aqueous biphasic systems. In addition, water-based systems are of little use for the extraction of target compounds and matrices of low-water solubility and cannot be used at all for compounds that are unstable in water. Typical applications of totally organic biphasic systems are the extraction of oil-based samples of natural or synthetic

origin, cosmetics, pharmaceutical products, spices, and foods.

A general scheme for the group fractionation of a sample soluble in a water-immiscible organic solvent by liquid–liquid extraction is shown in Fig. 24.1 [42]. By manipulating the pH of the aqueous solution, the sample is fractionated into neutral, basic, and acidic compounds. The acidic fraction can be further subdivided into strong and weak acids. Back-extraction of the acidic and basic fraction allows isolation of the compounds of interest in an organic solvent suitable for direct analysis or after further sample cleanup and/or derivatization. Additional fractionation of the neutral fraction is possible using functional-group selective reagents. For example, aldehydes and ketones can be isolated as water-soluble complexes with a sodium bisulfate solution or by using hydrazide reagents (Girard's reagent T). After hydrolysis of the complexes, the target compounds are back-extracted into an organic solvent for analysis. A more general

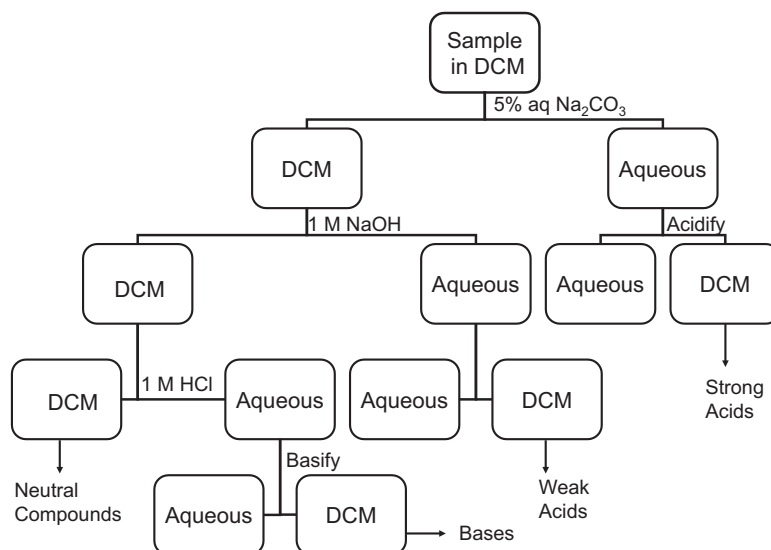


FIGURE 24.1 General scheme for the fractionation of samples soluble in a water-immiscible organic solvent by liquid–liquid extraction. Aqueous solutions of different pH are used to isolate neutral, basic, weak acid, and strong acid fractions. In the example shown DCM = dichloromethane.

fractionation based on polar interactions can be achieved by distribution in one of several totally organic biphasic systems [43,44].

The isolation of drugs and metabolites from biological fluids and tissues usually requires some form of sample pretreatment [33,45,46]. Basic drugs are typically extracted at $\text{pH} > 7$ from whole blood, while acidic drugs are usually extracted at $\text{pH} < 5$ from plasma or serum. Proteins are typically precipitated prior to liquid–liquid extraction by the addition of a polar organic solvent followed by centrifugation or by hydrolysis with a proteolytic enzyme. Lipids can be removed in a subsequent step by extraction with a low-polarity solvent. The protein and lipid content of urine is significantly lower than in plasma, and direct extraction of the filtered sample is possible for most drugs. Urine contains significant amounts of bound and conjugated drugs that may require acid or enzymatic hydrolysis prior to extraction. Tissue samples are typically homogenized with a water-miscible organic solvent and the supernatant used for analysis and sample cleanup.

The isolation of total lipids from biological samples is routinely performed using either the Folch method [47] or a common modification described by Bligh and Dyer [48]. The Folch and Bligh–Dyer methods utilize binary mixtures of chloroform and methanol (in different ratios) for the extraction of lipids followed by the addition of water for formation of a biphasic system. The spontaneous dissociation into two phases results in the partitioning of polar biological molecules (e.g., proteins, carbohydrates, salts, etc.) into the water-rich phase and neutral compounds of lower polarity, including most of the lipids, into the chloroform-rich phase. Insoluble particles and cellular debris are removed by filtration or centrifugation.

Pesticides of a wide polarity range can be isolated from low-fat commodities using the QuEChERS method [32,49,50]. This approach is based on a small-scale extraction using acetonitrile, salting out and dehydration of the

acetonitrile phase by magnesium sulfate and sodium acetate, and cleanup of the acetonitrile extract by dispersive solid-phase extraction. Numerous modifications of the generic method have been proposed for particular matrices. This approach has been adopted for a wide variety of environmental, forensic, industrial, pharmaceutical, and veterinary samples and is currently the go-to sample preparation approach for the determination of multiresidue contaminants by gas chromatography. Advantages include its streamlined sample processing and simplicity of adapting the general method to specific sample matrix problems. Parallel sample processing allows high sample throughput and low cost per sample making it an ideal choice for screening and survey programs.

24.2.2.6 *Liquid-phase microextraction*

The mid-1990s saw a paradigm shift in the practice of liquid–liquid extraction to address issues around the development of green analytical methods and to improve sample utilization in techniques such as gas chromatography. This research area became known as liquid-phase microextraction and comprises a number of small-scale and innovative approaches for solvent extraction [32,51,52]. In single-drop microextraction the extraction solvent is suspended as a single drop from the tip of a microsyringe needle immersed in an agitated aqueous sample solution or suspended in the headspace above the sample surface. The whole sample extract is introduced directly into the gas chromatograph overcoming the limitations of the low phase ratio and negligible sample depletion. The extraction rate is slow and equilibrium rarely achieved for standard sampling times. Calibration is required for quantitative methods. The selection of the extraction solvent is limited by the partial solubility of many organic solvents in the relatively large sample volume and the mechanical instability of the suspended drop in the agitated solution. To improve the robustness of the single-drop microextraction technique,

hollow-fiber liquid-phase microextraction was proposed [52,53]. The extraction solvent occupies the lumen and pores of a short microporous polymeric hollow fiber membrane, which is subsequently immersed in a stirred sample solution or suspended above it in the headspace. Solid-drop liquid-phase microextraction offers an alternative solution to the problem of mechanically unstable suspended solvent drops in a stirred solution [52,54]. In this case a small volume of an immiscible organic solvent is spread on the surface of a stirred aqueous sample solution followed by collection of the drop now formed in the vortex depression created by rapid stirring of the sample solution. After a suitable extraction time, the solvent drop is isolated by cooling the solution below the freezing point of the extraction solvent and removing the droplet with a microspatula. The extraction solvent must have a melting point near room temperature to facilitate its recovery as a solid drop as well as low solubility in the sample solution.

The most important of the current liquid-phase microextraction techniques is dispersive liquid–liquid microextraction [52,55–57]. This technique employs a ternary solvent system composed of a water-immiscible extraction solvent, a disperser solvent miscible with both the sample solution and extraction solvent, and the aqueous sample solution. A few percent of extraction solvent dissolved in the disperser solvent with a total volume of a few hundred microliters is rapidly injected into an aqueous sample solution forming a cloudy suspension consisting of microdroplets of extraction solvent uniformly dispersed throughout the sample solution. Centrifugation is typically used to isolate the extraction solvent by sedimentation for injection into the gas chromatograph. Formation of an emulsion phase creates the favorable conditions for the extraction reducing the extraction time and achieving useful preconcentration factors. The function of the disperser solvent is to promote droplet formation and to enhance the contact surface area between the extraction

solvent and the sample solution. Numerous modifications to the general technique aimed at simplifying sample handling or facilitating automation have been introduced and this remains an active research area. Liquid-phase microextraction techniques have so far not appeared in any regulatory or official methods of analysis but will probably do so in at least a limited way for aqueous samples analyzed by gas chromatography.

24.2.3 Liquid–solid extraction

The extraction of solids can be a challenge since the rate and extent of extraction typically depend on the properties of the matrix and the distribution of target compounds within the matrix as well as the ability of the extraction solvent to compete with the target compounds in sorptive interactions with the matrix [14]. Solid samples are usually processed initially to enhance the rate and extent of extraction [13,26,58]. Typical procedures are drying, grinding, homogenization, and sieving. Air-drying is suitable for plant materials and soil and freeze-drying for tissue and food commodities. Additional drying can be achieved by adding or grinding the sample with a desiccant (e.g., sodium sulfate) or diatomaceous earth, which also acts as a dispersion medium. Milling, chopping, and homogenization are used to reduce the particle size and to increase the surface area of the sample placed in contact with the solvent. Samples containing a large amount of fat usually require solidification prior to grinding by adding dry ice to the sample or by using a cryogenic mill. Sieving typically follows grinding to obtain a sample with a uniform particle size. Homogenization provides more efficient contact between solvent and sample and promotes a higher recovery of target compounds. Small-size samples, such as biological tissues, are usually homogenized in a probe-like high-speed homogenizer while large-scale samples, such as food commodities, are typically

homogenized together with the extraction solvent in a blender to simultaneously commute and extract the sample.

All analyses require a representative sample to achieve meaningful information about the sample. For heterogeneous samples using traditional methods, this has tended to favor sample sizes of 50–100 g, requiring 200 mL or more organic solvent for extraction. This is typical of regulatory methods except for biological tissues, for which only smaller sample sizes are typically available. Modern methods of solvent extraction tend to favor smaller sample sizes, 1–10 g, and solvent volumes of 10–20 mL, to achieve a better balance between obtaining a representative sample, extract utilization, and method economics. Even in this case, sample utilization is poor for gas chromatography since only a small fraction of the extract is used for the analysis, and a solvent reduction method may still be required to concentrate the extract.

24.2.3.1 *Traditional methods*

Traditional methods of solvent extraction for solids include shake flask, homogenization, and Soxhlet extraction. Shake flask methods are suitable for the extraction of target compounds of high solubility in the extraction solvent and only weakly bound to the matrix. Porous solids or semisolids are well suited to this technique. The sample and extraction solvent are placed in the same vessel and gently rocked or more vigorously agitated for a defined time using one of several common automated laboratory devices. The insoluble portion of the sample and the solvent extract are then separated by decantation, centrifugation, or filtration. Shake flask methods require a cooperative matrix and for many sample types, recovery is low or variable. The Soxhlet apparatus provides a more efficient extraction and until recently was the extraction technique for solids against which all other methods were compared [12,32,59,60]. Soxhlet extraction works best for samples in the form of a free-flowing powder; for matrices of low solubility in the

extraction solvent; for target compounds with a low vapor pressure at the extraction solvent boiling point; and for extraction solvents of low viscosity. The extraction solvent is vaporized, condensed, and allowed to percolate through the solid sample contained in a porous extraction thimble. The return of the solvent to the boiling flask is discontinuous, working on the siphon principle, and extracted material accumulates over time in the boiling flask as the sequence of vaporization, condensation, solid–liquid contact, return of solvent and extract to the boiling flask continues in a cyclic fashion. Typical conditions employ 10 g of sample, 50–200 mL of solvent, and a total extraction time of 1–6 h (or overnight) although smaller-scale extractors are available. The automated Soxhlet apparatus was developed to address some of the disadvantages of the traditional extraction method: a long extraction time; large volumes of extraction solvent; and the extracted compounds must be stable at the boiling point for the extraction solvent since they are accumulated in the boiling flask [60]. A faster extraction is achieved by commencing the extraction process with the sample in its thimble suspended in the boiling solvent rather than in contact with the condensed solvent, as is normally the case. At a suitable time the sample is raised above the boiling solvent and rinsed sequentially by condensed solvent, similar to the conventional extraction process, except that a shorter time is required. Finally the sample is concentrated by *in situ* distillation allowing collection and reuse of the solvent for other purposes. The extraction time is reduced 4–10-fold, largely as a result of the immersion step; solvent consumption is reduced by about 50%; and samples can be processed in parallel without operator intervention.

24.2.3.2 *Ultrasound- and microwave-assisted extraction*

Rapidly growing approaches for the extraction of solids utilize methods that afford improved energy transfer into the sample

together with further sample disintegration using ultrasound- or microwave-assisted devices. Sonic treatment, either by immersion of the sample and extraction solvent in a suitable vessel in a sonic water bath or by horn and probe devices, is commonly used to accelerate the extraction rate for porous solids and to disrupt the cellular structure of tissue samples releasing the cell contents [61–63]. The interaction between ultrasound and solvents is complex but generally results in enhanced solubility for target compounds, improved solvent penetration and transport within porous solids, and a slow increase in temperature favoring its use for the extraction of thermally labile compounds. Compared with Soxhlet extraction, it is faster, typically requires less solvent, generally extracts fewer matrix interferences, and affords similar recovery to classical Soxhlet extraction (although this does depend on the matrix). On the other hand, separation of the insoluble sample residue from the extraction solvent and rinsing steps is required at the end of the extraction, adding to the sample processing time. It is generally the method of choice for initial screening of samples as a fast and uncomplicated sample processing technique. Microwave-assisted solvent extraction requires purpose-designed apparatus for efficient heating and sample handling [58,64,65]. The absorption of microwave energy by either the sample or the solvent results in a rapid increase in temperature that in a sealed vessel can easily exceed the atmospheric pressure boiling point of the solvent. There are two general sample processing strategies generally employed. For microwave-absorbing samples surrounded by a solvent of low permittivity (low-polarity solvent), extraction occurs by expulsion of the target compounds from the hot sample into the (relatively) cool solvent. Alternatively, if the solvent is microwave-absorbing (polar solvent), heat is produced throughout the extraction system and flows from the solvent to the sample. Extractions are typically much faster compared with Soxhlet

extraction and solvent consumption is significantly reduced. On the other hand, the method is a poor choice for the extraction of thermally labile compounds, initial capital costs are relatively high, and after completion of the extraction, it is necessary to wait for the vessel to cool down before separating the solvent extract from insoluble sample by decantation, centrifugation, or filtration. The postextraction period adds significantly to the sample processing time and hinders full automation.

24.2.3.3 *Pressurized fluid extraction*

Pressurized liquid extraction and supercritical fluid extraction are further examples of closed-vessel extraction techniques typically performed at elevated pressures and temperatures using automated instrumentation. For pressurized liquid extraction, also known as accelerated solvent extraction, the sample as a free-flowing powder is placed in a stainless steel vessel and brought to an operating pressure (>100 bar) by pumping solvent into the vessel, which is heated to a temperature between 50 and 200°C. Initially, the sample is extracted under static conditions for a chosen time before relieving the pressure by allowing the solvent to escape to a collection vessel. The remaining extract is displaced from the vessel by fresh solvent followed by a nitrogen gas purge. Repeating the static extraction with fresh solvent in a cyclic fashion is an option for recalcitrant samples. An optimized extraction is a balance between the static extraction time and conditions, the number of cycles (if more than 1), and the total acceptable extraction time. Solvent usage is typically low (15 mL for a 10 g sample) and the extraction time is short (<20 min). Simultaneous extraction and cleanup are possible by adding a suitable sorbent to retain matrix components downstream of the sample (in-cell cleanup). The recovery of target compounds can exceed those for Soxhlet extraction, but the extract may be more complex due to matrix contamination. The process for supercritical fluid extraction is similar except that the

solvent in this case is a gas-like carbon dioxide raised to a temperature and pressure higher than its critical point for the extraction and purge steps [4,8,59,65,66]. Supercritical fluids have low viscosity, no surface tension, and favorable diffusion properties compared with liquids. These properties provide more favorable extraction kinetics for porous solids. The solvating capability of fluids can be changed over a useful range by varying temperature and pressure (density). However, the only supercritical fluid in common use is carbon dioxide and its low solvent strength means that small volumes of a polar organic solvent are required for the extraction of polar target compounds. A favorable feature of supercritical fluid extraction is that after depressurization in the collection vessel, carbon dioxide escapes as a gas resulting in concentration of the extract. Supercritical fluid extraction using carbon dioxide can be coupled directly to gas chromatography in which the depressurization step occurs in the injector of the gas chromatography, or in an interface module, and the separation is performed in the usual way [4,67,68]. This approach is made less attractive by low sample throughput (one sample at a time), instrument complexity, and the requirement for extensive optimization.

24.2.3.4 Matrix solid-phase dispersion

Matrix solid-phase dispersion is a widely used small-scale solvent extraction approach used to isolate contaminants or natural constituents from complex environmental, plant, and animal matrices [69,70]. Liquid samples are mixed and solid samples ground with an abrasive sorbent, typically an inorganic oxide or chemically bonded sorbent similar to materials used for solid-phase extraction. The sample matrix is disrupted and distributed into the sorbent by this pretreatment forming a free-flowing powder of uniform particle size. The powder is then packed into a short disposable column and the target compounds eluted with a small volume of solvent leaving sample debris in the column and

matrix components adsorbed to the sorbent. In addition, a cosorbent can be added at the bottom of the extraction column to facilitate *in situ* cleanup. In many cases, this method provides a sample suitable for direct analysis by gas chromatography or, if not, after further sample cleanup.

24.2.4 Gas-phase extraction

Gases can be utilized for the extraction of volatile compounds using gas-phase stripping techniques. Gases can also be a sample matrix, for example, in aerosols, from which volatile compounds are extracted and particulate matter isolated by filtration for subsequent analysis. Gas chromatography is the premier technique for the analysis of volatile organic compounds and is widely used for analysis of these samples.

Impingers, bubblers, and denuders are widely used solvent extraction devices for isolating high-boiling, reactive, or polar compounds from the gas phase [4]. They are typically used to isolate compounds difficult to recover from sorbent traps, the most common method for isolating volatile organic compounds from the gas phase, described in Chapter 10. Typical applications of gas-phase solvent extraction include personal sampling systems for monitoring workplace exposure to hazardous chemicals and in combination with filters solid-phase sampling devices for isolation of particulates, volatile organic compounds, and reactive gases from stack gases and engine exhaust, etc. Particulate matter accumulated on filters or collected with an impactor is typically treated by methods described for the solvent extraction of solids (Section 24.2.3). Liquid samples are usually analyzed directly by gas chromatography or after cleanup or derivatization [71].

Several gas-phase extraction methods for the isolation of volatile organic compounds from aqueous solution or solids can be coupled directly to gas chromatography as fully or

semiautomated systems. These are more fully described in Chapter 9 and only briefly mentioned here. The family of headspace methods provides an indirect approach for the analysis of volatile organic compounds from either a problematic matrix or dilute solution. Static headspace involves sampling the gas phase above a sample in an enclosed vessel in which equilibrium between the concentration of target compounds in the gas phase and sample has been established. Since only the gas phase is taken for analysis, matrix interference in the gas chromatographic separation is avoided. For dynamic headspace the gas phase is passed continuously over the sample and the extracted compounds accumulated in a cryogenic or sorbent trap prior to injection into the gas chromatograph. The target compounds are recovered by either thermal desorption or solvent elution from sorbent traps. Dynamic headspace offers a complementary approach to static headspace for the isolation of target compounds at lower concentrations than suitable for static headspace methods. Introducing the gas phase below the surface of an aqueous solution through a fritted orifice produces a continuous stream of freely dispersed bubbles maximizing the surface contact between the gas and liquid phases. As volatile organic compounds move into the gas phase, they are rapidly transported to a cryogenic or sorbent trap for accumulation and injection into the gas chromatograph, similar to dynamic headspace. This technique is referred to variously as purge-and-trap, gas-phase sparging, or gas-phase stripping. It is more efficient than dynamic headspace when the sample volume is small or the transfer of volatile compounds to the gas phase is inefficient. Typical volatile organic compounds isolated by this technique have low water solubility and an atmospheric boiling point $<200^{\circ}\text{C}$.

Common examples of the use of headspace methods include the analysis of volatile organic compounds where the matrix obscures the

compounds of interest in the chromatogram or contains late eluting peaks of no interest; the matrix contains inorganic compounds or polymers, which cannot be vaporized or dissolved in the usual way for solvent injection; and inhomogeneous samples, such as blood, sewage, colloids, etc., which would require extensive pretreatment prior to conventional gas chromatographic analysis. In these cases, the advantage of headspace methods is the isolation of the target compounds relatively free from its matrix without complicated sample treatment processes as well as a high level of automation. However, these methods generally require careful calibration, which can present its own problems.

24.2.5 Solid-phase extraction

Solid-phase extraction is based on the transfer of target compounds from a gas or liquid sample to the surface of a solid in intimate contact with the sample. The target compounds are isolated by their favorable interactions with the solid surface. The sorbent is separated from the sample matrix by various means and the target compounds recovered by solvent elution or thermally desorbed into the gas chromatograph. Porous polymers of high thermal stability and low water retention were responsible for revolutionizing the analysis of volatile organic compounds in air and purge gas samples from aqueous solution (see Chapter 10). Compounds of low mass ($<C_7$) are weakly retained at room temperature by polymeric sorbents such as Tenax, and a more active sorbent based on carbon is required to trap these compounds. Dual traps containing a porous polymer in the front section and a carbon-based sorbent in the rear can be used for the collection of compounds covering a wide volatility range.

Laboratory-scale, solid-phase extraction of liquids became an important technique with the introduction of disposable cartridge devices containing silica-based chemically bonded, porous polymer, or carbon sorbents of a suitable

particle size for sample processing by suction [70,72–74]. This downscaling and reoptimizing of column properties specifically for extraction quickly gained acceptance as an alternative to liquid–liquid extraction, initially as a replacement for classical liquid–liquid extraction, but more commonly today as a complementary technique to liquid-phase microextraction. Typical cartridge devices consist of short columns (generally an open syringe barrel) containing less than 1 g of sorbent with a nominal particle size between 20 and 60 μm , packed between porous frits. These remain the workhorse format for solid-phase extraction today available in sizes suitable for sample volumes from less than 1 mL to greater than 1 L. For large sample volumes (e.g., surface waters), the relatively slow sample processing rates and a low tolerance to blockage by suspended particles and sorbed matrix components spurred the development of alternative sampling formats based on disc technology in the form of particle-loaded membranes, particle-embedded glass fiber discs, and laminar discs [75]. Particle-loaded membranes consist of a web of polytetrafluoroethylene microfibrils, suspended in which are sorbent particles of about 8–10 μm in diameter. The membranes are flexible with a homogeneous structure formed into circular disks 0.5 mm thick with diameters from 4 to 96 mm. Small-size loose discs or discs housed in syringe barrels are used for small and intermediate sample volumes (similar to cartridges) as well as for special applications, such as on-disc derivatization and in-vial elution. The smaller discs are compatible with sample processing using suction, positive pressure, syringe filtration, and centrifugation. The large-size discs, supported on a sintered glass disc in a standard vacuum filtration apparatus, are used for sampling large sample volumes, such as surface waters free of the general problems associated with the cartridge format. Disc technology has contributed directly to the automation of solid-phase extraction through the development of multiwell extraction plates.

With an eye to further downsizing the extraction process and to facilitate automation, a number of low-volume devices and sorbents in the form of nanomaterials have been proposed [70]. Microextraction by packed sorbent (MEPS), for example, uses a conventional 100 or 250 μL syringe with a 1–2 mg sorbent bed located between the plunger and the needle or built into the needle as the sampling device [76]. The MEPS syringe facilitates low-dead volume sample processing by vertical movement of the plunger with sample and solvent flow possible in both directions through the bed in a cyclic fashion. The multiple contacts between the sorbent bed and sample or elution solvent improve the efficiency of the extraction process. The syringe-based device allows direct injection of the eluted target compounds into the gas chromatograph. Micro-solid-phase extraction ($\mu\text{-SPE}$) combines the advantages of porous membrane-based liquid-phase microextraction with solid-phase extraction in a small-scale device [77]. Solvents for the extraction of polar compounds from water are limited. Replacing such solvents (acceptor phase) with a sorbent material can overcome this deficiency. A small amount of sorbent is sealed inside a sheet of porous polymer membrane surrounding the sorbent whose edges are then sealed to secure the contents. The $\mu\text{-SPE}$ device (wetted with an organic solvent) is then suspended in the stirred sample solution for a suitable time to complete the extraction. The device is then removed, rinsed, and superficially dried, before recovery of the target compounds by ultrasound-assisted extraction with a small volume of organic solvent. The porous membrane acts as an impermeable barrier to macromolecules allowing the extraction of low-mass compounds without contamination of the sorbent or sample extracts for analysis by gas chromatography. The needle trap device is an extraction trap that contains a sorbent inside a small needle, through which a gas or liquid is drawn by gas-tight syringe or a pump, or it can be used for passive sampling

by diffusion [78,79]. Extracted compounds are recovered by thermal desorption of the needle in the hot injection port of a gas chromatograph. It is a small-scale version of sorbent cartridges employed for gas-phase sampling with certain advantages from an automation perspective. Typical sorbents are carbon-based or porous polymers similar to macroscale traps. Compared with solid-phase microextraction (SPME) (Section 24.2.6), quantitative extraction is achieved, which simplifies calibration strategies and the larger amount of sorbent provides a higher sample capacity. Needle traps are less fragile than the coated fibers used for SPME. Although aqueous samples can be processed, problems with particles and carryover due to strongly retained matrix components are difficult to manage, and often a better solution is to combine gas-phase stripping with trapping of organic volatiles from the gas phase. A version of this technique uses an immobilized liquid phase on the interior wall of the needle and is known as solid-phase dynamic extraction.

Nanoparticles with diameters from 1 to 100 nm are characterized by a large surface-to-volume ratio and are small enough for total dispersion in liquid samples. Magnetic core-shell nanoparticles have attracted the most attention since they simplify the handling of the nanoparticles throughout the extraction process with an external magnet [70,80]. Numerous approaches have been described for the synthesis of mainly iron oxide composite materials with a metal core and surface coating of carbon or silica gel, suitable for modification by bonding organic groups to the surface. These platforms have made possible the synthesis of sorbents with a wide range of properties for nonspecific, class-specific, and compound-specific extractions from predominantly aqueous solutions.

24.2.5.1 Sorbents for solid-phase extraction

Common sorbents for solid-phase extraction include inorganic oxides for extraction of nonaqueous samples containing target

compounds of low to intermediate polarity, low-specificity sorbents (alkylsiloxane-bonded silica, porous polymers, and carbon) for extraction of low to moderately polar target compounds from water, and molecularly imprinted polymers for the selective isolation of target compounds with a three-dimensional structure similar to the polymer imprinted cavities [70,74,81,82]. Their characteristic properties and typical applications in gas chromatography are summarized in Table 24.2. For inorganic oxide adsorbents (silica gel, alumina, Florisil, etc.), the properties that increase retention are a large surface area, the type of surface functional groups, and the adsorbent activity. Adsorbent activity is generally controlled by the intentional addition of water to the dry adsorbent prior to use and by drying samples with sodium sulfate, or a similar drying agent, prior to sample processing. A short column of sodium sulfate connected in tandem with the adsorbent cartridge can be used for this purpose also. Irreversible adsorption and catalytic degradation affect the recovery of labile compounds.

Low-specificity sorbents include siloxane-bonded silica sorbents, macroporous polymers, and different forms of carbon. Siloxane-bonded silica sorbents can be prepared with a wide range of bonding densities, pore sizes, and functional group types, although those of most importance are alkylsiloxane-bonded and polar siloxane-bonded silica sorbents containing cyano-, amino-, and propanediol functional groups. Alkylsiloxane-bonded silica sorbents with large surface areas, long alkyl chains (e.g., octadecyl or C₁₈), and high phase loading are generally used to isolate low-mass target compounds from aqueous solution. For polar compounds retention is often inadequate (environmental samples) and for basic compounds recovery may be low due to secondary ion-exchange interactions with ionized silanol groups (biomedical applications). Siloxane-bonded silica sorbents with polar functional groups are fairly ineffective at extracting

TABLE 24.2 Typical sorbents for solid-phase extraction and their general uses in gas chromatography.

(i) Inorganic oxides

Isolation of low- and medium-polarity compounds from nonaqueous solutions

- Organochlorine pesticides and polychlorinated biphenyls from oils and fats using Florisil
- Mycotoxins in feeds using silica gel
- Steroids and vitamins from creams and oil-based suspensions using silica gel or alumina
- Pesticides in foods, feeds, and soils using Florisil or silica gel
- Alkaloids, pigments, and flavor compounds from plant materials using alumina

Matrix simplification by fractionation into groups containing a similar number and type of functional groups

- Lipids on silica gel using chloroform to elute simple lipids, acetone to elute glycolipids, and methanol to elute phospholipids
- Polycyclic aromatic compounds (hydrocarbons, N-containing, and OH-containing) on alumina using a step solvent gradient

(ii) Low-specificity sorbents (aqueous solutions)

Isolation of neutral compounds and weak acids and bases after pH adjustment using alkylsiloxane-bonded silica, porous polymer, and carbon sorbents

- Agricultural and industrial chemicals from surface waters
- Drugs from biological fluids
- Pigments and color additives from beverages and foods

Polar chemically bonded phases

- Carbohydrates and nucleosides from biofluids using 3-aminopropylsiloxane-bonded silica sorbents
- Peptides and surfactants using spacer-bonded propanediol silica sorbents
- Drugs from biofluids using 3-cyanopropylsiloxane-bonded silica sorbents

(iii) Low-specificity sorbents (organic solvents)

Isolation of polar compounds with complementary properties to the sorbent

- 3-Cyanopropylsiloxane-bonded silica: Strong dipole-type interactions with weak hydrogen-bond acidity
- 3-aminopropylsiloxane-bonded silica: Strong hydrogen-bond base and weak hydrogen-bond acid with weak dipole-type interactions
- Spacer-bonded propanediol-bonded silica: Strong hydrogen-bond acid and moderate hydrogen-bond base with moderate dipole-type interactions
- Typical examples include the isolation of polar pesticides from fats and oils, polycyclic aromatic compounds from fuel oils, and active ingredients from ointments and suppositories

(iv) Application-specific molecularly imprinted polymers

Porous polymer sorbents with cavities specifically designed for the isolation of target compounds

Isolation of target compound(s) from organic solvents. Further sample cleanup may not be required before gas chromatographic analysis

low-mass compounds from water and are typically used for the isolation of polar compounds from organic solvents.

The common macroporous polymer sorbents are copolymers of styrene–divinylbenzene or acrylic esters and are used exclusively for extraction from aqueous solution [70,83]. Common formats include particle-packed beds and as monoliths in small-size sampling devices. They

are generally more retentive than siloxane-bonded silica sorbents. Highly cross-linked biporous polymers (hypercross-linked polymers) with large surface areas are favored for the extraction of low-mass polar compounds from water. Hydrophilic macroporous copolymers based on N-vinylpyrrolidone and divinylbenzene or methacrylate and divinylbenzene are water wettable simplifying typical sample

processing protocols. The common forms of carbon for solid-phase extraction are activated carbon and graphitized carbon blacks, supplemented by an expanding number of largely researched materials, such as carbon nanotubes, graphene, graphene oxide, and nanodiamonds [82,84,85]. Conventional carbon adsorbents have large surface areas and a heterogeneous surface containing active functional groups. Common uses are the large-scale isolation of dissolved organic compounds from surface waters and in personal monitoring devices for sampling workplace atmospheres. Poor reproducibility and variable chemical activity are common problems for these materials. Graphitized carbon blacks are more refined with a lower surface area and are used primarily for the gas-phase extraction of volatile organic compounds in combination with porous polymers in multibed sorbent sampling tubes.

Carbon nanotubes are nanomaterials with a different topology and morphology to active carbons. Single-walled and multiwalled carbon nanotubes (also cones, disks, horns, fibers) are characterized by a high surface-to-volume ratio and are easily modified by either physical adsorption of liquids or chemical reactions to create surface-bound organic groups. Carbon nanofibers have significantly larger dimensions and are preferred for solid-phase extraction using cartridge formats. Modified carbon nanotubes are used in solid-phase dispersion. Surface modification not only expands their potential applications but is used to overcome the strong intermolecular interactions between the carbon nanotubes, which prevent their dispersion in typical solvents. Magnetic core carbon composites are also receiving attention for solid-phase extraction.

Various sorbent types have been developed for compound and class-specific extractions, but only molecularly imprinted polymers are

used to a significant extent for gas chromatography [70,86]. Molecularly imprinted polymers are synthetic sorbents with artificially generated recognition sites designed to bind a single target compound or group of compounds with a common structural motif. They are typically more effective for samples dissolved in organic solvents, although techniques to accommodate aqueous samples have been developed, which usually require additional sample processing steps. The main application of molecularly imprinted polymers is the removal of the complex sample matrix, which would otherwise restrict the separation conditions for gas chromatography and to determine the amount of target compound(s) in the sample. Their high specificity can also be viewed as a disadvantage since a new sorbent is required for each group of related target compounds and multiresidue methods are usually impossible. Beyond a few high-volume applications commercial products are unavailable.

24.2.5.2 Sample processing conditions for cartridge and disc devices

Typical sample processing steps for the solid-phase extraction of liquids are summarized in [Table 24.3](#): these typically include sorbent conditioning to promote wetting of the sorbent by the sample solvent and removal of contaminants; application of the sample; rinsing of the sorbent to remove cosorbed matrix components; and recovery of the target compounds by solvent elution. These protocols lend themselves to automation using robotic platforms or special-purpose sample processing units that simultaneously extract and prepare samples for gas chromatographic analysis [33,70,74]. Multiwell plates with a sorbent bed at the bottom of the well or sorbent-containing pipette tips combined with liquid handling robots are suitable for high-throughput sample processing. However,

TABLE 24.3 Sample processing steps in solid-phase extraction using a vacuum manifold and their effect on the recovery of target compounds.

(i) Conditioning solvent (typically 3–5 bed volumes)	<ul style="list-style-type: none">• Ensures reproducible retention and stable flow during sample application• Helps to minimize contamination of extracts by sorbent impurities• Replace by sample solvent before processing samples
(ii) Sample considerations	<ul style="list-style-type: none">• Dilute viscous samples with a weak low viscosity solvent to reduce sample processing time• Remove excess particle matter by filtration or centrifugation to maintain constant sample flow rates• Add small volume of a miscible organic solvent (1%–3% v/v) to large-volume, aqueous samples to ensure sorbent remains solvated and to maintain a constant sample flow rate• Precipitate proteins from biological fluids for acceptable recovery of low-mass target compounds• Adjust pH to minimize ionization of weak acids and bases for aqueous samples• Typical sample flow rates 0.2–1.5 mm/s
(iii) Drying time after sample application is complete	<ul style="list-style-type: none">• Sufficient to remove all sample solvent trapped in sorbent pores• Typically 1–5 min, but sometimes considerably longer• Excessive drying may result in low recovery of target compounds from evaporation or retention in poorly solvated regions of the sorbent
(iv) Rinse solvent (optional)	<ul style="list-style-type: none">• Small volume of solvent of intermediate strength to elute matrix components. Target compounds remain immobilized on the sorbent• Biological fluids, plant and soil extracts often require a rinse step prior to separation while surface waters may not
(v) Solvent elution	<ul style="list-style-type: none">• Should be a strong solvent able to displace the target compounds from the sorbent in a small volume preferably compatible with gas chromatographic analysis without solvent exchange• Should normally be volatile and miscible with the sample solvent• May require desiccation to remove water (aqueous samples)• Ideal volume 2–3 times the bed volume but often larger

semiautomation using a vacuum manifold for parallel sample processing remains the approach used in most laboratories where sample numbers are small and the sample type changes frequently.

Compared with solvents, sorbents have some general disadvantages for extraction. Typical sorbent surfaces contain several functional groups not as easily replicated by synthesis and show greater variation than solvent properties. They also tend to have higher levels of contaminants originating from the manufacturing and packaging process. This can result in a significant chemical background in extract chromatograms. Sorbent retention is also affected by sample processing conditions, such as

overloading, displacement of target compounds by excess matrix, and blocking of sorbent pores restricting access to a portion of the sorbent surface area.

24.2.6 Solid-phase microextraction

SPME is the most important solid-phase extraction format for gas chromatography, integrating sampling, extraction, concentration, and sample introduction with a convenient syringe-based device [11,14,87,88]. The extraction phase is a thin layer of immobilized sorbent about 1 cm long and 10–100 μm thick coated on the outside of a fused-silica fiber or metal wire

support. The fiber is attached to the plunger of a modified microsyringe, which both protects and facilitates manipulation of the fiber during sampling. Sampling techniques include direct immersion, direct immersion with membrane protection, and headspace extraction. The key steps for extraction are the distribution of the target compounds between the extraction phase and the sample matrix and the recovery of target compounds by thermal desorption of the fiber in a standard gas chromatographic inlet with only minor modification. Direct immersion is suitable for sampling aqueous solutions with a low matrix burden. Otherwise the matrix accumulates on the fiber modifying its extraction properties and also may cause unstable baselines and appearance of ghost peaks in the chromatogram. Direct immersion with membrane protection is an active research area to address this issue for complex samples, such as biological fluids and foods. The headspace method is applicable to a wider range of sample types including solids, inhomogeneous suspensions, and solutions with unfavorable matrices for the direct immersion method. For semivolatile compounds, inadequate volatility and favorable water solubility inhibit rapid transfer to the headspace leading to long extraction times. Increasing the sample temperature may improve the rate of mass transfer from the sample solution to the headspace but may be offset by a reduction in the distribution constant of the target compounds between the headspace and the fiber coating. The main experimental variables that affect the extraction efficiency include the extraction-phase chemistry, extraction mode, agitation method, sample modification (pH, ionic strength, presence of organic solvent, etc.), extraction time, and conditions for thermal desorption. These factors should be optimized as a group to account for possible interactions among variables.

The commercially available extraction phases can be categorized as absorption coatings [poly(dimethylsiloxane), poly(acrylate), and poly(ethylene glycol)] and adsorption coatings

containing porous particles (divinylbenzene and Carboxen) with poly(dimethylsiloxane), typically, used as the binder. A selection guide for target compounds based on molecular weight and polarity is presented in [Table 24.4](#). Some authors consider the small number of fiber coatings commercially available a disadvantage and the development of new fiber coatings prepared in the laboratory is an active research area. Other problems are limited fiber reusability due to matrix contamination (mainly immersion sampling), short lifetime of physically coated fibers, and the fragile character of fibers during sampling and septum injection (non-septum-based sample inlets are preferred).

The extraction phase for SPME is extremely small compared to typical sample volumes and sampling occurs under conditions of negligible depletion unless the distribution constant is unusually large. The amount extracted increases with the extraction time finally reaching equilibrium. When the time to reach equilibrium is long, the preequilibrium region is selected for sampling. In this case the repeatability of the extraction time becomes a critical extraction parameter. Extraction in the preequilibrium region is kinetically controlled and mass transfer is dominated by diffusion (stagnant solution) or the method of agitation (agitated solution). Selectivity is usually limited for preequilibrium extraction compared with equilibrium extraction. For equilibrium sampling selectivity is determined by the distribution constants for the target compounds and the matrix. Calibration may require more effort than typical of conventional extraction techniques and is an important consideration for quantitative methods [89]. The small volume of extraction phase lends itself to field sampling (spot and time-weighted average) since it is independent of the sample volume (this is generally true as long as the product of the extraction-phase volume or surface area and the distribution constants of the target compounds are small compared with the sample volume). Although

TABLE 24.4 Selection guide for solid-phase microextraction fibers.

Fiber coating	Film thickness (μm)	Sample type	Desorption temperature ($^{\circ}\text{C}$)
PDMS	100	Volatile compounds with MW 60–275	200 to 280
	30	Nonpolar semivolatile compounds MW 80–500	200 to 280
	7	Low-polarity semivolatile compounds MW 125 to 600	220 to 320
PA	85	Polar semivolatile compounds MW 80–300	220 to 280
PEG	60	Polar volatile compounds MW 40–275	200 to 250
DVB/CAR (PDMS)	50/30	Volatile compounds MW 40–275	230 to 270
CAR/PDMS	75/85	Gases and low-molecular-weight compounds MW 30–225	250 to 310

CAR, Carboxen (a carbon molecular sieve); DVB, poly(divinylbenzene); MW, molecular weight; PA, poly(acrylate); PDMS, poly(dimethylsiloxane); PEG, Carbowax.

only small amounts of the target compounds are typically extracted by the fiber, the technique provides favorable detection limits compared to conventional extraction techniques since the total amount of extracted material is transferred to the column (eliminates solvent dilution).

24.2.6.1 Nonfiber formats

The extraction rate and detection levels of fiber-based techniques can be improved by increasing the volume and/or surface area of the extraction phase. Increasing the thickness of the extraction phase for fibers results in long extraction times and alternative formats in the form of thin films and coated stir bars have been developed for gas chromatography. Shorter extraction times can be obtained by adopting a geometry for the extraction phase with a higher surface-area-to-volume ratio than the cylindrical fiber geometry. The SPME arrow consists of a steel rod of larger diameter than a conventional coated fiber with a larger amount of extraction phase, while retaining compatibility with thermal desorption in a standard injection liner for gas chromatography [79]. Alternatively the surface-area-to-volume ratio can be enhanced by coating a thin film on a suitable laminar substrate of larger area than a cylindrical fiber [90].

Substrates of larger surface area usually require reversion to solvent desorption for the recovery of target compounds for gas chromatography. Stir bar sorptive extraction has become the accepted technique for SPME when a relatively large volume of extraction phase is required [70,91,92]. The extraction device consists of a magnetic stir bar in a glass sleeve externally coated with a 0.3–1.0 mm layer of extraction phase. Aqueous samples are analyzed by direct immersion of the stir bar with vigorous stirring and gas-phase samples by suspending the stir bar in the headspace above the sample. Target compounds are recovered by thermal desorption in a purpose-designed module connected directly to the gas chromatograph or by solvent desorption. The only extraction phases commercially available are poly(dimethylsiloxane), poly(acrylate), and an ethylene glycol/silicone copolymer suitable for the extraction of low- and intermediate-polarity compounds from water. On account of the larger volume of extraction phase, extraction times are long compared with fiber-based techniques. The relatively low selectivity of the available extraction phases results in significant matrix sorption and possible interference in the separation process. A reduced lifetime for the stir bar results from direct contact

with the extraction vessel together with rapid stirring. Common uses of direct immersion are the isolation of target compounds from surface waters and other samples with a low matrix burden while a wider range of sample types are analyzed in the headspace mode.

24.2.7 Membrane extraction

A number of membrane extraction techniques based on dialysis, reverse osmosis, ultrafiltration, and pervaporation have been used to prepare samples for gas chromatography [4,93–96]. None of these techniques are widely used at present. They typically require specific apparatus suitable for processing relatively large sample volumes and are out of favor with current developments in sample preparation for gas chromatography. This also applies to supported-liquid membrane extraction [97], although this technique has reappeared as a microextraction version known as hollow-fiber liquid-phase microextraction, requiring only simple equipment and compatible with small sample volumes, providing better sample utilization for gas chromatography [32,52,53,98,99]. Target compounds are extracted into a small volume of acceptor phase, 2–100 μL , contained in the lumen of a short length of a microporous polymeric hollow fiber. The membrane pores are impregnated with an organic solvent immiscible with the sample solvent, typically an aqueous solution, and the fiber either immersed in the stirred sample solution or suspended above it in the headspace. A major advantage of the porous membrane is that it provides a liquid barrier that protects the acceptor phase from leaking into the sample and the tubular configuration increases the surface contact with the sample. Either the two-phase (acceptor and membrane solvent are the same) or three-phase (membrane solvent is different to both the sample solution and the acceptor phase) modes are used for sampling. The two-phase mode requires

a large distribution constant for the target compounds for efficient extraction and the three-phase system a mechanism that prevents the extracted compounds from forming an unfavorable equilibrium between the sample solution and the acceptor phase. For example, neutral compounds tend to be distributed between all three phases at equilibrium but for ionizable compounds a change in pH can trap the target compounds in the acceptor phase promoting an efficient extraction. Electromembrane extraction provides faster extraction and higher selectivity for ionizable compounds by using an electric field to drive the ionized compounds through the liquid membrane [100]. In early studies the hollow fiber was either U-shaped or rod-shaped requiring a support structure to immobilize it in the sample solution. This restricted the possibilities for batch extractions and limited the contact between the sample solution and hollow fiber resulting in relatively long extraction times. Solvent-bar microextraction overcame these difficulties by using an impregnated fiber with sealed ends suspended freely in the stirred sample solution [101]. The tumbling motion of the hollow fiber promotes more favorable contact with the sample solution enhancing the rate of extraction as well as facilitating simultaneous sample extraction.

24.3 Sample cleanup by column chromatography

Column liquid chromatography is a common laboratory technique to isolate compounds with similar properties in a small volume of mobile phase (fractions) after solvent extraction. The basis for fractionation is separation by size, polarity, or ion-exchange capacity [4,5]. Large-scale gravity fed, short-bed gravity fed, medium- or high-pressure analytical and semipreparative columns are used for specific applications depending on the sample amount and

complexity. Large columns are appropriate for isolation studies while smaller columns are more commonly used for minimizing interferences in gas chromatography. The general trend toward downsizing sample preparation techniques allows solid-phase extraction cartridges and sorbent-dispersion techniques to be utilized as the cleanup step. The column dimensions are dictated by the amount of sample extract to be fractionated with wide-bore columns used for large samples and long columns for difficult separations at sample loadings of about 3% of the sorbent mass. Whenever the isolation of the target compounds from matrix interferences is inadequate for gravity-fed columns, medium- or high-pressure liquid chromatography is a suitable option. These systems minimize solvent consumption and time, reduce solvent contamination problems, and offer benefits through ease of automation and monitoring of fraction cuts [5]. Sample capacity is generally smaller than for gravity-fed columns. It is often necessary to include a wash cycle between injections for crude extracts, and if gradient elution is used, additional time to reequilibrate the column at the end of each cycle as columns are too expensive for single application use. Column-based approaches are generally one sample-at-time methods, further impacting sample throughput. Inorganic oxide sorbents are suitable for fractionating complex mixtures based on the type and number of polar functional groups by normal-phase chromatography [102]. Normal-phase chromatography on columns containing 3-aminopropylsiloxane-bonded silica can be used to isolate polycyclic aromatic hydrocarbons and their alkyl-substituted analogs in fractions ordered by increasing ring number [103]. Size-exclusion chromatography is a standard technique for the isolation of pesticides, herbicides, fungicides, aflatoxins, etc., from extracts containing high-mass polymers, lipids, fats, or oils [26,104]. Both polar and low-polarity target compounds elute in the same fraction in contrast to inorganic oxide

adsorbents. Its principal benefit is the removal of high-mass contaminants unsuitable for gas chromatography. Since samples rarely contaminate the column in size-exclusion chromatography, a high level of automation can be achieved.

24.3.1 Multidimensional and multimodal chromatography

Multidimensional gas chromatography offers several options for the simplification of complex mixtures and the fractionation of extracts containing interfering components. Some examples are summarized in Table 24.5. Multidimensional gas chromatography employs the separation of a sample using two columns of different capacity or selectivity connected in series via an appropriate interface for trapping and reinjection of target compounds [105–108]. The interface facilitates the selection of fractions to transfer from the first column to the second column with the diversion of other sample components from the second column. Typical operations are trace enrichment of target compounds, enhanced resolution of a group of target compounds, and increased sample throughput by heartcutting, backflushing, and foreflushing techniques. Heartcutting allows selected sections of the chromatogram from the first column to be isolated and transferred to the second column. Backflushing allows sample components with high retention factors to be removed from the first column by reversing the flow direction of the carrier gas, usually after isolating the target compounds by heartcutting. The objective is to minimize the additional separation time for the sample compared with the time required to separate the target compounds. Foreflushing is typically employed to divert solvent and reagents used in preparing the extract for analysis from the second column where these would have a deleterious effect on the separation or the detector response. It is useful for diverting

TABLE 24.5 Examples of the use of multidimensional gas chromatography for sample preparation.

Process	Observations
Solvent reduction	Large volumes of solvent and excess volatile derivatizing reagents can be vented in front of the interface to prevent deterioration of the second column or interference in detector operation
Trace enrichment	Large-volume injection or multiple injections of the sample extract with selective trapping and storage of the target compounds at the interface. To increase capacity a short column with a low phase ratio may be suitable for the first column.
Buried peaks	Divert from the interface the major portion of large peaks and transfer and trap the target compounds at the interface
Backflush	For extracts with a wide volatility range, the target compounds are transferred to the interface, the direction of the carrier gas flow for the first column is reversed, and its temperature possibly increased to expeditiously elute low-volatility matrix components.
Heartcut	Either single peaks or contiguous segments of the first-column chromatogram transferred to the interface and trapped for reinjection on the second column

excess derivatizing reagents or sample solvent from the second column and the detector and when large-volume injections are used to achieve trace enrichment. Multidimensional gas chromatography is an online technique requiring only simple modification to a modern gas chromatograph for automated operation. This technique is described more fully in Chapters 7 and 18.

Multimodal chromatography employs two complementary chromatographic processes to achieve the same goals as multidimensional gas chromatography but requires more complex instrumentation for online methods. Typical approaches are liquid chromatography–gas chromatography [109–111] and supercritical fluid chromatography–gas chromatography [4,58,67,112]. Either approach can be performed off-line with the manual or automated trapping of fractions from the first chromatographic system for subsequent reinjection into the second system. The online approach provides a sophisticated solution for sample cleanup but requires a high level of skill, which may not be available in all laboratories. Applications are limited to a few laboratories that are pioneers in the development of this technology.

Liquid chromatography provides efficient matrix simplification and transfer of defined fractions to the gas chromatography for high-resolution separation and detection. Direct transfer of fractions to the gas chromatograph reduces the possibility of contamination or losses during solvent removal improving sample detection limits and repeatability. Separations by liquid chromatography occur with concurrent dilution requiring the transfer of relatively large solvent volumes, from about 50 μL to 1 mL, using a loop interface with concurrent solvent evaporation or on-column interface with a retention gap and partial concurrent solvent evaporation [109]. Compared with conventional sample preparation techniques, the higher resolving power of liquid chromatography together with the possibility of online monitoring for fraction selection provides cleaner and well-defined extracts for separation by gas chromatography. While most practical applications are limited to normal-phase and size-exclusion chromatography employing volatile organic solvents. Reversed-phase methods can be used, albeit with some additional restrictions. Typical contemporary applications are found in food quality control for the determination of minor

components and contaminants in fats and oils and the analysis of essential oils and petroleum products [110,111].

24.4 Microchemical reactions for modification of target compound

Microchemical reactions referred to as derivatization are used to modify the properties of target compounds to achieve at least one of the following goals: to convert compounds with thermally or hydrolytically labile functional groups into stable products suitable for gas chromatography; to minimize undesirable column and system interactions resulting in peak asymmetry or mass loss by adsorption; to adjust the volatility of the target compounds to minimize peak overlaps or to displace the elution window for the target compounds to a region of the chromatogram unoccupied by matrix peaks; to introduce a detector-specific label into the target compounds to improve detection levels or increase selectivity; or to enhance the recovery of target compounds by increasing their distribution constant in the extraction system or to increase the selectivity of the extraction. Literally, thousands of reactions have been used to fulfill the aforementioned goals but more generally a smaller select group of reagents are used for most applications. Several books and review articles cover the topic adequately and are a good start to identify an appropriate reagent and experimental conditions for most compounds [110–116].

All derivatization reactions for gas chromatography are precolumn but not necessarily postextraction. Preextraction methods are employed for compounds with low distribution constants to facilitate their useful extraction into another phase, for example, low-mass polar compounds difficult to extract from aqueous solution. Common approaches include the addition of reagents to the aqueous sample and reaction prior to extraction or addition of

reagents for the reaction to the extraction phase to minimize redistribution of the product to the sample solution [117,118]. The later approach is favored for membrane separation and liquid-phase microextraction techniques [119–122]. Another variation is solid-phase analytical derivatization for cartridge techniques [123,124] and on-fiber derivatization for SPME [88,116,124,125]. Since the sample solution is invariable aqueous in these methods, the reactions employed, for example, acylation, alkylation, Schiff base formation, carbamylation, etc., must be tolerant to water as the reaction medium or in the reaction medium [117,118,125]. The target compounds must also form derivatives that are compatible with the subsequent approach for separation and detection. Reagent by-products or impurities can be a particular problem since the extracted target compounds are usually introduced directly into the gas chromatograph along with reagents, catalysts, by-products, and impurities. The latter should elute early in the chromatogram and leave an empty space for the modified target compounds. In addition, the reagents should not be a source of injection liner activity eventually leading to adsorption and peak tailing problems.

Postextraction reactions are typically performed in the solution phase and less commonly because of the smaller number of suitable reagents by injection-port derivatization. Equipment requirements for manual solution-phase reactions are generally simple, typically glass-tapered reaction or autosampler vials or culture tubes as reaction vessels; microliter syringes or autopipettors for reagent, catalyst, and solvent addition; hand agitation, vortex mixers, or mini magnetic stirrers for mixing; and convection ovens, drilled-block heaters, hot plates, or bath heaters for temperature control of reactions requiring elevated temperatures. Advanced programmable workstations allow addition of reagents, reaction at elevated temperatures, removal of excess reagents and solvents, solvent exchange, and injection of sequenced samples

into a gas chromatograph [122,126–128]. Alternatively, robotic sample preparation workstations allow the automation of manual reaction methods by mimicking the steps in the derivatization process without human intervention. Automated systems tend to provide better control of the experimental variables together with improved repeatability and facilitate further downsizing of the reaction. These systems are widely available in industry but manual methods are more common in academia because of the higher capital costs of automation and the smaller number of samples of a similar kind generally analyzed. A new approach to preparing derivatives makes use of microwave-assisted or ultrasound-assisted reactions [125,129–133]. Their main advantage is that reaction times can be reduced to a few minutes or less for moderately difficult functional groups. The faster reactions with microwave irradiation are a consequence of the higher reaction temperature that can be obtained in a sealed vessel and the more efficient heat transfer to the reaction mixture as a result of dielectric heating. There is some evidence that the choice of solvent and reagents for microwave-assisted derivatization affects the extent and rate of reaction differently to conventional methods, and a different choice of conditions can be beneficial.

In general, ultrasound-assisted reactions utilize milder conditions than microwave-assisted reactions that may suit some reactions better, particularly heterogeneous reactions or extraction with *in situ* derivatization [132,133]. Ultrasound irradiation causes cavitation in solutions resulting in high local pressures and temperatures responsible for the mechanical and chemical effects of ultrasound on particle disruption and reaction kinetics. Ultrasound-assisted reactions work best with redox-type reactions, especially for derivatizing inorganic and organometallic compounds [133]. There are a number of examples where ultrasound was employed for simultaneous extraction and derivatization in dispersive liquid–liquid

microextraction [121,133,134]. Microwave-assisted and ultrasound-assisted reactions require specialized equipment, although ultrasound-assisted reactions can be performed in standard ultrasound baths. The initial results for microwave- and ultrasound-assisted derivatization are impressive and these techniques could potentially morph into the preferred method for solution derivatization.

For injection-port derivatization the extract containing the target compounds and reagents are simply mixed and injected together into the gas chromatograph with the reaction occurring in the hot precolumn injector [135,136]. The residence time in the injector is short, which limits the range of reactions that produce (near) quantitative derivative formation. This reaction format is compatible with pyrolytic alkylation of acidic substances using tetraalkylammonium salts as the alkylating reagent.

Typical derivatizing reagents have varied structures but can be broadly described by considering two separate, but not necessarily independent parts, Fig. 24.2. The organic chain controls volatility, influences chemical and thermal stability, and contains the features required for a detector-oriented response. The reactive group provides the means to introduce the organic chain into a particular compound. The reactive group establishes the scope of the reagent for reaction with different functional groups, the selectivity of the reagent toward a

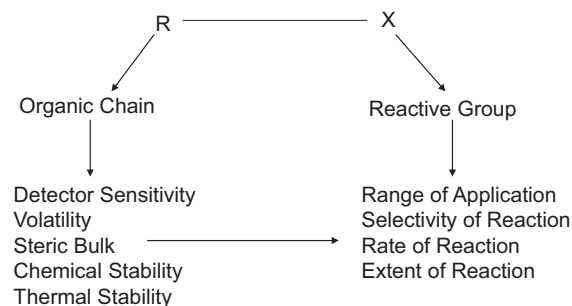


FIGURE 24.2 Anatomy of a derivatizing reagent.

target functional group in the presence of others, and the rate and extent of the reaction for each functional group. The size and shape of the organic chain can also influence the rate and extent of reaction with hindered functional groups. Volatility considerations favor the use of either short organic chains or organic chains with significant replacement of carbon–hydrogen bonds by carbon–fluorine bonds. This explains the rather large number of reagents with perfluorocarbon and pentafluorobenzene substituents. Their weak intermolecular interactions with common stationary phases allow multiple functional groups to be derivatized without a large change in retention. The two most common selective detectors for gas chromatography are the mass spectrometer and the electron-capture detector. Since fluorine-containing compounds are uncommon in natural samples, they have favorable mass selection properties when used as derivatizing reagents. Perfluorocarbon-containing derivatives with the further possibility of electron delocalization have a favorable response to the electron-capture detector [137]. These combinations of features allow reagents containing perfluorocarbon and pentafluorophenyl groups to be used as multipurpose derivatizing reagents for gas chromatography. Some common reagents and their typical applications are described further. This is only a sampling of the reagents that have been used for derivatization [113–116]. Specific reagents for the separation of enantiomers by formation of diastereomers are described in Chapter 23.

24.4.1 Alkylsilyl reagents

Alkylsilyl reagents are the most versatile and widely used general derivatizing reagents for gas chromatography [113,138–140]. They form thermally stable derivatives with polar compounds, usually, containing labile hydrogen atoms bound to electronegative elements, such as oxygen, nitrogen, sulfur, or phosphorous,

Table 24.6, as well as a wide range of oxyanions [141]. Numerous reagents have been suggested for the preparation of trimethylsilyl derivatives but only a smaller number have entered into general practice, Table 24.7. Newer reagents include trimethylsilyldiethylamine [139], trimethylsilyl *N,N*-dimethylcarbamate [139], trimethylsilylcyanide [142], and a mixture of hexamethyldisilazane–trifluoroacetic acid [143]. Whether these reagents will replace or simply supplement those in Table 24.7 is unclear at present, and the following discussion is based on the reagents in Table 24.7. The trimethylsilyl derivatives are reasonably volatile but are only moderately stable to hydrolytic conditions when subject to additional sample cleanup and some derivatives have limited stability when stored in the reaction medium. Alkyldimethylsilyl reagents were introduced to find an alternative compromise between volatility, hydrolytic stability, and reactivity. The *t*-butyldimethylsilyl reagents emerged as the best compromise with a view to improvement in hydrolytic stability. The *t*-butyldimethylsilyl derivatives are typically >1000 times more stable to hydrolytic conditions than the equivalent trimethylsilyl derivatives.

Typical silylation reactions are assumed to proceed by an S_N2 –Si mechanism with strong silylating reagents possessing a good leaving group (e.g., amides, imidazole), characterized as having a low basicity, an ability to stabilize a negative charge in the transition state, and little or no $p \rightarrow d$ bonding with silicon. Excess reagent, higher temperatures, polar solvents, and catalyst generally favor the formation of products and are optimized to overcome the slow and incomplete reaction of hindered functional groups. Trimethylchlorosilane is the preferred catalyst for reactions employing one of the stronger derivatizing reagents in Table 24.7. Reactions are typically performed under (near) anhydrous conditions as the silylating reagents react with water forming unreactive by-products along with a decrease in the rate and extent of the reaction. This can result in the need to adjust the

TABLE 24.6 Reagents forming derivatives with common functional groups.

Type	Target compound functional group	Derivative
Silylation (Section 24.4.1)	OH	OTMS
	SH	STMS
	COOH	COOTMS
	POH	POTMS
	SOH	SOTMS
	NOH	NOTMS
	BOH	BOTMS
	NH ₂	NHTMS → N(TMS) ₂
	= NH	= NTMS
	CH ₂ C=O	CH=CHOTMS
	C(O)NH ₂	C(O)NHTMS
Acylation (Section 24.4.2)	OH	OAc
	NH ₂	NHAc → N(Ac) ₂
	= NH	= NAc
	NOH	NOAc
	C(O)NH ₂	C(O)NHAc
	SH	SAc
	SO ₂ NHR	SO ₂ NRAc
	CH ₂ CHO	CH=CHOAc
Alkylation (section 24.4.3)	COOH	COOR
	SO ₂ H	SO ₂ R
	OH	OR
	SH	SR
	NH ₂	NR ₂
	NH	NR
	CONH ₂	CONR ₂
	SO ₂ NH ₂	SO ₂ NR ₂
	COCH ₂ COR	COCH=CR ₂
Chloroformate reagents (Section 24.4.4)	OH	OC(O)OR
		OC(O)OAR

(Continued)

TABLE 24.6 Reagents forming derivatives with common functional groups.—cont'd

Type	Target compound functional group	Derivative
	COOH	COOR
	NH ₂	OC(O)NHR
	SH	SOC(O)OR

TABLE 24.7 General reagents for preparing alkylsilyl derivatives.

Reagent	Structure	Abbreviation
Trimethylchlorosilane	TMSCl	TMCS
Trimethyliodosilane	TMSI	TMSI
<i>t</i> -Butyldimethylchlorosilane	<i>t</i> BDMSCl	TBDMCS
Hexamethyldisilazane	TMSNHTMS	HMDS
<i>N</i> -Trimethylsilylimidazole	TMSC ₃ H ₃ N ₂	TMSIm
<i>N</i> -Methyl- <i>N</i> -trimethylsilylacetamide	CH ₃ CON(CH ₃)TMS	MSTA
<i>N</i> -Methyl- <i>N</i> -trimethylsilyltrifluoroacetamide	CF ₃ CON(CH ₃)TMS	MSTFA
<i>N</i> - <i>t</i> -butyldimethylsilyl- <i>N</i> -methyltrifluoroacetamide	CF ₃ CON(CH ₃) <i>t</i> BDMS	MTBSTFA
<i>N,O</i> -Bis(trimethylsilyl)acetamide	CH ₃ C(OTMS) = NTMS	BSA
<i>N,O</i> -Bis(trimethylsilyl)trifluoroacetamide	CF ₃ C(OTMS) = NTMS	BSTFA
<i>N,O</i> -Bis(<i>t</i> -butyldimethylsilyl)trifluoroacetamide	CF ₃ C(O <i>t</i> BDMS) = N <i>t</i> BDMS	MTBSTFA

*t*BDMS, *t*-butyldimethylsilyl; TMS, trimethylsilyl.

reaction conditions to accommodate the properties of the matrix, to establish a defined protocol for drying and distributing the sample on the reaction vessel surface, and checking for variation in reaction conditions with different matrices. A notable exception with regard to the need for anhydrous reaction conditions is trimethylsilylimidazole, which can be used to derivatize hydroxyl groups in the presence of a reasonable amount of water, for example, to derivatize saccharides in syrups. Further considerations for selecting a reagent to derivatize different functional groups are summarized in Table 24.8. For alcohols the general order of reactivity is primary > secondary > tertiary and for amines primary > secondary. With primary amines the

introduction of one silyl group hinders access of a second, which can be introduced only with difficulty. Steric factors have a strong effect on reaction rates and the extent of reaction. Specific reagents, elevated temperatures, and long reaction times are required for quantitative reactions for hindered functional groups. Steric factors are more important for *t*-butyldimethylsilyl reagents. Most reactions occur without formation of secondary products [139,144].

Polyfunctional compounds with more than one type of functional group or the same functional group in different steric environments are the most challenging to obtain a complete reaction [139,145]. Since silylating reagents only react with functional groups containing a

TABLE 24.8 General considerations for the selection of alkylsilyl reagents for reactions with polyfunctional compounds.

Reagent	Comments
TMSIm	<p>Reacts with hindered alcohol and phenol groups, carboxylic acids, phosphates, and sulfonic acids</p> <p>Reacts with amines and amides that are weaker bases than imidazole (poor reagent for primary amines)</p> <p>Tolerates reasonable amounts of water in the derivatization of saccharides (e.g., syrups)</p> <p>Does not promote enol ether formation with unprotected ketone and aldehyde groups</p> <p>Used as a catalyst or component of mixed reagents for the reaction of highly hindered functional groups (e.g., TMSIm-BSTFA-TMCS 1:1:1 (v/v/v))</p> <p>Reagent and by-products may interfere in the separation of low-molecular-weight compounds</p>
BSTFA (or BSA)	<p>Reacts with most alcohols, phenols, carboxylic acids, amino acids, saccharides, thiols, amines, indoles, and nucleotides</p> <p>For complete reaction with hindered functional groups used as a mixture with 1% or 10% (v/v) trimethylchlorosilane (for amides, secondary amines, and hindered hydroxyl groups)</p> <p>Trifluoroacetic acid is sometimes used as a catalyst for reactions with hindered phenols and amino acids</p> <p>BSTFA produces volatile by-products that minimize interference in the separation of volatile compounds</p> <p>Fluorine-containing reagents reduce the buildup of silicon dioxide in flame-based detectors</p>
MSTFA	<p>Reacts with most alcohols, acids, amino acids, amides, amines, saccharides, nucleosides, and indoles.</p> <p>For complete reaction with hindered functional groups used as a mixture with 1% or 10% (v/v) trimethylchlorosilane</p> <p>Reaction properties are similar to BSTFA except that the reagent and by-products are the most volatile of all silylating reagents</p> <p>Minimizes buildup of silicon dioxide in flame-based detectors</p> <p>Promotes the formation of enol-TMS ethers with unprotected ketone and aldehyde groups (reactions usually incomplete in the absence of catalyst)</p>
HMDS	<p>Weak silylating reagent. Commonly used with trimethylchlorosilane (e.g., HMDS:TMCS 3:1 (v/v)) or trifluoroacetic acid (e.g., HMDS:TFAA 9:1(v/v)) in pyridine to expand its scope</p> <p>Mixed reagent with TMCS reacts with most alcohols, phenols, saccharides, carboxylic acids, and nucleotides</p> <p>Mixed reagent with TFAA has similar reactivity to BSTFA or MSTFA</p>
TMCS	<p>Poor silylating reagent in the absence of base (e.g., pyridine)</p> <p>Generally used as a catalyst with other silylating reagents</p>
MTBSTFA	<p>Reacts with most alcohol, phenol, carboxylic acid, thiol and amine functional groups where reaction is not prevented by steric factors</p> <p>Not as reactive as MSTFA with hindered functional groups</p> <p>Reaction rates and extent of reaction enhanced by addition of TBDMCS as a catalyst</p>

replaceable hydrogen atom, other functional groups may need to be protected, often by sequential reactions. For example, ketones and aldehydes do not typically require derivatization before gas chromatography but are partially derivatized or form unstable derivatives during the silylation of functional groups containing replaceable hydrogen atoms (see Table 24.8 for details). Reactions involving acid catalysts, such as trimethylchlorosilane, promote formation of enol-trimethylsilyl ether derivatives of aldehydes and ketones of poor stability. Stable derivatives suitable for gas chromatography require the reaction of aldehyde and ketone groups to form oximes followed by silylation of polar functional groups containing a replaceable hydrogen atom [138–140,144–147].

Electron ionization mass spectra of trimethylsilyl derivatives are commonly found in searchable mass spectrum libraries and fragmentation mechanisms for trimethylsilyl derivatives of common compounds are reasonably well understood [140,148,149]. Confidence in mass spectrum identification can be increased by simultaneously matching the retention indices for the derivatives. Molecular ions are often weak or absent in electron ionization mass spectra of trimethylsilyl derivatives. The molecular mass, however, can generally be inferred from relatively abundant ions of mass $[M-15]^+$ obtained by cleavage of a methyl group bound to silicon. In *t*-butyldimethylsilyl derivatives, cleavage of the *t*-butyl group from silicon results in a particularly abundant ion of high mass suitable for selected ion detection. This together with their higher hydrolytic stability is often the reason for the selection of *t*-butyldimethylsilyl derivatives for the trace analysis of polar compounds with unhindered functional groups by gas chromatography–mass spectrometry. Chemical ionization mass spectra of trimethylsilyl derivatives using proton donating reagents are rather simple with pseudomolecular ions $[M+H]^+$ as the base peak and little further fragmentation. Fragment ions for structural

elucidation or detection can be generated using tandem mass spectrometry. Deuterated reagents are available for the preparation of internal standards (d_9 -TMS) for quantitative analysis using selected ion monitoring.

24.4.2 Haloalkylacetyl reagents

Acylation reagents react with most types of common functional groups with replaceable hydrogen atoms except for carboxylic acids, Table 24.6 [113,114,137,150–152]. Acyl derivatives are typically more stable than trimethylsilyl derivatives, particularly for amines. This allows a wider range of methods to be used for their isolation from matrix components or excess reagent. Acyl reagents and derivatives are more tolerant of water than trimethylsilyl reagents and derivatives and some reactions can even be performed in aqueous solution. The most common acyl reagents contain trifluoromethyl, pentafluoropropyl, or heptafluorobutyryl groups with acid chloride, anhydride, or imidazole reactive groups. Other alkyl and haloalkyl reagents are less commonly used. These derivatives have relatively long retention times compared with the perfluorocarboxyl derivatives. The perfluorocarboxyl derivatives have favorable properties for electron-capture and negative ion chemical ionization mass spectrometry detection [137].

The perfluorocarboxyl derivatives are prepared from the anhydrides or acid chlorides, at elevated temperature in the presence of a basic solvent such as pyridine, triethylamine, or aqueous sodium bicarbonate, unless the derivatives are unstable to basic conditions. Excess reagent is removed by evaporation or extraction with a weak solution of an aqueous base. Under conditions where the anhydride might lead to undesirable side reactions (e.g., dehydration, enolization, etc.), the perfluorocarboxylimidazole reagents are used. The mass spectra of the perfluorocarboxyl derivatives frequently have

abundant high mass ions and characteristic fragment ions associated with the identity of the perfluorocarbon chain suitable for selected ion monitoring [152].

The main alternatives to acyl and trimethylsilyl reagents for reaction with alcohols, phenols, thiols, and amines are reagents containing a pentafluorophenyl group in the organic chain, Table 24.9 [114,137]. These derivatives are generally stable with favorable electron-capture properties and used for both solution and solid-phase analytical derivatization reactions pre- or postextraction [118,124,137].

24.4.3 Alkylation reagents

Alkylation is a chemical process in which the active hydrogen atoms of a functional group are replaced by an alkyl or aryl group under a variety of reaction conditions, Table 24.6 [113,114,151,153]. The most important reactions employ alkyl halides with catalyst, diazoalkanes, extractive alkylation, and pyrolytic alkylation and arylation (see injection-port derivatization in Section 24.4). Pentafluorobenzyl bromide is the most important alkylating reagent for use with the electron-capture detector, Table 24.9 [137]. Alkyl halides (methyl, ethyl, isopropyl, etc., or substituted benzyl bromides) in the presence of a catalyst (barium oxide, sodium borohydride, silver oxide, etc.) derivatize carboxylic acids, phenols, and thiol groups rapidly and hydroxyl groups slowly and not always to completion. The choice of catalyst affects the progress of side reactions, such as C-alkylation and O-acetyl migration, which is a consideration for selecting reaction conditions. Diazoalkanes alkylate acidic and enol groups virtually instantaneously. Lewis acid catalysts (e.g., boron trifluoride etherate) are used to promote the reaction of functional groups of low reactivity (e.g., alcohols). Because of the large difference in reaction rates, compounds

containing carboxylic acids and phenols can be selectively alkylated in the presence of less reactive functional groups. Health and safety concerns led to the introduction of trimethylsilyldiazomethane as a less hazardous replacement for diazomethane, the most widely used of the diazoalkanes [154,155]. Extractive alkylation is used to derivatize acids, phenols, alcohols, or amides in aqueous solution. The pH of the aqueous sample is adjusted to ionize the target compounds, which are then extracted as an ion pair with a tetraalkylammonium hydroxide into a suitable water-immiscible organic solvent. In the poorly solvating organic solvent the reaction with an alkyl halide occurs under favorable conditions. Extractive alkylation has the advantage of achieving extraction, concentration, and derivatization in a single step. Optimization of the experimental conditions may be lengthy but the high selectivity achievable has made this a popular technique for biomedical and environmental applications. Direct alkylation under (near) anhydrous conditions using potassium complexed with a crown ether or in the presence of a strong organic base is widely used for derivatizing phenols and carboxylic acids.

24.4.4 Chloroformate reagents

Alkylchloroformates (e.g., methyl, ethyl, isobutyl) and trichloroethyl- and pentafluorobenzyl chloroformates react rapidly with amines to form carbamates and phenols and carboxylic acids to form carbonate derivatives, Table 24.6, in both weakly basic aqueous solutions and in organic solvents [116,156]. They are popular reagents for microextraction with derivatization techniques [116,121,122]. In addition, trifluoroethyl chloroformate and heptafluorobutyl chloroformate efficiently and rapidly derivatize hydroxyl groups suitable for use with the electron-capture detector [157]. Chloroformates are the only general reagents for the

TABLE 24.9 Typical reagents for the introduction of the pentafluorophenyl group into target compounds.

Reagent	Functional group	Derivative
(i) General reagents		
Pentafluorobenzoyl chloride	OH, NH ₂	C ₆ F ₅ CH ₂ ·COOR C ₆ F ₅ CH ₂ ·COOAr C ₆ F ₅ CH ₂ CONHR
Pentafluorobenzyl bromide	CO ₂ H, OH, SH, SO ₂ NH ₂	C ₆ F ₅ CH ₂ COOR C ₆ F ₅ CH ₂ COOAr C ₆ F ₅ CH ₂ COR C ₆ F ₅ CH ₂ SR C ₆ F ₅ CH ₂ NHSO ₂ R
Pentafluorophenylacetyl chloride	OH, NH ₂	C ₆ F ₅ COOR C ₆ F ₅ COOAr C ₆ F ₅ CONHR
Pentafluorobenzenesulfonyl chloride	OH, NH ₂ , NH	C ₆ F ₅ SO ₃ Ar C ₆ F ₅ SO ₂ NHR C ₆ F ₅ SO ₂ NR ₂
Pentafluorobenzyl chloroformate	OH, NH ₂ , CO ₂ H, SH	C ₆ F ₅ CH ₂ OC(O)OAr C ₆ F ₅ CH ₂ OC(O)NHR C ₆ F ₅ CH ₂ OOCR C ₆ F ₅ CH ₂ OC(O)OSR
(ii) Functional group selective reagents		
Pentafluorophenylbenzoic anhydride	OH	C ₆ F ₅ COOR.
Pentafluorobenzyl alcohol	CO ₂ H	C ₆ F ₅ CH ₂ COOR
Pentafluorobenzaldehyde	NH ₂	C ₆ F ₅ CH = NR
Pentafluorophenylhydrazine	CO	C ₆ F ₅ NH = NCR ₂ C ₆ F ₅ NH = NCRH
Pentafluorobenzyl oxylamine	CO	C ₆ F ₅ CH ₂ ON = CR ₂ C ₆ F ₅ CH ₂ ON = CHR

derivatization of tertiary amines. Carbamates are formed with elimination of the shortest alkyl chains attached to the nitrogen atom of the tertiary amines. Not all reagents react as efficiently or in the same way with individual functional groups and these reagents require more customization of the reaction conditions, particularly for reactions that are near instantaneous.

24.4.5 Functional group selective reagents

Functional group selective reagents are used to derivatize a single, or similar functional groups, in the presence of other functional groups in the target compounds or matrix. Common applications are derivatization of selected target compounds to improve detection levels or to minimize matrix interference, or as a protecting group for sequential reactions for polyfunctional compounds. Some examples of pentafluorophenyl-containing reagents are given in Table 24.9. General reactions include esterification, Schiff base formation, and cyclic derivatives formed with bifunctional compounds.

Esterification is used to derivatize carboxylic acids and other acidic functional groups [113,114,151,158,159]. In a typical reaction the sample is dissolved in excess alcohol containing a small amount of acid catalyst, such as hydrogen chloride, acetyl chloride, thionyl chloride, boron trifluoride etherate, or boron trichloride, etc. Elevated temperatures are often used to accelerate the reaction. Several haloalkyl alcohols have been used to derivatize carboxylic acids but exhibit poor electron-capture properties. Esterification with pentafluorobenzyl alcohol or alkylation with pentafluorobenzyl bromide is the preferred approach for trace analysis of carboxylic acids with electron-capture detection or negative ion chemical ionization mass spectrometry [137]. Methyl esters and other alkyl esters are routinely used for the separation of fatty acids.

Ketone and aldehyde functional groups in polyfunctional compounds often form unstable by-products under conditions required for the derivatization of other functional groups [113,114,139,144–147,151]. Oximes formed with methylhydroxylamine and benzylhydroxylamine reagents are the most common protecting groups. For trace analysis pentafluorobenzylhydroxylamine [O-(2,3,4,5,6-pentafluorobenzyl) hydroxylamine] or pentafluorophenylhydrazone derivatives are commonly used with the electron-capture detector or negative ion chemical ionization mass spectrometry, Table 24.9 [113,114,137,160]. The pentafluorobenzyl oxime derivatives are generally preferred due to fewer problems with reagent contamination and by-product formation. Reactions can be carried out in organic or aqueous solution, on solid-phase sorbent traps, and on reagent-impregnated fibers for SPME [87,119,120,124,137]. Volatile aldehydes and ketones can be derivatized in aqueous solution and sampled from the headspace and solution-phase reactions accelerated using microwave-assisted reactions in aqueous solution or methanol. Under some chromatographic conditions two peaks may be observed for each aldehyde or ketone functional group due to the separation of the (E) and (Z) geometric isomers formed during the derivative reaction. Pentafluorobenzaldehyde reacts smoothly with primary amines to form stable derivatives with favorable electron-capturing properties [114,161]. Secondary amines form mixtures of ring-substituted products unsuitable for gas chromatography.

Bifunctional compounds are characterized by having a minimum of two functional groups in close proximity that can be simultaneously reacted with specific reagents to form cyclic derivatives with good gas chromatographic properties [113,151,162,163]. They consist of compounds across many families containing alkyl chains with functional groups on neighboring 1,2-, 1,3-, or 1,4-carbon atom series or aromatic rings with *ortho*-substituted functional

groups. Alkyl- (methyl, butane, t-butane), cyclohexyl, and aromatic [benzene, 3,5-bis(trifluoromethyl)benzene] boronic acids are the only general-purpose reagents for bifunctional compounds forming cyclic esters under mild reaction conditions for XH functional groups where X = O, N, S, or CO₂. Some derivatives have poor hydrolytic stability and boronate esters are not generally used in sequential reactions employing other common derivatizing reagents. The butaneboronate derivatives provide a convenient compromise between volatility and stability and are the most widely used for general applications and the 3,5-bis(trifluoromethyl)benzeneboronates and 2,4-dichlorobenzeneboronates for use with the electron-capture detector. Boronate derivatives have useful mass spectral properties with prominent molecular ions and high-mass fragment ions. There are numerous other reagents used to form cyclic derivatives with specific compounds in which the specific nature of the reaction is a source of selectivity as well as stabilizing the compounds to the hydrolytic conditions of extraction and thermal conditions of gas chromatography [116,162,163].

References

- [1] W.G. Jennings, A. Rapp, *Sample Preparation for Gas Chromatographic Analysis*, Huethig, Heidelberg, 1983.
- [2] C.F. Poole, S.A. Schuette, Isolation and concentration techniques for capillary column gas chromatographic analysis, *J. High Resolut. Chromatogr.* 6 (1983) 526–549.
- [3] K. Beyerman, *Organic Trace Analysis*, Horwood, Chichester, 1984.
- [4] S.K. Poole, T.A. Dean, J.W. Oudsema, C.F. Poole, Sample preparation for chromatographic separations: an overview, *Anal. Chim. Acta* 236 (1990) 3–42.
- [5] C.F. Poole, S.K. Poole, *Chromatography Today*, Elsevier, Amsterdam, 1991, pp. 738–946.
- [6] J. Tekel, S. Hatrik, Pesticide residue analysis in plant material by chromatographic methods: clean-up procedures and selective detectors, *J. Chromatogr. A* 754 (1996) 397–410.
- [7] J.G. Wilkes, E.D. Conte, Y. Kim, M. Holcomb, J.B. Sutherland, D.W. Miller, Sample preparation for the analysis of flavors and off-flavors in foods, *J. Chromatogr. A* 880 (2000) 3–33.
- [8] R.M. Smith, Before the injection – modern methods of sample preparation for separation techniques, *J. Chromatogr. A* 1000 (2003) 3–27.
- [9] T. Hyotylainen, Critical evaluation of sample preparation techniques, *Anal. Bioanal. Chem.* 394 (2009) 743–758.
- [10] S. de Konig, H.-G. Janssen, U.A.T. Brinkman, Modern methods of sample preparation for GC analysis, *Chromatographia* 69 (2009) 533–578.
- [11] J. Pawliszyn, H.L. Lord (Eds.), *Handbook of Sample Preparation*, Wiley-Blackwell, New York, 2010.
- [12] J. Pawliszyn (Ed.), *Comprehensive Sampling and Sample Preparation*, Elsevier, Amsterdam, 2012.
- [13] S. Moldoveanu, V. David, *Modern Sample Preparation for Chromatography*, Elsevier, Amsterdam, 2015.
- [14] C. Poole, Z. Mester, M. Miro, S. Pedersen-Bjergaard, J. Pawliszyn, Extraction for analytical scale sample preparation (IUPAC technical report), *Pure Appl. Chem.* 88 (2016) 649–687.
- [15] A. Gorak, H. Schoenmakers (Eds.), *Distillation: Operation and Applications*, Elsevier, Amsterdam, 2014.
- [16] T.J. Bruno, L.S. Ott, T.M. Lovestead, M.L. Huber, The composition-explicit distillation curve technique: relating chemical analysis and physical properties of complex fluids, *J. Chromatogr. A* 1217 (2010) 2703–2715.
- [17] K.D. Dix, J.S. Fritz, Simple steam distillation for sample preparation prior to gas-chromatographic determination of organic compounds, *J. Chromatogr.* 408 (1987) 201–210.
- [18] T.L. Peters, Steam distillation apparatus for concentration of trace-water soluble organics, *Anal. Chem.* 52 (1980) 211–213.
- [19] P. Rubiolo, B. Sgorbini, E. Liberto, C. Cordero, C. Bicchi, Essential oils and volatiles: sample preparation and analysis. A review, *Flav. Fragr. J.* 25 (2010) 282–290.
- [20] M.A. Ferhat, B.Y. Meklati, J. Smadja, F. Chemat, An improved microwave Clevenger apparatus for distillation of essential oils from orange peel, *J. Chromatogr. A* 1112 (2006) 121–126.
- [21] A.K. Kokolakis, S.K. Golfinopoulos, Microwave-assisted techniques (MATs), a quick way to extract a

- fragrance: a review, *Nat. Prod. Commun.* 8 (2013) 1493–1504.
- [22] T.A. Bouseta, S. Collin, Optimized Likens-Nickerson methodology for quantifying honey flavors, *J. Agric. Food Chem.* 43 (1995) 1890–1897.
- [23] M. Godefroot, P. Sandra, M. Verzele, New method for quantitative essential oil analysis, *J. Chromatogr.* 203 (1981) 325–335.
- [24] V. Seidel, W. Lindner, Universal sample enrichment technique for organochlorine pesticides in environmental and biological samples using a redesigned simultaneous steam distillation solvent-extraction apparatus, *Anal. Chem.* 65 (1993) 3677–3683.
- [25] A. Jayatilaka, S.K. Poole, C.F. Poole, T.M.P. Chichila, Simultaneous micro steam distillation/solvent extraction for the selective isolation of semivolatile flavor compounds from cinnamon and their separation by series-coupled column gas chromatography, *Anal. Chim. Acta* 302 (1995) 147–162.
- [26] S.M. Walters, Clean-up techniques for pesticides in fatty foods, *Anal. Chim. Acta* 236 (1990) 77–82.
- [27] Z. Ding, F.G.F. Qin, J. Yuan, S. Huang, R. Jiang, Y. Shao, Concentration of apple juice with an intelligent freeze concentrator, *J. Food Eng.* 256 (2019) 61–72.
- [28] Y. Pan, H. Li, X.R. Zhang, A.M. Li, Characterization of natural organic matter in drinking water: sample preparation and analytical approaches, *Trends Environ. Anal. Chem.* 12 (2016) 23–30.
- [29] D. Barcelo, M.F. Alpendurada, A review of sample storage and preservation of polar pesticides in water samples, *Chromatographia* 42 (1996) 704–712.
- [30] C.F. Poole, N.J. Evans, D.G. Wibberley, The determination of selenium in biological samples by gas-liquid chromatography with electron-capture detection, *J. Chromatogr.* 136 (1977) 63–72.
- [31] P. Haseley, G.-W. Oetjen, *Freeze-drying*, Wiley, New York, 2018.
- [32] C.F. Poole (Ed.), *Liquid-phase Extraction*, Elsevier, Amsterdam, 2020.
- [33] M. Alexovic, Y. Dotsikas, P. Bober, J. Sabo, Achievements in robotic automation of solvent extraction and related approaches for bioanalysis of pharmaceuticals, *J. Chromatogr. B* 1092 (2018) 402–421.
- [34] Y.Q. Tang, N.D. Weng, Salting-out assisted liquid-liquid extraction for bioanalysis, *Bioanalysis* 5 (2013) 1583–1598.
- [35] M. Anastassiades, S.J. Lehotay, D. Stanjnbaheer, F.J. Schenck, Fast and easy multiresidue method employing acetonitrile extraction/partitioning and “dispersive solid-phase extraction” for the determination of pesticide residues in produce, *J. AOAC Int.* 86 (2003) 412–431.
- [36] A. Samsidar, S. Siddiquee, S.M. Shaarani, A review of extraction, analytical and advanced methods for determination of pesticides in environment and foodstuffs, *Trends Food Sci. Technol.* 71 (2018) 188–2001.
- [37] C.F. Poole, T. Karunasekara, Solvent classification for chromatography and extraction, *J. Planar Chromatogr.* 25 (2012) 190–198.
- [38] C.F. Poole, T. Karunasekara, T.C. Ariyasena, Totally organic biphasic solvent systems for extraction and descriptor determination, *J. Sep. Sci.* 36 (2013) 95–109.
- [39] K.D. Clark, M.N. Emaus, M. Varona, A.N. Bowers, J.L. Anderson, Ionic liquids: solvents and sorbents in sample preparation, *J. Sep. Sci.* 41 (2018) 209–235.
- [40] C.F. Poole, S.K. Poole, Extraction of organic compounds with room temperature ionic liquids, *J. Chromatogr. A* 1217 (2010) 2268–2286.
- [41] C.F. Poole, N. Lenca, Green sample-preparation methods using room-temperature ionic liquids for the chromatographic analysis of organic compounds, *Trends Anal. Chem.* 71 (2015) 144–156.
- [42] S.G. Colgrove, H.J. Svec, Liquid-liquid fractionation of complex mixtures of organic components, *Anal. Chem.* 53 (1981) 1737–1742.
- [43] D.F.S. Natusch, B.A. Tomkins, Isolation of polycyclic organic compounds by solvent extraction with dimethyl sulfoxide, *Anal. Chem.* 50 (1976) 1429–1434.
- [44] C.F. Poole, Partition constant database for totally organic biphasic systems, *J. Chromatogr. A* 1527 (2017) 18–32.
- [45] G. Hendriks, D.R.A. Uges, J.P. Franke, Reconsideration of sample pH adjustment in bioanalytical liquid-liquid extraction of ionisable compounds, *J. Chromatogr. B* 853 (2007) 234–2441.
- [46] L. Novakova, H. Vickova, A review of current trends and advances in modern bio-analytical methods: chromatography and sample preparation, *Anal. Chim. Acta* 656 (2009) 8–35.
- [47] J. Folch, M. Lees, G.H. Sloane-Stanley, A simple method for the isolation and purification of total lipids from animal tissue, *J. Biol. Chem.* 226 (1957) 497–509.
- [48] E.G. Bligh, W.J. Dyer, A rapid method for total lipid extraction and purification, *Can. J. Biochem. Physiol.* 37 (1959) 911–917.
- [49] S.J. Lehotay, K.A. Son, H. Kwon, U. Koesukwiwat, W. Fu, K. Mastovoska, Comparison of QuEChERS sample preparation methods for the analysis of pesticide residues in fruits and vegetables, *J. Chromatogr. A* 1217 (2010) 2548–2560.
- [50] R. Perestrelo, P. Silva, P. Porto-Figueira, J.A.M. Pereira, C. Silva, S. Medina, J.S. Camara,

- QuEChERS – fundamentals, relevant improvements, applications and future, *Trends Anal. Chem.* 1070 (2019) 1–28.
- [51] J.M. Kokosa, A. Przyjazny, M.A. Jeannot, *Solvent Microextraction. Theory and Practice*, Wiley, Hoboken, 2009.
- [52] Y. Yamini, M. Rezazadeh, S. Seidi, Liquid-phase microextraction: the different principles and configurations, *Trends Anal. Chem.* 112 (2019) 264–272.
- [53] M. Ghambarian, Y. Yamini, A. Estrafill, Developments in hollow fiber based liquid-phase microextraction: principles and applications, *Microchim. Acta* 177 (2012) 271–294.
- [54] M.R. Ganjal, H.R. Sobhi, H. Farahani, P. Narouzi, R. Dinarvand, A. Kashtiaray, Solid drop based liquid-phase microextraction, *J. Chromatogr. A* 1217 (2010) 2337–2341.
- [55] M. Rezaee, Y. Yamani, M. Faraji, Evolution of dispersive liquid-liquid microextraction methods, *J. Chromatogr. A* 1217 (2010) 2342–2357.
- [56] M.-I. Leong, M.-R. Fuh, S.D. Huang, Beyond dispersive liquid-liquid microextraction, *J. Chromatogr. A* 1335 (2014) 2–14.
- [57] A. Zgola-Grzeskowiak, T. Grzeskowiak, Dispersive liquid-liquid microextraction, *Trends Anal. Chem.* 30 (2011) 1382–1399.
- [58] K. Ridgway, S.P.D. Lalljie, R.M. Smith, Sample preparation for the determination of trace residues and contaminants in foods, *J. Chromatogr. A* 1153 (2007) 36–53.
- [59] J.R. Dean, *Extraction Methods for Environmental Analysis*, Wiley, Chichester, 1998.
- [60] M.D.L. Castro, F. Priego-Capote, Soxhlet extraction: past and present panacea, *J. Chromatogr. A* 1217 (2010) 2383–2389.
- [61] B. Albero, J.L. Tadeo, R.A. Perez, Ultrasound-assisted extraction of organic contaminants, *Trends Anal. Chem.* 118 (2019) 739–750.
- [62] Y. Pico, Ultrasound-assisted extraction for food and environmental samples, *Trends Anal. Chem.* 43 (2013) 84–99.
- [63] F.P. Capote, M.D.L. de Castro, Ultrasound in analytical chemistry, *Anal. Bioanal. Chem.* 387 (2007) 249–257.
- [64] H. Wang, J. Ding, N.Q. Ren, Recent advances in microwave-assisted extraction of trace organic pollutants from food and environmental samples, *Trends Anal. Chem.* 75 (2016) 197–208.
- [65] V. Camel, Recent extraction techniques for solid matrices – supercritical fluid extraction, pressurized fluid extraction, and microwave-assisted extraction: their potential and pitfalls, *Analyst* 126 (2001) 1182–1193.
- [66] J.P. Jarvis, E.D. Morgan, Isolation of plant products by supercritical-fluid extraction, *Phytochem. Anal.* 8 (1997) 217–222.
- [67] T. Hyotylainen, On-line coupling of extraction with gas chromatography, *J. Chromatogr. A* 1186 (2008) 39–50.
- [68] A.D. Sanchez-Camargo, F. Parada-Alfonso, E. Ibanez, A. Cifuentes, On-line coupling of supercritical fluid extraction and chromatographic techniques, *J. Sep. Sci.* 40 (2017) 213–227.
- [69] A.L. Capriotti, C. Cavaliere, P. Foglia, R. Samperi, S. Stampachiacciere, S. Ventura, S. Lagana, Recent advances and developments in matrix solid-phase dispersion, *Trends Anal. Chem.* 71 (2015) 186–193.
- [70] C.F. Poole (Ed.), *Solid-phase Extraction*, Elsevier, Amsterdam, 2020.
- [71] J. Parshintsev, T. Hyotylainen, Methods for characterization of organic compounds in atmospheric aerosol particles, *Anal. Bioanal. Chem.* 407 (2015) 5877–5897.
- [72] A. Andrade-Eiron, M. Canle, V. Leroy-Cancellieri, V. Cerda, Solid-phase extraction of organic compounds. A critical review, *Trends Anal. Chem.* 80 (2016) 641–654.
- [73] C.F. Poole, New trends in solid-phase extraction, *Trends Anal. Chem.* 22 (2003) 362–373.
- [74] N.J.K. Simpson (Ed.), *Solid-phase Extraction: Principles, Strategies and Applications*, Marcel Dekker, New York, 2000.
- [75] C. Eger, T.C. Schmidt, Disk-based solid-phase extraction analysis of organic substances in water, *Trends Anal. Chem.* 61 (2014) 74–82.
- [76] M.M. Moein, A. Abdel-Rehim, M. Abdel-Rehim, Microextraction extraction by packed sorbent (MEPS), *Trends Anal. Chem.* 67 (2015) 34–44.
- [77] M. Sajid, Porous membrane protected micro-solid-phase extraction: a review of features, advancements and applications, *Anal. Chim. Acta* 965 (2017) 36–53.
- [78] H.L. Lord, W.Q. Zhan, J. Pawliszyn, Fundamentals and applications of needle trap devices: a critical review, *Anal. Chim. Acta* 677 (2010) 3–18.
- [79] K. Kedziora-Koch, W. Wasiaik, Needle-based extraction techniques with protected sorbent as powerful sample preparation tools to gas chromatographic analysis: trends in applications, *J. Chromatogr. A* 1565 (2018) 1–18.
- [80] M. Wlerucka, M. Biziuk, Application of magnetic nanoparticles for magnetic solid-phase extraction in preparing biological, environmental and food samples, *Trends Anal. Chem.* 59 (2014) 50–58.
- [81] J. Plotka-Wasyłka, N. Szczepanska, M. de la Guardia, J. Namiesnik, Modern trends in solid phase extraction: new sorbent media, *Trends Anal. Chem.* 77 (2016) 23–43.

- [82] Y. Wen, L. Chen, J. Li, D. Liu, L. Chen, Recent advances in solid-phase sorbents for sample preparation prior to chromatographic analysis, *Trends Anal. Chem.* 59 (2014) 26–41.
- [83] N. Fontanals, R.M. Marce, F. Borull, New hydrophobic materials for solid-phase extraction, *Trends Anal. Chem.* 24 (2005) 394–406.
- [84] L. Xu, X. Qi, X. Li, Y. Bai, H. Liu, Recent advances in applications of nanomaterials for sample preparation, *Talanta* 146 (2016) 714–726.
- [85] B.T. Zhang, X. Zheng, H.F. Li, J.M. Lin, Application of carbon-based nanomaterials in sample preparation: a review, *Anal. Chim. Acta* 784 (2013) 1–17.
- [86] E. Turiel, A. Martin-Esterban, Molecularly imprinted polymers for sample preparation: a review, *Anal. Chim. Acta* 688 (2010) 87–99.
- [87] N. Reyes-Garcés, E. Gionfriddo, M.- Gomez-Rios, N. Alam, E. Boyaci, B. Bojko, V. Singh, J. Gandy, J. Pawlisz, Advances in solid-phase microextraction and perspective on future directions, *Anal. Chem.* 90 (2018) 302–360.
- [88] J. Pawliszyn (Ed.), *Handbook of Solid-phase Microextraction*, Elsevier, Amsterdam, 2012.
- [89] G. Ouyang, J. Pawliszyn, A critical review in calibration methods for solid-phase microextraction, *Anal. Chim. Acta* 627 (2008) 184–197.
- [90] H. Piri-Moghadam, M.N. Alam, J. Pawliszyn, Review of geometries and coating materials in solid-phase microextraction: opportunities, limitations, and future perspectives, *Anal. Chim. Acta* 984 (2017) 42–65.
- [91] A. Prieto, O. Basauri, R. Rodil, A. Usobiaga, L.A. Fernandez, N. Etxebarria, O. Zuloaga, Stir bar sorptive extraction: a review on method optimization, novel applications, limitations and potential solutions, *J. Chromatogr. A* 1217 (2010) 2642–2666.
- [92] J.M.F. Nogueira, Stir bar sorptive extraction: 15 years making sample preparation more environmentally friendly, *Trends Anal. Chem.* 71 (2015) 214–223.
- [93] A.F. Ismail, M.A. Rahman, M.H.D. Othman, T. Matsuura (Eds.), *Membrane Separation Principles and Applications. From Material Selection to Mechanisms and Industrial Uses*, Elsevier, Amsterdam, 2019.
- [94] L.N. Moskvina, T.G. Nikitina, Membrane methods of substance separation in analytical chemistry, *J. Anal. Chem.* 59 (2004) 2–16.
- [95] O. Sae-Khow, S. Mitra, Pervaporation in chemical analysis, *J. Chromatogr. A* 1217 (2010) 2736–2746.
- [96] L.N. Gonclaves, I.M. Valente, J.A. Rodrigues, Recent advances in membrane-aided extraction and separation for analytical purposes, *Sep. Purif. Rev.* 46 (2017) 179–194.
- [97] J.A. Jonsson, L. Mathiasson, Membrane extraction in analytical chemistry, *J. Sep. Sci.* 24 (2001) 495–507.
- [98] J. Moreda-Pineiro, A. Moreda-Pineiro, Combined assisted extraction techniques as green sample pretreatments in food analysis, *Trends Anal. Chem.* 118 (2019) 1–18.
- [99] M. Havlikova, R. Cabala, V. Pacakova, Z. Bosakova, Critical evaluation of microextraction pretreatment techniques – part 2. Membrane-supported and homogeneous phase based techniques, *J. Sep. Sci.* 42 (2019) 303–318.
- [100] A. Gjelstad, S. Pedersen-Bjergaard, Recent developments in electromembrane extraction, *Anal. Methods* 5 (2013) 4548–4557.
- [101] J.A. Lopez-Lopez, C. Mendiguchia, J.J. Pinto, C. Moreno, Application of solvent-bar microextraction for the determination of organic and inorganic compounds, *Trends Anal. Chem.* 110 (2019) 57–65.
- [102] D. Schuetzle, T.L. Riley, T.J. Prater, T.M. Harver, D.F. Hunt, Analysis of nitrated polycyclic aromatic hydrocarbons in diesel particulates, *Anal. Chem.* 54 (1982) 265–271.
- [103] S.A. Wise, B.A. Benner, S.N. Chesler, L.R. Hilpert, C.R. Vogt, W.E. May, Characterization of the polycyclic aromatic hydrocarbons from two standard reference material air particulate samples, *Anal. Chem.* 58 (1986) 3067–3077.
- [104] F. David, C. Devos, E. Dumont, Z. Yang, P. Sandra, Determination of pesticides in fatty matrices using gel permeation clean-up followed by GC-MS/MS and LC-MS/MS analysis: a comparison of low- and high-pressure gel permeation columns, *Talanta* 165 (2017) 201–210.
- [105] N.H. Snow (Ed.), *Basic Multidimensional Gas Chromatography*, Elsevier, Amsterdam, 2020.
- [106] Y. Nolvachai, C. Kulsing, P.J. Marriott, Multidimensional gas chromatography in food analysis, *Trends Anal. Chem.* 96 (2017) 124–137.
- [107] D. Sciarrone, S. Panto, C. Ragonese, P. Dugo, L. Mondello, Evolution and status of preparative gas chromatography as a green sample-preparation technique, *Trends Anal. Chem.* 71 (2015) 65–73.
- [108] H.J. Cortes (Ed.), *Multidimensional Chromatography: Techniques and Applications*, Dekker, New York, 1990.
- [109] K. Grob, *On-line Coupled LC-GC*, Huethig, Heidelberg, 1991.
- [110] M. Biedermann, C. Munoz, K. Grob, Update of on-line coupled liquid chromatography – gas chromatography of mineral oil hydrocarbons in foods and cosmetics, *J. Chromatogr. A* 1521 (2017) 140–149.

- [111] G. Purcaro, S. Moret, L. Conte, Sample pre-fractionation of environmental and food samples using LC-GC multidimensional techniques, *Trends Anal. Chem.* 43 (2013) 146–160.
- [112] T. Greibrokk, Applications of supercritical-fluid extraction in multidimensional systems, *J. Chromatogr. A* 703 (1995) 523–536.
- [113] K. Blau, J. Halket (Eds.), *Handbook of Derivatives for Chromatography*, Wiley, Chichester, 1994.
- [114] D.R. Knapp, *Handbook of Analytical Derivatization Reactions*, Wiley, New York, 1979.
- [115] J.D. Drozd, *Chemical Derivatization in Gas Chromatography*, Elsevier, Amsterdam, 1981.
- [116] M.A. Farajzadeh, N. Nouri, P. Khorram, Derivatization and microextraction methods for determination of organic compounds by gas chromatography, *Trends Anal. Chem.* 55 (2014) 14–23.
- [117] A. Balinova, Strategies for chromatographic analysis of pesticide residues in water, *J. Chromatogr. A* 754 (1996) 125–135.
- [118] A.M.C. Ferreira, M.E.F. Laespada, J.L.P. Pavon, B.M. Cordero, *In situ* aqueous derivatization as sample preparation technique for gas chromatographic determinations, *J. Chromatogr. A* 1296 (2013) 70–83.
- [119] L. Xu, C. Basheer, H.K. Lee, Chemical reactions in liquid-phase microextraction, *J. Chromatogr. A* 1216 (2006) 701–707.
- [120] C.D. Stalikas, Y.C. Fiamegos, Microextraction combined with derivatization, *Trends Anal. Chem.* 27 (2008) 533–542.
- [121] H.Q. Lin, J.L. Wang, L.J. Zeng, G. Li, Y.F. Sha, D. Wu, B.Z. Liu, Development of solvent micro-extraction combined with derivatization, *J. Chromatogr. A* 1296 (2013) 235–242.
- [122] M. Sajid, Dispersive liquid-liquid microextraction coupled with derivatization: a review of different modes, applications, and green aspects, *Trends Anal. Chem.* 106 (2018) 169–182.
- [123] S.N. Atapattu, J.M. Rosenfeld, Solid phase analytical derivatization as a sample preparation method, *J. Chromatogr. A* 1296 (2013) 204–213.
- [124] S.N. Atapattu, J.M. Rosenfeld, Micro scale analytical derivatizations on solid phase, *Trends Anal. Chem.* 113 (2019) 351–356.
- [125] M. Sajid, J. Plotka-Wasylika, “Green” nature of the process of derivatization in analytical sample preparation, *Trends Anal. Chem.* 102 (2018) 16–31.
- [126] J. O’Reilly, O. Wang, I. Setkova, J.P. Hutchinson, Y. Chen, H.L. Lord, C.M. Linton, J. Pawliszyn, Automation of solid-phase microextraction, *J. Sep. Sci.* 28 (2005) 2010–2022.
- [127] A. Gonzalez, J. Avivar, V. Cerda, Estrogens determination in wastewater samples by automatic in-syringe dispersive liquid-liquid microextraction prior silylation and gas chromatography, *J. Chromatogr. A* 1413 (2015) 1–8.
- [128] H. Kataoka, Recent developments and applications of microextraction techniques in drug analysis, *Anal. Bioanal. Chem.* 396 (2010) 339–354.
- [129] I. Lavilla, V. Romero, I. Costas, C. Bendicho, Greener derivatization in analytical chemistry, *Trends Anal. Chem.* 61 (2014) 1–10.
- [130] S.L. Soderholm, M. Damm, C.O. Kappe, Microwave-assisted derivatization procedures for gas chromatography/mass spectrometry analysis, *Mol. Divers.* 14 (2010) 869–888.
- [131] M. Damm, G. Rechberger, M. Kollrosen, C.O. Kappe, Microwave-assisted high-throughput derivatization techniques utilizing silicon carbide microtiter platforms, *J. Chromatogr. A* 1217 (2010) 167–170.
- [132] M.D. Luque de Castro, F. Priego-Capote, A. Peralbo-Molina, The role of ultrasound in analytical derivatization, *J. Chromatogr. B* 879 (2011) 1189–1195.
- [133] M.M. Delgado-Provedano, M.D. Luque de Castro, Ultrasound assisted extraction and in-situ derivatization, *J. Chromatogr. A* 1296 (2013) 226–234.
- [134] A.A. Nuhu, C. Basheer, B. Saad, Liquid-phase and dispersive liquid-liquid microextraction techniques with derivatization: recent applications in bioanalysis, *J. Chromatogr. B* 879 (2011) 1180–1188.
- [135] Q. Wang, L. Ma, C.-R. Yin, L. Xu, Developments in injection port derivatization, *J. Chromatogr. A* 1296 (2013) 25–35.
- [136] E. Bizkarguenaga, A. Iparragirre, P. Navarro, M. Olivares, A. Prieto, A. Vallejo, O. Zuloaga, In-port derivatization after sorptive extractions, *J. Chromatogr. A* 1296 (2013) 36–46.
- [137] C.F. Poole, Derivatization reactions for use with the electron-capture detector, *J. Chromatogr. A* 1296 (2013) 15–24.
- [138] A.E. Pierce, *Silylation of Organic Compounds*, Pierce Chemical Company, Rockford, IL, 1968.
- [139] C.F. Poole, Alkylsilyl derivatives for gas chromatography, *J. Chromatogr. A* 1296 (2013) 2–14.
- [140] J.M. Halket, V.G. Zaikin, Derivatization in mass spectrometry – 1. Silylation, *Eur. J. Mass Spectrom.* 9 (2003) 1–21.
- [141] E. Pagliano, B. Campanella, A. D’Ulivo, Z. Mester, Derivatization chemistries for the determination of inorganic anions and structurally related compounds by gas chromatography – a review, *Anal. Chim. Acta* 1025 (2018) 12–40.
- [142] B. Khakimov, M.S. Motawia, S. Bak, S.B. Engelsens, The use of trimethylsilyl cyanide derivatization for robust and broad spectrum high-throughput gas

- chromatography-mass spectrometry based metabolomics, *Anal. Bioanal. Chem.* 405 (2013) 9193–9205.
- [143] B. Fodor, I. Boldizsar, I. Molnar-Perl, Alkylsilyl speciation and direct sample preparation of plant cannabinoids prior to their analysis by GC-MS, *Anal. Chim. Acta* 1021 (2018) 51–59.
- [144] J.L. Little, Artifacts in trimethylsilyl derivatization reactions and ways to avoid them, *J. Chromatogr. A* 844 (1999) 1–22.
- [145] V.G. Zaikin, Derivatization in mass spectrometry – 6. Formation of mixed derivatives of polyfunctional compounds, *Eur. J. Mass Spectrom.* 11 (2005) 611–636.
- [146] Z. Fuzfai, I. Boldizsar, I. Molnar-Perl, Characteristic fragmentation patterns of the trimethylsilyl and trimethylsilyl-oxime derivatives of various saccharides as obtained by gas chromatography coupled to ion-trap mass spectrometry, *J. Chromatogr. A* 1177 (2008) 183–189.
- [147] R.M. Flores, P.V. Doskey, Evaluation of multistep derivatization methods for identification and quantification of oxygenated species in organic aerosols, *J. Chromatogr. A* 1418 (2015) 1–11.
- [148] Z. Lai, O. Fiehn, Mass spectral fragmentation of trimethylsilylated small molecules, *Mass Spectrom. Revs.* 37 (2018) 245–247.
- [149] D.J. Harvey, P. Vouros, Mass spectrometric fragmentation of trimethylsilyl and related alkylsilyl derivatives, *Mass Spectrom. Revs.* 39 (2020) 105–211, <https://doi.org/10.1002/mass.21590> (in press).
- [150] H. Kataoka, Derivatization reactions for the determination of amines by gas chromatography and their applications in environmental analysis, *J. Chromatogr. A* 733 (1996) 19–34.
- [151] R.J. Wells, Recent advances in non-silylation derivatization techniques for gas chromatography, *J. Chromatogr. A* 843 (1999) 1–18.
- [152] V.G. Zaikin, J.M. Halket, Derivatization in mass spectrometry – 2. Acylation, *Eur. J. Mass Spectrom.* 9 (2003) 421–434.
- [153] J.M. Halket, V.G. Zaikin, Derivatization in mass spectrometry – 3. Alkylation (arylation), *Eur. J. Mass Spectrom.* 10 (2004) 1–19.
- [154] A. Ramz, J. Korpecka, E. Lankmayr, Optimized derivatization of acidic herbicides with trimethylsilyldiazomethane for GC analysis, *J. Sep. Sci.* 31 (2008) 746–752.
- [155] Y. Matsumoto, Y. Ando, Y. Hiraoka, A. Tawa, S. Ohshimo, A simplified gas chromatographic fatty-acid analysis by direct saponification/methylation procedure and its application on wild tuna larvae, *Lipids* 53 (2018) 919–929.
- [156] P. Husek, Chloroformates in gas chromatography as general purpose derivatizing agents, *J. Chromatogr. A* 717 (1998) 57–91.
- [157] L. Rimacova, P. Husek, P. Simek, A new method for immediate derivatization of hydroxyl groups by fluoroalkyl chloroformates and its application for the determination of sterols and tocopherols in human serum and amniotic fluid by gas chromatography-mass spectrometry, *J. Chromatogr. A* 1339 (2014) 154–167.
- [158] M. Kristensen, P. Christensen, J.H. Christensen, Optimization and validation of a derivatization method with boron trifluoride in ethanol for analysis of aromatic carboxylic acids in water, *J. Chromatogr. A* 1601 (2019) 21–26.
- [159] B. Fodor, I. Molnar-Perl, The role of derivatization techniques in the analysis of plant cannabinoids by gas chromatography mass spectrometry, *Trends Anal. Chem.* 95 (2017) 149–158.
- [160] J. Rousova, M.R. Lindahi, A. Casey, A. Kubatova, Simultaneous determination of trace concentrations of aldehydes and carboxylic acids in particulate matter, *J. Chromatogr. A* 1544 (2018) 49–61.
- [161] E. Gionfriddo, A. Passarini, J. Pawliszyn, A facile and fully automated on-fiber derivatization protocol for direct analysis of short-chain aliphatic amines using a matrix compatible solid-phase microextraction coating, *J. Chromatogr. A* 1457 (2016) 22–28.
- [162] C.F. Poole, A. Zlatkis, Cyclic derivatives for the selective chromatographic analysis of bifunctional compounds, *J. Chromatogr.* 184 (1980) 99–183.
- [163] V.G. Zaikin, J.M. Halket, Derivatization in mass spectrometry – 4. Formation of cyclic derivatives, *Eur. J. Mass Spectrom.* 10 (2004) 555–568.

Petrochemical applications of gas chromatography

*Juliana Crucello¹, Nathália de Aguiar Porto¹,
Rogério Mesquita Carvalho², Alexandre de Andrade Ferreira³,
Carlos Alberto Carbonexi³, Leandro Wang Hantao¹*

¹Institute of Chemistry, University of Campinas (UNICAMP), Campinas, SP, Brazil; ²Division of Chemistry, PETROBRAS Research and Development Center (CENPES), PETROBRAS, Rio de Janeiro, RJ, Brazil; ³Division of Geochemistry, PETROBRAS Research and Development Center (CENPES), PETROBRAS, Rio de Janeiro, RJ, Brazil

25.1 Introduction

Petroleum is a naturally occurring fluid resulting from years of decomposition of organic matter found beneath the Earth's surface under elevated temperature and pressure. It consists of a complex mixture of thousands of compounds, such as hydrocarbons, nitrogen-, oxygen-, sulfur-, and metal-containing species and metals [1,2]. Hydrocarbons are the dominant components of crude oil, with carbon numbers from C₁ to C₁₀₀₊, depending on the oil sample. Sulfur-containing compounds are the main class of heteroatom species in crude oil, while nitrogen- and oxygen-containing compounds are present in minor amounts. The proportion of heteroatom-containing compounds in crude oil depends on the geological origin of the oil [1]. Metals are also found in trace amounts, with vanadium and nickel typically present at orders

of magnitude higher than other metals [2]. Table 25.1 summarizes the principal chemical classes by crude oil constituents, along with their percentage content and examples of compounds for each class.

The petroleum industry traditionally classifies an oil according to its macroscopic properties; for example, the API (American Petroleum Institute) uses gravity, total sulfur content, viscosity, and total acidity number (TAN). Gravity is related to the oil density and is used to classify an oil as either light or medium (API > 20 degrees) or heavy (API < 20 degrees) according to ASTM D287 [1–3]. Such parameters are used in the evaluation of crude oil quality; however, they provide little information about the oil composition. For instance, an oil rich in lower-molecular-weight aromatics may exhibit an API gravity value greater than that of an oil composed predominantly of higher-molecular-

TABLE 25.1 Principal chemical classes with their percentage content and example of compounds present in petroleum [1].

Chemical class	Wt. %	Example of compounds
Hydrocarbon	90–95	Paraffins (<i>n</i> -alkanes), iso-paraffins (branched acyclic hydrocarbons), naphthenes (cyclic alkanes), and aromatic hydrocarbons.
S-compounds	0.04–5	Mercaptans, sulfides, disulphides, thiophenes, benzothiophenes, dibenzothiophenes, and naphthodibenzothiophenes.
N-compounds	0.1–0.9	Neutral N-compounds (pyrrole, indole, carbazole, and amide) and basic N-compounds (aniline, pyridine, quinoline, and acridine).
O-compounds	<2	Carboxylic acids, esters, phenols, furans, and benzofurans.
Metals	Trace amounts	Mostly vanadium and nickel.

weight paraffins [4]. Moreover, the oil composition is used to determine its destination during refining and processing, while it will also influence the properties of the final products, such as octane number, cetane number, and smoke point [4].

The molecular characterization of crude oils is considered one of the most important tasks to improve exploration and production processes, encompassing the earlier stages of geochemical background up to the final oil processing. For instance, molecular characterization may be employed to: (i) understand petroleum formation, migration, and accumulation; (ii) elaborate thermodynamic and kinetic models for flow assurance; (iii) predict crude oil physicochemical properties (e.g., API density); (iv) determine the petrochemical processes best suited for a particular petroleum; (v) quality assurance of petroleum-derived products; and (vi) identify

the origin of oil spills [1,4]. Hence, powerful analytical tools are mandatory to provide reliable molecular information of petroleum for the modern petroleum industry.

Instrumental analyses such as X-ray fluorescence, ultraviolet (UV), infrared (IR) absorption spectroscopy, and nuclear magnetic resonance (NMR) are employed to provide structural group-type analyses of the major constituents of petroleum [1,4]. Separation techniques, such as gas chromatography (GC), offer complementary compositional information compared to the aforementioned techniques [5,6]. A single GC run can provide valuable information about specific compounds or class-based groups. Additionally, the possibility of coupling GC with mass spectrometry (MS) expands the capability of experimental methods affording additional selectivity and sensitivity [1]. These features have led to the unequivocal consensus that GC is the most important analytical technique in the oil and gas industry. Accordingly, the American Society for Testing and Materials (ASTM) has standardized numerous procedures using GC-based methods for product testing [7]. Examples of GC standard test methods are summarized in Table 25.2.

Molecular characterization of petroleum is the most challenging task an analytical chemist can endure. First, the oil constituents exhibit a broad range of physical and chemical properties [8]. Second, petroleum presents an overwhelming number of isomers [4], as illustrated in Table 25.3. Such complexity makes the separation of the individual constituents a difficult task. Even if only a small number of the possible isomers were present in an oil sample, the number of analytes is still far higher than the average peak capacity of conventional GC using narrow-bore capillary columns (1D-GC) [1].

In this context, multidimensional gas chromatography (MDGC) was developed to effectively increase the peak capacity [9]. Introduced in the late 1950s, it has been steadily adopted ever since [4]. Most MDGC approaches combine

TABLE 25.2 Examples of standard test methods using gas chromatography [3].

ASTM	Objective
D2268	Analysis of high-purity <i>n</i> -heptane and isooctane
D2427	Determination of C ₂ through C ₅ hydrocarbons in gasolines
D5441	Standard test method for analysis of methyl <i>t</i> -butyl ether (MTBE) by gas chromatography
D5443	Paraffin, naphthene, and aromatic hydrocarbon type analysis in petroleum distillates through 200°C by multidimensional GC
D5623/ D5540	Determination of sulfur compounds in light petroleum liquids by GC and sulfur selective detection
D6839	Determination of hydrocarbon types, oxygenated compounds, and benzene in spark ignition engine fuels
D7900	Determination of light hydrocarbons in stabilized crude oils

TABLE 25.3 Number of possible isomers of paraffins with respect to the carbon number.

Carbon number	Number of isomers
5	3
10	75
20	3.66×10^5
30	4.11×10^9
40	6.24×10^{13}
60	2.21×10^{22}
80	1.06×10^{31}
100	5.92×10^{39}

Data retrieved from J. Beens, U.A.Th. Brinkman, *Trends Anal. Chem.* 19 (2000) 262.

two GC separation steps, providing the resolution of analytes based on their vapor pressure and by their capacity to undergo specific interactions with the stationary phase (SP). This results

in a structured chromatogram, wherein the peaks are distributed in the retention space based on the volatility and chemical family [1]. MDGC separations may exhibit two modes of operation: heart-cutting two-dimensional gas chromatography (GC-GC) and comprehensive two-dimensional gas chromatography (GC × GC).

GC-GC is a technique that was first developed in the petroleum industry to enhance the separation of oxygenated hydrocarbons in combustion products from automotive engines [10,11]. The development of a GC-GC method starts with an exploratory run emulating a 1D-GC analysis, wherein all effluent from the primary column is diverted to the first detector. Then, the analyst assigns the critical pairs of peaks that are overlapped and require further resolution. In the next run, all analytes experience the primary separation in the first column (¹D), but only selected fractions of the sample are transferred to the secondary column (²D) for additional separation. At this moment, the effluent of the ¹D is switched by an interface toward the ²D, where the second separation step takes place. After the selected fraction is loaded onto the secondary column, the effluent of the ¹D column is switched back to its initial pathway. So, the remainder of the analyte continues its original flow path to the first detector. The analytes that undergo the second separation stage are detected by a second detection module [9]. GC-GC is embodied by mechanical valves and flow-switching interfaces that evolved significantly over time [12]. Noteworthy, the Deans' switch is an interface that allows the transfer of the effluent from the ¹D to the ²D column by using pressure differences to switch flows between the two columns [13,14], as seen in Fig. 25.1A–B. Deans' switches have surpassed the limitations of mechanical interfaces, for example, surface adsorption and dead volume, and have extended the maximum allowable operating temperature (MAOT) [12].

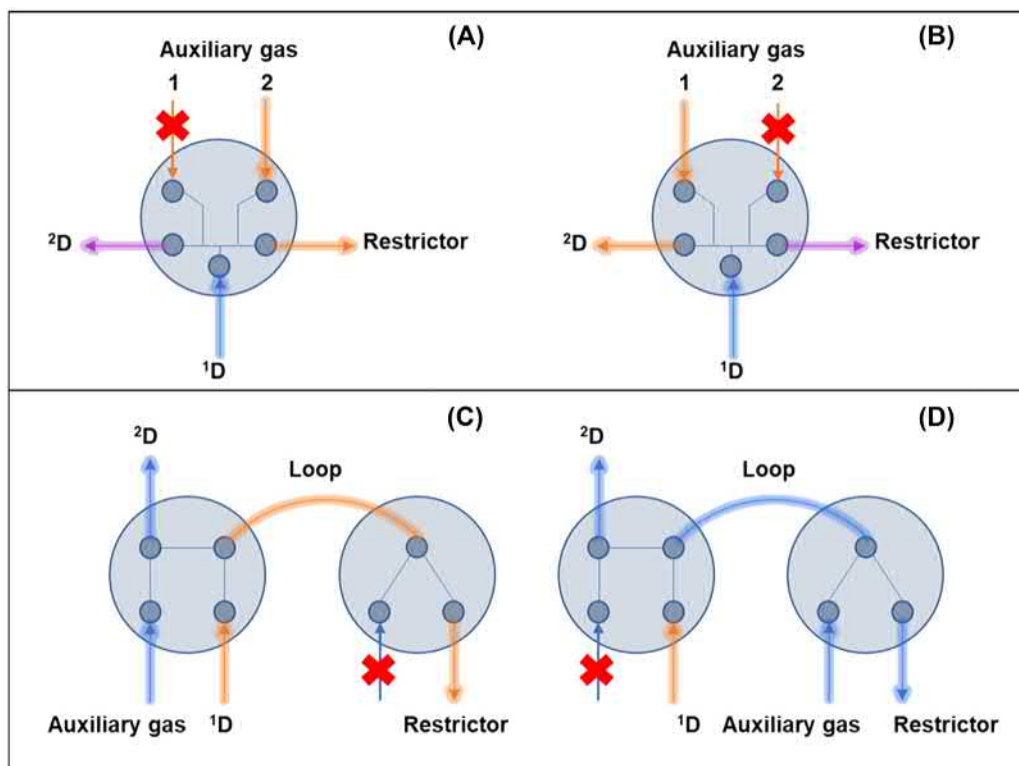


FIGURE 25.1 Flow-based interfaces for multidimensional gas chromatography (MDGC) highlighting the Deans' switch for heart-cutting two-dimensional gas chromatography (GC-GC) (A, B) and a reverse fill/flush assembly for comprehensive two-dimensional gas chromatography (GC \times GC) (C, D). Heart-cutting GC-GC: (A) ^1D chromatographic bands are eluted and diverted to the detection module and (B) ^1D bands are loaded onto the secondary column for separation followed by detection using an additional module. Reverse fill/flush flow modulator: (C) chromatographic band sampling (fill) and (D) band injection into the ^2D (flush).

GC \times GC was firstly introduced by Liu and Phillips in 1991 as a technique in which all the effluent from the ^1D separation is subjected to an additional separation on the ^2D [15]. The two separation columns are connected through an interface known as modulator, which continuously samples the effluent from the ^1D column and transfers the bands to the ^2D column as sharp pulses. A compression ratio of 120 can be attained by cryogenic modulation, where the original peak width of 6 s is focused to 50 ms. Each pulse is then subjected to a highly efficient and fast separation on the ^2D column, typically with durations of 2–12 s. The

modulation process will occur continuously throughout the analysis with a well-defined frequency to ensure reproducible separation. The time interval between successive reinjections by the modulator is defined as the modulation period. The modulation ratio provides a general guide for the selection of the modulation period. An average modulation ratio of 3 is recommended to maintain the resolution achieved in primary separation step, which ensures that components previously separated on the ^1D column do not recombine in the modulator, thus, maximizing the peak capacity of the composite system [9]. The interested reader is directed

elsewhere for further details of the modulation ratio [16]. The separation is visualized as contour plots, in which each peak is characterized by two retention coordinates (1t_R and 2t_R) and peak intensity by a user-defined color scale [17].

Modulation may be based on different principles, including thermal and flow-based interfaces. The best-performing thermal interfaces are the cryogenic modulators, which trap the 1D effluent in a cryogenically cooled region and reinject it into the 2D by thermal desorption [9]. Alternatively, differential flow modulators (FMs) provide suitable alternatives to thermal modulation. Flow-based modulators employ differential pressure to divert the 1D column effluent into an accumulation loop and subsequently reinject the bands to the 2D , as shown in Fig. 25.1C–D. Such interfaces exhibit a simple design allowing for robust operation at a lower cost [18]. Although the reinjection of cryogenic interfaces outperforms that of flow-based modulators, the latter have enabled high peak capacity separations providing similar qualitative results. Since the introduction of FM by Seeley [19], several FM designs have been proposed. Current commercial FMs use microfluidic devices in two operating modes: forward fill/flush (FFF) or reverse fill/flush (RFF). RFF modulators often exhibit an adjustable collection channel, which offers flexibility for the first-dimension flow rate and the modulation period. Another advantage of such an interface is the production of reduced dispersion in comparison to FFF and cryogenic modulators [20].

25.2 Column selection according to sample volatility

Column selection must consider the sample volatility to attain a balance between retention factors (k) and the MAOT of the GC column. The analysis of highly volatile compounds requires a retentive column, which relies on the use of solid adsorbents (gas–solid

chromatography) or thick liquid polymeric phases (gas–liquid chromatography) with a suitable phase ratio (β).

The ASTM D1945 method for analysis of permanent gases (e.g., oxygen, nitrogen, and methane) in natural gases uses an adsorption-based GC column. An alternative to traditional packed column is the porous-layer open tubular (PLOT) column for gas–solid chromatography, which exhibits higher resolution by improving the column efficiency. PLOT columns comprise a fused-silica capillary internally coated with a layer of solid adsorbent, which is bonded to the inner surface of the column [7]. Commercial PLOT columns include adsorbent phases based on aluminum oxides, molecular sieves, carbosieves, porous polymers (e.g., styrene-divinylbenzene), and silica [21]. The selected phase depends on the properties of the target compounds, as illustrated in Table 25.4, which presents some general applications for PLOT columns.

Wall-coated open tubular columns (WCOT) are used in gas–liquid chromatography and exhibit adjustable retention factors (k) depending on the column phase ratio (β). Hence, these columns are frequently employed in the oil and gas industry to characterize C_3 to C_{60+} hydrocarbons and heteroatom compounds. The general

TABLE 25.4 General applications of gas–solid chromatography.

Sorbent phase	Analytes
Molecular sieves	CO_2 ; O_2 ; N_2 ; CH_4 ; CO ; N_2O
Porous polymers	Volatile polar and nonpolar compounds
Alumina	Hydrocarbon impurities in C_1 – C_5 hydrocarbons
Carbosieve	Impurities in ethylene
Silica	C_1 – C_5 hydrocarbons; sulfur gases; hydrocarbons and semipolar impurities

Data retrieved from J. Zeeuw, J. Luong, *TrAC* (2002) 21, 595.

retention of a column can be estimated from its β value and length. While the retention time is directly proportional to the column length, the β value must take into account the analyte distribution constant in the biphasic system (K_D). The value of K_D is a thermodynamic property, which is dependent on the chemical potential of the system [22]. As shown by Eq. (25.1), K_D can be expressed a function of k and β . We find that an increase in k is expected by reducing the value of β , preserving the overall value of K_D —if the same phase chemistry is maintained. So, the β value contributes to the column retentiveness.

$$K_D = [A]_S/[A]_G = k \times \beta = k \times r/(2 \times d_f) \quad (25.1)$$

where K_D is distribution constant of the analyte between the SP (S) and gas phase (G), $[A]$ is the concentration of the analyte, k is the retention factor, β is the phase ratio, r is the column radius (μm), and d_f is the film thickness (μm).

Highly retentive GC columns exhibit low values of β (e.g., $\beta < 250$) and are characterized by a low ratio between the column radius and film thickness. Such columns are recommended for the analysis of highly volatile compounds [6]. Columns with high β values (e.g., $\beta > 250$) are less retentive and are recommended for heavier solutes (C_{30+}). A general-purpose column ($\beta = 250$) is frequently used for the analysis of a mixture with volatility comprised of C_6 – C_{30} [7].

SPs commonly used for oil and gas industry are based on poly(siloxane) and poly(ethylene glycol) (PEG). Most applications are carried out using poly(siloxane)-based phases either because they exhibit higher MAOT values compared to PEG-based phases or simply due to tradition. The most popular column is the $30 \text{ m} \times 0.25 \text{ mm}$ ($d_f = 0.25 \mu\text{m}$) coated with poly(diphenyldimethylsiloxane) with 5% diphenylsiloxane monomer incorporation. Selection of SP is not a trivial task, as it is highly dependent on the chemical nature of critical pairs. For

instance, SPs capable of engaging in strong dipole-type interactions are better suited to the separation of normal and branched chain alkanes, such as PEG and poly(diphenyldimethylsiloxane) with 50% diphenylsiloxane monomer incorporation. Highly cohesive phases are not typically used for the analysis of aliphatic hydrocarbons due to poor retention [23,24].

New types of SPs are being evaluated for oil analysis. For instance, those based on ionic liquids (ILs). A highly selective phase was developed to separate kerosene aliphatic hydrocarbons, namely saturated hydrocarbons, cycloalkanes, and olefins by structurally tuning the solvation properties of IL-based SPs [24,25], as well as demonstrating the ability to perform separations at high temperatures.

25.3 Introduction to organic geochemical analyses

Hydrocarbon analyses afford a means for understanding the relationship between crude oils and petroleum extracts from the corresponding source rocks, which can be used by geologists to interpret the characteristics of the petroleum source rocks when other information is unavailable [5]. The group of methods used for this purpose is coined “organic geochemical analyses.” Some hydrocarbons, such as “biomarkers,” are able to withstand processes such as weathering, biodegradation, and evaporation. Petroleum biomarkers can be used by geologists, alongside other information, to assess the organic matter in the source rock and the environmental conditions during its deposition, as well as the thermal maturity and degree of biodegradation of the petroleum [5].

Common activities in typical research and development facilities include the study of fluid inclusions, organic petrography, surface geochemistry, geochemical characterization of oil and gases, reservoir geochemistry, and

forensic investigations. The latter extends its scope to tracking the origin of petroleum in oil spills and monitoring illegal activities (e.g., theft of crude oil and petroleum products).

In this context, the most important methods used in organic geochemistry for hydrocarbon analyses are GC-based, since these constituents play an important role in such investigations. For example, C₁–C₅ hydrocarbons and their isotope distribution are quantified in natural gases present in exploratory wells [26]. The C₅–C₁₅ hydrocarbon fraction, in turn, may be used to investigate reservoir connectivity. Careful optimization of chromatographic conditions is required to resolve the complex cluster of peaks for C₇ and C₈ isomers. The most important aspects of GC-based methods used in the aforementioned applications are the precision and accuracy of retention times and response factors, because an extensive and reliable database is required for comparative data processing [5].

Recent advances in GC instrumentation have created interesting opportunities for hydrocarbon analysis. For example, online pyrolysis (Py) can be coupled to GC to assist in the determination of thermal maturity. Moreover, pyrolysis induces thermal cracking of hydrocarbons into smaller molecules under an inert atmosphere, which can then be separated and identified by GC-MS [27]. This chromatographic data is also used as a fingerprint, since pyrolysis products are closely related to the original organic matter. Online pyrolysis coupled to GC may use flame ionization detection (Py-GC-FID) and/or MS (Py-GC-MS). For complex mixtures, pyrolysis may be coupled to GC × GC, to enhance the available chemical information. The chromatographic profile of a petroleum extract from the Green River Shale obtained by Py-GC-MS exhibits extensive peak overlap, which is identified by a pronounced baseline drift called unresolved complex mixture (UCM), as shown in Fig. 25.2A. Improved resolution may be achieved by Py-GC × GC-MS, wherein a group-type separation

of the UCM becomes evident (Fig. 25.2B), namely linear and branched alkanes, aromatic hydrocarbons, and the isoprenoid-based petroleum biomarkers [28].

Although 1D-GC has been successfully used for pattern recognition and sample classification in organic geochemistry, GC × GC can provide additional information about the sample composition. Such information may improve data processing by accurately determining hydrocarbon ratios and pattern matching [22]. For instance, GC × GC-FID was employed to characterize hydrocarbons soluble in *n*-pentane (i.e., maltenes) [29]. Multiway principal component analysis (MPCA) was applied for data processing of the chromatographic data to distinguish between oils, which otherwise seemed very similar [22].

The hydrocarbon chromatographic profile can assist in determining the source of organic matter. A bimodal *n*-alkane distribution is usually associated with terrigenous higher-plant waxes. Predominance of even carbon-number *n*-alkanes in the chromatogram is related to carbonate source rocks. Odd carbon-number *n*-alkanes predominance is indicative of oils derived from shale source rocks [5]. Some hydrocarbons are considered petroleum biomarkers, for example, pristane (2,6,10,14-tetramethylpentadecane), phytane (2,6,10,14-tetramethylhexadecane), diasteranes, steranes, and homohopanes [30,31]. New biomarkers that are even more resistant to degradation are being characterized, specially from unconventional oil sources [32]. Diamondoids have gained attention as geochemical indicators because of their resistance to thermal stress and microbial activities [33]. They have a prominent structural rigidity owing to their diamond-like 3D cage structure, which enhances their resistance to thermal and microbial degradation [32].

In geochemical assays, a preliminary liquid chromatography (LC) step may be used to fractionate the crude oil into saturates, aromatics, resins, and asphaltenes (i.e., SARA fractionation). For routine analysis, a semipreparative

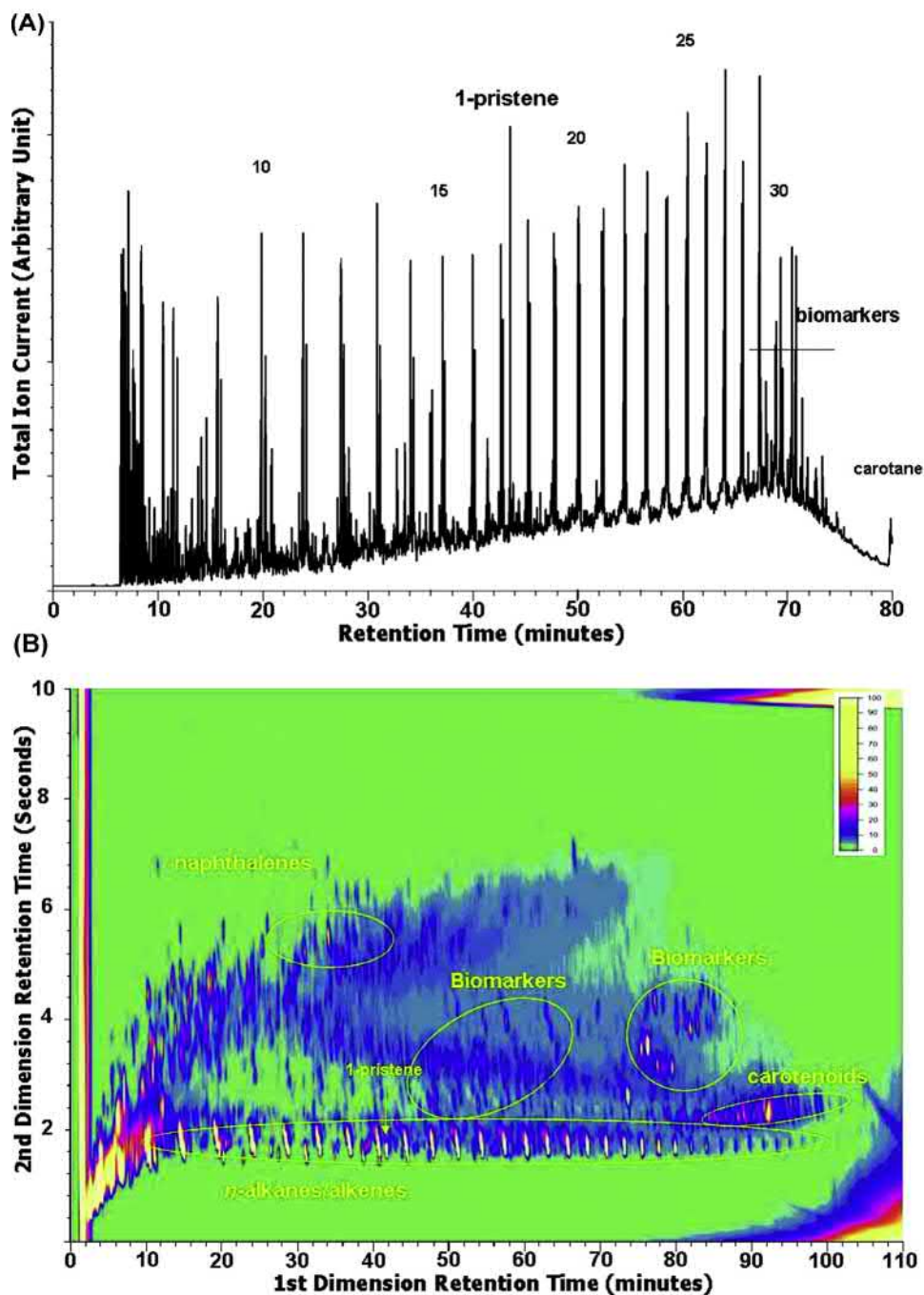


FIGURE 25.2 Improved resolution attained by MDGC. In (A) the 1D-GC total ion chromatogram of Green River Shale is shown. In (B), the chromatogram of the same sample using Py-GC×GC-FID. Reprinted from F.C.Y. Wang, C.C. Walters, *Anal. Chem.* 15 (2007) 5644. Copyright 2007, with permission from ACS Publications.

LC instrument fitted with a sample collector is typically used. However, this step may be bypassed if a high-peak capacity system (e.g., GC \times GC [32]) or if a highly selective detection system is used. Targeted analysis of diamondoids, saturate and aromatic petroleum biomarkers, and organosulfur compounds was performed by multiple reaction monitoring (MRM) using GC coupled to a triple quadrupole mass spectrometer (GC-MS/MS) [34].

Molecular stable isotopic analyses are typically performed using capillary GC (GC-IRMS). Postcolumn reactors for combustion and water removal are required to deliver a discrete pulse of the band to be analyzed by the isotope ratio mass spectrometer [35]. Typically, postcolumn peak broadening is minimized using a microfluidic valve for solvent diversion, a capillary combustion reactor, narrow-bore capillary transfer lines, and a cryogenic water trap [35]. High-precision isotope ratios such as carbon ($^{13}\text{C}/^{12}\text{C}$), sulfur ($^{34}\text{S}/^{32}\text{S}$), hydrogen ($^2\text{H}/^1\text{H}$) can be measured from small samples [36,37]. GC-IRMS data can be used to assess oil source and origin, as the compounds with common biological origin exhibit similar isotopic compositions.

A stable carbon isotope composition is preserved during diagenesis [5]. Low-molecular-weight aromatic compounds from petroleum fluids have not been widely studied for fluid-source correlations [38]. However, such aromatic compounds are important components in fluids, including condensates, which lack biomarkers. The results showed that fluvial-deltaic condensates with relatively high abundances of the *meta*-isomer of ethyltoluene are consistent with a mineral catalytic effect on the molecular distribution of such isomers, as it occurs during the clay-catalyzed synthesis of ethyltoluenes [38]. Continuous developments in the analyses of low-molecular-weight aromatic compounds are important to establish the evolution of the

organic matter to hydrocarbons in petroleum systems. Furthermore, GC-IRMS was used to determine compound-specific stable carbon isotope composition (CSIA) of crude oil samples from the Colombia region [39]. In this study, the composition and distribution of individual isoprenoids and *n*-alkanes were correlated to geochemical characteristics of crude oil and their depositional environment.

25.4 Refinery oil assays

The process in which crude oil is converted to useful products is known as the refinery of the oil. Such processes consist of a distillation step at atmospheric pressure, in which light distillates (such as light gases, kerosene, naphtha, and gas oil) are separated from heavier fractions. A second distillation under reduced pressure is used to produce flashed distillate and short residue, which are further processed in order to produce lighter products. Finally, to obtain the desired end products, a conversion process followed by another distillation are performed to either add hydrogen or remove carbon from the oil feeds, since products such as gasoline and diesel have a higher hydrogen-to-carbon ratio than the heavy oil fractions [10].

25.4.1 Simulated distillation (SimDist)

The boiling point range distribution of hydrocarbons is determined by simulated distillation (SimDist) using GC-based methods to evaluate petroleum for refining, providing information for optimization of the refinery processes [3]. Such GC analysis provides the most relevant information for vapor–liquid-related phase behavior [40]. Although boiling point range distribution can be accomplished by routine laboratory-scale distillation, such as atmospheric (ASTM D2892 and D86) and

vacuum distillation (ASTM D1160), such techniques suffer from poor reproducibility [1].

A SimDist method uses a GC column coated with a nonpolar phase, such as poly(dimethylsiloxane), wherein the retention of hydrocarbons is largely dominated by dispersive interactions. Hence, the hydrocarbon elution order is proportional to their boiling points. Such a retention mechanism allows the conversion of retention time into distillation temperatures. A calibration mixture with known boiling points (*e.g.*, a mixture of *n*-alkanes) is used for such conversions [40], enabling reliable petroleum analysis, as shown in Fig. 25.3.

The ASTM method D6352 for SimDist provides a boiling point distribution curve of petroleum fluids in the range of 174–700°C, which extends the range of a heavy oil characterization from 20% to 30% to 70%–85%. Such analyses only require a small sample amount compared to conventional distillation [40]. FID is employed in SimDist due to the constant

response factor toward hydrocarbons, which yields relative response factors close to 1. The evaluation of heteroatom-containing compounds may be performed by employing selective detectors, such as the atomic emission detector (AED), the nitrogen chemiluminescence detector (NCD), and the sulfur chemiluminescence detector (SCD) [41,42].

GC × GC can provide both the boiling point distribution and the composition of the distillation feedstock. The first attempt to employ GC × GC in SimDist analysis used a column combination consisting of a 10 m × 0.32 mm ($d_f = 0.1 \mu\text{m}$) nonpolar (poly(dimethylsiloxane)) ^1D column and a 1 m × 0.1 mm ($d_f = 0.1 \mu\text{m}$) mid-polar ^2D column [poly(diphenyldimethylsilyphenylenesiloxane) with 50% diphenylsiloxane monomer incorporation] [43]. The results were in accordance with ^1D -SimDist data and a complete group-type separation of saturates and aromatics was achieved, as well as a partial separation of aliphatic hydrocarbons [43,44].

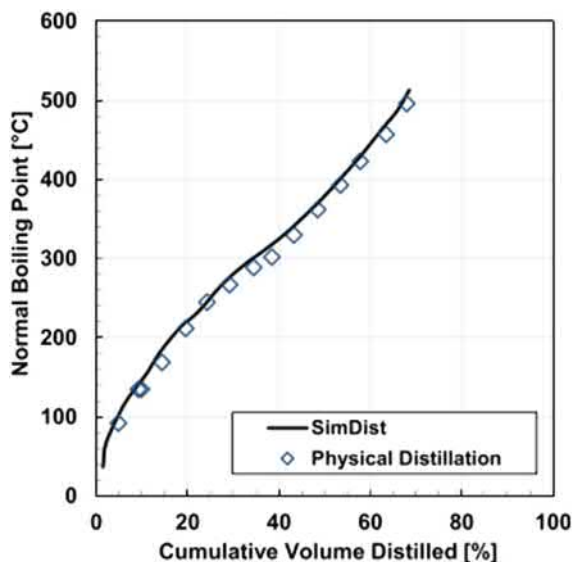


FIGURE 25.3 Comparison of conventional distillation and SimDist assays for an oil sample. Reprinted from O. Castellanos Diaz, H.W. Yarranton. *Energy & fuels*. 33 (2019) 6084. Copyright 2019, with permission from ACS Publications.

25.4.2 Analysis of light distillates (C_1 – C_9)

Light petroleum distillates consist of hydrocarbons from C_1 to C_9 with a boiling point range from -161°C to 150°C [6]. Natural gas (C_1 – C_4), light straight-run gasoline (C_4 – C_6), light (C_6 – C_7) and medium naphtha (C_7 – C_9) are the most important cuts of this fraction. Refinery analysis frequently focuses on the characterization of hydrocarbons and the monitoring of impurities such as S-, O-, and N-containing compounds [1,6].

GC assays for permanent gases typically use PLOT columns [45]. For example, 30 m × 0.32 mm id (20 μm particles) HP-PLOT Q (divinylbenzene-based phase) and 30 m × 0.32 mm id (10 μm particles) Rtx-Alumina BOND/MAPD (zeolite-based phase) columns, was used in parallel (in which a single injection is introduced into both columns) for the

separation of C_1 – C_3 hydrocarbons [46]. Similarly, the Rtx-Alumina BOND/MAPD column is used for the analysis of C_1 to C_5 in liquefied petroleum gas samples [47]. Furthermore, the use of a cryogenic trap for band focusing can also improve the performance of the GC instrument by increasing the signal-to-noise ratio of the peaks [48].

The standard methods of analysis for permanent gases, such as ASTM D1945 and D2163, use thermal conductivity detection (TCD), which is a concentration-sensitive detector with a wide linear range [49]. Alternatively, spectroscopic detection can be explored, such as IR or vacuum ultraviolet detection (VUV). The latter was successfully applied for the analysis of permanent gases [45]. The VUV detection module is able to detect C_1 – C_5 linear and branched hydrocarbons, water, oxygen, and nitrogen in gas samples.

Gasoline is the most important product of the light distillates and contains thousands of compounds. GC analysis is performed for quality assurance and to predict physicochemical properties. Typical GC assays for gasoline include its octane number, Reid vapor pressure, boiling point distribution, olefin content, and the concentration of aromatic hydrocarbons (i.e., benzene, toluene, and total aromatics) [50].

The composition of gasoline is far more complex than permanent gases. Thus, MDGC is often employed for a comprehensive analysis of gasoline. For instance, PIONA is a well-established method for determining paraffins, iso-paraffins, olefins, naphthenes, and aromatics in gasoline. PIONA data is a significant factor in determining the trade value for gasoline and to decide the nature and degree of additional treatment of the end product [51].

The PIONA method is described in ASTM D5443 and D6839 and uses an MDGC setup, as shown in Fig. 25.4. In the first step, the sample is directed through a polar OV-275 (dicyanoalkylsiloxane-based) column at 130°C , where aromatic hydrocarbons are retained, alongside binaphthenes and compounds with boiling points over 200°C . The unretained fraction is directed by a switching valve to a two-stage trapping system. The first stage consists of an olefin trap. The second stage is an n -alkane trap, where n -paraffins, iso-paraffins, and naphthenic hydrocarbons are adsorbed on a cartridge packed with molecular sieve (Molsieves) with a pore size of 5\AA . The unretained fraction is separated by gas–solid chromatography using a molecular sieve 13X-based column to resolve naphthenes and iso-paraffins based on molecular size and structure, followed

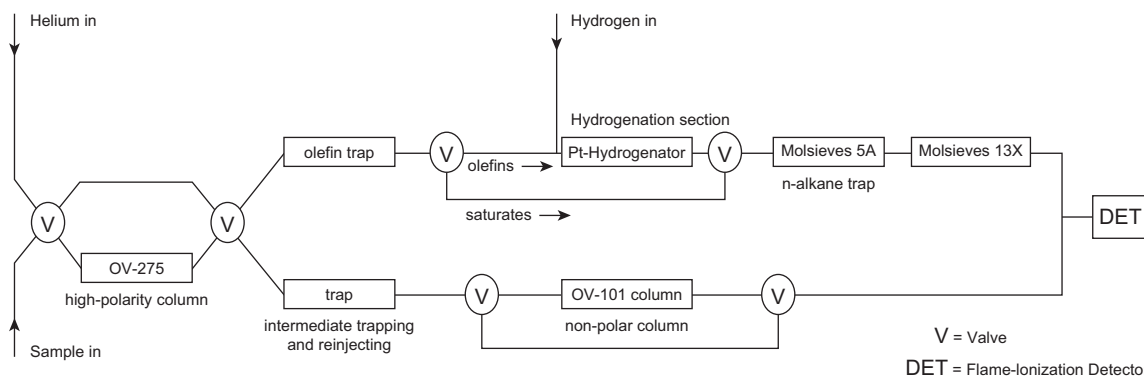


FIGURE 25.4 MDGC instrument configuration for PIONA analysis. This figure was published in J. Blomberg, P.J. Schoenmakers, U.A.Th. Brinkman, *Gas chromatographic methods for oil analysis*, *J. Chromatogr. A.* 972 (2002) 156. Copyright Elsevier (2002).

by FID detection. In the second step, analytes trapped in the *n*-alkane trap are thermally desorbed and also separated on the Molsieves 13X column. In the third step, olefins are desorbed from the olefin trap and pass through a platinum reactor, where they are hydrogenated and subsequently separated by the same gas–solid chromatographic processes described earlier. Lastly, aromatic hydrocarbons retained on the OV-275 column are eluted and refocused on a poly(2,6-diphenylphenylene oxide) (Tenax) cartridge. These compounds are thermally desorbed to a nonpolar poly(dimethylsiloxane) (OV-101) column, for separation at 130°C [5,52].

GC × GC provides a suitable alternative for the analysis of gasoline samples. Gasoline alkylation products and by-products formed after catalytic conversion of light sulfur compounds can be characterized by GC × GC-MS or GC × GC-FPD (FPD—flame photometric detector) [83]. The method enabled the detection of the various products derived from 3-methylthiophene for the first time. Also, GC × GC was evaluated for the prediction of the physicochemical properties of gasolines, such as distillation temperature range and density [53]. The results for both assays were in accordance with those obtained by standard methods.

Gasoline adulteration usually involves addition of organic solvents such as kerosene, diesel oil, ethanol, and other petrochemical distillates [54,55]. Due to the complexity of both gasoline and the adulterants, GC × GC was evaluated for this application. Data analysis involved chemometric methods such as multiway partial least squares (N-PLS) and parallel factor analysis (PARAFAC) to differentiate and quantify the adulterants in gasoline mixtures [54–56].

Selective detection is compulsory for element-specific information. GC-MS was used to characterize light distillates [57,58], assess adulteration in gasolines [59], and evaluate contamination by water or soil [60]. Target-compound analysis uses selective detectors, such as the FPD, nitrogen–phosphorous

(NPD), sulfur chemiluminescence (SCD), nitrogen chemiluminescence (NCD), and oxygen selective flame ionization (O-FID) detectors [10]. Noteworthy, the O-FID uses a two-stage postcolumn reaction module [61]. For example, the ASTM D5599 method mandates the use of an O-FID to determine oxygenated compounds, such as methyl *tert*-butyl ether (MTBE) and *tert*-amyl methyl ether (TAME), which are added to motor gasolines to increase their octane number [10,62].

25.4.3 Analysis of middle distillates (C₉–C₂₀)

Petroleum middle distillates contain C₉–C₂₀ hydrocarbons with a boiling point range from 150 to 370°C [4]. Important petroleum products are heavy naphtha (C₉–C₁₁); light (C₁₁–C₁₃) and heavy (C₁₃–C₁₅) kerosene; and atmospheric gas oil (C₁₅–C₂₀), which is used as feedstock for diesel fuel production [4,5].

Untargeted (group-type) analysis is frequently employed for the analysis of middle distillates instead of targeted analysis (i.e., individual analytes) [63]. An example of a group-type analysis is ASTM method D2425, which determines 11 classes of hydrocarbons by GC-MS. This method requires sample fractionation into saturates and aromatic fractions, according to the ASTM method D2549, prior to GC-MS analysis.

A comparative study of GC × GC and ASTM methods D2549 and D2425 demonstrated that the latter is a suitable alternative to the official methods [64]. Two column configurations were compared: nonpolar × polar and polar × nonpolar. The first comprised a 10 m × 0.2 mm-id ($d_f = 0.5 \mu\text{m}$) PONA (polydimethylsiloxane) primary column and a 0.8 m × 0.1 mm-id ($d_f = 0.1 \mu\text{m}$) BPX50 [poly(diphenylsilphenylene-siloxane) containing 50% diphenylsiloxane monomer] secondary column. The second column set was 10 m × 0.25 mm-id ($d_f = 0.25 \mu\text{m}$) BPX50 primary column and a 0.8 m × 0.1 mm-id

($d_f = 0.1 \mu\text{m}$) DB1 [poly(dimethylsiloxane)] secondary column. The nonpolar \times polar combination afforded the best resolution of the aromatic hydrocarbons, while the polar \times nonpolar combination was recommended for the separation of aliphatic hydrocarbons [64].

In addition, heteroatom-specific detection, for S- and N-containing compounds, is used for quality control of additives in refineries to improve fuel quality [1]. Quantitation of sulfur-containing compounds in fuels (e.g., kerosene, jet fuel, and diesel) is essential because of vehicle corrosion-related issues and the emission of SO_2/SO_3 during combustion [8].

Nitrogen-containing compounds are naturally occurring in fuels, but they are also added as additives to prevent oxidation/corrosion and as dispersants [3]. However, N-containing compounds negatively affect hydrodesulfurization processes for middle distillates [2]. Nitrogen-containing compounds can be selectively detected by NCD or NPD. For instance, the characterization of diesel samples by GC-NPD revealed that more than 90% of the nitrogen-containing compounds were neutral compounds (indoles and carbazoles), while in kerosene samples neutral compounds accounted for about 65% [65]. These results were corroborated by ASTM methods D4629 and D5762. This study showed that GC-NPD is an excellent tool for the monitoring and quantification of nitrogen-containing compounds in middle distillates, allowing for the development of a kinetic model of the hydrotreating process.

In addition, GC \times GC-NCD was successfully used to quantify N-containing compounds such as anilines, indoles, carbazoles, pyridines, quinolines, and acridines in middle distillates [66]. Solid-phase extraction (SPE) was used for sample fractionation. Sequential elution with dichloromethane and acetone separated the pairs pyridines/anilines, quinolines/indoles, and acridines/carbazoles, in accordance with ASTM method D4629.

25.4.4 Analysis of heavy distillates (C_{20+})

Heavy petroleum distillates consist of C_{20+} hydrocarbons with boiling points above 350°C [1]. Distillations cuts include vacuum gas oil (VGO) and atmospheric and vacuum residues [6]. The continuous demand for fuels created interest in the use of this fraction for diesel production using hydrocracking, hydrotreatment, fluid catalytic cracking, and retarded coking [44,67]. Such processes occur in two steps. First, the heteroatom-containing compounds are removed and the polyaromatic compounds are hydrogenated. In the second step, the naphthenic rings are selectively opened in order to improve the cetane number of the final product [68,82]. Compositional analysis of heavy distillates is necessary to evaluate its quality and processability [69]. Also, the occurrence of nitrogen- and sulfur-compounds determines the removal process to prevent catalyst poisoning [70].

Analysis of heavy distillates by GC is a twofold challenge. First, analyte discrimination is observed during sample preparation and introduction. Heavy hydrocarbons (C_{35+}) are not completely soluble or precipitate partially in CS_2 and *n*-hexane at room temperature, a problem with liquid injection systems. Also, isothermal vaporization-based injectors, such as split/splitless (SSL) injection, discriminate C_{20+} hydrocarbons [7]. Cold on-column injectors can provide reliable characterization for liquid injections [7]. Furthermore, multimode injection systems, such as the OPTIC-4, provide experimental flexibility by enabling PTV features, alongside thermal desorption capabilities. Such options are ideal for the analysis of heavy distillates, since slurries may be directly desorbed into the GC inlet.

Second, highly selective SPs are needed to resolve these complex samples. SPs with strong dipole-type interactions, such as poly(cyanopropylphenyldimethylsiloxane) and poly(ethylene-glycol), typically exhibit limited MAOT values

(ca. 250 to 260°C) [7]. However, a modified PEG phase with an MAOT value of 300°C (MEGA-WAX HT) recently became available as well as the DB-HeavyWAX column with an MAOT in the range of 280–290°C. The former has been used to separate heavy hydrocarbons in petroleum samples [71,72].

Recent research in column technology has aimed at the production of highly selective and thermally stable phases for GC and GC × GC. The MAOT value of a column is influenced by phase deterioration, which may be monitored by the column bleed and phase pooling at high temperatures resulting in peak broadening and tailing [73]. Highly cross-linked ionic liquid-based phases with MAOT values of 350°C were reported [74]. Such SPs can be structurally tuned to exhibit unique separation properties, such as high selectivity toward aromatic hydrocarbons [75]. Commercial columns that can operate at high temperatures are Phenomenex's Inferno columns with MAOT values up to 430°C and MEGA's low bleed columns with MAOT values of 400°C.

Alternative processes for the analysis of heavy distillates employ column back-flushing. The latter uses two GC columns, namely a guard column (or precolumn) and the separation column. The two columns are connected via a low-dead volume three-port connector. The third port is connected to an auxiliary gas supply from the GC instrument. This setup enables back-flushing of heavier matrix components from the first column after elution of the analytes. However, this approach is not applicable if the analytes are the latter eluting peaks.

Careful method development can decrease the elution temperature of analytes [43]. Short WCOT columns with high β values decreased analyte retention. The elution temperature of a series of *n*-alkanes was reduced by 30°C by increasing the β value from 100 to 800 [43]. Additionally, the same effect can be attained by using short capillary columns with a small internal diameter. This column configuration decreases

the impact of band broadening at high linear carrier gas velocities, Fig. 25.5 [7,76]. Noteworthy, a delicate balance between peak capacity and average column retention must be maintained during column selection to avoid peak overlap. The viscosity of the carrier gas also influences retention. Hydrogen carrier gas significantly lowers the elution temperature compared to helium [76].

Separations with a higher peak capacity are possible by GC × GC for heavy hydrocarbon separations. Hydrocarbons up to C₆₀ in VGO were obtained by cryogenic modulation and a nonpolar × mid-polar column set, consisting of a 10 m × 0.32 mm ($d_f = 0.1 \mu\text{m}$) ¹D column and a 1 m × 0.1 mm ($d_f = 0.1 \mu\text{m}$) ²D column [67]. GC×GC-NCD was used for group-type quantification of N-containing compounds by carbon

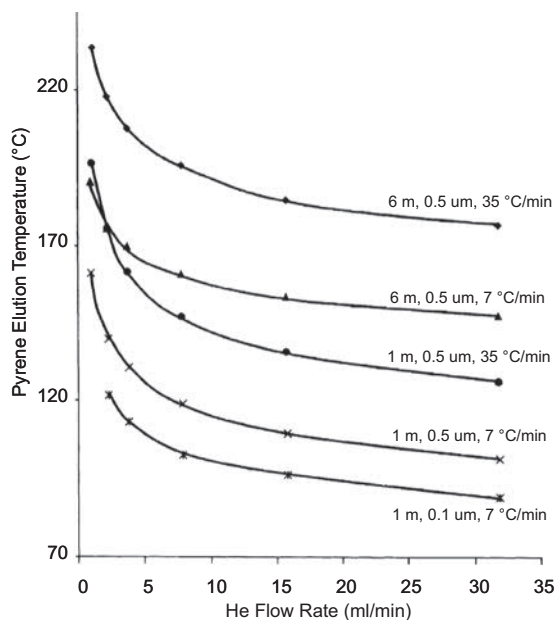


FIGURE 25.5 Impact of column length, internal diameter, film thickness, volumetric flow rate of carrier gas, and temperature programming in pyrene elution. This figure was published in A.B. Fialkov, A. Gordin, A. Amirav, *Extending the range of compounds amenable for gas chromatography—mass spectrometric analysis*, *J. Chromatogr. A*, 991 (2013) 221. Copyright Elsevier (2013).

number [77]. Furthermore, GC \times GC was used to determine the composition of both vapor and liquid samples of a feedstock conversion system using cryogenic modulation and a mid-polar \times nonpolar column setup [82].

Although cryogenic modulation is the most popular form of thermal modulation, it is difficult to optimize the separation conditions for samples of a wide volatility range in a single run, resulting in poor modulation of compounds at the extremes of the modulation interval [81]. In this context, consumable-free interfaces are attractive for cost-effective and flexible GC \times GC separations. Recent examples include the ZX-2 cooled two-stage loop interface and the solid-state modulator (SSM). The SSM was used for a group-type separation of bitumen [82], exhibiting a modulation range of C₈–C₄₀ [82]. Accordingly, FM is also a consumable-free interface for GC \times GC. RFF modulation was used in the analysis of VGO with efficient modulation up to C₄₀ [20]. The operational limits of FM-GC \times GC were improved by the FFF configuration, wherein successful modulation of hydrocarbons up to C₈₀ was reported [83].

References

- [1] F. Bertoncini, M. Courtiade-Tholance, D. Thiébaud, *Gas Chromatography and 2D-Gas Chromatography for Petroleum Industry*, Editions Technip, Paris, 2013.
- [2] J.G. Speight, *The Chemistry and Technology of Petroleum*, Taylor & Francis Group, New York, 2014.
- [3] J.G. Speight, *Handbook of Petroleum Product Analysis*, John Wiley & Sons, Inc., Hoboken, 2015.
- [4] J. Beens, U.A.Th. Brinkman, The role of gas chromatography in compositional analyses in the petroleum industry, *Trends Anal. Chem.* 19 (2000) 260–275, [https://doi.org/10.1016/S0165-9936\(99\)00205-8](https://doi.org/10.1016/S0165-9936(99)00205-8).
- [5] K.E. Peters, C.C. Walters, J.M. Moldowan, *The Biomarker Guide. Biomarkers and Isotopes in the Environment and Human History*, Cambridge University Press, New York, 2005.
- [6] B.J. Pollo, G.L. Alexandrino, F. Augusto, L.W. Hantao, The impact of comprehensive two-dimensional gas chromatography on oil & gas analysis: recent advances and applications in petroleum industry, *TrAC Trends Anal. Chem.* 105 (2018) 202–217, <https://doi.org/10.1016/j.trac.2018.05.007>.
- [7] R.L. Grob, E.F. Barry, in: *Modern Practice of Gas Chromatography*, John Wiley & Sons, Inc., New York, 2004.
- [8] L. Mondello, A.C. Lewis, K.D. Bartle, *Multidimensional Chromatography*, John Wiley & Sons, Ltd., West Sussex, 2002.
- [9] J.V. Seeley, S.K. Seeley, Multidimensional gas chromatography: fundamental advances and new applications, *Anal. Chem.* 85 (2013) 557–578, <https://doi.org/10.1021/ac303195u>.
- [10] J. Blomberg, P.J. Schoenmakers, U.A.Th. Brinkman, Gas chromatographic methods for oil analysis, *J. Chromatogr. A* 972 (2002) 137–173, [https://doi.org/10.1016/S0021-9673\(02\)00995-0](https://doi.org/10.1016/S0021-9673(02)00995-0).
- [11] M.C. Simmons, L.R. Snyder, Two-stage gas-liquid chromatography, *Anal. Chem.* 30 (1958) 32–35, <https://doi.org/10.1021/ac60133a007>.
- [12] P.Q. Tranchida, D. Sciarone, P. Dugo, L. Mondello, Heart-cutting multidimensional gas chromatography: a review of recent evolution, applications, and future prospects, *Anal. Chim. Acta* 716 (2012) 66–75, <https://doi.org/10.1016/j.aca.2011.12.015>.
- [13] D.R. Deans, Use of heart cutting in gas chromatography: a review, *J. Chromatogr. A* 203 (1981) 19–28, [https://doi.org/10.1016/S0021-9673\(00\)80278-2](https://doi.org/10.1016/S0021-9673(00)80278-2).
- [14] D.R. Deans, A new technique for heart cutting in gas chromatography [1], *Chromatographia* 1 (1968) 18–22, <https://doi.org/10.1007/BF02259005>.
- [15] Z. Liu, J.B. Phillips, Comprehensive two-dimensional gas chromatography using an on-column thermal modulator interface, *J. Chromatogr. Sci.* 29 (1991) 227–231, <https://doi.org/10.1093/chromsci/29.6.227>.
- [16] W. Khummueng, J. Harynuk, P.J. Marriott, Modulation ratio in comprehensive two-dimensional gas chromatography, *Anal. Chem.* 78 (2006) 4578–4587, <https://doi.org/10.1021/ac052270b>.
- [17] J.V. Seeley, Recent advances in flow-controlled multidimensional gas chromatography, *J. Chromatogr. A* 1255 (2012) 24–37, <https://doi.org/10.1016/j.chroma.2012.01.027>.
- [18] C. Cordero, P. Rubiolo, S.E. Reichenbach, A. Carretta, L. Cobelli, M. Giardina, C. Bicchi, Method translation and full metadata transfer from thermal to differential flow modulated comprehensive two dimensional gas chromatography: profiling of suspected fragrance allergens, *J. Chromatogr. A* 1480 (2017) 70–82, <https://doi.org/10.1016/j.chroma.2016.12.011>.
- [19] J.V. Seeley, N.J. Micyus, S.V. Bandurski, S.K. Seeley, J.D. McCurry, Microfluidic deans switch for

- comprehensive two-dimensional gas chromatography, *Anal. Chem.* 79 (2007) 1840–1847, <https://doi.org/10.1021/ac061881g>.
- [20] C. Duhamel, P. Cardinael, V. Peulon-Agasse, R. Firor, L. Pascaud, G. Semard-Jousset, P. Giusti, V. Livadaris, Comparison of cryogenic and differential flow (forward and reverse fill/flush) modulators and applications to the analysis of heavy petroleum cuts by high-temperature comprehensive gas chromatography, *J. Chromatogr. A* 1387 (2015) 95–103, <https://doi.org/10.1016/j.chroma.2015.01.095>.
- [21] J. de Zeeuw, J. Luong, Developments in stationary phase technology for gas chromatography, *TrAC Trends Anal. Chem.* 21 (2002) 594–607, [https://doi.org/10.1016/S0165-9936\(02\)00809-9](https://doi.org/10.1016/S0165-9936(02)00809-9).
- [22] J.C. Giddings, *Unified Separation Science*, John Wiley & Sons, Inc., New York, 1991.
- [23] J. Crucello, D.V. Pierone, L.W. Hantao, Simple and cost-effective determination of polychlorinated biphenyls in insulating oils using an ionic liquid-based stationary phase and flow modulated comprehensive two-dimensional gas chromatography with electron capture detection, *J. Chromatogr. A* 1610 (2019) 460530, <https://doi.org/10.1016/j.chroma.2019.460530>.
- [24] L.W. Hantao, A. Najafi, C. Zhang, F. Augusto, J.L. Anderson, Tuning the selectivity of ionic liquid stationary phases for enhanced separation of nonpolar analytes in kerosene using multidimensional gas chromatography, *Anal. Chem.* 86 (2014) 3717–3721, <https://doi.org/10.1021/ac5004129>.
- [25] T.D. Ho, C. Zhang, L.W. Hantao, J.L. Anderson, Ionic liquids in analytical chemistry: fundamentals, advances, and perspectives, *Anal. Chem.* 86 (2014) 262–285, <https://doi.org/10.1021/ac4035554>.
- [26] F. Hao, H. Zou, Cause of shale gas geochemical anomalies and mechanisms for gas enrichment and depletion in high-maturity shales, *Mar. Petrol. Geol.* 44 (2013) 1–12, <https://doi.org/10.1016/j.marpetgeo.2013.03.005>.
- [27] D.M. White, D.S. Garland, L. Beyer, K. Yoshikawa, Pyrolysis-GC/MS fingerprinting of environmental samples, *J. Anal. Appl. Pyrolysis* 71 (2004) 107–118, [https://doi.org/10.1016/S0165-2370\(03\)00101-3](https://doi.org/10.1016/S0165-2370(03)00101-3).
- [28] F.C.Y. Wang, C.C. Walters, Pyrolysis comprehensive two-dimensional gas chromatography study of petroleum source rock, *Anal. Chem.* 79 (2007) 5642–5650, <https://doi.org/10.1021/ac070166j>.
- [29] G.T. Ventura, G.J. Hall, R.K. Nelson, G.S. Frysinger, B. Raghuraman, A.E. Pomerantz, O.C. Mullins, C.M. Reddy, Analysis of petroleum compositional similarity using multiway principal components analysis (MPCA) with comprehensive two-dimensional gas chromatographic data, *J. Chromatogr. A* 1218 (2011) 2584–2592, <https://doi.org/10.1016/j.chroma.2011.03.004>.
- [30] C.R. Oliveira, A.A. Ferreira, C.J.F. Oliveira, D.A. Azevedo, E.V. Santos Neto, F.R. Aquino Neto, Biomarkers in crude oil revealed by comprehensive two-dimensional gas chromatography time-of-flight mass spectrometry: depositional paleoenvironment proxies, *Org. Geochem.* 46 (2012) 154–164, <https://doi.org/10.1016/j.orggeochem.2012.03.002>.
- [31] A. Casilli, R.C. Silva, J. Laakia, C.J.F. Oliveira, A.A. Ferreira, M.R.B. Loureiro, D.A. Azevedo, F.R. Aquino Neto, High resolution molecular organic geochemistry assessment of Brazilian lacustrine crude oils, *Org. Geochem.* 68 (2014) 61–70, <https://doi.org/10.1016/j.orggeochem.2014.01.009>.
- [32] R.C. Silva, R.S.F. Silva, E.V.R. De Castro, K.E. Peters, D.A. Azevedo, Extended diamondoid assessment in crude oil using comprehensive two-dimensional gas chromatography coupled to time-of-flight mass spectrometry, *Fuel* 112 (2013) 125–133, <https://doi.org/10.1016/j.fuel.2013.05.027>.
- [33] Z. Zhang, Y. Zhang, G. Zhu, J. Han, L. Chi, Variations of diamondoids distributions in petroleum fluids during migration induced phase fractionation: a case study from the Tazhong area, NW China, *J. Petrol. Sci. Eng.* 179 (2019) 1012–1022, <https://doi.org/10.1016/j.petrol.2019.05.016>.
- [34] M. Mei, K.K.A. Bissada, T.B. Malloy, L.M. Darnell, E.B. Szymczyk, Improved method for simultaneous determination of saturated and aromatic biomarkers, organosulfur compounds and diamondoids in crude oils by GC–MS/MS, *Org. Geochem.* 116 (2018) 35–50, <https://doi.org/10.1016/j.orggeochem.2017.09.010>.
- [35] A.A. Baczynski, P.J. Polissar, D. Juchelka, J. Schwieters, A. Hilkert, R.E. Summons, K.H. Freeman, Picomolar-scale compound-specific isotope analyses, *Rapid Commun. Mass Spectrom.* 32 (2018) 730–738, <https://doi.org/10.1002/rcm.8084>.
- [36] K. Grice, C. Eiserbeck, The analysis and application of biomarkers, in: *Treatise on Geochemistry*, 12, Elsevier Ltd., Amsterdam, 2014, pp. 47–78.
- [37] A. Amrani, A. Deev, A.L. Sessions, Y. Tang, J.F. Adkins, R.J. Hill, M.J. Moldowan, Z. Wei, The sulfur-isotopic compositions of benzothiophenes and dibenzothiophenes as a proxy for thermochemical sulfate reduction, *Geochem. Cosmochim. Acta* 84 (2012) 152–164, <https://doi.org/10.1016/j.gca.2012.01.023>.
- [38] J. Cesar, J. Eiler, B. Dallas, L. Chimiak, K. Grice, Isotope heterogeneity in ethyltoluenes from Australian condensates, and their stable carbon site-specific isotope analysis, *Org. Geochem.* 135 (2019) 32–37, <https://doi.org/10.1016/j.orggeochem.2019.06.002>.
- [39] J.E. Cortes, J.M. Rincon, J.M. Jaramillo, R.P. Philp, J. Allen, Biomarkers and compound-specific stable carbon isotope of n-alkanes in crude oils from Eastern Llanos Basin, Colombia, *J. South Am. Earth Sci.* 29 (2010) 198–213, <https://doi.org/10.1016/j.jsames.2009.03.010>.

- [40] O.C. Diaz, H.W. Yarranton, Applicability of simulated distillation for heavy oils, *Energy Fuels* 33 (2019) 6083–6087, <https://doi.org/10.1021/acs.energyfuels.9b00724>.
- [41] D.D. Link, P. Zandhuis, The distribution of sulfur compounds in hydrotreated jet fuels: Implications for obtaining low-sulfur petroleum fractions, *Fuel* 85 (2006) 451–455, <https://doi.org/10.1016/j.fuel.2005.08.029>.
- [42] R. Chakravarthy, G.N. Naik, A. Savalia, J. Kedia, C. Saravanan, A.K. Das, U. Sreedharan, K.B. Gudasi, Simultaneous determination of boiling range distribution of hydrocarbon, sulfur, and nitrogen in petroleum crude oil by gas chromatography with flame ionization and chemiluminescence detections, *Energy Fuels* 31 (2017) 3101–3110, <https://doi.org/10.1021/acs.energyfuels.6b03306>.
- [43] T. Dutriez, M. Courtiade, D. Thiébaud, H. Dulot, F. Bertoncini, J. Vial, M.C. Hennion, High-temperature two-dimensional gas chromatography of hydrocarbons up to nC60 for analysis of vacuum gas oils, *J. Chromatogr. A* 1216 (2009) 2905–2912, <https://doi.org/10.1016/j.chroma.2008.11.065>.
- [44] L. Boursier, V. Souchon, C. Dartiguelongue, J. Ponthus, M. Courtiade, D. Thiébaud, Complete elution of vacuum gas oil resins by comprehensive high-temperature two-dimensional gas chromatography, *J. Chromatogr. A* 1280 (2013) 98–103, <https://doi.org/10.1016/j.chroma.2012.12.059>.
- [45] L. Bai, J. Smuts, P. Walsh, H. Fan, Z. Hildenbrand, D. Wong, D. Wetz, K.A. Schug, Permanent gas analysis using gas chromatography with vacuum ultraviolet detection, *J. Chromatogr. A* 1388 (2015) 244–250, <https://doi.org/10.1016/j.chroma.2015.02.007>.
- [46] J. Luong, R. Gras, R.A. Shellie, H.J. Cortes, Applications of planar microfluidic devices and gas chromatography for complex problem solving, *J. Separ. Sci.* 36 (2013) 182–191, <https://doi.org/10.1002/jssc.201200789>.
- [47] S. Al-Zuhair, A. Khalil, M. Hassan, A. Abdulrazak, K. Basel, A. Fardoun, Performance evaluation of LPG desulfurization by adsorption for hydrogen production, *J. Energy Chem.* 24 (2015) 477–484, <https://doi.org/10.1016/j.jechem.2015.06.001>.
- [48] J.L. Burger, T.M. Lovestead, T.J. Bruno, Composition of the C6+ fraction of natural gas by multiple porous layer open tubular capillaries maintained at low temperatures, *Energy Fuels* 30 (2016) 2119–2126, <https://doi.org/10.1021/acs.energyfuels.6b00043>.
- [49] C.F. Poole, in: *Gas Chromatography*, Elsevier, Boston, 2013.
- [50] K. Altget, T. Gouw, *Chromatography in Petroleum Analysis*, Dekker, New York, 1979.
- [51] X. Zhu, L. Zhang, X. Che, L. Wang, The classification of hydrocarbons with factor analysis and the PONA analysis of gasoline, *Chemometr. Intell. Lab. Syst.* 45 (1999) 147–155, [https://doi.org/10.1016/S0169-7439\(98\)00098-7](https://doi.org/10.1016/S0169-7439(98)00098-7).
- [52] S.H. Ng, N.E. Heshka, C. Lay, E. Little, Y. Zheng, Q. Wei, F. Ding, FCC coprocessing oil sands heavy gas oil and canola oil. 2. Gasoline hydrocarbon type analysis, *Green Energy Environ.* 3 (2018) 286–301, <https://doi.org/10.1016/j.gee.2018.03.002>.
- [53] L.A.F. de Godoy, M.P. Pedroso, E.C. Ferreira, F. Augusto, R.J. Poppi, Prediction of the physicochemical properties of gasoline by comprehensive two-dimensional gas chromatography and multivariate data processing, *J. Chromatogr. A* 1218 (2011) 1663–1667, <https://doi.org/10.1016/j.chroma.2011.01.056>.
- [54] H. Parastar, S. Mostafapour, G. Azimi, Quality assessment of gasoline using comprehensive two-dimensional gas chromatography combined with unfolded partial least squares: a reliable approach for the detection of gasoline adulteration, *J. Separ. Sci.* 39 (2016) 367–374, <https://doi.org/10.1002/jssc.201500720>.
- [55] L.A.F. De Godoy, E.C. Ferreira, M.P. Pedroso, C.H.D.V. Fidélis, F. Augusto, R.J. Poppi, Quantification of kerosene in gasoline by comprehensive two-dimensional gas chromatography and N-way multivariate analysis, *Anal. Lett.* 41 (2008) 1603–1614, <https://doi.org/10.1080/00032710802122222>.
- [56] M.P. Pedroso, L.A.F. de Godoy, E.C. Ferreira, R.J. Poppi, F. Augusto, Identification of gasoline adulteration using comprehensive two-dimensional gas chromatography combined to multivariate data processing, *J. Chromatogr. A* 1201 (2008) 176–182, <https://doi.org/10.1016/j.chroma.2008.05.092>.
- [57] T. Veriotti, R. Sacks, High-speed GC/MS of gasoline-range hydrocarbon compounds using a pressure-tunable column ensemble and time-of-flight detection, *Anal. Chem.* 72 (2000) 3063–3069, <https://doi.org/10.1021/ac000081h>.
- [58] D.T. Quach, N.A. Ciszkowski, B.J. Finlayson-Pitts, A new GC-MS experiment for the undergraduate instrumental analysis laboratory in environmental chemistry: methyl-T-butyl ether and benzene in gasoline, *J. Chem. Educ.* 75 (1998) 1595–1598, <https://doi.org/10.1021/ed075p1595>.
- [59] L.S. Moreira, L.A. D'Avila, D.A. Azevedo, Automotive gasoline quality analysis by gas chromatography: study of adulteration, *Chromatographia* 58 (2003) 501–505, <https://doi.org/10.1365/s10337-003-0065-z>.
- [60] L. Zwank, T.C. Schmidt, S.B. Haderlein, M. Berg, Simultaneous determination of fuel oxygenates and

- BTEX using direct aqueous injection gas chromatography mass spectrometry (DAI-GC/MS), *Environ. Sci. Technol.* 36 (2002) 2054–2059, <https://doi.org/10.1021/es010270x>.
- [61] G.R. Verga, A. Sironi, W. Schneider, J.C. Frohne, Selective determination of oxygenates in complex samples with the O-FID analyzer, *J. High Resolut. Chromatogr.* 11 (1988) 248–252, <https://doi.org/10.1002/jhrc.1240110306>.
- [62] D.M. Lee, D.H. Lee, I.H. Hwang, Gasoline quality assessment using fast gas chromatography and partial least-squares regression for the detection of adulterated gasoline, *Energy Fuels* 32 (2018) 10556–10562, <https://doi.org/10.1021/acs.energyfuels.8b02368>.
- [63] M. Adahchour, J. Beens, R.J.J. Vreuls, U.A.Th. Brinkman, Recent developments in comprehensive two-dimensional gas chromatography (GC × GC). III. Applications for petrochemicals and organohalogens, *TrAC Trends Anal. Chem.* 25 (2006) 726–741, <https://doi.org/10.1016/j.trac.2006.03.005>.
- [64] C. Vendeuvre, R. Ruiz-Guerrero, F. Bertoncini, L. Duval, D. Thiébaud, M.C. Hennion, Characterisation of middle-distillates by comprehensive two-dimensional gas chromatography (GC × GC): a powerful alternative for performing various standard analysis of middle-distillates, *J. Chromatogr. A* 1086 (2005) 21–28, <https://doi.org/10.1016/j.chroma.2005.05.106>.
- [65] D. Singh, A. Chopra, M.B. Patel, A.S. Sarpal, A comparative evaluation of nitrogen compounds in petroleum distillates, *Chromatographia* 74 (2011) 121–126, <https://doi.org/10.1007/s10337-011-2027-1>.
- [66] K. Lissitsyna, S. Huertas, L.C. Quintero, L.M. Polo, Novel simple method for quantitation of nitrogen compounds in middle distillates using solid phase extraction and comprehensive two-dimensional gas chromatography, *Fuel* 104 (2013) 752–757, <https://doi.org/10.1016/j.fuel.2012.08.054>.
- [67] T. Dutriez, M. Courtiade, D. Thiébaud, H. Dulot, M.C. Hennion, Improved hydrocarbons analysis of heavy petroleum fractions by high temperature comprehensive two-dimensional gas chromatography, *Fuel* 89 (2010) 2338–2345, <https://doi.org/10.1016/j.fuel.2009.11.041>.
- [68] U. Nylén, J.F. Delgado, S. Järås, M. Boutonnet, Characterization of alkylated aromatic sulphur compounds in light cycle oil from hydrotreated vacuum gas oil using GC-SCD, *Fuel Process. Technol.* 86 (2004) 223–234, <https://doi.org/10.1016/j.fuproc.2004.03.001>.
- [69] B.N. Barman, Hydrocarbon type analysis by thin-layer chromatography with flame-ionization detection: vacuum gas oils, heavy feeds, and hydroprocessed products, *J. Separ. Sci.* 27 (2004) 311–315, <https://doi.org/10.1002/jssc.200201479>.
- [70] P. Wiwel, B. Hinnemann, A. Hidalgo-Vivas, P. Zeuthen, B.O. Petersen, J.O. Duus, Characterization and identification of the most refractory nitrogen compounds in hydroprocessed vacuum gas oil, *Ind. Eng. Chem. Res.* 49 (2010) 3184–3193, <https://doi.org/10.1021/ie901473x>.
- [71] K.M. Higa, A. Guilhen, L.C.S. Vieira, R.M. Carvalho, R.J. Poppi, M. Baptista, A.L. Gobbi, R.S. Lima, L.W. Hantao, Simple solid-phase extraction method for high efficiency and low-cost crude oil demulsification, *Energy Fuels* 30 (2016) 4667–4675, <https://doi.org/10.1021/acs.energyfuels.6b00553>.
- [72] É.M. Kataoka, R.C. Murer, J.M. Santos, R.M. Carvalho, M.N. Eberlin, F. Augusto, R.J. Poppi, A.L. Gobbi, L.W. Hantao, Simple, expendable, 3D-printed microfluidic systems for sample preparation of petroleum, *Anal. Chem.* 89 (2017) 3460–3467, <https://doi.org/10.1021/acs.analchem.6b04413>.
- [73] C. Yao, J.L. Anderson, Retention characteristics of organic compounds on molten salt and ionic liquid-based gas chromatography stationary phases, *J. Chromatogr. A* 1216 (2009) 1658–1712, <https://doi.org/10.1016/j.chroma.2008.12.001>.
- [74] J.L. Anderson, D.W. Armstrong, Immobilized ionic liquids as high-selectivity/high-temperature/high-stability gas chromatography stationary phases, *Anal. Chem.* 77 (2005) 6453–6462, <https://doi.org/10.1021/ac051006f>.
- [75] G.A. Odugbesi, H. Nan, M. Soltani, J.H. Davis, J.L. Anderson, Ultra-high thermal stability perarylated ionic liquids as gas chromatographic stationary phases for the selective separation of polyaromatic hydrocarbons and polychlorinated biphenyls, *J. Chromatogr. A* 1604 (2019) 460466, <https://doi.org/10.1016/j.chroma.2019.460466>.
- [76] A.B. Fialkov, A. Gordin, A. Amirav, Extending the range of compounds amenable for gas chromatography-mass spectrometric analysis, *J. Chromatogr. A* 991 (2003) 217–240, [https://doi.org/10.1016/S0021-9673\(03\)00247-4](https://doi.org/10.1016/S0021-9673(03)00247-4).
- [77] T. Dutriez, J. Borrás, M. Courtiade, D. Thiébaud, H. Dulot, F. Bertoncini, M.C. Hennion, Challenge in the speciation of nitrogen-containing compounds in heavy petroleum fractions by high temperature comprehensive two-dimensional gas chromatography, *J. Chromatogr. A* 1218 (2011) 3190–3199, <https://doi.org/10.1016/j.chroma.2010.10.056>.
- [78] R.B. Gaines, G.S. Frysinger, Temperature requirements for thermal modulation in comprehensive two-dimensional gas chromatography, *J. Separ. Sci.* 27 (2004) 380–388, <https://doi.org/10.1002/jssc.200301651>.

- [79] H. Boswell, K.T. Carrillo, T. Górecki, Evaluation of the performance of cryogen-free thermal modulation-based comprehensive two-dimensional gas chromatography-time-of-flight mass spectrometry (GC×GC-TOFMS) for the qualitative analysis of a complex bitumen sample, *Separations* 7 (2020) 1–12, <https://doi.org/10.3390/separations7010013>.
- [80] R.A. Shellie, H.J. Cortes, R. Gras, J. Luong, Planar microfluidic devices in flow modulated comprehensive two dimensional gas chromatography for challenging petrochemical applications, *Anal. Methods* 5 (2013) 6598–6604, <https://doi.org/10.1039/c3ay41198b>.
- [81] H. Obame, G. Toussaint, D. Laurenti, M. Tayakout, C. Geantet, Comprehensive GC×GC characterization of the catalytic alkylation of thiophenic compounds in a FCC gasoline, *Top. Catal.* 56 (2013) 1731–1739, <https://doi.org/10.1007/s11244-013-0109-z>.
- [82] P.T.M. Do, S. Crossley, M. Santikunaporn, D.E. Resasco, Catalytic strategies for improving specific fuel properties, *Catalysis* 20 (2008) 33–64, <https://doi.org/10.1039/B602366P>.
- [83] R. Henry, M. Tayakout-Fayolle, P. Afanasiev, F. Couenne, G. Lapisardi, L.J. Simon, V. Souchon, Methodology for the study of vacuum gas oil hydrocracking catalysts in a batch reactor - coupling of GC-2D data with vapour-liquid equilibrium, *Adv. Mater. Res.* 560-561 (2012) 207–213, <https://doi.org/10.4028/www.scientific.net/AMR.560-561.207>.

Gas chromatographic analysis of essential oils

K. Hüsnü Can Başer, Temel Özek

Anadolu University, Eskisehir, TR, Turkey

26.1 Definitions: what is essential oil? What are fragrances?

An essential oil, also known as volatile oil, or ethereal oil, is a liquid containing volatile aroma compounds obtained mainly from plant materials. Essential oils are biosynthesized by living organisms and are generally obtained from their matrix by water, steam, and dry distillation, or expression in the case of peel oils from citrus fruits [1–6]. There are some other processes involving extraction with organic solvents, fluidized gasses, or supercritical fluids. Concretes, absolutes, spice oleoresins, etc., obtained by extraction can be classified as aromatic extracts. They are not technically considered as essential oils [1,2,6].

Essential oils occur mainly in aromatic plants. However, a few of them are found in animal sources, such as Asian musk deer, North American beaver, civet, and sperm whale, or are produced by microorganisms [1,2,5,7,9]. The Council of Europe describes “*essential oil*” as a product obtained from “*vegetable raw material*.” Due to a ban on animal-based essential oils, and flavor and fragrance materials, the essential oil trade is entirely plant-based.

In plant materials, essential oils occur in oil cells, glandular hairs, and secretory cells within the epidermis or cavities [2,10]. However, they may also be bound with carbohydrates in glycosidic form. In such cases, hydrolysis should be applied to release the volatile moieties prior to distillation [2].

Essential oils are sources of substances as starting materials for different chemical syntheses. They can be fractionated to isolate aroma chemicals or used as fractions. These fractions and their isolates are widely used in different industrial applications in cosmetics, perfumery, pharmaceuticals, food, flavor, and fragrance sectors. Sometimes, essential oils are also associated with gums and/or resins. They can be liberated from such matrices by distillation [3].

Fragrance compounds are complex combinations of substances with characteristic and usually pleasant odor. They are added to products in order to impart a distinctive smell. Like all other ingredients, they are, therefore, used in a wide variety of products, such as foods, alcoholic and nonalcoholic beverages, cosmetics and toiletries, cleaning products, tobacco products, and a wide variety of pharmaceutical preparations

[1–5,7–9]. There are hundreds of fragrances created every year all over the world. Fragrances are thoroughly evaluated for safety prior to marketing [11]. They not only are composed of essential oils but may also contain natural or synthetic aroma chemicals or are diluted with carrier essential oils.

Essential oils may comprise volatile compounds that can be classified as terpenoids and nonterpenoid hydrocarbons and their oxygenated derivatives. However, some of them may also contain nitrogen or sulfur derivatives [12–14]. Essential oil compounds may exist in different forms such as alcohols, aldehydes, esters, ketones, acids, etc. The groups of compounds in essential oils are mainly monoterpenes, sesquiterpenes, and even diterpenes including their oxygenated derivatives [1–4,10]. In addition, phenylpropanoids, fatty acids and their esters, or their decomposition products are also encountered as volatiles in essential oils [1,2,15–17]. Essential oils should not be confused with fixed oils or fatty oils, which are composed of a naturally occurring mixture of lipids, which may not necessarily be volatile. Therefore, essential oils differ entirely both in chemical and in physical properties from fatty oils. Essential oil evaporates completely when dropped on filter paper; however, fixed oil leaves a permanent stain, which does not evaporate even when heated [2].

26.2 GC phases used in the analysis of essential oils and aroma chemicals

GC is the most important and common technique for the separation of essential oils [18]. Separation of components depends on the polarity and volatility of the analytes. Essentially, GC is based on differential partitioning of solutes between the mobile and stationary phase. It is quite simple, fast, reliable, and applicable to the separation of volatile materials, which are stable at a temperature up to 350–400 °C. If the sample or

the mixture is nonvolatile, then the sample should be derivatized appropriately to make it volatile e.g., silylation, acylation, and alkylation.

GC columns are categorized into two groups as packed and capillary columns. They are further classified according to their construction material, column length and diameter, type of stationary phase, and appropriate film thickness. Usually, preparative columns are made of glass, stainless steel, or fused silica [19]. One of the most important criteria for good GC separations is to select the most suitable stationary phase and column size (Table 26.1).

26.3 Separation criteria and techniques

26.3.1 Chiral columns

Enantiomers have identical physical properties such as boiling point, melting point, and spectroscopic features. Most of the essential oils contain enantiomeric compounds, and these enantiomers may possess different properties of interest in defining the quality of an essential oil. Enantiomers are preferably separated on capillary columns coated with a chiral stationary phases. There is no universal column for the separation of all enantiomeric compounds. Chiral stationary phases can only be applied for the separation of enantiomer pairs according to their structures [20,21]. The three main types of chiral GC stationary phases are chiral amino acid derivatives, chiral metal coordination compounds, and cyclodextrin derivatives (see Chapter 21). The latter have proven to be the most versatile for essential oil analysis.

26.3.2 Multidimensional techniques

Single-column GC applications are most commonly used for the analysis of essential oils. However, due to the limitations of one-dimensional chromatography for the separation of complex mixtures, interest in multidimensional

TABLE 26.1 GC column selection chart.

Column types		<ul style="list-style-type: none"> • Packed • Capillary
Column materials		<ul style="list-style-type: none"> • Glass • Stainless steel • Copper • Aluminum • Special alloy • Silica
Column polarity		<ul style="list-style-type: none"> • Nonpolar • Intermediate polarity • Polar • Highly polar
Stationary phases ^a	Nonpolar	<ul style="list-style-type: none"> • 100% dimethyl polysiloxane • 5% phenyl, 95% dimethyl polysiloxane
	Intermediate polarity	<ul style="list-style-type: none"> • 6% cyanopropyl phenyl, 94% dimethyl polysiloxane • 35% phenyl, 65% dimethyl polysiloxane • 35% phenyl, 65% dimethyl arylensiloxane • 14% cyanopropyl phenyl, 86% dimethyl polysiloxane
	Polar	<ul style="list-style-type: none"> • 50% cyanopropyl phenyl, 50% dimethyl polysiloxane • Polyethylene glycol
	Highly polar	<ul style="list-style-type: none"> • Poly(80% biscyanopropyl/20% cyanopropyl phenyl siloxane) • Poly(90% biscyanopropyl/10% cyanopropyl phenyl siloxane) • Poly(biscyanopropyl siloxane)
Column length	Packed	<ul style="list-style-type: none"> • 1–2 m (max. 10 m for special applications)
	Capillary	<ul style="list-style-type: none"> • 5–100 m
Column diameter	Packed	<ul style="list-style-type: none"> • 2–4 mm
	Capillary	<ul style="list-style-type: none"> • 0.10–0.53 mm
Column film thickness		<ul style="list-style-type: none"> • 0.1–5 μm

^a Summarized as most common.

(MDGC) and comprehensive two-dimensional gas chromatography (2D-GC) methods is increasing (see Chapter 7) [22–24]. In 2D-GC, the separation employs two capillary columns of different polarity in tandem. Each dimension

of separation gives specific information about the target compounds. Since an essential oil contains hundreds of compounds, this may be the only approach for complete characterization of complex oils. Comprehensive and multidimensional GC is also used for the efficient separation of enantiomers. In this case, the first column usually contains an achiral stationary phase and the separated components are directed to a chiral column to separate the enantiomers (see Chapter 21).

26.3.3 Headspace techniques

The gas space above the sample in a closed container is expressed as “*Headspace*” (HS). The HS technique is used in GC for the analysis of volatiles in solid, liquid, and gas samples (see Chapter 9).

The HS trapping technique is used to trap the odor of an aromatic material, such as a living flower, fragrance on the skin, or any other matrix. It requires a small amount of sample and is solvent-free. Odor can be sampled either directly or trapped on an adsorbent material. The trapped odorous components can be freed by either solvent extraction or thermal desorption prior to analysis by modern instrumental techniques (see Chapter 10). HS trapping techniques can be classified as follows [18,25]:

- static HS sampling,
- vacuum HS sampling, and
- dynamic HS sampling

In the **static HS sampling technique**, the sample is kept in a closed vial and HS air above the solid or a liquid sample is sampled by a gas syringe or directed onto the GC column. However, in common applications, the components in HS are first concentrated on an adsorbent trap. Heat may be applied to enhance the release of volatiles from the sample. Although a very rapid method, it does not give a comprehensive profile of the volatiles as some important components may not be detected.

Vacuum HS sampling technique involves suction of the headspace air via a vacuum pump through condensers cooled with liquid nitrogen to condense odorous principles. This technique is also used by some perfumery companies for commercial-scale production of fragrances.

Dynamic HS sampling involves sweeping the analyte with a stream of air or gas and adsorption of the volatiles from the gas stream on an adsorbent trap. Hydrophobic traps are preferred such as Tenax, Porapak Q, Chromosorb 101–105, or activated charcoal being the most popular. Volatiles from the trap can be removed either by thermal desorption or by solvent extraction. In fragrance analysis, solvent extraction is the preferred method. Dynamic HS sampling techniques can be applied in one of the following ways:

- **Closed-loop stripping method:** The analyte is placed in the middle of a closed circuit system in which clean air is continuously pumped through the analyte and odorous components in the HS air are trapped on an adsorbent material.
- **Direct sampling method:** The analyte, which may be a living flower, is placed in a glass container and the HS air is sucked via a suction pump through an adsorbent tube in which the odorous components are trapped [25].

26.3.4 Solid-phase microextraction (SPME)

Solid-phase microextraction (SPME) is a microsampling technique that has found wide application in flavor and fragrance research. It is a solvent-free method, which is used to trap flavors and fragrances either from aqueous samples (immersion SPME) or from the vapor space above a liquid or a solid sample (HS SPME) [25]. Since it is an equilibrium technique, it does not extract the analytes completely, hence does not

disturb the concentration of a liquid. Agitation of the liquid facilitates rapid extraction. For the HS samples, faster mass transport rates are attained and volatiles are extracted faster than semivolatiles.

Analytes adsorbed on the fiber are thermally desorbed directly in the injection port of a gas chromatograph for separation. The SPME assembly consists of a specially designed injector, also called SPME holder, which enables the coated fiber to move in and out of the needle. During injection into a vial for sampling or injection port for analysis, the fiber is concealed in the needle and exposed during sampling and thermal desorption. Several fiber coatings with different sorption properties are commercially available, such as polydimethylsiloxane (PDMS), polyacrylate (PA), polydimethylsiloxane/divinylbenzene (PDMS/DVB), carbowax (CW), carbowax/divinylbenzene (CW/DVB), and carboxene/polydimethylsiloxane (C/PDMS). SPME has proven itself to be a highly efficient and simple sample preparation technique, which may be expected to replace conventional HS techniques.

26.3.5 Preparative gas chromatography

This preparative technique is used when the analytical separation conditions have been established and large amounts of some components in high purity are required for further evaluation (see Chapter 16). Preparative gas chromatography (Prep-GC) is widely used for the isolation of terpenes and other volatiles from essential oils [19].

26.3.6 Gas chromatography—mass spectrometry (GC-MS)

In this commonly used technique for the analysis of essential oils and fragrances, a mass spectrometer coupled to a GC is used as a detector. Mass detection, unlike other common detection techniques, provides structural information for

the compound detected including its molecular mass as well as quantitative information. Detection of the compounds by peak matching with compounds in GC-MS Libraries is possible. Full characterization is completed by matching their retention indices with those of authentic compounds.

26.4 Retention index

In order to express the retention value of a compound reliably retention indices are used. There are two accepted retention index calculation methods depending on whether isothermal or temperature-programmed conditions are used [26,27]. A homologous series of n-alkanes is generally used as the standards for the calculation of retention index values. These are preferred for low-polarity stationary phases but owing to interfacial adsorption on polar phases ethyl esters are sometimes used as an alternative. The retention index for the standards is expressed as 100 times the number of carbon atoms. Thus, octane has a value of 800 and dodecane 1200 on all stationary phases. However, since the retention index values depend not only on the column temperature but also on the stationary phase used, retention index values change according to the polarity of stationary phase used. If the stationary phases are of the same polarity, the retention indices of the compounds remain the same within an acceptable range of ± 5 units for methyl silicone stationary phases and ± 10 units for polyethylene glycol phases [27].

26.5 Qualitative and quantitative aspects

The qualitative analysis of essential oils by GC is based on the comparison of the peaks in the chromatogram for the essential oil with those of authentic standards separated with the same chromatographic conditions. GC-MS is used for

correct identification of each peak (ideally single compound) separated from the essential oil. Spectroscopic information, in some cases, is an unavoidable alternative together with the use of retention indices and other relative retention parameters. The use of qualitative information alone is not sufficient to correctly characterize an essential oil, and quantitative data are also important. For this reason, selection of the detector is of extreme importance. Apart from the flame ionization detector (FID), each detector has associated with it a compound-specific response factor [4] (see Chapter 12). Since the FID has low selectivity, an electron-capture detector (ECD) is used to selectively detect compounds with a high electron affinity. Similarly, mass detector and FID do not have the same response, and FID is considered the more reliable and accurate. Therefore, GC-MS is preferred for qualitative identification except for the SIM mode in which only selected ions are quantified. In this mode, GC-MS gives the most accurate quantitative results for individual compounds. In recent years, hyphenated chromatographic and spectroscopic techniques have been used more extensively for the analysis of essential oils. In order to evaluate essential oil composition reliably both qualitative and quantitative data should be obtained from GC and/or GC-MS regarding detector response, column stationary phase (e.g., *some compounds such as thymoquinone decompose on a polar column*), and other retention factors [19].

26.6 GC-MS libraries

In GC, identification of a compound using retention indices is generally accepted when two successful matches are obtained from known and target compounds on at least two columns of different polarities. On the other hand, identification of the target compounds made on a single column can only be accepted if it is obtained in combination with

spectroscopic detection systems. In order to overcome this difficulty, it is necessary to have spectroscopic information of the compound simultaneously. When a suitable reference database (or library) is available, identification of target compounds will be much easier. Mass spectral data from GC-MS are generally considered as the key for component identification.

Three types of libraries are available for essential oil composition identification:

- commercial libraries,
- specific libraries, and
- in-house libraries.

26.6.1 Commercial libraries

These libraries contain nonspecific collections of spectra mainly taken from the literature. One has to be careful when evaluating data from commercial libraries since they contain mass spectral data taken under different conditions using different instruments. The main drawback of such libraries is the lack of retention data to compare with the retention indices. NIST has recently started providing such a service [28]. Among the commercially available GC-MS libraries for essential oil components and aroma chemicals, Wiley, NIST, NBS, TNO, EPA, NIH, Adams, MassFinder, FFNSC, and Tkachev can be mentioned.

26.6.2 Specific libraries

Some libraries are dedicated to specific applications or compound groups. Adams, MassFinder, FFNSC, and Joulain and Koenig collections are available for these applications. While the Adams and MassFinder are general essential oil libraries, FFNSC and Joulain and Koenig collections are prepared for flavors and fragrances of natural and synthetic compounds and sesquiterpene hydrocarbons, respectively. These libraries contain specific information for

the compounds of interest such as retention time, retention indices, and physicochemical information.

26.6.3 In-house libraries

Researchers dealing mainly with a certain group of products may develop their own libraries in order to facilitate and expedite compound characterization. Such libraries are more reliable since they are created using certified compounds under identical conditions and contain retention data. The BASER library of essential oil constituents is an example of an in-house library. In this library, retention time, retention index, source of mass spectrum, etc., are given for the polar HP-InnoWax column.

26.7 Conclusions

GC has proven its value as a useful, fast, and reliable separation technique for essential oils over the last few decades. Hyphenated techniques have broadened its usefulness. Especially, the GC-MS applications together with GC-MS libraries and retention index databases have revolutionized research into essential oils, flavors, and fragrances. Enantiomeric separations of optically active volatile chemicals through multidimensional techniques are possible and such useful information is highly regarded by the industry. HS analysis techniques are well advanced as a nondestructive analytical technique for capturing odor information. HS trapping can sample the odor of a living flower and continuous monitoring of diurnal changes of the odor is possible. GC in combination with an olfactometer can simultaneously evaluate the odor of sample components as they leave the column. A perfumer can also sniff the odor of the eluted compounds by attaching a sniffing port to the GC. Prep-GC is useful for isolating new compounds for further spectral

analyses and for accumulating enantiomers. GC-MS libraries facilitate and expedite the analyses of essential oils and fragrances. Instruments are only tools in the hands of a well-trained analyst. Therefore, specialization in a certain group of compounds or products is necessary for correct and accurate evaluation of instrumental data.

References

- [1] H. Surburg, J. Panten, *Common Fragrance and Flavor Materials: Preparation, Properties and Uses*, fifth ed., Wiley-VCH Verlag GmbH & Co. KGaA, Weinheim, 2006, p. 318.
- [2] K.H.C. Başer, F. Demirci, *Chemistry of essential oils*, in: R.G. Berger (Ed.), *Flavours and Fragrances: Chemistry, Bioprocessing and Sustainability*, Springer-Verlag, Heidelberg, 2007, pp. 43–86.
- [3] G.A. Reineccius, *Flavour-isolation techniques*, in: R.G. Berger (Ed.), *Flavours and Fragrances: Chemistry, Bioprocessing and Sustainability*, Springer-Verlag, Heidelberg, 2007, pp. 409–426.
- [4] K.H.C. Başer, G. Buchbauer (Eds.), *Handbook of Essential Oils*, CRC Press Taylor & Francis Group, Boca Raton, FL, 2010, pp. 3–38.
- [5] K.H.C. Başer, in: K.T. de-Silva (Ed.), *A Manual on Essential Oil Industry*, UNIDO, Vienna, 1995, p. 155.
- [6] K.H.C. Başer, F. Demirci, *Essential Oils*. *Kirk-Othmer Encyclopedia of Chemical Technology*, John Wiley & Sons, Inc, 2011, pp. 1–37.
- [7] M. Guentert, *The flavour and fragrance industry-past, present, and future*, in: R.G. Berger (Ed.), *Flavours and Fragrances: Chemistry, Bioprocessing and Sustainability*, Springer-Verlag, Heidelberg, 2007, pp. 1–14.
- [8] D.A. Müller, *Flavours: the legal framework*, in: R.G. Berger (Ed.), *Flavours and Fragrances: Chemistry, Bioprocessing and Sustainability*, Springer-Verlag, Heidelberg, 2007, pp. 15–24.
- [9] Anonymous, *Perfumes from Animal Sources*, Wikimedia Foundation, Inc., 2011 [updated May 15; cited 2011 May 15]; Available from: http://en.wikipedia.org/wiki/Perfume#Animal_sources2011.
- [10] E.J. Bowles, *The Chemistry of Aromatherapeutic Oils*, Allen & Unwin, Crows Nest, 2003, p. 236.
- [11] J.C.R. Demyttenaere, *Recent EU legislation on flavors and fragrances and its impact on essential oils*, in: K.H.C. Başer, G. Buchbauer (Eds.), *Handbook of Essential Oils*, CRC Press Taylor & Francis Group, Boca Raton, FL, 2010, pp. 917–948.
- [12] R.A. Clery, C.J. Hammond, A.C. Wright, *Nitrogen-containing compounds in black pepper oil (*Piper nigrum* L.)*, *J. Essent. Oil Res.* 18 (1) (2006) 1–3.
- [13] M. Iranshahi, G. Amin, M.S. Sourmaghi, A. Shafiee, A. Hadjiakhoondi, *Sulphur-containing compounds in the essential oil of the root of Ferula persica Willd. var. persica*, *Flavour Fragrance J.* 21 (2) (2006) 260–261.
- [14] D. Lopes, R.L.O. Godoy, S.L. Goncalves, M. Koketsu, A.M. Oliveira, *Sulphur constituents of the essential oil of nira (*Allium tuberosum* Rottl.) cultivated in Brazil*, *Flavour Fragrance J.* 12 (4) (1997) 237–239.
- [15] S. Bourgou, I. Bettaieb, M. Saidani, B. Marzouk, *Fatty acids, essential oil, and phenolics modifications of black cumin fruit under NaCl stress conditions*, *J. Agric. Food Chem.* 58 (23) (2010) 12399–12406.
- [16] C. Messaoud, M. Boussaid, *Myrtus communis* berry color morphs: a comparative analysis of essential oils, fatty acids, phenolic compounds, and antioxidant activities, *Chem. Biodivers.* 8 (2) (2011) 300–310.
- [17] N. Nasri, N. Tlili, S. Triki, W. Elfalleh, I. Cheraif, A. Khaldi, *Volatile constituents of *Pinus pinea* L. needles*, *J. Essent. Oil Res.* 23 (2) (2011) 15–19.
- [18] T. Cserhati, *Chromatography of Aroma Compounds and Fragrances*, Springer-Verlag, Heidelberg, 2010.
- [19] T. Özek, F. Demirci, *Isolation of natural products by preparative gas chromatography*, *Methods Mol. Biol.* 864 (2012) 275–300.
- [20] E. Francotte, *Chiral stationary phases for preparative enantioselective chromatography*, in: G.B. Cox (Ed.), *Preparative Enantioselective Chromatography*, Blackwell Publishing Ltd, Oxford, 2005, pp. 48–77.
- [21] T.E. Beesley, R.P.W. Scott, in: R.P.W. Scott, C. Simpson, E.D. Katz (Eds.), *Chiral Chromatography*, John Wiley & Sons Ltd, Chichester, 1998, p. 506.
- [22] L. Modello, A.C. Lewis, K.D. Bartle (Eds.), *Multidimensional Chromatography*, first ed., John Wiley & Sons, Inc, West Sussex, 2002, pp. 217–250.
- [23] P.Q. Tranchida, D. Sciarone, L. Mondello, *Multidimensional gas chromatography*, in: E. Grushka, N. Grinberg (Eds.), *Advances in Chromatography*, CRC Press Taylor & Francis Group, Boca Raton, 2010, pp. 289–328.
- [24] M.D.R.G.d. Silva, Z. Cardeal, P.J. Marriott, *Comprehensive two-dimensional gas chromatography: application to aroma and essential oil analysis*, in: H. Tamura, S.E. Ebeler, K. Kubota, G.R. Takeoka (Eds.), *Food Flavor*, American Chemical Society, Washington, DC, 2008, pp. 3–24.
- [25] N.C.D. Costa, S. Eri, *Identification of aroma chemicals*, in: D.J. Rowe (Ed.), *Chemistry and Technology of Flavors and Fragrances*, Blackwell Publishing Ltd., Boca Raton, FL, 2005, pp. 12–34.

- [26] T. Shibamoto, Retention indices in essential oil analysis, in: S. Sandra, C. Bicchi (Eds.), *Capillary Gas Chromatography in Essential Oil Analysis*, first ed., Alfred Huethig Verlag, Heidelberg, 1987.
- [27] V.I. Babushok, I.G. Zenkevich, Retention indices for most frequently reported essential oil compounds in gas chromatography, *Chromatographia* 69 (2009) 257–269.
- [28] V.I. Babushok, P.J. Linstrom, J.J. Reed, I.G. Zenkevich, R.L. Brown, W.G. Mallard, et al., Development of a database of gas chromatographic retention properties of organic compounds, *J. Chromatogr. A* 1157 (2007) 414–421.

Gas chromatographic analysis of lipids

*Cristina Cruz-Hernandez*¹, *Frédéric Destailats*²

¹Nestlé Research, Vers-Chez-Les-Blanc, Lausanne, Switzerland; ²Nestlé Nutrition Research, Vevey, Switzerland

Gas chromatography (GC) is one of the most widely used methods for resolving and quantifying lipids. GC almost exclusively uses methyl ester derivatives of fatty acids in conjunction with a flame ionization detector (FID). Other derivatives are discussed in order to enhance structural information for different lipid classes. GC-FID is also useful for analyzing free fatty acids and partial acylglycerols such as monoacylglycerols, diacylglycerols, and sterols after derivatization, which allow for the characterization of different fats and can be extended to the profiling of triacylglycerols, waxes, or sterol esters using heat-stable stationary phases. Complete separation of common fatty acids is typically achieved by using capillary columns with polar stationary phases but depending on the class of lipids to be separated, further separations and fractionations might be necessary or different columns required. Improvements in GC allow for faster analysis that offers many key benefits, such as increased laboratory productivity.

27.1 Introduction

Gas chromatography (GC) is the standard and certainly the most suitable tool to analyze

the fatty acid profile of simple and complex samples. The flame ionization detector (FID) is often used as a detector since it allows accurate quantification of fatty acid derivatives such as fatty acid methyl esters (FAMES). The evolution from packed columns to highly polar open-tubular capillary columns facilitated the progressive improvement in the resolution of complex mixtures of positional and geometrical isomers. Nowadays, fatty acid analysis on polar capillary columns is routinely used in the food sector to assess the quality of fats, oils, raw materials, and the fatty acid composition of food products. This type of analysis is widely used to assess the nutritional or health status in human subjects enrolled in nutritional interventions or in prospective epidemiological studies. Current developments in this field are focusing on the reduction of the separation time as well as the automation of sample preparation and data management.

GC-FID is used to analyze free fatty acids (FFA) and partial acylglycerols such as monoacylglycerols (MAG) or diacylglycerols (DAG) and sterols after derivatization. This type of analysis is useful to characterize the composition of fats and oils or emulsifiers and can be extended

to the profiling of triacylglycerols (TAG), waxes, or sterol esters using heat-stable stationary phases. Beyond the analysis of fatty acid esters with FID detection, GC is used in tandem with mass spectrometry (MS) for the structural analysis of fatty acids. Different techniques have been developed to identify and locate double bonds, rings, or other groups. Quantitative or structural analysis of more complex lipids such as glycerophospholipids (PL) or TAG is not achievable by GC and requires the use of liquid chromatography-based techniques. These topics have been recently addressed by Christie and Han in their book entitled "Lipid Analysis" and therefore will not be addressed in this chapter [1]. Also, applications of emerging multidimensional chromatographic techniques for lipid analysis will not be covered since this topic has been extensively recently reviewed by Tran-chida and coworkers [2].

27.2 Fatty acid analysis by GC as methyl ester derivatives

27.2.1 Preparation of fatty acid methyl esters

For many lipids, GC is the primary tool used in the determination of their fatty acid profile as their FAME derivatives; different considerations (i.e., response factor, retention time) have been evaluated to improve reliability [3]. During methylation, O-acyl- and N-acyl lipids are transesterified in the presence of a catalyst and a short-chain alcohol (i.e., methanol, ethanol, 2-propanol, or butanol) that replaces the glycerol or sphingosine moiety. Derivative formation is extensively used in lipid analysis; many other possibilities, including the preparation of FAME after transesterification or trimethylsilyl ethers (TMS) of hydroxyl groups, will be described later in this chapter. FAME can be prepared from isolated lipids or directly by

combining extraction and transesterification in a one-step procedure. The most commonly used catalysts are described further.

Hydrochloric acid (HCl), an acid catalyst, is required when substantial amounts of FFA, esters, alk-1-enyl ethers, amides, and glycosides (except ethers) are present in the sample to be analyzed. A solution of HCl/methanol (1–2 M), used widely in different matrices, converts the plasmalogen moiety (alk-1-enyl ethers) to dimethylacetals (DMA), and methylations are completed within minutes except for sphingolipids [4–6]. An alternative method was proposed to be effective with FAME yields >96% when toluene, methanol, and 8% of HCl solution are added sequentially to the lipid samples [7]. Sulfuric acid (H₂SO₄) has been used as a catalyst for the preparation of isopropyl, butyl, methyl, and other esters from dairy fats, blood, and animal fat [8–16]. The longer-chain esters have the advantage of providing FID responses that do not require correction factors for quantification and afford less inferences from solvent peaks, although short-chain fatty acids might be lost during aqueous washes and the resolution of closely eluting isomers may also appear to be compromised [17–19]. The acidic catalyst boron trifluoride (BF₃) in methanol is suitable for the methylation of all lipid classes, including amides, FFA, and plasmalogens. However, it is unstable and will produce artifacts if not fresh. In addition, acid-catalyzed methylation is generally not recommended for milk fat samples since it decreases the content of all the *cis/trans*-conjugated linoleic acid (*c/t*-CLA) isomers, producing *tt*-CLA isomers and methoxy artifacts, yet still commonly used in different matrices [20–29].

For oil samples containing primarily TAG, alkaline transesterification is recommended for direct formation of FAME and is usually performed using hexane and 2 M methanolic potassium or sodium hydroxide by GC or GC-MS [30–34]. For samples containing PL, a

method was recommended that allows the direct preparation of FAME and subsequent quantification of long-chain polyunsaturated fatty acids (LC-PUFA, 8), but does not apply to crude oil with acid values higher than 1.5%. Methylation using sodium methoxide (NaOCH_3) is recommended for the analyses of CLA-containing lipids. FAMEs are produced with the base (alkoxide), form an anionic intermediate, which is transformed in the presence of large excess of the alcohol (i.e., methanol, ethanol, 2-propanol, and butanol) into a new ester [4,35]. The most common reagent is 1–2 M sodium or potassium hydroxide in anhydrous methanol, which converts all esters to FAME within 10–15 min and is recommended to avoid isomerizations [3,18,36–39]. An aqueous-free system is preferred for the methylation of milk fat lipids [17,31,40].

Preparation of FAME is also common by direct methylation in different matrices such as plant materials, cultured cells, biological fluids such as total blood, plasma, bovine colostrum, and milk [22,41–46]. A direct transmethylation of dried blood spots with H_2SO_4 in methanol was compared to a standard and a microwaved-assisted method, with the second choice preferred for as it provided a higher yield in a shorter time [46]. When comparing direct methylation with extraction followed by methylation in egg, tissues, and plasma, fat extraction was preferred over direct derivatization [23,47–51]. For GC analysis of total blood HCl/MeOH 1.2% (w/v) at 45°C was selected, although other acid methylation methods have been also used and sometimes base methylation is recommended for other matrices such as blood lipids, serum phospholipids, fish, and vegetable oils, after initial solid-phase extraction (SPE) or thin-layer chromatography (TLC) fractionation for lipid classes [7,52–54]. Also, with anhydrous methanol HCl, a fast GC method was suggested with specific sample preparation for plasma and erythrocytes FAME analysis [55]. Additional sample preparation step, based on SPE, was also included in a method for lipids from plant

sources to obtain clean samples. This method used 5% HCl/methanol, 2 h at 70°C, and was preferred over several other methods of derivatization [56]. Different methods have been reported for fatty acid quantification in microalgae and for lipid-producing bacteria or microheterotrophs [57,58]. Efficient methods have been reported for oils, waxes, feedstuffs, plasma, or fresh, frozen, or lyophilized tissue samples, although no method is mentioned to inhibit the action of degradative enzymes when a mechanical grinder is used at room temperature [49,59–61]. Methylation was performed in the presence of up to 33% water and KOH in MeOH and H_2SO_4 or HCl as catalyst. Artifact formation or the isomerization of sensitive polyunsaturated fatty acids such as conjugated linoleic acid isomers was not mentioned [59]. When considering that no single methylation procedure adequately addresses the derivatization of all molecules, an optional approach is to perform two methylations in lipid matrices, i.e., first adding $\text{NaOCH}_3/\text{MeOH}$, followed by adding excess 5% HCl/MeOH [35]. A sequential base–acid catalyzed transesterification procedure with sodium (or potassium) methoxide in methanol followed by an acid reagent (e.g., sulfuric acid, HCl, BF_3) in methanol reaction was effective for different matrices (e.g., fish oil, ruminal digesta, extracted lipids, biological or foodstuff samples, biodiesel, edible oils) [22,62–68].

27.2.2 Analysis on conventional columns

Flexible fused-silica columns coated with a highly polar cyanoalkyl polysiloxane stationary phase are recommended for the analyses of fats that contain complex mixtures of geometric and positional isomers of monounsaturated fatty acids and CLA isomers as well as a range of FAs from butyric acid (4:0) to LC-PUFAs (e.g., milk fat). These columns are generally available in 100-m length from different suppliers and give improved separations of samples containing

fatty acids with different chain lengths; but shorter columns are also used for the same matrices [6,14,15,28,35,39,40,54,63,69–77]. The high cyanopropyl polysiloxane stationary phases are available as CP-Sil 88 (Varian Inc.), SP-2560 (Supelco Inc.), BPX-70 (SGE), and Rtx-2330 (Restek) columns. The CP-Sil 88 and SP-2560 columns provide similar elution orders for FAMES [5,20,22,50,54,64,70,72,73,75,76,78–82]. The BPX-70 column [36,65,83–86] provides a similar elution pattern for some fatty acids (e.g., CLA isomers) to those obtained using the CP-Sil 88 and the SP-2560 columns [20,29,35,38,70,72,74,80,87–89], although for other FAMES the order is different [1,90]. Some differences have been found, also in the order of elution as well as interferences of some fatty acids (21:0 and some 20:2 isomers), when the CP-Sil 88 and/or SP-2560 columns are used [3,80,87,90]. Differences are also observed for different temperature program rates as well as batch-to-batch variation for a given supplier [4]. Some variability on account of construction differences of the columns can occur, for example, some suppliers produce continuous 100-m capillary columns (i.e., SP-2560; RTX-2560; HP-88), while others join two 50-m capillary columns (i.e., CP-Sil 88), or two 100-m capillary columns (200 m Select FAME, Agilent). The BPX-70, Omegawax 250, and BP-20 (polyethylene glycol) columns were compared to omega-3 products for the separation of major fatty acids in serum, rat tissue, and fish oil. While all were suitable for these applications, the higher polarity of BPX-70 was beneficial for separations based on apparent polarity [36,45,91].

Retention of certain fatty acids can change depending on the column, its age, and the temperature program used. For example, the coelution of 21:0 with 9*c*11*c*- [80] or 10*t*12*c*- [90], and 11*c*13*t*- with 10*t*12*c*-CLA [86]. For routine analysis standards are recommended as well as GC-MS for a definitive identification. The 100-m ionic liquid (IL) capillary column SLB-1L111 was compared with the SP-2560 and CP-Sil 88

columns [92]. SLB-1L111 demonstrated improved separations for some *cis* and *trans* CLA isomers at 168°C and for 20:1 isomers in fish oil [25,93,94]. Improvements were observed also for the 14:1, 16:1 18:1, 20:1, and 18:3 acid isomers, as well as branched chain fatty acids, although the saturated fatty acids eluted between the *cis*- and *trans*-monounsaturated FAMES. An example using this column is shown in Fig. 27.1 [92,93]. The SLB-IL82 IL column supported large volume injection for GC with a vacuum ultraviolet (UV) spectroscopic detector for the quantification of 32 fatty acids in plasma samples [16]. Comparing IL columns of different polarity (IL- 59, 60, 65, and 111), further resolution of complex mixtures of *cis*- and *trans*-isomers was achieved with UV detection [5]. The medium-polarity SLB-IL60 column was useful for the characterization of fatty acid profiles in human blood [67]. A trihexyl(tetradecyl)phosphonium chloride column was suggested as an option to separate analytes with medium to low volatility including FAMES in different matrices (flavor, fragrance, and natural products to dry air) [94,95]. In comprehensive two-dimensional GC (GC × GC), various IL columns were evaluated for the separation of FAME mixtures [96]. Also, the SLB-IL100 column was compared with the medium BP-20 and DB-23 columns and the high-polarity BPX-70 columns and was found to be the best choice for the separation of positional and geometric isomers of monounsaturated FAMES, but the medium-polarity columns could be used when a particular selectivity is not required [21,29]. SLB-IL100 together with IL-82 was also better than SLB-IL61 for marine sources due to overlaps of different fatty acids [97,98]. A combination of a polar/less polar column set provided better separation of FAMES (e.g., SLB IL-111i and SLB IL-115) for GC × GC [99]. The TC-70-m, 60-m column (70% cyanopropyl polysilphenylene–siloxane liquid phase) was compared with other columns (e.g., SP-2560, 100 m, 100% cyanopropyl polysiloxane) for the

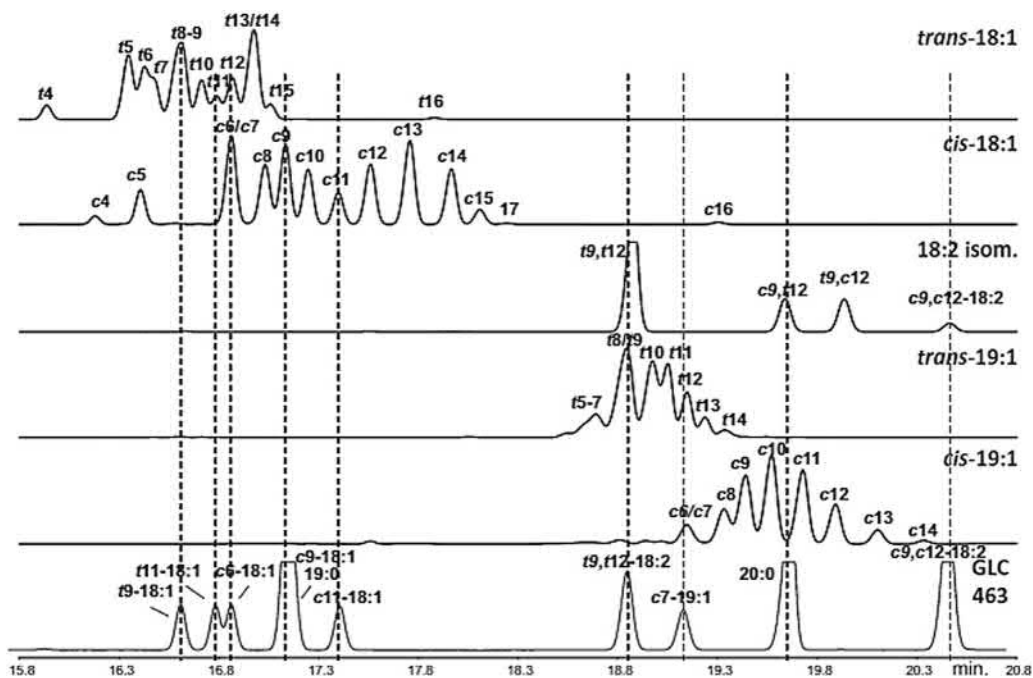


FIGURE 27.1 Partial GC chromatogram of the 18:1, 19:1, and 18:2 region. From top: *trans* and *cis* fractions of 18:1 obtained from a mixture of *cis* 6-, *cis* 9-, and *cis* 13–18:1 FAMES after two successive brominations and debrominations, linoleic acid FAME isomerized by PTSA, *trans* and *cis* fractions of 19:1 obtained by fractionating *cis* 10–19:1 FAME after six reactions, and reference FAME mixture GLC 463. From P. Delmonte et al. [45]

separation of *trans* isomers. In this example, the *trans* fatty acid content was reported to be quantitatively the same with both columns [100], although other reports suggest that these columns appear to be less efficient [90,101]. Similarly, the TRACE TR-FAME 60 m column was used for human milk and Indian snacks, without showing isomer separation (e.g., *trans*, 18:1, CLA) [27,102] as well as with the BD-23, 30 m column (50%-cyanopropyl)-methylpolysiloxane), used to separate FAMES in beef and milk fat [6,13]. Alternatively, although not as reliable, one can compare the results of different GC columns with different polarities. For example, the 60-m Supelcowax-10 capillary column was suggested as a complementary GC column mainly because of its intermediate polarity with a better resolution of the short-chain fatty acids and their monounsaturated fatty acids analogs, as well as

a complete separation of the 18:3 n-3 and 20:1 FAME isomers found in bovine tallow fat and olive oil. It was shown to provide confirmation of the identity of individual FAMES by comparison with a 100-m CP-Sil 88 column [33,66,74]. Columns with intermediate polarity (200-m Select FAME) have been used lately, although the increased length of this capillary column does not improve separations of the 18:1 isomer region [35,103]. A thorough systematic evaluation of the separation of these columns is needed to establish the elution pattern of most of the common FAMES including the positional and geometrical 18:1, 18:2, and 18:3 acid isomers and the identity of possible interfering FAMES in the CLA region. Partial separations were obtained on 120-m BPX-70 columns [90] as well as for the *trans*-18:1 isomers [104,105].

27.2.3 High-resolution analysis of positional isomers

Despite improvements in resolution using the 100-m highly polar columns, the separation of some fatty acids such as the geometric 18:1 acid isomers remains a challenge. Some FAMES are not separated, even when good resolution of other FAMES is accomplished using different columns and chromatographic conditions; therefore, having an optimum GC program to determine all the *cis* and *trans* isomers in lipid matrices has its limitations [72,90,106–108]. For example, the *trans*-18:1 isomers from 6*t*- to 11*t*-18:1 are not well resolved by GC in a typical temperature program, and the *trans*-18:1 isomers 12*t*- to 16*t*-18:1 may overlap extensively depending on the relative concentration of the major 9*c*-18:1 isomer, the sample size injected, and temperature program used. Underestimation of these peaks is sometimes reported due to incomplete separation [26,35,39,90]. Isothermal GC at 172, 160, and 150°C enables the resolution of almost all the *trans*-18:1 isomers by comparing the separations of total milk fat FAMES without previous separation [4,79]. This requires three separate GC analyses but all the *trans*-18:1 isomers can be resolved except for 13*t*/14*t*-18:1 and 6*t*-8*t*-18:1. The identification of individual *trans*-18:1 isomers is possible when the isomers are present at similar concentrations, but this becomes impossible when adjacent isomers are present at significantly different concentrations. The extent of the overlap of the 18:1 geometrical isomers is evident after prior fractionation using silver-ion chromatography followed by GC separations on long and polar columns [35,38,109].

Silver-ion thin-layer chromatography (Ag⁺-TLC) in tandem with GC is recommended for the complete analysis of the 18:1 isomers. Silver-ion-impregnated TLC plates (Ag⁺-TLC) are easily prepared and provide fractionation of fatty acid esters according to the number and geometry of the double bonds in the FAMES [110–113]. Hexane and diethyl ether are typically used as the mobile phase for the separation of

saturated from monounsaturated *trans*- and *cis*-FAMES and PUFAs. Fractionation is also possible by Ag⁺-HPLC and Ag⁺-SPE columns [12,62,114,115]. Eleven *trans*-18:1 acid isomers were separated by these techniques and, after the Ag⁺-TLC, a longer GC temperature program is recommended to complete the separation and resolution of *trans*-18:1 acid isomers [72,73,116]. Typical separation of the FAMES in the 18:0 to 18:2 n-6 region contains overlapping peaks associated with the *cis*-18:1, *trans*-18:1, and *c/t*-18:2 isomers as shown in Fig. 27.2. Of the *trans*-18:1 isomers, 4*t*-, 5*t*-, 6-8*t*-, 9*t*-, 10*t*-, 11*t*-, and 12*t*-18:1 can generally be resolved, while the 13*t*- and 14*t*-18:1 isomers are generally coeluted with the major 9*c*-18:1 isomer and poorly resolved. On the other hand, 15*t*-18:1 coelutes with 9*c*-/10*c*-18:1, and 16*t*-18:1 with 14*c*-18:1 [36]. By comparing the results of Ag⁺-TLC-GC analysis, it is possible to characterize the extent of the overlap of *cis*- and *trans*-18:1 isomers in the temperature-programmed separation of total milk fat FAMES [35]. The resolution of some *trans*-18:1 isomers is only partial (6*t*-8*t*- to 11*t*-18:1), and there is a lack of separation of the 6*t*-8*t*-18:1 and the 13*t*-/14*t*-18:1 isomers. Without prior Ag⁺-TLC separation, the *trans*-18:1 isomers are often misidentified. For example, the isomer 6*t*-18:1 was independently reported in a number of publications [117–120] even though its separation from 7*t*- and 8*t*-18:1 by GC is impossible.

After Ag⁺-TLC isolation, all the *trans*-18:1 isomers can be resolved except for 6*t*-8*t*-18:1. Precht and Molketin [72] suggested that the lack of separation of the 6*t*-8*t*-18:1 was due to the small content of the 6*t* and 7*t* isomers. Using Ag⁺-TLC and GC, this difficult pair of *trans*-18:1 isomers are separated, such as 13*t*-/14*t*-18:1, and 10*t*- and 11*t*-18:1 in samples high in either one of these isomers [35]. The analysis of the *trans*-isomers of *trans*-16:1, *trans*-20:1, and *trans*-22:1 requires injection of larger sample amounts, as demonstrated for *trans*-16:1 and the *trans*-20:1 acid isomers [90]. Various FAME isomers from milk fat, partially hydrogenated vegetable oil, algae, and fish oil were resolved after concentration

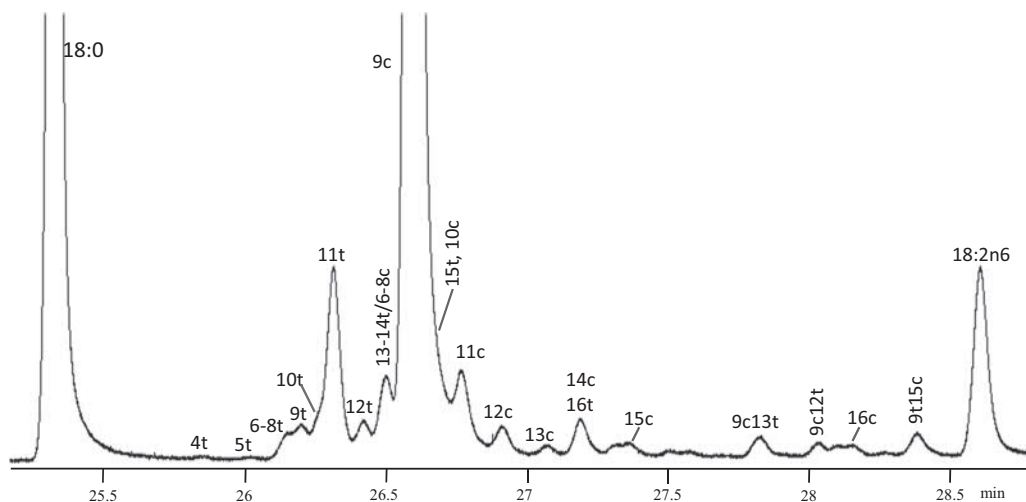


FIGURE 27.2 Gas-liquid chromatogram of butter on a 100 m capillary column with an enlarged view of the region from stearic (18:0) to linoleic (18:2 n-6) acids.

(Ag^+ -TLC), Ag^+ -SPE, and fractionation (Ag^+ -HPLC) with ionic liquid (SLB-IL100 and SLB-IL111) as well as non-IL columns [21,25,62,91,93,97,121–123]. Different multidimensional approaches (e.g., GC \times GC; Ag^+ -LC \times nonaqueous-LC or “off-line” Ag^+ -LC \times nonaqueous LC) were evaluated for the characterization of TAG [35]. Using an initial low temperature of 120°C and temperature programming improved the resolution of all *cis*-18:1 isomers, but even then 6*c*-8*c*-18:1 remains unresolved and most often 10*c*-18:1 is observed as an unresolved peak on the side of 9*c*-18:1 because of the large difference in their relative amounts. There is evidence that several of the minor *tt*- and *c/t*-18:2 isomers in milk fat elute starting with 13*c*-18:1 [20,76].

27.2.4 Fast and ultrafast analysis

Faster GC analysis of FAMES is possible using the new generation of columns and apparatus resulting in lower costs and increased laboratory productivity and sample throughput. In general, fast GC has been

defined based on peak widths obtained [124–127] as well as the separation of a sample in a shorter time than conventional GC methods [128,129]. Ultrafast GC belongs to the methods with separation times in the subsecond range and with average peak widths between 5 and 30 ms [124].

Fast GC without compromising resolution requires a shorter column, a different stationary phase film thickness, higher carrier gas velocity, faster temperature program rates, or flow programming. Columns of 100- μm internal diameter with a wide choice of stationary phases are available. Wide-bore capillary columns are of particular interest because they can be used as a direct replacement for packed columns without changing operating parameters or sample preparation. Modern instruments are equipped with electronic pressure/flow programming of the carrier gas that can be used to reduce the separation time. For wide-boiling-range samples, fast temperature programming is used to minimize the separation time. This is typically achieved using resistive heating at rates up to 1200°C min⁻¹ and cooling from 300 to 50°C in less than 30 s.

Different detection systems are compatible with fast GC such as FID, MS, and time-of-flight MS, useful for fast GC-MS [125,127,130–133]. Fast GC-MS with automated headspace solid-phase microextraction for the analysis of organic volatiles in fruits reduced significantly the time of analysis [130].

Evaluation of fatty acid composition by fast GC has been applied to different samples, such as essential oils [134–143], human plasma, and serum [129,144,145]. For the analysis of plasma lipids, Massod and Salem [146,147] developed an improved method for sample preparation. This method incorporates robotic transmethylation of samples and elution of n-3 PUFAs in under 6 min. Plasma and phospholipids isolated by SPE from total lipid extracts were analyzed with the identification of 37 fatty acids in 3.2 min and 25 fatty acids in 3.8 min, respectively [148]. Plasma and red blood cells [55,132,149] as well as five main polar lipid fractions (phosphatidylethanolamide, phosphatidylcholine, phosphatidylserine, phosphatidylinositol, and sphingomyelin) from brain lipids from rats [150] by fast GC in less than 5 min.

Analysis of menhaden oil, butter, lard, tallow, corn, dairy products peanut, olive, colza, sunflower, and soya samples by fast GC was achieved in about 2.9 min [133–135,151], significantly faster than previous GC separation times of about 70 and 15 min [142,151]. Vegetable oil analysis by ultrafast GC with FID detection was achieved in less than 2 min [134]. Shorter columns resulted in faster separations of cod liver extract on a 0.1 mm ID polar column segment of 2 m (1.45 min) or a 10 m × 0.1 mm ID column [139,152]. FAME analysis in seconds is possible with a low pressure GC-MS and low thermal mass resistive heating for rapid temperature ramping and cooling of the capillary column [131]. All methods and examples mentioned in this section can be taken into account to select specific conditions for fast GC, but the final parameters will depend always on the application.

27.3 Analysis of free fatty acids and acylglycerols

Acylglycerols are fatty acid esters of glycerol and comprise TAG, DAG, and MAG. The separation of TAGs by GC can be achieved using high-temperature conditions (>300°C). This technique allows good separations of TAGs according to the number of carbon atoms but is limited in terms of resolution for several reasons: such as the temperature required to elute TAGs, their thermal stability, and the thermal stability of stationary phases. Regardless of these limitations, the analysis of TAGs according to their carbon number can be performed to assess, for example, the authenticity of milk fat ([153]—a typical chromatogram of milk fat TAGs is shown in Fig. 27.3. This type of separation can be performed on short (<5 m) apolar capillary columns and is very useful for quality control of fats and oils. The use of more polar capillary columns such as RTX-65 (65% diphenyl/35% polydimethylsiloxane) provides improved resolution of TAGs in complex samples such as cocoa butter, palm oil, or butter [154].

Separation of TAG regioisomers such as POP and PPO (P and O standing for palmitic and oleic acid, respectively) cannot be obtained by high-

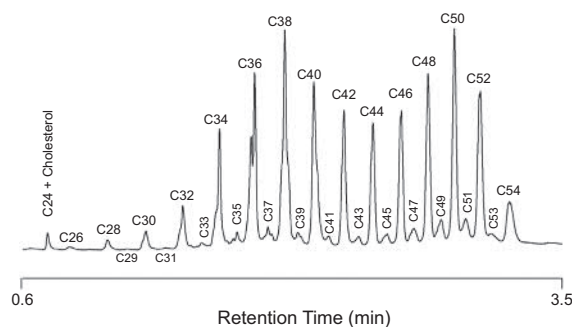


FIGURE 27.3 Separation of pure milk fat triacylglycerols (TAGs) on a short apolar capillary column. Adapted from F. Destailats, M. de Wispelaere, F. Joffre, *Authenticity of milk fat by fast analysis of triacylglycerols: application to the detection of partially hydrogenated vegetable oils*, *J. Chromatogr. A* 1131 (2006) 227–234.

temperature GC. Resolution of TAG regioisomers containing two butyric acid residues is possible on polar columns as demonstrated by Angers and Arul in studies of the regio-specific distribution of fatty acids in TAGs [155]. Separation of MAGs and DAGs in complex samples, such as emulsifiers or crude vegetable oils, can be achieved after silylation of the samples. The use of an appropriate internal standard allows the quantification of the different lipid classes by FID detection. This method has been standardized by the American Oil Chemist Society [156]. The separation can be achieved using apolar or medium polar columns. Glycerol can be separated simultaneously as its trimethylsilyl ether derivative. The separation of Sn-1,3 and Sn-1,2 DAG isomers with the same fatty acid residues is also possible. This feature is useful in studies of the hydrolysis of TAG in plant oils and milk fat [157,158]. Retention indices of TMS derivatives of MAGs and DAGs on nonpolar stationary phases (HP-5 and HP-1 type columns) are available [159]. Mass spectra of MAG and DAG TMS ethers have been reported [160] and GC-MS can be used to identify MAG regioisomers as their di-TMS derivatives [161]. Recently, GC analysis of soybean oil fractions containing FFAs, MAGs, DAGs, and TAGs was achieved using TMS derivatives and proposed as a quality control procedure to assess the quality of biofuels [162]. The chromatograms are generally complex as demonstrated by Torres and coworkers [163] or Verleyen and coworkers for deodorizer distillates [164]. In addition to the most abundant classes (FFAs, MAGs, DAGs, and TAGs), other liposoluble substances such as vitamins E, sterols, and hydrocarbons will also be present in the sample (see, for example, the study by L. Nang Lau et al. [157]). An alternative to the use of standards for identification is to use MS as a detector as described by Lytovchenko and coworkers for plant material [165] or Michael-Jubeli and coworkers for skin surface lipids—Fig. 27.4 [166]. It was demonstrated that

separation of partial acylglycerols as well as low volatility compounds (e.g., triterpenes) can be achieved without derivatization using comprehensive two-dimensional GC (GC × GC) with cryogenic modulation [167]. Comprehensive GC×GC with MS detection was used to analyze the neutral lipid profile of cancer cell extracts with outstanding resolution of more than 600 different species, including acylglycerols and other metabolites, such as nucleosides and nucleotides [168].

27.4 Analysis of sterols, sterol esters, stanyl esters, and steryl glycosides

Cholesterol or plant-derived sterols such as campesterol, stigmasterol, β -sitosterol, and their stanyl analogues are analyzed by GC as their TMS or other derivatives [169–175]. Separation of the unsaponifiable fraction from lipid extracts is required to isolate the sterols or stanols; this step also allows the hydrolysis of the steryl or stanyl esters and the fraction obtained can be analyzed after silylation [172]. Epicoprostanol is often used as an internal standard and a typical chromatogram of a dietary phytosterol formulation is shown in Fig. 27.5. This methodology is used to characterize the sterols and stanols in the characterization of vegetable oils and plant materials [173,174], ingredient authenticity [174], quality control of food products fortified with plant sterols or stanols and supplements [175–178], and clinical biology [179]. Sterol esters can be analyzed directly without prior hydrolysis of the acyl group and TMS derivatization as shown for cholesteryl esters in plasma lipids [180]. GC can also be used to analyze acyl steryl glycosides as proposed by Pieber and coworkers, who developed a methodology for their quantitative analysis in biodiesel using MS in the single-ion monitoring mode (SIM) as a detector [181]. The method involved a saponification step to release the fatty acid residue without alteration of the

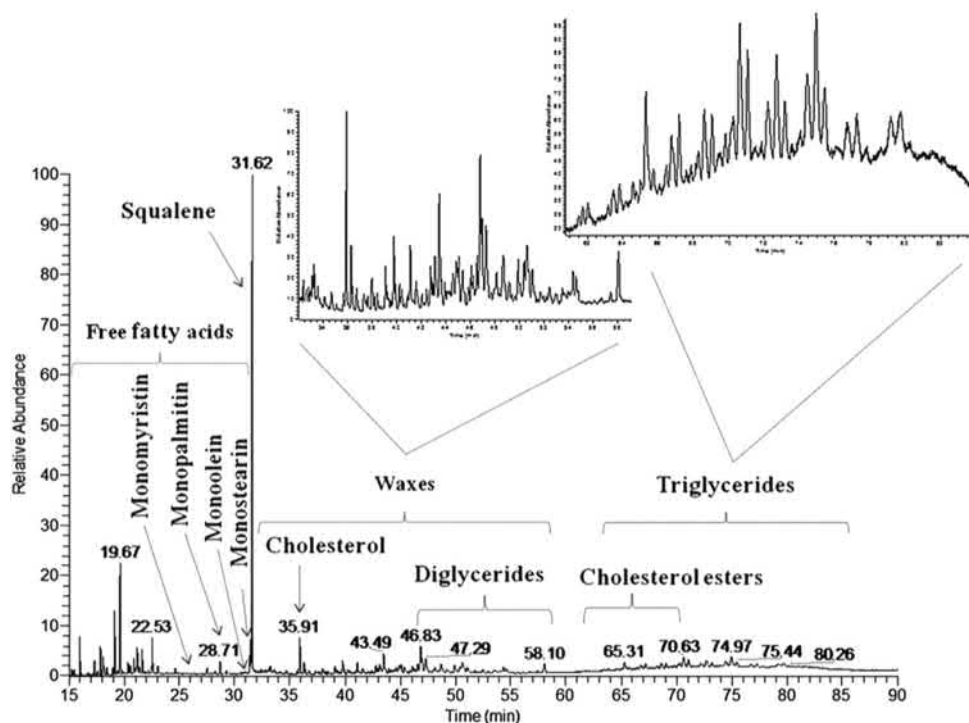


FIGURE 27.4 Separation of TMS derivatives of skin surface lipids by high-temperature gas chromatography–mass spectrometry. Adapted from R. Michael-Jubeli, J. Bleton, *High-temperature gas chromatography–mass spectrometry for skin surface lipid profiling*, *J. Lipid Res.* 52 (2011) 143–151.

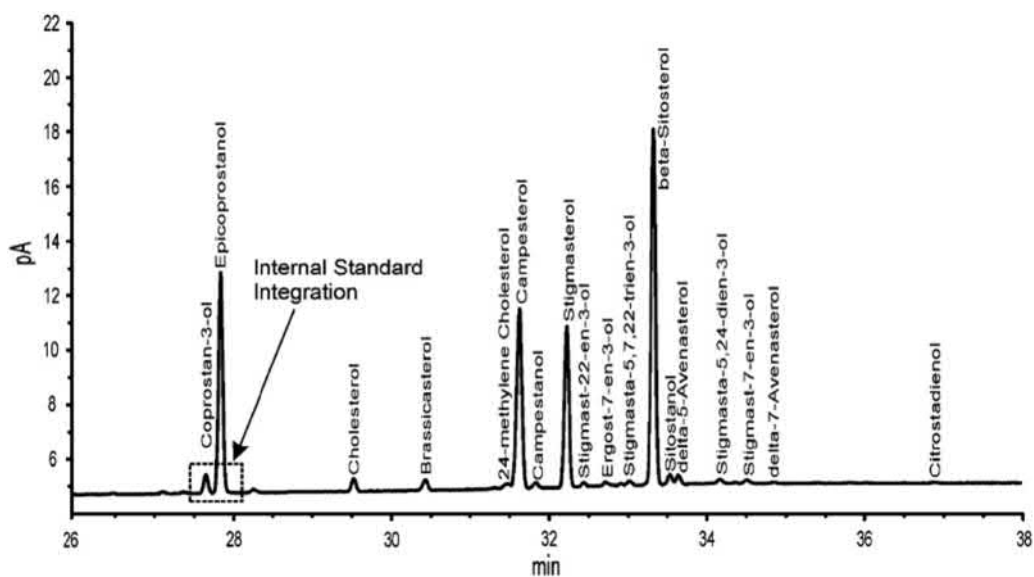


FIGURE 27.5 Separation of TMS derivative of phytosterols from milk formulated with emulsified sterol concentrate. Adapted from L.M. Clement, S.L. Hansen, C.D. Costin, *Quantitation of sterols and sterol esters in fortified foods and beverages by GC/FID*, *J. Am. Oil Chem. Soc.* 87 (2010) 973–980.

glycosidic bond. The fraction containing steryl glycosides is then trimethylsilylated using *N,O*-bis(trimethylsilyl)trifluoroacetamide (BSTFA) with 5% trimethylchlorosilane (TMCS) to ensure complete silylation of the glycoside groups [181]. Detection of complex steryl glycosides in microalgae was achieved by gas chromatography–triple quadrupole mass spectrometry (GC-QQQ-MS) of their TMS derivatives by Yu and coworkers [182].

27.5 Analysis of waxes

Waxes are fatty acid and fatty alcohol esters found in almost all natural lipid extracts. Their analysis is possible by GC, typically with MS detection [183,184]. The standard procedures for GC analysis involve as a first step the purification of the waxes from TAGs and other lipids by silica gel chromatography, thin-layer chromatography, or SPE as described by Christie [1]. This sample preparation step is required to reduce the complexity of the chromatogram and limit the coelution of waxes with other compounds. However, Michael-Jubeli et al. [166] reported a method for waxes and other lipids in skin surface lipid samples by GC-MS without prior isolation of the waxes. Alternatively, isolation of the wax fraction from the other lipids can be achieved online using liquid chromatography coupled with GC, as reported by Aragon et al. [184].

References

- [1] W.W. Christie, *Lipid Analysis. Isolation, Separation, Identification and Lipidomic Analysis*, fourth ed., The Oily Press, Bridgwater, UK, 2010.
- [2] P.Q. Tranchida, P. Donato, G. Dugo, *Comprehensive chromatographic methods for the analysis of lipids*, *Trends Anal. Chem.* 26 (3) (2007) 191–205.
- [3] R. Kapeller, Retention time correction in gas chromatography by modeling concentration related effects, applied to the analysis of fatty acid methyl esters, *J. Chromatogr. A* 1394 (2015) 118–127.
- [4] J.K.G. Kramer, J. Zhou, Conjugated linoleic acids and octadecenoic acids: extraction and isolation of lipids, *Eur. J. Lipid Sci. Technol.* 103 (2001) 594–600.
- [5] P. Gómez-Cortés, V. Rodríguez-Pino, A.L. Martínez Marín, M.A. de la Fuente, Identification and quantification of dimethyl acetals from plasmalogenic lipids in lamb intramuscular fat under different derivatization procedures, *J. Chromatogr. B. Anal. Technol. Biomed. Life Sci.* 1120 (2019) 24–28.
- [6] R. Jain, S.M. Bronkema, W. Yakah, J.E. Rowntree, C.A. Bitler, J. Fenton, Seasonal differences exist in the polyunsaturated fatty, mineral and antioxidant content of U.S. grass-finished beef, *PLoS One* 15 (2020) 1–14.
- [7] K. Ichihara, Y. Fukubayashi, Preparation of fatty acid methyl esters for gas-liquid chromatography, *J. Lipid Res.* 51 (2010) 635–640.
- [8] R.L. Wolff, C.C. Bayard, Improvement in the resolution of individual trans-18:1 isomers by capillary gas-liquid chromatography: use of a 100-m CP-Sil 88 column, *J. Am. Oil Chem. Soc.* 72 (1995) 1197–1201.
- [9] R.L. Wolff, C.C. Bayard, R.J. Fabien, Evaluation of sequential methods for the determination of butterfat fatty acid composition with emphasis on trans-18:1 acids. Application to the study of seasonal variations in French butters, *J. Am. Oil Chem. Soc.* 72 (1995) 1471–1483.
- [10] J.-M. Chardigny, R.L. Wolff, E. Mager, C.C. Bayard, J.-L. Sébédio, L. Martine, et al., Fatty acid composition of French infant formulas with emphasis on the content and detailed profile of trans fatty acids, *J. Am. Oil Chem. Soc.* 73 (1996) 1595–1601.
- [11] Y. Cui, X. Chen, L. Liu, W. Xie, Y. Wu, Q. Wu, D. Wang, Gas chromatography-mass spectrometry analysis of the free fatty acids in serum obtained from patients with Alzheimer's disease, *Biomed. Mater. Eng.* 26 (2015) S2165–S2177.
- [12] R. Sasaki, M. Umezawa, S. Tsukahara, T. Ishiguro, S. Sato, Y. Watanabe, Assignment of milk fat fatty acid propyl esters by GC-FID analysis with the aid of Ag-ion solid-phase extraction, *J. Oleo Sci.* 64 (2015) 1251–1258.
- [13] K. Yoshinaga, S. Sato, R. Sasaki, M. Asada, R. Hori, J. Imagi, et al., The collaborative study on the enzymatic analysis of positional distribution of short- and medium-chain fatty acids in milk fat using immobilized *Candida Antarctica* lipase, *J. Oleo Sci.* 65 (2016) 291–302.
- [14] D. Eibler, S. Krüger, K. Skírnisson, W. Vetter, Combined thin layer chromatography and gas chromatography with mass spectrometric analysis of lipid classes and fatty acids in malnourished polar bears (*Ursus maritimus*) which swam to Iceland, *J. Chromatogr. B. Anal. Technol. Biomed. Life Sci.* 1046 (2017) 138–146.
- [15] P.J. Watkins, Characterization of four alkyl-branched fatty acids as methyl, ethyl, propyl, and butyl esters using gas chromatography-quadrupole time of flight mass spectrometry, *Anal. Sci.* 36 (2020) 425–429.

- [16] I.C. Santos, J. Smuts, M.L. Crawford, R.P. Grant, K.A. Schug, Large-volume injection gas chromatography-vacuum ultraviolet spectroscopy for the qualitative and quantitative analysis of fatty acids in blood plasma, *Anal. Chim. Acta* 1053 (2019) 169–177.
- [17] P.Y. Chouinard, L. Corneau, D.M. Barbano, L.E. Metzger, D.E. Bauman, Conjugated linoleic acids alter milk fatty acid composition and inhibit milk fat secretion in dairy cows, *J. Nutr.* 129 (1999) 1579–1584.
- [18] W.W. Christie, A simple procedure for rapid transmethylation of glycerolipids and cholesterol esters, *J. Lipid Res.* 23 (1982) 1072–1075.
- [19] F. Ulberth, R.G. Gabernig, F. Schrammel, Flame-ionization detector response to methyl, ethyl, propyl, and butyl esters of fatty acids, *J. Am. Oil Chem. Soc.* 76 (1999) 263–266.
- [20] J.K.G. Kramer, V. Fellner, M.E.R. Dugan, F.D. Sauer, M.M. Mossoba, M.P. Yurawecz, Evaluating acid and base catalysts in the methylation of milk and rumen fatty acids with special emphasis on conjugated dienes and total trans fatty acids, *Lipids* 32 (1997) 1219–1228.
- [21] K. Shimizu, Y. Ando, Gas chromatographic separation of docosenoic acid positional isomers on an SLB-IL100 ionic liquid column, *J. Oleo Sci.* 61 (2012) 421–426.
- [22] P. Castro-Gómez, J. Fontecha, L.M. Rodríguez-Alcalá, A high-performance direct transmethylation method for total fatty acids assessment in biological and food-stuff samples, *Talanta* 128 (2014) 518–523.
- [23] I.S. Vieira de Melo, T. Da Rocha Ataíde, S. Lima de Oliveira, N. Bezerra Bueno, J. Duarte de Freitas, A.E. Goulart Sant'Ana, Hepatic fatty acid profile of rats fed a triheptanoin-based ketogenic diet, *Nutr. Hosp.* 32 (2015) 265–269.
- [24] P. Henry, O. Owopetu, D. Adisa, T. Nguyen, K. Anthony, D. Ijoni-Animadu, et al., Fatty acids composition of *Caenorhabditis elegans* using accurate mass GCMS-QTOF, *J. Environ. Sci. Health B.* 51 (2016) 546–552.
- [25] S. Senarath, K. Yoshinaga, T. Nagai, A. Yoshida, F. Beppu, C. Jayasinghe, et al., Quantitative analysis of the distribution of cis-eicosenoic acid positional isomers in marine fishes from the Indian ocean, *J. Oleo Sci.* 66 (2017) 187–197.
- [26] S. Lashkari, S.K. Jensen, Quantitative determination of conjugated linoleic acid and polyunsaturated fatty acids in milk with C17:0 as internal marker - evaluation of different methylation procedures, *Data Brief* 15 (2017) 106–110.
- [27] K. Joshee, T. Abhang, R. Kulkarni, Fatty acid profiling of 75 Indian snack samples highlights overall low trans fatty acid content with high polyunsaturated fatty acid content in some samples, *PLoS One* 14 (2019) 1–15.
- [28] P. Khrisanapant, B. Kebede, S.Y. Leong, I.A. Oey, A comprehensive characterisation of volatile and fatty acid profiles of legume seeds, *Foods* 8 (2019) 1–19.
- [29] H.D. Waktola, S.A. Mjøs, Chromatographic efficiency of polar capillary columns applied for the analysis of fatty acid methyl esters by gas chromatography, *J. Sep. Sci.* 41 (2018) 1582–1592.
- [30] S.W. Christopherson, R.L. Glass, Preparation of milk fat methyl esters by alcoholysis in an essential non-alcoholic solution, *J. Dairy Sci.* 52 (1969) 1289–1290.
- [31] W.W. Christie, *Gas Chromatography and Lipids: A Practical Guide*, The Oily Press, Ayr, 1989, p. 307.
- [32] M. Paolini, L. Bontempo, F. Camin, Compound-specific $\delta^{13}\text{C}$ and $\delta^2\text{H}$ analysis of olive oil fatty acids, *Talanta* 174 (2017) 38–43.
- [33] A. Kritioti, G. Menexes, C. Drouza, Chemometric characterization of virgin olive oils of the two major Cypriot cultivars based on their fatty acid composition, *Food Res. Int.* 103 (2018) 426–437.
- [34] M. Beccaria, R. Costa, G. Sullini, E. Grasso, F. Cacciola, P. Dugo, et al., Determination of the triacylglycerol fraction in fish oil by comprehensive liquid chromatography techniques with the support of gas chromatography and mass spectrometry data, *Anal. Bioanal. Chem.* 407 (2015) 5211–5225.
- [35] C. Cruz-Hernandez, Z. Deng, J. Zhou, A.R. Hill, M.P. Yurawecz, P. Delmonte, et al., Methods for analysis of conjugated linoleic acids and trans-18:1 isomers in dairy fats by using a combination of gas chromatography, silver-ion thin-layer chromatography/gas chromatography, and silver-ion liquid chromatography, *J. AOAC Int.* 87 (2004) 545–562.
- [36] J. Salimon, T.A. Omar, N. Salih, Comparison of two derivatization methods for the analysis of fatty acids and trans fatty acids in bakery products using gas chromatography, *Sci. World J.* 2014 (2014) 1–10.
- [37] K. Ichihara, C. Kohsaka, N. Tomari, T. Kiyono, J. Wada, K. Hirooka, et al., Fatty acid analysis of triacylglycerols: preparation of fatty acid methyl esters for gas chromatography, *Anal. Biochem.* 495 (2016) 6–8.
- [38] P. Vahmani, D.C. Rolland, K.E. Gzyl, M.E. Dugan, Non-conjugated cis/trans 18:2 in beef fat are mainly Δ -9 desaturation products of trans-18:1 isomers, *Lipids* 51 (2016) 1427–1433.
- [39] L. Deng, Q. Zou, B. Liu, W. Ye, C. Zhuo, L. Chen, et al., Fatty acid positional distribution in colostrum and mature milk of women living in Inner Mongolia, North Jiangsu and Guangxi of China, *Food Funct.* 9 (2018) 4234–4245.

- [40] Z. Liu, V. Ezernieks, S. Rochfort, B. Cocks, Comparison of methylation methods for fatty acid analysis of milk fat, *Food Chem.* 261 (2018) 210–215.
- [41] P. Risé, F. Salvetti, C. Galli, Application of a direct transmethylation method to the analysis of fatty acid profile in circulating and cultured cells, *Anal. Biochem.* 346 (1) (2005) 182–184.
- [42] A.I. Carrapiso, C. Garcia, Development in lipid analysis: some new extraction techniques and in situ transesterification, *Lipids* 35 (11) (2000) 1167–1177.
- [43] S. Yurchenko, A. Sats, V. Poikalainen, A. Karus, Method for determination of fatty acids in bovine colostrum using GC-FID, *Food Chem.* 212 (2016) 117–122.
- [44] A.D. Patterson, O. Maurhofer, D. Beyoglu, C. Lanz, K.W. Krausz, T. Pabst, et al., Aberrant lipid metabolism in hepatocellular carcinoma revealed by plasma metabolomics and lipid profiling, *Cancer Res.* 71 (2011) 6590–6600.
- [45] P. Delmonte, C.C. Lin, A. Sengee, S.A. Mjøs, Minor compounds and potential interferents in gas chromatographic analyses of human serum fatty acids, *J. Chromatogr. B Anal. Technol. Biomed. Life Sci.* 1138 (2020) 1–10.
- [46] A.H. Metherel, J.J. Aristizabal Henao, F. Ciobanu, A.Y. Taha, K.D. Stark, Microwave energy increases fatty acid methyl ester yield in human whole blood due to increased sphingomyelin transesterification, *Lipids* 50 (2015) 895–905.
- [47] E. Amusquivar, S. Schiffner, E. Herrera, Evaluation of two methods for plasma fatty acid analysis by GC, *Eur. J. Lipid Sci. Technol.* 113 (2011) 711–716.
- [48] M.R. Mazalli, N. Bragagnolo, Validation of two methods for fatty acids analysis in eggs, *Lipids* 42 (5) (2007) 483–490.
- [49] A.I. Ostermann, M. Müller, I. Willenberg, N.H. Schebb, Determining the fatty acid composition in plasma and tissues as fatty acid methyl esters using gas chromatography – a comparison of different derivatization and extraction procedures, *Prostaglandins Leukot. Essent. Fatty Acids* 91 (2014) 235–241.
- [50] D. Jamiol-Milc, E. Stachowska, T. Janus, A. Barcz, D. Chlubek, Elaidic acid and vaccenic acid in the plasma of pregnant women and umbilical blood plasma, *Pomeranian J. Life Sci.* 61 (1) (2015) 51–57.
- [51] S.F. Gallego, M. Hermansson, G. Liebisch, L. Hodson, C.S. Ejsing, Total fatty acid analysis of human blood samples in one minute by high mass spectrometry, *Biomolecules* 9 (2018) 1–16.
- [52] K. Ichihara, K. Yoneda, A. Takahashi, N. Hoshino, M. Matsuda, Improved methods for the fatty acid analysis of blood lipid classes, *Lipids* 46 (2011) 297–306.
- [53] J. Wattanakul, M. Sahaka, S. Amara, S. Mansor, B. Gontero, F. Carrière, et al., In vitro digestion of galactolipids from chloroplast-rich fraction (CRF) of postharvest, pea vine field residue (Haulm) and spinach leaves, *Food Funct.* 10 (2019) 7806–7817.
- [54] I. Criado-Navarro, A. Mena-Bravo, M. Calderón-Santiago, F. Priego-Capote, Profiling analysis of phospholipid fatty acids in serum as a complement to the comprehensive fatty acids method, *J. Chromatogr. A* 11 (2020). Feb:460965.
- [55] C. Cruz-Hernandez, S.K. Thakkar, I. Masserey-Elmelegy, W. Buosi, P. Fontannaz, F. Giuffrida, Quantification of fatty acids in erythrocytes and plasma by fast gas chromatography, *J. Sep. Sci.* 40 (2017) 3289–3300.
- [56] S.P. Alves, A.R.J. Cabrita, A.J.M. Fonseca, R.J.B. Bessa, Improved method for fatty acid analysis in herbage based on direct transesterification followed by solid-phase extraction, *J. Chromatogr. A* 1209 (2008) 212–219.
- [57] M.J. Griffiths, R.P. van Hille, S.T. Harrison, Selection of direct transesterification as the preferred method for assay of fatty acid content of microalgae, *Lipids* 45 (11) (2010) 1053–1060.
- [58] T. Lewis, P.D. Nichols, T.A. McMeekin, Evaluation of extraction methods for recovery of fatty acids from lipid-producing microheterotrophs, *J. Microbiol. Methods* 43 (2000) 107–116.
- [59] J.V. O Fallon, J.R. Busboom, M.L. Nelson, T. Gaskins, A direct method for fatty acid methyl ester synthesis: application to wet meat tissues, oils, and feedstuffs, *J. Anim. Sci.* 85 (2007) 1511–1521.
- [60] K.M. Maria John, S. Natarajan, D.L. Luthria, Metabolite changes in nine different soybean varieties grown under field and greenhouse conditions, *Food Chem.* 211 (2016) 347–355.
- [61] F. Xia, R. Feng, F.G. Xu, H. Su, C. He, Y.J. Hu, et al., Quantification of phospholipid fatty acids by chemical isotope labeling coupled with atmospheric pressure gas chromatography quadrupole- time-of-flight mass spectrometry (APGC/Q-TOF MS), *Anal. Chim. Acta* 1082 (2019) 86–97.
- [62] S. Shibamoto, A. Gooley, K. Yamamoto, Separation behavior of octadecadienoic acid isomers and identification of cis- and trans-isomers using gas chromatography, *Lipids* 50 (2015) 85–100.
- [63] P.G. Toral, G. Hervás, H. Leskinen, K.J. Shingfield, P. Frutos, In vitro ruminal biohydrogenation of eicosapentaenoic (EPA), docosapentaenoic (DPA), and docosahexaenoic acid (DHA) in cows and ewes: intermediate metabolites and pathways, *J. Dairy Sci.* 101 (7) (2018) 6109–6121.

- [64] W. Xia, S.M. Budge, Simultaneous quantification of epoxy and hydroxy fatty acids as oxidation products of triacylglycerols in edible oils, *J. Chromatogr. A* 1537 (2018) 83–90.
- [65] A. Sehl, L. Couédelo, L. Fonseca, C. Vaysse, M. Cansell, A critical assessment of transmethylation procedures for n-3 long-chain polyunsaturated fatty acid quantification of lipid classes, *Food Chem.* 251 (2018) 1–8.
- [66] E. Pereira, A. Napp, J.V. Braun, L.A.M. Fontoura, M. Seferin, J. Ayres, et al., Development and validation of analytical methodology by GC-FID using hexadecyl propanoate as an internal standard to determine the bovine tallow methyl esters content, *J. Chromatogr. B. Anal. Technol. Biomed. Life Sci.* 1093–1094 (2018) 134–140.
- [67] G. Micalizzi, E. Ragosta, S. Farnetti, P. Dugo, P.Q. Tranchida, L. Mondello, et al., Rapid and miniaturized qualitative and quantitative gas chromatography profiling of human blood total fatty acids, *Anal. Bioanal. Chem.* 412 (10) (2020) 2327–2337.
- [68] A.R. Behera, K. Dutta, P. Verma, A. Daverey, D.K. Sahoo, High lipid accumulating bacteria isolated from dairy effluent scum grown on dairy wastewater as potential biodiesel feedstock, *J. Environ. Manag.* 252 (2019) 1–10.
- [69] W. Stoffel, F. Chu, E.H. Ahrens, Analysis of long-chain fatty acids by gas-liquid chromatography. Micromethod for preparation of methyl esters, *Anal. Chem.* 31 (1959) 307–308.
- [70] K. Eulitz, M.P. Yurawecz, N. Sehat, J. Fritsche, J.A.G. Roach, M.M. Mossoba, et al., Preparation, separation, and confirmation of the eight geometrical cis/trans conjugated linoleic acid isomers 8,10 – through 11,13–18:2, *Lipids* 34 (1999) 873–877.
- [71] R.L. Wolff, N.A. Combe, F. Destailats, C. Boué, D. Precht, J. Molquentin, et al., Follow-up of the $\Delta 4$ to $\Delta 16$ Trans-18:1 isomer profile and content in French processed foods containing partially hydrogenated vegetable oils during the period 1995–1999. Analytical and nutritional implications, *Lipids* 35 (2000) 815–825.
- [72] D. Precht, J. Molquentin, C18:1, C18:2 and C18:3 trans and cis fatty acid isomers including conjugated cis $\Delta 9$, trans $\Delta 11$ linoleic acid (CLA) as well as total fat composition of German human milk lipids, *Nahrung* 43 (1999) 233–244.
- [73] J.K.G. Kramer, C. Cruz-Hernandez, J. Zhou, Conjugated linoleic acids and octadecenoic acids: analysis by GC, *Eur. J. Lipid Sci. Technol.* 103 (2001) 600–609.
- [74] J.K.G. Kramer, C.B. Blackadar, J. Zhou, Evaluation of two GC columns (60-m SUPELCOWAX 10 and 100-m CP Sil 88) for analysis of milkfat with emphasis on CLA, 18:1, 18:2 and 18:3 isomers, and short- and long-chain FA, *Lipids* 37 (2002) 823–835.
- [75] R.L. Wolff, D. Precht, A critique of 50-m CP Sil 88 capillary columns used alone to assess trans-unsaturated FA in foods: the case of the TRANSFAIR study, *Lipids* 37 (2002) 627–629.
- [76] D. Precht, J. Molquentin, Overestimation of linoleic acid and trans-C18:2 isomers in milk fats with emphasis on Δ trans 9, Δ trans 12-octadecadienoic acid, *Milchwissenschaft* 58 (2003) 30–34.
- [77] R.J.B. Bessa, P.V. Portugal, I.A. Mendes, J. Santos-Silva, Effect of lipid supplementation on growth performance, carcass and meat quality and fatty acid composition of intramuscular lipids of lambs fed dehydrated lucerne or concentrate, *Livest. Prod. Sci.* 96 (2005) 185–194.
- [78] K.S. Park, Y.J. Kim, E.K. Choe, Composition characterization of fatty acid zinc salts by chromatographic and NMR spectroscopic analyses on their fatty acid methyl esters, *J. Anal. Methods Chem.* 2019 (2019) 1–11.
- [79] R.L. Wolff, Analysis of alpha-linolenic acid geometrical isomers in deodorized oils by capillary gas-liquid chromatography on cyanoalkyl polysiloxane phases: a note of caution, *J. Am. Oil Chem. Soc.* 71 (1994) 907–909.
- [80] J.K.G. Kramer, N. Sehat, M.E.R. Dugan, M.M. Mossoba, M.P. Yurawecz, J.A.G. Roach, et al., Distribution of conjugated linoleic acid (CLA) isomers in tissue lipid classes of pigs fed a commercial CLA mixture determined by gas chromatography and silver ion-high performance liquid chromatography, *Lipids* 33 (1998) 549–558.
- [81] J.K.G. Kramer, N. Sehat, J. Fritsche, M.M. Mossoba, K. Eulitz, M.P. Yurawecz, et al., Separation of conjugated linoleic acid isomers, in: M.P. Yurawecz, M.M. Mossoba, J.K.G. Kramer, M.W. Pariza, G.J. Nelson (Eds.), *Advances in Conjugated Linoleic Acid Research*, vol. 1, AOCS Press, Champaign, IL, USA, 1999, pp. 83–109.
- [82] D. Precht, H. Hagemeister, W. Kanitz, J. Voigt, Trans fatty acids and conjugated linoleic acids in milk fat from dairy cows fed a rumen-protected linoleic acid rich diet, *Kiel. Milchwirtsch. Forschungsber.* 54 (2002) 225–242.
- [83] S. Banni, J.-C. Martin, Conjugated linoleic acid and metabolites, in: J.-L. Sébédio, W.W. Christie (Eds.), *Trans Fatty Acids in Human Nutrition*, The Oily Press, Dundee, UK, 1998, pp. 261–302.
- [84] F. Lavillonnière, J.C. Martin, P. Bougnoux, J.-L. Sébédio, Analysis of conjugated linoleic acid isomers and content in French cheeses, *J. Am. Oil Chem. Soc.* 75 (1998) 343–352.

- [85] F. Destaillets, P. Angers, Directed sequential synthesis of conjugated linoleic acid isomers from $\Delta 7,9$ to $\Delta 12,14$, *Eur. J. Lipid Sci. Technol.* 105 (2003) 3–8.
- [86] W.W. Christie, J.L. Sébédio, P. Juanéda, A practical guide to the analysis of conjugated linoleic acid, *Inform* 12 (2001) 147–152.
- [87] J.A.G. Roach, M.P. Yurawecz, J.K.G. Kramer, M.M. Mossoba, K. Eulitz, Y. Ku, Gas chromatography-high resolution selected-ion mass spectrometric identification of trace 21:0 and 20:2 fatty acids eluting with conjugated linoleic acid isomers, *Lipids* 35 (2000) 797–802.
- [88] AOCS Official Method Ce 1h-05, Determination of Cis-, Trans-, Saturated, Monounsaturated and Polyunsaturated Fatty Acids in Non-ruminant Animal Oils and Fats by Capillary GLC, Sampling and Analysis of Commercial Fats and Oils, AOCS, Champaign, IL, USA, 2005.
- [89] F. Destaillets, P. Angers, Base-catalyzed derivatization methodology for FA analysis. Application to milk fat and celery seed lipid TAG, *Lipids* 37 (2002) 527–532.
- [90] D. Precht, J. Molkenin, Frequency and distributions of conjugated linoleic acid and trans fatty acid contents in European bovine milk fats, *Milchwissenschaft* 55 (2000) 687–691.
- [91] Z. Wasta, S.A. Mjøs, A database of chromatographic properties and mass spectra of fatty acid methyl esters from omega-3 products, *J. Chromatogr. A* 1299 (2013) 94–102.
- [92] P. Delmonte, A.R.F. Kia, J.K.G. Kramer, M.M. Mossoba, L. Sidisky, J.I. Rader, Separation characteristics of fatty acid methyl esters using SLB-IL111, a new ionic liquid coated capillary gas chromatographic column, *J. Chromatogr. A* 1218 (3) (2011) 545–554.
- [93] A.R. Fardin-Kia, P. Delmonte, J.K. Kramer, G. Jahreis, K. Kuhnt, V. Santercole, et al., Separation of the fatty acids in menhaden oil as methyl esters with a highly polar ionic liquid gas chromatographic column and identification by time of flight mass spectrometry, *Lipids* 48 (12) (2013) 1279–1295.
- [94] C. Cagliero, M. Mazzucotelli, P. Rubiolo, A. Marengo, S. Galli, J.L. Anderson, et al., Can the selectivity of phosphonium based ionic liquids be exploited as stationary phase for routine gas chromatography? A case study: the use of trihexyl(tetradecyl) phosphonium chloride in the flavor, fragrance and natural product fields, *J. Chromatogr. A* (2020). Feb, 460969.
- [95] M.W.-H. Li, X. Huang, H. Zhu, K. Kurabayashi, X. Fan, Microfabricated ionic liquid column for separations in dry air, *J. Chromatogr. A*. (2020). Feb 27; 461002.
- [96] S. Pojjanapornpun, C. Kulsing, P. Kakanopas, Y. Nolvachai, K. Aryusuk, K. Krisnangkura, et al., Simulation of peak position and response profiles in comprehensive two-dimensional gas chromatography, *J. Chromatogr. A* 1607 (2019) 1–9.
- [97] C.C. Lin, Z. Wasta, S.A. Mjøs, Evaluation of the retention pattern on ionic liquid columns for gas chromatographic analyses of fatty acid methyl esters, *J. Chromatogr. A* 1350 (2014) 83–91.
- [98] A.X. Zeng, S.T. Chin, Y. Nolvachai, C. Kulsing, L.M. Sidisky, P.J. Marriott, Characterisation of capillary ionic liquid columns for gas chromatography-mass spectrometry analysis of fatty acid methyl esters, *Anal. Chim. Acta* 803 (2013) 166–173.
- [99] S. Pojjanapornpun, Y. Nolvachai, K. Aryusuk, C. Kulsing, K. Krisnangkura, P.J. Marriott, Ionic liquid phases with comprehensive two-dimensional gas chromatography of fatty acid methyl esters, *Anal. Bioanal. Chem.* 410 (2018) 4669–4677.
- [100] S. Shirasawa, A. Sasaki, Y. Saida, C. Satoh, A rapid method for trans-fatty acid determination using a single capillary GC, *J. Oleo Sci.* 56 (2) (2007) 53–58.
- [101] A.K. Vickers, M. Hastings, R. Lautamo, R. Davis, S. Watkins, New High Polarity bis(cyanopropyl) Siloxane Stationary Phase for GC Resolution of Positional and Geometric Isomers of Fatty Acid Methyl Esters, Agilent Technologies, November 11, 2004, 5989-181EN.
- [102] X. Dai, T. Yuan, X. Zhang, Q. Zhou, H. Bi, R. Yu, et al., Short-chain fatty acid (SCFA) and medium-chain fatty acid (MCFA) concentrations in human milk consumed by infants born at different gestational ages and the variations in concentration during lactation stages, *Food Funct.* 11 (2) (2020) 1869–1880.
- [103] J. Peene, J. de Zeeuw, F. Biermans, L. Joziassse, CP-Select CB for FAME, A New Highly Polar Bonded Stationary Phase with a Temperature Stability up to 290 °C Optimized for Analyzing Cis- and Trans FAME Isomers with GC, #P-147, Varian Inc, Middelburg, The Netherlands, 2004.
- [104] P. Juaneda, S. Brac de la Perriere, J.L. Sebedio, S. Gregoire, Influence of heat and refining on formation of CLA isomers in sunflower oil, *J. Am. Oil Chem. Soc.* 80 (2003) 937–940.
- [105] F. Destaillets, J.P. Trottier, J.M.G. Galvez, P. Angers, Analysis of alpha-linolenic acid biohydrogenation intermediates in milk fat with emphasis on conjugated linolenic acids, *J. Dairy Sci.* 88 (2005) 3231–3239.
- [106] K. Yoshinaga, Y. Kawamura, T. Kitayama, T. Nagai, H. Mizobe, K. Kojima, et al., Regiospecific distribution of trans-octadecenoic acid positional isomers in triacylglycerols of partially hydrogenated vegetable oil and ruminant fat, *J. Oleo Sci.* 64I (2015) 617–624.

- [107] P. Gómez-Cortés, M.A. de la Fuente, Classification of human milks based on their trans 18:1 fatty acid profile and effect of maternal diet, *Breastfeed. Med.* 12 (2017) 238–243.
- [108] R.S.S. Costa, F.S. Santos, D.B. Mucci, T.V. Souza, F.L.C. Sardinha, C.R.M.M. Chaves, et al., Trans fatty acids in colostrum, mature milk and diet of lactating adolescents, *Lipids* 51 (2016) 1363–1373.
- [109] J.K.G. Kramer, M.R. Hernandez, C. Cruz-Hernandez, J. Kraft, M.E.R. Dugan, Combining results of two GC separations partly achieves determination of all cis and trans 16:1, 18:1, 18:2, 18:3 and CLA isomers of milk fat as demonstrated using Ag-ion SPE fractionation, *Lipids* 43 (2008) 259–273.
- [110] G. Dobson, W.W. Christie, B. Nikolova-Damyanova, Silver ion chromatography of lipids and fatty acids, *J. Chromatogr. B* 671 (1995) 197–222.
- [111] B. Nikolova-Damyanova, W.W. Christie, B. Herslöf, Mechanistic aspects of fatty acid retention in silver ion chromatography, *J. Chromatogr. A* 749 (1996) 47–54.
- [112] L.J. Morris, Separations of lipids by silver ion chromatography, *J. Lipid Res.* 7 (1966) 717–732.
- [113] D. Precht, J. Molketin, Rapid analysis of the isomers of trans-octadecenoic acid in milk fat, *Int. Dairy J.* 6 (1996) 791–809.
- [114] B. Nikolova-Damyanova, B.G. Herslof, W.W. Christie, Silver ion high-performance liquid chromatography of derivatives of isomeric fatty acids, *J. Chromatogr. A* 609 (1992) 133–140.
- [115] P. Delmonte, J.K.G. Kramer, S. Banni, M.P. Yurawecz, New developments in silver ion and reverse phase HPLC of CLA, in: M.P. Yurawecz, J.K.G. Kramer, M.M. Mossoba, O. Gudmundsen, M.W. Pariza, S. Banni (Eds.), *Advances in Conjugated Linoleic Acid Research*, vol. 3, AOCS Press, Champaign, IL, USA, 2006, pp. 95–118.
- [116] R.L. Wolff, D. Precht, Comments on the resolution of individual trans-18:1 isomers by gas-liquid chromatography, *J. Am. Oil Chem. Soc.* 75 (1998) 421–422.
- [117] A.A. Abu-Ghazaleh, D.J. Schingoethe, A.R. Hippen, Conjugated linoleic acid and other beneficial fatty acids in milk fat from cows fed soybean meal, fish meal, or both, *J. Dairy Sci.* 84 (2001) 1845–1850.
- [118] R.J. Baer, J. Ryali, D.J. Schingoethe, K.M. Kasperson, D.C. Donovan, A.R. Hippen, et al., Composition and properties of milk and butter from cows fed fish oil, *J. Dairy Sci.* 84 (2001) 345–353.
- [119] D.C. Donovan, D.J. Schingoethe, R.J. Baer, J. Ryali, A.R. Hippen, S.T. Franklin, Influence of dietary fish oil on conjugated linoleic acid and other fatty acids in milk fat from lactating dairy cows, *J. Dairy Sci.* 83 (2000) 2620–2628.
- [120] A.A. Abu-Ghazaleh, D.J. Schingoethe, A.R. Hippen, L.A. Whitlock, Feeding fish meal and extruded soybeans enhances the conjugated linoleic acid (CLA) content of milk, *J. Dairy Sci.* 85 (2002) 624–631.
- [121] C.A. Weatherly, Y. Zhang, J.P. Smuts, H. Fan, C. Xu, K.A. Schug, et al., Analysis of long-chain unsaturated fatty acids by ionic liquid gas chromatography, *J. Agric. Food Chem.* 64 (6) (2016) 1422–1432.
- [122] K. Yoshinaga, M. Asanuma, H. Mizobe, K. Kojima, T. Nagai, F. Beppu, et al., Characterization of cis- and trans-octadecenoic acid positional isomers in edible fat and oil using gas chromatography-flame ionisation detector equipped with highly polar ionic liquid capillary column, *Food Chem.* 160 (2014) 39–45.
- [123] P. Gómez-Cortés, V. Rodríguez-Pino, M. Juárez, M.A. de la Fuente, Optimization of milk odd and branched-chain fatty acids analysis by gas chromatography using an extremely polar stationary phase, *Food Chem.* 231 (2017) 11–18.
- [124] P. Korytár, H.G. Jansen, E. Matisova, U.A.T. Brinkman, Practical fast gas chromatography: methods, instrumentation and applications, *Trends Anal. Chem.* 21 (2002) 558–572.
- [125] M. vanDeursen, J. Beens, C.A. Cramers, Possibilities and limitations of fast temperature programming as a route towards fast GC, *J. High Resolut. Chromatogr.* 22 (1999) 509–513.
- [126] L.M. Blumberg, M.S. Klee, Method translation and retention time locking in partition GC, *Anal. Chem.* 70 (1998) 3828–3839.
- [127] J. Ecker, M. Scherer, G. Schmitz, G. Liebisch, A rapid GC–MS method for quantification of positional and geometric isomers of fatty acid methyl esters, *J. Chromatogr. B* 15 (2012) 98–104.
- [128] J.M. Clemons, T.J. Thomas, Fast process gas chromatography, in: *Proceedings of the 45th annual ISA analysis division symposium, West Virginia, 45th Annual ISA analysis division symposium, Charleston, vol. 33, April 9–12, 2000*, pp. 115–128.
- [129] F. Magni, P.M. Piatti, L.D. Monti, P. Lecchi, A.E. Pontiroli, G. Pozza, et al., Fast gas chromatographic-mass spectrometric method for the evaluation of plasma fatty acid turnover using [1-¹³C] palmitate, *J. Chromatogr. B* 657 (1994) 1–7.
- [130] Y. Jiang, Y. Ni, H. Zhu, C. Zhu, Using fast gas chromatography-mass spectrometry with auto-headspace solid-phase microextraction to determine ultra trace residues of organophosphorus pesticides in fruits, *J. Chromatogr. Sci.* 49 (5) (2011) 353–360.

- [131] A.B. Fialkov, S.J. Lehotay, A. Amirav, Less than one minute low-pressure gas chromatography - mass spectrometry, *J. Chromatogr. A* 1612 (2020) 1–10.
- [132] S.F. Gallego, M. Hermansson, G. Liebisch, L. Hodson, C.S. Ejsing, Total fatty acid analysis of human blood samples in one minute by high-resolution mass spectrometry, *Biomolecules* 9 (2018) 1–16.
- [133] R. Inchingolo, V. Cardenia, M.T. Rodriguez-Estrada, Analysis of phytosterols and phytostanols in enriched dairy products by fast gas chromatography with mass spectrometry, *J. Sep. Sci.* 37 (20) (2014) 2911–2919.
- [134] T. Majchrzak, M. Lubinska, A. Różańska, T. Dymerski, J. Gebicki, J. Namieśnik, Thermal degradation assessment of canola and olive oil using ultra-fast gas chromatography coupled with chemometrics, *Monatsh. Chem.* 148 (9) (2017) 1625–1630.
- [135] W. Wojnowski, T. Majchrzak, T. Dymerski, J. Gebicki, J. Namieśnik, Poultry meat freshness evaluation using electronic nose technology and ultra-fast gas chromatography, *Monatsh. Chem.* 148 (9) (2017) 1631–1637.
- [136] C. Bicchi, C. Brunelli, C. Cordero, P. Rubiolo, M. Galli, A. Sironi, Direct resistively heated column gas chromatography (ultrafast module-GC) for high-speed analysis of essential oils of differing complexities, *J. Chromatogr. A* 1024 (2004) 195–207.
- [137] C. Bicchi, C. Brunelli, M. Galli, A. Sironi, Conventional inner diameter short capillary columns: an approach to speeding up gas chromatographic analysis of medium complexity samples, *J. Chromatogr. A* 931 (2001) 129–140.
- [138] L. Mondello, A. Casilli, P.Q. Tranchida, R. Costa, P. Dugo, G. Dugo, Fast GC for the analysis of citrus oils, *J. Chromatogr. Sci.* 42 (2004) 410–416.
- [139] L. Mondello, A. Casilli, P.Q. Tranchida, M. Furukawa, K. Komori, K. Miseri, et al., Fast enantiomeric analysis of a complex essential oil with an innovative multidimensional gas chromatographic system, *J. Chromatogr. A* 1105 (2006) 11–16.
- [140] M.J. Bogusz, S. Abu El Hajj, Z. Ehaideb, H. Hassan, M. Al-Tufail, Rapid determination of benzo(a)pyrene in olive oil samples with solid-phase extraction and low-pressure, wide-bore gas chromatography–mass spectrometry and fast liquid chromatography with fluorescence detection, *J. Chromatogr. A* 1026 (2004) 1–7.
- [141] F.L. Godoi, V. Wagner, R.H.M. Godoi, L.V. Vaeck, R.V. Grieken, Application of low-pressure gas chromatography–ion-trap mass spectrometry to the analysis of the essential oil of *Turnera diffusa* (Ward.) Urb., *J. Chromatogr. A* 1027 (2004) 127–130.
- [142] L. Mondello, P.Q. Tranchida, R. Costa, A. Casilli, G. Dugo, A. Cotroneo, et al., Fast GC for the analysis of fats and oils, *J. Sep. Sci.* 26 (2003) 1467–1473.
- [143] F. David, D.R. Gere, F. Scanlan, P. Sandra, Instrumentation and applications of fast high-resolution capillary gas chromatography, *J. Chromatogr. A* 842 (1999) 309–319.
- [144] I. Bondia-Pons, C. Moltó-Puigmartí, A.I. Castellote, M.C. López-Sabater, Determination of conjugated linoleic acid in human plasma by fast gas chromatography, *J. Chromatogr. A* 1157 (2007) 422–429.
- [145] Z. Meng, D. Wen, D. Sun, F. Gao, W. Li, Y. Liao, et al., Rapid determination of C12–C26 non-derivatized fatty acids in human serum by fast gas chromatography, *J. Sep. Sci.* 30 (2007) 1537–1543.
- [146] M.A. Masood, K.D. Stark, N. Salem Jr., A simplified and efficient method for the analysis of fatty acid methyl esters suitable for large clinical studies, *J. Lipid Res.* 46 (2005) 2299–2305.
- [147] M.A. Masood, N. Salem Jr., High-throughput analysis of plasma fatty acid methyl esters employing robotic transesterification and fast gas chromatography, *Lipids* 43 (2008) 171–180.
- [148] I. Bondia-Pons, S. Morera-Pons, A.I. Castellote, M.C. López-Sabater, Determination of phospholipid fatty acids in biological samples by solid-phase extraction and fast gas chromatography, *J. Chromatogr. A* 1116 (2006) 204–208.
- [149] F. Destailats, C. Cruz-Hernandez, Fast analysis by gas-liquid chromatography, *J. Chromatogr. A* 1169 (1–2) (2007) 175–178.
- [150] C. Cruz-Hernandez, F. Destailats, Recent advances in fast gas-chromatography: application to the separation of fatty acid methyl esters perspective on the resolution of complex fatty acid compositions, *J. Liq. Chromatogr. Relat. Technol.* 32 (2009) 1672–1688.
- [151] L. Mondello, R. Shellie, A. Casilli, P.Q. Tranchida, P. Marriott, G. Dugo, Ultra-fast essential oil characterization by capillary GC on a 50 microm ID column, *J. Sep. Sci.* 27 (2004) 699–702.
- [152] P.Q. Tranchida, M. Mondello, D. Sciarrone, P. Dugo, G. Dugo, L. Mondello, Evaluation of use of a very short polar microbore column segment in high-speed gas chromatography analysis, *J. Sep. Sci.* 31 (2008) 2634–2639.
- [153] F. Destailats, M. de Wispelaere, F. Joffre, Authenticity of milk fat by fast analysis of triacylglycerols: application to the detection of partially hydrogenated vegetable oils, *J. Chromatogr. A* 1131 (2006) 227–234.
- [154] R.J. Craven, R.W. Lencki, Rapid analysis of acylglycerols in low molecular weight milk fat fractions, *Lipids* 42 (2007) 473–482.
- [155] P. Angers, J. Arul, A simple method for regiospecific analysis of triacylglycerols by gas chromatography, *J. Am. Oil Chem. Soc.* 76 (4) (1999).

- [156] AOCS Official Method Cd 11b-91, Determination of Mono- and Diglycerides by Capillary Gas Chromatography, Sampling and Analysis of Commercial Fats and Oils, AOCS, Champaign, IL, USA, 2009.
- [157] H.L. Nang Lau, C.W. Pua, Y.M. Choo, A.N. Ma, Simultaneous quantification of free fatty acids, free sterols, squalene, and acylglycerol molecular species in palm oil by high-temperature gas chromatography-flame, *Lipids* 40 (5) (2005) 523–528.
- [158] P. Fagan, C. Wijesundera, Determination of mono- and di-acylglycerols in milk lipids, *J. Chromatogr. A* 1054 (2004).
- [159] V.A. Isidorov, Gas chromatographic retention indices of biologically and environmentally important organic compounds on capillary columns with low-polar stationary phases, *J. Chromatogr. A* 1216 (2009) 8998–9007.
- [160] V.A. Isidorov, M. Rusak, L. Szczepaniak, Gas chromatographic retention indices of trimethylsilyl derivatives of mono- and diglycerides on capillary columns with non-polar stationary phases, *J. Chromatogr. A* 1166 (2007) 207–211.
- [161] F. Destailats, C. Cruz-Hernandez, K. Nagy, Identification of monoacylglycerol regio-isomers by gas chromatography–mass spectrometry, *J. Chromatogr. A* 1217 (2010).
- [162] G. Flanagan, A.A. Andrianova, J. Casey, E. Hellrung, B.A. Diep, A. Seames, et al., Simultaneous high-temperature gas chromatography with flame ionization and mass spectrometric analysis of monocarboxylic acids and acylglycerols in biofuels and biofuel intermediate products, *J. Chromatogr. A* 1584 (2019) 165–178.
- [163] C.F. Torres, D. Tenllado, F.J. Señorans, A versatile GC method for the analysis of alkylglycerols and other neutral lipid classes, *Chromatographia* 269 (2009) 729–734.
- [164] T. Verleyen, R. Verhé, L. Garcia, K. Dewettinck, Gas chromatographic characterization of vegetable oil deodorization distillate, *J. Chromatogr. A* 921 (2001) 277–285.
- [165] A. Lytovchenko, R. Beleggia, N. Schauer, T. Isaacson, J.E. Leuendoff, H. Hellmann, et al., Application of GC-MS for the detection of lipophilic compounds in diverse plant tissues, *Plant Methods* 5 (2009) 1–11.
- [166] R. Michael-Jubeli, J. Bleton, High-temperature gas chromatography–mass spectrometry for skin surface lipids profiling, *J. Lipid Res.* 52 (2011) 143–151.
- [167] F.J.M. Novaes, C. Kulsing, H.R. Bizzo, F.R. de Aquino Neto, C.M. Rezende, P.J. Marriott, Analysis of underivatized low volatility compounds by comprehensive two-dimensional gas chromatography with a short primary column, *J. Chromatogr. A* 1536 (2018) 75–81.
- [168] Z. Yu, H. Huang, A. Reim, P.D. Charles, A. Northage, D. Jackson, et al., Optimizing 2D gas chromatography mass spectrometry for robust tissue, serum and urine metabolite profiling, *Talanta* 165 (2017) 685–691.
- [169] G. Brufau, R. Codony, M.A. Canela, Rapid and quantitative determination of total sterols of plant and animal origin in liver samples by gas chromatography, *Chromatographia* 64 (2006) 559–563.
- [170] M.L. Forchielli, G. Bersani, S. Tala, G. Grossi, The spectrum of plant and animal sterols in different oil-derived intravenous emulsions, *Lipids* 45 (2010) 63–71.
- [171] L.M. Clement, S.L. Hansen, C.D. Costin, Quantitation of sterols and sterol esters in fortified foods and beverages by GC/FID, *J. Am. Oil Chem. Soc.* 87 (2010) 973–980.
- [172] J.C. Bada, M. León-Camacho, M. Prieto, Characterization of walnut oils (*Juglans regia* L.) from Asturias, Spain, *J. Am. Oil Chem. Soc.* 87 (2010) 1469–1474.
- [173] Y. Liu, G. Yong, Y. Xu, D. Zhu, H. Tong, S. Liu, Simultaneous determination of free and esterified fatty alcohols, phytosterols and solanesol in tobacco leaves by GC, *Chromatographia* 71 (7–8) (2010) 727–732.
- [174] K.M. Al-Ismail, A.K. Alsaed, R. Ahmad, Detection of olive oil adulteration with some plant oils by GLC analysis of sterols using polar column, *Food Chem.* 121 (2010) 1255–1259.
- [175] S. Duong, N. Strobel, S. Buddhadasa, K. Stockham, M. Auldist, B. Wales, et al., Rapid measurement of phytosterols in fortified food using gas chromatography with flame ionization detection, *Food Chem.* 211 (2016) 570–576.
- [176] S. Duong, N. Strobel, S. Buddhadasa, K. Stockham, M.J. Auldist, M. Wales, et al., Influence of acid hydrolysis, saponification and sample clean-up on the measurement of phytosterols in dairy cattle feed using GC–MS and GC with flame ionization detection, *J. Separ. Sci.* 41 (17) (2018) 3467–3476.
- [177] S. Grasso, N.P. Brunton, F.J. Monahan, S.M. Harrison, Development of a method for the analysis of sterols in sterol-enriched deli-style Turkey with GC-FID, *Food Anal. Methods* 9 (3) (2016) 724–728.
- [178] A. Barnsteiner, T. Lubinus, A. Di Gianvito, W. Schmid, K.H. Engel, GC-based analysis of plant stanyl fatty acid esters in enriched foods, *J. Agric. Food Chem.* 59 (10) (2011) 5204–5214.
- [179] D. Noto, A.B. Cefalù, G. Barraco, E. Martino, Plasma non-cholesterol sterols: a useful diagnostic tool in pediatric hypercholesterolemia, *Pediatr. Res.* 67 (2) (2010) 200–204.

- [180] A. Kuksis, J.J. Myher, Quantitation of plasma lipids by gas-liquid chromatography on high temperature polarizable capillary columns, *J. Lipid Res.* 34 (1993) 1029–1038.
- [181] B. Pieber, S. Schober, C. Goebel, Novel sensitive determination of steryl glycosides in biodiesel by gas chromatography-mass spectroscopy, *J. Chromatogr. A* 1217 (2010) 6555–6561.
- [182] S. Yu, Y. Zhang, Y. Ran, W. Lai, Z. Ran, J. Xu, et al., Characterization of steryl glycosides in marine microalgae by gas chromatography-triple quadrupole mass spectrometry (GC-QQQ-MS), *J. Sci. Food Agric.* 98 (4) (2018) 1574–1583.
- [183] L. Zhang, Y. Yun, Y. Liang, Discovery of mass spectral characteristics and automatic identification of wax esters from gas chromatography mass spectrometry data, *J. Chromatogr. A* 1217 (2010) 3695–3701.
- [184] A. Aragon, J.M. Cortes, R.M. Toledano, J. Villen, Analysis of wax esters in edible oils by automated on-line coupling liquid chromatography-gas chromatography using the through oven transfer adsorption desorption, *J. Chromatogr. A* 1218 (2010) 4960–4965.

Gas chromatographic analysis of carbohydrates

A.C. Soria, A. Mena, A.I. Ruiz-Matute, M.L. Sanz

Instituto de Química Orgánica General (CSIC), Madrid, Spain

28.1 Introduction

Carbohydrates are biomolecules mainly composed of carbon, hydrogen, and oxygen, although they also include derivatives with other bioelements such as nitrogen, sulfur, and phosphorus. They are the most abundant form of organic carbon on the earth's surface, being present in the cells of all living organisms as free or bound molecules. They are involved in many vital functions; they act as the main source of cell energy and reserve, they are structural components and participate in a number of biological processes such as cell adhesion, cell signaling, and the regulation of biochemical pathways, etc. [1]. Moreover, carbohydrates have interesting technological functionalities that, in addition to their bioactive properties, are currently attracting a great deal of interest in the food, cosmetic, and pharmaceutical industries.

Carbohydrate bioactivities and functions are closely related to their structures. Therefore, characterization of the carbohydrate composition of a sample, in as much detail as possible, is of great interest for different applications.

Depending on the degree of polymerization (DP), carbohydrates can be classified as monosaccharides, oligosaccharides (usually DP 2–10), or polysaccharides. The wide number of structural isomers, associated with multiple linkage positions and different stereochemistry, together with the fact that carbohydrates are generally present in nature as heterogeneous and complex mixtures, make their characterization challenging. Moreover, the generic term “carbohydrate” also includes other derivatives obtained by reduction of carbonyl groups (alditols), by oxidation of one or more terminal groups to carboxylic acids, or by substitution of one or more hydroxyl groups by hydrogen, amino, thiol, etc., atoms [2].

High-resolution techniques such as gas chromatography (GC), and its coupling to mass spectrometry (GC-MS), which allows structural characterization, are widely used for the analysis of complex carbohydrate mixtures [3]. However, due to the low volatility of carbohydrates, GC is generally limited to the analysis of low-molecular-weight carbohydrates (LMWCs), and a derivatization process is mandatory to confer the required volatility and stability.

Before analysis, different sample pretreatments are utilized. Extraction and/or fractionation, cleanup, etc., are usually required to isolate target carbohydrates from the sample matrix. Other sample treatments such as hydrolysis are sometimes applied when the monomeric or linkage composition of carbohydrates of high molecular weight is to be determined.

This chapter covers the most recent developments in the application of GC to the analysis of carbohydrates, setting out not the different steps for sample preparation and chromatographic conditions usually employed, as well as the advantages of coupling GC to MS for the structural elucidation of unknown carbohydrates. Moreover, the utility of GC for the analysis of high-molecular-weight carbohydrates (oligo- and polysaccharides), after sample pretreatment, is also addressed. Finally, the potential of two-dimensional techniques for the characterization of complex carbohydrate mixtures and future perspectives are discussed.

28.2 Sample preparation

Fig. 28.1 illustrates the typical sample preparation steps required in the analysis of carbohydrates of different DP by gas chromatographic-based techniques.

28.2.1 Cleanup

Cleanup is carried out to remove impurities such as proteins and lipids and to eliminate potential interferences (carboxylic acids, polyphenols, etc.) during analysis. Depending on the state of aggregation of the sample, cleanup procedures can be directly applied to liquids or be implemented after the extraction of solid samples. Solid-phase extraction (SPE) is the most popular alternative for sample cleanup prior to gas chromatographic analysis of carbohydrates, but other approaches based on filtration, desalting, etc., can be used as well [5].

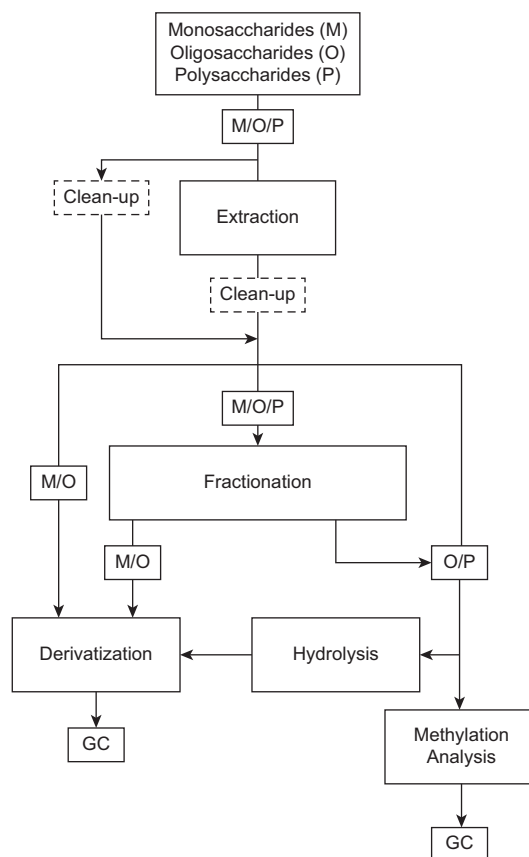


FIGURE 28.1 Scheme of sample preparation prior to gas chromatographic analysis of carbohydrates. Adapted with permission of Elsevier from M.L. Sanz, I. Martínez-Castro, Recent developments in sample preparation for chromatographic analysis of carbohydrates, *J. Chromatogr. A* 1153 (2007) 74–89.

28.2.2 Extraction and fractionation

Solvent selection is the most important step for extraction and fractionation affecting the efficiency and selectivity of the process. Most carbohydrates, except for those with high DP, are soluble in water. Despite advantages in terms of greenness and affordability of this solvent, water offers poor selectivity for carbohydrate extraction, and aqueous–alcohol mixtures (with different percentages of methanol or ethanol) are usually employed. Varying the

composition of these mixtures allows tuning the selectivity of the extraction for target carbohydrates [6–9]. Moreover, the addition of organic solvents after extraction is commonly used as a fractionation step for different purposes (e.g., lactulose *vs.* lactose fractionation [10], precipitation of polysaccharides [11], etc.). Acidic water improves the extraction of carbohydrates from plant matrices [12], but care should be taken as high concentrations of acid can cause the undesired hydrolysis of target carbohydrates.

As an alternative to conventional solvents, current research is mainly focused on evaluating solvents such as ionic liquids (ILs), deep eutectic solvents (DES), and natural deep eutectic solvents (NADES). ILs are organic salts formed by organic cations (e.g., imidazolium, pyridinium, pyrrolidinium, etc.) and organic or inorganic anions (e.g., chloride, dicyanamide, trifluoroacetate, etc.) with unique properties such as negligible vapor pressure over a wide temperature range, high thermal stability, high viscosity, and melting points lower than 100°C. DES are prepared by mixing hydrogen-bonding acceptors (HBA, mainly quaternary ammonium salts) and hydrogen-bonding donors (HBD, e.g., urea or a carboxylic acid) to form eutectic mixtures. They are considered NADES when molecules used as HBA and HBD are primary plant metabolites (e.g., sugars, alcohols, amino acids, organic acids, and choline derivatives) present in living organisms with important roles in cellular processes [13]. The availability of a large number of different combinations for their synthesis makes these solvents useful for selectivity tuning for target compound applications. Although DES and NADES have similar physical and chemical properties to ILs [14], eutectic solvents are easier to synthesize and more cost-competitive than conventional ILs, and most of them are environmentally friendly and nontoxic [15].

A number of studies have focused on the solubility of carbohydrates in different ILs [16–18], particularly on the solubilization of

polysaccharides such as lignocellulose, chitin, or starch for their recovery from biomass [19,20]. Several *in situ* transformations of these polysaccharides, such as esterification, acid-catalyzed hydrolysis, enzymatic transformations, or graft copolymerization, were reported to occur in IL media [20]. Moreover, combined procedures involving solubilization of polysaccharides in ILs (e.g., 1-butyl-3-methylimidazolium chloride, [C₄mim]Cl) followed by addition of different solvents (acetone/water, 3% (w/v) aqueous sodium hydroxide, etc.) were proposed for the selective precipitation of cellulose, hemicelluloses, and lignin from vegetable matrices, such as sugar cane bagasse [21].

However, the number of reports addressing the solubilization of LMWCs by ILs is much lower. Carrero-Carralero et al. [17] studied the solubility of LMWCs (mono-, di-, and trisaccharides) in different methylimidazolium-based ILs demonstrating a dependence on the structure of the target compounds. In general, ketoses were found to be more soluble than their corresponding aldoses, and trisaccharides showed a higher solubility than mono- and disaccharides. Teles et al. [22] evaluated the solubility of six monosaccharides in four ILs (dialkylimidazolium or tetraalkylphosphonium cations combined with dicyanamide, dimethylphosphate, or chloride anions) over the temperature range (15–75°C) to gain a better understanding of the anion and cation effects for the ILs, identifying some structure–property relationships. Among the ILs tested, [C₄C₁im][N(CN)₂] was the best solvent, providing a solubility value for D-(+)-glucose at 25°C higher (19 mol%) than for water (11 mol %). In general, enthalpic contributions were dominant and independent of the monosaccharide structure; however, the entropic contributions should also be taken into account, since they supported the differences observed in monosaccharide solubility. Moreover, the effect of the IL cation was found to be important.

Applications involving the use of ILs for fractionation of carbohydrates have been published, although further research is still required. As an example, methylimidazolium ILs allow the fractionation of bioactive ketoses from their corresponding aldoses [23] and the selective fractionation of polyols (acyclic sugar alcohols and inositols) from other LMWCs in binary mixtures [24]. Due to the low volatility of ILs, target compound recovery is a task worthy of further consideration since it also determines the reuse of the solvent. Several approaches were proposed for the recovery of carbohydrates; while selective precipitation is the most useful for polysaccharides [25,26]; approaches based on the use of active carbon [22], antisolvent effect [27], and column chromatography [28,29] were reported for LMWCs.

Similar to ILs, DES and NADES are useful for the solubilization of polysaccharides (lignin, cellulose, starch, chitin, chitosan, carrageenan, pectin, xylan, inulin, agar, and agarose) [30], mainly obtained from the delignification processes of agro-forest biowastes [31]. Solubilities for these polysaccharides are dependent on the DES composition. For instance, lignin was highly soluble (up to 14.9% at 100°C) in maleic acid/proline (1:3), whereas the solubility of cellulose was negligible in this solvent [32]. In a recent study by Häkkinen and Abbot [33], the solute-solvent interaction of mono-, di-, and polysaccharides in a variety of choline chloride-based DES was evaluated. In general, the solubility of carbohydrates in DES was good (up to 300 mg mL⁻¹); ethaline being the best solvent, with the lowest viscosity, and showing no degradation of carbohydrates compared with the more acidic DES tested. A eutectic mixture of choline chloride and glycolic and oxalic acids (1:1.7:0.3) was proposed to reduce the temperature of the thermal process for the valorization of alperujo, allowing the simultaneous extraction of alperujo polyphenols and sugars at 120°C [34].

Carbohydrates are typically extracted using conventional solid-liquid extraction (SLE) procedures. However, these methods present certain shortcomings associated with the use of high temperatures and extended extraction times, such as low efficiency and degradation of thermolabile carbohydrates, etc. To overcome these problems, a number of advanced extraction techniques have been trialed, such as ultrasound-assisted extraction (UAE), pressurized liquid extraction (PLE), microwave-assisted extraction (MAE), and supercritical fluid extraction (SFE) [35]. Among these, UAE and MAE are the most widely used for improved carbohydrate extraction before GC analysis.

The use of an additional source of energy, low-frequency (16–100 kHz) and high-power (80–200 W) ultrasounds in UAE and microwave radiation (2.45 GHz) in MAE, allows a more homogeneous heating of the solvent and an increase of cell disruption in the case of biological matrices. As a result, more efficient extractions in shorter times are accomplished. Advantages in terms of ease of use and moderate instrumentation investment have also contributed to the adoption of both techniques, in combination with GC, for the analysis of LMWCs [6–9,36,37] and, to a lesser extent, of polysaccharides [37–40].

Recent applications of MAE include the simultaneous extraction of inositols and galactooligosaccharides (GOS) from mung bean [36] or inositols and inulin from artichoke by-products [37], highlighting the faster extraction and yields of LMWC generally provided by this technique compared to SLE or PLE, respectively. Among others, UAE was utilized for the metabolomic analysis (including LMWCs) of *Salvia hispanica* [7,8], for the fingerprinting of polysaccharides from the genus *Astragalus* [39], and for the characterization of *Ziziphus jujuba* cv. Muzao galacturonic acid-rich polysaccharides [40], etc. Moreover, the sequential

use of MAE and UAE (MAE + UAE) was shown to be advantageous over the inverted approach (UAE + MAE), MAE, and UAE (yields in decreasing order) for the extraction of pectin from pomelo peels [41]. A commercial instrument for the simultaneous use of both techniques (Ultrasound-Microwave Assisted Extraction; UMAE) is now available and was used in a number of applications, for example, for extraction of oligosaccharides from lotus seeds [42] and water unextractable arabinoxylan from corn bran [11], etc.

The use of ILs, DES, NADES, in combination with advanced extraction techniques, was recently reported. As example, Brønsted acidic ILs (e.g., 3-methyl-1-(4-sulfonylbutyl)imidazolium hydrogensulfate) was employed in MAE [42] and UMAE [43] to obtain pectin-rich extracts from pomelo peels, demonstrating improved yields in a shorter time compared with traditional techniques using water and HCl solutions [43,44]. The use of malic acid:alanine:water (1:1:3) with MAE [45] and choline chloride:1,4-butanediol (1:4) with UAE [46] was also described to provide better extraction yields of soluble sugars and polysaccharides in banana puree and *Dioscorea opposita* samples, respectively, compared with hot water or ethanol as solvents.

In PLE, high temperatures combined with pressures high enough to keep the solvent in a liquid state above its atmospheric boiling point result in higher solvent diffusivity together with better solubilization and extraction kinetics of target compounds. Even though PLE commonly involves longer extraction times than UAE and MAE, it has been extensively used for the extraction of different types of carbohydrates, such as cyclitols and sugars [37,47–50], fructooligosaccharides [51], β -glucans [52,53], and inulin [37]. Most applications utilized water as a green solvent, in what is usually referred to as subcritical water extraction (SWE), but different choline chloride DES were also evaluated for the extraction of polysaccharides from

natural sources (e.g., alginate and fucoidan from brown seaweeds, [54]). The addition of an ultrasound device in the extraction system led to the development of ultrasound-assisted subcritical water extraction (USWE). USWE has shown to provide better yields than SLE, UAE, and SWE for the extraction of polysaccharide from *Lycium barbarum* [55]. Complex mixtures of carbohydrates may require the application of purification or fractionation techniques prior to their analysis. The techniques described earlier, however, lack sufficient selectivity to be used on their own for this purpose. Ethanol–water mixtures allowed sufficient selectivity using PLE for the purification of lactulose from a lactose mixture [56]. A more complex arrangement incorporating an in-cell packed bed of activated carbon, however, was necessary for the fractionation of honey monosaccharides and oligosaccharides using PLE [57]. SFE, using supercritical CO₂ with a percentage of organic modifier, was evaluated for the fractionation of β -glucans, chitins, and other bioactive compounds from *Lentinula edodes* [58], bioactive ketose from mixtures with aldoses [59], tagatose from mixtures with galactose [60], lactulose from aldoses [61], and oligosaccharides from dairy-based prebiotic ingredient [62].

The use of aqueous two-phase (ATP) systems in MAE and UAE is a recent trend for fractionation and purification of carbohydrates. ATP systems consist of ethanol and a polymer or salt saturated solution, which form a biphasic system with specific selectivity in each phase, acting as a liquid–liquid extraction system. As an example, a multiphase solvent consisting of 29% ethanol and 15% ammonium sulfate was evaluated for ultrasound-assisted aqueous two-phase extraction (UAATPE) of polysaccharides from *Z. jujuba* cv. Muzao fruits. This methodology provided higher extraction yields compared with UAE and allowed for the separation of ethanol-soluble polysaccharides from water-soluble polysaccharides [63]. In addition,

microwave-assisted aqueous two-phase extraction (MAATPE) was evaluated using a similar ethanol and salt system for the fractionation of polysaccharide from different plants [64,65], with higher yields and fewer impurities than other extraction techniques [66].

28.3 Derivatization

The GC analysis of carbohydrates requires a prior derivatization step in which the active hydrogens of hydroxyl, carboxyl, or amine groups are replaced by nonpolar groups. In addition to increasing the volatility and thermal stability of carbohydrates, derivatization can also enhance their detectability and change their chromatographic properties, which can be decisive for identification of isomers.

As general requirements, derivatization procedures should provide quantitative yields with minimal side reactions and chemically stable derivatives. Rapid and high specificity procedures based on a low number of reaction steps using low-cost reagents are preferred. Moreover, the number of derivatives per carbohydrate associated with the occurrence of different tautomeric forms in solution (open-chain, α - and β -furanoses, and α - and β -pyranoses) should be considered when selecting the most appropriate derivatization method, particularly for the chromatographic analysis of complex mixtures. A number of derivatization reactions have been proposed for the GC analysis of carbohydrates [67–70]; the most important are described further. A general reaction scheme together with advantages and disadvantages for each approach is provided in Table 28.1.

28.3.1 Alkylation

The per-*O*-methylated carbohydrates were the first derivatives to be used for GC analysis. In this one-pot reaction, a methyl group donor,

such as methyl iodide (iodomethane), is added to the carbohydrate dissolved in a polar aprotic solvent (e.g., dimethyl sulfoxide, *N,N*-dimethylformamide, etc.) [71]. Alternatively, iodomethane and methylsulfinyl carbanion catalyst [72] or iodomethane, and finely divided sodium hydroxide [73] can be used for the alkylation of carbohydrates up to oligosaccharides [68,74].

Although these derivatives lead to an improvement in volatility, the reaction is time-consuming and the methodology somewhat demanding. The chromatographic resolution of the *O*-methylated derivatives is often poor. As shown in Section 28.5.2, *O*-methylation is generally the first step in the structural characterization of oligosaccharides.

28.3.2 Alkylsilyl ethers

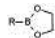
The favorable volatility and stability of trimethylsilyl ether (TMS) derivatives have maintained strong general interest in their use for the GC analysis of carbohydrates, long after they were first proposed by Sweeley [75]. Alkylsilyl ether formation is a simple procedure in which carbohydrates are dissolved in an aprotic solvent (usually pyridine) prior to silylation or the derivatization reagent is used as its own solvent.

A number of reagents have been described for alkylsilyl ether formation employing different temperature-time conditions [71]: *N*-methyl-*N*-trimethylsilylacetamide (MSA), *N*-trimethylsilyldimethylamine (TMSDMA), *N*-trimethylsilyldiethylamine (TMSDEA), *N*-methyl-*N*-trimethylsilyltrifluoroacetamide (MSTFA), *N*, *O*-bis(trimethylsilyl)acetamide (BSA), *N*, *O*-bis(trimethylsilyl)trifluoroacetamide (BSTFA), and *N*-trimethylsilylimidazole (TMSI) are most widely used. A combination of reagents is also used. Among these, hexamethyldisilazane (HMDS) + trimethylchlorosilane (TMCS) and trimethylsilylimidazole (TMSI) + TMCS are the most common. *t*-Butyldimethylsilyl (TBDMS) derivatives have

TABLE 28.1 Main derivatization procedures for GC analysis of carbohydrates.

Derivatives	Anomeric center	Derivatization reaction	Advantages	Disadvantages
Methyl ethers	Nonmodified (multiple peaks)	$R-OH + CH_3-X \rightarrow R-OCH_3 + HX$	<ul style="list-style-type: none"> - Analysis of LMWCs and structural characterization of polysaccharides 	<ul style="list-style-type: none"> - Complex chromatograms due to the different tautomeric forms of carbohydrates - Time-consuming procedure - Thermal degradation at high temperatures - Lack of good GC resolution
Acetates	Nonmodified (multiple peaks)	$R-OH + Ac-X \rightarrow R-OAc + HX$	<ul style="list-style-type: none"> - Analysis of LMWCs - Chemical and thermal stability 	<ul style="list-style-type: none"> - Complex chromatograms due to the different tautomeric forms of carbohydrates - Lower volatility than trimethylsilyl ethers
Trifluoroacetates	Nonmodified (multiple peaks)	$R-OH + CF_3CO-X \rightarrow R-O-COCF_3 + HX$	<ul style="list-style-type: none"> - More volatile than acetates or trimethylsilyl ethers - Suitable for carbohydrates in a wide range of molecular weights - Lower analysis temperatures can be used 	<ul style="list-style-type: none"> - Complex chromatograms due to the different tautomeric forms of carbohydrates - Difficulty in achieving satisfactory quantitation - Removal of acid by-products before analysis - Moisture-sensitive, hazardous and odorous reagents
Trimethylsilyl ethers	Nonmodified (multiple peaks)	$R-OH + (CH_3)_3Si-X \rightarrow R-O-Si(CH_3)_3 + HX$	<ul style="list-style-type: none"> - More volatile, less polar, and more thermally stable than methyl ethers and acetates - Rapid derivatization proceeding under mild conditions - Large number of silylating reagents available - Useful for quantifying equilibrium forms of carbohydrates in solution - Derivatives more widely utilized 	<ul style="list-style-type: none"> - Complex chromatograms due to the different tautomeric forms of carbohydrates - Samples must be completely dried - Silylation reagents are moisture sensitive
Trimethylsilyl oximes	Modified (two peaks)	<p>(1) $R-CHOH-CHO + NH_2OH \rightarrow R-CHOH-CH=NOH + H_2O$</p> <p>(2) $R-CHOH-CH=NOH + (CH_3)_3Si-X \rightarrow R-CHO-Si(CH_3)_3-CH=NO-Si(CH_3)_3 + HX$</p>	<ul style="list-style-type: none"> - Lower number of chromatographic peaks for reducing carbohydrates: <i>anti</i> (<i>E</i>)- and <i>syn</i> (<i>Z</i>)- oxime isomers - Applicable to both aldoses and ketoses - Derivatives are stable for a long time 	<ul style="list-style-type: none"> - Samples must be totally dry

TABLE 28.1 Main derivatization procedures for GC analysis of carbohydrates.—cont'd

Derivatives	Anomeric center	Derivatization reaction	Advantages	Disadvantages
Trimethylsilyl alkyl oximes	Modified (two peaks)	(1) $R-CHOH-CHO + NH_2OR' \rightarrow R-CHOH-CH=NOR' + H_2O$ (2) $R-CHOH-CH=NOR' + (CH_3)_3Si-X \rightarrow R-CHO-Si(CH_3)_3-CH=NO-R' + HX$	- Lower number of chromatographic peaks for reducing carbohydrates: <i>anti</i> (<i>E</i>)- and <i>syn</i> (<i>Z</i>)- oxime isomers - Applicable to both aldoses and ketoses	- Samples must be totally dry
Aldononitrile acetates	Modified (one peak)	(1) $R-CHOH-CHO + NH_2OH \rightarrow R-CHOH-C=NOH + H_2O$ (2) $R-CHOH-C=NOH + Ac-X \rightarrow R-CH-OAc-C\equiv N + HX$	- A single peak for each aldose - Water does not interfere with reaction	- Nonapplicable for ketoses - Nonappropriate for analysis of real samples where aldoses and ketoses coexist
Alditol acetates	Modified (one peak)	(1) $R-CHOH-CHO + NaBH_4 \rightarrow R-CHOH-CH_2OH$ (2) $R-CHOH-CH_2OH + Ac-X \rightarrow R-CH-OAc + HX$	- A single peak for each aldose - Very stable derivatives - Used for sugar composition analysis of macromolecules - Allows separation of complex mixtures	- Different sugars can lead to the same alditol - Each ketose yields a mixture of two alditols - Frequently, tedious and time-consuming procedure - Reaction products (acid by-products) often need to be removed before analysis - Acylation reagents are moisture sensitive
Dialkyl dithioacetals	Modified (one peak)	(1) $R-CHOH-CHO + R'-SH \rightarrow R-CHOH-CH(S-R')_2 + H_2O$ (2) $R-CHOH-CH(S-R')_2 + (CH_3)_3Si-X \rightarrow R-CHO-Si(CH_3)_3-CH(S-R')_2$	- A single peak for each aldose - Stable products	- Difficult procedure involving the use of a thiol as derivatization reagent - Variable yields - In some cases, formation of by-products contaminating the GC system
Cyclic alkane boronates	Nonmodified (one peak)	$R'-CHOH-CHOH-R'' + R-B(OH)_2 \rightarrow$ 	- Valid for aldoses and ketoses	- Multiple derivatives for oligosaccharides - Nonapplicable to uronic acids

Modified with permission of Elsevier from A.I. Ruiz-Matute, O. Hernández-Hernández, S. Rodríguez-Sánchez, M.L. Sanz, I. Martínez-Castro, *Derivatization of carbohydrates for GC and GC-MS analyses*, *J. Chromatogr. B* 879 (2011) 1226–1240.

certain advantages in terms of higher stability to hydrolysis than TMS ethers. Derivatization of LMWCs is usually carried out at room temperature with elevated temperatures typically used for oligosaccharides, for example, 60–100°C for 20–30 min [5,76].

Compared with the conventional approach for derivatizing LMWCs with pyridine as a solvent, different ILs also have been evaluated. In the latter case, the yield of derivatives was shown to depend on the selected reagent and target sugar. Thus, whereas TMSI under mild conditions (25°C, 1 h) provided yields close to 100% for different aldo- and ketosugars, other reagents (BSTFA + TMCS or BSTFA) were only useful for selected carbohydrates [77].

More recently, in a nontypical *in solution* approach, solid-phase microextraction (SPME) followed by on-fiber derivatization with BSTFA, was evaluated for the GC-MS analysis of simple carbohydrates as TMS derivatives. By this simple procedure, the presence of several minor LMWCs was detected for the first time in beer [78].

In spite of up to five TMS derivatives per reducing carbohydrate unit by silylation, as compared to nonreducing carbohydrates and sugar alcohols providing a single peak, their chromatographic resolution is good. Equilibrium of the sample in dry pyridine prior to the addition of the derivatization reagents has been used to stabilize tautomer ratios [79]. However, this preequilibrium step is not usually required if the addition of reagents is carried out without delay. Quantitative performance of TMS ethers under optimized reaction conditions is also satisfactory.

Since the stability of TMS derivatives is limited, their analysis shortly (within 1–2 days) after preparation is recommended. Alternatively, the extraction of TMS ethers with removal of the excess of derivatization reagents, by the consecutive addition of a nonpolar solvent (e.g., n-heptane) and water, together with drying the n-heptane solution

with anhydrous sodium sulfate, allows their preservation under refrigeration for several days [12,80].

28.3.3 Acyl esters

Acetates obtained by esterification of active OH groups with acid anhydrides or halides are useful derivatives for the GC separation of carbohydrates [81]. Although advantageous in terms of their chemical and thermal stability, their relatively low volatility compared with TMS derivatives and the preservation of the anomeric center giving rise to multiple peaks for reducing carbohydrates limits their application to simple mixtures of LMWCs. Perfluoroacetylation using trifluoroacetic anhydride (TFAA), pentafluoropropionic anhydride, heptafluorobutyric anhydride, or methylbis(trifluoroacetamide) (MBTFA) as esterifying agents was reported to afford derivatives with higher volatility than TMS and acetate derivatives [68,82]. This is particularly important for oligosaccharide analysis or when high analysis temperatures should be avoided. As shown in Section 28.3.9, acylation followed by alkylation is suitable for the GC analysis of enantiomers using chiral stationary phases. Apart from MBTFA, acylating reagents form acid by-products, which must be eliminated before GC analysis.

28.3.4 Oximes

In order to decrease the multiplicity of peaks in GC analysis of carbohydrate mixtures, several procedures have been proposed for modification of the anomeric center. Trimethylsilyl oximes (TMSO) obtained by conversion of the carbonyl group of reducing sugars into an oxime prior to trimethylsilylation result in only two peaks for each sugar: the *syn* (Z)- and *anti* (E)- oxime isomers [83,84]. Nonreducing sugars and polyalcohols give rise to a single trimethylsilyl

derivative as they do not undergo oximation. Also, the abundance and chromatographic resolution of oxime isomers were suggested as a tool to facilitate the identification of unknown carbohydrates [85,86].

Hydroxylamine hydrochloride (HACl) and a combination of HMDS + TFA are commonly used as oximation and trimethylsilylating reagents, respectively [69,70]. Although this requires a two-step derivatization reaction, it is easy to carry out and results in derivatives that are as volatile and more stable than TMS ethers (they can be stored under refrigeration for months). Oximes are applicable to both aldoses and ketoses and are widely used for the analysis of complex mixtures of carbohydrates in different matrices [87].

As an alternative to TMSO, a number of trimethylsilyl *O*-alkyloxime derivatives have been described [70,88,89]. For example, acetylation with TFAA of ethyloximes for the separation of monosaccharides in complex matrices with specific stationary phases [89]. However, derivatization of ketoses proved difficult and irreproducible. Sensitivity of detection and stability of these derivatives were lower than TMSO. The use of several oxime derivatives for the unambiguous characterization of complex monosaccharides also has been described. Haas et al. [70] used parallel derivatization by HACl/BSTFA and *O*-ethylhydroxylamine hydrochloride/BSTFA for the simultaneous identification of aldoses, ketoses, sugar alcohols, and sugar acids.

28.3.5 Aldonitrile acetates

Aldonitrile acetates (Wohl derivatives) are formed by reaction of sugars with HACl forming the corresponding unsubstituted oxime and further acetylation with acetic anhydride in the presence of either pyridine or 1-methylimidazole. The resulting acetyloxime is

dehydrated to the corresponding *per*-acetylaldonitrile (PAAN) derivative [68]. An advantage of PAAN derivatives is that they form a single peak for aldoses; with ketoses, however, the reaction is incomplete and this procedure is not recommended for the analysis of samples containing both type of sugars [12].

28.3.6 Alditol acetates

As an alternative approach to simplify the analysis of complex mixtures, reduction of the carbonyl group of monosaccharides and further acetylation of the corresponding alditols provide stable derivatives [90]. Sodium borohydride in dimethyl sulfoxide (DMSO) is typically used as the reducing agent. Alditol acetates provide a single peak for aldoses; however, two isomeric alditols are formed from ketoses (e.g., mannitol and glucitol are obtained from fructose). Moreover, the same alditol can be formed from different carbohydrates (e.g., mannitol may originate from both mannose and fructose; arabinitol from arabinose and lyxose, etc.). Although derivatives are stable for an extended time, the loss of information associated with the modification of the anomeric center and the fact that it is a rather tedious procedure limit applications for these derivatives.

28.3.7 Dialkylmercaptal derivatives

Dialkylthioacetals obtained by mercaptalation followed by trimethylsilylation or trifluoroacetylation provide single derivatives that are particularly useful for the analysis of high-molecular-weight carbohydrates, for example, uronic acids (that other methods fail) and aldoses [91]. Although the procedure is simpler than the alditol acetate method and stable derivatives are obtained, chromatographic resolution is poor and reaction yields variable. Moreover, by-products contaminating the GC

system are an occasional problem. The strong odor of thiol reagent is also a disadvantage for routine analysis.

28.3.8 Cyclic boronic esters

Cyclic boronic esters provide an alternative approach to prepare a single derivative per carbohydrate unit [68]. An alkyl (methyl-, butyl-, phenyl-) boronic acid reacts with sugar diols forming pentacyclic or hexacyclic boronic esters, depending on sugar stereochemistry. Free hydroxyl groups can be subsequently derivatized by trimethylsilyl ether or acetyl ester formation; however, optimization of reagents and conditions in this latter step is required to avoid *per*-silylation/acetylation or formation of by-products [92]. Although single peaks are obtained for aldoses and ketoses, multiple derivatives are possible for oligosaccharides. This method is not suitable for uronic acids. Reactions are rapid, repeatable, and generally quantitative and do not require further evaporation/extraction before GC analysis.

28.3.9 Chiral derivatives

Although a variety of applications rely on the chiral analysis of carbohydrates, a limited number of reports have addressed this issue for individual carbohydrates in complex mixtures. The resolution of sugar enantiomers is usually achieved after conversion of each enantiomer to a diastereomer by reaction with a chiral reagent (e.g., 2-butanol, 2-octanol, 1-phenylethanethiol, etc.) with subsequent separation on an achiral stationary phase (DB-5, DB-17). Among others examples of this approach are acetylated or trimethylsilylated acyclic dithioacetals, trifluoroacetylated 3-methyl-2-butyl esters, trimethylsilyl ethers or acetates of the diastereoisomeric

α -methylbenzylaminoalditols, etc. [93,94]. However, the utility of these methods for the quantitative analysis of enantiomers has been questioned at times.

Alternative procedures based on the use of chiral stationary phases also have been reported. For example, Cooper et al. [95] used different derivatization procedures (ethyl ester/*O*-trifluoroacetyl- (Et-TFA), isopropyl ester/*O*-trifluoroacetyl- and isopropyl ester/*O*-pentafluoropropionyl-derivatives), in combination with a permethylated β -cyclodextrin capillary column, for the enantioselective GC-MS analysis of C3–C6 straight-chain sugar acids. The Et-TFA derivatives provided suitable resolution of all sugars except for DL-glyceric acid and DL-erythronic acid. The same group evaluated different acetyl-trifluoroacetyl derivatives (ethyl-, 2-propyl-, and 2-butyl-TFA) on both chiral and achiral GC columns for the separation of complex mixtures of C3–C6 aldomonosaccharides [96]. Derivative formation occurred without loss of chiral information with only 1 or 2 abundant stereoisomers per carbohydrate, simplifying an otherwise crowded chromatogram. Although the different derivatives facilitated the separation of most target compounds, the selection of derivatives and column combination was made depending on the intended application.

28.4 Chromatographic conditions for the analysis of carbohydrates

28.4.1 Capillary columns

Most carbohydrate analyses are carried out on capillary columns coated with a nonpolar poly(dimethylsiloxane) stationary phases. These columns are thermally stable to temperatures around 320–350°C and suitable for the

separation of carbohydrates between DP1 and DP4. More polar poly(siloxane) stationary phases containing phenyl- [97,111], vinyl- [98,99], trifluoropropyl- [98,99], or cyanopropyl- [98,99] groups have been utilized as well [5]. Poly(ethylene glycol) stationary phases are rarely used for the separation of carbohydrates, mainly due to their limited thermal stability (up to 250–260°C) except for a few applications for monosaccharide [3,98,99]. An IL stationary phase SLB-IL60 [1,12-di(tripropylphosphonium)dodecane bis(trifluoromethylsulfonyl)imide] was used for the separation of mono- [92] and disaccharides [100]. More recently, a comprehensive survey of IL stationary phases for the analysis of mono-, di-, and trisaccharides, inositols, and iminosugars was reported [3]. Only the 1,12-di(2,3-dimethylimidazolium)dodecane bis(trifluoromethylsulfonyl)imide (SLB-IL82) stationary phase was able to elute a wide range of carbohydrates. Fig. 28.2 shows the chromatogram for the separation of a mixture of monosaccharide, iminosugars, and inositol standards on SLB-IL82 and, for comparison, on SUPELCOWAX 10 and HP-1 columns. As it can be seen, different elution orders are observed depending on the stationary phase; iminosugars were the most affected by column selectivity. Moreover, it was concluded that SLB-IL82 is a suitable alternative to conventional stationary phases for the analysis of LMWCs in complex plant extracts, such as those obtained from hyacinth and mulberry.

The carborane-containing poly(siloxane) stationary phases can withstand temperatures up to around 450°C and are suitable for the separation of oligosaccharides up to a molecular weight of about DP7 [101]. Among others, they were used for the analysis of prebiotic GOS [102], legume oligosaccharides [36], etc.

Capillary columns for the separation of carbohydrates typically vary in length from 2 to 30 m, internal diameter 0.25 or 0.32 mm, and film thickness of 0.05–0.25 μm . Capillary columns with ultrathin films (<0.05 μm) allow

the separation of maltodextrins up to DP7 and fructooligosaccharides up to about DP11 [103].

28.4.2 Separation conditions

Carbohydrate analysis typically requires the separation of complex mixtures in a wide volatility range (from mono- to oligosaccharides). Temperature programming is mandatory to shorten separation times. The temperature ramp usually ranges from 80 to 330°C; monosaccharides eluting from 80 to 140°C, disaccharides from 230 to 270°C, and tri- and tetrasaccharides from 290 to 330°C. For carborane-based stationary phases, temperatures up to 360–370°C can be used.

An injector temperature in the range 220–300°C is typically used for classical constant-temperature injectors. Rodríguez-Sánchez et al. [104] chose a temperature of 240°C for the analysis of iminosugars, inositol, and other LMWCs found in extracts of plant materials (hyacinth, mulberry, and buckwheat) as a compromise between the volatility of the carbohydrate derivatives, peak symmetry, and thermal stability for bioactive carbohydrates, including glycosyl inositols. The detector temperature should be equal to or higher than the maximum temperature reached in the column oven to avoid loss of resolution. An exception is when the column is connected to a mass spectrometer, as vacuum helps in the transfer of compounds into the MS, and the use of a lower interface temperature (around 270°C) is permissible. The use of helium as the carrier gas decreases the separation time compared with nitrogen without a substantial loss in column efficiency.

28.4.3 Detectors

The flame ionization detector (FID) provides high sensitivity although its identification capacity is low (positive identifications require the use of standard compounds not all of which are

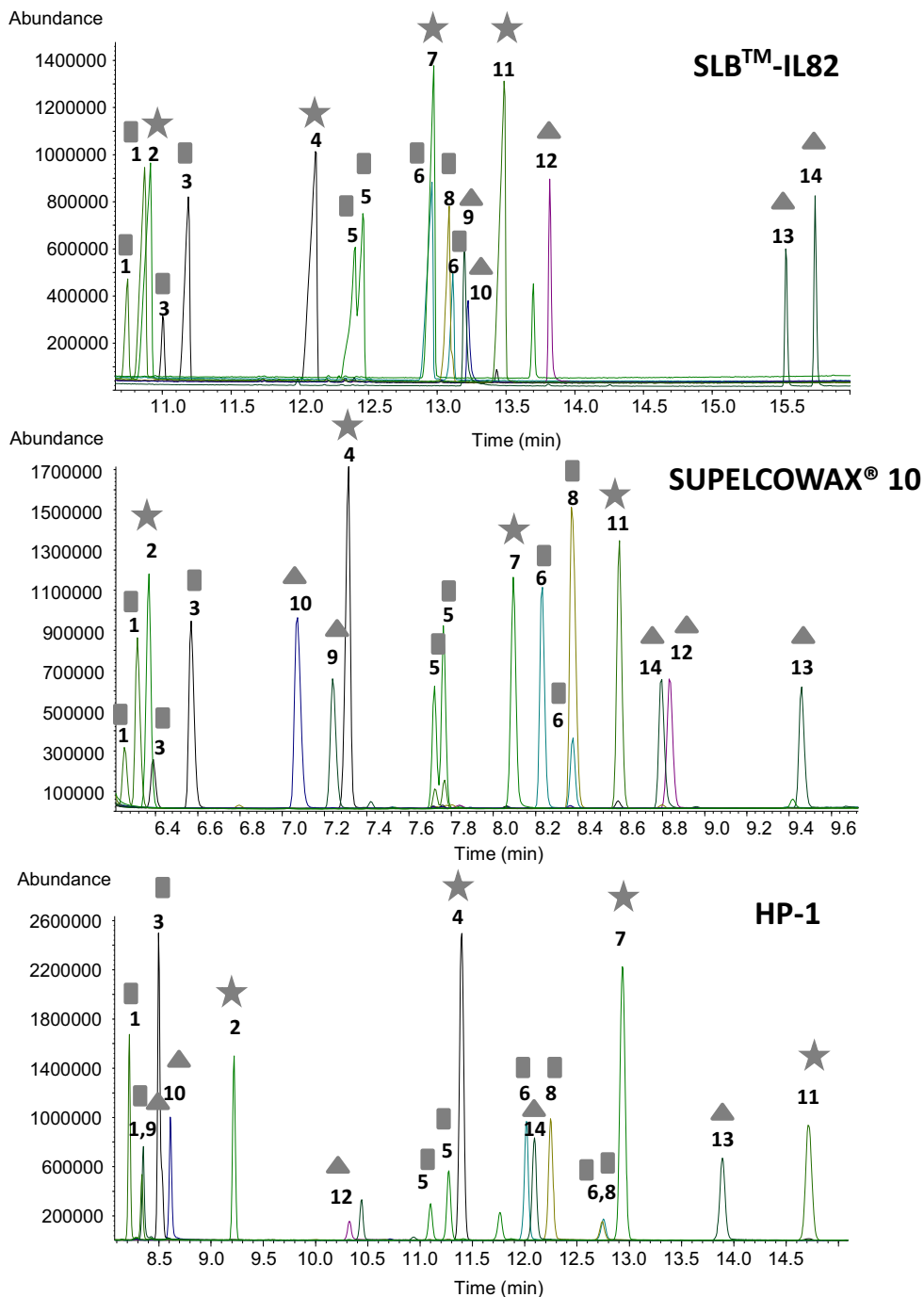


FIGURE 28.2 GC-MS chromatographic profiles obtained for derivatized monosaccharide (■), inimosugar (▲), and inositol (★) standards analyzed in SLB-IL82, SUPELCOWAX 10, and HP-1 columns: (1) arabinose (1 and 2), (2) pinitol, (3) ribose (1 and 2), (4) *chiro*-inositol, (5) fructose (1 and 2), (6) galactose (*E* and *Z*), (7) *scyllo*-inositol, (8) glucose (*E* and *Z*), (9) DMDP, (10) DMJ, (11) *myo*-inositol, (12) DNJ, (13) miglitol, and (14) α -HNJ. Reprinted with permission of Springer from S. Rodríguez-Sánchez, A.C. Soria, R. Lebron-Aguilar, M.L. Sanz, A.I. Ruiz-Matute, *Evaluation of different ionic liquid stationary phases for the analysis of carbohydrates by gas chromatography-mass spectrometry*, *Anal. Bioanal. Chem.* 411 (2019) 7461–7472.

likely to be commercially available) [105]. GC-MS has advantages for structural characterization, mainly when complex mixtures are analyzed. Electron impact (EI) ionization is typically used for carbohydrate analysis. In addition, positive chemical ionization (PCI) has been proposed for applications requiring the preservation of the pseudomolecular ion for the carbohydrates. The lack of structural information provided by PCI is overcome by coupling to tandem MS/MS analyzers [106]. Quadrupole mass analyzers are commonly used based on their relatively low cost and high sensitivity. However, some methods using ion traps (IT) have appeared [107].

More recently, vacuum ultraviolet (VUV) spectroscopy employing a deconvolution strategy

was proposed as an alternative to GC-MS for the identification of isomeric mono-, di-, and trisaccharides [108]. Fig. 28.3 illustrates GC-VUV chromatograms of permethylated aldopentoses (A), ketopentoses (B), aldohexoses (C), and ketohexoses (D). Although complex chromatograms were obtained, the proposed method was able to identify sugars in pharmaceutical samples.

28.5 Structural elucidation of low-molecular-weight carbohydrates

Despite the structural similarities of carbohydrates, the combination of GC retention data (linear retention indices, I^T) and mass spectrometric fragmentation patterns (abundances of characteristic EI m/z ions) can provide useful

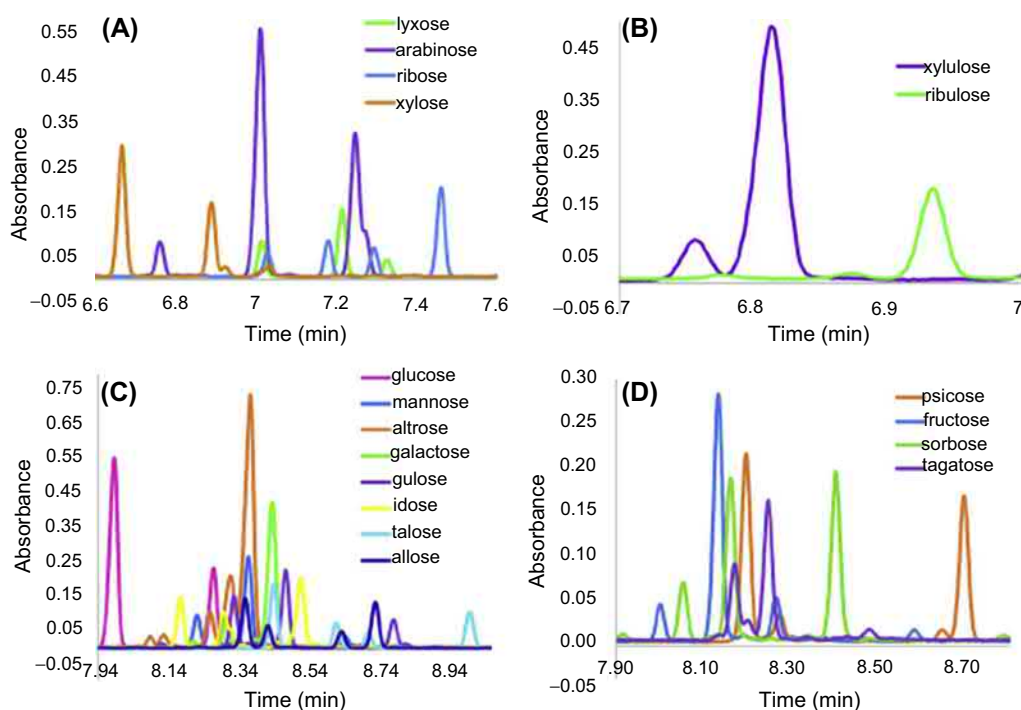


FIGURE 28.3 GC-VUV profiles of permethylated aldopentoses (A), ketopentoses (B), aldohexoses (C), and ketohexoses (D). Reprinted with permission of Elsevier from J. Schenk, G. Nagy, N.L.B. Pohl, A. Leghissa, J. Smuts, K.A. Schug, *Identification and deconvolution of carbohydrates with gas chromatography-vacuum ultraviolet spectroscopy*, *J. Chromatogr. A* 1513 (2017) 210–221.

information for the identification of unknown sugars. Carbohydrates with the same DP and differing in the position of their hydroxyl groups can have similar mass spectra but different retention indices. On the contrary, certain carbohydrates eluting at the same retention time can exhibit differences in their mass spectra. Therefore, both types of data are essential for carbohydrate identification. For quantitative purposes, the possibility of overlapping of unknown carbohydrates with expected sugars needs also be addressed. To that aim, in a study of the disaccharide composition of honey, de la Fuente et al. [109] developed an iterative approach, using as input data the relative contribution (percent values) of 15 disaccharide standards to several previously established retention time intervals on two chromatographic columns. This method took into account possible positive systematic errors caused by unknown compounds.

28.5.1 Retention

TMS and TMSO derivatives are commonly used for carbohydrate analysis. I^T values for many mono-, di-, and trisaccharides on different stationary phases can be found in the literature. As an example, Table 28.2 lists I^T ranges for different carbohydrates and derivatives on a variety of stationary phases.

Monosaccharides elute before disaccharides and disaccharides before trisaccharides on all columns. In general, for any carbohydrate derivative, retention is noticeably lower for polar stationary phases. Regarding IL columns, I^T values increase with the polarity of the stationary phase [3]. In this sense, I^T values on SLB-IL82 and SLB-IL76 are similar to poly(methylpolysiloxane) columns, whereas smaller values are observed for SLB-IL59 and SLB-IL60 columns.

Sanz et al. [110] evaluated the retention behavior (Kovats retention indices) of di- and

trisaccharides in honey on two columns with different stationary phases, a poly(dimethyldiphenylsiloxane) containing 65% diphenylsiloxane monomer and a poly(dimethylsiloxane). On the nonpolar column, nonreducing disaccharides (TMS derivatives) eluted before reducing disaccharides (TMSO derivatives) as a result of their lower molecular weight; some nonreducing disaccharides (e.g., trehaloses) eluted in between TMSO disaccharides on the more polar column. With respect to glycosidic linkages, although a specific elution order could not be established, TMSO carbohydrates with a 1→6 linkage were generally the last to elute of each carbohydrate group (e.g., gentiobiose and isomaltose eluted at the end of disaccharides). Chromatographic information can be enhanced by the combination of data from columns with complementary stationary phases.

For TMS iminosugars, a close relationship between I^T and the degree of hydroxylation was observed (i.e., iminosugars with two –OTMS groups are the first to elute, followed by iminosugars with three, four, etc., –OTMS groups [111,112]. For iminosugars with identical molecular formulas (e.g., fagomine and 1-deoxyfuconojirimycin), retention is affected by the type of substituents and the volatility of the compounds.

TMS methyl-inositols show lower retention indices than their corresponding inositols on nonpolar stationary phases. The same behavior is observed for TMS glycosyl-inositols and their corresponding methyl-inositol derivatives. Moreover, glycosyl-inositols derived from *chiro*-inositol elute earlier than those derived from *myo*-inositol, as for individual inositols [113]. For sugar acids, lactones show lower retention indices than their corresponding acid form (e.g., glucuronic acid γ -lactone 1840 and glucuronic acid 1 and 2 2021 and 2083, respectively) [114].

TABLE 28.2 Linear retention indices (I^T) of LMWCs.

Carbohydrates	Derivatives	Stationary phases/ I^T values	References
Monosaccharides	TMSO	ZB-5/1787-2130 SLB TM -IL82/1879-2155 SLB TM -IL76/1836-2068 SLB TM -IL60/1727-1990 SLB TM -IL59/1684-1938 Supelcowax 10/1331-1438 HP-1/1795-2078	Carrero-Carralero et al. [36] Rodríguez-Sánchez et al. [3]
	TMS	HP5/1523-2031	Isidorov and Szczepaniak [114]
	TMSEtO	HP5/1956-2011	Becker et al. [86,88]
Disaccharides	TMSO	ZB-5/2707-3018 SLB TM -IL82/2995-3508 SLB TM -IL76/2828-3278 SLB TM -IL60/2644-3042 SLB TM -IL59/2530-2906 Supelcowax 10/1841-2594 HP-1/2681-2857	Carrero-Carralero et al. [36] Rodríguez-Sánchez et al. [3]
	TMS	HP5/2714-3003	Isidorov and Szczepaniak [114]
	TMSEtO	HP5/2711-2964	Becker et al. [86,88]
Trisaccharides	TMSO	SLB TM -IL82/>4000 SLB TM -IL76/>4000 SLB TM -IL60/3546->4000 SLB TM -IL59/3372-3401 Supelcowax 10/2967-2996 HP-1/2857-3226 HT-5/3331-3631	Rodríguez-Sánchez et al. [3] Ruiz-Matute et al. [116]
	TMS	HP-5/3462-3627	Isidorov and Szczepaniak [114]
	TMS	SLB TM -IL82/1895-2207 SLB TM -IL76/1851-2169 SLB TM -IL60/1779-2109 SLB TM -IL59/1734-2052 Supelcowax 10/1334-1451 HP-1/1882-2146 HP5/1832-2466	Rodríguez-Sánchez et al. [3] Isidorov and Szczepaniak [114]
Glycosyl-inositols	TMS	HT5/2633-4236	Ruiz-Aceituno et al. [113]
Iminosugars	TMS	HP-1/1432-1903 BPX50/1525-1893 SLB TM -IL82/2170-2521 SLB TM -IL76/2227-2300 Supelcowax 10/1377-1503 HP-1/1808-2119	Rodríguez-Sánchez et al. [112] Rodríguez-Sánchez et al. [3]
	TMS	HP-5/1652-2494	Isidorov and Szczepaniak [114]
	TMS	HP-5/1652-2494	Isidorov and Szczepaniak [114]

HT5: 5% phenyl (equiv.) polycarborane-siloxane; HP-1: methylpolysiloxane; HP-5: 5% phenylmethylpolysiloxane; BPX50: 50% phenylmethylpolysiloxane. TMS, trimethylsilyl; TMSO, TMS oximes; TMSEtO, TMS ethoximes.

28.5.2 Mass spectra

EI mass spectra for numerous carbohydrate derivatives, such as TMS [112,113], TMSO [97,115,116], methyl acetates [117], etc., are available. For the same derivatization procedure, characteristic m/z fragments are similar for all carbohydrates, but their relative abundances might be different depending on structure, useful for the characterization of unknown carbohydrates. In this sense, the ratio of m/z 191:204:217 ions of 1.3:1:1.3 for TMS disaccharides is characteristic of nonreducing sugars with 1 \leftrightarrow 1 glycosidic linkages, such as trehalose and 1,1-galactobiose. A high abundant m/z 319 ion (corresponding to the loss of a TMSOH group from the chain C3–C4–C5–C6 of a hexose residue) is characteristic of TMSO reducing disaccharides with 1 \rightarrow 2 glycosidic linkages (e.g., kojibiose, sophorose, 1,2-galactobiose), whereas the m/z 422 ion (corresponding to C1–C2–C3–C4 of the oxime chain) is typical of TMSO carbohydrates with 1 \rightarrow 6 linkages (e.g., isomaltose, gentiobiose, 1,6-galactobiose). A mass spectrum with a relatively high m/z 307 ion is characteristic of TMSO carbohydrates with a reducing fructose substituent in C1 or C3 (e.g., trehalulose, turanose). Table 28.3 illustrates the relative abundances of the characteristic m/z fragments of TMSO derivatives of di- and trisaccharides of GOS derived from lactulose mixtures (GOSLu) [118]. The m/z data for each peak combined with their I^T values allowed the characterization of the different GOSLu present in the mixture.

28.6 GC-MS analysis of oligo- and polysaccharides

Oligosaccharides and polysaccharides are high-molecular-weight carbohydrates that can be degraded by thermal stress. However, GC-MS can be extremely useful for the characterization of these compounds. Two different

strategies are followed depending on the application. If only monosaccharide units of oligo- or polysaccharides are to be identified, a hydrolysis step followed by derivatization is used. If a comprehensive characterization is intended, methylation provides information on the glycosidic linkages. As both are well-known procedures used extensively for carbohydrate analysis, they are only briefly mentioned here.

28.6.1 Hydrolysis

Several hydrolytic treatments, either acidic or enzymatic, are used to break the glycosidic linkages and liberate the monomeric units of oligo- or polysaccharides. Acid hydrolysis uses different concentrations of either trifluoroacetic acid (TFA) or hydrochloric acid (HCl) at a variety of temperatures. Methanolysis using HCl in methanol also is used for hydrolysis. Specific enzymes for the depolymerization of high-molecular-weight carbohydrates are also widely used [5]. Willför et al. [119] compared the hydrolytic treatments mentioned earlier for the analysis of uronic acid-containing polysaccharides from plant materials; methanolysis provided the best results. A combination of methanolysis and hydrolysis methods was recommended for the determination of total sugar units, including cellulose, other noncrystalline hemicelluloses, and pectins. Microwave irradiation was also proposed to improve hydrolytic treatments to reduce time and increase yield.

28.6.2 Methylation analysis

Structural characterization of oligo- and polysaccharides involving the determination of glycosidic linkages is usually carried out by methylation analysis. It consists of three steps: (i) methylation of the free hydroxyl groups in the intact oligo- or polysaccharide; (ii) cleavage of the glycosidic links; and (iii) acetylation of

TABLE 28.3 Retention indices (I^T) and relative abundance for characteristic m/z ratios of galactooligosaccharide disaccharides derived from lactulose mixtures.

Identification	I^T	m/z ratios											
		191	204	205	217	244	305	307	319	361	422	451	538
Lactulose	2878–2887	22	76	24	37	2	4	1	15	41	–	1	1
1,1-Galactobiose	2903	66	37	14	46	3	3	–	6	50	–	–	–
1,4-Galactobiose <i>E</i>	2905	14	68	30	41	3	4	–	17	49	–	–	–
1,5-Galactosyl-fructose 1	2915	–	81	32	32	–	10	–	17	43	–	–	–
1,3-Galactobiose <i>E</i>	2932	10	51	21	41	6	3	4	14	38	–	1	–
1,2-Galactobiose <i>E</i>	2932	22	50	25	44	5	5	13	38	25	–	1	2
1,5-Galactosyl-fructose 2	2937	20	59	17	36	3	4	2	11	40	–	–	5
1,4-Galactobiose <i>Z</i> + unknown	2959	13	97	35	41	–	6	–	13	43	–	–	–
1,3-Galactobiose <i>Z</i> + 1,2-Galactobiose <i>Z</i>	2979	13	47	26	39	6	4	4	22	40	–	–	–
1,6-Glucosyl-fructose 1	3003	11	86	22	59	2	4	–	5	34	3	2	8
1,6-Glucosyl-fructose 2	3012	21	95	21	57	2	4	1	7	32	3	2	–
1,1-Galactosyl-fructose 1	3029	13	56	20	49	1	3	35	7	9	–	–	2
1,6-Galactobiose <i>E</i>	3046	32	67	19	42	2	5	6	7	–	1	2	3
1,1-Galactosyl-fructose 2	3049	20	54	17	71	2	3	26	5	13	–	–	2
1,6-Galactobiose <i>Z</i>	3094	30	65	20	41	2	5	8	8	53	–	2	–

Modified with permission of Elsevier from O. Hernández-Hernández, F.J. Moreno, A. Montilla, A. Clemente, A. Olano, M.L. Sanz, Characterization of novel galactooligosaccharides derived from lactulose, *J. Chromatogr. A* 1218 (2011) 7691–7696.

the new free hydroxyl groups. Retention times and characteristic m/z ions depend on the position of the acetyl groups in the resulting monosaccharides. Several methods have been described [72,73], most of which are based on the formation of monosaccharides with two different types of substituents; one indicating the position of the glycosidic linkage in the original polysaccharide, and the other aiding the volatility of the molecule [4,74]. Although it is a well-established procedure, methylation is sensitive to the reaction conditions (absence of water, temperature), reagents, and catalyst used. Thus, dry solvents, such as DMSO or *N,N*-dimethylformamide, are usually employed. Methyl iodide is typically selected as the

methylation reagent and either dimethyl base or sodium hydride as catalyst. The dimethyl base is preferred for the permethylation of β -cyclodextrins [120]. Methylation analysis was used for the characterization of several polysaccharides, such as those from fungi extracts [121–123], medicinal plants [124], food and beverages [125,126], etc.

28.7 Comprehensive two-dimensional gas chromatography

In spite of the high resolution provided by GC capillary columns, complex mixtures of carbohydrates may not be completely separated.

In comprehensive two-dimensional GC (GC \times GC), two columns of different selectivity are connected through a modulator resulting in a higher peak capacity. The main advantages of GC \times GC for carbohydrate analysis are improved resolution and an increase in sensitivity provided by the modulation process, which results in improved detection of minor compounds. When coupled to time-of-flight mass spectrometry (GC \times GC-TOF MS), additional information (mass spectrum) to retention times on the first (1t_R) and second dimension (2t_R) columns is obtained, making the identification of unknowns easier. The application of this technique to carbohydrate analysis is so far limited. After optimization of the method (1D and 2D columns, oven programs, modulation time, etc.), GC \times GC was applied to the analysis of disaccharides in different samples of honey [127] and several varieties of apple and peach fruits [100]. Several unknown carbohydrates were identified in these samples.

References

- [1] M. Hricovíni, Structural aspects of carbohydrates and the relation with their biological properties, *Curr. Med. Chem.* 11 (2004) 2565–2583.
- [2] S.J. Angyal, The composition of reducing sugars in solution, *Adv. Carbohydr. Chem. Biochem.* 42 (1984) 15–68.
- [3] S. Rodríguez-Sánchez, A.C. Soria, R. Lebron-Aguilar, M.L. Sanz, A.I. Ruiz-Matute, Evaluation of different ionic liquid stationary phases for the analysis of carbohydrates by gas chromatography-mass spectrometry, *Anal. Bioanal. Chem.* 411 (2019) 7461–7472.
- [4] M.L. Sanz, I. Martínez-Castro, Recent developments in sample preparation for chromatographic analysis of carbohydrates, *J. Chromatogr. A* 1153 (2007) 74–89.
- [5] A.C. Soria, S. Rodríguez-Sánchez, J. Sanz, I. Martínez-Castro, Gas chromatographic analysis of food bioactive oligosaccharides, in: F.J. Moreno, M. Sanz (Eds.), *Food Oligosaccharides: Production, Analysis and Bioactivity*, John Wiley & Sons, Inc, United States, 2014, pp. 370–398.
- [6] C. Christou, E. Poulli, S. Yiannopoulos, A. Agapiou, GC-MS analysis of D-pinitol in carob: syrup and fruit (flesh and seed), *J. Chromatogr. B Anal. Technol. Biomed. Life Sci.* 1116 (2019) 60–64.
- [7] B. de Falco, A. Fiore, R. Bochicchio, M. Amato, V. Lanzotti, Metabolomic analysis by UAE-GC MS and antioxidant activity of *Salvia hispanica* (L.) seeds grown under different irrigation regimes, *Ind. Crops Prod.* 112 (2018) 584–592.
- [8] B. de Falco, A. Fiore, R. Rossi, M. Amato, V. Lanzotti, Metabolomics driven analysis by UAEGC-MS and antioxidant activity of chia (*Salvia hispanica* L.) commercial and mutant seeds, *Food Chem.* 254 (2018) 137–143.
- [9] A. Mena-García, S. Rodríguez-Sánchez, A.I. Ruiz-Matute, M.L. Sanz, Exploitation of artichoke byproducts to obtain bioactive extracts enriched in inositols and caffeoylquinic acids by microwave assisted extraction, *J. Chromatogr. A* 1613 (2020) 460703.
- [10] A. Olano, Solubility of lactose and lactulose in alcohols, *J. Food Sci. Technol.* 16 (1979) 260–261.
- [11] Y. Jiang, X. Bai, S. Lang, Y. Zhao, C. Liu, L. Yu, Optimization of ultrasonic-microwave assisted alkali extraction of arabinoxylan from the corn bran using response surface methodology, *Int. J. Biol. Macromol.* 128 (2019) 452–458.
- [12] S. Rodríguez-Sánchez, O. Hernández-Hernández, A.I. Ruiz-Matute, M.L. Sanz, A derivatization procedure for the simultaneous analysis of iminosugars and other low molecular weight carbohydrates by GC-MS in mulberry (*Morus* sp.), *Food Chem.* 126 (2011) 353–359.
- [13] Y.H. Choi, J. van Spronsen, Y. Dai, M. Verberne, F. Hollmann, I.W.C.E. Arends, et al., Are natural deep eutectic solvents the missing link in understanding cellular metabolism and physiology? *Plant Physiol.* 156 (2011) 1701–1705.
- [14] A.P. Abbott, D. Boothby, G. Capper, D.L. Davies, R.K. Rasheed, Deep eutectic solvents formed between choline chloride and carboxylic acids: versatile alternatives to ionic liquids, *J. Am. Chem. Soc.* 126 (2004) 9142–9147.
- [15] Y.P. Mbous, M. Hayyan, W.F. Wong, C.Y. Looi, M.A. Hashim, Unraveling the cytotoxicity and metabolic pathways of binary natural deep eutectic solvent systems, *Sci. Rep.* 7 (2017) 1–14.
- [16] A.P. Carneiro, C. Held, O. Rodríguez, G. Sadowski, E.A. Macedo, Solubility of sugars and sugar alcohols in ionic liquids: measurement and PC-SAFT modeling, *J. Phys. Chem. B* 117 (2013) 9980–9995.
- [17] C. Carrero-Carralero, L. Ruiz-Aceituno, L. Ramos, F.J. Moreno, M.L. Sanz, Influence of chemical structure on the solubility of low molecular weight carbohydrates in room temperature ionic liquids, *Ind. Eng. Chem. Res.* 53 (2014) 13843–13850.

- [18] M.E. Zakrzewska, E. Bogel-Lukasik, R. Bogel-Lukasik, Solubility of carbohydrates in ionic liquids, *Energy Fuels* 24 (2010) 737–745.
- [19] X. Zhao, P. Cai, C. Sun, Y. Pan, Application of ionic liquids in separation and analysis of carbohydrates: state of the art and future trends, *TrAC Trends Anal. Chem.* 111 (2019) 148–162.
- [20] K. Wilpiszewska, T. Szychaj, Ionic liquids: media for starch dissolution, plasticization and modification, *Carbohydr. Polym.* 86 (2011) 424–428.
- [21] W. Lan, C.-F. Liu, R.-C. Sun, Fractionation of bagasse into cellulose, hemicelluloses, and lignin with ionic liquid treatment followed by alkaline extraction, *J. Agric. Food Chem.* 59 (2011) 8691–8701.
- [22] A.R.R. Teles, T.B.V. Dinis, E.V. Capela, L.M.N.B.F. Santos, S.P. Pinho, M.G. Freire, et al., Solubility and solvation of monosaccharides in ionic liquids, *Phys. Chem. Chem. Phys.* 18 (2016) 19722–19730.
- [23] C. Carrero-Carralero, L. Ruiz-Aceituno, L. Ramos, M.L. Sanz, F.J. Moreno, Use of room temperature ionic liquids for the selective fractionation of bioactive ketoses from aldoses, *Sep. Purif. Technol.* 149 (2015) 140–145.
- [24] L. Ruiz-Aceituno, C. Carrero-Carralero, L. Ramos, M.L. Sanz, Selective fractionation of sugar alcohols using ionic liquids, *Sep. Purif. Technol.* 209 (2019) 800–805.
- [25] M. Sharma, J. Prakash Chaudhary, D. Mondal, R. Meena, K. Prasad, A green and sustainable approach to utilize bio-ionic liquids for the selective precipitation of high purity agarose from an agarophyte extract, *Green Chem.* 17 (2015) 2867–2873.
- [26] N. Sun, H. Rodríguez, M. Rahman, R.D. Rogers, Where are ionic liquid strategies most suited in the pursuit of chemicals and energy from lignocellulosic biomass? *Chem. Commun.* 47 (2011) 1405–1421.
- [27] A.P. Carneiro, O. Rodríguez, E.A. Macedo, Separation of carbohydrates and sugar alcohols from ionic liquids using antisolvents, *Sep. Purif. Technol.* 132 (2014) 496–504.
- [28] D. Feng, L. Li, F. Yang, W. Tan, G. Zhao, H. Zou, et al., Separation of ionic liquid [Mmim][DMP] and glucose from enzymatic hydrolysis mixture of cellulose using alumina column chromatography, *Appl. Microbiol. Biotechnol.* 91 (2011) 399–405.
- [29] N.L. Mai, N.T. Nguyen, J.I. Kim, H.M. Park, S.K. Lee, Y.M. Koo, Recovery of ionic liquid and sugars from hydrolyzed biomass using ion exclusion simulated moving bed chromatography, *J. Chromatogr. A.* 1227 (2012) 67–72.
- [30] M. Zdanowicz, K. Wilpiszewska, T. Szychaj, Deep eutectic solvents for polysaccharides processing. A review, *Carbohydr. Polym.* 200 (2018) 361–380.
- [31] M. Jablonský, A. Škulcová, A. Malvis, J. Šima, Extraction of value-added components from food industry based and agro-forest biowastes by deep eutectic solvents, *J. Biotechnol.* 282 (2018) 46–66.
- [32] M. Francisco, A. van den Bruinhorst, M.C. Kroon, New natural and renewable low transition temperature mixtures (LTTMs): screening as solvents for lignocellulosic biomass processing, *Green Chem.* 14 (2012) 2153.
- [33] R. Häkkinen, A. Abbott, Solvation of carbohydrates in five choline chloride-based deep eutectic solvents and the implication for cellulose solubility, *Green Chem.* 21 (2019) 4673–4682.
- [34] M.Á. Fernández-Prior, A. Charfi, A. Bermúdez-Oria, E. Rodríguez-Juan, J. Fernández-Bolaños, G. Rodríguez-Gutiérrez, Deep eutectic solvents improve the biorefinery of alperujo by extraction of bioactive molecules in combination with industrial thermal treatments, *Food Bioprod. Process.* 121 (2020) 131–142.
- [35] A. Mena-García, A.I. Ruiz-Matute, A.C. Soria, M.L. Sanz, Green techniques for extraction of bioactive carbohydrates, *Trends Anal. Chem.* 119 (2019) 115612–115622.
- [36] C. Carrero-Carralero, D. Mansukhani, A.I. Ruiz-Matute, I. Martínez-Castro, L. Ramos, M.L. Sanz, Extraction and characterization of low molecular weight bioactive carbohydrates from mung bean (*Vigna radiata*), *Food Chem.* 266 (2018) 146–154.
- [37] L. Ruiz-Aceituno, M.J. García-Sarrió, B. Alonso-Rodríguez, L. Ramos, M.L. Sanz, Extraction of bioactive carbohydrates from artichoke (*Cynara scolymus* L.) external bracts using microwave assisted extraction and pressurized liquid extraction, *Food Chem.* 196 (2016) 1156–1162.
- [38] K.L. Cheong, D.T. Wu, Y. Deng, F. Leong, J. Zhao, W.J. Zhang, et al., Qualitation and quantification of specific polysaccharides from *Panax* species using GC–MS, saccharide mapping and HPSEC-RID-MALLS, *Carbohydr. Polym.* 153 (2016) 47–54.
- [39] Y.G. Xia, S.M. Yu, J. Liang, B.Y. Yang, H.X. Kuang, Chemical fingerprinting techniques for the differentiation of polysaccharides from genus *Astragalus*, *J. Pharm. Biomed. Anal.* 178 (2020) 112898.

- [40] X. Ji, Y. Yan, C. Hou, M. Shi, Y. Liu, Structural characterization of a galacturonic acid-rich polysaccharide from *Ziziphus Jujuba* cv. *Muzao*, *Int. J. Biol. Macromol.* 147 (2020) 844–852.
- [41] S.Q. Liew, G.C. Ngoh, R. Yusoff, W.H. Teoh, Sequential ultrasound-microwave assisted acid extraction (UMAE) of pectin from pomelo peels, *Int. J. Biol. Macromol.* 93 (2016) 426–435.
- [42] X. Lu, Z. Zheng, H. Li, R. Cao, Y. Zheng, H. Yu, et al., Optimization of ultrasonic-microwave assisted extraction of oligosaccharides from lotus (*Nelumbo nucifera* Gaertn.) seeds, *Ind. Crops Prod.* 107 (2017) 546–557.
- [43] Z. Liu, L. Qiao, H. Gu, F. Yang, L. Yang, Development of Brønsted acidic ionic liquid based microwave assisted method for simultaneous extraction of pectin and naringin from pomelo peels, *Sep. Purif. Technol.* 172 (2017) 326–337.
- [44] Z. Liu, L. Qiao, F. Yang, H. Gu, L. Yang, Brønsted acidic ionic liquid based ultrasound-microwave synergistic extraction of pectin from pomelo peels, *Int. J. Biol. Macromol.* 94 (2017) 309–318.
- [45] A.V. Gómez, C.C. Tadini, A. Biswas, M. Buttrum, S. Kim, V.M. Boddu, et al., Microwave-assisted extraction of soluble sugars from banana puree with natural deep eutectic solvents (NADES), *LWT* 107 (2019) 79–88.
- [46] L. Zhang, M. Wang, Optimization of deep eutectic solvent-based ultrasound-assisted extraction of polysaccharides from *Dioscorea opposita* Thunb, *Int. J. Biol. Macromol.* 95 (2017) 675–681.
- [47] H. Al-Suod, R. Gadzała-Kopciuch, B. Buszewski, Simultaneous HPLC-ELSD determination of sugars and cyclitols in different parts of *Phacelia tanacetifolia* Benth, *Biochem. Syst. Ecol.* 80 (2018) 32–38.
- [48] H. Al-Suod, I.A. Ratiu, R. Górecki, B. Buszewski, Pressurized liquid extraction of cyclitols and sugars: optimization of extraction parameters and selective separation, *J. Sep. Sci.* 42 (2019) 1–8.
- [49] K. Cai, D. Hu, B. Lei, H. Zhao, W. Pan, B. Song, Determination of carbohydrates in tobacco by pressurized liquid extraction combined with a novel ultrasound-assisted dispersive liquid-liquid microextraction method, *Anal. Chim. Acta* 882 (2015) 90–100.
- [50] I.-A. Ratiu, H. Al-Suod, M. Ligor, T. Ligor, V. Railean-Plugaru, B. Buszewski, Complex investigation of extraction techniques applied for cyclitols and sugars isolation from different species of *Solidago* genus, *Electrophoresis* 39 (2018) 1966–1974.
- [51] R. Vardanega, P.I.N. Carvalho, D.T. Santos, M.A.A. Meireles, Obtaining prebiotic carbohydrates and beta-ecdysone from Brazilian ginseng by subcritical water extraction, *Innov. Food Sci. Emerg. Technol.* 42 (2017) 73–82.
- [52] F.R. Smiderle, D. Morales, A. Gil-Ramírez, L.I. de Jesus, B. Gilbert-López, M. Iacomini, et al., Evaluation of microwave-assisted and pressurized liquid extractions to obtain β -d-glucans from mushrooms, *Carbohydr. Polym.* 156 (2017) 165–174.
- [53] E. Tejedor-Calvo, D. Morales, P. Marco, S. Sánchez, S. Garcia-Barreda, F.R. Smiderle, et al., Screening of bioactive compounds in truffles and evaluation of pressurized liquid extractions (PLE) to obtain fractions with biological activities, *Food Res. Int.* 132 (2020) 109054.
- [54] P.S. Saravana, Y.N. Cho, H.C. Woo, B.S. Chun, Green and efficient extraction of polysaccharides from brown seaweed by adding deep eutectic solvent in subcritical water hydrolysis, *J. Clean. Prod.* 198 (2018) 1474–1484.
- [55] Z. Chao, Y. Ri-fu, Q. Tai-qiu, Ultrasound-enhanced subcritical water extraction of polysaccharides from *Lycium barbarum* L, *Sep. Purif. Technol.* 120 (2013) 141–147.
- [56] A.I. Ruiz-Matute, M.L. Sanz, N. Corzo, P.J. Martín-Álvarez, E. Ibáñez, I. Martínez-Castro, et al., Purification of lactulose from mixtures with lactose using pressurized liquid extraction with ethanol-water at different temperatures, *J. Agric. Food Chem.* 55 (2007) 3346–3350.
- [57] A.I. Ruiz-Matute, L. Ramos, I. Martínez-Castro, M.L. Sanz, Fractionation of honey carbohydrates using pressurized liquid extraction with activated charcoal, *J. Agric. Food Chem.* 56 (2008) 8309–8313.
- [58] D. Morales, A.J. Piris, A. Ruiz-Rodríguez, M. Prodanov, C. Soler-Rivas, Extraction of bioactive compounds against cardiovascular diseases from *Lentinula edodes* using a sequential extraction method, *Biotechnol. Prog.* 34 (2018) 746–755.
- [59] F. Montañés, T. Fornari, P.J. Martín-Álvarez, A. Montilla, N. Corzo, A. Olano, et al., Selective fractionation of disaccharide mixtures by supercritical CO₂ with ethanol as co-solvent, *J. Supercrit. Fluids* 41 (2007) 61–67.
- [60] F. Montañés, T. Fornari, P.J. Martín-Álvarez, N. Corzo, A. Olano, E. Ibáñez, Selective recovery of tagatose from mixtures with galactose by direct extraction with supercritical CO₂ and different cosolvents, *J. Agric. Food Chem.* 54 (2006) 8340–8345.
- [61] F. Montañés, N. Corzo, A. Olano, G. Reglero, E. Ibáñez, T. Fornari, Selective fractionation of carbohydrate complex mixtures by supercritical extraction with CO₂ and different co-solvents, *J. Supercrit. Fluids* 45 (2008) 189–194.

- [62] F. Montañés, A. Olano, G. Reglero, E. Ibáñez, T. Fornari, Supercritical technology as an alternative to fractionate prebiotic galactooligosaccharides, *Sep. Purif. Technol.* 66 (2009) 383–389.
- [63] X. Ji, Q. Peng, Y. Yuan, F. Liu, M. Wang, Extraction and physicochemical properties of polysaccharides from *Ziziphus Jujuba* cv. Muzao by ultrasound-assisted aqueous two-phase extraction, *Int. J. Biol. Macromol.* 108 (2018) 541–549.
- [64] Z. Chen, W. Zhang, X. Tang, H. Fan, X. Xie, Q. Wan, et al., Extraction and characterization of polysaccharides from *Semen Cassiae* by microwave-assisted aqueous two-phase extraction coupled with spectroscopy and HPLC, *Carbohydr. Polym.* 144 (2016) 263–270.
- [65] Y. Lin, H. Zeng, K. Wang, H. Lin, P. Li, Y. Huang, et al., Microwave-assisted aqueous two-phase extraction of diverse polysaccharides from *Lentinus edodes*: process optimization, structure characterization and antioxidant activity, *Int. J. Biol. Macromol.* 136 (2019) 305–315.
- [66] Z. Cheng, H. Song, X. Cao, Q. Shen, D. Han, F. Zhong, et al., Simultaneous extraction and purification of polysaccharides from *Gentiana scabra* Bunge by microwave-assisted ethanol-salt aqueous two-phase system, *Ind. Crops Prod.* 102 (2017) 75–87.
- [67] I. Molnár-Perl, K. Horváth, Simultaneous quantitation of mono-, di- and trisaccharides as their TMS ether oxime derivatives by GC-MS: I. In model solutions, *Chromatographia* 45 (1997) 321–327.
- [68] D.J. Harvey, Derivatization of carbohydrates for analysis by chromatography; electrophoresis and mass spectrometry, *J. Chromatogr. B* 879 (2011) 1196–1225.
- [69] A.I. Ruiz-Matute, O. Hernández-Hernández, S. Rodríguez-Sánchez, M.L. Sanz, I. Martínez-Castro, Derivatization of carbohydrates for GC and GC-MS analyses, *J. Chromatogr. B* 879 (2011) 1226–1240.
- [70] M. Haas, S. Lamour, O. Trapp, Development of an advanced derivatization protocol for the unambiguous identification of monosaccharides in complex mixtures by gas and liquid chromatography, *J. Chromatogr. A* 1568 (2018) 160–167.
- [71] D.R. Knapp, *Handbook of Analytical Derivatization Reactions*, Wiley Interscience, New York, 1979.
- [72] S.I. Hakomori, A rapid permethylation of glycolipid, and polysaccharide catalyzed by methylsulfinyl carbanion in dimethyl sulfoxide, *J. Biochem.* 55 (1964) 205–208.
- [73] I. Ciucanu, F. Kerek, A simple and rapid method for the permethylation of carbohydrates, *Carbohydr. Res.* 131 (1984) 209–217.
- [74] I. Ciucanu, Per-O-methylation reaction for structural analysis of carbohydrates by mass spectrometry, *Anal. Chim. Acta* 576 (2006) 147–155.
- [75] C.C. Sweeley, R. Bentley, M. Makita, W.W. Wells, Gas-liquid chromatography of trimethylsilyl derivatives of sugars and related substances, *J. Am. Chem. Soc.* 85 (1963) 2497–2507.
- [76] R. Balogh, S. Szabolcs, B. Szabolcs, Determination and quantification of 2'-O-fucosyllactose and 3-O-fucosyllactose in human milk by GC-MS as O-trimethylsilyloxime derivatives, *J. Pharm. Biomed. Anal.* 115 (2015) 450–456.
- [77] L. Ruiz-Aceituno, C. Carrero-Carralero, L. Ramos, I. Martínez-Castro, M.L. Sanz, Development of a carbohydrate silylation method in ionic liquids for their gas chromatographic analysis, *Anal. Chim. Acta* 787 (2013) 87–92.
- [78] M. D'Auria, L. Emanuele, R. Racioppi, N. Stefanizzi, Determination of simple carbohydrates in beer using SPME, on fiber derivatization and gas chromatography mass spectrometry, *Food Res.* 4 (2020) 1156–1161.
- [79] N.H. Low, M. McLaughlin, H.J. Hofsommer, D.A. Hammond, Capillary gas chromatographic detection of invert sugar in heated, adulterated, and adulterated and heated apple juice concentrates employing the equilibrium method, *J. Agric. Food Chem.* 47 (1999) 4261–4266.
- [80] E. Troyano, A. Olano, M. Fernández-Díaz, J. Sanz, I. Martínez-Castro, Gas chromatographic analysis of free monosaccharides in milk, *Chromatographia* 32 (1991) 379–382.
- [81] S.W. Gunner, J.K.N. Jones, M.B. Perry, The gas-liquid partition chromatography of carbohydrate derivatives. Part 1. The separation of glycol and glucose acetates, *Can. J. Chem.* 39 (1961) 1892–1895.
- [82] J.E. Sullivan, L.R. Schewe, Preparation and gas chromatography of highly volatile trifluoroacetylated carbohydrates using *N*-methylbis[trifluoroacetamide], *J. Chromatogr. Sci.* 15 (1977) 196–197.
- [83] R.A. Laine, C.C. Sweeley, Analysis of trimethylsilyl O-methyl oximes of carbohydrates by combined gas-liquid chromatographic-mass spectrometry, *Anal. Biochem.* 43 (1971) 533–538.
- [84] N.H. Low, P. Sporns, Analysis and quantitation of minor disaccharides and trisaccharides in honey, using capillary gas-chromatography, *J. Food Sci.* 53 (1988) 558–561.
- [85] W. Funcke, C. Von Sonntag, *Syn* and *anti* forms of some monosaccharide O-methyl oximes: a ¹³C-n.m.r. and g.l.c. study, *Carbohydr. Res.* 69 (1979) 247–251.
- [86] M. Becker, F. Liebner, T. Rosenau, A. Potthast, Ethoximation-silylation approach for mono- and disaccharide analysis and characterization of their identification parameters by GC/MS, *Talanta* 115 (2013) 642–651.

- [87] M. Pokrzywnicka, R. Koncki, Disaccharides determination: a review of analytical methods, *Crit. Rev. Anal. Chem.* 48 (2018) 186–213.
- [88] M. Becker, T. Zweckmair, A. Forneck, T. Rosenau, A. Potthast, F. Liebner, Evaluation of different derivatization approaches for gas chromatographic-mass spectrometric analysis of carbohydrates in complex matrices of biological and synthetic origin, *J. Chromatogr. A* 1281 (2013) 115–126.
- [89] T. Zweckmair, S. Schiehser, T. Rosenau, A. Potthast, Improved quantification of monosaccharides in complex lignocellulosic biomass matrices: a gas chromatography-mass spectrometry based approach, *Carbohydr. Res.* 446–447 (2017) 7–12.
- [90] H. Bjorndal, B. Lindberg, S. Svensson, Gas-liquid chromatography of partially methylated alditols as their acetates, *Acta Chem. Scand.* 21 (1967) 1801–1804.
- [91] V. Pitthard, P. Finch, GC-MS analysis of monosaccharide mixtures as their diethylthioacetal derivatives: application to plant gums used in art works, *Chromatographia* 53 (2001) S317–S321.
- [92] M. Faraco, D. Fico, A. Pennetta, G.E. De Benedetto, New evidences on efficacy of boronic acid-based derivatization method to identify sugars in plant material by gas chromatography-mass spectrometry, *Talanta* 159 (2016) 40–46.
- [93] K.R. Kim, J. Lee, D. Ha, J. Jeon, H.G. Park, J.H. Kim, Enantiomeric separation and discrimination of 2-hydroxy acids as *O*-trifluoroacetylated (S)-(+)-3-methyl-2-butyl esters by achiral dual-capillary column gas chromatography, *J. Chromatogr. A* 874 (2000) 91–100.
- [94] A.C. Soria, M. Brokl, M.L. Sanz, I. Martínez-Castro, Sample preparation for the determination of carbohydrates in food and beverages, in: J. Pawliszyn (Ed.), *Comprehensive Sampling and Sample Preparation*, Academic Press, Elsevier, Amsterdam, 2012, pp. 213–243.
- [95] G. Cooper, S. Minakshi, C. Asiyó, Gas chromatography-mass spectrometry resolution of sugar acid enantiomers on a permethylated β -cyclodextrin stationary phase, *J. Chromatogr. A* 1216 (2009) 6838–6843.
- [96] G. Cooper, S. Yim, J. Lanoiselée, S. Sorden, F.G. Ramirez, The baseline resolution of aldo-monosaccharide enantiomers: simplified GC-MS analyses using acetal-trifluoroacetyl derivatives for complex samples, *J. Chromatogr. B* 1126–1127 (2019) 121761.
- [97] I. Molnár-Pearl, M. Pintér-Szakács, Á. Kövágó, J. Petróczy, Gas-liquid chromatographic determination of the raffinose family of oligosaccharides and their metabolites present in soy beans, *J. Chromatogr. A* 295 (1984) 433–443.
- [98] A. García-Raso, I. Martínez-Castro, M.I. Páez, J. Sanz, J. García-Raso, F. Saura-Calixto, Gas chromatographic behaviour of carbohydrate trimethylsilyl ethers: I. Aldopentoses, *J. Chromatogr. A* 398 (1987) 9–20.
- [99] A. García-Raso, M. Fernández-Díaz, M.I. Páez, J. Sanz, I. Martínez-Castro, Gas chromatographic retention of carbohydrate trimethylsilyl ethers: III. Keto-hexoses, *J. Chromatogr. A* 471 (1989) 205–216.
- [100] A. Marsol-Vall, M. Balcells, J. Eras, R. Canela-Garayoa, Comprehensive two-dimensional gas chromatography time-of-flight mass spectrometry to assess the presence of alpha, alpha-trehalose and other disaccharides in apple and peach, *Phytochem. Anal.* 26 (2015) 279–286.
- [101] K. Dettmer-Wilde, W. Engewald (Eds.), *Practical Gas Chromatography: A Comprehensive Reference*, Springer-Verlag, Berlin-Heidelberg, 2014.
- [102] O. Hernández, A.I. Ruiz-Matute, A. Olano, F.J. Moreno, M.L. Sanz, Comparison of fractionation techniques to obtain prebiotic galactooligosaccharides, *Int. Dairy J.* 19 (2009) 531–536.
- [103] N.G. Carlsson, H. Karlsson, A.S. Sandberg, Determination of oligosaccharides in foods, diets, and intestinal contents by high-temperature gas chromatography and gas chromatography/mass spectrometry, *J. Agric. Food Chem.* 40 (1992) 2404–2412.
- [104] S. Rodríguez-Sánchez, A.C. Soria, A.I. Ruiz-Matute, M.L. Sanz, Improvement of a gas chromatographic method for the analysis of iminosugars and other bioactive carbohydrates, *J. Chromatogr. A* 1289 (2013) 145–148.
- [105] F. Bartolozzi, G. Bertazza, D. Bassi, G. Cristoferi, Simultaneous determination of soluble sugars and organic acids as their trimethylsilyl derivatives in apricot fruits by gas-liquid chromatography, *J. Chromatogr. A* 758 (1997) 99–107.
- [106] R. Kubinec, P. Kotora, V. Ferenczy, J. Blaško, P. Podolec, A. Hengerics Szabo, et al., Simultaneous analysis of carbohydrates, polyols and amines in urine samples using chemical ionization gas chromatography with tandem mass spectrometry, *J. Sep. Sci.* 41 (2018) 449–458.
- [107] Z. Fuzfai, I. Molnár-Perl, Gas chromatographic-mass spectrometric fragmentation study of flavonoids as their trimethylsilyl derivatives: analysis of flavonoids, sugars, carboxylic and amino acids in model systems and in citrus juices, *J. Chromatogr. A* 1149 (2007) 88–101.
- [108] J. Schenk, G. Nagy, N.L.B. Pohl, A. Leghissa, J. Smuts, K.A. Schug, Identification and deconvolution of carbohydrates with gas chromatography-vacuum ultraviolet spectroscopy, *J. Chromatogr. A* 1513 (2017) 210–221.

- [109] E. de la Fuente, M.L. Sanz, I. Martínez-Castro, J. Sanz, Development of a robust method for the quantitative determination of disaccharides in honey by gas chromatography, *J. Chromatogr. A* 1135 (2006) 212–218.
- [110] M.L. Sanz, J. Sanz, I. Martínez-Castro, Gas chromatographic-mass spectrometric method for the qualitative and quantitative determination of disaccharides and trisaccharides in honey, *J. Chromatogr.* 1059 (2004) 143–148.
- [111] R.J. Nash, W.S. Goldstein, S.V. Evans, L.E. Fellows, Gas chromatographic method for separation of nine polyhydroxy alkaloids, *J. Chromatogr. A* 366 (1986) 431–434.
- [112] S. Rodríguez-Sánchez, A.I. Ruiz-Matute, M.L. Sanz, A.C. Soria, Characterization of trimethylsilyl ethers of iminosugars by gas chromatography-mass spectrometry, *J. Chromatogr. A* 1372 (2014) 221–227.
- [113] L. Ruiz-Aceituno, C. Carrero-Carralero, A.I. Ruiz-Matute, L. Ramos, M.L. Sanz, Characterization of cyclitol glycosides by gas chromatography coupled to mass spectrometry, *J. Chromatogr. A* 1484 (2017) 58–64.
- [114] V.A. Isidorov, L. Szczepaniak, Gas chromatographic retention indices of biologically and environmentally important organic compounds on capillary columns with low-polar stationary phases, *J. Chromatogr. A* 1216 (2009) 8998–9007.
- [115] M.L. Sanz, M.T. Díez-Barrio, J. Sanz, I. Martínez-Castro, GC behaviour of disaccharides trimethylsilyl oximes, *J. Chromatogr. A* 41 (2003) 205–208.
- [116] A.I. Ruiz-Matute, M. Brokl, A.C. Soria, M.L. Sanz, I. Martínez-Castro, Gas chromatographic-mass spectrometric characterization of tri- and tetrasaccharides in honey, *Food Chem.* 120 (2010) 637–642.
- [117] I. Stumm, W. Baltes, Analysis of the linkage positions in polydextrose by the reductive cleavage method, *Food Chem.* 59 (1997) 291–297.
- [118] O. Hernández-Hernández, F.J. Moreno, A. Montilla, A. Clemente, A. Olano, M.L. Sanz, Characterization of novel galactooligosaccharides derived from lactulose, *J. Chromatogr. A* 1218 (2011) 7691–7696.
- [119] S. Willför, A. Pranovich, T. Tamminen, J. Puls, C. Laine, A. Suurnäkki, B. Saake, et al., Carbohydrate analysis of plant materials with uronic acid-containing polysaccharides—A comparison between different hydrolysis and subsequent chromatographic analytical techniques, *Ind. Crops Prod.* 29 (2009) 571–580.
- [120] N.P.J. Price, Permethylated linkage analysis techniques for residual carbohydrates, *Appl. Biochem. Biotechnol.* 148 (2008) 271–276.
- [121] C.R.L.D. Costa, R.A. Menolli, E.F. Osaku, R. Tramontina, R.H. de Melo, A.E. Amaral, et al., Exopolysaccharides from *Aspergillus terreus*: production, chemical elucidation and immunoactivity, *Int. J. Biol. Macromol.* 139 (2019) 654–664.
- [122] H.Y. Ji, J. Yu, A.J. Liu, Structural characterization of a low molecular weight polysaccharide from *Grifola frondosa* and its antitumor activity in H22 tumor-bearing mice, *J. Funct. Foods* 61 (2019) 103472.
- [123] J. Li, F.F. Gu, C. Cai, M.H. Hu, L.D. Fan, J.J. Hao, G.L. Yu, Purification, structural characterization, and immunomodulatory activity of the polysaccharides from *Ganoderma lucidum*, *Int. J. Biol. Macromol.* 143 (2020) 806–813.
- [124] C.S. Wang, D.H. Hua, C.Y. Yan, Structural characterization and antioxidant activities of a novel fructan from *Achyranthes bidentata* Blume, a famous medicinal plant in China, *Ind. Crops Prod.* 70 (2015) 427–434.
- [125] Z. Guadalupe, B. Ayestarán, P. Williams, T. Doco, Determination of must and wine polysaccharides by gas chromatography-mass spectrometry and size-exclusion chromatography, in: K. Ramawat, J.M. Mérillon (Eds.), *Polysaccharides*, Springer, Cham, 2015.
- [126] C.P. Passos, A. Rudnitskaya, J.M.M.G.C. Neves, G.R. Lopes, M.A. Coimbra, Structural features of spent coffee grounds water-soluble polysaccharides: towards tailor-made microwave assisted extraction, *Carbohydr. Polym.* 214 (2019) 53–61.
- [127] M. Brokl, A.C. Soria, A.I. Ruiz-Matute, M.L. Sanz, L. Ramos, Separation of disaccharides by comprehensive two-dimensional gas chromatography-time-of-flight mass spectrometry. Application to honey analysis, *J. Agric. Food Chem.* 58 (2010) 11561–11567.

Gas chromatographic applications in metabolomics

*Sze Han Lee*¹, *Mainak Mal*², *Kishore Kumar Pasikanti*³,
*Eric Chun Yong Chan*¹

¹Department of Pharmacy, National University of Singapore, Singapore; ²Department of Pharmaceutical Technology, Brainware University, Kolkata, India; ³Accelerating Therapeutics for Opportunities in Medicine (ATOM) Consortium, San Francisco, CA, United States

29.1 Overview of metabonomics

Since its inception, the field of metabonomics has grown remarkably in terms of its applications and contributions to system biology research. Metabonomics provides a powerful tool for gaining valuable insight into functional biology, toxicology, pharmacology, diagnosis, and prognosis of diseases. The non-hypothesis-driven global metabolic profiling strategy or metabonomics is defined as the quantitative measurement of the dynamic multiparametric metabolic response of living systems to pathophysiological stimuli or genetic modification [1]. Metabonomics is complementary to genomics and proteomics as it measures the perturbed metabolic endpoints due to environmental, pharmacological, or pathological influences while in genomics and proteomics, more upstream biological events are typically profiled and studied [2]. Metabonomic studies involve the analysis of various biological matrices such as blood, urine, and tissues using

suitable analytical platforms. Metabolomics and metabolic fingerprinting are terms used in addition to metabonomics to describe the unbiased and nontargeted analysis of global metabolic profiles in biofluids and tissues [3,4]. In metabonomics, metabolites belonging to diverse metabolic pathways and comprising diverse chemical classes, such as organic acids, amino acids, fatty acids, amines, sugars, sugar alcohols, steroids, and nucleic acid bases, are profiled. Therefore, multiple complementary analytical platforms are often utilized for nontargeted metabonomic studies, in order to cover as large a metabolic space as possible [5]. In this chapter, application of gas chromatography–mass spectrometry (GC-MS)-based metabonomics is described for solid and liquid matrices. Notable biological matrices such as tissue, feces, plasma, or urine were chosen for discussion since the sample preparation procedures for these matrices are distinct and require special attention.

29.2 Analytical tools in metabonomic research

Ideally, an analytical tool for metabonomic research should allow analysis with minimal or no sample preparation, exhibit a high degree of robustness and reproducibility, and be high throughput and highly sensitive. Most importantly, for metabonomics, comprehensive coverage of metabolic space and ease of identification of profiled metabolites are additional desirable attributes of an analytical platform. Analytical platforms that are commonly used in metabonomics include nuclear magnetic resonance (NMR) spectroscopy- and MS-based techniques such as GC-MS, liquid chromatography–mass spectrometry (LC-MS), or capillary electrophoresis–mass spectrometry (CE-MS) [6]. In addition to these popular techniques, other methods such as Fourier transform infrared (FTIR) spectroscopy [7], LC with ultraviolet [8] or coulometric detection [9], and CE with ultraviolet detection [10] have also been used in metabonomic studies. In addition, hybrid platforms comprising LC, NMR spectroscopy, and MS have been explored in metabonomics. In such systems, the LC eluent is split into two parts and subjected to concomitant analysis by both NMR and MS. The resulting NMR- and MS-based data provide in-depth molecular information and aid in metabolite identification [11,12].

29.3 GC-MS-based metabonomics

29.3.1 GC-MS technologies

Among the various analytical methods utilized conventionally for metabonomics, GC-MS has emerged as an essential and complementary analytical technique because of its high sensitivity, reproducibility, and peak resolution. Moreover, the identification of metabolites can be performed straightforwardly using the electron ionization (EI) spectral libraries. However, chemical derivatization of the polar functional groups of metabolites is usually required in

GC-MS analysis to decrease their polarity and increase volatility and thermal stability. As a result of the extensive sample preparation process combined with long GC separation times, GC-MS is considered a relatively low-throughput technique compared to LC-MS or NMR spectroscopy [13]. However, sample throughput is significantly enhanced with the advent of gas chromatography/time-of-flight mass spectrometry (GC-TOFMS). Coupling of GC to the TOF analyzer offers several advantages compared with quadrupole MS. Software advances and the fast acquisition rate of TOFMS (up to 500 Hz) facilitate the deconvolution of the mass spectra of closely eluting analytes [14]. In other words, MS spectra of coeluting peaks can be extracted when chromatographic resolution of the metabolites is incomplete. Such an attribute of GC-TOFMS is pertinent to the analysis of complex biological matrices where coelution of metabolites is prevalent. Importantly, separation time can be reduced at lower chromatographic resolution employing the peak deconvolution function. In addition, spectral purity and sensitivity are enhanced significantly in GC-TOFMS compared to GC-MS analysis [14]. The advent of comprehensive two-dimensional gas chromatography time-of-flight mass spectrometry (GC \times GC-TOFMS) has significantly added to the metabolic space covered by conventional GC-MS. GC \times GC-TOFMS is noted for its ability to analyze complex mixtures in metabonomic investigations [15–19]. GC \times GC-TOFMS offers several advantages compared to GC-MS in metabonomic analyses. Firstly, peak capacity and peak resolution are significantly enhanced. Approximately 1000 peaks can be detected using GC \times GC-TOFMS. Therefore, a larger metabolic space can be covered using GC \times GC-TOFMS. Secondly, artifacts arising from column bleed or derivatizing agent can be separated from metabolite peaks using GC \times GC-TOFMS. Subsequently, artifact peaks can be automatically excluded from the data tables during data preprocessing. Thirdly, a fivefold increase in sensitivity was observed using GC \times GC-TOFMS compared to

GC-MS due to peak modulation. Finally, apart from the increased number of detectable peaks compared to GC-MS, spectral purity is significantly improved, which in turn aids in mass spectral deconvolution and compound identification [20–23].

Although comprehensive two-dimensional GC offers several advantages, it is important not to lose sight of some of the limitations of GC \times GC-TOFMS. Since short and narrow-bore columns are commonly used as second-dimension columns, column overloading is commonly observed in metabolomic studies [24]. Another issue requiring further investigation is retention time shifts in GC \times GC-TOFMS analysis. Although GC \times GC affords increased peak resolution, coelution of some metabolites remains inevitable due to the complex nature of biological matrices. The principles and instrumentation of comprehensive two-dimensional GC are reviewed in Chapter 7.

29.3.2 Metabonomic workflow

The overall workflow adopted in GC-MS-based metabolomics is summarized in Fig. 29.1.

29.3.2.1 GC-MS conditions and data acquisition

A sample injection volume of 0.5–2 μL is typically adopted in metabolomic studies, and the injector temperature is maintained at 200–250°C to facilitate rapid vaporization of the sample and subsequent mixing with the carrier gas. This is followed by the chromatographic separation of derivatized metabolites and subsequent detection by MS [25]. A split injection mode is usually preferred in metabolomic studies where metabolites vary widely in concentration. As discussed earlier, with the advent of TOFMS together with deconvolution software, the problem of coeluting analytes has been significantly suppressed resulting in faster GC separations [13].

Columns with varying polarities (DB-1 to DB-50) [25–27], varying internal diameters (0.25–0.18 mm) [25,28], and different lengths (10–60 m) have been utilized in metabolomic studies [29]. Nevertheless, DB-5MS columns or columns with similar separation properties are commonly used in metabolomic studies [30,31]. Generally, GC oven temperatures vary from 40 to 325°C [25,32] and the maximum column temperature that can be utilized depends on the type of GC column used. Helium is the most common carrier gas with typical column flow rates from 0.8 to 2 mL min^{-1} [26,31].

Although EI is the most common mode of ionization in metabolomic studies, chemical ionization (CI) has also been explored particularly for compounds that do not yield molecular ions in EI due to complete fragmentation [33]. In metabolomic studies, MS is typically operated in the full scan mode where a mass range of 50–700 is scanned [26]. Since metabolites are commonly subjected to derivatization prior to GC-MS analysis, various by-products are formed concurrently by the derivatizing agent. Such by-products can be present at high concentrations and therefore may cause saturation of the MS detector. Due to their high volatility, these by-products usually elute within the first few minutes of the separation. Therefore, an acquisition delay is commonly used, during which the MS detector is idled until these by-products are completely eluted [13].

Data acquisition is carried out by the software provided along with the instrument, and the raw data files are generated in a proprietary data format. However, for subsequent data preprocessing it is often necessary to convert the default data formats to common raw data formats, such as netCDF, ASCII, or mzXML. Some instrument software packages contain features for this purpose [34].

29.3.2.2 Data preprocessing and pretreatment

Data preprocessing in metabolomics analysis commonly refers to various steps involved in

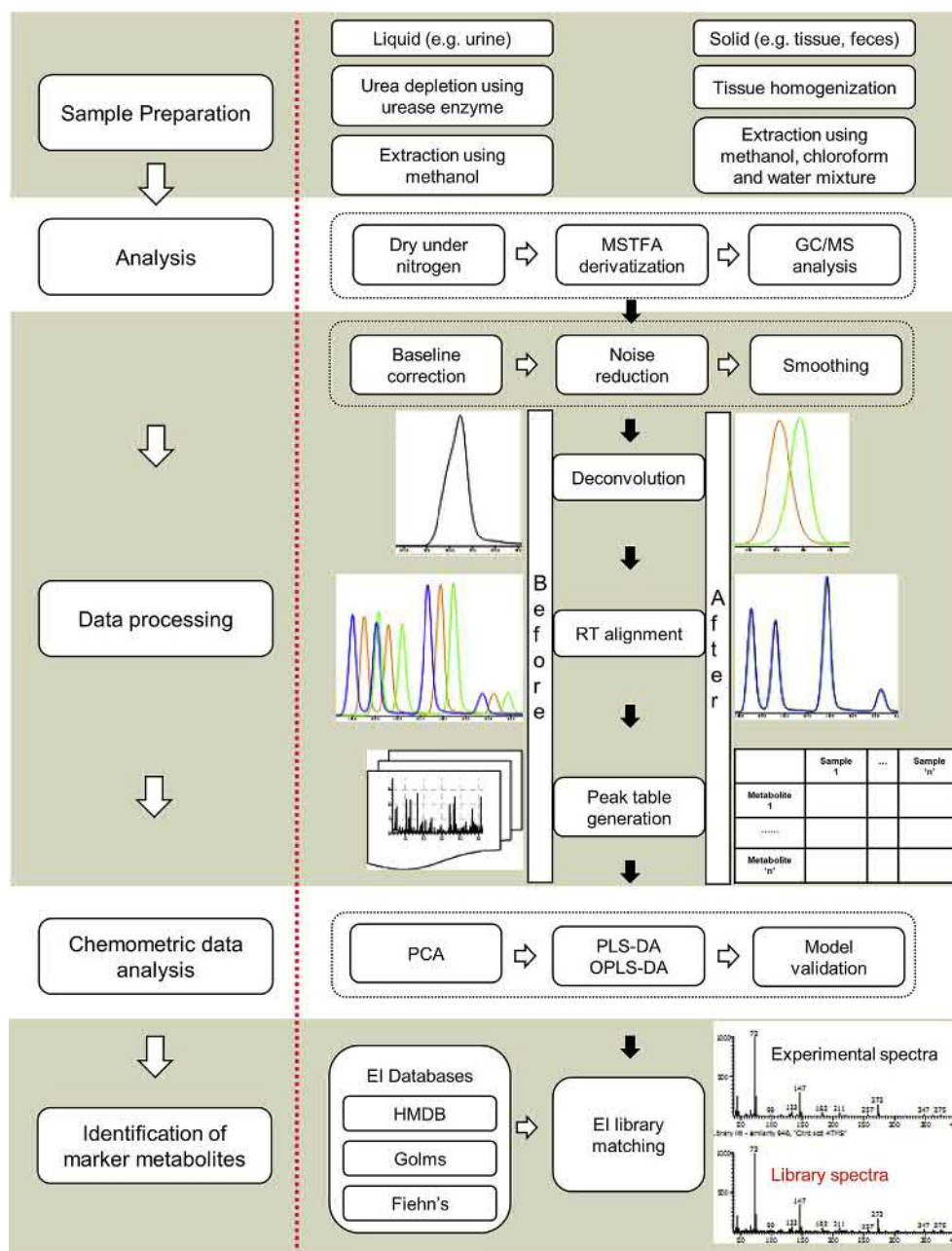


FIGURE 29.1 Summary of the main steps in liquid- and solid-based metabolomics. Subsequent to sample preparation, similar methodologies can be adopted for GC-MS data analysis, data preprocessing, chemometric data analysis, and metabolite identification.

converting GC-MS raw data into data tables amenable for chemometric analysis [35]. Data preprocessing includes steps such as noise reduction, baseline correction, deconvolution, and retention time alignment (see Chapter 20). Deconvolution is necessary to resolve coeluting peaks [36], and retention time alignment is important to negate variation in retention times as chemometric techniques are inherently sensitive to retention time precision [37]. Commercial software provided by GC-MS instrument vendors such as ChromaTOF (Leco Corp., USA) [38] as well as freely available software packages such as AMDIS (deconvolution only) [39], MathDAMP [40], MSFACTs [41], MZmine [42], XCMS [43], MetAlign [44], and TagFinder [45] can be used for GC-MS data preprocessing. Although these peak alignment algorithms reduce manual intervention significantly, each product has some limitations such as the mandatory conversion of chromatographic file formats to NetCDF and lack of all data preprocessing steps. For example, MetAlign provides retention time alignment features but does not offer deconvolution of chromatographic peaks [44]. In contrast, AnalyzerPro provides deconvolution but does not offer retention time alignment. In addition, most of the alignment software packages do not provide EI library matching for metabolite identification. Therefore, end users often have to depend on GC-MS vendor software to perform library matching. Recent online platform such as Workflow4Metabolomics 3.0 consolidates publicly available workflows for data processing, metabolite identification, and statistical analysis in a single product [46]. Finally, all the software packages require an in-depth understanding of the underlying algorithms, extensive optimization of parameters, and thorough validation before they can be utilized for peak alignment. Koh et al. evaluated retention time alignment accuracies of various algorithms for derivatized metabolite peaks and standard compounds [38]. Among the peak alignment algorithms evaluated in the study,

the calibration feature of the GC-MS software showed superior performance [38]. The use of a calibration feature for peak alignment requires greater manual intervention compared to peak alignment software. This limitation is acceptable, however, since the focus of metabolomics is data quality rather than throughput.

Data pretreatment involves steps such as normalization, centering, scaling, and transformation [35]. Normalization is necessary to counter minor variations in data arising from sample preparation and/or instrument response, while preserving the relevant inherent biological variation [34]. Although different normalization strategies exist, normalization to total area [13] and normalization using single or multiple internal standards [28] are used predominantly in the case of GC-MS-based metabolomics. Centering helps in balancing the difference between high- and low-abundance metabolites and mean centering is typically used for this purpose [47]. Scaling is used to account for the large concentration range of different metabolites by converting the data into a relative concentration using a scaling factor. Different scaling methods based on data dispersion such as auto-scaling, unit variance scaling, and Pareto scaling are typically used for metabolomic data [48]. Transformation involves nonlinear conversion of the data, for example, log transformation or power transformation to rectify heteroscedastic variation and to improve symmetry of skewed data [48]. Mathematical environments such as MATLAB (Mathworks, Natick, MA, USA) and R (open source GNU project) or commercial chemometric software such as SIMCA-P (Umetrics, Umeå, Sweden) have in-built features to carry out such data pretreatment steps prior to chemometric analysis.

29.3.2.3 Chemometric data analysis

Metabolomic studies result in the generation of huge and complex data sets containing a large number of observations (samples) and variables (metabolites). Multivariate statistical techniques

or chemometric tools are indispensable for the analysis of these data sets. Of the different chemometric methods available, hierarchical clustering, partitional clustering, artificial neural networks, support vector machine, evolutionary-based algorithms, and regression trees, projection-based methods are extensively used in metabolomics [35]. Projection-based methods include both unsupervised methods such as principal component analysis (PCA) and supervised methods such as partial least squares discriminant analysis (PLS-DA) and orthogonal PLS-DA (OPLS-DA). Projection-based methods are based on the assumption that the system in question is controlled by a few latent variables (LVs) or principal components. As PCA is useful for identifying outliers and inherent clustering trends, it is commonly used as the first step in chemometric analysis to investigate inherent data variability and clustering trends. Outliers can also be detected using the distance to model plot (DModX) based on residual variance of the PCA model [49]. PLS-DA is a supervised method in which class information for observations is included in the analysis to further enhance the investigation of class clustering trends. The OPLS-DA is a modified form of PLS-DA where orthogonal signal correction is used to split the variation in the X matrix into two parts, one that is unrelated or orthogonal to Y and the other that is related to Y [29]. This simplifies model interpretation and the identification of important variables contributing to the model as compared to PLS-DA [50]. Thus, PCA (to identify outliers and inherent clustering trends) is conventionally followed by PLS-DA or OPLS-DA to identify potential marker metabolites that are contributing significantly to the model and discriminating one class from another [51]. Chemometric software such as SIMCA-P and Unscrambler (CAMO software, Oslo, Norway) and mathematical environments such as MATLAB and R (open source GNU project)

are typically employed for chemometric data analysis in metabolomics.

29.3.2.4 Model validation

A typical chemometric model built in a metabolomic study is characterized by a relatively small number of observations compared to the number of variables [52]. Therefore, in some cases, it is possible that optimistic performance characteristics observed in a PLS-DA or OPLS-DA model could be due to specimen artifacts, overfitting of data, or chance correlation [51,53]. Therefore, validation of each model should be performed before it can be leveraged to predict the unknown observations or identification of marker metabolites. Model validation can be performed in two stages starting with internal validation and followed by external validation. Internal validation of PLS-DA models can be performed using a permutation test and receiver operating characteristic (ROC) analysis [54]. In the permutation test, goodness of fit (R^2 and Q^2) of the original model is compared with the goodness of fit of several PLS-DA models built using the data matrix where the order of the Y observations is randomly permuted, while the X matrix is kept intact [55,56]. Additionally, ROC analysis using the cross-validated predicted Y (predicted class) values can be further performed to verify the robustness of the model. The sensitivity and specificity trade-offs can be summarized for each model using the area under the ROC curve (AUC) and calculated using the trapezoidal rule [54]. ROC analysis can provide a good indication of sensitivity and specificity that can be achieved in predicting unknown samples.

Subsequent to confirmation of validity of each model using internal validation strategies, model validity can be further confirmed using external validation. To perform external validation, a subset of observations is randomly selected for building a training set and classification of the remaining samples is then predicted.

The selection of training and tests sets should be defined prior to chemometric analysis to represent actual prediction of unknown samples and to avoid bias related to data preprocessing and pretreatment. External validation can be performed iteratively by randomly selecting different combinations of training and test sets to estimate the predictive ability of the model. Most software packages (SIMCA-P or MetaboAnalyst) offer in-built features to perform internal and external validation. Once the validity of each model is confirmed using internal and external validation strategies, statistical significance of potential marker metabolites in control and treatment groups should be further verified by univariate statistical tests such as the Welch t-test [13].

29.3.2.5 Biomarker identification and pathway mapping

Subsequent to GC-MS analysis, preliminary identification of metabolites is carried out by library searching against mass spectral library databases provided with the instrument, such as the National Institute of Standards and Technology (NIST) database, as well as online databases such as the Human Metabolome Database (HMDB) [57], NIST Chemistry Web Book (webbook.nist.gov/chemistry), Madison Metabolomic Consortium Database (mmcd.nmrfam.wisc.edu), SpecInfo (<https://application.wiley-vch.de/stmdata/specinfo.php>), and Spectral Database for Organic Compounds (https://sdbs.db.aist.go.jp/sdbs/cgi-bin/cre_index.cgi). The identities of significant marker metabolites are further confirmed using commercially available standard compounds [13]. Subsequent to confirmation, it is pertinent to link the marker metabolites to metabolic pathways. Metabolic pathway mapping is important to identify significantly perturbed metabolic pathways in response to a diseased condition, or genetic modification, or pharmacological intervention. Various databases such as the Kyoto Encyclopedia of Genes and Genomes (KEGG), BioCyc

[58], and Reactome [59] and software packages such as KegArray (used with KEGG), Pathway Tools (used with BioCyc), and MetaCore (GeneGo, St Joseph, MI, USA) are available for metabolic pathway analysis. For the characterization of recurrent unidentified metabolites (potentially novel compounds), consensus mass spectra from untargeted GC-MS metabolomics data should be systemically constructed for eventual library building [60].

29.4 Metabonomics of solid samples

29.4.1 Sample preparation

The first step in sample preparation for GC-MS-based metabonomics of solid samples involves the effective extraction of metabolites from biological matrices such as tissues or feces. Different extraction strategies such as homogenization alone, or homogenization followed by ultrasonication, or ultrasonication alone (usually applicable for small amount of tissue, ≤ 20 mg) can be adopted [13,61]. The choice of extraction solvent depends on the nature of the matrix as well as the metabonomic study. In a heterogeneous solid matrix such as feces, isopropanol:acetonitrile:water (3:2:2 ratio) and 80% (v/v) aqueous methanol were the superior extraction solvents for adult and baby giant panda, respectively [62]. In the case of global metabonomics, a mixture of different solvents [for instance, chloroform/methanol/water 2.5:2 (v/v/v)] covering a wide polarity range is typically used for the extraction of as large a metabolic space as possible [61]. In the case of targeted metabolic profiling, a solvent or solvent mixture of narrow polarity range is used to selectively extract metabolites belonging to a specific chemical class. After extraction, the tissue extract is typically dried by using a nitrogen evaporator, followed by addition of a sufficient quantity of anhydrous toluene (about 100 μ L) to the extract. The mixture is evaporated to complete dryness using a nitrogen evaporator in order to eliminate any trace of

moisture that might interfere with GC-MS analysis. The dried extract thus obtained is then typically derivatized. Derivatization strategies include methoximation of metabolites using methoxyamine hydrochloride (MOX) reagent in pyridine (28–37°C, up to 2 or 16 h) followed by trimethylsilyl (TMS) derivatization using reagents such as N,O-bis-(trimethylsilyl)-trifluoroacetamide (BSTFA) with 1% trimethylchlorosilane (TMCS) or N-methyl-N-trifluoroacetamide (MSTFA) with 1% TMCS at 70°C for 30 min or 37°C for 1 h. Methoximation prior to TMS derivatization is considered necessary to prevent cyclization of sugars, decarboxylation of α -ketoacids, and stabilization of enolizable ketone groups [13,26,61].

29.4.2 Applications

Tissue-based metabonomics differs from plasma- or urine-based metabonomics as it provides anatomical site-specific information of the endogenous metabolites and is less susceptible to variation compared with plasma or urine. Therefore, tissues are suitable biomatrices for metabolic profiling where the main aim of the metabonomic study is to reveal the metabolic phenotype and deregulated metabolic pathways associated with a disease or pharmacological intervention rather than to diagnose or prognose a pathology. Tissue-based metabonomics using GC-MS either alone or in conjunction with other methods such as NMR, CE-MS, or LC-MS has shown promise in identifying metabolite-based biomarkers in different forms of cancer. Denkert et al. found that molecular changes in ovarian tumor tissues can be characterized by quantitative changes in metabolic profiles [63]. Tissue-based metabonomic studies in human colorectal cancer have revealed perturbations in various biochemical processes such as glycolysis, Krebs cycle, amino acid metabolism, fatty acid biosynthesis, steroid biosynthesis, eicosanoid

biosynthesis, bile acid biosynthesis, nucleotide metabolism, and osmoregulation. The majority of these observations were attributed to the high energy demand, tissue hypoxia, and altered synthetic rate of cellular components of rapidly proliferating tumor cells [61,63–65]. Moreover, in the study by Ong et al., distinct progressive changes in metabolite profiles accompanying the transformation of normal colonic mucosa to malignant tumor were found [65]. GC-MS-based metabonomic studies in human gastric cancer as well as in animal models of gastric cancer resulted in the identification of several marker metabolites with the potential for diagnosis and staging of gastric cancer as well as for prognosis of metastatic progression [66,67]. Wu et al. utilized GC-MS-based metabolic profiling of biopsied tissue specimens obtained from esophageal cancer patients, to identify several marker metabolites of diagnostic potential [68]. Similar studies have resulted in the identification of metabolite-based biomarkers of brain cancer [69,70].

GC-MS was utilized in the metabonomic studies of carbon tetrachloride-induced liver injury in mouse [71] and rat [72], metabolic syndrome using cardiac and adipose tissues of PPAR-alpha null mutant mouse [73], and microbial marker metabolites of endocarditis in human cardiac tissue [74]. The GC-MS was also used for tissue-based targeted metabonomic studies of L- β -methyl-aminoalanine in the human brain [75] and prostaglandins in human lung [76] and colorectal cancer [77,78]. GC-MS-based metabolic profiling was used to validate the 3-nitropropionic acid-induced early stage Huntington's disease rat model [79]. Recent advances in gut microbiome research have also revitalized efforts in fecal metabonomics, with identification of human and gut microbiota cometabolites allowing further exploration of host–gut microbiota metabolic interactions [80].

29.5 Metabonomics of liquid samples

Although solid tissue metabonomic studies are important in the mechanistic elucidation of diseases, harvesting tissue is an invasive process, often requiring biopsy. Compared with the analysis of tissue samples, liquid samples, such as urine and blood, offer several advantages. Urine collection is noninvasive and not limited by volume. In addition, urine can be used for measuring time-resolved, dynamic, or temporal data, an invaluable attribute for the investigation of the pathogenesis, progression, and prognosis of acute and chronic diseases. Blood is another useful matrix that carries biochemical signatures from perfused organs and tissues and may be processed to a simpler matrix such as serum or plasma. However, the choice of anti-coagulant has been shown to affect the plasma metabolome [81], and the use of blood has limitations in some cases since its metabolic composition can be affected by multiple organ systems and alterations detected in the serum and plasma may not be specific to a particular disease [82]. The application of GC-MS in urinary metabolic profiling is a long-standing practice. As expected, there were significant improvements in urine sample preparation and data processing over time. Shoemaker et al. contributed to a significant improvement in sample preparation by employing the urease enzyme to deplete urea that caused major chromatographic interference and masked many of the low-intensity metabolite peaks [83]. Remarkable improvement in analytical turnaround time in urine metabonomics was realized with the coupling of GC to TOFMS, as noted earlier.

The majority of recent reports describe the application of GC-MS in metabonomics rather than an advancement of the technique. This indicates a high level of acceptance and maturity of the GC-MS platform. Although the composition of urine may reflect a disease state or a pharmacological effect, it is important to

note that the urine metabotype is equally sensitive to other factors such as dietary intake [84] and physiological conditions such as age, gender, and demographic characteristics [85,86]. In some instances, urine may contain xenobiotics and their metabolites, which can introduce additional complexities in downstream data analysis. Furthermore, variation in metabolic composition can be introduced during sample collection and storage. Therefore, a proper study design is extremely important to obtain meaningful data. Baseline characteristics of study groups, sample collection, and storage conditions should be carefully controlled and standardized according to the research hypothesis. Variations due to diet and lifestyle factors can be minimized by collection of first-pass urine [84]. However, collection and storage of first-pass urine are challenging due to poor patient compliance. Evaluation of stability of urine samples using GC-MS [85] and other analytical platforms showed that urine samples are stable up to 6 months when stored at -20 or -80°C . No significant difference in urine metabolite compositions was observed when urine samples were subject to repeated freeze–thaw cycles (up to nine cycles) [85,87]. Lauridsen et al. showed that addition of a preservative is not mandatory provided urine samples are stored below -20°C [88]. On the other hand, instability of some of the metabolites was noted when urine was subject to freeze drying [88].

29.5.1 Sample preparation

Urine presents a wide dynamic range of metabolite concentrations, the occurrence of urea as a chromatographic interference, and the unpredictable degree of urinary dilution. Therefore, sample preparation for urinary metabolic profiling is distinct from other biological matrices. Sample preparation varies according to the derivatizing reagent utilized in a study.

Among several derivatizing reagents explored, TMS derivatizing agents such as BSTFA and MSTFA are used predominantly [89–92]. Recently, derivatization using ethyl chloroformate is gaining popularity particularly for urine metabolic profiling. In contrast to TMS reagents, which only work in the nonaqueous phase, ethyl chloroformate (ECF) remains reactive in aqueous medium. Briefly, urine preparation for TMS derivatization includes incubation of urine with urease enzyme, extraction using methanol, drying of the metabolic extract, and a two-step derivatization process with MOX and MSTFA, whereas ECF derivatization includes the addition of anhydrous ethanol and pyridine to urine samples followed by ECF. The mixture is then sonicated and subsequently extracted using chloroform, with the aqueous layer pH adjusted to 9–10 with sodium hydroxide. In some cases, the derivatization procedure is repeated with the addition of ECF to the mixture. After two successive ECF derivatizations, the aqueous layer is removed by aspiration, and the chloroform layer containing the derivatives is isolated, dried with anhydrous sodium sulfate, and analyzed by GC-MS [93].

Due to the wide adoption of TMS derivatization in metabolomic research, sample preparation employing TMS derivatization is presented in more detail here. Typically, a small volume of urine (200–500 μL) is utilized. Sample preparation is initiated by incubating individual urine samples with urease to deplete excess urea, which is a major chromatographic interferent. Up to 30–100 U of urease is used, depending on the volume of urine [85,94]. Termination of urease activity and extraction of metabolites are carried out using ethanol [94] or methanol [54]. Similar extraction efficiency for urinary metabolites by ethanol and methanol was noted [85]. Similar to tissue samples, the extracted metabolites are dried and subject to a two-step derivatization, first with MOX reagent, followed by a TMS derivatizing reagent such as MSTFA. However, it is important to note that silylation

can cause conversion reactions for some metabolites, for example, arginine is converted into ornithine by reaction with BSTFA or MSTFA [95].

29.5.2 Applications

Applications of GC-based urinary metabolic profiling are wide ranging, which include studying diseases of the renal system such as bladder, ovarian, and kidney cancers [31,54,96,97] and a host of other nonrenal-related studies [98]. Applications of GC-TOFMS-based metabolomic analyses were reported for biomarker discovery and elucidation of pathogenesis of various diseases such as diabetes [16,99], hepatocellular carcinoma [100], kidney cancer [31], bladder cancer [54], colorectal cancer [101], ovarian cancer [63], osteosarcoma [102], acute coronary syndrome [103], and Crohn's disease [104].

GC-based urinary metabolomics was also applied to toxicological evaluation. One way the biological systems adapt to maintain homeostasis in the face of a toxic challenge is to modulate the composition of biofluids by eliminating substances via the kidney [105]. Even when cellular homeostasis is maintained, subtle responses to toxicity or disease are expressed in altered biofluid composition such as the change in urinary metabolites [105]. Although GC-MS is less used toxicology compared to NMR and LC-MS, recent studies demonstrate the potential of urinary metabolic profiling by GC-MS as a complementary tool in toxicological evaluations, providing a comprehensive understanding of the response of biological system to xenobiotic intervention. Recently, Chen et al. utilized GC-MS-based urinary metabolic profiling to elucidate the toxicity induced by orally administered multiglycosides of *Tripterygium wilfordii* Hook. f. (GTW) in rats [106]. Urine samples at various time points and predose urine were collected from GTW-administered rats, and the samples were analyzed using both GC-MS and LC-MS. The study indicated that GTW caused a

time-dependent toxic effect at a high dose as revealed by the perturbed metabolic regulatory network [106]. This multiplatform metabolic profiling approach successfully aided in gaining insights into metabolic alterations associated with the onset and progression of multiorgan toxicity induced by GTW. GC-MS-based urinary metabonomics was applied in a nephrotoxicity investigation in rats, where the toxicity was induced by various xenobiotics such as aristolochic acid [30], gentamicin [107,108], cisplatin [108], and tobramycin [108]. Likewise, urinary metabonomics was utilized to understand hepatotoxicity caused by fenofibrate [109], atorvastatin [110], valproic acid [111], and carbon tetrachloride [112]. Other applications of urinary metabonomics include nutritional studies [113–115].

29.6 Future directions

Of the different sampling and transfer methods available for headspace GC-MS, solid-phase microextraction (SPME) has emerged as a promising technique because of its small sample size requirement, sensitivity, and minimal sample pretreatment compared to conventional methods. In headspace SPME, an SPME fiber is introduced as adsorbent into the headspace to trap volatile analytes. Various SPME fibers made of materials such as polydimethylsiloxane and polydimethylsiloxane/divinylbenzene are commercially available. In order to analyze more polar and nonvolatile analytes, the direct immersion mode is often preferred in which the SPME device (stir-bars or thin films) is brought into direct contact with the biological matrix of interest [116]. SPME in conjunction with headspace GC-MS has already been utilized in metabonomic studies involving human skin emissions [117,118], human sperm quality evaluation [119], breath in human lung cancer [120,121] and lung infections [122], colon cancer cells

[123], blood of liver cancer patients [124], and *Helicobacter pylori* infection in human gastric cancer [125]. Recent developments in SPME devices have further expanded its metabolic space coverage [126].

Gas chromatography–tandem mass spectrometry (GC-MS/MS) has emerged as a suitable technique for targeted analysis because of its higher selectivity and unambiguous metabolite identification capability compared with conventional GC-MS. Recently, GC-MS/MS was used for the analysis of marker metabolites related to alcohol and drug abuse in human hair [127–129], 4-aminobiphenyl hemoglobin adducts in smokers and nonsmokers [130], estrone sulfate in human plasma [131], endogenous anabolic steroids in human hair [132], endogenous organic acids in human urine [133], tyrosine metabolites in human urine [134], plasma [135], exhaled breath [136], and pyrimidine metabolites in human urine [137]. An increase in the use of GC-MS/MS for targeted profiling and validation of metabolite-based biomarkers is anticipated in the future.

References

- [1] J.K. Nicholson, J.C. Lindon, E. Holmes, 'Metabonomics': understanding the metabolic responses of living systems to pathophysiological stimuli via multivariate statistical analysis of biological NMR spectroscopic data, *Xenobiotica* 29 (1999) 1181–1189.
- [2] O. Fiehn, Combining genomics, metabolome analysis, and biochemical modelling to understand metabolic networks, *Comp. Funct. Genom.* 2 (2001) 155–168.
- [3] M. Morris, S.M. Watkins, Focused metabolomic profiling in the drug development process: advances from lipid profiling, *Curr. Opin. Chem. Biol.* 9 (2005) 407–412.
- [4] M. Urpi-Sarda, M. Monagas, N. Khan, R. Llorach, R.M. Lamuela-Raventos, O. Jauregui, et al., Targeted metabolic profiling of phenolics in urine and plasma after regular consumption of cocoa by liquid chromatography-tandem mass spectrometry, *J. Chromatogr. A* 1216 (2009) 7258–7267.
- [5] W.B. Dunn, N.J. Bailey, H.E. Johnson, Measuring the metabolome: current analytical technologies, *Analyst* 130 (2005) 606–625.

- [6] E.M. Lenz, I.D. Wilson, Analytical strategies in metabolomics, *J. Proteome Res.* 6 (2007) 443–458.
- [7] G.G. Harrigan, R.H. LaPlante, G.N. Cosma, G. Cockerell, R. Goodacre, J.F. Maddox, et al., Application of high-throughput Fourier-transform infrared spectroscopy in toxicology studies: contribution to a study on the development of an animal model for idiosyncratic toxicity, *Toxicol. Lett.* 146 (2004) 197–205.
- [8] H. Pham-Tuan, L. Kaskavelis, C.A. Daykin, H.G. Janssen, Method development in high-performance liquid chromatography for high-throughput profiling and metabolomic studies of biofluid samples, *J. Chromatogr. B Anal. Technol. Biomed. Life. Sci.* 789 (2003) 283–301.
- [9] K.E. Vigneau-Callahan, A.I. Shestopalov, P.E. Milbury, W.R. Matson, B.S. Kristal, Characterization of diet-dependent metabolic serotypes: analytical and biological variability issues in rats, *J. Nutr.* 131 (2001) 924S–932S.
- [10] S. Zomer, C. Guillo, R.G. Brereton, M. Hanna-Brown, Toxicological classification of urine samples using pattern recognition techniques and capillary electrophoresis, *Anal. Bioanal. Chem.* 378 (2004) 2008–2020.
- [11] J.C. Lindon, E. Holmes, J.K. Nicholson, Metabonomics in pharmaceutical R&D, *FEBS J.* 274 (2007) 1140–1151.
- [12] J.C. Lindon, J.K. Nicholson, I.D. Wilson, Directly coupled HPLC-NMR and HPLC-NMR-MS in pharmaceutical research and development, *J. Chromatogr. B Biomed. Sci. Appl.* 748 (2000) 233–258.
- [13] K.K. Pasikanti, P.C. Ho, E.C. Chan, Gas chromatography/mass spectrometry in metabolic profiling of biological fluids, *J. Chromatogr. B Anal. Technol. Biomed. Life Sci.* 871 (2008) 202–211.
- [14] J.W. Allwood, A. Erban, S. de Koning, W.B. Dunn, A. Luedemann, A. Lommen, et al., Inter-laboratory reproducibility of fast gas chromatography-electron impact-time of flight mass spectrometry (GC-EL-TOF/MS) based plant metabolomics, *Metabolomics* 5 (2009) 479–496.
- [15] M.F. Almstetter, I.J. Appel, M.A. Gruber, C. Lottaz, B. Timischl, R. Spang, et al., Integrative normalization and comparative analysis for metabolic fingerprinting by comprehensive two-dimensional gas chromatography-time-of-flight mass spectrometry, *Anal. Chem.* 81 (2009) 5731–5739.
- [16] X. Li, Z. Xu, X. Lu, X. Yang, P. Yin, H. Kong, et al., Comprehensive two-dimensional gas chromatography/time-of-flight mass spectrometry for metabolomics: biomarker discovery for diabetes mellitus, *Anal. Chim. Acta* 633 (2009) 257–262.
- [17] K. Ralston-Hooper, A. Hopf, C. Oh, X. Zhang, J. Adamec, M.S. Sepulveda, Development of GCxGC/TOF-MS metabolomics for use in ecotoxicological studies with invertebrates, *Aquat. Toxicol.* 88 (2008) 48–52.
- [18] R.E. Mohler, K.M. Dombek, J.C. Hoggard, K.M. Pierce, E.T. Young, R.E. Synovec, Comprehensive analysis of yeast metabolite GC × GC-TOFMS data: combining discovery-mode and deconvolution chemometric software, *Analyst* 132 (2007) 756–767.
- [19] R.A. Shellie, W. Welthagen, J. Zrostlikova, J. Spranger, M. Ristow, O. Fiehn, et al., Statistical methods for comparing comprehensive two-dimensional gas chromatography-time-of-flight mass spectrometry results: metabolomic analysis of mouse tissue extracts, *J. Chromatogr. A* 1086 (2005) 83–90.
- [20] M. Adahchour, J. Beens, U.A. Brinkman, Recent developments in the application of comprehensive two-dimensional gas chromatography, *J. Chromatogr. A* 1186 (2008) 67–108.
- [21] W. Khummueng, J. Harynuk, P.J. Marriott, Modulation ratio in comprehensive two-dimensional gas chromatography, *Anal. Chem.* 78 (2006) 4578–4587.
- [22] D. Ryan, P. Morrison, P. Marriott, Orthogonality considerations in comprehensive two-dimensional gas chromatography, *J. Chromatogr. A* 1071 (2005) 47–53.
- [23] J.M. Dimandja, G.C. Clouden, I. Colon, J.F. Focant, W.V. Cabey, R.C. Parry, Standardized test mixture for the characterization of comprehensive two-dimensional gas chromatography columns: the Phillips mix, *J. Chromatogr. A* 1019 (2003) 261–272.
- [24] M.M. Koek, B. Muilwijk, L.L. van Stee, T. Hankemeier, Higher mass loadability in comprehensive two-dimensional gas chromatography-mass spectrometry for improved analytical performance in metabolomics analysis, *J. Chromatogr. A* 1186 (2008) 420–429.
- [25] S.A. Fancy, O. Beckonert, G. Darbon, W. Yabsley, R. Walley, D. Baker, et al., Gas chromatography/flame ionisation detection mass spectrometry for the detection of endogenous urine metabolites for metabolomic studies and its use as a complementary tool to nuclear magnetic resonance spectroscopy, *Rapid Commun. Mass Spectrom.* 20 (2006) 2271–2280.
- [26] J. Lisec, N. Schauer, J. Kopka, L. Willmitzer, A.R. Fernie, Gas chromatography mass spectrometry-based metabolite profiling in plants, *Nat. Protoc.* 1 (2006) 387–396.

- [27] Q. Zhang, G. Wang, Y. Du, L. Zhu, A. Jiye, GC-MS analysis of the rat urine for metabonomic research, *J. Chromatogr. B Anal. Technol. Biomed. Life Sci.* 854 (2007) 20–25.
- [28] S. Bijlsma, I. Bobeldijk, E.R. Verheij, R. Ramaker, S. Kochhar, I.A. Macdonald, et al., Large-scale human metabolomics studies: a strategy for data (pre-) processing and validation, *Anal. Chem.* 78 (2006) 567–574.
- [29] S. Wiklund, E. Johansson, L. Sjöstrom, E.J. Mellerowicz, U. Edlund, J.P. Shockcor, et al., Visualization of GC/TOF-MS-based metabolomics data for identification of biochemically interesting compounds using OPLS class models, *Anal. Chem.* 80 (2008) 115–122.
- [30] Y. Ni, M. Su, Y. Qiu, M. Chen, Y. Liu, A. Zhao, et al., Metabolic profiling using combined GC-MS and LC-MS provides a systems understanding of aristolochic acid-induced nephrotoxicity in rat, *FEBS Lett.* 581 (2007) 707–711.
- [31] T. Kind, V. Tolstikov, O. Fiehn, R.H. Weiss, A comprehensive urinary metabolomic approach for identifying kidney cancer, *Anal. Biochem.* 363 (2007) 185–195.
- [32] K. Yuan, H. Kong, Y. Guan, J. Yang, G. Xu, A GC-based metabonomics investigation of type 2 diabetes by organic acids metabolic profile, *J. Chromatogr. B Anal. Technol. Biomed. Life Sci.* 850 (2007) 236–240.
- [33] H.J. Major, R. Williams, A.J. Wilson, I.D. Wilson, A metabonomic analysis of plasma from Zucker rat strains using gas chromatography/mass spectrometry and pattern recognition, *Rapid Commun. Mass Spectrom.* 20 (2006) 3295–3302.
- [34] M. Katajamaa, M. Oresic, Data processing for mass spectrometry-based metabolomics, *J. Chromatogr. A* 1158 (2007) 318–328.
- [35] R. Goodacre, D. Broadhurst, A.K. Smilde, B.S. Kristal, J.D. Baker, R. Beger, et al., Proposed minimum reporting standards for data analysis in metabolomics, *Metabolomics* 3 (2007) 231–241.
- [36] P. Jonsson, J. Gullberg, A. Nordstrom, M. Kusano, M. Kowalczyk, M. Sjöstrom, et al., A strategy for identifying differences in large series of metabolomic samples analyzed by GC-MS, *Anal. Chem.* 76 (2004) 1738–1745.
- [37] K.J. Johnson, B.W. Wright, K.H. Jarman, R.E. Synovec, High-speed peak matching algorithm for retention time alignment of gas chromatographic data for chemometric analysis, *J. Chromatogr. A* 996 (2003) 141–155.
- [38] Y. Koh, K.K. Pasikanti, C.W. Yap, E.C. Chan, Comparative evaluation of software for retention time alignment of gas chromatography/time-of-flight mass spectrometry-based metabonomic data, *J. Chromatogr. A* 1217 (2010) 8308–8316.
- [39] J.M. Halket, A. Przyborowska, S.E. Stein, W.G. Mallard, S. Down, R.A. Chalmers, Deconvolution gas chromatography/mass spectrometry of urinary organic acids—potential for pattern recognition and automated identification of metabolic disorders, *Rapid Commun. Mass Spectrom.* 13 (1999) 279–284.
- [40] R. Baran, H. Kochi, N. Saito, M. Suematsu, T. Soga, T. Nishioka, et al., MathDAMP: a package for differential analysis of metabolite profiles, *BMC Bioinf.* 7 (2006) 530.
- [41] A.L. Duran, J. Yang, L. Wang, L.W. Sumner, Metabolomics spectral formatting, alignment and conversion tools (MSFACTs), *Bioinformatics* 19 (2003) 2283–2293.
- [42] M. Katajamaa, J. Miettinen, M. Oresic, MZmine: toolbox for processing and visualization of mass spectrometry based molecular profile data, *Bioinformatics* 22 (2006) 634–636.
- [43] C.A. Smith, E.J. Want, G. O'Maille, R. Abagyan, G. Siuzdak, XCMS: processing mass spectrometry data for metabolite profiling using nonlinear peak alignment, matching, and identification, *Anal. Chem.* 78 (2006) 779–787.
- [44] A. Lommen, MetAlign: interface-driven, versatile metabolomics tool for hyphenated full-scan mass spectrometry data preprocessing, *Anal. Chem.* 81 (2009) 3079–3086.
- [45] A. Luedemann, K. Strassburg, A. Erban, J. Kopka, TagFinder for the quantitative analysis of gas chromatography–mass spectrometry (GC-MS)-based metabolite profiling experiments, *Bioinformatics* 24 (2008) 732–737.
- [46] Y. Guitton, et al., Create, run, share, publish, and reference your LC–MS, FIA–MS, GC–MS, and NMR data analysis workflows with the Workflow4Metabolomics 3.0 Galaxy online infrastructure for metabolomics, *Int. J. Biochem. Cell Biol.* 93 (2017) 89–101.
- [47] R. Bro, A.K. Smilde, Centering and scaling in component analysis, *J. Chemometr.* 17 (2003) 16–33.
- [48] R.A. van den Berg, H.C. Hoefsloot, J.A. Westerhuis, A.K. Smilde, M.J. van der Werf, Centering, scaling, and transformations: improving the biological information content of metabolomics data, *BMC Genom.* 7 (2006) 142.

- [49] J.C. Lindon, E. Holmes, J.K. Nicholson, Pattern recognition methods and applications in biomedical magnetic resonance, *Prog. Nucl. Magn. Reson. Spectrosc.* 39 (2001) 1–40.
- [50] M. Bylesjo, D. Eriksson, A. Sjodin, S. Jansson, T. Moritz, J. Trygg, Orthogonal projections to latent structures as a strategy for microarray data normalization, *BMC Bioinf.* 8 (2007) 207.
- [51] J. Trygg, E. Holmes, T. Lundstedt, Chemometrics in metabonomics, *J. Proteome Res.* 6 (2007) 469–479.
- [52] J. Westerhuis, H. Hoefsloot, S. Smit, D. Vis, A. Smilde, E. van Velzen, et al., Assessment of PLS-DA cross validation, *Metabolomics* 4 (2008) 81–89.
- [53] S. Smit, M.J. van Breemen, H.C. Hoefsloot, A.K. Smilde, J.M. Aerts, C.G. de Koster, Assessing the statistical validity of proteomics based biomarkers, *Anal. Chim. Acta* 592 (2007) 210–217.
- [54] K.K. Pasikanti, K. Esuvaranathan, P.C. Ho, R. Mahendran, R. Kamaraj, Q.H. Wu, et al., Noninvasive urinary metabonomic diagnosis of human bladder cancer, *J. Proteome Res.* 9 (2010) 2988–2995.
- [55] S. Wiklund, D. Nilsson, L. Eriksson, M. Sjöström, S. Wold, K. Faber, A randomization test for PLS component selection, *J. Chemometr.* 21 (2007) 427–439.
- [56] S. Mahadevan, S.L. Shah, T.J. Marrie, C.M. Slupsky, Analysis of metabolomic data using support vector machines, *Anal. Chem.* 80 (2008) 7562–7570.
- [57] D.S. Wishart, C. Knox, A.C. Guo, R. Eisner, N. Young, B. Gautam, et al., HMDB: a knowledgebase for the human metabolome, *Nucleic Acids Res.* 37 (2009) D603–D610.
- [58] R. Caspi, H. Foerster, C.A. Fulcher, P. Kaipa, M. Krummenacker, M. Latendresse, et al., The MetaCyc database of metabolic pathways and enzymes and the BioCyc collection of pathway/genome databases, *Nucleic Acids Res.* 36 (2008) D623–D631.
- [59] D. Croft, G. O’Kelly, G. Wu, R. Haw, M. Gillespie, L. Matthews, et al., Reactome: a database of reactions, pathways and biological processes, *Nucleic Acids Res.* 39 (2011) D691–D697.
- [60] X. Du, A. Smirnov, W. Jia, A preparatory study of how to construct consensus mass spectra of recurrent unknown metabolites from untargeted GC–MS metabolomics data, *Int. J. Mass Spectrom.* 427 (2018) 73–78.
- [61] M. Mal, P.K. Koh, P.Y. Cheah, E.C. Chan, Development and validation of a gas chromatography/mass spectrometry method for the metabolic profiling of human colon tissue, *Rapid Commun. Mass Spectrom.* 23 (2009) 487–494.
- [62] Y. Yang, et al., Evaluating different extraction solvents for GC-MS based metabolomic analysis of the fecal metabolome of adult and baby giant pandas, *Sci. Rep.* 9 (1) (2019) 1–9.
- [63] C. Denkert, J. Budczies, T. Kind, W. Weichert, P. Tablack, J. Sehoul, et al., Mass spectrometry-based metabolic profiling reveals different metabolite patterns in invasive ovarian carcinomas and ovarian borderline tumors, *Cancer Res.* 66 (2006) 10795–10804.
- [64] E.C. Chan, P.K. Koh, M. Mal, P.Y. Cheah, K.W. Eu, A. Backshall, et al., Metabolic profiling of human colorectal cancer using high-resolution magic angle spinning nuclear magnetic resonance (HR-MAS NMR) spectroscopy and gas chromatography mass spectrometry (GC-MS), *J. Proteome Res.* 8 (2009) 352–361.
- [65] E.S. Ong, L. Zou, S. Li, P.Y. Cheah, K.W. Eu, C.N. Ong, Metabolic profiling in colorectal cancer reveals signature metabolic shifts during tumorigenesis, *Mol. Cell. Proteomics* (2010), <https://doi.org/10.1074/mcp.M900551-MCP200>.
- [66] H. Wu, R. Xue, Z. Tang, C. Deng, T. Liu, H. Zeng, et al., Metabolomic investigation of gastric cancer tissue using gas chromatography/mass spectrometry, *Anal. Bioanal. Chem.* 396 (2010) 1385–1395.
- [67] J.L. Chen, H.Q. Tang, J.D. Hu, J. Fan, J. Hong, J.Z. Gu, Metabolomics of gastric cancer metastasis detected by gas chromatography and mass spectrometry, *World J. Gastroenterol.* 16 (2010) 5874–5880.
- [68] H. Wu, R. Xue, C. Lu, C. Deng, T. Liu, H. Zeng, et al., Metabolomic study for diagnostic model of esophageal cancer using gas chromatography/mass spectrometry, *J. Chromatogr. B Anal. Technol. Biomed. Life Sci.* 877 (2009) 3111–3117.
- [69] S. Wold, E. Johansson, E. Jellum, I. Björnson, R. Nesbakken, Application of Simca multivariate data-analysis to the classification of gas-chromatographic profiles of human-brain tissues, *Anal. Chim. Acta Comp.* 5 (1981) 251–259.
- [70] E. Jellum, I. Björnson, R. Nesbakken, E. Johansson, S. Wold, Classification of human cancer-cells by means of capillary gas-chromatography and pattern-recognition analysis, *J. Chromatogr.* 217 (1981) 231–237.
- [71] G.Y.F.H. Xin, Y. Ke, C. Yi Yu, Gas chromatography-mass spectrometry based on metabonomic study of carbon tetrachloride-induced acute liver injury in mice, *Chin. J. Anal. Chem.* 27 (2006) 1736–1740.
- [72] L. Pan, Y. Qiu, T. Chen, J. Lin, Y. Chi, M. Su, et al., An optimized procedure for metabonomic analysis of rat liver tissue using gas chromatography/time-of-flight mass spectrometry, *J. Pharm. Biomed. Anal.* 52 (2010) 589–596.

- [73] H.J. Atherton, N.J. Bailey, W. Zhang, J. Taylor, H. Major, J. Shockcor, et al., A combined H-1-NMR spectroscopy- and mass spectrometry-based metabolomic study of the PPAR-alpha null mutant mouse defines profound systemic changes in metabolism linked to the metabolic syndrome, *Physiol. Genom.* 27 (2006) 178–186.
- [74] O.N. Khabib, N.V. Beloborodova, G.A. Osipov, Detection of bacterial molecular markers in the tissue of cardiac valves in normal and pathological states by gas chromatography and mass spectrometry, *Zh. Mikrobiol. Epidemiol. Immunobiol.* (2004) 62–68.
- [75] L.R. Snyder, J.C. Hoggard, T.J. Montine, R.E. Synovec, Development and application of a comprehensive two-dimensional gas chromatography with time-of-flight mass spectrometry method for the analysis of L-beta-methylamino-alanine in human tissue, *J. Chromatogr. A* 1217 (2010) 4639–4647.
- [76] W.C. Hubbard, C.L. Litterst, M.C. Liu, E.R. Bleecker, J.C. Eggleston, T.L. McLemore, et al., Profiling of prostaglandin biosynthesis in biopsy fragments of human lung carcinomas and normal human lung by capillary gas chromatography-negative ion chemical ionization mass spectrometry, *Prostaglandins* 32 (1986) 889–906.
- [77] A. Bennett, A. Civier, C.N. Hensby, P.B. Melhuish, I.F. Stamford, Measurement of arachidonate and its metabolites extracted from human normal and malignant gastrointestinal tissues, *Gut* 28 (1987) 315–318.
- [78] V.W. Yang, J.M. Shields, S.R. Hamilton, E.W. Spannhake, W.C. Hubbard, L.M. Hyland, et al., Size-dependent increase in prostanoid levels in adenomas of patients with familial adenomatous polyposis, *Cancer Res.* 58 (1998) 1750–1753.
- [79] K.L. Chang, L.S. New, M. Mal, C.W. Goh, C.C. Aw, E.R. Browne, et al., Metabolic profiling of 3-nitropropionic acid early-stage Huntington's disease rat model using gas chromatography time-of-flight mass spectrometry, *J. Proteome Res.* 10 (2011) 2079–2087.
- [80] L. Zhao, et al., High throughput and quantitative measurement of microbial metabolome by gas chromatography/mass spectrometry using automated alkyl chloroformate derivatization, *Anal. Chem.* 89 (10) (2017) 5565–5577.
- [81] A.P. Siskos, et al., Interlaboratory reproducibility of a targeted metabolomics platform for analysis of human serum and plasma, *Anal. Chem.* 89 (1) (2017) 656–665.
- [82] D. Ng, K. Pasikanti, E. Chan, Trend analysis of metabolomics and systematic review of metabolomics-derived cancer marker metabolites, *Metabolomics* (2010) 1–24.
- [83] J.D. Shoemaker, W.H. Elliott, Automated screening of urine samples for carbohydrates, organic and amino acids after treatment with urease, *J. Chromatogr.* 562 (1991) 125–138.
- [84] M.C. Walsh, L. Brennan, J.P.G. Malthouse, H.M. Roche, M.J. Gibney, Effect of acute dietary standardization on the urinary, plasma, and salivary metabolomic profiles of healthy humans, *Am. J. Clin. Nutr.* 84 (2006) 531–539.
- [85] K.K. Pasikanti, P.C. Ho, E.C. Chan, Development and validation of a gas chromatography/mass spectrometry metabolomic platform for the global profiling of urinary metabolites, *Rapid Commun. Mass Spectrom.* 22 (2008) 2984–2992.
- [86] M. Assfalg, I. Bertini, D. Colangiuli, C. Luchinat, H. Schafer, B. Schutz, et al., Evidence of different metabolic phenotypes in humans, *Proc. Natl. Acad. Sci. U.S.A.* 105 (2008) 1420–1424.
- [87] H.G. Gika, G.A. Theodoridis, I.D. Wilson, Liquid chromatography and ultra-performance liquid chromatography-mass spectrometry fingerprinting of human urine: sample stability under different handling and storage conditions for metabolomics studies, *J. Chromatogr. A* 1189 (2008) 314–322.
- [88] M. Lauridsen, S.H. Hansen, J.W. Jaroszewski, C. Cornett, Human urine as test material in 1H NMR-based metabolomics: recommendations for sample preparation and storage, *Anal. Chem.* 79 (2007) 1181–1186.
- [89] K. Dettmer, P.A. Aronov, B.D. Hammock, Mass spectrometry-based metabolomics, *Mass Spectrom. Rev.* 26 (2007) 51–78.
- [90] M. Chen, L. Zhao, W. Jia, Metabolomic study on the biochemical profiles of a hydrocortisone-induced animal model, *J. Proteome Res.* 4 (2005) 2391–2396.
- [91] S.H. Lee, H.M. Woo, B.H. Jung, J. Lee, O.S. Kwon, H.S. Pyo, et al., Metabolomic approach to evaluate the toxicological effects of nonylphenol with rat urine, *Anal. Chem.* 79 (2007) 6102–6110.
- [92] J.L. Little, Artifacts in trimethylsilyl derivatization reactions and ways to avoid them, *J. Chromatogr. A* 844 (1999) 1–22.
- [93] Y. Qiu, M. Su, Y. Liu, M. Chen, J. Gu, J. Zhang, et al., Application of ethyl chloroformate derivatization for gas chromatography-mass spectrometry based metabolomic profiling, *Anal. Chim. Acta* 583 (2007) 277–283.
- [94] T. Kuhara, Diagnosis and monitoring of inborn errors of metabolism using urease-pretreatment of urine, isotope dilution, and gas chromatography-mass spectrometry, *J. Chromatogr. B Anal. Technol. Biomed. Life. Sci.* 781 (2002) 497–517.

- [95] K.R. Leimer, R.H. Rice, C.W. Gehrke, Complete mass spectra of N-trifluoroacetyl-n-butyl esters of amino acids, *J. Chromatogr.* 141 (1977) 121–144.
- [96] H.J. Issaq, O. Nativ, T. Waybright, B. Luke, T.D. Veenstra, E.J. Issaq, et al., Detection of bladder cancer in human urine by metabolomic profiling using high performance liquid chromatography/mass spectrometry, *J. Urol.* 179 (2008) 2422–2426.
- [97] K. Kim, P. Aronov, S.O. Zakharkin, D. Anderson, B. Perroud, I.M. Thompson, et al., Urine metabolomics analysis for kidney cancer detection and biomarker discovery, *Mol. Cell. Proteomics* 8 (2009) 558–570.
- [98] J.C. Lindon, J.K. Nicholson, E. Holmes, H. Antti, M.E. Bollard, H. Keun, et al., Contemporary issues in toxicology the role of metabolomics in toxicology and its evaluation by the COMET project, *Toxicol. Appl. Pharmacol.* 187 (2003) 137–146.
- [99] Y. Bao, T. Zhao, X. Wang, Y. Qiu, M. Su, W. Jia, Metabonomic variations in the drug-treated type 2 diabetes mellitus patients and healthy volunteers, *J. Proteome Res.* 8 (2009) 1623–1630.
- [100] H. Wu, R. Xue, L. Dong, T. Liu, C. Deng, H. Zeng, et al., Metabolomic profiling of human urine in hepatocellular carcinoma patients using gas chromatography/mass spectrometry, *Anal. Chim. Acta* 648 (2009) 98–104.
- [101] Y. Qiu, G. Cai, M. Su, T. Chen, X. Zheng, Y. Xu, et al., Serum metabolite profiling of human colorectal cancer using GC-TOFMS and UPLC-QTOFMS, *J. Proteome Res.* 8 (2009) 4844–4850.
- [102] Z. Zhang, Y. Qiu, Y. Hua, Y. Wang, T. Chen, A. Zhao, et al., Serum and urinary metabonomic study of human osteosarcoma, *J. Proteome Res.* 9 (2010) 4861–4868.
- [103] M. Vallejo, A. Garcia, J. Tunon, D. Garcia-Martinez, S. Angulo, J.L. Martin-Ventura, et al., Plasma fingerprinting with GC-MS in acute coronary syndrome, *Anal. Bioanal. Chem.* 394 (2009) 1517–1524.
- [104] H.M. Lin, S.I. Edmunds, N.A. Helsby, L.R. Ferguson, D.D. Rowan, Nontargeted urinary metabolite profiling of a mouse model of Crohn's disease, *J. Proteome Res.* 8 (2009) 2045–2057.
- [105] J.C. Lindon, E. Holmes, J.K. Nicholson, So what's the deal with metabolomics? *Anal. Chem.* 75 (2003) 384A–391A.
- [106] M. Chen, Y. Ni, H. Duan, Y. Qiu, C. Guo, Y. Jiao, et al., Mass spectrometry-based metabolic profiling of rat urine associated with general toxicity induced by the multiglycoside of *Tripterygium wilfordii* hook. f., *Chem. Res. Toxicol.* 21 (2008) 288–294.
- [107] M. Sieber, D. Hoffmann, M. Adler, V.S. Vaidya, M. Clement, J.V. Nonventre, et al., Comparative analysis of novel noninvasive renal biomarkers and metabonomic changes in a rat model of gentamicin nephrotoxicity, *Toxicol. Sci.* 109 (2009) 336–349.
- [108] K.J. Boudonck, M.W. Mitchell, L. Nemet, L. Keresztes, A. Nyska, D. Shinar, et al., Discovery of metabolomics biomarkers for early detection of nephrotoxicity, *Toxicol. Pathol.* 37 (2009) 280–292.
- [109] T. Ohta, N. Masutomi, N. Tsutsui, T. Sakairi, M. Mitchell, M.V. Milburn, et al., Untargeted metabolomic profiling as an evaluative tool of fenofibrate-induced toxicology in Fischer 344 male rats, *Toxicol. Pathol.* 37 (2009) 521–535.
- [110] B.S. Kumar, Y.J. Lee, H.J. Yi, B.C. Chung, B.H. Jung, Discovery of safety biomarkers for atorvastatin in rat urine using mass spectrometry based metabolomics combined with global and targeted approach, *Anal. Chim. Acta* 661 (2010) 47–59.
- [111] M.S. Lee, B.H. Jung, B.C. Chung, S.H. Cho, K.Y. Kim, O.S. Kwon, et al., Metabolomics study with gas chromatography-mass spectrometry for predicting valproic acid-induced hepatotoxicity and discovery of novel biomarkers in rat urine, *Int. J. Toxicol.* 28 (2009) 392–404.
- [112] X. Huang, L. Shao, Y. Gong, Y. Mao, C. Liu, H. Qu, et al., A metabonomic characterization of CCl₄-induced acute liver failure using partial least square regression based on the GC-MS metabolic profiles of plasma in mice, *J. Chromatogr. B Anal. Technol. Biomed. Life. Sci.* 870 (2008) 178–185.
- [113] W.S. Law, P.Y. Huang, E.S. Ong, C.N. Ong, S.F. Li, K.K. Pasikanti, et al., Metabonomics investigation of human urine after ingestion of green tea with gas chromatography/mass spectrometry, liquid chromatography/mass spectrometry and (1)H NMR spectroscopy, *Rapid Commun. Mass Spectrom.* 22 (2008) 2436–2446.
- [114] Z. Wu, M. Li, C. Zhao, J. Zhou, Y. Chang, X. Li, et al., Urinary metabolomics study in a rat model in response to protein-energy malnutrition by using gas chromatography-mass spectrometry and liquid chromatography-mass spectrometry, *Mol. Biosyst.* 6 (2010) 2157–2163.
- [115] F.A. van Dorsten, C.H. Grun, E.J. van Velzen, D.M. Jacobs, R. Draijer, J.P. van Duynhoven, The metabolic fate of red wine and grape juice polyphenols in humans assessed by metabolomics, *Mol. Nutr. Food Res.* 54 (2010) 897–908.
- [116] D. Vuckovic, X. Zhang, E. Cudjoe, J. Pawliszyn, Solid-phase microextraction in bioanalysis: new devices and directions, *J. Chromatogr. A* 1217 (2010) 4041–4060.
- [117] Y. Xu, S.J. Dixon, R.G. Brereton, H.A. Soini, M.V. Novotny, K. Trebesius, et al., Comparison of human axillary odour profiles obtained by gas chromatography/mass spectrometry and skin microbial profiles obtained by denaturing gradient gel electrophoresis using multivariate pattern recognition, *Metabolomics* 3 (2007) 427–437.

- [118] M. Gallagher, C.J. Wysocki, J.J. Leyden, A.I. Spielman, X. Sun, G. Preti, Analyses of volatile organic compounds from human skin, *Br. J. Dermatol.* 159 (2008) 780–791.
- [119] V. Longo, et al., HS-SPME-GC-MS metabolomics approach for sperm quality evaluation by semen volatile organic compounds (VOCs) analysis, *Biomed. Phys. Eng. Express* 5 (1) (2018) 015006.
- [120] H. Yu, L. Xu, P. Wang, Solid phase microextraction for analysis of alkanes and aromatic hydrocarbons in human breath, *J. Chromatogr. B Anal. Technol. Biomed. Life Sci.* 826 (2005) 69–74.
- [121] X. Chen, F. Xu, Y. Wang, Y. Pan, D. Lu, P. Wang, et al., A study of the volatile organic compounds exhaled by lung cancer cells in vitro for breath diagnosis, *Cancer* 110 (2007) 835–844.
- [122] M. Syhre, J.M. Scotter, S.T. Chambers, Investigation into the production of 2-Pentylfuran by *Aspergillus fumigatus* and other respiratory pathogens in vitro and human breath samples, *Med. Mycol.* 46 (2008) 209–215.
- [123] D. Zimmermann, M. Hartmann, M.P. Moyer, J. Nolte, J.I. Baumbach, Determination of volatile products of human colon cell line metabolism by GC-MS analysis, *Metabolomics* 3 (2007) 13–17.
- [124] R. Xue, L. Dong, S. Zhang, C. Deng, T. Liu, J. Wang, et al., Investigation of volatile biomarkers in liver cancer blood using solid-phase microextraction and gas chromatography/mass spectrometry, *Rapid Commun. Mass Spectrom.* 22 (2008) 1181–1186.
- [125] B. Buszewski, A. Ulanowska, T. Ligor, M. Jackowski, E. Klodzinska, J. Szeliga, Identification of volatile organic compounds secreted from cancer tissues and bacterial cultures, *J. Chromatogr. B Anal. Technol. Biomed. Life Sci.* 868 (2008) 88–94.
- [126] D. Vuckovic, J. Pawliszyn, Systematic evaluation of solid-phase microextraction coatings for untargeted metabolomic profiling of biological fluids by liquid chromatography-mass spectrometry, *Anal. Chem.* 83 (2011) 1944–1954.
- [127] C.M. Zimmermann, G.P. Jackson, Gas chromatography tandem mass spectrometry for biomarkers of alcohol abuse in human hair, *Ther. Drug Monit.* 32 (2010) 216–223.
- [128] H. Kharbouche, F. Sporkert, S. Troxler, M. Augsburg, P. Mangin, C. Staub, Development and validation of a gas chromatography-negative chemical ionization tandem mass spectrometry method for the determination of ethyl glucuronide in hair and its application to forensic toxicology, *J. Chromatogr. B Anal. Technol. Biomed. Life Sci.* 877 (2009) 2337–2343.
- [129] A. Orfanidis, et al., A GC–MS method for the detection and quantitation of ten major drugs of abuse in human hair samples, *J. Chromatogr. B* 1047 (2017) 141–150.
- [130] T.H. Seyler, L.R. Reyes, J.T. Bernert, Analysis of 4-aminobiphenyl hemoglobin adducts in smokers and nonsmokers by pseudo capillary on-column gas chromatography-tandem mass spectrometry, *J. Anal. Toxicol.* 34 (2010) 304–311.
- [131] F. Giton, P. Caron, R. Berube, A. Belanger, O. Barbier, J. Fiet, Plasma estrone sulfate assay in men: comparison of radioimmunoassay, mass spectrometry coupled to gas chromatography (GC-MS), and liquid chromatography-tandem mass spectrometry (LC-MS/MS), *Clin. Chim. Acta* 411 (2010) 1208–1213.
- [132] M. Shen, P. Xiang, B. Shen, M. Wang, Determination of endogenous anabolic steroids in hair using gas chromatography-tandem mass spectrometry, *Se Pu* 26 (2008) 454–459.
- [133] M. Pacenti, S. Dugheri, F. Villanelli, G. Bartolucci, L. Calamai, P. Boccalon, et al., Determination of organic acids in urine by solid-phase microextraction and gas chromatography-ion trap tandem mass spectrometry previous ‘in sample’ derivatization with trimethylxonium tetrafluoroborate, *Biomed. Chromatogr.* 22 (2008) 1155–1163.
- [134] D. Tsikas, A. Mitschke, M.T. Suchy, F.M. Gutzki, D.O. Stichtenoth, Determination of 3-nitrotyrosine in human urine at the basal state by gas chromatography-tandem mass spectrometry and evaluation of the excretion after oral intake, *J. Chromatogr. B Anal. Technol. Biomed. Life Sci.* 827 (2005) 146–156.
- [135] J.P. Gaut, J. Byun, H.D. Tran, J.W. Heinecke, Artifact-free quantification of free 3-chlorotyrosine, 3-bromotyrosine, and 3-nitrotyrosine in human plasma by electron capture-negative chemical ionization gas chromatography mass spectrometry and liquid chromatography-electrospray ionization tandem mass spectrometry, *Anal. Biochem.* 300 (2002) 252–259.
- [136] M. Larstad, A.S. Soderling, K. Caidahl, A.C. Olin, Selective quantification of free 3-nitrotyrosine in exhaled breath condensate in asthma using gas chromatography/tandem mass spectrometry, *Nitric Oxide* 13 (2005) 134–144.
- [137] U. Hofmann, M. Schwab, S. Seefried, C. Marx, U.M. Zanger, M. Eichelbaum, et al., Sensitive method for the quantification of urinary pyrimidine metabolites in healthy adults by gas chromatography-tandem mass spectrometry, *J. Chromatogr. B Anal. Technol. Biomed. Life Sci.* 791 (2003) 371–380.

Applications of gas chromatography in forensic science

Abuzar Kabir, Kenneth G. Furton

Department of Chemistry and Biochemistry, Florida International University, Miami, FL, United States

Gas chromatography (GC) is now a mature and indispensable analytical instrument in investigational forensic science. High sensitivity, selectivity, resolution and speed, good accuracy and precision, wide dynamic concentration range, simple and robust instrument design, and its ability to easily interface with many established and emerging detection systems have made GC the instrument of choice in many facets of investigational forensic science. A continuous influx of new column chemistries, development of high-precision thermal and pneumatic instrument control systems, introduction of the programmable temperature vaporizer (PTV) injector, and the large number of available detection systems have positioned GC in a unique place in forensic analytical laboratories. Although the applications of GC are limited to volatile and semivolatile organic compounds, rapid development in derivatization chemistry, technology, and high-temperature capabilities have made hundreds of new organic compounds with forensic significance amenable to GC and thus extended its horizon.

The introduction of comprehensive two-dimensional GC (GC \times GC), GC–isotope ratio mass spectrometry, and fast GC has contributed significantly in expanding forensic applications by their unmatched separation capability; high data quality and relatively low operational cost are additional advantages.

30.1 Introduction and scope

Forensic science applies scientific principles, tools, and methodologies to resolve legal issues and disputes. Although forensic science depends on the contributions from almost all branches of science, the contributions from chemistry have undoubtedly played a pivotal role in uplifting forensic science to its current state. Forensic chemists not only analyze a wide variety of forensic samples, but also extract and interpret information from the analytical data that may potentially have to withstand rigorous challenges when presented in civil and/or criminal judicial proceedings. As such, it is imperative

that any analytical methodology developed for solving forensic problems should meet, at a bare minimum, the required standard set forth by the court of law.

Among all analytical instruments currently used in routine forensic sample analyses as well as in basic and applied forensic research, gas chromatography (GC) is one of the most widely used analytical tools. High sensitivity, selectivity, resolution, speed, good accuracy and precision, wide dynamic concentration range, simple and robust instrument design, and its ability to interface with many established and emerging detection systems have made GC the instrument of choice in many facets of forensic science. In addition to its numerous advantageous features, the basic principle and the theory of GC have been well studied and comprehended since its inception more than half a century ago. As such, new GC instruments (hardware) along with their operating systems (software) are sufficiently simple and user-friendly that even a novice operator can operate it with confidence.

Due to the inherent advantages of GC, applications of this technique are on a continuous rise. Major application areas in forensic science include bulk seized drug analysis, drug screening from biological specimens, postmortem toxicology, trace evidence analysis, man-made environmental pollution investigation, human odor profiling, explosive analysis, analysis of ignitable liquid residues from fire debris, etc. The application areas of GC in forensic science and commonly used sample preparation techniques that precede GC analysis are illustrated in [Fig. 30.1](#).

Sampling and sample preparation profoundly impact the validity and integrity of GC analysis of forensic samples, especially when dealing with trace and ultratrace levels of the target analyte(s) present in various complex matrices (e.g., biological, environmental, fire debris, and explosive residues). In addition, in the majority

of the forensic cases, the amount of available sample is generally limited. Therefore, a scientifically sound sampling and sample preparation strategy should be adopted prior to beginning the analytical workflow in order to ensure that the analyzed samples are truly representative of the evidence matrix and no substantial chemical information, pertinent to the forensic investigation, is lost. Due to the complex nature of the sample matrix where the analytes of interest are present, most often, forensic samples cannot be introduced directly into the GC. This incompatibility stems primarily from two factors. First, the complex sample matrix, if introduced directly into the GC without employing any sample treatment/cleanup procedure, may exert a detrimental impact on the performance of the GC. Second, the concentration of the analyte(s) of interest in the sample matrix may be too low to be detected by the GC unless the analytes are preconcentrated using a suitable sample preparation technique. Since every forensic case is unique, standardization of the sampling and sample preparation techniques for forensic samples is difficult and often dependent upon the knowledge, experience, and judgment of the analyst.

Sample preparation techniques frequently employed in processing forensic samples prior to GC analysis include solvent extraction, solid-phase extraction (SPE), purge and trap, liquid-liquid extraction (LLE), supercritical fluid extraction (SFE), steam distillation, accelerated solvent extraction (ASE), microwave-assisted extraction (MAE), solid-phase microextraction (SPME), liquid-phase microextraction (LPME), stir-bar sorptive extraction (SBSE), solid-phase dynamic extraction (SPDE), and fabric phase sorptive extraction (FPSE).

GC may be interfaced with a large variety of detectors for the detection, quantification, and/or identification of the analyte(s), which include flame ionization detector (FID), nitrogen-phosphorus detector (NPD), sulfur and nitrogen

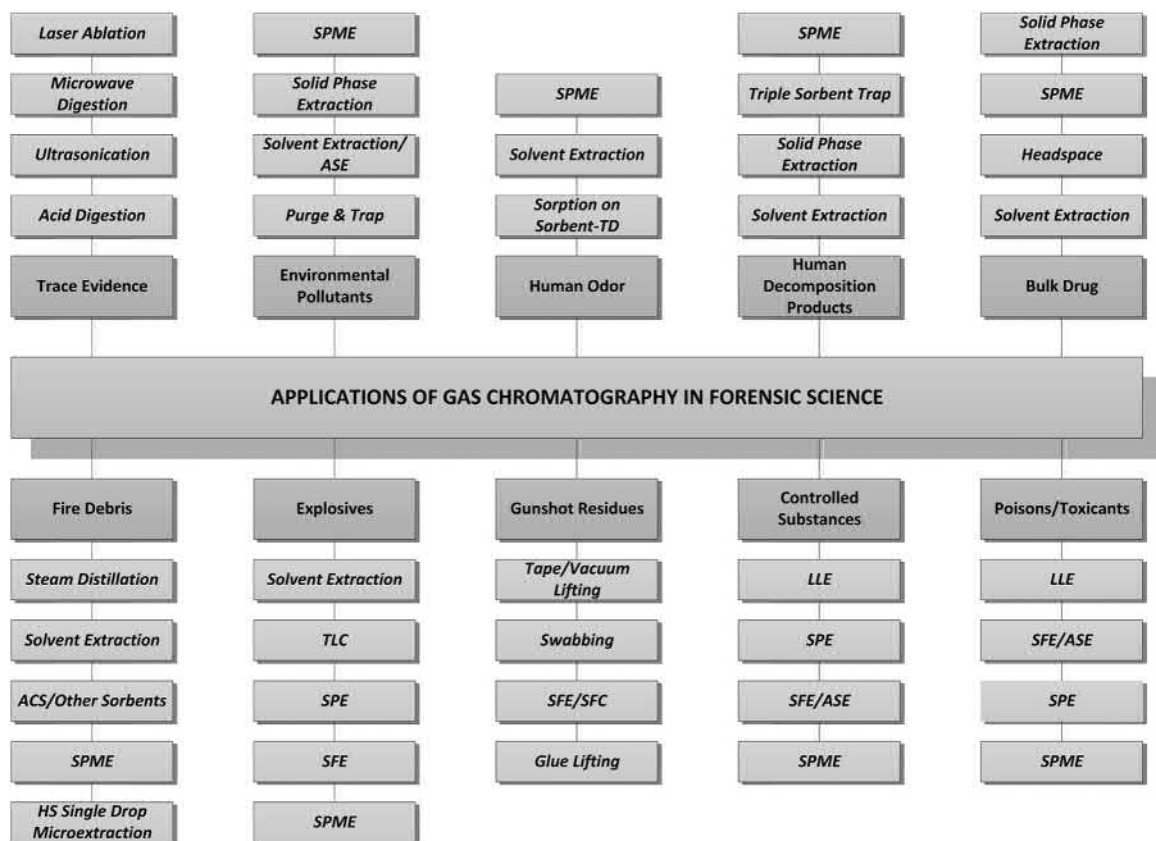


FIGURE 30.1 Major application areas of gas chromatography in forensic science with principal sample preparation techniques.

chemiluminescence detector, flame-photometric detector (FPD), atomic emission detector (AED), thermal energy analyzer (TEA), electron-capture detector (ECD), ion mobility spectrometry (IMS), time-of-flight mass spectrometry (TOFMS), vacuum ultraviolet spectroscopy (VUV), and isotope ratio mass spectrometry (IRMS). However, the most popular detector is the mass spectrometer (MS) as it simultaneously offers identification and quantification of an unknown substance with high confidence. In some cases, tandem mass spectrometry, MS/MS, is used as a detector to increase selectivity and sensitivity.

30.2 Analysis of bulk drug for identification, impurity profiling, and drug intelligence purpose

The scope of bulk drug analysis includes seized illicit drugs, as well as counterfeit and traditional medicines in which synthetic medicinal products are occasionally added to boost their pharmacological potency. Being illicit or inadequately regulated, these products pose substantial risks to public health. The following section discusses the applications of GC for analyzing illicit drugs, counterfeit drugs, as well as traditional medicines.

30.2.1 Analysis of confiscated illicit drugs

Law enforcement agencies seek information from the forensic chemists regarding the analysis of confiscated drugs as to: (1) whether the submitted sample contains any controlled substance(s) in it; (2) if yes, then how much of the controlled substance does it contain; and (3) is the sample similar to other seized samples? To address these questions, the seized drug samples require both qualitative (screening) and quantitative analyses (confirmation and quantification) of the illicit component. Federal and state drug trafficking penalties vary with the type and quantity of the drug seized. Both identification and quantification data of seized drug samples are frequently demanded by the prosecution. Drug intelligence often requires impurity profiling, identification of the precursors, reaction by-products, and isotopic profile analysis to establish possible origin of the substance, sources of the raw materials, precursors, and solvents used in the manufacturing process that may lead to tracking down clandestine manufacturing facilities of the illicit drugs.

GC has been the technique of choice for the analysis of confiscated drug for many years. Although GC-FID is still the most frequently used approach, chromatographic profiling procedures have been continuously shifting toward GC-MS due to its higher analytical performance [1] and rapidly decreasing cost. Among others, one major advantage of GC-MS is its ability to use the *target ion* quantification functionality that helps in situations where coelution of structurally related compounds is a problem. Based on a drug's acceptable medical use or its potential abuse or dependence, United States Drug Enforcement Administration (US DEA) has classified drugs into five distinct categories: Schedule 1–V. Table 30.1 presents a list and chemical structures of the most common scheduled drugs [2].

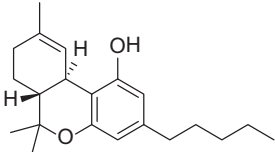
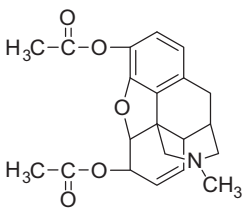
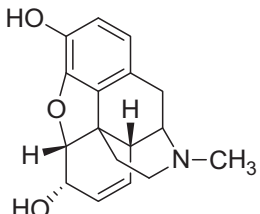
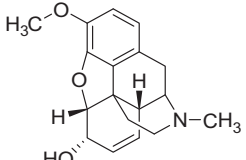
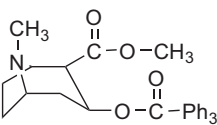
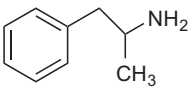
Cannabis is one of the most widely cultivated and abused flowering plants that produces a

wide range of illicit drugs including marijuana, sinsemilla, Thai sticks, ditch weed, hashish, hash oil, etc. Although Δ^9 -tetrahydrocannabinol (Δ^9 -THC) is the main psychoactive ingredient in cannabis, other cannabinoids present in cannabis also demonstrate different pharmacological activities. Cannabinoids are extracted from confiscated cannabis using solvent extraction. The extracted samples can be analyzed by GC-FID [3] or GC-MS [4,5]. Marijuana can be easily recognized by its distinct volatile profile obtained using a new device known as the Capillary Microextractor of Volatiles (CMV) followed by GC-MS [6]. A new synthetic cannabinoid, 4F-MDMB-BINACA was recently characterized using GC-MS and other analytical instruments [7].

Heroin is a commonly abused drug. It is a semisynthetic product derived from morphine. Due to the differences in agricultural and manufacturing procedures, there is a significant difference in the type and concentration of opium alkaloid content in heroin samples. In addition to that, insertion of diluents and adulterants makes the illicit drug sample matrix even more complicated. However, profiling of the seized drugs provides information regarding origin, as well as the adulterants and diluents used in the manufacturing process. Although FID continues to be a major detector for screening and quantitation of the opium alkaloids and adulterants, due to the higher selectivity and its ability to identify unknown albeit important impurities, MS is used frequently with GC [8–10]. When conventional approaches fail to obtain information about the origins of confiscated illicit heroin samples, elemental analysis/isotope ratio mass spectrometry (EA-IRMS) and gas chromatography/combustion/IRMS (GC-C-IRMS) may be used to obtain isotopic information such as delta C-13, delta N-15, delta O-18, and delta H-2 values of the alkaloids to predict geographical or temporal origins of the confiscated samples [11].

Opium contains more than 20 different types of alkaloids that constitute from a small amount

TABLE 30.1 Classification of DEA scheduled drugs and their chemical structures.

Drug class	Commercial name	DEA schedule	Chemical structure
Cannabinoids	Marijuana	I	
	Hashish	I	
Opioids	Heroin	I	
	Opium	II, III, V	<div style="display: flex; justify-content: space-around; align-items: flex-end;"> <div style="text-align: center;">  <p>Morphine</p> </div> <div style="text-align: center;">  <p>Codeine</p> </div> </div>
Stimulants	Cocaine	II	
	Amphetamine	II	

(Continued)

TABLE 30.1 Classification of DEA scheduled drugs and their chemical structures.—cont'd

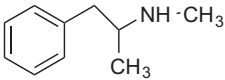
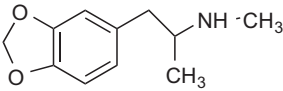
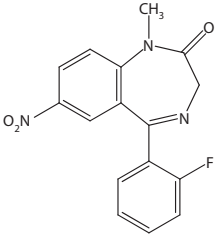
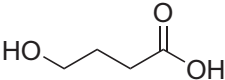
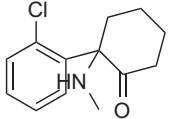
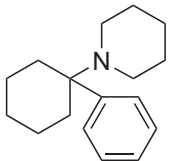
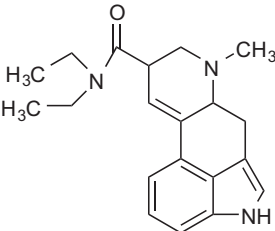
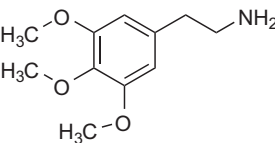
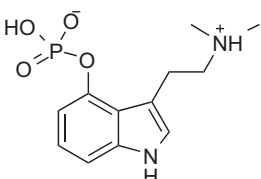
Drug class	Commercial name	DEA schedule	Chemical structure
	Methamphetamine	II	
Club drugs	MDMA	I	
	Flunitrazepam	IV	
	GHB	I	
Dissociative drugs	Ketamine	III	
	PCP and analogs	I, II	

TABLE 30.1 Classification of DEA scheduled drugs and their chemical structures.—cont'd

Drug class	Commercial name	DEA schedule	Chemical structure
Hallucinogens	LSD	I	
	Mescaline	I	
		3	
	Psilocybin	I	
		4	

to as high as 10% of its weight [12]. Analysis of these alkaloids is carried out using GC-FID or GC-MS. Alkaloid components are extracted from opium samples by solvent extraction. The solution is then treated with 20% (v/v) trifluoroacetic anhydride (TFAA) in order to transform alkaloids into trifluoroacetylated derivatives before GC analysis. A relatively simpler way is to use thermal desorption (TD) in combination with GC to analyze volatile and semivolatile alkaloids, impurities, synthetic by-products, and residual solvents simultaneously. This approach reduces the use of toxic organic solvents and eliminates the tedious sample preparation process. A new arsenal, GC coupled to vacuum

ultraviolet spectrophotometry (GC-VUV) is now used to identify opiates as well their common adulterants and diluents [13].

Bulk cocaine samples, in the form of hydrochloride salts and free base, are routinely analyzed by GC-MS or GC-FID [14]. For drug intelligence purposes, cocaine samples are profiled to determine major cutting agents [15] and cocaine alkaloids present in the sample that include ecgonine methyl ester, ecgonine, tropacocaine, benzoylecgonine, norcocaine, *cis*- and *trans*-cinnamoylcocaine, and 3,4,5-trimethoxycocaine. Profiling of cocaine requires derivatization. *N*-methyl-*N*-trimethylsilyltrifluoroacetamide (MSTFA), *N,O*-bis(trimethylsilyl)

acetamide (BSA), trimethylchlorosilane (TMSCl), *N,O*-bis(trimethylsilyl)trifluoroacetamide (BSTFA) + 1% (v/v) trimethylchlorosilane (TMCl) are commonly used for this purpose. However, if the cocaine sample contains lactose or mannitol as the cutting agent, derivatization with MSTFA is advised [16]. Analysis of solvent residues in illicit cocaine may also provide valuable information regarding the clandestine manufacturing process and can be used for source discrimination purposes. Residual solvent is analyzed by extracting it onto an SPME fiber followed by analysis by GC-MS [17] or directly by static headspace-GC-MS [18]. If identification, profiling, or residual solvent analysis alone or in combination does not offer conclusive information about the source of the drug, GC-MS-IRMS has been used to obtain $\delta^{13}\text{C}$ and/or $\delta^{15}\text{N}$ values that can be used, independently or in combination with other relevant information, as an efficient tool for source discrimination [19].

Methamphetamine (MA) can be manufactured using a number of synthetic routes. Consequently, it exhibits different impurity profiles [20] based on the synthetic route, as well as the reaction conditions employed in the manufacturing process. Impurity profiling of seized MA is carried out by GC-FID or GC-MS. Impurities present in MA are extracted by LLE under alkaline conditions or by SPME. Comparison between LLE and SPME reveals [21] that the relative intensity of impurities in MA appears to be much higher for SPME, thus establishing it as an efficient solventless sampling tool for impurity profiling. In addition, a larger number of volatiles are observed for SPME-GC-MS. TD GC-MS may be used as a green alternative for impurity profiling of MA [22]. Comparing the performance of TD and LLE in MA impurity profiling revealed that both the chromatographic signal intensity and the number of detected peaks are higher when TD is used [22].

Amphetamine-type stimulants (ATs), e.g., ecstasy, are a global problem due to their ubiquitous availability and abuse around the world.

Ecstasy, a synthetic drug, composed primarily of 3,4-methylenedioxy-*N*-methylamphetamine (MDMA) and other sympathomimetic amines such as amphetamine (AP) and MA. The majority of the methods used for ecstasy profiling are based on GC-FID or GC-MS [23,24]. Sample preparation for ecstasy seizures includes LLE, SPE, and SPME. Due to its operational simplicity and solvent-free nature, SPME has gained much interest in recent years among forensic chemists. To identify the clandestine production facility of AP, aqueous waste characterization using GC-MS can be used [25].

Designer drugs are synthetic versions of drugs that are designated as controlled substance as per the US DEA schedule. They are similar in structure and efficacy to controlled substances. Common designer drugs include fentanyl and meperidine analogs, phencyclidine (PCP), APs, and MA. Designer drugs are screened, identified, and quantified using GC-MS. Prior to chromatographic analysis, the drug sample is often derivatized with trifluoroacetic acid (TFA). Comparison of the chromatographic separation between TFA derivatives of phenethylamine-type drugs and their free base demonstrates that derivatization facilitates the complete separation of some critical components, which are not separated in their free-base state [26]. A new designer drug, deschlorketamine, a ketamine analogue possessing more potency and longer-lasting impact than ketamine was characterized by Frison et al. using GC-MS and other analytical techniques so that the forensic analysts may easily identify this new drug [27].

Methaqualone (MTQ) is a sedative-hypnotic drug commonly sold in South Africa as *Mandrax*. GC-MS is routinely used to identify and quantify the concentration of MTQ in seized drugs. Studies show that only chromatographic profiles of multiple batches of seized samples (some of them are similar in appearance and tablet weight), obtained by GC-MS analysis, are not sufficient to associate them with the same

manufacturer; hence, identification of precursors or reaction by-products is recommended to make any definitive conclusion [28].

p-Fluorofentanyl (pFF), a potent synthetic narcotic analgesic, is often used illicitly and can be found in tablet and capsule form. For gas chromatographic analysis, it is first solubilized in aqueous solution of potassium hydroxide and sodium sulfate followed by extraction into diethyl ether. The organic extract is then evaporated to dryness and reconstituted in methanol. pFF can be analyzed by GC-MS without derivatization [29].

In addition to the use of conventional one-dimensional GC with suitable detectors for drug screening, comprehensive two-dimensional GC coupled with TOFMS (GC × GC-TOFMS) [30,31] and GC-Fourier transform infrared spectroscopy (GC-FTIR) [32] have shown promise for faster screening and confirmation of illicit drugs.

30.2.2 Analysis of counterfeit drugs and traditional medicinal products

Both counterfeit drugs and inadequately regulated traditional medicines pose significant risk to human health and public safety. Counterfeit drugs account for at least 10% of the medicines sold worldwide [33]. Forensic analysis of counterfeit medicines plays a key role in determining the presence of potentially toxic ingredients, establishing possible association between different counterfeit medicines, and providing valuable clues to the drug regulatory and law enforcement agencies regarding the potential sources. Although HPLC and other analytical instruments are frequently employed for screening of the suspect samples, GC-MS is also used when the analyte of interest is thermally stable [34].

Traditional medicinal products occasionally contain undisclosed synthetic medicinal compounds added to increase their efficacy. They are available in various forms including tablet,

capsule, powder, and syrup. Since the addition of potent medicinal compounds is not disclosed, consumers are often unaware of the risk associated with the consumption of these products. GC-MS is generally used for the identification of the presence of synthetic medicinal products in traditional medicines [35]. An overview of different methodologies used in the United States for the determination of organic volatile impurities in pharmaceutical products is presented by Mulligan et al. [36]. Some of these approaches are designed to detect counterfeit bulk pharmaceutical products using their volatile impurity profile by GC.

30.3 Gas chromatography in forensic toxicology

Toxicology is the *science of poison*. It deals with chemical and physical properties of poisons, their physiological or behavioral effects on living organisms, their qualitative and quantitative methods of analysis, and the development of procedures for the treatment of poisoning [37]. Forensic toxicology, a subunit of the broader field of toxicology, deals with the application of toxicology to cases and issues where the adverse effects of poison have administrative or medico-legal consequences, and subsequently, there is a potential likelihood that the results will be used in a court of law.

Forensic toxicology has applications in five major areas: (1) postmortem toxicology/death investigation toxicology, (2) human performance toxicology, (3) doping control, (4) forensic workplace drug testing, and (5) abuse of recreational drugs with malice intent.

30.3.1 Postmortem toxicology/death investigation toxicology

Analysis of postmortem samples to determine the probable cause of death is always challenging due to the intrinsic variability of the

concentration of drugs/toxicants within the body, different degrees of corpse degradation before it reaches the morgue, and the inconsistency in the availability of sample specimens submitted for toxicological analysis. Collection of biological samples should strictly follow relevant protocols developed to minimize site-to-site variability. When possible, peripheral blood and at least one other specimen, e.g., urine, vitreous humor, liver, or gastric content should be collected.

In order to isolate target analytes from the collected biological specimens, different sample preparation techniques are employed. Commonly used sample preparation techniques include SPE, SPME, single-drop microextraction, and solvent extraction. The selection of an appropriate sample preparation technique normally depends on the type of biological specimen.

The samples are generally screened using GC equipped with NPD or FID. Confirmatory tests are often carried out using MS or MS/MS. As the effectiveness of GC is largely dependent upon sampling and sample preparation techniques, as well as chromatographic parameters, e.g., column type and quality, column temperature, and analysis time [38], developing a GC method requires careful consideration of all of the listed and other important parameters that may substantially influence the analytical results.

The extent and type of postmortem toxicological analysis are dependent upon jurisdiction of death, age of the deceased, availability of medical history, and many other factors. Depending on the availability of information regarding the deceased, a psychoactive drug screening or a comprehensive drug screening may be carried out [39]. Drug screening determines the type and quantity of the drug present in the biological specimen and often includes alcohol, drugs of abuse, and a variety of toxic substances.

When the screening test provides a positive result for a particular drug/toxicant, a confirmatory test is carried out. Often, a different chromatographic technique is recommended for

confirmatory test in order to minimize systematic errors.

The following section discusses typical uses of GC in postmortem toxicology.

Nicotine, a water-soluble alkaloid, is the addictive ingredient in cigarettes. A number of poison cases are reported every year instigated by accidental ingestion of cigarettes, cigarette end, or their liquid extract. In some cases, these ingestions claim human lives. A gas chromatographic method was developed by Moriya et al. that allows the detection of nicotine and its major metabolite cotinine from blood and urine samples with a limit of detection (LOD) of 2.1 ng mL^{-1} for both analytes [40].

Due to its sedative and euphoric effects, gamma-hydroxybutyric acid (GHB) is popular as a recreational drug. GHB is also an endogenous compound, produced as a by-product of gamma-aminobutyric acid (GABA) metabolism. Therefore, it is important to know the endogenous concentration of GHB in humans. GHB can be extracted from plasma and urine samples in chloroform for analysis by GC-FID and in ethyl acetate for analysis by GC-MS. GHB can be detected by GC-FID without derivatization; however, derivatization using BSTFA containing 1% (v/v) TMCS improves the method sensitivity by at least one order of magnitude when analysis is carried out by GC-MS. The LOD is 2.5 mg L^{-1} by GC-FID and 0.2 mg L^{-1} by GC-MS [41].

Frequently abused drugs, e.g., AP, morphine, codeine, opiates, cocaine, and their metabolites can be extracted from human postmortem tissues including brain [42]. The analytes are extracted from homogenized brain tissues by SPE. Following SPE, extracted drug samples and their metabolites are derivatized in two steps, first using a mixture of *N*-methyl-*N*-(*t*-butyldimethylsilyl) trifluoroacetamide (MTBSTFA) +1% (v/v) *tert*-butyldimethylchlorosilane (TBDMCS) and later a mixture of BSTFA + 1% (v/v) TMCS. MTBSTFA helps in reducing the loss of APs due to volatility, during

the sample preparation steps. TBDMS derivatizes primary amines of APs while sterically hindered functional groups are derivatized with BSTFA. As such, this dual derivatization process provides a mixture of thermally stable derivatives amenable to GC. The analytes are finally quantified by GC-MS operated in positive chemical ionization (PCI) mode. ATS can be monitored in plasma using direct immersion SPME followed by GC-MS [43]. An interesting method for the simultaneous monitoring of five drugs (morphine, 6-monoacetylmorphine, cyamemazine, meprobamate, and caffeine) with substantially different physicochemical properties in 11 different biological fluids and tissues using automated SPE and GC-MS/MS was described [44]. Basic drugs, e.g., amitriptyline, citalopram, clozapine, diazepam, dihydrocodeine, methadone, and tramadol, from postmortem blood samples are extracted using LLE under basic condition (pH 10) with diethyl ether as the extraction solvent. These analytes can be analyzed by GC-MS without derivatization [45].

Acidic and neutral drugs including analgesics, anticoagulants, antidiabetics, antiepileptics, barbiturates, diuretics, hypnotics, and muscle relaxants are also screened from blood samples. The drugs are extracted from blood samples using ethyl acetate and analyzed by GC-FID or GC-MS [46]. To determine “new psychoactive substances” in postmortem matrices, a new method comprised of mixed-mode SPE, microwave fast derivatization, and GC-MS operated in selected ion monitoring mode was presented by Margalho et al. [47]. Due to the high popularity and demand of cocaine, adulterants are often added to cocaine. Gameiro et al. analyzed 97 real blood samples tested positive for cocaine and/or its metabolites using GC-MS to investigate the presence of any adulterants [48]. In total, 31 samples contained adulterants.

Organophosphorus insecticides, substances commonly used in suicide attempts, are analyzed from postmortem blood samples [49,50]. Omethoate, dimethoate, diazinon,

chlorpyrifos, parathion-ethyl, and chlorfenvinphos are some of the members of this insecticide family. Sample preparation for extracting these insecticides from blood samples includes protein precipitation, SPME, LLE, and SPE. Since organophosphorus pesticides are thermally stable, generally no derivatization is required prior to GC-MS analysis.

Fentanyl, a synthetic narcotic anesthetic 80–100 times more potent than morphine, can be determined in urine using dispersive liquid–liquid microextraction (DLLME) followed by GC-MS [51]. Drug screening in blood is often impacted by the presence of triglycerides (TG) and their concentration. Huang et al. studied the impact of TGs on the extraction of 19 commonly used drugs when LLE is employed on whole blood prior to GC-MS analysis. The study revealed that LLE with diethyl ether, ethyl acetate/hexane (9:1), and chlorobutane is effective when TGs are at low concentration (0.63–6.85 mmol L⁻¹). However, when TGs are at high concentration, chlorobutane should be used as the extraction solvent [52]. Karlons et al. developed a sensitive and selective method for simultaneous monitoring of 15 benzodiazepines in human whole blood using a mixed-mode cation-exchange polymer sorbent for extracting the analytes, derivatization with *N*-(*t*-butyldimethylsilyl)-*N*-methyl trifluoroacetamide, and GC-MS analysis in the negative ion chemical ionization mode [53]. Limits of detection varied from 0.24 to 0.62 ng mL⁻¹.

Zanaboni et al. compared different analytical methods for the determination of carbon monoxide in postmortem blood and concluded that HS-GC-TCD was the best method among those considered [54]. 2,4-Dinitrophenol (2,4-DNP), a prohibited drug known for its weight-loss effect, appears to be reemerging in forensic casework. To facilitate easy monitoring of 2,4-DNP in blood and urine samples, de Campos et al. reported a new method using GC-MS that was applied to six suspected cases in the United States with three positive results [55]. One criterion to assess

the performance of a forensic toxicological laboratory is its capability to rapidly screen drugs and poisons from different biological samples. Pan et al. developed a high-throughput screening method for 288 drugs and poisons in human blood using GC–high-resolution accurate mass spectrometry (GC-HRMS) [56]. The blood samples were extracted with a diethyl ether and buffer solution, centrifuged, and an aliquot of the supernatant analyzed by GC-HRMS.

30.3.2 Human performance toxicology

Human performance toxicology primarily deals with driving under the influence of drugs and alcohol. Upon request from a Law Enforcement Officer, a suspect must take chemical DUI (driving under the influence) tests, which include breathalyzers, blood tests, and urine tests to establish his/her sobriety.

Ethanol is the most widely abused drug in the world. However, unlike other common drugs of abuse, ethanol poses enormous analytical challenges due to its high volatility, as well as its ability of being produced *in situ* in poorly handled samples or as a natural product of the postmortem process [57]. Due to its high volatility, ethanol cannot be efficiently isolated from complex biological matrices by classical extraction techniques nor can it be introduced directly, along with the matrix, into the GC system. As a result, headspace sampling remains the only viable alternative sampling and sample preparation technique. To make headspace sampling more reliable and efficient, an HS-GC-FID method was developed utilizing a dual-role robotic autosampler, one for sample preparation and the other for headspace sample introduction into the GC. A DB-624 column successfully baseline-separated all known analytes that normally appear with ethanol, providing LOQ and LOD values of 17 mg dL^{-1} and 5 mg dL^{-1} , respectively [57]. Taylor et al. developed a new method to monitor ethanol in blood using

headspace GC that requires 10–100 μL of blood. The study also compared the alcohol concentration between capillary and venous blood and statistically significant alcohol concentration difference between capillary and venous blood. Venous blood samples were found to contain higher alcohol levels compared to capillary blood, which was also observed by other researchers [58]. A method developed by Diekmann et al. utilized headspace GC coupled to VUV (HS-GC-VUV) to monitor ethanol and other inhalant compounds in whole blood [59].

Kristoffersen et al. studied the effects of blood storage and headspace conditions on the ethanol concentration in plasma, hemolyzed blood, and nonhemolyzed blood using HS-GC-FID [60]. A decrease in ethanol concentration was observed after a few days of storage at room temperature with nearly equivalent increase in aldehyde concentration. The diminishing value of ethanol concentration with prolonged storage at room temperature is attributed to the oxidation of ethanol to acetaldehyde. In addition, high headspace equilibration temperature was found to contribute to a higher ethanol value.

Considering the fact that ethanol can be detected in the body for only a relatively short time after consumption, ethyl glucuronide (EtG), a metabolite of ethanol, is frequently used to investigate alcohol addiction (as opposed to social consumption). Monitoring ethyl glucuronide offers an extended window for assessing alcohol consumption and can be detected in body fluids, tissues, and hair samples. Ethyl glucuronide is nonvolatile and stable upon storage. It can be extracted from urine samples using MAE with chloroform followed by evaporation to dryness [61]. Due to its nonvolatile nature, analysis of ethyl glucuronide by GC requires derivatization. All hydroxyl functional groups present in EtG can be trimethylsilylated with BSTFA and pyridine. Analysis of EtG extracts by GC-MS in the selected ion monitoring (SIM) mode provided LOQ and LOD values of $0.1 \mu\text{g mL}^{-1}$ and 5 ng mL^{-1} , respectively, with

recovery in the range of 80%–92%. A similar MAE with n-hexane-water (1:1) was used for a hair matrix [62]. Due to the advantage of obtaining a greater retrospective window for the detection of chronic use of alcohol, EtG may be monitored using hair samples rather than bodily fluids (urine, blood, and saliva). Several analytical methods using GC-NCI-MS [63], GC-NCI-MS/MS [64], and GC-MS/MS [65] have been developed for this purpose.

A recent development in EtG analysis from hair samples is the use of a protein precipitation (PPT) technique. EtG was extracted from hair samples in deionized water by sonication for 1 h, incubated overnight, centrifuged, and the supernatant evaporated to dryness. The residue was reconstituted in a mixture of acetonitrile and deionized water (7:1 v/v), then passed through a Sirocco protein precipitation plate. EtG residue was derivatized using a mixture of pyridine and BSTFA for GC analysis. In addition to using a PPT technique for matrix simplification, large-volume injection (LVI) with a programmable temperature vaporization (PTV) injector was used to improve sensitivity (liquid injections of up to 50 μL). LOQ and LOD values of 10 pg mg^{-1} and 5 pg mg^{-1} , respectively, by GC-MS/MS were observed [66]. Although BSTFA is the most common derivatization reagent for EtG, other derivatization reagents, e.g., pentafluoropropionic anhydride (PFPA) and heptafluorobutyric anhydride (HFBA), were also tested [67]. PFPA was shown to offer improved sensitivity for GC-MS analysis [64].

Extraction of EtG from hair samples is generally carried out using water as the extraction solvent, followed by matrix cleanup by SPE, derivatization, and finally GC analysis. An alternative method that utilized SPME for preconcentration and sample introduction was developed [68]. Following the typical procedure of EtG extraction in water followed by SPE for matrix cleanup and derivatization using HFBA, the derivatized EtG was exposed to HS-SPME. Carboxen-polydimethylsiloxane (CAR-PDMS, 75 μm) SPME fiber demonstrated the best

performance in terms of analyte yield with minimal matrix effects. The HS-SPME-GC-MS/MS method provided LLOQ and LLOD values of 2.8 pg mL^{-1} and 0.6 pg mL^{-1} , respectively, which were significantly lower than the previously reported values for liquid sample introduction [66]. To monitor residues of stimulants including fenproporex (FEN), diethylpropion (DIE) and sibutramine (SIB) in urine samples of professional drivers and other consumers, Cunha et al. described a DLLME and GC-MS based method capable of detecting 0.1 ng mL^{-1} of FEN and DIE and 0.05 ng mL^{-1} of SIB [69]. A new psychoactive drug AM-694, a synthetic cannabinoid, has seen increased interests in recent years. A method consisting of SPE of AM-694 from urine and subsequent GC-MS analysis was developed by Bertol et al. The parent drug and its metabolites can also be monitored using LC-MS/MS [70]. Chericoni et al. used LLE, direct aqueous derivatization, and subsequent GC-MS analysis to monitor morphine, codeine, and 6-acetyl morphine in human urine and blood samples. This approach will help forensic cases involving drug impaired driving [71]. Wozniak et al. presented a method based on GC-MS/MS for simultaneously monitoring 11 APs and 34 synthetic cathinones in whole blood using only 200 μL of sample. The method involves LLE followed by pentafluoropropionyl derivatization prior to GC-MS/MS analysis affording a low limit of quantification (1–2.5 ng mL^{-1}).

30.3.3 Doping control

The use of performance-enhancing drugs in sports is commonly known as doping and is considered a widespread problem within the athletic community. These drugs are frequently used by athletes to improve their athletic performance. World Anti-Doping Agency (WADA) strictly monitors the presence of performance-enhancing drugs in urine samples collected from athletes and publishes a list of prohibited substances each year. The prohibited substances

include (1) anabolic agents; (2) peptide hormones, growth factors, and related substances; (3) β -2 agonists; (4) hormone antagonists and modulators; and (5) diuretics and other masking agents. Anabolic agents, commonly known as anabolic steroids, have been the most frequently detected performance-enhancing drugs for many years [72]. Because of the ever-increasing number of performance-enhancing drugs, the structural similarity of exogenous and endogenous steroids, the inherent complexity of the urine matrix, and the low concentration of these drugs in urine samples, their analysis is always challenging [73].

For doping control purposes, urine samples are collected from the athletes and are divided into two portions, one is sent for analysis and the other is kept under secure custody so that it can be used in case there is a dispute of the analytical results. The analyses of the urine samples are carried out in two levels: (1) screening analysis for all samples and (2) confirmatory analysis of suspicious samples that provide positive test results during screening [73]. For both screening and confirmatory analysis, GC-MS is frequently used. However, due to the low concentration of these drugs in urine samples and their low thermal stability, sample preparation (preconcentration, derivatization, etc.) always precedes the chromatographic analysis. For sample preparation, aliquots of the urine samples are first enzymatically hydrolyzed using β -glucuronidase for deconjugating the steroids. The deconjugated steroids are then extracted from the urine sample matrix by either LLE or SPE. Prior to analysis by GC-MS, the extracted analytes are derivatized with typically trimethylsilyl reagents such as MSTFA, although other approaches using methoxime, trifluoroacetyl, heptyfluorobutryl derivatives and mixed modifications have been reported [72–78].

The use of comprehensive two-dimensional GC coupled with combustion-IRMS (GC \times GC-C-IRMS) is a recent development for doping control [79]. This system offers a viable alternative to

already-established GC-MS methods with better separation of the target compounds and simpler urine cleanup procedures.

30.3.4 Forensic workplace drug testing

Due to the continuous increase in the use of illicit drugs among workers, resulting in poor job performance, tardiness, frequent absence from work, and other behavioral issues, the importance of workplace drug testing (pre- and postemployment) is on the rise. Workplace drug testing includes collection and analysis of a biological specimen, e.g., urine, hair, blood, sweat, and oral fluid to determine the presence or absence of selected drugs or their metabolites. In addition to drug screening in the workplace, biological specimens for drug screening can also be collected from schools, military, and prisons. Purschke et al. developed an automated LLE followed by GC-MS analysis for monitoring THC, 11-OH-THC, and free THC-carboxylic acid (THC-COOH) from serum [80]. A new method for the simultaneous identification and quantification of five new psychoactive substances (bupropion, desoxypipradrol, mephedrone, methylone, and naphyrone) in blood by GC with nitrogen chemiluminescence detection (GC-NCD) and atmospheric-pressure chemical ionization quadrupole TOFMS was presented by Ojanpera et al. The method does not require authentic reference standards [81].

Drug screening using urine samples may include a standard five-panel drug test for marijuana (THC), cocaine, PCP, opiates, and amphetamine or a ten-panel drug test for methamphetamine, barbiturates, benzodiazepines, MDMA, and methadone in addition to the five-panel drugs. Hair samples are frequently tested using either a standard five-panel or seven-panel drug test. A seven-panel drug test includes barbiturates and benzodiazepines, as well as the five-panel drug test. Fig. 30.2 represents a typical chromatogram from a clinical sample tested positive for codeine, morphine,

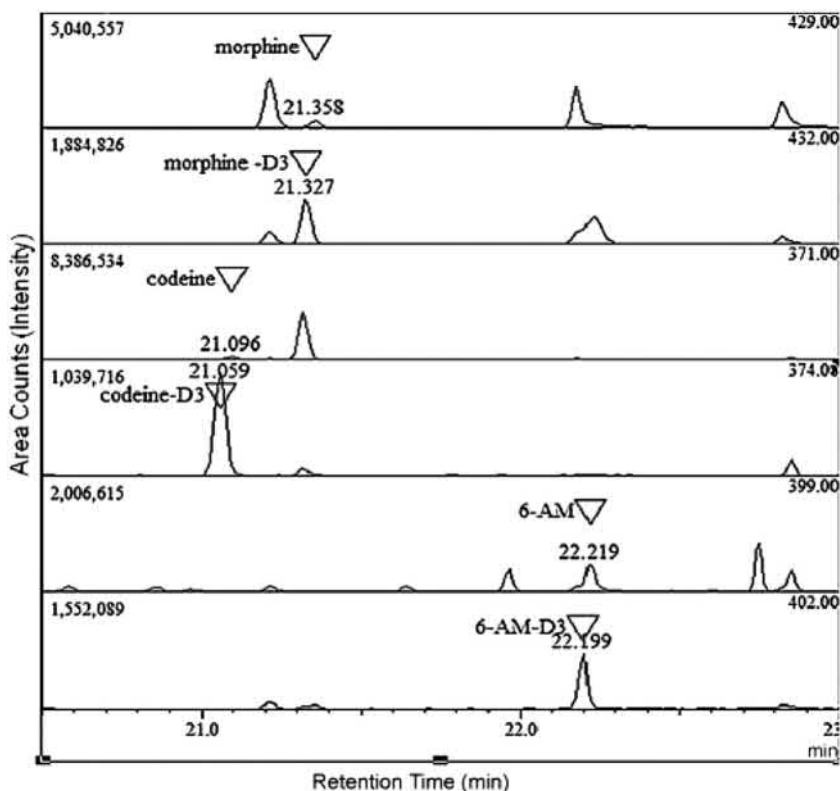


FIGURE 30.2 Chromatogram obtained from a clinical sample testing positive for codeine, morphine, and 6-monoacetylmorphine. Reproduced with permission from Reference M. Moller, K. Aleksa, P. Walasek, T. Karaskov, G. Koren, Solid-phase microextraction for the detection of codeine, morphine and 6-monoacetylmorphine in human hair by gas chromatography-mass spectrometry, *Forensic Sci. Int.* 196 (2010) 64–69; Copyright 2010, Elsevier Science.

and 6-monoacetylmorphine (6-MAM) [82]. Abuse of Marijuana is often detected by its metabolite 11-nor-carboxy-Delta (9) tetrahydrocannabinol (THC-COOH) in urine. Eller et al. recently introduced hollow-fiber LPME (HF-LPME)-based sample preparation and GC-MS analysis with a LOD of 1.5 ng mL^{-1} [83].

30.3.5 Abuse of recreational drugs to facilitate crime

One out of every five teens is a victim of date rape, which is often facilitated by recreational drugs known as date rape drugs such as flunitrazepam (Rohypnol), GHB, gamma-butyrolactone

(GBL), and ketamine. These drugs are sometimes called “club drugs” since they are frequently used at dance clubs, concerts, bars, or parties. Several reviews cover the current state of date rape drug analysis from biological samples [84–86].

Determination of GHB in humans is challenging because of its endogenous nature. As such, unless the forensic toxicologist has a clear knowledge of the basal level of endogenous GHB concentration, it is impossible to assess the exogenous concentration. Vaiano et al. studied the GHB baseline in hair samples from 150 volunteers. The GHB concentration was determined by incubating hair samples

overnight with sodium hydroxide, LLE using ethyl acetate, trimethylsilyl derivatization, and GC-MS analysis in the single-ion monitoring mode. Average GHB levels were higher in males than in females (0.829 ng mg^{-1} vs. 0.596 ng mg^{-1} , respectively). The study also revealed that the endogenous concentration of GHB is higher for males >30 years old, whereas the concentrations are quite similar throughout all other age categories [87]. Ketamine and its major metabolite norketamine can be monitored in urine and plasma samples of victims using microextraction by packed sorbent and GC-MS/MS with a detection limit of 5 ng mL^{-1} [88]. Zolpidem, a member of Z-drugs, is frequently used in date rape, robbery, extortion as well as in drugged driving. Kenan et al. developed a GC-MS method to monitor the residue of Zolpidem in urine [89]. The workflow requires a one-step LLE using ethyl acetate as the extractant. The method is sensitive with an LOQ of $0.35 \text{ } \mu\text{g mL}^{-1}$.

30.4 Analysis of ignitable liquid residues from fire debris

Unlike other crime scenes, it is often difficult, if not impossible, to obtain direct physical evidence related to the arsonist (e.g., DNA, fingerprint) from the fire scene as they are most often destroyed by the fire. As such, in a majority of arson cases, the investigators heavily depend on collecting, analyzing, and tracking the potential sources of ignitable liquid residues (ILRs) or accelerants that the arsonists use to aid the fire.

ASTM International has classified ignitable liquids into nine primary classes, which include gasoline, petroleum distillates, isoparaffinic products, aromatic products, naphthenic paraffinic products, n-alkanes products, dearomatized distillates, oxygenated solvents, and others/miscellaneous [90]. Gasoline, kerosene, paint thinners, charcoal lighter fluids, alcohols, mineral spirits, fuel oils, and vegetable oils are

the most common accelerants used by arsonists. Detection and identification of ILRs obtained from the fire scene provide the investigator with crucial information about the type of accelerants used, helping them to track down the suspected arsonist(s). Two recent books *Analysis and Interpretation of Fire Scene Evidence* [91] and *Fire Debris Analysis* [92] extensively cover various important aspects of fire science from a forensic perspective. Some review articles also cover important aspects within this field [92–94].

ASTM International has developed a number of standard practices for screening, isolating, and quantifying ILRs and archiving of extracts recovered from fire debris prior to instrumental analysis.

Due to the complex nature of the sample matrix and high volatility of ignitable liquids, sample collection from the crime scene requires extreme care and attention. On top of that, proper documentation is required in every step to meet any potential future legal challenges. The fire debris samples, as a source of ILRs, are collected from the fire scene in clean, airtight containers and are immediately transported to the laboratory for analysis. Commercial containers, e.g., metal paint cans, glass mason jars, and copolymer bags, are among those most frequently used as fire debris evidence collection and storage containers. Sample preparation techniques prior to injection of ILR samples into GC include dynamic headspace concentration, passive headspace concentration with activated charcoal, solvent extraction, and passive headspace concentration with SPME. SPME has gained increased attention in recent years as a viable sample preparation technique for fire debris analysis [95–99].

Separation of ILR samples is predominantly carried out by GC coupled with different detectors, e.g., FID, FTICR-HRMS, PID, ECD, MS, MS/MS, DMS, and AED, with MS being the most frequently used detection system [100,101]. ASTM has adopted GC-MS as the preferred analytical tool for fire debris analysis

and established a standard test method for investigators (ASTM E1618-11).

Interpretation of the overly complex chromatographic information obtained from ILR analysis is always challenging and most often requires application of multivariate statistical techniques for data analysis, such as principal component analysis (PCA), discriminant analysis (DA), and Pearson product moment correlation (PPMC) coefficients [95,102].

In addition to the continuous attempt to develop superior gas chromatographic methods, some researchers addressed different aspects of fire debris analysis to gain a better understanding of the fire scenes. Almirall and Furton characterized the background and pyrolysis products to assess their potential interferences in fire debris analysis. Many of the compounds identified by combustion/pyrolysis of common substrates, e.g., alkanes and aromatics, are the target compounds commonly found in ILR mixtures [103]. R. Borusiewicz et al. studied the impact of different factors, e.g., type of substrate or burned materials, type of accelerant, length of time between the lighting and extinguishing of the fire, and the level of air availability on the possibility of identifying trace accelerants. The study revealed that the type of burned material exerts the greatest influence in identifying trace accelerants [104]. In an attempt to develop a less expensive and more reliable onsite detection tool for ignitable liquid residues, Lu and Harrington [105] investigated GC–differential mobility spectrometry (GC-DMS). Headspace SPME was used as the sample preconcentration technique. GC-DMS was used to classify samples into one of seven ignitable liquids using a fuzzy rule building expert system, which had an 82.3% accurate classification rate for burned samples. Headspace GC-IMS (HS-GC-IMS) was used to determine ignitable liquids from fire debris [106].

Due to the high abundance of natural background compounds along with the pyrolysis by-products formed during the combustion

process, identification of ignitable liquid residues is now preferentially carried out using comprehensive GC × GC-TOFMS with substantially higher probability of detecting marker compounds [107,108]. In suspected arson case, if an intact or partially intact human cadaver is recovered, sampling of the fire debris alongside the human remains is challenging. Nizio et al. developed a body bag as an alternative sampling container to collect and analyze ILR from the burnt remains without losing any valuable analytical information. Using the body bag followed by dynamic headspace sampling and subsequent TD-GC × GC-TOFMS provided information as to whether any ILR was involved or not [109].

30.5 Analysis of explosives

Since September 11, 2001, terrorist attacks in the United States, the importance and significance of the identification and quantification of traces of explosives, particularly compounds used in making homemade explosives (HME), have been overwhelmingly recognized among the law enforcement agencies. As such, new instrumental methods, a majority of which are based on GC, have emerged in recent years. Table 30.2 provides a list of common organic explosives with their pertinent properties [110]. The low vapor pressures of many organic explosives present tremendous challenges in their detection by GC.

Identification and determination of postblast organic residues of explosives is an important topic in forensic science as the chemical profile of postblast residues provides valuable information with regard to the explosive type, their tentative origin, as well as an assessment of the severity of environmental pollution.

Organic explosive compounds can be arbitrarily classified as nitro-containing and non-nitro-containing explosives based on the presence or absence of nitro/nitroso functional

TABLE 30.2 List of organic explosives with their pertinent properties.

Explosive class	Name of the explosive	Abbreviation	Molecular weight	Vapor pressure at 25°C (Torr)
Nitroaliphatic	Nitromethane	NM	61.04	2.8×10^1
	2,3-Dimethyl-2,3-dinitrobutane	DMNB	176.17	2.1×10^{-3}
Nitroaromatic	2,4-Dinitrotoluene	2,4-DNT	182.13	2.1×10^{-4}
	2,4,6-Trinitrotoluene	TNT	227.13	5.8×10^{-6}
	2,4,6-Trinitrophenol	Picric acid	229.10	5.8×10^{-9}
Nitrate ester	Ethylene glycol dinitrate	EGDN	152.06	7.0×10^{-2}
	Nitroglycerine	NG	227.09	3.1×10^{-4}
	Pentaerythritol tetranitrate	PETN	316.14	1.4×10^{-8}
Nitramine	2,4,6,N-Tetranitro-N-methylaniline	Tetryl	287.14	5.7×10^{-9}
	Trinitro triazacyclohexane	RDX	222.12	4.6×10^{-9}
	1,3,5,7-Tetranitro-1,3,5,7-	HMX	296.16	1.6×10^{-13}
	Tetraazacyclooctane	CL20	438.18	Not available
	Hexatrinetrohexaazaisowurtzitane			
Peroxide	Triacetone triperoxide	TATP	222.24	3.7×10^{-1}
	Hexamethylene triperoxide diamine	HMTD	208.17	Not available
By-product	2-Ethyl-1-hexanol		130.23	1.4×10^{-1}
	Hydrogen peroxide		34.03	1.4×10^0
	Acetone		58.08	2.3×10^2

groups in their structure. Trinitrotoluene (TNT) and nitroglycerine (NG) are examples of nitro-containing explosives, whereas triacetone triperoxide (TATP) and hexamethylene triperoxide diamine (HMTD) are examples of non-nitro-containing explosives.

Over the years, TATP has increased in popularity among terrorist groups, as indicated by multiple bombings that have occurred within the United States and throughout the world, where TATP was the explosive compound that was used. Sigman et al. [111] developed a method for analyzing TATP by GC-MS (using ammonia positive-ion chemical ionization, electron ionization, and methane negative-ion chemical ionization). Comparison among the

different ionization methods revealed that ammonia positive-ion chemical ionization results in the lowest LLOD in the picogram range compared to 15 ng by GC-FID.

Since HME are generally made by commercially available ingredients, one possible way to track the origin of the used precursors is to obtain the impurity profile of the precursor and to match the impurity profile with commercial precursors from different manufacturers. As manufacturers use different starting materials, solvent, and synthetic routes for synthesizing precursor chemicals, each of the precursors should possess a unique impurity profile that can be easily differentiated from the others. Partridge et al. [112] utilized some off-the-shelf

precursors to prepare TATP and HMTD. Following detonation, SPME was used to obtain postblast by-products. Analysis of the postblast residues by GC-MS indicated the persistence of the same impurities present in the precursors, validating the potential application of profiling to trace back the raw materials/precursors used to manufacture the explosive.

A majority of the explosives, except peroxide-based explosives, contains either nitro (NO_2) or nitrate (NO_3) functional groups and therefore is compatible with a chemiluminescence-based detector known as thermal energy analyzer (TEA). The TEA pyrolyzes the explosive vapors at high temperatures to produce an NO radical, which is later oxidized by ozone to form the excited state of nitrogen dioxide (NO_2^*), which then emits a photon as it returns to the ground state. The emission of photons can be detected using a photomultiplier tube. Since TEA is only sensitive to nitrogen-containing compounds, the presence of other organic compounds in the sample matrix does not influence the sensitivity of TEA in detecting such explosives in complex environmental matrices [113]. DNT, TNT, NG, and PETN explosives have been analyzed using solvating GC in a packed column with CO_2 as the mobile phase and detected with TEA. Compared to the detection sensitivity of FID, TEA can detect 10 times more NG, with a linear range from 0.1 to 0.5 ppb [114]. In addition to TEA, other detectors, e.g., FID, ECD, NPD, and MS, are frequently used for nitrogen-containing explosives, with the ECD being the most common. The ECD is less selective but more sensitive for nitroaromatic explosives than TEA or NPD [115]. Impurity profiling of trinitrotoluene can be performed in just 4 min using vacuum-outlet GC [116].

Routon et al. [117] developed a GC-MS method in order to discriminate Hodgdon Pyrodex and Triple Seven, two black powder substitutes frequently used as fillers in improvised explosive devices (IEDs). The method

utilizes derivatization using BSTFA +1% (v/v) TMCS. The derivatization process converts organic fuel compounds (benzoic acid, nitrobenzoic acid, and dicyandiamide) into trimethylsilyl derivatives, which are easily separated and identified by GC-MS.

Emulsion explosives, a new explosive class widely used in China that accounts for 40%–50% of Chinese explosive output, consist of an aqueous solution of inorganic oxidizing salt, an organic fuel, and emulsifiers. Postblast residues of these explosives can be analyzed by first reacting the residues with methanolic potassium hydroxide solution to convert the emulsifiers into fatty acid methyl esters, followed by derivatization with BSTFA containing 1% (v/v) TMCS. The GC-MS profile offers sufficient information to recognize the original explosive [118].

With the rapid increase in the use of organic explosives, it is important to trace the clandestine manufacturing units. As such, Partridge et al. [112] developed a method to detect impurities in the commercially available precursor chemicals. Detection of those impurities provides valuable information regarding the potential sources of the precursor chemicals and eventually to be able to retrospectively track down the potential wrongdoer.

Although IMS is considered as a reliable field detection tool for explosive detection and is routinely used by law enforcement and military personnel, its deficiency to handle chemical mixtures (as opposed to a single pure compound) poses a serious limitation to its effectiveness as a field detection technique. Cook et al. [119] offered a unique approach to boost the capability of IMS by interfacing it to a GC. GC-IMS resolved the problem of separating components from a complex mixture, thus accomplishing enhanced linear dynamic range (LDR). As such, the new system was able to screen both single- and multicomponent explosive systems with the ability to detect trace to high concentrations of target analytes.

Although commonly used by law enforcement agencies to disperse large groups of protesters, aerosol defense sprays, also known as pepper spray, can be used, with criminal intention as a weapon. Among other irritants, oleoresin capsicum (OC) is one of the major active ingredients used in defense sprays. In forensic investigations, pepper spray residuals have been recovered from the fabrics of the victim/offender by LLE. However, low and inconsistent recovery in solvent extraction has prompted the development of a new method based on headspace SPME-GC-MS. Both PDMS/DVB and DVB/CAR/PDMS SPME fibers were found to be suitable for extracting capsaicin and its analog dihydrocapsaicin with LODs of 1.08 and 0.73 ng, respectively, and about 70% recovery from spiked samples.

Due to the low concentration of explosives that are present in an overly complex matrix, explosive samples often require sample preparation and/or matrix cleanup prior to analysis by GC. Water and soil samples are generally prepared by using US Environmental Protection Agency SW-846 Method 8330 [120], which utilizes SPE or salting out. However, SPE often involves multiple steps, utilizing toxic organic solvents and indiscriminately extracting numerous organic interferents that are present in the sample matrix.

Explosive traces can also be recovered from different surfaces near the explosion site using solvent-wetted cotton swabs. Analytes are extracted from the swab by adding additional organic solvent. The volume of the extracting solvent is often reduced by evaporation to increase the analyte concentration.

Being simple, solvent-free, and fast, SPME has been employed for selective extraction of explosive analytes from different matrices. Both direct immersion SPME [120] and headspace SPME [121] can be used with PDMS/DVB and CW/DVB as the preferred fiber chemistry. Headspace SPME can also be used to analyze volatile

compounds from smokeless powder by GC-FID [122].

Investigations on improvised explosives, their assembling places, vehicles used for their transportation require efficient swabbing system that can collect traces of the explosive substances. Romolo et al. studied different swabbing systems including isopropanol: water (7:3) prewetted commercial swabs, dry paper swabs, and cotton swab prewetted with isopropanol to collect residues of TATP. Among the tested swabs, wetted swabs performed better [123].

Recently, Andrasko et al. reported the use of GC-UV to monitor TNT, DNT, EGDN, NG, TATP and PETN [124].

30.6 Gas chromatographic analysis of organic gunshot residues (OGSRs)

In any criminal case involving actual or suspected use of firearms, the detection and identification of residues from the firearm discharge are of prime importance as they provide invaluable information in estimating the firing distance, identifying the bullet holes, and determining whether or not the suspect was involved in the shooting [125]. Gunshot residue (GSR), also known as cartridge discharge residue (CDR) or firearm discharge residue (FDR), is composed of unburned or partially burned propellant powder, particles from the ammunition primer, grease, lubricants, and tiny metal fragments from the cartridge [125–127]. GSR comprises both organic and inorganic compounds. However, we will limit our discussion to the organic components of the GSR as GC is only used to detect and identify those compounds. Table 30.3 provides a list of organic compounds commonly encountered in GSR.

Some of the compounds in Table 25.3 are almost obsolete, as they are no longer being used in current firearm formulations [127]. However, they may still be detected in cases where

TABLE 30.3 Common organic compounds identified in gunshot residues.

Compound	Function
2,4-Dinitrophenylamine (2,4-DPA)	Propellant
2,3-Dinitrotoluene (2,3-DNT)	
2,4-Dinitrotoluene (2,4-DNT)	
2,6-Dinitrotoluene (2,6-DNT)	
2-Nitrophenylamine (2-NDPA)	
4-Nitrophenylamine (4-NDPA)	
Carbazole	
Carbanilide	
Camphor	
Butyl centralite	
Butyl phthalate	
Akardite II (AKII)	
Cresol	
Methyl cellulose	
Methyl centralite	
Methyl phthalate	
Nitroguanidine	
Nitrotoluene	
N-Nitrosodiphenylamine (N-NDPA)	
Picric acid	
RDX	
Resorcinol	
Triacetin	
Dextrin	Primer
Diazodinitrophenol	
Diazonitrophenol	
Gum Arabic	
Gum tragacanth	
Karaya gum	
Sodium alginate	

(Continued)

TABLE 30.3 Common organic compounds identified in gunshot residues.—cont'd

Compound	Function
Pentaerythritol tetranitrate (PETN)	Propellant/primer
2,4,6-Trinitrotoluene	
Nitrocellulose (NC)	
Nitroglycerine (NG)	
Tetracene	
Tetryl	

old ammunitions are used. The major sources of organic compounds in GSR include the propellant powder and the primer mix. Although black powder was the first propellant used in firearms, it has been discontinued with the introduction of a better propellant known as smokeless powder. As the name implies, it produces negligible smoke when fired unlike the black powder. Smokeless powders are classified into (1) single-base powder if only nitrocellulose is used as the explosive; (2) double-base powder if both nitrocellulose and nitroglycerine are used as the explosive components; and (3) triple-base powder when nitroglycerine, nitrocellulose, and nitroguanidine are used as the explosive components. In addition to the explosive components, other ingredients that are commonly used in the firearm formulations are additives, stabilizers, plasticizers, flash inhibitors, coolants, surface lubricants, and antiwear additives, which are all contributors to the source of organic compounds in the GSR.

For investigative purposes, GSRs are often collected from different areas and surfaces, e.g., skin, hair, body parts, and clothing of the suspect, as well as vehicles, surroundings of the incident, and surfaces of different objects, which are in proximity of the incident [128]. Depending upon the objects and the type of surfaces from where GSR is collected, different sampling procedures and strategies are applied, with a common goal of maximizing the amount

of GSR collected and minimizing the collection of matrix interferences, as well as to reduce the risk of cross-contamination. The most frequently used sampling procedure includes tape lifts, glue lifts, swabbing, vacuum lifts, combing, nose blowing, etc. [127]. Recent developments in organic GSR analysis have been reviewed by Goudsmits et al. [129] and Chang et al. [130].

Analysis of the organic compounds present in GSR is generally carried out using GC coupled with a variety of different detectors, e.g., FID, ECD, MS, and TEA, with TEA being the most frequently used detector. Andrasko et al. [131] investigated various organic compounds and degradation products from smokeless powders in the barrels of firearms after test shooting. GSRs were extracted onto an SPME fiber and introduced into a GC-TEA for analysis. The compounds were later identified by GC-MS. As SPME is a nondestructive equilibrium-based sampling and sample preconcentration technique, the same sample can be investigated multiple times in order to validate the analytical results. In another study performed by Zeichner et al. [132], analysis of the organic constituents of GSR was carried out by GC-TEA, GC-MS, and IMS in order to assess their relative performances. GSR was collected on fiberglass and Teflon filters using a portable vacuum sampler. Collected samples were solvent extracted, centrifuged or filtered and evaporated. GC-TEA was found to offer a good level of sensitivity for

organic compounds in GSR. However, the sensitivity for nitroglycerine (NG) compared to dinitrotoluene (DNT) was low and was attributed to the on-column thermal decomposition of NG. The sensitivity for GC-MS was at least one or two orders of magnitude lower than GC-TEA. On the other hand, IMS had comparable sensitivity for organic GSR.

Zeichner et al. [133] investigated the potential of analyzing both inorganic and organic components of GSR by first utilizing scanning electron microscopy/energy dispersive X-ray spectroscopy (SEM-EDX) for inorganic GSR and then GC-TEA and IMS for organic GSR. The GSR samples were collected from the suspect's body or clothing using double-sided adhesive stubs. The collected GSR on the adhesive stub was extracted with a solution containing 80% v v⁻¹ aqueous solution of 0.1% w v⁻¹ sodium azide and 20% v v⁻¹ ethanol by sonication at 80°C for 15 min. The residues from the first extraction were then extracted with methylene chloride and concentrated. One major drawback of this combined analysis was its low extraction efficiency (30%–90%) for NG and DNT.

Although GC is compatible with a majority of the compounds in Table 30.3, some compounds cannot be analyzed by this system for various reasons. For example, nitrocellulose (NC) is not compatible with GC because it is insufficiently volatile. Similarly, nitrate esters, a common GSR constituent, are incompatible with GC due to their poor thermal stability.

Another interesting application of GC with forensic implication in GSR analysis is the estimation of time since discharge from the firearm and spent cartridges. This application utilizes SPME to sample for volatile organic compounds (VOCs) inside the barrel of the firearm and cartridge case followed by analyzing the extract by GC-TEA, GC-FID, or GC-MS. Estimation of time since last discharge is based on the assumption that the dissipation rate of VOCs from the firearm and the cartridge case is a function of time [134–138]. Goudsmits et al. developed a

method capable of analyzing both organic and inorganic GSRs from a single sample. GSR samples are collected using an adhesive carbon aluminum stub. The organic portion is analyzed by SPME-GC-MS and the inorganic components by SEM-EDX [139]. Tarifa et al. developed a fast detection and characterization of organic and inorganic GSRs collected from the hand of suspects by capillary microextraction of volatiles followed by GC-MS analysis [140].

30.7 Analysis of forensic trace evidence

Forensic trace evidence includes both microscopic and macroscopic physical evidence that is left behind at a crime scene by the perpetrator, which can link him/her to the scene. Hairs, fibers, paint, soil, polymeric materials, glass, and impressions are among commonly encountered trace evidence. Trace evidence is often evaluated by visual and microscopical means to assess their physical characteristics to obtain a potential match with the suspect. When chemical analysis of the trace evidence is inevitable, GC is among a few analytical techniques utilized to aid in establishing a possible associative relationship with the suspect. Although pyrolysis-gas chromatography/mass spectrometry (py-GC-MS) has been considered as the gold standard for organic trace analysis, GC-MS is also used quite frequently. Synthetic polymeric materials, e.g., polyurethane foam [141], automobile body fillers and paints [142–144], and spray paints on plasters [145], are routinely analyzed by py-GC-MS. Trace evidences, e.g., fragments of photocopied paper [146], amino acids in fingerprint residues [147], and condom lubricants for sexual assault cases [148], are also analyzed by py-GC-MS. Verification of the authenticity and integrity of written documents is carried out by analyzing the ink from the questioned document. This analysis may be performed either by thermal desorption of ink volatiles followed by GC-MS (Fig. 30.3)

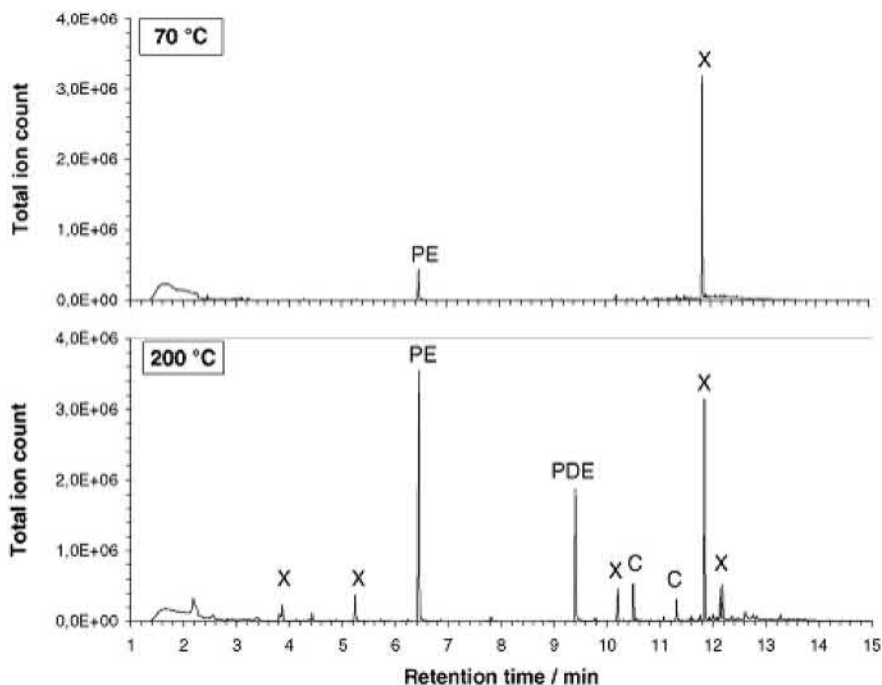


FIGURE 30.3 Chromatogram obtained for age determination of ballpoint pen ink by thermal desorption gas chromatography–mass spectrometry. Reprinted with permission from Reference J.H. Bugler, H. Buchner, A. Dallmayer, *Age determination of ballpoint pen ink by thermal desorption and gas chromatography-mass spectrometry*, *J. Forensic Sci.*, 53 (2008) 982–988; Copyright 2011, Elsevier Science.

[149,150] or by SPME of extractable volatiles from the ink sample and subsequent analysis by GC-MS [151]. Yang et al. have developed a new method using py-GC-MS to quantify vehicle paint components containing polystyrene [152].

30.8 Forensic environmental analysis

The primary motivation behind developing and applying environmental forensic methodologies in the United States originated from the need to determine the environmental liability of a suspected individual/group or business entity in response to a specific law. Most common laws passed in order to safeguard the

environment include Comprehensive Environmental Response Compensation and Liability Act (CERLA) and Resource Conservation and Recovery Act (RCRA). Environmental forensics is a very broad field and is growing rapidly with the advent of numerous sophisticated instrumental and mathematical techniques that help in determining the extent of environmental pollution, as well as to ascertain the source(s) for potential legal action. GC is an invaluable tool in many areas of environmental forensics, including analysis of pesticides, polychlorinated biphenyls (PCBs), dioxins and furans, polycyclic aromatic hydrocarbons (PAHs), and automobile gasoline. Fingerprinting of crude oil and refined products is another major area that relies upon GC.

30.8.1 Analysis of pesticides

Pesticides are chemical agents used to destroy or control pests. Common pesticides include organochlorines, organophosphates, carbamates, pyrethroids, photosynthesis inhibitors, dithiocarbamates, and benzimidazoles. Pesticides and their degradation products are analyzed from different complex matrices, e.g., soil, water, and biological tissue, to determine their concentration and fate in the environment, as well as to study exposure and ecological effects [153]. Forensic samples for pesticide analysis often undergo LLE and liquid–solid extraction. Solid samples are generally treated with sodium sulfate to eliminate moisture followed by extraction with methylene chloride using Soxhlet extraction, ultrasonic extraction, or other suitable extraction techniques. Extracted samples are then subjected to cleanup procedures to reduce matrix interferences, which eventually helps with detecting and quantifying the target analyte(s). Cleanup processes include gel permeation chromatography, adsorption on solid adsorbents, and adsorption on charcoal. Depending upon the target pesticides, different gas chromatographic detectors are employed. For example, organochlorine pesticides and phenoxy acid herbicide are analyzed by GC-ECD, organophosphate pesticides by GC-FPD, and organonitrogen pesticides by GC-NPD. In addition to that, mass spectrometry is widely used for its capability to detect pesticides and provides valuable structural information [154].

30.8.2 Analysis of polychlorinated biphenyls

PCBs belong to the list of persistent organic contaminants, which, once released into the environment, remain intact for an exceptionally long time by resisting photolytic, chemical, and biological degradation. Due to their widespread use in transformers and condensers as dielectrics,

as well as in glues, dyes, and construction materials as additives, along with other industrial applications, their presence in the environment is ubiquitous. PCBs are highly toxic. The danger of PCBs is synergized with the presence of polychlorinated dibenzodioxines (PCDDs) and polychlorinated dibenzofurans (PCDFs). About 209 congeners of PCBs have been enormously challenging to detect and identify. GC is routinely used for analyzing PCBs, with ECD and MS being the preferred detectors. For identification of individual PCB congeners, MS is used [155]. Due to the high number of PCB congeners, as well as matrix interferences, coelution is always a problem. Tandem mass spectrometry (MS/MS) may also be used for separating coeluting congener pairs, which are not separated by GC-MS. Parallel GC may be used to accomplish a better separation among closely eluted PCB congeners. Two chromatographic columns with different stationary phases (DB-1 and DB-XLB) are attached in parallel to the GC inlet. The analytes are detected by two ECD detectors connected to the other ends. Such a technique reduces the separation time significantly for critical congeners [156]. Multidimensional GC is a viable alternative where separation of closely eluted PCB congeners is required [157]. Fingerprinting of PCBs in environmental samples is also possible using GC × GC-TOFMS [158].

30.8.3 Analysis of dioxins and furans

Dioxins (polychlorinated dibenzo-*p*-dioxins) and furans (PCDFs) are among the most toxic compounds reported. Dioxins and furans have structural similarities; both are planar compounds containing chlorine-substituted benzene rings connected by one (furan) or two (dioxin) oxygen [159]. Furan and dioxin may have as many as 75 and 135 congeners, respectively. Due to the complex nature of environmental samples, different sample preparation techniques are employed based on the availability

and the nature of the sample in order to reduce matrix interferences and preconcentrate the analytes. Major sample preparation techniques include Soxhlet extraction, ASE, MAE, and SPE.

GC-HRMS is considered the gold standard being the only acceptable detector, per several US Environmental Pollution Agency (US EPA) methods [160]. GC-MS is also used frequently. Other gas chromatographic techniques commonly used in dioxin and furan analysis are large volume injection GC-MS/MS [161], fast GC-TOFMS [162], GC \times GC-TOFMS [163], and GC \times GC-ECD [164].

30.8.4 Analysis of polycyclic aromatic hydrocarbons

PAHs represent a large class of organic compounds containing two or more fused aromatic rings. PAHs are ubiquitous environmental pollutants and are commonly found in air, soil, sediment, and water samples [165]. PAHs can originate from either natural source (diagenesis of organic material and biosynthesis by plants and animals) or anthropological sources (combustion of fossil fuels, refuse burning, and automobile exhaust). Hundreds of PAHs have been identified, many of which are known or suspect carcinogens. PAHs can enter into the environment on local, regional, and a global scale. Environmental forensic scientists often deal with the challenging tasks of (1) chemical profiling of PAHs, (2) determining the potential source types, (3) determining the specific source(s) of PAHs from many possible candidates, and (4) allocating fractions of the PAHs to the suspected source(s).

Since PAHs can originate from both natural and anthropological sources, establishing a scientifically sound association between the PAHs extracted and identified from a study area and a suspected source requires a combination of robust analytical techniques as well as advanced statistical tools.

Considering the enormous challenges involved in isolating PAHs from different overly complicated environmental matrices, the US EPA has developed multiple analytical methods for different environmental matrices, e.g., drinking water, municipal and industrial discharges, soils, sludge, solid waste, and ambient air [166]. Each method has been designed to provide particular information regarding the PAHs or volatile/semivolatile organic compounds present in the sample matrix, as well as to address sample preparation issues, as oftentimes sample preparation is needed to preconcentrate the PAHs, eliminate, or reduce the matrix interferences before it can be introduced into GC. EPA Method 610 applies to 16 priority pollutants, which are known to be of high risk for human health [167]. Due to the combined advantages of high selectivity, resolution, and sensitivity for PAH analysis, GC finds itself favorable over LC. As such, GC-FID and GC-MS are considered as the workhorse in PAHs analysis. Due to the presence of a high number of PAHs, structurally similar to each other in environmental samples, careful selection of a GC column is of high importance if complete separation of each PAH is a goal. Methyl and phenyl-substituted polysiloxane stationary phases are the most common stationary phases for PAH analysis [168]. GC-TOFMS is recommended for complex samples as TOF-MS offers better structural conformations, as well as signal-to-noise ratios [169]. When a complete separation of all PAHs is critical for the investigation, GC \times GC with FID, MS, or TOF-MS should be considered [170]. Sources of the origin of environmental PAHs can be established by employing GC-IRMS, which enables the calculation of compound-specific carbon isotope ratios ($^{13}\text{C}/^{12}\text{C}$) of individual PAHs to trace back the origin of that particular PAH [171].

In addition to the techniques mentioned earlier, large-volume injection using PTV for increased sensitivity [172], fast GC (approximately 3 min

total analysis time) [173], and LC-GC-MS [174] have been used as well to analyze PAHs from environmental samples.

30.8.5 Fingerprinting of crude and refined petroleum

Crude and refined petroleum fingerprinting is a globally adopted technique aimed at determining an oil source by matching the collected samples with the suspected candidate sources and includes differentiating the background hydrocarbons with the alleged spilled oil,

monitoring the changes in composition of the spilled oil over time, and assessing the impact on the ecosystem in order to impose monetary liability to the responsible entity. Due to the chemical makeup of the crude and refined petroleum (predominantly hydrocarbons), GC is considered the gold standard for petroleum fingerprinting. GC-FID is frequently used in preliminary screenings of environmental samples. Fig. 30.4 represents a decision tree that is often used in a typical environmental laboratory to process suspected oil-spill samples [175].

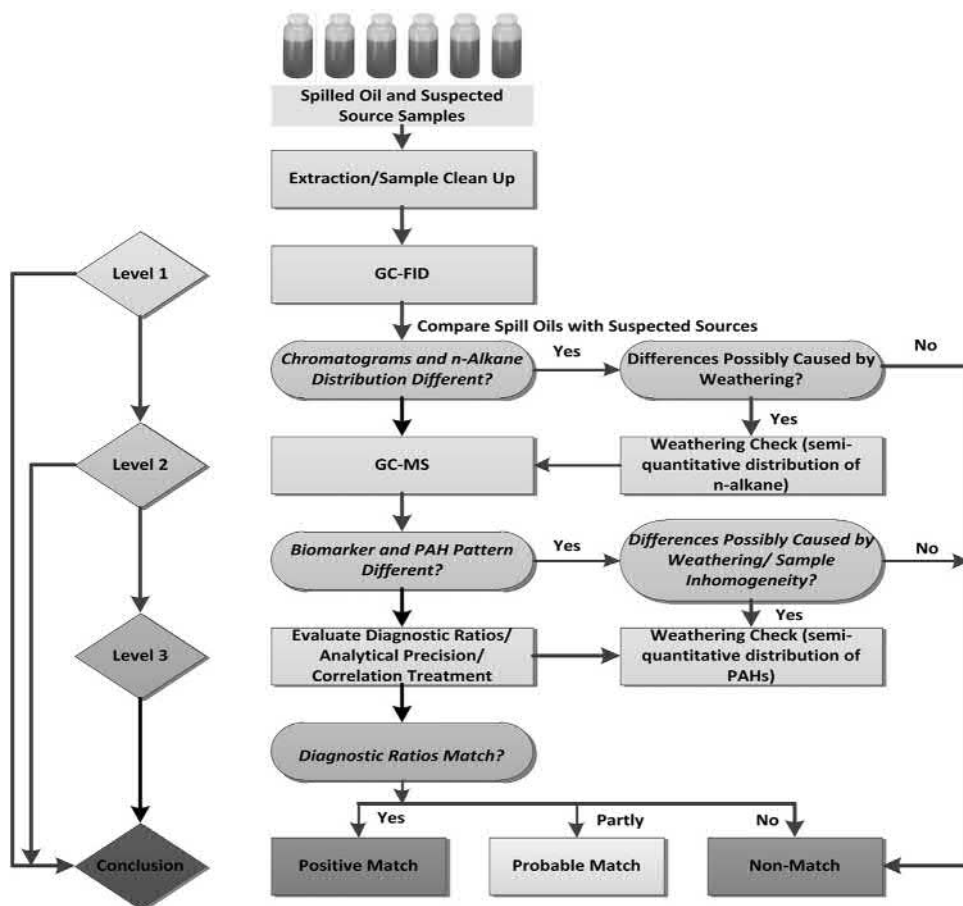


FIGURE 30.4 Decision chart used in oil-spill identification. Adopted with permission from Reference Z.D. Wang, M.F. Fingas, *Development of oil hydrocarbon fingerprinting and identification techniques*, *Mar. Pollut. Bull.* 47 (2003) 423–452; Copyright 2011, Elsevier Science.

Identification and quantification of an individual compound in the sample matrix are carried out by GC-MS [176,177], py-GC-MS [178], comprehensive GC \times GC coupled to high-resolution TOFMS [179], and GC coupled with triple quadrupole mass spectrometry in multiple reaction monitoring (MRM) mode (GC-MS/MS) [180]. Oftentimes, GC-IRMS is employed to obtain information regarding geographical origin of the spilled oil by calculating isotope ratios of selected elements. When environmental samples are found overly complex with many coeluted compounds, GC \times GC in combination with different detectors, e.g., FID [181,182], TOFMS [157], NCD, sulfur chemiluminescence detector (SCD) [183], atomic emission detector (AED) [184], and MS [185] may be employed.

30.9 Analysis of human odor profile

In recent years, research on the analysis of human odor profile has garnered a great deal of interest among forensic chemists [186–196]. Human odor has been reported [186,188,197] as being a unique characteristic of an individual and an individualistic parameter potentially useful as a biometric identifier similar to that of a fingerprint.

Human odor is believed to be the product of body's metabolism, hormones, gland secretions, and bacterial interactions [198]. It consists of a range of VOCs, e.g., aldehydes, ketones, aliphatic and aromatic hydrocarbons, fatty acids, and carboxylic acid methyl esters. An individual odor profile is dependent upon several factors, e.g., genetic makeup, environmental and physiological conditions, age, and sex, and can be classified as primary, secondary, and tertiary odor [186]. Primary odor contains VOCs that are characteristic to an individual and is stable over time regardless of diet or environmental factors (surroundings). Secondary odor consists of VOCs that originate from within the body similar to primary odor, but is functionally

related to diet and various environmental factors. Tertiary odor contains VOCs that originate from outside sources (e.g., cosmetics, lotions, perfumes, and smoke). From a forensic viewpoint, human odor collection is of primary interest to law enforcement officers because it can be collected from evidence and then subsequently provided to scent-discriminating canines where they can compare the collected scent to the scent left at a crime scene [187,199].

GC is the most common technique used in human odor research. Due to the low concentration of compounds present in human odor, a sample preparation technique is required to preconcentrate the analyte(s) prior to GC-MS analysis. A detailed summary of human skin volatiles and different approaches for their sampling was provided by Dormont et al. [193]. SPME [186,200–203], SBSE [204], sorption on solid sorbents [190,205,206], and solvent extraction [207] have been reported as a sample preparation/preconcentration techniques, with SPME being the most popular. Some researchers [187] collect human odor on selected sorbent materials (e.g., cotton, polyester, rayon, and blend fabrics) by placing the collection material in between the palms of the hands allowing the material to remain in contact with the palms for a predefined time. The collection materials are then immediately enclosed in a glass vial in order to equilibrate the collected odor with the headspace inside the enclosed vial. Human odor compounds are then extracted onto an SPME fiber and introduced into the inlet of the GC where the VOCs are thermally desorbed onto the column. Some researchers [194,199] have implemented a specially designed sampling tool known as a Scent Transfer Unit 100 (STU-100). STU-100 is a device that produces a dynamic airflow and is comprised of a vacuum pump and a scent collection head to hold the sorbent media (most often, a piece of cotton gauze) on the surface so that odor can be collected without coming into direct contact with the evidence (or palms of the hands). The airflow speed of this

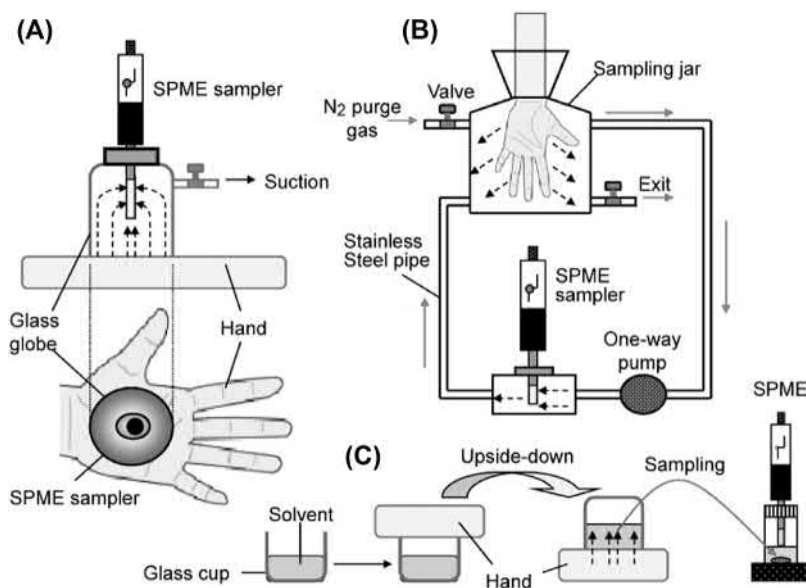


FIGURE 30.5 Illustration of hand odor sampling and preconcentration using solid-phase microextraction (SPME). (A) Direct SPME in sealed glass globe, (B) direct SPME in flow sampling chambers, and (C) liquid sampling in glass cup. *Reproduced with permission from Reference H. Kataoka, K. Saito, Recent advances in SPME techniques in biomedical analysis, J. Pharmaceut. Biomed. Anal. 54 (2011) 926–950; Copyright 2011, Elsevier Science.*

instrument can be adjusted, which will influence the accumulation of VOCs on the sorbent media. Additionally, time for odor collection, sorbent media, and the distance between the STU-100 and the object of interest can be optimized in order to achieve the desired odor collection efficiency. Upon scent collection, the sorbent is then stored in a vial so that SPME can be performed and subsequently analyzed using GC-MS. In addition, instead of collecting odors on the surface of sorbents, SPME of VOCs emanating from the hand can be directly carried out by placing a sealed glass globe on the palm to enclose the extraction surface [207], or by enclosing the hand in a sampling chamber [201] where a continuous and steady nitrogen gas flow carries the human odor to the SPME fiber for preconcentration. Another approach for hand odor collection is to wash the hands with a solvent (water) to transfer the VOCs into the solvent. The solvent containing the washed-hand

odor compounds is then analyzed by SPME-GC-MS. This approach is recommended for extracting more polar and less volatile compounds (Fig. 30.5.) [208].

Considering the broad polarity range of human volatile compounds, a single GC column may not be sufficient to separate all the compounds. As such, Choi et al. presented a method combining SPME with separation in GC columns connected in parallel followed by MS identification. In total, 574 compounds were identified in a sweat sample [209]. Hand odor samples may be analyzed by comprehensive GC \times GC-MS and subjected to Bayesian Hypothesis Testing that provides a probability estimate as to whether two odor samples originated from the same person [210].

Human scent evidence collected from objects at crime scenes is often quickly presented to human scent canines in order to identify a criminal from a pool of suspects. Hudson et al. [195]

studied the stability of human scent collected on a pretreated cotton sorbent. Cotton material retaining human scent volatiles was subjected to moderate to extreme environmental conditions (room temperature, -80°C , dark, UV light) for a period. SPME-GC-MS analysis was used to monitor the change in retaining human scent. The results revealed that the scent profile changed with time, with the maximum changes occurring within the first 3 weeks.

Different human scent collection media (cotton, cotton blend, and natural and synthetic composite materials) have also been tested to evaluate their capability for retaining human scent volatile compounds [195,199,211]. Commercial sorbent materials were found to contain volatile compounds that were recognized as being human scent compounds. Therefore, these materials require effective cleaning prior to human scent collection. Supercritical fluid extraction, subcritical water extraction, Soxhlet extraction, and steam sterilization were investigated to identify the best extraction method to clean the sorbent media. Headspace SPME-GC-MS of the sorbent media before and after the cleaning demonstrated that supercritical fluid extraction outperformed all the other extraction methods [211].

30.10 Analysis of human decomposition products

Within the last several years, there has been increased interest in the decomposition process, in particular the evolution of VOCs, in both human and animal. Research has been conducted on the chemical processes that occur during the decomposition process, as well as identifying biomarker(s) that may aid in estimating the postmortem interval with high precision [212–220]. Some research groups have also engaged in developing advanced techniques to uncover buried human remains from clandestine graves.

Human remains and their analogues (often used as an investigational sample matrix) are extremely complex, and when they decompose the proteins, lipids, and carbohydrate macromolecules that are found within the body breakdown producing VOCs with a range of functional groups, such as aldehydes, ketones, sulfur-containing compounds, nitrogen-containing compounds, hydrocarbons, carboxylic acids, just to name a few.

The human body differs in composition (different protein/fat ratio) in comparison to human cadaver analogues. As a result, obtaining a representative sample from a decaying body is quite challenging. Sampling and sample preparation for human remains are mostly dependent upon broad objectives of study, which are, in general, classified into the following categories: (1) estimating the postmortem interval, (2) understanding the complex decomposition pathways, including the impact of different environmental and geochemical factors on the decomposition process, as well as the decomposition products at various stages, (3) developing human remains detector canine training aids to train them without handling hazardous materials, and (4) assessing the environmental impacts on the decomposition process.

Research on human remains volatiles is largely reliant on GC-MS [143]. However, comprehensive GC \times GC-TOFMS is steadily replacing conventional GC-MS owing to its unambiguous advantages of increased sensitivity and additional peak capacity [212,214,215,218,220–223].

30.10.1 Estimation of postmortem interval (PMI)

There are research groups that are focusing on identifying suitable biomarker(s) that could be used to estimate the postmortem interval of a deceased individual with high precision. Such a biomarker would not only minimize the

possibility of human error, but also aid in providing a more reliable and precise means for the estimation of the postmortem interval.

Among other analytes, amino acids, putrescine, and cadaverine were reported in some human remains studies [224]. Target analytes were extracted from human remains sample in an EDTA buffer solution. After extracting the analytes from the human remains samples, the extract was subjected to drying followed by derivatization. Analysis of amino acids was carried out by derivatizing a fraction of dried extract using pyridine and MTBSTFA. On the other hand, cadaverine and putrescine were analyzed after derivatization with pyridine and methyl-8 (DMF dimethyl acetal).

30.10.2 Characterization of decomposition products

The decomposition process begins immediately after death and may continue for years depending upon the environmental conditions and surroundings in which the body is placed [225]. One of the major decomposition products is adipocere, a white soap-like material consisting of saturated fatty acids, unsaturated fatty acids, triglycerides, hydroxyl fatty acids, and other minor ingredients [226]. Formation of adipocere can be affected by environmental conditions, including temperature, pH, and microbial activity. Characterization of adipocere provides valuable information pertaining to the state of decomposition of the body, as well as to assess the impact of the burial environment on the decomposition process. Characterization of adipocere involves both identification and quantification of its individual constituents, and GC-MS is most often used for this purpose. Oftentimes, adipocere is extracted from soil samples by solvent extraction using chloroform, hexane, or another suitable organic solvent. Due to the high polarity of the majority of the adipocere constituents, derivatization is required prior to GC-MS. Hexamethyldisilazane (HMDS) [227]

and *N,O*-bis(trimethylsilyl)trifluoroacetamide BSTFA [226] are commonly used derivatizing reagents. Free fatty acids (FFAs) can be isolated from adipocere by SPE using disposable cartridges [228]. The extracted FFAs are then derivatized for GC-MS analysis. GC-IRMS can be used to obtain $\delta^{13}\text{C}$ values. The $\delta^{13}\text{C}$ values ($\Delta^{13}\text{C}_{18.0-16.0}$) are characteristic of an individual and can be used in combination with other information to aid in identifying decomposing remains [229].

Formation of VOCs is an integral part of the decomposition process. During the course of decomposition a variety of VOCs are produced. For example, carbohydrates produce oxygen-rich compounds, including alcohols, aldehydes, ketones, acids, esters, and ethers; proteins yield nitrogen-, sulfur-, and phosphorous-containing compounds; lipids break down into hydrocarbons, nitrogen-, phosphorous-, and oxygen-containing compounds. VOCs are often collected from decomposing remains using different solid sorbents (Carbograph, Carbosieve, Carbotrap, Carbosieve S-III, and Carbotrap-C) [224,230]. After collecting the volatiles on the sorbent tubes for a predetermined time, the analytes are thermally desorbed and analyzed by GC-MS. Vass et al. demonstrated that air sampling followed by GC-MS of carpet samples and other parts of a vehicle can be utilized to confirm the presence of human decomposition products even though the remains are no longer present [231].

Human remains detection canines are often trained using tissue, blood, bone, and decomposition fluids, which are biohazardous and difficult to obtain. Attempts have been made to identify key odor-producing constituents from decomposing remains to produce nonhazardous canine training aids [199,232]. Due to lack of easy access to human remains, cadaver detection dogs are often trained using pig remains as an alternative training aid. Knobel et al. compared the VOCs emanated from four human cadavers and four pig carcasses using comprehensive GC \times GC-TOFMS. The results demonstrated

substantial variations in the composition and VOC profile of pig and human remains. This finding will encourage revisiting the justification of using porcine-based training aid for cadaver detection dogs [212]. Cadaver dogs are frequently used to locate human remains on land and in water with a presumption that human remains on land and in water would emanate same VOCs, regardless of the depositional environment. Irish et al. studied the VOC profile released by whole porcine cadavers deposited on the surface and submerged in water using SPME-GC-MS. The cadavers on the land provided 70 identifiable VOCs, whereas the cadavers submerged in water provided 40 identifiable VOCs in the headspace. This study highlighted the necessity to accommodate the stark difference in the VOC profile due to the depositional condition so that the cadaver dogs do not fail to locate the dead body of a missing person [213]. A noncontact sampling instrument is shown in Fig. 30.6 [196].

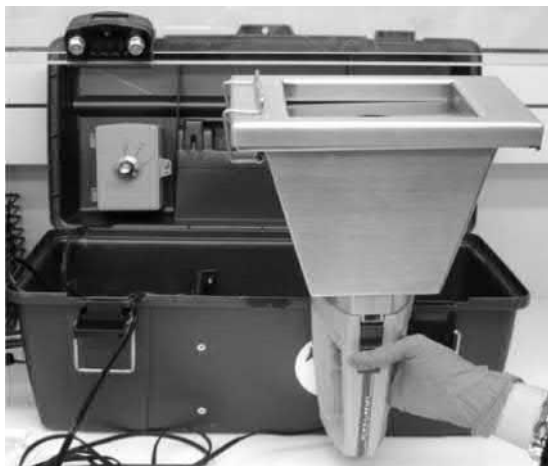


FIGURE 30.6 A noncontact sampling device used for collecting VOCs from human remains. Reprinted with permission from Reference P.A. Prada, A.M. Curran, K.G. Furton, *The evaluation of human hand odor volatiles on various textiles: a comparison between contact and noncontact sampling methods*, *J. Forensic Sci.* 56 (2011) 866–881; Copyright 2011, Elsevier Publications.

SPME is employed to extract VOCs from cotton gauze pads that were used to collect odor from decomposing remains and then analyzed by GC-MS. Alumina-coated porous-layer open-tubular (PLOT) columns were used to analyze ninhydrin-reactive nitrogen (NRN) compounds collected from the headspace air above grave soil [233].

30.11 Field-portable gas chromatograph for onsite sample analysis

Following September 11, 2001, the demand for portable and rapid field-deployable gas chromatographic systems that are capable of detecting lethal, hazardous, and toxic chemicals, such as chemical warfare agents (CWAs) and toxic industrial chemicals (TICs), has increased significantly. Since then, a number of portable and rapid field-deployable gas chromatographic systems have emerged, each of which has its own characteristic properties.

Lewis et al. [234] developed a microfabricated planar gas chromatograph using two chemically etched 95×95 mm glass substrates sandwiched together resulting in a 7.5 m-long capillary channel. The channel was coated with a nonpolar PDMS stationary phase. A standard FID and a modified lightweight photoionization detector (PID) served as the detector for the miniaturized planar GC. Test mixtures containing selected VOCs demonstrated detection sensitivity at the subnanogram level for monoaromatics.

Man-portable fast gas chromatographs coupled with a TOFMS (GC-TOFMS) have been developed. These instruments have low power consumption, high speed, a quadrupole ion trap TOFMS, and are lightweight (30 lbs.). These field-portable systems can screen a sample rapidly by photoionization MS or full-scale confirmatory analysis using GC-MS in the EI mode. Such a system can be conveniently deployed in the field for detecting hazardous chemicals including CWAs [235].

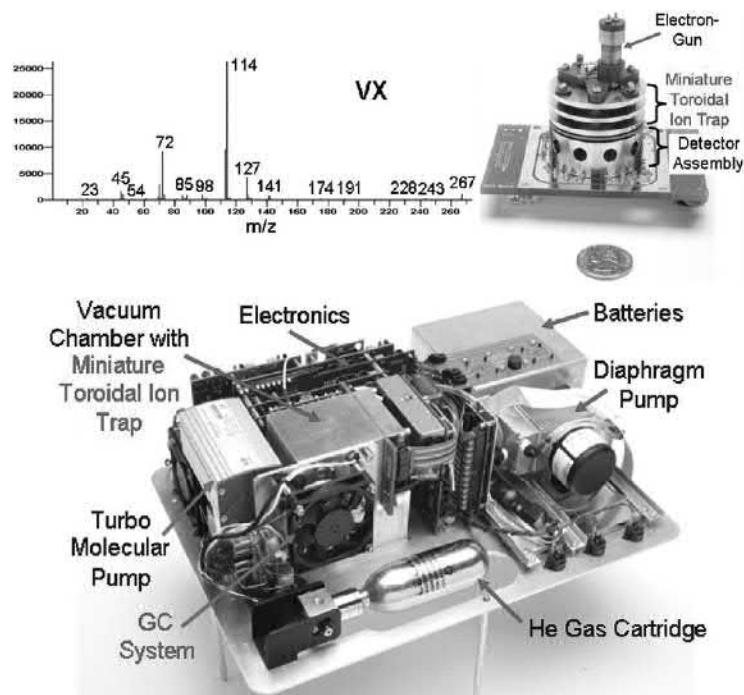


FIGURE 30.7 Internal components of portable Guardion-7 gas chromatograph–toroidal ion trap mass spectrometer (GC-TMS). Reproduced with permission from Reference J.A. Contreras, J.A. Murray, S.E. Tolley, J.L. Oliphant, H.D. Tolley, S.A. Lammert, E.D. Lee, D.W. Later, M.L. Lee, *Hand-portable gas chromatograph-toroidal ion trap mass spectrometer (GC-TMS) for detection of hazardous compounds*, *J. Am. Soc. Mass Spectrom.* 19 (2008) 1425–1434; Copyright 2011, Elsevier Science.

GC-IMS-MS was shown to decrease the false-positive rates for explosives in comparison to a stand-alone conventional IMS device. In addition, GC-IMS-MS has the capability of detecting TNT, RDX, HMTD, and TATP even in the presence of highly concentrated interferences and is considered a good candidate for field deployment [119].

Modifying commercially available HAPSITE Smart GC-MS system, Fair et al. [236] enhanced its capability for rapid sampling and onsite analysis of VOCs at low parts per billion concentration (ppb). The modifications include the addition of a Tenax microtrap concentrator between the GC inlet and the column. A GC- μ FID system was developed [237] to cater to identification of environmental contaminants from polluted water in conjunction with SPME.

Focusing on the capability of detecting CWAs and TICs, a hand-portable GC coupled with a toroidal ion trap mass spectrometer (GC-TMS) that operates on batteries was developed (Fig. 30.7). The system uses SPME for sample collection and introduction into the GC, thereby enabling it to handle target analytes from both air and water matrices [238]. Lam et al. developed a portable GC-MS capable of identifying hazardous organic compounds in air and water at fire scenes [239].

30.12 Gas chromatography in food forensics

Food forensics is an emerging discipline that focuses on determining authenticity, adulteration,

and safety of foodstuffs to protect consumer's safety and well-being and to enforce food-related laws. Unlike other forensic fields, food forensics has broader implications on the personal level as it is designed to safeguard what we eat or drink. Although food authenticity is primarily determined by various methods based on DNA analysis, proteomics, and metabolomics, the use of GC is also a common practice.

In response to the report of melamine-tainted Chinese infant formula, which allegedly inflicted severe adverse health effects in babies, a confirmatory GC-MS method was developed to confirm the presence of melamine in cow milk (CM) and milk-based powdered infant formula [240]. Melamine was extracted from milk-based infant formula using SPE and derivatized using BSTFA-TMCS (99:1 v v⁻¹). A low LOD (0.009 mg kg⁻¹), high recovery (95%–101%), and fair reproducibility were indicative of the method's performance for confirming melamine in the selected matrices.

Olive oils are often subjected to adulteration and if the adulterant is similar in nature (e.g., hazelnut oil in virgin olive oils), then determining authenticity of the claimed substance is challenging. L. Cercaci et al. [241] developed a method that combines SPE, thin-layer chromatography, and GC to confirm the authenticity of virgin olive oil by recognizing the presence of hazelnut in the tested sample. The method was built on the principle that authentic virgin olive oils possess a unique value range of an esterified sterol fraction known as the Mariani ratio (R_{MAR}), which is significantly different in adulterated samples. An SPE silica cartridge was used to separate esterified sterols from the oil sample. The adsorbed analytes were eluted first in n-hexane and then by a mixture of n-hexane and diethyl ether (8:2 v v⁻¹). Both the fractions were then combined, dried, and subjected to cold saponification. The unsaponifiable fraction was fractionated on a silica TLC plate, which extracted the sterol band, and then derivatized with a mixture of pyridine, HMDS,

and trimethylchlorosilane (TMCS) prior to GC-MS analysis. The study suggested that calculating the Mariani ratio of any suspected oil by GC-MS might provide reliable information about its authenticity.

U.S. Food and Drug Administration's Forensic Chemistry Center received 25 cases during 1992–2004 involving the tampering of beverage products, infant formula, and raw meat, with bleach. Exposure to bleach may cause serious physical damage to the consumer. Jackson et al. [242] developed a method to detect bleach in beverages by headspace GC-FID based on the formation of chloroform. Chloroform is produced in an aqueous solution of sodium hypochlorite and is easily detected by GC-FID.

Other interesting applications of GC with forensic significance include recognition of beer brand [243], determination of the geographic origin of Emmental cheese [244], and investigating the adulteration of wine by GC-IRMS [245].

30.13 Analysis of chemical warfare agents (CWAs)

A chemical warfare/weapon agent (CWA) is a substance intended for use in military operations to kill, seriously injure, or incapacitate the enemy because of its physiological effects. CWAs are classified into four major classes based on their functional characteristics: (1) nerve agents, (2) blister agents, (3) blood agents, and (4) choking agents. Table 30.4 describes the classification and characteristics of major CWAs. Recent development in monitoring CWAs and their degradation products was summarized by Valdez et al. [246].

Nerve agents have a short life span and are readily hydrolyzed under environmental conditions to stable degradation products, e.g., alkylphosphonic acids (APAs). A rapid and reliable GC method is necessary to screen and identify the presence of APAs. Although LC-MS can be

TABLE 30.4 List of chemical warfare agents (CWAs) and their characteristics.

List of chemical warfare agents		
Agent classes	Example	Characteristics
Nerve agents	Tabun (GA) Sarin (GB) Soman (GD) Cyclosarin VX	Attack nervous system. Can enter body through inhalation or skin
Blister agents	Mustard gas Lewisite	Attack skin. Rapidly absorbed into skin
Choking agents	Phosgene chloropicrin Chlorine	Attack respiratory track
Blood agents	Hydrogen cyanide Cyanogen chloride	Attack blood circulatory system

used for this purpose, it is not compatible with mobile laboratories utilized for onsite testing. Subramaniam et al. [247] addressed this problem by developing a fast, only 5 min, for sample preparation before GC-MS using negative chemical ionization. Sample preparation included derivatization with a new reagent 1-(diazomethyl)-3,5-bis(trifluoromethyl)benzene. Plausible forensic signatures can be obtained by impurity profiling of chemical weapon precursors using comprehensive GC \times GC-TOFMS [248]. Eyison et al. developed a rapid method using SPE followed by GC-MS/MS to monitor 1,1' sulfonylbis [2-(methylthio) ethane] (SBMTE), a biomarker of sulfur mustard exposure. The method has a limit of quantification of 1 ng mL⁻¹ [249].

Sampling of potential CWAs from a suspected surface poses a great health risk. Imran et al. developed a three-layered composite wipe fabricated by laminating nonwoven polypropylene, activated carbon fabric (ACF), and aramid fabric together. Extraction efficiency, wiping efficacy, and adsorption capacity of the new sampling device were assessed using blister and nerve agent. The sampling device was effective for both porous and nonporous surfaces [250]. Terzic et al. developed a rapid method

for monitoring Lewisite in aqueous sample matrices with a LOD of ~100 ng mL⁻¹ [251].

30.14 New developments in gas chromatography with forensic implications

In addition to the continuous improvements in the GC hardware, pneumatics, electronics, control software, as well as GC column chemistries, the addition of fast GC, GC \times GC, and GC-IRMS has significantly augmented the overall analytical power that conventional GC offers to the forensic community. GC is considered the workhorse in forensic laboratories due to its ability for separating and detecting volatile and semivolatile organic compounds of forensic interests; however, it often suffers from long separation times, from typically 10 to 60 min. With the growing number of samples in forensic laboratories, faster analysis remains a pressing issue. To address such a demand, fast GC has emerged. The primary goal of the fast GC is to maintain resolving power of the column by manipulating several chromatographic parameters, e.g., column length and internal diameter; stationary phase chemistry and film thickness; carrier gas type and its linear velocity; and oven

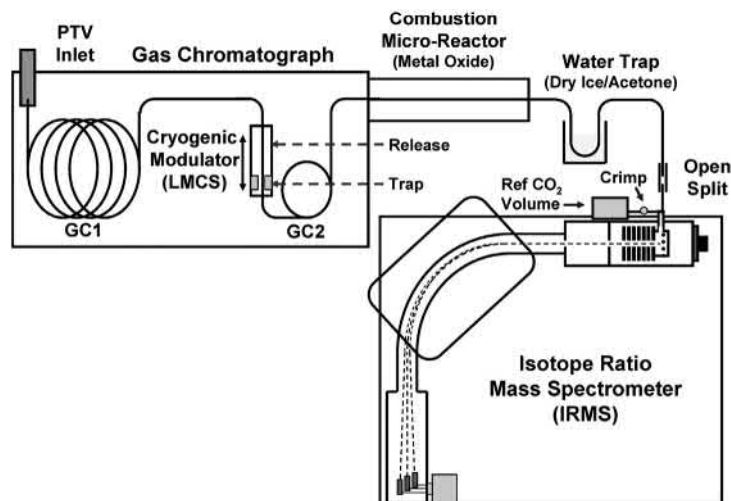


FIGURE 30.8 Schematic representation of a GC \times GCC-IRMS system. Reproduced with permission from Reference H.J. Tobias, G.L. Sacks, Y. Zhang, J.T. Brenna, *Comprehensive two-dimensional gas chromatography combustion isotope ratio mass spectrometry*, *Anal. Chem.* 80 (2008) 8613–8621; Copyright 2011, American Chemical Society.

temperature program rate. Fast GC generally uses 100 μm internal diameter columns with hydrogen as the carrier gas. A decrease of 3–10 fold is possible for the separation time without compromising resolution.

Another development in the field of GC is the advent of comprehensive GC \times GC. Samples are first separated on a nonpolar column and trapped in a modulator for reinjection as a series of short pulses on a shorter and generally polar second column. Each analyte peak is now defined by two different retention parameters. When MS is used as the detector a third dimension of information is obtained. Two recent review articles have eloquently covered recent progresses in GC \times GC-MS for forensic applications [210,252].

GC-IRMS has had a tremendous impact on forensic science [253–255]. GC-IRMS provides unique information regarding geographic, chemical, and biological origin of the analyzed sample. The underlying principle of GC-IRMS is that based on the geographic, chemical, or biological origin, samples collected can be characterized by its C, O, H, N, and S isotope ratio. As a result,

even though two samples are apparently identical, they can be discriminated from each other if they are sourced from two different geographic locations. Fig. 30.8 represents the schematic of a GC \times GC-C-IRMS instrument [256].

References

- [1] P. Esseiva, L. Gaste, D. Alvarez, F. Anglada, Illicit drug profiling, reflection on statistical comparisons, *Forensic Sci. Int.* 207 (2011) 27–34.
- [2] Lists of scheduling actions controlled substances regulated chemicals, in: U.S.D.o.J. Drug Enforcement Administration, 2020, pp. 1–91.
- [3] Z. Mehmedic, S. Chandra, D. Slade, H. Denham, S. Foster, A.S. Patel, S.A. Ross, I.A. Khan, M.A. ElSohly, Potency trends of delta 9-THC and other cannabinoids in confiscated cannabis preparations from 1993 to 2008, *J. Forensic Sci.* 55 (2010) 1209–1217.
- [4] J. Broseus, F. Anglada, P. Esseiva, The differentiation of fibre- and drug type Cannabis seedlings by gas chromatography/mass spectrometry and chemometric tools, *Forensic Sci. Int.* 200 (2010) 87–92.
- [5] Z. Muccio, C. Wockel, Y. An, G.P. Jackson, Comparison of bulk and compound-specific $\delta^{13}\text{C}$ isotope ratio analyses for the discrimination between cannabis samples, *J. Forensic Sci.* 57 (2012) 757–764.

- [6] N. Wiebelhaus, D. Hamblin, N.M. Kreitals, J.R. Almirall, Differentiation of marijuana headspace volatiles from other plants and hemp products using capillary microextraction of volatiles (CMV) coupled to gas-chromatography-mass spectrometry (GC-MS), *Forensic Chem.* 2 (2016) 1–8.
- [7] A.J. Krotulski, A.L.A. Mohr, S.L. Kacinko, M.F. Fogarty, S.A. Shuda, F.X. Diamond, W.A. Kinney, M.J. Menendez, B.K. Logan, 4F-MDMB-BINACA: a new synthetic cannabinoid widely implicated in forensic casework, *J. Forensic Sci.* 64 (2019) 1451–1461.
- [8] S. Klemenc, In common batch searching of illicit heroin samples - evaluation of data by chemometrics methods, *Forensic Sci. Int.* 115 (2001) 43–52.
- [9] R. Dams, T. Benijts, W.E. Lambert, D.L. Massart, A.P. De Leenheer, Heroin impurity profiling: trends throughout a decade of experimenting, *Forensic Sci. Int.* 123 (2001) 81–88.
- [10] M. Usman, T. Jamshaid, A. Naseer, Y. Baig, Z. Mehmood, M. Shahwar, S. Akhtar, M.T. Chaudhary, M. Sarwar, M.A. Tahir, Component analysis of illicit morphia tablets (clandestine laboratory preparation) using gas chromatography mass spectrometry: a case study, *Egypt. J. Food Sci.* 8 (2018) 5.
- [11] F.A. Idoine, J.F. Carter, R. Sleeman, Bulk and compound-specific isotopic characterisation of illicit heroin and cling film, *Rapid Commun. Mass Spectrom.* 19 (2005) 3207–3215.
- [12] M. Hida, T. Mitsui, S. Tsuge, H. Ohtani, Rapid and sensitive determination of morphine in street opium samples by thermal desorption gas chromatography using a microfurnace pyrolyzer, *J. Separ. Sci.* 27 (2004) 1030–1032.
- [13] Z.R. Roberson, H.C. Gordon, J.V. Goodpaster, Instrumental and chemometric analysis of opiates via gas chromatography-vacuum ultraviolet spectrophotometry (GC-VUV), *Anal. Bioanal. Chem.* 412 (2020) 1123–1128.
- [14] J. Eliaerts, N. Meert, F. Van Durme, N. Samyn, K. De Wael, P. Dardenne, Practical tool for sampling and fast analysis of large cocaine seizures, *Drug Test. Anal.* 10 (2018) 1039–1042.
- [15] T.R. Fiorentin, M. Fogarty, R.P. Limberger, B.K. Logan, Determination of cutting agents in seized cocaine samples using GC-MS, GC-TMS and LC-MS/MS, *Forensic Sci. Int.* 295 (2019) 199–206.
- [16] S. Locicero, P. Hayoz, P. Esseiva, L. Dujourdy, F. Besacier, P. Margot, Cocaine profiling for strategic intelligence purposes, a cross-border project between France and Switzerland - Part I. Optimisation and harmonisation of the profiling method, *Forensic Sci. Int.* 167 (2007) 220–228.
- [17] M. Chiarotti, R. Marsili, A. Moreda-Pineiro, Gas chromatographic-mass spectrometric analysis of residual solvent trapped into illicit cocaine exhibits using head-space solid-phase microextraction, *J. Chromatograph. B-Analytic. Technol. Biomed. Life Sci.* 772 (2002) 249–256.
- [18] J.R. Mallette, J.F. Casale, Headspace-gas chromatographic-mass spectrometric analysis of South American commercial solvents and their use in the illicit conversion of cocaine base to cocaine hydrochloride, *J. Forensic Sci.* 60 (2015) 45–53.
- [19] Z. Muccio, G.P. Jackson, Simultaneous identification and delta 13C classification of drugs using GC with concurrent single quadrupole and isotope ratio mass spectrometers, *J. Forensic Sci.* 56 (2011) S203–S209.
- [20] A. Shekari, M. Akhgari, F. Jokar, Z. Mousavi, Impurity characteristics of street methamphetamine crystals seized in Tehran, Iran, *J. Subst. Use* 21 (2016) 501–505.
- [21] H. Inoue, Y.T. Iwata, K. Kuwayama, Characterization and profiling of methamphetamine seizures, *J. Health Sci.* 54 (2008) 615–622.
- [22] K. Kuwayama, H. Inoue, T. Kanamori, K. Tsujikawa, H. Miyaguchi, Y. Iwata, N. Kamo, T. Kishi, Contribution of thermal desorption and liquid-liquid extraction for identification and profiling of impurities in methamphetamine by gas chromatography-mass spectrometry, *Forensic Sci. Int.* 171 (2007) 9–15.
- [23] M. Morelato, A. Beavis, M. Tahtouh, O. Ribaux, P. Kirkbride, C. Roux, The use of organic and inorganic impurities found in MDMA police seizures in a drug intelligence perspective, *Sci. Justice* 54 (2014) 32–41.
- [24] L.R. Togni, R. Lanaro, R.R. Resende, J.L. Costa, The variability of ecstasy tablets composition in Brazil, *J. Forensic Sci.* 60 (2015) 147–151.
- [25] F.M. Hauser, J.W. Hulshof, T. Rossler, R. Zimmermann, M. Putz, Characterisation of aqueous waste produced during the clandestine production of amphetamine following the Leuckart route utilising solid-phase extraction gas chromatography-mass spectrometry and capillary electrophoresis with contactless conductivity detection, *Drug Test. Anal.* 10 (2018) 1368–1382.
- [26] K. Kanai, K. Takekawa, T. Kumamoto, T. Ishikawa, T. Ohmori, Simultaneous analysis of six phenethylamine-type designer drugs by TLC, LC-MS, and GC-MS, *Forensic Toxicol.* 26 (2008) 6–12.
- [27] G. Frison, L. Zamengo, F. Zancanaro, F. Tisato, P. Traldi, Characterization of the designer drug deschloroketamine (2-methylamino-2-phenylcyclohexanone) by gas chromatography/mass spectrometry, liquid chromatography/high-resolution mass spectrometry, multi-stage mass spectrometry, and nuclear magnetic resonance, *Rapid Commun. Mass Spectrom.* 30 (2016) 151–160.

- [28] A.A. Grove, E.R. Rohwer, J.B. Laurens, B.C. Vorster, The analysis of illicit methaqualone containing preparations by gas chromatography-mass spectrometry for forensic purposes, *J. Forensic Sci.* 51 (2006) 376–380.
- [29] D. de Boer, W.P.J. Goemans, V.R. Ghezavat, R.D. van Ooijen, R.A.A. Maes, Seizure of illicitly produced para-fluorofentanyl: quantitative analysis of the content of capsules and tablets, *J. Pharmaceut. Biomed. Anal.* 31 (2003) 557–562.
- [30] S.M. Song, P. Marriott, P. Wynne, Comprehensive two-dimensional gas chromatography-quadrupole mass spectrometric analysis of drugs, *J. Chromatogr. A* 1058 (2004) 223–232.
- [31] M. Schaffer, T. Groger, M. Putz, S. Dieckmann, R. Zimmermann, Comparative analysis of the chemical profiles of 3,4-methylenedioxymethamphetamine based on comprehensive two-dimensional gas chromatography-time-of-flight mass spectrometry (GCxGC-TOFMS), *J. Forensic Sci.* 57 (2012) 1181–1189.
- [32] M. Praisler, I. Dirinck, J. Van Boclaer, A. De Leenheer, D.L. Massart, Pattern recognition techniques screening for drugs of abuse with gas chromatography-Fourier transform infrared spectroscopy, *Talanta* 53 (2000) 177–193.
- [33] R. Martino, M. Malet-Martino, V. Gilard, S. Balayssac, Counterfeit drugs: analytical techniques for their identification, *Anal. Bioanal. Chem.* 398 (2010) 77–92.
- [34] K. Soltaninejad, M. Faryadi, M. Akhgari, L. Bahmanabadi, Chemical profile of counterfeited buprenorphine vials seized in Tehran, Iran, *Forensic Sci. Int.* 172 (2007) E4–E5.
- [35] S.Y. Liu, S.O. Woo, H.L. Koh, HPLC and GC-MS screening of Chinese proprietary medicine for undeclared therapeutic substances, *J. Pharmaceut. Biomed. Anal.* 24 (2001) 983–992.
- [36] K.J. Mulligan, T.W. Brueggemeyer, D.F. Crockett, J.B. Schepman, Analysis of organic volatile impurities as a forensic tool for the examination of bulk pharmaceuticals, *J. Chromatogr. B Biomed. Appl.* 686 (1996) 85–95.
- [37] L.J. Langman, B.M. Kapur, Toxicology: then and now, *Clin. Biochem.* 39 (2006) 498–510.
- [38] H. Schütz, F. Erdmann, M.A. Verhoff, G. Weiler, Pitfalls of toxicological analysis, *Leg. Med.* 5 (2003) S6–S19.
- [39] O.H. Drummer, Requirements for bioanalytical procedures in postmortem toxicology, *Anal. Bioanal. Chem.* 388 (2007) 1495–1503.
- [40] F. Moriya, Y. Hashimoto, Nicotine and cotinine levels in blood and urine from forensic autopsy cases, *Leg. Med.* 6 (2004) 164–169.
- [41] S.P. Elliott, Gamma hydroxybutyric acid (GHB) concentrations in humans and factors affecting endogenous production, *Forensic Sci. Int.* 133 (2003) 9–16.
- [42] R.H. Lowe, A.J. Barnes, E. Lehmann, W.J. Freed, J.E. Kleinman, T.M. Hyde, M.M. Herman, M.A. Huestis, A validated positive chemical ionization GC/MS method for the identification and quantification of amphetamine, opiates, cocaine, and metabolites in human postmortem brain, *J. Mass Spectrom.* 41 (2006) 175–184.
- [43] K.D. Mariotti, R.S. Schuh, P. Ferranti, R.S. Ortiz, D.Z. Souza, F. Pechansky, P.E. Froehlich, R.P. Limberger, Simultaneous analysis of amphetamine-type stimulants in plasma by solid-phase microextraction and gas chromatography-mass spectrometry, *J. Anal. Toxicol.* 38 (2014) 432–437.
- [44] F. Bevalot, C. Bottinelli, N. Cartiser, L. Fanton, J. Guitton, Quantification of five compounds with heterogeneous physicochemical properties (morphine, 6-monoacetylmorphine, cyamemazine, meprobamate and caffeine) in 11 fluids and tissues, using automated solid-phase extraction and gas chromatography-tandem mass spectrometry, *J. Anal. Toxicol.* 38 (2014) 256–264.
- [45] S. Paterson, R. Cordero, S. Burlinson, Screening and semi-quantitative analysis of postmortem blood for basic drugs using gas chromatography/ion trap mass spectrometry, *J. Chromatogr. B-Analytic. Technol. Biomed. Life Sci.* 813 (2004) 323–330.
- [46] D.S.T. Lo, T.C. Chao, S.E. Ng-Ong, Y.J. Yao, T.H. Koh, Acidic and neutral drugs screen in blood with quantitation using microbore high-performance liquid chromatography diode array detection and capillary gas chromatography flame ionization detection, *Forensic Sci. Int.* 90 (1997) 205–214.
- [47] C. Margalho, A. Castanheira, F.C. Real, E. Gallardo, M. Lopez-Rivadulla, Determination of “new psychoactive substances” in postmortem matrices using microwave derivatization and gas chromatography-mass spectrometry, *J. Chromatogr. B-Analytic. Technol. Biomed. Life Sci.* 1020 (2016) 14–23.
- [48] R. Gameiro, S. Costa, M. Barroso, J. Franco, S. Fonseca, Toxicological analysis of cocaine adulterants in blood samples, *Forensic Sci. Int.* 299 (2019) 95–102.
- [49] R. Raposo, M. Barroso, S. Fonseca, S. Costa, J.A. Queiroz, E. Gallardo, M. Dias, Determination of eight selected organophosphorus insecticides in postmortem blood samples using solid-phase extraction and gas chromatography/mass spectrometry, *Rapid Commun. Mass Spectrom.* 24 (2010) 3187–3194.

- [50] N.I.P. Valente, S. Tarelho, A.L. Castro, A. Silvestre, H.M. Teixeira, Analysis of organophosphorus pesticides in whole blood by GC-MS-mu ECD with forensic purposes, *J. Forensic Leg. Med.* 33 (2015) 28–34.
- [51] M.A. Gardner, S. Sampsel, W.W. Jenkins, J.E. Owens, Analysis of fentanyl in urine by DLLME-GC-MS, *J. Anal. Toxicol.* 39 (2015) 118–125.
- [52] Z.B. Huang, T.F. Yu, L. Guo, Z.B. Lin, Z.Q. Zhao, Y.W. Shen, Y. Jiang, Y.H. Ye, Y.L. Rao, Effects of triglycerides levels in human whole blood on the extraction of 19 commonly used drugs using liquid-liquid extraction and gas chromatography-mass spectrometry, *Toxicol. Rep.* 2 (2015) 785–791.
- [53] N. Karlonas, A. Padaruskas, A. Ramanavicius, A. Ramanaviciene, Mixed-mode SPE for a multi-residue analysis of benzodiazepines in whole blood using rapid GC with negative-ion chemical ionization MS, *J. Separ. Sci.* 36 (2013) 1437–1445.
- [54] M. Zanaboni, G. Roda, S. Arnoldi, E. Casagni, V. Gambaro, M. Dei Cas, Comparison of different analytical methods for the determination of carbon monoxide in postmortem blood, *J. Forensic Sci.* 65 (2020) 636–640.
- [55] E.G. de Campos, M. Fogarty, B.S. De Martinis, B.K. Logan, Analysis of 2,4-Dinitrophenol in postmortem blood and urine by gas chromatography-mass spectrometry: method development and validation and report of three fatalities in the United States, *J. Forensic Sci.* 65 (2020) 183–188.
- [56] M.R. Pan, P. Xiang, Z.G. Yu, Y.L. Zhao, H. Yan, Development of a high-throughput screening analysis for 288 drugs and poisons in human blood using Orbitrap technology with gas chromatography-high resolution accurate mass spectrometry, *J. Chromatogr. A* 1587 (2019) 209–226.
- [57] C.L. Morris-Kukoski, E. Jagerdeo, J.E. Schaff, M.A. LeBeau, Ethanol analysis from biological samples by dual rail robotic autosampler, *J. Chromatogr. B-Analytic. Technol. Biomed. Life Sci.* 850 (2007) 230–235.
- [58] L. Taylor, V. Remeskevicius, L. Saskoy, T. Brodie, J. Mahmud, H. Moir, J. Brouner, C. Howe, B. Thatti, S. O'Connell, G. Trotter, B. Rooney, Determination of ethanol in micro-volumes of blood by headspace gas chromatography: statistical comparison between capillary and venous sampling sites, *Med. Sci. Law.* (2020) 1–11, <https://doi.org/10.1177/0025802420928632>.
- [59] J.A. Diekmann, J. Cochran, J.A. Hodgson, J. Smuts, Quantitation and identification of ethanol and inhalant compounds in whole blood using static headspace gas chromatography vacuum ultraviolet spectroscopy, *J. Chromatogr. A* 1611 (2020) 6.
- [60] L. Kristoffersen, L.E. Stormyhr, A. Smith-Kielland, Headspace gas chromatographic determination of ethanol: the use of factorial design to study effects of blood storage and headspace conditions on ethanol stability and acetaldehyde formation in whole blood and plasma, *Forensic Sci. Int.* 161 (2006) 151–157.
- [61] I.A. Freire, A.M.B. Barrera, P.C. Silva, M.J.T. Duque, P.F. Gomez, P.L. Eijo, Microwave assisted extraction for the determination of ethyl glucuronide in urine by gas chromatography-mass spectrometry, *J. Appl. Toxicol.* 28 (2008) 773–778.
- [62] I. Alvarez, A.M. Bermejo, M. Jesus, P. Fernandez, P. Cabarcos, P. Lopez, Microwave-assisted extraction: a simpler and faster method for the determination of ethyl glucuronide in hair by gas chromatography-mass spectrometry, *Anal. Bioanal. Chem.* 393 (2009) 1345–1350.
- [63] M. Yegles, A. Labarthe, V. Auwarter, S. Hartwig, H. Vater, R. Wennig, F. Pragst, Comparison of ethyl glucuronide and fatty acid ethyl ester concentrations in hair of alcoholics, social drinkers and teetotallers, *Forensic Sci. Int.* 145 (2004) 167–173.
- [64] H. Kharbouche, F. Sporkert, S. Troxier, M. Augsburg, P. Mangin, C. Staub, Development and validation of a gas chromatography-negative chemical ionization tandem mass spectrometry method for the determination of ethyl glucuronide in hair and its application to forensic toxicology, *J. Chromatogr. B-Analytic. Technol. Biomed. Life Sci.* 877 (2009) 2337–2343.
- [65] R. Paul, R. Kingston, L. Tsanaclis, A. Berry, A. Guwy, Do drug users use less alcohol than non-drug users? A comparison of ethyl glucuronide concentrations in hair between the two groups in medico-legal cases, *Forensic Sci. Int.* 176 (2008) 82–86.
- [66] Y. Shi, B.H. Shen, P. Xiang, H. Yan, M. Shen, Determination of ethyl glucuronide in hair samples of Chinese people by protein precipitation (PPT) and large volume injection-gas chromatography-tandem mass spectrometry (LVI-GC/MS/MS), *J. Chromatogr. B-Analytic. Technol. Biomed. Life Sci.* 878 (2010) 3161–3166.
- [67] C. Jurado, T. Soriano, M.P. Gimenez, M. Menendez, Diagnosis of chronic alcohol consumption - hair analysis for ethyl-glucuronide, *Forensic Sci. Int.* 145 (2004) 161–166.
- [68] R. Agius, T. Nadulski, H.G. Kahl, J. Schrader, B. Dufaux, M. Yegles, F. Pragst, Validation of a headspace solid-phase microextraction-GC-MS/MS for the determination of ethyl glucuronide in hair according to forensic guidelines, *Forensic Sci. Int.* 196 (2010) 3–9.

- [69] R.L. Cunha, W.A. Lopes, P.A.P. Pereira, Determination of free (unconjugated) amphetamine-type stimulants in urine samples by dispersive liquid-liquid microextraction and gas chromatography coupled to mass spectrometry (DLLME-GC-MS), *Microchem. J.* 125 (2016) 230–235.
- [70] E. Bertol, F. Vaiano, M.G. Di Milia, F. Mari, In vivo detection of the new psychoactive substance AM-694 and its metabolites, *Forensic Sci. Int.* 256 (2015) 21–27.
- [71] S. Chericoni, F. Stefanelli, V. Iannella, M. Giusiani, Simultaneous determination of morphine, codeine and 6-acetyl morphine in human urine and blood samples using direct aqueous derivatisation: validation and application to real cases, *J. Chromatogr. B-Analytic. Technol. Biomed. Life Sci.* 949 (2014) 127–132.
- [72] M.K. Parr, W. Schanzer, Detection of the misuse of steroids in doping control, *J. Steroid Biochem. Mol. Biol.* 121 (2010) 528–537.
- [73] E.M. Brun, R. Puchades, A. Maquieira, Analytical methods for anti-doping control in sport: anabolic steroids with 4,9,11-triene structure in urine, *Trac. Trends Anal. Chem.* 30 (2011) 771–783.
- [74] J. Marcos, J.A. Pascual, X. de la Torre, J. Segura, Fast screening of anabolic steroids and other banned doping substances in human urine by gas chromatography/tandem mass spectrometry, *J. Mass Spectrom.* 37 (2002) 1059–1073.
- [75] H.H. Maurer, Position of chromatographic techniques in screening for detection of drugs or poisons in clinical and forensic toxicology and/or doping control, *Clin. Chem. Lab. Med.* 42 (2004) 1310–1324.
- [76] H.H. Maurer, Role of gas chromatography-mass spectrometry with negative ion chemical ionization in clinical and forensic toxicology, doping control, and biomonitoring, *Ther. Drug Monit.* 24 (2002) 247–254.
- [77] M. Mazzarino, M. Oreggia, F. Botre, Application of fast gas chromatography/mass spectrometry for the rapid screening of synthetic anabolic steroids and other drugs in anti-doping analysis, *Rapid Commun. Mass Spectrom.* 21 (2007) 4117–4124.
- [78] H.H. Maurer, Systematic toxicological analysis procedures for acidic drugs and/or metabolites relevant to clinical and forensic toxicology and/or doping control, *J. Chromatogr. B* 733 (1999) 3–25.
- [79] H.J. Tobias, Y. Zhang, R.J. Auchus, J.T. Brenna, Detection of synthetic testosterone use by novel comprehensive two-dimensional gas chromatography combustion-isotope ratio mass spectrometry, *Anal. Chem.* 83 (2011) 7158–7165.
- [80] K. Purschke, S. Heintz, O. Lerch, F. Erdmann, F. Veit, Development and validation of an automated liquid-liquid extraction GC/MS method for the determination of THC, 11-OH-THC, and free THC-carboxylic acid (THC-COOH) from blood serum, *Anal. Bioanal. Chem.* 408 (2016) 4379–4388.
- [81] I. Ojanpera, S. Mesihä, I. Rasanen, A. Pelander, R.A. Ketola, Simultaneous identification and quantification of new psychoactive substances in blood by GC-APCI-QTOFMS coupled to nitrogen chemiluminescence detection without authentic reference standards, *Anal. Bioanal. Chem.* 408 (2016) 3395–3400.
- [82] M. Moller, K. Aleksa, P. Walasek, T. Karaskov, G. Koren, Solid-phase microextraction for the detection of codeine, morphine and 6-monoacetylmorphine in human hair by gas chromatography-mass spectrometry, *Forensic Sci. Int.* 196 (2010) 64–69.
- [83] S. Eller, L.G. Flaiban, B. Paranhos, J.L. da Costa, F.R. Lourenco, M. Yonamine, Analysis of 11-nor-9-carboxy-Delta(9)-tetrahydrocannabinol in urine samples by hollow fiber-liquid phase microextraction and gas chromatography-mass spectrometry in consideration of measurement uncertainty, *Forensic Toxicol.* 32 (2014) 282–291.
- [84] R.J. Dinis-Oliveira, T. Magalhaes, Forensic toxicology in drug-facilitated sexual assault, *Toxicol. Mech. Method.* 23 (2013) 471–478.
- [85] A.N. Lad, A. Pandya, Y.K. Agrawal, Overview of nano-enabled screening of drug-facilitated crime: a promising tool in forensic investigation, *Trac. Trends Anal. Chem.* 80 (2016) 458–470.
- [86] B. Madea, F. Musshoff, Knock-out drugs: their prevalence, modes of action, and means of detection, *Dtsch. Arztebl. Int.* 106 (2009). 341-U312.
- [87] F. Vaiano, G. Serpelloni, S. Furlanetto, D. Palumbo, F. Mari, A. Fioravanti, E. Bertol, Determination of endogenous concentration of gamma-hydroxybutyric acid (GHB) in hair through an ad hoc GC-MS analysis: a study on a wide population and influence of gender and age, *J. Pharmaceut. Biomed. Anal.* 118 (2016) 161–166.
- [88] I. Moreno, M. Barroso, A. Martinho, A. Cruz, E. Gallardo, Determination of ketamine and its major metabolite, norketamine, in urine and plasma samples using microextraction by packed sorbent and gas chromatography-tandem mass spectrometry, *J. Chromatogr. B-Analytic. Technol. Biomed. Life Sci.* 1004 (2015) 67–78.

- [89] N. Kenan, S. Mercan, M. Acikkol, Development and validation of a practical analytical method for Zolpidem as a drug facilitated crime tool, *J. Chem. Metrol.* 13 (2019) 68–74.
- [90] A. International, ASTM Book of Standards Volume 14.02 Particle Spray Characterization; Forensic Sciences; Accreditation & Certification; Forensic Psychophysiology; Nanotechnology; Forensic Engineering, in, ASTM International, Pennsylvania, USA, 2020, pp. 1–890.
- [91] J.R. Almirall, K.G. Furton, *Analysis and Interpretation of Fire Scene Evidence*, Taylor & Francis, 2004.
- [92] E. Stauffer, J.A. Dolan, R. Newman, *Fire Debris Analysis*, Elsevier Science Bv, Amsterdam, 2008.
- [93] P. Mark, L. Sandercock, Fire investigation and ignitable liquid residue analysis - a review: 2001-2007, *Forensic Sci. Int.* 176 (2008) 93–110.
- [94] A.D. Pert, M.G. Baron, J.W. Birkett, Review of analytical techniques for arson residues, *J. Forensic Sci.* 51 (2006) 1033–1049.
- [95] M. Monfreda, A. Gregori, Differentiation of unevaporated gasoline samples according to their brands, by SPME-GC-MS and multivariate statistical analysis, *J. Forensic Sci.* 56 (2011) 372–380.
- [96] A.C. Harris, J.F. Wheeler, GC-MS of ignitable liquids using solvent-desorbed SPME for automated analysis, *J. Forensic Sci.* 48 (2003) 41–46.
- [97] M. Tankiewicz, C. Morrison, M. Biziuk, Application and optimization of headspace solid-phase microextraction (HS-SPME) coupled with gas chromatography-flame-ionization detector (GC-FID) to determine products of the petroleum industry in aqueous samples, *Microchem. J.* 108 (2013) 117–123.
- [98] A. Aqel, A.M. Dhabbah, K. Yusuf, N.M. Al-Harbi, Z.A. Al Othman, A.Y. Badjah-Hadj-Ahmed, Determination of gasoline and diesel residues on wool, silk, polyester and cotton materials by SPME-GC-MS, *J. Anal. Chem.* 71 (2016) 730–736.
- [99] A.M. Dhabbah, S.S. Al-Jaber, A.H. Al-Ghamdi, A. Aqel, Determination of gasoline residues on carpets by SPME-GC-MS technique, *Arabian J. Sci. Eng.* 39 (2014) 6749–6756.
- [100] A. Choodum, N.N. Daeid, Evaluating the performance of three GC columns commonly used for the analysis of ignitable liquid mixtures encountered in fire debris, *Analytical Method.* 3 (2011) 1525–1534.
- [101] B.J. de Vos, M. Froneman, E. Rohwer, D.A. Sutherland, Detection of petrol (gasoline) in fire debris by gas chromatography/mass spectrometry/mass spectrometry (GC/MS/MS), *J. Forensic Sci.* 47 (2002) 736–756.
- [102] J.M. Baerncopf, V.L. McGuffin, R.W. Smith, Association of ignitable liquid residues to neat ignitable liquids in the presence of matrix interferences using chemometric procedures, *J. Forensic Sci.* 56 (2011) 70–81.
- [103] J.R. Almirall, K.G. Furton, Characterization of background and pyrolysis products that may interfere with the forensic analysis of fire debris, *J. Anal. Appl. Pyrol.* 71 (2004) 51–67.
- [104] R. Borusiewicz, J. Zieba-Palus, G. Zadora, The influence of the type of accelerant, type of burned material, time of burning and availability of air on the possibility of detection of accelerants traces, *Forensic Sci. Int.* 160 (2006) 115–126.
- [105] Y. Lu, P.B. Harrington, Forensic application of gas chromatography - differential mobility spectrometry with two-way classification of ignitable liquids from fire debris, *Anal. Chem.* 79 (2007) 6752–6759.
- [106] M.J. Aliano-Gonzalez, M. Ferreiro-Gonzalez, G.F. Barbero, M. Palma, C.G. Barroso, Application of headspace gas chromatography-ion mobility spectrometry for the determination of ignitable liquids from fire debris, *Separations* 5 (2018) 9.
- [107] L.N. Kates, P.I. Richards, C.D. Sandau, The application of comprehensive two-dimensional gas chromatography to the analysis of wildfire debris for ignitable liquid residue, *Forensic Sci. Int.* 310 (2020).
- [108] A.A.S. Sampat, B. van Daelen, M. Lopatka, H. Mol, G. van der Weg, G. Vivo-Truyols, M. Sjerps, P.J. Schoenmakers, A.C. van Asten, Detection and characterization of ignitable liquid residues in forensic fire debris samples by comprehensive two-dimensional gas chromatography, *Separations* 5 (2018) 27.
- [109] K.D. Nizio, S.L. Forbes, Developing a method for the collection and analysis of burnt remains for the detection and identification of ignitable liquid residues using body bags, *Dynamic Headspace Samp. TD-GCxGC-TOFMS, Separat.* 5 (2018) 13.
- [110] R.J. Harper, K.G. Furton, Chapter 13 - biological detection of explosives, in: J. Yinon (Ed.), *Counterterrorist Detection Techniques of Explosives*, Elsevier Science B.V., Amsterdam, 2007, pp. 395–431.
- [111] M.E. Sigman, C.D. Clark, R. Fidler, C.L. Geiger, C.A. Clausen, Analysis of triacetone triperoxide by gas chromatography/mass spectrometry and gas chromatography/tandem mass spectrometry by electron and chemical ionization, *Rapid Commun. Mass Spectrom.* 20 (2006) 2851–2857.
- [112] A. Partridge, S. Walker, D. Armit, Detection of impurities in organic peroxide explosives from precursor chemicals, *Aust. J. Chem.* 63 (2010) 30–37.

- [113] M.S. Meaney, V.L. McGuffin, Luminescence-based methods for sensing and detection of explosives, *Anal. Bioanal. Chem.* 391 (2008) 2557–2576.
- [114] C.R. Bowerbank, P.A. Smith, D.D. Fetterolf, M.L. Lee, Solvating gas chromatography with chemiluminescence detection of nitroglycerine and other explosives, *J. Chromatogr. A* 902 (2000) 413–419.
- [115] M.E. Walsh, Determination of nitroaromatic, nitramine, and nitrate ester explosives in soil by gas chromatography and an electron capture detector, *Talanta* 54 (2001) 427–438.
- [116] H. Brust, S. Willemse, T.Y. Zeng, A. van Asten, M. Koeberg, A. van der Heijden, A. Bolck, P. Schoenmakers, Impurity profiling of trinitrotoluene using vacuum-outlet gas chromatography-mass spectrometry, *J. Chromatogr. A* 1374 (2014) 224–230.
- [117] B.J. Routon, B.B. Kocher, J.V. Goodpaster, Discriminating Hodgdon Pyrodex (R) and triple seven (R) using gas chromatography-mass spectrometry, *J. Forensic Sci.* 56 (2011) 194–199.
- [118] F.F. Tian, J. Yu, J.L. Hu, Y. Zhang, M.X. Xie, Y. Liu, X.F. Wang, H.L. Liu, J. Han, Determination of emulsion explosives with Span-80 as emulsifier by gas chromatography-mass spectrometry, *J. Chromatogr. A* 1218 (2011) 3521–3528.
- [119] G.W. Cook, P.T. LaPuma, G.L. Hook, B.A. Eckenrode, Using gas chromatography with ion mobility spectrometry to resolve explosive compounds in the presence of interferents, *J. Forensic Sci.* 55 (2010) 1582–1591.
- [120] F. Monteil-Rivera, C. Beaulieu, J. Hawari, Use of solid-phase microextraction/gas chromatography-electron capture detection for the determination of energetic chemicals, in marine samples, *J. Chromatogr. A* 1066 (2005) 177–187.
- [121] S. Calderara, D. Gardebas, F. Martinez, Solid phase micro extraction coupled with on-column GC/ECD for the post-blast analysis of organic explosives, *Forensic Sci. Int.* 137 (2003) 6–12.
- [122] K.H. Chang, C.H. Yew, A.F.L. Abdullah, Optimization of headspace solid-phase microextraction technique for extraction of volatile smokeless powder compounds in forensic applications, *J. Forensic Sci.* 59 (2014) 1100–1108.
- [123] F.S. Romolo, L. Cassioli, S. Grossi, G. Cinelli, M.V. Russo, Surface-sampling and analysis of TATP by swabbing and gas chromatography/mass spectrometry, *Forensic Sci. Int.* 224 (2013) 96–100.
- [124] J. Andrasko, L. Lagesson-Andrasko, J. Dahlen, B.H. Jonsson, Analysis of explosives by GC-UV, *J. Forensic Sci.* 62 (2017) 1022–1027.
- [125] F.S. Romolo, P. Margot, Identification of gunshot residue: a critical review, *Forensic Sci. Int.* 119 (2001) 195–211.
- [126] E.B. Morales, A.L.R. Vazquez, Simultaneous determination of inorganic and organic gunshot residues by capillary electrophoresis, *J. Chromatogr. A* 1061 (2004) 225–233.
- [127] O. Dalby, D. Butler, J.W. Birkett, Analysis of gunshot residue and associated materials-A review, *J. Forensic Sci.* 55 (2010) 924–943.
- [128] A.J. Schwoeble, D.L. Exline, *Current Methods in Forensic Gunshot Residue Analysis*, CRC Press, Boca Raton, 2000.
- [129] E. Goudsmits, G.P. Sharples, J.W. Birkett, Recent trends in organic gunshot residue analysis, *Trac. Trends Anal. Chem.* 74 (2015) 46–57.
- [130] K.H. Chang, P.T. Jayaprakash, C.H. Yew, A.F.L. Abdullah, Gunshot residue analysis and its evidential values: a review, *Aust. J. Forensic Sci.* 45 (2013) 3–23.
- [131] J. Andrasko, J. Oskarsson, S. Stahling, Ammunition used in the latest shooting, *Forensic Sci. Int.* 136 (2003), 146–146.
- [132] A. Zeichner, B. Eldar, B. Glattstein, A. Koffman, T. Tamiri, D. Muller, Vacuum collection of gunpowder residues from clothing worn by shooting suspects, and their analysis by GC/TEA, IMS, and GC/MS, *J. Forensic Sci.* 48 (2003) 961–972.
- [133] A. Zeichner, B. Eldar, A novel method for extraction and analysis of gunpowder residues on double-side adhesive coated stubs, *J. Forensic Sci.* 49 (2004) 1194–1206.
- [134] J. Andrasko, T. Norberg, S. Stahling, Time since discharge of shotguns, *J. Forensic Sci.* 43 (1998) 1005–1015.
- [135] J. Andrasko, S. Stahling, Time since discharge of spent cartridges, *J. Forensic Sci.* 44 (1999) 487–495.
- [136] J. Andrasko, S. Stahling, Time since discharge of rifles, *J. Forensic Sci.* 45 (2000) 1250–1255.
- [137] J.D. Wilson, J.D. Tebow, K.W. Moline, Time since discharge of shotgun shells, *J. Forensic Sci.* 48 (2003) 1298–1301.
- [138] J. Andrasko, S. Stahling, Time since discharge of pistols and revolvers, *J. Forensic Sci.* 48 (2003) 307–311.
- [139] E. Goudsmits, L.S. Blakey, K. Chana, G.P. Sharples, J.W. Birkett, The analysis of organic and inorganic gunshot residue from a single sample, *Forensic Sci. Int.* 299 (2019) 168–173.
- [140] A. Tarifa, J.R. Almirall, Fast detection and characterization of organic and inorganic gunshot residues on the hands of suspects by CMV-GC-MS and LIBS, *Sci. Justice* 55 (2015) 168–175.

- [141] N.S. Parsons, M.H.W. Lam, S.E. Hamilton, F. Hui, A preliminary investigation into the comparison of dissolution/digestion techniques for the chemical characterization of polyurethane foam, *Sci. Justice* 50 (2010) 177–181.
- [142] S.C. McNorton, G.W. Nutter, J.A. Siegel, The characterization of automobile body fillers, *J. Forensic Sci.* 53 (2008) 116–124.
- [143] J. Zieba-Palus, G. Zadora, J.M. Milczarek, P. Koscieniak, Pyrolysis-gas chromatography/mass spectrometry analysis as a useful tool in forensic examination of automotive paint traces, *J. Chromatogr. A* 1179 (2008) 41–46.
- [144] B.K. Kochanowski, S.L. Morgan, Forensic discrimination of automotive paint samples using pyrolysis-gas chromatography-mass spectrometry with multivariate statistics, *J. Chromatogr. Sci.* 38 (2000) 100–108.
- [145] J.M. Milczarek, J. Zieba-Palus, Examination of spray paints on plasters by the use of pyrolysis-gas chromatography/mass spectrometry for forensic purposes, *J. Anal. Appl. Pyrol.* 86 (2009) 252–259.
- [146] Y. Higashikawa, H. Kanno, T. Kaneko, S. Suzuki, Forensic discrimination of trace fragments of photocopied materials, *Bunseki Kagaku* 56 (2007) 1147–1152.
- [147] A. Richmond-Aylor, S. Bell, P. Callery, K. Morris, Thermal degradation analysis of amino acids in fingerprint residue by pyrolysis GC-MS to develop new latent fingerprint developing reagents, *J. Forensic Sci.* 52 (2007) 380–382.
- [148] G.P. Campbell, A.L. Gordon, Analysis of condom lubricants for forensic casework, *J. Forensic Sci.* 52 (2007) 630–642.
- [149] J.H. Bugler, H. Buchner, A. Dallmayer, Characterization of ballpoint pen inks by thermal desorption and gas chromatography-mass spectrometry, *J. Forensic Sci.* 50 (2005) 1209–1214.
- [150] J.H. Bugler, H. Buchner, A. Dallmayer, Age determination of ballpoint pen ink by thermal desorption and gas chromatography-mass spectrometry, *J. Forensic Sci.* 53 (2008) 982–988.
- [151] L. Brazeau, M. Gaudreau, Ballpoint pen inks: the quantitative analysis of ink solvents on paper by solid-phase microextraction, *J. Forensic Sci.* 52 (2007) 209–215.
- [152] S.H. Yang, J.Y. Shen, M.S. Chang, G.J. Wu, Quantification of vehicle paint components containing polystyrene using pyrolysis-gas chromatography/mass spectrometry, *Analytical Method.* 4 (2012) 1989–1995.
- [153] E.A. Scribner, E.M. Thurman, L.R. Zimmermann, Analysis of selected herbicide metabolites in surface and ground water of the United States, *Sci. Total Environ.* 248 (2000) 157–167.
- [154] S.M. Mudge, I. ebrary, *Methods in Environmental Forensics*, CRC Press, Boca Raton, 2009.
- [155] O.N. Zabelina, V.I. Saloutin, O.N. Chupakhin, Analysis of polychlorinated biphenyl mixtures by gas chromatography, *J. Anal. Chem.* 65 (2010) 1098–1108.
- [156] J.W. Cochran, G.M. Frame, Recent developments in the high-resolution gas chromatography of polychlorinated biphenyls, *J. Chromatogr. A* 843 (1999) 323–368.
- [157] G.S. Frysinger, R.B. Gaines, C.M. Reddy, GC x GC - a new analytical tool for environmental forensics, *Environ. Forensics* 3 (2002) 27–34.
- [158] D. Megson, R. Kalin, P.J. Worsfold, C. Gauchotte-Lindsay, D.G. Patterson, M.C. Lohan, S. Comber, T.A. Brown, G. O'Sullivan, Fingerprinting polychlorinated biphenyls in environmental samples using comprehensive two-dimensional gas chromatography with time-of-flight mass spectrometry, *J. Chromatogr. A* 1318 (2013) 276–283.
- [159] E.J. Reiner, The analysis of dioxins and related compounds, *Mass Spectrom. Rev.* 29 (2010) 526–559.
- [160] J.F. Focant, G. Eppe, M.L. Scippo, A.C. Massart, C. Pirard, G. Maghuin-Rogister, E. De Pauw, Comprehensive two-dimensional gas chromatography with isotope dilution time-of-flight mass spectrometry for the measurement of dioxins and polychlorinated biphenyls in foodstuffs - comparison with other methods, *J. Chromatogr. A* 1086 (2005) 45–60.
- [161] K. Saito, A. Ohmura, M. Takekuma, R. Sasano, Y. Matsuki, H. Nakazawa, Application of a novel large-volume injection method using a stomach-shaped inlet liner in capillary gas chromatographic trace analysis of dioxins in human milk and plasma, *Anal. Sci.* 23 (2007) 661–666.
- [162] E. Matisova, M. Domotorova, Fast gas chromatography and its use in trace analysis, *J. Chromatogr. A* 1000 (2003) 199–221.
- [163] J.F. Focant, A. Sjodin, D.G. Patterson, Improved separation of the 209 polychlorinated biphenyl congeners using comprehensive two-dimensional gas chromatography-time-of-flight mass spectrometry, *J. Chromatogr. A* 1040 (2004) 227–238.
- [164] P. Haglund, P. Korytar, C. Danielsson, J. Diaz, K. Wiberg, P. Leonards, U.A.T. Brinkman, J. de Boer, GCxGC-ECD, A promising method for the determination of dioxins and dioxin-like PCBs in food and feed, *Anal. Bioanal. Chem.* 390 (2008) 1815–1827.
- [165] S. Dahle, V. Savinov, J. Klungsoyr, S. Boitsov, N. Plotitsyna, A. Zhilin, T. Savinova, V. Petrova, Polycyclic aromatic hydrocarbons (PAHs) in the Barents Sea sediments: small changes over the recent 10 years, *Mar. Biol. Res.* 5 (2009) 101–108.

- [166] D.L. Poster, M.M. Schantz, L.C. Sander, S.A. Wise, Analysis of polycyclic aromatic hydrocarbons (PAHs) in environmental samples: a critical review of gas chromatographic (GC) methods, *Anal. Bioanal. Chem.* 386 (2006) 859–881.
- [167] W.A. Lopes, G.O. da Rocha, P.A.D. Pereira, F.S. Oliveira, L.S. Carvalho, N.D.C. Bahia, L.D. Conceicao, J.B. de Andrade, Multivariate optimization of a GC-MS method for determination of sixteen priority polycyclic aromatic hydrocarbons in environmental samples, *J. Separ. Sci.* 31 (2008) 1787–1796.
- [168] S.P. Wu, S. Tao, F.L. Xu, R. Dawson, T. Lan, B.G. Li, J. Cao, Polycyclic aromatic hydrocarbons in dustfall in Tianjin, China, *Sci. Total Environ.* 345 (2005) 115–126.
- [169] D.Z. Zou, K.L. Liu, W.P. Pan, J.T. Riley, Y.Q. Xu, Rapid analysis of PAHs in fly ash using thermal desorption and fast GC-TOF-MS, *J. Chromatogr. Sci.* 41 (2003) 245–250.
- [170] O. Panic, T. Gorecki, Comprehensive two-dimensional gas chromatography (GCxGC) in environmental analysis and monitoring, *Anal. Bioanal. Chem.* 386 (2006) 1013–1023.
- [171] A. Stark, T. Abrajano, J. Hellou, J.L. Metcalf-Smith, Molecular and isotopic characterization of polycyclic aromatic hydrocarbon distribution and sources at the international segment of the St. Lawrence River, *Org. Geochem.* 34 (2003) 225–237.
- [172] F.M. Norlock, J.K. Jang, Q.M. Zou, T.M. Schoonover, A. Li, Large-volume injection PTV-GC-MS analysis of polycyclic aromatic hydrocarbons in air and sediment samples, *J. Air Waste Manag. Assoc.* 52 (2002) 19–26.
- [173] G.L. Reed, K. Clark-Baker, H.M. McNair, Fast gas chromatography of various sample types using fast oven temperature programming, *J. Chromatogr. Sci.* 37 (1999) 300–305.
- [174] A. Christensen, C. Ostman, R. Westerholm, Ultrasound-assisted extraction and on-line LC-GC-MS for determination of polycyclic aromatic hydrocarbons (PAH) in urban dust and diesel particulate matter, *Anal. Bioanal. Chem.* 381 (2005) 1206–1216.
- [175] Z.D. Wang, M.F. Fingas, Development of oil hydrocarbon fingerprinting and identification techniques, *Mar. Pollut. Bull.* 47 (2003) 423–452.
- [176] Z.D. Wang, M. Fingas, L. Sigouin, Using multiple criteria for fingerprinting unknown oil samples having very similar chemical composition, *Environ. Forensics* 3 (2002) 251–262.
- [177] C.G. Barroso, Characterization of petroleum-based products in water samples by HS-MS, *Fuel* 222 (2018) 506–512.
- [178] B.J. Riley, C. Lennard, S. Fuller, V. Spikmans, Pyrolysis-GC-MS analysis of crude and heavy fuel oil asphaltene for application in oil fingerprinting, *Environ. Forensics* 19 (2018) 14–26.
- [179] P.K. Piotrowski, B.A. Weggler, D.A. Yoxtheimer, C.N. Kelly, E. Barth-Naftilan, J.E. Saiers, F.L. Dorman, Elucidating environmental fingerprinting mechanisms of unconventional gas development through hydrocarbon analysis, *Anal. Chem.* 90 (2018) 5466–5473.
- [180] P.L. Adhikari, R.L. Wong, E.B. Overton, Application of enhanced gas chromatography/triple quadrupole mass spectrometry for monitoring petroleum weathering and forensic source fingerprinting in samples impacted by the Deepwater Horizon oil spill, *Chemosphere* 184 (2017) 939–950.
- [181] R.B. Gaines, G.S. Frysinger, M.S. Hendrick-Smith, J.D. Stuart, Oil spill source identification by comprehensive two-dimensional gas chromatography, *Environ. Sci. Technol.* 33 (1999) 2106–2112.
- [182] G.T. Ventura, G.J. Hall, R.K. Nelson, G.S. Frysinger, B. Raghuraman, A.E. Pomerantz, O.C. Mullins, C.M. Reddy, Analysis of petroleum compositional similarity using multiway principal components analysis (MPCA) with comprehensive two-dimensional gas chromatographic data, *J. Chromatogr. A* 1218 (2011) 2584–2592.
- [183] R.X. Hua, Y.Y. Li, W. Liu, J.C. Zheng, H.B. Wei, J.H. Wang, X. Lu, H.W. Kong, G.W. Xu, Determination of sulfur-containing compounds in diesel oils by comprehensive two-dimensional gas chromatography with a sulfur chemiluminescence detector, *J. Chromatogr. A* 1019 (2003) 101–109.
- [184] L.L.R. van Stee, J. Beens, R.J.J. Vreuls, U.A.T. Brinkman, Comprehensive two-dimensional gas chromatography with atomic emission detection and correlation with mass spectrometric detection: principles and application in petrochemical analysis, *J. Chromatogr. A* 1019 (2003) 89–99.
- [185] G.T. Ventura, B. Raghuraman, R.K. Nelson, O.C. Mullins, C.M. Reddy, Compound class oil fingerprinting techniques using comprehensive two-dimensional gas chromatography (GC x GC), *Org. Geochem.* 41 (2010) 1026–1035.
- [186] A.M. Curran, P.A. Prada, K.G. Furton, The differentiation of the volatile organic signatures of individuals through SPME-GC/MS of characteristic human scent compounds, *J. Forensic Sci.* 55 (2010) 50–57.
- [187] A.M. Curran, C.F. Ramirez, A.A. Schoon, K.G. Furton, The frequency of occurrence and discriminatory power of compounds found in human scent across a population determined by SPME-GEMS, *J. Chromatogr. B-Analytic. Technol. Biomed. Life Sci.* 846 (2007) 86–97.

- [188] V. Cuzuel, G. Cognon, I. Rivals, C. Sauleau, F. Heulard, D. Thiebaut, J. Vial, Origin, analytical characterization, and use of human odor in forensics, *J. Forensic Sci.* 62 (2017) 330–350.
- [189] V. Cuzuel, R. Leconte, G. Cognon, D. Thiebaut, J. Vial, C. Sauleau, I. Rivals, Human odor and forensics: towards Bayesian suspect identification using GC x GC-MS characterization of hand odor, *J. Chromatogr. B-Analytic. Technol. Biomed. Life Sci.* 1092 (2018) 379–385.
- [190] V. Cuzuel, E. Portas, G. Cognon, I. Rivals, F. Heulard, D. Thiebaut, J. Vial, Sampling method development and optimization in view of human hand odor analysis by thermal desorption coupled with gas chromatography and mass spectrometry, *Anal. Bioanal. Chem.* 409 (2017) 5113–5124.
- [191] V. Cuzuel, A. Sizun, G. Cognon, I. Rivals, F. Heulard, D. Thiebaut, J. Vial, Human odor and forensics. Optimization of a comprehensive two-dimensional gas chromatography method based on orthogonality: how not to choose between criteria, *J. Chromatogr. A* 1536 (2018) 58–66.
- [192] P. Dolezal, K.G. Furton, J. Lnenickova, P. Kyjakova, V. Skerikova, I. Valterova, L. Pinc, S. Urban, Multiplicity of human scent signature, *Egypt. J. Food Sci.* 9 (2019).
- [193] L. Dormont, J.M. Bessiere, A. Cohuet, Human skin volatiles: a review, *J. Chem. Ecol.* 39 (2013) 569–578.
- [194] B.A. Eckenrode, S.A. Ramsey, R.A. Stockham, G.J. Van Berkel, K.G. Asano, D.A. Wolf, Performance evaluation of the scent transfer Unit (TM) (STU-100) for organic compound collection and release, *J. Forensic Sci.* 51 (2006) 780–789.
- [195] D.T. Hudson, A.M. Curran, K.G. Furton, The stability of collected human scent under various environmental conditions, *J. Forensic Sci.* 54 (2009) 1270–1277.
- [196] P.A. Prada, A.M. Curran, K.G. Furton, The evaluation of human hand odor volatiles on various textiles: a comparison between contact and noncontact sampling methods, *J. Forensic Sci.* 56 (2011) 866–881.
- [197] A.M. Curran, S.I. Rabin, P.A. Prada, K.G. Furton, Comparison of the volatile organic compounds present in human odor using SPME-GC/MS, *J. Chem. Ecol.* 31 (2005) 1607–1619.
- [198] S.K. Pandey, K.H. Kim, Human body-odor components and their determination, *Trac. Trends Anal. Chem.* 30 (2011) 784–796.
- [199] L.E. DeGreeff, A.M. Curran, K.G. Furton, Evaluation of selected sorbent materials for the collection of volatile organic compounds related to human scent using non-contact sampling mode, *Forensic Sci. Int.* 209 (2011) 133–142.
- [200] M. Kusano, E. Mendez, K.G. Furton, Development of headspace SPME method for analysis of volatile organic compounds present in human biological specimens, *Anal. Bioanal. Chem.* 400 (2011) 1817–1826.
- [201] Z.M. Zhang, J.J. Cai, G.H. Ruan, G.K. Li, The study of fingerprint characteristics of the emanations from human arm skin using the original sampling system by SPME-GC/MS, *J. Chromatogr. B-Analytic. Technol. Biomed. Life Sci.* 822 (2005) 244–252.
- [202] J.S. Brown, P.A. Prada, A.M. Curran, K.G. Furton, Applicability of emanating volatile organic compounds from various forensic specimens for individual differentiation, *Forensic Sci. Int.* 226 (2013) 173–182.
- [203] M. Kusano, E. Mendez, K.G. Furton, Comparison of the volatile organic compounds from different biological specimens for profiling potential, *J. Forensic Sci.* 58 (2013) 29–39.
- [204] D.J. Penn, E. Oberzaucher, K. Grammer, G. Fischer, H.A. Soini, D. Wiesler, M.V. Novotny, S.J. Dixon, Y. Xu, R.G. Brereton, Individual and gender fingerprints in human body odour, *J. R. Soc. Interface* 4 (2007) 331–340.
- [205] E. Woolfenden, Sorbent-based sampling methods for volatile and semi-volatile organic compounds in air Part 1: sorbent-based air monitoring options, *J. Chromatogr. A* 1217 (2010) 2674–2684.
- [206] B. Grabowska-Polanowska, P. Miarka, M. Skowron, J. Sulowicz, K. Wojtyna, K. Moskal, I. Sliwka, Development of sampling method and chromatographic analysis of volatile organic compounds emitted from human skin, *Bioanalysis* 9 (2017) 1465–1475.
- [207] M. Gallagher, J. Wysocki, J.J. Leyden, A.I. Spielman, X. Sun, G. Preti, Analyses of volatile organic compounds from human skin, *Br. J. Dermatol.* 159 (2008) 780–791.
- [208] H. Kataoka, K. Saito, Recent advances in SPME techniques in biomedical analysis, *J. Pharmaceut. Biomed. Anal.* 54 (2011) 926–950.
- [209] M.J. Choi, C.H. Oh, 2nd Dimensional GC-MS analysis of sweat volatile organic compounds prepared by solid phase micro-extraction, *Technol. Health Care* 22 (2014) 481–488.
- [210] B. Gruber, B.A. Weggler, R. Jaramillo, K.A. Murrell, P.K. Piotrowski, F.L. Dorman, Comprehensive two-dimensional gas chromatography in forensic science: a critical review of recent trends, *Trac. Trends Anal. Chem.* 105 (2018) 292–301.
- [211] P.A. Prada, A.M. Curran, K.G. Furton, Comparison of extraction methods for the removal of volatile organic compounds (VOCs) present in sorbents used for human scent evidence collection, *Analytical Method.* 2 (2010) 470–478.

- [212] Z. Knobel, M. Ueland, K.D. Nizio, D. Patel, S.L. Forbes, A comparison of human and pig decomposition rates and odour profiles in an Australian environment, *Aust. J. Forensic Sci.* 51 (2019) 557–572.
- [213] L. Irish, S.R. Rennie, G.M.B. Parkes, A. Williams, Identification of decomposition volatile organic compounds from surface-deposited and submerged porcine remains, *Sci. Justice* 59 (2019) 503–515.
- [214] A. Deo, S.L. Forbes, B.H. Stuart, M. Ueland, Profiling the seasonal variability of decomposition odour from human remains in a temperate Australian environment, *Aust. J. Forensic Sci.* 52 (6) (2019).
- [215] K.D. Nizio, M. Ueland, B.H. Stuart, S.L. Forbes, The analysis of textiles associated with decomposing remains as a natural training aid for cadaver-detection dogs, *Forensic Chem.* 5 (2017) 33–45.
- [216] M.A. Iqbal, K.D. Nizio, M. Ueland, S.L. Forbes, Forensic decomposition odour profiling: a review of experimental designs and analytical techniques, *Trac. Trends Anal. Chem.* 91 (2017) 112–124.
- [217] S. Stadler, J.F. Focant, S.L. Forbes, Forensic analysis of volatile organic compounds from decomposed remains in a soil environment, in: H. Kars, L. VanDenEijkel (Eds.), *Soil in Criminal and Environmental Forensics*, 2016, pp. 297–316.
- [218] K.A. Perrault, P.H. Stefanuto, B.H. Stuart, T. Rai, J.F. Focant, S.L. Forbes, Detection of decomposition volatile organic compounds in soil following removal of remains from a surface deposition site, *Forensic Sci. Med. Pathol.* 11 (2015) 376–387.
- [219] K.A. Perrault, K.D. Nizio, S.L. Forbes, A comparison of one-dimensional and comprehensive two-dimensional gas chromatography for decomposition odour profiling using inter-year replicate field trials, *Chromatographia* 78 (2015) 1057–1070.
- [220] S. Stadler, P.H. Stefanuto, M. Brokl, S.L. Forbes, J.F. Focant, Characterization of volatile organic compounds from human analogue decomposition using thermal desorption coupled to comprehensive two-dimensional gas chromatography-time-of-flight mass spectrometry, *Anal. Chem.* 85 (2013) 998–1005.
- [221] L.M. Dubois, P.H. Stefanuto, K.A. Perrault, G. Delporte, P. Delvenne, J.F. Focant, Comprehensive approach for monitoring human tissue degradation, *Chromatographia* 82 (2019) 857–871.
- [222] P.H. Stefanuto, J.F. Focant, GCxGC-TOFMS, the Swiss knife for VOC mixtures analysis in soil forensic investigations, in: H. Kars, L. VanDenEijkel (Eds.), *Soil in Criminal and Environmental Forensics*, Springer Int Publishing Ag, Cham, 2016, pp. 317–329.
- [223] A. Agapiou, E. Zorba, K. Mikedi, L. McGregor, C. Spiliopoulou, M. Statheropoulos, Analysis of volatile organic compounds released from the decay of surrogate human models simulating victims of collapsed buildings by thermal desorption-comprehensive two-dimensional gas chromatography-time of flight mass spectrometry, *Anal. Chim. Acta* 883 (2015) 99–108.
- [224] A.A. Vass, R.R. Smith, C.V. Thompson, M.N. Burnett, N. Dulgerian, B.A. Eckenrode, Odor analysis of decomposing buried human remains, *J. Forensic Sci.* 53 (2008) 384–391.
- [225] A.A. Vass, S.A. Barshick, G. Segal, J. Caton, J.T. Skeen, J.C. Love, J.A. Synsteliien, Decomposition chemistry of human remains: a new methodology for determining the postmortem interval, *J. Forensic Sci.* 47 (2002) 542–553.
- [226] S.L. Forbes, J. Keegan, B.H. Stuart, B.B. Dent, A gas chromatography-mass spectrometry method for the detection of adipocere in grave soils, *Eur. J. Lipid Sci. Technol.* 105 (2003) 761–768.
- [227] S.L. Forbes, B.H. Stuart, B.B. Dent, The identification of adipocere in grave soils, *Forensic Sci. Int.* 127 (2002) 225–230.
- [228] S.J. Notter, B.H. Stuart, B.B. Dent, J. Keegan, Solid-phase extraction in combination with GC/MS for the quantification of free fatty acids in adipocere, *Eur. J. Lipid Sci. Technol.* 110 (2008) 73–80.
- [229] I.D. Bull, R. Berstan, A. Vass, R.P. Evershed, Identification of a disinterred grave by molecular and stable isotope analysis, *Sci. Justice* 49 (2009) 142–149.
- [230] M. Statheropoulos, C. Spiliopouliou, A. Agapiou, A study of volatile organic compounds evolved from the decaying human body, *Forensic Sci. Int.* 153 (2005) 147–155.
- [231] A.A. Vass, Death is in the air: confirmation of decomposition without a corpse, *Forensic Sci. Int.* 301 (2019) 149–159.
- [232] L.E. DeGreeff, K.G. Furton, Collection and identification of human remains volatiles by non-contact, dynamic airflow sampling and SPME-GC/MS using various sorbent materials, *Anal. Bioanal. Chem.* 401 (2011) 1295–1307.
- [233] T.M. Lovestead, T.J. Bruno, Detecting gravesoil with headspace analysis with adsorption on short porous layer open tubular (PLOT) columns, *Forensic Sci. Int.* 204 (2011) 156–161.
- [234] A.C. Lewis, J.F. Hamilton, C.N. Rhodes, J. Halliday, K.D. Bartle, P. Homewood, R.J.P. Grenfell, B. Goody, A.M. Harling, P. Brewer, G. Vargha, M.J.T. Milton, Microfabricated planar glass gas chromatography with photoionization detection, *J. Chromatogr. A* 1217 (2010) 768–774.
- [235] J.A. Syage, B.J. Nies, M.D. Evans, K.A. Hanold, Field-portable, high-speed GC/TOFMS, *J. Am. Soc. Mass Spectrom.* 12 (2001) 648–655.

- [236] J.D. Fair, W.F. Bailey, R.A. Felty, A.E. Gifford, B. Shultes, L.H. Volles, Method for rapid on-site identification of VOCs, *J. Environ. Sci.* 21 (2009) 1005–1008.
- [237] H.Q. Li, C.H. Deng, X.M. Zhang, Fast field analysis of short-chain aliphatic amines in water using solid-phase microextraction and a portable gas chromatograph, *J. Separ. Sci.* 31 (2008) 3225–3230.
- [238] J.A. Contreras, J.A. Murray, S.E. Tolley, J.L. Oliphant, H.D. Tolley, S.A. Lammert, E.D. Lee, D.W. Later, M.L. Lee, Hand-portable gas chromatograph-toroidal ion trap mass spectrometer (GC-TMS) for detection of hazardous compounds, *J. Am. Soc. Mass Spectrom.* 19 (2008) 1425–1434.
- [239] R. Lam, C. Lennard, G. Kingsland, P. Johnstone, A. Symons, L. Wythes, J. Fewtrell, D. O'Brien, V. Spikmans, Person-portable equipment in environmental forensic investigations: application to fire scenes, *Aust. J. Forensic Sci.* 50 (2018) 672–681.
- [240] P. Lutter, M.C. Savoy-Perroud, E. Campos-Gimenez, L. Meyer, T. Goldmann, M.C. Bertholet, P. Mottier, A. Desmarchelier, F. Monard, C. Perrin, F. Robert, T. Delatour, Screening and confirmatory methods for the determination of melamine in cow's milk and milk-based powdered infant formula: validation and proficiency-tests of ELISA, HPLC-UV, GC-MS and LC-MS/MS, *Food Contr.* 22 (2011) 903–913.
- [241] L. Cercaci, M.T. Rodriguez-Estrada, G. Lercker, Solid-phase extraction-thin-layer chromatography-gas chromatography method for the detection of hazelnut oil in olive oils by determination of esterified sterols, *J. Chromatogr. A* 985 (2003) 211–220.
- [242] D.S. Jackson, D.F. Crockett, K.A. Wolnik, The indirect detection of bleach (Sodium hypochlorite) in beverages as evidence of product tampering, *J. Forensic Sci.* 51 (2006) 827–831.
- [243] T. Cajka, K. Riddellova, M. Tomaniova, J. Hajslova, Recognition of beer brand based on multivariate analysis of volatile fingerprint, *J. Chromatogr. A* 1217 (2010) 4195–4203.
- [244] L. Pillonel, S. Ampuero, R. Tabacchi, J.O. Bosset, Analytical methods for the determination of the geographic origin of Emmental cheese: volatile compounds by GC/MS-FID and electronic nose, *Eur. Food Res. Technol.* 216 (2003) 179–183.
- [245] A.I. Cabanero, J.L. Recio, M. Ruperez, Isotope ratio mass spectrometry coupled to liquid and gas chromatography for wine ethanol characterization, *Rapid Commun. Mass Spectrom.* 22 (2008) 3111–3118.
- [246] C.A. Valdez, R.N. Leif, S. Hok, B.R. Hart, Analysis of chemical warfare agents by gas chromatography-mass spectrometry: methods for their direct detection and derivatization approaches for the analysis of their degradation products, *Rev. Anal. Chem.* 37 (2018) 26.
- [247] R. Subramaniam, C. Astot, L. Juhlin, C. Nilsson, A. Ostin, Direct derivatization and rapid GC-MS screening of nerve agent markers in aqueous samples, *Anal. Chem.* 82 (2010) 7452–7459.
- [248] J.C. Hoggard, J.H. Wahl, R.E. Synovec, G.M. Mong, C.G. Fraga, Impurity profiling of a chemical weapon precursor for possible forensic signatures by comprehensive two-dimensional gas chromatography/mass spectrometry and chemometrics, *Anal. Chem.* 82 (2010) 689–698.
- [249] R.K. Eyison, S. Sezigen, M. Ortatatli, L. Kenar, Optimized gas chromatography-tandem mass spectrometry for 1,1'-sulfonylbis 2-(methylthio)ethane quantification in human urine, *J. Chromatogr. Sci.* 57 (2019) 397–402.
- [250] M. Imran, N. Kumar, V.B. Thakare, A.K. Gupta, J. Acharya, P. Garg, Sampling and analyses of surfaces contaminated with chemical warfare agents by using a newly developed triple layered composite wipe, *Anal. Bioanal. Chem.* 412 (2020) 1097–1110.
- [251] O. Terzic, S. Bartenbach, P. de Voogt, Determination of Lewisites and their hydrolysis products in aqueous and multiphase samples by in-sorbent tube butyl thiolation followed by thermal desorption-gas chromatography-full scan mass spectrometry, *J. Chromatogr. A* 1304 (2013) 34–41.
- [252] A. Sampat, M. Lopatka, M. Sjerps, G. Vivo-Truyols, P. Schoenmakers, A. van Asten, Forensic potential of comprehensive two-dimensional gas chromatography, *Trac. Trends Anal. Chem.* 80 (2016) 345–363.
- [253] K.D.B. Bezemer, M. Koeberg, A. van der Heijden, C.A. van Driel, C. Blaga, J. Bruinsma, A.C. van Asten, The potential of isotope ratio mass spectrometry (IRMS) and gas chromatography-IRMS analysis of triacetone triperoxide in forensic explosives investigations, *J. Forensic Sci.* 61 (2016) 1198–1207.
- [254] S.D. Harvey, K.H. Jarman, J.J. Moran, C.M. Sorensen, B.W. Wright, Characterization of diesel fuel by chemical separation combined with capillary gas chromatography (GC) isotope ratio mass spectrometry (IRMS), *Talanta* 99 (2012) 262–269.
- [255] S.P. Sharma, S.C. Lahiri, Chemical characterization and quantitative estimation of narcotic drugs in the seized illicit samples by GC-MS and GC-FTIR, identification of source and possibility of isotopic substitution, *J. Indian Chem. Soc.* 93 (2016) 1299–1312.
- [256] H.J. Tobias, G.L. Sacks, Y. Zhang, J.T. Brenna, Comprehensive two-dimensional gas chromatography combustion isotope ratio mass spectrometry, *Anal. Chem.* 80 (2008) 8613–8621.

Applications of gas chromatography to multiresidue methods for pesticides and related compounds in food

*Milagros Mezcuá, M. Angeles Martínez-Uroz,
Amadeo R. Fernández-Alba*

Pesticide Residue Research Group, University of Almería, La Canada de San Urbano, Almería, Spain

31.1 Introduction

Plant production yield is being continually affected by harmful organisms. It is essential to protect plants and plant products against such organisms in order to prevent a reduction in yield or damage to the plants or plant products and to ensure both the quality of the products harvested and high agricultural productivity. The use of active substances in plant protection products is one of the most common methods of protecting plants and plant products from the effects of harmful organisms. In some cases, these products act by confusing insects or making crops less palatable for pests. However, more commonly, the damaging insects, weeds, or fungi are killed by chemicals. Such pesticides have potentially severe undesirable effects if they are not strictly regulated. A possible consequence of their use may be the presence of residues in the treated

products, in animals feeding on those products, and in products of animal origin.

Maximum residue levels (MRLs) are the upper legal concentration levels acceptable for pesticide residues in or on food or feed based on Good Agricultural Practices (GAP) and which ensure the lowest consumer exposure possible.

Regulatory and public concern over pesticide residues in food has been increasing due to the potential health hazards. Measuring trace levels of pesticides in the presence of large amounts of sample matrix components that occur naturally is a challenging task. There is growing interest in developing simple, rapid, cost-effective, and reliable analytical methods to ensure that the levels of toxic pesticides incurred in produce are below tolerance levels.

Multiresidue methods (MRMs) are undoubtedly one way of addressing the problem of

pesticide determination and are worth evaluating given the great diversity of these groups of compounds. However, the complex sample matrix may contain abundant quantities of components that can interfere with good sample analysis.

For the development of an MRM, two important aspects must be taken into account. The first issue to consider is the extraction method employed. Next, compounds with different physicochemical properties and different structural characteristics are included in the scope of an MRM, making it necessary to employ extraction methods with a wide versatility.

The first notable MRM was the Mills method developed in the 1960s for the determinations of nonpolar organochlorine pesticides in nonfatty food. The Mills method was based on acetonitrile extraction, the extract was then diluted with water, and the pesticides were partitioned into a nonpolar solvent. The follow-up research was oriented toward extending the analytical polarity range to cover a wider range of polarity of pesticides analyzed in a single procedure. New solvents for initial extraction and addition of sodium chloride for the partitioning step were used and were tested to reach higher recoveries of the more polar analytes. In the 1980s, environmental and health concerns led to the avoidance of dangerous solvents; later, solid-phase extraction (SPE) was established and to avoid liquid–liquid partitioning and as a cleanup step. Increased urgency to further reduce solvent usage and manual labor led to the introduction of several alternative extraction approaches: matrix solid-phase dispersion (MSPD), supercritical fluid extraction (SFE), and solid-phase microextraction (SPME). In 2003, Anastassiades et al. developed a quick, easy, inexpensive, effective, rugged, and safe method (QuEChERS) based on solid–liquid extraction (SLE) using AcN as the extraction solvent, aimed to overcome critical flaws and practical limitations of existing methods [1].

On the other hand, the instrumental methods need to be able to identify a multiclass group of compounds; in this sense, mass spectrometry detectors offer a greater advantage than traditional detectors. To ensure the desired level of analytical selectivity and sensibility by gas chromatography–mass spectrometry (GC-MS), the regulatory and commercial testing laboratories usually adopt selective techniques such as tandem mass spectrometry (MS/MS) or selected ion monitoring (SIM) to get better sensitivity as compared to full scan techniques. Due to wide diversity in the natural and indirect sources of contamination in food, target-oriented residue monitoring by MS/MS or SIM often fails to provide holistic assessment of the contamination status of any food sample.

This overview focuses on a revision of MRMs based on GC-MS published for the determination of pesticides in different groups of food: crops, animal origin food, processed food, and baby food. Within these groups of food, published work from 2005 until recently has been reviewed. Due to the large amount of published MRMs for pesticides in food, especially for crops, not all published work has been referenced in this chapter; a selection has been made detailing the most representative techniques.

31.2 Multiresidue methods for pesticides in crops

Plant food can be contaminated by pesticides under a great variety of circumstances and at different times preceding their consumption. Many factors can reduce such contamination (e.g., rainfall, wind, chemical reactions induced by oxygen, moisture, light, or plant enzymes). The number of publications that describe MRMs for the determination of pesticides in crops is very high; from 2009 to now there are more than 30 publications describing MRMs

for determination of pesticides in crops by GC-MS, and most of them are for fruits and vegetables. The past few years have been reviewed in this work. An overview of these methods is shown in [Table 31.1](#).

The scope of multiresidue revised methods varies between 14 and 346 pesticides, the limits of detection (LOD) published for all authors meet with the actual legislation, and very good recoveries are achieved for all employed methods. In this section, we will describe the more critical aspects that can affect the obtained results after the application of an MRM.

Most of the extraction methods are employed for the determination of pesticides based on SLE; acetonitrile is the solvent of choice for most authors [2–13]. SLE methods have been developed in general miniaturized methods with a small amount of sample and extraction solvent, with the exception of Chen et al. [14], SLE allows recoveries between 70% and 120%, as can be seen in [Table 31.1](#).

Stir bar sorptive extraction is employed for the determination of 20 pesticides in different vegetables [15]; this technique provides very good LOD but recoveries are in the range of 10%–110%, and recoveries were even lower than 20% for matrices such as green beans, onions, tomatoes, and green peppers.

Other extraction techniques such as microwave-assisted extraction (MAE) [16], SPME [17], and MSPD [18,19] have been employed for the determination of pesticides in crops. Cleanup steps are employed in some cases; the technique of choice is dispersive SPE using PSA as a dispersive agent.

Regarding sample injection, 1 μL is, in general, injected in a splitless mode, but various authors select a large volume injection mode (20 μL) using a temperature program in the injection ports when programmed-temperature vaporizing injectors are used; however, no significant differences in LOD can be assigned to the different volumes of injection, as can be observed in [Table 31.1](#).

Regarding chromatographic separation, a nonpolar analytical column has been employed in most methods with a stationary phase composition of 5% phenyl/95% dimethylpolysiloxane.

The selection of the instrumental method, together with the selection of the extraction methods, is the most important choice for the correct identification and quantification of target compounds; MRMs for determination of pesticides in crops in past years have been focused on the use of MS as a detection system. The ionization mode in MS is one of the aspects to consider when a method must be selected. The most current methods for multiresidue analysis in crops are based on electron impact ionization; however, the compounds with highly electronegative elements, such as halogen, oxygen, etc., afforded high sensitivity in the pesticide analysis with the negative chemical ionization (NCI) mode. If the chemical ionization mode is used, the chromatograms obtained are cleaner due to the minimization of background interferences from ions derived from the sample matrix than when using electron ionization. NCI is specially recognized for improved selectivity and sensitivity for organochlorine and organophosphorus compounds. The MS methods developed in NCI [4,10,11,20] show very low LOD and quantification.

Different analyzers have been used, such as MRMs, quadrupole, ion trap (IT), triple quadrupole, and time-of-flight (TOF). When a TOF analyzer was used [9], 150 pesticides were analyzed in less than 10 min. The selectivity that provides the measurement of exact mass in full scan mode without the need to create a retention time window makes this analyzer an excellent tool for high-scope MRMs. However, the absence of fragments by collision induced in some pesticides makes necessary the confirmation of pesticides with another technique; this is a limitation in the use of these detectors in target methods. In recent years, they are used for the development of screening methods [21].

TABLE 31.1 Overview of multiresidue methods for determination of pesticides in crops.

Matrix	Analytical technique	Injection	Column	Cleanup	Extraction method	Scope	LOD/LOQ	Recoveries%	References
Grapes	GC-MS-SIM (EI) quadrupole	1 μ L splitless	DB-1701	Dispersive SPE (PSA)	Solid–liquid with acetonitrile	346	1.7–266/Nd μ g kg ⁻¹	60–120	[2]
Green vegetables	GC-MS-SIM (EI) ion trap	1 μ L on column injection	ZB-5MS	Dispersive SPE (PSA)	Solid–liquid with acetonitrile	16	0.03–0.1/0.1–0.5 μ g kg ⁻¹	85–112	[3]
Lettuce, orange, strawberry, plum	GC-MS-SIM (NCI) quadrupole	2 μ L solvent vent	CP-Sil 8 CB	Dispersive SPE (PSA)	Solid–liquid with acetonitrile	26	0.00015–0.619/ 0.0005–2.356 μ g L ⁻¹	70–110	[4]
Orange, grape, pear, and apple	GC-MS-(EI) quadrupole SCAN and SIM simultaneously	1 μ L splitless	ZB-5MS		MSPD	31	9–250/N ⁻¹ .d μ g kg ⁻¹	62–116	[18]
Corn muffin and cocoa beans	GC-MS-(SIM) (EI) quadrupole	5 μ L solvent vent mode	RTX5MS	Disposable pipette extraction (DPX)	Solid–liquid with acetonitrile	27	0.90–12.48/2.73–37.8 μ g kg ⁻¹	87–135	[5]
Grape, pomegranate, mango	GC-MS-MRM (EI) ion trap	20 μ L PTV LVI	VF 5MS	Dispersive SPE (PSA and GCB)	Solid–liquid with acetonitrile	50	Nd/10–20 μ g kg ⁻¹	70–120	[6]
Lettuce, spinach, green bean, green pepper, tomato, broccoli, potato, carrot, and onion	GC-MS-(SIM) (EI) quadrupole	20 μ L solvent vent mode	TRB 5MS		Stir bar sorptive extraction followed by liquid desorption	20	0.01–10 μ g kg ⁻¹	10–110	[15]
Leeks	GC-MS/MS (EI) (triple quadrupole)	1 μ L in splitless mode.	TR-5MS	Dispersive SPE (PSA and GCB)	Solid–liquid with acetonitrile (pretreatment with microwave)	20	0.07–1.5/0.25–5 μ g kg ⁻¹	81–109	[7]
Tomato, strawberry, potato, orange, and lettuce	LP-GC-MS (EI) (time-of-flight)	10 μ L in solvent vent mode	Rti-5MS	Dispersive SPE (PSA) and DPX	Solid–liquid with acetonitrile	150	25 μ g kg ⁻¹	70–120	[56]
Rice, soybean, potato, spinach, cabbage, apple, orange, cacao pumpkin, and green tea			DB-17			10	10 μ g kg ⁻¹	72–120	[8]
Mix of vegetables	GC-MS/MS (EI) (triple quadrupole)	1 μ L in splitless mode	TR-5MS		MSPD	15	0.7–32 μ g kg ⁻¹	73–111	[9]

Garlic, onion, spring onion, and chili	GC-MS-(SIM) (NCI) quadrupole	1 μ L in pulsed splitless mode	HP-5MS	Dispersive SPE (PSA and GCB) additionally C18 for chili	Solid-liquid with acetonitrile-hexane	17	0.02–6 μ g kg ⁻¹	54–129.8	[19]
Wheat grains, flour, and bran	GC-MS-(SIM) (NCI) triple quadrupole	2 μ L no data mode	VF-5MS	Dispersive SPE (C18)	Solid-liquid with acetonitrile	24	2.5/5–10 μ g kg ⁻¹	70–120	[18]
Fruits and vegetables (1-year survey)	GC-MS/MS (EI) triple quadrupole	6 μ L large volume injection technique	VF-5MS	Dispersive SPE (PSA)	Solid-liquid with acetonitrile	121	1–3/10 μ g kg ⁻¹	80–116	[10]
Pak choi, cabbage, legumes, leaf mustard (3-year survey)	GC-MS-(SIM) (EI) quadrupole (only for confirmation)	1 μ L no data mode	DB-1701		Solid-liquid with ethyl acetate	22	10 μ g kg ⁻¹	80–120	[11]
Berries (raspberry, strawberry, blueberry, and grape)	GC-MS-(SIM) (EI) quadrupole	1 μ L in splitless mode	DB-1701	SPE	Solid-liquid with acetonitrile	88	6–50/20–150 μ g kg ⁻¹	63–137	[12]
Grape	GC-MS-(SIM) (EI) quadrupole	Splitless mode (no data about volume)	AT.RPA-1	Extraction and cleanup in one step with SiO ₂ fiber	25	0.48–1.4/ 1.6–28 μ g L ⁻¹	61–108	24	[14]
Fruits and vegetables	GC-MS-(SIM) for quantitation GC-MS-(full scan) for screening (EI) quadrupole	20 μ L in solvent vent mode	HP-5MS	Dispersive SPE	MAE with acetone and acetonitrile	72	2–20/25–100 μ g kg ⁻¹	72–114	[57]
Carrot and orange	GC-MS-(SIM) (EI) quadrupole	2 μ L in splitless mode	DB-17	Disposable pipette extraction	Solid-liquid with acetonitrile	36	0.2–28.6/0.4–96.2 μ g kg ⁻¹	72–116	[58]
Grapes	GC-MS/MS (EI) ion trap	20 μ L PTV-LVI program	TR-5MS	Dispersive SPE (PSA)	Solid-liquid with ethyl acetate	21	0.5–3.1/2.5–10 μ g kg ⁻¹	77–115	[59]
Mangoes	GC-MS-(SIM) (EI) quadrupole	Splitless mode, injection by desorption of fiber	RTX-1		SPME	14	1.0–3.3/3.3–33.3 μ g kg ⁻¹	71.6–117.5	[60]
Cabbage and apples	GC-MS/MS (NCI) triple quadrupole	10 μ L PTV LVI program	RTX-5MS	Dispersive SPE (PSA and C18)	Solid-liquid with acetonitrile	82	0.01–1.82/0.03–6.46 μ g kg ⁻¹	58.7–124.4	[17]

The use of a quadrupole analyzer in the SIM mode is an excellent tool for the target method because of the good selectivity in comparison to full scan. The problem with this configuration is that when the scope of the required method is high, it is more convenient to develop various SIM methods in order to assure good selectivity [2], which involves increased processing time since it involves several injections per sample.

Therefore, the best tool for MRMs is the use of triple quadrupole or IT with the capacity to work in MS-MS, which provides good sensitivity and selectivity.

It is well known [22,23] that suppression in the signal in GC is due to a gradual accumulation of nonvolatile matrix components in the GC system, resulting in the formation of new active sites and a gradual decrease in analyte responses. The presence of matrix effects and their extent are simultaneously influenced by several factors (matrix concentration, pesticide concentration, matrix type, and analytical range). The matrix sample diversity and the different possibilities of interactions that can occur within the sample/pesticide/chromatographic system make it difficult to establish a trend for the matrix effect of each pesticide in each matrix. Therefore, the quantitation based on the use of analytical standards prepared in a blank matrix extract (matrix-matched calibration) to compensate for the matrix effect and to obtain more accurate results is commonly used in MRMs for pesticides in crops and in the other groups of food commodities considered in this chapter.

The average in the reported limits of quantification is 10 $\mu\text{g kg}^{-1}$; the lowest limits of quantification are achieved when NCI is employed.

31.3 Multiresidue methods for pesticides in animal origin products

The diversity of matrices in animal origin products makes it difficult to establish general trends in MRMs, especially in the extraction stage of the method.

In this section, MRMs reviewed will be commented upon while focusing on the class of pesticides in order to give a homogeneous point of view.

A nonpolar analytical column has been used in all cases with a stationary phase composition of 5% phenyl/95% dimethylpolysiloxane.

Concerning organochlorinated pesticides, they have been analyzed in eggs [24], honey [25], and fish [26]; the extraction methods employed were MSPD, ASE, and SEME, respectively; better LOD were achieved in honey. In all cases, good recoveries were achieved; IT or quadrupole, in electron impact ionization and SIM mode, has been selected for all methods.

Organophosphorus pesticides have been analyzed in cow milk by HS-SPME [27]; LOD between 2.2 and 10.9 and limits of quantification between 6.5 and 32.9 $\mu\text{g kg}^{-1}$ have been reported. A quadrupole mass spectrometer operated in the electron ionization SIM mode was employed. A group of organophosphate pesticides has been analyzed in honey [28], the extraction method employed is coacervative microextraction ultrasound-assisted back-extraction procedure, with LOD between 0.03 and 0.47 $\mu\text{g kg}^{-1}$ and recoveries higher than 90%. An IT has been used in the electron ionization mode.

Different MRMs have been developed for the determination of pyrethrins and pyrethroids in fish [29], porcine muscle, and pasteurized milk [30]. For fish, SLE with acetonitrile was performed followed by DSPE with PSA and C18 for cleanup, the injection was in splitless mode, and analysis was made by GC-MS in NCI and SIM modes. Recoveries were in the range 70%–115%, LOD achieved were between 0.3 and 0.5 $\mu\text{g kg}^{-1}$. For porcine muscle and pasteurized milk, a liquid–liquid extraction (LLE) was employed, the identification was made by GC-MS with electron ionization in the SIM mode, recoveries were in the range of 83%–109%, and very high LOD and quantification were reported, between 3 and 9 mg kg^{-1} and between 10 and 24.6 mg kg^{-1} , respectively.

Multiclass MRMs have also been developed for the determination of pesticides in animal origin products. For determination of pesticides in honey, single drop microextraction, LLE [31], and LLE and low-temperature purification [32] were used. In animal fat, SLE with AcN and n-hexane followed by dispersive SPE [33] has been developed. In honey, MS was used only for confirmation; 1 μ L was injected in the splitless mode, and analyses were performed in full scan and electron impact ionization modes. For animal fat, 4 μ L was injected in a PTV inlet in a solvent vent mode, a quadrupole was used for identification and quantification in electron impact ionization in the SIM mode.

31.4 Multiresidue methods for pesticides in processed food

31.4.1 Juice

Fruit juices are low-fat and nutritious beverages, and their consumption can help to fulfill the recommendation to eat more fruits and vegetables. Fruit juice sales in the two major markets, Europe (EU) and United States of America (USA), show a steady increase with sales volumes in both regions at some 11 billion liters per year. Simultaneously, safety concerns have increased in consumers and authorities about these products. Pesticide residues resulting from the treatment of raw fruits or from the water used in the processing are undoubtedly one of the major problems to human health due to their toxicity. Despite the progressive introduction of good practices in production, regulation, and scrutiny in the fruit juice industry to prove that the fruit juices are safe for consumption, the presence of pesticide residues remains a real problem.

In EU and other countries in the world, the MRLs of pesticides are established for raw agricultural commodities and not for processed products. However, pesticide residue levels

found in a fruit juice depend on the various factors such as the type of pesticide, process applied, commodity, and degradation process involved. Thus far, EU and USA have prepared recommendations on principles and practices to the establishment of MRLs for fruit juice and other processed food [34].

Different extraction methods have been developed for the determination of pesticides in juices. In Zuin et al. [35], SBSE and MASE are compared for the determination of 18 pesticides in sugar cane juice. SBSE provides better LOD values, precision, and linearity, whereas MASE resulted in better recoveries, being faster, simpler, and fully automated.

Other extraction techniques employed for pesticides in juices are: dispersive LLE for analysis of 25 pesticides in apple [36], in which an efficient and highly reproducible extraction was achieved for all pesticides assayed; SPE [37] for the determination of 52 pesticides in carrot, peach, grape, orange, pineapple, and apple; and extraction with acetonitrile for the determination of 141 pesticides in apple juice [38].

The scope of the reviewed methods is between 18 and 141 pesticides, electron impact ionization is the technique of choice for the determination of pesticides in juice, and most of authors select the SIM mode for method development in order to achieve a good sensitivity. However, for a high number of pesticides, this mode of work does not allow the selectivity required for MRMs in food commodities [39]; similar LODs are achieved working in full scan and SIM mode, as shown in Fig. 31.1 [internal communication]. In a method developed for the determination of 141 pesticides in the SIM mode, the method was divided in two methods, which include 62 and 79 pesticides, respectively, in order to achieve good results [38].

One of the major obstacles in the effective GC-MS analysis is the complexity of food matrixes and the presence of interferences that increase the need for cleanup steps, limit the ruggedness

of the instrumental methods, and make low-level pesticide identification and quantification difficult. The use of multidimensional GC (with two different mechanisms of separation) can help solve this problem due to the effective increase in the selectivity and, consequently, in the resolution of the analytes. Cunha et al. [36] have developed and validated a fast analytical

MD-GC-MS method for evaluation of multiple pesticide residues in apple juice; the potential of a dual GC column system connected by a Deans' switch device was tested in combination with fast GC-MS.

Albero et al. [37] describe a method based on SPE followed by GC-MS (SIM) in which many compounds presented an increase in their

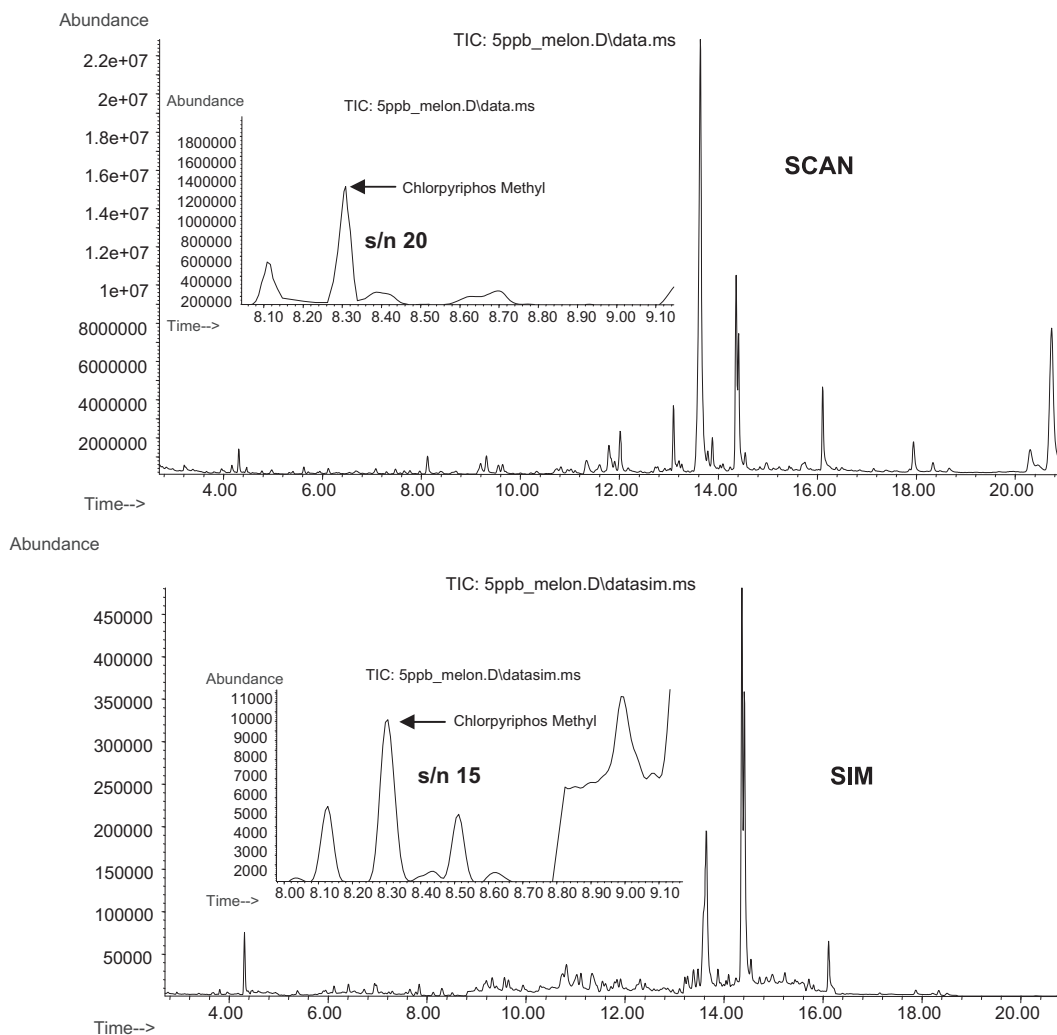


FIGURE 31.1 Total ion chromatograms in full scan and SIM of a melon extract spiked at $5 \mu\text{g kg}^{-1}$ with a mixture of 95 pesticides. The areas of the chromatograms where chlorpyrifos methyl elutes are magnified are shown. Signal-to-noise ratios of chlorpyrifos methyl are shown in the chromatograms.

chromatographic response, some of them from two- to fivefold, although organochlorine pesticides were the compounds that presented the lowest matrix effect. Sample components may compete for the active sites of the glass liner, decreasing the interaction between the active sites of the glass liner and the analyte, and thus a larger amount of analyte is transferred to the chromatographic column.

In general, LOD achieved by the authors for the determination of pesticides in juices are between 0.06 and 5 $\mu\text{g L}^{-1}$; the method that allows better sensitivity is DLLME followed by MD-GC-MS [36].

31.4.2 Wine

Fungicides, insecticides, and herbicides are commonly used in viticulture. Vineyards are treated with these products in the final stage of vegetation to prevent attack, which may occur shortly before the harvest.

Different MRMs have been developed for the determination of pesticides in wine; most of the research describes development of methods for wine, grapes, and must.

The reviewed bibliography involves very different extraction methods: extraction with solvent, SPE, and solvent bar microextraction. Dasgupta et al. developed an extraction with ethyl acetate for the determination of 160 pesticides followed by cleanup by dispersive SPE with PSA [40]; Cunha et al. employed acetonitrile as a solvent for the extraction of 16 pesticides; and the cleanup is performed by dispersive solid extraction as well, but with PSA and C18 [41].

SPE [42] has been optimized for the determination of 16 organochlorinated pesticides in wine; the sorbent and the percentage of ethanol in the sample were optimized for a quantitative extraction of the selected compounds, 30% of ethanol and HySphere Resin SH Cartridges were selected as optima.

Solvent bar microextraction was developed for the determination of only six pesticides in

wine [43]; different aspects of the extraction were optimized: hollow fiber, extraction solvents, extraction time, temperature, and finally the effect of ionic strength and ethanol addition. Once optimized, the limits of detection at the fg ml^{-1} level were achieved. Obviously, this extraction method allows better sensitivity than others, but the number of compounds analyzed is low.

Residue monitoring by unit-resolution GC-MS can be suitably performed on either a quadrupole or TOF instrument. For a complex mixture of analytes, a TOF mass spectrometer, when coupled with a fast GC system, can perform simultaneous analyses of a large number of compounds within a reasonably short time period with sufficient accuracy, which is otherwise not possible with slower, scanning type mass detector (MS) such as quadrupoles or ITs. In the case of multiresidue screening by GC-MS full scan, the separation of a large component mixture is often a challenging task due to limited peak capacity and the resulting coelution of interfering matrix compounds. Since peak deconvolution algorithms require sufficient sampling to resolve complex peaks, correct identification of residues at trace levels becomes less likely as more compounds coelute at a single location in the chromatogram. Such analytical problems can however be resolved with comprehensive two-dimensional gas chromatography ($\text{GC} \times \text{GC}$).

Two-dimensional GC-TOF-MS has been developed for the determination of 160 pesticides in wine [40]; it provides advantages in terms of sensitivity, precision, and accuracy. In addition, the possibility of false negatives is reduced with the lower detection limits offered. Matrix effects can be solved by using $\text{GC} \times \text{GC}$ since baselines of compounds with common ions with matrix components can be separated.

A fast low-pressure GC-MS method [41] was optimized for the determination of 27 pesticides in wine; in this method, using a column of 15 m length and 0.32 mm internal diameter, the carrier

gas was set at 2.6 mL min^{-1} constant flow; with this condition, a shorter run time can be obtained than with conventional GC. The acquisition was performed in the SIM mode and matrix effects were resolved by the use of matrix match solutions.

GC-MS in tandem is the most commonly used MRM method for the determination of pesticides in wine, such as heptachlor, aldrin, endrin, endosulfan, and dieldrin [42,43].

31.4.3 Oil

The development of sample-treatment procedures for the isolation of pesticides in samples with relatively high fat content ($>15\%$), such as olive samples, by chromatographic techniques, requires the complete removal of the high-molecular-mass fat from the sample to maintain the chromatographic system in working order. The main problem associated when working with these kinds of matrices is that dirty extracts with even small amounts of fat may harm the whole system (columns and detectors). For this reason, an additional cleanup step is usually included in MRMs for the determination of pesticides in processed food, such as oil. In addition, the development of MRMs to control a large number of compounds is highly desirable. However, the different natures and physicochemical properties of the classes of compounds to be studied (e.g., organochlorines, organophosphorus compounds, and triazines) make it even more complex to establish extraction methodologies.

For the analysis of pesticides in the oil samples, several methods were used, such as SPE, gel permeation chromatography (GPC), SPME, MSPD, and SFE.

A total of 95 pesticides including organophosphate, organochlorines, carbamates, triazines, triadiazines, and pyrethroid compounds were extracted from soybean oil by LLE (oil solved in n-hexane was extracted with acetonitrile

followed by centrifugation, freezing, and dispersive SPE as a cleanup step, using florisil as a sorbent [44]). Determination of 33 pesticides in peanut oil used low-temperature cleanup at -20°C for oil precipitation after extraction with ACN and dispersive SPE using PSA and C18 as a sorbent [45].

Eight pesticides in virgin olive oil were determined by carbon nanotube-based SPE [46] without additional cleanup steps.

Extraction with n-hexane and acetonitrile followed by a cleanup step of GPC was applied for the determination of 26 pesticides from olive oil [47,48]. An MSPD method was validated for the determination of nine pesticides in olive oil; aminopropyl was used to prepare the dispersion with the oil, and florisil was employed for the cleanup in one unique step [49]. A nonpolar analytical column has been used with a stationary-phase composition of 5% phenyl/95% dimethylpolysiloxane.

For analytical determination, most authors develop MRMs using quadrupole in electron impact ionization in the SIM mode; in general, $1 \mu\text{L}$ is injected in the splitless mode [44–46,49]; however, there are some applications in which an IT is employed in the determination of 30 pesticides using electron impact ionization in the MS/MS mode [48]. Other applications have been developed using electron impact ionization and chemical ionization simultaneously [47].

31.5 Multiresidue methods for pesticides in baby food

Baby food is any food that is made specifically for infants, roughly between the ages of 6 months and 2 years. Baby foods combine a wide range of different matrices: nonfatty baby foods based on fruits and vegetables, fatty food based on meat/egg/cheese, and cereal-based foods. Moreover, breast milk and infant formulas are also included. The EU Baby Food Directive 2006/

125/EC on processed cereal-based foods and processed foods for infants and young children places emphasis on the control of pesticides or transformation products (including metabolites) of pesticides with a maximum acceptable daily intake of $0.0005 \text{ mg kg}^{-1}$ body weight. Pesticides are either designated as prohibited, and considered not to have been used if their residue does not exceed $3 \text{ } \mu\text{g kg}^{-1}$, or have MRLs set between 4 and $8 \text{ } \mu\text{g kg}^{-1}$. Twelve of the pesticides and breakdown products listed in the Directive (cadusafos, ethoprophos, fipronil, fipronil-desulfinyl, heptachlor, trans-heptachlor epoxide, hexachlorobenzene, nitrofen, aldrin, dieldrin, endrin, and dimethoate) are suitable for multiresidue analysis by GC-MS. The remaining compounds specified in the Directive, because of their physicochemical properties, require analysis either by multiresidue liquid chromatography-mass spectrometry (LC-MS) or by specific single residue methods.

MRLs applied to the analysis of baby food need to be sensitive enough to meet the current directives mentioned earlier. In this chapter, MRLs based on GC-MS have been reviewed; the most common matrices analyzed are processed fruits such as purees, milk infant formulas, meat, and vegetables [50–52].

The scope of the MRM for baby food is between 12 and 17; nonpolar columns are employed in most of the cases.

Special attention is focused to development of methods for pesticides listed in the Directive 2006/125/EC [53].

Regarding the extraction techniques, SLE with acetonitrile followed by different variations concerning the cleanup step in the extraction is the extraction method of choice for most authors when meat, fruits and vegetables are analyzed.

However, other different extraction methods have been developed for multiresidue determination of pesticides in baby food. DI-SPME-GC-MS has been employed for analysis of carrots, vegetables, chicken with rice, chicken

with vegetables, and lamb with vegetables. SPME is an environmentally nonharmful pre-concentration system that avoids the use of organic solvents and cleanup steps, thus reducing the sample preparation time and allowing low detection limits [54].

SLE as a modification of the QuEChERS method by using a triple partitioning extraction between water, can, and hexane to considerably reduce lipophilic coextracts generally present at high levels in baby food is used for the multiresidue analysis of pesticides in meat-based baby food. A wide scope is achieved and 236 pesticides are analyzed [52]; this method allows a pre-concentration factor of 10 and very low LOD and quantification are achieved, 0.03 and 0.1, respectively.

For apple and apple purée, four sample preparation methods were tested [50]: a modified QuEChERS method utilizing column-based SPE cleanup instead of dispersive SPE provides lower recoveries, but slightly better LOQs. The modified Schenck's method with the best cleaning efficiency provides the lowest LOQs, while MSPD provides the worst cleaning related to the highest LOQs. The QuEChERS method, without any evaporation step, offers extreme improvement in rapidity and simplicity in comparison with the other methods tested. This makes the QuEChERS method the most attractive and useful in the ultratrace analysis of pesticides.

An SLE method (modified QuEChERS citrate) has been evaluated and applied to samples of fruits intended to be baby food [55]; the method has proven to be fast, easy to conduct, and used only small quantities of reagents. The results showed quite good analytical performance in terms of good repeatability, and recovery was achieved in almost all cases for the studied matrices.

When analyzing milk infant formulas, one of the main problems associated with the analysis is the high lipid content, lipids often coextracted with the analytes of interest. It is well known

that, in GC, large amounts of injected fat may cause problems in the injector and at the top of the column. To avoid some of the main disadvantages of the cleanup steps, such as reducing sample treatment time and minimizing the organic solvents consumed, modern extraction techniques are being applied. Such is the case with the pressurized liquid extraction (PLE) technique, which allows the combination of selective extraction with integrated cleanup strategies, by using fat-retainer compounds placed in the PLE extraction cell [51].

Recoveries achieved in the employed method are generally between 70% and 120%.

The analytical determinations in MRMs for pesticides in baby food have been performed by using different analyzers; ion trap (IT) in full scan mode has been employed by Cieslik et al. [55] and Przybyloski et al. [52]. Quadruple in the SIM mode has been used by Viñas et al. [54] and Hercegová et al. [50]. A more selective and sensitive technique has been used by Leandro et al. [53], who employ TSQ in the MS/MS mode, and Mezcuca et al. [51], who employ IT in the MS/MS mode.

Few pesticides have been found in baby food and concentrations are lower than the established limits; the highest concentration in milk infant formula was $5.03 \mu\text{g kg}^{-1}$ of alpha endosulfan.

31.6 Conclusions

Attending to the extraction procedure in the selected MRMs for determination of pesticides in food commodities, for crops the extraction technique of choice is SLE with acetonitrile as a solvent, followed in some cases by dispersive solid extraction as cleanup; MRMs in products of animal origin are characterized by the diversity in extraction strategies, depending on the specific matrix.

In oil matrices, the main characteristic in the extraction procedure is the need to remove the high molecular compounds that can interfere in the determination of pesticides; this is mainly performed by GPC in the selected MRMs for determination of pesticides in food commodities.

Low-volume injection ($1 \mu\text{L}$) in the splitless mode is generally the injection technique of choice for most authors. The chromatographic separation is performed by the use of a nonpolar analytical column with a stationary-phase composition of 5% phenyl/95% dimethylpolysiloxane. In all reviewed papers, a higher number of methods describe the analytical determination using quadrupole as an analyzer in the SIM mode, followed by a lower number of publications that employ an IT analyzer in the MS/MS mode; electron impact ionization is the ionization mode selected by most authors. In general, there are a scarce number of methods that employ chemical ionization as the ionization mode.

Recoveries achieved are generally in the range 70%–120%. Limits of quantification range between 10 and $25 \mu\text{g kg}^{-1}$.

Acknowledgments

The authors acknowledge funding support from the Junta de Andalucía-FEDER (Project ref. AGR-4047) and from the EU, DG SANCO Specific Agreement No. 5 to Framework Partnership Agreement No. SANCO/2005/FOOD SAFETY/0025-Pesticides in Fruit and Vegetables. Milagros Mezcuca acknowledges the research contract to Junta de Andalucía-FEDER.

References

- [1] A. Hercegová, M. Domotorava, E. Matisová, *J. Chromatogr. A* 1153 (2007) 54–73.
- [2] Y.-J. Lian, G.-F. Pang, H.-R. Shu, C.-L. Fan, Y.-M. Liu, J. Feng, et al., *J. Agric. Food Chem.* 58 (2010) 9428–9453.
- [3] C. Przybylski, V. Bonnet, *Anal. Bioanal. Chem.* 394 (2009) 1147–1159.

- [4] R. Huskova, E. Matisova, S. Hrouzkava, L. Svorc, J. Chromatogr. A 1216 (2009) 6326–6334.
- [5] H. Guan, W.E. Brewer, S.L. Morgan, J. Agric. Chem. 57 (2009) 10531–10538.
- [6] R.H. Savant, K. Banerjee, S.C. Utture, S.H. Patil, S. Dasgupta, M.S. Ghaste, et al., J. Agric. Chem. 58 (2010) 1447–1454.
- [7] J.W. Wong, K. Zhang, K. Tech, D.G. Hayward, C.M. Malovi, A.J. Krynskiy, et al., J. Agric. Food Chem. 58 (2010) 5868–5883.
- [8] L.-J. Qu, H. Zhang, J.-H. Zhu, G.-S. Yang, H.Y. Aboul-Enein, Food Chem. 122 (2010) 327–332.
- [9] U. Koesukwivat, S.J. Lehotay, S. Miao, N. Leepipatpiboon, J. Chromatogr. A 1217 (2010) 6692–6703.
- [10] C.-Y. Shen, X.-W. Cao, W.-J. Shen, Y. Jiang, Z.-Y. Zhao, B. Wu, et al., Talanta 84 (2010) 141–147.
- [11] D.I. Kolberg, O.D. Prestes, M.B. Adaime, R. Zanella, Food Chem. 125 (2010) 1436–1442.
- [12] F.J. Camino Sanchez, A. Zafra-Gomez, J. Ruiz-Garcia, R. Bermudez-Peinado, O. Ballesteros, A. Navalon, et al., J. Food Compos. Anal. 24 (2010) 427–440.
- [13] X. Yang, H. Zhang, Y. Liu, J. Wang, Y.C. Zhang, A.J. Dong, et al., Food Chem. 127 (2011) 855–865.
- [14] C. Chen, Y. Qian, Q. Chen, C. Tao, C. Li, Y. Li, Food Contr. 22 (2011) 114–1120.
- [15] M. Barriada-Pereira, P. Serodio, M.J. Gonzalez-Castro, J.M.F. Nogueira, J. Chromatogr. A 1217 (2010) 119–126.
- [16] G. Satpathy, Y. Kumar Tyagi, R.K. Gupta, Food Chem. 127 (2011) 1300–1308.
- [17] A. Menezes Filho, F. Neves dos Santos, P. Alfonso de Paula Pereira, Talanta 81 (2010) 346–354.
- [18] J.J. Ramos, M.J. Gonzalez, L. Ramos, J. Chromatogr. A 1216 (2009) 7307–7313.
- [19] Q.-B. Lin, H.-J. Shi, P. Xue, Chromatographia 72 (2010) 1143–1148.
- [20] J. Dong, Y.X. Pan, J.-X. Lv, J. Sun, X.-M. Gong, K. Li, Chromatographia 74 (2011) 109–119.
- [21] M. Mezcua, O. Malato, J.F. Garcia-Reyes, A. Molina-Diaz, A.R. Fernandez-Alba, Anal. Chem. 81 (2009) 913–929.
- [22] D.R. Erny, A.M. Gillespie, D.M. Gilvydis, J. Chromatogr. 57 (1993) 638.
- [23] H. Jana, C. Tomas, Food toxicant analysis-Y, in: Picó (Ed.), Gas Chromatography-Mass Spectrometry (GC-MS), Elsevier, 2007 (Chapter 12).
- [24] V.I. Valsamaki, V.I. Boti, V.A. Sakkas, T.A. Albanis, Anal. Chim. Acta 573 (2006) 195–201.
- [25] J. Wang, M.M. Kliskis, S. Jun, Food Res. Int. 144 (2010) 147–151.
- [26] K. Shrivastava, H.-F. Wu, J. Sep. Sci. 38 (2008) 380–386.
- [27] F. de M. Rodrigues, P.R.R. Mesquita, L.S. De Oliveira, S. Fabio, De Oliveira, A. Menezes Filho, A. Pedro, De P. Pereira, et al., Microchem. J. 98 (2011) 56–61.
- [28] A.R. Fontana, A.B. Camargo, J.C. Altamirano, J. Chromatogr. A 1217 (2010) 6334–6341.
- [29] D.F.K. Rawn, J. Judge, V. Roscoe, Anal. Bioanal. Chem. 397 (2010) 2525–2531.
- [30] S. Khay, A.M. Abdel-Aty, J.-H. Choi, E.-H. Shin, H.-C. Shin, J.-S. Kim, et al., J. Sep. Sci. 32 (2009) 244–251.
- [31] N.G. Tsiropoulos, E.G. Amvrazi, J. AOAC Int. 94 (2011) 634–644.
- [32] G. Paulino de Pinho, A. Augusto Neves, M. Eliana Lopes Ribeiro de Queiroz, F. Oliveira Silverio, Food Contr. 21 (2010) 1307–1311.
- [33] M. Castillo, C. González, A. Miralles, Anal. Bioanal. Chem. 400 (2011) 1315–1328.
- [34] A.R. Fernandez-Alba, Beijing, 2009. <http://www.crl.pesticides.eu/library/docs/fv/Beijing2009pdf>.
- [35] V. Gomes Zuin, M. Schellin, L. Montero, J.H. Yariwake, F. Augusto, P. Popp, J. Chromatogr. A 1114 (2006) 180–187.
- [36] S.C. Cunha, J.O. Fernandez, M.B.P.P. Oliveira, J. Chromatogr. A 1216 (2009) 8835–8844.
- [37] B. Albero, C. Sánchez-Brunete, L. José, Tadeo Talanta 66 (2005) 917–924.
- [38] J.-H. Wang, Y.-B. Zhang, X.-L. Wang, J. Sep. Sci. 29 (2006) 2330–2337.
- [39] M. Mezcua, M.A. Martinez-Uroz, P.L. Wylie, A.R. Fernandez-Alba, J. AOAC Int. 92 (2009) 1790–1860.
- [40] S. Dasgupta, K. Banerjee, S.H. Patil, M. Ghaste, K.N. Dhumal, P.G. Adsule, J. Chromatogr. A 1217 (2010) 3881–3889.
- [41] S.C. Cunha, J.O. Fernandes, A. Alves, M.B.P.P. Oliveira, J. Chromatogr. A 1216 (2009) 119–126.
- [42] J. Antonio Perez-Serradilla, J.M. Mata-Granados, M. Dolores Duque de Castro, Chromatographia 71 (2010) 899–905.
- [43] K.-J. Chia, S.-D. Huang, Rapid Comm. Mass Spectrom. 20 (2006) 118–124.
- [44] T. Dong Nguyen, M.H. Lee, G.H. Lee, Microchem. J. 95 (2010) 113–119.
- [45] L. Li, H. Zhang, C. Pan, Z. Zhou, S. Jiang, F. Liu, J. Sep. Sci. 30 (2007), 2097–2104.
- [46] S. López-Feria, S. Cárdenas, M. Valcarcel, J. Chromatogr. A 1216 (2009) 7346–7350.
- [47] E. Ballesteros, A. Garcia Sánchez, N. Ramos Martos, J. Chromatogr. A 1111 (2006) 89–96.
- [48] M. Guardi-Rubio, M.L. Fernández-De Córdoba, M.J. Ayora-Cañada, A. Ruiz-Medina, J. Chromatogr. A 1108 (2006) 231–239.

- [49] C. Ferrer, M.J. Gómez, M. Jose Gómez, J.F. García-Reyes, I. Ferrer, E. Michael Thurman, A.R. Fernández-Alba, *J. Chromatogr. A* 1069 (2005) 183–194.
- [50] A. Hercegová, M. Domotorová, S. Hrouzková, E. Matisová, *Int. J. Anal. Chem.* 87 (2007) 957–969.
- [51] M. Mezcua, M.R. Repetti, A. Agüera, C. Ferrer, J.F. García-Reyes, A.R. Fernández-Alba, *Anal. Bioanal. Chem.* 389 (2007) 1833–1840.
- [52] C. Przbyski, S. Christophe, *J. Sep. Sci.* 32 (2009) 1858–1867.
- [53] C.C. Leandro, R.J. Fussell, B.J. Keely, *J. Chromatogr. A* 1085 (2005) 207–212.
- [54] P. Viñas, N. Campillo, N. Martínez-Castillo, M. Hernández-Córdoba, *J. Chromatogr. A* 1216 (2009) 140–146.
- [55] E. Cieslik, S. Anna, J. Manuel Molina Ruiz, M. Surma-Zamdora, *Food Chem.* 125 (2011) 773–778.
- [56] M.I. Cervera, C. Medina, T. Portolés, E. Pitarch, J. Beltrán, E. Serrahima, et al., *Anal. Bioanal. Chem.* 397 (2010) 2873–2891.
- [57] M. Nakamura, S. Noda, M. Kosugi, N. Ishiduka, K. Mizukoshi, M. Taniguchi, et al., *Food Hyg. Saf. Sci.* 51 (2010) 213–219.
- [58] H.R. Norli, A. Christiansen, B. Holen, *J. Chromatogr. A* 1217 (2010) 2056–2064.
- [59] H. Guan, W.E. Brewer, S.T. Garris, S.L. Morgan, *J. Chromatogr. A* 1217 (2010) 1867–1874.
- [60] K. Banerjee, R.H. Savant, S. Dasgupta, S.H. Patil, D.P. Oulkar, P.G. Adsule, *J. AOAC Int.* 93 (2010) 369–379.

Gas chromatographic analysis of wine*

Susan E. Ebeler

Department of Viticulture and Enology, One Shields Avenue, University of California, Davis,
CA, United States

32.1 Introduction

Following the development of gas chromatography (GC) described in the seminal works of James and Martin in the early 1950s [1–7], among the early applications of GC were studies on the volatile composition of wines [8–12]. GC has continued to be important for understanding wine chemistry, and currently, the applications of GC for analysis of wine are vast. As with other applications, GC analysis of wines has benefited from advances in column technology, improved stationary phases, and new detection methods. Early GC analyses with packed columns and flame ionization detectors provided insights into the alcohol, ester, and aldehyde components that were present in relatively high concentrations and that influenced wine aroma [8–12]. In the mid- to late-1980s, the introduction of capillary columns with high resolving power and

efficiencies resulted in a flurry of research activity and identification of hundreds of new volatile compounds in grapes and wines, including many that are present at trace levels [13,14]. Since the beginning of the 21st century and particularly, over the past decade, there has been a resurgence of activity as multidimensional separations and new hyphenated detection techniques are allowing even greater resolution and sensitivity with more than 200 compounds being detected in a single run [15–17]. Several articles reviewing the gas chromatographic analysis of wine have been published [e.g., 14, 18–22]. This chapter will focus on selected recent applications of GC analysis of wines and alcoholic beverages with a focus on novel stationary phases, detection methods, multidimensional separations, and sample preparation methodologies. The goal of this review is to highlight some selected and emerging trends and to provide insight into some of the

* Dedicated to the memory of Dr. Walt Jennings—a wonderful mentor and friend.

future opportunities and challenges associated with gas chromatographic analysis of wines.

32.2 Stationary phases

The majority of GC separations for wine analysis continue to use poly(dimethylsiloxane)-based and poly(ethylene glycol)-based stationary phases, as reviewed in other chapters of this volume. Since the first edition of this volume, interest in novel GC stationary phases continues [23]. Carbon-based phases, including nanotubes/nanofibers and graphene oxide nanosheets, and ionic liquids have received attention and have been explored as GC stationary phases for wine analysis.

Carbon-based sorbents have been used for isolation and separation of volatiles for many years [24,25]. *Nanostructured carbon-based sorbents* with fullerene-like structures have received attention as stationary phases due to their excellent adsorption and mass transfer properties for a wide range of compounds [26–29]. The nanotubes typically have diameters of <1–50 nm and their structures are generally single-walled or multiwalled with concentric layers (Fig. 32.1) [30–32]. As discussed by Kwon and Park [33], the curved internal surface of nanotubes provides for stronger binding affinities for molecules, as compared to planar carbon surfaces.

Merli et al. [27] used functionalized multiwalled carbon nanotubes to separate alcohols and esters in distilled spirits. The columns gave good separation and quantitation of ethyl acetate, methanol, ethanol, 1-propanol, 2-butanol, 2-methyl-1-propanol, and 3-methyl-1-butanol in these beverages. Analysis of methanol and ethanol can be challenging due to their poor retention on many GC stationary phases; however, with the functionalized nanotube phases, excellent retention and separation of these compounds were obtained. The columns are easy to prepare, reproducible, and less expensive

than traditional stationary phases. However, the functionalized materials have a limited operational temperature range (<200°C) and are currently limited to analysis of low-boiling analytes. In a novel application, Reid et al. [26] designed a microfabricated chip containing a carbon nanotube stationary phase for high-speed micro-GC analyses. Using the microchip, a series of C₆–C₁₁ hydrocarbons were separated in less than 2.5 s. Although further work is required before these columns can be used for more complex separations, such as are required for wine analysis, the nanotube stationary phases show promise for rapid chromatographic analysis of volatile compounds.

Graphene oxide nanosheets have also been proposed as carbon-based stationary phases for GC [34]. When coated on the surface of a fused-silica capillary column, the graphene oxide column was characterized as having a polarity similar to that of a nonpolar DB-1 column while providing the potential for enhanced separation efficiency of a series of straight-chain alcohols (ethanol, 1-butanol, 1-pentanol) and aromatic compounds (benzene, chlorobenzene, m-xylene, anisole, phenol, naphthalene). While these analytes, particularly the straight-chain and aromatic alcohols are of interest for wine and other foods and beverages, such applications of graphene oxide as a GC stationary phase have not been widely explored [29].

In the past 10 years, applications of *ionic liquids* as GC stationary phases for a number of food and beverage analyses, including wine, have increased significantly. Ionic liquids are salts with melting points below 100°C; for GC applications, salts with melting points between –40 and 50°C provide the best characteristics for GC separations [35–39]. Cross-linking of the ionic liquids provides stability for both low- and high-temperature separations (up to 350°C). A distinct advantage of many ionic liquid stationary phases is their ability to separate both polar and nonpolar analytes, and

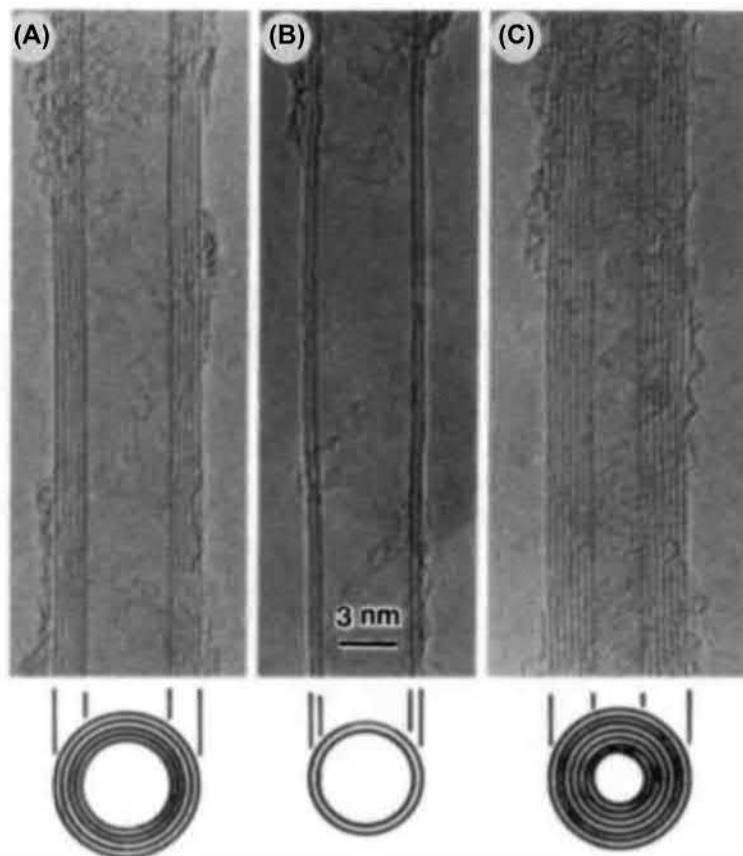


FIGURE 32.1 Electron micrographs of multiwall coaxial nanotubes. Parallel *dark lines* correspond to the lattice images of graphite. A cross section of each tubule is illustrated. (A) Tube consisting of five graphitic sheets, diameter 6.7 nm; (B) two-sheet tube, diameter 5.5 nm; and (C) seven-sheet tube, diameter 6.5 nm, which has the smallest hollow diameter (2.2 nm). With permission from S. Iijima, *Helical microtubules of graphitic carbon*, *Nature* 354 (1991) 56–58.

they have also been applied to chiral separations. With simple modifications to the salt (i.e., by changing the cation, anion, or substituents), a high degree of analyte selectivity can be obtained; in some cases, the ionic liquid may provide novel selectivity impossible with current GC stationary phases, making them particularly promising [37,38,40–42].

Cationic imidazolium-based ionic liquids were able to separate a complex mixture of hydrocarbons, alcohols, aldehydes, esters, terpenes, and ketones typical of those found in wines [43]. Analysis of fatty acid esters (including *cis*- and

trans-fatty acid isomers) and pesticides in a variety of food and beverage matrices has been demonstrated [37,39,43,44]. Schmarr et al. [45] quantified 2,4,6-trichloroanisole (TCA), the compound responsible for cork-taint off-aromas in wines, using GC with an ionic liquid stationary phase and showed an interesting normal isotope effect for the separation between the native and deuterated TCA isotopologue used as an internal standard. Differences in van der Waal dispersion forces of the ionic liquid compared to siloxane phases were thought to impact the separation and point to the need to carefully evaluate the

separations when using these novel phases. Several ionic liquid GC stationary phases are commercially available providing a range of selectivity [46–48]. Further studies are needed to fully characterize the ionic liquid stationary phases and to fully evaluate their applications for complex matrices such as wines.

In an interesting application, Zhao et al. [49] combined a cationic imidazolium-based ionic liquid stationary phase with a single-walled carbon nanotube. The nanotubes themselves can have chiral properties due to spatial arrangements of the graphene sheets [32]. Zhao et al. [49] demonstrated enhanced separations of racemic mixtures of terpenes (e.g., citronellal, limonene, carvone, camphor) and alcohols (e.g., phenylethanol, 2-phenyl-1-propanol, 2-methyl-1-butanol) when the GC capillary column was first coated with a single-wall nanotube and then coated with the ionic liquid. The nanotubes were thought to increase the surface area available for interactions between the analytes and the ionic liquid. While not directly applied to a wine sample, the compounds studied are key grape and fermentation-derived compounds, indicating potential applications for chiral analyses of wine matrices.

32.3 Multidimensional separations

Two- or multidimensional separations and the development of comprehensive GC \times GC analyses have provided the opportunity for improved resolution of the hundreds of volatile compounds that are found in grapes and wines [20,50–52]. In the most common application of *multidimensional GC*, a chromatographic peak (or region) from one column is passed to a second column with a different stationary phase. Components that are not separated on the first column are separated on the second column by choosing a stationary phase for the second column that is different from and complementary to that of the first column. By using a chiral

stationary phase in the second column, stereoisomers of selected compounds can be effectively separated in complex mixtures without prior isolation. Analysis of chiral compounds with aroma active properties is an important application of multidimensional GC for wine analysis [53–55]. In one application, Barba et al. [56] used multidimensional GC-MS to separate the stereoisomers of 2,3-butanediol and linalool in white wines. Since the different isomers of linalool have different sensory properties, this separation may provide an improved chemical characterization of wine aroma. Langen et al. [57] used multidimensional GC-MS with chiral separation on the second column to characterize the enantiomeric ratio of α -ionone, a norisoprenoid compound that contributes important floral and raspberry notes in wines. The authors proposed this approach as a way to determine whether flavorings were added to the wines since the *R*-isomer predominated in authentic wines.

In other selected wine applications, multidimensional GC-MS has been used for analysis of methoxy-pyrazines, which contribute vegetal/bell pepper aromas at low-ng/L levels [58]; quantitation of 2-aminoacetophenone (responsible for atypical aging off-aroma) at levels below the sensory threshold [59]; analysis of the oxygenated sesquiterpene rotundone, which contributes peppery aromas in Syrah wines [60]; quantitation of the carcinogen ethyl carbamate [61]; and identification of a new lactone, 2-nonen-4-olide, that contributes an “overripe orange” aroma to Bordeaux dessert wines [62]. Excellent overviews of the theory and applications of multidimensional GC are available [63–66]. Other chapters of this volume also provide more detailed discussions of multidimensional GC.

Comprehensive GC (or GC \times GC) is a variation of multidimensional GC where the entire effluent from the first analytical column is placed on the second column and separated in the second dimension. Pulses of effluent from the first

column are trapped over a defined time and then injected onto the second column. Modulation of the pulses requires careful optimization of instrumental parameters and, as with conventional two-dimensional GC, the two separation columns are chosen to be complementary. The second column for comprehensive GC must also provide a rapid separation so that pulses of effluent remain focused and separated from each other, therefore the second column is often shorter and has a narrower diameter and thinner film thickness than the first column. Ionic liquid stationary phases are of particular interest for multidimensional separations because the ionic liquids can be designed to provide a wide range of selectivity for the optimal separation of specific analytes [37,42,45–48]. Excellent reviews of comprehensive GC are available, including advantages and disadvantages of conventional and comprehensive GC [63,64,67–73].

Comprehensive GC applications for wine analysis can be classified as targeted analyses, focusing on quantitation of specific compounds, and nontargeted analyses, aimed at profiling large numbers of peaks in a sample without prior knowledge of their identity. An early application of comprehensive GC was the targeted analysis of 3-isobutyl-2-methoxypyrazine (IBMP) in wines [74–77]. IBMP is usually the most abundant methoxypyrazine found in grapes and wine, although other methoxypyrazines (e.g., 3-isopropyl-2-methoxypyrazine and 3-*sec*-butyl-2-methoxypyrazine) are also often present (reviewed in Ref. [78]). IBMP is found only in selected grape varieties (e.g., Cabernet Sauvignon, Sauvignon blanc, Merlot) [79] and contributes a bell pepper aroma when present at concentrations above the sensory threshold ($\sim 2\text{--}10\ \mu\text{g L}^{-1}$ in water; [80]). The low sensory threshold requires very sensitive analyses, which were achieved by extensive solvent extraction combined with chemical ionization mass spectrometry [81] or more recently, by solid-phase microextraction (SPME) of the headspace followed by GC–electron impact (EI)-MS in the

selected ion mode (SIM) [82]. The one-dimensional GC-(EI)MS-SIM analysis often suffers from interferences with the methoxypyrazine peaks, however, making quantitation difficult [74,77]. Comprehensive GC improves the separation of IBMP from matrix interferences and using this technique, highly sensitive methods for analysis of IBMP have been reported in wines and grape berries, with limits of detection of $0.5\ \text{ng L}^{-1}$ and $0.6\text{--}1.8\ \text{pg g}^{-1}$, respectively [74,76].

Schmarr et al. [77], however, observed that matrix interferences can also occur in the comprehensive GC analysis of IBMP in grapes and wines. These authors proposed that additional sample cleanup, combined with online high-performance liquid chromatography (HPLC) followed by multidimensional GC-MS, provided the best approach for removing matrix interferences in the analysis of IBMP. As the authors note, this hyphenated LC-GC approach is expensive and complex and may not be feasible for many applications. However, these results point to the need to carefully evaluate peak purity in such analyses, particularly for trace analytes such as IBMP. The development of standard protocols for monitoring analyte ion ratios and internal standard responses is necessary for ensuring that valid and accurate data is being obtained.

Comprehensive GC \times GC combined with SPME was also used for the analysis of ethyl carbamate (urethane) in wines [83]. Ethyl carbamate is a potential carcinogen formed in wines from urea and ethanol [84]. Voluntary limits for ethyl carbamate in wines have been established in the United States (weighted average $<15\ \mu\text{g L}^{-1}$; [85]) while in Canada, maximum levels ($30\ \mu\text{g L}^{-1}$) have been set (limits are higher for fortified wines, distilled spirits, and fruit brandies and liquors [86]). The high peak capacity of GC \times GC allowed for direct analysis of ethyl carbamate in Spanish Madeira wines without solvent extraction or derivatization as used in most previous methods, including the multidimensional GC-

MS method described by Tu et al. [61]. Limits of detection for the comprehensive GC \times GC method were well below the maximum allowed levels (LOD = 2.75–4.31 $\mu\text{g L}^{-1}$ for dry and sweet model wine solutions, respectively).

Dasgupta et al. [87] separated an impressive 185 pesticides and organic pollutants in grape and wine extracts in less than 38 min using GC \times GC-TOFMS. The authors report that the method provided improved sensitivity for a wider range of targeted analytes compared to previous reported procedures. While the high peak capacity of GC \times GC minimized many matrix interferences observed with other methods, some matrix enhancement or suppression was still observed for some analytes, requiring use of matrix matched standards for accurate quantitation. In addition, deconvolution algorithms could not separate two pairs of coeluting analytes (diazinon and fluchloralin; pyrimethanil and etrimphos) when these compounds were present at low concentrations ($<25 \mu\text{g L}^{-1}$).

Using GC \times GC with either time-of-flight (TOF) or quadrupole MS detection, the nontargeted, simultaneous analysis of over 200 volatile compounds in wines has been reported [17,88–90]. Approximately 2–4 times more compounds were detected in these studies compared to typical one-dimensional analyses [17,91]. The limitation of these analyses is the extensive time required for peak identification and data analysis and interpretation [88–91]. Rocha et al. [92] profiled only the monoterpene compounds in grapes using GC \times GC-TOFMS and by extracting ions that were characteristic of the terpenes (m/z 93, 121, 136). When retention times of the extracted ion peaks from both separation columns were plotted against each other, the terpenes with similar structures clustered together; this clustering aided in compound identification. Comprehensive GC \times GC analysis of sesquiterpenes in Cabernet Sauvignon wines allowed identification of 10 new sesquiterpenes not previously reported in *V. vinifera* wines [91]. Schmarr et al. [88] used an

isotopically labeled internal standard to provide quantitative information on volatiles measured in their study. Although internal standards were used in the studies of Robinson et al. [17] and Rocha et al. [92], no quantitation data was reported.

The extensive characterization of volatile composition that is possible with comprehensive GC \times GC separation provides the opportunity for a more detailed understanding of wine components that may contribute to sensory properties, as well as the ability to better discriminate among wines based on variety, growing region, viticultural practices, vintage, or processing variables [17,88–90,93]. Critical challenges remain in the availability of software and chemometric tools for analysis of the complex GC \times GC data that are obtained. Research into the development of new data analysis and statistical tools continues in order to efficiently process these large data sets, to allow for automated and accurate peak identifications, and to provide for sophisticated pattern recognition for sample classification.

32.4 Detectors and hyphenated techniques

Among the most common GC detectors for wine analysis are the flame ionization (FID) and mass spectrometric (MS) detectors. Other detectors can provide improved sensitivity and/or selectivity for some analytes relative to these “universal” detectors. For example, flame photometric (FPD) and chemiluminescence detectors are widely used for analysis of sulfur-containing volatiles that may contribute to off-aromas of wines [94–96]. Electron-capture detectors are used for analysis of trace levels of haloanisoles (e.g., 2,4,6-trichloroanisole responsible for cork-taint aromas [97]), pesticide residues [98–102], and volatile aldehydes (as their pentafluorobenzyl hydroxylamine oximes) [103]. Nitrogen–phosphorous detectors (NPDs) have also seen applications for the analysis of

pesticide residues [102,104] as well as for analysis of methoxypyrazines that contribute a bell pepper aroma to some wine varieties such as Cabernet Sauvignon [74,105]. The NPD detector has also been used for the analysis of thiazolidine derivatives of aldehydes, including acetaldehyde, that contribute oxidative aromas to wines [106–108]. In an interesting application, an atomic emission detector (AED) was used to identify and quantify eight organic sulfur and two organic selenium species (dimethyl selenide, dimethyl diselenide) in wines [109]. Finally, the GC effluent is coupled to an olfactory port and the human nose as a detector is widely used to identify important odor active compounds in wines (reviewed by Refs. [19–21,110]).

Over the past ten years, wine analyses increasingly use detector technologies that provide the potential for rapid analyses with improved selectivity and sensitivity compared to traditional GC detectors. These detector technologies include time of flight (TOF) mass spectrometry and hyphenated techniques, such as tandem mass spectrometry (MS/MS) for the analysis of a wide range of wine components.

Time-of-flight (TOF) MS detectors offer very fast acquisition rates yielding a larger number of spectra across chromatographic peaks compared to quadrupole instruments. This aids in analyte resolution, quantitation, and identification. Several commercial GCs with TOF detectors provide nominal mass accuracy (unit mass resolution), although high-resolution instruments with accurate mass capabilities are also available. Studies by Setkova et al. [15,16] highlighted the potential for GC-TOFMS to provide rapid analysis of large numbers of analytes. In these studies ~201 volatile components in ice wine were identified and quantitated in <5 min; the volatile profile was used to classify a range of ice wines according to their origin, grape variety, and processing conditions.

GC-TOFMS analysis is also widely used for metabolomic applications, often employing a two-step methoximation-silylation protocol to

derivatize metabolites including amino acids, organic acids, sugars, sugar alcohols, sugar acids, and fatty acids contained in biological samples [111–114]. Skogerson et al. [115] identified 108 metabolites in several white wines (Chardonnay, Pinot gris, Riesling, Sauvignon blanc, and Viognier) using GC-TOFMS. Differences in metabolite profiles were apparent among the different wines and could be used to predict differences in the sensory perception of wine “body” or viscous mouthfeel. Ding et al. [116] used GC-TOFMS profiling to characterize metabolic changes occurring during *Saccharomyces cerevisiae* fermentations. Atanasov et al. [117] reviewed the potential for metabolomics research to improve winemaking practices and grapevine breeding programs for producing high-quality wines.

The hyphenated technique, *tandem GC-MS (GC-MS/MS)*, continues to gain increasing acceptance for targeted quantitation of trace analytes in wines. In tandem MS, effluent from the GC column is ionized and enters the first MS where precursor ions are selected and transferred to a collision or reaction cell. In the collision cell, the precursor ions are bombarded with energy causing them to further fragment into product ions, which are then detected. The GC-MS/MS experiment can be performed in several ways: (a) all precursor ion masses are scanned in MS1 and, following fragmentation in the collision cell, only selected product ions are monitored in MS2; (b) only a selected precursor ion from MS1 is allowed to pass into the collision cell and all product ions from the reaction are monitored; (c) similar to (a), all precursor masses are scanned in MS2 and fragmented in the collision cell; however, MS2 scans for masses associated with a constant neutral loss from the precursor ions; and (d) both MS1 and MS2 are set to select only for specific preidentified masses. Two types of GC-MS/MS instruments are available, quadrupole instruments where the ions travel through the mass separators and collision cell sequentially in space, and ion-trap

instruments, which contain an ion trap that manipulates the precursor ions in time to sequentially perform the functions of MS1, the collision cell, and MS2. With GC-MS/MS analyses, the high degree of selectivity for both precursor and product ions typically provides sensitive analysis of trace compounds. In addition, analyte structural information can be obtained by monitoring the product ions produced from specific precursor ions. Theory and applications of tandem GC-MS have been reviewed [118–121].

One of the most widely used applications of GC-MS/MS for wine analysis is for multiresidue pesticide screening [122–127]. These methods provide rapid and simultaneous screening for a large number of pesticides, and depending on the sample preparation procedures, limits of detection in the low pg mL^{-1} range have been reported [123]. GC-MS/MS is also used for quantitation of trace levels of aroma and off-aroma compounds. Selected applications include analysis of (a) compounds responsible for cork taint (2,4,6-trichloroanisole, 2,3,4,6-tetrachloroanisole, 2,4,6-tribromoanisole, and pentachloroanisole) [128–135]; (b) *Brettanomyces*-related off-aromas (4-ethylguaiacol, 4-ethylphenol, 4-vinylguaiacol, 4-vinylphenol) [133,134]; (c) methoxypyrazines associated with bell-pepper varietal aromas (2-methoxy-3-isobutylpyrazine, 2-methoxy-3-isopropylpyrazine, 2-methoxy-3-sec-butylpyrazine, 2-methoxy-3-ethylpyrazine) [136,137]; (d) 1-octen-3-one, which has a mushroom-like aroma [138]; (e) rotundone, an oxygenated sesquiterpene, which is associated with a peppery aroma in some wine varieties [139]; (f) lactones in wines [140]; (g) volatile thiols, which contribute tropical fruit aromas to wines, particularly Sauvignon blanc wines (3-sulfanylhexanol, 3-sulfanylhexyl acetate, 4-methyl-4-sulfanylpentan-2-one, benzenemethanethiol, and ethyl 2-sulfanylacetate) [141,142];

and (h) sesquiterpenes in grapes [143]. The majority of these compounds have aroma thresholds in the ng L^{-1} range and therefore require highly sensitive and selective methods for their analysis.

The diastereoisomers of S-3-(hexan-1-ol) cysteine in grape juice were analyzed by ion trap GC-MS/MS following isolation by affinity chromatography and derivatization with heptafluorobutyric anhydride and heptafluorobutanol [144]. Using this method, the authors observed that the diastereomeric ratio of this cysteinylated compound changed as a result of infection of the juice with the noble rot fungus, *Botrytis cinerea*. During fermentation, the cysteinylated precursor is enzymatically cleaved to form the important aroma compound 3-sulfanylhexan-1-ol. Thibon et al. [144] observed that the diastereomeric ratio of the precursor did not change during fermentation and the aglycone that was released also had a nearly identical isomeric ratio to that of the precursor. The diastereomers of the aglycone 3-sulfanylhexan-1-ol have similar and very low aroma thresholds of $50\text{--}60 \text{ ng L}^{-1}$; however, the aroma quality is dependent on the enantiomeric form; the R-form has a grapefruit-like character, while the aroma of the S-form is described as passion fruit [145]. The results of this study demonstrate the application of GC-MS/MS as an important tool for accurately measuring low levels of diastereomeric precursors that can impact wine sensory properties.

Jelen et al. [146] compared GC-MS/MS, comprehensive GC \times GC-TOFMS, and GC-MS in selected ion monitoring mode (SIM) for the analysis of six haloanisoles, which contribute musty aromas to wines. GC-MS/MS provided the lowest limits of detection for the compounds analyzed, often an order of magnitude lower than for GC \times GC-TOFMS. Comprehensive GC \times GC-TOFMS provided improved detection limits relative to GC-MS(SIM) and also provided

spectral information for identification of a broader range of analytes in the wines.

32.5 Sample preparation

No discussion of gas chromatographic analysis of wines would be complete without mention of sample preparation. Jennings and Filsoof [147] used a model solution containing compounds with a range of functional groups and boiling points to elegantly demonstrate the dramatic qualitative and quantitative effects of different sample preparation techniques on measured GC responses. The importance of sample preparation was further emphasized by Flath [148]:

Numerous approaches have been developed for the concentration and isolation of volatile materials, but all have shortcomings which limit their universal applicability. It is necessary to be aware of these limitations and reduce their impact if possible by modifying and improving the most appropriate method, or by applying complementary techniques to compensate for shortcomings of any one method.

Sample preparation techniques for wine analysis have been briefly reviewed [10–22]. In many cases, sample preparations that include derivatization reactions can be used to enhance the volatility and/or stability of analytes that are not normally amenable to GC (due to their strong polarity, high boiling point, and/or thermal instability). Selected applications of derivatization reactions for analysis of wine components include analysis of amines [149,150]; organic and inorganic metals such as arsenic [151]; phenols and polyphenols, including resveratrol [152–154]; amino acids [155]; and sugars [156]. Derivatization reactions are also used to add functional groups to analytes to enhance selectivity (and sensitivity) with detectors such as the NPD and ECD as discussed. While not a comprehensive listing, these applications and other discussed throughout this chapter show

the wide range of analytes in wines that can be analyzed by GC previously.

Currently most sample preparation/extraction approaches for wine analysis are aimed at providing rapid analysis with minimal or no solvent usage. Two areas in particular have received much attention during recent years: sorptive extraction methods (e.g., solid-phase microextraction or SPME, solid-phase dynamic extraction or SPDE, stir-bar sorptive extraction or SBSE, and solid-phase extraction or SPE) and liquid microextraction methods (e.g., single-drop microextraction, membrane extraction, and dispersive liquid–liquid microextraction). Kloskowski et al. [157] have provided a general overview of sample preparation techniques. Sorptive sample preparation techniques are the focus of reviews by Baltussen et al. and Nongonierma et al. [158–160]; single-drop liquid microextraction was reviewed by Xu et al. [161].

32.5.1 Sorptive extraction methods

Since its introduction in the 1990s, *SPME* has become one of the most widely used sample preparation techniques for GC, and *SPME* extraction from the headspace (HS) is commonly used for analysis of wine volatiles. HS-*SPME* extractions are easy to perform, sensitive, and rapid (most extractions are completed in less than 1 h). Several fiber coatings are commercially available offering some selectivity in analyte extraction, and novel phases, including ionic liquid and carbon-based nanomaterials, continue to be evaluated [162–165]. However, with coating materials containing Carboxen, where competition for sorption sites can occur, matrix effects can impact extraction efficiencies; this matrix effect is particularly important for the analysis of volatile organic sulfur compounds [94,96,166] and for direct analysis of aldehydes in wines [167].

On-fiber derivatization, where sample extraction, concentration, and derivatization are accomplished simultaneously, has received attention over several years. Here, derivatizing agent is deposited on the SPME fiber, the fiber is exposed to the sample headspace, and analytes sorb to the fiber and either react directly with the derivatizing reagent, or after sorption the fiber is inserted into the hot GC inlet where the derivatization reaction occurs; the derivatized analyte is then thermally desorbed from the fiber and is analyzed in the normal manner. Headspace-SPME analysis combined with on-fiber derivatization (e.g., *O*-(2,3,4,5,6-pentafluorobenzyl)hydroxylamine (PFBHA) hydrochloride) was utilized for the sensitive and selective analysis of aldehydes (e.g., alkanals, including acetaldehyde, (*E*)-2-alkenals, (*E,E*)-2,4-alkadienals, and furfural) and ketones (e.g., 2,3-butanedione, and 3-hydroxy-2-butanone), in wines and distilled beverages [168–171]. These aldehydes can impact wine flavor, and in some cases, their levels can be associated with oxidative conditions during processing or storage. On-fiber derivatization of polyphenols including resveratrol was accomplished using silylating reagents (e.g., bis(trimethylsilyl)trifluoroacetamide, BSTFA) [153,154]. Polyphenols impact wine bitterness and astringency and have antioxidant properties that affect wine stability and the health effects of wine.

Zapata et al. [172] compared on-fiber derivatization of wine carbonyls with a method where the carbonyls were first sorbed on an SPE cartridge, derivatized with PFBHA, and eluted with solvent for GC analysis. While the SPME method was overall relatively fast and easy to perform, the SPE isolation/derivatization procedure was more reproducible (repeatability relative standard deviations of <10% for SPE vs. <20% for SPME). Sensitivity (limits of detection) for the two methods depended on the type of detector used and the analyte studied.

Excellent reviews of HS-SPME measurements of volatile and semivolatile constituents in wine

samples are available [173–177]. There continues to be interest in faster, high-throughput sample preparation methods, and HS-SPME sampling under reduced pressure has been proposed as one way to significantly decrease sampling times and increase analyte partitioning into the headspace [178]. Risticvec et al. [173,174] describe a rapid HS-SPME protocol using preequilibrium, short extraction times (2–5 min extraction time with agitation at 500 rpm) combined with preloading of a known amount of internal standard onto the fiber, for accurate and reproducible analysis of wine volatiles. Using this procedure, combined with GC-TOFMS analysis and detection, the authors stated they were able to analyze 200–500 analytes in wines with a total analysis time of 10–15 min per sample.

SPDE is a variation of SPME, where the polymeric extracting material is coated on the inside of a needle, sample (liquid or gas phase) is repeatedly drawn into the needle core for analyte sorption to occur, and then the needle is placed into the GC inlet for desorption, separation, and detection. SPDE offers increased sorbent capacity compared to SPME, therefore providing better extraction efficiencies and improved sensitivity (reviewed by Ref. [179–181]). SPDE needles are often made of stainless steel, rather than fused silica, so are less fragile than SPME fibers. SPDE was used for analysis of short-chain, volatile alcohols (fusel oils) and esters in wines and other alcoholic beverages, to monitor pesticides in grapes, and to profile volatiles in fermenting musts in order to compare formation of volatiles in normal and problem fermentations, and to classify white wines [179,182,183].

SBSE (also known as Twister), like SPME, uses a polymeric material for analyte sorption (currently only poly(dimethylsiloxane) and poly(ethylene glycol) modified phases are commercially available); however, in the case of SBSE, the polymeric material is coated on the outside of a magnetic stir bar. The amount

of SBSE sorbent is significantly greater, compared to SPME; therefore, extraction capacities are greater [157,184,185]. Either the liquid or headspace/vapor phase of the sample can be extracted. Following extraction, the stir bar is removed from the sample (rinsed with water if extraction was from the liquid phase), placed into a special thermal desorption GC inlet for analyte desorption, and the analytes cryofocused at the front of the column for GC analysis. While the desorption and cryofocusing steps are fully automated, insertion and removal of the stir bar into the sample vials for sampling must be done manually. SBSE has been widely adopted for analysis of grape and wine volatiles associated with wine aroma [186–194].

Arbulu et al. [195] used a dual SBSE method to evaluate the volatile profile of wine. Here, two stir bars were used simultaneously, one placed in the liquid phase and one in the headspace of the wine sample. After the sorption step, both stir bars were placed in the thermal desorption inlet for desorption and cryofocusing, followed by GC-MS analysis. Over 200 volatiles and semivolatiles were characterized in the wine sample, including several previously unidentified wine components: three organic acids (*cis*-vaccenic acid, 12-methylaminolauric acid, 17-octadecynoic acid), two sesquiterpenes (mansonone C, ledene oxide-(II)), and one C13-norisoprenoid ketone (tabanone or megastigmatrienone).

Rather than thermally desorbing analytes from the stir bar, Coelho et al. [196] used solvent desorption of the stir bar, combined with large volume injection, to profile and quantify 71 volatiles in sparkling wines. Vestner et al. [197] combined microwave-assisted extraction of cork stoppers with SBSE to quantify 2,4,6-trichloroanisole from the cork. Solvent extraction from the cork matrix is typically slow (24 h); however, Vestner et al. reported total extraction times of $\sim 4\frac{1}{2}$ h ($3\frac{1}{2}$ h for microwave-assisted extraction, 1 h for SBSE) and up to 10 samples could be extracted simultaneously.

SPE is widely used for isolation of volatiles and nonvolatiles in wines. A variety of SPE stationary phases are available providing a range of analyte selectivity, and typically only small amounts of solvent are needed for extractions. Reversed-phase (C_{18}) SPE extraction cartridges are widely used to extract glycosidically bound aroma precursors from grapes and wine. Following isolation of the glycoside fraction, the volatile aglycone aroma compounds are released by acid or enzyme hydrolysis and the free aglycones analyzed by GC [198–200]. Other applications include isolation of terpenes in wines followed by GC analysis of the extract [201], isolation of methoxypyrazines [202], complexing trace levels (ng L^{-1}) of polyfunctional thiol aroma compounds on cartridges containing *p*-hydroxymercurybenzoate [203], and isolation followed by direct GC analysis of 10 different organic acids in red and white wines (the method detects up to 29 acids in foods; [204]). Although extensively used for many years, new SPE stationary phases and applications continue to be developed [160,205–207]. Automation of SPE where the extraction is performed online followed by gas chromatographic separations has been reviewed [208]. Using switching valves, analytes extracted on the SPE column are directly introduced to the GC system resulting in reduced analysis times and improvements in precision and sensitivity compared to manual SPE sample preparation [208].

32.5.2 Liquid-phase microextractions

Liquid-phase microextraction techniques that use very small amounts of solvents that are amenable to injection for GC are of growing interest as replacements for traditional liquid–liquid extractions. As reviewed by Kloskowski [157] and Pena-Pereira [209], these methods generally fall into one of the following three categories: (1) *single-drop microextraction* where a drop of extracting solvent is suspended into the

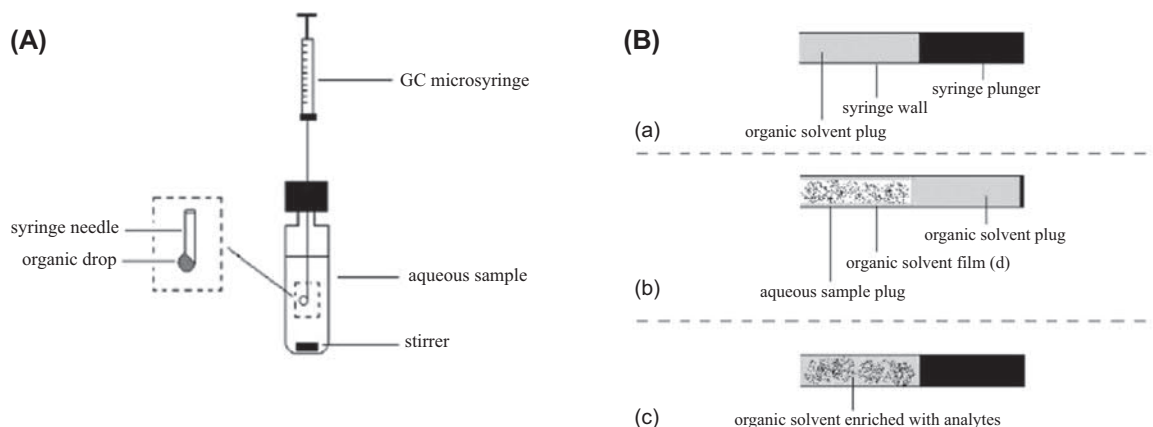


FIGURE 32.2 Schematic for single-drop liquid microextractions. (A) Equilibrium single-drop extraction in liquid phase. (B) Dynamic, nonequilibrium single-drop extraction performed in syringe with repeated retraction of plunger. **Step a:** Syringe is filled with organic extracting solvent. **Step b:** Plunger is retracted to withdraw aqueous sample into syringe; extracting solvent forms thin film on inner surface of the syringe. **Step c:** Expulsion of sample by pushing plunger back into syringe; solvent remains in syringe. Steps a–c repeated several times to extract analytes from sample. With permission from L. Xu, C. Basheer, H. K. Lee, *Developments in single-drop microextraction*, *J. Chromatogr. A* 1152 (2007) 184–192.

sample (or the headspace above the sample) from the tip of a rod (often made of polytetrafluoroethylene, PTFE) or a syringe needle, and extraction from the sample occurs under equilibrium or nonequilibrium conditions (Fig. 32.2), i.e., sample flows past the solvent drop or the solvent drop and sample is repeatedly withdrawn into the needle where the solvent forms a thin layer with increased extraction surface area along the sides of the needle (Fig. 32.2B); (2) **membrane extraction** where the sample and extracting solvent are separated by a porous membrane. The membranes are typically hydrophobic polymeric materials and/or are filled with extracting solvent and are typically assembled using a hollow fiber; these extractions can be either static or dynamic; and (3) **dispersive liquid–liquid microextraction** where a high-density organic extracting solvent and a dispersing solvent that is miscible in both the organic solvent and the aqueous sample phase are rapidly added to the sample forming small dispersed, emulsified droplets of the organic solvent within the sample. The dispersed droplets have a high surface area and rapidly extract the

analytes from the aqueous phase; following centrifugation, the heavier organic layer, containing the extracted analytes, sinks and is isolated for GC analysis. Dispersive liquid–liquid extractions were introduced by Rezaee et al. in 2006 for analysis of hydrophobic pollutants and pesticides in water [210]. Further modifications of the dispersive liquid–liquid extraction method by Regueiro et al. [211] eliminated the emulsifier phase and used ultrasound to assist in droplet formation. General advantages and disadvantages of these microextraction methods are reviewed elsewhere [157,209,212–216]. Using these methods, high analyte enrichment factors can typically be obtained, particularly with the dispersive liquid extractions and membrane extractions; however, some sample is typically lost in the membrane when performing membrane extractions, and extraction kinetics for the single droplet and membrane extractions can be slow depending on the analytes, the solvents, and the configurations used.

All of these liquid-phase microextraction techniques have been applied to wine analysis. Droplet microextraction was used for the

determination of ethanol and pesticides in wines [217–219] and polyphenols in grapes [220]. Membrane extraction was used to test for leaching of 2-ethylhexyl 4-(dimethylamino)benzoate from sterile Tetra Pak packaging materials into wines [221]. Dispersive liquid–liquid microextraction appears to be among the most widely tested of these methods with applications for analysis of pesticides in wines [222,223]; phenols, halophenols, and haloanisoles in wines and corks [132,133,224,225]; biogenic amines [226]; varietal-sulfur aroma compounds in wines (methylmercaptoacetate, methyl(methylthio)acetate, 2-methylthioethanol, 3-methylthiopropanol, 3-methylthiohexanol, 4-methylthio-4-methyl-2-pentanone and hexanethiol) [227]; the aroma compounds geosmin and methylisoborneol in wines [228]; and more than 140 volatile and semi-volatile compounds in grape marc distillate (e.g., grappa) [229]. All of the liquid-phase microextraction methods provide rapid and simple sample preparation procedures; however, in some cases the complex wine matrices can result in significant interferences such as precipitation of matrix components in the dispersive liquid–liquid microextraction of fungicides from red wines [222]. Automation of these techniques to improve the robustness and reproducibility of these approaches will be critical for further use and more widespread acceptance [213–215].

32.5.3 Other sample preparation methods and comparisons of methods

A sample technique that combines both liquid–liquid extraction and SPE is the so-called QuEChERS (quick, easy, cheap, effective, rugged, and safe) procedure [230]. The sample is first extracted with a solvent (e.g., acetonitrile), salt (MgSO_4 , NaCl) is added to separate the phases, and a sorbent (e.g., primary secondary amine (PSA), C_{18}) is then added to remove matrix interferences and the supernatant is analyzed by

GC-MS (or LC-MS) [231–237]. QuEChERS is most widely used for analysis of pesticide residues in foods and has been applied to the multi-residue analysis of pesticide in grapes and wines [238–241]. The method is rapid, simple to perform, requires minimal solvent, is easily transferable among different laboratories, and yields high analyte recoveries; however, acetonitrile solvent is not ideal for GC and a Programmable Temperature Vaporization-Large Volume Injection (PTV-LVI) inlet is recommended for best sensitivity [232]. Application of QuEChERS for multiresidue pesticide analysis of foods has been recognized as an official method by the American Association of Official Analytical Chemists (AOAC 2007.01; [242]) and by the European Committee for Standardization (CEN Standard Method EN 15662; [243]).

All of the aforementioned sample preparation methods are highly versatile, with applications to many types of analytes and matrices. However, only in a relatively few cases have these different sample preparation methods been compared. For analysis of halophenols and haloanisols in wines, Maggi et al. [131] observed that SBSE (extracting from the liquid) gave lower limits of detection for most of the tested compounds compared to both HS-SPME and direct immersion SPME. Perestrelo et al. [244] also observed that SBSE (sampling from the liquid) had lower limits of detection and quantitation for a range of target analytes compared to SPME (sampling from the headspace); analysis of volatiles in red and white wines showed that more volatile esters were identified and quantitated using the SBSE method compared to HS-SPME (25 vs. 16). Hjelmeland et al. [137] compared headspace SPME and SBSE from both the headspace and the liquid phase of wines for quantitation of methoxypyrazines responsible for vegetative aromas. All methods provided excellent sensitivity, reproducibility, and accuracy, while the headspace sorptive

extraction overall provided the lowest sensitivity in terms of quantitation limits. As noted by Hjelmeland et al. [137], all sampling methods evaluated, provided limits of quantitation that were at or below the sensory thresholds for the analytes measured and so would provide sufficient sensitivity for monitoring the impacts of a range of viticultural and winemaking practices on methoxypyrazine levels in wines. Andujar-Ortiz et al. [245] compared SPME and SPE with traditional liquid–liquid extraction for the analysis of wine volatiles. Based on results from 30 volatile compounds, SPME showed the lowest recovery among the three methods for polar volatiles such as 1-hexanol, furfural, and geraniol. However, the SPME method used significantly less sample (8 vs. 50 mL), was faster (extraction times of 20 min), and required no organic solvents. Fontana et al. [229] observed that dispersive liquid–liquid microextraction generally provided higher extraction efficiencies compared to SPME for a range of volatile and semivolatile compounds in grape marc distillates. In summary, as new sample preparation methods continue to evolve, comparisons of these types will be critical so that appropriate sample preparation methods can be chosen based on both the experimental objectives and an understanding of how the analytes of interest respond to various sample preparation procedures.

For all of these methods, accurate quantitative analysis requires careful consideration of analyte recoveries and matrix effects (e.g., matrix components interfering with the chromatographic separations or causing ion suppression or enhancement in the MS). Stable isotope dilution analysis (SIDA) offers the most effective way to minimize matrix effects on analyte recovery and reproducibility [19–21]. An internal standard (IS) that structurally matches the analyte of interest but contains one or more stable isotope atoms (typically ^2H or ^{13}C) is added to

the sample at the beginning of the analysis. The IS and analyte theoretically respond similarly to any matrix interactions and so the response will be comparable for both the analyte and the IS. The analyte and IS can be measured by MS and the response ratios used to calculate concentrations. One of the most comprehensive applications of SIDA was reported by Siebert et al. [246] where 31 compounds in wine (including fatty acids, alcohols, acetate esters, and ethyl esters) were quantitated by SPME-GC-MS using 29 different deuterated compounds as internal standards. However, Koch et al. [79] have indicated that even with an isotopically matched IS, changes in the grape matrix during ripening influenced recovery and reproducibility of the analysis of IBMP using HS-SPME-GC-MS. In these cases, standard addition calibration methods may provide the most accurate method of quantitation, even though large numbers of analyses are required [79]. Lavignini et al. [247] compared the analysis of sulfur compounds in wines using both isotopically labeled and nonisotopically labeled internal standards. They report the application of a statistical variance component model to effectively account for matrix effects when using nonisotopically labeled internal standards that are typically cheaper and more readily available than isotopically labeled compounds.

Although use of one or sometimes two internal standards is common for most analyses, Rebiere et al. [248] reported that reproducibility of SPME methods can be enhanced by application of four internal standards (nonisotopically labeled) to monitor for fiber performance as well analyte extraction and quantitation. More recently, Ferreira et al. [249] used 13 different internal standards combined with multivariate calibration to minimize matrix effects for the HS-SPME analysis of 47 volatile compounds typically found in wines. Finally, Gómez-Ríos

et al. [250] proposed an “in-fiber” SPME calibration using six different compounds that are loaded onto the fiber prior to extraction of the analytes of interest from the sample matrix. This approach is applicable to samples where addition of an internal standard to the matrix may alter the sample properties and provides a rapid method for controlling for instrument and measurement responses over time.

As noted at the beginning of this section, no sample preparation technique is without bias, sample preparation and quantitation methods should be chosen to meet experimental objectives, and in some cases, more than one sample preparation method may be needed to yield the most complete information. Although there have been many recent advances, additional research on sample preparation techniques and statistical approaches that will enhance data analysis and interpretation is still needed.

Summary

Since its development in the 1950s, GC has proven to be a critical tool for the identification and quantitation of many wine analytes. This review has largely focused on research and applications that have occurred in the past ~15 years and from this overview, several trends become apparent: (1) There is increasing focus on development of sustainable and environmentally friendly stationary phase materials, such as ionic liquids and carbon nanotubes, that give the same performance as today’s siloxane- and polyethylene glycol-based phases; (2) Development of multidimensional separations and sensitive new detectors and hyphenated techniques allows for the analysis of more compounds in a given chromatographic run than was possible even 10 years ago; (3) The new separation modes and detectors also allow for faster analysis times; along with research focused on faster, high throughput sample preparation methods, total analysis times of only a few seconds or minutes are now often possible; and (4) There is

increasing interest in miniaturization of columns (see for example a recent review by Sidelnikov et al. [251]) and sample preparation techniques; this miniaturization contributes to faster analysis times in some cases, and also reduces solvent and chemical use and costs. There is also increasing focus on miniaturization of GC instruments (see also review by Regmi and Agah [252] but this was not a focus of the current review. These active areas of research are providing an improved understanding of wine composition and chemistry, however many challenges remain: (1) While the stationary phases being developed may be cheaper and offer unique selectivities compared to existing stationary phases, many of the newer column materials do not have the thermal stability and chromatographic efficiencies of traditional columns, therefore much research is still needed before these stationary phases will be widely used for analysis of complex matrices such as wines; (2) The development of software tools and approaches for identifying, aligning, deconvoluting, and integrating the hundreds of peaks in multi-dimensional GC analyses remains challenging; new multivariate statistical approaches are needed to analyze the large amounts of data that are obtained from the profiling and metabolomic analyses; (3) Comparisons and optimization of sample preparation procedures for different analytes is still needed, and for the most accurate quantitation, the ability to understand and account for variable matrix effects remains difficult for some grape and wine matrices. As analytical chemists strive to meet these challenges, new advances in the GC analysis of wines will most surely occur. Over the past ~65 years, GC analysis has provided critical information about grape and wine composition and the changes that occur as grapes are transformed into wine. However, much remains unknown and future improvements in GC separations, detection, sample preparation, and data handling processes will be needed as scientists continue to push the boundaries of our knowledge of grape and wine chemistry.

References

- [1] A.T. James, Gas-liquid partition chromatography: the separation of volatile aliphatic amines and of the homologues of pyridine, *Biochem. J.* 52 (1952) 242–247.
- [2] A.T. James, A.J.P. Martin, Gas-liquid partition chromatography: the separation and micro-estimation of volatile fatty acids from formic acid to dodecanoic acid, *Biochem. J.* 50 (1952) 679–690.
- [3] A.T. James, A.J.P. Martin, G.H. Smith, Gas-liquid partition chromatography: the separation and micro-estimation of ammonia and the methylamines, *Biochem. J.* 52 (1952) 238–242.
- [4] A.T. James, A.J.P. Martin, Gas-liquid chromatography: a technique for the analysis and identification of volatile materials, *Br. Med. Bull.* 10 (1954) 170–176.
- [5] A.J.P. Martin, A.T. James, Gas-liquid chromatography: the gas-density meter, a new apparatus for the detection of vapours in flowing gas streams, *Biochem. J.* 63 (1956) 138–143.
- [6] A.T. James, A.J.P. Martin, Gas-liquid chromatography: the separation and identification of the methyl esters of saturated and unsaturated acids from formic acid to *n*-octadecanoic acid, *Biochem. J.* 63 (1956) 144–152.
- [7] A.T. James, A.J.P. Martin, The separation and identification of some volatile paraffinic, naphthenic, olefinic, and aromatic hydrocarbons, *J. App. Chem.* 6 (1956) 105–115.
- [8] E. Bayer, Anwendung Chromatographischer Methoden zur Qualitätsbeurteilung von Weien and Mosten, *Vitis* 1 (1958) 298–312.
- [9] E. Bayer, L. Bässler, Systematische Identifizierung von Estern im Weinroma. II. Mitteilung zur systematischen Identifizierung verdampfbarer organischer Substanzen, *Z. für Anal. Chem.* 181 (1961) 418–424.
- [10] A. Castille, Methanol in spirits, *An. Bromatologia* 12 (1960) 335–340.
- [11] A.D. Webb, R.E. Kepner, Fusel oil analysis by means of gas-liquid partition chromatography, *Am. J. Enol. Vitic.* 12 (1961) 51–59.
- [12] A.D. Webb, R.E. Kepner, The aroma of flor sherry, *Am. J. Enol. Vitic.* 13 (1962) 1–14.
- [13] P. Schreier, Flavor compositions of wines: a review, *CRC Crit. Rev. Food Sci. Nutr.* 12 (1979) 59–111.
- [14] A. Rapp, Wine aroma substances from gas chromatographic analysis, in: H.F. Linskens, J.F. Jackson (Eds.), *Modern Methods of Plant Analysis, Wine Analysis*, vol. 6, Springer-Verlag, Berlin, Germany, 1988, pp. 29–66.
- [15] L. Setkova, S. Risticovic, J. Pawliszyn, Rapid headspace solid-phase microextraction-gas chromatographic-time-of flight mass spectrometric method for qualitative profiling of ice wine volatile fraction I. Method development and optimization, *J. Chromatogr. A* 1147 (2007) 213–223.
- [16] L. Setkova, S. Risticovic, J. Pawliszyn, Rapid headspace solid-phase microextraction-gas chromatographic-time-of-flight mass spectrometric method for qualitative profiling of ice wine volatile fraction II: classification of Canadian and Czech ice wines using statistical evaluation of the data, *J. Chromatogr. A* 1147 (2007) 224–240.
- [17] A.L. Robinson, P.K. Boss, H. Heymann, P.S. Solomon, R.D. Trengove, Development of a sensitive non-targeted method for characterizing the wine volatile profile using headspace solid-phase microextraction comprehensive two-dimensional gas chromatography time-of-flight mass spectrometry, *J. Chromatogr. A* 1218 (2011) 505–517.
- [18] I.L. Francis, J.L. Newton, Determining wine aroma from compositional data, *Austr. J. Grape Wine Res.* 11 (2005) 114–126.
- [19] P. Polaskova, J. Herszage, S.E. Ebeler, Wine flavor: chemistry in a glass, *Chem. Soc. Rev.* 37 (2008) 2478–2489.
- [20] S.E. Ebeler, J.H. Thorngate, Wine chemistry and flavor: looking into the crystal glass, *J. Agric. Food Chem.* 57 (2009) 8098–8108.
- [21] A.L. Robinson, P.K. Boss, P.S. Solomon, R.D. Trengov, H. Heymann, S.E. Ebeler, Origins of grape and wine aroma. Part 2. Chemical and sensory analysis, *Am. J. Enol. Vitic.* 65 (2014) 25–42.
- [22] H. Heymann, S.E. Ebeler, *Sensory and Instrumental Evaluation of Alcoholic Beverages*, Academic Press, London, United Kingdom, 2016, p. 265, 2016.
- [23] M.M. Rahman, A.M.A. El-Aty, J.-H. Choi, H.-C. Shin, S.C. Shin, J.-H. Shim, Basic overview on gas chromatography columns. Chapter 3, in: J.L. Anderson, A. Berthod, V.P. Estévez, A.M. Stalcup (Eds.), *Analytical Separation Science*, first ed., Wiley-VCH Verlag GmbH & Co. KGaA, Weinheim, Germany, 2015, pp. 823–834.
- [24] T. Cserhádi, Carbon-based sorbents in chromatography. New achievements, *Biomed. Chromatogr.* 23 (2009) 111–118.
- [25] Z.A. AlOthman, S.M. Wabaidur, Application of carbon nanotubes in extraction and chromatographic analysis: a review, *Arabian J. Chem.* 12 (2018) 633–651.
- [26] V.R. Reid, M. Stadermann, O. Bakajin, R.E. Synovec, High-speed, temperature programmable gas chromatography utilizing a microfabricated chip with an improved carbon nanotube stationary phase, *Talanta* 77 (2009) 1420–1425.
- [27] D. Merli, A. Speltini, D. Ravelli, E. Quartarone, L. Costa, A. Profumo, Multi-walled carbon nanotubes

- as the gas chromatographic stationary phase: role of their functionalization in the analysis of aliphatic alcohols and esters, *J. Chromatogr. A* 1217 (2010) 7275–7281.
- [28] M.L. Castillo-García, M.P. Aguilar-Caballos, A. Gómez-Hens, Nanomaterials as tools in chromatographic methods, *Trend Anal. Chem.* 82 (2016) 385–393.
- [29] V.N. Postnov, O.V. Rodinkov, L.N. Moskvin, A.G. Novikov, A.S. Bugaichenko, O.A. Krokhina, From carbon nanostructures to high-performance sorbents for chromatographic separation and preconcentration, *Russian Chem. Rev.* 85 (2016) 115–138.
- [30] S. Iijima, Helical microtubules of graphitic carbon, *Nature* 354 (1991) 56–58.
- [31] M.S. Dresselhaus, G. Dresselhaus, P. Avouris (Eds.), *Carbon Nanotubes. Synthesis, Structure, Properties, and Application*, Springer, New York, 2001.
- [32] A.L. Hemasa, N. Naumovski, W.A. Maher, A. Ghanem, Application of carbon nanotubes in chiral and achiral separations of pharmaceuticals, biologics and chemicals, *Nanomaterials* 7 (2017) 186, <https://doi.org/10.3390/nano7070186>, 2017.
- [33] S.H. Kwon, J.H. Park, Intermolecular interactions on multiwalled carbon nanotubes in reversed-phase liquid chromatography, *J. Sep. Sci.* 29 (2006) 945–952.
- [34] Q. Qu, Y. Shen, C. Gu, Z. Gu, Q. Gu, C. Wang, X. Hu, Capillary column coated with graphene oxide as stationary phase for gas chromatography, *Anal. Chim. Acta* 757 (2012) 83–87.
- [35] S.A. Shamsi, N.D. Danielson, Utility of ionic liquids in analytical separations, *J. Sep. Sci.* 30 (2007) 1729–1750.
- [36] B. Buszewski, S. Studzinska, A review of ionic liquids in chromatographic and electromigration techniques, *Chromatographia* 68 (2008) 1–10.
- [37] D.W. Armstrong, T. Payagala, L.M. Sidisky, The advent and potential impact of ionic liquid stationary phases in GC and GC \times GC, LC-GC *N. Am.* 27 (2009) 596–605.
- [38] A. Berthod, M.J. Ruiz-Ángel, S. Carda-Broch, Recent advances on ionic liquid uses in separation techniques, *J. Chromatogr. A* 1559 (2018) 2–16.
- [39] H. Nan, J.L. Anderson, Ionic liquid stationary phases for multidimensional gas chromatography, *Trends Anal. Chem.* 105 (2018) 367–379.
- [40] C.F. Poole, N. Lenca, Gas chromatography on wall-coated open-tubular columns with ionic liquid stationary phases, *J. Chromatogr. A* 1357 (2014) 87–109.
- [41] M.S.S. Amaral, P.J. Marriott, H.R. Bizzo, C.M. Rezende, Ionic liquid capillary columns for analysis of multi-component volatiles by gas chromatography-mass spectrometry: performance, selectivity, activity and retention indices, *Anal. Bioanal. Chem.* 410 (2018) 4615–4632.
- [42] C. Cagliero, C. Bicchi, Ionic liquids as gas chromatographic stationary phases: how can they change food and natural product analyses? *Anal. Bioanal. Chem.* 412 (2020) 17–25.
- [43] J. González Álvarez, D. Blanco Gomis, P. Aria Abrodo, D. Díaz Llorente, E. Busto, N. Rios Lombardía, V. Gotor Fernández, M.D. Gutiérrez Álvarez, Evaluation of new ionic liquids as high stability selective stationary phases in gas chromatography, *Anal. Bioanal. Chem.* 400 (2011) 1209–1216.
- [44] Y. Meng, V. Pino, J.L. Anderson, Exploiting the versatility of ionic liquids in separation science: determination of low-volatility aliphatic hydrocarbons and fatty acid methyl esters using headspace solid-phase microextraction coupled to gas chromatography, *Anal. Chem.* 81 (2009) 7107–7112.
- [45] H.-G. Schmarr, P. Slabizki, S. Müntnich, C. Metzger, E. Gracia-Moreno, Ionic liquids as novel stationary phases in gas liquid chromatography: inverse or normal isotope effect? *J. Chromatogr. A* 1270 (2012) 310–317.
- [46] W. Weber, J.T. Andersson, Ionic liquids as stationary phases in gas chromatography—an LSER investigation of six commercial phases and some applications, *Anal. Bioanal. Chem.* 406 (2014) 5347–5358.
- [47] C. Cagliero, C. Bicchi, C. Cordero, E. Liberto, B. Sgorbini, P. Rubiolo, Room temperature ionic liquids: new GC stationary phases with a novel selectivity for flavor and fragrance analyses, *J. Chromatogr. A* 1268 (2012) 130–138.
- [48] C. Cagliero, C. Bicchi, C. Cordero, E. Liberto, P. Rubiolo, B. Sgorbini, Analysis of essential oils and fragrances with a new generation of highly inert gas chromatographic columns coated with ionic liquids, *J. Chromatogr. A* 1495 (2017) 64–75.
- [49] L. Zhao, A. Ping, A.-H. Duan, L.M. Yuan, Single-walled carbon nanotubes for improved enantioseparations on a chiral ionic liquid stationary phase in GC, *Anal. Bioanal. Chem.* 399 (2011) 143–147, 2011.
- [50] J.V. Seeley, S.K. Seeley, Multidimensional gas chromatography: Fundamental advances and new applications, *Anal. Chem.* 85 (2013) 557–578.
- [51] Y. Nolvachai, C. Kulsing, P.J. Marriott, Multidimensional gas chromatography in food analysis, *Trends Anal. Chem.* 96 (2017) 124–137.
- [52] H.G. Schmarr, Heart-cutting two-dimensional gas chromatography. Chapter 6, in: P.Q. Tranchida (Ed.), *Food Chemistry, Function and Analysis* No. 17, Royal Society of Chemistry, London, England, 2020, pp. 201–236.

- [53] P. Bouchilloux, P. Darriet, D. Dubourdieu, R. Henry, S. Reichert, A. Mosandl, Stereodifferentiation of 3-mercapto-2-methylpropanol in wine, *Eur. Food Res. Technol.* 210 (2000) 349–352.
- [54] P. Darriet, S. Lamy, S. La Guerche, M. Pons, D. Dubourdieu, D. Blancard, P. Steliopoulos, A. Mosandl, Stereodifferentiation of geosmin in wine, *Eur. Food Res. Technol.* 213 (2001) 122–125.
- [55] L. Fernandes, A.M. Relva, M.D.R. Gomes da Silva, C. Freitas, Different multidimensional chromatographic approaches applied to the study of wine malolactic fermentation, *J. Chromatogr. A* 995 (2003) 161–169.
- [56] C. Barba, G. Flores, M. Herraiz, Stereodifferentiation of some chiral aroma compounds in wine using solid phase microextractions and multidimensional gas chromatography, *Food Chem.* 123 (2010) 846–861.
- [57] J. Langen, P. Wegmann-Herr, H.-G. Schmarr, Quantitative determination of α -ionone, β -ionone, and β -damascenone and enantiodifferentiation of α -ionone in wine for authenticity control using multidimensional gas chromatography with tandem mass spectrometric detection, *Anal. Bioanal. Chem.* 408 (2015) 6483–6496.
- [58] Y. Wen, I. Ontañón, V. Ferreira, R. Lopez, Determination of ppq-levels of alkylmethoxypyrazines in wine by stirbar sorptive extraction combined with multidimensional gas chromatography-mass spectrometry, *Food Chem.* 255 (2018) 235–241.
- [59] H.G. Schmarr, J. Keiser, S. Krautwald, An improved method for the analysis of 2-aminoacetophenone in wine based on headspace solid-phase microextraction and heart-cut multidimensional gas chromatography with selective detection by tandem mass spectrometry, *J. Chromatogr. A* 1477 (2016) 64–69.
- [60] H. Takase, K. Sasaki, H. Shinmori, A. Shinohara, C. Mochizuki, H. Kobayashi, H. Saito, H. Matsuo, S. Suzuki, R. Takata, Analysis of rotundone in Japanese Syrah grapes and wines using stir bar sorptive extraction (SBSE) with heart-cutting two-dimensional GC-MS, *Am. J. Enol. Vitic.* 66 (2015) 398–402.
- [61] Q. Tu, W. Qi, J. Zhao, J. Zhao, L. Zhang, Y. Guo, Quantification ethyl carbamate in wines using reaction-assisted-extraction with 9-xanthidrol and detection by heart-cutting multidimensional gas chromatography-mass spectrometry, *Anal. Chim. Acta* 1001 (2018) 86–92.
- [62] P. Stamatopoulos, E. Frérot, S. Tempère, A. Pons, P. Darriet, Identification of a new lactone contributing to overripe orange aroma in Bordeaux dessert wines via perceptual interaction phenomena, *J. Agric. Food Chem.* 62 (12) (2014) 2469–2478.
- [63] W. Bertsch, Two-dimensional gas chromatography. Concepts, instrumentation, and applications—Part 1: fundamentals, conventional two-dimensional gas chromatography, selected applications, *J. High Resolut. Chromatogr.* 22 (1999) 647–665.
- [64] L. Mondello, P.Q. Tranchida, P. Dugo, G. Dugo, Comprehensive two-dimensional gas chromatography-mass spectrometry: a review, *Mass Spec. Rev.* (27) (2008) 101–124.
- [65] P.J. Marriott, S.-T. Chin, B. Maikunthod, H.G. Schmarr, S. Bieri, Multidimensional gas chromatography, *Trends Anal. Chem.* 34 (2012) 1–21, 2012.
- [66] P.J. Marriott, Y. Nolvachai, A better way to separate the wheat from the chaff. Progression from single-dimension gas chromatography to multidimensional gas chromatography, *Sep. Sci. Technol.* 12 (2020) 41–68.
- [67] W. Bertsch, Two-dimensional gas chromatography. Concepts, instrumentation, and applications—Part 2: comprehensive two-dimensional gas chromatography, *J. High Resolut. Chromatogr.* 23 (2000) 167–181.
- [68] P.J. Marriott, P.D. Morrison, R.A. Shellie, M.S. Dunn, E. Sari, D. Ryan, Multidimensional and Comprehensive Two-Dimensional Gas Chromatography, LCGC Europe, December 2003, pp. 2–10.
- [69] C. Cordero, J. Kiefl, P. Schieberle, S. Reichenback, C. Bicchi, Comprehensive two-dimensional gas chromatography and food sensory properties: potential and challenges, *Anal. Bioanal. Chem.* 407 (2015) 169–191.
- [70] M.S. Klee, J. Chochran, M. Merrick, L.M. Blumberg, Evaluation of conditions of comprehensive two-dimensional gas chromatography that yields a near-theoretical maximum in peak capacity gain, *J. Chromatogr. A* 1383 (2015) 151–159.
- [71] S.E. Prebihalo, K.L. Berrier, C.E. Freye, H.D. Bahaghighat, N.R. Moore, D.K. Pinkerton, R.E. Synovec, Multidimensional gas chromatography: advances in instrumentation, chemometrics, and applications, *Anal. Chem.* 90 (2018) 505–532, 2018.
- [72] M.S.S. Amaral, Y. Nolvachai, P.J. Marriott, Comprehensive two-dimensional gas chromatography advances in technology and applications: biennial update, *Anal. Chem.* 92 (2020) 85–104.
- [73] P.Q. Tranchida, L. Mondello, Comprehensive two-dimensional gas chromatography, Chapter 7, in: P.Q. Tranchida (Ed.), *Food Chemistry, Function and Analysis No. 17*, Royal Society of Chemistry, 2020, pp. 237–282.
- [74] D. Ryan, P. Watkins, J. Smith, M. Allen, P. Marriott, Analysis of methoxypyrazines in wine using

- headspace solid phase microextraction with isotope dilution and comprehensive two-dimensional gas chromatography, *J. Sep. Sci.* 28 (2005) 1075–1082.
- [75] I. Ryona, B.S. Pan, D.S. Intrigliolo, A.N. Lakso, Effects of cluster light exposure on 3-isobutyl-2-methoxy-pyrazine accumulation and degradation patterns in red wine grapes (*Vitis vinifera* L. cv. Cabernet Franc), *J. Agric. Food Chem.* 56 (2008) 10838–10846.
- [76] I. Ryona, B.S. Pan, G.L. Sacks, Rapid measurement of 3-alkyl-2-methoxy-pyrazine content of winegrapes to predict levels in resultant wines, *J. Agric. Food Chem.* 57 (2009) 8250–8257.
- [77] H.-G. Schmarr, S. Ganß, S. Koschinski, U. Fischer, C. Riehle, J. Kinnart, T. Potouridis, M. Kutyrév, Pitfalls encountered during quantitative determination of 3-alkyl-2-methoxy-pyrazines in grape must and wine using gas chromatography-mass spectrometry with stable isotope dilution analysis comprehensive two-dimensional gas chromatography-mass spectrometry and on-line liquid chromatography-multidimensional gas chromatography-mass spectrometry as potential loopholes, *J. Chromatogr. A* 1217 (2010) 6769–6777.
- [78] M.S. Allen, M.J. Lacy, S. Boyd, Methoxy-pyrazines of grapes and wines, in: A.L. Waterhouse, S.E. Ebeler (Eds.), *Chemistry of Wine Flavor*, ACS Symposium Series No. 714, American Chemical Society, Washington, DC, 1999, pp. 31–38.
- [79] A. Koch, C.L. Doyle, M.A. Matthews, L.E. Williams, S.E. Ebeler, 2-Methoxy-3-isobutylpyrazine in grape berries and its dependence on genotype, *Phytochem* 71 (2010) 2190–2198.
- [80] R.G. Buttery, R.M. Seifert, D.G. Guadagni, L.C. Ling, Characterization of some volatile constituents of bell peppers, *J. Agric. Food Chem.* 17 (1969) 1322–1327.
- [81] R.L.N. Harris, M.J. Lacey, W.V. Brown, M.S. Allen, Determination of 2-methoxy-3-alkylpyrazines in wine by gas chromatography/mass spectrometry, *Vitis* 26 (1987) 201–207.
- [82] D.M. Chapman, J.H. Thorngate, M.A. Matthews, J.-X. Guinard, S.E. Ebeler, Yield effects on 2-methoxy-3-isobutylpyrazine concentration in Cabernet Sauvignon using a solid phase microextraction gas chromatography/mass spectrometry method, *J. Agric. Chem.* 52 (2004) 5431–5435.
- [83] R. Perestrelo, S. Petronilho, J.S. Camara, S.M. Rocha, Comprehensive two-dimensional gas chromatography with time-of-flight mass spectrometry combined with solid phase microextraction as a powerful tool for quantification of ethyl carbamate in fortified wines. The case study of Madeira wine, *J. Chromatogr. A* 1217 (2010) 3441–3445.
- [84] C.E. Butzke, L.F. Bisson, *Ethyl Carbamate Preventative Action Manual*, 1997. Available on-line, <https://www.fda.gov/food/chemicals/ethyl-carbamate-preventative-action-manual>. (Accessed 18 July 2020).
- [85] J. Alexander, G.A. Guðjón, D. Benford, A. Cockburn, J.-P. Cravedi, et al., Ethyl carbamate and hydrocyanic acid in food and beverages. Scientific opinion of the panel on contaminants, *EFSA J.* 551 (2007) 1–44.
- [86] Health Canada, Canadian Standards (“Maximum Levels”) for Various Chemical Contaminants in Foods. <http://www.hc-sc.gc.ca/fn-an/secureit/chem-chim/contaminants-guidelines-directives-eng.php>. (Accessed on-line 19 July, 2020).
- [87] S. Dasgupta, K. Banerjee, S.H. Patil, M. Ghaste, K.N. Dhumal, P.G. Adsule, Optimization of two-dimensional gas chromatography time-of-flight mass spectrometry for separation and estimation of the residues of 160 pesticides and 25 persistent organic pollutants in grape and wine, *J. Chromatogr. A* 1217 (2010) 3881–3889.
- [88] H.-G. Schmarr, J. Bernhardt, U. Fischer, A. Stephan, P. Müller, D. Durner, Two-dimensional gas chromatographic profiling as a tool for a rapid screening of the changes in volatile composition occurring due to microoxygenation of red wines, *Anal. Chim. Acta* 672 (2010) 114–123.
- [89] B.T. Weldegergis, A. de Villiers, C. McNeish, S. Seethapathy, A. Mostafa, T. Górecki, A.M. Crouch, Characterisation of volatile components of pinotage wines using comprehensive two-dimensional gas chromatography coupled to time-of-flight mass spectrometry (GC × GC-TOFMS), *Food Chem.* 129 (2011) 188–199.
- [90] J.E. Welke, M. Zanús, M. Lazzarotto, F.H. Pulgati, C.A. Zini, Main differences between volatiles of sparkling and base wines accessed through comprehensive two dimensional gas chromatography with time-of flight mass spectrometric detection and chemometric tools, *Food Chem.* 164 (2014) 427–437.
- [91] S. Petronilho, M.A. Coimbra, S.M. Rocha, A critical review on extraction techniques and gas chromatography based determination of grapevine derived sesquiterpenes, *Anal. Chim. Acta* 846 (2014) 8–35.
- [92] S.M. Rocha, E. Coelho, J. Zrostlíková, I. Delgado, M.A. Coimbra, Comprehensive two-dimensional gas chromatography with time-of-flight mass spectrometry of monoterpenoids as a powerful tool for grape

- origin traceability, *J. Chromatogr. A* 1161 (2007) 292–299.
- [93] K.P. Nicolli, A.C.T. Biasoto, E.A. Souza-Silva, C.C. Guerra, H.P. dos Santos, J.E. Welke, C.A. Zini, Sensory, olfactometry and comprehensive two-dimensional gas chromatography analyses as appropriate tools to characterize the effects of vine management on wine aroma, *Food Chem.* 243 (2018) 103–117.
- [94] R. López, A.C. Lapeña, J. Cacho, V. Ferreira, Quantitative determination of wine highly volatile sulfur compounds by using automated headspace solid-phase microextraction and gas chromatography-pulsed flame photometric detection. Critical study and optimization of a new procedure, *J. Chromatogr. A* 1143 (2007) 8–15.
- [95] Y. Fang, M.C. Qian, Sensitive quantification of sulfur compounds in wine by headspace solid-phase microextraction technique, *J. Chromatogr. A* 1080 (2005) 177–185.
- [96] J. Herszage, S.E. Ebeler, Analysis of volatile organic sulfur compounds in wine using headspace solid-phase microextraction gas chromatography with sulfur chemiluminescence detection, *Am. J. Enol. Vitic.* 62 (2011) 1–8.
- [97] D. Özhan, R.E. Anli, N. Vural, M. Bayram, Determination of chloroanisoles and chlorophenols in cork and wine by using HS-SPME and GC-ECD detection, *J. Inst. Brew.* 115 (2009) 71–77.
- [98] S. Navarro, A. Barba, G. Navarro, N. Vela, J. Oliva, Multiresidue method for the rapid determination—in grape, must and wine—of fungicides frequently used on vineyards, *J. Chromatogr. A* 882 (2000) 221–229.
- [99] J. Oliva, A. Barba, N. Vela, F. Melendreras, S. Navarro, Multiresidue method for the rapid determination of organophosphorus insecticides in grapes, must and wine, *J. Chromatogr. A* 882 (2000) 213–220.
- [100] M. Correia, C. Delerue-Matos, A. Alves, Multi-residue methodology for pesticide screening in wines, *J. Chromatogr. A* 889 (2000) 59–67.
- [101] M. Correia, C. Delerue-Matos, A. Alves, Development of a SPME-GC-ECD methodology for selected pesticides in must and wine samples, *Fresenius' J. Anal. Chem.* 369 (2001) 647–651.
- [102] J.J. Jiménez, J.L. Bernal, M.J. del Nozal, L. Toribio, E. Arias, Analysis of pesticide residues in wine by solid-phase extraction and gas chromatography with electron capture and nitrogen-phosphorus detection, *J. Chromatogr. A* 919 (2001) 147–156.
- [103] V. Ferreira, L. Culleré, N. Loscos, J. Cacho, Critical aspects of the determination of pentafluorobenzyl derivatives of aldehydes by gas chromatography with electron-capture or mass spectrometric detection: validation of an optimized strategy for the determination of oxygen-related odor-active aldehydes in wine, *J. Chromatogr. A* 1122 (2006) 255–265.
- [104] L. Vaquero-Fernández, J. Sanz-Asensio, P. Fernández-Zurbano, M. Sainz-Ramírez, M. López-Alonso, S.-I. Epifanio-Fernández, M.-T. Martínez-Soria, Development of a liquid-liquid extraction method for the determination of pyrimethanil, metalaxyl, dichlofluanid, and penconazol during the fermentative process of must by GC-NPD, *J. Sci. Food Agric.* 89 (2009) 750–757.
- [105] P.J. Hartmann, H.M. McNair, B.W. Zoecklein, Measurement of 3-alkyl-2-methoxypyrazine by headspace solid-phase microextraction in spiked model wines, *Am. J. Enol. Vitic.* 53 (2002) 285–288.
- [106] S.E. Ebeler, R.S. Spaulding, Characterization and measurement of aldehydes in wine, in: A.L. Waterhouse, S.E. Ebeler (Eds.), *Chemistry of Wine Flavor*, ACS Symposium Series No. 714, American Chemical Society, Washington, DC, 1999, pp. 166–179.
- [107] M. Lau, J.D. Ebeler, S.E. Ebeler, Gas chromatographic analysis of aldehydes in alcoholic beverages using a cysteamine derivatization procedure, *Am. J. Enol. Vitic.* 50 (1999) 324–333.
- [108] S.K. Frivik, S.E. Ebeler, Influence of sulfur dioxide on the formation of aldehydes in white wine, *Am. J. Enol. Vitic.* 54 (2003) 31–38.
- [109] N. Campillo, R. Peñalver, I. López-García, M. Hernández-Córdoba, Headspace solid-phase microextraction for the determination of volatile organic sulphur and selenium compounds in beers, wines and spirits using gas chromatography and atomic emission detection, *J. Chromatogr. A* 1216 (2009) 6735–6740.
- [110] S.-T. Chin, G.T. Eyres, P.J. Marriott, Application of integrated comprehensive/multidimensional gas chromatography with mass spectrometry and olfactometry for aroma analysis in wine and coffee, *Food Chem.* 185 (2015) 355–361.
- [111] J. Lisec, N. Schauer, J. Kopka, L. Willmitzer, A.R. Fernie, Gas chromatography mass spectrometry-based metabolite profiling in plants, *Nat. Protoc.* 1 (2006) 387–396.
- [112] D. Steinhauser, J. Kopka, Methods, applications and concepts of metabolite profiling: primary metabolism, *EXS* 97 (2007) 171–194.
- [113] O. Fiehn, G. Wohlgenuth, M. Scholz, T. Kind, D.Y. Lee, Y. Lu, S. Moon, B. Nikolau, Quality control for plant metabolomics: reporting MSI-compliant studies, *Plant J.* 53 (2008) 691–704.
- [114] J.W. Allwood, A. Erban, S. de König, W.B. Dunn, A. Luedemann, A. Lommen, L. Kay, R. Löscher, J. Kopka, R. Goodacre, Inter-laboratory reproducibility of fast gas chromatography-electron impact-time of flight mass spectrometry (GC-EI-TOF/MS)

- based plant metabolomics, *Metabolomics* 5 (2009) 479–496.
- [115] K. Skogerson, R. Runnebaum, G. Wohlgemuth, J. de Ropp, H. Heymann, O. Fiehn, Comparison of gas chromatography-coupled time-of-flight mass spectrometry and ¹H nuclear magnetic resonance spectroscopy metabolite identification in white wines from a sensory study investigating wine body, *J. Agric. Food Chem.* 57 (2009) 6899–6907.
- [116] M.-Z. Ding, J.S. Cheng, W.-H. Xiao, B. Qiao, Y.-J. Yuan, Comparative metabolomic analysis on industrial continuous and batch ethanol fermentation processes by GC-TOF-MS, *Metabolomics* 5 (2009) 229–238.
- [117] I. Atanassov, T. Hvarleva, K. Rusanov, I. Tsvetkov, A. Atanassov, Wine metabolite profiling: possible application in winemaking and grapevine breeding in Bulgaria, *Biotechnol. Biotechnol. Eq.* 23 (2009) 1449–1452.
- [118] J.H. Gross, *Mass Spectrometry. A Textbook*, Springer-Verlag, Berlin, 2004.
- [119] E. de Hoffmann, V. Stroobant, *Mass Spectrometry: Principles and Applications*, third ed., Wiley and Sons, West Sussex England, 2007.
- [120] M.C. McMaster, *GC/MS. A Practical User's Guide*, second ed., Wiley and Sons, NJ, 2008.
- [121] H.-J. Hübschmann, *Handbook of GC/MS. Fundamentals and Applications*, second ed., Wiley-VCH Verlag GmbH & Co, Weinheim, 2009.
- [122] M. Nantangelo, S. Tavazzi, E. Benfenati, Evaluation of solid phase microextraction-gas chromatography in the analysis of some pesticides with different mass spectrometric techniques: application to environmental waters and food samples, *Anal. Lett.* 35 (2002) 327–338.
- [123] K.J. Chia, S.D. Huang, Analysis of organochlorine pesticides in wine by solvent bar microextraction coupled with gas chromatography with tandem mass spectrometric detection, *Rapid Comm. Mass. Spec.* 20 (2006) 118–124.
- [124] P. Paya, M. Anastassiades, D. Mack, I. Sigalova, B. Tasdelen, J. Oliva, A. Barba, Analysis of pesticide residues using the Quick Easy Cheap Effective Rugged and Safe (QuEChERS) pesticide multiresidue method in combination with gas and liquid chromatography and tandem mass spectrometric detection, *Anal. Bioanal. Chem.* 389 (2007) 1697–1714.
- [125] J.A. Perez-Serradilla, J.M. Mata-Granados, M.D.L. de Castro, Low-level determination of organochlorine pesticides in wines by automatic preconcentration and GC-MS-MS detection, *Chromatographia* 71 (2010) 899–905.
- [126] J. Martins, C. Esteves, A. Limpo-Faria, P. Barros, N. Ribeiro, T. Simoes, M. Correia, C. Delerue-Matos, Multiresidue method for the determination of organophosphorus pesticides in still wine and fortified wine using solid-phase microextraction and gas chromatography-tandem mass spectrometry, *Anal. Lett.* 44 (2011) 1021–1035.
- [127] J.V. Dias, M.G.P. Nunes, I.R. Pizzutti, B. Reichert, A.A. Jung, C.D. Cardoso, Simultaneous determination of pesticides and mycotoxins in wine by direct injection and liquid chromatography-tandem mass spectrometry analysis, *Food Chem.* 293 (2019) 83–91.
- [128] J.L. Gomez-Ariza, T. Garcia-Barrera, F. Lorenzo, Analysis of anisoles in wines using pervaporation coupled to gas chromatography-mass spectrometry, *J. Chromatogr. A* 1049 (2004) 147–153.
- [129] J.L. Gomez-Ariza, T. Garcia-Barrera, F. Lorenzo, Simultaneous separation, clean-up and analysis of musty odorous compounds in wines by on-line coupling of a pervaporation unit to gas chromatography-tandem mass spectrometry, *Anal. Chim. Acta* 516 (2004) 165–170.
- [130] J.L. Gomez-Ariza, T. Garcia-Barrera, F. Lorenzo, Dynamic headspace coupled to pervaporation for the analysis of anisoles in wine by gas chromatography-ion-trap tandem mass spectrometry, *J. Chromatogr. A* 1056 (2004) 243–247.
- [131] L. Maggi, A. Zalacain, V. Mazzoleni, G.L. Alonso, M.R. Salinas, Comparison of stir bar sorptive extraction and solid-phase microextraction to determine halophenols and haloanisoles by gas chromatography-ion trap tandem mass spectrometry, *Talanta* 75 (2008) 753–759.
- [132] A.R. Fontana, S.H. Patil, K. Banerjee, J.C. Altamirano, Ultrasound-assisted emulsification microextraction for determination of 2,4,6-trichloroanisole in wine samples by gas chromatography tandem mass spectrometry, *J. Agric. Food Chem.* 58 (2010) 4576–4581.
- [133] C. Pizarro, C. Saenz-Gonzalez, N. Perez-del-Notario, J.M. Gonzalez-Saiz, Development of a dispersive liquid-liquid microextraction method for the simultaneous determination of the main compounds causing cork taint and Brett character in wines using gas chromatography-tandem mass spectrometry, *J. Chromatogr. A* 1218 (2011) 1576–1584.
- [134] C. Pizarro, N. Perez-del-Notario, J.M. Gonzalez-Saiz, Multiple headspace solid-phase microextraction for

- eliminating matrix effect in the simultaneous determination of haloanisoles and volatile phenols in wines, *J. Chromatogr. A* 1166 (2007) 1–8.
- [135] A.K. Hjelmeland, T.S. Collins, J.L. Miles, P.L. Wylie, A.E. Mitchell, S.E. Ebeler, High-throughput, sub ng/L analysis of haloanisoles in wines using HS-SPME with GC-triple quadrupole MS, *Am. J. Enol. Vitic.* 63 (2012) 494–499.
- [136] R. Godelman, S. Limmert, T. Kuballa, Implementation of headspace solid-phase-microextraction-GC-MS/MS methodology for determination of 3-alkyl-2-methoxy-pyrazines in wine, *Eur. Food Res. Technol.* 227 (2008) 449–461.
- [137] A.K. Hjelmeland, P.L. Wylie, S.E. Ebeler, A comparison of sorptive extraction techniques coupled to a new quantitative, sensitive, high throughput GC-MS/MS method for methoxy-pyrazine analysis in wine, *Talanta* 148 (2016) 336–345, 2016.
- [138] L. Cullere, J. Cacho, V. Ferreira, Validation of an analytical method for the solid phase extraction, in cartridge derivatization and subsequent gas chromatographic-ion trap tandem mass spectrometric determination of 1-ocen-3-one in wines at ng L⁻¹ level, *Anal. Chim. Acta* 563 (2006) 51–57.
- [139] F. Mattivi, L. Caputi, S. Carlin, T. Lanza, M. Minozzi, D. Nanni, L. Valenti, U. Vrhovsek, Effective analysis of rotundone at below-threshold levels in red and white wines using solid-phase microextraction gas chromatography/tandem mass spectrometry, *Rapid Comm. Mass Spec.* 25 (2011) 483–488.
- [140] J. Langen, C.-Y. Wang, P. Slabizki, K. Wall, H.-G. Schmarr, Quantitative analysis of γ - and δ -lactones in wines using gas chromatography with selective tandem mass spectrometric detection, *Rapid Commun. Mass Spectrom.* 27 (2013) 2751–2759, 2013.
- [141] L. Dagan, F. Reillon, A. Roland, R. Schneider, Development of a routine analysis of 4-mercapto-4-methylpentan-2-one in wine by stable isotope dilution assay and mass tandem spectrometry, *Anal. Chim. Acta* 821 (2014) 48–53.
- [142] C. Thibon, A. Pons, N. Mouakka, P. Redon, R. Méreau, P. Darriet, Comparison of electron and chemical ionization modes for the quantification of thiols and oxidative compounds in white wines by gas chromatography-tandem mass spectrometry, *J. Chromatogr. A* 1415 (2015) 123–133.
- [143] N. Duhamel, D. Slaghenaufi, L.I. Pilkington, M. Herbst-Johnstone, R. Larcher, D. Barker, B. Fedrizzi, Facile gas chromatography-tandem mass spectrometry stable isotope dilution method for the quantification of sesquiterpenes in grape, *J. Chromatogr. A* 1537 (2018) 91–98.
- [144] C. Thibon, S. Shinkaruk, T. Tominaga, B.E. Bennetau, D. Dubourdieu, Analysis of the diastereoisomers of the cysteinylated aroma precursor of 3-sulfanylhexanol in *Vitis vinifera* grape must by gas chromatography coupled with ion trap tandem mass spectrometry, *J. Chromatogr. A* 1183 (2008) 150–157.
- [145] D. Dubourdieu, T. Tominaga, Polyfunctional thiol compounds, Chapter 8B, in: M.V. Moreno-Arribas, M.C. Polo (Eds.), *Wine Chemistry and Biochemistry*, Springer, New York, 2009, pp. 275–293.
- [146] H.H. Jelen, M. Dziadas, M. Majcher, Different headspace solid phase microextraction—gas chromatography/mass spectrometry approaches to haloanisoles analysis in wine, *J. Chromatogr. A* 1313 (2013) 185–193.
- [147] W.G. Jennings, M. Filsoof, Comparison of sample preparation techniques for gas chromatographic analysis, *J. Agric. Food Chem.* 25 (1977) 440–445.
- [148] R. Flath, Symposium on methods for the isolation of trace volatile constituents, *J. Agric. Food Chem.* 25 (1977) 439.
- [149] K.K. Ngim, S.E. Ebeler, M.E. Lew, D.G. Crosby, J.W. Wong, Optimized procedures for analyzing primary alkylamines in wines by pentafluorobenzaldehyde derivatization and GC-MS, *J. Agric. Food Chem.* 48 (2000) 3311–3316.
- [150] A. Pendem, V.M. Pawar, S. Jayaraman, development of a gas chromatography method for the estimation of alkylamines in foods, *J. Agric. Food Chem.* 58 (2010) 8904–8910.
- [151] N. Campillo, R. Peñalver, P. Viñas, I. López-García, M. Hernández-Cordoba, Speciation of arsenic using capillary gas chromatography with atomic emission detection, *Talanta* 77 (2008) 793–799.
- [152] R. Montes, M. García-López, I. Rodríguez, R. Cela, Mixed-mode solid-phase extraction followed by acetylation and gas chromatography mass spectrometry for the reliable determination of *trans*-resveratrol in wine samples, *Anal. Chim. Acta* 673 (2010) 47–53.
- [153] L. Cai, J.A. Koziel, M. Dharmadhikari, J.H. van Leeuwen, Rapid determination of *trans*-resveratrol in red wine by solid-phase microextraction with on-fiber derivatization and multidimensional gas chromatography-mass spectrometry, *J. Chromatogr. A* 1216 (2009) 281–287.
- [154] P. Vinas, N. Campillo, N. Martinez-Castillo, M. Hernandez-Cordoba, Solid-phase microextraction on-fiber derivatization for the analysis of some polyphenols in wine and grapes using gas chromatography-mass spectrometry, *J. Chromatogr. A* 1216 (2009) 1279–1284.
- [155] H.S.M. Ali, R. Patzold, H. Bruckner, Gas chromatographic determination of amino acid enantiomers in

- bottled and aged wines, *Amino Acids* 38 (2010) 951–968.
- [156] A.I. Ruiz-Matute, M.L. Sanz, M.V. Moreno-Arribas, I. Martínez-Castro, Identification of free disaccharides and other glycosides in wine, *J. Chromatogr. A* 1216 (2009) 7296–7300.
- [157] A. Kloskowski, W. Chrzanowski, M. Pilarczyk, J. Namiesnik, Modern techniques of sample preparation for determination of organic analytes by gas chromatography, *Crit. Rev. Anal. Chem.* 37 (2007) 15–38.
- [158] E. Baltussen, C.A. Cramers, P.J.F. Sandra, Sorptive sample preparation—a review, *Anal. Bioanal. Chem.* 373 (2002) 3–22.
- [159] A. Nongonierma, A. Voilley, P. Cayot, J.-L. Le Quééré, M. Springett, Mechanisms of extraction of aroma compounds from foods, using adsorbents. Effect of various parameters, *Food Rev. Internat.* 22 (2006) 51–94.
- [160] C.F. Poole, Core concepts and milestones in the development of solid-phase extraction, in: C.F. Poole (Ed.), *Solid-Phase Extraction: Handbooks in Separation Science*, Elsevier, London, UK, 2020, pp. 1–36, 2020.
- [161] L. Xu, C. Basheer, H.K. Lee, Developments in single-drop microextraction, *J. Chromatogr. A* 1152 (2007) 184–192.
- [162] H. Piri-Moghadam, M.N. Alam, J. Pawliszyn, Review of geometries and coating materials in solid phase microextraction: opportunities, limitations, and future perspectives, *Anal. Chim. Acta* 984 (2017) 42–65.
- [163] E. Gionfriddo, É.A. Souza-Silva, T.D. Ho, J.L. Anderson, J. Pawliszyn, Exploiting the tunable selectivity features of polymeric ionic liquid-based SPME sorbents in food analysis, *Talanta* 188 (2018) 522–530.
- [164] A. Piñeiro-García, G. González-Alatorre, F. Tristan, J.C. Fierro-Gonzalez, S.M. Vegga-Díaz, Simple preparation of reduced graphene oxide coatings for solid phase micro-extraction (SPME) of furfural to be detected by gas chromatography/mass spectrometry, *Mater. Chem. Phys.* 213 (2018) 556–561.
- [165] J. Zheng, J. Huang, Q. Yang, C. Ni, X. Xie, Y. Shi, J. Sun, F. Zhu, G. Ouyang, Fabrications of novel solid phase microextraction fiber coatings based on new materials for high enrichment capability, *Trends Anal. Chem.* 108 (2018) 135–153, 2018.
- [166] R.A. Murray, Limitations to the use of solid-phase microextraction for quantitation of mixtures of volatile organic sulfur compounds, *Anal. Chem.* 73 (2001) 1646–1649.
- [167] S.J. Pérez Olivero, J.P. Pérez Trujillo, A new method for the determination of carbonyl compounds in wines by headspace solid-phase microextraction coupled to gas chromatography-ion trap mass spectrometry, *J. Agric. Food Chem.* 58 (2010) 12976–12985.
- [168] R. Flamini, A. Dalla Vedova, A. Panighel, N. Perchiazzi, S. Ongarato, Monitoring of the principal carbonyl compounds involved in malolactic fermentation of wine by solid-phase microextraction and positive ion chemical ionization GC/MS analysis, *J. Mass Spectrom.* 40 (2005) 1558–1564.
- [169] W.K. Carlton, B. Gump, K. Fugelsang, A.S. Hasson, Monitoring acetaldehyde concentrations during micro-oxygenation of red wine by headspace solid-phase microextraction with on-fiber derivatization, *J. Agric. Food Chem.* 55 (2007) 5620–5625.
- [170] H.-G. Schmarr, W. Sang, S. Ganß, U. Fischer, B. Köpp, C. Schulz, T. Potouridis, Analysis of aldehydes *via* headspace SPME with on-fiber derivatization to their O-(2,3,4,5,6-pentafluorobenzyl)oxime derivatives and comprehensive 2D-GC-MS, *J. Sep. Sci.* 31 (2008) 3458–3465.
- [171] G.M. Valtierra, R.J. Ciprés, A.P. Álvarez, Identification and quantification of aldehydes in mezcal by solid phase microextractions with on-fiber derivatization-gas chromatography, *J. Mex. Chem. Soc.* 55 (2011) 84–88.
- [172] J. Zapata, L. Mateo-Vivaraco, J. Cacho, V. Ferreira, Comparison of extraction techniques and mass spectrometric ionization modes in the analysis of wine volatile carbonyls, *Anal. Chim. Acta* 660 (2010) 197–205.
- [173] S. Risticvic, H. Lord, T. Górecki, C.L. Arthur, J. Pawliszyn, Protocol for solid-phase microextraction method development, *Nat. Protoc* 5 (2010) 122–139.
- [174] S. Risticvic, Y. Chen, L. Kudlejova, R. Vatinno, B. Baltensperger, J.R. Stuff, D. Hein, J. Pawliszyn, Protocol for the development of automated high-throughput SPME-GC methods for the analysis of volatile and semivolatile constituents in wine samples, *Nat. Protoc* 5 (2010) 162–176.
- [175] A. Panighel, R. Flamini, Applications of solid-phase microextraction and gas chromatography/mass spectrometry (SPME-GC/MS) in the study of grape and wine volatile compounds, *Molecules* 19 (2014) 21291–21309.
- [176] É.A. Sluza-Silva, E. Gionfriddo, J. Pawliszyn, A critical review of the state of the art of solid-phase microextraction of complex matrices II. Food analysis, *Trends Anal. Chem.* 71 (2015) 236–248.
- [177] S. Azzi-Achkouty, N. Estephan, N. Ouaini, D.N. Rutledge, Headspace solid-phase microextraction for wine volatile analysis, *Crit. Rev. Food Sci. Nutr.* 57 (2017) 2009–2020.
- [178] E. Psillakis, The effect of vacuum: an emerging experimental parameter to consider during headspace

- microextraction sampling, *Anal. Bioanal. Chem.* 412 (2020) 5989–5997, <https://doi.org/10.1007/s00216-020-02738-x>.
- [179] M.A. Jochman, M.P. Kmiecik, T.C. Schmidt, Solid-phase dynamic extraction for the enrichment of polar volatile organic compounds from water, *J. Chromatogr. A* 1115 (2006) 208–216.
- [180] J. Plotka-Wasyłka, N. Szczepanska, M. de la Guardia, J. Namiesnik, Miniaturized solid-phase extraction techniques, *Trends Anal. Chem.* 73 (2015) 19–38.
- [181] K. Kedziora-Koch, W. Wasiak, Needle-based extraction techniques with protected sorbent as powerful sample preparation tools to gas chromatography analysis: trends in application, *J. Chromatogr. A* 1565 (2018) 1–18.
- [182] S. Malherbe, V. Watts, H.H. Nieuwoudt, F.F. Bauer, M. du Toit, Analysis of volatile profiles of fermenting grape must by headspace solid-phase dynamic extraction coupled with gas chromatography-mass spectrometry (HS-SPDE GC-MS): novel application to investigate problem fermentations, *J. Agric. Food Chem.* 57 (2009) 5161–5166.
- [183] D. Djozan, M.A. Farajzadeh, S.M. Sorouraddin, T. Baheri, J. Norouzi, Inside-needle extraction method based on molecularly imprinted polymer for solid-phase dynamic extraction and preconcentration of triazine herbicides followed by GC-FID determination, *Chromatographia* 75 (2012) 139–148.
- [184] J.M.F. Nogueira, Stir-bar sorptive extraction: 15 years making sample preparation more environment-friendly, *Trends Anal. Chem.* 71 (2015) 214–223, 2015.
- [185] F. David, N. Ochiai, P. Sandra, Two decades of stir bar sorptive extraction: a retrospective and future outlook, *Trends Anal. Chem.* 112 (2019) 102–111, 2019.
- [186] Y. Hayasaka, K. MacNamara, G.A. Baldock, R.L. Taylor, A.P. Pollnitz, Application of stir bar sorptive extraction for wine analysis, *Anal. Bioanal. Chem.* 375 (2003) 948–955.
- [187] J. Diez, C. Dominguez, D.A. Guillen, R. Veas, C.G. Barroso, Optimisation of stir bar sorptive extraction for the analysis of volatile phenols in wines, *J. Chromatogr. A* 1025 (2004) 263–267.
- [188] R.F. Alves, A.M.D. Nascimento, J.M.F. Nogueira, Characterization of the aroma profile of Madeira wine by sorptive extraction techniques, *Anal. Chim. Acta* 546 (2005) 11–21.
- [189] A. Zalacain, J. Marin, G.L. Alonso, M.R. Salinas, Analysis of wine primary aroma compounds by stir bar sorptive extraction, *Talanta* 71 (2007) 1610–1615.
- [190] Y. Fang, M.C. Qian, Quantification of selected aroma-active compounds in Pinot noir wines from different grape maturities, *J. Agric. Food Chem.* 54 (2006) 8567–8573.
- [191] T. Kosmerl, E. Zlatic, Determination of 2-aminoacetophenone in wines using the stir bar sorptive extraction method coupled with GC-MS and GC-NPD, *Mitt. Klosterneubg.* 59 (2009) 121–126.
- [192] R. Delgado, E. Duran, R. Castro, R. Natera, C.G. Barroso, Development of a stir bar sorptive extraction method coupled to gas chromatography-mass spectrometry for the analysis of volatile compounds in Sherry brandy, *Anal. Chim. Acta* 672 (2010) 130–136.
- [193] C. Franc, F. David, G. de Revel, Multi-residue off-flavour profiling in wine using stir bar sorptive extraction-thermal desorption-gas chromatography-mass spectrometry, *J. Chromatogr. A* 1216 (2009) 3318–3327.
- [194] D.J. Caven-Quantrill, A.J. Buglass, Comparison of volatile constituents extracted from model grape juice and model wine by stir bar sorptive extraction-gas chromatography-mass spectrometry, *J. Chromatogr. A* 1218 (2011) 875–881.
- [195] M. Arbulu, M.C. Sampdero, A. Sanchez-Ortega, A. Gómez-Caballero, N. Unceta, M.A. Goicolea, R.J. Barrio, Characterisation of the flavor profile from Graciano *Vitis vinifera* wine variety by a novel dual stir bar sorptive extraction methodology coupled to thermal desorption and gas chromatography-mass spectrometry, *Anal. Chim. Acta* 777 (2013) 41–48, 2013.
- [196] E. Coelho, M.A. Coimbra, J.M.F. Nogueira, S.M. Rocha, Quantification approach for assessment of sparkling wine volatiles from different soils, ripening stages, and varieties by stir bar sorptive extraction with liquid desorption, *Anal. Chim. Acta* 635 (2009) 214–221.
- [197] J. Vestner, S. Fritsch, D. Rauhut, Development of a microwave assisted extraction method for the analysis of 2,4,6-trichloroanisole in cork stoppers by SIDA-SBSE-GC-MS, *Anal. Chim. Acta* 660 (2010) 76–80.
- [198] M.J. Ibarz, V. Ferreira, P. Hernández-Orte, N. Loscos, J. Cacho, Optimization and evaluation of a procedure for the gas chromatographic-mass spectrometric analysis of the aromas generated by fast acid hydrolysis of flavor precursors extracted from grapes, *J. Chromatogr. A* 1116 (2006) 217–229.
- [199] N. Loscos, P. Hernández-Orte, J. Cacho, V. Ferreira, Release and formation of varietal aroma compounds during alcoholic fermentation from nonfloral grape odorless flavor precursors fractions, *J. Agric. Food Chem.* 55 (2007) 6674–6684.
- [200] N. Loscos, P. Hernandez-Orte, J. Cacho, V. Ferreira, Comparison of the suitability of different hydrolytic strategies to predict aroma potential of different grape varieties, *J. Agric. Food Chem.* 57 (2009) 2468–2480.

- [201] Z. Piñero, M. Palma, C.G. Barroso, Determination of terpenoids in wines by solid phase extraction and gas chromatography, *Anal. Chim. Acta* 513 (2004) 209–214.
- [202] R. López, E. Gracia-Moreno, J. Cacho, V. Ferreira, Development of a mixed-mode solid phase extraction method and further gas chromatography mass spectrometry for the analysis of 3-alkyl-2-methoxy-pyrazines in wine, *J. Chromatogr. A* 1218 (2010) 842–848.
- [203] L. Mateo-Vivaracho, J. Cacho, V. Ferreira, Selective preconcentration of volatile mercaptans in small SPE cartridges: quantitative determination of trace odor-active polyfunctional mercaptans in wine, *J. Sep. Sci.* 32 (2009) 3845–3853.
- [204] B. Jurado-Sánchez, E. Ballesteros, M. Gallego, Gas chromatographic determination of 29 organic acids in foodstuffs after continuous solid-phase extractions, *Talanta* 84 (2011) 924–930.
- [205] R.E. Majors, New chromatography columns and accessories at Pittcon 2011: Part II, LC-GC N. Am. 29 (2011) 301–316.
- [206] A. Panighel, R. Flamini, Solid phase extraction and solid phase microextraction in grape and wine volatile compounds analysis, *Sample Prep.* 2 (2015) 55–65.
- [207] J. Feng, H.M. Loussala, S. Han, X. Ji, C. Li, M. Sun, Recent advances of ionic liquids in sample preparation, *Trends Anal. Chem.* 125 (2010) 115833.
- [208] E.V.S. Maciel, A.L. de Toffoli, F.M. Lanças, Current status and future trends on automated multidimensional separation techniques employing sorbent-based extraction columns, *J. Sep. Sci.* 42 (2019) 258–272.
- [209] F. Pena-Pereira, I. Lavilla, C. Bendicho, Miniaturized preconcentration methods based on liquid-liquid extraction and their application in inorganic ultratrace analysis and speciation: a review, *Spectrochim. Acta B* 54 (2009) 1–15.
- [210] M. Rezaee, Y. Assadi, M.-R.M. Hosseini, E. Aghaee, F. Ahmadi, S. Berijani, Determination of organic compounds in water using dispersive liquid-liquid microextraction, *J. Chromatogr. A* 1116 (2006) 1–9.
- [211] J. Regueiro, M. Llompert, C. Garcia-Jares, J.C. Garcia-Monteagudo, R. Cela, Ultrasound-assisted emulsification-microextraction of emergent contaminants and pesticides in environmental waters, *J. Chromatogr. A* 1190 (2008) 27–38.
- [212] A. Spietulun, L. Marcinkowski, M. de la Guardia, J. Namiesnik, Green aspects, developments and perspectives of liquid phase microextraction techniques, *Talanta* 119 (2014) 34–45.
- [213] M. Alexovic, B. Horstkotte, P. Solich, J. Sabo, Automation of static and dynamic non-dispersive liquid phase microextraction. Part 1: approaches based on extractant drop-, plug-, film- and microflow-formation, *Anal. Chim. Acta* 906 (2016) 22–40.
- [214] M. Alexovic, B. Horstkotte, P. Solich, J. Sabo, Automation of static and dynamic non-dispersive liquid phase microextraction. Part 2: approaches based on impregnated membranes and porous supports, *Anal. Chim. Acta* 907 (2016) 18–30.
- [215] M. Alexovic, B. Horstkotte, I. Sramkova, P. Solich, J. Sabo, Automation of dispersive liquid-liquid microextraction and related techniques. Approaches based on flow, batch, flow-batch and in-syringe modes, *Trends Anal. Chem.* 86 (2017) 39–55, 2017.
- [216] J. Soares da Silva Burato, D.A. Vargas Medina, A.L. de Toffoli, E. Vasconcelos Soares Maciel, F. Mauro Lancas, Recent advances and trends in miniaturized sample preparation techniques, *J. Sep. Sci.* 43 (2020) 202–225.
- [217] A. Garbi, V. Sakkas, Y.C. Fiamegos, C.D. Stalikas, T. Albanis, Sensitive determination of pesticides residues in wine samples with the aid of single-drop microextraction and response surface methodology, *Talanta* 82 (2010) 1286–1291.
- [218] I. Sramkova, B. Horstkotte, P. Solich, H.H. Sklenarova, Automated in-syringe single-drop head-space micro-extraction applied to the determination of ethanol in wine samples, *Anal. Chim. Acta* 828 (2014) 53–60.
- [219] J. Pereira dos Anjos, J.B. Andrade, Simultaneous determination of pesticide multiresidues in white wine and rosé wine by SDME/GC-MS, *Microchem. J.* 120 (2015) 69–76.
- [220] P. Viñas, N. Martínez-Castillo, N. Campillo, M. Hernández-Córdoba, Directly suspended droplet microextraction with in injection-port derivatization coupled to gas chromatography-mass spectrometry for the analysis of polyphenols in herbal infusions, fruits and functional foods, *J. Chromatogr. A* 1218 (2011) 639–646.
- [221] J.G. March, C. Genestar, B.M. Simonet, Determination of 2-ethylhexyl 4-(dimethylamino) benzoate using membrane-assisted liquid-liquid extraction and gas chromatography-mass spectrometric detection, *Anal. Bioanal. Chem.* 394 (2009) 883–891.
- [222] R. Montes, I. Rodríguez, M. Ramil, E. Rubi, R. Cela, Solid-phase extraction followed by dispersive liquid-liquid microextraction for the sensitive determination of selected fungicides in wine, *J. Chromatogr. A* 1216 (2009) 5459–5466.
- [223] B. Chen, F.-Q. Wu, W.-D. Wu, B.-H. Jin, L.-Q. Xie, W. Feng, G. Ouyang, Determination of 27 pesticides in wine by dispersive liquid-liquid microextraction

- and gas chromatography-mass spectrometry, *Microchem. J.* 126 (2016) 415–422, 2016.
- [224] N. Campillo, P. Viñas, J. I. Cacho, R. Peñalver, M. Hernández-Córdoba, Evaluation of dispersive liquid-liquid microextraction for the simultaneous determination of chlorophenols and haloanisoles in wines and cork stoppers using gas chromatography-mass spectrometry, *J. Chromatogr. A* 1217 (2010) 7323–7330.
- [225] C. Pizarro, C. Sáenz-González, N. Perez-del-Notario, J.M. González-Sáiz, Optimisation of a dispersive liquid-liquid microextraction method for the simultaneous determination of halophenols and haloanisoles in wines, *J. Chromatogr. A* 1217 (2010) 7630–7637.
- [226] J. Plotka-Wasyłka, V. Simeonov, J. Namiesnik, An *in situ* derivatization-dispersive liquid-liquid microextraction combined with gas chromatography-mass spectrometry for determining biogenic amines in home-made fermented alcoholic drinks, *J. Chromatogr. A* 1453 (2016) 10–18.
- [227] V.P. Jofré, M.V. Assof, M.L. Fanzone, H.C. Goicoechea, L.D. Martínez, M.F. Silva, Optimization of ultrasound assisted-emulsification-dispersive liquid-liquid microextraction by experimental design methodologies for the determination of sulfur compounds in wines by gas chromatography-mass spectrometry, *Anal. Chim. Acta* 683 (2010) 126–135.
- [228] C. Cortada, L. Vidal, A. Canals, Determination of geosmin and 2-methylisoborneol in water and wine samples by ultrasound-assisted dispersive liquid-liquid microextraction coupled to gas chromatography-mass spectrometry, *J. Chromatogr. A* 1218 (2011) 17–22.
- [229] A. Fontana, I. Rodríguez, R. Cela, Dispersive liquid-liquid microextraction and gas chromatography accurate mass spectrometry for extraction and non-targeted profiling of volatile and semi-volatile compounds in grape marc distillates, *J. Chromatogr. A* 1546 (2018) 36–45.
- [230] M. Anastassiades, S.J. Lehotay, D. Stajnbaher, F.J. Schenck, Fast and easy multiresidue method employing acetonitrile extraction/partitioning and “dispersive solid-phase extraction” for the determination of pesticide residues in produce, *J. AOAC Int.* 86 (2003) 412–431.
- [231] R.E. Majors, QuEChERS—a new sample preparation technique for multiresidue analysis of pesticides in foods and agricultural samples, *LC GC* 25 (2007) 436–446.
- [232] S.J. Lehotay, M. Anastassiades, R.E. Majors, QuEChERS, a sample preparation technique that is “catching on”: an up-to-date interview with the inventors, *LC GC* 28 (2010) 504–516.
- [233] J. Fenik, M. Tankiewicz, M. Biziuk, Properties and determination of pesticides in fruits and vegetables, *Trends Anal. Chem.* 30 (2011) 814–826.
- [234] T. De Souza Vargas, N. de Andrade Salustriano, B. Klein, W. Romão, S. Riberio Campos da Silva, R. Wagner, R. Scherer, Fungicides in red wines produced in South America, *Food Addit. Contam. A* 35 (2018) 2135–2144.
- [235] Á. Santana-Mayor, B. Socas-Rodríguez, A.V. Herrera-Herrera, M.A. Rodríguez-Delgado, Current trends in QuEChERS method. A versatile procedure for food, environmental and biological analysis, *Trends Anal. Chem.* 116 (2019) 214–235.
- [236] R. Perestrelo, P. Silva, P. Porto-Figueira, J.A.M. Pereira, C. Silva, S. Medina, J.S. Câmara, QuEChERS-Fundamentals, relevant improvements, applications and future trends, *Anal. Chim. Acta* 1070 (2019) 1–28.
- [237] R. Urkude, V. Dhurvey, S. Kochhar, Pesticide residues in beverages, in: A.M. Grumezescu, A.M. Holban (Eds.), *Quality Control in the Beverage Industry*, vol. 17, Elsevier, London, United Kingdom, 2019, pp. 529–560, 2019.
- [238] S.C. Cunha, J.O. Fernandes, A. Alves, M.B.P. P Oliveira, Fast low-pressure gas chromatography-mass spectrometry method for the determination of multiple pesticides in grapes, musts, and wines, *J. Chromatogr. A* 1216 (2009) 110–126.
- [239] Y. Jiang, X. Li, J. Xu, C. Pan, J. Zhang, W. Niu, Multi-residue method for the determination of 77 pesticides in wine using QuEChERS sample preparation and gas chromatography with mass spectrometry, *Food Addit. Contam. A* 26 (2009) 859–866.
- [240] Y.-J. Lian, G.-F. Pang, H.-R. Shu, C.-L. Fan, Y.-M. Liu, J. Feng, Y.-P. Wu, Q.-Y. Chang, Simultaneous determination of 346 multiresidue pesticides in grapes by PSA-MSPD and GC-MS-SIM, *J. Agric. Food Chem.* 58 (2010) 9428–9453.
- [241] W.-J. Kong, Q.-T. Liu, D.D. Kong, Q.Z. Liu, X.-P. Ma, M.-H. Yang, Trace analysis of multi-class pesticide residues in Chinese medicinal health wines using gas chromatography with electron capture detection, *Sci. Rep.* 6 (2016) 21558.
- [242] S.J. Lehotay, M. O’Neil, J. Tully, A.V. García, M. Contreras, H. Moi, V. Heinke, T. Anspach, G. Lach, R. Fussell, K. Mastovska, M.E. Poulsen, A. Brown, W. Hammack, J.M. Cook, L. Alder, K. Lindtner, M.G. Vila, M. Hopper, A. De Kok, M. Hiemstra, F. Schenck, A. Williams, A. Parker, Determination of pesticide residues in foods by acetonitrile extraction and partitioning with magnesium sulfate: collaborative study, *J. AOAC Int.* 90 (2007) 485–520.

- [243] EN 15662, Foods of plant origin-Multimethod for the determination of pesticide residues using GC- and LC-based analysis following extraction/partitioning and clean-up by dispersive SPE-Modular QuEChERS-method, in: European Committee for Standardization, CEN/TC 275-Food Analysis-Horizontal Methods, ISG 67.050-General Methods of Tests and Analysis for Food Products, 2018. Accessed via, www.cen.eu. (Accessed 18 July 2020).
- [244] R. Perestrelo, J.M.F. Nogueira, J.S. Camara, Potentialities of two solventless extraction approaches-stir bar sorptive extraction and headspace solid-phase micro-extraction for determination of higher alcohol acetates, isoamyl esters and ethyl esters in wines, *Talanta* 80 (2009) 622–630.
- [245] I. Andujar-Ortiz, M.V. Moreno-Arribas, P.J. Martín-Alvarez, M.A. Pozo-Bayón, Analytical performance of three commonly used extraction methods for the gas chromatography-mass spectrometry analysis of wine volatile compounds, *J. Chromatogr. A* 1216 (2009) 7351–7357.
- [246] T.E. Siebert, H.E. Smyth, D.L. Capone, C. Neuwöhner, K.H. Pardon, G.K. Skouroumounis, M.J. Herderich, M.A. Sefton, A.P. Pollnitz, Stable isotope dilution analysis of wine fermentation products by HS-SPME-GC-MS, *Anal. Bioanal. Chem.* 382 (2005) 937–947.
- [247] I. Lavignini, B. Fedrizzi, G. Versini, F. Magno, Effectiveness of isotopically labeled and non-isotopically labeled internal standards in the gas chromatography/mass spectrometry analysis of sulfur compounds in wines: use of a statistically based matrix comprehensive approach, *Rapid Comm. Mass Spec.* 23 (2009) 1167–1172.
- [248] L. Rebiere, A.C. Clark, L.M. Schmidtke, P.D. Prenzler, G.R. Scollary, A robust method for quantification of volatile compounds within and between vintages using headspace-solid-phase micro-extraction coupled with GC-MS-Application on Semillon wines, *Anal. Chim. Acta* 660 (2010) 149–157.
- [249] V. Ferreira, P. Herrero, J. Zapata, A. Escudero, Coping with matrix effects in headspace solid phase microextraction gas chromatography using multivariate calibration strategies, *J. Chromatogr. A* 1407 (2015) 30–41.
- [250] G.A. Gómez-Ríos, N. Reyes-Garcés, J. Pawliszyn, Development of a new in-vial standard gas system for calibrating solid-phase microextraction in high-throughput and on-site applications, *J. Sep. Sci.* 36 (2013) 2939–2945.
- [251] V.N. Sidelnikov, O.A. Nikolaeva, I.A. Platonov, V.N. Parmon, Gas chromatography of the future: columns whose time has come, *Russ. Chem. Rev.* 85 (2016) 1033–1055.
- [252] B.P. Regmi, M. Agah, Micro gas chromatography: an overview of critical components and their integration, *Anal. Chem.* 90 (2018) 13133–13150.

Gas chromatographic analysis of emerging and persistent environmental contaminants

Frank L. Dorman, Eric J. Reiner

Biochemistry and Molecular Biology, The Pennsylvania State University, University Park, PA,
United States

Humans have been using chemicals for more than 100 years. There currently are about 100,000 chemicals of commerce in use today [1]. Almost 3000 of them are high-production-volume chemicals (production volumes of more than 1 million pounds per year). For example, lindane was first synthesized in 1833, polychlorinated naphthalenes (PCNs) in 1833, and DDT in 1873, but these compounds were not used for practical applications until many years later [2,3]. PCNs were used to flame retard military uniforms and airplane cloth in World War 1. PCNs were also used as flame retardants for cloth electrical cabling prior to the development of polymeric cable coatings and as antifungal agents for rubber as recently as 2003 [4]. In the early 1900s, halogenated organic compounds were analyzed by boiling them in the presence of silver nitrate and then measuring their concentration gravimetrically (Carius method) or treating the halide with sodium in the presence of ethanol and the chloride concentration determined by titration using

the Volhard method. Due to the toxicity of these compounds, spectrophotometric methods were developed in the 1940s to reduce detection limits, but these methods were still not sensitive or selective enough to be used for the protection of human health or the environment. PCNs were replaced by polychlorinated biphenyls (PCBs) as they were less toxic than the dioxin-like PCNs. In the late 1940s, a number of chemicals including DDT were identified as having pesticide properties. DDT was used to control mosquitoes, lice, and ticks that can carry malaria, typhus, and typhoid. Many other pesticides were developed and used in the late 1940s and up to early 1970s [4]. Rachel Carson's efforts and book, *Silent Spring* [5], were a major cause in the banning of these materials by the mid-1970s. The extensive bird deaths resulted from eating highly contaminated earthworms that break down contaminated foliage. Carson's efforts are considered the beginning of the environmental movement.

33.1 Introduction

The discovery of gas chromatography (GC) in the early 1950s [6] was a very important development as it enabled the separation and detection of the many components present in environmental samples. Early detectors such as the thermal conductivity detector were not very sensitive or selective. The electron-capture detector (ECD), very sensitive and selective to organohalogen compounds, and the mass spectrometer, a universal detector, were both first used in the late 1950s. The ECD [7] is still used in many applications, but the development of cheaper, more rugged, and user-friendly mass spectrometers has made them the GC detector of choice for most applications [8]. Packed GC columns were used from the 1950s to the 1970s. For these types of columns, the stationary phase was coated onto a support material that was packed in a column (see Chapter 4). The separating power was quite poor as compared to today's standards with peak capacities of less than 10. The wall-coated open-tubular column (WCOT) or capillary column was developed in the early 1960s, but not commonly used until the late 1970s or early 1980s following the development of fused silica, which enabled long columns (30 m and longer) to be wound on a support cage that could be placed in an oven [9,10]. The separating power of capillary columns is significantly greater than packed columns with peak capacities ranging from 50 to 100 (see Chapter 3). Standard configurations are 0.25 mm id, 0.25 μm d_f and are used for most applications. By decreasing the inner diameter and reducing the film thickness while keeping the phase ratio (inner diameter to film thickness) constant, the relative retention times remain the same. Narrower-bore columns have a greater number of theoretical plates per meter enabling shorter columns to be used resulting in shorter analysis times. The GC peaks become taller and narrower, which increases sample detectability. This technique is termed "fast GC" and chromatographic run times can be reduced by up to 80%. The main

challenge with the narrow peaks produced using fast GC is to obtain the necessary 7–10 sampling points across a GC peak to ensure accurate determination of peak area. Comprehensive two-dimensional gas chromatography (GC \times GC) [11,12] is a relatively new technique where two GC columns of different phases are linked using a device called a modulator (see Chapter 7). The modulator traps the eluent from the first (dimension) column and reinjects it into the second (dimension) column. The peaks eluting from the second column are very narrow (a few hundred milliseconds wide) resulting in significant improvement in separations. A schematic of a GC \times GC system is shown in Fig. 33.1. Peak capacities of GC \times GC analyses can be over 1000.

Although many thousands of chemicals are used, only a small number are regulated on an international scale. The Stockholm Agreement [13], first ratified in 2001, included only 12 halogenated compounds or compound groups (see Table 33.1). An additional nine were added in 2009 and three more are currently under review. All of the original and recently added compounds are persistent, bioaccumulative, and toxic organic compounds. To analyze these compounds, samples must be quantitatively extracted and the extract must be simplified to remove matrix coextractables so that a portion of the cleaned extract can be injected into the analytical instrument without affecting or biasing the results or damaging the instrument. Compounds such as dioxin, polychlorinated biphenyls (PCBs), polychlorinated naphthalenes (PCNs), polychlorinated diphenylethers (PCDEs), or polybrominated diphenyl ethers (PBDEs) are multicomponent mixtures comprised of congeners (a series of related compounds where hydrogen atoms are serially replaced by chlorine or bromine atoms—see Fig. 33.2). The toxicity of the specific congeners can vary significantly [14]. For example, the toxicity of the two major dioxins present in Agent Orange, 1,3,6,8-tetrachlorodibenzo-p-dioxin (TCDD) and 2,3,7,8-TCDD, can vary by

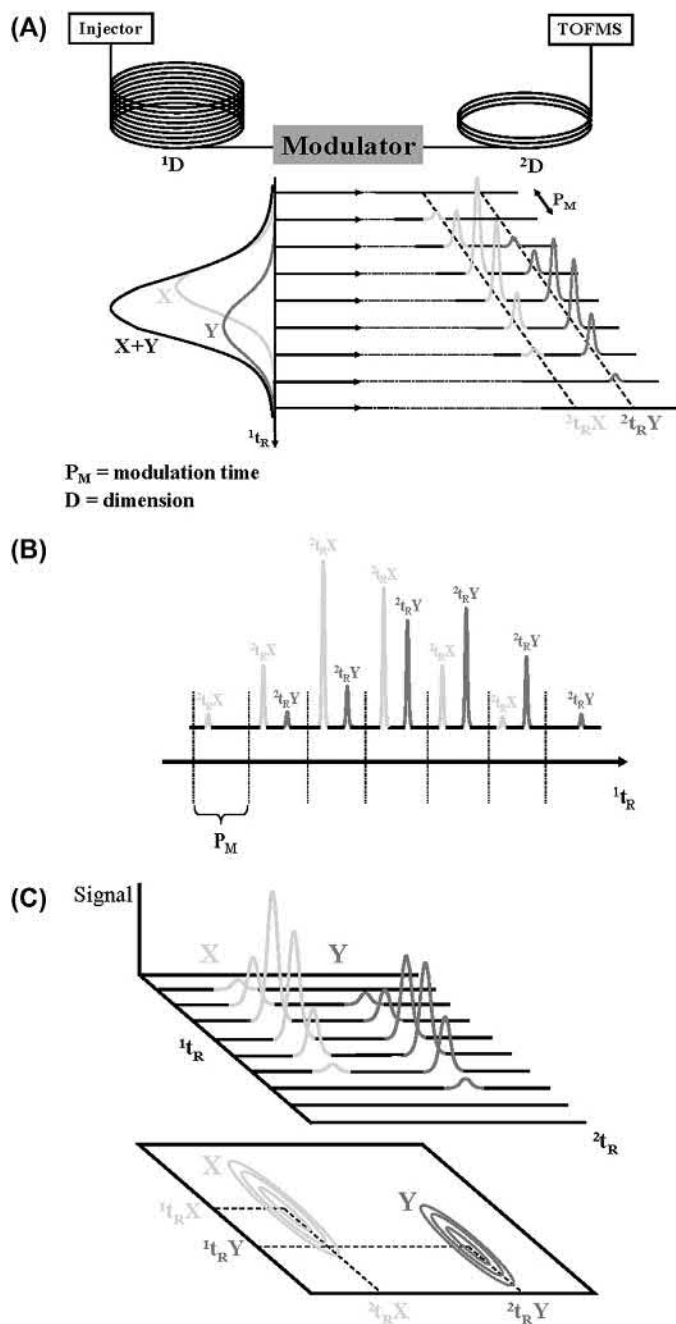


FIGURE 33.1 Schematic of the GC \times GC-TOFMS apparatus and how chromatograms are produced. (A) The modulator allows sampling of the analytes eluting from the first-dimension GC (1D) and reinjects them into the second-dimension column (2D). The modulation process is illustrated for two coeluting compounds in 1D (X and Y) retention time 1t_R in the first dimension. As the modulation process occurs during the modulation period P_m , narrow bands of analytes enter 2D and elute with different second-dimension retention times $^2t_R(X)$ and $^2t_R(Y)$. (B) Raw data signals are recorded by the TOFMS throughout the entire separation process. (C) Construction of a two-dimensional contour plot from the high-speed secondary chromatograms obtained in (B), in which similar signal intensities are connected by the contour lines. Modified from J.F. Focant, E.J. Reiner, K. MacPherson, T. Kolic, A. Sjodin, D.G. Patterson Jr, et al., *Measurement of PCDD, PCDFs, and non-ortho-PCBs by comprehensive multidimensional gas chromatography-isotope dilution time-of-flight mass spectrometry (GcxGC-IDTOFMS)*, *Talanta* 63 (2004) 1231–1240.

TABLE 33.1 Stockholm convention POPs.

Category	Compounds
Pesticides	<ul style="list-style-type: none"> • Aldrin • Chlordane • Dieldrin • DDT • Endrin • Heptachlor • Hexachlorobenzene (HCB) • Mirex • Toxaphene
Industrial chemicals	<ul style="list-style-type: none"> • Polychlorinated biphenyls (PCBs)
Unintentional production	<ul style="list-style-type: none"> • Polychlorinated dibenzodioxins (PCDDs) and dibenzofurans (PCDF) • PCBs • HCB
Added, May 2009	<ul style="list-style-type: none"> • Chlordecone • ?-Hexachlorocyclohexane • ?-Hexachlorocyclohexane • Hexabromobiphenyl • Hexabromodiphenyl ether and heptabromodiphenyl ether • Lindane (gamma-hexachlorocyclohexane) • Pentachlorobenzene • Perfluorooctanesulfonic acid (PFOS), its salts and perfluorooctanesulfonyl fluoride • Tetrabromodiphenyl ether and pentabromodiphenyl ether
Compounds under review nominated for addition, October 2009	<ul style="list-style-type: none"> • Short-chain chlorinated paraffin (SCCPs) • Endosulfan • Hexabromocyclododecane (HBCD)

six orders of magnitude, with the 2,3,7,8 congener being the most toxic of all dioxin congeners. Mass spectrometry (MS) is considered the most selective of all detectors. A major drawback in the analysis of isomers (and congeners if they fragment to common ions) is that they cannot be distinguished if their mass spectra are identical or very similar. This is frequently the case with the persistent environmental pollutants described in this chapter and therefore requires a separation technique such as GC to be used in conjunction with MS detection. In general, the combination of GC and MS is considered the most sensitive and selective analytical technique for these types of compounds.

33.2 Polychlorinated biphenyls

PCBs were first synthesized in 1881. Commercial production began in 1929, by the Anniston Ordnance Company (Anniston, Alabama), whose name was later changed to the Theodore Swann Company after the founder Theodore Swann. In 1935, this facility was purchased by Monsanto, who became one of the largest manufacturers of PCBs with production levels peaking in 1970. Manufacturing continued until 1977 when production was halted. During this time, estimates are that over 1 million tons of PCBs were produced, a considerable amount of which unfortunately has entered the environment through a variety of pathways [15]. PCBs had a wide variety of potential uses, including extenders in insecticide production, paint ingredients, insulators for electrical devices such as transformers and capacitors, and heat exchange fluids [16].

PCBs are a family of chlorinated organic compounds that consist of two benzene rings linked by a carbon-carbon bond. Chlorine is substituted on the two rings from 1 to 10 available positions (Fig. 33.2), which accounts for

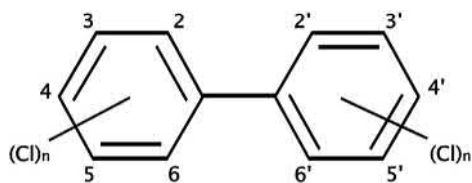


FIGURE 33.2 Structure and naming for PCBs.

209 possible congeners in the family of PCBs. A PCB is then commonly referred to either by its specific congener structure (e.g., 2,2',4,4' tetra-chlorobiphenyl) as in the case of a specific compound or by the commercial product itself.

Since individual congeners were not manufactured and isolated in the commercial process, many PCB analytical methods are based around the identification and quantification of the commercial mixture. Commercial mixtures were sold under a variety of trade names, as listed in Table 33.2. Among these commercial names, "Aroclor" is one of the most prevalent, and, within each family of commercial mixtures, there are typically several different products [17]. These products were developed for a variety of uses and range both in overall distribution of congeners and in the degree of chlorination. For the Aroclor family, each mixture is given a numerical identifier that denotes its chlorination range. Specifically the last two digits of the Aroclor number denote the percent chlorine substitution by weight (except for Aroclor 1016). Table 33.3 lists the common Aroclor mixtures.

33.2.1 Analytical considerations

When developing an analytical method for PCBs, it is important to first determine the reason for performing the work: identification and quantification of the specific congeners or determination of the commercial mixture. Since PCBs were used as commercial mixtures, not as specific congeners, many methods have been focused on the identification of the commercial mixture or mixtures present in a sample,

TABLE 33.2 PCB commercial mixtures and primary country of use.

APIROLIO	(Italy)
AROCLOR	(UK, USA)
ASBESTOL	(USA)
ASKAREL	(UK, USA)
BAKOLA 131	(USA)
CHLOREXTOL	(USA)
CLOPHEN	(Germany)
DELOR	(Czechoslovakia)
DK	(Italy)
DIACLOR	(USA)
DYKANOL	(USA)
ELEMEX	(USA)
FENCLOR	(Italy)
HYDOL	(USA)
INTERTEEN	(USA)
KANECLOR	(Japan)
NOFLAMOL	(USA)
PHENOCOLOR	(France)
PYRALENE	(France)
PYRANOL	(USA)
PYROCLOR	(UK)
SAFT-KUHL	(USA)
SOVOL	(USSR)
SOVTOL	(USSR)

Adapted from *PCB Transformers and Capacitors: From Management to Reclassification and Disposal*. UNEP Chemicals, Geneva, Switzerland. www.chem.unep.ch/pops/pdf/PCBtrnsacap.pdf.

followed by their quantification [18]. Methods employing this approach use commercial mixtures as calibration standards and typically identify several of the highest responding components, which are characteristic for each of the mixtures. Several difficulties arise from these so-called "Aroclor" methods. Most

TABLE 33.3 Common Aroclor formulations.

CA #	Formulation	Approximate weight% Cl
12674-11-2	Aroclor 1016	40
11104-28-2	Aroclor 1221	21
11141-16-5	Aroclor 1232	32
53469-21-9	Aroclor 1242	42
12672-29-6	Aroclor 1248	48
11097-69-1	Aroclor 1254	54
11096-82-5	Aroclor 1260	60
37324-23-5	Aroclor 1262	62
11100-14-4	Aroclor 1268	68

Table adapted from *Aroclor and Other PCB Mixtures*, USEPA Web Document. <http://www.epa.gov/osw/hazard/tsd/pubs/aroclortable.pdf>.

notably, weathering of the PCB mixture since its introduction into the environment can cause significant distortion of the pattern of the individual congeners relative to the original commercial mixture. It is easily possible to determine the most significant congeners in the original Aroclor from the calibration standards, and a calibration curve can be developed for each of these. If the pattern or distribution of these congeners changes as a result of weathering of the samples, however, the Aroclor may be misidentified or incorrectly quantified.

The individual identification and quantification of the PCB congeners are a possible solution to issues of weathering; however, this approach is arguably more difficult. Since there are 209 possible congeners, all of which are chemically similar, the complete separation of these has been a goal of the analytical community for quite some time. Even though there are some very sophisticated methods for analysis, to date, nobody has separated all 209 PCB congeners in a single separation, even when employing dual-column separations and/or mass spectrometric detection. One significant advantage of

the congener-based analysis is that the individual PCBs range considerably in toxicological effect. Many of the PCBs are considered relatively nontoxic, but some are of considerable concern. PCB congeners without chlorine substitution at the ortho-positions on the two rings are able, via rotation, to align in a planar geometry. This causes these specific congeners to adopt a structure more similar to the toxic dioxin and furan congeners, discussed in another section. These congeners may be termed "dioxin-like" or "coplanar" congeners. A detailed congener analysis is, therefore, the method of choice if the goal of the analysis is to measure PCBs based on their toxic qualities to arrive at a toxic equivalent (TEQ) value. There are generally 12 PCB congeners that are considered to have these properties as listed in Table 33.4.

TABLE 33.4 PCB congeners with TEF values as assigned by the World Health Organization (WHO) [19].

Non-ortho-PCB congener	IUPAC name	WHO-TEF
PCB77	3,4,4',5-TeCB	0.0001
PCB 81	3,3',4,4'-TeCB	0.0003
PCB 126	3,3',4,4',5-PeCB	0.1
PCB 169	3,3',4,4',5,5'-HxCB	0.03
Mono-ortho PCB congener		
PCB 105	2',3,4,4',5-PeCB	0.00003
PCB 114	2,3',4,4',5-PeCB	0.00003
PCB 118	2,3,4,4',5-PeCB	0.00003
PCB 123	2,3,3',4,4'-PeCB	0.00003
PCB 156	2,3,3',4,4',5'-HxCB	0.00003
PCB 157	2,3',4,4',5,5'-HxCB	0.00003
PCB 167	2,3,3',4,4',5-HxCB	0.00003
PCB 189	2,3,3',4,4',5,5'-HpCB	0.00003

33.2.2 Analysis of PCBs based on commercial mixtures

Each of the commercial mixtures (Aroclors, Kaneclors, etc.) contains a distribution of individual congeners. Several studies have been conducted to determine the individual congener composition of these mixtures using either GC-ECD or GC-MS. Current regulatory methods simplify the analytical methodology either by specifying quantification as a combination of one or more commercial-product congener distributions or by specifying short lists of target congeners for individual quantification. There have been studies to detail the congener composition of the various commercial mixtures so that, in theory, identification of the actual commercial mixture would not be necessary [20]. Even so, "Aroclor" methods still abound. These methods rely on the analysis of chemical reference materials that are the commercial mixtures. These standards are analyzed over a range of concentrations with enough chromatographic resolution to allow for the identification of the most significant congeners in the distribution.

For calibration, standards of the possible commercial mixtures are analyzed to allow for pattern identification as shown in Fig. 33.3. Aroclors identified in the samples are then quantified against a multipoint calibration curve for each Aroclor based on the 3–5 of the most significant congeners for each. Each congener chosen must be characteristic for each Aroclor; however, in general, the later-eluting congeners are subject to less weathering or breakdown.

Unknowns must first then be qualitatively identified as to which commercial mixture or mixtures represent the PCB distribution in the sample. Provided this is successful, the same significant congeners are used to provide 3–5 separate estimates of concentration through the use of the previously mentioned calibrations. The lowest value (assumed to have the least bias from possible interference) is then used for final

quantification of the sample. Many methods employ some sort of QA/QC criterion in terms of the variance of the quantified values. Quantification is considered to be more valid if the 3–5 chosen congeners all yield similar results for a sample.

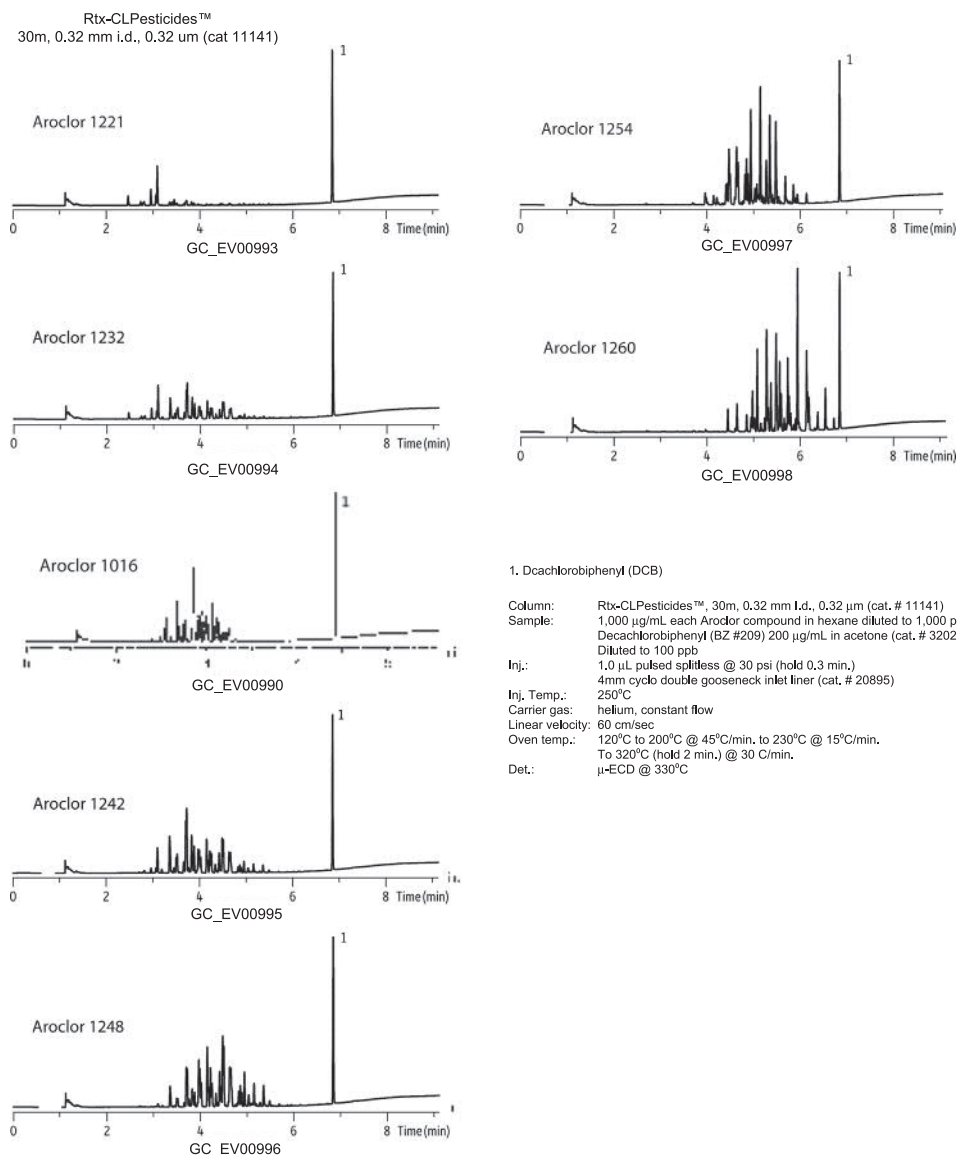
Methods employing ECD detection are generally subject to a second-column conformational analysis. This may be done at the time of initial sample analysis through the use of a dual-column instrumental setup, or sample with positive analyses for PCBs may be reanalyzed using a secondary, or confirmation, column. The confirmatory column must have a dissimilar elution order to minimize the possibility of interference from pesticides and other compounds commonly found in some PCB-containing samples.

The quantitation of PCBs as Aroclors is appropriate for many regulatory compliance determinations, but is particularly difficult when the Aroclors have been weathered by long exposure in the environment. Since PCBs were eliminated from production many years ago, most samples have undergone some amount of weathering. In addition, when mixtures of PCBs are in a single sample, identification of the Aroclors may be difficult and, if identification is incorrect, then the quantification will be inaccurate as the sample may be compared to the wrong standard. These reasons, in addition to the common need to determine toxicological-based data, have led to the ever-increasing adoption of congener-based analytical methods.

33.2.3 Analysis of PCBs based on individual congeners

The individual PCB congeners are named according to the convention of their single-ring chlorine substitution. This yields their IUPAC name. Due to the complexity of these names, there have been PCB numbering systems based on the positional substitution of chlorine on the

Aroclor PCB's
Rtx-CLPesticides



Restek Corporation 110 Benner Circle Bellefonte, PA 16823
 814-353-1300 800-356-1688 Fax 814-353-1309 www.restek.com

FIGURE 33.3 Common Aroclor standard chromatograms showing the distribution of PCB congeners.

two rings of the molecule [21,22]. It should be noted that the two listed naming systems differ for congeners 107, 108, 109, 199, 100, and 201.

What must first be determined in the development of a congener-specific analysis is the intended target compound list. For all the Aroclors, approximately 150 congeners may be present [20]. Numerous GC column combinations were evaluated in order to determine the chromatographic conditions that resulted in the best overall separation, but in general “XLB-type” phases are considered the best as far as single-column separations using GC-MS. For two-column chromatographic separations using electron-capture detection, numerous column combinations have been evaluated, but in general 5% diphenyl polydimethylsiloxane columns, or XLB columns as the primary column and either carborane phases (e.g., HT-8 or SGE) [23], or other functionalized polysiloxane phases as confirmatory columns are preferred. In the case of congener-specific analysis, each compound is treated as an individual. If a total PCB quantity is required, the congeners are merely summed following individual quantification. If the identification of specific Aroclor is desired from a congener-specific analysis, the congener distribution as a function of Aroclor must be considered (Fig. 33.4) [20]. While this reconstitution is possible, it can be difficult especially in complex samples and in cases of weathering.

33.2.4 Recent improvements to chromatographic separation of PCBs

As previously mentioned, comprehensive GC (GC × GC) is a technique that has been used to increase the peak capacity of a GC separation. This technique has allowed for a further increase in the total number of PCB congeners resolved in a single analysis [24]. Using two GC columns with considerably different selectivity (ca. HT-8 and BPX-50), it is possible to separate 188 of the 209 PCB congeners. Further, by using

time-of-flight MS (TOFMS) as a detector, it is currently possible to separate 192 of the 209 PCB congeners. This required an analysis time of 146 min, but represents the current state of the art at the time of writing for PCB congener analysis. It may be only a matter of time before the complete separation of all 209 congeners becomes possible—a feat that has been attempted by analytical chemists for quite a long time.

33.2.5 PCB summary

PCB analysis is still one of the most common environmental analyses performed in US commercial laboratories, despite the fact that PCB manufacturing voluntarily ceased in the United States in the 1970s. Due to the fact that there is no “consensus method” for the analysis of PCBs, they can be especially demanding. Numerous congener and Aroclor methods have been reported, but analytically the congener methods are preferred. Considering the total number of possible congeners, this analysis is complex, but unless sample fractionation is being performed (to isolate the coplanar PCBs, for example), it is best that the entire list of environmentally found PCBs be the minimum target compound list and possibly the entire list of 209 congeners.

33.3 Dioxins

Polychlorinated dibenzo-p-dioxins (PCDDs) and polychlorinated dibenzofurans (PCDFs) are structurally related planar compounds with two chlorine-substituted benzene rings connected by one (furan) or two oxygen atoms (dioxin). There are 75 possible dioxin congeners and 135 possible furan congeners where up to eight chlorines can replace hydrogen atoms in the three-ring structure. Congeners with chlorines in the 2,3,7,8 positions can bind with the aryl hydrocarbon receptor (AhR), which can

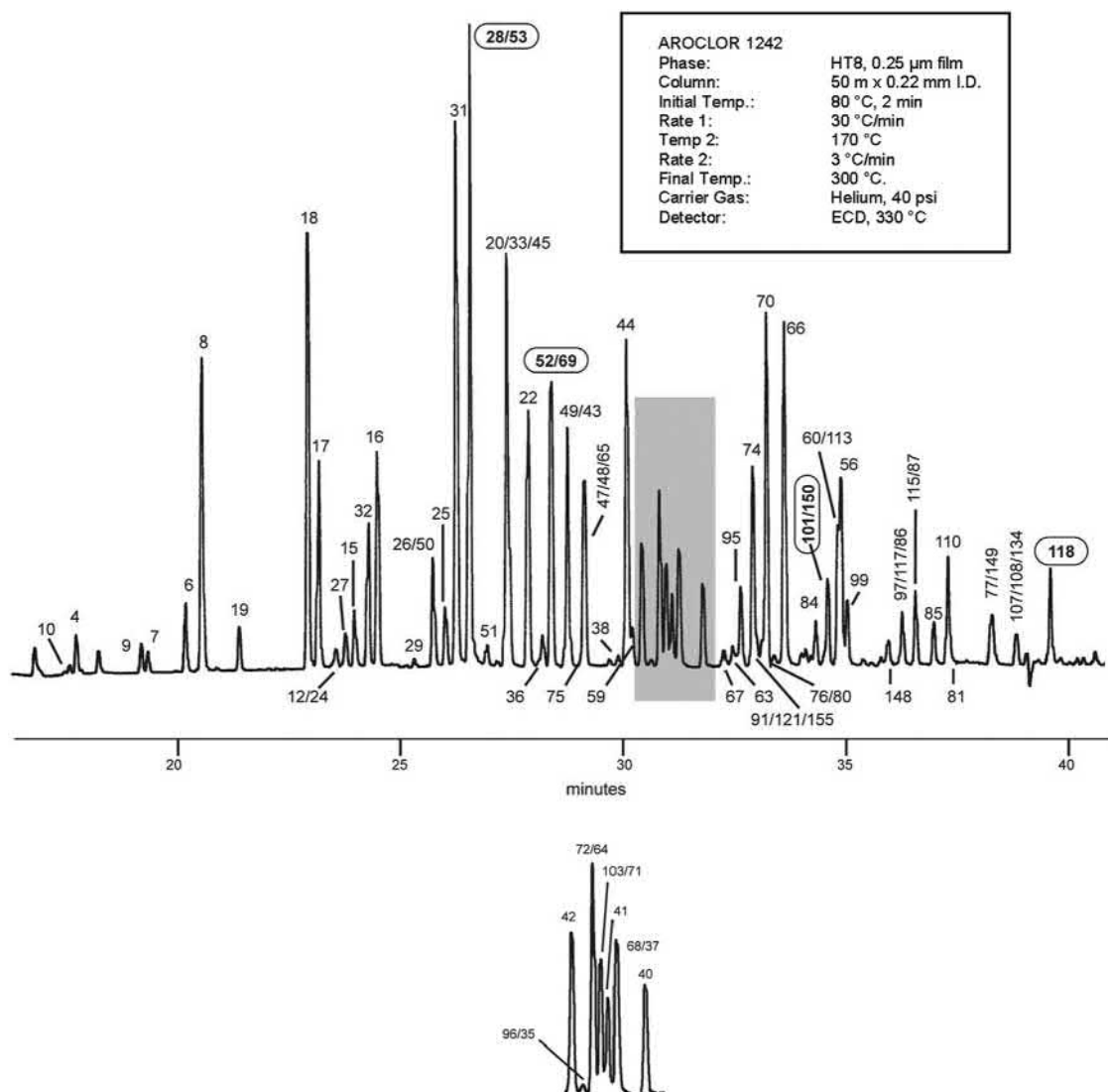


FIGURE 33.4 Aroclor 1242 separation. Adapted from SGE Application Note. http://www.sge.com/uploads/eb/cc/ebcee7536aa32ddab2c44fcbac67f33/AP-0040-C_RevB.pdf. The bottom chromatogram is expansion of shaded area in the chromatogram above.

promote a number of toxic effects including weight loss, immune impairment, reproductive disorders, development toxicity, and cancer [25]. Dioxin-like compounds (DLCs) all act through a common mechanism (examples—Fig. 33.5); therefore, the degree of their

toxicological potency can be determined and compared using a relative toxicity scheme normalized to 2,3,7,8-TCDD, the most toxic congener. The toxic equivalent factor (TEF) is a value assigned to each 2,3,7,8-substituted congener representative of its relative potency

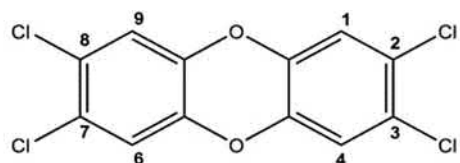
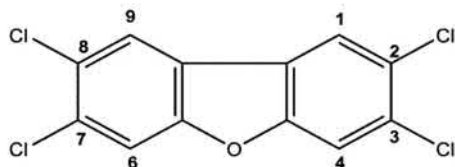
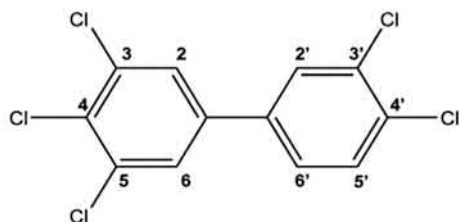
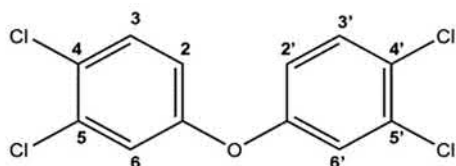
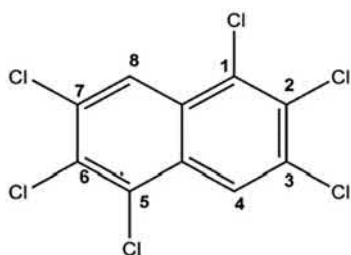
**2,3,7,8-tetrachlorodibenzo-p-dioxin****2,3,7,8-tetrachlorodibenzofuran****3,3',4,4',5-pentachlorobiphenyl (PCB-126)****3,3',4,4'-tetrachlorodiphenylether****1,2,3,5,6,7-tetrachloronaphthalene (PCN-67)**

FIGURE 33.5 Structures of a number of dioxin-like compounds.

compared to 2,3,7,8-tetrachlorodibenzo-p-dioxin. The sum of the concentration of each individual DLC multiplied by its TEF can be expressed as the toxic equivalent quantity (TEQ) of 2,3,7,8-TCDD in the sample:

$$\text{TEQ} = \sum [\text{PCDD}_i \times \text{TEF}_i] \sum [\text{PCDF}_j \times \text{TEF}_j] \\ \sum [\text{PCB}_k \times \text{TEF}_k] \sum \text{DLC}_l \times \text{TEF}_l$$

The analysis of dioxins is one of the most challenging in analytical chemistry [14,26]. Due to very high toxicity of these compounds, complex sample preparation procedures and very sensitive and selective instrumentation are required. Isotope dilution with $^{13}\text{C}_{12}$ -labeled 2,3,7,8-congeners is used to account for losses due to the extensive sample cleanup, act as chromatographic time markers for the toxic congeners, increase linearity, and help increase sensitivity for low-level samples. The analytical steps for PCDD/F are similar to those for analytical methods of most compounds. These steps include the following:

- Subsampling representative aliquot for analysis.
- Addition of isotopically labeled PCDD/F internal standards to the sample aliquot.
- Quantitative extraction of PCDD/Fs and other matrix coextractives from sample by one or more extraction methods (see further).
- Removal of interfering coextractives from the sample extracts using a series of sample cleanup procedures (see further).
- Concentration of cleaned extract (in suitable solvent) to amount needed to meet required detection limits for analytical determinations. Final extract volumes typically range from 10 to 50 μL .
- Injection of 0.5–5 μL (or more if a large-volume injector is used) into GC–MS detection system.
- Review of data and determination of areas of analytical peaks that meet positive

identification criteria in chromatograms (see further).

- Correction of raw data based on recovery of isotopically labeled PCDD/F internal standards added to samples before extraction.
- Use of MS calibration curves to determine concentrations of all 17 2,3,7,8-substituted PCDD/Fs.
- Review of all available quality control data to ensure that analytical run passes required quality assurance criteria.

Samples can be extracted using standard procedures. Solid samples including soils and sediments can be extracted using Soxhlet extraction, sonication, microwave extraction, or pressurized liquid extraction (PLE). Biological samples (tissue and vegetation) can be extracted using the same techniques after drying with sodium sulfate or diatomaceous earth or acid digested followed by liquid–liquid extraction. Liquid samples can be extracted using solid-phase extraction, liquid–liquid extraction, or using passive samplers. Air samples are typically extracted using high-volume samplers with a glass fiber filter to capture the particulates and a polyurethane foam plug (PUFF) to capture the vapor phase.

Due to the high sample concentration factors (10^6 or more) required to meet the very low detection limits for PCDD/Fs, extensive sample cleanup is required to remove matrix coextractable and interfering compounds. The classical cleanup procedure is a three-stage cleanup based on the Smith–Stallings procedure, which involves an acid- and base-impregnated layered silica column to remove polar compounds and alumina column to remove the remaining compounds of lower polarity and begin to separate compounds such as ortho-substituted PCBs from the other DLCs. The third stage is an activated carbon column that is used to separate the planar compounds (all DLCs are planar) from the nonplanar ones. Nonplanar compounds (PBDEs, ortho-substituted PCBs) are

eluted through the carbon column in the forward direction and the planar dioxin-like compounds (PCDD/Fs, non-ortho-PCBs, and PCNs) are strongly retained and must be removed with a strong elution solvent such as toluene, typically in the reverse direction. Biological samples and other samples with significant amounts of coextractable matrix compounds are often treated by acid and/or base wash or gel permeation chromatography (GPC) prior to the three-stage cleanup.

Chromatographic separation of isomers is a very important step in dioxin analysis due to the very large difference in toxicity [27,28]. There is currently no single GC column that can uniquely resolve all of the 17 toxic congeners from all others. The classical method involves initial analysis on a 60 m \times 0.25 mm id 0.25 μ m 5% diphenyl polydimethylsiloxane column with confirmation using a polar phase (e.g., DB-225). In most cases, phases such as arylene-based 5% diphenyl polydimethylsiloxane, DB-Dioxin, or Rtx-Dioxin-2 (Chapter 3) can provide results that are not significantly different when confirmation on a secondary column is done, and many laboratories no longer routinely perform confirmation analysis, especially on biological and human samples where only 2,3,7,8-isomers bioaccumulate. Table 33.5 shows various combinations of chromatographic columns that have been used to analyze PCDD/Fs and their ability to resolve the specific 2,3,7,8-congeners. Shorter columns, e.g., 40 m, 0.18 mm id, and 0.15 μ m film thickness, have been used to reduce run times by 30%–40%. Shorter columns tend to compromise GC peak capacity because often the dioxin-like PCBs are analyzed with the dioxins, and up to 20 ions are monitored in the tetra-dioxin/furan window precluding the ability to obtain a minimum of 7–10 data points across the narrower GC peaks obtained with microbore columns. Comprehensive two-dimensional GC (GC \times GC) [29,30] has been used to enhance chromatographic resolution. Very fast detectors such as TOFMS are

TABLE 33.5 Isomeric specific separation of 2,3,7,8-substituted dioxins and furans using various gas chromatographic phases.

	DB-5, Rtx-5MS HP5-MS, Equity-5	CP-Sil 8 CB/MS	DB-5MS ZB-5MS	Rtx-Dioxin2	ZB5UMS	DB-XLB	DB-225	SP-2331
<i>PCDDs</i>								
2,3,7,8-TCDD	++	+-	++	++	++	+-	+-	+-
1,2,3,7,8-PeCDD	++	+-	+-	--	--	--	--	--
1,2,3,4,7,8-HxCDD	++	++	++	++	++	++	++	++
1,2,3,6,7,8-HxCDD	++	++	++	++	++	++	++	++
1,2,3,7,8,9-HxCDD	--	+-	+-	++	++	++	++	++
1,2,3,4,6,7,8-HpCDD	++	++	++	++	++	++	++	++
1,2,3,4,6,7,8,9-OCDD	++	++	++	++	++	++	++	++
<i>PCDFs</i>								
2,3,7,8-TCDF	--	+-	+-	++	++	++	++	+-
1,2,3,7,8-PeCDF	++	++	++	++	++	++	--	--
2,3,4,7,8-PeCDF	--	--	--	--	--	--	++	++
1,2,3,4,7,8-HxCDF	--	++	++	++	++	++	++	--
1,2,3,6,7,8-HxCDF	++	++	++	++	++	++	--	++
1,2,3,7,8,9-HxCDF	++	--	--	--	--	++	++	++
2,3,4,6,7,8-HxCDF	+-	--	--	--	--	+-	--	++
1,2,3,4,6,7,8-HpCDF	++	++	++	++	++	++	++	++
1,2,3,4,7,8,9-HpCDF	++	++	++	++	++	++	++	++
1,2,3,4,6,7,8,9-OCDF	++	++	++	++	++	++	++	++

Reproduced with permission from Fishman, J. *Chromatogr. A* 1139 (285) (2007).

required for GC × GC due to the narrow GC peaks (<1 s wide) that are produced. Unfortunately, current TOF mass spectrometers are less selective (nominal mass resolution) and at least an order of magnitude less sensitive than high-resolution mass spectrometers (HRMS).

Magnetic sector instruments running at 10,000 resolution are still the gold standard for PCDD/F analysis. Modern sector instruments are able to detect PCDD/Fs at subfemtogram

levels. The carrier effect of $^{13}\text{C}_{12}$ -labeled surrogates helps to minimize adsorption and carry the 2,3,7,8-native congeners through the gas chromatograph. A resolving power of 10,000 is used because this is the best compromise between sensitivity and selectivity. At resolutions greater than 10,000, sensitivity drops off exponentially. Electron ionization (EI) using a reduced electron energy of about 35 eV is typically used. Dioxins are very stable compounds

showing little fragmentation and therefore the molecular ion is monitored. Negative chemical ionization (NCI) is not used for PCDD/F analysis. The vast majority of dioxins are more sensitive in NCI than EI, except for 2,3,7,8-TCDD, which is significantly less sensitive because the molecular ion readily fragments with the charge located on the stable chloride anion. Single ion monitoring (SIM) is typically used to enhance sensitivity, because the detector is set only to scan for masses (mass to charge ratios of the dioxin and furan ions of interest, see [Table 33.5](#)) where PCDD/Fs can be detected. Magnetic sector instruments can scan by either varying the magnetic field or accelerating voltage to switch between ions of interest. In order to scan as fast as possible, accelerating voltage is scanned. In order to obtain the greatest sensitivity, the analytical run is broken into groups or windows consisting of congeners of the same degree of chlorination. If too wide a mass range is scanned, sensitivity will be lost with reduced accelerating voltage. [Table 33.6](#) lists the specific ions of interest for PCDD/Fs and dl-PCBs. Typically, only the tetra- to octa-PCDD/Fs and 12 WHO PCBs are analyzed because they are the only compounds with TEFs.

Tandem quadrupole MS [31] or ion trap MS can be used with single reaction monitoring (MS/MS) for PCDD/F analysis and has been shown to be very selective. The dioxin molecular ion uniquely fragments by the loss of COCl (63 Da) resulting in a very clean mass chromatogram with very few interferences. dl-PCBs can also be analyzed using SRM; however, the loss of Cl₂ (70 Da) is not unique for PCBs, therefore interferences can be observed in the SRM traces for PCB analysis.

Dioxin analysis involves a significant amount of quality control. Instruments are tuned to 10,000 resolution (10% valley at $M/\Delta M$) and group windows are determined using a window setting standard containing the first- and last-eluting PCDD/F for each congener group. In addition, a column performance mixture

containing the closest eluting congeners for 2,3,7,8-TCDD and 1,2,3,7/1,2,3,8-TCDD are analyzed to ensure that 2,3,7,8-TCDD can be separated from 1,2,3,7/1,2,3,8-TCDD with at least a 25% valley [26]. Following a multipoint calibration typically containing five points or more, sample analysis can be carried out. Normally isotopic peaks of the molecular ion cluster are monitored, such that the most abundant ion becomes the target mass for quantification, and the next most abundant ion becomes a qualifier ion. A positive identification must include the elution of the two isotopic peaks within ± 2 s of each other as well as the corresponding ¹³C₁₂-labeled surrogate standard within the correct time window. The peak shapes must be Gaussian and have a signal-to-noise ratio of at least 3:1. Details are listed in EPA method 1613, MOE method 3418, or ISO 18703/ISO 17858 (see [Table 33.7](#))

33.4 Organochlorine pesticides

Also listed as compounds in the Stockholm Convention, many of the organochlorine pesticides (OCs) are persistent and bioaccumulative. Compounds such as DDT, endrin, dieldrin, and others are also mentioned by name in *Silent Spring*. Most of these types of compounds are now banned from use, but due to their nature are frequently found in many solid matrices from plant and animal tissue through the range of soils commonly analyzed. There are still some locations around the globe that use some of these compounds (South Africa for malaria control, for example); so discussion of their analysis is still relevant, unfortunately.

Similar sample preparation strategies as mentioned earlier are also amenable to OCs. As hydrophobic compounds they are more commonly found in solid matrices, or organic matrices, as opposed to aqueous ones. Following extraction, there are many extract cleanup techniques, details of which can be found in the cited

TABLE 33.6 HRMS multiple ion monitoring program for CDDs/CDFs (DPE = chlorinated diphenyl ethers).

Ion group	m/z (quantification ions)	Compound	Dwell (ms)	Delay (ms)	Theoretical isotope ratio	Acceptable range
1	303.9016, 305.8987	TCDF	50	10	0.77	0.65–0.89
	315.9419, 317.9389	¹³ C ₁₂ -TCDF	25	10	0.77	0.65–0.89
	316.9824	PFK LockMass	30	10		
	319.8965, 321.8936	TCDD	50	10	0.77	0.65–0.89
	327.8847	³⁷ C ₁₂ -TCDD	25	10		
	331.9368, 333.9339	¹³ C ₁₂ -TCDD	25	10	0.78	0.65–0.89
	375.8364	Hexa-DPE	25	10		
2	339.8597, 341.8567	Penta-CDF	50	10	1.61	1.32–1.78
	351.9000, 353.8970	¹³ C ₁₂ -Penta-CDF	25	10	1.56	1.33–1.79
	354.9792	PFK LockMass	30	10		
	353.8576, 355.8546, 357.8517	Penta-CDD	50	10	1.55	1.31–1.78
	367.8949, 369.8919	¹³ C ₁₂ -Penta-CDD	25	10	1.56	1.32–1.79
	409.7974	Hexa-DPE	25	10		
3	373.8208, 375.8178	Hexa-CDF	50	10	1.24	1.06–1.43
4	383.8369, 385.8610	¹³ C ₁₂ - Hexa-CDF	25	10	0.52	0.44–0.60
	389.8157, 391.8127	Hexa-CDD	50	10	1.24	1.05–1.43
	392.9760	PFK LockMass	30	10		
	401.8559, 403.8529	¹³ C ₁₂ - Hexa-CDD	25	10	1.25	1.06–1.43
	445.7555	Octa-DPE	25	10		
	407.7818, 409.7789	Hepta-CDF	50	10	1.04	0.88–1.19
5	417.8250, 419.8220	¹³ C ₁₂ - Hepta-CDF	25	10	0.45	0.38–0.51
	423.7766, 425.7737	Hepta-CDD	50	10	1.03	0.88–1.19
	435.8169, 437.8140	¹³ C ₁₂ - Hepta-CDD	25	10	1.04	0.88–1.20
	442.9729	PFK LockMass	30	10		
	479.7165	Nona-DPE	25	10		
	441.7428, 443.7400	Octa-CDF	50	10	0.89	0.76–1.02
6	457.7377, 459.7348	Octa-CDD	50	10	0.89	0.75–1.02
	469.7779, 471.7750	¹³ C ₁₂ - Octa-CDD	25	10	0.89	0.76–1.03
	480.9697	PFK LockMass	30	10		

TABLE 33.7 Selected methods for analysis of POPs.

Method	Analytes/comments	References
USEPA1613	Seventeen 2,3,7,8-substituted dioxins and furans with congener group totals in water and wastewater. Uses isotope dilution—GC-HRMS	USEPA, 1994b
USEPA1614	Brominated diphenyl ethers in water soil, Sediment and tissue by HRGC/HRMS	USEPA, 2007
USEPA1668a	209 PCB congeners. 12 WHO dioxin-like PCBs by GC-HRMS, the remaining 197 by GC-MS	USEPA, 1999
USEPA23	Seventeen 2,3,7,8-substituted dioxins and furans with congener group totals in incinerator stack gasses. Uses isotope dilution—GC-HRMS	USEPA, 1995
USEPA 8290 (SW-846)	Seventeen 2,3,7,8-substituted dioxins and furans with congener group totals in materials and waste. Uses isotope dilution—GC-HRMS	USEPA, 1994a
ISO 18073	Seventeen 2,3,7,8-substituted dioxins and furans with congener group totals in water and wastewater. Uses isotope dilution—GC-HRMS. Allows GC-MS as an alternate detection method	ISO, 2004
ISO 17858	12 WHO dioxin-like PCBs in environmental matrices by GC-HRMS. Allows GC-MS as an alternate detection method	ISO, 2006
ISO 22032	Water quality—determination of selected polybrominated diphenyl ethers in sediment and sewage sludge—method using extraction and gas chromatography/mass spectrometry	ISO, 2006
EN 1948	Seventeen 2,3,7,8-substituted dioxins and furans and congener group totals in stationary sources by isotope dilution—GC-HRMS	European Standard, 1997
MOE3418	Seventeen 2,3,7,8-substituted dioxins and furans including congener group totals and 12 WHO dioxin-like PCBs by GC-HRMS. Uses isotope dilution—GC-HRMS	Ontario Ministry of the Environment, 2010
MOE 3430	Polybrominated diphenyl ethers in environmental matrices using GC-HRMS	Ontario Ministry of the Environment, 2010
MOE3136	The determination of polychlorinated biphenyls (PCBs), organochlorines (OCs), and chlorobenzenes (CBs) in fish, clams, and mussels by fast GC-ECD	Ontario Ministry of the Environment, 2009
MOE3487	The determination of polychlorinated biphenyls (PCBs), organochlorines (OCs), and chlorobenzenes —(CBs) in solids by GC × GC- μ ECD.	Ontario Ministry of the Environment, 2010
ENVCAN 1/RM/19	Seventeen 2,3,7,8-substituted dioxins and furans and congener group totals in pulp and paper effluents by isotope dilution—GC-HRMS	Environment Canada, 1992
JIS K0311	Seventeen 2,3,7,8-substituted dioxins and furans including congener group totals in incinerator stack gasses by isotope dilution—GC-HRMS	JIS, 1999a
JIS K0312	Seventeen 2,3,7,8-substituted dioxins and furans including congener group totals in wastewater by isotope dilution—GC-HRMS	JIS, 1999b

methodology in Table 33.7. Preparatory gel permeation chromatography (prep-GPC) can be extremely helpful in cleanup of these extracts prior to analysis. Prep-GPC is a relatively simple

technique that easily removes both sulfur and larger hydrocarbons typically found in biota and samples taken from locations that are high in concentration of various tar-like materials.

Analysis using either MS or ECD is common, but, if using ECD, then a confirmatory analysis must be performed on a GC column exhibiting different selectivity so as to change the elution profile of the compounds; this helps to minimize quantification bias as well as misidentification. Due to the relatively recent increase in MS sensitivity and ruggedness, MS-based methods seem to be increasing in popularity. Even with this increase in sensitivity, it can still be challenging to reach desired detection limits without additional sample extract concentration (as in done with dioxin samples) or without using SIM, or mass spectrometers that are designed to be especially sensitive (TOFMS or high-resolution sector instruments).

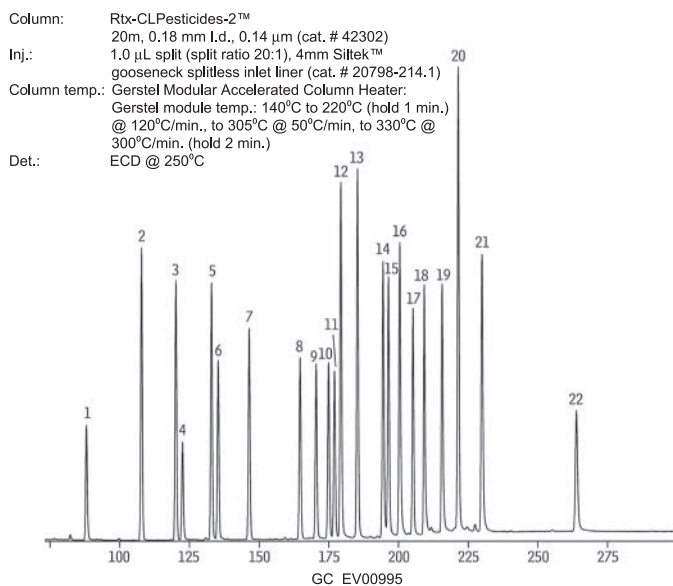
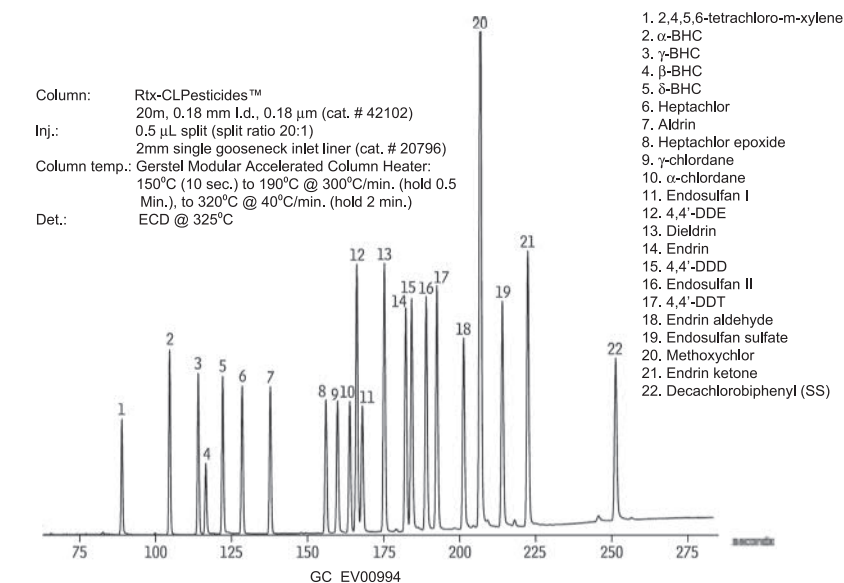
For GC columns, many manufacturers now offer primary and confirmation columns designed for this separation that employ proprietary stationary-phase chemistries. The Rtx-CLPesticides and Rtx-CLPesticides2 columns (Restek Corporation) were developed in 1997 and are used frequently for this analysis. Since this time, there have been a number of other options including the MR-1 and MR-2 (Phenomex). These columns all have relatively short analysis times, with complete separation of the common OCs. They may also be used for GC-MS analysis of the OCs, but, in addition, many users also use more common 5% diphenyl polydimethylsiloxane or XLB-type stationary phases. An example of this separation can be found in Fig. 33.6 coupled with a fast GC option using resistive heating. As observed from the figure, this analysis can be conducted in a short time (less than 5 min) provided the samples have been prepared in a manner that removes many of the common interferents.

33.5 Halogenated flame retardants

Flame retardants have been used for thousands of years [32]. Halogenated flame

retardants (HFRs) have been used since the 1960s mainly because they are significantly more compatible with the many polymeric materials we use today and are much better at causing charring and reducing smoke, which allows more time for escape [33,34]. Hundreds of different brominated and chlorinated flame retardants have been developed and are being detected in the environment. PBDEs are the most commonly known and widely used HFRs and along with the hexabromobiphenyls are the only HFRs currently on the Stockholm Convention list. Hexabromocyclododecane (HBCD) and tetrabromobisphenyl-A (TBBPA) are also high-production-volume brominated flame retardants (BFRs) used in numerous applications. There are also a number of chlorinated flame retardants including dechlorane plus (DP) and other dechloranes developed for specific polymer uses such as electrical cabling. A number of the more common HFRs and their applications are shown in Table 33.8.

The properties that make HFRs very good at retarding flames also make them a real challenge to analyze. Most HFRs readily decompose during the analytical process as they have been designed to easily release a radical halogen that combines with the radicals formed in the preignition stage of combustion. Analytical methods must therefore be designed to minimize the exposure to elevated temperatures, which can be a real problem for GC analysis. Surprisingly enough, most HFRs have a significant vapor pressure and can be analyzed using lower temperatures (<300°C) and shorter GC columns. Most HFRs are also light-sensitive and care must be taken to reduce exposure to light during the analytical process to minimize dehalogenation. In addition, many of the HFRs are present in building materials, furniture, and electronic equipment present in the laboratory. Great care must be taken to minimize exposure to dust, as levels of HFRs in dust can be high and a significant source of contamination.



Sample: Organochlorine Pesticide Mix AB #2 (8-80 µg/mL each component
In hexane/toluene 1:1, cat.# 32292),
Pesticide Surrogate Mix (200 µg/mL each component in acetone, cat.# 32000)
Inj.: 0.5µL, split (split ratio 20:1), 2mm single gooseneck inlet liner (cat. # 20796)
Inj. Temp.: 250°C
Carrier gas: helium, constant flow
Flow rate: 1.5 mL/min.
Oven temp.: 275°C

FIGURE 33.6 OC's separated on Rtx-CL Pesticides and Rtx-Cl Pesticides2 GC columns using Gerstel Mach Fast GC system.

33.6 Polybrominated diphenyl ethers

Sample extraction methods are similar to dioxins, PCBs, and other halogenated organics and can include PLE, Soxhlet, microwave, and sonification for solid samples, acid digestion, or extraction by PLE/Soxhlet for biological samples and SPE or liquid–liquid extraction for liquid samples. Sample preparation also involves conditions similar to PCDD/F analysis. In fact, sample preparation for PBDEs, dl-PCBs, PCDD/Fs, and other organic compounds can be combined. Silica is typically used as a sample preparation material with alumina or Florisil as an optional cleanup step depending on the amount of matrix coextractable materials in the sample. In a combined analyte method (PBDEs, dl-PCBs, PCDD/Fs, and other HFRs), the silica eluent can be loaded onto activated carbon. The PBDEs, ortho-PCBs, and other nonplanar compounds are eluted in the forward direction in one fraction and the PCDD/Fs, non-ortho-PCBs, and other planar compounds such as PCNs can be eluted in the reverse direction. Most methods analyze at least 7–10 congeners, including 17, 28, **47**, 49, **99**, **100**, 119, **153**, **154**, **189**, and **209 (key congeners in bold)**, and some methods analyze for more than 30 congeners. The majority of the concentration comes from the ones listed earlier. Earlier methods did not analyze for BDE209 because analyses were carried out on 30 m × 0.25 mm id film thickness 0.25 μm columns and BDE209 degrades on these columns due to the prolonged residence at elevated temperatures. In addition, unless extreme care is taken, significant degradation could occur resulting in large biases because labeled standards were not available. With the development of labeled internal BDE standards, the use of shorter, thinner film columns, and a better understanding of the conditions required, results for BDE209 are more accurate. The major problem is still extensive contamination, which can be random and often no reason can be

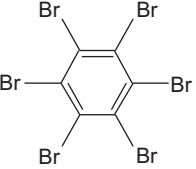
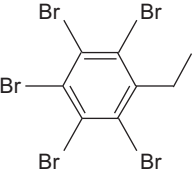
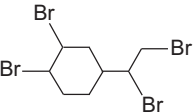
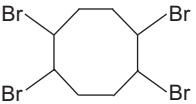
found. Levels of 10 ng or more in a blank can be randomly detected after obtaining multiple blanks at levels below 100 pg.

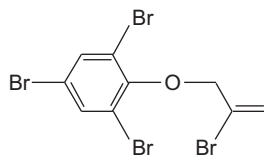
The standard column for PBDE analysis is a 5% diphenyl polydimethylsiloxane, 15 m × 0.25 mm id and 0.10 μm film thickness. Short thin-film columns are used to enable high-molecular-weight PBDEs such as decaBDE (BDE209) to pass through the injector to detector. Most laboratories now only use the 15 m column for analysis. It is able to resolve most major interferences and runs can be completed in less than 20 min. A variety of different methods including HRMS, NCI, and MS/MS are used, with HRMS and NCI being the most common. In HRMS methods, isotope dilution using the $^{13}\text{C}_{12}$ -labeled surrogates for the main congeners is the method of choice where the $\text{M}^+ - \text{Br}_2$ ion is monitored for hexa and higher substituted congeners and M^+ for mono- to penta-congeners. In the NCI method, the bromine anion is monitored. This method is much less selective and possibly less accurate depending on the amount of matrix interferences that are present because isotope dilution cannot be used. It is however less expensive as a much simpler low-resolution mass spectrometer can be used. More details are in EPA 1614, MOE 3430, or ISO 22032 (Table 33.7).

33.7 Other halogenated flame retardants

There are many other HFRs with many different physical and chemical properties [35]. A number of the more common ones are shown in Table 33.8. These compounds range from polar to nonpolar and have a significant range in molecular weights ranging from just over 100 Da to about 1000. Many of them can be analyzed by GC-MS, but due to their polar nature, e.g., TBBPA or tendency for isomer interconversion at GC temperatures (e.g., HBCD), a number of them must be analyzed using liquid chromatography–tandem MS (LC-MS/MS).

TABLE 33.8 Various halogenated flame retardants.

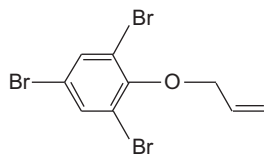
Compound	Chemical formula	Uses [3,4,27]	Analytical method
 <p>Hexabromobenzene (HBB)</p>	C_6Br_6	Paper; electrical goods; polyamides; polypropylene	GC-MS
 <p>Pentabromoethylbenzene (PBEb)</p>	$C_8H_5Br_5$	Unsaturated polyesters; polyethylene; polypropylenes; polystyrene; SBR-latex; textiles, rubbers, ABS	GC-MS
 <p>1,2,5-Tetrabromoethylcyclohexane (TBECH)</p>	$C_8H_{12}Br_4$	Expandable polystyrene beads	GC-MS LC-MSMS
 <p>1,2,5,6-Tetrabromocyclooctane (TBCO)</p>	$C_8H_{12}Br_4$	Polystyrene	GC-MS LC-MSMS



$C_9H_6Br_4O$ High-impact plastic

GC-MS LC-MSMS

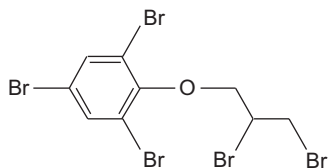
2-Bromoallyl 2,4,6-tribromophenyl ether (BATE)



$C_9H_7Br_3O$ Polyamide; polyester; polyethylene;
polypropylene; polystyrene; polycarbonates

GC-MS LC-MSMS

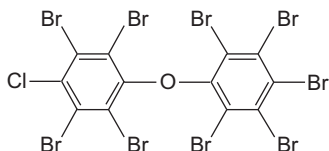
Allyl 2,4,6-tribromophenyl ether (ATE)



$C_9H_7Br_5O$ Polypropylene

GC-MS LC-MSMS

2,3-Dibromopropyl 2,4,6-tribromophenyl ether (DPTE)



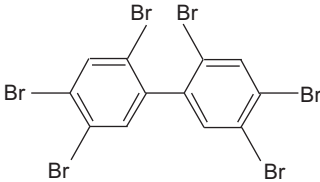
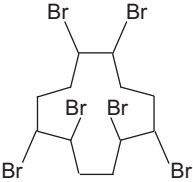
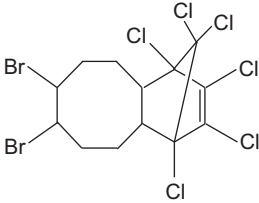
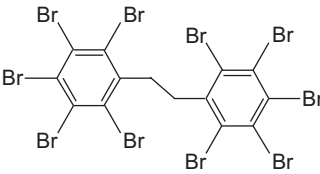
$C_{12}Br_9ClO$ Potential instrument injection Standard for
BDE209, DBDPE

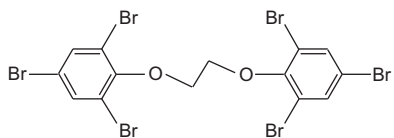
GC-MS LC-MSMS

2,2',3,3',4,5,5',6,6'-Nonabromo-4'-chlorodiphenyl ether
(4 PC-BDE208)

Continued

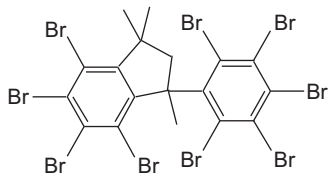
TABLE 33.8 Various halogenated flame retardants.—cont'd

Compound	Chemical formula	Uses [3,4,27]	Analytical method
 2,2',4,4',5,5'-Hexabromobiphenyl (BB-153)	$C_{12}H_4Br_6$	Molded plastics and synthetic fibers	GC-MS
 Hexabromocyclododecane (HBCD)	$C_{12}H_{18}Br_6$	Polystyrene; latex; textiles; adhesives; coatings; polyesters	LC-MSMS
 Hexachlorocyclopentadienyl-dibromocyclooctane (HCBDO)	$C_{13}H_{12}Br_2Cl_6$	Styrenic polymer	GC-MS
 Decabromodiphenylethane (DBDPE)	$C_{14}H_4Br_{10}$	High-impact plastic; polyamide; polypropylenes; polystyrene; polyester/cotton	GC-MS LC-MSMS



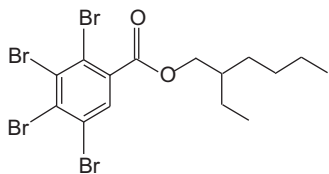
1,2-bis(2,4,6-Tribromophenoxy)ethane (BTBPE)

$C_{14}H_8Br_6O_2$ Thermoplastics; ABS polymer systems, high-impact polystyrene GC-MS LC-MSMS



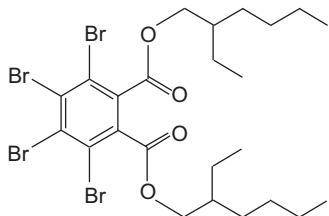
Octabromotrimethylphenylindane (OBIND)

$C_{18}H_{12}Br_8$ High-impact polystyrene (HIPS); Acrylonitrile butadiene styrene (ABS); Polyethylene; polyamides GC-MS



2-Ethylhexyl-2,3,4,5-tetrabromobenzoate (EHTeBB)

$C_{15}H_{18}Br_4O_2$ Thermoplastics; PVC; rubber GC-MS LC-MSMS

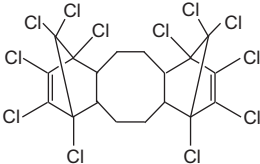
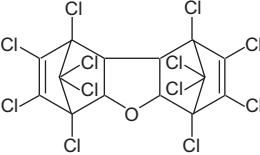
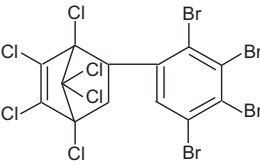


Bis(2-ethyl-1-hexyl)tetrabromophthalate (BEHTBP)

$C_{24}H_{34}Br_4O_4$ Thermoplastics; PVC; rubber GC-MS LC-MSMS

Continued

TABLE 33.8 Various halogenated flame retardants.—cont'd

Compound	Chemical formula	Uses [3,4,27]	Analytical method
	$C_{18}H_{12}Cl_{12}$	Polyamides; polystyrene	GC-MS
Dechlorane plus (DP)	$C_{13}H_2Cl_{12}O$	Thermoplastics; PVC, high-voltage electrical cabling	GC-MS
			
Dechlorane 602	$C_{12}H_4Br_4Cl_6$	Thermoplastics; PVC; high-voltage electrical cabling, silicon grease	GC-MS
			
Dechlorane 604			

Extraction methods are similar to the other halogenated compounds discussed earlier. Sample preparation can be slightly different for each compound or compounds being analyzed. Some compounds, bis(2-ethyl-1-hexyl)tetrabromophthalate (BEHTBP) and 2-ethylhexyl-2,3,4,5-tetrabromobenzoate (EHTeBB), for example, are acid-sensitive, and HBCD isomers are strongly retained on alumina and therefore neutral silica and/or Florisil are used for sample cleanup. It is important to perform recovery studies to ensure that compounds of interest are recovered quantitatively for the method and procedures being used.

In most cases, the same columns as for PBDEs are used for the brominated and chlorinated flame retardants—5% diphenyl polydimethylsiloxane, 15 m × 0.25 mm id, film thickness 0.10 (μ)m. Longer columns are also used for the more volatile compounds, e.g., HBB, PBEB, BATE, and ATE, as they are not retained as strongly as some of the higher-molecular-weight compounds DPBPE and BTBPE. Most methods use GC-ECNI-MS for analysis for the non-BDE BFRs as many of them fragment extensively under GC-EI-MS conditions. The chlorinated dechlorane-type flame retardants exhibit strong retro-Diels–Alder fragments at $m/z = 272$ and $m/z = 237$ characteristic of this group of compounds. Many of the OC pesticides also exhibit these peaks. Most OC pesticides were produced by forming an adduct of hexachlorocyclopentadiene (HCCPD) with another nonhalogenated cyclohexadiene. Adding a second HCCPD to the diene through a Diels–Alder addition produced a much less toxic compound with excellent flame-retarding properties. Both GC-EI-HRMS and GC-NCI-MS are used to analyze the dechlorane compounds.

33.8 Perfluorinated compounds

Perfluorinated compounds (PFCs) are a broad range of compounds used in numerous applications including stain repellents for textiles,

additive to paper products, and in aqueous film forming foams used to fight electrical fires [36–39]. They have been added to the Stockholm list because they are persistent, bioaccumulative, and toxic, and have been detected globally. The most common are the perfluorinated carboxylic acids (PFCAs) and perfluorocarbonsulfonic acids (PFSAs) of which perfluorooctanoic acid (PFOA) and perfluorooctane sulfonate (PFOS) are the most well known. Other PFC compounds include fluorotelomer alcohols (FTOHs), fluorotelomer methacrylates (FTMACs), fluorotelomer acrylates (FTACs), perfluorooctane sulfonamides (FOSAs), perfluorooctane sulfonamidoethanols (FOSEs), polyfluoroalkyl phosphoric acid diesters (diPAPs), and perfluorinated phosphonic acids (PFPAAs).

The method of choice for PFCs is LC-MS/MS as the majority of these compounds are polar and require derivatization to be analyzed by GC. Except for the PFCAs, obtaining a stable derivative is a significant challenge. Methyl or 2,4 difluoroanilide derivatives may be used to analyze PFCA on a 30 m × 0.25 mm id, film thickness 0.25 (μ)m 5% diphenyl polydimethylsiloxane column. The less polar PFCs, FTMAC, FTACs, FTOHs, FOSAs, and FOSEs, can be analyzed underivatized on a poly(ethylene glycol) phase—a 30 m × 0.25 mm id, film thickness 0.25 μm. GC-MS is typically used only if specific isomer information is required or compounds such as PFOA where background contamination from Teflon lines in liquid chromatographs can cause issues with accurate quantification.

33.9 Polycyclic aromatic hydrocarbons

Polycyclic aromatic hydrocarbons (PAHs) are widespread environmental contaminants present in fossil fuels and formed through combustion of biomass [40]. They are made of multifused benzene rings up to 1000 in molecular weight or more. PAHs with less than 10 benzene rings are known as carcinogens and are toxic to humans and wildlife. Early methods

TABLE 33.9 Selected PAHs reported for environmental and health effects studies.

WHO EHC ^a	GENO ^{a,b}	CARC ^{a,b}	US EPA ^c	U.S. ATSDR ^d	MOE 3418	ISO 17993 ^e
Acenaphthene	(?)	(?)	X	X	X	X
Acenaphthylene	(?)	No data	X	X	X	X
Anthracene	–	–	X	X	X	X
Benz[a]anthracene	+	+	X	X	X	X
Benzo[b]fluoranthene	+	+	X	X	X	X
Benzo[j]fluoranthene	+	+		X		
Benzo[ghi]fluoranthene	(+)	(–)			X	X
Benzo[k]fluoranthene	+	+	X	X	X	X
Benzo[ghi]perylene	+	–	X	X	X	X
Benzo[a]pyrene	+	+	X	X	X	X
Benzo[e]pyrene	+	?	X*	X	X	X
Chrysene	+	+	X	X	X	X
Coronene	(+)	(?)	X*			
Dibenz[a,h]anthracene	+	+	X	X	X	X
Fluoranthene	+	(+)	X	X	X	X
Fluorene	–	–	X	X	X	X
Indeno[1,2,3-cd]pyrene	+	+	X	X	X	X
Naphthalene	–	(?)	X		X	X
Perylene	+	(–)				
Phenanthrene	(?)	(?)	X	X	X	X
Pyrene	(?)	(?)	X	X	X	X
Triphenylene	+	(–)				

^a Reviewed in World Health Organization (WHO) Environmental Health Criteria Monograph on PAHs.

^b GENO = genotoxicity; CARC = carcinogenicity; +, positive; –, negative; ?, questionable; parentheses, result derived from small database.

^c US Environmental Protection Agency (EPA) Method 610 PAHs; PAHs noted with asterisk (*) included in Method TO-13A for PAHs in air.

^d US Agency for Toxic Substances and Disease Registry (ATSDR) Toxicological Profile for PAHs.

^e International Organization for Standardization (<http://www.iso.org>) Method 17993:2002 Water quality—determination of 15 PAH in water by HPLC–FL after liquid–liquid extraction.

Modified from D.L. Poster, M.M. Schantz, L.C. Sander, S.A. Wise, Analysis of polycyclic aromatic hydrocarbons (PAHs) in environmental samples: a critical review of gas chromatographic (GC) methods, *Anal. Bioanal. Chem.* 386 (2006) 859–881.

used high-performance LC with fluorescence detection because of the strong fluorescent properties of these compounds. With the development of capillary columns, GC-MS is often the method of choice. Most methods include 16–20

compounds containing at least the 16 priority PAHs (see Table 33.9). There are many different alkyl-substituted PAHs and hetero-PAHs (PAH with S, N, or O). Hetero-PAHs are typically not regulated except if they are halo substituted

e.g., PCDD/F or PCNs because there are too many compounds and a lack of analytical standards.

Extraction methods are similar to those used for PCDD/Fs, PBDEs, and other organic compounds. Because they are typically present in the environment at levels higher than those discussed earlier, a simple cleanup, typically a silica SPE cartridge cleanup, is used. PAHs contain no halogens and therefore are mass sufficient (accurate mass is greater than nominal mass). There are fewer interfering compounds at these higher masses of these highly unsaturated hydrocarbons. As a result, low-resolution MS (single quadrupole or ion trap) is used. In order to increase sensitivity, SIM is used. Deuterium-labeled internal standards and in some cases a full isotope dilution method are used. ^{13}C -labeled internal standards are rarely used because of cost. The most common column is a 5% diphenyl polydimethylsiloxane phase with a $30\text{ m} \times 0.25\text{ mm}$ id, film thickness $0.25\text{ }\mu\text{m}$ column. Fast GC with 20 and 10 m columns has been used to reduce run times [41]. Other stationary phases, most commonly 50% diphenyl polydimethylsiloxane and their arylene equivalents (Chapter 3), are also used. EI is used. PAHs are very stable and for most compounds the molecular ion is the base peak and also the quantifier ion. The major problem is selection of a second ion that can be used for a qualifier ion. It is typically the $\text{M} - \text{H}^+$ or $\text{M} + 1^+$ (^{13}C isotope) ion. In some cases, the doubly charged molecular ion at half of the M^+ is also used. Challenging separations include the anthracene/phenanthrene pair and the benzo[b]fluoranthene/benzo[k]fluoranthene pair. Benzo[j]fluoranthene can elute between the benzo[b]fluoranthene/benzo[k]fluoranthene pair and often bias the results of these two PAHs. An alternate phase like DB-17 can separate the benzofluoranthenes.

33.10 Other compounds not specifically discussed

Obviously, there are many other compounds of environmental importance. The ones discussed are those identified by the Stockholm Convention and therefore constitute those with the highest importance. In addition to these, however, there are many other important compound classes such as organophosphate pesticides, hydrocarbons, and herbicides that are of equal interest to commercial laboratories; however, because these compounds are not considered bioaccumulative, they were deliberately not discussed here. Finally, many analytical methods are based not on compound class (PCBs, dioxins, etc.) but on general chemical properties. Volatile and semivolatile compound methods are also quite common and typically performed with general-purpose GC columns using MS detection to allow for the identification of target compounds without the need for multiple confirmatory columns.

33.11 Summary

This chapter discusses several different classes of environmentally significant chemicals and their analysis. It must be noted that there are entire texts devoted to each of these compound classes, and this information is intended to be a starting point for the interested reader. Even with GC and GC-MS being considered mature, the rate of advancement of analytical methods is still fairly fast. Finally, GC \times GC shows considerable promise for the possible combination of these individual methods into one or two analyses. Fig. 33.7 is the GC \times GC-ECD chromatogram of most of the compound classes mentioned in this chapter, resolved in a

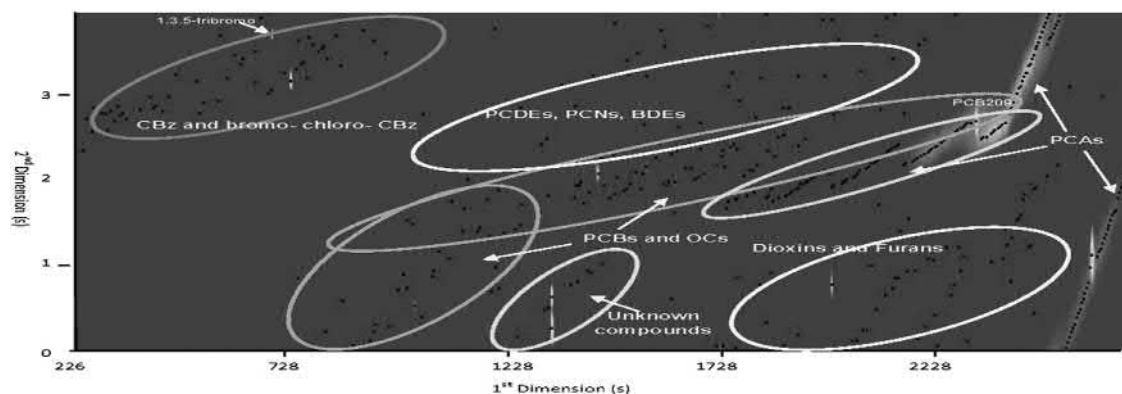


FIGURE 33.7 Two-dimensional chromatogram of a sediment sample showing the presence of a variety of halogenated organic compounds. From A.M. Musalu, E.J. Reiner, S.N. Liss, T. Chen, G. Ladwig, D. Morse, A routine method for the analysis of polychlorinated biphenyls, organochlorine pesticides, chlorobenzenes and screening of other halogenated organics in soil, sediment and Sludge by GC \times GC- μ ECD, *Anal. Bioanal. Chem.* (2011). <http://dx.doi.org/10.1007/s00216-011-5114-0> (in press).

single injection. This will likely continue to be explored as a way of increased resolution and sensitivity for many analyses. There has been considerable refinement in the methods discussed here relative to where a lot of this first began in the 1970s. It is certain that this will continue to evolve.

References

- [1] D.C.G. Muir, P.H. Howard, Are there other persistent organic pollutants? A challenge for environmental chemists, *Environ. Sci. Technol.* 40 (2006) 7157–7166.
- [2] D. Hayward, Identification of bioaccumulating polychlorinated naphthalenes and their toxicological significance, *Environ. Res.* 76 (1998) 1–18.
- [3] E.J. Reiner, A.R. Boden, T. Chen, T. Chen, K.A. MacPherson, A.M. Muscalu, Advances in the analysis of persistent halogenated organic compounds, *LC-GC Eur.* 23 (2) (2010) 60–70.
- [4] N. Yamashita, S. Taniyasu, N. Hanari, Y. Horii, J. Falandysz, Polychlorinated naphthalene contamination of some recently manufactured industrial products and commercial goods in Japan, *J. Environ. Sci. Health A Toxic/Hazardous Substances Environ. Eng.* 38 (2003) 1745–1759.
- [5] R. Carson, *Silent Spring*, Houghton Mifflin, Boston, USA, 1962.
- [6] A.T. James, A.J.P. Martin, Gas-liquid partition chromatography; the separation and micro-estimation of volatile fatty acids from formic acid to dodecanoic acid, *Biochem. J.* 35 (1952) 679–690.
- [7] J.E. Lovelock, Ionization methods for the analysis of gases and vapors, *Anal. Chem.* 33 (1961) 162–178.
- [8] K.D. Bartle, P. Myers, History of gas chromatography, *Trends Anal. Chem.* 21 (2002) 547–557.
- [9] P. Korytar, H.-G. Janssen, E. Matisova, U.A.T. Brinkman, Practical fast gas chromatography: methods, instrumentation and applications, *Trends Anal. Chem.* 21 (2002) 558–572.
- [10] K. Mastovska, S.J. Lehotay, A practical approaches to fast gas chromatography-mass spectrometry, *J. Chromatogr.* 1000 (2003) 153–180.
- [11] M. Adahchour, J. Beens, J.J. Vreuls, U.A.T. Brinkman, Recent developments in the application of comprehensive two-dimensional gas chromatography, *J. Chromatogr. A* 1186 (2008) 67–108.
- [12] O. Panic, T. Gorecki, Comprehensive, two-dimensional gas chromatography (GC \times GC) in environmental analysis and monitoring, *Anal. Bioanal. Chem.* 386 (2006) 1013–1023.
- [13] Stockholm Convention Secretariat, UNEP, 2001. <http://chm.pops.int/>.
- [14] E.J. Reiner, R.E. Clement, A.B. Okey, C.H. Marvin, Advances in analytical techniques for polychlorinated dibenzo-p-dioxins, polychlorinated dibenzofurans and dioxin-like PCBs *Anal. Bioanal. Chem.* 386 (2006) 791–806.

- [15] PCB Transformers and Capacitors: From Management to Reclassification and Disposal. UNEP Chemicals, Geneva, Switzerland. www.chem.unep.ch/pops/pdf/PCBtrnscap.pdf.
- [16] M.D. Erickson, Analytical Chemistry of PCB's, Butterworth Pub., Stoneham, MA, 1986.
- [17] Aroclor and Other PCB Mixtures, USEPA Web Document. <http://www.epa.gov/osw/hazard/tsd/pcbs/pubs/aroclorable.pdf>.
- [18] USEPA SW-846, Method 8082A, Revision 1, February 2007.
- [19] World Health Organization, Re-evaluation of Human and Mammalian Toxic Equivalency Factors for Dioxins and Dioxin-like Compounds, 2005. http://www.who.int/ipcs/assessment/tef_update/en/.
- [20] G.M. Frame, J.W. Cochran, et al., Complete PCB congener distributions for 17 aroclor mixtures determined by 3 HRGC systems optimized for comprehensive, quantitative, congener-specific analysis, HRC J. High Resolut. Chromatogr. 19 (12) (1996) 657–668.
- [21] R. Guitart, P. Puig, et al., Requirement for a standardized nomenclature criterium for PCB's – computer assisted assignment of correct congener denomination and numberings, Chemosphere 27 (8) (1993) 1451–1459.
- [22] K. Ballschmiter, M. Zell, Analysis of polychlorinated-biphenyls (PCB) by glass-capillary gas-chromatography - composition of technical Aroclor-PCB and Clophen-PCB mixtures, Fresenius Z. Anal. Chem. 302 (1) (1980) 20–31.
- [23] SGE Application Note. http://www.sge.com/uploads/eb/ce/ebcee7536aa32ddab2c44fcbaac67f33/AP-0040-C_RevB.pdf.
- [24] J.F. Focant, A. Sjodin, D.G. Patterson Jr., Improved separation of the 209 polychlorinated biphenyl congeners using comprehensive two-dimensional gas chromatography-time-of-flight mass spectrometry, J. Chromatogr. A 1040 (2004) 227–238.
- [25] A.B. Okey, An aryl hydrocarbon receptor odyssey to the shores of toxicology: the Deichmann lecture, International Congress of Toxicology-XI, Toxicol. Sci. 98 (2007) 5–38.
- [26] E.J. Reiner, The analysis of dioxins and related compounds, Mass Spectrom. Rev. 29 (2010) 526–559.
- [27] J. Boer, Capillary gas chromatography for the determination of halogenated micro-contaminants, J. Chromatogr. A 843 (1999) 179–198.
- [28] S.P.J. Van Leeuwen, J. de Boer, Advances in the gas chromatographic determination of persistent organic pollutants in the aquatic environment, J. Chromatogr. A 1186 (2008) 116–182.
- [29] J. DeVos, P. Gorst-Allman, E. Rowher, Establishing an alternative method for the quantitative analysis of polychlorinated dibenzo-p-dioxins and polychlorinated dibenzofurans by comprehensive two dimensional gas chromatography-time-of-flight mass spectrometry for developing countries, J. Chromatogr. A 1218 (2011) 3282–3290.
- [30] J.F. Focant, E.J. Reiner, K. MacPherson, T. Kolic, A. Sjodin, D.G. Patterson Jr., et al., Measurement of PCDD, PCDFs, and non-ortho-PCBs by comprehensive multidimensional gas chromatography-isotope dilution time-of-flight mass spectrometry (GcxGC-IDTOFMS), Talanta 63 (2004) 1231–1240.
- [31] E.J. Reiner, D.H. Schellenberg, V.Y. Taguchi, Environmental applications for the analysis of chlorinated dibenzo-p-dioxins and dibenzofurans using mass spectrometry/mass spectrometry, Environ. Sci. Technol. 25 (1991) 110–117.
- [32] M. Alae, P. Arias, A. Sjodin, A. Bergman, An overview of commercially used flame retardants, their applications, their use patterns in different countries/regions and possible modes of release, Environ. Int. 29 (2003) 683–689.
- [33] T.M. Kolic, L. Shen, K. MacPherson, L. Fayez, T. Gobran, P. Helm, et al., The analysis of halogenated flame retardants by GC-HRMS in environmental samples, J. Chromatogr. Sci. 47 (2009) 83–91.
- [34] A. Covaci, S. Harrad, M.A.-E. Abdallah, N. Ali, R.J. Law, D. Herzke, et al., Novel brominated flame retardants: a review of their analysis, environmental fate and behaviour, Environ. Int. 37 (2011) 532–556.
- [35] A. Covaci, S. Voorspoels, J. de Boer, Determination of brominated flame retardants, with emphasis on polybrominated diphenyl ethers (PBDEs) in environmental and human samples – a review, Environ. Int. 29 (2003) 735–756.
- [36] S.P.J. van Leeuwen, J. de Boer, Extraction and clean-up strategies for the analysis of poly- and perfluoroalkyl substances in environmental and human matrices, J. Chromatogr. A 1153 (2007) 172–185.
- [37] M. Villagrasa, M. López De Alda, D. Barceló, Environmental analysis of fluorinated alkyl substances by liquid chromatography-(tandem) mass spectrometry: a review, Anal. Bioanal. Chem. 386 (2006) 953–972.
- [38] J.C. D'Eon, P.W. Crozier, V.I. Furdui, V.I.E.J. Reiner, E.L. Libelo, S.A. Mabury, Observation of a commercial fluorinated material, the polyfluoroalkyl phosphoric acid diesters, in human sera, wastewater treatment plant sludge, and paper fibers, Environ. Sci. Technol. 43 (2009) 4589–4594.

- [39] J.P. Benskin, A.O. De Silva, J.W. Martin, Isomer profiling of perfluorinated substances as a tool for source tracking: a review of early findings and future applications, *Rev. Environ. Contam. Toxicol.* 208 (2010) 111–160.
- [40] D.L. Poster, M.M. Schantz, L.C. Sander, S.A. Wise, Analysis of polycyclic aromatic hydrocarbons (PAHs) in environmental samples: a critical review of gas chromatographic (GC) methods, *Anal. Bioanal. Chem.* 386 (2006) 859–881.
- [41] A.R. Boden, E.J. Reiner, Development of an isotope-dilution gas chromatographic-mass spectrometric method for the analysis of polycyclic aromatic compounds in environmental matrices, *Polycycl. Aromat. Comp.* 24 (2004) 309–323.

Gas chromatography in space exploration

Maria Chiara Pietrogrande

Department of Chemistry, University of Ferrara, Ferrara, Italy

Gas chromatography (GC) is the preferred analytical technique for the in situ search for organic molecules in extraterrestrial environments since it meets the severe requirements imposed by flight conditions: short analysis time and low energy consumption, robustness, storage for long periods under extreme conditions, high efficiency and sensitivity, automation, and remote control operations. Exploration of our solar system has been fundamentally motivated by the search for chemical biomarkers that could provide evidence of extinct or extant life. GC instruments have been successfully installed on probes for in situ space exploration: the payloads have even included pyr-GC-MS systems composed of a pyrolyzer (pyr) device for analyzing organic compounds in atmospheres and soils at ppb concentration levels.

This chapter describes three relevant applications concerning the onboard GC instruments used in the Cassini–Huygens mission to Titan, the Rosetta mission to Comet P/Churyumov–Gerasimenko, and the Mars space exploration program.

34.1 Introduction

Space missions are designed to study the physics and chemistry of extraterrestrial environments

in the hopes of shedding light on the origins, evolution, distribution, and future of life in the Universe; more specifically, such missions seek to understand the origins of life and to test the hypothesis that life does indeed exist elsewhere and not just on the Earth (this is the realm of astrobiology) [1–3]. With this aim, planetary atmospheres and surfaces are directly investigated using remote-sensing techniques (usually spectroscopy) from orbiting observatories and in situ chemical analysis using atmospheric or surface-landing probes [4,5].

Gas chromatography (GC) has been, and remains, one of the most frequently used techniques for such in situ chemical analyses. This is because it offers great efficiency at high speed, it takes advantage of the enormous separation power provided by capillary GC columns, its formats are sensitive and straightforward, and it can be hyphenated with spectrometric and spectroscopic devices as well as with multicolumn operations. In combination with laboratory simulation, experiments, and computation of theoretical models, in situ GC analyses provide accurate information on the elemental-isotopic and chemical composition of the atmospheres and soils of various bodies within the solar system, useful in identifying the chemical signature of extinct or extant life (or proto-life) processes [6–14].

This chapter reviews the relevant applications of onboard GC instrumentation used in space missions to Titan, with its complex atmosphere resembling that of the primitive Earth [10,13,14], to comets that retain traces of the Earth's early evolution [7–9], and to Mars as the planet that most closely resembles the Earth [11,12].

34.2 Technological and operating constraints in space GC

Flight conditions that restrict mass, size, and energy consumption do indeed require specially designed gas chromatographic instruments and specific operative conditions if they are to meet space-mission-imposed constraints [6–10]. An overview of the GC instruments installed on probes of in situ space missions is reported in Table 34.1.

It must be underlined that the comprehensive definition of instrument design—i.e., the selection of chromatographic columns and detectors, as

well as the definition of the sampling system—is vitally important in space analysis, as hardware configuration cannot be changed after the probe is launched and no significant modification of its working conditions can be implemented.

To fulfill the important criterion of the robustness—resistance to vibrations and temperature variations—metallic capillary columns with cross-linked and bonded phases are the selection of choice because they are highly efficient and require short analysis times (Table 34.1, third column). Shock and vibration resistance is one of the main criteria for the selection of a detector: thermal conductivity (TCD) and electron-capture (ECD) detectors are the detectors of choice for space GC [6–10]. In addition, over the last 10 years, progress in mass spectrometer (MS) design has resulted in miniaturized, onboard MS detectors that provide additional information relevant to peak identification (Table 34.1, fourth column).

Another limitation encountered when operating in space is the restricted amounts of power

TABLE 34.1 Overview of the GC Instruments Installed on probes of in situ space missions.

Mission, launch, arrival year	Experiment, sample type	GC columns	Detectors
NASA viking to Mars, 1975, 1976	GEX, gas GC-MS, soil	Pairs of packed porapak Q Tenax coated with polymetaphenoxylene	Thermistore TCD MS
NASA and ESA Cassini–Huygens to Titan 1997, 2004	GC-MS; gas or aerosol	Six columns in parallel: packed columns (carbon molecular sieve, glassy carbon) and three capillary WCOTs	Five MS sources in parallel
ESA Rosetta mission to Comet 2003, 2011	GC-MS; comet nucleus	Six WCOTs and two PLOTs in parallel, three chiral columns	One time-of-flight MS and eight nanoTCDs in parallel
Phoenix mission, 2007, 2008	TEGA; Mars soil	Six GC capillary columns	
NASA Mars Science Laboratory mission, 2011, 2012	Sample analysis at Mars (SAM); Mars soil	Six GC capillary columns for C1–C15 hydrocarbons, including a Chirasil-Dex for separation of chiral compounds	TCD, QMS
ESA ExoMars Mission to Mars biological environment of the Martian surface, 2013	Sample preparation and distribution system (SPDS); Mars soil	Mars Organic Analyzer (MOA), a portable microfabricated capillary electrophoresis (CE) instrument	

and carrier gas available for the instrument. Consequently, short analysis runs—i.e., less than 30 min—and low operating temperatures—historically in the 20–70°C range—are used in isothermal conditions, since temperature-programming operations increase power consumption [7,9,10]. These operating conditions strongly limit the selection of a column's dimensions and stationary phases—i.e., column length and polymer film thickness. To overcome the power supply limitation, space probes are fitted with solar cells, which provide greater amounts of energy than the electric batteries used in the past.

In addition, data storage and transmission in space are another problem for space GC analyses since onboard electronic and data handling systems suffer from analysis time (generally limited to 10–20 min) and data acquisition rate restrictions, factors of primary importance if one has to define and interpret a chromatogram [8,13].

All these constraints present challenges for the development of new GC equipment for future explorations.

34.3 Prebiotic chemistry in Titan's atmosphere: the Cassini–Huygens mission

It is assumed that the atmosphere on Titan, the largest moon of the planet Saturn, strongly resembles that of the primitive Earth, before the appearance of life, and this makes it one of the most interesting places to search for extinct or extant life in extraterrestrial environments. The joint NASA-ESA Cassini mission was launched on October 15, 1997 to explore Saturn and Titan: after the Huygens probe landed on Titan on January 14, 2005 (two distinct atmospheric samples were collected at separate altitudes as the probe descended), the Cassini spacecraft completed its initial 4-year mission to explore the Saturn System in June 2008 and a Cassini Equinox Mission was extended through 2010 [10,13–19]. A GC-MS instrument was installed

on the Cassini probe: three capillary columns operated in parallel to detect and identify organic compounds by connecting each column to an independent MS ion source (Table 34.1, third row). It was coupled to an aerosol and collector pyrolyzer (ACP) to investigate the composition (including isotope ratio) of refractory materials such as aerosols and soil [6,10].

The GC-MS analyses on the Huygens probe found evidence of a moist surface, with ethane (among other volatiles) evaporating from the surface heated by the warm bottom of the probe itself. Taken together with remote sensing from a visual and infrared mapping spectrometer and from radar instruments on the Cassini orbiter, these observations of surface features suggest that a “methallogical” cycle exists on Titan, with methane playing a role similar to that of water in the hydrological cycle seen on the Earth. The ACP result is the first evidence of the presence of complex macromolecular organic matter constituting the solid organic refractory core of the aerosol particles in Titan's atmosphere (tholins) [18,19]. These results were predicted by theoretical models and supported by simulation studies on laboratory analogs representative of the hydrocarbon and nitrile gases in Titan's aerosols, i.e., tholins generated either by photochemistry or by cold plasma discharges [14–17].

34.4 Prebiotic chemistry in comet environments: Rosetta mission

Being among the most primitive objects in the solar system, comets are assumed to conserve the solar system's average composition and to contain a great abundance of extraterrestrial organic material, the prebiotic building blocks for the emergence of life on the Earth. The European Space Agency (ESA) Rosetta space mission was launched on March 2, 2004 and its main objective was a rendezvous with Comet 67P/Churyumov–Gerasimenko. Over a period of nearly 2 years, it studied the comet's nucleus

and environment in great detail and sent a probe to the comet's surface to gain vital insight into our origins, just as the Rosetta stone enabled us to decipher hieroglyphics [7–9,20].

Among the eight instruments aboard the Rosetta lander, the cometary sampling and composition (COSAC) experiment was dedicated to the in situ analysis of compounds obtained by thermal volatilization of the material in the comet's nucleus by a pyrolyzer (maximum heating temperature: 800°C). GC detection was achieved by a miniaturized TCD connected to each column and a miniaturized (<1 kg), high-resolution TOF MS with a mass range of 12–1500 amu [7,9]. The GC system contained eight capillary columns for chemical

characterization, mounted in parallel: five capillary columns with different polarities were selected to unambiguously identify the broad range of compounds expected in comets. In addition, three chiral columns were installed for enantiomeric separation of chiral aliphatic hydrocarbons and cometary amino acids (Table 34.1, fourth row).

Chromatograms recovered from space missions are interpreted by comparing them with laboratory calibration measurements under operating conditions simulating those present in the probe mission, i.e., isothermal condition or a slow temperature-increasing program [8–10]. As an example, Fig. 34.1 shows a GC-MS chromatogram of a standard mixture

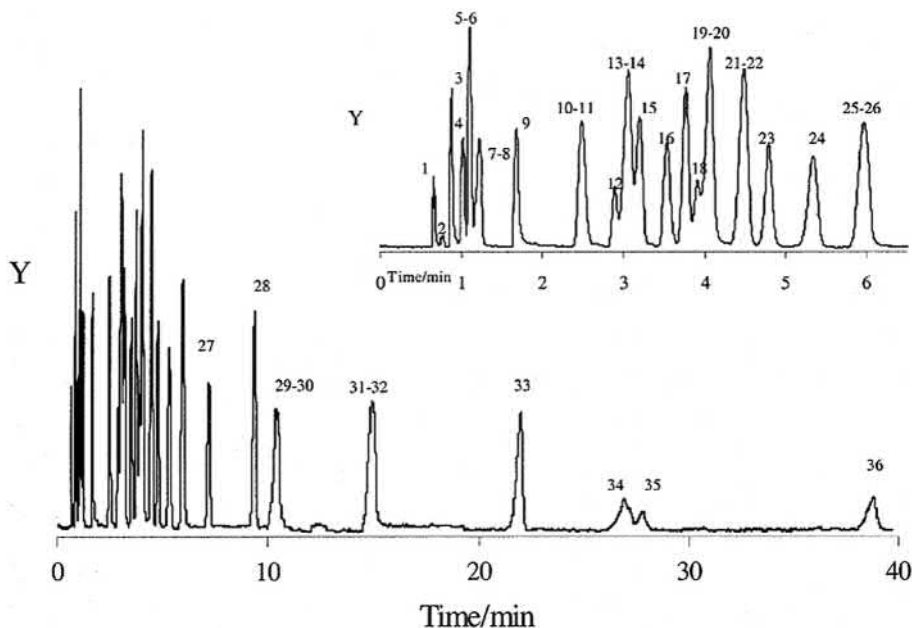


FIGURE 34.1 Chromatogram of a complex mixture of VOCs representative of the targeted chemical species in space in situ analysis. Column: MXT-1 column. Operating conditions: isothermal at 30°C and flow rate 25.6 cm/s⁻¹. FID detector. 1; methanol; 10; n-hexane; 11, ethyl acetate; 12, methyl propionate; 13, 2,2 dimethylpentane; 14, methylcyclopentane; 15, 2,4-dimethylpentane; 16, isopropyl methyl ketone; 17, benzene; 18, isopropyl acetate; 19, cyclohexane; 2, 2,3-dimethylpentane; 2, methyl formate; 20, 1-butanol; 22, 2-methyl hexane; 23, 3-methyl hexane; 24, isooctane; 25, n-heptane; 26, propyl acetate; 27, methyl butyl ketone; 28, toluene; 29, isobutyl acetate; 3, ethanol; 30, 1-pentanol; 31, n-octane; 32, butyl acetate; 33, ethylbenzene; 34, 1-hexanol; 35, isoamyl acetate; 36, amyl acetate, acetone; 5, 1-pentene; 6, isopropanol; 7, n-pentane; 8, ethyl formate; 9, 1-propanol. Reprinted with Permission from Reference M.C. Pietrogrande, I. Tellini, A. Felinger, F. Dondi, C. Szopa, R. Sternberg, et al., *Decoding of complex isothermal chromatograms: application to chromatograms recovered from space missions*, *J. Sep. Sci.* 26 (2003) 569–577.

containing 36 organic compounds representative of extraterrestrial atmospheres, i.e., 36 hydrocarbons and oxygenated compounds with carbon numbers ranging from 2 to 8. The column used was the MXT-1 silanized stainless-steel column selected for space missions (Huygens probe, COSAC experiment) and the operating temperature was the same isothermal condition at 30°C planned for use in the COSAC experiments [8].

34.5 Search for key chemical biomarkers: Mars exploration

Mars is of great interest to astrobiologists because it is the planet that most closely resembles the Earth and may still retain the original prebiotic organic compounds that led to life. Mars exploration started in 1976 with the first NASA Viking mission when, for the first time ever, a pyrolysis-based GC-MS instrument was installed on the Viking space probe (Table 34.1, first, second rows). However, at that time, GC-MS instrumentation lacked the detection

sensitivity needed to catch low levels of organics on Mars and only detected CO₂ and water [21,22]. Later, Mars exploration continued with the detailed data from rovers such as Opportunity and Spirit [12,21].

The upcoming Mars Science Laboratory (MSL) mission will be the most comprehensive search thus far for organic molecules in Martian rocks and soil. The MSL spacecraft was launched on November 26, 2011 and the rover Curiosity is expected to land on Mars in August 2012 and operate for 2 years [11,12,23–28]. Curiosity's scientific payload includes the Sample Analysis at Mars (SAM, scheme reported in Fig. 34.2) instrument package composed of three instruments: a GC, an MS, and a tunable laser spectrometer (TLS), i.e., to measure carbon isotope ratios (¹³C/¹²C) and to identify biotic or abiotic organic compounds. The GC and MS systems allow high mass and volume availability using six GC columns to identify a broader range of organic species, taking advantage of the significant advances in throughput and sensitivity over what the instruments on the

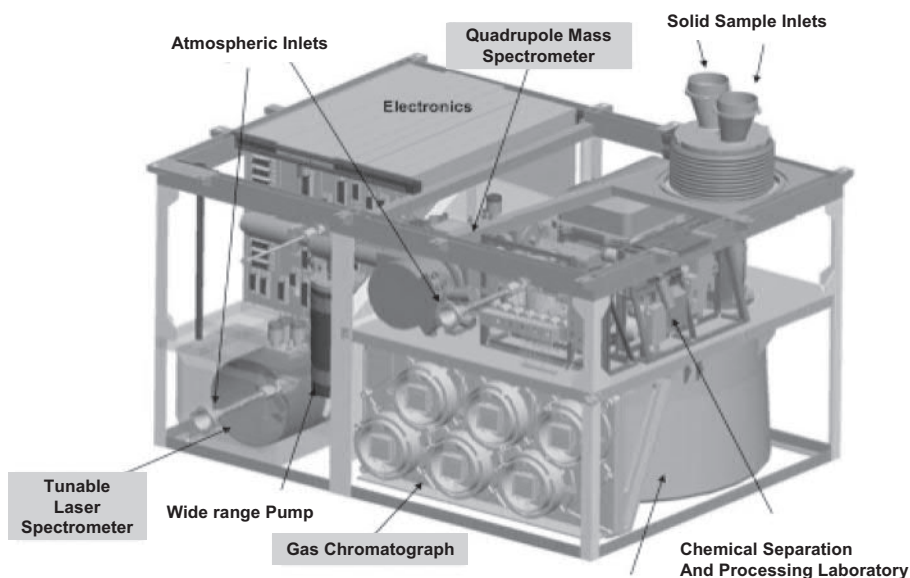


FIGURE 34.2 Outline of the sample analysis at Mars (SAM) included in Curiosity's scientific payload [23].

Viking were able to provide (Table 34.1, sixth row). Moreover, to gain better access to samples, the SAM will be housed on a rover rather than inside a lander as the Viking GC-MS was.

In addition, the SAM instruments are supported by a sample manipulation system (SMS) and a Chemical Separation and Processing Laboratory (CSPL) that include different sample handling and pretreatment devices, i.e., high conductance and microvalves, gas manifolds with heaters and temperature monitors, chemical and mechanical pumps, pyrolysis ovens, and chemical scrubbers and getters [11,12,24–26]. CSPL subsystems will also be

implemented to analyze nonvolatile compounds in the Martian soil, i.e., carboxylic acids and amino acids, as such compounds play an important role in terrestrial biochemistry. For GC in situ analysis of such molecules, a chemical reactor has been developed based on one-pot, one-step extraction (either by solvent extraction with isopropanol or by pyrolysis) and derivatization reaction using the chemical derivatizing reagent already developed in the Rosetta mission, i.e., MTBSTFA (N-methyl-N-(tert-butyldimethylsilyl)trifluoroacetamide) [24–26]. As an example, Fig. 34.3 shows the GC-MS signal obtained by analyzing an analog

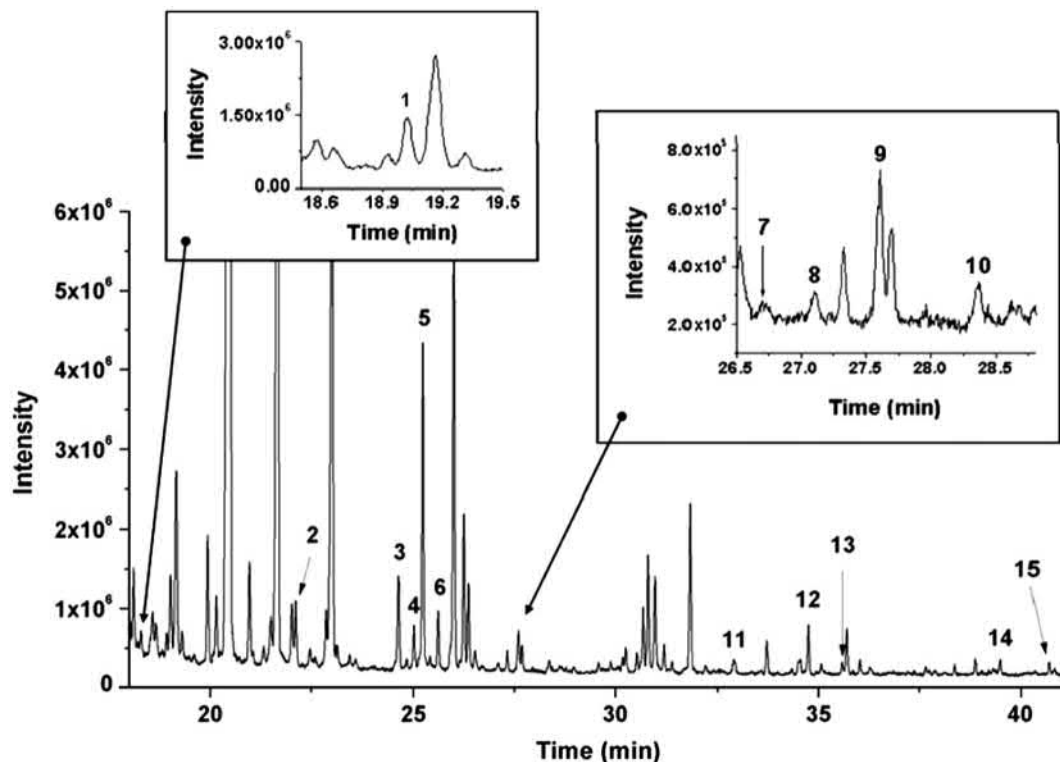


FIGURE 34.3 GC-MS analysis of Atacama soil sample spiked with a mixture of standard acids (10^{-3} M each), under representative space operating conditions. The sample was heated at 500°C for 5 min and derivatized by MTBSTFA reagent. GC column: RTX 5MS capillary column; programmed ramp temperature from 100 to 270°C at $4^{\circ}\text{C min}^{-1}$; MS detection in EI mode. Standard compounds: 1, 4-methyl pentanoic acid; 10, valine; 11, dodecanoic acid; 12, phosphoric acid; 13, 1,2 benzenedicarboxylic acid; 14, pentadecanoic acid; 15, 1,2 benzenedicarboxylic acid bis(2-methylpropyl)ester; 2, heptanoic acid; 3, benzoic acid; 4, octanoic acid; 5, hydroxyethanoic acid; 6, 2-hydroxypropanoic acid; 7, alanine; 8, glycine; 9, nonanoic acid. Reprinted from Reference A. Buch, R. Sternberg, C. Szopa, C. Freissinet, C. Garnier, El J. Bekri, et al., *Development of a gas chromatography compatible sample processing system (SPS) for the in-situ analysis of refractory organic matter in Martian soil: preliminary results*, *Adv. Space Res.* 43 (2009) 143–151.

material of the Mars surface—Atacama Desert soil, from the aridest part of the desert located in Chile—spiked with a standard mixture of carboxylic and amino acids (10^{-3} M each): 15 target compounds can be separated under representative space operating conditions (miniaturization, automation, and low energy consumption) [26]. Further developments are currently under investigation to design a GC-MS instrument for future Mars missions [27,28].

34.6 Search for chirality in space

The next step in the search for the signature of the prebiotic/biotic materials and the occurrence of life will be the detection of enantiomeric excess of amino acids or sugars in extraterrestrial environments. In fact, these molecules are known to be present in one enantiomer in living macromolecules (L for amino acids and D for sugars), whereas they are found as racemic mixtures

(equal parts of L and D) in abiotic systems [29,30]. Chirality discrimination requires amino acid derivatization using a one-step derivatization reaction able to preserve the enantiomeric configuration and prevent racemization [31–33].

A single-step derivatization strategy using a DMF-DMA (N,N-dimethylformamide dimethylacetal) reagent has proved useful in in situ space analysis to search for homochirality in extraterrestrial space: it is a rapid, one-step reaction (without any cofactors) that can occur at relatively low temperatures (140°C); the reaction can easily be automated, and it yields low-molecular-weight products compatible with space MS performance (limited mass range for detection). Enantioseparation and characterization of DMF-DMA derivatives can be achieved using the Chirasil-Dex chiral capillary column, the most effective chiral capillary column used in the SAM experiments. As an example, Fig. 34.4 reports the enantiomeric separation of 20 proteinic amino acids with

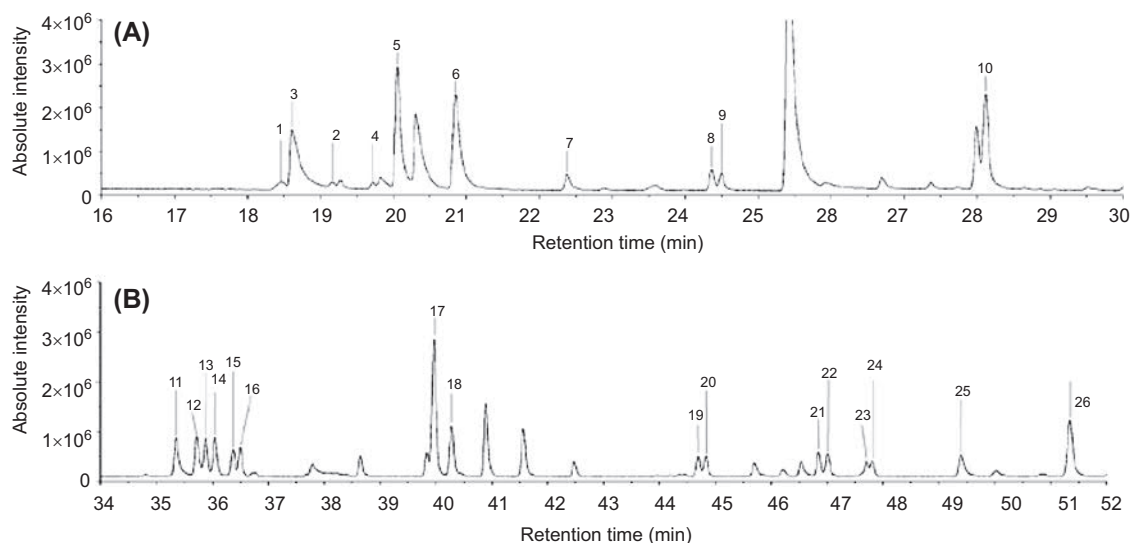


FIGURE 34.4 Chromatogram of 20 separated amino acids (1–10 10–7 mol of each enantiomer). Derivatization with 20 μL DMF-DMA, 3 min at 140°C . GC column: CP-Chirasil-DEX CB capillary column; temperature program: 70°C for 5 min, increasing temperature rate $3^{\circ}\text{C min}^{-1}$ up to 190°C , isotherm for 10 min at 190°C . MS detection in EI mode (m/z range from 40 to 350 $u\text{ma}$). 1, l-Thr; 10, d + l Ile; 11, l-Pro; 12, d-Pro; 13, d-Asp; 14, l-Asp; 15, d-Cys; 16, l-Cys; 17, d + l Met; 18, d + l Glu; 19, d-Phe; 2, d-Thr; 20, l-Phe; 21, d + l-Lys; 22, d + l Lys; 23, d or l Tyr; 24, l or d Tyr; 25, d + l His; 26, d + l Arg; 3, l-Ser; 4, d-Ser; 5, d-Ala; 6, l-Ala; 7, Gly; 8, d-Val; 9, l-Val. Reprinted from Reference C. Freissinet, A. Buchi, R. Sternberg, C. Szopa, C. Geffroy-Rodier, C. Jelinek, et al., *Search for evidence of life in space: analysis of enantiomeric organic molecules by N, N dimethylformamide dimethylacetal derivative dependant gas chromatography–mass spectrometry*, *J. Chromatogr. A* 1217 (2010) 731–740.

good enantiomer resolution (R_s values ≥ 0.8) and high sensitivity (LOD values ~ 1 pmol) [32]. Coupled with miniaturized GC-MS (SIM) formats, the DMF-DMA procedure has been incorporated in the Rosetta mission's COSAC experiment and the SAM Mars experiments [6,7,24,25].

34.7 Conclusions and perspectives

The experience of GC instruments used in space missions has proven the feasibility of the GC technique for the in situ analysis of extraterrestrial environments, providing good chemical characterization of extraterrestrial environments and thus making a fundamental contribution to our understanding of the Earth and planetary systems.

Space research has shown positive synergism with technological developments in GC instrumentation. Dramatic improvements in sophisticated space instruments have taken advantage of all the technological advances made in conventional GC used in terrestrial laboratories. Likewise, these improvements—mainly in terms of miniaturization, automation, and energy saving—have, in turn, led to developments in benchtop-scale GC equipment. In the future, the experiments performed on onboard space landers should become increasingly similar to what analytical chemists generally perform in terrestrial laboratories.

It is, however, true that new breakthroughs are required to further enhance space GC techniques. The most pressing demands are to: (i) extend the techniques to higher temperatures and temperature programming and (ii) shorten elution times for most compounds analyzed. Moreover, new stationary phases must be tailored to broaden the range of compounds targeted in such missions. Last, but not least, detector sensitivity must be further enhanced: improving the dynamic MS analysis range, miniaturization, and making detection limits as low

as possible are the main goals for mass spectrometers i.e., currently, the detectors of choice because they can provide more structural information than traditional detectors. In addition, new sample-enrichment procedures should be explored to develop reliable, fully automated sample pretreatment methods that meet space requirements, i.e., trapping and thermal desorption, as well as liquid extraction techniques.

Other new breakthroughs in GC space application concern the development of miniaturized equipment and methods: lab-on-a-chip systems are actively being studied because they may be able to provide high-performance chemical analysis in a miniaturized format. As an alternative, complementary techniques such as high-performance liquid chromatography, capillary electrophoresis, and supercritical fluid chromatography should also be adapted to space applications.

For these reasons, in the next space exploratory missions, sophisticated GC instruments will be specially designed for integration into space instrument subsystems so they can gather a wide range of chemical signatures of present or extinct life in extraterrestrial environments.

References

- [1] S.A. Benner, Defining life, *Astrobiology* 10 (2010) 1021–1030.
- [2] B.S. Blumberg, Astrobiology, space and the future age of discovery, *Philos. Transact. A Math. Phys. Eng. Sci.* 1936 (2011) 508–515.
- [3] C.H. Gibson, R.E. Schild, N.C. Wickramasinghe, The origin of life from primordial planets, *Int. J. Astrobiol.* 10 (2011) 83–98.
- [4] M. Fridlund, Extra-terrestrial life in the European space agency's cosmic vision plan and beyond, *Philos. Transact. A Math. Phys. Eng. Sci.* 1936 (2011) 582–593.
- [5] M. Carr, Astronomy: martian illusions, *Nature* 470 (2011) 172–173.
- [6] C. Szopa, R. Sternberg, C. Rodier, D. Coscia, F. Raulin, Development and Analytical Aspects of Gas Chromatography for Space Exploration, LC•GC Europe, February 2001, pp. 1–6.

- [7] R. Sternberg, C. Szopa, C. Rodier, Analyzing a comet nucleus by capillary GC, *Anal. Chem.* 74 (17) (2002) 481A–487A.
- [8] M.C. Pietrogrande, I. Tellini, A. Felinger, F. Dondi, C. Szopa, R. Sternberg, et al., Decoding of complex isothermal chromatograms: application to chromatograms recovered from space missions, *J. Separ. Sci.* 26 (2003) 569–577.
- [9] C. Szopa, M. De Pra, I. Tellini, R. Sternberg, M.C. Pietrogrande, C. Vidal-Madjar, et al., Dual column capillary gas chromatographic system for the in situ analysis of volatile organic compounds on a cometary nucleus, *J. Separ. Sci.* 27 (2004) 495–503.
- [10] C. Szopa, G. Freguglia, R. Sternberg, M.J. Nguyen, P. Coll, F. Raulin, et al., Performances under representative pressure and temperature conditions of the gas chromatography–mass spectrometry space experiment to investigate Titan's atmospheric composition, *J. Chromatogr. A* 1131 (2006) 215–226.
- [11] M.N. Heinrich, B.N. Khare, C.P. McKay, Prebiotic organic synthesis in early Earth and Mars atmospheres: laboratory experiments with quantitative determination of products formed in a cold plasma flow reactor, *Icarus* 191 (2007) 765–778.
- [12] R. Navarro-Gonzalez, E. Iniguez, J. de la Rosa, C.P. McKay, Characterization of organics, microorganisms, desert soils, and Mars-like soils by thermal volatilization coupled to mass spectrometry and their implications for the search for organics on Mars by Phoenix and future space missions, *Astrobiology* 8 (2009) 703–715.
- [13] M.C. Pietrogrande, P. Coll, R. Sternberg, C. Szopa, R. Navarro-Gonzalez, C. Vidal-Madjar, et al., Analysis of complex mixtures recovered from space missions: statistical approach to the study of Titan atmosphere analogues (tholins), *J. Chromatogr. A* 939 (2001) 69–77.
- [14] N.T. Buu, C.J. Jeffrey, M. Force, R.G. Briggs, V. Vuitton, J.P. Ferris, Photochemical processes on Titan: irradiation of mixtures of gases that simulate Titan's atmosphere, *Icarus* 177 (2005) 106–115.
- [15] M. McGuigan, J.H. Waite, H. Imanaka, R.D. Sacks, Analysis of Titan tholin pyrolysis products by comprehensive two-dimensional gas chromatography–time-of-flight mass spectrometry, *J. Chromatogr. A* 1132 (2006) 280–288.
- [16] M. Ruiz-Bermejo, C. Menor-Salván, E. Mateo-Martí, S. Osuna-Esteban, J. Á Martín-Gago, S. Veintemillas-Verdaguer, CH₄/N₂/H₂-spark hydrophobic tholins: a systematic approach to the characterisation of tholins, *Icarus* 198 (2008) 232–241.
- [17] M. Ruiz-Bermejo, C. Menor-Salván, J.L. de la Fuente, E. Mateo-Martí, S. Osuna-Esteban, J. Á Martín-Gago, et al., CH₄/N₂/H₂-spark hydrophobic tholins: a systematic approach to the characterisation of tholins, Part II, *Icarus* 204 (2009) 672–680.
- [18] E.H. Wilson, S.K. Atreya, Titan's carbon budget and the case of the missing ethane, *J. Phys. Chem.* 113 (2009) 11221–11226.
- [19] E. Sciamma-O'Brien, N. Carrasco, C. Szopa, A. Buch, G. Cernogora, Titan's atmosphere: an optimal gas mixture for aerosol production? *Icarus* 209 (2010) 704–714.
- [20] J.F.J. Todd, S.J. Barber, I.P. Wright, G.H. Morgan, A.D. Morse, S. Sheridan, et al., Ion trap mass spectrometry on a comet nucleus: the Ptolemy instrument and the Rosetta space mission, *J. Mass Spectrom.* 42 (2007) 1–10.
- [21] B.E. DiGregorio, The search for organic molecules on Mars, *Anal. Chem.* 77 (2005) 348A–353A.
- [22] R. Mukhopadhyay, The Viking GC-MS and the search for organics on Mars, *Anal. Chem.* 79 (2007) 7249–7256.
- [23] <u><http://msl-scicorner.jpl.nasa.gov/Instruments/SAM/></u>.
- [24] M.C. Pietrogrande, M.G. Zampolli, F. Dondi, C. Szopa, R. Sternberg, A. Buch, et al., *In situ* analysis of the Martian soil by gas chromatography: decoding of complex chromatograms of organic molecules of exobiological interest, *J. Chromatogr. A* 1071 (2005) 255–261.
- [25] D. Meunier, R. Sternberg, F. Mettetal, A. Buch, D. Coscia, C. Szopa, et al., A laboratory pilot for in situ analysis of refractory organic matter in Martian soil by gas chromatography–mass spectrometry, *Adv. Space Res.* 39 (2007) 337–344.
- [26] A. Buch, R. Sternberg, C. Szopa, C. Freissinet, C. Garnier, El J. Bekri, et al., Development of a gas chromatography compatible sample processing system (SPS) for the in-situ analysis of refractory organic matter in Martian soil: preliminary results, *Adv. Space Res.* 43 (2009) 143–151.
- [27] L.M. Pratt, C. Allen, A. Allwood, A. Anbar, S. Atreya, M. Carr, et al., The mars astrobiology explorer-cacher (MAX-C): a potential rover mission for 2018. Final report of the mars mid-range rover science analysis group (MRR-SAG) october 14, 2009, *Astrobiology* 10 (2010) 127–163.
- [28] S.A. Getty, L.F. Inge, L. Feng, W.B. Brinckerhoff, E.H. Cardiff, V.E. Holmes, et al., Development of an evolved gas-time-of-flight mass spectrometer for the volatile analysis by Pyrolysis of Regolith (VAPoR) instrument, *Int. J. Mass Spectrom.* 295 (2010) 124–132.

- [29] T.J. Ward, Chiral separations, *Anal. Chem.* 74 (2002) 2863–2872.
- [30] L. Caglioti, O. Holczknecht, N. Fujii, C. Zucchi, G. Palyi, *Astrobiology and biological chirality, Orig. Life Evol. Biosph.* 36 (2006) 459–466.
- [31] M.G. Zampolli, G. Basaglia, F. Dondi, R. Sternberg, C. Szopa, M.C. Pietrogrande, Gas chromatography–mass spectrometry analysis of amino acid enantiomers as methyl chloroformate derivatives: application to space analysis, *J. Chromatogr. A* 1150 (2007) 162–172.
- [32] C. Freissinet, A. Buch, R. Sternberg, C. Szopa, C. Geffroy-Rodier, C. Jelinek, et al., Search for evidence of life in space: analysis of enantiomeric organic molecules by N, N dimethylformamide dimethylacetal derivative dependant gas chromatography–mass spectrometry, *J. Chromatogr. A* 1217 (2010) 731–740.
- [33] M.C. Pietrogrande, G. Basaglia, Enantiomeric resolution of biomarkers in space analysis: chemical derivatization and signal processing for gas chromatography–mass spectrometry analysis of chiral amino acids, *J. Chromatogr. A* 1217 (2010) 1126–1133.

Gas chromatographic analysis of chemical warfare agents

Philip A. Smith

US Department of Labor, Salt lake Technical Center, Sandy, UT, United States

Gas chromatography (GC) has been used to detect and quantify chemical warfare agent (CWA)-related compounds in a variety of matrices since shortly following early advances in the widely used method that occurred in the 1950s. A general description of nerve agents, vesicants, blood and pulmonary agents, toxins, and incapacitating agents is provided, along with issues related to GC analysis of these compounds and CWA degradation products. Specialized sample introduction methods such as solid-phase microextraction and thermal desorption of sorbent tubes are discussed, along with derivatization, retention index systems, and specialized detectors. As high-performance open-tubular GC columns and highly useful GC detectors based on flame photometry and mass spectrometry have become routinely available, those interested in CWA detection have come to increasingly rely on GC methods to monitor CWA-related analytes. Analysis methods based on GC are routinely used in support of the multi-lateral Chemical Weapons Convention, forensic efforts, public health and military force protection capabilities and to study markers for CWA exposures or metabolites found in biomedical

samples. The rapid defensive detection of CWA-related analytes outside of the laboratory is important to protect the health of civilian populations and deployed military personnel, and this need has driven research and development efforts to use GC in increasingly smaller field detection devices with both element-selective and mass spectrometric detection. Important milestones in GC instrument development that enable potentially high-performance GC analysis in such an instrument are discussed, such as the development of restively heated low thermal mass column assemblies. The development of very small mass spectrometers for detection of CWA-related analytes in a field setting has led to the use of internal ionization ion trap detectors in several commercially available GC instruments, and details relevant to this are also discussed.

35.1 Introduction and background

35.1.1 The use of gas chromatography for analysis of CWA materials

When James and Martin first performed gas-liquid chromatography to separate a series of

n-alkyl fatty acids, their packed column stationary phase consisted of diatomaceous earth coated with stearic acid dissolved in silicone oil. The column temperature was controlled by passing an isothermally heated liquid through a jacket surrounding the column. For detection, column effluent was passed through a pH indicator solution and base was dispensed from a dropper when the operators noted a color change. Elution time was manually recorded, along with the amount of titration reagent needed to bring the pH indicator solution back to its initial state [1,2].

Important developments in gas chromatography (GC) theory and column design followed in succession, leading by the early 1980s to the current state-of-the-art open-tubular fused-silica GC column with, for example, a cross-linked covalently bonded siloxane-based liquid stationary phase. These advances have allowed GC to become a tool routinely used for many applications, both in and out of the laboratory, including for analysis of chemical warfare agent (CWA) compounds. Broadly defined, CWA materials are chemical compounds used historically or designed and created to kill or injure members of an opposing military force. Several instances have also occurred where CWA materials have been used by governments or terrorists against civilian populations. Specific substances historically used or created for chemical warfare use are the subjects of an international treaty that requires declaration and elimination of existing CWA stockpiles and prohibits the creation of certain listed chemical compounds [3].

Due to the speed and relatively simple analysis procedures inherent to GC, this is now one of the most used methods for CWA analysis. Even in high-concern situations where detection of any CWA-related analyte is imperative, initial screening by GC "shows you which samples are interesting, and should be further investigated" [4]. The use of selective GC detectors is possible due to the presence of either sulfur or phosphorus in many CWA compounds. Mass spectrometric detection is desirable for GC analysis

of CWA materials due to the need for certainty in identification, and mass spectrometric detectors are widely available at reasonable cost to meet this need.

One of the earliest reports of GC analysis for a CWA analyte in the peer-reviewed literature appeared in 1970, as Albro and Fishbein reported both isothermal and temperature program analysis of bis(2-chloroethyl sulfide) (sulfur mustard, or HD) and several related analytes [5]. They used a 0.2-cm I.D., 1.5-m glass column packed with Gas-Chrom Q, which had been coated with 3% cyclohexanedimethanol, and a flame ionization detector (FID).

Writing in 1972 of the need for rapid detection of sulfur mustard during permeability testing of chemical protective clothing, Erickson et al. [6]

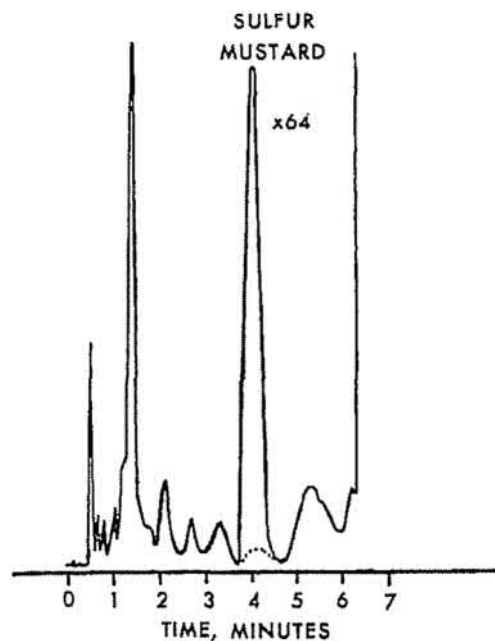


FIGURE 35.1 Gas chromatogram resulting from analysis of sulfur mustard using packed column GC and isothermal column temperature (125°C) to obtain required speed of analysis. Reprinted from Ref. R.L. Erickson, R.N. Macnair, R.H. Brown, H.D. Hogan, Determination of bis(2-chloroethyl)sulfide in a Dawson apparatus by gas chromatography, *Anal. Chem.* 44 (1972) 1040–1041. Copyright (1972) American Chemical Society.

described temperature program analytical performance in GC that seemed impossible to attain at that time “A total elution time of 2 min was allowed per sample injection ... Consequently, it was not possible to use such time-consuming techniques as temperature programming.”

A chromatogram produced by these researchers is shown in Fig. 35.1, with relatively hot isothermal conditions selected to allow their required sample throughput. Thirty years later, advances in GC column design and column heating have produced small, lightweight column modules capable of temperature programming at rates up to several hundred °C per minute with resistive heating of a low thermal mass (LTM) open-tubular fused-silica column [7]. In 2003, this column heating approach demonstrated that GC performance unimagined by Erickson et al. in the early 1970s is now possible, both in the laboratory and for use in field analysis. A standard open-tubular fused-silica column with bonded liquid stationary phase was used with LTM resistive heating in a small field-portable gas chromatography–mass spectrometry (GC-MS) instrument to separate CWA analytes sampled from water by solid-phase microextraction (SPME). These included *O*-isopropylmethylphosphonofluoridate (sarin or GB), *O*-pinacolylmethylphosphonofluoridate (soman or GD), ethyl-*N,N*-dimethylphosphoramidocyanidate (tabun or GA), HD, *O*-ethyl *S*-[2-(diisopropylamino)ethyl] methyl phosphonothiolate (VX), and T-2 mycotoxin (466 u), and the GC-MS analysis was completed in <4 min. The first four of these (including sulfur mustard) were eluted in <1.5 min (Fig. 35.2) [8].

This chapter summarizes important developments in GC for analysis of CWA compounds, the GC detectors often used, as well as the development of field-portable GC instrumentation largely driven by a demand to detect CWA analytes in near real time to protect deployed military forces, first responder personnel, and civilian populations.

35.1.2 Chemical weapons convention

The convention on the prohibition of the development, production, stockpiling, and use of chemical weapons and of their destruction (chemical weapons convention or CWC) became operative in 1997. The various state parties bound by this multilateral treaty have agreed to declare and destroy CWA materials previously stockpiled and related production facilities and to create a means to verify that compounds controlled under the CWC are not used in a prohibited fashion.

To complete the verification tasks defined by the CWC, the Organisation for the Prohibition of Chemical Weapons (OPCW) has been established. Substantial work has been done to define the analytical capabilities required to support verification efforts. A major part of these capabilities includes laboratory GC, including GC-MS [4,9], as well as transportable GC-MS [10].

35.1.3 Types of CWA and related material

35.1.3.1 Nerve agents

Nerve agent CWA compounds typically contain organophosphorus functional groups. Nerve agents bind to the mammalian enzyme acetylcholinesterase, deactivating this enzyme. In neurons where acetylcholine (Fig. 35.3) is the neurotransmitter, transmission of a nerve signal between two neurons occurs with the release of this compound from the axon of one of the neurons. Diffusion of acetylcholine across a synapse to the dendrite structure of a second neuron may initiate an electrochemical signal that travels down the length of that neuron. In the case of nerve signals initiated to stimulate the activity of muscles (e.g., for breathing), acetylcholine also signals between the final neuron and the muscle tissue. If the acetylcholinesterase enzyme is deactivated, fundamental and necessary activities of the body can be

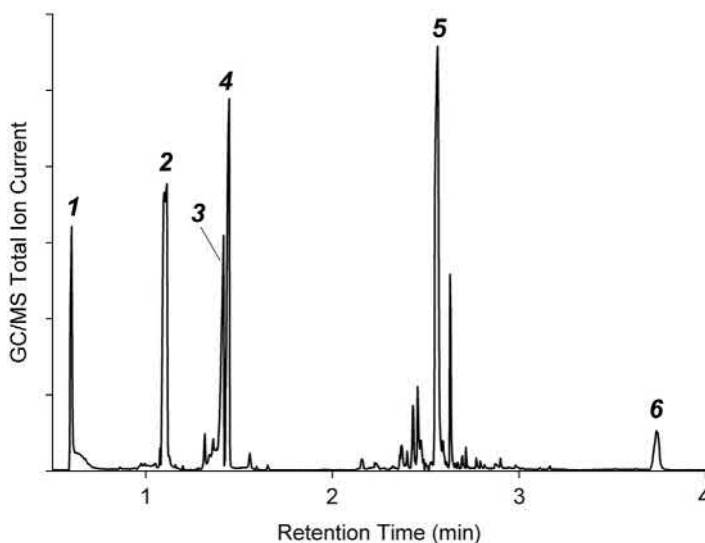


FIGURE 35.2 Direct 5 min SPME sampling of water spiked with (1) sarin, (2) soman, (3) tabun, (4) sulfur mustard, (5) VX, and (6) T-2 toxin. A 100% polydimethylsiloxane stationary-phase GC column was used, having a length of 15 m, 0.25 mm I.D., and 25 μm film thickness. Column temperature program: 40°C for 5 s, 80°C min^{-1} to 100°C, 20°C min^{-1} to 115°C, then 200°C min^{-1} to 300°C, which was maintained until the run was completed. Carrier gas was H_2 at constant pressure with initial linear velocity of 100 cm s^{-1} . Reprinted from Ref. P.A. Smith, M.T. Sng, B.A. Eckenrode, S.Y. Leow, D. Koch, R.P. Erickson, et al., *Towards smaller and faster gas chromatography–mass spectrometry systems for field chemical detection*, *J. Chromatogr. A* 1067 (2005) 285–294, Copyright (2005), with permission of Elsevier.

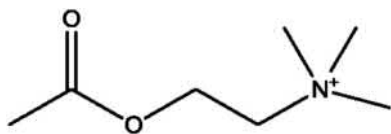


FIGURE 35.3 Acetylcholine.

severely impaired as nerve impulses will tend to continue in an uncontrolled fashion at affected synapses.

Fig. 35.4 provides the structure for the nerve agent VX, and the similarities to acetylcholine are readily apparent. In normal function, a serine residue in the acetylcholinesterase enzyme forms a transient covalent bond with acetylcholine to cleave the acetyl group from the neurotransmitter molecule. With nerve agent poisoning, a permanent covalent bond between

the serine residue and the nerve agent causes loss of enzymatic function.

In pursuit of effective insecticides, the German chemist Gerhard Schroeder is reported to have synthesized the first nerve agent tabun (Fig. 35.5) in 1936 [11]. This chemical was discovered to have unacceptable mammalian toxicity, and its military potential was recognized. A report was sent to the German Army in 1937, and this resulted in related patents being made secret. German efforts to develop additional nerve agents resulted in the discovery of other compounds with anticholinesterase activity, including sarin and soman (Fig. 35.5). During World War II, thousands of tons of tabun and hundreds of tons of sarin were produced by the German military [11], although it is widely held that these stockpiles were not used during the war.

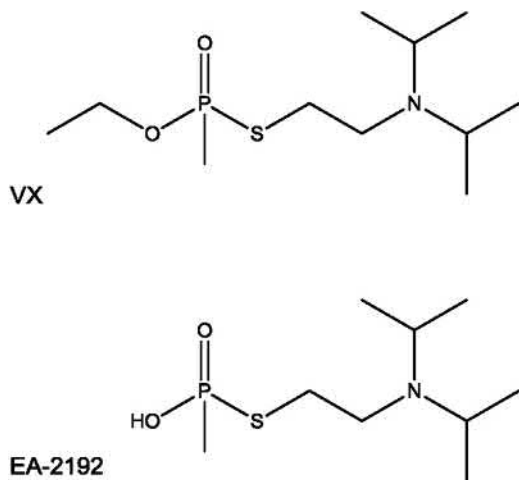


FIGURE 35.4 VX and the VX degradation product EA-2192.

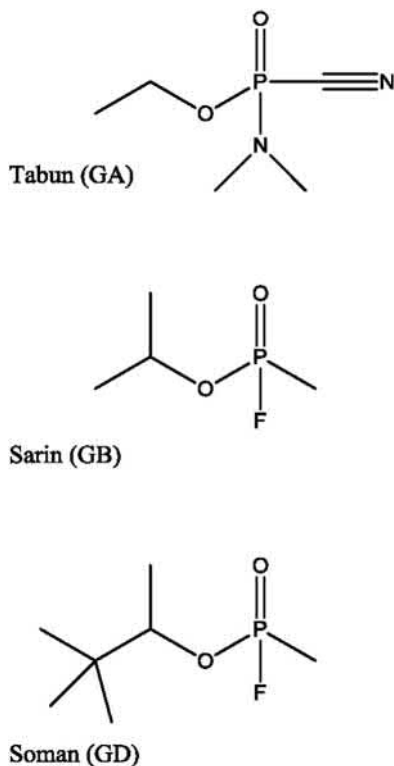


FIGURE 35.5 G agents.

The nerve agents tabun, sarin, cyclohexyl sarin, soman, and VX are all suitable for analysis by GC without the need for derivatization, and GC has been used for analysis of these types of compounds since at least the early 1960s. However, as development of GC occurred during the height of the cold war years, the early GC analyses of nerve agents completed at military research facilities were not well documented in peer-reviewed literature sources. As an example of typical GC instrumentation and methods used in the 1960s for CWA analysis, Baier and Seller describe the use of packed column GC with FID and thermal conductivity detector (TCD) to identify thermal degradation of sarin with and without catalysis [12].

Exemplary of more current approaches, D'Agostino et al. describe the use of capillary column GC with mass spectrometric detection for separation and identification of numerous VX degradation products as well as the parent material [13]. For detection by GC under field conditions, early person-portable GC-MS systems capable of self-contained (i.e., battery powered) operation were able to detect the more volatile G agents directly from air. However, detection of VX required conversion to a more volatile species by reaction of gas-phase VX with AgF. Without the need for a so-called V-to-G conversion step, fast GC separation of degraded VX compounds and the parent material from SPME with mass spectrometric detection was recently described using a small person-portable GC-MS instrument [14] (Fig. 35.6). The second-generation person-portable GC-MS instrument used is capable of stand-alone operation on battery power for several hours, with GC separation by a well-insulated resistively heated 5-m metal capillary column with liquid film stationary phase (0.10 mm I.D., 1 μm d_f).

35.1.3.2 Vesicants

The prototypical CWA vesicant is sulfur mustard (Fig. 35.7). This compound was reportedly first created by Despretz in 1822 by mixing

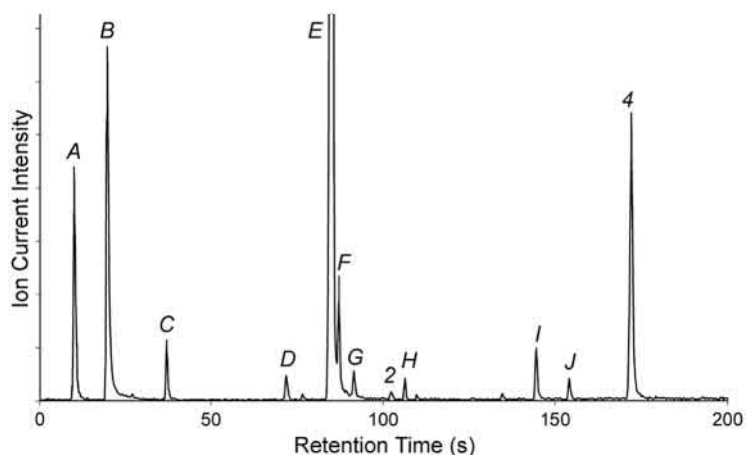
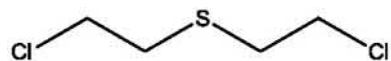
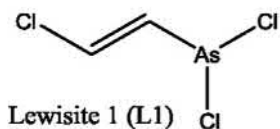


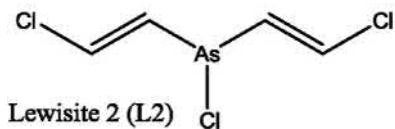
FIGURE 35.6 Chromatogram produced by analysis of sample collected after VX was added to AgF and maintained at 70°C overnight. The person-portable GC-MS system described in Refs. [14] was used for analysis of SPME samples collected from the headspace of a vial containing the VX material. Peak identities in order of elution: *A*, thiirane; *B*, diisopropylamine; *C*, *O*-ethyl methylphosphonofluoridate; *D*, diethyl methylphosphonate; *E*, 2-(diisopropylamino)ethanethiol; *F*, unknown analyte, probable $M^+ \cdot 159 \text{ m z}^{-1}$; *G*, *O,S*-diethyl methylphosphonothioate; *2*, 2-(diisopropylaminoethyl)sulfide; *H*, unknown analyte, probable $M^+ \cdot 157 \text{ m z}^{-1}$; *I*, VX; *J*, unknown analyte, likely bis(diisopropylaminoethyl)sulfide from presence of 114 m z^{-1} base peak and elution order; *4*, bis(diisopropylaminoethyl)disulfide. Reprinted from Ref. P.A. Smith, C.R. Jackson Lepage, B. Savage, C.R. Boverbank, E.D. Lee, M.J. Lukacs, Use of a hand-portable gas chromatograph-toroidal ion trap mass spectrometer for self-Cl identification of degradation products related to *O*-ethyl *S*-2-diisopropylaminoethyl methyl phosphonothiolate (VX), *Anal. Chim. Acta* 690 (2011) 215–220, Copyright (2011), with permission from Elsevier.



Sulfur Mustard (HD)



Lewisite 1 (L1)



Lewisite 2 (L2)

FIGURE 35.7 Vesicants sulfur mustard, lewisite 1, and lewisite 2.

sulfur chloride and ethylene [11]. Despretz did not recognize the toxic properties of the resulting compound, but noted a horseradish or mustard smell. The synthesis of purified sulfur mustard was reported by Meyer in 1866 [11].

Sulfur mustard was used during armed conflict in 1917, and unlike the permanent gases used as CWA materials in the war prior to this (e.g., Cl_2 deployed from compressed gas cylinders), the effects of sulfur mustard were not limited to pulmonary exposure [11], and thus a chemical protective mask alone no longer offered adequate protection against CWA exposures. Sulfur mustard produced a large number of injuries from pulmonary, dermal, and ocular exposure, and treatment of these casualties required the expenditure of significant logistical and medical efforts. Analysis of sulfur mustard by GC has been routine for some time [5]. Analysis of the primary hydrolysis product of this

compound, thiodiglycol, is usually completed by GC analysis following derivatization.

The organoarsenical vesicant 2-chloroethenyldichloroarsine (lewisite 1, Fig. 35.7) was produced near the end of the World War I but was not used in that conflict. Lewisite is a fast-acting blister agent and has been produced for inclusion in a mixture with sulfur mustard to cause more rapid onset of blister formation and also for use in cold environments where sulfur mustard alone would remain a solid. As produced, lewisite consists of a mixture with three major components, of which lewisite 1 is the dominant species. In contrast to the nerve agents and sulfur mustard, derivatization is required for analysis of lewisite 1 by GC, and Muir et al. described thermal desorption GC-MS analysis for derivatives of these compounds and for underivatized sulfur mustard from sorbent tubes. Derivatization of lewisite 1 and lewisite 2 was completed by reaction with either butanethiol or 3,4-dimercaptotoluene, which had been preloaded onto a sorbent tube (Fig. 35.8) [15]. When using the dimercaptotoluene reagent both lewisite 1 and lewisite 2 yielded the same reaction product.

35.1.3.3 Blood and pulmonary agents

Mentioned here for completeness, the blood agents include systemic metabolic poisons, such as hydrogen cyanide (HCN), and the pulmonary (choking) agents include Cl₂ and phosgene, which damage pulmonary tissues. While these agents are highly dangerous in certain circumstances, they are also used extensively for legitimate industrial applications and

furthermore are extremely volatile and thus nonpersistent. This makes these types of compounds less useful in armed conflict where opposing forces are found in close proximity to each other and also tends to limit severe health effects to those who are heavily exposed over a brief period. The low environmental persistence of blood and pulmonary agents also lessens the analytical demands associated with their detection and identification.

35.1.3.4 Toxins

Toxins are harmful compounds produced by biological organisms. In the case of toxins produced by a microorganism such as trichothecene mycotoxins, a state wishing to illicitly use a toxin as a CWA could dismiss allegations of deliberate use due to the possibility that a recovered toxin material could have been produced by natural processes. Illustrative of the political and diplomatic ramifications that may be attendant with analysis of samples related to CWA use or production is the reported use of CWA materials against anticommunist resistance fighters in Southeast Asia in the 1970s. This allegation surfaced and gained credence when it was officially disclosed by the US Secretary of State. At that time the cold war was an important focus for many governments, and the alleged use of trichothecene mycotoxins (eventually termed “yellow rain”) against the backdrop of the cold war struggle subjected the allegations to intense scrutiny, and the topic remains controversial.

A sample allegedly collected from an area in Laos where numerous animal deaths had reportedly occurred was analyzed by Rosen and Rosen [16]. These researchers used packed column GC with mass spectrometric detection to identify the presence of the mycotoxins T-2, diacetoxyscirpenol, 4-deoxynivalenol, and zearalenone in the sample as trimethylsilyl esters. A separate sample was analyzed by Mirocha, who also detected the presence of mycotoxins using GC-MS [17].

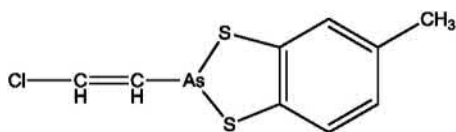


FIGURE 35.8 3,4-Dimercaptotoluene derivative of lewisite 1.

Referring to mycotoxins as putative agents causing the reported CWA incidents, Watson et al. [18] summarized the following questions and answered them in the affirmative:

1. Were the chemical and physical properties of these compounds suited for their use as warfare agents?
2. Could the toxins be produced in the large quantities that would be needed for such operations?
3. Was there any evidence that these toxins had been the subjects of classified research projects at institutes involved in chemical or biological warfare research?

An alternative explanation for the “yellow rain” material found in Southeast Asia was put forward by Nowicke and Messelson [19], who argued that the material was likely fecal material produced by honeybees.

Gas chromatographic analysis for trichothecene mycotoxins had been reported as early as 1971 [20]. The methods described by Ikediobi et al. involved trimethylsilyl (TMS) derivatization, and both isothermal and temperature program methods using packed pyrex glass columns and flame ionization detection. The favored liquid film for the larger toxins (e.g., T-2 and HT-2) was SE-30, due to a relatively high upper temperature limit [20].

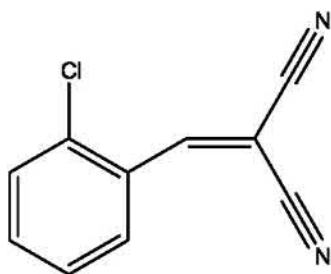
Following the initial yellow rain papers published by Rosen and Rosen [16] and Mirocha et al. [17], considerable interest in GC analysis of trichothecene mycotoxins was raised in the chemical defense community as shown by the work published in 1986. D'Agostino et al. [21] used capillary column GC (DB-1 and DB-5 liquid films) with both FID and MS for analysis of six underivatized mycotoxins. Peak shape was initially poor when the toxins were dissolved in methanol, and the substitution of acetone provided improved chromatographic performance. Electron ionization (EI) allowed detection of mycotoxins spiked in human blood at $\mu\text{g g}^{-1}$ concentrations, although the mass spectra lacked

diagnostic high-mass ions. Using selected ion monitoring, and ammonia chemical ionization (CI), T-2 toxin and diacetoxyscirpenol were detected at levels as low as 2 ng g^{-1} . Begley et al. [22] also used capillary column GC (SE-54) with single ion monitoring mass spectrometric detection to detect trichothecenes in the same spiked human blood sample set analyzed by D'Agostino et al., observing similar detection limits. Negative ion CI was employed, with sensitivity aided by pentafluoropropionyl esterification prior to GC analysis. Development of an SPME method for sampling underivatized T-2 toxin from water for subsequent GC analysis with flame ionization detection was described by Lee et al. [23]. Detection was possible at levels as low as 10 ppb (v/v).

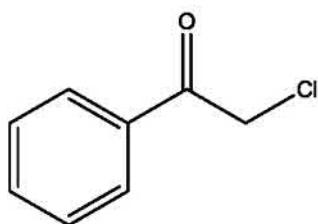
Demonstrating the potential use of SPME and a field-portable GC-MS instrument for rapid sampling and analysis of a range of CWA materials under field conditions, Smith et al. [8] completed SPME sampling for T-2 toxin and several CWA compounds from water, with GC-MS analysis in <4 min using high-velocity H_2 carrier gas and a rapidly heated LTM GC column.

35.1.3.5 Riot control/incapacitating agents

The characteristics of an ideal incapacitating agent include rapid onset of physiological effects that render targeted individuals incapable of performing routine functions, with rapid reversibility when exposure to the agent ceases, and lack of short- and long-term health effects from exposure. Two broad classes of incapacitating agents include those that are routinely used by civil authorities for riot and crowd control and compounds developed through military research for use on the battlefield. The effects of the latter category (intense nausea or psychological disturbance) are somewhat morally objectionable, and thus this type of incapacitating agent is not used for civilian riot-control situations. Several readily available incapacitating agents that produce intense pain for a brief period are routinely used



o-Chlorobenzylidenemalononitrile (CS)



o-Chlorobenzylidenemalononitrile (CN)

FIGURE 35.9 Riot-control agents.

by law enforcement personnel in many countries, including o-chlorobenzylidenemalononitrile (CS) and phenacyl chloride (CN), shown in Fig. 35.9. Beswick [24] describes the use of chemical incapacitating agents in both military conflicts and civil disturbances.

Some controversy exists concerning the categorization of incapacitating agents such as CS and CN among CWA materials. Both CS and CN are considered to be relatively safe, nonlethal agents routinely used in civil disturbances for crowd dispersal. Such use is typically judged to be moral, as alternative means of crowd dispersal would cause a greater risk for harm or loss of life. Wils and Hulst described GC-MS methods for analysis of CS and related compounds [25] and provided relevant mass spectra.

The dispersal of CS and CN is often accomplished by heating. For example, a small thermal

CS canister “grenade” contains lactose fuel, permanganate oxidizer, and CS. In a commercially available CS canister, when the mixture was lit by a fuse mechanism, temperatures of about 700°C were measured inside the canister [26]. Kluchinsky et al. recognized the potential for thermal production of organic degradation products and characterized a number of these recovered as airborne contaminants produced by incendiary-type CS grenades used in riot control [27]. One of the principal degradation products recovered suggested the loss of hydrogen cyanide (HCN) from the parent CS material, and further work confirmed the presence of airborne HCN produced by high-temperature dispersion of CS [28].

35.1.3.6 Environmental degradation products of CWA compounds

Most analytical methods for detection of CWA materials would deal with either analysis of bulk chemicals (i.e., from a suspected CWA process stream) or with environmental samples collected from air, soil, or water sources. A comprehensive discussion regarding the environmental fate of nerve and blister agents has been provided by Munro et al. [29], who listed the well-known degradation products. The literature cited by these authors refers to numerous papers where GC analysis was used for CWA-related products produced through hydrolysis. Many of these CWA degradation products are not suitable for direct analysis by GC, but, in most cases, this may be accomplished following derivatization.

Many of the nerve agent hydrolysis products contain acidic phosphorus functional groups, while sulfur mustard produces thiodiglycol, and a principal degradation product of lewisite 1 is chlorovinyl arsenous acid. Production of thiodiglycol from sulfur mustard occurs via hydrolytic dehydrochlorination, and a number of related sulfoxide and sulfone compounds are also known to result from hydrolysis of the parent material. Militarized vesicants may

include both sulfur mustard and longer-chain-length compounds with biological effects similar to sulfur mustard, such as bis(2-chloroethylthio)ethane (sesquimustard) and bis[(2-chloroethylthio)ethyl] ether. D'Agostino and Provost demonstrated the usefulness of GC for these analytes as well by subjecting samples of HQ (a mixture of sulfur mustard and sesquimustard) and HT (a mixture of sulfur mustard and the ether) to hydrolysis. This was followed by GC-MS analyses using both EI and ammonia CI to directly identify a number of the resulting degradation products and numerous TMS derivatives [30].

Most of the nerve agent hydrolysis products are considerably less dangerous than the intact parent CWA materials. The VX degradation product *S*-2-(*N,N*-diisopropylaminoethyl) methylphosphonothiolate (EA-2192, Fig. 35.4) is a zwitterion and is not directly extractable as at least one of the two possible EA-2192 ionization sites remains substantially ionized at all pH conditions. The ability to identify this product in waste streams from declared VX destruction processes is important as this compound is a potent cholinesterase inhibitor in its own right [29]. Derivatization approaches for GC analysis of CWA-related compounds are discussed later, under "Analytical Considerations."

35.1.4 CWA detection needs as drivers for field-portable GC instrumentation

An impetus for the development of early field-portable GC systems was the need to analyze CWA materials in near real time. Early instruments (see Chapter 15) used for analyses in the field employed technology relevant to the early years of GC such as packed columns. Due to the power requirements for temperature program operation, the early field-portable GC instruments used low temperatures and often isothermal column temperature. At the other extreme, the Viking 572 and Bruker EM 640S

GC-MS designs developed in the 1990s are exemplary of high-capability field-portable GC instrumentation. Both of these instruments borrowed from typical laboratory-based GC designs, although with miniaturized components when possible. Each design employed a small air bath oven for column heating, for example, and each employed an ion beam quadrupole detector with two-stage vacuum pumping. The Bruker instrument was adopted by the OPCW for official on-site analyses [10]. In addition to the needs for orthogonal analysis driven by forensic [31] and CWC treaty compliance concerns [10], substantial resources have been applied to the development of field-portable GC-based methods with element-selective detectors for analysis of CWA in field settings to protect the health of workers involved in destruction of declared CWA stockpiles and the public.

Development of a second generation of commercial field-portable GC instruments has primarily been driven by the need to detect and identify CWA materials in the field. Arguably, the most important improvement in this area is the use of LTM column heating. Several low-power consumptive approaches to this end have been described in the literature and have engendered commercial ventures [7,32]. Since the events of September 11, 2001, increased interest in field-portable GC-MS for detection of CWA compounds or other dangerous chemicals has led to commercialization of at least four GC-MS instruments that use the LTM heating approach first described by Sloan et al. [7] for control of GC column temperature, and the general approach for this is discussed further as follows.

35.1.4.1 MINICAMS

The MINICAMS is a commercially available GC instrument designed specifically for field detection of CWA materials at very low levels during operations to destroy declared CWA stockpiles. This system may automatically pass ambient air through a sorbent trap for

subsequent thermal desorption or through a sample loop if preconcentration is not required. In addition to analysis of airborne nerve or vesicant CWA compounds that contain either sulfur or phosphorus, the instrument may be set up to monitor lewisite using gas-phase dithiol derivatization prior to analysis [33]. The MINICAMS is compact and completes analyses quickly, but access to stable external power is required. Several detectors are available, but flame photometric or pulsed flame photometric types are the logical choices for detection of CWA analytes.

35.1.4.2 Low thermal mass GC column heating

The movement away from packed GC columns toward the open-tubular design for use in a laboratory setting was driven by the improved chromatographic performance made possible by the improved design. However, the modern fused-silica, open-tubular GC column that has resulted is also much smaller than the typical packed column. As the open-tubular GC column design (which happens coincidentally to also have a low thermal mass) became accepted and widely used, this also opened up the potential to move away from convection oven heating to quickly change the temperature of a standard open-tubular column using relatively little power.

Several research groups independently demonstrated rapid heating and cooling of a typical fused-silica, open-tubular GC column using very little power [7,32]. With the approach of Sloan et al. [7] thermal control is provided by measuring the temperature-dependent resistance in a thin platinum wire threaded within a small circular column bundle. Column heating is provided by several additional insulated wires intertwined with the coiled GC column (Fig. 35.10), which are resistively heated using electrical current under microprocessor feedback control. The commercial availability of high-performance resistively heated LTM GC column modules beginning in the early 2000s has led to

adoption of this column heating method in several GC-MS systems designed for both field transportability and person portability. In most of these cases, funding from US military organizations spurred the development of these due to the need for small, fast field-portable instruments to protect the health of deployed forces.

The LTM column heating approach replaced a small convection oven present in earlier versions of the person-portable Hapsite GC-MS instrument that was first marketed in the 1990s. Later adoption of this heating approach resulted in lower power consumption. This first-generation person-portable GC-MS instrument uses an ion beam quadrupole detector, with primary mass spectrometer vacuum pumping provided by a nonevaporative getter (NEG) pump and an ion sputter pump to remove residual noble gases. Due to the need for a reasonable NEG service life, a polymer membrane GC-MS interface is used in this instrument. This challenges the instrument's chromatographic performance, and the use of an approximately 1-m air sample probe heated to only about 40°C limits this instrument to direct air sampling and analysis of airborne analytes with *n*-alkane linear program temperature retention index values less than about 1300. For air sampling, an onboard sorbent tube may be used to trap analytes when the air sample probe inlet is used. Additional modules to allow desorption of an SPME fiber or an externally collected sorbent tube sample have been added to this instrument's capabilities recently. A chromatogram produced from analysis of volatile CWA analytes by a Hapsite instrument is shown in Fig. 35.11. The GC-MS membrane interface used in this instrument is the primary cause of the GC peak tailing seen in the chromatogram.

Smith et al. [8] described a transportable GC-MS capable of very fast analysis of CWA compounds (similar to Fig. 35.2). Construction of this instrument was funded by the US military with the specific intention that it be built with an LTM column assembly mounted to a

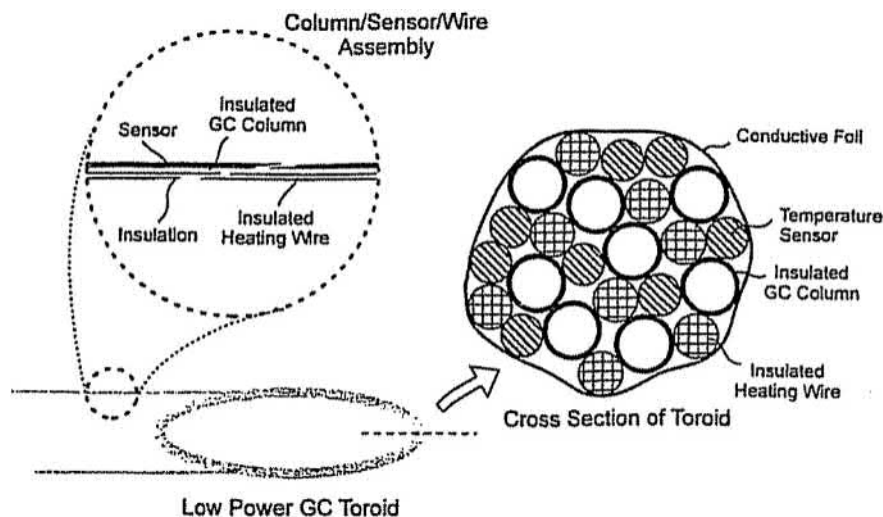


FIGURE 35.10 Diagram illustrating the low thermal mass (LTM) resistive heating design for a standard open-tubular capillary column. Reprinted from Ref. K.M. Sloan, R.V. Mustacich, B.A. Eckenrode, *Development and evaluation of a low thermal mass gas chromatograph for rapid forensic GC-MS analyses*, *Field Anal. Chem. Technol.* 5 (2001) 288–301, © 2002 Wiley Periodicals, Inc., with permission from Wiley Periodicals.

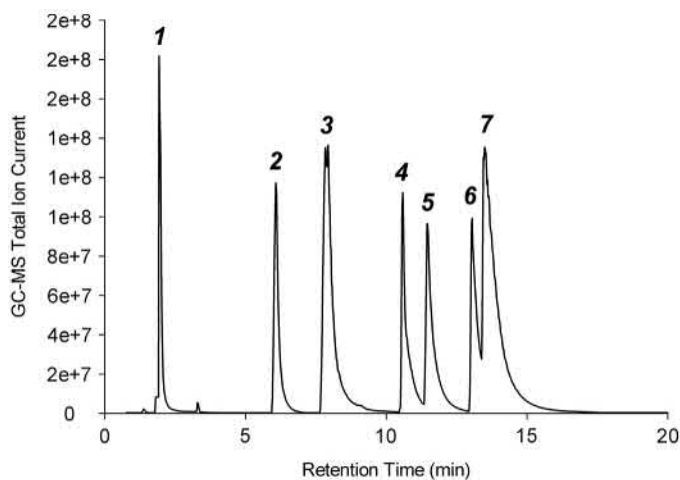


FIGURE 35.11 Hapsite sampling/analysis GC-MS chromatogram: 5.0 mg m^{-3} air concentration for each of four volatile CWAs. Sample time was 1.0 min, nominal sample rate was 250 mL min^{-1} with Tenax concentrator module used. Initial column temperature was 70°C , ramped to 180°C at $30^\circ\text{C min}^{-1}$: 1: Air, methylene chloride; 2: Sarin; 3: N,N-dimethylacetamide (artifact present in clean Tedlar bags); 4: phenol (artifact present in clean Tedlar bags); 5: soman (two diastereomers not resolved here); 6: sulfur mustard; and 7: cyclohexylmethylphosphonofluoridate. Reprinted from Ref. P. Smith, C. Jackson Lepage, D. Koch, H. Wyatt, B. Eckenrode, G. Hook, et al., *Detection of gas phase chemical warfare agents using field-portable gas chromatography-mass spectrometry systems: instrument and sampling strategy considerations*, *Trends Anal. Chem.* 23 (2004) 296–306, Copyright (2004), with permission from Elsevier.

standard quadrupole mass filter heavily used for laboratory GC-MS analyses. A refined LTM GC-MS design based on this approach was commercialized in 2010 by Agilent Technologies, using the 5975 mass spectrometric detector, with the resulting instrument designated as the 5975T (“transportable”) GC-MS system. In the early 2000s, an additional GC-MS instrument designed primarily for field use incorporated the same basic LTM GC column design as the separation method for a transportable cylindrical ion trap detector GC-MS manufactured by Griffin Analytical (now part of FLIR Systems Inc.).

Beginning in 2008, a GC-MS instrument designed for person portability incorporating LTM GC has been commercially produced by Torion Technologies [35]. The current version of this instrument weighs 14.5 kg and is small enough to travel onboard commercial aircraft as a carry-on luggage item (after removing the onboard high-pressure He cylinder for transportation safety). Due to the use of a small, well-insulated injector and transfer line components, and a 5-m GC column with 0.10-mm I.D. that is resistively heated as per Sloan et al. [7], the rechargeable battery used in this instrument is adequate to complete about 20 analysis cycles. Vacuum in the mass spectrometer is maintained by a small turbomolecular pump, backed by an onboard membrane roughing pump. As initially designed, sample introduction was limited to desorption from an SPME fiber. The small GC column diameter limits carrier gas flow into the toroidal ion trap detector, allowing direct interface of the GC to the mass spectrometer. A chromatogram produced by this instrument from analysis of a degraded VX sample is shown in Fig. 35.6.

35.1.4.3 Volatility constraints for field-portable GC

A significant challenge exists for gas-phase sampling of the nerve agent VX, a compound with limited volatility. For qualitative screening

using SPME, Hook et al. showed that with gentle heating of cloth material contaminated with a drop of VX liquid, adequate analyte loading may be rapidly obtained from the headspace of a sealed vial [36]. The use of a sealed vial contributes to increased analyst safety, although it would be wise to use this sampling method with full personal protective measures and a scrubber-equipped fume hood. For quantitative sampling of airborne VX for GC analysis, a different approach has been used for years where airborne VX is passed through a porous material coated with silver fluoride. The reaction shown in Fig. 35.12 occurs readily as demonstrated by Fowler and Smith [37], producing a much more volatile (and still quite dangerous) “G analog” that differs from the G agent sarin only in the presence of an *O*-ethyl group instead of an *O*-isopropyl group. The reaction to produce the G analog is used for field GC analysis methods where the capability to quantify VX vapor concentration is desired. The removal of the diisopropylamine functional group and the sulfur atom from the VX molecule results in not only a more volatile analyte, but also one that is also less susceptible to interactions with active sites [38]. Prior to the work documented by Fowler and Smith, quantitative VX measurements were often completed using liquid impinger sampling and spectrophotometric measurements or involved wet chemistry titration of cholinesterase activity.

35.2 Analytical considerations for sampling and gas chromatographic analysis of CWA-related compounds

35.2.1 Derivatization

As discussed earlier for analysis of CWA degradation products, hydrolysis and metabolism of these generally produce degradation products and metabolites that are quite polar. Many of these compounds may be derivatized

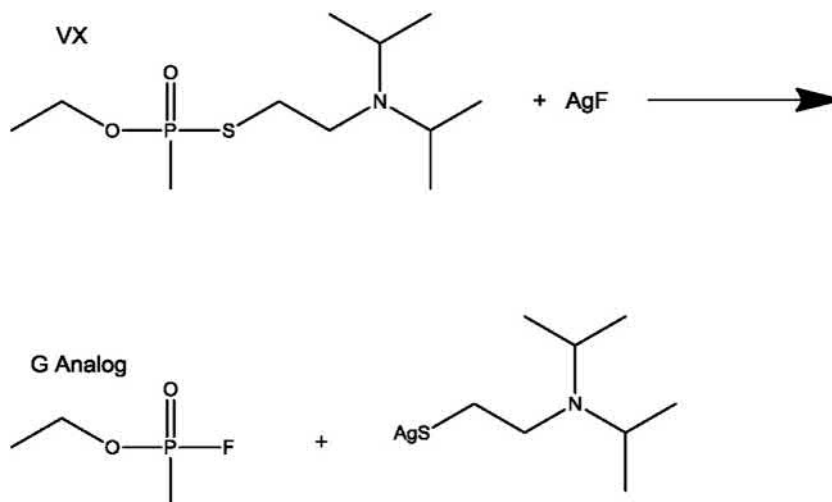


FIGURE 35.12 Conversion of airborne VX to a more volatile and less reactive G analog by reacting VX vapor with AgF, initially described by Fowler and Smith [37].

for GC analysis following routine procedures to add TMS or *tert*-butyldimethylsilyl (TBDMS) groups to mask amine or hydroxyl sites. A comprehensive review of derivatization for analysis of CWA-related materials was completed by Black and Muir in 2003, who covered derivatization for GC as well as for liquid chromatography analysis [38].

35.2.1.1 G agents

The suitability of alkylphosphonic and alkyl methylphosphonic acids for TBDMS derivatization and quantitative GC analysis was investigated by Purdon et al. in 1989 [39]. Trimethylsilylation is also a possibility for analysis of G agent degradation products, and both approaches are discussed by Kuitunen for use in OPCW analytical procedures [40]. Recovery of alkylphosphonic acid compounds is problematic in aqueous samples or soil matrices where inorganic cations are present unless a cation-exchange cleanup is included [38]. Other derivatization approaches (e.g., methylation and pentafluorobenzyl esterification) for G agent degradation products are summarized by Black and Muir [38].

For confirmation of exposure, GC analysis of the sarin metabolite *O*-isopropyl methylphosphonic acid, the *O*-ethyl methylphosphonic acid sarin analog, and methylphosphonic acid was completed for the TMS derivatives by Minami et al. [41]. Urine to be tested was first passed through an ion-exchange column to remove metal ions, followed by drying of the eluate under vacuum. The acid metabolites were derivatized as trimethylsilyl esters for analysis using flame photometric detection. Limits of detection as low as 25 parts per billion for the isopropyl and ethyl phosphonic acid species were reported.

35.2.1.2 VX

Many degradation products of VX do not require derivatization for GC analysis [13,42]. Hydrolytic degradation of VX can produce several acidic phosphorus compounds, including ethyl methylphosphonic acid, ethyl methylthiophosphonic acid, and EA-2192 (Fig. 35.4) [43]. Creasy et al. [44] showed that TMS derivatization of alkyl methylphosphonic acids and alkyl methylphosphonothioic acids may be routinely completed for GC analysis.

Analysis of EA-2192 as the TMS derivative was problematic, although methylation with trimethylphenylammonium hydroxide (TMPAH) allowed GC analysis of this analyte [45]. Pardasani et al. [43] showed recently that the TMS derivative of EA-2192 may be successfully analyzed by GC if column temperatures that favor gas-phase activity of the derivative are maintained throughout an entire analytical run. These researchers hypothesized that decomposition of the derivative occurred on the column after initial condensation at the relatively cool column temperatures typically used at the beginning of a linear temperature program.

35.2.1.3 Sulfur mustard

As is the case for all of the nerve and vesicant compounds except for lewisite 1, the parent sulfur mustard compound is well suited for GC analysis. However, virtually all of the mustard degradation products are best analyzed following derivatization. Wils and Hulst [46] reported EI mass spectra for numerous TMS derivatives of analytes related to sulfur mustard, as well for many of the underivatized degradation products.

35.2.1.4 Lewisite

Muir et al. reported that GC analysis of underivatized lewisite 1 and lewisite 2 (both of which contain reactive As–Cl bonds) quickly leads to column degradation [15]. Derivatization of lewisite 1, lewisite 2, and the lewisite hydrolysis products such as chlorovinyl arsenous acid is usually accomplished using a thiol or dithiol reagent. Early work by Fowler et al. used 1,2-ethanedithiol to derivatize chlorovinyl arsenous acid in water for GC analysis with flame photometric detection. Excess reagent was precipitated by treating the aqueous sample with AgNO₃ prior to solvent extraction [47]. Butanethiol and 3,4-dimercaptotoluene were used by Muir and co-workers, who spiked derivatizing reagent into an air stream passing over tenax packed in a thermal desorption tube prior to sampling air

that contained lewisite 1 and lewisite 2. While the dithiol reagent provided better detection limits, its use resulted in the production of the same derivative for both lewisite 1 and lewisite 2, restricting the use of this reagent to the simultaneous quantification of the total combined airborne concentration of both analytes [15]. Due to the confusing production of degradation product derivatives with the same identity as those produced from the parent CWA compounds, Hanaoka et al. analyzed samples containing lewisite and sulfur mustard without derivatization using GC with either atomic emission or mass spectrometric detection. This approach is unusual for lewisite, and the authors used a guard column and on-column injection with frequent column solvent washes to allow analysis of the underivatized lewisite compounds [48].

35.2.2 Thermal desorption

Desorption of air sampling sorbent media is often carried out with liquid solvents [40]. However, when very low airborne concentrations are to be sampled, thermal desorption becomes an attractive alternative as this avoids dilution of the relevant analytes. In 1979, Fowler et al. reported thermal desorption for analysis of CWA-related analytes after sampling sulfur mustard onto a packed tube that was later placed into a heated GC injector, followed by flow of carrier gas through the sorbent to an isothermally heated packed column [49]. Commercially available instrumentation was not an option for thermal desorption of analytes trapped on sorbent tubes when Fowler et al. completed this work.

The apparatus for the thermal desorption of sampling tubes directly into the analytical column of a gas chromatograph can be purchased from commercial sources or fabricated in-house (see Chapter 10). However, commercially available equipment is often prohibitively expensive

for those who wish merely to engage in limited experimentation or who expect to use the method only occasionally [49].

Later work by Steinhanses and Schoene demonstrated the usefulness of a commercially available thermal desorption inlet for GC analysis of sulfur mustard and several organophosphorus compounds, including sarin and soman, using flame photometric detection [50]. Black et al. used a commercially available thermal desorption inlet interfaced to laboratory GC-MS to successfully sample sulfur mustard from the headspace above soil collected by an investigative journalist where CWAs had allegedly been used by the government of Iraq against civilians [51]. Hancock and Peters used a custom-built thermal desorption inlet for GC analysis of compounds "of chemical defense interest," sampled from the gas phase by purging spiked water, and by sampling the headspace above spiked soil. Simultaneous flame ionization and flame photometric detection were used [52].

Several field-portable GC systems available today include an integrated sorbent tube air sampler to preconcentrate airborne analytes for thermal desorption to introduce analytes into GC instrumentation, including the MINICAMS fixed-location instrument as well as the Hapsite person-portable GC-MS instrument. In both cases, the use of thermal desorption and compact thermal desorption components allows for detection of trace contaminant levels using relatively little power.

35.2.3 SPME sampling/sample introduction for GC analysis

In 1990, Arthur and Pawliszyn described SPME [53]. Analysis of samples collected onto a typical SPME fiber is most often completed by GC, and thousands of papers have described the use of SPME sampling from a wide range of matrices for GC analysis, including a number with a focus on detection and identification of

CWA materials. The use of SPME for sampling and sample introduction relevant to GC analysis of CWA-related compounds may follow two broad approaches: (1) quantitative GC analysis and (2) qualitative screening. Zygmunt et al. [54] reviewed the use of SPME for CWA sampling and GC analysis in 2007, summarizing numerous sample matrices that have been addressed. Updating their list, CWA compounds that have been sampled from soil or sediment or their extracts by SPME for GC analysis include sulfur mustard [55], lewisite degradation products [56,57], and VX degradation products [42]. Those sampled from aqueous systems include sulfur mustard [8,58], nerve agents [8,59,60], T-2 toxin [8,23], degradation products of sulfur mustard and nerve agents [58,61], and lewisite degradation products [57]. Those sampled from air include G nerve agents [34,60,62] and sulfur mustard [34]. Hook et al. also demonstrated the potential to detect VX on contaminated cloth material by short-duration SPME sampling from a closed vial kept at 50°C, with GC-MS analysis completed in the field [36].

Quantitative GC analysis of SPME samples may employ either passive equilibrium or dynamic air sampling. The former approach is most typically used, although for some analytes attainment of equilibrium between the SPME fiber coating and the matrix sampled can be lengthy. Sampling may stop before equilibrium is attained as long as adequate analyte is available on the fiber and sample duration is consistent from one sampling event to another. It is advisable to avoid termination of sampling in the area of an SPME uptake curve where the curve is steep (sample duration on x -axis, mass loaded to fiber on y -axis), as small errors in sample timing can cause relatively large errors in quantification. The dynamic quantitative air sampling approach uses an adsorptive SPME fiber coating as described by Koziel et al. [63]. An example of equilibrium sampling followed by quantitative analysis of CWA-related materials in water was provided by Lakso and Ng,

who used SPME with GC-MS (selected ion monitoring). They obtained detection limits for sarin, soman, and tabun of about $0.05 \mu\text{g mL}^{-1}$, while the detection limit for VX was reported to be about $0.5 \mu\text{g mL}^{-1}$ [59]. With the exception of the value for VX, these are below or slightly above the respective short-term exposure limits promulgated by the US army for their presence in water to be consumed by deployed troops. In another example, Kimm et al. used passive headspace SPME sampling to demonstrate that sulfur mustard spiked in soil at several hundred ng g^{-1} soil could be detected with GC-MS analysis [55]. In the soil system, equilibrium sampling was approached at room temperature, with a sampling time of 20 min. For dynamic quantitative air sampling using SPME, Hook et al. used a carboxen/polydimethylsiloxane SPME fiber coating and GC-MS analysis to quantify airborne sarin concentrations as low as about 20 ppb (v/v) [62].

The speed and simplicity of SPME, and the ability to desorb GC analytes from an SPME fiber within the heated injector of an unmodified GC system, make SPME useful for rapidly screening large numbers of potentially contaminated items and environmental samples for the presence of relatively concentrated (mg quantities) CWA materials. Additionally, the use of SPME avoids the need for solvent extraction to obtain target analytes from various matrices and also avoids extensive sample handling. Both of these attributes lessen the likelihood for exposure to technicians using SPME and field-portable GC instrumentation to complete qualitative screening for CWA contaminants. For qualitative CWA screening, GC-MS is usually used to identify analytes sampled quickly and safely using SPME [8,34,42,57]. The U.S. Marine Corps Chemical Biological Incident Response Force (CBIRF), tasked with counterterrorism responsibilities for detection and mitigation of chemical, biological, and radiological attack, uses SPME and GC analysis with fast resistive column heating and mass spectrometric detection to quickly

screen samples potentially contaminated with CWA materials. In the field, a limited amount of a liquid sample suspected of being a CWA may be collected by a properly protected individual using a cotton-tipped swab to be sealed inside a vial with a septum top. The exterior of the vial is then decontaminated, and insertion of an SPME fiber through the septum under a portable fume hood allows headspace sampling with low potential for exposure to the GC operator. This approach is attractive for field use in a mobile laboratory or other transportable platform equipped with GC-MS capability, and sample times of 1 min or less are possible if mg quantities of CWA materials such as the G agents, sulfur mustard [58], or even VX [36] are present.

35.2.4 GC detectors for CWA analyses

35.2.4.1 Flame ionization detector (FID)

Numerous papers describe GC analysis of CWA materials with detection by FID. In situations where samples are to be screened for the possible presence of CWA compounds, the general usefulness of this detector for virtually all hydrocarbon-containing analytes necessitates the consideration of relative retention information such as the linear temperature program retention index (LTPRI) system proposed by Van den Dool and Kratz [64]. D'Agostino and Provost used GC with flame ionization detection to obtain this type of retention index information relative to a homologous series of *n*-alkanes for organophosphorus compounds (including sarin, soman, tabun, and VX), vesicants, irritants, simulants, and precursors [65]. With little information on analyte identity provided by the detector, the FID is useful only for screening samples where CWA compounds, precursors, or degradation products are expected or to specifically rule out their presence. As GC with mass spectrometric detection has become more widely used, this has reduced the need to rely on broadly responding types of detectors for general screening.

Extensive tables of LTPRI data for CWA-related GC analytes have been compiled for use in the work of the OPCW [4]. The usefulness of such information is not limited to GC analysis using a nonorthogonal detector such as the FID. LTPRI information is also useful in those cases where EI mass spectra fail to provide an unambiguous identification [13].

35.2.4.2 *Detectors with selectivity toward phosphorus, sulfur, and arsenic*

The presence of phosphorus and sulfur in nerve agents, sulfur mustard, precursors, and degradation products allows the use of GC detectors with selectivity toward these elements. In addition to the use of a homologous *n*-alkane series, LTPRI information relative to a homologous series of alkyl bis(trifluoromethyl)phosphine sulfides (the M-series) has also been tabulated for many CWA-related GC analytes [4,66]. The use of the M-series for LTPRI measurement of CWA analytes supports the use of detectors with element-specific selectivity.

Lakso and Ng used GC with both mass spectrometric and nitrogen–phosphorus detection to detect nerve agents sampled from water by SPME with detection limits of $0.05 \mu\text{g L}^{-1}$ for the G agents and $0.5 \mu\text{g L}^{-1}$ for VX [59]. Flame photometric detection has been used extensively to detect compounds related to both nerve agents and sulfur mustard. Sass and Parker reported the use of flame photometric detection for GC analyses of a number of nerve agents and other organophosphorus compounds in 1980. In that work, they cited an early defense community technical report on the use of this GC detector as early as 1969 [67], only a few years after it was described by Brody and Chaney [68]. A more recent publication details detection of methyl phosphonic acid metabolites for sarin and the ethyl sarin analog in the urine of patients exposed during the 1995 Tokyo subway chemical terrorism incident [41]. Analysis with flame photometric detection followed TMS derivatization of these analytes.

Derivatization of lewisite compounds with thiol reagents conveniently produces analytes that are suitable for analysis using flame photometric detection [56]. While offering excellent sensitivity for both sulfur and phosphorus compounds (better for phosphorus than for sulfur), it is well known that the flame photometric detector response is not linear for sulfur [68].

Atar et al. described pulsed flame photometric detection in 1991 [69]. This detector improves on the classical flame photometric detector in several ways, primarily through separation of emission information in time with the use of a pulsed flame, as heteroatoms tend to emit following carbon. In a continuous flame detector, coeluting hydrocarbon compounds can lead to quenching of the desired signal derived from sulfur or phosphorus. In addition, the pulsed flame photometric detector uses less hydrogen than a continuous flame detector, a plus for use in a field-portable detection system [70]. Jing and Amirav [71] discussed the ability of the pulsed flame photometric detector to selectively detect a range of heteroatoms (including arsenic) as well as carbon.

35.2.4.3 *Atomic emission detection*

The atomic emission detector has been used for GC analysis of CWA-related compounds on numerous occasions due to its ability to provide information on the empirical formula of an unknown analyte. Since this detector was described in 1989 [72], it has been used repeatedly to assist in the identification of CWA-related compounds separated by GC. In combination with MS, Mazurek et al. used atomic emission detection to identify a number of compounds related to the presence of sulfur mustard in an item caught in the nets of fishermen in the Baltic Sea [73].

35.2.4.4 *Mass spectrometric detection*

As in other fields where correct analyte identification is important, the mass spectrometer is commonly acknowledged to be the most useful detector for GC analysis of CWA-related

compounds. As the interface of GC with the ion beam quadrupole mass spectrometer was attaining commercial significance in the 1960s, widespread recognition of the need to control environmental pollution was taking hold in the United States and other developed nations. In the United States, this led to the creation of the Environmental Protection Agency in 1970, and the quadrupole mass filter rapidly became the most important GC detector for applications where both detection and identification of organic pollutants were required. As recounted by Finnigan, "the combination of GC retention time and MS spectrum gave unambiguous proof of the presence of pollutants. Any technique that left ambiguity in the analytical results was likely to lead to continual controversy and litigation" [74].

Heller et al. described the usefulness of the newly commercialized GC-MS systems available at that time: "The identification of pollutants at the part-per billion level with a high degree of confidence in the result has become nearly routine in several EPA laboratories. What was once an impossible task for a staff of 100 working 6 months sometimes can be accomplished by a skilled individual in a few hours" [75].

Confirmation of analyte identity where OPCW treaty compliance is in question necessarily follows a conservative approach. A positive identification is confirmed with analysis by two independent methods [9]. Often, this may be obtained with mass spectrometric detection using (sequentially) both electron and chemical ionization (EI and CI), requiring pure analytes as optimally provided by the use of a gas chromatographic inlet.

35.2.4.4.1 EI

The majority of GC-MS analyses for CWA-related materials has used an ion beam quadrupole detector and 70 eV EI conditions. The quadrupole mass filter and EI produce reasonably standard mass spectra that may be compared to large-mass spectral databases. In some cases, EI data alone are inconclusive, e.g.,

for identification of VX and degradation products of VX having the diisopropylaminoethyl functional group [13]. The presence of this structure typically imparts a base peak at m/z^{-1} 114, and, in the case of VX and related compounds, signal for M^{+} and other high-mass ions is either completely absent or very weak, resulting in a number of very similar EI mass spectra that may not be easily differentiated either by automated mass spectral searching or by manual examination.

35.2.4.4.2 CI

The use of CI for GC-MS is important to confirm EI results in forensic and OPCW analyses. Sass and Fisher reported the use of EI, as well as methane, isobutane, and ethylene CI reagents for GC-MS detection of nerve agents in 1979 [76]. When this work was carried out, packed GC columns were still commonly used and a GC-MS interface required the diversion of most of the column flow away from the high vacuum region of a mass spectrometric detector. In the cited work, a membrane interface was used to accomplish this, while later work has been predominantly carried out using capillary columns where a direct interface is possible. D'Agostino et al. demonstrated the use of CI detection for GC-MS using a capillary column and ammonia reagent gas to supplement EI data for the successful identification of VX and a number of its degradation products possessing the diisopropylaminoethyl functional group. The use of ammonia reagent provided soft ionization of the targeted amine compounds, producing mass spectra with abundant $[M+H]^+$ pseudomolecular ions and little fragmentation [13]. The high proton affinity of CI reagent ions produced from ammonia relative to ions produced from other typical CI reagent gases provides some selectivity against the ionization of uninteresting analytes such as hydrocarbon compounds that may also be present in a CWA-related sample. Rohrbaugh used methanol as CI reagent for GC-MS analyses of VX

and related degradation products and discussed the relative merits of this liquid reagent for use in a field-portable system to avoid the need to transport compressed gas reagents [77]. Methanol CI generally produced more intense signals for $[M+H]^+$ and less fragmentation compared to spectra obtained using methane or ammonia reagent.

35.2.4.4.3 Self-CI

The phenomenon of self-CI is commonly seen when an ion trap mass spectrometric detector is used and ionization occurs within the trapping region (internal ionization) [78]. At least two such ion trap GC-MS instruments with internal ionization have been commercialized for use in the field, driven in large part by the need for defensive detection of CWA analytes by military forces [35,79]. While ion beam instruments operated with EI at typically low pressures produce unimolecular decomposition, the simultaneous presence of ions and neutral species within an ion trap using internal ionization may lead to an additional dimension of information related to specific ion/molecule chemistry. When analyzed using an internal ionization ion trap GC-MS detector, numerous CWA analytes produce either protonated pseudomolecular ions or protonated dimer ions [14,80]. When this occurs the resulting mass spectra are not directly comparable to those obtained from large-mass spectral databases mostly produced using ion beam instruments. Nevertheless, the addition of ion/molecule interactions to the EI process may be useful in identifying unknown analytes, as long as the basis for the ion/molecule reactions is understood.

The formation of protonated dimers has been observed when ionization occurs at a phosphoryl or carbonyl oxygen atom [80]. Protonation at this location is thought to occur through self-CI interaction between M^+ and neutral molecules. This is then followed by reaction of a resulting electrophilic phosphorus or carbon atom with the nucleophilic neutral

species [80]. Even when a phosphoryl oxygen atom is present, if a different site on the molecule is more readily ionized (e.g., the diisopropylamino functional group of VX), the formation of a dimer ion is not observed, presumably as the phosphoryl oxygen remains uncharged and thus unactivated for reaction with the neutral molecule. Self-CI protonation at the amine group without the formation of a dimer may be observed in this situation and is also possible for amine compounds that lack a phosphoryl oxygen as well [14]. Further work is needed to verify the reactivity of additional functional groups or elements as well as to incorporate this information into automated algorithms for identification of unknown chemicals using this information combined with existing mass spectral libraries.

35.2.4.4.4 Tandem mass spectrometry

Selective detection with tandem MS using either a triple quadrupole or an ion trap mass spectrometer is available to many of the chemical defense community laboratories and has been used for high-certainty detection of targeted compounds present at low levels in matrices with high concentrations of interferents. D'Agostino et al. described early efforts using GC with a highly specialized triple quadrupole mass spectrometer to selectively detect targeted CWA analytes at pg levels in an extract of charcoal that had been used to sample a diesel exhaust environment [81]. The use of ion trap instrumentation allows for similar MS/MS detection with lower overall instrumentation cost compared to the more specialized triple quadrupole detector. Riches et al. described the use of a benchtop ion trap mass spectrometric GC detector operated in the negative ion chemical ionization (NICI) MS/MS mode to detect pentafluorobenzyl derivatives of nerve agent alkyl alkylphosphonic acid metabolites in urine [82]. The primary negative ion from an alkyl alkylphosphonic acid pentafluorobenzyl derivative results from loss of the pentafluorobenzyl group and thus structural

information relevant to the remaining alkyl groups is retained. Full scan and selected ion monitoring NICI data provided detection limits in the low ng mL^{-1} range, while the use of selected reaction monitoring MS-MS mode improved the sensitivity of the method by about an additional order of magnitude.

35.3 GC applications for biomedical CWA analyses

In 1994, Black et al. described the use of GC-MS for “the first documented unequivocal identification of nerve agent residues in environmental samples collected after a chemical attack” [83]. In addition to the need for unequivocal detection of CWA-related compounds in environmental matrices, a similar need exists with regard to biological matrices, for both forensic and clinical purposes. Two instances are amply demonstrated in the literature: detection of sulfur mustard hydrolysis products in those reportedly exposed to this CWA material during the Iran–Iraq conflict of the 1980s and detection of hydrolysis products related to the G agent sarin, found in various tissues of individuals exposed to this compound during the Tokyo subway terrorism incident of 1995, as well as the less-well-known 1994 incident in Matsumoto Japan.

In 1984, Wils et al. found thiodiglycol through GC-MS analyses of urine collected from Iranian soldiers allegedly attacked with the CWA sulfur mustard in 1984 during the Iran–Iraq war [84]. However, “thiodiglycol concentrations from 10 to 100 ng mL^{-1} in the urine of both the Iranian patients and the controls precluded an unambiguous verification of the use of mustard gas against the Iranian patients” [85]. In 1985, Vycudilik reported the GC-MS detection of sulfur mustard in the urine of two patients 1 week after they were reportedly exposed to this CWA material in the Iran–Iraq war [86]. In a subsequent paper, GC with high-resolution MS was used to again identify this analyte in the urine of six out of 12 patients reporting exposure [87].

However, Vycudilik noted that the methods used did not specifically differentiate between thiodiglycol and the nonhydrolyzed agent, as “this compound is also synthesized via a nucleophilic substitution from thiodiglycol and chloride ions in the course of the extraction procedure” [87]. Hard evidence for the use of CWA materials in this conflict was a goal for numerous chemical defense laboratories, and additional work was performed to examine the usefulness of thiodiglycol as a marker for exposure to sulfur mustard. Black and Read noted that “the detection of free sulfur mustard in the body fluids of hospitalized casualties is unlikely, due to its chemical reactivity and extensive metabolism” [88]. These researchers used pentafluorobenzyl chloride derivatization, followed by NICI GC-MS analysis to detect thiodiglycol in spiked blood and urine samples, allowing detection at levels as low as 1 ng mL^{-1} . Thiodiglycol was found at concentrations up to 16 and $<1 \text{ ng mL}^{-1}$ in the blood and urine, respectively, of healthy nonexposed control subjects, allowing Black and Read to hypothesize that the reported analytical method could be useful to differentiate exposed and nonexposed individuals with the caveat that additional work was needed to carefully examine the incidence and magnitude of endogenously produced thiodiglycol ... “clearly a much larger number of control subjects will need to be analyzed for thiodiglycol before any firm conclusions can be drawn about endogenous levels” [88].

Minami et al. extracted alkyl methylphosphonic acid metabolites present in the urine of patients exposed to sarin and related impurities in the Tokyo subway incident of 1995 [41]. Ion exchange cleanup was required, and this was followed by TMS derivatization and analysis by GC with flame photometric detection. The time course for the presence of isopropyl methylphosphonic acid in the urine of two exposed patients was followed, demonstrating relatively high concentrations at 12 h following exposure and a rapid decline thereafter.

Nagao et al. found that for four victims they examined from the Tokyo subway incident "postmortem examinations revealed no macroscopic and microscopic findings specific to sarin poisoning and sarin and its hydrolysis products were almost undetectable in their blood" [89]. To provide information of use to future forensic or clinical work, these researchers described the recovery of isopropyl methylphosphonic acid from sarin-bound acetylcholinesterase enzyme present in peripheral blood of the victims. The sarin-bound enzyme was released by trypsin and alkaline phosphatase digestion, and the free acid was then subjected to TMS derivatization for GC-MS analysis [89].

The less-well-known terrorist release of sarin in the Japanese city of Matsumoto caused seven deaths, compared to the 12 deaths attributed to the Tokyo incident the following year. Nakajima et al. described GC analysis methods that were similar to those reported by Minami et al. [41] to follow the exponential decay of isopropyl methylphosphonic acid and methylphosphonic acid excreted in the urine of a single case [90]. This person lived in a third floor apartment said to be 50 m away from the sarin release point. He recalled "blurriness of vision immediately after opening the window at ~2300 h on the 27th of June 1994, and then he went to bed. At 0100 h the next day, he was found unconscious by a rescuer team, and was transferred to a hospital" [90]. The victim's total sarin dose was estimated by extrapolating the decay curves obtained for the urinary metabolites, arriving at a value of $\sim 0.05 \text{ mg kg}^{-1}$, slightly above the accepted lethal dose for humans. Noting this information and the clinical findings, Nakajima et al. stated that this victim "...fortunately had a narrow escape from death."

35.4 Conclusion

GC rapidly became an important method for detection and identification of chemical compounds related to CWAs in the decade

immediately following the initial experiments completed by James and Martin. With the development of the modern fused-silica, open-tubular GC column and the widespread availability of mass spectrometric detectors, GC-based detection approaches have assumed increased importance to the OPCW treaty compliance laboratories, the chemical defense research community, and technician-level users of field-portable GC instrumentation. The availability of selective detectors well suited to the CWA-related analytes and the ability to analyze many of the intact CWA compounds by GC without derivatization further add to the usefulness of GC for a variety of applications ranging from OPCW treaty compliance verification of process stream or environmental samples, to clinical efforts focused on the protection of human health. Where derivatization is required for GC analysis, substantial well-documented efforts have resulted in sensitive methods that are suitable for use in many circumstances.

While the ability to complete GC-MS analyses using person-portable instrumentation can extend the capabilities of frontline users who need highly definitive answers in high-stakes situations, the supporting systems, methods, and identification algorithms must be improved to fully realize the potential of the faster, smaller, and more capable instruments that continue to be developed to meet this need.

References

- [1] A.T. James, A.J.P. Martin, Gas-liquid partition chromatography: the separation and micro-estimation of volatile fatty acids from formic to dodecanoic acid, *Biochem. J.* 50 (1951) 679-690.
- [2] L.S. Ettre, A. Zlatkis, A.J.P. Martin (Eds.), 75 Years of Chromatography, a Historical Dialogue, Elsevier, Amsterdam, 1979, pp. 285-296.
- [3] Convention on the Prohibition of the Development, Production, Stockpiling and Use of Chemical Weapons and on Their Destruction, Technical Secretariat of the Organisation for Prohibition of Chemical Weapons, The Hague, 1997.

- [4] O. Kostianen, Gas chromatography in screening of chemicals related to the chemical weapons convention, in: M. Mesilaakso (Ed.), *Chemical Weapons Convention Chemical Analysis, Sample Collection, Preparation, and Analytical Methods*, John Wiley and Sons, Chichester, UK, 2005.
- [5] P.W. Albro, L. Fishbein, Gas chromatography of sulfur mustard and its analogs, *J. Chromatogr.* 46 (1970) 202–203.
- [6] R.L. Erickson, R.N. Macnair, R.H. Brown, H.D. Hogan, Determination of bis(2-chloroethyl)sulfide in a Dawson apparatus by gas chromatography, *Anal. Chem.* 44 (1972) 1040–1041.
- [7] K.M. Sloan, R.V. Mustacich, B.A. Eckenrode, Development and evaluation of a low thermal mass gas chromatograph for rapid forensic GC-MS analyses, *Field Anal. Chem. Technol.* 5 (2001) 288–301.
- [8] P.A. Smith, M.T. Sng, B.A. Eckenrode, S.Y. Leow, D. Koch, R.P. Erickson, et al., Towards smaller and faster gas chromatography–mass spectrometry systems for field chemical detection, *J. Chromatogr. A* 1067 (2005) 285–294.
- [9] E.R.J. Wils, Gas chromatography/mass spectrometry in analysis of chemicals related to the chemical weapons convention, in: M. Mesilaakso (Ed.), *Chemical Weapons Convention Chemical Analysis, Sample Collection, Preparation, and Analytical Methods*, John Wiley and Sons, Chichester, UK, 2005.
- [10] M. Sokolowski, The OPCW gas chromatograph/mass spectrometer for on-site analysis. Instrumentation, AMDIS software, and preparations for use, in: M. Mesilaakso (Ed.), *Chemical Weapons Convention Chemical Analysis, Sample Collection, Preparation, and Analytical Methods*, John Wiley and Sons, Chichester, UK, 2005.
- [11] L. Szinicz, History of chemical and biological warfare agents, *Toxicology* 214 (2005) 167–181.
- [12] R.W. Baier, S.W. Weller, Catalytic and thermal decomposition of isopropyl methyl fluorophosphonate, *Ind. Eng. Chem. Process Des. Dev.* 6 (1967) 380–385.
- [13] P.A. D'Agostino, L.R. Provost, J. Visentini, Analysis of O-ethyl S-[2-(diisopropylamino)ethyl] methylphosphonothiolate (VX) by capillary column gas chromatography-mass spectrometry, *J. Chromatogr.* 402 (1987) 221–232.
- [14] P.A. Smith, C.R. Jackson Lepage, B. Savage, C.R. Bowerbank, E.D. Lee, M.J. Lukacs, Use of a hand-portable gas chromatograph-toroidal ion trap mass spectrometer for self-CI identification of degradation products related to O-ethyl S-2-diisopropylaminoethyl methyl phosphonothiolate (VX), *Anal. Chim. Acta* 690 (2011) 215–220.
- [15] B. Muir, S. Quick, B.J. Slater, D.B. Cooper, M.C. Moran, C.M. Timperly, et al., Analysis of chemical warfare agents II. Use of thiols and statistical experimental design for the trace level determination of vesicant compounds in air samples, *J. Chromatogr. A* 1068 (2005) 315–326.
- [16] R.T. Rosen, J.D. Rosen, Presence of four Fusarium mycotoxins and synthetic material in “yellow rain”, *Bio-med. Mass Spectrom.* 9 (1982) 443–450.
- [17] C.J. Mirocha, R.A. Pawlosky, K. Chatterjee, S. Watson, W. Hayes, Analysis for Fusarium toxins implicated in biological warfare in Southeast Asia, *J. Assoc. Off. Anal. Chem.* 66 (1983) 1485–1499.
- [18] S.A. Watson, C.J. Mirocha, A.W. Hayes, Analysis for trichothecenes in samples from Southeast Asia associated with “yellow rain”, *Fund. Appl. Toxicol.* 4 (1984) 700–717.
- [19] J.W. Nowicke, M. Messelson, Yellow rain – a palynological analysis, *Nature* 309 (1984) 205–206.
- [20] C.O. Ikediobi, I.C. Hsu, J.R. Bamburg, F.M. Strong, Gas-liquid chromatography of mycotoxins of the trichothecene group, *Anal. Biochem.* 43 (1971) 327–340.
- [21] P.A. D'Agostino, L.R. Provost, D.R. Drover, Analysis of trichothecene mycotoxins in human blood by capillary column gas chromatography-ammonia chemical ionization mass spectrometry, *J. Chromatogr.* 367 (1986) 77–86.
- [22] P. Begley, B.E. Foulger, P.D. Jeffery, R.M. Black, R.W. Read, Detection of trace levels of trichothecenes in human blood using capillary gas chromatography-electron-capture negative chemical ionization mass spectrometry, *J. Chromatogr.* 367 (1986) 87–101.
- [23] P.K. Lee, S.Y.K. Kee, W. Ng, P. Gopalakrishnakone, Determination of trichothecene toxin (T2 mycotoxin) in aqueous sample with solid phase microextraction technique followed by gas chromatography with flame ionization detection, *J. High Resolut. Chromatogr.* 22 (1999) 424–426.
- [24] F.W. Beswick, Chemical agents used in riot control and warfare, *Hum. Toxicol.* 2 (1983) 247–256.
- [25] E.R.J. Wils, A.G. Hulst, Mass spectra of some derivatives of the irritant o-chlorobenzylidenemalononitrile (CS), *Fresenius Z. Anal. Chem.* 320 (1985) 357–360.
- [26] T.A. Kluchinsky Jr., M.V. Sheely, P.B. Savage, P.A. Smith, Formation of 2-chlorobenzylidenemalononitrile (CS riot control agent) thermal degradation products at elevated temperatures, *J. Chromatogr. A* 952 (2002) 205–213.
- [27] T.A. Kluchinsky Jr., P.B. Savage, M.V. Sheely, R.J. Thomas, P.A. Smith, Identification of CS-derived compounds formed during heat-dispersion of CS riot control agent, *J. Microcolumn Sep.* 13 (2001) 186–190.

- [28] P.A. Smith, M.V. Sheely, T.A. Kluchinsky Jr., Solid phase microextraction with analysis by gas chromatography to determine short term hydrogen cyanide concentrations in a field setting, *J. Separ. Sci.* 25 (2002) 917–921.
- [29] N.B. Munro, S.S. Talmage, G.D. Griffin, L.C. Waters, A.P. Watson, J.F. King, et al., The sources, fate, and toxicity of chemical warfare agent degradation products, *Environ. Health Perspect.* 107 (1999) 933–974.
- [30] P.A. D'Agostino, L.R. Provost, Capillary column electron impact and ammonia chemical ionization gas chromatographic-mass spectrometric and gas chromatographic-tandem mass spectrometric analysis of mustard hydrolysis products, *J. Chromatogr.* 645 (1993) 283–292.
- [31] B.A. Eckenrode, Environmental and forensic applications of field-portable GC-MS: an overview, *J. Am. Soc. Mass Spectrom.* 12 (2001) 683–693.
- [32] E.U. Ehrmann, H.P. Dharmasena, K. Carney, E.B. Overton, Novel column heater for fast capillary gas chromatography, *J. Chromatogr. Sci.* 34 (1996) 533–539.
- [33] J. Padayhag, Vapor validation of monitoring systems for detection of trace levels of chemical warfare agents in air, in: V.M. Kolodkin (Ed.), *NATO Security through Science Series, Ecological Risks Associated with the Destruction of Chemical Weapons*, Springer, The Netherlands, 2006.
- [34] P. Smith, C. Jackson Lepage, D. Koch, H. Wyatt, B. Eckenrode, G. Hook, et al., Detection of gas phase chemical warfare agents using field-portable gas chromatography-mass spectrometry systems: instrument and sampling strategy considerations, *Trends Anal. Chem.* 23 (2004) 296–306.
- [35] J.A. Contreras, J.A. Murray, S.E. Tolley, J.L. Oliphant, H.D. Tolley, S.A. Lammert, et al., Hand-portable gas chromatograph-toroidal ion trap mass spectrometer (GC-TMS) for detection of hazardous compounds, *J. Am. Soc. Mass Spectrom.* 19 (2008) 1425–1434.
- [36] G.L. Hook, G. Kimm, G. Betsinger, P.B. Savage, A. Swift, T. Logan, et al., Solid phase microextraction sampling and gas chromatography/mass spectrometry for field detection of the chemical warfare agent O-ethyl S-(2-diisopropylaminoethyl) methylphosphonothiolate (VX), *J. Separ. Sci.* 26 (2003) 1091–1096.
- [37] W.K. Fowler, J.E. Smith, Indirect determination of O-ethyl S-(2-diisopropylaminoethyl) methylphosphonothioate in air at low concentrations, *J. Chromatogr.* 478 (1989) 51–61.
- [38] R.M. Black, B. Muir, Derivatization reactions in the chromatographic analysis of chemical warfare agents and their degradation products, *J. Chromatogr. A* 1000 (2003) 253–281.
- [39] J.G. Purdon, J.G. Pagotto, R.K. Miller, Preparation, stability and quantitative analysis by gas chromatography and gas chromatography-electron impact mass spectrometry of tert-butyl dimethylsilyl derivatives of some alkylphosphonic and alkyl methylphosphonic acids, *J. Chromatogr.* 475 (1989) 261–272.
- [40] M.-L. Kuitunen, Sample preparation for analysis of chemicals related to the chemical weapons convention in an off-site laboratory, in: M. Mesilaakso (Ed.), *Chemical Weapons Convention Chemical Analysis, Sample Collection, Preparation, and Analytical Methods*, John Wiley and Sons, Chichester, UK, 2005.
- [41] M. Minami, D.-M. Hui, M. Katsumata, H. Inagaki, C.A. Boulet, Method for the analysis of the methylphosphonic acid metabolites of sarin and its ethanol-substituted analogue in urine as applied to the victims of the Tokyo sarin disaster, *J. Chromatogr. B* 695 (1997) 237–244.
- [42] G.L. Hook, G. Kimm, D. Koch, P.B. Savage, B. Ding, P.A. Smith, Detection of VX in soil through solid-phase microextraction sampling and gas chromatography/mass spectrometry of the VX degradation product bis(diisopropylaminoethyl)disulfide, *J. Chromatogr. A* 992 (2003) 1–9.
- [43] D. Pardasani, A. Purohit, A. Mazumder, D.K. Dubey, Gas chromatography-mass spectrometric analysis of toxic hydrolyzed products of nerve agent VX and its analogues for verification of chemical weapons convention, *Anal. Methods* 2 (2010) 661–667.
- [44] W.R. Creasy, A.A. Rodriguez, J.R. Stuff, R.W. Warren, Atomic emission detection for the quantitation of trimethylsilyl derivatives of chemical-warfare-agent related compounds in environmental samples, *J. Chromatogr. A* 709 (1995) 333–344.
- [45] W.R. Creasy, J.R. Stuff, B. Williams, K. Morrissey, J. Mays, R. Duevel, et al., Identification of chemical-weapons-related compounds in decontamination solutions and other matrices by multiple chromatographic techniques, *J. Chromatogr. A* 774 (1997) 253–263.
- [46] E.R.J. Wils, A.G. Hulst, Mass spectra of some derivatives of 2,2'-dichlorodiethyl sulphide (mustard gas), *Fresenius Z. Anal. Chem.* 321 (1985) 471–474.
- [47] W.K. Fowler, D.C. Stewart, D.S. Weinberg, E.W. Sarver, Gas chromatographic determination of the lewisite hydrolysate, 2-chlorovinylarsonous acid, after derivatization with 1,2-ethanedithiol, *J. Chromatogr.* 558 (1991) 235–246.
- [48] S. Hanaoka, K. Nomura, T. Wada, Determination of mustard and lewisite related compounds in abandoned chemical weapons (Yellow shells) from sources in

- China and Japan, *J. Chromatogr. A* 1101 (2006) 268–277.
- [49] W.K. Fowler, C.H. Duffey, H.C. Miller, Modification of a gas chromatographic inlet for thermal desorption of adsorbent-filled sampling tubes, *Anal. Chem.* 51 (1979) 2333–2336.
- [50] J. Steinhanses, K. Schoene, Thermal desorption-gas chromatography of some organophosphates and S-mustard after trapping on Tenax, *J. Chromatogr.* 514 (1990) 273–278.
- [51] R.M. Black, R. Claarke, D.B. Cooper, R.W. Read, D. Utley, Application of headspace analysis, solvent extraction, thermal desorption and gas chromatography-mass spectrometry to the analysis of chemical warfare samples containing sulphur mustard and related compounds, *J. Chromatogr.* 673 (1993) 71–80.
- [52] J.R. Hancock, G.W. Peters, Retention index monitoring of compounds of chemical defence interest using thermal desorption gas chromatography, *J. Chromatogr.* 538 (1991) 249–257.
- [53] C.L. Arthur, J. Pawliszyn, Solid phase microextraction with thermal desorption using fused silica optical fibers, *Anal. Chem.* 62 (1990) 2145–2148.
- [54] B. Zygmunt, A. Zaborowska, J. Świattłowska, J. Namieśnik, Solid phase microextraction combined with gas chromatography - a powerful tool for the determination of chemical warfare agents and related compounds, *Curr. Org. Chem.* 11 (2007) 241–253.
- [55] G.L. Kimm, G.L. Hook, P.A. Smith, Application of headspace solid-phase microextraction and gas chromatography-mass spectrometry for detection of the chemical warfare agent bis(2-chloroethyl) sulfide in soil, *J. Chromatogr. A* 971 (2002) 185–191.
- [56] B.A. Tomkins, G.A. Sega, C.-H. Ho, Determination of lewisite oxide in soil using solid phase microextraction followed by gas chromatography with flame photometric or mass spectrometric detection, *J. Chromatogr. A* 909 (2001) 13–28.
- [57] B. Szostek, J.H. Aldstadt, Determination of organoarsenicals in the environment by solid-phase microextraction-gas chromatography-mass spectrometry, *J. Chromatogr. A* 807 (1998) 253–263.
- [58] J.-A.M. Creek, A.M. McAnoy, C.S. Brinkworth, Rapid monitoring of sulfur mustard degradation in solution by headspace solid-phase microextraction and gas chromatography mass spectrometry, *Rapid Commun. Mass Spectrom.* 24 (2010) 3419–3424.
- [59] H.A. Lakso, W.F. Ng, Determination of chemical warfare agents in natural water samples by solid-phase microextraction, *Anal. Chem.* 69 (1997) 1866–1872.
- [60] J.F. Schneider, A.S. Boparai, L.L. Reed, Screening for sarin in air and water by solid-phase microextraction-gas chromatography-mass spectrometry, *J. Chromatogr. Sci.* 39 (2001) 420–424.
- [61] M.T. Sng, W.F. Ng, In-situ derivatisation of degradation products of chemical warfare agents in water by solid-phase microextraction and gas chromatography-mass spectrometric analysis, *J. Chromatogr. A* 832 (1999) 173–182.
- [62] G.L. Hook, C.J. Lepage, S.I. Miller, P.A. Smith, Dynamic solid phase microextraction for sampling of airborne sarin with gas chromatography-mass spectrometry for rapid field detection and quantification, *J. Separ. Sci.* 27 (2004) 1017–1022.
- [63] J. Koziel, M. Jia, J. Pawliszyn, Air sampling with porous solid-phase microextraction fibers, *Anal. Chem.* 72 (2000) 5178–5186.
- [64] H. Van Den Dool, P.D. Kratz, A generalization of the retention index system including linear temperature programmed gas-liquid partition chromatography, *J. Chromatogr.* 11 (1963) 463–471.
- [65] P.A. D'Agostino, L.R. Provost, Gas chromatographic retention indices of chemical warfare agents and simulants, *J. Chromatogr.* 331 (1985) 47–54.
- [66] A. Manninen, M.-L. Kuitunen, L. Julin, Gas chromatographic properties of the M-series of universal retention index standards and their application to pesticide analysis, *J. Chromatogr.* 394 (1987) 465–471.
- [67] S. Sass, R.J. Steger, Gas chromatographic differentiation and estimation of some sulfur and nitrogen mustards using a multidetector technique, *J. Chromatogr.* 238 (1982) 121–132.
- [68] S.S. Brody, J.E. Chaney, Flame photometric detector. The application of a specific detector for phosphorous and for sulfur compounds-sensitive to subnanogram quantities, *J. Gas Chromatogr.* 4 (1966) 42–46.
- [69] E. Atar, S. Cheskis, A. Amirav, Pulsed flame - a novel concept for molecular detection, *Anal. Chem.* 63 (1991) 2064–2068.
- [70] G. Frishman, A. Amirav, Fast GC-PFPD system for field analysis of chemical warfare agents, *Field Anal. Chem. Technol.* 4 (2000) 170–194.
- [71] H. Jing, A. Amirav, Pulsed flame photometric detector - a step forward towards universal heteroatom selective detection, *J. Chromatogr. A* 805 (1998) 177–215.

- [72] J.J. Sullivan, B.D. Quimby, Detection of C, H, N, and O in capillary gas chromatography by atomic emission, *J. High Resolut. Chromatogr.* 12 (1989) 282–286.
- [73] M. Mazurek, Z. Witkiewicz, S. Popiel, M. Śliwakowski, Capillary gas chromatography-atomic emission spectroscopy-mass spectrometry analysis of sulphur mustard and transformation products in a block recovered from the Baltic Sea, *J. Chromatogr. A* 919 (2001) 133–145.
- [74] R.E. Finnigan, Quadrupole mass spectrometers, from development to commercialization, *Anal. Chem.* 66 (1994) 969A–975A.
- [75] S.R. Heller, J.M. McGuire, W.L.W.L. Budde, Trace organics by GC/MS, *Environ. Sci. Technol.* 9 (1975) 210–213.
- [76] S. Sass, T.L. Fisher, Chemical ionization and electron impact mass spectrometry of some organophosphate compounds, *Org. Mass Spectrom.* 14 (1979) 257–264.
- [77] D.K. Rohrbaugh, Methanol chemical ionization quadrupole ion trap mass spectrometry of O-ethyl S-[2-(diisopropylamino)ethyl] methylphosphonothiolate (VX) and its degradation products, *J. Chromatogr. A* 893 (2000) 393–400.
- [78] S.A. McLuckey, G.L. Glish, K.G. Asano, G.J. Van Berkel, Self chemical ionization in an ion trap mass spectrometer, *Anal. Chem.* 60 (1988) 2312–2314.
- [79] G.E. Patterson, A.J. Guymon, L.S. Riter, M. Everly, J. Griep-Raming, B.C. Laughlin, et al., Miniature cylindrical ion trap mass spectrometer, *Anal. Chem.* 74 (2002) 6145–6153.
- [80] P.A. Smith, C. Jackson Lepage, M. Lukacs, N. Martin, A. Shufutinsky, P.B. Savage, Field-portable gas chromatography with transmission quadrupole and cylindrical ion trap mass spectrometric detection: chromatographic retention index data and ion/molecule interactions for chemical warfare agent identification, *Int. J. Mass Spectrom.* 295 (2010) 113–118.
- [81] P.A. D'Agostino, L.R. Provost, J.F. Anacleto, P.W. Brooks, Capillary column gas chromatography–tandem mass spectrometry detection of chemical warfare agents in a complex airborne matrix, *J. Chromatogr.* 504 (1990) 259–268.
- [82] J. Riches, I. Morton, R.W. Read, R.M. Black, The trace analysis of alkyl alkylphosphonic acids in urine using gas chromatography-ion trap negative ion tandem mass spectrometry, *J. Chromatogr. B* 816 (2005) 251–258.
- [83] R.M. Black, R.J. Clarke, R.W. Read, M.T.J. Reid, Application of gas chromatography–mass spectrometry and gas chromatography–tandem mass spectrometry to the analysis of chemical warfare samples, found to contain residues of the nerve agent sarin, sulphur mustard and their degradation products, *J. Chromatogr. A* 662 (1994) 301–321.
- [84] E.R.J. Wils, A.G. Hulst, A.L. de Jong, A. Verweij, H.L. Boter, Analysis of thiodiglycol in urine of victims of an alleged attack with mustard gas, *J. Anal. Toxicol.* 9 (1985) 254–257.
- [85] E.R.J. Wils, A.G. Hulst, J. van Laar, Analysis of thiodiglycol in urine of victims of an alleged attack with mustard gas, part II, *J. Anal. Toxicol.* 12 (1988) 15–19.
- [86] W. Vycudilik, Detection of mustard gas bis(2-chloroethyl)-sulfide in urine, *Forensic Sci. Int.* 28 (1985) 131–136.
- [87] W. Vycudilik, Detection of bis(2-chloroethyl)-sulfide (Yperite) in urine by high resolution gas chromatography-mass spectrometry, *Forensic Sci. Int.* 35 (1987) 67–71.
- [88] R.M. Black, R.W. Read, Detection of trace levels of thiodiglycol in blood, plasma and urine using gas chromatography–electron-capture negative-ion chemical ionisation mass spectrometry, *J. Chromatogr.* 449 (1988) 261–270.
- [89] M. Nagao, T. Takatori, Y. Matsuda, M. Nakajima, H. Iwase, K. Iwadate, Definitive evidence for the acute sarin poisoning diagnosis in the Tokyo subway, *Toxicol. Appl. Pharmacol.* 144 (1997) 198–203.
- [90] T. Nakajima, K. Sasaki, H. Ozawa, Y. Sekijima, H. Morita, Y. Fukushima, et al., Urinary metabolites of sarin in a patient of the Matsumoto sarin incident, *Arch. Toxicol.* 72 (1998) 601–603.

Index

Note: Page numbers followed by “f” indicate figures and “t” indicate tables.

A

- Absolute heating rate, 42
- Absolute method, 388
- Absolute temperature, 23
- Absorption spectra, 371
- Accelerants in fire debris, 306
- Accuracy profiles, data analysis methods, 559, 559f
- Acrylics, 331–332
- Acylglycerols, 690–691
- Additive absorption, 387
- Adsorbents, behavior of, 122–123
- Adsorption
 - chromatography, 117
 - materials, 117
 - stabilization of, 121–122
- Advanced applications, 337–341
- Advanced data mining for GC-MS, 315–316
- Air
 - gas sampling, 282–284
 - GC-ICPMS for, 459–460
 - monitoring, 291–295
 - industrial (fugitive) emissions, 293–294
 - industrial (occupational) hygiene or workplace air monitoring, 291
 - monitoring ambient outdoor air and indoor air quality (IAQ), 291
 - monitoring vehicle interior air quality (VIAQ), 292–293
- Alkali metal salts, 158–159
- Alkylation reagents, 645, 646t
- Alkylimidazolium-based ionic (CD), 594–595
- Alkylsilyl reagents, 640–644, 642t–643t
 - polyfunctional compounds, 642–644
 - trimethylchlorosilane, 640–642
 - trimethylsilyldiethylamine, 640
 - trimethylsilylimidazole, 640–642
- Alternative detector design, 355–356, 360
- Alternative protective coatings, 104–105
- Alumina, 124–127
 - behavior of, 124–127
- Aluminum-clad fused silica, 105
- Ambient outdoor air and indoor air quality (IAQ), 291
- α -Amino acid derivatives, 583–584
- Amphetamine-type stimulants (ATs), 752
- Analog-to-digital converter (ADC), 506, 507f
- Analysis of variance (ANOVA), 552, 555
- Analyte recovery during thermal desorption, 314
- Analytical gas chromatography (GC), 19–20
- Antimony, in soil, 459
- Apolane 87, 143–145
 - stationary phases and, 6
- Aromatic composition of gasoline, 209–211
- Arsenic detectors, 892
- Association of Official Analytical Chemists (AOAC), 548
- Asymmetry, 510
- Atmospheric pressure chemical ionization (APCI), 390–393
- Atmospheric research, 294
- Atomic diffusion volume increments, 32
- Atomic emission detector (AED), 365–366, 365f, 812–813, 892
- Atomic emission spectrometry (AES)
 - GC-GD-AES, 454–457
 - GD and, 449–450
 - ICP and, 449–450

- Automated dry purging, 276
- Automated Mass spectral Deconvolution and Identification System (AMDIS), 315, 539–540
- Autosampler, liquid injectors, 221

B

- Baby food
 - multiresidue methods, 802–804
 - pesticides, 802–804
- Bacillus amylobacter*, 587
- Backflushing
 - 2D GC, 195–200
 - basic mode of operation, 195–197
 - for gasoline oxygenates, 197–200
 - “Backflush” mode, 276–277
- Backpressure regulator, 222
 - GSV and, 246
 - in split injection, 236–237
- Band-broadening mechanisms, 155–158
- Barrier-discharge ionization detector (BID), 357–358
- Baseline correction, 528–529, 529f
- Battlefield protection, 299
- Beer’s Law, 387
- Best-fit spectra, 419–420
- Biomarker identification, 733
- Biomass, 336–337
- Body fluids, GC-ICPMS for, 460–461
- Bond dissociation and free radicals, 326
- Bonded stationary phase, 6
- Borderline inlet pressure, 37
- Borosilicate, 100
- Breath monitoring, 290–291
- Breath testing, 290–291
- Brightly enhanced sample transfer (BEST), 240
- Bulk drug analysis, 747–753

- Bulk physical property detectors,
358–360
thermal conductivity detector,
358–360
- Bunching, 515
- tert*-Butyldimethylsilyl (TBDMS), 589
- C**
- Calibration methods, 540–541
partial least squares (PLS) regression,
540
principal component regression
(PCR), 540–541
- Cannabis, 748
- Capillary columns, 23, 713–714
- Capillary (open-tubular) columns, 20
- Capillary electrophoresis (CE)
ICPMS and, 449–450, 454
- Capillary tubing, types of, 123–124
- Carbohydrates
bioactivities, 703
chromatographic conditions, 713–716
capillary columns, 713–714
detectors, 714–716
separation conditions, 714
comprehensive two-dimensional gas
chromatography, 720–721
degree of polymerization (DP), 703
derivatization, 708–713, 709t–710t
acyl esters, 711
alditol acetates, 712
aldonitrile acetates, 712
alkylation, 708
alkylsilyl ethers, 708–711
chiral derivatives, 713
cyclic boronic esters, 713
dialkylmercaptal derivatives,
712–713
oximes, 711–712
functions, 703
high-resolution techniques, 703
hydrolysis, 719
low-molecular-weight
carbohydrates, 716–719
mass spectra, 719
methylation analysis, 719–720
oligosaccharides, 719–720
polysaccharides, 719–720
retention, 717, 718t
sample preparation, 704–708, 704f
cleanup, 704
extraction, 704–708
fractionation, 704–708
- Carbon, 131–134
adsorbents, 159
molecular sieves, 159
- Carbowax 20M, 147
- Carrier gas flows, 9–11, 19, 313
- Carrier gas local velocity, 23
- Cartridge discharge residue (CDR),
764
- Cassini–Huygens mission, 867
- “Catalyst-killers”, 135
- Cavity formation, 168
- Characteristic thermal constant,
27–29
- Chelates as chiral selectors, 584–587
- Chemical ionization (CI), 385
- Chemical release/emission testing,
299
- Chemical warfare agent (CWA)
blood and pulmonary agents, 881
chemical weapons convention, 877
derivatization, 887–889
environmental degradation
products, 883–884
field-portable GC instrumentation,
887
- G agents, 888
gas chromatography, 875–877
GC applications, 895–896
GC detectors, 891–895
arsenic detectors, 892
atomic emission detection, 892
CI, 893–894
EI, 893
flame ionization detector (FID),
891–892
mass spectrometric detection,
892–895
phosphorus detectors, 892
self-CI, 894
sulfur detectors, 892
tandem mass spectrometry,
894–895
- GC instrumentation, 884–887
lewisite, 889
low thermal mass GC column
heating, 885–887
MINICAMS, 884–885
nerve agents, 877–879, 879f
riot control/incapacitating agents,
882–883
sample introduction for, 890–891
sampling and gas chromatographic
analysis, 887–895
- specialized sample introduction
methods, 875
SPME sampling, 890–891
sulfur mustard, 889
thermal desorption, 889–890
toxins, 881–882
vesicants, 879–881, 880f
volatility constraints, 887
VX, 888–889
- Chemical warfare agents (CWAS),
778–779
- Chemiluminescent detector (CLD),
363–364
- Chemistry, 117–119
- Chemometric data analysis, 731–732
- ChemStation software programs, 533
- Chinese environmental standards,
282–284
- Chiral columns, 676
- Chiral covalent organic frameworks
(COFs), 593
- Chiral ionic liquids, 594–595
- Chiral mesoporous silica, 593–594
- Chiral nematic mesoporous silica
(CNMS), 593–594
- Chiral recognition
column efficiency, 596–598
complex samples by gas
chromatography, 598–601
enantiomers analysis, 598–601
enantioselective gas
chromatography, 602–604, 603f
enantioselectivity, 596–598
gas chromatography with mass
spectrometry, 598–601
mass spectrometry, 601–602
multidimensional gas, 598
strategy for, 596–604
total analysis system (TAS), 604
- Chiral stationary phases, 583–595
- Chlorine-containing compounds, 419
- Chloroformate reagents, 645–647
- ChromAlign software, 532–533
- Chromatogram, 550–551
- Chromatographic conditions,
713–716
capillary columns, 713–714
detectors, 714–716
separation conditions, 714
- Chromatographic resolution, 380
- Chromatographic separation,
846–847
- Chromatographic system, 20f

- Chromatography data system (CDS)
 analog-to-digital converter (ADC),
 506, 507f
 constant and variable data rates,
 507–508
 control of devices, 505
 conversion, 512–513
 data preprocessing, 505
 discretization, errors caused by,
 512–513
 duty cycle, 506
 equipment control, 506–508
 external standard calculations,
 519–520, 519f
 internal standard calculations,
 520–521
 relative calibration, 521
 relative concentration, 520–521
 measurement of signals, 505
 measuring, 506–507
 overlapped peaks handling, 518
 peak identification, 505, 517–518
 peak parameters, 505
 peak search, 508–511
 convolution, 509
 integration, 508
 moving weighted average, 509
 peak parameters, 509–511
 peak shape, 509
 statistical moments, 508
 quantification, 518–521
 quantitative calculations, 505
 signal measurement, 506–508
 smoothing, 514–517
 area, 516–517
 height, 516–517
 smoother comparison, 516
 zeroth peak moment, 513
Chromosorb P-AW-DMCS, 499
Classical least squares (CLS), 540
Classical liquid–liquid extraction,
 618
 applications, 620–622
Classical molecular spectroscopy
 methods, 371
Cleanroom environment, 105
Closed-loop stripping method, 678
Coating and packing techniques,
 149–150
Coatings
 static, 112
 for WCOT, 103
“Coating solution”, 111
Coating stationary phase
 leaching, 108–109
 rinsing and dehydration, 109
 surface deactivations, 109–110
 surface preparations, 108
Coating techniques, 112–114
Cohesive energy density, 572
Coiled glass capillaries, 4
Cold EI, 384–385
Cold on-column injection (COCI), 223f
 elution in, 225
 with PTV, 243–244
 retention gap in, 226–229, 228f
 sample introduction and, 223–229
 samples for, 223–224
 solvents in, 224–226
Collision cross section (CCS), 427
Collision induced dissociation (CID),
 410
Column chromatography, 55
Column diameter and pressure,
 82–83
Column efficiency, 150, 596–598
Column heating, 9–11
Column liquid chromatography
 multidimensional gas
 chromatography, 636–638, 637t
 multimodal gas chromatography,
 636–638
Column power
 isothermal, 478–479, 478f–479f
 programmed, 480, 482f
Column technology, 99–100
 alternative protective coatings,
 104–105
 cleanroom environment, 105
 coating stationary phase
 leaching, 108–109
 rinsing and dehydration, 109
 surface deactivations, 109–110
 surface preparations, 108
 coating techniques, 112–114
 drawing capillary from preform,
 101–103
 fused-silica capillary tubing,
 107–108
 fused-silica drawing process, 100
 preform–draw material, 100–101
 protective coating, 103–104
 quality evaluation, 114–115
 quality monitoring, 105–107
 stationary phases, 111–112
 surface chemistry, 101
Column tubing internal diameter, 23
Commercial column manufacturers,
 5–6
Commercial libraries, 680
Commercially available extraction
 phases, 633
“Committee on Analytical
 Requirements” (CAR),
 270–271
Common packed-column
 applications of porous
 polymers, 161t
Complement TD applications,
 314–316
Complexation gas chromatography,
 586f
Complex liquid and solid samples,
 285–288
Comprehensive 2D gas
 chromatography (GC X GC),
 200–203, 204f
 basic mode of operation,
 203–206
 DS for, 210f
 elution times and, 205f
 for environment, 836
 for gasoline aromatic composition,
 209–211
 modulators, 206–209
 separations for
 detectors in, 209
 quantification in, 209
 with TOFMS, 212f, 837f
 for yeast extracts, 211
 wine, 801
Comprehensive gas chromatography,
 14–15
Comprehensive techniques, 180–181
Comprehensive two-dimensional gas
 chromatography, 720–721
Computer-aided structural
 elucidation (CASE), 498
Computer-assisted stationary-phase
 design, 180
Computer processing of spectra
 ion chromatograms, 418–419
 library searching, 419–420
 spectrum addition and subtraction,
 417–418
Concentration-dependent detector,
 353
Concentration-sensitive detector,
 343–344

- Condensation polymers, 335
Confidence interval (CI), 516
Confiscated illicit drugs, 748–753, 749t–751t
Contact time, 109
N-containing compounds, 667
Continuous online monitoring, 285
Continuous proof testing machine, 512f
Control of devices, 505
Conventional columns analysis, 685–687
Conventional detectors for gas chromatography, 343–345, 344t
 bulk physical property detectors, 358–360
 thermal conductivity detector, 358–360
 electrochemical detectors, 366–367
 ionization-based detectors
 barrier-discharge ionization detector (BID), 357–358
 electron-capture detector (ECD), 350–354
 flame ionization detector (FID), 345–348
 helium ionization detector (HID), 356–357
 photoionization detector, 354–356
 thermionic ionization detector (TID), 348–350
 optical detectors
 atomic emission detector (AED), 365–366
 flame photometric detector (FPD), 360–363
 gas-phase chemiluminescence detector, 363–365
Conventional glasses, 100, 102
Conventional polyimide-clad fused silica, 104–105
Cooley–Tukey FFT, 380–381
Copolymers, 328–329
Corona discharge sources, 429
Costructure-directing agents (CSDA), 594
Countercurrent chromatography, 618–620
Counterfeit drugs, 753
Critical “analytical” injection, 313
Cross-linked stationary phase, 6
 Cross-sectional average, 33–34
 Crude and refined petroleum fingerprinting, 771
 Crude oils, molecular characterization of, 656
 Cryogen-free retention, 280f
 Cryogenic loop modulator, 207f
 Curie-point pyrolyzer, 329–330
 Curie-point system, 330
 Cyanoalkyl groups, 145–146
 3-Cyanopropylmethylsiloxane monomers, 174–175
 3-Cyanopropylphenylsiloxane, 174–175
 Cyclofructans (CFs), 590–591, 591f
- D**
Darcy’s law, 33–34
Data acquisition, 729
Data analysis methods, 525–546
 accuracy profiles, 559, 559f
 analyte quantification, 525–526
 calibration, 540–541
 chemometrics, 525
 experimental method optimization, 541–542
 one-dimensional (1D) gas chromatography (GC), 526
 pattern recognition, 533–540
 pixel-level data, 526–527
 precision, 554–555
 preprocessing, 527–533
 pseudointegration, 525–526
 robustness, 556–557
 sample stability, 557
 specificity, 556
 three-dimensional (3D) data, 526–527
 trueness, 555–556
Data handling, 14
“Data mining” algorithms, 315
Data preprocessing, 505, 729–731
Data pretreatment, 437, 729–731
Data processing software for GC-MS, 315–316
2D chromatogram, 211
Deans switch (DS), 200–201
 for GC X GC, 210f
Decomposition products
 characterization, 775–776
Decompression-related zone
 expansion, 51
Deconvolution, 379–380
Degree of polymerization (DP), 703
Dehydration, 109
Dendrograms, 534
Density, cohesive energy, 572
Derivatives suitable for GC/MS, 372t, 420
Derivatization, 708–713, 709t–710t
 acyl esters, 711
 alditol acetates, 712
 aldonitrile acetates, 712
 alkylation, 708
 alkylsilyl ethers, 708–711
 chiral derivatives, 713
 cyclic boronic esters, 713
 dialkylmercaptal derivatives, 712–713
 oximes, 711–712
Derivatized cyclodextrins, 587–590
 chiral stationary phases based, 587–590
 mechanism of chiral recognition, 590
 overview, 587
Derivatizing reagents, 639–640, 639f
Detection limit, 19
Detection modes, 433
Detectors, 6–7, 13–14, 476–477, 714–716
 differential mobility spectrometers (DMS), 477
 electron capture detectors (ECD), 476–477
 emission detectors, 477
 field asymmetric ion mobility spectrometers (IMS), 477
 flame ionization detector (FID), 477
 in GC X GC separations, 209
 Ion mobility spectrometers (IMS), 477
 mass spectrometer (MS), 477
 nitrogen–phosphorus detectors (NPD), 477
 photoionization detector (PID), 476
 pulsed-discharge photoionization detector (PDD), 476
 surface acoustic wave detector (SAW), 477
 thermal conductivity detector (TCD), 477
2D GC separations, graphical representation of, 193–195
Diacylglycerols (DAG), 683–684
Dialkyl phthalates, 147

- Diatomite (diatomaceous earth), 148–149
- Di-butyltin (DBT), 458
- Dichloromethane (DCM), 490–491
- Diethylene glycol succinate (DEGS), stationary phases and, 6
- Differential flow modulation, 207
- Differential mobility spectrometers (DMS), 477
- Digilab LP-GC-FTIR system, 378
- Diisocyanates, 335
- Dimensionless heating rate, 41–43
- Dimensionless plate height, 61
- 4,6-dimethyldibenzothiophene (4,6-DMDBT), 202
- Dimethylselenide (DMSe), 461
- Dinitrophenylhydrazine (DNPH) sampling, 284
- Dinitrotoluene (DNT), 766–767
- Diodearray detector (DAD), 373
- Dioxins, 769–770, 843–848, 845f
- Direct deposition (DD), 376
- Direct desorption of materials, 312–313
- Direct sampling method, 678
- Direct thermal desorption of residual volatiles, 299–301
- Discretization, errors caused by, 512–513
- Discriminant analysis, 536–538, 537f
- Dispersive liquid-liquid microextraction (DLLME), 755, 817–818
- Distance-averaged immobility, 44
- 2,6-di-*t*-butylpyridine (2,6-DtBP), 426
- 4,6-DMDBT in diesel fuel, 202
- Do-it-yourself glass capillary columns, 4
- Doping control, 757–758
- Dorris–Gray procedure, 564
- Double splitting, 273–274
- Drift tube, 429–430
- Drugs of abuse, 306–307
- 2D separation techniques, 192
- Dual-cell thermal conductivity detector, 359f
- Dual-detector designs, 360–362
- Dual-plasma burner functions, 364–365
- Dynamic coating, 113, 120
- Dynamic diffusion constant, 49
- Dynamic headspace extraction, 257
- Dynamic HS sampling, 678
- E**
- Early column developments, 3–6, 353
- Early commercial instruments, 3
- Early instrumentation, 2–3
- Effective carbon number concept, 348
- Effective diffusion coefficient, 49
- Efficiency-optimized flow (EOF), 74–75, 602–604
- Effusion or Watson–Biemann separator, 378–379, 381f
- Electric precision controllers, 481
- Electrochemical detectors, 366–367
- Electrolytic conductivity detector (ELCD), 366–367
- Electron-capture detector (ECD), 3–4, 130, 350–354, 432
- Electron capture detectors (ECD), 476–477, 812–813
- Electron-capturing compounds, 351–353
- Electronically temperature controlled (ETC), 377
- Electronic control of flows and pressures, 280–282
- Electron ionization (EI), 382–384, 389f, 802, 847–848
- cold, 384–385
- mass spectra, 416f
- Electrospray ionization (ESI), 427
- Electrospray sources, 429
- Element-selective detectors, 345, 360–362
- Elution times
- in COCI, 225
- comprehensive gas chromatography and, 205f
- immobility, 43
- inverse gas chromatography (IGC), 561–562
- order, peak spacing and reversal of, 45–48
- solute migration and, 37–45
- dimensionless heating rate and void temperature increment, 41–43
- general equations of, 38–39
- isobaric analysis, 39–40
- linear heating ramp and linear retention model, 41
- method translation and retention time locking, 40
- migration and elution parameters, 43–45
- temperatures, 43
- Emission detectors, 477
- Enantiomeric composition, 596
- Enantiomeric excess, 596
- Enantiomeric purity, 596
- Enantiomers analysis, 598–601
- Enantiomers, separation
- α -amino acid derivatives, 583–584
- chelates as chiral selectors, 584–587
- chiral covalent organic frameworks (COFs), 593
- chiral ionic liquids, 594–595
- chiral mesoporous silica, 593–594
- chiral recognition, strategy for, 596–604
- chiral stationary phases, 583–595
- complexation gas chromatography, 586f
- cyclofructans, 590–591, 591f
- derivatized cyclodextrins, 587–590
- determination of, 595–596
- direct approach, 582
- hydrogenbonding CSPs, 584, 585f
- indirect approach, 582
- MCP (4-chloro-2-methylphenoxy) propionic acid, 581
- metal–organic cages, 593
- metal–organic frameworks, 591–593, 592f
- micropreparative enantioselective gas chromatography, 604–606
- porous organic cages, 593
- recognition, 582
- total analysis system (TAS), 604
- Enantioselective gas chromatography, 602–604, 603f
- Enantioselectivity, 596–598
- Endocrine disruptor, 299
- Enhanced automation, 268
- Enhanced desorption efficiency, 269
- Environmental analysis, 768–772
- Environmental applications, 441–442
- Environment, GC for, 836
- Epoxyes, 336
- Essential functions and performance characteristics, 270–274
- automation, 273
- double splitting, 273–274
- two-stage desorption, 271–272
- Essential oils, gas chromatographic analysis of commercial libraries, 680

- Essential oils, gas chromatographic
 analysis of (*Continued*)
 definitions, 675–676
 fragrances, 675–676
 GC-MS libraries, 679–680
 GC phases, 676
 in-house libraries, 680
 qualitative and quantitative aspects,
 679
 retention index, 679
 separation criteria, 676–679
 chiral columns, 676
 closed-loop stripping method, 678
 direct sampling method, 678
 dynamic HS sampling, 678
 gas chromatography–mass
 spectrometry (GC-MS), 678–679
 headspace techniques, 677–678
 multidimensional techniques,
 676–677
 preparative gas chromatography,
 678
 solid-phase microextraction
 (SPME), 678
 vacuum HS sampling technique,
 678
 specific libraries, 680
 Ethyl chloroformate (ECF), 735–736
 European Medicines Agency (EMA),
 548
 Experimental method optimization,
 541–542
 Explosives, 442, 761–764, 762t
 shotgun propellant residues, 307
 Exponential peaks, 48
 Extended temperature range, 31
 External standard calculations,
 519–520, 519f
 Extraction phase, 633–634
- F**
 Far-UV detector (FUVD), 373
 Fast Fourier transform (FFT), 380
 algorithm, 372–373
 Fast gas chromatography, for
 environment, 836
 Fatty acid analysis, 684–690
 Fatty acid methyl esters (FAMES),
 683–685
 Fentanyl, 755
 Field and portable instruments
 column configurations, 474–476, 475f
 isothermal operation, 475
 isothermal packed columns, 475
 multiple columns with flow
 modulation, 476
 multiple columns with multiport
 valves, 475–476, 476f
 temperature programming, 475
 commercial portable GCs, 482
 design challenges, 472, 472f
 detectors, 476–477
 differential mobility spectrometers
 (DMS), 477
 electron capture detectors (ECD),
 476–477
 emission detectors, 477
 field asymmetric ion mobility
 spectrometers (IMS), 477
 flame ionization detector
 (FID), 477
 Ion mobility spectrometers
 (IMS), 477
 mass spectrometer (MS), 477
 nitrogen–phosphorus detectors
 (NPD), 477
 photoionization detector (PID),
 476
 pulsed-discharge photoionization
 detector (PDD), 476
 surface acoustic wave detector
 (SAW), 477
 thermal conductivity detector
 (TCD), 477
 future trends, 482–485
 gas supply, 477–478
 history of, 469–470, 470f–471f
 multiport valves, column switching
 with, 473–474, 473f
 power management,
 478–481
 column power (isothermal),
 478–479, 478f–479f
 column power (programmed),
 480, 482f
 electric precision controllers, 481
 pumps—pressure or vacuum, 481
 prototyping, 481–482, 483f–484f
 sample introduction, 472–474
 six-port valve, 474f
 Field asymmetric ion mobility
 spectrometers (IMS), 477
 Field ionization, 394, 408f
 Field-portable gas chromatograph,
 776–777
 Field-portable GC instrumentation, 887
 Fire debris, 760–761
 accelerants in, 306
 First responders, 299
 Fixed pressure, 81–82
 Flame ionization, 345–346, 346t, 347f
 Flame ionization detection (FID),
 3–4, 345–348, 349t, 373, 432,
 477, 683, 812–813, 891–892
 Flame photometric detector (FPD),
 360–363
 Flame sealing, 109
 Flash vaporization injector, 230f
 for gasoline, 231f
 with rubber septum, 3
 sample introduction and, 229–231
 “Floating-point operations”, 381–382
 Flory–Huggins equation, 570
 Flory–Huggins interaction
 parameter, 569
 Flow and split ratio selection,
 310–311
 Flow transducer, 222
 Fluorine-containing compounds,
 639–640
 Fluorocarbon powders, 149
 Food. *See also* Baby food
 forensic science, 777–778
 GC for, 793–806
 MRMs, 799
 pesticides in, 793–806
 Food analysis, 439–441
 Food and Drug Administration
 (FDA), 548
 Forensic applications
 accelerants in fire debris, 306
 drugs of abuse, 306–307
 explosives and shotgun propellant
 residues, 307
 forensic (characterization) of
 inks, paper, and other materials,
 308–309
 monitoring manufacturing and other
 industrial chemical processes,
 309
 Forensic (characterization) of
 inks, paper, and other
 materials, 308–309
 Forensic science
 bulk drug analysis, 747–753
 chemical warfare agents (CWAS),
 778–779
 decomposition products
 characterization, 775–776

- dioxins, 769–770
doping control, 757–758
environmental analysis, 768–772
explosives, 761–764, 762t
facilitate crime, 759–760
field-portable gas chromatograph, 776–777
fire debris, 760–761
food, 777–778
furans, 769–770
gas chromatography (GC), 753–760
 new developments in, 779–780
human decomposition products, 774–776
human odor profile, 772–774, 773f
organic gunshot residues (OGSRS), 764–767, 765t–766t
pesticides analysis, 769
polychlorinated biphenyls analysis, 769
postmortem interval (PMI), 774–775
recreational drugs, 759–760
toxicology
 death, 753–756
 human performance, 756–757
 trace evidence, 767–768, 768f
 workplace drug testing, 758–759
Formaldehyde, 284–285
Forward pressure regulator, 222
 in split injection, 236
Fourier transform ion cyclotron resonance (FT-ICR) mass spectrometers, 411
Fourier transform infrared spectroscopy (FIR), 372–374, 376–377, 379, 390, 394
 gas chromatography, 373–382
Free fatty acids (FFA), 683–684, 690–691
Free radical generation, 327f
Freeze concentration, 617–618
Freeze-drying, 617–618
Fuller–Giddings empirical expression, 32
Full width at half maxima (FWHM), 378
“Functional group regional reconstruction”, 380–381
Functional group selective reagents, 647–648
Functionalized polysiloxanes, 111–112
Fused-silica capillary material, 100
Fused-silica capillary tubing, 103, 107–108
Fused-silica columns, 7–9, 108, 127
 drawing process for, 100
 preforms for, 100–101
 tensile strength of, 8
 wide-bore, 12
Fused-silica drawing process, 100
Fused-silica draw tower
 configuration, 104f
Fused-silica tubing, 123–124
- G**
G agents, 888
“G-analogue”, 299
Gas chromatography (GC), 19–20, 99, 142–143, 157–158, 191–193, 385, 425, 505, 683
 backflushing 2D GC, 195–200
 analysis of oxygenates in gasoline, 197–200
 basic mode of operation, 195–197
 complex samples by, 598–601
 comprehensive, 14–15
 detectors, 343
 2D GC
 basic mode of operation, 203–206
 detection and quantitation in GC 3
 GC separations, 209
 GC x GC modulators, 206–209
 drift tube, 434, 434f
 early column developments, 3–6
 early instrumentation, 2–3
 for environment, 835–864
 expertise decline for, 15–16
 flow of ideal gas in open tubes, 33–37
 food, 793–806
 forensic science, 753–760
 fused-silica column, 7–9
 GC-DMS, 434
 GC-FAIMS coupling, 434
 general definitions and conventions, 23
 glass capillary columns, 6–7
 graphical representation of 2D GC separations, 193–195
 heartcutting 2D GC, 200–203
 basic mode of operation, 200–202
 4,6-DMDBT in diesel fuel, 202
 multiple heartcuts and independent column heating, 202–203
 Hindelang conferences, 7–9
 instrumentation, sophistication of
 column heating, 9–11
 comprehensive gas chromatography, 14–15
 data handling, 14
 detectors, 13–14
 instruments, 434–435
 invention of, 1–2
 mass spectrometry, 598–601
 nomenclature and other conventions, 20–22
 abbreviations, 20–21
 subscripts, 21
 symbols, 21–22
 optimization
 detection limit and trade-off triangle, 89–92
 optimal flow rate, 74–84
 optimal heating rate, 84–89
 targets of column optimization, 73–74
 peak spacing and reversal of elution order, 45–48
 peak width
 in nonuniform dynamic chromatography, 50–67
 plate height in uniform static chromatography, 48–50
 performance metrics
 benchmarks, 71–73
 metrics, 67–71
 pesticides in, 793–806
 plasma-based detectors for, 449–467
 properties of ideal gas
 solute diffusivity in gas, 31–33
 theoretical relations, 29–30
 viscosity, 30–31
 reactant ion peak (RIP), 435f
 sample introduction for, 232–235
 choosing, 218
 solid-phase microextraction (SPME), 434
 solute–column interaction
 characteristic parameters of, 24–29
 relations between characteristic parameters, 29
 solute distribution between mobile and stationary phases, 23–24
 solute migration and elution, 37–45

- Gas chromatography (GC) (*Continued*)
dimensionless heating rate and void temperature increment, 41–43
general equations of, 38–39
isobaric analysis, 39–40
linear heating ramp and linear retention model, 41
method translation and retention time locking, 40
migration and elution parameters, 43–45
TD for, 267–270
validation for, 547–560
accuracy profiles, 559
characteristics and guidelines for, 549t
linearity, 550–553
method items for, 548–557
regulatory aspects, 548
steps, 548f
- Gas chromatography Fourier transform infrared spectroscopy (GC-FTIR), 373–382, 390, 391t–393t, 394
data analysis and interpretation, 379–380
data treatment, 380–382
instrumentation, 374–377
library search methods, 379
performance characteristics, 378–379
- Gas chromatography–mass spectrometry (GC-MS), 123, 678–679
- Gas chromatography vacuum ultraviolet spectroscopy (GC-VUV), 382–390, 391t–393t, 394
data analysis and interpretation, 385
data treatment, 385–390
instrumentation, 382–384
performance characteristics, 384–385
- Gas chromatography with glow discharge (GC-GD), 450–451
- Gas chromatography with glow discharge and atomic emission spectroscopy (GC-GD-AES), 454–457
- Gas chromatography with glow discharge and mass spectrometry (GC-GD-MS), 454–457
- Gas chromatography with inductively coupled plasma (GC-ICP), 450–451
- Gas chromatography with inductively coupled plasma mass spectrometry (GC-ICPMS), 449–451
advances in applications for, 457–462
for air, 459–460
biological applications for, 460–462
for body fluids, 460–461
elements analyzed by, 454, 455t
interface between, 453–454, 453f
for microbes, 460
for plants, 460
samples for, 457
for urine, 461
- Gas chromatography with mass spectrometry (GC-MS), 13–14
baby food, 803
juice, 799–801
MRMs, 794
wine, 801
- Gas chromatography with microwave-induced plasma (GC-MIP), 449–451
- Gas chromatography with microwave-induced plasma and atomic emission spectroscopy (GC-MIP-AES), 454
elements analyzed by, 456t
- Gas discharge detector, 356
- Gas-liquid chromatography (GLC), 24, 142–158, 166–167
- Gas-liquid partition coefficient, 168
- Gas-liquid partition constant, 154
- Gasoline, 665
aromatic composition of, GC X GC for, 209–211
flash vaporization injector for, 231f
hydrocarbons, 197–198
oxygenates in, 2D GC backflushing for, 197–200
- Gas-phase chemiluminescence detector, 363–365
- Gas-phase diffusion coefficients, 166–167
- Gas-phase extraction, 626–627
- Gas sampling valve (GSV)
PLOT and, 247
sample introduction and, 246–247
- Gas–solid chromatography, 141, 157–158, 160
carbon adsorbents, 159
inorganic oxides, 158–159
molecular sieves, 159–160
porous organic polymers, 160
- Gas–solid Inverse gas chromatography (IGC), 562–569
- Gas supply, field and portable instruments, 477–478
- Gaussian functions, 387–388, 513
- Gaussian model, 156t
- Gaussian peaks, 48
- GC 3 GC application, 209–211
- GC-GD-AES. *See* Gas chromatography with glow discharge and atomic emission spectroscopy (GC-GD-AES)
- GC-MS, advanced data mining and data processing software for, 315–316
- GC x GC modulators, 206–209
- Gel permeation chromatography (GPC)
oils, 802
- Generalized rank annihilation method (GRAM), 538–539
- General separation performance, 73
- Generic characteristic thermal constant, 29
- Generic temperature program, 88–89
- Gibbs free energy, 24
- Giddings compressibility factor, 51, 55
- Giddings equation, 55
- Glass capillary columns, 6–7
- Glass conical vials, 420
- Glow discharge (GD), 449–450
GC-GD, 450–451
GC-GD-AES, 454–457
GC-GD-MS, 454–457
- Glow dischargeatomic emission spectrometry (GD-AES), 450
- “Glue” trapping particles, 118
- Gold-coated LP interfaces, 374–375
- Good Agricultural Practices (GAP), 793
- Gram–Schmidt Orthogonalization (GSO) technique, 372–373
algorithm, 381–382
- Graphitized carbon, 159

- Gravity, 655–656
Greatly enhanced sensitivity, 268–269
“Greenhouse gases”, 282–284
Grob mix, 114
Grob test mixture compounds, 114t
Gunshot residue (GSR), 764
Gutmann’s model, 566–567
- H**
Habgood–Harris definition, 61–62
Halás–Hartmann–Heine compressibility factor, 36–37
Halide anions, 147
Haloalkylacyl reagents, 644–645
Halogenated flame retardants, 851, 853–859, 854t–858t
Hansen’s solubility parameters (HSPs), 572
Headspace extraction
 dynamic, 257
 MHE, 255
 sample-loop system in, 260
 SHE, 253–255
 partition coefficient and, 254–255
 phase ratio and, 254
 sample-loop system in, 260
 sensitivity with, 254
 transfer-line-based systems and, 259–260
Headspace-gas chromatography (HS-GC), 251–253
 fundamentals of, 253–257
 history of, 252
 instrumentation and practice for, 257–262
 method development for, 262–264
 sample solvent and, 263–264
 sample volume and, 263
 syringes for, 258–259
 vial temperature and, 263
Headspace (HS) GC-VUV, 393
Headspace sampling (HS), 604
Headspace single-drop microextraction (HS-SDME), 257
Headspace techniques, 677–678
Heartcutting
 2D GC, 200–203
 basic mode of operation, 200–202
 4,6-DMDBT in diesel fuel, 202
 multiple heartcuts and independent column heating, 202–203
 Heated filament pyrolyzers, 330
 Heated uniformly, 39
 Heated valve technology for thermal desorption, 277
 Height of equivalent theoretical plate (HETP), 50
 Helium (He), 450
 MIP and, 450
 Helium ionization detector (HID), 356–357
 Hierarchical cluster analysis, 178–180
 Hierarchical cluster analysis (HCA), 534, 535f
 High-boiling semivolatiles, recovery of, 276
 Higher-molecular-weight compounds, 159
 Highly fluorinated liquids, 145
 High-molecular-weight hydrocarbons, 143–145
 High-performance liquid chromatography (HPLC), 384, 494–498
 High-purity hydrogen, 351–353
 High-resolution mass spectrometers (HRMS), 846–847
 High-resolution techniques, 703
 Hindelang conferences, 7–9
 Horning’s system, 385
 Hot on-column injection, 243–244
 Humidity, Inverse gas chromatography (IGC), 564–566, 565f
 Hybrid methods, 186
 Hybrid powdercoats, 336
 Hydride generation (HG)-ICPMS, 458
 Hydride ion extraction, 405
 Hydrocarbon chromatographic profile, 661
 Hydrocarbon impurities, 124
 Hydrocarbon stationary phases, 143–145
 Hydrochloric acid (HCl), 684
 Hydrogen–air diffusion flames, 347, 360
 Hydrogen-bond basicity, 147
 Hydrogen-rich plasma, 349–350
 Hydrolysis, 719
- I**
Ideal basic separation, 65
Ideal gas
 in open tubes, 33–37
 solute diffusivity in gas, 31–33
 theoretical relations, 29–30
 viscosity, 30–31
Ideal thermodynamic equilibrium model, 24
Ideal thermodynamic model, 25–26, 44–45
Immobilized stationary phases, 6
Incorrect plate height equation, 65–67
Incremental separation capacity, 69
Independent column heating, 2D GC and, 202–203
Independent of pressure, 30–31
Indoor and in-vehicle air, 295–299
Inductively coupled plasma (ICP), 449–450
 AES and, 449–450
 GC-ICP, 450–451
Inductively coupled plasma mass spectrometry (ICPMS), 449–450
 advantages and limitations of, 452–453
 GC-ICPMS, 450–454
 advances in applications for, 457–462
 for air, 459–460
 biological applications for, 460–462
 as detector between, 454, 455t
 elements analyzed by, 454, 455t
 for microbes, 460
 for plants, 460
 samples for, 457
 for urine, 461
 HG, 458
 HPLC and, 454
 interface between, 453–454, 453f
 schematic of, 452f
Industrial chemical processes, 309
Industrial (fugitive) emissions, 293–294
Industrial (occupational) hygiene, 291
Inertness, 276
In-house libraries, 680
Injection-port derivatization, 639
“Injection”/transfer volumes, 271
Injectors, 219t
 glass capillary columns, 6–7
 PTV, 12

- Injectors (*Continued*)
in transfer-line-based systems and,
259–260
- Inorganic oxides, 158–159
- Inorganic salts, 135, 158–159
- Instrumentation, pyrolysis-gas
chromatography
programmed pyrolysis, 330
pulse pyrolysis, 329–330
- Instrumentation, sophistication of
column heating, 9–11
comprehensive gas chromatography,
14–15
data handling, 14
detectors, 13–14
- Intercorrelation, 568
- Interfacial adsorption, 154–155
- Intermediate film thickness, 55–56
- Internal standard (IS), 276, 550
- Internal standard calculations,
520–521
relative calibration, 521
relative concentration, 520–521
- International Conference on
Harmonisation of Technical
Requirements for the
Registration of
Pharmaceuticals for Human
Use (ICH), 548
- International Organization for
Standardization (ISO), 548
- International Union of Pure and
Applied Chemistry (IUPAC),
548
- Intuitive plate number, 53
- Inverse fast Fourier transform (IFFT)
function, 529–531
- Inverse gas chromatography (IGC),
561–579
gas–solid, 562–569
humidity, 564–566, 565f
nonspecific interactions, 562–564
polymer bulk properties and,
569–573
polymers blends, 569–573
solubility parameter, 572–573
specific surface properties, 566–569
- Ion chromatograms, 418–419
- Ionic liquids (ILs), 147, 175–176, 178,
594
- Ionization-based detectors
barrier-discharge ionization detector
(BID), 357–358
electron-capture detector (ECD),
350–354
flame ionization detector (FID),
345–348
helium ionization detector (HID),
356–357
photoionization detector, 354–356
thermionic ionization detector (TID),
348–350
- Ionization process, 348
- Ionization sources, 427–429
- Ionization techniques
atmospheric pressure chemical
ionization (APCI), 390–393
chemical ionization (CI), 385
cold EI, 384–385
electron ionization (EI), 382–384
field ionization, 394
photoionization, 408
- Ion mobility spectrometers (IMS), 477
applications, 439–442
clinical applications, 441
collision cross section (CCS), 427
data pretreatment, 437
detection modes, 433
detector, 430
device components, 427–430, 428f
corona discharge sources, 429
electrospray ionization (ESI), 427
electrospray sources, 429
ionization sources, 427–429
other ionization sources, 429
photoionization sources, 428–429
radioisotope sources, 427–428
2,6-di-*t*-butylpyridine (2,6-DtBP),
426
DMS/FAIMS, 431–432, 431f
drift tube, 429–430
electron-capture detector (ECD), 432
environmental applications,
441–442
explosives, 442
flame ionization detector (FID), 432
food analysis, 439–441
gas chromatography (GC), 425
columns, 433
coupled to, 433–434
drift tube, 434, 434f
GC-DMS, 434
GC-DMS coupling, 434
GC-FAIMS coupling, 434
instruments, 434–435
reactant ion peak (RIP), 435f
solid-phase microextraction
(SPME), 434
- GC-IMS analysis
advantages, 438–439
disadvantages, 439
isothermal separations, 433
limitations of, 432
mass spectrometry (MS), 425
multicapillary columns
(MCC), 433
operation, 426–427
partial least squares discriminant
analysis (PLS-DA), 438
statistical analysis, 437–438
supervised multivariate analysis, 438
treatment, 435–438, 437f
types of, 430–432
unsupervised analysis, exploratory
analysis by, 437–438
validation and interpretation, 438
- Isobaric analysis, 39–40
- Isophorone diisocyanate, 335
- Isothermal GC, 20
- Isothermal separations, 433
- Isotope ratio mass spectrometry
(IRMS), 601–602
- J**
- James–Martin compressibility factor,
35, 562
- Jet molecular separator, 374–377,
375f
- Juice, 799–801
- J&W Scientific, founding of, 5–6
- K**
- Kovats retention indices, 191–192
- Kyoto Encyclopedia of Genes and
Genomes (KEGG), 733
- L**
- Large-scale preparative GC, 488
- Large-volume injection (LVI), 757
with PTV, 244–245
- Laser ablation (LA), 451
- Laser radiation source, 373–374
- Leaching, 108–109
- Least-squares regression, 552
- Least-squares smoothing, 514
- Lewis acid–base interactions,
566–567
- Lewisite, 889
- Library-search methods, 379,
419–420

- Lifshitz–van der Waals component, 563
- Light pipe (LP) interface, 372–373
- Lignin, 336–337
- Limit of detection (LOD), 553–554, 795
for juices, 799
for SDME, 458
- Limit of quantification (LOQ), 553–554
- Linear discriminant analysis (LDA), 537–538
- Linear dynamic range, 91
- Linear heating ramp, 41
- Linear ion traps, 411
- Linearity
assessment of linearity, 552–553, 552t
classic calibration, 550–551
standard addition, 551, 551f
- Linear model has chromatographic justification, 26
- Linear quadrupole filter, 409–410, 410f
- Linear retention index (LRI), 185
- Linear retention model, 26–27, 41
- Liners
in liquid injectors, 220–221
in split injection, 235–236
in splitless injection, 239
- Lipids
acylglycerols, 690–691
conventional columns analysis, 685–687
diacylglycerols (DAG), 683–684
fast and ultrafast analysis, 689–690
fatty acid analysis, 684–690
fatty acid methyl esters (FAMES), 683–685
flame ionization detector (FID), 683
free fatty acids (FFA), 683–684, 690–691
gas chromatography (GC), 683
hydrochloric acid (HCl), 684
mass spectrometry (MS), 683–684
monoacylglycerols (MAG), 683–684
positional isomers, high-resolution analysis of, 688–689
stanyl esters, 691–693
sterol esters, 691–693
sterols, 691–693
steryl glycosides, 691–693
thin-layer chromatography (TLC), 685
triacylglycerols (TAG), 683–684
waxes analysis, 693
- Lipsky–Horvath separator, 373–374, 379–380, 383f
- Liquid chromatography (LC), 505, 661–663
- Liquid chromatography with mass spectrometry (LC-MS)
for baby food, 802–803
- Liquid-crystal stationary phases, 147
- Liquid injectors, 218
autosampler, 221
liners in, 220–221
pneumatic systems, 221–222
septa in, 221
syringes in, 218–220
- Liquid-liquid partitioning, 794
- Liquid N₂-cooled MCT detector response, 377
- Liquid-phase columns, 119–120
- Liquid-phase microextraction, 622–623
- Liquid samples, 735–737
applications, 736–737
ethyl chloroformate (ECF), 735–736
sample preparation, 735–736
- Liquid sampling valve (LSV), 248f
sample introduction and, 247
- Liquid–solid extraction, 623–626
matrix solid-phase dispersion, 626
pressurized fluid extraction, 625–626
traditional methods, 624
ultrasound- and microwave-assisted extraction, 624–625
- Liquid stationary phases, 122
- Longitudinal velocity, 33
- Low-duty-cycle modulators, 206
- Lower cost per analysis, 269
- Lower-energy ionization, 314–315
- Lower limit of quantification (LLOQ), 553–554
- Low-molecular-weight carbohydrates, 716–719
- Low quantitative precision, 206
- Low spatial frequency–baseline features, 381–382
- LP-GC-FTIR, 390
- M**
- Magnetic sector instruments, 409, 847–848
- Mars exploration, 869–871, 869f–870f
- MASE, for juices, 799
- Mass and their uses, definitions of, 417
- Mass flow controller, 222
- Mass-sensitive detectors, 343–344
- Mass spectra, 719
- Mass spectrometer (MS), 477
- Mass spectrometric detection, 892–895
- Mass spectrometric detectors, 314
- Mass spectrometric detectors for gas chromatography, 371–372
data analysis
computer processing of spectra, 417–420
definitions of mass and their uses, 417
interfaces, 372–373
Effusion or Watson–Biemann separator, 378–379, 381f
jet molecular separator, 374–377, 375f
Lipsky–Horvath separator, 379–380, 383f
membrane separator, 380–382, 386f
open split interface, 373–382
ionization techniques
atmospheric pressure chemical ionization (APCI), 390–393
chemical ionization (CI), 385
cold EI, 384–385
electron ionization (EI), 382–384
field ionization, 394
photoionization, 408
methods of
Fourier transform ion cyclotron resonance (FT-ICR) mass spectrometers, 411
magnetic sector instruments, 409
orbitrap mass spectrometers, 412
quadrupole (Q) mass filters, 409–411
tandem mass spectrometers, 413–414
time-of-flight (TOF) mass spectrometers, 412–413, 412f
modes of operation
full scan spectra, 414
selected ion monitoring (SIM), 414–417
sample preparation, 420

- Mass spectrometry (MS), 209, 425, 683–684
GC-MS, 13–14
GD and, 450–451
wine, 801
- Mathematical hyperbola, 66
- Matrix-induced response enhancement, 551
- Matrix solid-phase dispersion, 626
- Matrix solid-phase dispersion (MSPD), 794
for baby food, 803
for MRMs, 794
- Maximum allowable operating temperature (MAOT), 657, 660
- McLafferty rearrangement, 377
- MCCP (4-chloro-2-methylphenoxy) propionic acid, 581
- Mean squares (MS), 552
- Membrane extraction, 635, 817–818
- Membrane separator, 380–382, 386f
- Mercury
in body fluids, 460–461
contamination, 458
food, 461–462
urine, 461
in water, 457–459
- Metabolomics
analytical tools, 728
biomarker identification, 733
chemometric data analysis, 731–732
data acquisition, 729
data preprocessing, 729–731
data pretreatment, 729–731
future directions, 737
GC-MS-based metabolomics, 728–733
GC-MS conditions, 729
GC-MS technologies, 728–729
Kyoto Encyclopedia of Genes and Genomes (KEGG), 733
liquid samples, 735–737
applications, 736–737
ethyl chloroformate (ECF), 735–736
sample preparation, 735–736
metabonomic workflow, 729–733
model validation, 732–733
non-hypothesis-driven global metabolic profiling strategy, 727
overview, 727
pathway mapping, 733
solid samples
applications, 734
sample preparation, 733–734
- Metabonomics, workflow, 729–733
- Metal–organic cages, 593
- Metal–organic frameworks, 591–593, 592f
- Metal–organic polygons or polyhedra (MOPs), 593
- Methacrylate polymers, 326–327
- Methamphetamine (MA), 752
- Methane monitoring, 288
- Methaqualone (MTQ), 752–753
- Method translation software, 184–185
- Methoxyamine hydrochloride (MOX), 733–734
- Methylation analysis, 719–720
- 3,4-Methylenedioxymethamphetamine, 550
- Methylmercury, 458
- Michelson interferometer, 376–377
- Microbes, GC-ICPMS for, 460
- Microfurnace pyrolyzers, 329–330
- Micropreparative enantioselective gas chromatography, 604–606
- Microwave-assisted extraction (MAE), 624–625, 795
for MRMs, 795
- Microwave-induced helium plasmas, 360
- Microwave-induced plasma (MIP), 449–450, 456f
GC-MIP, 450–451
- Migration and elution parameters, 43–45
- Mills method, 794
- MINICAMS, 884–885
- Minimal detectable amount (MDA), 90
- Minimal detectable concentration (MDC), 90
- Minimum detectable amount (MDA), 89
- MIP-AES, GC-MIP-AES, 454
elements analyzed by, 456f
- MIP-AES/MS, 450
- Mixed retention mechanisms, 183
- Mobile and stationary phases, 23–24
- Mobile-phase velocity, 156–158
- Modern commercial columns, 112
- Modern data systems, 345
- Modes of operation
full scan spectra, 414
selected ion monitoring (SIM), 414–417
- Modulators
for GC X GC, 206–209
low-duty-cycle, 206
thermal, 207
- Molar cohesive energy, 572
- Molar gas constant, 24
- Molecular characterization, 656
- Molecular diffusion volume, 32
- Molecular polarizability, 567
- Molecular sieve–coated PLOT column, 130f
- Molecular sieves, 127–130, 159–160
- Molecular spectroscopic detectors for gas chromatography, 371–372
comparison of techniques, applications, 390–393
gas chromatography Fourier transform infrared spectroscopy (GC-FTIR), 373–382
data analysis and interpretation, 379–380
data treatment, 380–382
instrumentation, 374–377
performance characteristics, 378–379
gas chromatography vacuum ultraviolet spectroscopy (GC-VUV), 382–390
data analysis and interpretation, 385
data treatment, 385–390
instrumentation, 382–384
performance characteristics, 384–385
milestones, 372–373
- Molecular spectroscopy detection, 371–372
- Molecular theory
pyrolysis-gas chromatography bond dissociation and free radicals, 326
copolymers, 328–329
no oligomers, 328
oligomer formation, 326–328
- Monoacylglycerols (MAG), 683–684
- “Monoisotopic” masses, 417
- MS detection, innovations in, 314–315
- Multipillar columns (MCC), 433

- Multidimensional chromatography (MDC), 489–490
- Multidimensional gas chromatography (MDGC), 191–193, 489–490, 490f, 500–501, 501f, 598, 636–638, 637t
- Multidimensional techniques, 676–677
- Multimodal gas chromatography, 636–638
- Multiple headspace extraction (MHE), 255
sample-loop system in, 260
- Multiple heartcuts, 202–203
- Multiple injections with pre-collection, GC column, 502
- Multiple ion chromatograms, 419
- Multiple ion monitoring, 415–416
- Multiple linear regression analysis, 169
- Multiple reaction monitoring (MRM), 416–417
- Multiple smoothing, 515
- Multiport valves, column switching with, 473–474, 473f
- Multiresidue methods (MRMs), 793–806
animal origin products, 798–799
baby food, 802–804
pesticides, 794–798, 796t–797t
processed food, 799–802
- Multivariate curve resolution (MCR), 538–539
- N**
- N-alkane reference compounds, 185
- Nanocrystalline cellulose (NCC), 593–594
- Naphthenes, 128–129
- Narrow-bore columns, 207
- Narrow peaks, 513
- National Institute of Standards and Technology (NIST), 539–540
- Natural products, 494–498
- Near-real time monitoring technologies, 291
- Needle valve, 222
- Negative chemical ionization (NCI), 795, 847–848
- Negative ion CI, 390–393
- Nernst Glower source, 377
- Nerve agents, 877–879, 879f
- Net velocity, 23
- New GC-related technology developments, 314–316
- New-generation alumina columns, 124
- Nicotine, 754
- Nitrogen-containing compounds, 364–365, 667
- Nitrogen–phosphorous detectors (NPDs), 477, 812–813
- Nitrous oxide/stack injection, 129–130
- Noise reduction, 529–531, 530f
- Nomenclature and other conventions, 20–22
abbreviations, 20–21
subscripts, 21
symbols, 21–22
- Nonfiber formats, 634–635
- Nonnegative matrix factorization (NMF), 390
- Nonoptimized flame conditions, 362
- Nonpolar polysiloxanes, 111
- Nonpolar stationary phases, 182–183
- Non-radioisotope-based detectors, 351
- Nontargeted algorithms, 539–540
- Nontube-form sorptive samplers, 312
- Nonuniform dynamic chromatography, peak width in, 50–67
- Nonuniform static chromatography
plate height and plate number in, 52–55
plate height in, 55–61
- Nonuniform static medium, 53
- Nonvaporizing injectors, 218
- Nonvolatiles, 288
- Nonylphenol (NP), 498
- Normalization, 531–532
- Normal-phase liquid chromatography (NPLC), 499
- Nuclear magnetic resonance (NMR) spectroscopy, 728
- Nucleophilic displacement reactions, 147
- Nylons, 335
- O**
- Occupational exposure limits (OELs), 291
- Odor/fragrance profiling and VOC “fingerprinting”, 301–303
- Off-line sampling options, 291
- Off-line thermal desorption technology, 299
- Oil, 802
- Oleoresin capsicum (OC), 764
- Oligomer formation, 326–328
- Oligomers, 327–328
- Oligosaccharides, 719–720
- One-dimensional (1D) gas chromatography (GC), 526
- “One-shot” limitation of TD, 270
- One-variable-at-a-time (OVAT) approach, 557
- On-fiber derivatization, 816
- Online air/gas monitoring, 282–284
- Open split interface, 373–382
- Open-tubular columns (OTC), 23, 141–142, 166t
- Optical detectors, 362, 363t
atomic emission detector (AED), 365–366
flame photometric detector (FPD), 360–363
gas-phase chemiluminescence detector, 363–365
- Optimal dimensionless plate height, 76
- Optimal flow rate, 74–84
column diameter and pressure, 82–83
fixed pressure, 81–82
practical recommendations, 78–79
strong gas decompression, 75–78
weak gas decompression, 79–81
- Optimal length, 76
- Optimization
detection limit and trade-off triangle, 89–92
focusing trap, 276–277
optimal flow rate, 74–84
column diameter and pressure, 82–83
fixed pressure, 81–82
practical recommendations, 78–79
strong gas decompression, 75–78
weak gas decompression, 79–81
optimal heating rate, 84–89
targets of column optimization, 73–74
- Optimum mobile-phase velocity, 166–167
- Orbitrap mass spectrometers, 412, 412f
- Organic compounds, 288, 348

- Organic compounds (*Continued*)
isolation, 619t
- Organic gunshot residues (OGSRS),
764–767
- Organochlorine pesticides, 848–851,
850t
- Organophosphorus insecticides, 755
- Organotins, 458
- Orthogonality, 180–181, 181t
- Orthogonal signal correction (OSC),
537–538
- Overlapped peaks handling, 518
- Overloaded peaks, 223
- Oxygenates, in gasoline, 198f
- Oxygen-selective columns, 135
- P**
- Packed-column gas chromatography,
143–146, 143t–144t,
153–154, 160t
- Packed columns, 3, 141–142
band-broadening mechanisms,
155–158
classification of stationary phases,
151–153
coating and packing techniques,
149–150
frequently used stationary phases,
142–148
gas–liquid chromatography,
142–158
gas–solid chromatography
carbon adsorbents, 159
inorganic oxides, 158–159
molecular sieves, 159–160
porous organic polymers, 160
GC-MS and, 13–14
for preparative-scale gas
chromatography, 150–151
retention models, 153–155
stationary phases, 145t–146t
supports, 148–149, 148t
- Paraffins, 128–129
- Parallel factor analysis (PARAFAC),
539
- Partial least squares discriminant
analysis (PLS-DA), 438,
536–537, 731–732
- Partial least squares (PLS) regression,
540
- Partition coefficient, SHE and, 254–255
- Patent enforcement, 4
- Pattern recognition, 533–540
- automated mass spectral purification
and identification system
(AMDIS), 539–540
discriminant analysis, 536–538, 537f
generalized rank annihilation
method (GRAM), 538–539
hierarchical cluster analysis (HCA),
534, 535f
linear discriminant analysis (LDA),
537–538
multivariate curve resolution (MCR),
538–539
nontargeted algorithms,
539–540
orthogonal signal correction (OSC),
537–538
parallel factor analysis (PARAFAC),
539
principal component analysis (PCA),
534–536, 536f
resolution methods, 538–540
singular value decomposition (SVD),
538–539
trilinear decomposition (TLD), 539
- Paul-type quadrupole ion trap, 410f
- Peak area, MHE and, 255
- Peak formation factor, 62
- Peak identification, 517–518
- Peak parameters, 505
- Peak purity, 511
- Peak search
convolution, 509
integration, 508
moving weighted average, 509
peak parameters, 509–511
peak shape, 509
statistical moments, 508
- Peak width
in nonuniform dynamic
chromatography, 50–67
plate height in uniform static
chromatography, 48–50
- PEEK jacketed material (PEEKsil),
106–107
- Perfluorinated compounds
(PFCs), 859
- Performance metrics
benchmarks, 71–73
metrics, 67–71
- Perimeter monitoring, 293–294
- PerkinElmer ATD 50 unit, 272
- Permanent gases/carbon monoxide,
127–128
- Pesticides
for baby food, 802–803
in food, 793–806
GC for, 793–806
MRMs, 793–806
- Petrochemical applications
crude oils, molecular
characterization of, 656
gravity, 655–656
hydrocarbon chromatographic
profile, 661
hydrocarbons, 655
instrumental analyses, 656
maximum allowable operating
temperature (MAOT), 657, 660
molecular characterization, 656
molecular stable isotopic analyses,
663
multidimensional gas
chromatography (MDGC),
656–657
organic geochemical analyses,
660–663
porous-layer open tubular (PLOT),
659, 659t
preliminary liquid chromatography
(LC), 661–663
refinery oil assays, 663–669
heavy distillates analysis,
667–669, 668f
light distillates analysis, 664–666,
665f
middle distillates analysis,
666–667
simulated distillation (SimDist),
663–664, 664f
thermal conductivity detection
(TCD), 665
vacuum ultraviolet detection
(VUV), 665
sample volatility, column selection
to, 659–660
stable carbon isotope composition,
663
stationary phase (SP), 656–657
total acidity number (TAN), 655–656
wall-coated open tubular columns
(WCOT), 659–660
- Petroleum studies, 500
- p*-Fluorofentanyl (pFF), 753
- Pharmaceutical samples, impurities
in, 498, 499f
- Phase ratio, SHE and, 254

- Phencyclidine (PCP), 752
Pheromones, 494–498
Phosphorus detectors, 892
Photoionization, 408
 detection, 355t
Photoionization detector (PID),
 354–356, 476
Photoionization sources, 428–429
Pinpoint deactivation, 110
Pixel-level data, 526–527
Plackett–Burman (PB) design, 557
Plasma-based detectors, for GC,
 449–467, 451f
“Plate number”, 54
PLOT, GSV and, 247
Plunger in barrel syringe, 218
Plunger in needle syringe, 218
Pneumatic systems
 in split injection, 236–237
 in splitless injection, 239
Polar nonionic stationary phases, 178
Polar porous polymer U-type
 column, 134
Polar stationary phases, 183, 200
Poly(2-hydroxyethyl methacrylate)
 (PHEMA), 566
Poly(dimethyldiphenylsiloxane), 173t
Poly(dimethylsiloxanes), 145–146
Poly(ethylene glycols), 147
Poly(ethylene glycols) (PEG),
 170–172
Poly(methyl methacrylate) (PMMA),
 566
Poly(siloxane), 145–146, 589
Poly(styrene-co-methacrylic acid)
 (PSMA-12), 571
Polyamides, 335–336
Polybrominated diphenyl ethers, 853
Polychlorinated biphenyls (PCB),
 836–838
 analytical considerations, 839–840
 chromatographic separation, 843
 commercial mixtures, 841
 for environment, 836
 individual congeners analysis,
 841–843
Polycyclic aromatic hydrocarbons
 (PAHs), 185, 859–861
Polydimethylsiloxane, 103
Polyester polyols, 335
Polyethylene glycol, 420
Polyfunctional compounds, 642–644
Polyimide, 103–105
Polyimide resin, 103–104
Polymers blends, inverse gas
 chromatography (IGC),
 569–573
Polymers, bulk properties of,
 569–573
Polyolefins, 332–334
Poly(cyanoalkylsiloxane) phases,
 145–146
Polypropylene, 332–333
Polysaccharides, 719–720
Polysiloxane, stationary phases and,
 6
Poly(cyanopropylphenyldimethylsi-
 loxane) stationary phase,
 170–172, 172f
Poly(dimethylsiloxane) stationary
 phase, 174–175
Poly(methyloctylsiloxane) stationary
 phase, 180–181
Poly(dimethyldiphenylsiloxane)
 stationary phases (PMPS),
 172–174
Poly(ester) stationary phases, 147
Poly(ethylene glycol) stationary
 phases, 175
Poly(siloxane) stationary phases,
 151–152, 172–174
Polystyrene (PS), 330–331, 566
Polytetrafluoroethylene, 326–327
Polyurethanes, 335
Polyvinylacetate (PVA), 334
Polyvinylchloride (PVC), 334, 334f
Porous-layer open tubular (PLOT), 23
 , 117, 141–142, 659, 659t
 behavior of adsorbents, 122–123
 chemistry, 117–119
 in gas chromatography–mass
 spectrometry, 123
 manufacture of, 119–121
 measurement of restriction, 119
 most commonly used adsorbents,
 124–138
 alumina, 124–127
 carbon, 131–134
 inorganic salts, 135
 molecular sieves, 127–130
 porous polymers, 135–138
 silica gel, 134–135
 stabilization of adsorption layers,
 121–122
 types of capillary tubing, 123–124
Porous organic cages, 593
Porous organic polymers, 160
Porous polymers, 135–138
 common packed-column
 applications of, 161t
Positional isomers, high-resolution
 analysis of, 688–689
Positive chemical ionization (PCI),
 754–755
Positive ion CI, 385–390
Postinjection effect, 234–235, 237f
Potassium bromide, 375–376
Power management, 478–481
 column power (isothermal),
 478–479, 478f–479f
 column power (programmed),
 480, 482f
 electric precision controllers, 481
 pumps–pressure or vacuum, 481
Practical recommendations,
 78–79
Prebiotic chemistry, 867–869
Precision, data analysis methods,
 554–555
Preform–draw material, 100–101
Preforms, for fused-silica columns,
 100–101
Preinjection effect, 232, 237f
Preparative fraction collector (PFC),
 490–491
Preparative gas chromatography
 (Prep-GC), 678
 analytical-scale prep-GC, 488–489
 1D GC, 489, 490f
 multidimensional gas
 chromatography (MDGC),
 489–490, 490f
 spectroscopic methods, 494,
 495t–497t
 trapping systems, 490–493
 applications, 494–502, 495t–497t
 scale, 488–489
 case studies, 494–502
 chiral studies, 499–500
 environmental pollutant studies,
 498–499
 large-scale preparative GC, 488
 multidimensional gas
 chromatography (MDGC),
 500–501, 501f
 multiple injections with
 prep-collection, GC column, 502
 natural products, 494–498
 petroleum studies, 500

- Preparative gas chromatography
(Prep-GC) (*Continued*)
 pharmaceutical samples, impurities
 in, 498, 499f
 pheromones, 494–498
 prep-scale enrichment, GC analysis,
 501
 trace components, 487
 X-ray analysis, 499–500
- Preparative-scale gas
 chromatography, 150–151
- Preprocessing chromatographic data,
 527–533
 baseline correction, 528–529, 529f
 noise reduction, 529–531, 530f
 normalization, 531–532
 retention time alignment, 532–533
 software platforms, 533
- Prep-scale enrichment, GC analysis,
 501
- Pressure gauge/transducer, 222
- Pressure-pulsed injection, 239–240
 splitless injection and, 243f
- Pressurized fluid extraction, 625–626
- Pressurized liquid extraction (PLE),
 for baby food, 803–804
- Pressurizing phase, in transfer-
 linebased systems, 259
- Primary free radicals, 326
- Principal component analysis (PCA),
 534–536, 536f
- Principal component regression
 (PCR), 540–541
- “Product ion spectrum”, 413–414
- Programmable split splitless injector
 (PSS), 240
- Programmable temperature
 vaporizer (PTV) injector,
 240–245, 271, 745
 COCl with, 243–244
 injection modes for, 241t
 with LVI, 244–245
 sample introduction and, 240–245
- Programmed pyrolysis, 330
- Programmed split injection, 241–242
- Programmed splitless injection,
 242–243
- Programmed-temperature vaporizer
 (PTV) injector, 12
- Protective coating, 103–104
- Prototyping, 481–482, 483f–484f
 “Pseudo-absolute”, 388
- Pseudoabsolute quantification, 388
- Pseudointegration, 525–526
- “Pulling toffee”, 101
- Pulsed discharge electron-capture
 detector (PDECD), 353
- Pulsed-discharge HID (PDHID),
 356–357
- Pulsed-discharge photoionization
 detector (PDD), 476
- Pulse pyrolysis, 329–330
- Pumps—pressure or vacuum, 481
- 3-Pyridyl carbinol derivative, 420,
 422f
- Pyrolysis-gas chromatography, 325
 applications
 acrylics, 331–332
 advanced applications, 337–341
 biomass, 336–337
 epoxies, 336
 polyamides, 335–336
 polyolefins, 332–334
 polystyrene, 330–331
 polyurethanes, 335
 vinyl polymers, 334–335
 instrumentation
 programmed pyrolysis, 330
 pulse pyrolysis, 329–330
 molecular theory
 bond dissociation and free
 radicals, 326
 copolymers, 328–329
 no oligomers, 328
 oligomer formation, 326–328
- Q**
- Quadrupole-collision celleTOF (Q-
 TOF) instrument, 414
- Quadrupole ion trap (QIT), 410–411
- Quadrupole (Q) mass filters, 409–411
- Qualitatively polarity, 167
- Quality evaluation, 114–115
- Quality monitoring, 105–107
- Quantitative calculations, 505
- Quantitative sample re-collection, 280
- Quick, easy, cheap, effective, rugged,
 and safe (QuEChERS), 794
 baby food, 803
- R**
- Racemic isoleucine, 592f
- Radioisotope-based detectors, 351,
 353, 356
- Radioisotope sources, 427–428
- Rapid data acquisition, 377
- Rapid scan interferometry, 378
- Reactant ion peak (RIP), 435f
- Reagents forming derivatives,
 641t–642t
- Receiver operating characteristic
 (ROC), 732
- Reduced analytical interference, 269
- Reduced exposure risk, 269
- Reference void time, 39
- Regional reconstruction, 380–381
- Regression models, 181–182
- Relative humidity (RH), 564–565,
 565f
- relative response factors (RRFs), 388
- Relative retention measurements,
 181–182
- Reliable extraction efficiency, 269
- Reliable gas standards, 313
- Repeatability, 554–555
- Reproducible analyte retention, 103
- Residual volatiles, direct thermal
 desorption of, 299–301
- Resolution methods, 538–540
- Resonance enhanced multiphoton
 ionization (REMPI), 408
- Retardation factor, 23
- Retention gap in COCl,
 226–229, 228f
- Retention index, 679
- Retention models, 153–155
- Retention projection, 184–185
 methodology, 184–185
- Retention time alignment, 532–533
- Retention time locking (RTL), 40,
 184–185, 598–601
- Reusable samplers, 269
- Reversed-flow gas chromatography,
 158
- Reversed-phase liquid
 chromatography (RP-LC),
 498–499
- Reverse solvent effect, 226, 226f
- Rinsing, 109
- Riot control/incapacitating agents,
 882–883
- Robustness, data analysis methods,
 556–557
- Rohrschneider/McReynolds system,
 142–143, 167–168
- Rosetta mission, 867–869
- Rtx-CLPesticides, 176–177
- Rtx-OPPesticides, 176–177
- Rubber septum, flash vaporizer
 with, 3
- Rule of thumb, 507
- Rydberg transitions, 385

- S**
- SACPS, 174–175
- Salmeterol xinafoate (SX), 566
- Salting out, 264
- Salting-out-assisted liquid–liquid extraction, 620
- Sample, 19
- Sample introduction
- COCI and, 223–229
 - flash vaporization injector and, 229–231
 - for GC
 - choosing, 218
 - supporting devices for, 218
- GSV and, 246–247
- LSV and, 247
- and PTV, 240–245
- split injection and, 231–240
- splitless injection and, 237–240
- Sample-loop system
- in MHE, 260
 - in SHE, 260
- Sample preparation
- column chromatography, sample cleanup by, 635–638
 - multidimensional gas chromatography, 636–638
 - multimodal gas chromatography, 636–638
 - isolation and concentration techniques
 - gas-phase extraction, 626–627
 - liquid–solid extraction, 623–626
 - membrane extraction, 635
 - solid-phase extraction, 627–632
 - solid-phase microextraction, 632–635
 - solvent extraction, 618–623
 - traditional methods, 616–618
- microchemical reactions, 638–648
- alkylation reagents, 645, 646t
 - alkylsilyl reagents, 640–644, 642t–643t
 - chloroformate reagents, 645–647
 - functional group selective reagents, 647–648
 - haloalkylacyl reagents, 644–645
 - reagents forming derivatives, 641t–642t
- Samples
- for COCI, 223–224
 - for GC-ICPMS, 457
 - introduction of, for GC, 217–218
 - Sample stability, data analysis methods, 557
 - Sample-storage interfacing techniques, 378–379
 - Sampling and gas chromatographic analysis, 887–895
 - Saturated hydrocarbons, 209–211
 - Savitzky–Golay smoothing, 515–516
 - Scanning tunneling microscopy (STM), 563
 - Selected ion-monitoring (SIM) juice, 799
 - MRMs, 794, 798
 - SPE, 794
- Selective elimination of interferents, 269
- Selenium, 460
- in urine, 461
- Self-CI, 894
- Sensitivity, of SHE, 254
- Separability-averaged immobility, 71
- Separation
- 2D GC and, 193–195
 - graphical representation for, 193–195, 197–200
- efficiency, 55
- enantiomers
- α -amino acid derivatives, 583–584
 - chelates as chiral selectors, 584–587
 - chiral covalent organic frameworks (COFs), 593
 - chiral ionic liquids, 594–595
 - chiral mesoporous silica, 593–594
 - chiral recognition, strategy for, 596–604
 - chiral stationary phases, 583–595
 - complexation gas chromatography, 586f
 - cyclofructans, 590–591, 591f
 - derivatized cyclodextrins, 587–590
 - determination of, 595–596
 - direct approach, 582
 - hydrogenbonding CSPs, 584, 585f
 - indirect approach, 582
- MCPP (4-chloro-2-methylphenoxy) propionic acid, 581
- metal–organic cages, 593
 - metal–organic frameworks, 591–593, 592f
 - micropreparative enantioselective gas chromatography, 604–606
 - porous organic cages, 593
 - recognition, 582
 - total analysis system (TAS), 604
 - GC-MS and, 13–14
 - for GC X GC, detectors in, 209
- Septa
- flash vaporizer with, 3
 - in liquid injectors, 221
- Septum-equipped temperature programmable capillary injector (SPI), 240
- Signal measurement, 506–508
- Signal-to-noise ratio, 90, 511
- Silanol groups, 148–149
- Silarylen–esiloxane copolymers, 173t
- Silica as packed precolumn, 135
- Silica-coated columns, 134
- Silica gel, 134–135
- Simpson's rule, 513
- Simulated distillation (SimDist), 663–664, 664f
- Single-beam interferometer, 376–377
- Single-drop liquid-phase microextraction (SDME), 457
- Single-drop microextraction (SDME), 458, 817–818
- HS-SDME, 257
- Single ion chromatograms, 418–419
- Single-ion (SIM) detection limits, 314
- Single ion monitoring (SIM), 847–848
- Single stationary phases, 148
- Singular value decomposition (SVD), 538–539
- Six-port valve, 474f
- Smoothing, 514–517
- adaptive smoothing, 516
 - area, 516–517
 - bunching, 515
 - height, 516–517
 - linear filters, 515
 - median filter, 516
 - moving average, 515
 - moving weighted average, 515
 - multiple smoothing, 515
 - Savitzky–Golay filter, 515–516
 - smoother comparison, 516
- Smooth medium, 51
- Société Française des Sciences et Techniques Pharmaceutiques (SFSTP), 548, 554
- Soda glass, 100

- Sodium tetrahydroborate (NaBH₄), 458
- “Softer” ionization technique, 379
- Software platforms, 533
- Soil
- antimony in, 459
 - arsenic in, 459
 - GC-ICPMS for, 459
 - mercury in, 459
- Soil gas and vapor intrusion into buildings, 294
- Solid-phase extraction (SPE), 627–632, 667, 794
- sample processing conditions, 631–632, 632t
 - sorbents for, 629–631, 630t
 - wine, 794
- Solid phase microextraction (SPME), 267, 434, 457–458, 604, 632–635, 678, 737
- commercially available extraction phases, 633
 - extraction phase, 633–634
 - for MRMs, 794
 - nonfiber formats, 634–635
 - selection guide, 634t
- Solubility parameter, inverse gas chromatography (IGC), 572–573
- Solute asymptotic migration immobility, 43
- Solute–column interaction
- characteristic parameters of, 24–29
 - relations between characteristic parameters, 29
 - solute distribution between mobile and stationary phases, 23–24
- Solute diffusion, 31–33
- Solute distribution, 24
- Solute elution temperature, 38
- Solute hydrogen-bond acid, 168
- Solute linear retention model, 26
- Solute migration and elution, 37–45
- dimensionless heating rate and void temperature increment, 41–43
 - general equations of, 38–39
 - isobaric analysis, 39–40
 - linear heating ramp and linear retention model, 41
 - method translation and retention time locking, 40
 - migration and elution parameters, 43–45
- Solute mobile time, 38–39
- Solute–solvent interactions, 168
- Solvation parameter model, 169t, 182–183
- Solvent bar microextraction, 801
- Solvent extraction, 618–623
- air monitoring, 268–270
 - classical liquid–liquid extraction, 618
 - applications, 620–622
 - countercurrent chromatography, 618–620
 - liquid-phase microextraction, 622–623
 - organic compounds isolation, 619t
 - salting-out-assisted liquid–liquid extraction, 620
 - solvent selection, 620
- Solvents
- boiling points of, 221t
 - in COCl₂, 224–226
 - extraction, for wine, 801
 - flooding effect, 225, 225f
 - samples of, HS-GC and, 263–264
 - selection, 620
 - split injection and, 232
 - in splitless injection, 237
 - vapor volumes for, 221t
- Sorbent-packed injector liners, 270
- Sorbent tubes, 288
- Sorptive extraction (SP), 255–257, 815–817
- Space
- Cassini–Huygens mission, 867
 - chirality, 871–872, 871f
 - future perspectives, 872
 - mars exploration, 869–871, 869f–870f
 - mission, 865
 - operating constraints, 866–867, 866t
 - prebiotic chemistry, 867–869
 - Rosetta mission, 867–869
 - technological constraints, 866–867, 866t
- Specialized sample introduction methods, 875
- Special zeolites for argon and oxygen, 130
- Specificity, data analysis methods, 556
- Specific speed-optimized flow rate (SSOF), 74–75
- Spectroscopic methods, 494, 495t–497t
- Spectrum addition and subtraction, 417–418
- Speed optimization, 74
- Speed-optimized flow (SOF), 74–75, 602–604
- Split flow, recollection of, 278–280
- Split injection, 11–12, 236
- backpressure regulator in, 236–237
 - forward pressure regulator in, 236
 - liners in, 235–236
 - pneumatic systems in, 236–237
 - programmed, 241–242
 - sample introduction and, 231–240
 - solvents and, 232
 - syringes in, 232–237
 - vaporizing, 243
- Splitless injection, 11–12
- liners in, 239
 - pneumatic systems in, 239
 - pressure-pulsed injection and, 243f
 - programmed, 242–243
 - sample introduction and, 237–240
 - solvents in, 237
 - syringes in, 239
 - vaporizing, 243
- Split ratio, 236
- SPME sampling, 890–891
- Squalane, stationary phases and, 6
- S-Swafer, 198–199
- Stable carbon isotope composition, 663
- Stack (flue) gases, 293–294
- “Stand-alone” sampling devices, 288
- Standard addition, 551
- Standard furnace heating system, 102
- Standard SGE dimensional specifications, 105t
- Stanyl esters, 691–693
- Static coating, 112–113, 120
- Static headspace extraction (SHE), 253–255
- partition coefficient and, 254–255
 - phase ratio and, 254
 - sample-loop system in, 260
 - sensitivity with, 254
 - transfer-line-based systems and, 259–260
- Stationary phase (SP), 6, 19, 111–112, 167–181, 170t–171t, 176t, 656–657
- classification of, 151–153

- classification of stationary phases, 177–180
compositions, 176–177
interactions, 169–170
moieties, 111
molecules, 109
polymer, 112
polysiloxane and, 6
selection, 192–193
solvation parameter model, 168–169
stationary-phase selectivity tuning, 180–181
structure–retention relationships, 181–186
isothermal retention index, 182–183
quantitative structure/retention relationships, 185–186
temperature-programmed retention and retention indices, 183–185
system constants database for open-tubular columns, 169–177, 170t–171t
- Sterol esters, 691–693
Sterols, 691–693
Steryl glycosides, 691–693
Stir bar sorptive extraction (SBME), 255–256, 261–262, 457, 493, 795
Strong gas decompression, 75–78
Structure-selective detectors, 345, 350–351, 351t
Styrene divinylbenzene derivative, 122
Sulfur detectors, 892
Sulfur gases, 137–138
Sulfur mustard, 889
Sum of the squared residuals (SSR), 387
Supercritical fluid extraction (SFE), for MRMs, 794
Supervised multivariate analysis, 438
Supervised pattern recognition methods, 533–534
Support coated open-tubular capillary columns (SCOT), 3–4, 142
Surface acoustic wave detector (SAW), 477
Surface chemistry, 101
Surface deactivations, 109–110
Surface free energy, 563
Surface preparations, 108
Synthesized functional group interferograms, 380–381
Synthetic fused-silica material, 100
Syringes
for HS-GC, 258–259
in liquid injectors, 218–220
in split injection, 232–237
in splitless injection, 239
System constants, 151, 170t–171t
- T**
Tandem configurations, 414
Tandem mass spectrometers, 413–414, 894–895
for MRMs, 794
t-Butyldimethylsilyl (TBDMS) derivatives, 414–415
Temperature
program conditions, 185
vial, headspace-gas chromatography and, 263
Temperature domain (T-domain) representation, 43
Temperature-programmed GC, 183–184, 184t
plate height, efficiency, and optimal flow in, 61–64
Temperature-programmed retention indices, 185
Temperature programming, 20
Temperature vaporizing injector (TPI), 240
Temporal spacing, 45
Tensile strength, of fused-silica capillary columns, 8
Tert-amyl methyl ether (TAME), 198–199
Tertiary free radical, 331
1,3,6,8-tetrachlorodibenzo-p-dioxin (TCDD), 836–838
Tetramethoxysilane (TMOS), 593–594
Tetramethylammonium hydroxide (TMAH), 337–338
Theoretical relations, 29–30
Thermal conductivity detection (TCD), 477, 665
Thermal desorption (TD), 338–340, 748–751, 889–890
applications, 288
calibration of, 313–314
gas chromatography, 267–270
air monitoring, 291–295
industrial (fugitive) emissions, 293–294
industrial (occupational) hygiene or workplace air monitoring, 291
monitoring ambient outdoor air and indoor air quality (IAQ), 291
monitoring vehicle interior air quality (VIAQ), 292–293
breath monitoring, 290–291
of complex liquid and solid samples, 285–288
direct thermal desorption of residual volatiles, 299–301
essential functions and performance characteristics, 270–274
automation, 273
double splitting, 273–274
two-stage desorption, 271–272
evolution of
air/gas sampling, 282–284
continuous online monitoring, 285
electronic control of flows and pressures, 280–282
formaldehyde, 284–285
heated valve technology for thermal desorption, 277
limitations of early systems, 276
optimization of focusing trap, 276–277
recollection of split flow, 278–280
tube sealing for automation, 277–278
forensic applications
accelerants in fire debris, 306
drugs of abuse, 306–307
explosives and shotgun propellant residues, 307
forensication (characterization) of inks, paper, and other materials, 308–309
monitoring manufacturing and other industrial chemical processes, 309
general principles, 267–268

- Thermal desorption (TD) (*Continued*)
indoor and in-vehicle air, 295–299
odor/fragrance profiling and VOC
“fingerprinting”, 301–303
sampling options for, 288
with solvent extraction for air
monitoring, 268–270
thermal desorption applications,
288
toxic chemical agents and civil
defense, 299
method development, 309–314
Thermal gradient GC, 24, 38
Thermally assisted hydrolysis,
337–338
Thermal modulation GC x GC, 209
Thermal modulators, 207
Thermal spacing, 45
Thermionic ionization detector (TID),
345–346, 346t, 348–350
Thermodynamic function, 165
Thermostating phase, in transferline-
based systems, 259
Thick-film columns, 165–167
Thin-film columns, 55–56
Thin-layer chromatography (TLC),
685
Thin-wall fused-silica capillary
tubing, 100
Three-dimensional (3D) data,
526–527
Threshold limit values (TLVs),
291
Time-averaged velocity, 35
Time-consuming calculations, 380
Time-dependent density functional
theory (TDDFT), 387–388
Time interval deconvolution (TID),
388
Time-of-flight mass spectrometry
(TOFMS), 209, 412–413, 412f,
813
GC X GC with, 212f
for yeast extracts, 211
for wine, 801
Toluene diisocyanate (TDI), 335
Total acidity number (TAN), 655–656
Total analysis system (TAS), 604
Total current vaporization, 239
Total ion chromatograms (TIC), 418
Toxic chemical agents and civil
defense, 299
Toxins, 881–882
Trace components, 487
Trace evidence, forensic science,
767–768, 768f
Tracer gases, monitoring, 294–295
Traditional liquid extraction
methods, 285
Traditional methods
distillation, 616–617
freeze concentration, 617–618
freeze-drying, 617–618
Traditional pulse pyrolysis, 337–338
Transfer-line-based systems, SHE
and, 259
Transport efficiency, 55
Trapping systems, 490–493
capillary trapping, 491, 492f–493f
Gerstel preparative fraction collector,
490–491, 492f
sorber trapping method, 493, 494f
Triacylglycerols (TAG), 683–684
Tributyltin (TBT), 458
Trifluoroacetic anhydride (TFAA),
748–751
3,3,3-Trifluoropropyl-methylsiloxane
monomers, 174
Trilinear decomposition (TLD), 539
Trimethylchlorosilane, 640–642
Trimethylsilyl (TMS), 378,
733–734
Trimethylsilyldiethylamine, 640
Trimethylsilylimidazole, 640–642
Trinitrotoluene (TNT), 761–762
“Triple quadrupole”, 413
Triple quadrupole instruments,
413–414
Triple quadrupole mass
spectrometer, 413f
1,2,3-tris-(2-cyanoethoxy)propane
(TCEP), 199
Trueness, data analysis methods,
555–556
Tube sealing for automation,
277–278
Two-dimensional gas
chromatography (2D GC),
191–192, 200
backflushing for, 195–200
for gasoline oxygenates,
197–200
heartcutting, 200–203
independent column heating and,
202–203
multiple heartcuts and, 200–203
separation and graphical
representation for, 193–195
Two-stage desorption, 271–272
Two-stage thermal desorption,
272f–273f, 277f
Two-stage thermal modulation,
207–208, 208f
Typical gas-phase CLD, 364–365
- U**
Ultimate trade-off triangle, 92
Ultra-high-purity helium, 356
Ultrasound-assisted extraction,
624–625
Ultrasound irradiation, 639
Ultravolatile organics, 276
Uniform heating of columns, 51
Uniform static chromatography,
plate height in, 48–50
United States Pharmacopeia (USP),
252, 556–557
Unresolved complex mixture
(UCM), 500
Unsupervised analysis, exploratory
analysis by, 437–438
Upper limit of quantification
(ULOQ), 553–554
Urine, GC-ICPMS for, 461
US Environmental Pollution Agency
(US EPA), 770
- V**
Vacuum gas oil (VGO), 667
Vacuum HS sampling technique, 678
Vacuum ultraviolet (VUV), 373, 390,
394, 665
detection, 384
gas chromatography, 382–390
software, 387
Validation, gas chromatography
(GC), 547–560
accuracy profiles, 559
characteristics and guidelines for,
549t
linearity, 550–553
method items for, 548–557
regulatory aspects, 548
steps, 548f
Valve-based modulation, 206
van Deemter equation, 158
Vaporizing injectors, 218
Vaporizing split injection, 243
Vaporizing splitless injection, 243

- Vehicle interior air quality (VIAQ),
292–293
- Vesicants, 879–881, 880f
- Vial temperature, HS-GC and, 263
- Vinyl polymers, 334–335
- Viscosity, 30–31
- Void temperature increment, 41–43
- Void time, 510
- Volatile metal halides, 145
- Volatility constraints, 887
- Volatility range, 276
- Volumetric flow rate, 35
- VX, 888–889
- W**
- Wall-coated open-tubular capillary
columns (WCOT), 3–5, 23, 99,
141–142, 659–660
- coatings for, 103
- for environment, 836
- Water, 457–459
- Waxes analysis, 693
- Weak gas decompression, 79–81
- Wide-bore fused-silica capillary
columns, 12
- Wine, 801–802
- carbon-based sorbents, 808
- cationic imidazolium-based ionic
liquids, 809–810
- comparisons of methods,
819–821
- detectors, 812–815
- gas chromatography (GC),
807–808
- graphene oxide, 808
- hyphenated techniques, 812–815
- liquid-phase microextractions,
817–819, 818f
- multidimensional separations,
810–812
- sample preparation, 815–821
- sorptive extraction methods,
815–817
- stationary phases, 808–810
- Workplace air monitoring,
291
- Workplace drug testing, forensic
science, 758–759
- World Anti-Doping Agency
(WADA), 757–758
- X**
- X-ray analysis, 499–500
- Y**
- Yeast extracts, GC X GC-TOFMS for,
211, 212f
- Z**
- Zeroth peak moment, 513

GAS Chromatography

Edited by **Colin F. Poole**

Professor Colin F. Poole (Wayne State University) is internationally known in the field of thin-layer chromatography and is an editor of the *Journal of Chromatography* and former editor of the *Journal of Planar Chromatography – Modern TLC*. He has authored several books on chromatography. He is the author of approximately 400 research articles, many of which deal with thin-layer chromatography, and is co-chair of the biennial "International Symposium on High-Performance Thin-Layer Chromatography".

A single source of authoritative information on all aspects of the practice of gas chromatography

Gas Chromatography, Second Edition, offers a single source of authoritative information on all aspects of the practice of gas chromatography. A focus on short, topic-focused chapters facilitates identifying information of immediate interest for familiar or emerging uses of gas chromatography. It gives those working in both academia and industry the opportunity to learn, refresh, and deepen their understanding of fundamental and instrumental aspects of gas chromatography and tools for the interpretation and management of chromatographic data. It provides a consolidated guide to the selection of separation conditions and the use of auxiliary techniques approached by the reader for possibly the first time or after some time.

This new edition restores the contemporary character of the book with respect to those involved in advancing the technology, analyzing the data produced or applying the technique to new application areas. New topics covered include hyphenated spectroscopic detectors, micromachined instrument platforms, derivatization and related microchemical techniques, petrochemical applications, volatile compounds in the atmosphere, and more.

Key Features

- Provides an overview and focused treatment of single topics in individual chapters written by recognized authoritative and visionary experts in the field
- Offers comprehensive coverage of modern gas chromatography from theory, to methods, to selected applications
- Places modern developments in research literature into a general context not always apparent to inexperienced users of the technique

Science / Chemistry / Analytic



ELSEVIER

elsevier.com/books-and-journals

ISBN 978-0-12-820675-1



9 780128 206751